Barnes, Paul W., Bornman, Janet F., Pandey, Krishna K., Bernhard, Germar H., Bais, Alkiviadis F., Neale, Rachel E., Robson, Matthew ORCID: https://orcid.org/0000-0002-8631-796X and et. al. (2023) Environmental effects of stratospheric ozone depletion, UV radiation, and interactions with climate change: 2022 assessment report.

Environmental Effects of Stratospheric Ozone Depletion, UV Radiation, and Interactions with Climate Change

2022 Assessment Report

UN environment programme | ozone secretariat

Montreal Protocol on Substances that Deplete the Ozone Layer

Montreal Protocol
On Substances that Deplete the Ozone Layer

UNEP
2022 Assessment Report of the
Environmental Effects Assessment Panel

The text of this report is composed in Gibson.

Disclaimer

The United Nations Environment Programme (UNEP), the Environmental Effects Assessment Panel (EEAP) Co-chairs and members, and the companies and organisations t in furnishing or distributing this information, do not make any warranty or representation, either express or implied, with respect to the accuracy, completeness, or utility; nor do they assume any liability of any kind whatsoever resulting from the use or reliance upon any information, material, or procedure contained herein,including but not limited to any claims regarding health, safety, environmental effect or fate, efficacy, or performance, made by the source of information.

Mention of any company, association, or product in this document is for information purposes only and does not constitute a recommendation of any such company, association, or product, either express or implied by UNEP, the Environmental Effects Assessment Panel Co-chairs or members, or organisations that employ them.

Acknowledgement

The Environmental Effects Assessment Panel, Co-chairs and members acknowledge with thanks the outstanding contributions from all of the individuals and organisations who provided support to the Panel. The opinions expressed are those of the Panel and do not necessarily reflect the reviews of any sponsoring or supporting organisation.

HIGHLIGHTS

Environmental Effects Assessment Panel
2022 Quadrennial Assessment

Environmental effects of stratospheric ozone depletion, UV radiation, and interactions with climate change

The highlights of the 2022 Quadrennial Assessment focus on major findings since the last assessment, acknowledging the contribution of the Montreal Protocol on Substances that Deplete the Ozone Layer to several of the United Nations Sustainable Development Goals and the alignment of the Panel with these Goals. The strong interconnected effects of stratospheric ozone depletion, ultraviolet (UV) radiation, and climate change are increasingly evident and complex, with consequences for life on Earth and a sustainable future. Within this context, the Highlights cover current and projected consequences for human health (including the COVID-19 pandemic), terrestrial and aquatic ecosystems, air quality, natural and synthetic materials, and microplastics.

1 Ultraviolet radiation, stratospheric ozone depletion, and climate change

- Concentrations of stratospheric ozone in the future will depend on the decrease in ozone-depleting substances (ODSs) controlled by the Montreal Protocol, other substances currently not controlled, and on emissions of greenhouse gases, such as carbon dioxide, methane and nitrous oxide. The trajectory of these emissions depends greatly on policy decisions.
- Large increases in UV radiation were observed during the 2020 Antarctic and Arctic springs, when the UV Index rose by to 80% and 70%, respectively, above the historical means.
- In the Antarctic, these anomalously high amounts of UV radiation extended over spring and the start of summer, and may have had negative consequences for migrating animals returning to breed, which may not have been adapted to the unusually high UV irradiation.
- Increasing warming will lead to more ice melt and increased exposure of ecosystems to UV radiation on land and in water bodies, especially in polar and high-elevation regions.
- Thawing of permafrosts will result in the release of UV-absorbing organic carbon into aquatic ecosystems and enhanced emissions of carbon dioxide and methane to the atmosphere.
- The concurrence of heat waves with drought and high UV-B irradiance (280-315 nm) may negatively affect food security and biodiversity of crops and animals. These climatic conditions can disrupt formerly favourable habitats and may shift habitats to locations with different conditions, to which plants and animals may not be adapt. Tropical coral reefs under naturally high UV irradiance are of particular concern, since an increase in sea surface temperatures of 1 °C to 2 °C can cause bleaching of corals, enhanced by high amounts of UV radiation.

2 Human health

- Exposure to UV radiation has multiple harms and benefits. Harms include skin cancer, inflammatory skin disorders, sunburn, and eye disorders such as cataract. Benefits include production of vitamin D, reduced autoimmune disease and, possibly, lowered blood pressure and decreased risk of metabolic disorders.
- The Montreal Protocol has resulted in significant reductions in UV-related diseases. The United States Environmental Protection Agency has estimated that, due to the Montreal Protocol, 11 million cases of melanoma, 432 million cases of keratinocyte skin cancers, and 63 million cases of cataract will have been avoided for those born between 1890 and 2100 in the United States.

- The Montreal Protocol may have benefits for UV-induced inflammatory skin disorders. In some people these lead to large decreases in quality of life. Many diuretic and anti-inflammatory drugs can cause photosensitivity when skin is exposed to UV radiation, although the global incidence of drug-induced photosensitivity is unclear. Some drugs used for decreasing blood pressure may increase the risk of keratinocyte skin cancer through UV-induced DNA damage.

- By avoiding large increases in the UV Index, the Montreal Protocol may have enabled people, especially those with light skin, to spend time outdoors without incurring sunburn, thereby gaining the benefits of sun exposure. One of these benefits is the generation of vitamin D in the skin. Vitamin D plays an important role in maintaining musculoskeletal health, and there is increasing evidence of benefits for diseases related to immune function, including autoimmune diseases (e.g., multiple sclerosis), infection, and for cardiovascular disease, cancer mortality, and all-cause mortality.

- Decreases in UV radiation under the Montreal Protocol may have resulted in a lower rate at which pathogens are inactivated, including the SARS-CoV-2 virus responsible for COVID-19. However, the positive outcomes of the Montreal Protocol outweigh any potential advantage for disinfection by higher amounts of solar UV radiation.

3 Role of UV radiation in the troposphere

- Outdoor air pollution (e.g., from sulfate, nitrate, ozone, and particulate matter) results in ca 4 million premature deaths per year, and also damages vegetation and crops.

- Increasing concentrations of greenhouse gases are partly responsible for enhanced atmospheric circulation resulting in a downward transport of additional ozone ('good' UV-B-absorbing ozone) from the stratosphere to the troposphere ('bad' ozone, part of smog).

- In the troposphere (the layer of the atmosphere extending from the Earth's surface to a height of 8-15 km), UV-B radiation generates the cleaning agent of the atmosphere, the hydroxyl radical (OH). This radical removes many compounds released by human activity and natural sources, such as carbon monoxide, methane, and HFOs, HFCs and HCFCs[1] (widely used as refrigerants). HFCs and HCFCs have high global warming potential contributing to climate change. When broken down by hydroxyl radicals, these compounds can form halogenated chemicals, including trifluoroacetic acid (TFA).

- TFA has a long environmental lifetime, accumulates in surface and ground waters, and has been found in blood, drinking water, beverages, dust, plants, and agricultural soils. However, it does not interact with biological molecules and, due to its high solubility in water, it does not bioaccumulate. It is unlikely to cause adverse effects in terrestrial and aquatic organisms. Continued monitoring and assessment are nevertheless advised due to uncertainties in the deposition of TFA and its potential effects on marine organisms.

- UV radiation also plays a key role in creating harmful photochemical smog by reacting with pollutants such as nitrogen oxides, and volatile organic compounds (e.g., fuel, solvent vapours) mostly from industry and transport. Even low concentrations of pollutants are detrimental to human health, prompting the World Health Organization to recommend average annual decreases in key air pollutants, including halving the maximum current level ($10~\mu g/m^3$) of small particulate matter to $5~\mu g/m^3$, and that of nitrogen dioxide from 40 to $10~\mu g/m^3$.

4 Global challenges of increasing plastic debris in the environment

- Many materials, including plastics, are susceptible to solar UV radiation, high temperature, and moisture, resulting in degradation, loss in strength, discolouration, decreased service life and environmental pollution due to the release of potentially environmentally harmful by-products. UV-stabilisers and other additives are being used to counteract photodegradation and release of toxic by-products.

- UV-degradation of plastics leads to generation of microplastics (<5 mm) and nanoplastics (<0.001 mm), which have been found in ecosystems, bottled drinking water, table salt, seafood, and wastewater. Microfibres, including textile fibre fragments, are common contaminants of the environment. However, the biological effects of micro- and nanoplastics remain uncertain.

- New UV-stabilisation technologies that block UV radiation through treatment of textiles with certain oxide nanoparticles (e.g., zinc oxide, titanium oxide), are being developed for next-generation synthetic (e.g., polyester fabric) and natural textiles (e.g. cotton fabric).

A sustainable future requires continued adherence to the Montreal Protocol, with particular attention paid to mitigation of climate change, since recovery of stratospheric ozone is highly dependent on changes in greenhouse gas emissions and atmospheric concentrations of ozone-depleting substances, which will also determine future UV radiation at the Earth's surface.

---

[1] ODS replacements: HFCs, hydrofluorocarbons; HCFCs, hydrochlorofluorocarbons; HFOs, hydrofluoroolefins.

PREFACE

Background

The Montreal Protocol on Substances that Deplete the Ozone Layer was established 35 years ago following the 1985 Vienna Convention for protection of the environment and human health against excessive amounts of harmful ultraviolet-B (UV-B, 280-315 nm) radiation reaching the Earth's surface due to a reduced UV-B-absorbing ozone layer. The Montreal Protocol, ratified globally by all 198 Parties (countries), controls ca 100 ozone-depleting substances (ODS). These substances have been used in many applications, such as in refrigerants, air conditioners, aerosol propellants, fumigants against pests, fire extinguishers, and foam materials.

The Montreal Protocol has phased out nearly 99% of ODS, including ODS with high global warming potentials such as chlorofluorocarbons (CFC), thus serving a dual purpose. However, some of the replacements for ODS also have high global warming potentials, for example, the hydrofluorocarbons (HFCs). Several of these replacements have been added to the substances controlled by the Montreal Protocol. The HFCs are now being phased down under the Kigali Amendment. As of December 2022, 145 countries have signed the Kigali Amendment, exemplifying key additional outcomes of the Montreal Protocol, namely, that of also curbing climate warming and stimulating innovations to increase energy efficiency of cooling equipment used industrially as well as domestically.

As the concentrations of ODS decline in the upper atmosphere, the stratospheric ozone layer is projected to recover to pre-1980 levels by the middle of the 21st century, assuming full compliance with the control measures of the Montreal Protocol. However, in the coming decades, the ozone layer will be increasingly influenced by emissions of greenhouse gases and ensuing global warming. These trends are highly likely to modify the amount of UV radiation reaching the Earth's surface with implications for the effects on ecosystems and human health.

Role of the Assessment Panels

Against this background, four Panels of experts were established in 1988 to support and advise the Parties to the Montreal Protocol with up-to-date information to facilitate decisions for protecting the stratospheric ozone layer. In 1990 the four Panels were consolidated into three, the Scientific Assessment Panel, the Environmental Effects Assessment Panel, and the Technology and Economic Assessment Panel.

Every four years, each of the Panels provides their Quadrennial Assessments as well as a Synthesis Report that summarises the key findings of all the Panels. In the in-between years leading up to the quadrennial, the Panels continue to inform the Parties to the Montreal Protocol of new scientific information.

The Environmental Effects Assessment Panel

The Environmental Effects Assessment Panel (EEAP) evaluates the consequences of stratospheric ozone depletion in the context of a changing global climate in line with its Terms of Reference (decision XXXI/2, November 2019) and within the framework of the United Nations Sustainable Development Goals (SDGs). The EEAP also alerts the Parties to additional areas of potential importance to the Montreal Protocol. The 2022 Quadrennial Assessment focusses on the following:

Interactive effects of stratospheric ozone and climate change on:

1. Solar ultraviolet radiation
2. Human health
3. COVID-19 and the Montreal Protocol
4. Terrestrial ecosystems and biogeochemical cycles
5. Aquatic ecosystems
6. Composition of the troposphere and air quality
7. Natural and synthetic materials
8. Microplastics in the environment

This 2022 EEAP Quadrennial Assessment was written by 48 individuals and reviewed by 65 reviewers from 20 countries. The Assessment includes Highlights, Executive Summary, contribution to the above topics, and a Question & Answer (Q&A) document.

Particular attention is given to the linkages between stratospheric ozone depletion and UV radiation, and climate change, with respect to the broad effects on the environment and human health. Key areas of concern are the increased frequency and intensity of extreme climate events that are occurring together with the ongoing increases in emissions of greenhouse gases and consequent rising temperatures in many parts of the world. These changes also change the exposure to UV radiation of humans, other animals, and ecosystems, with implications for human well-being, food security, biodiversity, and overall sustainability of life on our planet.

Janet F. Bornman, Paul W. Barnes, Krishna Pandey

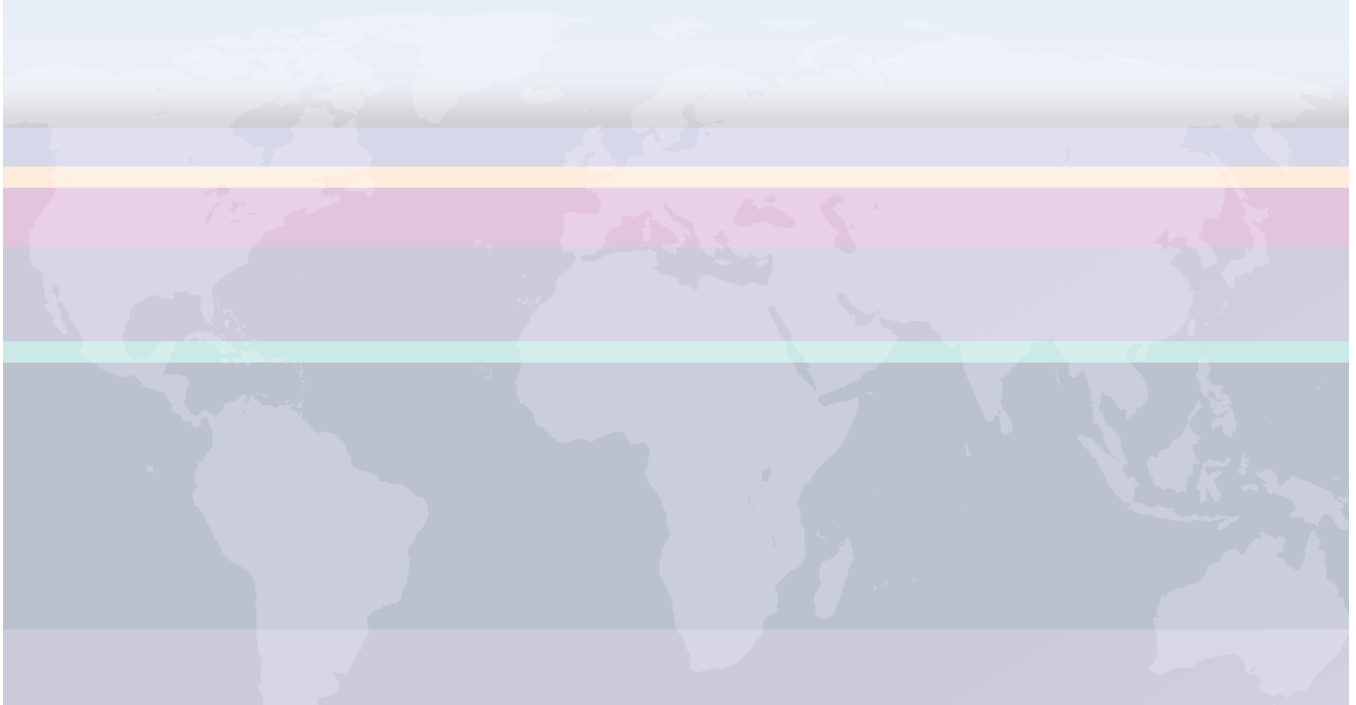*Co-Chairs of the Environmental Effects Assessment Panel, United Nations Environment Programme*

TABLE OF CONTENTS

Table of contents

EXECUTIVE SUMMARY

EXECUTIVE SUMMARY

Environmental Effects Assessment Panel
2022 Quadrennial Assessment

Environmental Effects of Stratospheric Ozone Depletion, UV Radiation, and Interactions with Climate Change

Paul W. Barnes, Janet F. Bornman, Krishna K. Pandey [Co-Chairs], Germar H. Bernhard, Alkiviadis F. Bais, Rachel E. Neale, T. Matthew Robson, Patrick J. Neale, Craig E. Williamson, Sasha Madronich, Stephen R. Wilson, Anthony L. Andrady, Anu M. Heikkilä, Marcel A.K. Jansen, Sharon A. Robinson, Richard G. Zepp, Chris C. White, Pieter J. Aucamp, Anastazia T. Banaszak, Laura S. Bruckman, Marianne Berwick, Scott N. Byrne, Bente Foereid, Donat-P. Häder, Loes M. Hollestein, Wen-Che Hou, Samuel Hylander, Rachael Ireland, Andrew R. Klekociuk, J. Ben Liley, Janice D. Longstreth, Robyn M. Lucas, Roy Mackenzie, Javier Martinez-Abaigar, Richard L. McKenzie, Catherine M. Olsen, Rachele Ossola, Nigel D. Paul, Lesley E. Rhodes, Kevin C. Rose, Tamara Schikowski, Keith R. Solomon, Mads P. Sulbaek Andersen, Barbara Sulzberger, Qing-Wei Wang, Sten-Åke Wängberg, Seyhan Yazar, Antony R. Young, Liping Zhu, Meifang Zhu

1 Introduction

The Montreal Protocol on Substances that Deplete the Ozone Layer and its Amendments and Adjustments (hereafter referred to simply as the 'Montreal Protocol') have proven highly effective in protecting the stratospheric ozone layer and preventing global-scale increases in solar ultraviolet-B radiation (UV-B; wavelengths between 280-315 nm) at the Earth's surface [1,2]. This global treaty, including the Kigali Amendment, has also been one of the most important societal actions taken to date to mitigate global warming, since many of the ozone-depleting substances (ODS) and their substitutes that are controlled by the Montreal Protocol are also potent greenhouse gases (GHGs) [3-5]. The Antarctic ozone hole is contributing to climate change in the Southern Hemisphere, and climate change is modifying the exposure of humans, other animals, plants, and materials to UV-B and UV-A radiation (315-400 nm) [6,7]. Thus, changes in stratospheric ozone, UV radiation, and climate are inextricably linked in a number of ways that have the potential to affect human health and the environment.

In this Executive Summary we highlight and summarise key findings from the 2022 Quadrennial Assessment by the Environmental Effects Assessment Panel (EEAP; Box 1) of the Montreal Protocol under the United Nations Environment Programme (UNEP). The 2022 Qudrennial Assessment presents the most recent, comprehensive assessment since the 2018 Quadrennial Assessment (available at https://ozone.unep.org/science/assessment/eeap and also for the wider scientific community in Photochemical & Photobiological Sciences 18, 595-828). The current assessment addresses the interactive environmental effects of changes in the stratospheric ozone layer, solar UV radiation, and climate on human health, terrestrial, and aquatic ecosystems, biogeochemical cycles, air quality, materials, and microplastics in accordance with the Terms of Reference from the Parties to the Montreal Protocol (Box 1). Additionally, we assess the linkages between solar UV radiation, the Montreal Protocol, and the Coronavirus (COVID-19) pandemic.

> **Box 1. The UNEP Environmental Effects Assessment Panel (EEAP) and its Terms of Reference.**
>
> - *The EEAP is one of the three Assessment Panels established by the Montreal Protocol to assess various aspects of stratospheric ozone depletion (https://ozone.unep.org/science/overview). The EEAP considers the full range of potential effects of stratospheric ozone depletion, UV radiation and the interactive effects of climate change on human health, aquatic, terrestrial ecosystems, biogeochemical cycles (e.g., movement and transformation of carbon and other elements through the biosphere and atmosphere), air quality, and materials for construction, and other uses.*
>
> - *The Terms of Reference of the EEAP, according to decision XXXI/2, Meeting of the Parties to the Montreal Protocol, are as follows:*
>
> - *The Parties to the Montreal Protocol request the Environmental Effects Assessment Panel, in drafting its 2022 report, to pay particular attention to the most recent scientific information together with future projections and scenarios, to assess the effects from changes in the ozone layer and ultraviolet radiation, and their interaction with the climate system, as well as the effects of breakdown products of controlled substances and their alternatives on:*
>
> 1. *The biosphere, biodiversity and ecosystem health, including on biogeochemical processes and global cycles;*
>
> 2. *Human health;*
>
> 3. *Ecosystem services, agriculture, materials for construction, transport, and photovoltaic use, as well as the generation of environmental microplastics.*

The findings in the 2022 Quadrennial Assessment, which are summarised here, demonstrate that the Montreal Protocol continues to play a vital role in preserving human health and maintaining healthy, diverse ecosystems on land and in the water. New findings refine and quantify the negative consequences on human health and ecosystem productivity of extreme levels of solar UV-B radiation that would have occurred without the Montreal Protocol. However, other findings show that in regions of the Earth that are not currently experiencing appreciable ozone depletion (i.e., outside polar regions), levels of solar UV-B radiation can have some beneficial effects. For example, beneficial effects may include those for human health, crop vigour and defence against pests and pathogens, food quality, and important ecosystem services, such as the disinfection of surface waters and the breakdown of environmental toxins and contaminants. Evidence that climate change is playing an increasingly important role in altering the exposure to UV radiation of organisms, ecosystems, and materials continues to mount. Changes in exposure to UV radiation are occurring through changes in extreme climate events[2] , cloud cover, aerosols, snow and ice cover, mixing of ocean waters, species distributions, the seasonal patterns of growth and development (phenology), and human behaviour.

2 Ultraviolet radiation and climate change

The Montreal Protocol continues to play a critical role in protecting the stratospheric ozone layer and climate, and in preventing large increases in surface UV-B radiation. While UV-B irradiances remain high under the Antarctic ozone hole, changes in UV-B radiation outside polar regions over the past several decades have been small. However, substantial interannual variability in stratospheric ozone and UV-B radiation are occurring due to changes in climate caused by increases in atmospheric greenhouse gases (GHGs). Despite large year-to-year variability, recovery of the Antarctic ozone hole by the middle of this century is still projected. Future changes in stratospheric ozone and UV-B irradiance outside polar regions are expected to be small. Recent anomalous changes in stratospheric ozone over polar regions, particularly over Antarctica, have likely contributed to extreme events, such as heat waves and wildfires, in the Southern Hemisphere. The elevated UV-B radiation together with these extreme events have the potential to significantly affect organisms and ecosystems in polar regions, especially as the climate continues to change.

---

[2] An extreme climate event has been defined as "an episode or occurrence in which a statistically rare or unusual climatic period alters ecosystem structure and/or function well outside the bounds of what is considered typical or normal variability" [8]; or similarly, according to the Intergovernmental Panel on Climate Change (IPCC), "if the value of a variable exceeds (or lies below) a threshold" that is exceeded [9]. Compound extreme events are the "combination of multiple drivers and/or hazards that contribute to societal or environmental risk." An example of a compound extreme event would be fire weather conditions which are the combination of hot, dry, and windy conditions [9].

Key findings

- **Nearly all studies published since our last Quadrennial Assessment have confirmed that changes in biologically effective UV radiation at the Earth's surface outside polar regions have been small (< 4% per decade) during the last 25 years.** Some locations showed small increases in the UV Index (UVI[3]), while others showed small decreases. Over the last 2–3 decades, changes in the erythemal UV radiation outside the polar regions were mainly governed by variations in clouds, aerosols, and surface reflectivity (for areas usually covered by snow or ice) rather than long-term trends in total column ozone.

- **The Antarctic ozone hole has resulted in large increases in surface UV-B radiation, with peak irradiances sometimes exceeding those observed in subtropical locations.** Results from an updated analysis [10] confirm previous conclusions that the Antarctic ozone hole has led to large increases in the UVI at Palmer Station, Antarctica (64° S) year-round, with the largest increases occurring during spring (between 15 September and 15 November) (Fig. 1). During spring, the maximum UVI that has been observed at this site since the early 1990s is 2.5 times higher than it was in the pre-ozone-hole period (years 1970-1976) and sometimes exceeds values observed at subtropical locations (e.g., San Diego, California; 32° N). During summer and autumn (21 December – 21 June; the time of the year when there is no ozone hole); UVI maxima measured between 1990 and 2020 exceeded maxima estimated for years prior to 1976 by 20%.
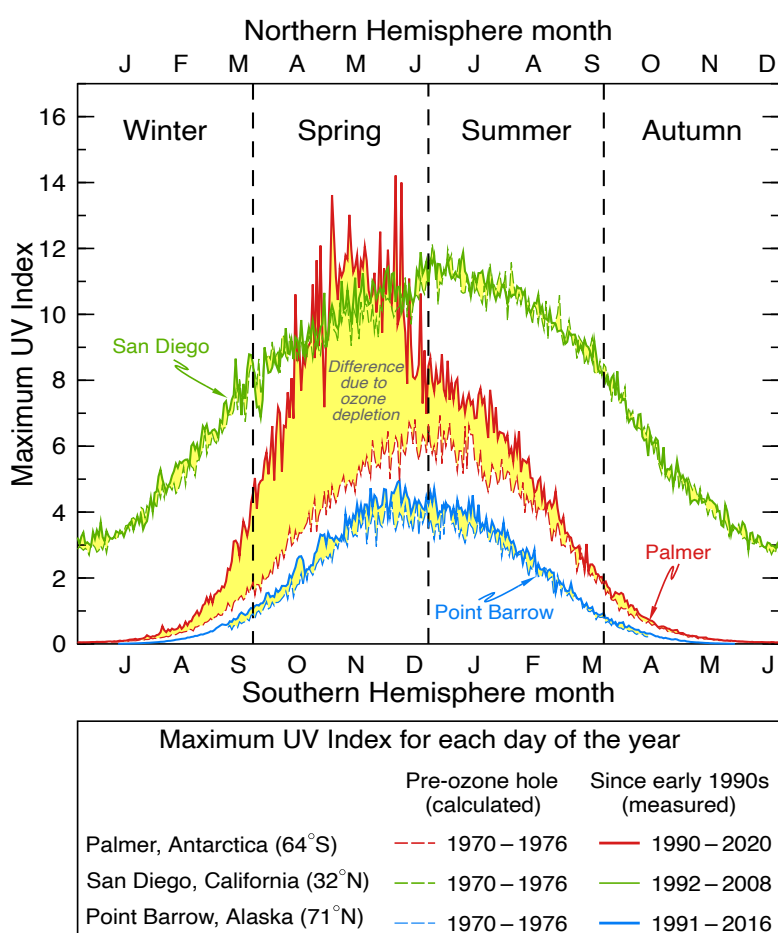
Fig. 1. Comparison of the highest UV Index (UVI) ever measured for each day of the year at Palmer Station (a station at the Antarctic coast), San Diego (a city near the border of the United States and Mexico) and near Point Barrow (the northern-most point in Alaska) since the early 1990s (solid lines) with reconstructed data for the pre-ozone-hole period 1970–1976 (broken lines). Yellow shading indicates the change between historical and contemporary UVI. The difference is particularly large for Palmer Station during spring, the period affected by the Antarctic ozone hole. The highest UVIs observed at Palmer since the 1990s exceed those measured at San Diego despite that city's much lower latitude. Adapted from [10].

---

[3] The UV Index is a measure of UV irradiance in terms of its effectiveness in causing sunburn (reddening of human skin; medically known as erythema).

- **Large inter-annual variability in the UV Index over polar regions has been observed in recent years.** For example, in spring 2019, the UVI was at the minimum of the historical (1991–2018) range at the South Pole, while near record-high values, of up to 80% above the historical mean, were observed in spring 2020 (Fig. 2). A persistent Antarctic ozone hole in 2020 resulted in spikes in the UVI (red arrow in Fig. 2) in late spring when young animals are born or hatched and when plants are actively growing. The loss of protective snow cover, due to continued global warming, could further exacerbate the deleterious effects of these high spring-time UV irradiances on organisms in this region [11].
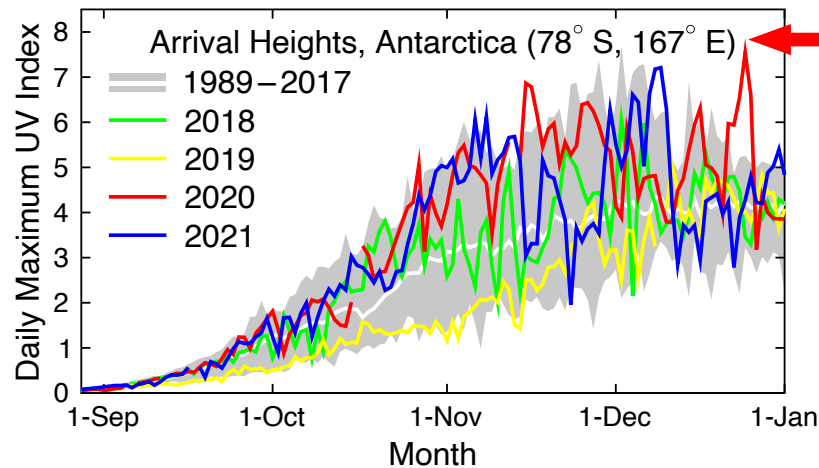
Fig. 2. Daily maximum UV Index (UVI) measured at Arrival Heights, Antarctica in 2018 (green), 2019 (yellow), 2020 (red), and 2021 (blue) compared with the average (white line) and the range (grey shading) of daily maximum observations of the years indicated in the legends. The UVI was calculated from spectra measured by a SUV-100 spectroradiometer. Up to 2009, the instrument was part of the NSF UV Monitoring Network [12] and it is now a node in the NOAA Antarctic UV Monitoring Network (https://gml.noaa.gov/grad/antuv/). Consistent data processing methods were applied for all years [13,14].

- **Recent warming and widespread heatwave events in Antarctica may have increased the exposure of plants and animals to UV-B radiation and disrupted ecosystems in this region.** Since our last assessment there have been two widespread heatwave events in Antarctica. The first occurred in summer 2019/2020 when temperature records were broken around the continent [15]. The second was in March 2022 (austral autumn) when extreme temperatures, almost 40 ˚C higher than normal (-48.6° C), were reported when an atmospheric river, or plume of warm, moist air, moved onto the Antarctic plateau. Heatwaves such as these accelerate melting of snow and ice cover [16] and can expose vegetation to high springtime UV-B radiation from which they have previously been protected [17]. Warming temperatures on the Antarctic Peninsula are also opening up ice-free areas [16], causing the expansion of habitats of vascular plants [18] and increasing the possibility of new plant and animal species invading the continent [19,20].

- **In the Arctic, some of the highest UV-B irradiances on record were measured in March and April 2020.** The monthly average UVI over the Canadian Arctic in March 2020 was up to 70% higher than the historical (2005–2019) average, often exceeding this mean by three standard deviations. Because most Arctic organisms are protected by snow and sea ice at this time of year, they likely were not exposed to these high UV-B irradiances; however, changes in snow and ice cover resulting from climate change could expose these organisms to elevated UV-B radiation if these pronounced ozone depletion events continue to occur into the future.

- **Recent ozone depletion events in the Arctic have been linked to extreme weather events and melting of sea ice in this region.** Heatwave conditions that occurred in the Siberian Arctic in early 2020 [21] appeared to have been aided by atmospheric circulation patterns that were affected by the strong ozone depletion of 2020 [22,23]. Ozone depletion in March 2020 may also have contributed to the prevailing reduction of sea ice in the Arctic Ocean bordering Siberia [24].

- **The Montreal Protocol has prevented large increases in surface UV-B radiation, with greatest benefits at high latitudes.** Modelling studies indicate that without the Montreal Protocol, the UVI at northern and southern latitudes of less than 50° would have increased by 10–20% between 1996 and 2020. For latitudes exceeding 50° S, the UVI would have increased by 25% at the southern tip of South America and by more than 100% at the South Pole in spring-time (Fig. 3).

Fig. 3. Comparison of relative changes in the UVI between 1996 and 2020 for (a) summer and (b) spring, derived from observations at nine ground stations (black symbols) and calculated from results of two chemistry-climate models (blue lines). Both climate models assume the "World Avoided" scenario where emissions of ozone depleting substances are not controlled by the Montreal Protocol. Blue shading indicates the range of these model projections. Ground stations include South Pole (90° S), Arrival Heights (78° S), Palmer Station (65° S), Lauder (45° S), Alice Springs (24° S), Mauna Loa (20° N), Boulder (40° N), Thessaloniki (41° N), and Barrow (71° N). Ground stations with a near-complete data record for 1996–2020 are indicated by solid symbols. Sites with less than 24 years of data are shown with open symbols. Error bars indicate the 95% confidence interval of the regression model. Updated from [1].

- **Surface UV radiation is expected to decrease 2–6% by 2090 at mid-latitudes with variable changes in the tropics of less than 3%.** Assuming full compliance with the Montreal Protocol and constant atmospheric aerosol concentrations, modelling indicates that the UVI at mid-latitudes (30–60°) will decrease between 2015 and 2090 by 2–5% in the north and by 4–6% in the south due to recovery of the ozone layer. Changes in the UVI at the tropics over this time period are estimated to be less than 3%.

- **The Montreal Protocol has made direct contributions to the mitigation of global warming.** Since most substances controlled by the Montreal Protocol are also potent greenhouse gases, the phase-out of these substances may have prevented warming by 0.5 to 1.0 °C over mid-latitude regions, and by more than 1.0 °C in the Arctic. According to some studies, ODSs likely contributed half of the climate-forced loss of Arctic sea ice in the latter half of the 20th century, although there are large uncertainties associated with these estimates.

- **The Montreal Protocol is indirectly mitigating climate change by protecting the global vegetation carbon sink.** If the production of ODSs had not been controlled by the Montreal Protocol, effective UV-B radiation, when weighted according to damaging effects on plants, could have increased by about a factor of five over the 21st century[4] [25]. Plants exposed to this extreme UV-B radiation would have experienced reduced photosynthesis and growth, which would have resulted in an estimated 325–690 billion tonnes less carbon held in terrestrial vegetation by the end of this century. This reduction in carbon sequestration would have resulted in an additional 115–235 parts per million of carbon dioxide (CO_2) in the atmosphere, causing an additional rise of global-mean surface temperature of 0.5–1.0 °C (Fig. 4).

---

[4] "World Avoided" scenarios, such as the scenario discussed here, are inevitably only estimates based on the state of current knowledge. They cannot consider possible changes in human behaviour and policies that may come about when large changes in UV irradiance and their consequences become more obvious in the future. Nevertheless, these projections allow us to put the crucial benefits that the Montreal Protocol has brought to date into perspective.
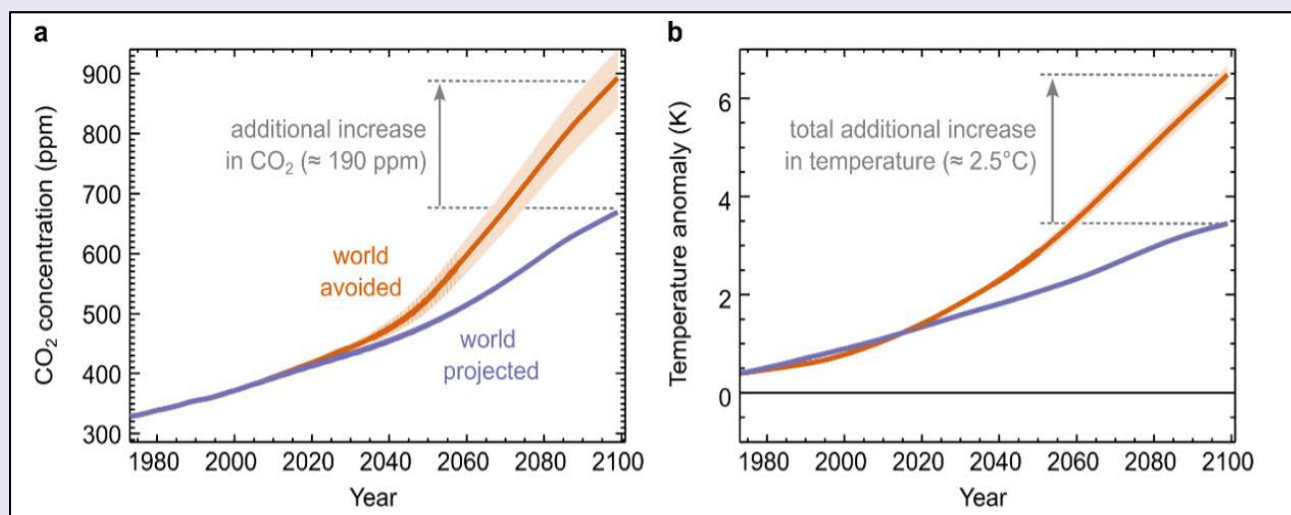
Fig. 4. Changes in atmospheric CO_2 concentrations (a) and surface temperature (b) resulting from UV-B radiation under scenarios with (violet line) and without (orange line) the Montreal Protocol. Shading around the orange line represents the range of responses from simulations assuming a 50-150% range of plant responses to UV radiation. The additional 2.5 °C (range = 2.4-2.7 °C) in temperature shown in panel (b) includes the ODS warming effect (1.7 °C) and the UV plant effect (0.85 °C). Figure adapted from Young et al. [25].

3 Human health

Exposure to excessive UV radiation can result in a number of deleterious effects on human health, including skin cancer (Fig. 5) and cataract. However, it is estimated that millions of cases of these diseases have been avoided due to the Montreal Protocol. Moderate exposure to UV radiation can have some beneficial effects on human health, most notably the production of vitamin D. It is likely that by avoiding large increases in UV-B radiation, the Montreal Protocol has allowed humans to safely tolerate time outdoors, thereby gaining the benefits of sun exposure. This may have reduced the risk or severity of several diseases, particularly those related to immune function, such as multiple sclerosis. Solar UV radiation may also have played a role in inactivating the virus responsible for the COVID-19 pandemic (SARS-CoV-2) and in influencing people's immune system responses to viral infection. However, available evidence suggests it to be unlikely that the Montreal Protocol has had a major effect on the COVID-19 pandemic.

Key findings

- **Modelling studies indicate that the Montreal Protocol is contributing to the prevention of skin cancer.** Results from an updated study [26] indicate that the Montreal Protocol will have prevented millions of cases of skin cancers (melanoma and keratinocyte cancers) in the United States for people born between 1890 – 2100 (Table 1). The model estimated that people born in 2040 or later will not experience excess risk of skin cancer caused by the effect of ozone depletion on UV-B radiation, assuming continued compliance with the Montreal Protocol. While this study highlights the critical importance of the Montreal Protocol, an important limitation is that these estimates assume no changes in sun exposure behaviour, skin screening or population structure, such as in the distribution of skin types. Other limitations include uncertainty regarding stratospheric ozone trends and the choice of the action spectrum for DNA damage.
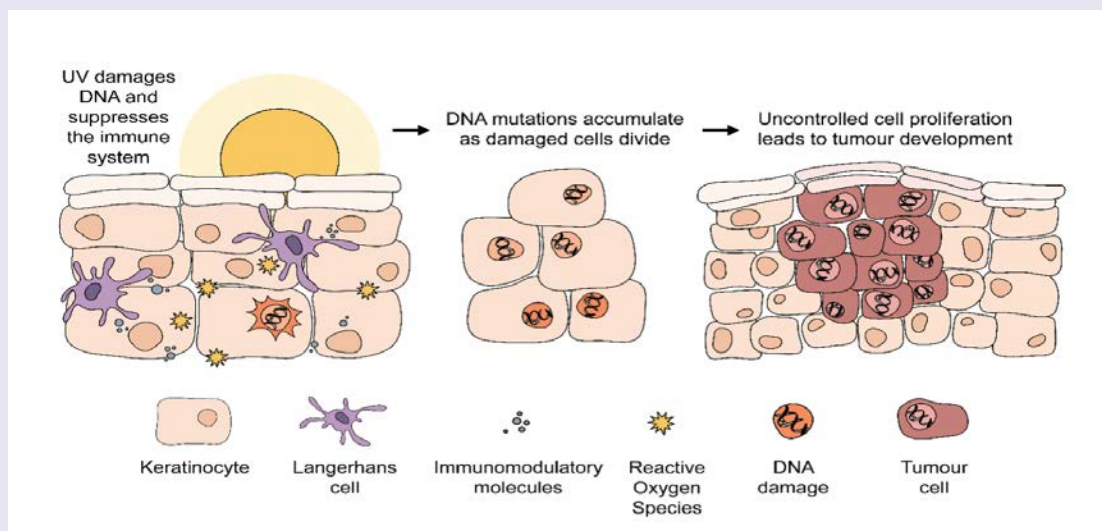
Fig. 5. Skin cancer resulting from exposure to UV radiation occurs primarily as a consequence of direct and indirect (via reactive oxygen species) DNA damage and immune suppression.

- **The incidence of malignant melanoma continues to increase in many developed countries, but trends vary with population and age.** Incidence has increased in some countries (e.g., United Kingdom, Sweden, Canada, Norway, France, and Lithuania), but declined or stabilised in others (e.g., Hungary, Australia, and Denmark) [27-32]. In Canada, Italy and England the incidence of melanoma increased in older age groups but declined or stabilised in younger age groups [33-35]. The increases in the rates of skin cancer in older age groups are most likely the result of high lifetime sun exposure, rather than to changes in stratospheric ozone. The stabilising or decreasing incidence in younger age groups in some jurisdictions may reflect migration patterns, increased use of sun protection strategies, and a social shift in occupational and recreational activities from outdoors to indoors. In the absence of the Montreal Protocol, these declines may not have been observed.

- **Keratinocyte skin cancers are the most common cancer in the world and pose a significant burden on human health and economies.** Keratinocyte skin cancers (KC) include basal cell carcinoma (BCC) and squamous cell carcinoma (SCC). An analysis of Global Burden of Disease (GBD) data found that in 2019 KC was the most common cancer globally, affecting almost 3 times as many people as the next most common cancer (lung, 2.2 million people) [36,37]. Death due to BCC is very rare, but ~56,000 people died due to SCC. The burden of disease, as measured by disability-adjusted life years (DALYs), increased by almost 25% between 2010 and 2019. The incidence of KC has increased in many locations, including Australia, New Zealand, Iceland, and the United Kingdom, but in the United States the incidence remained fairly stable from 2005 to 2019. The lifetime risk of KC is much higher in populations living in conditions with high ambient UV radiation; for example, the lifetime risk is 3.5 times higher in Australia than in the United Kingdom [38,39]. The cost of KC in terms of medical treatment and lost worker productivity is very high and increasing. For example, the average paid and unpaid productivity loss per premature death from melanoma in Europe are the second highest of all cancers, and in the United States between 1997 and 2015, total expenditure for treatment of melanoma increased at a faster rate than for other cancers. In Australia, skin cancer (KC and melanoma combined) costs more to treat than any other cancer. These high costs point to the potential economic benefits of the Montreal Protocol with respect to skin cancer prevention.

- **Solar UV radiation causes or worsens inflammatory skin disorders (photodermatoses) and can contribute to phototoxicity of certain medications.** Photodermatoses are inflammatory skin disorders that are induced or exacerbated by exposure to UV radiation (UV-B and UV-A radiation) and sometimes visible radiation. These disorders can lead to substantial decreases in the quality of life, due both to the morbidity associated with the conditions and to the reduction in work and recreational activities that are needed to manage these conditions. A considerable number of common oral medications (e.g., diuretics and anti-inflammatory drugs) [40] exhibit photosensitising potential, whereby individuals exposed to sufficient doses of these drugs together with UV radiation can experience skin reddening, swelling and burning. Photosensitising drugs may increase the risk of skin cancer through UV-induced DNA damage, but further studies are required to adequately assess this risk.

- **Modelling studies indicate that the Montreal Protocol will reduce the incidence of cataract.** Long-term exposure of eyes to UV radiation can cause cataract, which is the leading cause of blindness world-wide [41-45]. Access to care is the main determinant of vision loss due to cataract, and individuals living in regions with high ambient UV radiation and limited access to care (such as in parts of Asia, Oceania and Sub-Saharan Africa) experience above average incidences of moderate to severe vision impairment [41,43,45]. In the United States, model estimates indicate that the Montreal Protocol will prevent 63 million cases of cataract for individuals born between 1890 – 2100 (Table 1).

Table 1. Estimated number of skin cancers and cataracts avoided due to implementation of the Montreal Protocol, relative to no regulation of ODS through the lifetimes of people born between 1890 and 2100 in the United States. From [26].

		Health effects avoided by the Montreal Protocol as amended and adjusted, compared to no ODS regulation
Incidence of skin cancer	Keratinocyte	432,000,000
	Melanoma	11,000,000
	Total	**443,000,000**
Mortality from skin cancer	Keratinocyte	800,000
	Melanoma	1,500,000
	Total	**2,300,000**
Incidence of cataract		63,000,000

Notes:

The incidence estimates shown here are rounded to the nearest million; mortality estimates are rounded to the nearest hundred thousand. Totals may not sum due to independent rounding.

- **Exposing the skin and eyes to solar radiation leads to the production of vitamin D, modulates the immune system, and can have other beneficial effects on health.** The best known benefit of exposing the skin to the sun, and in particular UV-B radiation, is production of vitamin D. Vitamin D is essential for maintaining musculoskeletal health but recent findings also indicate that low levels of 25-hydroxy vitamin D (25(OH)D), the molecule measured to assess vitamin D status, may also be associated with increased risk of a range of health outcomes, including multiple sclerosis [46], respiratory tract infections [47], and coronary heart disease [48]. Separately from vitamin D, exposing the skin to UV radiation modulates the immune system, both locally within the skin and at distant body sites. This has dual effects, increasing the risk of skin cancer, but downregulating inflammation. There is emerging evidence that UV-A radiation (and possibly UV-B), can release nitric oxide from the skin with benefits for blood pressure and metabolism. Exposing the eyes to the sun reduces the risk of short-sightedness. Balancing the risks and benefits of sun exposure is challenging. In the absence of the Montreal Protocol the high UV indices that would have occurred would have caused skin damage in a very short time, limiting the time people could spend outdoors and reducing the benefits of sun exposure.

- **Solar UV radiation can inactivate SARS-CoV-2, the virus responsible for COVID-19, but the Montreal Protocol has likely had a minimal effect on COVID-19 transmission.** A newly-developed action spectrum indicates that both UV-B and UV-A radiation can inactivate the SARS-CoV-2 virus [49]. Estimates of the exposure time required for virus inactivation vary among studies, but the most reliable data suggest that 90% of viral particles embedded in saliva are inactivated within *ca*. 7 minutes by solar radiation under optimal high-sun conditions, as would occur under clear skies near midday during summer at mid- to low latitudes. Longer exposures to solar UV radiation (exceeding ~13 minutes) would be required for inactivation early or late in the day during winter at higher latitudes [50-52]. Slightly longer inactivation times were found for aerosolised virus particles, and inactivation times would be longer for cloudy conditions or if virus particles are shielded from solar radiation. As the primary mode of transmission of this virus from person to person appears to occur through respiratory droplets and aerosols generated by breathing, sneezing, and coughing in crowded indoor conditions [53-57], disinfection by UV radiation of outdoor surfaces is unlikely to have played a significant part in controlling COVID-19.

- **Exposure to ambient levels of solar UV radiation may contribute to a reduced incidence or severity of COVID-19, but causal mechanisms are unclear and uncertainty is high.** A number of studies have shown that the incidence or severity of COVID-19 is inversely related to ambient solar UV radiation (i.e., fewer cases and less severe COVID-19 with greater intensity of UV radiation), but there are many possible confounding factors (e.g., other environmental factors such as temperature, humidity and total solar radiation, as well as factors affecting viral transmission and disease management). The causal nature of these relationships is therefore unclear. Some studies have found inverse associations between vitamin D (25(OH)D) concentration in the blood and the risk of SARS-CoV-2 positivity or severity of COVID-19. If vitamin D is found to be causally associated with COVID-19 risk or outcomes, or if other effects of UV radiation on the immune system are important, extreme care would be required to balance these beneficial effects of sun exposure against the risks of sunburn and skin cancer in people with light skin. In general, the far-reaching, positive outcomes of the implementation of the Montreal Protocol for human health outweigh any potential advantage that might have been gained by the effects of solar UV radiation on the transmission and severity of COVID-19 that would have occurred in the absence of the Montreal Protocol. Perhaps most importantly, the Montreal Protocol has avoided large increases in UV-B radiation that would likely have caused people to spend less time outdoors, and more time indoors where the risk of COVID-19 infection is much higher.

4 Terrestrial ecosystems and biogeochemical cycles

Changes in UV radiation and climate interact to affect terrestrial ecosystems and biogeochemical cycles (i.e., the cycling of nutrients such as carbon and nitrogen), with potential consequences for food security, biodiversity, and climate. Exposure to extreme solar UV radiation, as would have occurred without the Montreal Protocol, would have had pronounced deleterious effects on many plants, animals, and microorganisms. However, most species in terrestrial environments have evolved mechanisms to tolerate or avoid the harmful effects of solar UV radiation, at least at levels within the range experienced without significant ozone depletion. Nonetheless, these moderate levels of solar UV radiation together with climate change can affect the productivity and biodiversity of terrestrial ecosystems, including agroecosystems, by altering food quality, plant defence against pests and pathogens, plant vigour and tolerances to other abiotic stresses, and the photodegradation of plant litter and pesticides. Importantly, the photodegradation of plant litter by UV and short-wavelength visible radiation can enhance decomposition and nutrient cycling, resulting in emission of GHGs, such as carbon dioxide and nitrous oxide, with positive feedbacks on the climate system.

Key findings

- **Extreme climate events are becoming more prevalent with climate change, and these events are likely to alter the exposure of organisms to UV radiation and disrupt terrestrial ecosystems.** Globally, stronger storms, catastrophic floods, protracted droughts, anomalous heat waves, more intense wildfires, and other extreme climate events (ECEs[5]) are causing long-term disruption to the structure and function of many terrestrial ecosystems [58,59]. Together with changes in cloud cover and aerosols, these ECEs are likely altering the UV radiation received by terrestrial organisms outside polar regions to a greater degree than current or projected changes in stratospheric ozone concentrations (Fig. 6). While these alterations in solar UV irradiation have the potential to affect biodiversity, productivity, emissions of GHGs [60-62], and ecosystem carbon storage [63], the magnitude of these impacts are unknown at the present time.

- **Ongoing changes in climate are exposing plants to new combinations of UV radiation and other environmental factors that can affect stress tolerances and food quality.** A combination of particular concern is high UV-B irradiance and drought, as climate change is increasing the frequency and severity of drought. Drought periods frequently coincide with high UV radiation, particularly at mid to low latitudes [9]. Because of shared molecular pathways in stress tolerance mechanisms, the response of plants to moderate levels of UV radiation may confer some cross-protection against drought [64,65]. This cross-tolerance might mitigate some of the detrimental effects of drought on crop growth and yield, unless both stress factors are excessive. UV radiation and climate factors can also interact to have both positive and negative effects on nutritional quality of food, depending on type of crop and environmental conditions [66].
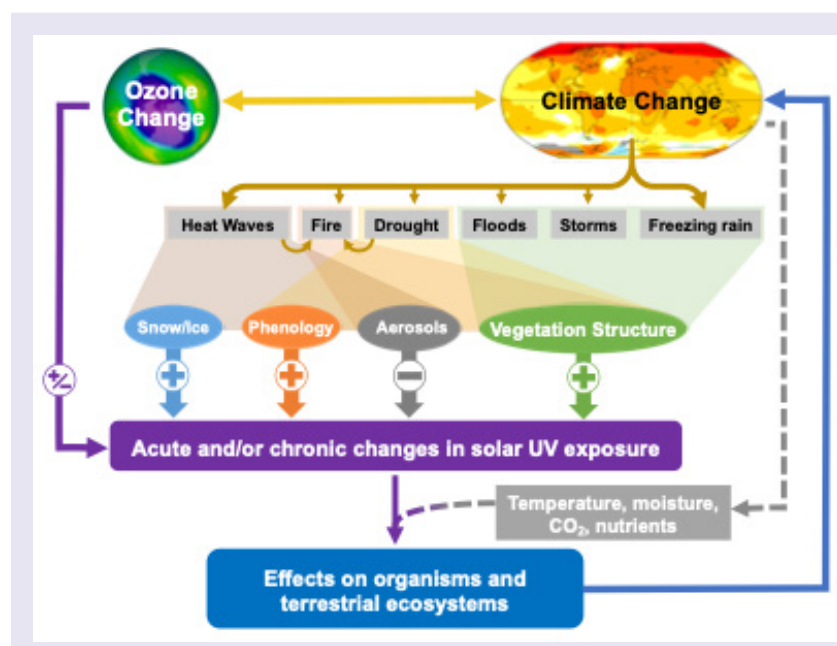
Fig 6. Pathways by which extreme climate events (ECEs) driven by changes in stratospheric ozone and climate can affect UV radiation exposure and terrestrial organisms and ecosystems. Changes in stratospheric ozone and climate interact to influence the frequency and intensity of a number of ECEs (upper-most grey rectangles). These ECEs in turn affect atmospheric and surface intermediaries (multi-coloured ovals connected with ECEs by overlapping shaded regions) which can increase (+) or decrease (-) the solar UV radiation reaching terrestrial organisms and ecosystems. Solid arrows show direct mediation by climate, ozone and UV radiation on ECEs and potential interactive and feedback effects. Dashed arrows show chronic effects of climate change factors.

---

[5] An extreme climate event has been defined as "an episode or occurrence in which a statistically rare or unusual climatic period alters ecosystem structure and/or function well outside the bounds of what is considered typical or normal variability" [8]; or similarly, according to the Intergovernmental Panel on Climate Change (IPCC), "if the value of a variable exceeds (or lies below) a threshold" that is exceeded [9]. Compound extreme events are the "combination of multiple drivers and/or hazards that contribute to societal or environmental risk." An example of a compound extreme event would be fire weather conditions which are the combination of hot, dry, and windy conditions [9].

- **Certain crops, especially those grown in the tropics and montane environments, may be vulnerable to relatively small increases in UV-B radiation.** Because of shifting bioclimatic zones with climate change, certain crops are being grown at higher elevations than was previously possible [e.g., 67,68]. For some species of crop plants, especially those grown in the tropics, the intense UV radiation at higher elevations may exceed their UV tolerances, resulting in damage to DNA and proteins with negative consequences for their physiology and growth [69]. As crop species are grown in new habitats, they also encounter new weeds, pests, and pathogens [70,71]. Exposure to UV radiation is known to influence competition between plants and defence against herbivores [72,73] such that the altered UV radiation conditions may further disrupt the structure and function of these agroecosystems by affecting interactions of crop plants with weeds and pests. Differential effects of climate change on range shifts and phenology can also lead to spatial and/or temporal or seasonal mismatches between pollinators and their plant hosts [74,75], posing a risk to both agroecosystem function and food security.

- **Climate change can contribute to declines in biodiversity by reducing the availability of suitable habitats for species and by shifting their distribution ranges, which alters exposure to UV radiation and may disrupt species interactions.** Plant and animal species are migrating and shifting their distribution ranges to higher elevations and latitudes in response to on-going changes in climate [76-78], and these changes can decrease (poleward shifts) or increase (elevational shifts) exposures to solar UV radiation. Some models suggest that UV radiation can interact with climate change to influence species distributions, although the mechanisms underlying these effects are unclear. Nonetheless, changes in UV irradiances resulting from these shifts will likely modify plant growth forms and secondary chemistry (e.g., flavonoids and other phenolic compounds), which may affect the competitive ability of plants and their defence against herbivores [79,72]. Depending on location, these changes in species interactions have the potential to negatively affect biodiversity [80].

- **Solar UV radiation can accelerate the decomposition of dead plant matter (litter) in many terrestrial ecosystems with implications for carbon storage and climate.** The decomposition of plant litter is a key biogeochemical process determining rates of nutrient cycling, energy flow, and carbon storage in terrestrial ecosystems. Exposure of litter to solar UV radiation and short-wavelength visible radiation (i.e., blue and green light), can increase rates of litter decomposition via the direct photochemical breakdown of lignin and other plant cell wall constituents (i.e., photomineralisation), and indirectly, by enhancing microbial decomposition (i.e., photofacilitation). Photodegradation of litter is now recognised to be important in a wide variety of ecosystems across a range of climatic regions (e.g., deserts, grasslands, forests), although the relative importance of photomineralisation *vs* photofacilitation may differ among habitats [81]. A newly developed action spectrum for photomineralisation indicates that UV-A is more effective than UV-B radiation in driving this process. Thus, ozone depletion likely has minimal effect on this aspect of photodegradation [82]. Photodegradation influences the cycling and storage of carbon as well as other elements (e.g., nitrogen and phosphorous) and can be an important pathway of GHG emissions by terrestrial ecosystems [83,84].

- **Thawing of permafrost is destabilising Arctic ecosystems and exposing ancient sources of organic carbon to photodegradation by solar UV radiation.** The world's soils store large amounts of carbon, approximately two-to-three times more than the atmosphere (Fig. 7A). Therefore, even small instabilities or degradation of soils driven by perturbations in climate can lead to large releases of carbon. A large proportion of soil carbon is stored at high northern latitudes, where it has remained stable in peatlands and permafrost soils over long time periods, often many thousands of years. As climate warms, permafrost is thawing [85], leading to the decomposition of this ancient organic matter and the release of carbon dioxide, methane and other GHGs. The organic matter from thawed permafrost soils enters aquatic ecosystems as dissolved organic matter (DOM) where it becomes susceptible to photodegradation by solar UV radiation [86]. Reductions in ice and snow or changes in vegetation and cloud cover are further modifying exposures to UV irradiation, which affect the magnitude of these photodegradation processes and Arctic organisms (Fig. 7B).

- **Photodegradation of dissolved organic matter by UV radiation in aquatic ecosystems releases greenhouse gases that may exacerbate climate change.** Climate change is enhancing terrestrial runoff rich in dissolved organic matter (DOM) to lakes, rivers, and coastal waters, which increases the amount of DOM that is subjected to photodegradation. Another important source of DOM is the permafrost soils of the Northern Hemisphere (Fig. 7). Emissions of CO_2 resulting from photodegradation of DOM at mid-latitudes are generally negligible compared to emissions from microbial mineralisation of DOM but may play a large role at high latitudes. The magnitude of the direct abiotic photochemical degradation (i.e., photomineralisation) of DOM in Arctic watersheds rich in yedoma (organic-rich permafrost, [87]) is still uncertain, with estimates ranging from negligible [88-90] to 75–90% of total CO_2 emissions [91-93]. Understanding how DOM photoreactivity varies across seasons and with water chemistry is crucial to predicting the extent of photochemical CO_2 emissions in high latitude ecosystems and their variations induced by changes in climate and UV radiation.
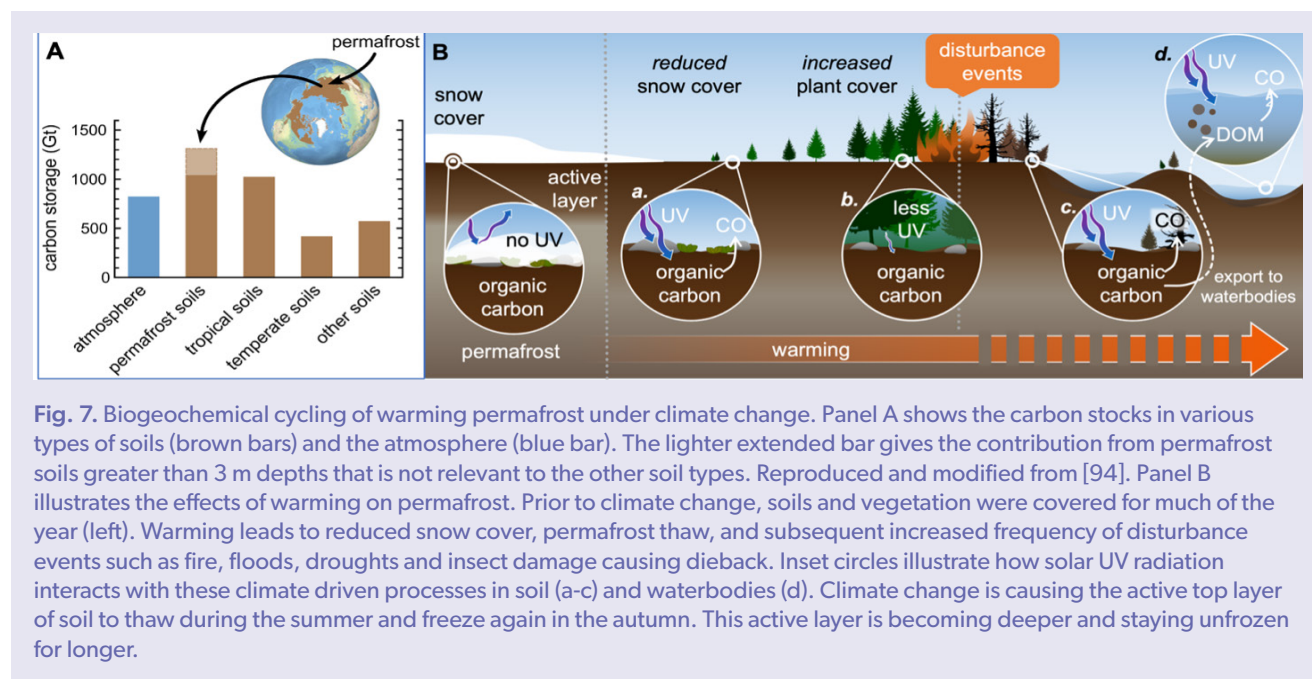
Fig. 7. Biogeochemical cycling of warming permafrost under climate change. Panel A shows the carbon stocks in various types of soils (brown bars) and the atmosphere (blue bar). The lighter extended bar gives the contribution from permafrost soils greater than 3 m depths that is not relevant to the other soil types. Reproduced and modified from [94]. Panel B illustrates the effects of warming on permafrost. Prior to climate change, soils and vegetation were covered for much of the year (left). Warming leads to reduced snow cover, permafrost thaw, and subsequent increased frequency of disturbance events such as fire, floods, droughts and insect damage causing dieback. Inset circles illustrate how solar UV radiation interacts with these climate driven processes in soil (a-c) and waterbodies (d). Climate change is causing the active top layer of soil to thaw during the summer and freeze again in the autumn. This active layer is becoming deeper and staying unfrozen for longer.

5 Aquatic ecosystems

Changes in stratospheric ozone along with climate change and human activity are altering the aquatic environment and modifying the exposure of aquatic ecosystems to UV radiation with potential consequences for species distributions, biogeochemical cycles, and services provided by these ecosystems. Climate change results in variations in the depth of mixing, thickness of ice cover, the duration of ice-free conditions, and inputs of dissolved organic matter, all of which can either increase or decrease exposure to UV radiation (Fig. 8). Human activities release contaminants such as oil, UV filters in sunscreens, and microplastics into the aquatic environment, which are then modified by UV radiation, frequently amplifying adverse effects on aquatic organisms and aquatic environments. These changes combine with other environmental changes such as global warming and ocean acidification to impact microorganisms, macroalgae, and plants and animals in aquatic environments. Minimising the disruptive consequences of these effects on critical services provided by the world's rivers, lakes, and oceans (e.g., freshwater supply, recreation, transport, and food security) will not only require continued adherence to the Montreal Protocol but also a wider inclusion of solar UV radiation and its effects in studies and/or models of aquatic ecosystems under conditions of the future global climate.

Key findings

- **Ozone depletion and climate change are altering exposure to UV radiation in the ocean's surface layers by changing the depth of the mixed layer, but effects vary with latitude.** An analysis of almost 50 years (1970-2018) of data from sensors on free-floating devices and ships show a deepening of the water circulation over the global ocean. The maximum depth of circulation from the surface, the mixed layer depth (MLD; Fig. 8), has deepened, on average, by 2.9 % per decade, adding around 5-10 m per decade to the MLD [95]. The deeper organisms circulate, the less they are exposed to UV radiation. Deepening trends do vary regionally, with greater deepening in much of the Southern Ocean and less deepening in the North Atlantic, whereas shallowing is occurring for some areas near the Equator and in high Arctic latitudes. Deeper mixing in the Southern Ocean is linked to the strengthening of surface winds associated with the positive phase of the Southern Annular Mode, which is influenced by ozone depletion [96].
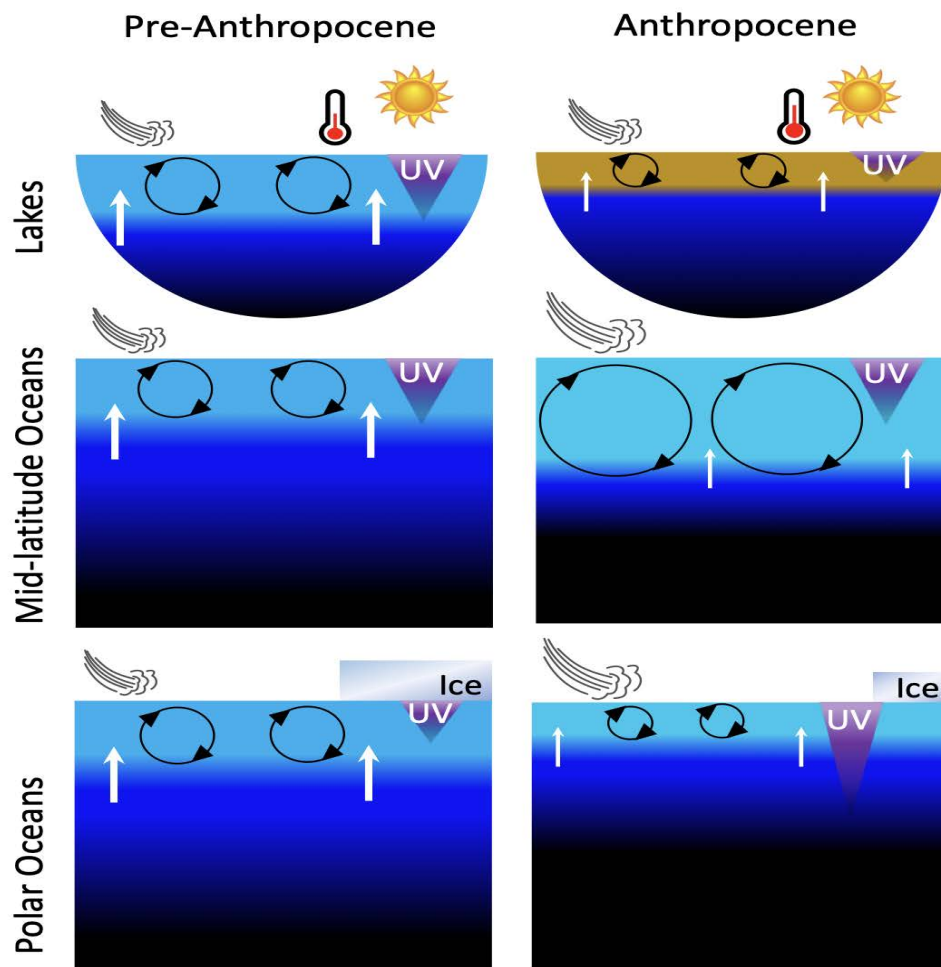
Fig. 8. Schematic depiction of processes controlling exposure to UV-B radiation in aquatic ecosystems comparing before and after the Anthropocene (i.e., the current period of significant human impact on the Earth's ecosystems). In general, exposure to UV-B radiation is limited to the surface layer (light blue/brown), the mixing of which depends on the stratifying effect of surface warming and inputs of fresh water *vs* the stirring effects of surface winds and currents. Ice cover shields the polar ocean and wintertime lakes (not shown). In oceans in the Anthropocene, generally there is more warming, more wind, and a greater mixed layer depth (MLD), while sharpening the density barrier (pycnocline, dark blue) to nutrient transport (arrows) from deep water (black). However, ice melt reduces shielding and freshens the polar ocean reducing the MLD. Terrestrial run-off from rain events browns lake surface water, lowers transparency to UV-B radiation and warms surface waters due to enhanced absorption of solar radiation. Drought would have the opposite effect. The warming results in shallower mixed layers in lakes, as do weaker winds. Dimensions are not to scale.

- **Anthropogenic factors in combination with UV radiation are exacerbating stresses on aquatic ecosystems, especially tropical coral reef ecosystems.** Tropical coral reefs, which are based on the symbiotic association between reef-building corals and symbiotic dinoflagellates (Family Symbiodiniaceae), are highly diverse and economically important ecosystems that are naturally exposed to high levels of UV radiation because they occur in clear, tropical waters close to the surface. Findings from some studies indicate that exposure to UV-B radiation can have detrimental effects on symbionts, although negative effects are often not evident on the coral host [97]. Stress on symbionts can lead to their expulsion from the coral host and coral bleaching. These negative effects on symbiont health are a concern as coral bleaching is becoming more common as sea surface waters continue to warm and become more acidic. These effects may exacerbate the impact of UV-B radiation on coral ecosystems. Coral reefs may also be vulnerable to oil pollutants and chemicals from sunscreens, the toxic effects of which can be enhanced by UV-B radiation and climate change [98,99] (Fig. 9).
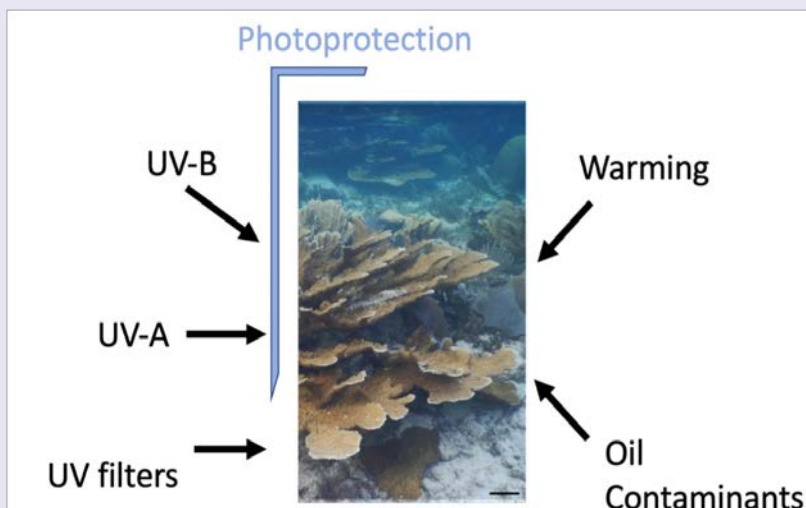
Fig 9. Coral reef-dwelling organisms, such as reef-building corals, are affected by stressors such as warming of sea surface waters and by contaminants such as oil and UV filters (e.g., sunscreens). In near-surface waters, corals are also exposed to high levels of UV radiation, the potentially damaging effects of which are moderated by photoprotection mechanisms. Nevertheless, the negative impacts of stressors and contaminants are exacerbated by co-exposure to UV-A and UV-B radiation. Photo: Sandra Mendoza Quiroz.

- **Solar UV radiation degrades oil pollutants but enhances their toxicity to aquatic organisms.** Recent studies have confirmed that solar UV radiation is a key factor contributing to the removal of pollutants from oil spills (reviewed by [100]). For example, during the 102 days of the Deepwater Horizon spill, UV-driven production of water soluble organic carbon (also referred to as photo-dissolution) accounted for about 8% (estimated range: 3-17%) of overall oil removal, an amount comparable to other widely acknowledged removal processes (evaporation and coastal stranding) [101]. Exposure to high amounts of UV radiation can also increase the toxicity of some oil components for corals, sponges, molluscs, polychaetes, and crustaceans [99]. Typically, exposure to UV radiation has not been a part of oil toxicity studies, but these results suggest that including such exposures in future studies would improve our understanding of the fate and toxicity of oil spills occurring at or near the ocean's surface [102].

6 Air quality and contaminants

Solar UV radiation is a major contributor to the formation of air pollution (tropospheric ozone (O_3) and some particulate matter (PM)), which has been identified as a critical issue in human health world-wide. However, UV radiation also plays a role in cleansing the atmosphere of pollutants, and air pollution can affect the penetration of UV radiation to the Earth's surface. Thus, changes in stratospheric ozone and climate can have complex and sometimes opposing effects on different types of air pollution. Solar UV radiation also plays an important role in the breakdown of contaminants in aquatic and terrestrial ecosystems, but the ecological and human health consequences of these transformations are not yet well understood. Contamination of the environment by compounds used to replace ODS remains a concern.

Key findings

- **Solar UV radiation, particularly UV-B radiation, can worsen tropospheric air quality with appreciable harmful effects on human health.** Globally, poor outdoor air quality causes extensive morbidity and over 4 million premature deaths per year related to respiratory, cardiovascular, reproductive and neurological disorders. Improvements in some aspects of air quality (e.g., PM) have occurred in some regions (e.g., China), because stringent measures to control pollution have led to long-term reductions in emissions of nitrogen oxides (NOx) and sulfur dioxide (SO_2)—necessary ingredients for the UV-driven formation of tropospheric O_3 and PM. Decreases in UV-B radiation, as a result of the Montreal Protocol, would be expected to result in a reduced net production of O_3 near sources of pollution (e.g., cities with large emissions of NOx from traffic) and a slower consumption of O_3 with increasing distance from polluted areas. Future scenarios in which stratospheric O_3 returns to 1980 values or even exceeds them, could help ameliorate urban O_3 pollution but may worsen O_3 pollution reaching rural areas. For PM, sensitivity to changes in UV radiation is expected based on knowledge of the relevant photochemical processes, but has not been studied systematically and hence remains unquantified.

- **Tropospheric ozone and particulate matter can have adverse effects on forests and the yields of crops in rural areas, with important economic consequences.** Tropospheric O_3 is known to contribute to significant losses in growth, quality and yield of crops and other plants, and recent studies have further quantified these effects. For example, a recent meta-analysis of 48 studies examining the effects of chronic tropospheric O_3 exposure on soybeans conducted between 1980 and 2019 showed that O_3 reduced leaf-area by 21%, leaf, shoot and root biomass by 14%, 23% and 17%, respectively, and seed yield by 28% [103]. A study on the historical losses to air pollutants in maize and soybean grown in the United States showed that improvements in the control of O_3, SO_2, PM, and NO_2 have increased yields by an average of 20% [104]. Of these pollutants, PM and NO_2 appeared to cause more damage than O_3 and SO_2. Overall, the improvement in yields from stricter controls of the pollutants was equivalent to ca US$ 5 billion.

- **Solar UV radiation also plays a major role in cleansing the troposphere of pollutants and greenhouse gases.** UV-generated hydroxyl radicals (OH), the major cleaning agents of the troposphere, remove many atmospheric pollutants and GHGs (Fig. 10). Research has shown that increases in UV radiation caused by stratospheric ozone depletion over 1980-2020 have contributed a small increase (*ca*. 3%) to the concentration of globally averaged OH, alongside several other variables that affect OH (e.g., temperature, humidity, and increased emissions of precursors of tropospheric O_3). Hydroxyl radicals react with many environmentally important chemicals including some GHGs (e.g., methane; CH_4) and some ODSs, such as the so-called very-short-lived substances (VSLSs; halo-organics with an atmospheric lifetime of less than or equal to 6 months). These reactions control both the lifetimes and the amounts of such chemicals in the atmosphere. For CH_4, the UV-related increase in OH is the equivalent of offsetting increases in the concentration by 40 ppb or decreasing emissions by ~15 Tg y^{-1}. For the VSLSs, the changes in OH are part of a complex feedback (Fig. 10) that is not yet fully quantified.
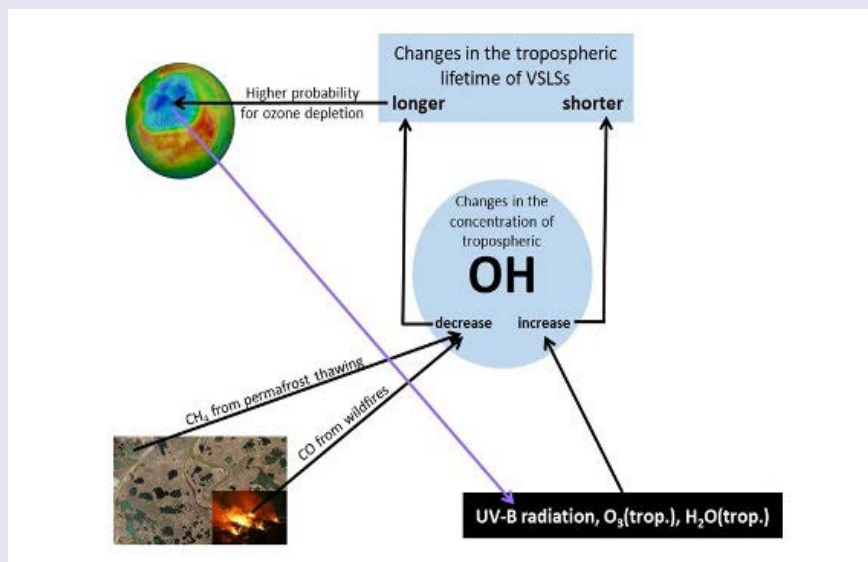
Fig. 10. Interacting effects of UV-B radiation and tropospheric O_3 and water (H_2O) on tropospheric concentrations of OH and on the lifetime of very-short-lived substances (VSLSs). Effects of climate change include more frequent wildfires and thawing of permafrost soils with the formation of thermokarst lakes, which are important sources of CO and CH_4, respectively. Increased emissions of CO and CH_4 tend to decrease the tropospheric OH concentration, which in turn results in longer lifetime of VSLSs and thus a higher probability of stratospheric ozone depletion.

- **The increases in trifluoroacetic acid concentrations due to replacements of the ozone-depleting substances are not expected to pose significant risk to humans or the environment at the present time.** Trifluoroacetic acid (TFA) continues to be found in the environment, including in remote regions, although concentrations are so low that they are currently very unlikely to have adverse toxicological consequences for humans and ecosystems [105,106]. The accumulated amount of TFA is expected to increase because of the planned replacement of ODS with short-lived fluorinated chemicals (Fig. 11). However, based on projected future use of these precursors of TFA, no harm is anticipated. There is a large uncertainty associated with the magnitude of other sources of TFA (e.g., potential natural sources, fluorinated pesticides, and pharmaceuticals), which do not fall under the purview of the Montreal Protocol. Trifluoroacetic acid has biological properties that differ significantly from the longer chain polyfluoroalkyl substances (PFAS) and inclusion of TFA in this larger group of chemicals for regulation would be inconsistent with the risk assessment of TFA.
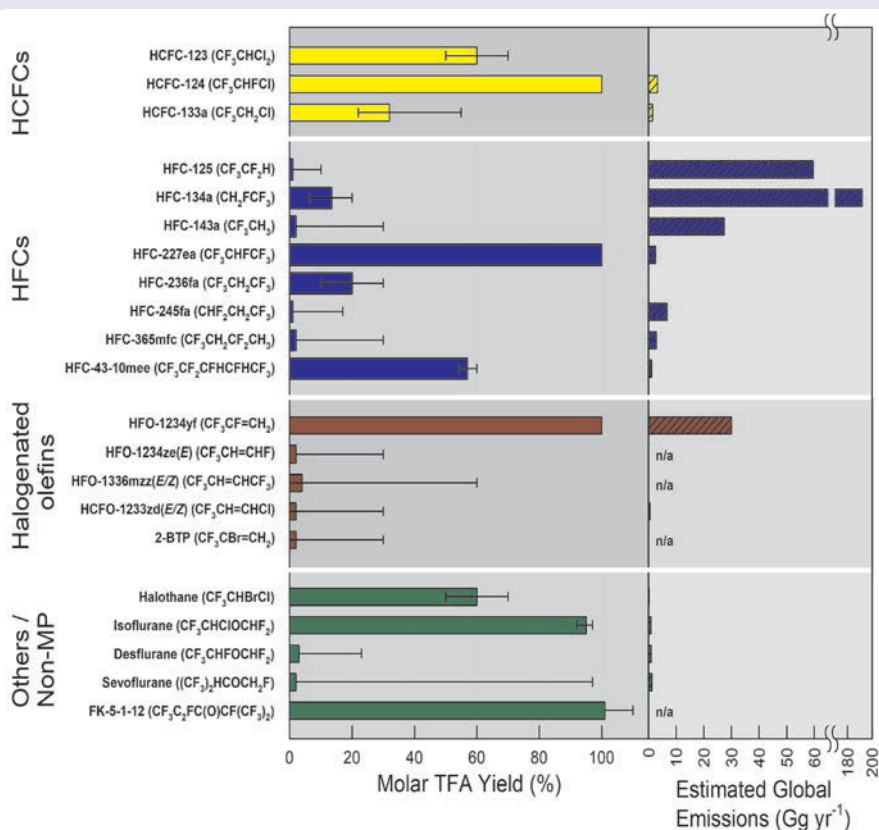
Fig. 11. Yields of trifluoroacetic acid (TFA) from selected individual chlorofluorocarbon (CFC) replacement compounds, as well as the estimated global emissions of these compounds. The figure also includes selected compounds not under the purview of the Montreal Protocol. Error bars represent both experimental uncertainties and upper and lower yield ranges due to competing reaction channels that depend on environmental conditions. The yields of TFA from individual compounds are estimated based on evaluations of the available literature. Note split scale for the emission of HFC-134a is much higher than that of other compounds.

7 Materials and plastics

Solar UV radiation contributes to the aging and degradation of textiles as well as natural and synthetic materials, such as wood and plastics used in building materials. This degradation occurs on the surface of materials that then allows for other environmental agents, such as heat and moisture, to enter and deteriorate deeper layers. Superficial changes caused by UV radiation therefore lead to an overall ageing of a material. Thus, ozone depletion and climate change interact to affect the ageing process of materials and their service lifetimes. New technologies have been developed that can minimise these ageing effects, thereby resulting in longer lifetimes, diminished use of natural resources and waste, and reduced release of potentially harmful micro- and nano-plastics. However, the production of plastics and accumulation of micro- and nano-plastics in the environment, especially aquatic environments, continues to be of concern. Secondary microplastics can be generated in the environment during fragmentation of plastic litter that is photo-oxidised by solar UV radiation. By preventing increases in UV radiation, the Montreal Protocol has likely resulted in a slower generation and accumulation of microplastics in the environment than would have occurred without this treaty.

Key findings

- **More environmentally-friendly additives are being developed and used in plastics and wood to reduce the degradation of these materials by solar UV radiation.** The recent trend towards development of environmentally sustainable technologies and building materials has necessitated the use of plant-based, non-toxic additives in coatings, plastics, and sunscreens [107-109]. In selecting additives, including UV-stabilisers [110], for plastics or coatings, increasing attention is being paid to minimising their potential ecotoxicity as these additives often leach out to contaminate the environment [111]. Some wood extractives and lignin nanoparticles have been tested for their efficacy as UV shielding material against surface discolouration of wood. Nanoparticles of lignin applied to coatings and even sunscreens have shown promise for substituting or complementing synthetic UV-absorbers. However, the undesirable dark colour of lignin is a drawback in lignin-based UV-shielding products and needs to be addressed.

- **New technologies are being developed to increase the lifespan of photovoltaic modules used in solar panels.** Polymers in photovoltaic (PV) modules undergo oxidation when exposed to solar UV irradiation and this causes brittleness, degradation and reduced lifetime of these systems [112-115] (Fig. 12). While accelerated laboratory testing has improved understanding of the different degradation mechanisms in PV modules, accurate prediction of degradation of these systems in the outdoors and under actual in-use conditions is still lacking [116]. Efforts to find a better replacement for the encapsulant material used in these systems has yielded several candidate polymers, such as ionomers and thermoplastic polyolefin [117]; and novel transparent backsheets designed to work specifically with bifacial PV cells and modules are being introduced. These modules will collect reflected sunlight on the back side of the module to increase power generation per unit area [118].
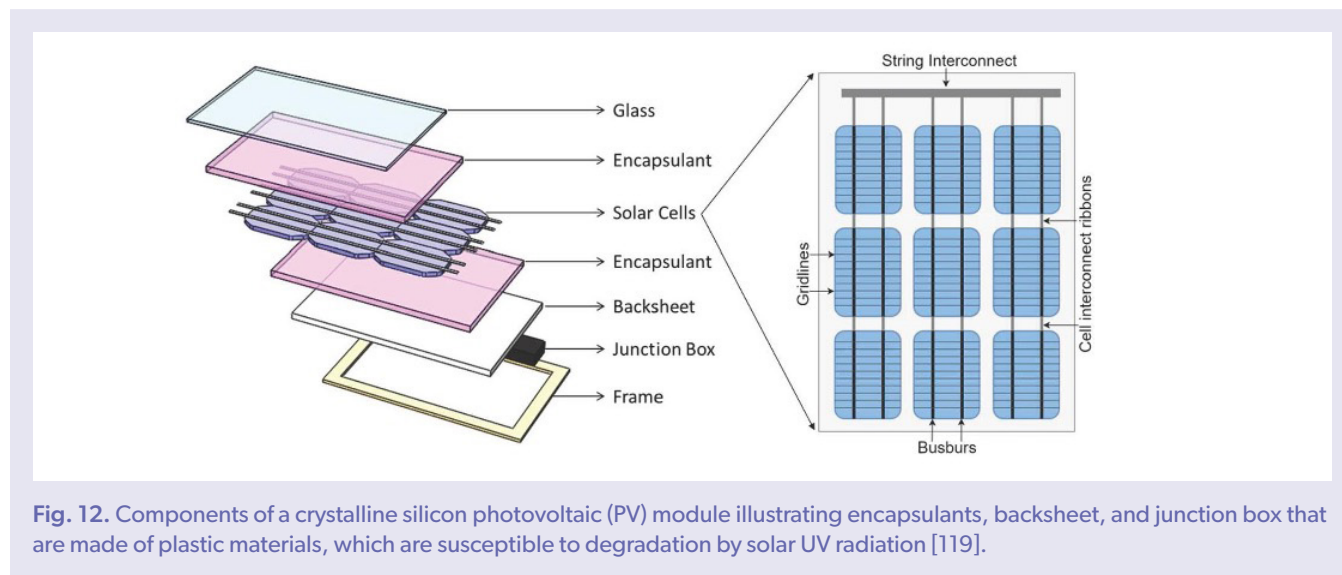
Fig. 12. Components of a crystalline silicon photovoltaic (PV) module illustrating encapsulants, backsheet, and junction box that are made of plastic materials, which are susceptible to degradation by solar UV radiation [119].

- **Solar UV radiation causes weathering of plastics, which ultimately results in fragmentation and the formation of micro- and nano-plastics.** Plastic debris in the environment is perceived as an increasing pollution problem with an estimated 8300 million metric tons being produced since the 1950s, of which ca 80% have ended in landfills and the natural environment [120]. In the natural environment, micro- (<5 mm) and nano-plastics (<0.1 μm) are generated as a result of solar UV-driven weathering of plastic debris in combination with fragmentation due to exposure to mechanical forces [121] (Fig. 13). Exposure to solar UV radiation is a primary weathering mechanism of plastics debris. Such photo-oxidation of plastic debris under extended outdoor exposure makes the material weak, brittle and prone to subsequent fragmentation [122,123]. Fragmentation then occurs when plastics are subjected to factors such as wave action or encounters with animals, resulting in the generation of secondary micro- or nano-particles. While there are concerns about potential effects of micro- and nanoplastics, the risks of these pollutants to human health and the environment are at present unclear. Nonetheless, there are calls for a global treaty on plastics towards a more sustainable future [124].

- **The implementation of the Montreal Protocol, and consequent avoidance of high solar UV-B radiation, has likely prevented increases in the generation of microplastics in the environment.** Large increases in terrestrial solar UV-B radiation, which have been avoided by the Montreal Protocol, would have increased the rates of UV-driven photo-oxidation, and consequently fragmentation of plastic debris that produces microplastics. However, estimates of the impact of the Montreal Protocol on microplastic production are limited by uncertainties in the UV dose-response of photo-oxidative reactions, and the distribution of plastics within different environments (soil, water, etc.), which affect exposure to UV radiation. Thus, while UV driven photo-oxidation of plastics, and subsequent fragmentation are well documented, the quantitative impact of this process on plastic longevity, microplastic generation, and ecological impacts remains unknown at present
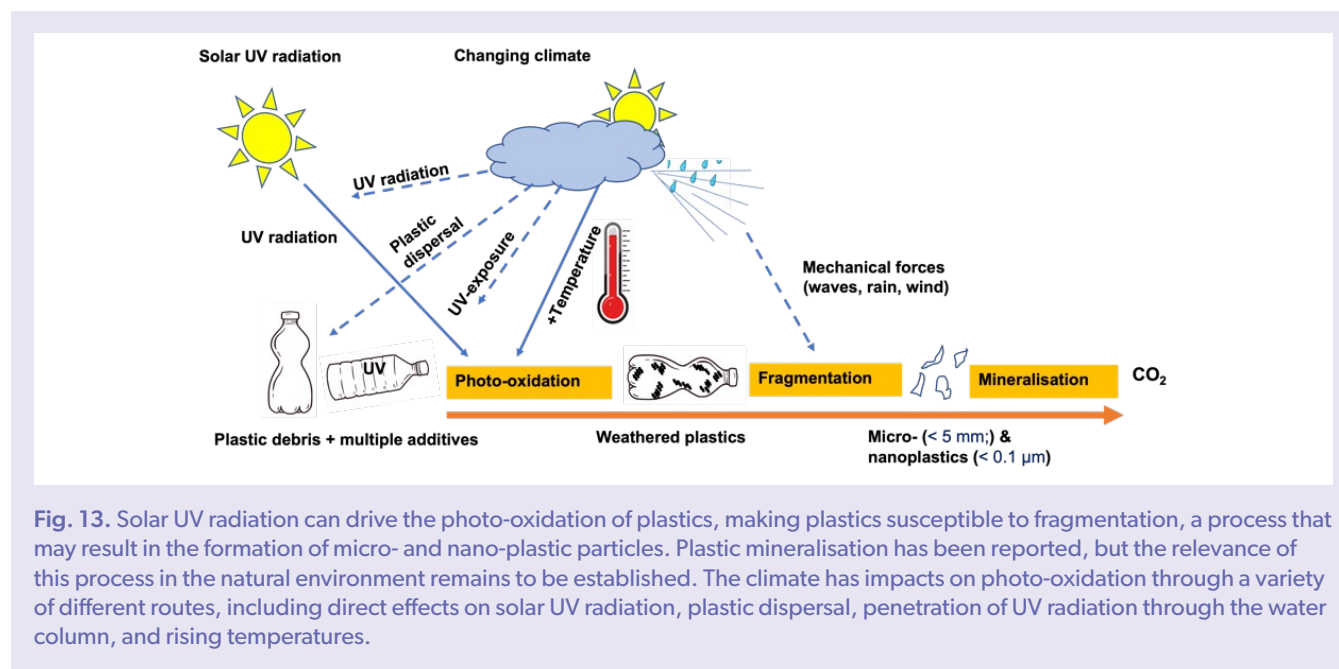
Fig. 13. Solar UV radiation can drive the photo-oxidation of plastics, making plastics susceptible to fragmentation, a process that may result in the formation of micro- and nano-plastic particles. Plastic mineralisation has been reported, but the relevance of this process in the natural environment remains to be established. The climate has impacts on photo-oxidation through a variety of different routes, including direct effects on solar UV radiation, plastic dispersal, penetration of UV radiation through the water column, and rising temperatures.

8 Conclusions

The Executive Summary, together with the full Quadrennial Assessment, illustrate the diversity of ways that changes in stratospheric ozone, UV radiation and climate interact to affect human health and the environment. While exposure to solar UV radiation, and, in particular, UV-B radiation, can have deleterious effects on humans and other organisms, modest exposure to UV radiation can have beneficial effects on human health, food quality and plant defence against pests, the disinfection of waters, and the conversion of toxic contaminants to more benign by-products [125,60,126]. Maintaining an optimal balance between the positive and negative effects of solar UV radiation would have been difficult to achieve, if not impossible, without the Montreal Protocol. Evidence also continues to mount showing that the Montreal Protocol is directly and indirectly protecting the Earth's climate and mitigating some of the negative consequences of climate change [5,25].

Since our last Quadrennial Assessment, the world has experienced continued increases in global temperatures, additional extreme climate events (ECEs, e.g., heat waves, droughts, and hurricanes) and events resulting from a combination of weather extremes and other drivers (e.g., wildfires) that have all contributed to increasing societal and environmental risk. As recently reported by the Intergovernmental Panel on Climate Change [9], ECEs are expected to increase in frequency and intensity in the future because of anthropogenic climate change. The ECEs, together with other aspects of climate change (e.g., changing cloud cover and aerosols), alter the exposure to UV radiation of humans, plants, animals, and materials to a greater degree than the expected changes in the stratospheric ozone layer—assuming continued and full compliance with the Montreal Protocol.

While our knowledge of the interactive effects of ozone depletion, UV radiation, and climate change has advanced since our last Quadrennial Assessment, a number of uncertainties persist that limit our ability to precisely and quantitatively assess the full extent and magnitude of these effects. Notably, it is uncertain how surface UV radiation will change in the future as the climate continues to change and to what degree the environmental and human effects of climate change are modulated by concurrent changes in stratospheric ozone and UV radiation. These factors are especially important considering future scenarios that might involve solar radiation management and climate intervention [127-130]. Despite these uncertainties, it is clear from this Quadrennial Assessment that the Montreal Protocol has been vital in protecting humans, aquatic and terrestrial ecosystems, air quality, and natural and synthetic materials from the deleterious consequences of stratospheric ozone depletion [131,1].

By protecting the stratospheric ozone layer and mitigating some of the effects of climate change, the Montreal Protocol continues to contribute to the implementation of the United Nations Sustainable Development Goals (SDGs). Specifically, the EEAP shows the alignment of the Montreal Protocol and its Amendments by addressing 21 targets in 11 of the 17 SDGs (Box 2). These SDGs address

targets in the areas of climate change, air and water quality, biodiversity and ecosystems, contaminants and materials, and human health. Thus, the Montreal Protocol has wide ranging significance for sustainability by protecting human health and maintaining healthy, diverse ecosystems on land and in the water.

Box 2. The following UN Sustainable Development Goals (SDGs) and their specific targets are addressed in the 2022 EEAP Quadrennial Assessment.

SDG	Targets
2 ZERO HUNGER	2.3 increase productivity of small-scale food producers 2.4 ensure sustainable food production systems 2.5 maintain genetic diversity of agricultural plants and animals
3 GOOD HEALTH AND WELL-BEING	3.3 end epidemics of communicable diseases 3.9 reduce deaths caused by air, soil and water contamination
6 CLEAN WATER AND SANITATION	6.1 achieve access to safe drinking water 6.3 reduce water pollution 6.6 protect water-related ecosystems
7 AFFORDABLE AND CLEAN ENERGY	7.A enhance international cooperation around clean energy
9 INDUSTRY, INNOVATION AND INFRASTRUCTURE	9.4 upgrade industries to be sustainable
11 SUSTAINABLE CITIES AND COMMUNITIES	11.5 reduce deaths caused by disasters 11.6 reduce the environmental impact of cities
12 RESPONSIBLE CONSUMPTION AND PRODUCTION	12.4 achieve environmentally sound management of chemicals and wastes 12.5 reduce waste generation
13 CLIMATE ACTION	13.2 integrate climate change measures into policy 13.3 improve education on climate-change mitigation
14 LIFE BELOW WATER	14.1 reduce marine pollution 14.3 minimise impacts of ocean acidification
15 LIFE ON LAND	15.1 ensure the conservation of terrestrial ecosystems 15.3 combat desertification
17 PARTNERSHIPS FOR THE GOALS	17.14 enhance policy coherence for sustainable development

References

1. McKenzie, R. L., Bernhard, G. H., Liley, B., Disterhoft, P., Rhodes, S., Bais, A. F., Morgenstern, O., Newman, P., Oman, L., Brogniez, C., & Simic, S. (2019). Success of Montreal Protocol demonstrated by comparing high-quality UV measurements with "World Avoided" calculations from two chemistry-climate models. *Scientific Reports, 9*(1), 12332, https://doi.org/10.1038/s41598-019-48625-z

2. WMO (2022). Scientific Assessment of Ozone Depletion: (2022).GAW Report No. 278. World Meteorological Organization, Geneva, Switzerland. https://ozone.unep.org/science/assessment/sap

3. Velders, G. J. M., Andersen, S. O., Daniel, J. S., Fahey, D. W., & McFarland, M. (2007). The importance of the Montreal Protocol in protecting climate. *Proceedings of the National Academy of Sciences of the United States of America, 104*(12), 4814–4819, https://doi.org/10.1073/pnas.0610328104

4. Purohit, P., Borgford-Parnell, N., Klimont, Z., & Höglund-Isaksson, L. (2022). Achieving Paris climate goals calls for increasing ambition of the Kigali Amendment. *Nature Climate Change, 12*(4), 339-342, https://doi.org/10.1038/s41558-022-01310-y

5. Goyal, R., England, M. H., Sen Gupta, A., & Jucker, M. (2019). Reduction in surface climate change achieved by the 1987 Montreal Protocol. *Environmental Research Letters, 14*(12), 124041, https://doi.org/10.1088/1748-9326/ab4874

6. Barnes, P. W., Williamson, C. E., Lucas, R. M., Robinson, S. A., Madronich, S., Paul, N. D., Bornman, J. F., Bais, A. F., Sulzberger, B., Wilson, S. R., Andrady, A. L., McKenzie, R. L., Neale, P. J., Austin, A. T., Bernhard, G. H., Solomon, K. R., Neale, R. E., Young, P. J., Norval, M., Rhodes, L. E., Hylander, S., Rose, K. C., Longstreth, J., Aucamp, P. J., Ballaré, C. L., Cory, R. M., Flint, S. D., de Gruijl, F. R., Häder, D.-P., Heikkilä, A. M., Jansen, M. A. K., Pandey, K. K., Robson, T. M., Sinclair, C. A., Wängberg, S.-Å., Worrest, R. C., Yazar, S., Young, A. R., & Zepp, R. G. (2019). Ozone depletion, ultraviolet radiation, climate change and prospects for a sustainable future. *Nature Sustainability, 2*(7), 569-579, https://doi.org/10.1038/s41893-019-0314-2

7. Williamson, C. E., Zepp, R. G., Lucas, R. M., Madronich, S., Austin, A. T., Ballaré, C. L., Norval, M., Sulzberger, B., Bais, A. F., McKenzie, R. L., Robinson, S. A., Häder, D.-P., Paul, N. D., & Bornman, J. F. (2014). Solar ultraviolet radiation in a changing climate. *Nature Climate Change, 4*(6), 434-441, https://doi.org/10.1038/nclimate2225

8. Smith, M. D. (2011). The ecological role of climate extremes: current understanding and future prospects. *Journal of Ecology, 99*(3), 651-655, https://doi.org/10.1111/j.1365-2745.2011.01833.x

9. IPCC (2021). Climate Change 2021: The Physical Science Basis. Contribution of Working Group I to the Sixth Assessment Report of the Intergovernmental Panel on Climate Change. [V. Masson-Demotte, P. Zhai, A. Pirani, S.L. Connors, C.Péan, S. Berger, N. Caud, Y. Chen, L. Goldfarb, M.I. Gomis, M. Huang, K. Leitzell, E. Lonnoy, J.B.R. Matthews, T.K. Maycock, T. Waterfield, O. Yelekçi, R. Yu and B. Zhou (Eds)], https://doi.org/10.1017/9781009157896

10. Bernhard, G. H., McKenzie, R. L., Lantz, K., & Stierle, S. (2022). Updated analysis of data from Palmer Station, Antarctica (64° S), and San Diego, California (32° N), confirms large effect of the Antarctic ozone hole on UV radiation. *Photochemical & Photobiological Sciences, 21*(3), 1-12, https://doi.org/10.1007/s43630-022-00178-3

11. Robinson, S. A., & Erickson III, D. J. (2015). Not just about sunburn -- the ozone hole's profound effect on climate has significant implications for Southern Hemisphere ecosystems. *Global Change Biology, 21*(2), 515-527, https://doi.org/10.1111/gcb.12739

12. Booth, C. R., Lucas, T. B., Morrow, J. H., Weiler, C. S., & Penhale, P. A. (1994). The United States National Science Foundation's polar network for monitoring ultraviolet radiation. In C. S. Weiler, & P. A. Penhale (Eds.), *Ultraviolet radiation in Antarctica: Measurements and biological effects* (Vol. 62, pp. 17-37, Antarc. Res. Ser.): American Geophysical Union, Washington, D.C.

13. Bernhard, G., Booth, C. R., & Ehramjian, J. C. (2004). Version 2 data of the National Science Foundation's ultraviolet radiation monitoring network: South Pole. *Journal of Geophysical Research: Atmospheres, 109*(D21), D21207, https://doi.org/10.1029/2004jd004937

14. Bernhard, G., & Stierle, S. (2020). Trends of UV radiation in Antarctica. *Atmosphere, 11*(8), 795, https://doi.org/10.3390/atmos11080795

15. Robinson, S. A., Klekociuk, A. R., King, D. H., Pizarro Rojas, M., Zúñiga, G. E., & Bergstrom, D. M. (2020). The 2019/2020 summer of Antarctic heatwaves. *Global Change Biology, 26*(6), 3178-3180, https://doi.org/10.1111/gcb.15083.

16. Lee, J. R., Waterman, M. J., Shaw, J. D., Bergstrom, D. M., Lynch, H. J., Wall, D. H., & Robinson, S. A. (2022). Islands in the ice: Potential impacts of habitat transformation on Antarctic biodiversity. *Global Change Biology*, https://doi.org/10.1111/gcb.16331.

17. Robinson, S. A., Wasley, J., & Tobin, A. K. (2003). Living on the edge - plants and global change in continental and maritime Antarctica. *Global Change Biology, 9*(12), 1681-1717, https://doi.org/10.1046/j.1365-2486.2003.00693.x.

18. Cannone, N., Malfasi, F., Favero-Longo, S. E., Convey, P., & Guglielmin, M. (2022). Acceleration of climate warming and plant dynamics in Antarctica. *Current Biology, 32*(7), 1599-1606, https://doi.org/10.1016/j.cub.2022.01.074.

19. IPCC (2022). Climate Change 2022: Impacts, adaptation, and vulnerability. Contribution of Working Group II to the Sixth Assessment Report of the Intergovernmental Panel on Climate Change. [H.-O. Pörtner, D.C. Roberts, M. Tignor, E.S. Poloczanska, K. Mintenbeck, A. Alegría, M. Craig, S. Langsdorf, S. Löschke, V. Möller, A. Okem, B. Rama (eds.)]. Cambridge University Press. Cambridge University Press, Cambridge, UK and New York, NY, USA,3056 pp., doi:10.1017/9781009325844

20. Chown, S. L., Leihy, R. I., Naish, T. R., Brooks, C. M., Convey, P., Henley, B. J., Mackintosh, A. N., Phillips, L. M., Kennicutt II, M. C., & Grant, S. M. (Eds.). (2022). *Antarctic climate change and the environment: A decadal synopsis and recommendations for action*. Cambridge, United Kingdom: Scientific Committee on Antarctic Research, www.scar.org

21. Overland, J. E., & Wang, M. (2021). The 2020 Siberian heat wave. *International Journal of Climatology, 41*, E2341-E2346, https://doi.org/10.1002/joc.6850.

22. Xia, Y., Hu, Y., Huang, Y., Zhao, C., Xie, F., & Yang, Y. (2021). Significant contribution of severe ozone loss to Siberian-Arctic surface warming in spring 2020. *Geophysical Research Letters, 48*(8), e2021GL092509, https://doi.org/10.1029/2021GL092509.

23. Domeisen, D. I. V., & Butler, A. H. (2020). Stratospheric drivers of extreme events at the Earth's surface. *Communications Earth & Environment, 1*(1), https://doi.org/10.1038/s43247-020-00060-z.

24. Zhang, J., Tian, W., Pyle, J. A., Keeble, J., Abraham, N. L., Chipperfield, M. P., Xie, F., Yang, Q., Mu, L., Ren, H.-L., Wang, L., & Xu, M. (2022). Responses of Arctic sea ice to stratospheric ozone depletion. *Science Bulletin, 67*(11), 1182-1190, https://doi.org/10.1016/j.scib.2022.03.015.

25. Young, P. J., Harper, A. B., Huntingford, C., Paul, N. D., Morgenstern, O., Newman, P. A., Oman, L. D., Madronich, S., & Garcia, R. R. (2021). The Montreal Protocol protects the terrestrial carbon sink. *Nature, 596*(7872), 384-388, https://doi.org/10.1038/s41586-021-03737-3.

26. Madronich, S., Lee-Taylor, J. M., Wagner, M., Kyle, J., Hu, Z., & Landolfi, R. (2021). Estimation of skin and ocular damage avoided in the United States through implementation of the Montreal Protocol on substances that deplete the ozone layer. *ACS Earth and Space Chemistry, 5*(8), 1876-1888, https://doi.org/10.1021/acsearthspacechem.1c00183.

27. Olsen, C. M., Thompson, J. F., Pandeya, N., & Whiteman, D. C. (2020). Evaluation of sex-specific incidence of melanoma. *JAMA Dermatology, 156*(5), 1-8, https://doi.org/10.1001/jamadermatol.2020.0470.

28. Defossez, G., Uhry, Z., Delafosse, P., Dantony, E., d'Almeida, T., Plouvier, S., Bossard, N., Bouvier, A. M., Molinié, F., Woronoff, A. S., Colonna, M., Grosclaude, P., Remontet, L., & Monnereau, A. (2021). Cancer incidence and mortality trends in France over 1990-2018 for solid tumors: the sex gap is narrowing. *BMC Cancer, 21*(1), 726, https://doi.org/10.1186/s12885-021-08261-1.

29. Korovin, S., Fedorenko, Z., Michailovich, Y., Kukushkina, M., Sekerija, M., & Ryzhov, A. (2020). Burden of malignant melanoma in Ukraine in 2002-2013: incidence, mortality and survival. *Experimental Oncology, 42*(4), 324-329, https://doi.org/10.32471/exp-oncology.2312-8852.vol-42-no-4.15334.

30. Pehalova, L., Krejci, D., Snajdrova, L., & Dusek, L. (2021). Cancer incidence trends in the Czech Republic. *Cancer Epidemiology, 74*, 101975, https://doi.org/10.1016/j.canep.2021.101975.

31. Liszkay, G., Kiss, Z., Gyulai, R., Oláh, J., Holló, P., Emri, G., Csejtei, A., Kenessey, I., Benedek, A., Polányi, Z., Nagy-Erdei, Z., Daniel, A., Knollmajer, K., Várnai, M., Vokó, Z., Nagy, B., Rokszin, G., Fábián, I., Barcza, Z., & Polgár, C. (2020). Changing trends in melanoma incidence and decreasing melanoma mortality in Hungary between 2011 and 2019: A nationwide epidemiological study. *Frontiers in Oncology, 10*, 612459, https://doi.org/10.3389/fonc.2020.612459.

32. Dulskas, A., Cerkauskaite, D., Vincerževskiene, I., & Urbonas, V. (2021). Trends in incidence and mortality of skin melanoma in Lithuania 1991-2015. *International Journal of Environmental Research and Public Health, 18*(8), https://doi.org/10.3390/ijerph18084165.

33. Heer, E. V., Harper, A. S., Sung, H., Jemal, A., & Fidler-Benaoudia, M. M. (2020). Emerging cancer incidence trends in Canada: The growing burden of young adult cancers. *Cancer, 126*(20), 4553-4562, https://doi.org/10.1002/cncr.33050.

34. Bucchi, L., Mancini, S., Crocetti, E., Dal Maso, L., Baldacchini, F., Vattiato, R., Giuliani, O., Ravaioli, A., Caldarella, A., Carrozzi, G., Ferretti, S., Filiberti, R. A., Fusco, M., Gatti, L., Gili, A., Magoni, M., Mangone, L., Mazzoleni, G., Michiara, M., Panato, C., Piffer, S., Piras, D., Rosso, S., Rugge, M., Scala, U., Tagliabue, G., Tumino, R., Stanganelli, I., & Falcini, F. (2021). Mid-term trends and recent birth-cohort-dependent changes in incidence rates of cutaneous malignant melanoma in Italy. *International Journal of Cancer, 148*(4), 835-844, https://doi.org/10.1002/ijc.33259.

35. Memon, A., Banniser, P., Rogers, I., Sundin, J., Al-Ayadhy, B., James, P. W., & McNally, R. J. Q. (2021). Changing epidemiology and age-specific incidence of cutaneous malignant melanoma in England: An analysis of the national cancer registration data by age, gender and anatomical site, 1981–2018. *The Lancet Regional Health - Europe, 2*, 100024.

36. Global Burden of Disease 2019 Cancer Collaboration (2021). Cancer incidence, mortality, years of life lost, years lived with disability, and disability-adjusted life years for 29 cancer groups from 2010 to 2019: A systematic analysis for the global burden of disease study 2019. *JAMA Oncology, 8*(2), 420, https://doi.org/10.1001/jamaoncol.2021.6987.

37. Zhang, W., Zeng, W., Jiang, A., He, Z., Shen, X., Dong, X., Feng, J., & Lu, H. (2021). Global, regional and national incidence, mortality and disability-adjusted life-years of skin cancers and trend analysis from 1990 to 2019: An analysis of the Global Burden of Disease Study 2019. *Cancer Medicine, 10*(14), 4905-4922, https://doi.org/10.1002/cam4.4046.

38. Kwiatkowska, M., Ahmed, S., Ardern-Jones, M. R., Bhatti, L. A., Bleiker, T. O., Gavin, A., Hussain, S., Huws, D. W., Irvine, L., Langan, S. M., Millington, G. W. M., Mitchell, H., Murphy, R., Paley, L., Proby, C. M., Thomson, C. S., Thomas, R., Turner, C., Vernon, S., & Venables, Z. C. (2022). A summary of the updated report on the incidence and epidemiological trends of keratinocyte cancers in the UK 2013–2018. *British Journal of Dermatology, 186*(2), 367-369, https://doi.org/10.1111/bjd.20764.

39. Olsen, C. M., Pandeya, N., Green, A. C., Ragaini, B. S., Venn, A. J., & Whiteman, D. C. (2022). Keratinocyte cancer incidence in Australia: a review of population-based incidence trends and estimates of lifetime risk. *Public Health Research & Practice, 32*(1), https://doi.org/10.17061/phrp3212203.

40. Hofmann, G. A., Gradl, G., Schulz, M., Haidinger, G., Tanew, A., & Weber, B. (2020). The frequency of photosensitizing drug dispensings in Austria and Germany: a correlation with their photosensitizing potential based on published literature. *Journal of the European Academy of Dermatology and Venereology, 34*(3), 589-600, https://doi.org/10.1111/jdv.15952.

41. Cheng, C.-Y., Wang, N., Wong, T. Y., Congdon, N., He, M., Wang, Y. X., Braithwaite, T., Casson, R. J., Cicinelli, M. V., Das, A., Flaxman, S. R., Jonas, J. B., Keeffe, J. E., Kempen, J. H., Leasher, J., Limburg, H., Naidoo, K., Pesudovs, K., Resnikoff, S., Silvester, A. J., Tahhan, N., Taylor, H. R., Bourne, R. R. A., on behalf of the Vision Loss Expert Group of the Global Burden of Disease, S. (2020). Prevalence and causes of vision loss in East Asia in 2015: magnitude, temporal trends and projections. *British Journal of Ophthalmology, 104*(5), 616-622, https://doi.org/10.1136/bjophthalmol-2018-313308.

42. Kahloun, R., Khairallah, M., Resnikoff, S., Cicinelli, M. V., Flaxman, S. R., Das, A., Jonas, J. B., Keeffe, J. E., Kempen, J. H., Leasher, J., Limburg, H., Naidoo, K., Pesudovs, K., Silvester, A. J., Tahhan, N., Taylor, H. R., Wong, T. Y., Bourne, R. R. A., & Vision Loss Expert Group of the Global Burden of Disease Study. (2019). Prevalence and causes of vision loss in North Africa and Middle East in 2015: magnitude, temporal trends and projections. *British Journal of Ophthalmology, 103*(7), 863-870, https://doi.org/10.1136/bjophthalmol-2018-312068.

43. Keeffe, J. E., Casson, R. J., Pesudovs, K., Taylor, H. R., Cicinelli, M. V., Das, A., Flaxman, S. R., Jonas, J. B., Kempen, J. H., Leasher, J., Limburg, H., Naidoo, K., Silvester, A. J., Stevens, G. A., Tahhan, N., Wong, T. Y., Resnikoff, S., & Bourne, R. R. A. , on behalf of the Vision Loss Expert Group of the Global Burden of Disease Study. (2019). Prevalence and causes of vision loss in South-east Asia and Oceania in 2015: magnitude, temporal trends and projections. *British Journal of Ophthalmology, 103*(7), 878-884, https://doi.org/10.1136/bjophthalmol-2018-311946.

44. Leasher, J. L., Braithwaite, T., Furtado, J. M., Flaxman, S. R., Lansingh, V. C., Silva, J. C., Resnikoff, S., Taylor, H. R., Bourne, R. R. A., on behalf of the Vision Loss Expert Group of the Global Burden of Disease Study. (2019). Prevalence and causes of vision loss in Latin America and the Caribbean in 2015: magnitude, temporal trends and projections. *British Journal of Ophthalmology, 103*(7), 885-893, https://doi.org/10.1136/bjophthalmol-2017-311746.

45. Naidoo, K., Kempen, J. H., Gichuhi, S., Braithwaite, T., Casson, R. J., Cicinelli, M. V., Das, A., Flaxman, S. R., Jonas, J. B., Keeffe, J. E., Leasher, J., Limburg, H., Pesudovs, K., Resnikoff, S., Silvester, A. J., Tahhan, N., Taylor, H. R., Wong, T. Y., Bourne, R. R. A., & Vision Loss Expert Group of the Global Burden of Disease, S. (2020). Prevalence and causes of vision loss in sub-Saharan Africa in 2015: magnitude, temporal trends and projections. *British Journal of Ophthalmology, 104*(12), 1658-1668, https://doi.org/10.1136/bjophthalmol-2019-315217.

46. Sintzel, M. B., Rametta, M., & Reder, A. T. (2018). Vitamin D and multiple sclerosis: A comprehensive review. *Neurology and Therapy, 7*(1), 59-85, https://doi.org/10.1007/s40120-017-0086-4.

47. Pham, H., Waterhouse, M., Baxter, C., Duarte Romero, B., McLeod, D. S. A., Armstrong, B. K., Ebeling, P. R., English, D. R., Hartel, G., Kimlin, M. G., Martineau, A. R., O'Connell, R., van der Pols, J. C., Venn, A. J., Webb, P. M., Whiteman, D. C., & Neale, R. E. (2021). The effect of vitamin D supplementation on acute respiratory tract infection in older Australian adults: an analysis of data from the D-Health Trial. *The Lancet Diabetes & Endocrinology, 9*(2), 69-81, https://doi.org/10.1016/S2213-8587(20)30380-6.

48. Emerging Risk Factors Collaboration/EPIC-CVD/Vitamin D Studies Collaboration (2021). Estimating dose-response relationships for vitamin D with coronary heart disease, stroke, and all-cause mortality: observational and Mendelian randomisation analyses. *Lancet Diabetes Endocrinol, 9*(12), 837-846, https://doi.org/10.1016/S2213-8587(21)00263-1.

49. Biasin, M., Strizzi, S., Bianco, A., Macchi, A., Utyro, O., Pareschi, G., Loffreda, A., Cavalleri, A., Lualdi, M., Trabattoni, D., Tacchetti, C., Mazza, D., & Clerici, M. (2022). UV and violet light can neutralize SARS-CoV-2 infectivity. *Journal of Photochemistry and Photobiology, 10*, 100107, https://doi.org/10.1016/j.jpap.2021.100107.

50. Ratnesar-Shumate, S., Williams, G., Green, B., Krause, M., Holland, B., Wood, S., Bohannon, J., Boydston, J., Freeburger, D., Hooper, I., Beck, K., Yeager, J., Altamura, L. A., Biryukov, J., Yolitz, J., Schuit, M., Wahl, V., Hevey, M., & Dabisch, P. (2020). Simulated sunlight rapidly inactivates SARS-CoV-2 on surfaces. *The Journal of Infectious Diseases, 222*(2), 214-222, https://doi.org/10.1093/infdis/jiaa274.

51. Schuit, M., Ratnesar-Shumate, S., Yolitz, J., Williams, G., Weaver, W., Green, B., Miller, D., Krause, M., Beck, K., Wood, S., Holland, B., Bohannon, J., Freeburger, D., Hooper, I., Biryukov, J., Altamura, L. A., Wahl, V., Hevey, M., & Dabisch, P. (2020). Airborne SARS-CoV-2 is rapidly inactivated by simulated sunlight. *The Journal of Infectious Diseases, 222*(4), 564-571, https://doi.org/10.1093/infdis/jiaa334.

52. Sagripanti, J. L., & Lytle, C. D. (2020). Estimated inactivation of coronaviruses by solar radiation with special reference to COVID-19. *Photochemistry and Photobiology, 96*(4), 731-737, https://doi.org/10.1111/php.13293.

53. Stadnytskyi, V., Bax, C. E., Bax, A., & Anfinrud, P. (2020). The airborne lifetime of small speech droplets and their potential importance in SARS-CoV-2 transmission. *Proceedings of the National Academy of Sciences, 117*(22), 11875-11877, https://doi.org/10.1073/pnas.2006874117.

54. Medicine, T. L. R. (2020). COVID-19 transmission — up in the air. *The Lancet Respiratory Medicine, 8*(12), 1159, https://doi.org/10.1016/S2213-2600(20)30514-2.

55. Rahman, H. S., Aziz, M. S., Hussein, R. H., Othman, H. H., Salih Omer, S. H., Khalid, E. S., Abdulrahman, N. A., Amin, K., & Abdullah, R. (2020). The transmission modes and sources of COVID-19: A systematic review. *International Journal of Surgery Open, 26*, 125-136, https://doi.org/10.1016/j.ijso.2020.08.017.

56. Zhou, L., Ayeh, S. K., Chidambaram, V., & Karakousis, P. C. (2021). Modes of transmission of SARS-CoV-2 and evidence for preventive behavioral interventions. *BMC Infectious Diseases, 21*(1), 496, https://doi.org/10.1186/s12879-021-06222-4.

57. Zhang, R., Li, Y., Zhang, A. L., Wang, Y., & Molina, M. J. (2020). Identifying airborne transmission as the dominant route for the spread of COVID-19. *Proceedings of the National Academy of Sciences, 117*(26), 14857-14863, https://doi.org/10.1073/pnas.2009637117.

58. Dodd, R. J., Chadwick, D. R., Harris, I. M., Hines, A., Hollis, D., Economou, T., Gwynn-Jones, D., Scullion, J., Robinson, D. A., & Jones, D. L. (2021). Spatial co-localisation of extreme weather events: a clear and present danger. *Ecology Letters, 24*(1), 60-72, https://doi.org/10.1111/ele.13620.

59. Filazzola, A., Matter, S. F., & MacIvor, J. S. (2021). The direct and indirect effects of extreme climate events on insects. *Science of the Total Environment, 769*, 145161, https://doi.org/10.1016/j.scitotenv.2021.145161.

60. Neale, R. E., Barnes, P. W., Robson, T. M., Neale, P. J., Williamson, C. E., Zepp, R. G., Wilson, S. R., Madronich, S., Andrady, A. L., Heikkilä, A. M., Bernhard, G. H., Bais, A. F., Aucamp, P. J., Banaszak, A. T., Bornman, J. F., Bruckman, L. S., Byrne, S. N., Foereid, B., Häder, D. P., Hollestein, L. M., Hou, W.-C. C., Hylander, S., Jansen, M. A. K., Klekociuk, A. R., Liley, J. B., Longstreth, J., Lucas, R. M., Martinez-Abaigar, J., McNeill, K., Olsen, C. M., Pandey, K. K., Rhodes, L. E., Robinson, S. A., Rose, K. C., Schikowski, T., Solomon, K. R., Sulzberger, B., Ukpebor, J. E., Wang, Q.-W., Wängberg, S.-Å., White, C. C., Yazar, S., Young, A. R., Young, P. J., Zhu, L., & Zhu, M. (2021). Environmental effects of stratospheric ozone depletion, UV radiation, and interactions with climate change: UNEP Environmental Effects Assessment Panel, Update 2020. *Photochemical & Photobiological Sciences, 20*, 1-67, https://doi.org/10.1007/s43630-020-00001-x.

61. Silva, C. A., Santilli, G., Sano, E. E., & Laneve, G. (2021). Fire occurrences and greenhouse gas emissions from deforestation in the Brazilian Amazon. *Remote Sensing, 13*(3), https://doi.org/10.3390/rs13030376.

62. Shiraishi, T., & Hirata, R. (2021). Estimation of carbon dioxide emissions from the megafires of Australia in 2019-2020. *Scientific Reports, 11*(1), 8267, https://doi.org/10.1038/s41598-021-87721-x.

63. Walsh, J. E., Ballinger, T. J., Euskirchen, E. S., Hanna, E., Mård, J., Overland, J. E., Tangen, H., & Vihma, T. (2020). Extreme weather and climate events in northern areas: A review. *Earth-Science Reviews, 209*, https://doi.org/10.1016/j.earscirev.2020.103324.

64. Jansen, M. A. K., Ač, A., Klem, K., & Urban, O. (2022). A meta-analysis of the interactive effects of UV and drought on plants. *Plant, Cell & Environment, 45*(1), 41-54, https://doi.org/10.1111/pce.14221.

65. Verdaguer, D., Díaz-Guerra, L., Font, J., González, J. A., & Llorens, L. (2018). Contrasting seasonal morphological and physio-biochemical responses to UV radiation and reduced rainfall of two mature naturally growing Mediterranean shrubs in the context of climate change. *Environmental and Experimental Botany, 147*, 189-201, https://doi.org/10.1016/j.envexpbot.2017.12.007.

66. Robson, T. M., Aphalo, P. J., Banas, A. K., Barnes, P. W., Brelsford, C. C., Jenkins, G. I., Kotilainen, T., Labuz, J., Martínez-Abaigar, J., Morales, L. O., Neugart, S., Pieristè, M., Rai, N., Vandenbussche, F., & Jansen, M. (2019). A perspective on ecologically relevant plant-UV research and its practical application. *Photochemical & Photobiological Sciences, 18*, 970-988, https://doi.org/10.1039/c8pp00526e.

67. Mansour, G., Ghanem, C., Mercenaro, L., Nassif, N., Hassoun, G., & Del Caro, A. (2022). Effects of altitude on the chemical composition of grapes and wine: a review. OENO One, 56(1), 227-239, https://doi.org/10.20870/oeno-one.2022.56.1.4895.

68. Hinojos Mendoza, G., Gutierrez Ramos, C. A., Heredia Corral, D. M., Soto Cruz, R., & Garbolino, E. (2020). Assessing suitable areas of common grapevine (Vitis vinifera l.) for current and future climate situations: The CDS Toolbox SDM. *Atmosphere, 11*(11), 1201, https://doi.org/10.3390/atmos11111201.

69. Derebe, A. D., Gobena Roro, A., Tessfaye Asfaw, B., Worku Ayele, W., & Hvoslef-Eide, A. K. (2019). Effects of solar UV-B radiation exclusion on physiology, growth and yields of taro (*Colocasia esculenta* (L.)) at different altitudes in tropical environments of Southern Ethiopia. *Scientia Horticulturae, 256*, 108563, https://doi.org/10.1016/j.scienta.2019.108563.

70. Tonnang, H. E., Sokame, B. M., Abdel-Rahman, E. M., & Dubois, T. (2022). Measuring and modelling crop yield losses due to invasive insect pests under climate change. *Current Opinion in Insect Science, 100873*, https://doi.org/10.1016/j.cois.2022.100873.

71. Wallingford, P. D., Morelli, T. L., Allen, J. M., Beaury, E. M., Blumenthal, D. M., Bradley, B. A., Dukes, J. S., Early, R., Fusco, E. J., Goldberg, D. E., Ibáñez, I., Laginhas, B. B., Vilà, M., & Sorte, C. J. B. (2020). Adjusting the lens of invasion biology to focus on the impacts of climate-driven range shifts. *Nature Climate Change, 10*(5), 398-405, https://doi.org/10.1038/s41558-020-0768-2.

72. Pierik, R., & Ballaré, C. L. (2021). Control of plant growth and defense by photoreceptors: From mechanisms to opportunities in agriculture. *Molecular Plant, 14*(1), 61-76, https://doi.org/10.1016/j.molp.2020.11.021.

73. Robson, T. M., Klem, K., Urban, O., & Jansen, M. A. K. (2015). Re-interpreting plant morphological responses to UV-B radiation. *Plant, Cell & Environment, 38*(5), 856-866, https://doi.org/10.1111/pce.12374.

74. Schweiger, O., Biesmeijer, J. C., Bommarco, R., Hickler, T., Hulme, P. E., Klotz, S., Kühn, I., Moora, M., Nielsen, A., Ohlemüller, R., Petanidou, T., Potts, S. G., Pyšek, P., Stout, J. C., Sykes, M. T., Tscheulin, T., Vilà, M., Walther, G.-R., Westphal, C., Winter, M., Zobel, M., & Settele, J. (2010). Multiple stressors on biotic interactions: how climate change and alien species interact to affect pollination. *Biological Reviews, 85*(4), 777-795, https://doi.org/10.1111/j.1469-185X.2010.00125.x.

75. Weaver, S. A., & Mallinger, R. E. (2022). A specialist bee and its host plants experience phenological shifts at different rates in response to climate change. *Ecology, e3658*, https://doi.org/10.1002/ecy.3658.

76. Pecl, G. T., Araújo, M. B., Bell, J. D., Blanchard, J., Bonebrake, T. C., Chen, I.-C., Clark, T. D., Colwell, R. K., Danielsen, F., Evengård, B., Falconi, L., Ferrier, S., Frusher, S., Garcia, R. A., Griffis, R. B., Hobday, A. J., Janion-Scheepers, C., Jarzyna, M. A., Jennings, S., Lenoir, J., Linnetved, H. I., Martin, V. Y., McCormack, P. C., McDonald, J., Mitchell, N. J., Mustonen, T., Pandolfi, J. M., Pettorelli, N., Popova, E., Robinson, S. A., Scheffers, B. R., Shaw, J. D., Sorte, C. J. B., Strugnell, J. M., Sunday, J. M., Tuanmu, M.-N., Vergés, A., Villanueva, C., Wernberg, T., Wapstra, E., & Williams, S. E. (2017). Biodiversity redistribution under climate change: Impacts on ecosystems and human well-being. *Science, 355*(6332), eaai9214, https://doi.org/10.1126/science.aai9214.

77. Vitasse, Y., Ursenbacher, S., Klein, G., Bohnenstengel, T., Chittaro, Y., Delestrade, A., Monnerat, C., Rebetez, M., Rixen, C., Strebel, N., Schmidt, B. R., Wipf, S., Wohlgemuth, T., Yoccoz, N. G., & Lenoir, J. (2021). Phenological and elevational shifts of plants, animals and fungi under climate change in the European Alps. *Biological Reviews, 96*(5), 1816-1835, https://doi.org/10.1111/brv.12727.

78. Chowdhury, S., Fuller, R. A., Dingle, H., Chapman, J. W., & Zalucki, M. P. (2021). Migration in butterflies: a global overview. *Biological Reviews, 96*(4), 1462-1483, https://doi.org/10.1111/brv.12714.

79. Fraser, D. P., Sharma, A., Fletcher, T., Budge, S., Moncrieff, C., Dodd, A. N., & Franklin, K. A. (2017). UV-B antagonises shade avoidance and increases levels of the flavonoid quercetin in coriander (*Coriandrum sativum*). *Scientific Reports, 7*(1), 17758, https://doi.org/10.1038/s41598-017-18073-8.

80. Seastedt, T., & Oldfather, M. (2021). Climate change, ecosystem processes and biological diversity responses in high elevation communities. *Climate, 9*(5), https://doi.org/10.3390/cli9050087.

81. Wang, Q.-W., Pieristè, M., Kotilainen, T., Forey, E., Chauvat, M., Kurokawa, H., Robson, M., & Jones, A. (2022). Meta-analysis of ecological studies attenuating solar radiation illustrates the importance of blue light over ultraviolet radiation in driving photodegradation of litter in terrestrial ecosystems. https://doi.org/10.21203/rs.3.rs-1377521/v1.

82. Day, T. A., & Bliss, M. S. (2019). A spectral weighting function for abiotic photodegradation based on photochemical emission of CO_2 from leaf litter in sunlight. *Biogeochemistry, 146*(2), 173-190, https://doi.org/10.1007/s10533-019-00616-y.

83. Wang, Q.-W., Robson, T. M., Pieristè, M., Kenta, T., Zhou, W., & Kurokawa, H. (2022). Canopy structure and phenology modulate the impacts of solar radiation on C and N dynamics during litter decomposition in a temperate forest. *Science of the Total Environment, 820*, 153185, https://doi.org/10.1016/j.scitotenv.2022.153185.

84. Day, T. A., & Bliss, M. S. (2020). Solar photochemical emission of CO_2 from leaf litter: Sources and significance to C loss. *Ecosystems, 23*, 1344-1361, https://doi.org/10.1007/s10021-019-00473-8.

85. Hugelius, G., Loisel, J., Chadburn, S., Jackson, R. B., Jones, M., MacDonald, G., Marushchak, M., Olefeldt, D., Packalen, M., Siewert, M. B., Treat, C., Turetsky, M., Voigt, C., & Yu, Z. (2020). Large stocks of peatland carbon and nitrogen are vulnerable to permafrost thaw. *Proceedings of the National Academy of Sciences, 117*(34), 20438-20446, https://doi.org/10.1073/pnas.1916387117.

86. Gagné, K. R., Ewers, S. C., Murphy, C. J., Daanen, R., Walter Anthony, K., & Guerard, J. J. (2020). Composition and photo-reactivity of organic matter from permafrost soils and surface waters in interior Alaska. *Environmental Science: Processes & Impacts, 22*(7), 1525-1539, https://doi.org/10.1039/d0em00097c.

87. Zimov, S. A., Schuur, E. A. G., & Chapin, F. S. (2006). Permafrost and the global carbon budget. *Science, 312*(5780), 1612-1613, https://doi.org/10.1126/science.1128908.

88. Grunert, B. K., Tzortziou, M., Neale, P., Menendez, A., & Hernes, P. (2021). DOM degradation by light and microbes along the Yukon River-coastal ocean continuum. *Scientific Reports, 11*(1), 10236, https://doi.org/10.1038/s41598-021-89327-9.

89. Rocher-Ros, G., Harms, T. K., Sponseller, R. A., Väisänen, M., Mörth, C.-M., & Giesler, R. (2021). Metabolism overrides photo-oxidation in CO_2 dynamics of Arctic permafrost streams. *Limnology and Oceanography, 66*(S1), 11564, https://doi.org/10.1002/lno.11564.

90. Stubbins, A., Mann, P. J., Powers, L., Bittar, T. B., Dittmar, T., McIntyre, C. P., Eglinton, T. I., Zimov, N., & Spencer, R. G. M. (2017). Low photolability of yedoma permafrost dissolved organic carbon. *Journal of Geophysical Research: Biogeosciences, 122*(1), 200-211, https://doi.org/10.1002/2016JG003688.

91. Bowen, J. C., Ward, C. P., Kling, G. W., & Cory, R. M. (2020). Arctic amplification of global warming strengthened by sunlight oxidation of permafrost carbon to CO_2. *Geophysical Research Letters, 47*(12), e2020GL087085, https://doi.org/10.1029/2020GL087085.

92. Cory, R. M., Ward, C. P., Crump, B. C., & Kling, G. W. (2014). Sunlight controls water column processing of carbon in Arctic fresh waters. *Science, 345*(6199), 925-928, https://doi.org/10.1126/science.1253119.

93. Mazoyer, F., Laurion, I., & Rautio, M. (2022). The dominant role of sunlight in degrading winter dissolved organic matter from a thermokarst lake in a subarctic peatland. *Biogeosciences Discussions, 1-28*, https://doi.org/10.5194/bg-2022-26.

94. Strauss, J., Schirrmeister, L., Grosse, G., Fortier, D., Hugelius, G., Knoblauch, C., Romanovsky, V., Schädel, C., Schneider von Deimling, T., Schuur, E. A. G., Shmelev, D., Ulrich, M., & Veremeeva, A. (2017). Deep Yedoma permafrost: A synthesis of depositional characteristics and carbon vulnerability. *Earth-Science Reviews, 172*, 75-86, https://doi.org/10.1016/j.earscirev.2017.07.007.

95. Sallée, J. B., Pellichero, V., Akhoudas, C., Pauthenet, E., Vignes, L., Schmidtko, S., Garabato, A. N., Sutherland, P., & Kuusela, M. (2021). Summertime increases in upper-ocean stratification and mixed-layer depth. *Nature, 591*(7851), 592-598, https://doi.org/10.1038/s41586-021-03303-x.

96. Waugh, D. W., Garfinkel, C. I., & Polvani, L. M. (2015). Drivers of the recent tropical expansion in the southern hemisphere: Changing SSTs or ozone depletion? *Journal of Climate, 28*(16), 6581-6586, https://doi.org/10.1175/jcli-d-15-0138.1.

97. van de Water, J. A. J. M., Courtial, L., Houlbrèque, F., Jacquet, S., & Ferrier-Pagès, C. (2018). Ultraviolet radiation has a limited impact on seasonal differences in the *Acropora muricata* holobiont. *Frontiers in Marine Science, 5*, 275, https://doi.org/10.3389/fmars.2018.00275.

98. He, T., Tsui, M. M. P., Tan, C. J., Ma, C. Y., Yiu, S. K. F., Wang, L. H., Chen, T. H., Fan, T. Y., Lam, P. K. S., & Murphy, M. B. (2019). Toxicological effects of two organic ultraviolet filters and a related commercial sunscreen product in adult corals. *Environmental Pollution, 245*, 462-471, https://doi.org/10.1016/j.envpol.2018.11.029.

99. Nordborg, F. M., Jones, R. J., Oelgemoller, M., & Negri, A. P. (2020). The effects of ultraviolet radiation and climate on oil toxicity to coral reef organisms - A review. *Science of the Total Environment, 720*, 137486, https://doi.org/10.1016/j.scitotenv.2020.137486.

100. Ward, C. P., & Overton, E. B. (2020). How the 2010 Deepwater Horizon spill reshaped our understanding of crude oil photochemical weathering at sea: a past, present, and future perspective. *Environmental Science: Processes & Impacts, 22*(5), 1125-1138, https://doi.org/10.1039/d0em00027b.

101. Freeman, D. H., & Ward, C. P. (2022). Sunlight-driven dissolution is a major fate of oil at sea. *Science Advances, 8*(7), eabl7605, https://doi.org/10.1126/sciadv.abl7605.

102. Nielsen, K. M., Alloy, M. M., Damare, L., Palmer, I., Forth, H. P., Morris, J., Stoeckel, J. A., & Roberts, A. P. (2020). Planktonic fiddler crab (Uca longisignalis) are susceptible to photoinduced toxicity following in ovo exposure in oiled mesocosms. *Environmental Science & Technology, 54*(10), 6254-6261, https://doi.org/10.1021/acs.est.0c00215.

103. Li, C., Gu, X., Wu, Z., Qin, T., Guo, L., Wang, T., Zhang, L., & Jiang, G. (2021). Assessing the effects of elevated ozone on physiology, growth, yield and quality of soybean in the past 40 years: A meta-analysis. *Ecotoxicology and Environmental Safety, 208*, 111644, https://doi.org/10.1016/j.ecoenv.2020.111644.

104. Lobell, D. B., & Burney, J. A. (2021). Cleaner air has contributed one-fifth of US maize and soybean yield gains since 1999. *Environmental Research Letters, 16*(7), 074049, https://doi.org/10.1088/1748-9326/ac0fa4.

105. Chen, H., Zhang, L., Li, M., Yao, Y., Zhao, Z., Munoz, G., & Sun, H. (2019). Per-and polyfluoroalkyl substances (PFASs) in precipitation from mainland China: Contributions of unknown precursors and short-chain (C2-C3) perfluoroalkyl carboxylic acids. *Water Research, 153*, 169-177, https://doi.org/10.1016/j.watres.2019.01.019.

106. Pickard, H. M., Criscitiello, A. S., Persaud, D., Spencer, C., Muir, D. C., Lehnherr, I., Sharp, M. J., De Silva, A. O., & Young, C. J. (2020). Ice core record of persistent short-chain fluorinated alkyl acids: Evidence of the impact from global environmental regulations. *Geophysical Research Letters, 47*(10), e2020GL087535S, https://doi.org/10.1029/2020GL087535.

107. Hassan, A. A., Abbas, A., Rasheed, T., Bilal, M., Iqbal, H. M., & Wang, S. (2019). Development, influencing parameters and interactions of bioplasticizers: An environmentally friendlier alternative to petro industry-based sources. *Science of the Total Environment, 682*, 394–404, https://doi.org/10.1016/j.scitotenv.2019.05.140.

108. Gunaalan, K., Fabbri, E., & Capolupo, M. (2020). The hidden threat of plastic leachates: A critical review on their impacts on aquatic organisms. Water Research, 184, 116170, https://doi.org/10.1016/j.watres.2020.116170.

109. Najafi, V., & Abdollahi, H. (2020). Internally plasticized PVC by four different green plasticizer compounds. *European Polymer Journal, 128*, 109620, https://doi.org/10.1016/j.eurpolymj.2020.109620.

110. Tipton, D. A., & Lewis, J. W. (2008). Effects of a hindered amine light stabilizer and a UV light absorber used in maxillofacial elastomers on human gingival epithelial cells and fibroblasts. *The Journal of Prosthetic Dentistry, 100*(3), 220–231, https://doi.org/10.1016/S0022-3913(08)60182-1

111. Barrick, A., Champeau, O., Chatel, A., Manier, N., Northcott, G., & Tremblay, L. A. (2021). Plastic additives: challenges in ecotox hazard assessment. *PeerJ, 9*, e11300, https://doi.org/10.7717/peerj.11300.

112. Lokanath, S. V., Skarbek, B., & Schindelholz, E. J. (2019). 9 - Degradation processes and mechanisms of PV wires and connectors. In H. E. Yang, R. H. French, & L. S. Bruckman (Eds.), *Durability and reliability of polymers and other materials in photovoltaic modules,* pp. 217–233, Plastics Design Library. William Andrew Publishing.

113. Santhakumari, M., & Sagar, N. (2019). A review of the environmental factors degrading the performance of silicon wafer-based photovoltaic modules: Failure detection methods and essential mitigation techniques. *Renewable and Sustainable Energy Reviews, 110*, 83–100, https://doi.org/10.1016/j.rser.2019.04.024.

114. Han, H., Yan, H., Wang, X., Zhang, K., Huang, J., Sun, Y., Liu, J., Verlinden, P. J., Altermatt, P., Liang, Z., & Shen, H. (2019). Analysis of the degradation of encapsulant materials used in photovoltaic modules exposed to different climates in China. *Solar Energy, 194*, 177–188, https://doi.org/10.1016/j.solener.2019.10.014.

115. Correa-Puerta, J., Ferrada, P., Häberle, P., Díaz-Almeida, D., Sanz, A., Zubillaga, O., Marzo, A., Portillo, C., & del Campo, V. (2021). Comparing the effects of ultraviolet radiation on four different encapsulants for photovoltaic applications in the Atacama Desert. *Solar Energy, 228*, 625–635, https://doi.org/10.1016/j.solener.2021.10.003.

116. IEA (2021). World Energy Outlook 2021. International Energy Agency Paris, France.

117. Tracy, J., Bosco, N., Delgado, C., & Dauskardt, R. (2020). Durability of ionomer encapsulants in photovoltaic modules. *Solar Energy Materials and Solar Cells, 208*, 110397, https://doi.org/10.1016/j.solmat.2020.110397.

118. Smith, S., Perry, L., Watson, S., Moffitt, S. L., Shen, S.-J., Mitterhofer, S., Sung, L.-P., Jacobs, D., & Gu, X. (2022). Transparent backsheets for bifacial photovoltaic (PV) modules: Material characterization and accelerated laboratory testing. *Progress in Photovoltaics: Research and Applications, 30*(8), 959-969, https://doi.org/10.1002/pip.3494.

119. Gok, A., Gordon, D. A., Wang, M., French, R. H., & Bruckman, L. S. (2019). 3 - Degradation science and pathways in PV systems. In H. E. Yang, R. H. French, & L. S. Bruckman (Eds.), *Durability and reliability of polymers and other materials in photovoltaic modules*, pp. 47–93, Plastics Design Library. William Andrew Publishing.

120. Geyer, R., Jambeck, J. R., & Law, K. L. Production, use, and fate of all plastics ever made. *Science Advances, 3*(7), e1700782, https://doi.org/10.1126/sciadv.1700782.

121. Andrady, A. L., Barnes, P. W., Bornman, J. F., Gouin, T., Madronich, S., White, C. C., Zepp, R. G., & Jansen, M. A. K. (2022). Oxidation and fragmentation of plastics in a changing environment; from UV-radiation to biological degradation. *Science of the Total Environment, 851*, 158022, https://doi.org/10.1016/j.scitotenv.2022.158022.

122. Garvey, C. J., Impéror-Clerc, M., Rouzière, S., Gouadec, G., Boyron, O., Rowenczyk, L., Mingotaud, A. F., & ter Halle, A. (2020). Molecular-scale understanding of the embrittlement in polyethylene ocean debris. *Environmental Science & Technology, 54*(18), 11173-11181, https://doi.org/10.1021/acs.est.0c02095.

123. Alimi, O. S., Claveau-Mallet, D., Kurusu, R. S., Lapointe, M., Bayen, S., & Tufenkji, N. (2022). Weathering pathways and protocols for environmentally relevant microplastics and nanoplastics: What are we missing? *Journal of Hazardous Materials, 423*, 126955, https://doi.org/10.1016/j.jhazmat.2021.126955.

124. Geneva-Environment-Network (2022). Update plastics and the environment. https://www.genevaenvironmentnetwork.org/resources/updates/plastics-and-the-environment/. Accessed 21 June 2022 2022.

125. Barnes, P. W., Robson, T. M., Neale, P. J., Williamson, C. E., Zepp, R. G., Madronich, S., Wilson, S. R., Andrady, A. L., Heikkilä, A. M., Bernhard, G. H., Bais, A. F., Neale, R. E., Bornman, J. F., Jansen, M. A. K., Klekociuk, A. R., Martinez-Abaigar, J., Robinson, S. A., Wang, Q. W., Banaszak, A. T., Häder, D. P., Hylander, S., Rose, K. C., Wängberg, S. Å., Foereid, B., Hou, W. C., Ossola, R., Paul, N. D., Ukpebor, J. E., Andersen, M. P. S., Longstreth, J., Schikowski, T., Solomon, K. R., Sulzberger, B., Bruckman, L. S., Pandey, K. K., White, C. C., Zhu, L., Zhu, M., Aucamp, P. J., Liley, J. B., McKenzie, R. L., Berwick, M., Byrne, S. N., Hollestein, L. M., Lucas, R. M., Olsen, C. M., Rhodes, L. E., Yazar, S., & Young, A. R. (2022). Environmental effects of stratospheric ozone depletion, UV radiation, and interactions with climate change: UNEP Environmental Effects Assessment Panel, Update 2021. *Photochemical & Photobiological Sciences*, *21*, 275-301, https://doi.org/10.1007/s43630-022-00176-5.

126. Bernhard, G. H., Neale, R. E., Barnes, P. W., Neale, P. J., Zepp, R. G., Wilson, S. R., Andrady, A. L., Bais, A. F., McKenzie, R. L., Aucamp, P. J., Young, P. J., Liley, J. B., Lucas, R. M., Yazar, S., Rhodes, L. E., Byrne, S. N., Hollestein, L. M., Olsen, C. M., Young, A. R., Robson, T. M., Bornman, J. F., Jansen, M. A. K., Robinson, S. A., Ballare, C. L., Williamson, C. E., Rose, K. C., Banaszak, A. T., Hader, D. P., Hylander, S., Wangberg, S. A., Austin, A. T., Hou, W. C., Paul, N. D., Madronich, S., Sulzberger, B., Solomon, K. R., Li, H., Schikowski, T., Longstreth, J., Pandey, K. K., Heikkila, A. M., & White, C. C. (2020). Environmental effects of stratospheric ozone depletion, UV radiation and interactions with climate change: UNEP Environmental Effects Assessment Panel, update 2019. *Photochemical & Photobiological Sciences, 19*, 542-584, https://doi.org/10.1039/d0pp90011g.

127. Crutzen, P. J. (2006). Albedo enhancement by stratospheric sulfur injections: A contribution to resolve a policy dilemma? *Climatic Change, 77*(3-4), 211-220, https://doi.org/10.1007/s10584-006-9101-y.

128. Kravitz, B., & MacMartin, D. G. (2020). Uncertainty and the basis for confidence in solar geoengineering research. *Nature Reviews Earth & Environment, 1*(1), 64-75, https://doi.org/10.1038/s43017-019-0004-7.

129. Madronich, S., Tilmes, S., Kravitz, B., MacMartin, D., & Richter, J. (2018). Response of surface ultraviolet and visible radiation to stratospheric SO_2 injections. *Atmosphere, 9*(11), https://doi.org/10.3390/atmos9110432.

130. Tilmes, S., Müller, R., & Salawitch, R. (2008). The sensitivity of polar ozone depletion to proposed geoengineering schemes. *Science, 320*(5880), 1201, https://doi.org/10.1126/science.1153966.

131. Barnes, P. W., Bornman, J. F., Pandey, K. K., Bernhard, G. H., Bais, A. F., Neale, R. E., Robson, T. M., Neale, P. J., Williamson, C. E., Zepp, R. G., Madronich, S., Wilson, S. R., Andrady, A. L., Heikkilä, A. M., & Robinson, S. A. (2021). The success of the Montreal Protocol in mitigating interactive effects of stratospheric ozone depletion and climate change on the environment. *Global Change Biology, 27*(22), 5681-5683, https://doi.org/10.1111/gcb.15841

1

STRATOSPHERIC OZONE, UV RADIATION, AND CLIMATE INTERACTIONS

G. H. Bernhard[6], A. F. Bais[7], P. J. Aucamp[8], A. R. Klekociuk[9], J. B. Liley[10], and R. L. McKenzie[9]

[6] Biospherical Instruments Inc., San Diego, California, USA.

[7] Laboratory of Atmospheric Physics, Department of Physics, Aristotle University, Thessaloniki, Greece.

[8] Ptersa Environmental Consultants, Pretoria, South Africa.

[9] Antarctic Climate Program, Australian Antarctic Division, Kingston, Australia.

[10] National Institute of Water & Atmospheric Research, Lauder, New Zealand.

Table of contents

Summary

This assessment provides a comprehensive update of the effects of changes in stratospheric ozone and other factors (aerosols, surface reflectivity, solar activity, and climate) on the intensity of ultraviolet (UV) radiation at the Earth's surface. The assessment is performed in the context of the Montreal Protocol on Substances that Deplete the Ozone Layer and its Amendments and Adjustments. Changes in UV radiation at low- and mid-latitudes (0–60°) during the last 25 years have generally been small (e.g., typically less than 4% per decade, increasing at some sites and decreasing at others) and were mostly driven by changes in cloud cover and atmospheric aerosol content, caused partly by climate change and partly by measures to control tropospheric pollution. Without the Montreal Protocol, erythemal (sunburning) UV irradiance at northern and southern latitudes of less than 50° would have increased by 10–20% between 1996 and 2020. For southern latitudes exceeding 50°, the UV Index (UVI) would have surged by between 25% (year-round at the southern tip of South America) and more than 100% (South Pole in spring). Variability of erythemal irradiance in Antarctica was very large during the last four years. In spring 2019, erythemal UV radiation was at the minimum of the historical (1991–2018) range at the South Pole, while near record-high values were observed in spring 2020, which were up to 80% above the historical mean. In the Arctic, some of the highest erythemal irradiances on record were measured in March and April 2020. For example in March 2020, the monthly average UVI over a site in the Canadian Arctic was up to 70% higher than the historical (2005–2019) average, often exceeding this mean by three standard deviations. Under the presumption that all countries will adhere to the Montreal Protocol in the future and that atmospheric aerosol concentrations remain constant, erythemal irradiance at mid-latitudes (30–60°) is projected to decrease between 2015 and 2090 by 2–5% in the north and by 4–6% in the south due to recovering ozone. Changes projected for the tropics are ≤3%. However, in industrial regions that are currently affected by air pollution, UV radiation will increase as measures to reduce air pollutants will gradually restore UV radiation intensities to those of a cleaner atmosphere. Since most substances controlled by the Montreal Protocol are also greenhouse gases, the phase-out of these substances may have avoided warming by 0.5 to 1.0 °C over mid-latitude regions of the continents, and by more than 1.0 °C in the Arctic; however, the uncertainty of these calculations is large. We also assess the effects of changes in stratospheric ozone on climate, focusing on the poleward shift of climate zones, and discuss the role of the small Antarctic ozone hole in 2019 on the devastating "Black Summer" fires in Australia. Additional topics include the assessment of advances in measuring and modelling of UV radiation; methods for determining personal UV exposure; the effect of solar radiation management (stratospheric aerosol injections) on UV radiation relevant for plants; and possible revisions to the vitamin D action spectrum, which describes the wavelength dependence of the synthesis of previtamin D_3 in human skin upon exposure to UV radiation.

1 Introduction

Chapter 1 focuses on the effects of changes in the ozone layer on climate and ultraviolet (UV) radiation at the Earth's surface, the interactions between UV radiation and climate, and on the influence of other geophysical parameters affecting UV radiation. The Chapter sets the stage for the subsequent Chapters of this Quadrennial Assessment that address the consequences of the interconnected effects of stratospheric ozone depletion, UV radiation, and climate change on human health [1] (including the COVID-19 pandemic [2]), terrestrial [3] and aquatic [4] ecosystems, the carbon cycle [3,4], air quality [5], natural and synthetic materials [6], and the fate of environmental plastic debris [7]. The 2022 Quadrennial Assessment focuses on new scientific knowledge up to August 2022 that has accumulated since our last comprehensive assessment of 2018 (see the website, Quadrennial Assessment 2018; and was also made available in Photochem. Photobiol. Sci., 2019, 18, 595–828). Many of these effects are assessed in terms of the benefits for life on Earth resulting from the implementation of the Montreal Protocol on Substances that Deplete the Ozone Layer [8] and its Amendments and Adjustments (henceforth "the Montreal Protocol"). These benefits were achieved by curbing depletion of stratospheric ozone, thereby limiting increases of UV radiation, and mitigating climate change. Further topics include assessments of observed trends in UV radiation, projections of UV radiation into the future, and advances in the monitoring and modelling of UV radiation.

2 State of the science in 2018

The previous comprehensive assessment of the EEAP [9], which was based on the state of knowledge in 2018, concluded that the Montreal Protocol was highly beneficial for protecting the stratospheric ozone layer and limiting the rise of solar UV-B (280–315 nm) radiation at the Earth's surface. Therefore, increases in erythemal (sunburning) UV radiation between the late 1970s (at the onset of anthropogenically induced stratospheric ozone depletion) and 2018 were negligible in the tropics, small (< 10%) at mid-latitudes (30–60°), and large (> 50%) only in polar regions.[11] Furthermore, the implementation of the Montreal Protocol[12] prevented increases in UV-B radiation since the mid-1990s. As a result, observed changes in UV radiation at mid-latitudes during the last ~3 decades were mainly controlled by clouds and aerosols instead of changes in stratospheric ozone. Statistically significant decreases in UV-B radiation consistent with ozone recovery had not yet been detected at mid- and low-latitudes at the time of the previous assessment because of the large variability in UV-B radiation caused by factors other than ozone. Conversely, continuing decreases in clouds and aerosols (rather than changes in ozone) observed since the mid-1990s led to positive trends of UV radiation at several sites between 30° and 60° N. Several independent satellite records indicated that changes in large-scale patterns of clouds occurred between the 1980s and 2000s with consequences on UV radiation at the Earth's surface.

In contrast to the tropics and mid-latitudes, variability of UV-B radiation in Antarctica remained very large, with near record-high erythemal UV radiation observed at the South Pole in spring 2015 and well below average values in spring 2016. The Arctic remained vulnerable to large decreases in total column ozone[13] (TCO) and concomitant increases in UV-B irradiance whenever meteorological conditions led to a cold lower stratosphere in late winter and early spring. For example, greatly reduced stratospheric ozone concentrations during the second half of February 2016 led to increases of erythemal UV radiation of up to 60% above the climatological average over northern Scandinavia and northern Siberia.

By preventing the further growth of the Antarctic ozone hole, the Montreal Protocol also helped to reduce its effects on atmospheric circulation, which include shifts of climate zones in the Southern Hemisphere and associated changes in weather patterns. For example, changes in tropospheric circulation contributed to a decrease in summer temperatures over southeast and south-central Australia, and inland areas of the southern tip of Africa. Anomalously high TCO in the spring were significantly correlated with hotter-than-normal summers over large regions of the Southern Hemisphere and vice versa.

With the predicted recovery of stratospheric ozone over the next several decades, UV-B radiation was expected to decrease at all latitudes outside the tropics, with the greatest decreases predicted over Antarctica. A projection of the erythemal irradiance[14] (quantified in terms of the UV Index[15] or UVI) for the end of the 21ˢᵗ century (average of 2085−2095) relative to the current decade (average of 2010−2020) suggested that ozone-recovery will lead to a decrease in the UVI by about 30% over Antarctica, and up to 6% over mid-latitudes. These projections were uncertain because future concentrations of stratospheric ozone will depend not only on the decrease of ozone-depleting substances (ODSs) controlled by the Montreal Protocol but also on the trajectory of concentrations of other greenhouse gases such as carbon dioxide and methane, which will greatly depend on policy decisions implemented in the coming decades. Changes in cloudiness were projected to result in small (up to 4%) localised increases in UVI over the mid-latitudes and tropics, and to decreases exceeding 10% in the Arctic. Reductions in reflectivity due to melting of snow and sea ice as well as shifting of the melting season were predicted to decrease above-surface UVI by up to 10% in the Arctic and by 2–3% around Antarctica. However, the increasingly ice-free Arctic Ocean and reductions in snow cover would lead to increases in UV radiation penetrating the water column and reaching land surfaces formerly covered by snow. Decreases in concentrations of aerosols over urban areas of the Northern Hemisphere were projected to increase the UVI by typically 5–10% and by up to 30% over heavily industrialised regions (e.g., southern and eastern Asia) as measures to control air pollution start to reduce contamination from aerosols towards pre-industrial levels. The extent of these changes was again determined to be greatly contingent on policy decisions.

---

[11] If not stated otherwise, the latitude ranges for both the Northern and Southern Hemispheres are defined as: polar latitudes (80°–90°); high-latitudes (60°–80°); mid-latitudes (30°–60°); low-latitudes or tropics (0°–30°).

[12] The Montreal Protocol was adopted in 1987 and was implemented in 1989 when it entered into force.

[13] Total column ozone or TCO is the amount of ozone in a vertical column extending from the Earth's surface to the top of the atmosphere. TCO is reported in Dobson Units or DU. One DU corresponds to a hypothetical layer of pure ozone with a thickness of 0.01 millimetre that would ensue if all ozone molecules in the vertical column were compressed to standard pressure (1013.25 hPa) and temperature (273.15 K or 0 °C). One DU corresponds to 2.69×10^{16} molecules per square centimetre of area at the base of this column. Averaged over the Earth's surface, the TCO is about 300 DU, which relates to a layer of pure ozone that is three millimetres thick.

[14] Irradiance is the radiant power (or radiant flux) received by a surface per unit area. "Radiant" indicates that the energy is received as electromagnetic radiation, and the surface is assumed horizontal unless otherwise specified.

[15] The UV Index is calculated by weighting solar UV spectra with the action spectrum of erythema [10] and multiplying the result with 40 m²/ W. See also Sect. 11.

3 Current and future status of atmospheric ozone

Changes in atmospheric ozone concentrations in general and TCO in particular are regularly being assessed by the Scientific Assessment Panel (SAP) of the Montreal Protocol in coordination with the World Meteorological Organization (WMO) and UNEP. The information provided in this section is largely based on the SAP's latest assessment [11] and provides the background for our assessment of the various effects resulting from changes in the ozone layer. We note that trends in TCO assessed by the SAP and summarised here refer to trends resulting mainly from human activities. The effects of natural cycles and events that affect TCO have been removed as part of the trend analysis. Such cycles and events include the solar cycle; the quasi-biennial oscillation (QBO; a pattern of alternating zonal winds in the tropical stratosphere); the El Niño-Southern Oscillation (ENSO; a pattern of alternating warm and cold sea surface temperatures of the tropical Pacific Ocean); the Arctic Oscillation (AO) and the Antarctic Oscillation (AAO), which both describe the back-and-forth shifting of atmospheric pressure between the poles and the mid-latitudes; the Brewer-Dobson circulation (a global-scale meridional circulation in the stratosphere); and aerosols from major volcanic eruptions [12].

3.1 Changes in total column ozone outside the polar regions

Signs of the ozone layer's recovery outside the polar regions are now more robust compared to the SAP's previous assessment [13] owing to updated trend models and additional four years of data. For the first time, small but statistically significant increases in TCO (of 0.4±0.2% per decade) for the period 1996–2020 are now evident for the latitude band 60° S–60° N [12]. However, this positive trend is mostly driven by TCO changes in the Southern Hemisphere (Fig. 1). In the tropics (20° S–20° N) and northern mid-latitudes (35°–60° N), increases in TCO since 1996 have not been observed with certainty (Fig. 1a and b), and statistically significant trends (of 0.7±0.6% per decade) have only been found for the southern mid-latitudes (35°–60° S) (Fig. 1c). Even though the Montreal Protocol entered into force more than 30 years ago, it was expected that the recovery of the ozone layer at mid-latitudes would only now start to become evident because the removal rate of ODSs controlled by the Montreal Protocol from the stratosphere is three to four times slower than the rate at which they were added [14]. Furthermore, year-to-year variability in TCO obscures the attribution of trends to declining concentrations of ODSs. Detecting significant increases in TCO outside Antarctica therefore requires much more time than the detection of its previous decline. In the upper stratosphere, however, the rate of increase in the ozone concentrations is larger, ranging between 1.5% and 2.2% per decade over the mid-latitudes of both hemispheres, and between 1% and 1.5% per decade in the tropics [11]. Since ozone column amounts in the upper stratosphere (above 32 km) are relatively small (typically less than 25% of the TCO at mid-latitudes), these increases contribute only modestly to the growth of TCO. Over the mid-latitudes, the present day TCO (2018–2020 average) is still below the average of the period 1964–1980 by ~4% in the Northern Hemisphere and by ~5% in the Southern Hemisphere [11]. Reasons for these latitude-dependent changes in TCO are discussed in SAP's 2022 assessment [11].

3.2 Changes in total column ozone over Antarctica

Several studies have provided evidence that the Antarctic ozone hole is starting to recover [15-21]. Signs of recovery are strongest for the month of September, which is the key month for chemical destruction of ozone. Both ground-based and satellite data indicate a statistically significant positive trend in TCO of 12% per decade in September since 2000 (Fig. 1e). These increases are consistent with the decrease in the concentration of ODSs controlled by the Montreal Protocol [20]. However, there are still no significant trends for October (Fig. 1f) or later months because TCO in late spring is less sensitive to decreasing ODSs in the stratosphere compared to September. In a typical Antarctic winter, ozone is almost completely destroyed in the lower stratosphere by the end of September, which may explain why no recovery has yet been observed in October over the polar cap [12]. In addition, year-to-year variability is also larger later in the year [11].

Assuming continued adherence to the Montreal Protocol, concentrations of ODSs are projected to decline further, eventually resulting in the disappearance of the annually recurring ozone hole in the second half of the 21st century [11]. Until that time, large year-to-year variations in various ozone hole metrics are expected because of the sensitivity of chemical ozone destruction to temperature in the lower stratosphere in the presence of ODSs. Especially during the last few years, the depth and size of the Antarctic ozone hole have exhibited particularly large variability:

In September and October 2019, the Antarctic ozone hole was the smallest on record since the early 1980s due to abnormally strong planetary wave[16] activity originating in the subtropical Pacific Ocean east of Australia and over the eastern South Pacific [22-24]. These waves weakened the stratospheric polar vortex, which led to a warming of the polar stratosphere, starting in mid-August [25]. The resulting above-normal temperature in the lower stratosphere reduced the occurrence of polar stratospheric clouds (PSCs), which provide the surfaces for heterogeneous[17] chemical reactions involving chlorine that result in catalytic destruction of ozone. The volume of PSCs dropped to almost zero by mid-September and the chemical processes leading to ozone depletion were therefore suppressed far earlier than usual. The average TCO over the polar cap (60°–90° S) in September and October 2019 was the highest over the last 40 years, and the minimum TCO for September 2019 was the highest since 1988.

---

[16] Large-scale perturbations in atmospheric circulation, typically manifesting as meandering of the jet stream.

[17] Heterogeneous chemical reactions are chemical reactions between substances of different phases, e.g., gaseous, liquid, solid.

For the months of September, October, and November, the polar cap average TCO was higher by 29%, 28%, and 26%, respectively, compared to the mean of the 2008–2018 period [26].
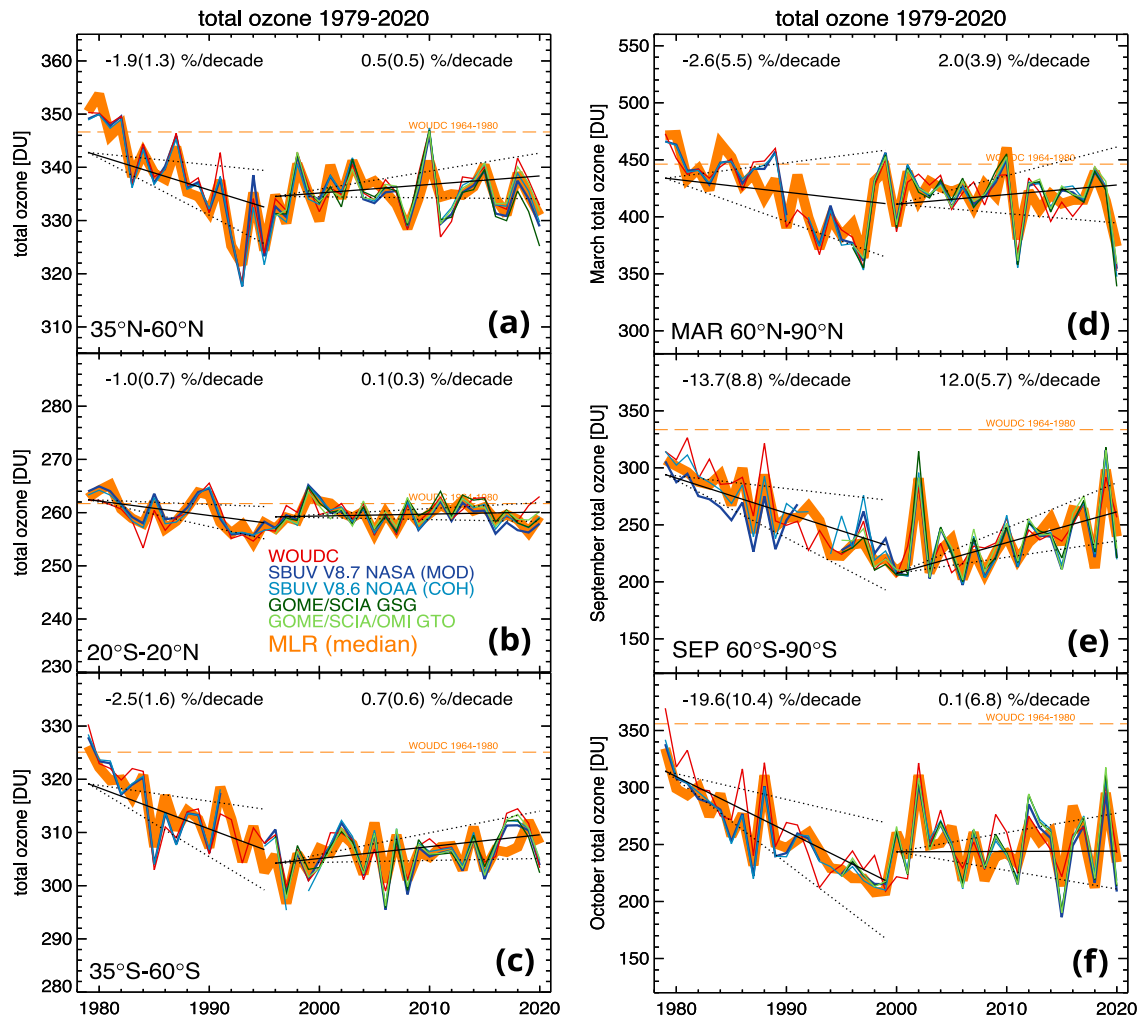
Fig. 1 Time series of annual mean TCO for the latitude bands (a) 35° N−60° N, (b) 20° S−20° N, and (c) 35° S−60° S; and monthly mean TCO for (d) March in the Arctic (60° N−90° N), (e) September in the Antarctic (60° S−90° S), and (f) October in the Antarctic (60° S−90° S). Colours indicate different ground- and satellite-based datasets. These are identified in the legend of panel (b) and defined as follows: WOUDC: ground-based measurements from the World Ozone and UV data centre (https://woudc.org/); SBUV V8.7 NASA (MOD): NASA Merged Ozone Data from the series of space-borne Solar Backscatter Ultraviolet (SBUV) instruments; SBUV V8.6 NOAA (COH): the NOAA cohesive dataset from several satellite sensors; GOME/SCIA GSG: the merged dataset from the space-borne Global Ozone Monitoring Experiment (GOME), the SCanning Imaging Absorption spectroMeter for Atmospheric CHartographY (SCIAMACHY), GOME-2A, and GOME-2B; and GOME/SCIA/OMI GTO: the merged data set from GOME, SCIAMACHY, the Ozone Monitoring Instrument (OMI), GOME-2A, GOME-2B, and TROPOspheric Monitoring Instrument (TROPOMI). The MLR (heavy orange line) dataset is the median of the five datasets described above and represents the input to the regression model applied by Weber et al. [12]. Solid black lines indicate linear trends calculated with this regression model before and after the peak in ODSs in 1996, respectively, and dotted lines indicate the two standard deviation (2σ) uncertainty of the estimated trends. Trend numbers are indicated for the pre (1979–1995) and post (1996–2020) ODS peak period in the top part of the plot. Numbers in parentheses are the 2σ trend uncertainty. The dashed orange line shows the mean TCO from 1964 until 1980 from the WOUDC data. Note that the scales of the ordinates are different in the six panels. Adapted from Weber et al. [12].

- In contrast, the Antarctic ozone holes in spring 2020 and 2021 were amongst the largest and longest-lived in the observational record [27,28]. These long-lasting ozone holes, extending to times when snow has melted, may have had impacts on Antarctic organisms [29]. Yook et al. [28] provided evidence that injection of smoke originating from the Australian "Black Summer" wildfires of early 2020 (Sect. 5.1.2) may have contributed to the large ozone hole of 2020, while aerosols from the eruption of La Soufrière

(13° N) on Saint Vincent in April 2021 may have played a role in the large ozone hole of 2021. (Aerosols injected into the tropical stratosphere disperse rapidly to high latitudes [30].) Furthermore, the lack of planetary waves during both years resulted in a cold and stable stratospheric vortex over Antarctica, which created conditions favourable for persistent ozone depletion [11,20,31]. Additionally, loss of ozone in early spring 2020 enhanced the strength and persistence of the vortex later in that year [32]. Even though large ozone holes will likely continue to occur in the future, either through dynamical variability alone, or exacerbated by large volcanic eruptions or major inputs of smoke into the stratosphere, the recovery of the ozone hole is expected to continue [27].

The large year-to-year variability in the TCO observed thus far resulted in large year-to-year variations in UV radiation in Antarctica (Sect. 7.1.1). For example, the UVIs measured at the South Pole in 2019 were some of the lowest since the start of measurements in 1991, while those in 2020 set new record highs. The recovery of the Antarctic ozone hole is generally more difficult to detect with UV-B radiation than ozone data because signs of recovery are most pronounced in September [15,33] when the UVI in Antarctica is still very low. Factors other than ozone that affect UV radiation (Sect. 6) lead to additional variability, hampering detection of recovery further.

Using observations from satellites between 1978 and 2020, a recent study [34] compared annual averages of the depth and area of the Antarctic ozone hole for early spring (1 September – 15 October) and late spring (16 October – 30 November). This analysis is of high relevance for assessing trends in UV radiation over Antarctica because UV radiation is generally much greater later in spring when the Sun is higher in the sky even though TCO is typically much lower earlier in spring. Figure 2a shows TCO averaged from 1 September to 15 October (red line) and from 16 October to 30 November (blue line) at King George Island (62° S), located near the northern tip of the Antarctic Peninsula. For the earlier period, the 11-year moving average of TCO was lowest around the year 2000, when the concentration of ozone-depleting chlorine and bromine compounds in the stratosphere was close to its maximum, and average TCO appears to be increasing since this time. The observation at this station is consistent with the positive trend in Antarctic TCO for September shown in Fig. 1e. Conversely, and consistent with Fig. 1f, there is no clear indication that TCO is also recovering in the later period. Similarly, the size of the ozone hole—quantified as the area with TCO below 220 Dobson Units (DU)—appears to be decreasing faster in early spring (Fig. 2b).
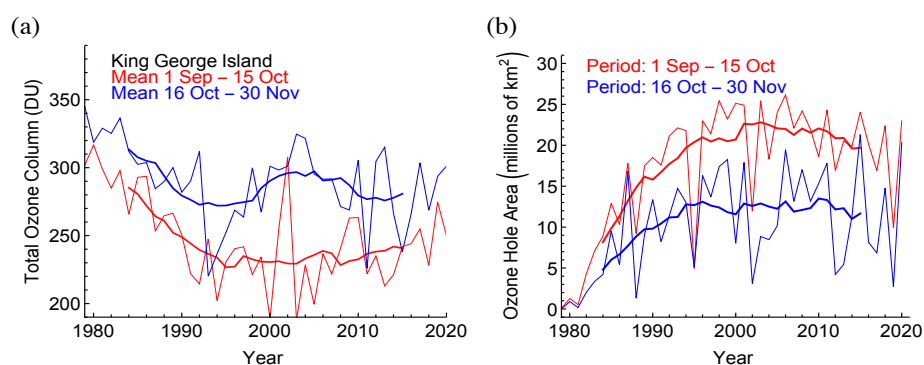
Fig. 2 (a) Time series of TCO at King George Island (62° S), averaged from 1 September to 15 October (red line) and from 16 October to 30 November (blue line). (b) Evolution of the ozone hole area averaged from 1 September to 15 October (red line) and from 16 October to 30 November (blue line). Bold lines indicate 11-year centred moving averages calculated from annual data. Adapted from Cordero et al. [34].

3.3   Changes in total column ozone over the Arctic

While there is still no clear evidence of ozone recovery in the Arctic, it is expected that signs of recovery would first be detected in March because chemical ozone loss in the Arctic is typically largest in this month [35]. Figure 1d indicates that TCO in March averaged over the northern polar cap (63°–90° N) is indeed increasing by 2% per decade, but this small positive trend is not statistically significant because of the large interannual dynamical variability observed for this latitude belt [11].

Sporadic ozone depletion events continue to occur in the Arctic. An exceptionally large episode of stratospheric ozone depletion was observed in late winter and early spring (February–April) of 2020 [36], exceeding in severity the previously reported event of 2011 [37]. The TCO averaged over 63°–90° N for this 3-month period was 340 Dobson Units (DU), which is 100 DU below the mean of the period 1979–2019 and the lowest since the start of satellite measurements in 1979. These low values of TCO in 2020 were partially caused by a strong and long-lived polar vortex, which provided ideal conditions for chemical ozone destruction to take place. Temperatures

low enough to form PSCs within the vortex developed early in the season, and on average enclosed about a third of the vortex volume [35,36,38-41]. Furthermore, the strong vortex also inhibited replenishment of Arctic ozone from lower latitudes [11]. These conditions are unique in the ~40 years of measurements, making 2020 the year with the largest loss of Arctic ozone on record. The large ozone hole observed over Antarctica six months later is a coincidence and cannot be attributed to a known common cause.

The unprecedented depletion of Arctic ozone in winter/spring of 2019/2020 contrasts with the conditions in the boreal winters of 2018/2019 and 2020/2021. In both winters, major stratospheric warmings occurred in January [42-44], which limited overall ozone loss. As a result, the minimum TCO in March 2019 (defined as the minimum of the daily mean TCO within an area that encloses the Arctic polar vortex and is surrounded by the 63° N contour of "equivalent latitude" [45]) was the highest since 1988 [46], and the minimum TCO in March 2021 was identical to its average value since the start of satellite observations in 1979 [47]. Such large year-to-year variations in Arctic ozone depletion, which are driven by differences in meteorological conditions, are expected to continue for as long as concentrations of ODSs remain elevated [11,41,48]. Furthermore, winters with a warm stratosphere (and little ozone depletion) will likely randomly alternate with winters with a cold stratosphere (and large ozone depletion). A recent study [49] provides evidence that years with a cold stratospheric Arctic vortex are getting colder. Reduced stratospheric temperatures will likely result in more PSC formation and lead to more chemical ozone loss via catalytic processes. As a consequence, ozone-depletion events as large or even larger than the one observed in 2020 [e.g., 36] will likely re-occur throughout the 21st century until concentrations of ODSs have substantially decreased. The magnitude of stratospheric cooling in the future will critically depend on the development of greenhouse gas (GHG) concentrations and on variability in the amount of water (H_2O) vapour in the stratosphere [11,49]. Under the scenario with the highest concentration of GHGs and H_2O, sporadic springtime increases in UV radiation in the Arctic could be somewhat larger at the end of the 21st century than those observed in 2020 [49].

3.4   Effects of greenhouse gases on stratospheric ozone

This section briefly discusses the effects of changes in the atmospheric concentration of GHGs that are responsible for global warming but are also relevant to stratospheric ozone changes. The SAP's latest report [11] discusses these processes in more detail. Increases in GHGs affect ozone depletion in several key ways [50]. First, radiative cooling of the polar stratosphere (promoted by GHGs during winter months) enhances the formation of PSCs. These clouds provide the surfaces for heterogeneous chemical reactions that lead to the destruction of ozone, thereby decreasing ozone concentrations. Second, cooling of the upper stratosphere at extrapolar latitudes reduces the rates of gas-phase chemical reactions that lead to ozone loss, thereby increasing ozone concentrations in the upper stratosphere. Third, changes in the concentrations of nitrous oxide (N_2O) and methane (CH_4), which are both GHGs, also affect ozone concentrations chemically because both gases are also key sources of reactive species in catalytic cycles (the NOx and HOx cycles, respectively) that destroy ozone. The NOx cycle dominates in the middle stratosphere (approximately 25-35 km) while the HOx cycle is mostly contributing in the lower stratosphere. Fourth, increases in GHG concentrations are expected to strengthen the Brewer–Dobson circulation, which describes the redistribution of ozone from tropical to extratropical regions [51]. Fifth, global warming induced by increases in GHGs increases the flux of "very short-lived substances" (VSLS) into the stratosphere as further explained in the following.

VSLS are ozone-depleting halogen-containing substances with a lifetime of less than six months that are mostly produced by natural processes, for example, by macroalgae (seaweed) and phytoplankton. About 25% of bromine entering the stratosphere in 2016 was from VSLS [13], with the majority originating from oceanic sources. While stratospheric bromine is a relatively minor constituent by volume, it is an important contributor to ozone depletion. Per atom, bromine is about 60–75 times (depending on the concentration of GHGs) more effective in destroying ozone than is chlorine [52]. A recent modelling study [53] examined the effect of climate change on changes in bromine from oceanic sources. The study assumed the Representative Concentration Pathway[18] RCP 6.0 GHG scenario and concluded that the flux of brominated VSLS compounds from the ocean to the atmosphere will increase by about 10% over the 21st century for all latitudes with the exception of the Arctic. The increase will be even greater over the Arctic because of the projected decrease in sea ice, which is currently hindering the escape of brominated compounds from the ocean. By the end of the 21st century, almost the entire polar ocean will likely be exposed in August and September and sea ice will no longer curtail ocean–atmosphere fluxes of brominated compounds. This study is one example of an indirect effect of climate change on the concentration of substances that promote stratospheric ozone depletion.

3.5   Estimates of total column ozone during the 21st century

Projections of TCO into the future are available from chemistry-climate models (CCMs), which were run for different future emissions scenarios as part of a coordinated, multi-model activity where all models follow the same protocols to perform a comparable set of simulations [11,54]. Uncertainties associated with these projections arise mainly from the assumed future trajectories of emissions of GHGs and pollutants. The models were run in the framework of CMIP6[19] simulations and follow a new set of future emissions scenarios,

---

[18] Representative Concentration Pathways are greenhouse gas concentration (not emission) trajectories adopted by the Intergovernmental Panel on Climate Change (IPCC) for its fifth Assessment Report. The pathways are used for climate modelling and research. They describe four climate futures, which differ in the amount of greenhouse gases that are emitted in years to come. The four RCPs, RCP 2.6, RCP 4.5, RCP 6, and RCP 8.5, are named after a possible range of radiative forcing values in the year 2100 relative to pre-industrial values (+2.6, +4.5, +6.0, and +8.5 W m^{-2}, respectively).

[19] Coupled Model Intercomparison Project Phase 6.

the Shared Socioeconomic Pathways (SSP[20]) [55], which assume compliance with the Montreal Protocol and its Amendments. The ozone projections for the different SSPs are therefore based on the same evolution of controlled ODSs and depend only on the evolution of GHGs and other pollutants.

The new simulations for the evolution of TCO towards the year 2100 support conclusions similar to those presented in a previous assessment of the SAP [13]. Figure 3 depicts the evolution of the annual-mean TCO averaged over different latitude bands for the period 1950–2100. The projections are based on a set of CMIP6 CCMs, which were run for the historical period 1950–2015 as well as for different scenarios for the future period 2015–2100. Year-to-year variability in these simulations is the result of internal variability (sometimes called "weather noise" [13]).

In summary, for scenarios with stabilising or slightly decreasing concentrations of GHGs (SSP2-4.5, SSP4-3.4, and SSP4-6.0), the near-global mean (60° S–60° N) TCO is projected to return to historic levels (year 1980) by the middle of the 21st century (around year 2040) and remain at those levels until 2100. For scenarios with continued GHG increases (SSP3-7.0 and SSP5-8.5), the TCO is projected to return to 1980 levels sooner and significantly exceed historic levels throughout the latter half of the 21st century. This overshoot, which has also been termed "super-recovery", results from the fact that increases in GHGs cool the upper stratosphere. This cooling reduces the rates of gas-phase chemical reactions that destroy ozone, and as a result, ozone concentrations increase. In contrast, and despite the assumption that halogenated ODSs will continue to decline throughout this century, TCO is not projected to return to historic levels by 2100 for scenarios with small GHG emissions (SSP1-1.9 and SSP1-2.6) and is projected to decrease in the tropics [11]. The consequences of these changes in TCO on UV radiation at the Earth's surface, and its dependence on the GHG scenario, are discussed in Sect. 8.

Fig. 3 Regional average CMIP6 multi-model annual mean TCO for the historical period (1950–2015) (black line), and the future (2015–2100) based on seven SSP scenarios (coloured lines). The six panels show results for different latitudinal bands, indicated in the top left of each panel. The number of models participating in each simulation is shown in parentheses in the legend. The light grey envelope indicates the model spread for the historical simulations (calculated as the standard error). Total ozone columns for the 1960 and 1980 annual means are given by the solid and dashed horizontal grey lines respectively. Note that the scales of the ordinates are different in the six panels. Reprinted from Keeble et al. [54].

4 Benefits of the Montreal Protocol

Benefits of the Montreal Protocol can be both direct (curbing stratospheric ozone depletion and limiting increases of UV radiation) and indirect (effects on climate). This section provides new information on both benefits.

4.1   Direct effects of the Montreal Protocol on stratospheric ozone depletion and UV radiation

The phase-out of ODSs mandated by the Montreal Protocol has already limited increases in UV radiation at the Earth's surface. To demonstrate this beneficial effect, McKenzie et al. [56] compared seasonal means of the daily maximum UVI measured at the Earth's surface with UVI data derived from results of two CCMs that assumed either the "World Avoided" scenario, where emissions of ODSs would have continued without regulation, or the "World Expected" scenario, where ODSs are curbed in compliance with the Montreal Protocol and its Amendments. The ground-based measurements were made at 17 mostly clean-air sites (latitude range 73° N–90° S) by state-of-the-art spectroradiometers. Trends in the UVI over 1996–2018 derived from measurements at sites with sufficiently long data records were found to be either small (< ±10% per decade at Antarctic sites) or not significantly different from zero. These estimates matched calculations following the World Expected scenario within the limits of the measurement uncertainty. In contrast, without the Montreal Protocol, the UVI at northern and southern latitudes of less than 50° would have increased by 10–20% between the early 1990s and 2018. For southern latitudes exceeding 50°, UVI values would have surged by between 25% (year-round at the southern tip of South America) and more than 100% (South Pole in spring and summer).

Figure 4 shows an update of the work by McKenzie et al. [56] including also UVI measurements from 2019 and 2020, and focusing on sites with at least 15 years of observations between 1996 and 2020. With the exception of Thessaloniki (41° N), changes in the UVI over this time period have been smaller than ±11% at all sites for both summer (Fig. 4a) and spring (Fig. 4b), and smaller than the "World Avoided" scenarios projected by the two CCMs (GEOSCCM[21] [57] and NIWA-UKCA[22] [58]), confirming that the Montreal Protocol has prevented large increases in UV radiation, in particular at southern latitudes higher than 60°. For example, without the Montreal Protocol (blue lines in Fig. 4), the UVI at the South Pole would by now have more than doubled in spring, while the ground-based measurements indicate a decrease of 10±34% (±2 standard deviations). Projected changes for high latitudes in the Northern Hemisphere are generally smaller because ozone depletion over the Arctic is less severe than that over the Antarctic (Sect. 3.2 and 3.3). The relatively large increases in the measured UVI at Thessaloniki (16% for spring and 8% for summer) are mostly caused by reductions in atmospheric aerosols at this urban site resulting from air pollution control measures (Sect. 6.1) and are not the result of decreases in ozone.

Fig. 4 Comparison of relative changes in the UVI between 1996 and 2020 for (a) summer and (b) spring, derived from observations at nine ground stations (black symbols) and calculated from results of two chemistry-climate models (blue lines). Both climate models assume the "World Avoided" scenario where emissions of ozone depleting substances are not controlled by the Montreal Protocol. Blue shading indicates the range of these model projections. Ground stations include South Pole (90° S), Arrival Heights (78° S), Palmer Station (65° S), Lauder (45° S), Alice Springs (24° S), Mauna Loa (20° N), Boulder (40° N), Thessaloniki (41° N), and Barrow (71° N). Ground stations with a near-complete data record for 1996–2020 are indicated by solid symbols. Sites with less than 24 years of data are shown with open symbols. Error bars indicate the 95% confidence interval of the regression model. Updated from McKenzie et al. [56].

4.2   Indirect effects of the Montreal Protocol on climate

Most ODSs controlled by the Montreal Protocol are also potent GHGs with Global Warming Potentials (GWPs) that are substantially larger than those of carbon dioxide (CO_2) on a molecule-by-molecule basis. The climate forcing of halocarbons has greatly increased during the last century. For example, over the second half of the 20th century, the combined direct radiative effect of all ODSs was the

---

[21] Goddard Earth Observing System Chemistry-Climate Model.

[22] REF-C2 simulation of the NIWA-UKCA model (Implementation of the United Kingdom Chemistry and Aerosols (UKCA) model by New Zealand's National Institute of Water & Atmospheric Research (NIWA)) [58] with exponentially increasing concentrations of ODSs at 3% per year added from 1974 onwards

second largest contributor to global warming after CO_2, with approximately one third of the radiative forcing[23] (RF) of CO_2 [59]. The climate effects of ODSs were already anticipated during the establishment of the Montreal Protocol [60], and their impact on climate has been continuously revised since the ratification of the Montreal Protocol [13,61,62]. Work on assessing the contribution of ODSs to global warming has continued during the last four years; however, the net effect of ODSs on global temperatures is still highly uncertain [Chapters 6 and 7 of 63] because some of the warming that ODSs induce is offset by their effect on stratospheric ozone. Specifically, since ozone is also a GHG, depletion of ozone caused by ODSs has a cooling effect, but the magnitude of this effect (hereinafter termed "indirect forcing from ozone depletion") is uncertain. On one hand, two single-model studies have reported a very large cancellation of the direct forcing by ODSs by the indirect forcing from ozone depletion of up to 80% [64,65], and two multi-model studies using an "emergent constraint approach"[24] based on CMIP6 models came to a similar conclusion [66,67]. On the other hand, additional studies, which were part of several model intercomparison projects, concluded that the climatic effect from ODS-induced ozone depletion is either small or negligible [68-72]. According to Chiodo and Polvani [72], the four studies that have calculated a large effect on climate from ozone depletion have weaknesses (e.g., one study was based on a short time period, one study had a large ozone bias, and the remaining two studies assumed unrealistically strong ozone depletion), while the other studies that indicate a small indirect forcing from ozone depletion are more reliable because they are consistent with multi-model means of the CMIP5 and CMIP6 models, as summarised by Checa-Garcia et al. [68]. However at this time, results from the two groups of studies cannot be reconciled. Because of these discrepancies, the latest (6th) report of the Intergovernmental Panel on Climate Change (IPCC) [specifically, Chapter 7 of 63] does not attempt to quantify the indirect forcing from ozone depletion, in contrast to previous IPCC reports [e.g., 73].

In the following, we summarise results of recent studies that evaluate the amount of global warming that has been avoided due to the Montreal Protocol's control of ODSs. All studies implicitly calculate the indirect forcing from ozone depletion and take this forcing into account when computing the net effect of the Montreal Protocol on surface temperatures. However, because of the uncertainty in calculating this feedback, the resulting effect on temperature is also uncertain. Still, taken together, these new studies further demonstrate the effectiveness of the Montreal Protocol in limiting temperature rise at the Earth's surface.

Goyal et al. [74] used a coupled atmosphere-ocean-land-sea-ice model to re-evaluate the Montreal Protocol's effect on global warming from the control of ODSs. The study considered ODSs that have contributed substantially to stratospheric chlorine concentrations, namely the chlorofluorocarbons (CFCs) CFC-11 and CFC-12, as well as the CFC substitutes HCFC-22, HFC-125 and HFC-134a. Increases in GHG concentrations (including the concentrations of these ODSs) were described in this model by RCP 8.5, which leads to the strongest warming at the surface of the Earth. The study determined that, as of 2019, the Montreal Protocol has avoided warming between 0.5 to 1.0 °C over mid-latitude regions of Africa, North America, and Eurasia and as much as 1.1 °C warming in the Arctic. In addition to quantifying the benefits from the Montreal Protocol that have already been realised, Goyal et al. [74] also assessed the Montreal Protocol's effect on the future climate for the RCP 8.5 scenario. Projected temperature increases that are likely to be averted by 2050 are in the order of 1.5 °C to 2 °C over most extrapolar land areas, and between 3 °C and 4 °C over the Arctic. Averaged over the globe (including the oceans), about 1 °C warming would be avoided by 2050, which corresponds to about 25% mitigation of global warming expected from all GHGs.

A separate study [59] found that, over the period 1955–2005, ODSs were responsible for about one third of warming globally and about half of the warming in the Arctic. Since changes in Arctic temperatures have a direct effect on sea ice loss, Polvani et al. [59] concluded that ODSs contributed half of the forced Arctic sea ice loss in the latter half of the 20th century. These results were recently confirmed [75], showing that Arctic warming and sea-ice loss from ODSs are slightly more than half (52-59%) of those from CO_2.

More recently, Chiodo and Polvani [72] calculated that stratospheric ozone depletion from ODSs only cancels about 25% of the RF from ODSs, in agreement with recent studies [e.g., 68]. The net RF of ODS is 0.24 W/m^2 accordingly, which amounts to nearly one third of the RF of CO_2 over the period 1955–2005, emphasising the large RF effect of ODSs on tropospheric temperatures.

In summary, recent model calculations demonstrate a large effect of the Montreal Protocol in limiting global warming, but these results are subject to large uncertainties because the cooling effect resulting from ODS-induced ozone depletion is quantitatively not well reproduced by CCMs. The influence of ODSs on climate is an area of active research and it is expected that refinements to chemistry-climate models will further reduce uncertainties in estimating the effect of the Montreal Protocol on surface temperature.

In one of the latest Amendments of the Montreal Protocol (the 2016 Kigali Amendment [76]), the phase-down of hydrofluorocarbons (HFCs)—replacement chemicals of ODSs that do not harm the ozone layer but have a large GWP—is regulated.

Without this amendment, the continued increase in atmospheric HFC concentrations would have contributed 0.28–0.44 °C to global surface warming by 2100. In contrast, the controls established by the Kigali Amendment are expected to limit surface warming from HFCs to about 0.04 °C in 2100 [77].

An unexpected slowdown in the decline of the atmospheric concentration of CFC-11 was observed after 2012 [78] and was partially caused by new emissions from eastern China (primarily the northeastern provinces of Shandong and Hebei). These emissions were likely due to new production and use [79]. They were initially of concern as they would delay recovery of ozone [80] and make a small but significant contribution to global warming [81]. The emissions appear to have been eliminated [82-84] and likely did not have a

---

[23] Radiative forcing quantifies the change in Earth's energy balance (in W m^{-2}) between incoming short-wave solar radiation and outgoing long-wave (thermal) IR radiation, either at the tropopause or at the top of atmosphere. If radiative forcing is positive at the tropopause, the temperature of the troposphere will increase.

[24] Emergent constraints are physically explainable empirical relationships between characteristics of the current climate and long-term climate prediction that emerge in large ensembles of climate model simulations.

significant effect on dates of recovery of the ozone hole [85-88]. However, if similar emissions were to reoccur and last longer, effects on climate could be significant.

If the production of ODSs had not been controlled by the Montreal Protocol, biologically active UV-B radiation causing plant damage [89] could have increased by about a factor of five over the 21st century[25] [90]. The ensuing harmful effects on plant growth were estimated to result in 325–690 billion tonnes less carbon held in plants by the end of this century. This reduction in carbon sequestration would have resulted in an additional 115–235 parts per million of CO_2 in the atmosphere, causing an additional rise of global-mean surface temperature of 0.5–1.0 °C. However, these estimates have large uncertainties and should be viewed with caution because the "generalised plant damage action spectrum" [89] used in the calculations does not account for the variety of plant responses across species and ecosystems. Furthermore, experiments (summarised by Ballaré et al. [91]) have not yet established whether the assumed sensitivity of plants to increases in UV-B radiation (i.e., a 3% reduction in biomass for every 10% increase in UV-B radiation for the "reference" scenario considered by Young et al. [90]) can be extrapolated to the very large increases in UV-B radiation simulated in this study. For example, Young et al. [90] did not consider that plants have protective mechanisms against damaging amounts of UV radiation, e.g., by synthesising UV-absorbing compounds [e.g., 29,92-95]. Such adaptation would mitigate the net CO_2 flux into the atmosphere. Conversely, enhanced photodegradation of organic matter under elevated UV radiation would release additional CO_2 into the atmosphere [96]. For more details, see Box 1, Chapter 4 [3].

In conclusion, the studies assessed above provide further evidence that the Montreal Protocol is not only vital for the recovery of the ozone layer, but also for the reduction of global warming. The Montreal Protocol is therefore considered to be one of the most successful international treaties to date mitigating anthropogenic climate change.

5 Effects of recent changes in stratospheric ozone on climate and weather

An in-depth assessment of the two-way interactions between changes in stratospheric ozone and climate is part of the SAP's latest report [11]. Here we focus on a subset of this assessment and emerging topics. We also highlight the effects of Antarctic and Arctic ozone depletion on the climates of the Southern and Northern Hemisphere, respectively, and assess how these changes impact temperature and precipitation at the Earth's surface as well as the extent of Antarctic sea ice and snow coverage.

5.1 Effects of Antarctic ozone depletion on Southern Hemisphere climate

By enhancing cooling of the stratosphere, Antarctic ozone depletion has caused a poleward shift of climate zones and has been the primary driver of climate change in the Southern Hemisphere during summer in recent decades [97 and Sect. 5.1.1]. An influence of stratospheric ozone changes on sea surface temperature (SST) of the Southern Ocean may also be expected. However, current climate models have generally not been able to reliably reproduce observed changes in SST at high southern latitudes [98]. Recent modelling has provided evidence that changes in atmospheric ozone during the latter half of the 20th century may be responsible for about one third of the observed warming in the upper 2,000 m of the Southern Ocean (30°–60° S) [99]. About 60% of this contribution can be attributed to increases in tropospheric ozone—partly caused by increasing downward transport of ozone from the stratosphere to the troposphere and partly by enhanced production of ozone in the troposphere [100]—and the other 40% to stratospheric ozone depletion [99].

Antarctic sea ice cover increased between 1978 and 2015 [101,102] and has subsequently shown a general decline with large year-to-year variability [103], which is still not completely understood (Sect. 5.1.3). Atmosphere-ocean interactions are intimately linked to the formation and dissipation of sea ice. However, the influence of ozone depletion on Antarctic sea ice is largely masked by other climate processes.

5.1.1 Shifting of climate zones

The effect of stratospheric ozone depletion on the summertime large-scale atmospheric circulation in the Southern Hemisphere has recently been confirmed and substantiated [97]. The primary effect has been the poleward shift of the tropospheric westerly winds over

---

[25] "World Avoided" scenarios such as the scenario discussed here are inevitably only estimates based on the state of current knowledge. They cannot consider possible changes in human behaviour and policies that may come about when large changes in UV irradiance and their consequences would have become more obvious in the future. Nevertheless, these projections allow us to put the crucial benefits that the Montreal Protocol has brought to date into perspective.

the Southern Ocean during the latter part of the 20th century. The location of these tropospheric winds is quantified with the Southern Annular Mode (SAM[26]) index. The poleward shift of these winds has led to a more positive state of the SAM during summer [104-106]. This shift has affected regional temperature patterns [104] as well as precipitation in parts of Australia and South America [107], and Antarctica [105]. Specifically, stratospheric ozone depletion led to a tendency for more precipitation in parts of Australia, and less rain in South America. As an example, Yook et al. [28] provide evidence that the large Antarctic ozone holes of 2020 and 2021 (Sect. 3.2)—which were likely influenced by the Australian wildfires of early 2020 and the eruption of La Soufrière in April 2021, respectively— contributed to anomalously strong westerly winds over much of the Southern Ocean, anomalously cool conditions over the Antarctic plateau, anomalously warm conditions over the Antarctic peninsula, and anomalously cool conditions over much of Australia with flooding rains across the south-east of the continent. These anomalies are consistent with those observed in other years with large Antarctic ozone holes [105].

As a direct result of the Montreal Protocol, recovery of stratospheric ozone observed since the end of the 20th century reversed cooling trends of the Southern Hemisphere's lower stratosphere [21,108]. However, warming trends observed post-2001 are about 50–75% smaller in magnitude than the cooling trends during the era of progressing ozone depletion. These changes in stratospheric temperature have also halted or partially reversed the poleward shift of climate zones [97].

Projections of the future climate for the Antarctic region under the 6th phase of the Coupled Model Intercomparison Project (CMIP6) [109] suggest that ozone recovery over the first half of the 21st century will tend to shift the westerly jet[27] equatorward during summer. This would lead to a reversal of the changes in air and sea temperature at the surface—as well as in precipitation and in the zonal wind speed over Antarctica and the Southern Ocean— that were observed during the period of progressively worsening ozone depletion in the late 20th century. However, this shift in the westerly jet is countered by the effects of both tropospheric warming and stratospheric cooling associated with increases in GHGs. The magnitude of this effect will depend on the GHG scenario defined by SSPs. Low-emissions scenarios (SSP1-2.6 and SSP2-4.5) tend to result in little overall change in the jet's position, while high emissions scenarios (e.g., SSP5-8.5) tend to cause an overall poleward forcing, particularly outside of the summer season. In the second half of the 21st century, GHG effects dominate under all emissions scenarios, with the westerly jet strengthened and placed further poleward than before the ozone hole era. However, projections of how this shift will affect weather patterns at southern mid and high latitudes (including South America, South Africa and Australia) are subject to the strong dependence on GHG scenario and climate feedbacks (e.g., changes in sea ice and ocean temperatures), which may develop over the next 50 years, plus the limited ability of models to take all these processes into account on a regional scale.

5.1.2 Causes and consequences of the 2019/2020 "Black Summer" fires

A topic that has emerged since our previous assessment [9] is the role played by Antarctic ozone variability in recent extreme weather and climatic conditions, and the follow-on effects of these extremes for stratospheric ozone concentrations.

From mid-2019 to early-2020, a series of devastating wildfires occurred in Australia, particularly along parts of the eastern coast, affecting over 10 million hectares. The overall severity of these 2019/2020 "Black Summer" fires was exacerbated by exceptionally hot and dry weather conditions combined with rainfall deficits over several years. As shown by Lim et al. [110], anomalously hot and dry conditions in subtropical eastern Australia from austral spring to early summer are favoured in years when the Antarctic stratospheric winter vortex is weak. Weak vortex conditions are promoted when planetary-scale (Rossby) waves disturb and warm the Antarctic atmosphere and reduce the overall amount of stratospheric ozone depletion in spring. The strong warming of the Antarctic stratosphere that occurred in September 2019 is a specific case of a weak vortex that has been linked with the 2019/2020 Black Summer fires [25,111-117]. Specifically, downward coupling from the Antarctic stratosphere promoted a strong negative phase of the tropospheric SAM at mid-latitudes in summer, which reduced precipitation over Australia and further exacerbated fire conditions [115].

While the fires were mainly promoted by the weak polar vortex, the reduced ozone depletion resulting from the weak vortex may have been an exacerbating factor. This connection was studied by Jucker and Goyal [117] who found that surface conditions were influenced by anomalously high concentrations of ozone in the lower stratosphere that accompanied the stratospheric warming event and delayed the stratosphere-to-troposphere coupling. This suggests that ozone recovery could further promote a seasonal delay in stratosphere-to-troposphere coupling under weak vortex conditions. On the other hand, stratospheric warming events, such as that observed in 2019, appear to be less likely in a future climate [118] as increasing concentrations of GHGs will cool the stratosphere.

One consequence of the Black Summer fires was that superheated air from the these fires produced large-scale pyrocumulonimbus clouds, which forced injection of an unprecedented amount of smoke and tropospheric air into the lower stratosphere [119-125]. From there, this air rose to heights of up to 35 km where it had persistent effects across a wide latitude band for several months [123,126]. Ozone-poor tropospheric air in the rising plume reduced TCO by up to 100 DU locally [119,123,127], with impacts on UV radiation at the Earth's surface. The rising air also increased mixing ratios of water vapour in the lower stratosphere at southern mid-latitudes [123,127] where it may have depleted ozone through enhanced heterogeneous reactions [128], although the magnitude of this effect is unclear [129]. The plume also contained significant quantities of black carbon aerosol and reactive gases, which affect stratospheric chemistry

---

[26] The SAM is the leading mode of Southern Hemisphere extratropical climate variability describing a seesaw of atmospheric mass between the mid- and high-latitudes, with corresponding impacts on the strength of the circumpolar westerly winds. A positive SAM index corresponds to a poleward shift of the maximum wind speed, which results in weaker-than-normal westerly winds in the southern mid-latitudes.

[27] The term "westerly jet" refers in the context to the maximum of westerly winds (i.e., winds blowing from west to east) close to the surface, not the jet stream in the upper troposphere. The jet's latitude is defined as the latitude with the largest wind speed.

[31,130-132]. Quantifying the overall effect of the Black Summer fires on stratospheric ozone is still the subject of ongoing research.

Additional information on the fire's impact on stratospheric chemistry is provided in SAP's latest assessment [11].

5.1.3   Effects on sea ice extent and snow coverage

The effects of ozone depletion on temperature and air circulation over Antarctica may also change snow and ice cover on the Antarctic continent and the extent of sea ice. For example, interactive climate models [97,133], which are state-of-the-art in representing the complex interplay between effects of transport and dynamics [134], have demonstrated that ozone depletion has influenced near-surface winds over the Southern Ocean during summer and could thus potentially affect sea ice extent. However, as discussed below, these linkages are still not well understood. Changes in ice or snow coverage are important because they modify the reflectivity of the surface, which in turn changes downwelling UV radiation (Sect. 6.2).

The sea ice zone surrounding Antarctica shows strong seasonal variability [101,102,135]. There has been marked interannual variability during the last four decades, particularly in the last years, with regionally opposing patterns of change [Chapter 2 of 63]. Antarctic sea ice expanded between 1979 (the start of satellite measurements) and 2015, although only in the transitional seasons. Trends in both summer and winter were not significant. After this period of increase, the extent of Antarctic sea ice declined dramatically during the austral springs of 2016 and 2017 [101], reaching a record low on 1 March 2017, which was 27% below the mean of annual minima calculated for 1978–2016. However, a partial recovery was observed between 2017 and 2021 (https://climate.nasa.gov/ask-nasa-climate/2861/arctic-and-antarctic-sea-ice-how-are-they-different/). Several studies examined the reasons for this recovery [136-138]; however, none of these studies found robust evidence that trends or variations in stratospheric ozone contributed to this phenomenon.

As discussed in Sect. 5.1, the effect of stratospheric ozone depletion on temperatures at the surface of the Southern Hemisphere is primarily mediated by changes in the SAM during summer. Observational studies have shown that the seasonal response to trends in the SAM has resulted in the cooling of the SST around Antarctica in autumn, which should have promoted an overall increase in sea ice extent in that season, consistent with observations between 1979 and 2015 [139-141]. Furthermore, ozone depletion has been linked to a reduction in downwelling long-wave[28] radiation. This reduction would also cool the Southern Ocean [142,143]. In contrast to these studies, results from state-of-the-art earth-system models clearly indicate that ozone depletion in the second half of the 20th century should have caused a reduction in sea ice extent, mainly by promoting the redistribution of ocean heat content [140,141,143-145]. However, only a subset of leading climate models can adequately capture the observed link between the SAM and autumn changes in sea ice [133]. In general, current climate models do not provide a consistent representation of the observed long-term trends in sea ice. As concluded by Polvani et al. [133], this appears to be the consequence of the relatively small fraction of variance explained by the seasonal coupling of the SAM and sea ice, which is surpassed by the larger fractions attributable to natural variations and the models' internal variability. The effect of ozone depletion on changes in sea ice is therefore still not well understood.

Over much of the Antarctic continent, only relatively small seasonal changes in the short-wave albedo[29] of the ice sheet occur and are primarily caused by deposition of snow and melting at the surface [146]. Local exceptions occur in the regions of exposed rock, which account for approximately 0.4% of the surface area of the continent. Here, varying coverage by ice, snow, and surface water can strongly influence albedo [147]. Changes in snowfall over Antarctica have been attributed to changes in atmospheric circulation resulting from the depletion of ozone [148], although patterns of relative change are heterogeneous [149].

5.2   Associations between Arctic stratospheric ozone losses and the climate of the Northern Hemisphere

Years with a strong Arctic polar vortex and associated significant stratospheric ozone depletion have been linked to widespread climate anomalies across the Northern Hemisphere based on targeted model experiments with CCMs [150]. As an example, the exceptionally large ozone depletion that occurred in March–April 2020 (Sect. 3.3) not only led to record-breaking increases in Arctic solar UV radiation (Sect. 7.1.2) but also affected weather patterns in the Northern Hemisphere during spring. Specifically, it helped to keep the Arctic Oscillation (or AO[30]) in a record-high positive state through April [36], thus contributing to abnormally high temperatures across Asia and Europe [151]. Furthermore, loss of stratospheric ozone modified circulation patterns of winds around the Arctic, thereby affecting the stability of the upper troposphere in the Siberian sector of the Arctic. In turn, this led to more high-level clouds that enhanced downwelling long-wave (thermal) radiation [152]. The associated anomalous warming of the surface in April 2020 was further amplified by a reduction in albedo caused by melting of snow and sea ice. Monthly anomalies (relative to the 1981–2010 climatology) in air temperature of up to +6 °C were observed over Siberia from January through May 2020 [153]. The temperature in the Siberian town of Verhojansk (68° N, 133° E) set a new record of 38 °C on 20 June 2020, which is the highest temperature ever documented near the Arctic Circle. Depletion of stratospheric ozone over the Arctic in March may cause reductions in the sea ice concentration and the sea

---

[28] Long-wave radiation is electromagnetic radiation with wavelengths between 3 and 100 µm that is emitted from the Earth and its atmosphere in the form of thermal radiation. Long-wave radiation contrasts with short-wave radiation with wavelengths between ~0.3 and ~3 µm originating from the Sun.

[29] Albedo is the proportion of the incident radiation that is reflected by a surface. Short-wave albedo refers to the fraction of the total incident solar irradiance in the wavelength range of ~0.3–3 µm that is reflected by the Earth's surface. Albedo may also refer to the reflectivity in a certain wavelength range, such as the UV range.

[30] The Arctic Oscillation (AO) or Northern Annular Mode (NAM) is analogous to the Southern Annular Mode (SAM) and characterises the pattern of winds circulating around the Arctic. When the AO is in its positive phase, a ring of strong winds circulating the North Pole acts to confine colder air in the polar regions.

ice thickness over the Arctic Ocean north of Siberia from spring to summer [154].

The unprecedented depletion of Arctic ozone in the spring of 2020 contrasts with the boreal winter of 2020/2021, when a major sudden stratospheric warming (SSW) occurred on 5 January 2021 [42,43] and limited overall ozone loss (Sect. 3.3). During an SSW event, the westerly winds of the wintertime polar stratosphere decelerate and temperatures in the polar stratosphere rapidly increase [155]. The 2021 SSW event warmed the lower stratosphere, interrupted the catalytic cycles associated with ozone depletion [47], and also affected the polar atmospheric circulation from the upper stratosphere to the surface for six weeks after the event. During this period, surface temperatures were anomalously high over Greenland and the Canadian Arctic and anomalously low over Europe, northern Asia, and the United States, with a cold air outbreak first occurring over Eurasia in January and then over North America in the first two weeks of February [156]. SSWs generally increase the likelihood of such weather anomalies [157]; however, it is still unclear to what degree the cold weather events in early 2021 were linked to the SSW on 5 January 2021. There is some evidence that the cold outbreak in Siberia on 22–24 January 2021 was associated with the SSW [158]. However, simulations with a climate model did not find evidence that this SSW event caused or influenced the record-breaking cold in North America during February 2021.

Precipitation in Central China in April–May has been linked to Arctic stratospheric ozone changes in February–March by combining observations, reanalysis data, and a CCM [159]. Specifically, positive Arctic ozone anomalies enhance precipitation in central China and negative anomalies reduce precipitation. Another study, using the same CCM, demonstrated a negative relationship between Arctic ozone anomalies in March and surface temperature anomalies in central Russia and, a weaker positive relationship in southern Asia [160]. Furthermore, variations in precipitation occurring during April in the northwestern United States (mainly the states of Washington and Oregon) are strongly linked to changes in Arctic stratospheric ozone during March [161]. Specifically, higher-than-normal Arctic ozone concentrations in March lead to less precipitation in April and vice versa.

Despite these advances in the understanding, assessing linkages between Arctic ozone depletion and weather in the Northern Hemisphere remains difficult and is subject to large uncertainties. It is anticipated that future studies will refine the conclusions summarised above.

6 Factors other than ozone affecting UV radiation

Solar UV-B radiation at the Earth's surface is mostly controlled by the height of the Sun above the horizon (i.e., the solar elevation[31]); TCO; clouds; aerosols; the reflectivity of the surface, also called albedo; and altitude. Less important factors include: the vertical distribution of ozone in the atmosphere (i.e., the ozone profile) for fixed TCO; other trace gases such as sulphur dioxide (SO_2) and nitrogen dioxide (NO_2); seasonal changes in the Earth-Sun distance; changes in solar activity, which influence both stratospheric ozone concentrations and the UV-B irradiance at the top of the atmosphere; topography; and volcanic eruptions. Except for determinants related to the Sun and volcanic activity, all these factors are influenced by human activities—such as the release of GHGs and air pollutants—and are coupled with changes in the climate. For example, higher temperatures will lead to less sea ice in the Arctic, which will in turn reduce surface reflectivity and UV radiation at or above the surface. The effects of these factors have been described at length in previous assessments [9,162,163]. No studies published in the last four years provide new insights into the effect of clouds on UV radiation. We therefore focus in the following sections on new understandings into the roles of aerosols, albedo, solar activity, volcanic eruptions, and climate interactions on UV radiation.

6.1   Aerosols

Natural and anthropogenic aerosols (solid and liquid particles suspended in the atmosphere) play a major role in controlling the intensity of UV radiation at the Earth's surface. Although effects of aerosols have been discussed in numerous studies, the magnitude of these effects is still uncertain. The attenuation of surface UV radiation by aerosols depends on their amount, as measured by aerosol optical depth (AOD), and on their efficiency of absorption, as discussed at length in our last assessments [9,162]. To quantify these effects further, Campanelli et al. [164] analysed optical properties of aerosols and spectral irradiance in Rome, Italy, and correlated the variability of the UVI (adjusted for variations in TCO) with the AOD at 340 nm for two groups of either strongly or weakly absorbing aerosols.

---

[31] The position of the Sun in the sky is typically either described by the solar elevation, which is counted from the horizon, or the solar zenith angle (SZA), which is counted from the zenith (the imaginary point directly above a particular location). The solar elevation can be calculated as 90° – SZA.

Absorption for the two classes was quantified with the single scattering albedo[32] (SSA). For strongly absorbing aerosols (SSA < 0.9), an increase of the AOD by one unit resulted in a decrease of the UVI by 2.7 units (about 30%) for a solar zenith angle (SZA) of 30° and by 1.65 units (about 25%) for a SZA of 40°. For less absorbing aerosols (SSA > 0.9), the UVI decreased only by one unit (about 12%) per unit of AOD increase for both SZAs. The study illustrates the importance of the absorption properties of aerosols.

The paucity of measurements of the properties of aerosols (including the SSA) in the UV-B range [9] hampers our ability to accurately assess the effects of aerosols on a global scale as well as for urban regions with a diverse mix of aerosol types [5]. Global networks, such as the Aerosol Robotic Network (AERONET), which measure AOD and other aerosol properties, do not perform observations at UV-B wavelengths. While the technology for measuring AOD and SSA in the UV-B range exists and has been tested at a few sites [165-169], there are at present no reliable data to assess aerosol properties in this critical wavelength range on a global scale. However, the European Brewer Network (EUBREWNET) [170] has recently started to provide AOD in the wavelength range from 306 to 320 nm [167] and a preliminary analysis confirms the good quality of the data. It is anticipated that this network will expand globally.

In areas with elevated levels of air pollution and small variability in TCO, the attenuation of solar UV radiation under cloudless skies is mainly controlled by aerosols. In such areas, abatement of air pollution can lead to increases in the intensity of UV radiation towards levels that would normally occur in unpolluted areas at similar latitudes and altitudes. An example of this is the observed increase of ~25% in UVI over Mexico City between 2000 and 2019, which was attributed to reductions in pollutants; in order of importance, aerosols, tropospheric ozone, NO_2, and SO_2 [171]. Because of high historical levels of air pollution in Mexico City, the UVI under cloud-free conditions was lower by ~40% in 2000 and ~25% in 2019 relative to values expected for an unpolluted clear atmosphere. Monthly averages of the daily maximum UVI from the 11 stations distributed across the Mexico City Metropolitan Area considered in this study show a clear upward trend of 0.9% per year between 2000 and 2019, and an overall increase in monthly maximum UVI of 1.5 over the two decades (Fig. 5). Since 2016, the rate of increase is greater, possibly reflecting more aggressive measures in reducing air pollutants. Human health benefits resulting from the decrease in air pollution [5,172] outweigh risks—such as the potential increase in skin cancer incidence—stemming from the gradual return of UV radiation intensities to more natural levels prevailing at unpolluted areas[33].

The effects of air quality measures implemented in Mexico City may help to project changes in UV radiation for regions that are currently still affected by heavy smog, such as South and East Asia [9,173]. Finally, the study for Mexico City also confirmed earlier findings [e.g., 174] that the UVI at the surface of heavily polluted areas cannot be reliably estimated from satellite observations, emphasising the importance of ground-based measurements. A similar finding was reported by Roshan et al. [175] for the city of Doha, Qatar, when extreme dust storms resulted in a measured UVI of 6–7 compared to a UVI of 10–11 estimated by the OMI satellite on the same days.
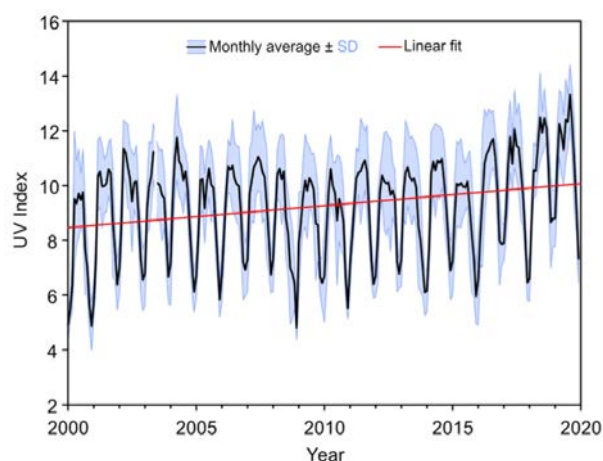
Fig. 5 Monthly average noontime UVI in the Mexico City Metropolitan Area (black line) ± 1 standard deviation (blue shading), and linear fit (red line) to average data. Reprinted from Ipiña et al. [171] with permission from the American Chemical Society, Copyright © 2021.

The effect of increased aerosols and tropospheric ozone on surface UV radiation during the biomass burning[34] season in Pretoria, South Africa, was investigated by du Preez et al. [176]. The simulations included different scenarios with and without increased levels of aerosols and tropospheric ozone from biomass burning. For cloudless days during the height of the biomass burning period in September, aerosols and tropospheric ozone reduced the noontime UVI by 13% and 1%, respectively, demonstrating that changes in

---

[32] The AOD is the sum of the aerosol scattering optical depth τ_{sca} and the absorption optical depth τ_{abs}, which quantifies the attenuation of the direct solar beam due to scattering and absorption of photons: $\tau = \tau_{sca} + \tau_{abs}$. Instead of specifying τ and τ_{abs}, the single scattering albedo (SSA) is often reported instead: $SSA = \tau_{sca} / (\tau_{sca} + \tau_{abs}) = \tau_{sca} / \tau$, resulting in $\tau_{abs} = (1 - SSA) \times \tau$. A decrease in SSA, therefore, corresponds to an increase in absorption of radiation.

[33] The global number of deaths from air pollution (particulate matter and gases such as tropospheric ozone and nitrous oxides) has been estimated at 4.2 million per year [5]. In comparison, the number of deaths from skin cancer was about 120,000 in 2020 (https://gco.iarc.fr/today/fact-sheets-cancers, accessed 13 November 2022).

[34] Biomass burning is the burning of living and dead vegetation. It generally includes the human-initiated burning of vegetation for land clearing and land-use change as well as natural, lightning-induced fires.

the UVI were dominated by the effects from aerosols.

Smog from the Black Summer wildfires in Australia (Sect. 5.1.2) led to extreme air pollution and low visibility. However, even during days with a visibility of less than 5 km, the intensity of UV radiation may have still been harmful to human health. For example, on 10 December 2019, the visibility near Sydney, Australia, dropped to about 1 km around noon. Despite this low visibility, the cumulative erythemal UV dose measured at this location over a one-hour period at noon was still more than 4 SED[35] or about 46% of the one-hour dose measured on the cloud and haze-free day of 27 November 2019. During the eight hours between early morning and late afternoon the dose on 10 December 2019 was 17 SED. The corresponding dose of 27 November was 48 SED [180]. These UV doses far exceed the maximum daily UV dose recommended by ICNIRP for outdoor workers [181]. While most people stayed indoors during the fires because the air pollution was so extreme, emergency workers, who had to be outside despite adverse conditions, may have been exposed to UV radiation levels harmful to human health, potentially without being aware of it and without applying appropriate sun protection measures.

Despite increases of aerosols in specific regions (e.g., from bushfires, burning of biomass or dust storms), over most populated areas of the globe, there is a general decrease in aerosols. Trends of aerosol optical and chemical properties on global and regional scales have been reported from observations with several ground-based networks [182]. Most of the properties related to loading of aerosols exhibit negative trends in the period 2000–2014 in regions covered by observations, both at the surface and in the total atmospheric column. Significant decreases in AOD were found in areas with intense anthropogenic activity (Europe, North America, South America, North Africa and Asia), ranging from −1.2% per year to −3.1% per year. These data were used to validate various aerosol models (six AeroCom[36] phase III models, four CMIP6 models and the CAMS[37] reanalysis dataset) showing good agreement in the AOD trends. When these models were used to estimate the global AOD trend by filling the gaps in regions not covered by observations, a global increase in AOD of about 0.2% per year between 2000 and 2014 was found, primarily caused by an increase in the loads of organic aerosols, sulphate, and black carbon. These findings highlight differences between regional and global effects of aerosols on UV radiation, which must be considered, especially when projecting into the future.

In a modelling study [183] exploring China's future anthropogenic emission pathways, it was projected that emissions of major air pollutants (i.e., SO_2, NOx, $PM_{2.5}$ aerosols, and non-methane volatile organic compounds) in China will be lower by 34–66% in 2030 and by 58–87% in 2050 compared to 2015. These estimates were derived by considering a combination of strong low-carbon and air pollution control policies. A second study [184] investigated the evolution of different types of aerosols over the Euro-Mediterranean region between 1971–2000 and 2021–2050 according to three different scenarios representing a wide range of possible future pathways. The study showed a decrease in AOD of between 30% and 40% over Europe, mainly from decreasing emissions of sulphur dioxide. However, these reductions are partly (~30%) compensated by increases in the optical depth from nitrate and ammonium particles.

Attenuation of UV radiation by aerosols can sometimes also mask the effect of "ozone mini-holes" (defined as a synoptic-scale[38] region with strongly decreased TCO resulting from dynamical processes [185]) that would otherwise lead to increases in UV radiation. One example is an event that occurred in Athens, Greece, during 8 days in May 2020 [186]. On 15 May 2020, TCO was 43 DU (or more than 2 standard deviations) below the climatological mean, which would have normally led to an increase in the UVI by ~29%. However, the AOD on this day was 0.31 (47%) higher than the climatological mean due to the intrusion of Saharan dust, and measured UVIs agreed to within ~2% with the climatological mean. Hence the opposing effects of low TCO and high AOD nearly cancelled each other. This study highlights the important role of aerosols in modifying the effects of changes in TCO on surface UV-B radiation. There is some evidence that the weather pattern that led to the transport of dust from Africa towards Athens was also responsible for the occurrence of the ozone mini-hole and the low TCO over Athens that ensued.

6.2   Surface reflectivity

Changes in the reflectivity of the Earth's surface (both land and ocean) can change the downwelling UV radiation because radiation that is reflected upward by the surface may subsequently be scattered downward by air molecules, aerosols, and cloud droplets. Topography can modify the reflectivity resulting in complex effects on UV radiation, as for example in narrow valleys with snow covered slopes. The largest effect of surface reflectivity occurs in areas with variable snow and ice cover because of the large difference in the albedo of bare and snow/ice covered ground. This variability is often linked to climate change. For example, because of the warming of the Arctic, the start date of the spring snow melt at Ny-Ålesund (79° N), Svalbard, has advanced by three days per decade over the last 40 years [187], so now begins about two weeks earlier than in the early 1980s.

Figure 6 illustrates the effect of surface albedo on UV radiation by comparing UV irradiance in the 337.5–342.5 nm range measured at Arrival Heights (78° S), Antarctica, with the extent of land-fast ice—defined as sea ice fixed in place by attachment to land, glaciers, grounded icebergs, or ice shelves—covering McMurdo Sound 1 km west of Arrival Heights. In 2000, a mega-iceberg calved from the

---

[35] The standard erythemal dose (SED) is a measure of cumulative erythemal UV radiation [177]. One SED is equivalent to an erythemally effective radiant exposure of 100 J m⁻². Two SED may lead to erythema in individuals with freckled pale skin (Skin Type I, defined by the Fitzpatrick scale [178]). Longer exposure times are required for individuals with darker skin [179].

[36] Aerosol Comparisons between Observations and Models (https://aerocom.met.no/)

[37] Copernicus Atmosphere Monitoring Service (https://atmosphere.copernicus.eu/)

[38] In meteorology, synoptic scale refers to a high- or low-pressure area with a horizontal length scale of the order of 1000 km or more.

Ross Ice Shelf, became temporarily trapped, and persisted in the entrance to McMurdo Sound for five years [188]. The tabular iceberg interrupted the normal movement of sea ice, resulting in McMurdo Sound remaining covered by ice with high albedo until April in some years [189]. As a consequence, UV irradiance was elevated in March between 2001 and 2007 when the ice edge was more than 13 km away from McMurdo, while less UV radiation was observed between 2011 and 2015 when McMurdo Sound was free from land-fast ice [190]. Since similar data are not available before 2000 and after 2016, sea ice cannot be correlated with UV radiation over a longer time period at this location. However, Kim et al. [189] reported that the dates of the retreat of land-fast ice in McMurdo Sound have not changed over the last 37 years except for years affected by mega-icebergs.
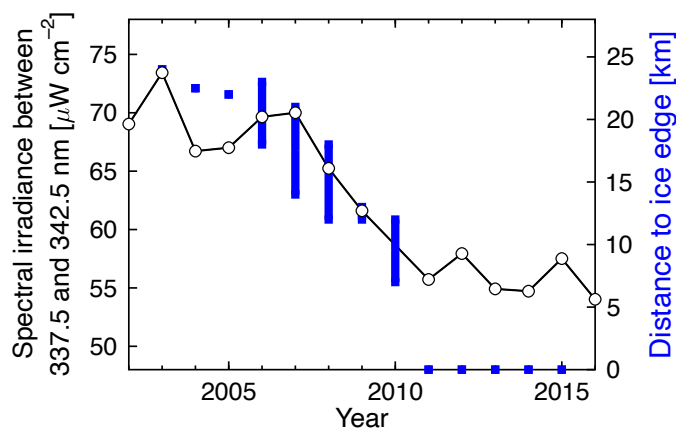
Fig. 6 Comparison of monthly mean spectral irradiance between 337.5 and 342.5 nm for March (left axis) at Arrival Heights, Antarctica, and approximate distance of the outer edge of the land-fast ice from Arrival Heights (right axis) during March. Distance data are based on Fig. 3 of Kim et al. [189]. The vertical extension of the blue bars indicates the variability of the distance within the month of March. A distance of zero km from the ice edge means that McMurdo Sound, 1 km west of Arrival Heights, was free of ice. In years when the ice edge was far from the station and the ocean surrounding the station was covered by sea ice, the albedo was greatly enhanced and UV radiation in these years tended to be higher compared to years when McMurdo Sound adjacent to the station was free of ice. Adapted from Bernhard and Stierle [190].

6.3   Solar activity

Variability in the solar activity can indirectly affect UV radiation at the Earth's surface through changes induced in atmospheric ozone, particularly in the stratosphere. These changes in ozone are caused by two different mechanisms, which are both related to the 11-year variability of solar activity. One mechanism is mediated through photochemical processes in the upper atmosphere that are modified by changes in solar UV-C (100–280 nm) radiation. The other process is driven by changes in the rate of energetic particle[39] precipitation (EPP), which mainly affect ozone over the polar regions [191,192].

The increase in emissions of solar UV-C radiation between the minimum and maximum of the solar cycle leads to increases in ozone concentrations in the upper stratosphere (altitude of 30–60 km) and decreases in the lower stratosphere (15–30 km), mainly at lower latitudes [193]. Using a CCM, Xiao et al. [194] estimated that for a 5% (10%) increase in solar output in the spectral range of 200–370 nm, the globally averaged ozone increases by up to 4.5% (9.0%) in the upper stratosphere, and decreases by up to 1.5% (3.3%) in the lower stratosphere. It was further noticed that the response of ozone to the variability of UV-C radiation during a solar cycle is non-linear, confirming earlier results [195].

Our previous assessment [9] discussed the effects of reduced solar activity in the future (e.g., from a Grand Solar Minimum[40]) on UV-B radiation received at the Earth's surface. Based on the work by Arsenovic et al. [196], we concluded that UV-B radiation at the top of the atmosphere would decrease slightly due to weaker emission from the Sun; however, the reduced solar activity would also lead to decreases of ozone production in the stratosphere, resulting in an overall increase of UV-B radiation at the surface. This conclusion is still valid.

Solar activity has recently shown a declining tendency, suggesting that the Sun has entered into a modern Grand Solar Minimum period, from about 2020 to 2053, which would lead to a significant reduction of the solar magnetic field and magnetic activity by about 70%, similar to the Maunder minimum that occurred in the period 1645–1710 [197]. The influence of such reductions in total solar irradiance (TSI[41]) on surface temperatures was investigated using a climate model run under the RCP 8.5 scenario, which predicted a decrease in the global average temperature for the second half of the 21st century of 0.13 °C due to atmospheric effects of the upcoming Grand Solar Minimum [198]. Simulations by Arsenovic et al. [196], which were based on the RCP 4.5 GHG scenario, estimated that a stronger

---

[39] Energetic particles considered here are highly energetic electrons, protons, neutrons, and ions that are accelerated into the atmosphere through various heliophysical and geomagnetic processes. They enter the atmosphere mainly in the geomagnetic polar regions (https://lasp.colorado.edu/home/mag/research/energetic-particle-precipitation).

[40] Grand solar minima are defined as periods when several solar cycles exhibit lesser than average activity for decades or centuries.

[41] Total Solar Irradiance (TSI) is the solar radiative power per area integrated over all wavelengths that is incident on the Earth's upper atmosphere.

solar minimum with reduction in TSI of 0.48% would only compensate for about 15% of GHG-induced warming by 2100. Hence, the estimated decreases in temperature by 2100 due to reduced solar activity are small compared to the projected increases due to GHG emissions. Therefore, the reduction of solar irradiance during a possible Grand Solar Minimum would only partly offset the anthropogenic change in climate caused by continuing GHG emissions.

The upcoming maximum of Solar Cycle 25 is expected to be weaker than the current Cycle 24, which was the weakest in at least the past 100 years [199,200]; however, the uncertainty of this prediction is large. Model results [199] estimated a deep extended solar activity minimum for 2019–2021, and a weak solar activity maximum in 2024–2025. This modelling study is based on analysis of magnetograms that contain information on the evolution of magnetic fields on the solar surface, allowing forecasting of the solar activity in the future. The reduced activity in the period of the solar maximum will lead to less photochemical production of stratospheric ozone at low latitudes, but also to reduced polar ozone destruction due to fewer energetic particles.

Although none of the studies discussed above addressed effects on surface UV-B radiation, the upcoming weaker solar activity period would lead to decreases in stratospheric ozone and consequently to increases in UV-B radiation at the surface, despite the reduced solar irradiance entering the Earth's atmosphere. This effect has not been considered in the projections of UV radiation described in Sect. 8.

6.4   Volcanic eruptions

Throughout the Earth's history, major volcanic eruptions or impacts of meteors have perturbed the climate, affected the stratosphere, and caused regional and global environmental disasters. Global effects are mainly caused by the reflection of incoming solar radiation by the aerosol layer that forms in the stratosphere after a large volcanic eruption, but also by the destruction of stratospheric ozone involving heterogeneous chemical reactions on the surfaces of volcanic aerosols in the presence of halogens [201-203]. Volcanic aerosols are dispersed zonally to other latitudes and can persist for several years, resulting in cooling of the troposphere. Such eruptions can either reduce solar UV-B irradiance at the Earth's surface through scattering of radiation back to space or increase it through reduced absorption by the depleted ozone layer. The magnitude of these effects depends on the strength of the eruption and on the amounts of aerosols and halogenated compounds involved. Large tropical volcanos in the last ~200 years, e.g., Mt. Pinatubo in 1991 and Mt. Tambora in 1815, have caused globally averaged cooling of 0.3 and 0.7 °C at the Earth's surface, respectively [204]. Conversely, stratospheric aerosols from Mt. Pinatubo warmed the lower tropical stratosphere by up to 4 °C in the 2 to 3 years following the eruption [205].

Recent studies used chemistry-climate models to investigate the effects of different amounts of SO_2 and halogens injected into the tropical stratosphere by volcanic eruptions [204,206,207]. Brenna et al. [206] assumed an explosive eruption at 14° N, rich in sulphur, chlorine, and bromine compounds, occurring during preindustrial times. The assumed amount of SO_2 injected represents the average of 28 historical volcanic eruptions in the Central American Volcanic Arc (CAVA; extending parallel to the Pacific coastline from Mexico to Panama), comparable in magnitude with the Mt. Pinatubo eruption. However, the amount of bromine and chlorine deposited in the stratosphere was assumed to be much larger than the amount estimated for Mt. Pinatubo. (The Mt. Pinatubo eruption was unusual because it occurred at a time when the Philippines were also inundated by a typhoon. Water droplets from the storm likely adsorbed halogen compounds in the plume and prevented them from reaching the stratosphere [208,209].) The ozone depletion calculated by Brenna et al. [206] led to increases in the clear-sky summertime UVI of more than 50% in the NH during the first two years after the eruption. Maximum increases in the UVI were modelled to exceed 7 units in the NH tropics and subtropics, and peak at 4 units in the NH mid-latitudes. Much of the mid-latitudes would have experienced a UVI above 15, which is similar to present-day peak values in the tropics [210]. This simulation was based on the injection of large amounts of halogens, which are thought to be representative for volcanic eruptions in the CAVA. Simulated increases in UV radiation are therefore much larger than those observed after the eruption of Mt. Pinatubo.

Another modelling study [204] investigated the effect on the atmosphere of the eruption of a super volcano like Toba, which erupted 74,000 years ago. It has been estimated that Toba injected 100 times more SO_2 into the stratosphere than Mt. Pinatubo. According to this study[42], such an event could lead to the collapse of the ozone layer in the tropics with ~50% reduction in TCO, which would increase the daily maximum UVI by more than a factor of two. Even with one fifth of the injected SO_2 amount, ozone depletion in the tropics would be similar to that currently occurring in Antarctica and would last for nearly a year.

These studies show that massive but rare volcanic eruptions can lead to severe depletion of stratospheric ozone, changes in atmospheric circulation and temperature patterns, and large increases in UV-B radiation at the Earth's surface.

These increases can by far exceed those associated with ozone depletion from ODSs in the 1980s and 1990s as well as the expected rise in UV B radiation to more natural levels over urban regions that may occur when measures to reduce air pollution are implemented

---

[42] The study did not include the chemical impact of halogen compounds, as there is no reliable information on their emissions from Toba. The modelled effect on ozone mainly occurs because absorption by SO_2 and scattering by the aerosol layer reduces the flux of solar UV C radiation reaching the lower stratosphere. Solar UV-C radiation with wavelengths shorter than 242 nm initiates the formation of ozone in the stratosphere because it leads to the photolysis of oxygen molecules (O_2). The resulting oxygen atoms react with O_2 to form ozone (O_3). Less UV-C flux below the aerosol layer therefore leads to less ozone production. If ozone loss by halogen compounds had been included also, the modelled ozone decline and increase in UV-B radiation at the Earth's surface would have been even larger.

(Sect. 6.1).

6.5   Climate change

In the absence of changes in the TCO, climate-change-induced trends in the properties of clouds, atmospheric aerosols and surface albedo have the potential to strongly influence the long-term behaviour of UV radiation at the Earth's surface.

The optical properties of clouds, aerosols, and surface albedo, and the interactions between these components, are active areas of research because of their importance in the radiative balance at the surface. Global warming is expected to influence cloudiness because of the atmosphere's ability to hold more water as temperatures increase [211]. However, patterns of change in cloud cover, height, and optical depth are difficult to assess because of the inherent internal variability in regional climate forcing combined with the short length of available climate data records. The physical understanding of cloud processes continues to advance. For example, the better understanding of the microphysics of supercooled liquid water has reduced the bias in the modelled short-wave cloud radiative effect over the Southern Ocean [212]. Climate models also continue to improve in their representation of aerosols, which cool the lower troposphere and counter some of the warming resulting from GHGs [63]. Reductions in air pollution have generally occurred in Europe and North America as the result of regulations; however, economic growth has caused large regional increases in aerosol emissions in Asia and Africa [213]. Interactions between aerosols and clouds remain the largest uncertainty in climate projections. Changing patterns of coverage of the surface with snow, ice, and vegetation under global warming are also relevant to surface UV irradiance, with observed darkening of the Arctic surface over 2000–2019 attributed to summertime loss of sea ice, while mixed trends in albedo have occurred over this period in Antarctica [214] (see also Sect. 6.2).

The complexity in accurately accounting for all relevant processes, particularly on small scales where observations are influenced by local effects (e.g., UV enhancement under broken clouds), limits the ability to attribute trends in UV irradiance to specific climate change effects. However, several recent studies have quantified local-scale influences, with examples provided below.

The occurrence of cloud-free conditions is very important for total UV exposure. Atmospheric blocking systems, which are large-scale patterns of stationary atmospheric pressure fields that "block" or redirect migratory cyclones or anti-cyclones, can lead to prolonged periods of clear skies at mid and high latitudes. In a blocking event, a high-pressure weather system can persist for days or even weeks over some geographical regions, inhibiting cloud formation and causing moisture in the westerly zonal flow to be deflected around it. Hence, clouds are often more persistent than usual outside regions with high pressure resulting in lower UV irradiance at the Earth's surface. A recent example where surface UV radiation was exceptionally affected by atmospheric blocking occurred during May–July 2018 in Norway and Finland [215]. The monthly mean noontime UVI was 20–40% above the long-term mean as a direct result of decreased cloud cover. For example at Sodankylä (67° N), the mean temperature in July 2018 was 5.6 °C above the 1981–2010 average for the same month and the duration of sunshine in 2018 was 405 hours, exceeding the 1981–2010 average of 245 hours by 65%. This particular event was associated with a record heat-wave in central and northern Europe [216]. Recent studies examining trends and variability in atmospheric blocking at high latitudes have found mixed patterns of change, with regional shifts in trends in the Antarctic Peninsula region over the satellite era [217], and no significant trends over Greenland [218]. For high-emissions SSP scenarios, a clear decrease in future blocking over Greenland and the north Pacific was found, but seasonal and regional projections are generally unclear [219].

It has been known for decades that changes in tropopause height are inversely linked to changes in TCO [220,221]. If the tropopause is shifted up, some lower stratospheric ozone is horizontally transported to surrounding regions with lower tropopause height. The result is a decrease of TCO in areas where the tropopause is elevated [221]. Furthermore, mid-latitude regions with elevated tropopause may also be influenced by the advection of stratospheric ozone-poor air masses from lower latitudes (ozone mini-holes) [185,222].

In a new study, Fountoulakis et al. [223] quantified the effect of changes in the geopotential height (GPH) at 250 hPa (a quantity similar to tropopause height) on TCO and spectral irradiances at 307.5 and 324 nm at three locations across Italy: Aosta (46° N), Rome (42° N), and Lampedusa (36° N). Statistically significant anti-correlations were found between GPH and monthly anomalies in TCO for all locations and months. Conversely, positive correlations between GPH and monthly anomalies in spectral irradiance at 307.5 nm were detected for most months. The study makes a strong case that increases in GPH or tropopause height that are expected from the warming of the troposphere due to climate change [224,225] would reduce TCO and subsequently lead to increases in UV-B radiation.

Additional effects of climate change on TCO and the vertical distribution of ozone in the atmosphere—such as the expected strengthening of the Brewer-Dobson circulation, unexpected declines in lower stratospheric ozone in the extratropics [226], and the dependence of TCO on GHG scenarios (Sect. 3.5)—are discussed in great detail in SAP's latest report [11] and are therefore not addressed here.

7 Variability in UV radiation and trends from observations

This section assesses observed variations in UV radiation on various time scales as well as long-term trends in the UVI observed by ground-based and space-borne instruments over several decades.

7.1   Variations in UV radiation with time and altitude

Year-to-year and seasonal variability in UV radiation is mainly controlled by variations in the TCO, cloud cover, and aerosols. For example, TCO at mid-latitudes is higher in the spring and lower in the autumn. As a result, the UVI near the autumn equinox can exceed that at the spring equinox by nearly a factor of two for matching SZAs [227]. The effect from ozone is most pronounced at high latitudes of the Southern Hemisphere during spring but variability in stratospheric ozone in the Arctic has also led to larger variability in UV radiation at northern high latitudes in recent years during the late winter and early spring season. Both regions are discussed in the following sections.

7.1.1   Temporal variations of UV radiation in Antarctica

We reported in our previous assessment [9] that the variability of UV-B radiation in Antarctica observed between 2014 and 2017 was very large, with near record-high UVIs observed at the South Pole in spring 2015, and well below average values in spring 2016. Variability during the period discussed in this report (2018–2021) was equally large, despite evidence that stratospheric ozone concentrations over Antarctica are now recovering (Sect. 3.2).

Figure 7 shows the daily maximum UVI observed at three Antarctic stations (South Pole (90° S), Arrival Heights (78° S), and Palmer (65° S)) for September–December, the months most affected by the ozone hole. Observations in 2018, 2019, 2020, and 2021 were compared with the average and range of measurements between ~1990 and 2017. UVIs in October 2018 were well above the long-term mean and approached historical maxima at the South Pole but remained within the range of typical variability at the other two sites. Conversely, unusually low UVIs were observed at the South Pole and Arrival Heights in spring 2019 due to a record high TCO during this period. Between October and mid-November 2019, the UVI at the South Pole was at the minimum of the historical (1991–2017) range and remained close to this minimum between mid-November 2019 and January 2020. At Arrival Heights, the UVI in 2019 was close to the minimum between September and mid-November, and stayed below the long-term mean until mid-December, except for two short periods.

In contrast to 2019, near record-high UVI maxima were observed in spring 2020 and 2021 because of large and persistent Antarctic ozone holes in these years (Sect. 3.2). In both years, the UVI at the South Pole tracked or exceeded the historical range between September and mid-November and set new records in mid-November and mid-December 2020. On 21 November 2020, the maximum UVI measured on this day exceeded the average of the daily maxima for 21 November, calculated from measurements of the years 1991–2017, by 83%. At Arrival Heights, the UVI reached a new all-time site record of 7.8 on 23 December 2020, exceeding the previous record for this day by nearly 50%. Measurements at Palmer Station were highly variable, as is typical for this site, but new records were also set at this site in the second half of November 2020 when the centre of the ozone hole was above the station. High UV radiation at this time, which coincides with the start of the growing season for plants and the peak breeding season for most animals, is a concern [3].

The record-high UVIs in 2020 were not only confined to the three stations shown in Fig. 7 but also observed at other Antarctic research stations. At the Australian Antarctic bases Casey (66° S), Mawson (68° S), and Davis (69° S), UVIs measured with broadband radiometers between October and December 2020 were generally well above the 2007–2019 climatological mean, with new record-high values set on several days in November and December [31]. The number of days when TCO dropped below 220 DU and led to spikes in UVI was the highest ever observed at the three sites. The daily maximum UVI at Marambio, a station located near the Antarctic Peninsula at 64° S, exceeded 12 on several days in late November and early December 2020 [20]. Similarly, extreme UVI values were measured at King George Island (62° S), near the northern tip of the Antarctic Peninsula [34]. The UVI exceeded 11 on four days between 24 November and 4 December 2020 and peaked at 14.3 on 2 December. This value ties, within the measurement uncertainty, with the highest value of 14.2 (recorded on 4 December 1998) ever measured at Palmer Station ([230] and Sect. 7.3). On 3 December 2020, the erythemal daily dose at King George Island was 8.1 kJ/m^2, which is among the highest on Earth and only comparable to those recorded at high altitude sites such as the Atacama Desert, Chile [231], or at Mauna Loa, Hawaii, where the highest dose ever observed was 9.5 kJ/m^2 [232]. These extreme levels of UV radiation were a result of solar elevations close to their annual maximum; close to 24 hours of daylight at King George Island; broken clouds, which can enhance radiation levels at the surface beyond the clear-sky level when the solar disk is free of clouds and additional radiation is scattered by clouds to the observer; and low TCO. For example, on 1 December 2020 the TCO over King George Island was 180 DU, which is the lowest value ever recorded for December at this site [34]. UVI data for 2021 from stations other than those shown in Fig. 7 are not yet available.
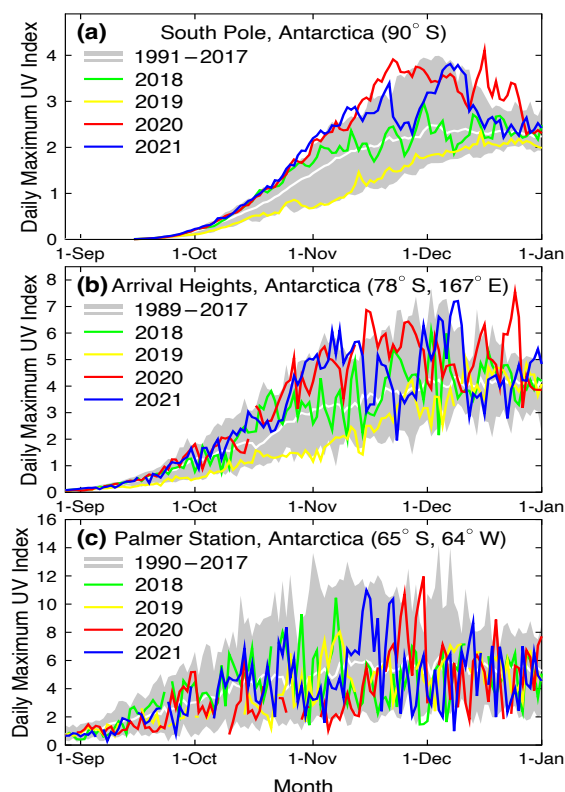
Fig. 7 Daily maximum UVI measured at (a) the South Pole, (b) Arrival Heights, and (c) Palmer Station in 2018 (green), 2019 (yellow), 2020 (red), and 2021 (blue) compared with the average (white line) and the range (grey shading) of daily maximum observations of the years indicated in the legends. The UVI was calculated from spectra measured by SUV-100 spectroradiometers. Up to 2009, the instruments were part of the NSF UV Monitoring Network [228] and they are now a node in the NOAA Antarctic UV Monitoring Network (https://gml.noaa.gov/grad/antuv/). Consistent data processing methods were applied for all years [190,229].

The findings of the studies discussed above show that variability of springtime UV-B radiation in Antarctica is large despite ongoing reduction of ODSs and signs of ozone recovery. This surprisingly high variability is mainly driven by changes in meteorological conditions and in particular the persistently low temperature of the lower stratosphere.

When the Antarctic polar vortex breaks up at the end of the austral spring, ozone-depleted air masses disperse to lower latitudes, which may lead to large increases in UV radiation over populated areas in the Southern Hemisphere [233]. However, a recent study found that the breakup of the polar vortex had only a small effect on UV radiation at Cape Town, South Africa (34° S). Elevated levels of UV radiation at this location were more frequently associated with low-ozone air masses of tropical origin [234].

7.1.2 Temporal variations of UV radiation in the Arctic

As discussed in Sect. 3.3, an exceptionally large episode of stratospheric ozone depletion was observed in late winter and early spring (February–April) of 2020 in the Arctic [35,36,39,41]. Figure 8a shows deviations of monthly average TCO from past (2005–2019) averages north of 45° N for March, April, May, and June, and their effects on UVI. In March 2020, relative TCO anomalies of up to −40% and exceeding 3 standard deviations (σ) were measured over northern Canada and the adjacent Arctic Ocean. In April, relative TCO anomalies of up to −35% and exceeding 3σ were observed for virtually all areas north of 60° N. During the breakup of the polar vortex in May [35], areas with abnormally low (> 3σ) TCO still persisted over Siberia.

The low TCO led to record-breaking anomalies in solar UV-B radiation over the Arctic measured by ground-based instruments at ten Arctic and subarctic locations and observed by the Ozone Monitoring Instrument (OMI) on NASA's Aura satellite [235,236]. Relative UV-B radiation anomalies were particularly large between early March and mid-April 2020. However, absolute anomalies for this period remained small (e.g., below 0.6 UVI units) because solar elevations for March and April are still low in the Arctic. In the following, we only discuss relative anomalies.

In March 2020, the monthly average UVI over the Canadian Arctic and the adjacent Arctic Ocean was between 30% and 70% higher than the historical (2005–2019) averages, often exceeding the climatological average by 3σ. By April 2020, they were positive over a vast area, including northern Canada, Greenland, northern Europe, and Siberia. The maximum anomaly was 78% and anomalies exceeded 3σ almost everywhere north of 70° N. In May 2020, UVI anomalies of up to 60% and exceeding 3σ were measured over Siberia. The UVIs in June were elevated by up to 30% over parts of Norway, Sweden, and Finland, resulting from a combination of negative TCO anomalies and unusually fair weather with several cloudless days [236]. Ground-based measurements generally confirm UVI anomalies derived from satellite data (Fig. 8c). However, notable differences between the ground-based and satellite data sets exist for Sodankylä (Finland), and Trondheim and Finse (Norway) in May.

These discrepancies are likely caused by a mismatch between the albedo climatology used in the satellite retrieval and the actual albedo. Albedo in May is affected by the timing of snow melting, which was unusually late at Sodankylä and Finse in 2020.

In contrast to 2020, Arctic UVI anomalies in 2019 and 2021 remained within 2σ of the climatological mean, with few exceptions [46,47]. One exception is the large UVI anomalies of up to 65% in the period 15–30 April 2019 in Norway, Sweden, and Finland, when a persistent high-pressure system with clear skies was centred over the Nordic countries. As the TCO in the Arctic is projected to have large year-to-year variability for the remainder of the 21st century (Sect. 3.5), large variations in UV radiation are likely to occur over the next decades.
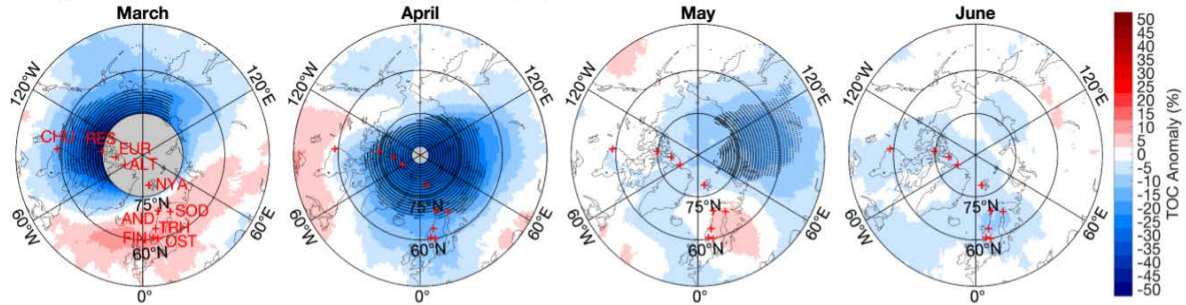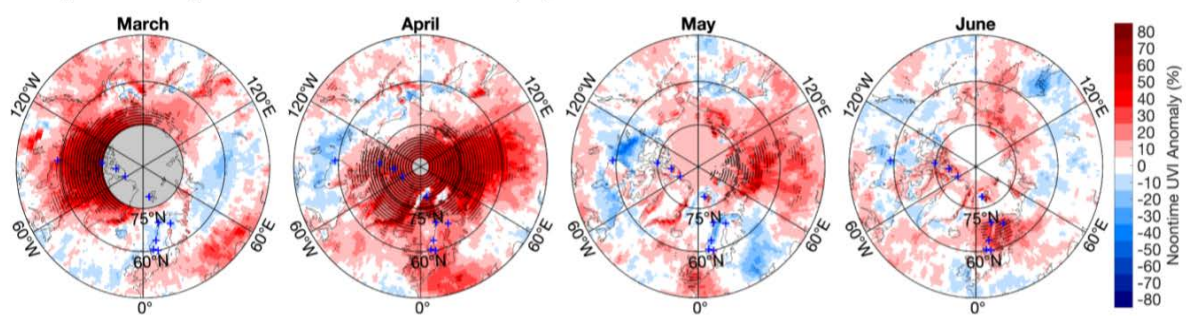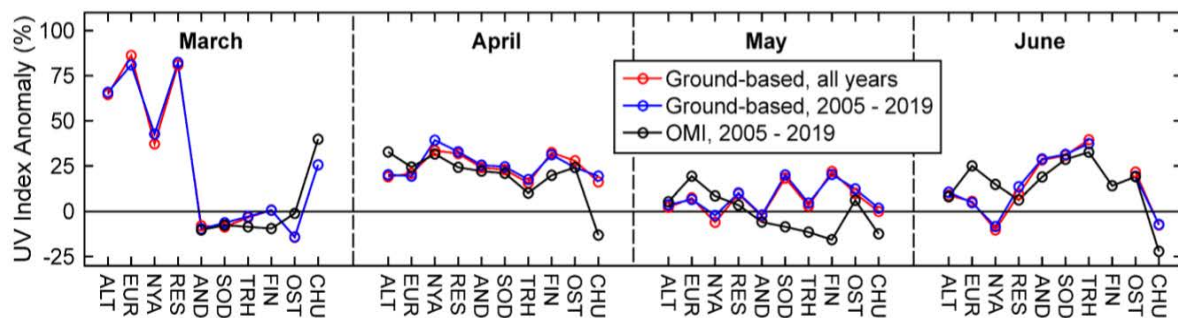
Fig. 8 Monthly mean anomaly maps (in %) of **(a)** TCO and **(b)** noontime UVI for March, April, May, and June 2020 relative to 2005–2019 means. Stippling indicates pixels where anomalies exceed three standard deviations (3σ). Grey-shaded areas centred at the North Pole in the maps for March and April indicate latitudes with no OMI data because of polar darkness. Locations of ground stations are indicated by crosses in every map, with labels added to the first panel. Maps are based on the OMTO3 Level 3 TCO product [237]. **(c)** Percentage anomalies in monthly means of the noontime UVI for 2020 derived from measurements at 10 ground stations (North to South along the x-axis) relative to all years with available data (red) and 2005–2019 (blue). The black datasets indicate anomalies for the same stations derived from OMI measurements relative to 2005–2019. Site acronyms are ALT: Alert (83° N); EUR: Eureka (80° N); NYA: Ny-Ålesund (79° N); RES: Resolute (75° N); AND: Andøya (69° N); SOD: Sodankylä (67° N); TRH: Trondheim (63° N); FIN: Finse (61° N); OST: Østerås (60° N); and CHU: Churchill (59° N). Figure adapted from Bernhard et al. [235].

7.1.3 Dependence of UV radiation on altitude

Measurements from satellites suggest that the highest UVI values observed during the year at the Earth's surface range from less than 3 at the poles to about 25 at high altitudes within the tropics of the Southern Hemisphere, such as the Altiplano Region of Peru and Bolivia [210]. The average altitude of this region is 3,750 m and the highest peak (Illimani) is at 6,438 m above sea level (asl). Ground-based measurements of UV radiation in this area are sparse despite their importance for human health and ecosystems. Recent measurements at Quito, Ecuador (2,850 m asl), established a maximum UVI of 21 at this location [238]. This value is consistent with the highest value of 21.2 measured at Mauna Loa (3,397 m asl) [232] and supports the maximum value of ~25 for the highest UVI that may occur on Earth considering that Quito is at a considerably lower elevation than the highest peaks of the Andes. The extreme UVI values at high-altitude locations close to the equator may have significant health effects for people moving to these regions for work or recreation without taking appropriate precautions to protect themselves from UV radiation [239].

7.2 Observed long-term changes in UV radiation

In the last four years, new trends in UV radiation derived from ground-based measurements have been published for several regions [190,223,238,240-245]. These studies confirm that changes in UV radiation during the last 25 years have generally been small—typically less than 4% per decade, increasing at some sites and decreasing at others, with few exceptions—consistent with the multi-site study by McKenzie et al. [56] discussed in Sect. 4.1. Results from these studies are assessed in more detail below. While only studies that appeared to be of high quality according to our assessment were included, the measurement uncertainty of the various datasets varies and the reader is referred to the original publications for details.

Trends in solar spectral irradiance at 307.5 nm, which is a reasonable proxy for trends in erythemally weighted UV radiation, were calculated at several stations in Europe, Canada, and Japan over a 25-year (1992–2016) period [240]. Long-term changes at this wavelength vary by location and are mostly driven by changes in aerosols and TCO. However, at high northern latitudes, changes in the surface reflectivity are also an important factor. Over Japan, the spectral irradiance at 307.5 nm has increased significantly by about 3% per decade over this 25-year period and this increase is attributed to a decrease in absorbing aerosols. The only European station with a significant trend was Thessaloniki, Greece, where spectral irradiance at 307.5 nm rose by 3.5% per decade with an increasing rate of change during the last decade, possibly because of decreasing absorption by aerosols.

Updated estimates of trends in UV-B irradiance at four European stations (Reading (51° N), Uccle (51° N), Sodankylä (67° N), and Thessaloniki (41° N)) have been reported for the period 1996–2017, i.e., starting after the global peak of ODSs [245]. The study concluded that the variability of UV-B radiation at these European sites was mainly governed by variations in clouds, aerosols, and surface reflectivity, while changes in TCO were less important. Statistically significant (95% confidence level (CL)) positive trends in noontime spectral irradiance at 307.5 nm were found for Thessaloniki (8% per decade) and Uccle (5% per decade), while, for Reading, the trend was negative (−7% per decade). These trends were again attributed to the effects of aerosols and clouds. No statistically significant trend was found at Sodankylä; however, the decreasing tendency of −5% per decade at this site was found to be consistent with changes in surface reflectivity due to declining snow cover in late winter and spring. In a follow-on study [223], a similar trend analysis was performed for Rome (42° N), Italy. A statistically significant negative trend in TCO of –1% per decade was found, but there was no corresponding significant increase in spectral irradiance at 307.5 nm over the period 1996–2020. However for certain months, positive trends in UV irradiance were observed, which were predominantly caused by changes in clouds and/or aerosols.

Several other studies reported estimates of trends for erythemal irradiance (or erythemal doses) at northern European sites. No statistically significant trends in erythemal UV radiation were observed at Moscow, Russia (56° N), over the period from 1999 to 2015 [243]; at Chilton, England (52° N), between 1991 and 2015 [246]; and at Tõravere, Estonia (58° N), between 2004 and 2016 [244]. At the last site, there were also no trends in the main factors influencing UV radiation, namely TCO; aerosol optical depth; and global short-wave radiation, which is a proxy for the effect of clouds.

Trends in erythemal irradiance at the Earth's surface over the period of 2005–2017 have been calculated for the continental United States using satellite-based (OMI) measurements and ground-based measurements at 31 sites distributed throughout the United States by the Department of Agriculture's UV-B Monitoring and Research Program [241]. The study concluded that trends in noontime erythemal irradiance estimated from these satellite- and ground-based measurements cannot be reconciled. Specifically, trends derived from the satellite-based dataset were not significant for most of the continental United States, except for a small region in the New England states of Maine, Vermont, New Hampshire, and Massachusetts. In those regions, small (about 5% per decade) positive trends were calculated from OMI data, and they were significant at the 95% CL. However, data from the two ground-based stations located in this region indicated a significant decrease in erythemal UV over the same period. This discrepancy can be explained, either by calibration issues of the ground-based sensors and OMI [247], or by increasing attenuation of UV radiation in the lowest part of the atmosphere, which cannot be adequately probed by OMI. While trends calculated for several other stations were also significant, the magnitude of these trends is generally within the measurement uncertainty range so that no firm conclusions about changes in levels of erythemal irradiance across the continental United States can be drawn.

In a similar study based on OMI measurements, trends in noontime erythemal irradiance, TCO, and cloud and haze transmission were calculated for 191 cities located between latitudes of 60° N and 60° S over the period 2005−2018 [248]. Significant changes in erythemal irradiance were found at the 95% CL for 40 of the 191 sites over this period. When data were averaged over 15° latitude bands, correlations between erythemal irradiance and short- and long-term changes in cloud and absorbing aerosols, as well as inverse correlations between UV radiation and TCO, became apparent. Estimates of changes in atmospheric transmission at 340 nm show

increases of 1.1±1.2% per decade between 60° S and 45° S, almost no change between 45° S and 20° N, decreases of 3% per decade at 22° and 32° N, an increase of 2.5% per decade near 25° N, and increases of 1±0.9% per decade from 35° N to 60° N. Changes in zonally averaged (~15° latitude bins) erythemal irradiance between 60° N and 60° S range between –4 and 5% per decade and are predominantly caused by changes in cloud and aerosol transmission. However, judging from the error bars in the figures provided by Herman et al. [248], changes in zonally averaged transmission and erythemal irradiance are generally not significant at the 95% CL.

Trends in erythemal daily doses (D_{ery}) were calculated for the period 1979–2015 over Northern Eurasia (a region between 40° and 80° N and extending in longitude from Scandinavia to Siberia) using simulations by a climate chemistry model (INM-RSHU[43]), re-analyses of atmospheric data (ERA-Interim[44]), and data from satellite measurements (TOMS/OMI) [242]. For cloud-free conditions, statistically significant increases in D_{ery} of up to 3% per decade were found for spring and summer over large areas and attributed to decreases in TCO. When clouds were included in the analysis, greater trends of 6–8% per decade were found over Eastern Europe and several regions in Siberia and Northeast Asia. This observation suggests that over this 36-year period, changes in cloud attenuation had larger effects on UV-B radiation than changes in TCO at high latitudes of the Northern Hemisphere extending to 80° N.

An analysis of UVI data computed from satellite-based measurements for local noon and clear skies by the Tropospheric Emission Monitoring Internet Service (TEMIS) indicated that there is no long-term trend in UVI at the equatorial high-altitude site of Quito, Ecuador (0° S, 2,850 m asl), for the period 1979–2018 [238]. This conclusion was corroborated by ground-based measurements at this site. For 2010–2014, the measured UVI was within the range of variability inferred for 1979–2009 from TEMIS data. This is consistent with the observation that there are no significant trends in TCO in the tropics (Sect. 3.1).

Trends in the UVI measured by spectroradiometers at three Antarctic sites (South Pole (90° S), Arrival Heights (78° S), and Palmer Station (65° S)) have recently been reassessed for the period of 1996–2018 [190]. At the South Pole (a site representative of the Antarctic Polar Plateau), significant (95% CL) decadal trends of −3.9% and −3.1% were calculated for January and February, respectively, which can mostly be explained by concomitant trends in TCO. At Arrival Heights, the recalculated trend for summer is −3.3% per decade and is significant at the 90% CL. This downward trend is caused by a significant upward trend in TCO of 1.5% per decade for January plus the effect of reductions in land-fast ice covering the sea adjacent to the instrument site (Sect. 6.2). No significant trends were reported for Palmer Station. The study provides further evidence that the UVI in Antarctica is starting to decrease during summer months. However, statistically significant reductions for spring (October and November), when the ozone hole leads to large UVI variability, were not detected.

All studies summarised above paint a consistent picture: changes in UV-B radiation outside the polar regions over the last 2–3 decades are mainly governed by variations in clouds, aerosols, and surface reflectivity (for snow- or ice-covered areas), while changes in TCO are less important. These results corroborate the conclusion by McKenzie et al. [56] discussed in Sect. 4.1 that changes in TCO have not led to significant changes in UV-B radiation over this period.

7.3   Reconstruction of historical changes in UV radiation

Systematic measurements of surface UV radiation suitable for trend analysis began only in the late 1980s. In the absence of direct measurements, knowledge of UV irradiance levels prior to the onset of ozone depletion relies on radiative transfer model calculations in combination with inputs such as TCO and other proxy data. At very few locations, ground-based TCO measurements commenced before the 1960s and UV irradiances have been reconstructed from these measurements [249-252]. The erythemal UV irradiance was recently reconstructed for Moscow, Russia, for the warm season (May–September) over the period 1968–2016 [253] using data of TCO, AOD at 550 nm, surface albedo, cloud cover, and cloud transmission. Results were validated against measurements of broadband instruments emulating the erythemal response of human skin (Sect. 10.1), which were available from 1999 onward. Reconstructed and measured data for the overlap period agreed well; the coefficient of determination R^2 was 0.89. Results indicate statistically significant decadal trends in erythemal UV irradiance of –11.6±1.6% for the period 1968–1978 and 5.1±1.9 for the period 1979–2016, which were predominantly driven by changes in cloud transmission. One important shortcoming of the study is that the consistency of cloud data of this 48-year data record was not independently verified; hence, trend estimates could be affected by spurious trends in the measures of cloudiness.

Daily erythemal UV doses were reconstructed for Novi Sad, Serbia [254]. Using a radiative transfer model with inputs of TCO and snow cover data, plus empirical relations between erythemal doses and sunshine duration, statistically significant increases in erythemal UV doses of 8.8% and 13.1% per decade over the period 1980–1997 were found for summer and winter, respectively, which were linked to the statistically significant decline in TCO over this period.

Satellite measurements of TCO became available in the late 1970s and have also been used for reconstructing the UVI at several ground stations under the assumption that changes in aerosol and clouds were small during this period [56]. These reconstructions imply that considerable increases in the summer UVI occurred between 1978 and 1990, ranging from about 5% at northern mid-latitudes, up to 10% at southern mid-latitudes, and up to 20% at the three Antarctic sites considered in this study.

Starting in 2010, the "Twenty Questions and Answers About the Ozone Layer" component of assessment reports prepared by the SAP

---

[43] INM-RSHU: Institute of Numerical Mathematics – Russian State Hydrometeorological University; ERA-Interim: European Centre for Medium-Range Weather Forecasts Re-Analysis; TOMS: Total Ozone Mapping Spectrometer.

[44] ERA-Interim is a global atmospheric reanalysis published by the European Centre for Medium-Range Weather Forecasts (ECMWF, https://www.ecmwf.int/) that is available from 1 January 1979 to 31 August 2019.

have included a plot comparing reconstructed UVIs at Palmer Station, Antarctica (64° S), for the pre-ozone-hole period 1978–1980 with UVIs measured between 1990 and 2006 [13,255,256]. This plot has recently been updated [230] and is reproduced in Fig. 9. The revised plot is similar to the legacy one but includes data up to 2020 and also compares recent measurements with reconstructed pre-ozone-hole UVIs for San Diego, California (32° N), and Barrow, Alaska (79° N). Furthermore, historical UVIs at the three sites have been calculated from TCO measurements by the Backscatter Ultraviolet (BUV) experiment on the Nimbus-4 satellite between 1970 and 1976. While trends in TCO were already negative in the 1970s over polar regions [67], analysis presented by Bernhard et al. [230] did not show clear evidence that the developing ozone hole affected Palmer Station before 1976. In contrast, the period 1978–1980 used for the legacy plot was already somewhat influenced by ozone depletion. The new results confirm the previous conclusion that the ozone hole led to large increases in the UVI at Palmer Station year-round, with the largest increases occurring during spring (between 15 September and 15 November). The maximum UVI at this site is now larger by a factor of 2.50±0.37 (±1σ) on average compared to the pre-ozone-hole period. During summer and autumn (21 December – 21 June), i.e., the seasons least affected by the ozone hole, UVI maxima measured between 1990 and 2020 exceed maxima estimated for years prior to 1976 by 20±13%. Measured and reconstructed pre-ozone depletion data for San Diego (a subtropical site), are almost indistinguishable: on average, the UVI has increased by 3±7% (±1σ) since the 1970s. This modest growth is consistent with the small change in TCO observed at subtropical latitudes (Sect. 3.1) and with the conclusion of McKenzie et al. [56] that maximum daily UVI values have remained essentially constant at mid-latitudes over the last ~20 years due to the phase-out of ODSs controlled by the Montreal Protocol. At the Arctic site of Barrow, the UVI increased by 18±15% (±1σ) since the 1970s. The largest spikes in the UVI of up to 40% relative to the 1970s were measured during spring in years with abnormally strong Arctic ozone depletion, such as 2011 [257]. We note that these reconstructions are subject to uncertainty because they assume that surface albedo and attenuation by clouds and aerosols have not changed over the last 50 years in this area. However, at Palmer and Barrow, the TCO is by far the most important factor in controlling the UVI, while changes in albedo at San Diego can be considered negligible. Note that changes in the UVI discussed here do not contradict the conclusion in Sect. 7.2 that long-term changes in UV-B radiation outside the polar regions have generally been small over the last 2–3 decades. Changes shown in Fig. 9 are by and large attributable to changes in TCO occurring in the 1970s and 1980s (Fig. 1).
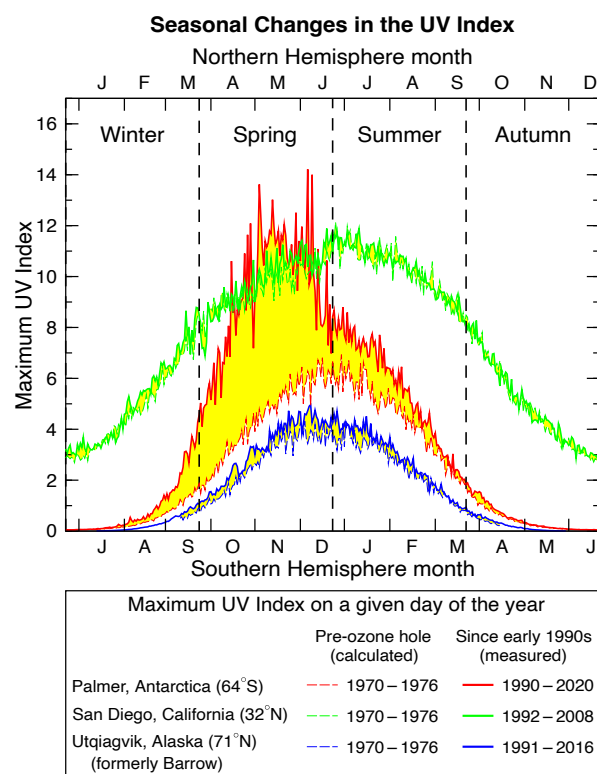
Fig. 9 Comparison of the highest UVIs ever measured for each day of the year at Palmer Station, San Diego, and Barrow since the early 1990s (solid lines) with reconstructed data for the pre-ozone-hole period 1970–1976 (broken lines). Yellow shading indicates the change between historical and contemporary UVI. The difference is particularly large for Palmer Station during spring, the period affected by the Antarctic ozone hole. The highest UVIs observed at Palmer since the 1990s exceed those measured at San Diego despite that city's much lower latitude. Reprinted from Bernhard et al. [230].

At Athens, Greece, records of the duration of sunshine were used to reconstruct monthly averages of short-wave (wavelength range ~300–3,000 nm) solar irradiance at the surface between 1900–2012 [258]. There were very small (0.02%) changes between 1900 and 1953, followed by a negative trend of 2% per decade during a "dimming" period of 1955–1980 and a positive trend of 1.5% per decade during a "brightening" period of 1980–2012. Measurements of short-wave irradiance at Potsdam (52°), Germany, show distinct dimming and brightening periods between 1947–1986 and 1986–2016, respectively, with measurements in 1986 about 10 W/m² lower compared to those at the start and end of the time series [259]. Changes for "all-sky" (cloudy and cloud-free) and clear-sky (cloud-free) conditions were similar, suggesting that changes in aerosols were mostly responsible for these variations in short-wave irradiance. While

these trend estimates are unrelated to changes in TCO and do not directly translate to changes in UV radiation, they qualitatively capture variations in the effect of clouds and aerosols on solar irradiance over the period studied, which are also relevant for changes in UV radiation. Trends in UV radiation related to changes in aerosols are likely larger than trends in short-wave irradiance because attenuation by aerosols is generally larger in the UV region than at visible wavelengths.

8 Projections of UV radiation

Projections of solar UV radiation at the Earth's surface for the 21st century have been reported in new studies published during the last four years. These new projections are generally in agreement with those reported in our last assessment [9]. They confirm the projected reductions in UV radiation, particularly at high and polar latitudes, due to the recovery of stratospheric ozone, as well as the increases in UV radiation due to decreasing concentrations of aerosols over regions with intense urban or industrial activities. Furthermore, projected decreases in surface reflectivity due to reduction in ice cover and decreases in cloudiness, both associated with climate change, are also important drivers leading to regional changes (decreases and increases, respectively) in surface UV radiation.

One of the new studies [260] reports global projections of UVI that were calculated with a radiative transfer model using TCO, temperature, and aerosol fields provided by 17 CCMs. These CCMs were included in the first phase of the Chemistry-Climate Model Initiative (CCMI-1) [58,261]. The CCM simulations were performed for four future GHG scenarios described by RCPs 2.6, 4.5, 6.0 and 8.5. Zonal-mean noontime UVI for cloudless skies were calculated for the period 1960–2100.

According to this study, noontime UVI in 2100 is projected to increase relative to calculations for the 1960s for RCPs 2.6, 4.5 and 6.0. These increases depend on latitude and the RCP scenario, and range between 1% (northern high latitudes for RCP 6.0) and 8% (northern mid-latitudes for RCP 2.6) as shown in Table 1. Trends calculated for the worst-case scenario RCP 8.5 show a different pattern with UVI projected to increase only in the tropics and to decrease elsewhere, with the largest decrease of 8% at northern high latitudes.

Only three of the 17 CCMs provided outputs of the AOD and its wavelength-dependence. The AOD used in projections of UV radiation is therefore based on the median of AODs derived from these three CCMs. According to these calculations, AODs are projected to decrease by almost 80% between 2000 and 2100 at northern high- and mid-latitudes, resulting in concomitant increases in the UVI of about 2% and 6%, respectively. These changes in UVI due to changes in AOD are of similar magnitude to those caused by changes in stratospheric ozone. However, these AOD estimates as well as the absorption properties of aerosols used in these CCMs are highly uncertain because future changes in atmospheric aerosols depend greatly on policy choices, such as measures to reduce air pollution [262]. Moreover, changes in optical depth and absorption properties of aerosols are highly dependent on region, hence zonal mean changes in UVI, like those discussed above, are not necessarily representative for most regions.

To address these concerns, Lamy et al. [260] also provide UVI projections for temporally invariant or "fixed" AODs based on a current climatology [263]. Using this climatology and the RCP 6.0 scenario, noontime UVIs in 2100 are projected to change relative to 1960 by −5% at Northern Hemisphere (NH) high latitudes, −2% at NH mid latitudes, +3% in the tropical belt, 0% at Southern Hemisphere (SH) mid-latitudes, and −2% at SH high latitudes (Table 1, column 6). These changes in UVI are mainly driven by changes in TCO. Assuming time-invariant aerosol amounts for the future, the clear-sky UVI is projected to decrease from 2015 to 2090 by 3% at NH and 6% at SH mid-latitudes. However, in regions that are currently affected by air pollution, the UVI is projected to increase if emissions of air pollutants are curtailed in the future.

Table 1 also shows a comparison of projected changes in zonal mean UVIs between 2015 and 2090 inferred from the study by Lamy et al. [260] and as published in our last assessment [9]. In both cases, UVI projections were based on results from the CCMI-1 initiative; however, different subsets of models were used, as well as methods to calculate the UVI from parameters provided by the CCMs. Furthermore, Bais et al. [9] provided projections for different months while Lamy et al. [260] only considered annual averages. Despite these differences, changes in UVI calculated by the two studies for fixed AODs are consistent (see last five columns of Table 1) and project a decrease of 2–5% for northern mid-latitudes, a decrease of 4–6% for southern mid-latitudes, and almost no change for the tropics. Both studies also predict large decreases in the UVI over southern high latitudes due to the expected healing of the stratospheric ozone hole.

Projections provided in the above studies were corroborated by another study where long-term changes in erythemal UV radiation were calculated over Eurasia (latitudes 40–80° N, longitudes 10° W–180° E) based on results of a CCM developed by the Russian State Hydrometeorological University (RSHU) [264]. These calculations considered only changes in TCO (i.e., excluding effects of aerosols and clouds) and predict that erythemal UV radiation levels in the years 2055–2059 will be lower over Eurasia by 4 to 8% relative to the reference period 1979–1983.

Table 1 Comparison of zonal-mean changes in clear-sky UVI calculated by Lamy et al. [260] and Bais et al. [9].

Latitudes	Lamy et al. [260] Change [%] 1960 to 2100[a]					Change [%] 2015 to 2090[b]		Bais et al. [9] Change [%] 2015 to 2090[c]			
	Transient AODs, RCP =				Fixed AODs	Transient AODs	Fixed AODs	Fixed AODs			
	2.6	4.5	6.0	8.5	RCP 6.0	RCP 6.0	RCP 6.0	RCP 6.0			
	Annual mean[e]							Jan	Apr	Jul	Oct
High N[d]	6	2	1	-8	-5	0	-6	-3	-7	-5	-4
30–60° N	8	5	5	-1	-2	5	-3	-4	-5	-3	-2
0–30° N[f]	3	3	3	1	3	-	1	-1	0	-1	-1
0–30° S[f]	3	3	3	2	3	0	0				
30–60° S	3	3	2	-2	0	-5	-6	-5	-4	-5	-6
High S[d]	7	6	4	0	-2	-18	-18	-8	-6	-6	-23

All values are rounded.

[a] According to Table 5 of Lamy et al. [260]

[b] Inferred from Fig. 4 and 6 of Lamy et al. [260]

[c] Table 1 of Bais et al. [9]

[d] Latitude range of "High N" and "High S" refer to 60–90° in Lamy et al. [260] and 60–80° in Bais et al. [9]

[e] Changes reported by Lamy et al. [260] refer to trends averaged over all months; Bais et al. [9] provide changes for the months of January, April, July, and October.

[f] Lamy et al. [260] report changes separately for 0–30° N and 0–30° S while Bais et al. [9] provide changes for 30° N to 30° S.

Simulations with one of the CCMs (EMAC[45]) for the period 1960–2100 were used to derive trends in DNA-damaging radiation at four mid-latitude locations and one tropical high-altitude site [265]. Weighting the spectral irradiance with the action spectrum for DNA-damage [266] yields dose rates that are more sensitive to changes in radiation at shorter (UV-B) wavelengths than the erythemal UV dose rates or the UVI; hence it is more sensitive to changes in TCO. DNA-damaging irradiance averaged over the five locations considered in this study is projected to increase by 1.3% per decade between 2050 and 2100. To isolate the effect of GHGs on climate, one simulation assumed increasing GHGs according to RCP 6.0 and the second adopted constant GHGs at 1960 levels. No trend in TCO was detected by the model after 2050, and the trend detected in DNA-damaging irradiance was attributed to a statistically significant (95% CL) decrease in cloud cover of 1.4% per decade resulting from increasing GHGs. The study suggests that changes in UV-B irradiance at low- and mid-latitudes during the second half of the 21st century will be dominated by factors other than changes in stratospheric ozone. However, these projections depend on the accuracy of simulating the cloud fields by climate models because uncertainties in the modelling of clouds propagate to the projected changes in solar UV-B radiation.

The SAP's latest assessment [11] also evaluates the effect of a fleet of commercial supersonic aircraft on stratospheric ozone concentrations. Such a fleet is currently being considered by different organisations and companies. Depending on scenario and flight altitudes, emissions of water vapour and nitrogen oxides from such a fleet could reduce TCO by up to 25 DU at high northern latitudes.

---

[45] EMAC CCM is the European Centre for Medium-Range Weather Forecasts–Hamburg (ECHAM)/Modular Earth Submodel System (MESSy) Atmospheric Chemistry Model.

Reductions in TCO at mid and low latitudes of the Northern Hemisphere would be considerably smaller, and the Southern Hemisphere is less affected because most flights take place in the Northern Hemisphere. While no study has quantified the effect of a future fleet of supersonic aircraft on UV radiation, the estimated decrease in TCO suggests that erythemal UV irradiance could increase by several percent at mid-latitudes of the Northern Hemisphere.

New model calculations examined the effect on stratospheric ozone (and by implication on UV radiation) of quadrupling concentrations of atmospheric CO_2 [267]. Such an increase would lead to a dynamically-driven decrease in concentrations of ozone in the tropical lower stratosphere, an increase of ozone in the lower stratosphere over the high latitudes, and a chemically-driven increase of ozone (via stratospheric cooling) throughout the upper stratosphere. In the tropics, opposite changes in ozone in the upper and lower stratosphere result in small changes in the TCO, and, in turn, to small changes in tropical UV-B radiation in the future, if effects from all other factors remain the same. A quadrupling of atmospheric CO_2 concentrations during the 21st century is currently not expected, but could occur in the 22nd century if emissions of CO_2 were to continue unabated according to the RCP 8.5 scenario [268]. The study suggests that even "worst-case" increases in CO_2 will not result in significant increases in UV-B radiation in the tropics.

All studies discussed above confirm the understanding of UV radiation in the 21st century established in our last assessment [9]. Simulations with a new generation of CCMs that have only recently been performed are expected to provide updated projections of UV radiation but are not yet available for assessment in this report.

A recent study used a state-of-the-art climate model with interactive chemistry [269] to calculate the effects on TCO and UV radiation resulting from a regional or global nuclear war. A global-scale nuclear war would cause a 15 year-long reduction in the TCO with a peak loss of 75% globally and 65% in the tropics. Initially, soot would shield the surface from UV-B radiation, but eventually the UVI would become extreme: greater than 35 in the tropics for 4 years, and greater than 45 during the summer in the southern polar regions for 3 years. For a regional nuclear war, global TCO could be reduced by 25% with recovery taking 12 years.

9 Implications of solar radiation management on UV radiation

Over the last decade, global warming from increasing GHGs has accelerated, and global mean air temperatures near the surface have risen by about 1.1 °C above pre-industrial levels [Chapter 2 of 63]. The resulting changes in climate observed worldwide have stimulated discussions on strategies to mitigate warming through artificially forced reduction of solar radiation entering the troposphere. Impacts of such solar radiation management (SRM) interventions on the atmosphere and the environment have been investigated in numerous modelling studies and discussed in current assessments by the SAP [11] and IPCC [Chapter 4 of 63], and the last EEAP assessment [9]. The latest SAP report [11] extensively addresses the potential impacts on TCO from stratospheric aerosol injection (SAI) under different scenarios. Here, we focus on the effects of the possible implementation of SAI on surface UV radiation. The effects are driven by changes in TCO but also by the redistribution of solar radiation from the direct to diffuse component, plus the global dimming effect expected from back-scattering of solar radiation to space by the aerosol layer.

The TCO is affected both by SAI-induced changes in heterogeneous chemical reactions, which depend on the surface area density of the aerosol (e.g., in $\mu m^2/cm^3$), and by changes in atmospheric dynamics (including transport, temperature, and water vapour changes). These effects on TCO differ with latitude and season, and depend on the future SAI scenario because they act in addition to the effects of decreasing ODSs and increasing GHGs. During the Antarctic ozone hole season, destruction of ozone in the stratosphere resulting from SAI would mainly be controlled by halogen chemistry on the surface of aerosols, while transport of ozone through circulation becomes important in other seasons [11].

Using models that participated in the Geoengineering Large ENSemble (GLENS) project, Tilmes et al. [270] estimated the effect on TCO in the latitude band 63°–90° S from SAI designed to achieve a reduction of 1.5 and 2.0 °C in global surface temperature. They found a reduction of up to 70 DU in the Antarctic TCO at the start of the SAI application (2020–2030), followed by an increase in TCO towards 2100 with a pattern like the projected changes in TCO without the application of SAI. In a more recent study, Tilmes et al. [271] estimated the initial abrupt decrease in TCO to be between 8% and 20% in 2030–2039 compared to 2010–2019, depending on injection strategy and model. All scenarios assumed in these studies result in a delayed recovery of Antarctic ozone to pre-ozone-hole levels by 20 to ~40 years. The TCO for these SAI scenarios remains below the levels projected by the worst case GHG scenario (SSP5-8.5) until the end of the 21st century, which would lead to increased levels of UV-B radiation during the entire period in Antarctica.

In a similar study, Tilmes et al. [272] estimated the effects of SAI also in the Northern Hemisphere and the tropics based on simulations of the G6 Geoengineering Model Intercomparison Project (GeoMIP). The models agree that sulphur injections result in a robust increase in TCO in winter at middle and high latitudes of the Northern Hemisphere of up to 20 DU over the 21st century compared to simulations based on the SSP5-8.5 scenario without SAI. This increase in TCO, which is linearly related to the increase in the amount of sulphur injections, is driven by the warming of the tropical lower stratosphere and would eventually result in decreasing UV-B radiation at these latitudes during the remainder of the 21st century. The magnitude of these changes in UV-B radiation depends on the SAI scenario. The

Arctic TCO is initially projected to decrease by 13 to 22 DU depending on the scenario, which is a much smaller decrease than that projected by Tilmes et al. [270] for the Antarctic discussed above. By the end of the 21st century, the Arctic TCO with and without SAI are approximately the same. Finally for the tropics, changes in ozone due to SAI would be small. The initial reduction in TCO projected by Tilmes et al. [270] and Tilmes et al. [272] for the Antarctic and Arctic is attributable to heterogeneous reactions on aerosol particles in the presence of ODSs. Robrecht et al. [273] showed that this effect is far less important for mid-latitudes and the tropics compared with polar regions.

While the above studies have focused on the consequences of SAI on ozone, effects on UV and visible radiation from SAI also depend on the attenuation (dimming) and redistribution of solar radiation. These effects have been quantified with a radiative transfer model using inputs from the GLENS project [271] designed to counteract warming from increased GHGs under the RCP 8.5 scenario [274]. Estimated changes in the UVI are predominantly driven by the attenuation of solar radiation by the artificial aerosol layer (with concentrations peaking above ~30 km in the tropics and above ~25 km in the high latitudes). Reduced direct radiation due to aerosol scattering results in substantial reductions in solar irradiance at the Earth's surface despite an enhanced contribution from diffuse radiation. However, the larger diffuse component may allow more efficient penetration of UV irradiance through forest and crop canopies [275], offsetting, to some extent, the reduced irradiance on top of the canopies. The intervention is estimated to reduce the daily average above-canopy UVI in 2080 relative to 2020 by about 15% at 30° N and by 6–22% at 70° N, depending on season. About one third of the reduced UVI at 30° N is due to the relative increase in TCO (~3.5%) between the reference and the SRM scenario. The corresponding increase in TCO for 70° N is less than 1% and explains only a very small fraction of the decrease in the UVI. The calculated changes in the UVI are therefore primarily caused by the scattering effect of sulphate aerosols, with a very small contribution from the absorption by sulphur dioxide (SO_2). Finally, reductions in photosynthetically active radiation (PAR) are estimated to range from 9% to 16% at 30° N and from 20% to 72% at 70° N, depending on season, with the largest proportional changes occurring in December, when the absolute levels of radiation are small. Such large changes in the UVI and PAR would likely have important consequences for ecosystem services and food security; however, such repercussions have not yet been quantified. While the study only characterised changes in UV radiation and PAR for the NH, similar results can be expected for the SH.

10 Advances in UV monitoring and modelling

In this section, we provide a summary of advances in measuring and modelling UV radiation at the Earth's surface and in assessing personal exposure to UV radiation, which is controlled both by ambient UV radiation and personal behaviour.

10.1   Ground-based systems

UV radiation at the Earth's surface is normally measured with scanning spectroradiometers, such as those installed in the Network for the Detection Atmospheric Composition Change (NDACC) [276]; broadband instruments, which typically emulate the erythemal response of human skin [277]; multi-filter instruments, which measure the spectral irradiance at several wavelengths (typically 4–7) in the UV range [278]; array spectroradiometers, which record the entire UV spectrum within seconds; dosimeters, which measure the UV dose that accumulates over a given amount of time; and specialised systems designed for a specific research question such as the measurement of the angular distribution of sky radiance [279]. The different instruments have been discussed in detail in previous assessments [9,162]. In brief, scanning spectroradiometers using double monochromators are the most accurate instruments but are expensive to acquire and maintain, and the recording of a UV spectrum may take several minutes. Broadband radiometers are relatively inexpensive, and their spectral response is tailored to a specific effect (e.g., erythema) under study, but because they do not provide spectral information, the factors driving changes in UV radiation (e.g., ozone, clouds, and aerosols) cannot be unambiguously separated. Multi-filter instruments can be used for studying a specific effect and the factors it depends upon, but require elaborate characterisations and calibrations in order to provide accurate data of solar irradiance [280]. Array spectroradiometers (or spectrographs) use single monochromators for physical reasons, and measurements at wavelengths shorter than 310 nm are often affected by stray light [281]. An instrument combining an array spectrometer with narrow-band filters that mitigate this problem has recently been introduced [282] and evaluated [283], indicating good performance at wavelengths longer than 305 nm. Finally, dosimeters are simple, low-cost, small devices that measure the UV dose electronically [284], chemically [285,286], or both [287], and are further discussed in Sect. 10.5.2. Their accuracy is typically less than that of high-end spectrometers [288]; however, they are frequently used for exposure studies (Sect. 10.5.2) where they can be easily attached, for example, to the forehead, wrist or clothing of test subjects.

The quality of measurements of UV radiation from these systems or sensors has historically been assessed with intercomparison campaigns where instruments are either compared with each other or a reference instrument. An example of the latter is a campaign with 75 participating broadband radiometers with erythemal response [277]. The instruments' solar measurements were first compared with data from the QASUME (Quality Assurance of Spectral Ultraviolet Measurements in Europe) reference spectroradiometer

[289]. The QASUME instrument has been used since 2002 to assess the quality of UV radiation measurements from more than 250 spectroradiometers at more than 40 stations worldwide (https://www.pmodwrc.ch/en/world-radiation-center-2/wcc-uv/qasume-site-audits/). New calibrations were subsequently transferred from QASUME to the 75 broadband radiometers. Furthermore, the angular and spectral response of the instruments was measured and functions for correcting deviations from the ideal response were established. With their original calibration applied, measurements of 32 (43%) of the 75 instruments agreed to within ±5% with measurements of the reference spectroradiometer while 48 (64%) agreed to within ±10%. Twenty-seven (35%) datasets deviated by more than ±10% from the reference and two datasets differed by 70%. After instruments were recalibrated, 73 (97%) of the 75 instruments agreed to within ±5% with the reference. This example demonstrates that proper quality control, quality assurance, and calibration procedures are vital for obtaining accurate measurements of UV radiation. A similar intercomparison involving four broadband radiometers and a reference spectroradiometer was conducted between March 2018 and February 2019 at Saint-Denis, La Réunion (21° S) [290]. Data from three of the four instruments agreed to within ±3% with the reference while data from one instrument exhibited a systematic error of 14%.

Even high-end spectroradiometers require meticulous characterisation and calibration for obtaining measurements with low uncertainty [291]. Finally, the development of a rigorous uncertainty budget (i.e., the calculation, tallying and combination of all uncertainty components) is a demanding task [292], but is necessary for obtaining high quality data.

10.2   Modelling of UV radiation

The transfer of radiation through the Earth's atmosphere is affected by absorption and scattering by gases, aerosols, and clouds; the reflection of radiation by the Earth's surface; and several other factors (Sect. 6). These factors are taken into account in computer simulations of UV radiation by radiative transfer models. Physically correct radiative transfer codes for modelling the UV radiation at the Earth's surface have been available for many years [e.g., 293,294-297] and can be considered reliable and mature. Most models assume that the atmosphere is homogeneous in both horizontal directions and only varies in the vertical direction, but newer models (e.g., [298,299]) that are based on the Monte Carlo technique [300] can also account for the three-dimensional structure of the atmosphere, topography, surface condition (e.g., patchy snow) or illumination geometry (e.g., the inhomogeneous irradiation during a solar eclipse). The greatest challenge in radiative transfer calculations is not the physical description of the transfer of radiation through the atmosphere but the specification of the input parameters that interact with radiation and are often not completely known, such as the single scattering albedo (SSA) of aerosols in the UV-B range or the structure of clouds.

One source of uncertainty in determining the UV radiation at the Earth's surface with models is the uncertainty of the solar spectrum outside the Earth's atmosphere. The extraterrestrial solar spectra (ETS) used in legacy model implementations sometimes differed by several percent at certain wavelengths [301,302]. These surprisingly large discrepancies for a fundamental quantity such as the ETS can be explained by the difficulty in measuring this spectrum. In one method, several solar spectra are observed at the Earth's surface at different path lengths of the direct solar beam through the atmosphere. These measurements are then extrapolated using the Langley technique [303] to a path length of zero for deriving the ETS. The method is subject to large uncertainties at wavelengths where atmospheric attenuation is large, such as at wavelengths shorter than 310 nm (where ozone absorbs strongly) or in strong water vapour absorption bands. Another method is the direct measurement from space. The challenge of this method is to prevent changes in an instrument's calibration during transport from the calibration laboratory to space. Both methods have advanced greatly during the last years.

Gröbner et al. [304] applied the Langley technique to radiometrically accurate measurements of QASUME (Sect. 10.1) and a "Fourier-transform spectroradiometer," which measures spectra at high resolution, to derive an ETS over the wavelength range of 300–500 nm with a spectral resolution of 0.025 nm, a wavelength accuracy of 0.01 nm, and a radiometric accuracy of 2% (95% CL) between 310 and 500 nm and 4% at 300 nm. Richard et al. [305] measured the ETS from the International Space Station with the Total and Spectral Solar Irradiance Sensor / Spectral Irradiance Monitor (TSIS-1 SIM) between 200 and 2,400 nm with an accuracy of 0.5% (95% CL) and a spectral resolution of 5 nm between 280 and 400 nm. The high accuracy is achieved by calibrating the system against a cryogenic radiometer and monitoring the instrument's stability in space with an on-board, detector-based reference electrical substitution radiometer. Finally, by combining the superior spectral resolution of the spectrum by Gröbner et al. [304] with the greater radiometric accuracy of the TSIS-1 SIM spectrum, Coddington et al. [306] developed a composite spectrum (named TSIS-1 HSRS) with a spectral resolution of 0.025, a sampling resolution of 0.01 nm and a radiometric accuracy of better than 1.3% (68% CL) at wavelengths shorter than 400 nm, representative of solar minimum conditions between solar cycles 24 and 25. This spectrum can be considered a new benchmark for modelling applications.

An important application of radiative transfer models is the calculation of UV irradiances at the Earth's surface from backscattered radiances measured by satellites (Sect. 10.3). Typically, measurements at different wavelengths by a single space-based instrument such as OMI are used to first derive the TCO and then apply corrections to account for the effects of clouds and aerosols [307].

10.3   Satellite observations of UV radiation

The TCO and UV radiation at the ground have been estimated from measurements of various space-borne sensors since the 1970s, starting with the Backscatter Ultraviolet (BUV) experiment on the Nimbus-4 satellite [308]. These measurements have been continued, amongst others, by several Solar Backscatter UV (SBUV) instruments [309]; Total Ozone Monitoring Spectrometers (TOMS) [310,311]; Global Ozone Monitoring Experiments (GOME and GOME-2) [312,313]; the Ozone Monitoring Instrument (OMI) [314] on the Aura

satellite; and the Earth Polychromatic Imaging Camera (EPIC) installed on the Deep Space Climate Observatory (DSCOVR), which is located at the Lagrange Point L1 between the Earth and Sun [315].

Several of these types of instruments have been installed on various satellites. Estimates of UV radiation are derived from backscattered radiances measured by these sensors and radiative transfer model calculations (Sect. 10.2). Uncertainties of these estimates are typically larger than those of UV measurements at the Earth's surface because the conditions on the ground cannot be completely characterised from space, in particular in the presence of clouds [316], absorbing aerosols in the boundary layer [317], or snow and ice [318]. The validation of satellite data with ground-based measurements from many sites has been discussed in our previous assessment [9]. In general, UV data from satellites are accurate within a few percent under low-aerosol and clear-sky conditions, but can be affected by systematic errors exceeding 50% for less ideal observing conditions.

Data of UV radiation at the Earth's surface estimated from satellite observations typically have the spatial resolution of the satellite sensor (e.g., 13 × 24 km at nadir for OMI) and are typically based on one satellite-measured spectrum per day at low and mid latitudes. As an alternative, Kosmopoulos et al. [319] have used inputs from various data sources to calculate real-time and forecasted UVIs for Europe with a spatial and temporal resolution of 5 km and 15 min, respectively. The new data product agrees with measurements at 17 ground-based stations distributed across Europe to within ±0.5 UVI units for 80% of clear-sky and 70% of all-sky conditions. Similarly, Vuilleumier et al. [320] calculated erythemal irradiance for Switzerland with a spatial resolution of 1.5–2 km and a temporal resolution of one hour for 2004–2018, using data from several European satellites. A validation of these data with ground-based measurements at three meteorological stations in Switzerland (Locarno, Payerne, and Davos) indicates that the expanded uncertainty of hourly UVI values of the new data products is about 0.3 UVI units for UVI <3 and up to 1.5 UVI units for UVI > 6.

Measurements with OMI started in 2004 and their quality has degraded recently [247]. The future of the Aura spacecraft is uncertain beyond 2023 [321]. Fortunately, several alternative satellite instruments have become operational within the last years to continue monitoring of ozone and UV radiation from space. For example, the Ozone Mapping and Profiler Suite (OMPS) [322] is installed on NOAA's Suomi NPP (launched in 2011) and the NOAA-20 (launched in 2017) satellites. The TROPOspheric Monitoring Instrument (TROPOMI) [323], which is installed on the Sentinel-5 Precursor satellite (launched in 2017), will continue ozone-monitoring efforts by the European Space Agency. TROPOMI may also fly on future Sentinel satellites [324]. TROPOMI observations of UV radiation have recently been compared with ground-based measurements at 25 sites [325]. For snow-free surface conditions, the median relative difference between UVI measurements by TROPOMI and these ground stations was within ±10% at 18 of 25 sites. For 10 sites, the agreement was at the ±5% level. These differences are comparable to those reported for OMI [316,318,326,327]. Larger differences were observed at locations with challenging conditions, such as mountainous areas or sites in the Arctic and Antarctic with variable snow cover. A comprehensive comparison between OMI and TROPOMI surface UV products is planned [314] to ensure that there is no step-change in the time series of UV radiation measurements when transitioning from OMI to TROPOMI.

In preparation for new satellite missions (e.g., Sentinel-4 and Sentinel-5 of the European Space Agency), Lipponen et al. [328] developed an approach to assimilate input data from geosynchronous and low Earth orbit satellite measurements with the goal to provide high-resolution UVI and UV-A data. Zhao and He [329] combined TCO data from OMI with top-of-the-atmosphere reflectance data from MODIS for quantifying attenuation by clouds and aerosols and surface reflectance data from MODIS and used a machine learning algorithm to calculate erythemal irradiances at 1 km resolution. The system is trained and tested with UV measurements of NOAA's Surface Radiation Budget Network (SURFRAD) and UV data from the United States Department of Agriculture's (USDA) UV-B Monitoring and Research Program. For most stations, calculated and measured data agreed to within ±5% (mean bias calculated from match-up data). However, the system was trained with data from the continental United States only, and the fidelity of the method for sites that are different in terms of latitude, ozone climatology, pollution levels, and surface albedo has not yet been demonstrated.

10.4   Forecasting of the UV Index

The UVI is now part of weather forecasts in many countries. National weather services and other agencies use models to predict the diurnal course of the UVI (e.g., every hour) for one or several days into the future (e.g., the Israel Meteorological Service (https://ims. gov.il/en/UVIHourly), the German Meteorological Service (https://kunden.dwd.de/uvi/index.jsp), and the Copernicus Atmosphere Monitoring Service (https://climate-adapt.eea.europa.eu/observatory/evidence/projections-and-tools/cams-uv-index-forecast). New methods for improving UVI forecasts have recently been proposed based on an "ensemble member" approach, where a model is executed multiple times with different initial conditions [330], and a machine learning algorithm [331].

10.5   Personal exposure

Our 2014 and 2018 assessments [9,162] discussed advances in the understanding of personal exposure to ambient solar UV radiation and how personal exposure relates to measurements of UV irradiance, which are typically referenced to a horizontal surface. Exposure studies address needs for both research and public advice and quantify UV radiation on non-horizontal surfaces, and how the effects of shade, clothing, and human behaviour affect UV doses in real-world settings. Exposure studies have shown that adults working outdoors receive only about 10% of the total available annual UV radiation dose while indoor-working adults and children get only about 2–4% of the available UV dose [332,333]. This shows that standard irradiance measurements are a poor proxy for realistic exposures. While there could be a good correlation between ambient and personal UV dose at the population level, exposure of individuals depends greatly on lifestyle.

Reviews of a large number of studies on personal exposure to UV radiation during non-occupational [334] and occupational [335] activities concluded that understanding of human exposure to UV radiation has greatly increased during the last 4–5 decades. However, for most activities, our ability to accurately calculate the UV exposure of exposed body sites is still limited for many conditions.

10.5.1 Exposure models

Models of human morphology can quantify the protection afforded by attire, for example, from wearing various hats [336] and sunglasses [337]. These models often use the "predictive protection factor" (PPF), which is akin to the sun protection factor (SPF) developed for sunscreens, except that the PPF also depends on the direct-to-diffuse ratio of incident radiation. These models may be validated using mannequin torsos or heads equipped with UV sensors [338]. The sky view factor derived from all-sky imagery in the visible range together with the calculated clear-sky UV irradiance has recently been utilised to accurately estimate UV irradiance in partially shaded settings [339].

Doses of erythemal radiation received by the human body during holidays at the beach have recently been modelled [340]. Taking into account all confounding factors affecting exposure (e.g., clothing, behaviour, photo-protection), these models predict that the forearm typically receives about 170 standard erythemal doses (SED) in a week, which is comparable with the average annual exposure of a citizen in Europe or North America. Furthermore, for a full day sun-bathing at the beach or pool, multiple body sites can receive more than 50 SED.

10.5.2 Personal dosimetry

The three types of dosimeters previously identified [162]—polysulphone (a plastic film that changes its transmission following exposure to UV radiation), biofilm, and electronic devices—are still in use, and their relative merits in different contexts have recently been reviewed [341,342]. These measurement technologies were further described in a review that also proposes a future course for development and regulation of wearable UV sensors [343].

Some authors [e.g., 344] distinguish between "radiometers," which give an instantaneous flux reading such as the UVI, and "dosimeters," which measure cumulative dose such as the standard erythemal dose (SED). However, the distinction is irrelevant for many electronic sensors, which measure flux but also accumulate it electronically. The same can apply to photochromic sensors in combination with smartphones or other electronic logging. Hereafter we use the term "dosimeter" for all types of sensors.

The history and characteristics of polysulphone dosimeters have been reviewed by one of their pioneers [285]. They are useful whenever water resistance is necessary, as in a study of triathletes [286]. Alternative photochromic sensors have been developed using the photodegradable dye DTEC[46] [345] and xanthommatin [344].

A new development of a biofilm dosimeter that mimics the photoreaction resulting in previtamin D_3 synthesis in human skin has recently been presented [346]. Biofilm sensors of a similar type were used to measure exposure to UV radiation of lifeguards, demonstrating that this group receives high doses of erythemal UV radiation, averaging over 6 SEDs per day [347].

Electronic dosimeters have some advantages for research involving personal dosimetry compared to other sensors. They can be engineered to have a spectral responsivity and a directional response approaching those of research-grade radiometers measuring erythemal irradiance [284]. The time resolution and ability to interface wirelessly with smartphones allows feedback to users, and has supported research on how such information can influence sun exposure amongst melanoma survivors [348], dockworkers and fishermen [349], or young adults in general [350]. In a small study of outdoor workers in Romania, dosimeters measured up to 6 SEDs per day and led the authors to suggest that UV dosimeters should be compulsory for outdoor workers, similar to personal dosimetry for ionising radiation in relevant professions [351].

A 14-year study with electronic dosimeters showed that participants that are in continued employment maintained their sun exposure behaviour, retirees increased their exposure, and high school students reduced their exposure when starting work [352]. Additional exposure studies confirmed expectations that outdoor workers [351]; participants in triathlons [286]; and elite surfers, windsurfers, and Olympic sailors [353] are at high risk of overexposure to UV radiation. In general, staying outdoors for long periods, even at low UV irradiance levels, can result in risk of damage from UV radiation [232].

Airline pilots have long been known to have twice the incidence rate of malignant melanoma and keratinocyte skin cancers than the general population, but UV-B radiation is almost entirely blocked by cockpit windows [354]. Other factors explaining this elevated risk of skin cancer, like ionising radiation and disrupted circadian rhythms, have been largely ruled out.

Measurements with dosimeters that are sensitive to both erythemal and UV-A radiation suggested that cockpit windows are partially transparent to UV-A radiation and pilots are therefore exposed to levels of UV-A radiation that exceed guidelines for eye protection established by ICNIRP [355], in particular if sunglasses are not worn or visors are not deployed [356].

---

46 (2Z,6Z)-2,6-bis(2-(2,6-diphenyl-4H-thiopyran-4-ylidene)ethylidene)cyclohexanone

10.5.3 Low-cost / crowd-sourced sensors and cell phone apps

Our last assessment [9] described a wide range of new tools for research and for getting information to users, including electronic sensors, photochromic films with associated software, and forecasts or "nowcasts" of UV radiation using cell phone apps. A review of developments in this area [357] describes the promise of these new technologies, but a comparison of UV radiation reported by cell phone apps with actual UV measurements found that many of these apps have poor accuracy [358]. For example, of the six apps reviewed in this study, only one was able to predict the actual UVI to within ±30% in most cases. A further miniaturisation of sensors to millimetre scale with wireless communication to standard consumer devices [359] will widen the scope of how these sensors can be deployed. Other studies have also shown that useful personal exposures to UV radiation can be achieved from satellite-based UV radiation estimates combined with exposure ratio modelling to account for individual factors [360] or by leveraging UV data from local research stations [361].

11 Action spectra

Action spectra describe the wavelength dependence of biological effects caused by UV radiation. A biological effect is quantified by first multiplying the action spectrum for this effect by the spectrum of the incident irradiance and then integrating this product over wavelength. The result is the biologically effective UV irradiance, UV_{BE}. Most action spectra decrease by several orders of magnitude towards longer wavelengths in the UV-B range. Since solar spectra increase by a similar amount in this wavelength range, a given biological effect is very sensitive to the wavelength intervals within the UV-B range over which this decrease (action spectrum) or increase (solar spectrum) occurs. This implies that action spectra must be very accurately measured.

The most widely used action spectrum is that for erythema [10], which is the basis of UVI calculations. In sunlight, the strongest contribution to erythema is from UV-B wavelengths, peaking near 307 nm. UV-A wavelengths also contribute, especially at the shorter end of the UV-A region (e.g., 315–340 nm). A small-scale study with 10 participants [362] found clinically perceptible erythema after exposure to UV radiation in the 370–400 nm range plus visible light (400–700 nm), confirming that longer UV-A wavelengths can also cause erythema. The study also suggests that the erythema action spectrum, which is currently defined only up to 400 nm [10], should possibly be extended into the visible range. This finding is also supported by a recent assessment by Diffey and Osterwalder [363].

Another important action spectrum for human health defines the wavelength dependence of the conversion of 7-dehydrocholesterol in the skin to previtamin D_3, which is subsequently transformed to the active form of vitamin D (1,25-dihydroxycholecalciferol or calcitriol) involving isomerisation and hydroxylations in the skin, liver, and kidneys. This spectrum was measured 40 years ago [364] and was standardised by the International Commission on Illumination (CIE) [365] by interpolating the original data, plus extending the end of the spectrum from 315 nm to 330 nm via an exponential extrapolation. The spectrum has been widely used for developing recommendations for optimal solar exposure [179]; however, its validity has been questioned [179,366]. Specifically, the CIE standard [365] is based on a scanned figure from a single publication that does not include a complete description of the experiment such as the UV doses used. Furthermore, the source used for irradiation had a large bandwidth of 5 nm, which leads to noticeable broadening of the spectrum, and the extrapolation from 315 to 330 nm is questionable because there are no experimental data in this wavelength range.

Young et al. [367] have recently provided evidence that shifting the CIE action spectrum for previtamin D_3 synthesis by 5 nm to shorter wavelengths (Fig. 10) would produce a more realistic action spectrum for the production of previtamin D_3 in human skin. They exposed 75 volunteers to five lamp spectra with different spectral composition, and correlated the observed increase in serum 25(OH)D levels (the form of vitamin D used to assess vitamin D status) with the effective UV irradiance, UV_{BE}. The action spectrum for calculating UV_{BE} was either the CIE spectrum in its unaltered form or a variant shifted in wavelength. The shift by 5 nm is plausible because the absorption spectrum of 7-dehydrocholesterol is also found to be shifted by about 5 nm to shorter wavelengths relative to the CIE action spectrum, even after adjusting for the spectral transmission of the skin's outermost layer, the stratum corneum [366]. Furthermore, results obtained with the shifted action spectrum are consistent with calculations using alternative vitamin D action spectra proposed by Bolsée et al. [368], Olds [369], and van Dijk et al. [370], which are also shifted to shorter wavelengths relative to the CIE spectrum. These results suggest that the CIE standard [365] may need revision. However, the spectral change of solar spectra observed on the Earth (e.g., the difference between summer at the equator and winter in the Northern Hemisphere) is smaller than the difference in the spectral composition of the various artificial light sources used in the new experiment. The effect of the shift is therefore less important for natural sunlight, leading to the conclusion by Young et al. [367] that the CIE action spectrum (with no shift) remains adequate for risk-benefit calculations and the development of recommendations for healthy solar exposure. Along the same line, a recent assessment [371] concluded that the current CIE action spectrum [365] probably needs to be amended, but that it is acceptable to continue using this action spectrum for risk-benefits assessments until that work is completed.

An action spectrum for the inhibition of SARS-CoV-2 (the virus responsible for the COVID-19 disease) was recently measured. This spectrum is discussed in Chapter 2 [2].
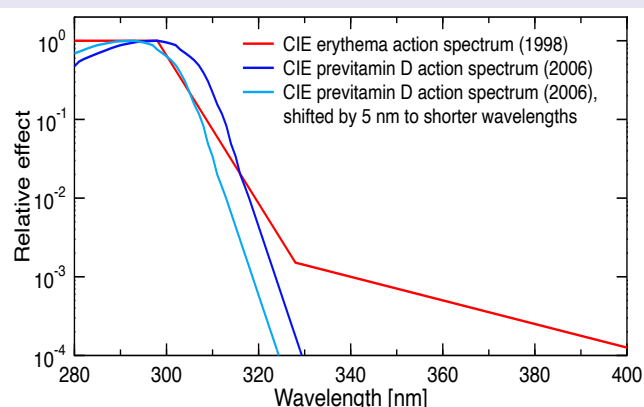
Fig. 10 Comparison of CIE action spectra for erythema [10] and the cutaneous synthesis of previtamin D_3 [365]. The effect of a 5-nm blue shift on the previtamin D_3 action spectrum is also shown.

12 Gaps in knowledge

Our assessment identified the following gaps in knowledge:

- Most ODSs are also GHGs and have a large effect on global warming. However, since ozone is also a GHG, depletion of ozone caused by ODSs has a cooling effect (Sect. 4.2). The net effect on temperatures at the Earth's surface resulting from the direct (warming) effect of ODSs and the indirect (cooling) effect from ozone depletion induced by ODSs is uncertain because climate models disagree on the magnitude of the latter effect. While the balance of all studies suggests that the Montreal Protocol is highly effective in limiting temperature rise at the Earth's surface, the magnitude of the effect remains uncertain.

- The effect of Antarctic ozone depletion on changes in sea ice surrounding Antarctica is not well understood.

- The effect of the Antarctic ozone hole on summertime weather in the Southern Hemisphere is uncertain. In particular, it is difficult to quantify if changes in weather are more affected by the year-to-year variability of the polar vortex, which is partly driven by changes in sea surface temperature of the Southern Ocean, or by the actual depletion of ozone within the vortex. It is also not clear how the coupling between the stratosphere and troposphere in weak vortex conditions will evolve under ozone recovery.

- While several studies have identified correlations between Arctic ozone changes and weather in the Northern Hemisphere, knowledge on how these linkages are mediated is incomplete.

- The paucity of measurements of the properties of aerosols in the UV-B range hampers our ability to accurately assess the effects of aerosols on a global scale as well as for urban regions. While efforts to improve this situation are underway—for example, EUBREWNET has recently started to provide AOD in the wavelength range from 306 to 320 nm (Sect. 6.1)—aerosol data in the UV-B range are currently available only for a few locations.

- Atmospheric blocking systems (stagnant high- or low-pressure synoptic systems) can cause week-long anomalies of UV radiation. It is not well understood how climate change may alter the frequency, persistence, and geographical extent and location of these blocking patterns, and their effect on UV radiation.

- One of the largest uncertainties in projecting changes to ozone and UV radiation during the 21st century is the evolution of GHG trajectories, which mostly depend on policy decisions and societal behaviour.

- Uncertainties in projections of UV radiation arising from incomplete knowledge of future changes in aerosol and cloud optical properties are significant.

- The number of stations with high-quality spectral UV measurements has been declining during the last decade and the funding for many of the remaining stations is uncertain. If this trend continues, the scientific community may lose the ability to assess changes of UV radiation at the Earth's surface and associated impacts, in order to verify new satellite UV data products with ground-based observations and to validate model projections.

13 Conclusions

Virtually all studies published during the last four years confirmed that changes in UV radiation (typically assessed with the UVI) during the last 25 years have been small: less than 4% per decade for the UVI at the majority of ground stations, increasing at some sites and decreasing at others. Changes in the UVI outside the polar regions over the last 2–3 decades were mainly governed by variations in clouds, aerosols, and surface reflectivity (for snow- or ice-covered areas), while changes in TCO are less important. Variability in the UVI in Antarctica continued to be very large. In spring 2019, the UVI was at the minimum of the historical (1991–2018) range at the South Pole, while near record-high values were observed in spring 2020 and 2021, which were up to 80% above the historical mean. In the Arctic, some of the highest UV-B irradiances on record were measured in March and April 2020. For example in March 2020, the monthly average UVI over the Canadian Arctic was up to 70% higher than the historical (2005–2019) average, often exceeding this mean by three standard deviations.

Without the Montreal Protocol, the UVI at northern and southern latitudes of less than 50° would have increased by 10–20% between 1996 and 2020. For southern latitudes exceeding 50°, the UVI would have surged by between 25% (year-round at the southern tip of South America) and more than 100% (South Pole in spring).

Under the presumption that all countries will adhere to the Montreal Protocol in the future and that atmospheric aerosol concentrations remain constant, the UVI at mid-latitudes (30–60°) is projected to decrease between 2015 and 2090 by 2–5% in the north and by 4–6% in the south due to recovering ozone. Changes projected for the tropics are smaller than 3%.

Since most substances controlled by the Montreal Protocol are also greenhouse gases, the phase-out of these substances may have avoided warming by 0.5 to 1.0 °C over mid-latitude regions of the continents, and by more than 1.0 °C in the Arctic. ODSs contributed one-half of the forced Arctic sea ice loss in the latter half of the 20th century. The uncertainty of changes in temperature and sea ice simulated by these models is still large.

Assessing the Montreal Protocol's impact on solar UV radiation and climate, and their interaction, is impeded by several gaps in knowledge. The net temperature change at the Earth's surface resulting from the direct (warming) effect of ODSs and the indirect (cooling) effect from ozone depletion is uncertain, because climate models disagree on the magnitude of the latter effect. While all studies support the role of the Montreal Protocol in limiting global warming, the magnitude of increases in temperatures that were averted remains uncertain. There is evidence that in both hemispheres polar ozone depletion in spring has an influence on weather; however, the mechanisms and magnitude of the effect are not fully understood. The lack of measurements of absorption properties of aerosols in the UV-B range hinders the assessment of the aerosols' impact on UV-B radiation. One of the largest uncertainties in projecting changes in UV radiation during the 21st century is the incomplete knowledge of how GHGs will increase over time. Uncertainties in UV projections arising from inadequate understanding of future changes in aerosols and clouds are also significant.

Our assessment addresses several United Nations Sustainable Development Goals (SDGs) and their targets (https://sdgs.un.org/goals). Owing to the Montreal Protocol, large increases in UV-B radiation have been avoided and global warming reduced. By assessing how ozone depletion affects climate change, we contribute to SDGs 13.1 (strengthen resilience to climate-related hazards and disasters) and 13.2 (integrate climate change measures into policy, strategy and planning). Furthermore, by providing up-to-date information on the interactive effects of ozone depletion on UV radiation and climate, both in this assessment and the companion document titled "Questions and Answers about the effects of ozone depletion on humans and the environment" we address SDGs 13.3 (improve education on climate-change mitigation) and 17.14 (enhance policy coherence for sustainable development).

List of abbreviations

AAO	Antarctic Oscillation
AeroCom	Aerosol Comparisons between Observations and Models
AERONET	Aerosol Robotic Network
AO	Arctic Oscillation
AOD	aerosol optical depth
asl	above sea level
BUV	Backscatter Ultraviolet
CAMS	Copernicus Atmosphere Monitoring Service
CAVA	Central American Volcanic Arc
CCM	chemistry-climate model
CCMI	Chemistry-Climate Model Initiative
CFC	Chlorofluorocarbon
CIE	Commission Internationale de l' Éclairage (Eng.: International Commission on Illumination)
CL	confidence level
CMIP6	Coupled Model Intercomparison Project Phase 6
COVID-19	Coronavirus disease 2019
DSCOVR	Deep Space Climate Observatory
DTEC	((2Z,6Z)-2,6-bis(2-(2,6-diphenyl-4H-thiopyran-4-ylidene)ethylidene)cyclohexanone
EEAP	Environmental Effects Assessment Panel
EMAC	European Centre for Medium-Range Weather Forecasts–Hamburg (ECHAM)/Modular Earth Submodel System (MESSy) Atmospheric Chemistry model
ENSO	El Niño-Southern Oscillation
EPIC	Earth Polychromatic Imaging Camera
EPP	energetic particle precipitation
ERA	ECMWF (European Centre for Medium-Range Weather Forecast) Re-Analysis
ETS	Extraterrestrial (solar) spectrum
EUBREWNET	European Brewer Network
GeoMIP	Geoengineering Model Intercomparison Project
GHG	Greenhouse gas
GLENS	Geoengineering Large Ensemble
GOME	Global Ozone Monitoring Experiment
GPH	geopotential height
GWP	global warming potential
HSRS	Hybrid Solar Reference Spectrum
ICNIRP	International Commission on Non-Ionizing Radiation Protection
IPCC	Intergovernmental Panel on Climate Change
MODIS	Moderate Resolution Imaging Spectroradiometer
NASA	National Aeronautics and Space Administration (of the United States)
NDACC	Network for the Detection of Atmospheric Composition Change
NH	Northern Hemisphere
NIWA	National Institute of Water & Atmospheric Research (of New Zealand)
NOAA	National Oceanic and Atmospheric Administration (of the United States)
NPP	National Polar-orbiting Partnership
NSF	National Science Foundation (of the United States)
ODS	ozone-depleting substances
OMI	Ozone Monitoring Instrument
OMPS	Ozone Mapping and Profiler Suite

PAR	photosynthetically active radiation (400-700 nm)
PM$_{2.5}$	particulate matter 2.5 (fine inhalable particles, with diameters that are generally 2.5 μm or smaller)
PPF	predictive protection factor
PSC	polar stratospheric clouds
QASUME	Quality Assurance of Spectral Ultraviolet Measurements in Europe
QBO	quasi-biennial oscillation
RAF	Radiation Amplification Factor
RCP	Representative Concentration Pathways
RF	Radiative forcing
RSHU	Russian State Hydrometeorological University
SAI	stratospheric aerosol injection
SAM	Southern Annular Mode
SAP	Scientific Assessment Panel
SARS-CoV-2	Severe acute respiratory syndrome coronavirus 2
SBUV	Solar Backscatter Ultraviolet Radiometer
SED	standard erythemal dose
SH	Southern Hemisphere
SIM	Spectral Irradiance Monitor
SPE	solar proton events
SPF	sun protection factor
SRM	solar radiation management
SSA	single scattering albedo
SSP	Shared Socioeconomic Pathways
SST	sea surface temperature
SSW	sudden stratospheric warming
SURFRAD	Surface Radiation Budget Network
SZA	solar zenith angle
TEMIS	Tropospheric Emission Monitoring Internet Service
TCO	total column ozone
TOMS	Total Ozone Mapping Spectrometer
TROPOMI	Tropospheric Monitoring Instrument
TSI	total solar irradiance
TSIS	Total and Spectral Solar Irradiance Sensor
UNEP	United Nations Environment Programme
USDA	United States Department of Agriculture
UV	Ultraviolet (100–400 nm)
UV-A	Ultraviolet-A (315–400 nm)
UV-B	Ultraviolet-B (280–315 nm)
UV-C	Ultraviolet-C (100–280 nm)
UVI	Ultraviolet Index
VIS	Visible (radiation)
VSLS	very short-lived substances
WMO	World Meteorological Organization

Author contributions All authors contributed to the conception and assessment and carried out extensive revisions of content.

Conflict of interest The authors declare no conflicts of interest.

References

1. Neale, R. E., Lucas, R. M., Byrne, S., Hollestein, L., Rhodes, L. E., Yasar, S., Young, A. R., Ireland, R., & Olsen, C. M. (2022). The effects of exposure to solar radiation on human health. *Chapter 3*

2. Bernhard, G. H., Madronich, S., M., L. R., Byrne, S. N., Schikowski, T., & Neale, R. E. (2022). Linkages between COVID-19, solar UV radiation, and the Montreal Protocol. *Chapter 2*

3. Barnes, P. W., Robson, T. M., Zepp, R. G., Bornman, J. F., Jansen, M. A. K., Ossola, R., Wang, Q.-W., Robinson, S. A., Foereid, B., Klekociuk, A. R., Martinez-Abaigar, J., Hou, W. C., & Paul, N. D. (2022). Interactive effects of changes in UV radiation and climate on terrestrial ecosystems, biogeochemical cycles, and feedbacks to the climate system. *Chapter 4*

4. Neale, P. J., Williamson, C. E., Banaszak, A. T., Häder, D. P., Hylander, S., Ossola, R., Rose, K. A., Wängberg, S.-Å., & Zepp, R. G. (2022). The response of aquatic ecosystems to the interactive effects of stratospheric ozone depletion, UV radiation, and climate change. *Chapter 5*

5. Madronich, S., Sulzberger, B., Longstreth, J., Schikowski, T., Andersen, M. P. S., Solomon, K. R., & Wilson, S. R. (2022). Changes in tropospheric air quality related to the protection of stratospheric ozone and a changing climate. *Chapter 6*

6. Andrady, A. L., Heikkila, A. M., Pandey, K. K., Bruckman, L. S., White, C. C., Zhu, M., & Zhu, L. (2022). Effects of UV radiation on natural and synthetic materials. *Chapter 7*

7. Jansen, M. A. K., Barnes, P. W., Bornman, J. F., Rose, K. A., Madronich, S., White, C. C., Zepp, R. G., & Andrady, A. L. (2023). The Montreal Protocol and the fate of environmental plastic debris. *Chapter 8*

8. United Nations. (1987). Montreal Protocol on Substances that Deplete the Ozone Layer. *United Nations Treaty Series*, Number 1522. https://treaties.un.org/Pages/showDetails.aspx?objid=080000028003f7f7

9. Bais, A. F., Bernhard, G., McKenzie, R. L., Aucamp, P. J., Young, P. J., Ilyas, M., Jockel, P., & Deushi, M. (2019). Ozone-climate interactions and effects on solar ultraviolet radiation. *Photochemical & Photobiological Sciences, 18*(3), 602–640. https://doi.org/10.1039/c8pp90059k

10. CIE. (1998). *Erythema reference action spectrum and standard erythema dose*. CIE Standard Bureau, Vol. ISO 17166:1999(E), CIE DS 007.1/E-1998. Commission Internationale de l'Eclairage, Vienna, Austria.

11. WMO. (2022). Scientific Assessment of Ozone Depletion: 2022, GAW Report No. 278. World Meteorological Organization, Geneva, Switzerland. https://ozone.unep.org/science/assessment/sap

12. Weber, M., Arosio, C., Coldewey-Egbers, M., Fioletov, V. E., Frith, S. M., Wild, J. D., Tourpali, K., Burrows, J. P., & Loyola, D. (2022). Global total ozone recovery trends attributed to ozone-depleting substance (ODS) changes derived from five merged ozone datasets. *Atmospheric Chemistry and Physics, 22*(10), 6843-6859. https://doi.org/10.5194/acp-22-6843-2022

13. WMO. (2018). *Scientific Assessment of Ozone Depletion: 2018*, Global Ozone Research and Monitoring Project-Report No. 58, 588 pp., Geneva, Switzerland, https://ozone.unep.org/science/assessment/sap

14. Steinbrecht, W., Hegglin, M. I., Harris, N., & Weber, M. (2018). Is global ozone recovering? *Comptes Rendus Geoscience, 350*(7), 368-375. https://doi.org/10.1016/j.crte.2018.07.012

15. Solomon, S., Ivy, D. J., Kinnison, D., Mills, M. J., Neely, R. R., & Schmidt, A. (2016). Emergence of healing in the Antarctic ozone layer. *Science, 353*(6296), 269-274. https://doi.org/10.1126/science.aae0061

16. Kuttippurath, J., Kumar, P., Nair, P. J., & Pandey, P. C. (2018). Emergence of ozone recovery evidenced by reduction in the occurrence of Antarctic ozone loss saturation. *npj Climate and Atmospheric Science, 1*(1), 42. https://doi.org/10.1038/s41612-018-0052-6

17. Pazmiño, A., Godin-Beekmann, S., Hauchecorne, A., Claud, C., Khaykin, S., Goutail, F., Wolfram, E., Salvador, J., & Quel, E. (2018). Multiple symptoms of total ozone recovery inside the Antarctic vortex during austral spring. *Atmospheric Chemistry and Physics, 18*(10), 7557-7572. https://doi.org/10.5194/acp-18-7557-2018

18. Tully, M. B., Krummel, P. B., & Klekociuk, A. R. (2019). Trends in Antarctic ozone hole metrics 2001–17. *Journal of Southern Hemisphere Earth Systems Science, 69*(1), 52-56. https://doi.org/10.1071/es19020

19. Bodeker, G. E., & Kremser, S. (2021). Indicators of Antarctic ozone depletion: 1979 to 2019. *Atmospheric Chemistry and Physics, 21*(7), 5289-5300. https://doi.org/10.5194/acp-21-5289-2021

20. Kramarova, N., Newman, P. A., Nash, E. R., Strahan, S. E., Long, C. S., Johnson, B., Pitts, M., Santee, M. L., Petropavlovskikh, I., Coy, L., de Laat, J., Bernhard, G. H., Stierle, S., & Lakkala, K. (2021). 2020 Antarctic ozone hole. In J. Blunden, & T. Boyer (Eds.), "State of the Climate in 2020", *Bulletin of the American Meteorological Society, 102*(8), S345–S349. https://doi.org/10.1175/BAMS-D-21-0081.1

21. Zambri, B., Solomon, S., Thompson, D. W. J., & Fu, Q. (2021). Emergence of Southern Hemisphere stratospheric circulation changes in response to ozone recovery. *Nature Geoscience, 14*(9), 638-644. https://doi.org/10.1038/s41561-021-00803-3

22. Kramarova, N., Newman, P. A., Nash, E. R., Strahan, S. E., Long, C. S., Johnson, B., Pitts, M., Santee, M. L., Petropavlovskikh, I., Coy, L., & de Laat, J. (2020). 2019 Antarctic ozone hole. In J. Blunden, & D. S. Arndt (Eds.), "State of the Climate in 2019", *Bulletin of the American Meteorological Society, 101*(8), S310-S312. https://doi.org/10.1175/BAMS-D-20-0090.1

23. Milinevsky, G., Evtushevsky, O., Klekociuk, A., Wang, Y., Grytsai, A., Shulga, V., & Ivaniha, O. (2019). Early indications of anomalous behaviour in the 2019 spring ozone hole over Antarctica. I*nternational Journal of Remote Sensing, 41*(19), 7530-7540. https://doi.org/10.1080/2150704X.2020.1763497

24. Shen, X., Wang, L., & Osprey, S. (2020). Tropospheric forcing of the 2019 Antarctic sudden stratospheric warming. *Geophysical Research Letters, 47*(20). https://doi.org/10.1029/2020gl089343

25. Yamazaki, Y., Matthias, V., Miyoshi, Y., Stolle, C., Siddiqui, T., Kervalishvili, G., Laštovička, J., Kozubek, M., Ward, W., Themens, D. R., Kristoffersen, S., & Alken, P. (2020). September 2019 Antarctic sudden stratospheric warming: quasi-6-Day wave burst and ionospheric effects. *Geophysical Research Letters, 47*(1). https://doi.org/10.1029/2019gl086577

26. Safieddine, S., Bouillon, M., Paracho, A. C., Jumelet, J., Tencé, F., Pazmino, A., Goutail, F., Wespes, C., Bekki, S., Boynard, A., Hadji-Lazaro, J., Coheur, P. F., Hurtmans, D., & Clerbaux, C. (2020). Antarctic ozone enhancement during the 2019 sudden stratospheric warming event. *Geophysical Research Letters, 47*(14). https://doi.org/10.1029/2020gl087810

27. Stone, K. A., Solomon, S., Kinnison, D. E., & Mills, M. J. (2021). On recent large Antarctic ozone holes and ozone recovery metrics. *Geophysical Research Letters, 48*(22). https://doi.org/10.1029/2021gl095232

28. Yook, S., Thompson, D. W. J., & Solomon, S. (2022). Climate impacts and potential drivers of the unprecedented Antarctic ozone holes of 2020 and 2021. *Geophysical Research Letters, 49*(10). https://doi.org/10.1029/2022gl098064

29. Barnes, P.W., Robson, T.M., Neale, P.J., Williamson, C.E., Madronich, S., Wilson, S.R., Heikkilä, A.M., Bernhard, G.H., Bais, A.F., Neale, R.E., Bornman, J. F., Jansen, M. A. K., Klekociuk, A. R., Martinez-Abaigar, J., Robinson, S.A., Wang, Q.-W., Banaszak, A.T., Häder, D.-P., Hylander, S., Rose, K.C., Wängberg, S.-Å., Føreid, B., Hou, W.-C., Ossola, R., Paul, N.D., Ukpebor, J.E., Andersen, M.P.S., Longstreth, J., Schikowski, T., Solomon, K.R., Sulzberger, B., Bruckman, L.S., Pandey, K.K., Zhu, L. & Zhu, M., Aucamp, P.J., Liley, J.B., McKenzie, R.L., Berwick, M., Byrne, S.N., Hollestein, L. M., Lucas, R.M., Olsen, C.M., Rhodes, L.E., Yazar, S., & Young, A.R. (2022). Environmental effects of stratospheric ozone depletion, UV radiation, and interactions with climate change: UNEP Environmental Effects Assessment Panel, Update 2021. *Photochemical & Photobiological Sciences, 21*, 275–301. https://doi.org/10.1007/s43630-022-00176-5

30. Zhuo, Z., Kirchner, I., Pfahl, S., & Cubasch, U. (2021). Climate impact of volcanic eruptions: the sensitivity to eruption season and latitude in MPI-ESM ensemble experiments. *Atmospheric Chemistry and Physics, 21*(17), 13425-13442. https://doi.org/10.5194/acp-21-13425-2021

31. Klekociuk, A. R., Tully, M. B., Krummel, P. B., Henderson, S. I., Smale, D., Querel, R., Nichol, S., Alexander, S. P., Fraser, P. J., & Nedoluha, G. (2022). The Antarctic ozone hole during 2020. *Journal of Southern Hemisphere Earth Systems Science, 72*(1), 19-37. https://doi.org/10.1071/es21015

32. Ivanciu, I., Matthes, K., Wahl, S., Harlaß, J., & Biastoch, A. (2021). Effects of prescribed CMIP6 ozone on simulating the Southern Hemisphere atmospheric circulation response to ozone depletion. *Atmospheric Chemistry and Physics, 21*(8), 5777-5806. https://doi.org/10.5194/acp-21-5777-2021

33. Strahan, S. E., Douglass, A. R., & Damon, M. R. (2019). Why do Antarctic ozone recovery trends vary? *Journal of Geophysical Research: Atmospheres, 124*(15), 8837-8850. https://doi.org/10.1029/2019jd030996

34. Cordero, R. R., Feron, S., Damiani, A., Redondas, A., Carrasco, J., Sepúlveda, E., Jorquera, J., Fernandoy, F., Llanillo, P., Rowe, P. M., & Seckmeyer, G. (2022). Persistent extreme ultraviolet irradiance in Antarctica despite the ozone recovery onset. *Scientific Reports, 12*(1). https://doi.org/10.1038/s41598-022-05449-8

35. Manney, G. L., Livesey, N. J., Santee, M. L., Froidevaux, L., Lambert, A., Lawrence, Z. D., Millán, L. F., Neu, J. L., Read, W. G., Schwartz, M. J., & Fuller, R. A. (2020). Record-low Arctic stratospheric ozone in 2020: MLS observations of chemical processes and comparisons with previous extreme winters. *Geophysical Research Letters, 47*(16). https://doi.org/10.1029/2020gl089063

36. Lawrence, Z. D., Perlwitz, J., Butler, A. H., Manney, G. L., Newman, P. A., Lee, S. H., & Nash, E. R. (2020). The remarkably strong Arctic stratospheric polar vortex of winter 2020: Links to record-breaking Arctic oscillation and ozone loss. *Journal of Geophysical Research: Atmospheres*, 125(22), e2020JD033271. https://doi.org/10.1029/2020JD033271

37. Manney, G. L., Santee, M. L., Rex, M., Livesey, N. J., Pitts, M. C., Veefkind, P., Nash, E. R., Wohltmann, I., Lehmann, R., Froidevaux, L., Poole, L. R., Schoeberl, M. R., Haffner, D. P., Davies, J., Dorokhov, V., Gernandt, H., Johnson, B., Kivi, R., Kyrö, E., Larsen, N., et al. (2011). Unprecedented Arctic ozone loss in 2011. *Nature, 478*(7370), 469-475. https://doi.org/10.1038/nature10556

38. Varotsos, C. A., Efstathiou, M. N., & Christodoulakis, J. (2020). The lesson learned from the unprecedented ozone hole in the Arctic in 2020; a novel nowcasting tool for such extreme events. *Journal of atmospheric and solar-terrestrial physics, 207*, 105330. https://doi.org/10.1016/j.jastp.2020.105330

39. Dameris, M., Loyola, D. G., Nützel, M., Coldewey-Egbers, M., Lerot, C., Romahn, F., & van Roozendael, M. (2021). Record low ozone values over the Arctic in boreal spring 2020. *Atmospheric Chemistry and Physics, 21*(2), 617-633. https://doi.org/10.5194/acp-21-617-2021

40. Grooß, J. U., & Müller, R. (2021). Simulation of Record Arctic Stratospheric Ozone Depletion in 2020. *Journal of Geophysical Research: Atmospheres, 126*(12). https://doi.org/10.1029/2020JD033339

41. Wohltmann, I., Gathen, P., Lehmann, R., Maturilli, M., Deckelmann, H., Manney, G. L., Davies, J., Tarasick, D., Jepsen, N., Kivi, R., Lyall, N., & Rex, M. (2020). Near complete local reduction of Arctic stratospheric ozone by severe chemical loss in spring 2020. *Geophysical Research Letters, 47*, e2020GL089547. https://doi.org/10.1029/2020gl089547

42. Lee, S. H. (2021). The January 2021 sudden stratospheric warming. *Weather, 76*(4), 135-136. https://doi.org/10.1002/wea.3966

43. Lu, Q., Rao, J., Liang, Z., Guo, D., Luo, J., Liu, S., Wang, C., & Wang, T. (2021). The sudden stratospheric warming in January 2021. *Environmental Research Letters, 16*(8), 084029. https://doi.org/10.1088/1748-9326/ac12f4

44. Lee, S. H., & Butler, A. H. (2019). The 2018–2019 Arctic stratospheric polar vortex. *Weather, 75*(2), 52-57. https://doi.org/10.1002/wea.3643

45. Butchart, N., & Remsberg, E. E. (1986). The area of the stratospheric polar vortex as a diagnostic for tracer transport on an isentropic surface. *Journal of the Atmospheric Sciences, 43*(13), 1319-1339. https://doi.org/10.1175/1520-0469(1986)0432.0.CO;2

46. Bernhard, G., Fioletov, V., Grooß, J.-U., Ialongo, I., Johnsen, B., Lakkala, K., Manney, G., & Müller, R. (2020). Ozone and UV radiation. In J. Richter-Menge, & M. L. Druckenmiller (Eds.), *"State of the Climate in 2019", Bulletin of the American Meteorological Society, 101*(8), S274-S277. https://doi.org/10.1175/BAMS-D-20-0086.1

47. Bernhard, G., Fioletov, V., Grooß, J.-U., Ialongo, I., Johnsen, B., Lakkala, K., Manney, G., & Müller, R. (2022). Ozone and UV radiation. In R. Thoman, M. L. Druckenmiller, & T. Moon (Eds.), *"State of the Climate in 2021", Bulletin of the American Meteorological Society, 103*(9), S293-S296. https://doi.org/10.1175/BAMS-D-22-0082.1

48. Feng, W., Dhomse, S. S., Arosio, C., Weber, M., Burrows, J. P., Santee, M. L., & Chipperfield, M. P. (2021). Arctic ozone depletion in 2019/20: Roles of chemistry, dynamics and the Montreal Protocol. *Geophysical Research Letters, 48*(4). https://doi.org/10.1029/2020GL091911

49. von der Gathen, P., Kivi, R., Wohltmann, I., Salawitch, R. J., & Rex, M. (2021). Climate change favours large seasonal loss of Arctic ozone. *Nature Communications, 12*(1), 1-17. https://doi.org/10.1038/s41467-021-24089-6

50. Langematz, U. (2018). Future ozone in a changing climate. *Comptes Rendus Geoscience, 350*(7), 403-409. https://doi.org/10.1016/j.crte.2018.06.015

51. Oberländer, S., Langematz, U., & Meul, S. (2013). Unraveling impact factors for future changes in the Brewer-Dobson circulation. *Journal of Geophysical Research: Atmospheres, 118*(18), 10,296-210,312. https://doi.org/10.1002/jgrd.50775

52. Klobas, J. E., Weisenstein, D. K., Salawitch, R. J., & Wilmouth, D. M. (2020). Reformulating the bromine alpha factor and equivalent effective stratospheric chlorine (EESC): evolution of ozone destruction rates of bromine and chlorine in future climate scenarios. *Atmospheric Chemistry and Physics, 20*(15), 9459-9471. https://doi.org/10.5194/acp-20-9459-2020

53. Falk, S., Sinnhuber, B.-M., Krysztofiak, G., Jöckel, P., Graf, P., & Lennartz, S. T. (2017). Brominated VSLS and their influence on ozone under a changing climate. *Atmospheric Chemistry and Physics, 17*(18), 11313-11329. https://doi.org/10.5194/acp-17-11313-2017

54. Keeble, J., Hassler, B., Banerjee, A., Checa-Garcia, R., Chiodo, G., Davis, S., Eyring, V., Griffiths, P. T., Morgenstern, O., Nowack, P., Zeng, G., Zhang, J., Bodeker, G., Burrows, S., Cameron-Smith, P., Cugnet, D., Danek, C., Deushi, M., Horowitz, L. W., Kubin, A., et al. (2021). Evaluating stratospheric ozone and water vapour changes in CMIP6 models from 1850 to 2100. *Atmospheric Chemistry and Physics, 21*(6), 5015-5061. https://doi.org/10.5194/acp-21-5015-2021

55. Meinshausen, M., Nicholls, Z. R. J., Lewis, J., Gidden, M. J., Vogel, E., Freund, M., Beyerle, U., Gessner, C., Nauels, A., Bauer, N., Canadell, J. G., Daniel, J. S., John, A., Krummel, P. B., Luderer, G., Meinshausen, N., Montzka, S. A., Rayner, P. J., Reimann, S., Smith, S. J., et al. (2020). The shared socio-economic pathway (SSP) greenhouse gas concentrations and their extensions to 2500. *Geoscientific Model Development, 13*(8), 3571-3605. https://doi.org/10.5194/gmd-13-3571-2020

56. McKenzie, R., Bernhard, G., Liley, B., Disterhoft, P., Rhodes, S., Bais, A., Morgenstern, O., Newman, P., Oman, L., Brogniez, C., & Simic, S. (2019). Success of Montreal Protocol demonstrated by comparing high-quality UV measurements with "World Avoided" calculations from two chemistry-climate models. *Scientific Reports, 9*(1), 12332. https://doi.org/10.1038/s41598-019-48625-z

57. Newman, P. A., Oman, L. D., Douglass, A. R., Fleming, E. L., Frith, S. M., Hurwitz, M. M., Kawa, S. R., Jackman, C. H., Krotkov, N. A., Nash, E. R., Nielsen, J. E., Pawson, S., Stolarski, R. S., & Velders, G. J. M. (2009). What would have happened to the ozone layer if chlorofluorocarbons (CFCs) had not been regulated? *Atmospheric Chemistry and Physics, 9*(6), 2113-2128. https://doi.org/10.5194/acp-9-2113-2009

58. Morgenstern, O., Hegglin, M. I., Rozanov, E., O'Connor, F. M., Abraham, N. L., Akiyoshi, H., Archibald, A. T., Bekki, S., Butchart, N., Chipperfield, M. P., Deushi, M., Dhomse, S. S., Garcia, R. R., Hardiman, S. C., Horowitz, L. W., Jöckel, P., Josse, B., Kinnison, D., Lin, M., Mancini, E., et al. (2017). Review of the global models used within phase 1 of the Chemistry–Climate Model Initiative (CCMI). *Geoscientific Model Development, 10*(2), 639-671. https://doi.org/10.5194/gmd-10-639-2

59. Polvani, L. M., Previdi, M., England, M. R., Chiodo, G., & Smith, K. L. (2020). Substantial twentieth-century Arctic warming caused by ozone-depleting substances. *Nature Climate Change, 10*(2), 130-133. https://doi.org/10.1038/s41558-019-0677-4

60. Wigley, T. M. L. (1988). Future CFC concentrations under the Montreal Protocol and their greenhouse-effect implications. *Nature, 335*(6188), 333-335. https://doi.org/10.1038/335333a0

61. Myhre, G., Shindell, D., Bréon, F. M., Collins, W., Fuglestvedt, J., Huang, J., Koch, D., Lamarque, J. F., Lee, D., Mendoza, B., Nakajima, T., Robock, A., Stephens, G., Takemura, T., & Zhang, H. (2013). Anthropogenic and natural radiative forcing. In T. F. Stocker, D. Qin, G. K. Plattner, M. Tignor, S. K. Allen, J. Doschung, A. Nauels, Y. Xia, V. Bex, & P. M. Midgley (Eds.), *Climate change 2013: The physical science basis. Contribution of Working Group I to the fifth assessment report of the Intergovernmental Panel on Climate Change, 659-740*. Cambridge, UK: Cambridge University Press. https://doi.org/10.1017/CBO9781107415324.018

62. Velders, G. J. M., Andersen, S. O., Daniel, J. S., Fahey, D. W., & McFarland, M. (2007). The importance of the Montreal Protocol in protecting climate. *Proceedings of the National Academy of Sciences of the United States of America, 104*(12), 4814–4819. https://doi.org/10.1073/pnas.0610328104

63. IPCC. (2021). *Climate Change 2021: The Physical Science Basis. Contribution of Working Group I to the Sixth Assessment Report of the Intergovernmental Panel on Climate Change*, [V. Masson-Delmotte, P. Zhai, A. Pirani, S. L. Connors, C. Péan, S. Berger, N. Caud, Y. Chen, L. Goldfarb, M. I. Gomis, M. Huang, K. Leitzell, E. Lonnoy, J. B. R. Matthews, T. K. Maycock, T. Waterfield, O. Yelekçi, R. Yu, & B. Zhou (Eds.)]. Cambridge University Press, Cambridge, United Kingdom and New York, NY, USA. https://doi.org/10.1017/9781009157896.

64. Ramaswamy, V., Schwarzkopf, M. D., & Shine, K. P. (1992). Radiative forcing of climate from halocarbon-induced global stratospheric ozone loss. *Nature, 355*(6363), 810-812. https://doi.org/10.1038/355810a0

65. Shindell, D., Faluvegi, G., Nazarenko, L., Bowman, K., Lamarque, J.-F., Voulgarakis, A., Schmidt, G. A., Pechony, O., & Ruedy, R. (2013). Attribution of historical ozone forcing to anthropogenic emissions. *Nature Climate Change, 3*(6), 567-570. https://doi.org/10.1038/nclimate1835

66. Morgenstern, O., O'Connor, F. M., Johnson, B. T., Zeng, G., Mulcahy, J. P., Williams, J., Teixeira, J., Michou, M., Nabat, P., Horowitz, L. W., Naik, V., Sentman, L. T., Deushi, M., Bauer, S. E., Tsigaridis, K., Shindell, D. T., & Kinnison, D. E. (2020). Reappraisal of the climate impacts of ozone depleting substances. *Geophysical Research Letters, 47*(20), e2020GL088295. https://doi.org/10.1029/2020gl088295

67. Morgenstern, O., Frith, S. M., Bodeker, G. E., Fioletov, V., & A, R. J. (2021). Reevaluation of total-column ozone trends and of the effective radiative forcing of ozone depleting substances. *Geophysical Research Letters, 48*(21). https://doi.org/10.1029/2021GL095376

68. Checa-Garcia, R., Hegglin, M. I., Kinnison, D., Plummer, D. A., & Shine, K. P. (2018). Historical tropospheric and stratospheric ozone radiative forcing using the CMIP6 database. *Geophysical Research Letters, 45*(7), 3264-3273. https://doi.org/10.1002/2017GL076770

69. Cionni, I., Eyring, V., Lamarque, J. F., Randel, W. J., Stevenson, D. S., Wu, F., Bodeker, G. E., Shepherd, T. G., Shindell, D. T., & Waugh, D. W. (2011). Ozone database in support of CMIP5 simulations: results and corresponding radiative forcing. *Atmospheric Chemistry and Physics, 11*(21), 11267-11292. https://doi.org/10.5194/acp-11-11267-2011

70. Skeie, R. B., Myhre, G., Hodnebrog, Ø., Cameron-Smith, P. J., Deushi, M., Hegglin, M. I., Horowitz, L. W., Kramer, R. J., Michou, M., Mills, M. J., Olivié, D. J. L., Connor, F. M. O., Paynter, D., Samset, B. H., Sellar, A., Shindell, D., Takemura, T., Tilmes, S., & Wu, T. (2020). Historical total ozone radiative forcing derived from CMIP6 simulations. *npj Climate and Atmospheric Science, 3*(1). https://doi.org/10.1038/s41612-020-00131-0

71. Conley, A. J., Lamarque, J. F., Vitt, F., Collins, W. D., & Kiehl, J. (2013). PORT, a CESM tool for the diagnosis of radiative forcing. *Geoscientific Model Development, 6*(2), 469-476. https://doi.org/10.5194/gmd-6-469-2013

72. Chiodo, G., & Polvani, L. M. (2022). New Insights on the Radiative Impacts of Ozone Depleting Substances. *Geophysical Research Letters, 49*(10). https://doi.org/10.1029/2021gl096783

73. IPCC. (2013). *Climate change 2013: The physical science basis. Contribution of Working Group I to the fifth assessment report of the Intergovernmental Panel on Climate Change*, [T. F. Stocker, D. Qin, G.-K. Plattner, M. Tignor, S. K. Allen, J. Boschung, A. Nauels, Y. Xia, V. Bex, & P. M. Midgle (Eds.)]. Cambridge University Press, Cambridge, United Kingdom and New York, USA.

74. Goyal, R., England, M. H., Sen Gupta, A., & Jucker, M. (2019). Reduction in surface climate change achieved by the 1987 Montreal Protocol. *Environmental Research Letters, 14*(12), 124041. https://doi.org/10.1088/1748-9326/ab4874

75. Liang, Y.-C., Polvani, L. M., Previdi, M., Smith, K. L., England, M. R., & Chiodo, G. (2022). Stronger Arctic amplification from ozone-depleting substances than from carbon dioxide. *Environmental Research Letters, 17*(2). https://doi.org/10.1088/1748-9326/ac4a31

76. United Nations. (2016). Amendment to the Montreal Protocol on Substances that Deplete the Ozone Layer. *United Nations Treaty Series*, Number C.N.872.2016.TREATIES-XXVII.2.f. https://treaties.un.org/doc/Treaties/2016/10/20161015%2003-23%20PM/Ch_XXVII-2.f-English%20and%20French.pdf

77. Velders, G. J. M., Daniel, J. S., Montzka, S. A., Vimont, I., Rigby, M., Krummel, P. B., Muhle, J., O'Doherty, S., Prinn, R. G., Weiss, R. F., & Young, D. (2022). Projections of hydrofluorocarbon (HFC) emissions and the resulting global warming based on recent trends in observed abundances and current policies. *Atmospheric Chemistry and Physics, 22*(9), 6087-6101. https://doi.org/10.5194/acp-22-6087-2022

78. Montzka, S. A., Dutton, G. S., Yu, P., Ray, E., Portmann, R. W., Daniel, J. S., Kuijpers, L., Hall, B. D., Mondeel, D., Siso, C., Nance, J. D., Rigby, M., Manning, A. J., Hu, L., Moore, F., Miller, B. R., & Elkins, J. W. (2018). An unexpected and persistent increase in global emissions of ozone-depleting CFC-11. *Nature, 557*(7705), 413-417. https://doi.org/10.1038/s41586-018-0106-2

79. Rigby, M., Park, S., Saito, T., Western, L. M., Redington, A. L., Fang, X., Henne, S., Manning, A. J., Prinn, R. G., Dutton, G. S., Fraser, P. J., Ganesan, A. L., Hall, B. D., Harth, C. M., Kim, J., Kim, K. R., Krummel, P. B., Lee, T., Li, S., Liang, Q., et al. (2019). Increase in CFC-11 emissions from eastern China based on atmospheric observations. *Nature, 569*(7757), 546-550. https://doi.org/10.1038/s41586-019-1193-4

80. Dhomse, S. S., Feng, W., Montzka, S. A., Hossaini, R., Keeble, J., Pyle, J. A., Daniel, J. S., & Chipperfield, M. P. (2019). Delay in recovery of the Antarctic ozone hole from unexpected CFC-11 emissions. *Nature Communications, 10*(1), 5781. https://doi.org/10.1038/s41467-019-13717-x

81. Lickley, M., Solomon, S., Fletcher, S., Velders, G. J. M., Daniel, J., Rigby, M., Montzka, S. A., Kuijpers, L. J. M., & Stone, K. (2020). Quantifying contributions of chlorofluorocarbon banks to emissions and impacts on the ozone layer and climate. *Nature Communications, 11*(1), 1380. https://doi.org/10.1038/s41467-020-15162-7

82. Park, S., Western, L. M., Saito, T., Redington, A. L., Henne, S., Fang, X., Prinn, R. G., Manning, A. J., Montzka, S. A., Fraser, P. J., Ganesan, A. L., Harth, C. M., Kim, J., Krummel, P. B., Liang, Q., Mühle, J., O'Doherty, S., Park, H., Park, M.-K., Reimann, S., et al. (2021). A decline in emissions of CFC-11 and related chemicals from eastern China. *Nature, 590*(7846), 433-437. https://doi.org/10.1038/s41586-021-03277-w

83. Chipperfield, M. P., Hegglin, M. I., Montzka, S. A., Newman, P. A., Park, S., Reimann, S., Rigby, M., Stohl, A., Velders, G. J. M., & Walter-Terrinoni, H. (2021). *Report on unexpected emissions of CFC-11*. WMO Report No. 1268. World Meteorological Organization, Geneva, Switzerland.

84. Montzka, S. A., Dutton, G. S., Portmann, R. W., Chipperfield, M. P., Davis, S., Feng, W., Manning, A. J., Ray, E., Rigby, M., Hall, B. D., Siso, C., Nance, J. D., Krummel, P. B., Mühle, J., Young, D., O'Doherty, S., Salameh, P. K., Harth, C. M., Prinn, R. G., Weiss, R. F., et al. (2021). A decline in global CFC-11 emissions during 2018−2019. *Nature, 590*(7846), 428-432. https://doi.org/10.1038/s41586-021-03260-5

85. Solomon, S., Alcamo, J., & Ravishankara, A. R. (2020). Unfinished business after five decades of ozone-layer science and policy. *Nature Communications, 11*(1), 4272. https://doi.org/10.1038/s41467-020-18052-0

86. Dameris, M., Jöckel, P., & Nützel, M. (2019). Possible implications of enhanced chlorofluorocarbon-11 concentrations on ozone. *Atmospheric Chemistry and Physics, 19*(22), 13759-13771. https://doi.org/10.5194/acp-19-13759-2019

87. Fleming, E. L., Newman, P. A., Liang, Q., & Daniel, J. S. (2020). The Impact of Continuing CFC 11 Emissions on Stratospheric Ozone. *Journal of Geophysical Research: Atmospheres, 125*(3). https://doi.org/10.1029/2019jd031849

88. Keeble, J., Abraham, N. L., Archibald, A. T., Chipperfield, M. P., Dhomse, S., Griffiths, P. T., & Pyle, J. A. (2020). Modelling the potential impacts of the recent, unexpected increase in CFC-11 emissions on total column ozone recovery. *Atmospheric Chemistry and Physics, 20*(12), 7153-7166. https://doi.org/10.5194/acp-20-7153-2020

89. Caldwell, M. M. (1971). Solar UV irradiation and the growth and development of higher plants. In A. C. Giese (Ed.), Current Topics in Photobiology and Photochemistry, *Photophysiology, VI, 131-177*. New York, U.S.A.: Academic Press. https://doi.org/10.1016/B978-0-12-282606-1.50010-6

90. Young, P. J., Harper, A. B., Huntingford, C., Paul, N. D., Morgenstern, O., Newman, P. A., Oman, L. D., Madronich, S., & Garcia, R. R. (2021). The Montreal Protocol protects the terrestrial carbon sink. *Nature, 596*(7872), 384-388. https://doi.org/10.1038/s41586-021-03737-3

91. Ballaré, C. L., Caldwell, M. M., Flint, S. D., Robinson, S. A., & Bornman, J. F. (2011). Effects of solar ultraviolet radiation on terrestrial ecosystems. Patterns, mechanisms, and interactions with climate change. *Photochemical & Photobiological Sciences, 10*(2), 226-241. https://doi.org/10.1039/C0PP90035D

92. Day, T. A. (1993). Relating UV-B radiation screening effectiveness of foliage to absorbing-compound concentration and anatomical characteristics in a diverse group of plants. *Oecologia, 95*(4), 542-550. https://doi.org/10.1007/BF00317439

93. Jansen, M. A. K., Ač, A., Klem, K., & Urban, O. (2022). A meta-analysis of the interactive effects of UV and drought on plants. *Plant, Cell & Environment, 45*(1), 41-54. https://doi.org/10.1111/pce.14221

94. Rozema, J., Björn, L. O., Bornman, J. F., Gaberščik, A., Häder, D. P., Trošt, T., Germ, M., Klisch, M., Gröniger, A., & Sinha, R. P. (2002). The role of UV-B radiation in aquatic and terrestrial ecosystems—an experimental and functional analysis of the evolution of UV-absorbing compounds. *Journal of Photochemistry and Photobiology B: Biology, 66*(1), 2-12. https://doi.org/10.1016/S1011-1344(01)00269-X

95. Waterman, M. J., Nugraha, A. S., Hendra, R., Ball, G. E., Robinson, S. A., & Keller, P. A. (2017). Antarctic moss biflavonoids show high antioxidant and ultraviolet-screening activity. *Journal of Natural Products, 80*(8), 2224-2231. https://doi.org/10.1021/acs.jnatprod.7b00085

96. Williamson, C. E., Zepp, R. G., Lucas, R. M., Madronich, S., Austin, A. T., Ballare, C. L., Norval, M., Sulzberger, B., Bais, A. F., McKenzie, R. L., Robinson, S. A., Häder, D.-P., Paul, N. D., & Bornman, J. F. (2014). Solar ultraviolet radiation in a changing climate. [Review]. *Nature Climate Change, 4*(6), 434-441. https://doi.org/10.1038/nclimate2225

97. Son, S.-W., Han, B.-R., Garfinkel, C. I., Kim, S.-Y., Park, R., Abraham, N. L., Akiyoshi, H., Archibald, A. T., Butchart, N., Chipperfield, M. P., Dameris, M., Deushi, M., Dhomse, S. S., Hardiman, S. C., Jöckel, P., Kinnison, D., Michou, M., Morgenstern, O., O'Connor, F. M., Oman, L. D., et al. (2018). Tropospheric jet response to Antarctic ozone depletion: An update with Chemistry-Climate Model Initiative (CCMI) models. *Environmental Research Letters, 13*(5), 054024. https://doi.org/10.1088/1748-9326/aabf21

98. Seviour, W. J. M., Codron, F., Doddridge, E. W., Ferreira, D., Gnanadesikan, A., Kelley, M., Kostov, Y., Marshall, J., Polvani, L. M., Thomas, J. L., & Waugh, D. W. (2019). The Southern Ocean sea surface temperature response to ozone depletion: a multimodel comparison. *Journal of Climate, 32*(16), 5107-5121. https://doi.org/10.1175/jcli-d-19-0109.1

99. Liu, W., Hegglin, M. I., Checa-Garcia, R., Li, S., Gillett, N. P., Lyu, K., Zhang, X., & Swart, N. C. (2022). Stratospheric ozone depletion and tropospheric ozone increases drive Southern Ocean interior warming. *Nature Climate Change, 12*(4), 365-372. https://doi.org/10.1038/s41558-022-01320-w

100. Lu, X., Zhang, L., Zhao, Y., Jacob, D. J., Hu, Y., Hu, L., Gao, M., Liu, X., Petropavlovskikh, I., McClure-Begley, A., & Querel, R. (2019). Surface and tropospheric ozone trends in the Southern Hemisphere since 1990: possible linkages to poleward expansion of the Hadley circulation. *Science Bulletin, 64*(6), 400-409. https://doi.org/10.1016/j.scib.2018.12.021

101. Turner, J., & Comiso, J. (2017). Solve Antarctica's sea-ice puzzle. *Nature, 547*, 275–277. https://doi.org/10.1038/547275a

102. Turner, J., Phillips, T., Marshall, G. J., Hosking, J. S., Pope, J. O., Bracegirdle, T. J., & Deb, P. (2017). Unprecedented springtime retreat of Antarctic sea ice in 2016. *Geophysical Research Letters, 44*(13), 6868-6875. https://doi.org/10.1002/2017gl073656

103. Parkinson, C. L. (2019). A 40-y record reveals gradual Antarctic sea ice increases followed by decreases at rates far exceeding the rates seen in the Arctic. *Proceedings of the National Academy of Sciences, 116*(29), 14414-14423. https://doi.org/10.1073/pnas.1906556116

104. Gillett, Z. E., Arblaster, J. M., Dittus, A. J., Deushi, M., Jöckel, P., Kinnison, D. E., Morgenstern, O., Plummer, D. A., Revell, L. E., Rozanov, E., Schofield, R., Stenke, A., Stone, K. A., & Tilmes, S. (2019). Evaluating the relationship between interannual variations in the Antarctic ozone hole and Southern Hemisphere surface climate in chemistry–climate models. *Journal of Climate, 32*(11), 3131-3151. https://doi.org/10.1175/jcli-d-18-0273.1

105. Fogt, R. L., & Marshall, G. J. (2020). The Southern Annular Mode: Variability, trends, and climate impacts across the Southern Hemisphere. *WIREs Climate Change, 11*(4), e652. https://doi.org/10.1002/wcc.652

106. Morales, M. S., Cook, E. R., Barichivich, J., Christie, D. A., Villalba, R., LeQuesne, C., Srur, A. M., Ferrero, M. E., Gonzalez-Reyes, A., Couvreux, F., Matskovsky, V., Aravena, J. C., Lara, A., Mundo, I. A., Rojas, F., Prieto, M. R., Smerdon, J. E., Bianchi, L. O., Masiokas, M. H., Urrutia-Jalabert, R., et al. (2020). Six hundred years of South American tree rings reveal an increase in severe hydroclimatic events since mid-20th century. *Proceedings of the National Academy of Sciences of the United States of America, 117*(29), 16816-16823. https://doi.org/10.1073/pnas.2002411117

107. Damiani, A., Cordero, R. R., Llanillo, P. J., Feron, S., Boisier, J. P., Garreaud, R., Rondanelli, R., Irie, H., & Watanabe, S. (2020). Connection between Antarctic ozone and climate: interannual precipitation changes in the Southern Hemisphere. *Atmosphere, 11*(6). https://doi.org/10.3390/atmos11060579

108. Banerjee, A., Fyfe, J. C., Polvani, L. M., Waugh, D., & Chang, K.-L. (2020). A pause in Southern Hemisphere circulation trends due to the Montreal Protocol. *Nature, 579*(7800), 544-548. https://doi.org/10.1038/s41586-020-2120-4

109. Bracegirdle, T. J., Krinner, G., Tonelli, M., Haumann, F. A., Naughten, K. A., Rackow, T., Roach, L. A., & Wainer, I. (2020). Twenty first century changes in Antarctic and Southern Ocean surface climate in CMIP6. *Atmospheric Science Letters, 21*(9), e984. https://doi.org/10.1002/asl.984

110. Lim, E.-P., Hendon, H. H., Boschat, G., Hudson, D., Thompson, D. W. J., Dowdy, A. J., & Arblaster, J. M. (2019). Australian hot and dry extremes induced by weakenings of the stratospheric polar vortex. *Nature Geoscience, 12*(11), 896-901. https://doi.org/10.1038/s41561-019-0456-x

111. Hendon, H. H., Thompson, D. J. W., Lim, E.-P., Butler, A. H., Newman, P. A., Coy, L., Scaife, A., Polichtchouk, I., Garreaud, R. S., T.G., S., & Nakamura, H. (2019). Rare forecasted climate event under way in the Southern Hemisphere. *Nature, 573*(7775), 495. https://doi.org/10.1038/d41586-019-02858-0

112. Lim, E.-P., Hendon, H. H., Butler, A. H., Garreaud, R. D., Polichtchouk, I., Shepherd, T. G., Scaife, A., Comer, R., Coy, L., Newman, P. A., Thompson, D. J. W., & Nakamura, H. (2020). The 2019 Antarctic sudden stratospheric warming. *SPARC Newsletter, 54*, 10-13.

113. Noguchi, S., Kuroda, Y., Kodera, K., & Watanabe, S. (2020). Robust enhancement of tropical convective activity by the 2019 Antarctic sudden stratospheric warming. *Geophysical Research Letters, 47*(15), e2020GL088743. https://doi.org/10.1029/2020GL088743

114. Robinson, S. A., Klekociuk, A. R., King, D. H., Pizarro Rojas, M., Zúñiga, G. E., & Bergstrom, D. M. (2020). The 2019/2020 summer of Antarctic heatwaves. *Global Change Biology, 26*(6), 3178-3180. https://doi.org/10.1111/gcb.15083

115. Newman, P., Nash, E. R., Kramarova, N., & Butler, A. (2020). The 2019 southern stratospheric warming. In T. Scambos, & S. Stammerjohn (Eds.), *"State of the Climate in 2019", Bulletin of the American Meteorological Society, 101*(8), S297-S298. https://doi.org/10.1175/BAMS-D-20-0090.1

116. Lim, E.-P., Hendon, H. H., Butler, A. H., Thompson, D. W. J., Lawrence, Z., Scaife, A. A., Shepherd, T. G., Polichtchouk, I., Nakamura, H., Kobayashi, C., Comer, R., Coy, L., Dowdy, A., Garreaud, R. D., Newman, P. A., & Wang, G. (2021). The 2019 Southern Hemisphere stratospheric polar vortex weakening and its impacts. *Bulletin of the American Meteorological Society, 102*(6), E1150–E1171. https://doi.org/10.1175/BAMS-D-20-0112.1

117. Jucker, M., & Goyal, R. (2022). Ozone-Forced Southern Annular Mode During Antarctic Stratospheric Warming Events. *Geophysical Research Letters, 49*(4). https://doi.org/10.1029/2021gl095270

118. Jucker, M., Reichler, T., & Waugh, D. W. (2021). How frequent are Antarctic sudden stratospheric warmings in present and future climate? *Geophysical Research Letters, 48*(11), e2021GL093215. https://doi.org/10.1029/2021GL093215

119. Kablick III, G. P., Allen, D. R., Fromm, M. D., & Nedoluha, G. E. (2020). Australian PyroCb smoke generates synoptic-scale stratospheric anticyclones. *Geophysical Research Letters, 47*(13), e2020GL088101. https://doi.org/10.1029/2020GL088101

120. Ohneiser, K., Ansmann, A., Kaifler, B., Chudnovsky, A., Barja, B., Knopf, D. A., Kaifler, N., Baars, H., Seifert, P., Villanueva, D., Jimenez, C., Radenz, M., Engelmann, R., Veselovskii, I., & Zamorano, F. (2022). Australian wildfire smoke in the stratosphere: the decay phase in 2020/2021 and impact on ozone depletion. *Atmospheric Chemistry and Physics, 22*(11), 7417-7442. https://doi.org/10.5194/acp-22-7417-2022

121. Ohneiser, K., Ansmann, A., Baars, H., Seifert, P., Barja, B., Jimenez, C., Radenz, M., Teisseire, A., Floutsi, A., Haarig, M., Foth, A., Chudnovsky, A., Engelmann, R., Zamorano, F., Bühl, J., & Wandinger, U. (2020). Smoke of extreme Australian bushfires observed in the stratosphere over Punta Arenas, Chile, in January 2020: optical thickness, lidar ratios, and depolarization ratios at 355 and 532 nm. *Atmospheric Chemistry and Physics, 20*(13), 8003-8015. https://doi.org/10.5194/acp-20-8003-2020

122. Boone, C. D., Bernath, P. F., & Fromm, M. D. (2020). Pyrocumulonimbus stratospheric plume injections measured by the ACE-FTS. *Geophysical Research Letters, 47*(15), e2020GL088442. https://doi.org/10.1029/2020GL088442

123. Khaykin, S., Legras, B., Bucci, S., Sellitto, P., Isaksen, L., Tencé, F., Bekki, S., Bourassa, A., Rieger, L., Zawada, D., Jumelet, J., & Godin-Beekmann, S. (2020). The 2019/20 Australian wildfires generated a persistent smoke-charged vortex rising up to 35 km altitude. *Communications Earth & Environment, 1*(1), 1-12. https://doi.org/10.1038/s43247-020-00022-5

124. Hirsch, E., & Koren, I. (2021). Record-breaking aerosol levels explained by smoke injection into the stratosphere. *Science, 371*(6535), 1269-1274. https://doi.org/10.1126/science.abe1415

125. Allen, D. R., Fromm, M. D., Kablick III, G. P., & Nedoluha, G. E. (2020). Smoke with Induced Rotation and Lofting (SWIRL) in the stratosphere. J*ournal of the Atmospheric Sciences, 77*(12), 4297-4316. https://doi.org/10.1175/JAS-D-20-0131.1

126. Yu, P., Davis, S. M., Toon, O. B., Portmann, R. W., Bardeen, C. G., Barnes, J. E., Telg, H., Maloney, C., & Rosenlof, K. H. (2021). Persistent stratospheric warming due to 2019–2020 Australian wildfire smoke. *Geophysical Research Letters, 48*(7), e2021GL092609. https://doi.org/10.1029/2021GL092609

127. Schwartz, M. J., Santee, M. L., Pumphrey, H. C., Manney, G. L., Lambert, A., Livesey, N. J., Millán, L., Neu, J. L., Read, W. G., & Werner, F. (2020). Australian new year's pyroCb impact on stratospheric composition. *Geophysical Research Letters, 47*(24), e2020GL090831. https://doi.org/10.1029/2020GL090831

128. Anderson, J. G., Wilmouth, D. M., Smith, J. B., & Sayres, D. S. (2012). UV dosage levels in summer: Increased risk of ozone loss from convectively injected water vapor. *Science, 337*(6096), 835-839. https://doi.org/10.1126/science.1222978

129. Schwartz, M. J., Read, W. G., Santee, M. L., Livesey, N. J., Froidevaux, L., Lambert, A., & Manney, G. L. (2013). Convectively injected water vapor in the North American summer lowermost stratosphere. *Geophysical Research Letters, 40*(10), 2316-2321. https://doi.org/10.1002/grl.50421

130. Bernath, P., Boone, C., & Crouse, J. (2022). Wildfire smoke destroys stratospheric ozone. *Science, 375*(6586), 1292-1295. https://doi.org/10.1126/science.abm5611

131. Solomon, S., Dube, K., Stone, K., Yu, P., Kinnison, D., Toon, O. B., Strahan, S. E., Rosenlof, K. H., Portmann, R., Davis, S., Randel, W., Bernath, P., Boone, C., Bardeen, C. G., Bourassa, A., Zawada, D., & Degenstein, D. (2022). On the stratospheric chemistry of midlatitude wildfire smoke. *Proceedings of the National Academy of Sciences, 119*(10), e2117325119. https://doi.org/10.1073/pnas.2117325119

132. Santee, M. L., Lambert, A., Manney, G. L., Livesey, N. J., Froidevaux, L., Neu, J. L., Schwartz, M. J., Millán, L. F., Werner, F., Read, W. G., Park, M., Fuller, R. A., & Ward, B. M. (2022). Prolonged and pervasive perturbations in the composition of the Southern Hemisphere midlatitude lower stratosphere from the Australian New Year's fires. *Geophysical Research Letters, 49*(4). https://doi.org/10.1029/2021GL096270

133. Polvani, L. M., Banerjee, A., Chemke, R., Doddridge, E. W., Ferreira, D., Gnanadesikan, A., Holland, M. A., Kostov, Y., Marshall, J., Seviour, W. J. M., Solomon, S., & Waugh, D. W. (2021). Interannual SAM modulation of Antarctic sea ice extent does not account for its long-term trends, pointing to a limited role for ozone depletion. *Geophysical Research Letters, 48*(21). https://doi.org/10.1029/2021gl094871

134. Haase, S., & Matthes, K. (2019). The importance of interactive chemistry for stratosphere–troposphere coupling. *Atmospheric Chemistry and Physics, 19*(5), 3417-3432. https://doi.org/10.5194/acp-19-3417-2019

135. Zhou, C., Zhang, T., & Zheng, L. (2019). The characteristics of surface albedo change trends over the Antarctic sea ice region during recent decades. *Remote Sensing, 11*(7). https://doi.org/10.3390/rs11070821

136. Meehl, G. A., Arblaster, J. M., Chung, C. T. Y., Holland, M. M., DuVivier, A., Thompson, L., Yang, D., & Bitz, C. M. (2019). Sustained ocean changes contributed to sudden Antarctic sea ice retreat in late 2016. *Nature Communications, 10*(1), 14. https://doi.org/10.1038/s41467-018-07865-9

137. Wang, G., Hendon, H. H., Arblaster, J. M., Lim, E.-P., Abhik, S., & van Rensch, P. (2019). Compounding tropical and stratospheric forcing of the record low Antarctic sea-ice in 2016. *Nature Communications, 10*(1), 13. https://doi.org/10.1038/s41467-018-07689-7

138. Wang, Z., Turner, J., Wu, Y., & Liu, C. (2019). Rapid decline of total Antarctic sea ice extent during 2014–16 controlled by wind-driven sea ice drift. *Journal of Climate, 32*(17), 5381-5395. https://doi.org/10.1175/jcli-d-18-0635.1

139. Doddridge, E. W., & Marshall, J. (2017). Modulation of the seasonal cycle of Antarctic sea ice extent related to the southern annular mode. *Geophysical Research Letters, 44*(19), 9761-9768. https://doi.org/10.1002/2017gl074319

140. Ferreira, D., Marshall, J., Bitz, C. M., Solomon, S., & Plumb, A. (2015). Antarctic ocean and sea ice response to ozone depletion: A two-time-scale problem. *Journal of Climate, 28*(3), 1206–1226. https://doi.org/10.1175/jcli-d-14-00313.1

141. Seviour, W. J. M., Codron, F., Doddridge, E. W., Ferreira, D., Gnanadesikan, A., Kelley, M., Kostov, Y., Marshall, J., Polvani, L.M., Thomas, J. L., & Waugh, D. W. The Southern Ocean sea surface temperature response to ozone depletion: A multimodel comparison. *Journal of Climate, 32*(16), 5107–5121. https://doi.org/10.1175/jcli-d-19-0109.1

142. Xia, Y., Hu, Y., Liu, J., Huang, Y., Xie, F., & Lin, J. (2020). Stratospheric ozone-induced cloud radiative effects on Antarctic sea ice. *Advances in Atmospheric Sciences, 37*(5), 505-514. https://doi.org/10.1007/s00376-019-8251-6

143. Li, S., Liu, W., Lyu, K., & Zhang, X. (2021). The effects of historical ozone changes on Southern Ocean heat uptake and storage. *Climate Dynamics, 57*(7-8), 2269-2285. https://doi.org/10.1007/s00382-021-05803-y

144. England, M., Polvani, L., & Sun, L. (2018). Contrasting the Antarctic and Arctic atmospheric responses to projected sea ice loss in the late twenty-first century. *Journal of Climate, 3*1(16), 6353-6370. https://doi.org/10.1175/jcli-d-17-0666.1

145. Doddridge, E. W., Marshall, J., Song, H., Campin, J.-M., & Kelley, M. (2021). Southern Ocean heat storage, reemergence, and winter sea ice decline induced by summertime winds. *Journal of Climate, 34*(4), 1403-1415. https://doi.org/10.1175/jcli-d-20-0322.1

146. Jakobs, C. L., Reijmer, C. H., van den Broeke, M. R., van de Berg, W. J., & van Wessem, J. M. (2021). Spatial variability of the snowmelt albedo feedback in Antarctica. *Journal of Geophysical Research: Earth Surface, 126*(2). https://doi.org/10.1029/2020jf005696

147. Bergstrom, A., Gooseff, M. N., Myers, M., Doran, P. T., & Cross, J. M. (2020). The seasonal evolution of albedo across glaciers and the surrounding landscape of Taylor Valley, Antarctica. *The Cryosphere, 14*(3), 769-788. https://doi.org/10.5194/tc-14-769-2020

148. Schneider, D. P., Kay, J. E., & Lenaerts, J. (2020). Improved clouds over Southern Ocean amplify Antarctic precipitation response to ozone depletion in an earth system model. *Climate Dynamics, 55*(5-6), 1665-1684. https://doi.org/10.1007/s00382-020-05346-8

149. Lenaerts, J. T. M., Fyke, J., & Medley, B. (2018). The signature of ozone depletion in recent Antarctic precipitation change: a study with the Community Earth System Model. *Geophysical Research Letters, 45*(23). https://doi.org/10.1029/2018gl078608

150. Friedel, M., Chiodo, G., Stenke, A., Domeisen, D. I. V., Fueglistaler, S., Anet, J. G., & Peter, T. (2022). Springtime arctic ozone depletion forces northern hemisphere climate anomalies. *Nature Geoscience, 15*(7), 541-547. https://doi.org/10.1038/s41561-022-00974-7

151. Domeisen, D. I. V., & Butler, A. H. (2020). Stratospheric drivers of extreme events at the Earth's surface. *Communications Earth & Environment, 1*(1), 1-8. https://doi.org/10.1038/s43247-020-00060-z

152. Xia, Y., Hu, Y., Huang, Y., Zhao, C., Xie, F., & Yang, Y. (2021). Significant contribution of severe ozone loss to the Siberian-Arctic surface warming in spring 2020. *Geophysical Research Letters, 48*(8), e2021GL092509. https://doi.org/10.1029/2021GL092509

153. Overland, J. E., & Wang, M. (2021). The 2020 Siberian heat wave. *International Journal of Climatology, 41*, E2341-E2346. https://doi.org/10.1002/joc.6850

154. Zhang, J., Tian, W., Pyle, J. A., Keeble, J., Abraham, N. L., Chipperfield, M. P., Xie, F., Yang, Q., Mu, L., Ren, H.-L., Wang, L., & Xu, M. (2022). Responses of Arctic sea ice to stratospheric ozone depletion. *Science Bulletin, 67*(11), 1182-1190. https://doi.org/10.1016/j.scib.2022.03.015

155. Baldwin, M. P., Ayarzagüena, B., Birner, T., Butchart, N., Butler, A. H., Charlton-Perez, A. J., Domeisen, D. I. V., Garfinkel, C. I., Garny, H., Gerber, E. P., Hegglin, M. I., Langematz, U., & Pedatella, N. M. (2021). Sudden Stratospheric Warmings. *Reviews of Geophysics, 59*(1). https://doi.org/10.1029/2020rg000708

156. Butler, A. H., & Lee, S. H. (2022). The 2020 Arctic Sudden Stratospheric Warming. In R. Thoman, M. L. Druckenmiller, & T. Moon (Eds.), *"State of the Climate in 2021", Bulletin of the American Meteorological Society, 103*(8), S296-S298. https://doi.org/10.1175/BAMS-D-22-0082.1

157. Huang, J., Hitchcock, P., Maycock, A. C., McKenna, C. M., & Tian, W. (2021). Northern hemisphere cold air outbreaks are more likely to be severe during weak polar vortex conditions. *Communications Earth & Environment, 2*(1). https://doi.org/10.1038/s43247-021-00215-6

158. Zhang, M., Yang, X. Y., & Huang, Y. (2022). Impacts of Sudden Stratospheric Warming on extreme cold events in early 2021: An ensemble based sensitivity analysis. *Geophysical Research Letters, 49*(2). https://doi.org/10.1029/2021GL096840

159. Xie, F., Ma, X., Li, J., Huang, J., Tian, W., Zhang, J., Hu, Y., Sun, C., Zhou, X., Feng, J., & Yang, Y. (2018). An advanced impact of Arctic stratospheric ozone changes on spring precipitation in China. *Climate Dynamics, 51*(11-12), 4029-4041. https://doi.org/10.1007/s00382-018-4402-1

160. Stone, K. A., Solomon, S., Kinnison, D. E., Baggett, C. F., & Barnes, E. A. (2019). Prediction of Northern Hemisphere regional surface temperatures using stratospheric ozone information. *Journal of Geophysical Research: Atmospheres, 124*(12), 5922-5933. https://doi.org/10.1029/2018jd029626

161. Ma, X., Xie, F., Li, J., Zheng, X., Tian, W., Ding, R., Sun, C., & Zhang, J. (2019). Effects of Arctic stratospheric ozone changes on spring precipitation in the northwestern United States. *Atmospheric Chemistry and Physics, 19*(2), 861-875. https://doi.org/10.5194/acp-19-861-2019

162. Bais, A. F., McKenzie, R. L., Bernhard, G., Aucamp, P. J., Ilyas, M., Madronich, S., & Tourpali, K. (2015). Ozone depletion and climate change: Impacts on UV radiation. *Photochemical & Photobiological Sciences, 14*(1), 19-52. https://doi.org/10.1039/c4pp90032d

163. McKenzie, R. L., Aucamp, P. J., Bais, A. F., Björn, L. O., Ilyas, M., & Madronich, S. (2011). Ozone depletion and climate change: impacts on UV radiation. *Photochemical & Photobiological Sciences, 10*(2), 182-198. https://doi.org/10.1039/c0pp90034f

164. Campanelli, M., Diémoz, H., Siani, A. M., di Sarra, A., Iannarelli, A. M., Kudo, R., Fasano, G., Casasanta, G., Tofful, L., Cacciani, M., Sanò, P., & Dietrich, S. (2022). Aerosol optical characteristics in the urban area of Rome, Italy, and their impact on the UV index. *Atmospheric Measurement Techniques, 15*(5), 1171-1183. https://doi.org/10.5194/amt-15-1171-2022

165. Mok, J., Krotkov, N. A., Arola, A., Torres, O., Jethva, H., Andrade, M., Labow, G., Eck, T. F., Li, Z., & Dickerson, R. R. (2016). Impacts of brown carbon from biomass burning on surface UV and ozone photochemistry in the Amazon Basin. *Scientific Reports, 6*, 36940. https://doi.org/10.1038/srep36940

166. Carlund, T., Kouremeti, N., Kazadzis, S., & Gröbner, J. (2017). Aerosol optical depth determination in the UV using a four-channel precision filter radiometer. *Atmospheric Measurement Techniques, 10*(3), 905-923. https://doi.org/10.5194/amt-10-905-2017

167. López-Solano, J., Redondas, A., Carlund, T., Rodriguez-Franco, J. J., Diémoz, H., León-Luis, S. F., Hernández-Cruz, B., Guirado-Fuentes, C., Kouremeti, N., Gröbner, J., Kazadzis, S., Carreño, V., Berjón, A., Santana-Díaz, D., Rodríguez-Valido, M., De Bock, V., Moreta, J. R., Rimmer, J., Smedley, A. R. D., Boulkelia, L., et al. (2018). Aerosol optical depth in the European Brewer Network. *Atmospheric Chemistry and Physics, 18*(6), 3885-3902. https://doi.org/10.5194/acp-18-3885-2018

168. Mok, J., Krotkov, N. A., Torres, O., Jethva, H., Li, Z., Kim, J., Koo, J.-H., Go, S., Irie, H., Labow, G., Eck, T. F., Holben, B. N., Herman, J., Loughman, R. P., Spinei, E., Lee, S. S., Khatri, P., & Campanelli, M. (2018). Comparisons of spectral aerosol single scattering albedo in Seoul, South Korea. *Atmospheric Measurement Techniques, 11*(4), 2295-2311. https://doi.org/10.5194/amt-11-2295-2018

169. Fountoulakis, I., Natsis, A., Siomos, N., Drosoglou, T., & Bais, A. F. (2019). Deriving Aerosol Absorption Properties from Solar Ultraviolet Radiation Spectral Measurements at Thessaloniki, Greece. *Remote Sensing, 11*(18), 2179. https://doi.org/10.3390/rs11182179

170. Rimmer, J. S., Redondas, A., & Karppinen, T. (2018). EuBrewNet – A European Brewer network (COST Action ES1207), an overview. *Atmospheric Chemistry and Physics, 18*(14), 10347-10353. https://doi.org/10.5194/acp-18-10347-2018

171. Ipiña, A., López-Padilla, G., Retama, A., Piacentini, R. D., & Madronich, S. (2021). Ultraviolet radiation environment of a tropical megacity in transition: Mexico City 2000–2019. *Environmental Science & Technology, 55*(16), 10946-10956. https://doi.org/10.1021/acs.est.0c08515

172. Wilson, S. R., Madronich, S., Longstreth, J. D., & Solomon, K. R. (2019). Interactive effects of changing stratospheric ozone and climate on tropospheric composition and air quality, and the consequences for human and ecosystem health. *Photochemical & Photobiological Sciences, 18*(3), 775-803. https://doi.org/10.1039/c8pp90064g

173. Moses, E., Cardenas, B., Nagpure, A., & Pai, M. (2020). *Can An Airshed Governance Framework in India Spur Clean Air for All? Lessons from Mexico City and Los Angeles: Policy Brief*, CCAPC/2020/01, Collaborative Clean Air Policy Centre, New Delhi, India.

174. Cabrera, S., Ipiña, A., Damiani, A., Cordero, R. R., & Piacentini, R. D. (2012). UV index values and trends in Santiago, Chile (33.5°S) based on ground and satellite data. *Journal of Photochemistry & Photobiology B: Biology, 115*, 73-84. https://doi.org/10.1016/j.jphotobiol.2012.06.013

175. Roshan, D. R., Koc, M., Abdallah, A., Martin-Pomares, L., Isaifan, R., & Fountoukis, C. (2020). UV Index forecasting under the influence of desert dust: evaluation against surface and satellite-retrieved data. *Atmosphere, 11*(1). https://doi.org/10.3390/atmos11010096

176. du Preez, D. J., Bencherif, H., Portafaix, T., Lamy, K., & Wright, C. Y. (2021). Solar ultraviolet radiation in Pretoria and its relations to aerosols and tropospheric ozone during the biomass burning season. *Atmosphere, 12*(2). https://doi.org/10.3390/atmos12020132

177. Diffey, B. L., Jansén, C. T., Urbach, F., & Wulf, H. C. (1997). The standard erythema dose: a new photobiological concept. *Photodermatology, Photoimmunology and Photomedicine, 13*(1-2), 64-66. https://doi.org/10.1111/j.1600-0781.1997.tb00110.x

178. Fitzpatrick, T. B. (1988). The Validity and Practicality of Sun-Reactive Skin Types I Through VI. *Archives of Dermatology, 124*(6), 869-871. https://doi.org/10.1001/archderm.1988.01670060015008

179. McKenzie, R. L., Liley, J. B., & Björn, L. O. (2009). UV Radiation: Balancing Risks and Benefits. *Photochemistry and Photobiology, 85*, 88-98. https://doi.org/10.1111/j.1751-1097.2008.00400.x

180. Igoe, D. P., Parisi, A. V., Downs, N. J., & Butler, H. (2022). A case study of UV exposure risk in Sydney during the 2019/2020 New South Wales bushfires. *Photochemistry and Photobiology, 98*(5), 1236-1244. https://doi.org/10.1111/php.13603

181. ICNIRP (2010). ICNIRP Statement—Protection of workers against ultraviolet radiation. *Health Physics, 99*(1), 66-87. https://doi.org/10.1097/HP.0b013e3181d85908

182. Mortier, A., Gliß, J., Schulz, M., Aas, W., Andrews, E., Bian, H., Chin, M., Ginoux, P., Hand, J., Holben, B., Zhang, H., Kipling, Z., Kirkevåg, A., Laj, P., Lurton, T., Myhre, G., Neubauer, D., Olivié, D., von Salzen, K., Skeie, R. B., et al. (2020). Evaluation of climate model aerosol trends with ground-based observations over the last 2 decades – an AeroCom and CMIP6 analysis. *Atmospheric Chemistry and Physics, 20*(21), 13355-13378. https://doi.org/10.5194/acp-20-13355-2020

183. Tong, D., Cheng, J., Liu, Y., Yu, S., Yan, L., Hong, C., Qin, Y., Zhao, H., Zheng, Y., Geng, G., Li, M., Liu, F., Zhang, Y., Zheng, B., Clarke, L., & Zhang, Q. (2020). Dynamic projection of anthropogenic emissions in China: methodology and 2015–2050 emission pathways under a range of socio-economic, climate policy, and pollution control scenarios. *Atmospheric Chemistry and Physics, 20*(9), 5729-5757. https://doi.org/10.5194/acp-20-5729-2020

184. Drugé, T., Nabat, P., Mallet, M., & Somot, S. (2021). Future evolution of aerosols and implications for climate change in the Euro-Mediterranean region using the CNRM-ALADIN63 regional climate model. *Atmospheric Chemistry and Physics, 21*(10), 7639-7669. https://doi.org/10.5194/acp-21-7639-2021

185. Millán, L. F., & Manney, G. L. (2017). An assessment of ozone mini-hole representation in reanalyses over the Northern Hemisphere. *Atmospheric Chemistry and Physics, 17*(15), 9277-9289. https://doi.org/10.5194/acp-17-9277-2017

186. Raptis, I.-P., Eleftheratos, K., Kazadzis, S., Kosmopoulos, P., Papachristopoulou, K., & Solomos, S. (2021). The combined effect of ozone and aerosols on erythemal irradiance in an extremely low ozone event during May 2020. *Atmosphere, 12*(2). https://doi.org/10.3390/atmos12020145

187. Becherini, F., Vitale, V., Lupi, A., Stone, R. S., Salvatori, R., Salzano, R., di Carlo, P., Viola, A. P., & Mazzola, M. (2021). Surface albedo and spring snow melt variations at Ny-Ålesund, Svalbard. *Bulletin of Atmospheric Science and Technology, 2*(1-4). https://doi.org/10.1007/s42865-021-00043-8

188. Brunt, K. M., Sergienko, O., & MacAyeal, D. R. (2017). Observations of unusual fast-ice conditions in the southwest Ross Sea, Antarctica: preliminary analysis of iceberg and storminess effects. *Annals of Glaciology, 44*, 183-187. https://doi.org/10.3189/172756406781811754

189. Kim, S., Saenz, B., Scanniello, J., Daly, K., & Ainley, D. (2018). Local climatology of fast ice in McMurdo Sound, Antarctica. *Antarctic Science, 30*(2), 125-142. https://doi.org/10.1017/s0954102017000578

190. Bernhard, G., & Stierle, S. (2020). Trends of UV radiation in Antarctica. *Atmosphere, 11*(8), 795. https://doi.org/10.3390/atmos11080795

191. Gordon, E. M., Seppälä, A., Funke, B., Tamminen, J., & Walker, K. A. (2021). Observational evidence of energetic particle precipitation NOx (EPP-NOx) interaction with chlorine curbing Antarctic ozone loss. *Atmospheric Chemistry and Physics, 21*(4), 2819-2836. https://doi.org/10.5194/acp-21-2819-2021

192. Gordon, E. M., Seppälä, A., & Tamminen, J. (2020). Evidence for energetic particle precipitation and quasi-biennial oscillation modulations of the Antarctic NO_2 springtime stratospheric column from OMI observations. *Atmospheric Chemistry and Physics, 20*(11), 6259-6271. https://doi.org/10.5194/acp-20-6259-2020

193. Haigh, J. D., Winning, A. R., Toumi, R., & Harder, J. W. (2010). An influence of solar spectral variations on radiative forcing of climate. *Nature, 467*(7316), 696-699. https://doi.org/10.1038/nature09426

194. Xiao, Z.-N., Dong, S., & Zhong, Q. (2019). Numerical simulation of climate response to ultraviolet irradiation forcing. *Advances in Climate Change Research, 10*(3), 133-142. https://doi.org/10.1016/j.accre.2019.07.001

195. Roy, I., & Haigh, J. D. (2011). The influence of solar variability and the quasi-biennial oscillation on lower atmospheric temperatures and sea level pressure. *Atmospheric Chemistry and Physics, 11*(22), 11679-11687. https://doi.org/10.5194/acp-11-11679-2011

196. Arsenovic, P., Rozanov, E., Anet, J., Stenke, A., Schmutz, W., & Peter, T. (2018). Implications of potential future grand solar minimum for ozone layer and climate. *Atmospheric Chemistry and Physics, 18*(5), 3469-3483. https://doi.org/10.5194/acp-18-3469-2018

197. Miyahara, H., Tokanai, F., Moriya, T., Takeyama, M., Sakurai, H., Horiuchi, K., & Hotta, H. (2021). Gradual onset of the Maunder Minimum revealed by high-precision carbon-14 analyses. *Scientific Reports, 11*(1). https://doi.org/10.1038/s41598-021-84830-5

198. Ineson, S., Maycock, A. C., Gray, L. J., Scaife, A. A., Dunstone, N. J., Harder, J. W., Knight, J. R., Lockwood, M., Manners, J. C., & Wood, R. A. (2015). Regional climate impacts of a possible future grand solar minimum. *Nature Communications, 6*(1). https://doi.org/10.1038/ncomms853

199. Kitiashvili, I. N. (2020). Application of synoptic magnetograms to global solar activity forecast. *The Astrophysical Journal, 890*(1). https://doi.org/10.3847/1538-4357/ab64e7

200. Zharkova, V. (2020). Modern grand solar minimum will lead to terrestrial cooling. *Temperature, 7*(3), 217-222. https://doi.org/10.1080/23328940.2020.1796243

201. Stone, K. A., Solomon, S., Kinnison, D. E., Pitts, M. C., Poole, L. R., Mills, M. J., Schmidt, A., Neely, R. R., Ivy, D., Schwartz, M. J., Vernier, J.-P., Johnson, B. J., Tully, M. B., Klekociuk, A. R., König-Langlo, G., & Hagiya, S. (2017). Observing the impact of Calbuco volcanic aerosols on south polar ozone depletion in 2015. *Journal of Geophysical Research: Atmospheres, 122*(21), 11862-11879. https://doi.org/10.1002/2017JD026987

202. Arnold, F., Bührke, T., & Qiu, S. (1990). Evidence for stratospheric ozone-depleting heterogeneous chemistry on volcanic aerosols from El Chichón. *Nature, 348*(6296), 49-50. https://doi.org/10.1038/348049a0

203. Brasseur, G., & Granier, C. (1992). Mount Pinatubo aerosols, chlorofluorocarbons, and ozone depletion. *Science, 257*(5074), 1239-1242. https://doi.org/10.1126/science.257.5074.1239

204. Osipov, S., Stenchikov, G., Tsigaridis, K., LeGrande, A. N., Bauer, S. E., Fnais, M., & Lelieveld, J. (2021). The Toba supervolcano eruption caused severe tropical stratospheric ozone depletion. *Communications Earth & Environment, 2*(1). https://doi.org/10.1038/s43247-021-00141-7

205. Labitzke, K., & McCormick, M. P. (1992). Stratospheric temperature increases due to Pinatubo aerosols. *Geophysical Research Letters, 19*(2), 207-210. https://doi.org/10.1029/91GL02940

206. Brenna, H., Kutterolf, S., & Krüger, K. (2019). Global ozone depletion and increase of UV radiation caused by pre-industrial tropical volcanic eruptions. *Scientific Reports, 9*(1). https://doi.org/10.1038/s41598-019-45630-0

207. Ming, A., Winton, V. H. L., Keeble, J., Abraham, N. L., Dalvi, M. C., Griffiths, P., Caillon, N., Jones, A. E., Mulvaney, R., Savarino, J., Frey, M. M., & Yang, X. (2020). Stratospheric ozone changes from explosive tropical volcanoes: modeling and ice core constraints. *Journal of Geophysical Research: Atmospheres, 125*(11). https://doi.org/10.1029/2019JD032290

208. Krüger, K., Kutterolf, S., Hansteen, T. H., Schmidt, A., Fristad, K. E., & Elkins-Tanton, L. T. (2015). Halogen release from Plinian eruptions and depletion of stratospheric ozone. In *Volcanism and Global Environmental Change*, 244-259: Cambridge Univ. Press. https://doi.org/10.1017/cbo9781107415683.020

209. Mankin, W. G., Coffey, M. T., & Goldman, A. (1992). Airborne observations of SO_2, HCl, and O_3 in the stratospheric plume of the Pinatubo volcano in July 1991. *Geophysical Research Letters, 19*(2), 179-182. https://doi.org/10.1029/91gl02942

210. Zaratti, F., Piacentini, R. D., Guillén, H. A., Cabrera, S. H., Liley, J. B., & McKenzie, R. L. (2014). Proposal for a modification of the UVI risk scale. *Photochemical & Photobiological Sciences, 13*(7), 980-985. https://doi.org/10.1039/C4PP00006D

211. Norris, J. R., Allen, R. J., Evan, A. T., Zelinka, M. D., O'Dell, C. W., & Klein, S. A. (2016). Evidence for climate change in the satellite cloud record. *Nature, 536*(7614), 72-75. https://doi.org/10.1038/nature18273

212. Bodas-Salcedo, A., Hill, P. G., Furtado, K., Williams, K. D., Field, P. R., Manners, J. C., Hyder, P., & Kato, S. (2016). Large contribution of supercooled liquid clouds to the solar radiation budget of the Southern Ocean. *Journal of Climate, 29*(11), 4213-4228. https://doi.org/10.1175/JCLI-D-15-0564.1

213. Cherian, R., & Quaas, J. (2020). Trends in AOD, clouds, and cloud radiative effects in satellite data and CMIP5 and CMIP6 model simulations over aerosol source regions. *Geophysical Research Letters, 47*(9). https://doi.org/10.1029/2020gl087132

214. Wu, D. L., Lee, J. N., Kim, K.-M., & Lim, Y.-K. (2020). Interannual variations of TOA albedo over the Arctic, Antarctic and Tibetan Plateau in 2000–2019. *Remote Sensing, 12*(9). https://doi.org/10.3390/rs12091460

215. Bernhard, G. H., Fioletov, V. E., Grooß, J.-U., Ialongo, I., Johnsen, B., Lakkala, K., Manney, G. L., & Müller, R. (2019). Ozone and UV radiation. In J. Richter-Menge, E. Osborne, M. Druckenmiller, & M. O. Jeffries (Eds.), *"State of the Climate in 2018", Bulletin of the American Meteorological Society, 100*(9), S165-S168. https://doi.org/10.1175/2019BAMSStateoftheClimate.1

216. Rösner, B., Benedict, I., Van Heerwaarden, C., Weerts, A., Hazeleger, W., Bissolli, P., & Trachte, K. (2019). The long heat wave and drought in Europe in 2018. In *"State of the Climate in 2018", Bulletin of the American Meteorological Society, 100*(9), S222-S223. https://doi.org/10.1175/2019BAMSStateoftheClimate.1

217. Marín, J. C., Bozkurt, D., & Barrett, B. S. (2022). Atmospheric blocking trends and seasonality around the Antarctic Peninsula. *Journal of Climate, 35*(12), 3803-3818. https://doi.org/10.1175/jcli-d-21-0323.1

218. Wachowicz, L. J., Preece, J. R., Mote, T. L., Barrett, B. S., & Henderson, G. R. (2020). Historical trends of seasonal Greenland blocking under different blocking metrics. I*nternational Journal of Climatology, 41*(S1). https://doi.org/10.1002/joc.6923

219. Woollings, T., Barriopedro, D., Methven, J., Son, S.-W., Martius, O., Harvey, B., Sillmann, J., Lupo, A. R., & Seneviratne, S. (2018). Blocking and its response to climate change. *Current Climate Change Reports, 4*(3), 287-300. https://doi.org/10.1007/s40641-018-0108-z

220. Dobson, G. M. B., Brewer, A. W., & Cwilong, B. M. (1946). Bakerian Lecture: Meteorology of the lower stratosphere. Proceedings of the Royal Society of London. Series A. *Mathematical, Physical and Engineering Sciences, 185*(1001), 144-175. https://doi.org/10.1098/rspa.1946.0010

221. Steinbrecht, W., Claude, H., Köhler, U., & Hoinka, K. P. (1998). Correlations between tropopause height and total ozone: Implications for long-term changes. *Journal of Geophysical Research: Atmospheres, 103*(D15), 19183-19192. https://doi.org/10.1029/98JD01929

222. Hommel, R., Eichmann, K. U., Aschmann, J., Bramstedt, K., Weber, M., von Savigny, C., Richter, A., Rozanov, A., Wittrock, F., Khosrawi, F., Bauer, R., & Burrows, J. P. (2014). Chemical ozone loss and ozone mini-hole event during the Arctic winter 2010/2011 as observed by SCIAMACHY and GOME-2. *Atmospheric Chemistry and Physics, 14*(7), 3247-3276. https://doi.org/10.5194/acp-14-3247-2014

223. Fountoulakis, I., Diémoz, H., Siani, A. M., di Sarra, A., Meloni, D., & Sferlazzo, D. M. (2021). Variability and trends in surface solar spectral ultraviolet irradiance in Italy: on the influence of geopotential height and lower-stratospheric ozone. *Atmospheric Chemistry and Physics, 21*(24), 18689-18705. https://doi.org/10.5194/acp-21-18689-2021

224. Lin, P., Paynter, D., Ming, Y., & Ramaswamy, V. (2017). Changes of the tropical tropopause layer under global warming. *Journal of Climate, 30*(4), 1245-1258. https://doi.org/10.1175/JCLI-D-16-0457.1

225. Meng, L., Liu, J., Tarasick, D. W., Randel, W. J., Steiner, A. K., Wilhelmsen, H., Wang, L., & Haimberger, L. (2021). Continuous rise of the tropopause in the Northern Hemisphere over 1980–2020. *Science Advances, 7*(45). https://doi.org/10.1126/sciadv.abi8065

226. Ball, W. T., Alsing, J., Mortlock, D. J., Staehelin, J., Haigh, J. D., Peter, T., Tummon, F., Stübi, R., Stenke, A., Anderson, J., Bourassa, A., Davis, S. M., Degenstein, D., Frith, S., Froidevaux, L., Roth, C., Sofieva, V., Wang, R., Wild, J., Yu, P., et al. (2018). Evidence for a continuous decline in lower stratospheric ozone offsetting ozone layer recovery. *Atmospheric Chemistry and Physics, 18*(2), 1379-1394. https://doi.org/10.5194/acp-18-1379-2018

227. McKenzie, R., Liley, B., Kotkamp, M., Geddes, A., Querel, R., Stierle, S., Lantz, K., Rhodes, S., & Madronich, S. (2022). Relationship between ozone and biologically relevant UV at 4 NDACC sites. *Photochemical & Photobiological Sciences*. https://doi.org/10.1007/s43630-022-00281-5

228. Booth, C. R., Lucas, T. B., Morrow, J. H., Weiler, C. S., & Penhale, P. A. (1994). The United States National Science Foundation's polar network for monitoring ultraviolet radiation. In C. S. Weiler, & P. A. Penhale (Eds.), *Ultraviolet radiation in Antarctica: Measurements and biological effects, 62*, 17-37: American Geophysical Union, Washington, D.C. https://doi.org/10.1029/AR062p0017

229. Bernhard, G., Booth, C. R., & Ehramjian, J. C. (2004). Version 2 data of the National Science Foundation's ultraviolet radiation monitoring network: South Pole. Journal of Geophysical Research: *Atmospheres, 109*(D21), D21207. https://doi.org/10.1029/2004jd004937

230. Bernhard, G. H., McKenzie, R. L., Lantz, K., & Stierle, S. (2022). Updated analysis of data from Palmer Station, Antarctica (64° S), and San Diego, California (32° N), confirms large effect of the Antarctic ozone hole on UV radiation. *Photochemical & Photobiological Sciences, 21*(3), 373-384. https://doi.org/10.1007/s43630-022-00178-3

231. Cordero, R. R., Damiani, A., Jorquera, J., Sepúlveda, E., Caballero, M., Fernandez, S., Feron, S., Llanillo, P. J., Carrasco, J., Laroze, D., & Labbe, F. (2018). Ultraviolet radiation in the Atacama Desert. *Antonie van Leeuwenhoek, 111*(8), 1301-1313. https://doi.org/10.1007/s10482-018-1075-z

232. McKenzie, R. L., & Lucas, R. M. (2018). Reassessing impacts of extended daily exposure to low level solar UV radiation. *Scientific Reports, 8*(1), 13805. https://doi.org/10.1038/s41598-018-32056-3

233. Kirchhoff, V. W. J. H., Sahai, Y., Casiccia S., C. A. R., Zamorano B., F., & Valderrama V., V. (1997). Observations of the 1995 ozone hole over Punta Arenas, Chile. *Journal of Geophysical Research, 102*(D13), 16,109-116,120. https://agupubs.onlinelibrary.wiley.com/doi/abs/10.1029/97JD00276

234. du Preez, D. J., Ajtić, J. V., Bencherif, H., Bègue, N., Cadet, J.-M., & Wright, C. Y. (2019). Spring and summer time ozone and solar ultraviolet radiation variations over Cape Point, South Africa. *Annales Geophysicae, 37*(2), 129-141. https://doi.org/10.5194/angeo-37-129-2019

235. Bernhard, G. H., Fioletov, V. E., Grooß, J.-U., Ialongo, I., Johnsen, B., Lakkala, K., Manney, G. L., Müller, R., & Svendby, T. (2021). Ozone and ultraviolet radiation. In J. Blunden, & T. Boyer (Eds.), *"State of the Climate in 2020", Bulletin of the American Meteorological Society, 102*(8), S299–S303. https://doi.org/10.1175/BAMS-D-21-0086.1

236. Bernhard, G. H., Fioletov, V. E., Grooß, J. U., Ialongo, I., Johnsen, B., Lakkala, K., Manney, G. L., Müller, R., & Svendby, T. (2020). Record-Breaking Increases in Arctic Solar Ultraviolet Radiation Caused by Exceptionally Large Ozone Depletion in 2020. *Geophysical Research Letters, 47*(24), e2020GL090844. https://doi.org/10.1029/2020gl090844

237. Bhartia, P. K., & Wellemeyer, C. W. (2002). TOMS-V8 total O_3 algorithm. In *OMI Algorithm Theoretical Basis Document Volume II.*, 15–31. NASA Goddard Space Flight Center Tech. Doc. ATBD-OMI-02

238. Parra, R., Cadena, E., & Flores, C. (2019). Maximum UV index records (2010–2014) in Quito (Ecuador) and its trend inferred from remote sensing data (1979–2018). *Atmosphere, 10*(12), 787. https://doi.org/10.3390/atmos10120787

239. Rivas, M., Rojas, E., & Madronich, S. (2008). Aumento Del Índice Solar Ultravioleta Con La Altura. *Ingeniare. Revista chilena de ingeniería, 16*(2). https://doi.org/10.4067/S0718-33052008000200013

240. Fountoulakis, I., Zerefos, C. S., Bais, A. F., Kapsomenakis, J., Koukouli, M.-E., Ohkawara, N., Fioletov, V., De Backer, H., Lakkala, K., Karppinen, T., & Webb, A. R. (2018). Twenty-five years of spectral UV-B measurements over Canada, Europe and Japan: Trends and effects from changes in ozone, aerosols, clouds, and surface reflectivity. *Comptes Rendus Geoscience, 350*(7), 393-402. https://doi.org/10.1016/j.crte.2018.07.011

241. Zhang, H., Wang, J., Castro García, L., Zeng, J., Dennhardt, C., Liu, Y., & Krotkov, N. A. (2019). Surface erythemal UV irradiance in the continental United States derived from ground-based and OMI observations: quality assessment, trend analysis and sampling issues. *Atmospheric Chemistry and Physics, 19*(4), 2165-2181. https://doi.org/10.5194/acp-19-2165-2019

242. Chubarova, N. E., Pastukhova, A. S., Zhdanova, E. Y., Volpert, E. V., Smyshlyaev, S. P., & Galin, V. Y. (2020). Effects of ozone and clouds on temporal variability of surface UV radiation and UV resources over Northern Eurasia derived from measurements and modeling. *Atmosphere, 11*(1), 59. https://doi.org/10.3390/atmos11010059

243. Chubarova, N. E., Pastukhova, A. S., Galin, V. Y., & Smyshlyaev, S. P. (2018). Long-term variability of UV irradiance in the Moscow region according to measurement and modeling data. Izvestiya, *Atmospheric and Oceanic Physics, 54*(2), 139-146. https://doi.org/10.1134/s0001433818020056

244. Aun, M., Eerme, K., Ansko, I., & Aun, M. (2019). Daily, seasonal, and annual characteristics of UV radiation and its influencing factors in Tõravere, Estonia, 2004–2016. *Theoretical and Applied Climatology, 138*(1-2), 887-897. https://doi.org/10.1007/s00704-019-02865-1

245. Fountoulakis, I., Diémoz, H., Siani, A.-M., Laschewski, G., Filippa, G., Arola, A., Bais, A. F., De Backer, H., Lakkala, K., Webb, A. R., De Bock, V., Karppinen, T., Garane, K., Kapsomenakis, J., Koukouli, M.-E., & Zerefos, C. S. (2020). Solar UV irradiance in a changing climate: Trends in Europe and the significance of spectral monitoring in Italy. *Environments, 7*(1), 1. https://doi.org/10.3390/environments7010001

246. Hunter, N., Rendell, R. J., Higlett, M. P., amp, apos, Hagan, J. B., & Haylock, R. G. E. (2019). Relationship between erythema effective UV radiant exposure, total ozone, cloud cover and aerosols in southern England, UK. *Atmospheric Chemistry and Physics, 19*(1), 683-699. https://doi.org/10.5194/acp-19-683-2019

247. Torres, O., Bhartia, P. K., Jethva, H., & Ahn, C. (2018). Impact of the ozone monitoring instrument row anomaly on the long-term record of aerosol products. *Atmospheric Measurement Techniques, 11*(5), 2701-2715. https://doi.org/10.5194/amt-11-2701-2018

248. Herman, J., Cede, A., Huang, L., Ziemke, J., Torres, O., Krotkov, N., Kowalewski, M., & Blank, K. (2020). Global distribution and 14-year changes in erythemal irradiance, UV atmospheric transmission, and total column ozone for 2005–2018 estimated from OMI and EPIC observations. *Atmospheric Chemistry and Physics, 20*(14), 8351-8380. https://doi.org/10.5194/acp-20-8351-2020

249. Lindfors, A., & Vuilleumier, L. (2005). Erythemal UV at Davos (Switzerland), 1926-2003, estimated using total ozone, sunshine duration, and snow depth. *Journal of Geophysical Research, 110*(D2, D02104). https://doi.org/10.1029/2004JD005231

250. Krzyścin, J. W., & Sobolewski, P. S. (2018). Trends in erythemal doses at the Polish Polar Station, Hornsund, Svalbard based on the homogenized measurements (1996–2016) and reconstructed data (1983–1995). *Atmospheric Chemistry and Physics, 18*(1), 1-11. https://doi.org/10.5194/acp-18-1-2018

251. Posyniak, M., Szkop, A., Pietruczuk, A., Podgórski, J., & Krzyścin, J. (2016). The long-term (1964–2014) variability of aerosol optical thickness and its impact on solar irradiance based on the data taken at Belsk, Poland. *Acta Geophysica, 64*(5), 1858-1874. https://doi.org/10.1515/acgeo-2016-0026

252. Čížková, K., Láska, K., Metelka, L., & Staněk, M. (2018). Reconstruction and analysis of erythemal UV radiation time series from Hradec Králové (Czech Republic) over the past 50 years. *Atmospheric Chemistry and Physics, 18*(3), 1805-1818. https://doi.org/10.5194/acp-18-1805-2018

253. Volpert, E. V., & Chubarova, N. E. (2021). Long-term changes in solar radiation in Northern Eurasia during the warm season according to measurements and reconstruction model. *Russian Meteorology and Hydrology, 46*(8), 507-518. https://doi.org/10.3103/S1068373921080021

254. Malinović-Milićević, S., Radovanović, M. M., Mijatović, Z., & Petrović, M. D. (2022). Reconstruction and variability of high daily erythemal ultraviolet doses and relationship with total ozone, cloud cover, and albedo in Novi Sad (Serbia). *International Journal of Climatology*. https://doi.org/10.1002/joc.7803

255. WMO. (2011). *Scientific Assessment of Ozone Depletion: 2010*, [A.-L. Ajavon, P. A. Newman, J. A. Pyle, & A. R. Ravishankara (Eds.)]. Global Ozone Research and Monitoring Project – Report No. 52. World Meteorological Organisation, Geneva, Switzerland.

256. WMO. (2014). *Scientific Assessment of Ozone Depletion: 2014*, [A.-L. N. Ajavon, P. A. Newman, J. A. Pyle, & A. R. Ravishankara (Eds.)]. Global Ozone Research and Monitoring Project – Report No. 55. World Meteorological Organisation, Geneva, Switzerland.

257. Bernhard, G., Dahlback, A., Fioletov, V., Heikkilä, A., Johnsen, B., Koskela, T., Lakkala, K., & Svendby, T. (2013). High levels of ultraviolet radiation observed by ground-based instruments below the 2011 Arctic ozone hole. *Atmospheric Chemistry and Physics, 13*(21), 10573-10590. https://doi.org/10.5194/acp-13-10573-2013

258. Kazadzis, S., Founda, D., Psiloglou, B. E., Kambezidis, H., Mihalopoulos, N., Sanchez-Lorenzo, A., Meleti, C., Raptis, P. I., Pierros, F., & Nabat, P. (2018). Long-term series and trends in surface solar radiation in Athens, Greece. *Atmospheric Chemistry and Physics, 18*(4), 2395-2411. https://doi.org/10.5194/acp-18-2395-2018

259. Wild, M., Wacker, S., Yang, S., & Sanchez-Lorenzo, A. (2021). Evidence for clear-sky dimming and brightening in Central Europe. *Geophysical Research Letters, 48*(6). https://doi.org/10.1029/2020gl092216

260. Lamy, K., Portafaix, T., Josse, B., Brogniez, C., Godin-Beekmann, S., Bencherif, H., Revell, L., Akiyoshi, H., Bekki, S., Hegglin, M. I., Jöckel, P., Kirner, O., Liley, B., Marecal, V., Morgenstern, O., Stenke, A., Zeng, G., Abraham, N. L., Archibald, A. T., Butchart, N., et al. (2019). Clear-sky ultraviolet radiation modelling using output from the Chemistry Climate Model Initiative. *Atmospheric Chemistry and Physics, 19*(15), 10087-10110. https://doi.org/10.5194/acp-19-10087-2019

261. Eyring, V., Lamarque, J.-F., Hess, P., Arfeuille, F., Bowman, K., Chipperfiel, M. P., Duncan, B., Fiore, A., Gettelman, A., & Giorgetta, M. A. (2013). Overview of IGAC/SPARC Chemistry-Climate Model Initiative (CCMI) community simulations in support of upcoming ozone and climate assessments. *SPARC Newsletter, 40*(1), 48-66.

262. van Vuuren, D. P., Edmonds, J., Kainuma, M., Riahi, K., Thomson, A., Hibbard, K., Hurtt, G. C., Kram, T., Krey, V., Lamarque, J.-F., Masui, T., Meinshausen, M., Nakicenovic, N., Smith, S. J., & Rose, S. K. (2011). The representative concentration pathways: an overview. *Climatic Change, 109*(1-2), 5-31. https://doi.org/10.1007/s10584-011-0148-z

263. Kinne, S., O'Donnel, D., Stier, P., Kloster, S., Zhang, K., Schmidt, H., Rast, S., Giorgetta, M., Eck, T. F., & Stevens, B. (2013). MAC-v1: A new global aerosol climatology for climate studies. *Journal of Advances in Modeling Earth Systems, 5*(4), 704-740. https://doi.org/10.1002/jame.20035

264. Pastukhova, A. S., Chubarova, N. E., Zhdanova, Y. Y., Galin, V. Y., & Smyshlyaev, S. P. (2019). Numerical simulation of variations in ozone content, erythemal ultraviolet radiation, and ultraviolet resources over Northern Eurasia in the 21st century. Izvestiya, *Atmospheric and Oceanic Physics, 55*(3), 242-250. https://doi.org/10.1134/s0001433819030058

265. Eleftheratos, K., Kapsomenakis, J., Zerefos, C. S., Bais, A. F., Fountoulakis, I., Dameris, M., Jöckel, P., Haslerud, A. S., Godin-Beekmann, S., Steinbrecht, W., Petropavlovskikh, I., Brogniez, C., Leblanc, T., Liley, J. B., Querel, R., & Swart, D. P. J. (2020). Possible effects of greenhouse gases to ozone profiles and DNA active UV-B irradiance at ground level. *Atmosphere, 11*(3), 228. https://doi.org/10.3390/atmos11030228

266. Setlow, R. B. (1974). The wavelengths in sunlight effective in producing skin cancer: a theoretical analysis. *Proceedings of the National Academy of Sciences of the United States of America, 71*(9), 3363-3366. https://doi.org/10.1073/pnas.71.9.3363

267. Chiodo, G., Polvani, L. M., Marsh, D. R., Stenke, A., Ball, W., Rozanov, E., Muthers, S., & Tsigaridis, K. (2018). The response of the ozone layer to quadrupled CO_2 concentrations. *Journal of Climate, 31*(10), 3893-3907. https://doi.org/10.1175/jcli-d-17-0492.1

268. IPCC. (2014). *Climate change 2014: synthesis report*. Contribution of Working Groups I, II and III to the fifth assessment report of the Intergovernmental Panel on Climate Change, [Core Writing Team, R. K. Pachauri, & L. A. Meyer (Eds.)]. IPCC, Geneva, Switzerland.

269. Bardeen, C. G., Kinnison, D. E., Toon, O. B., Mills, M. J., Vitt, F., Xia, L., Jägermeyr, J., Lovenduski, N. S., Scherrer, K. J. N., Clyne, M., & Robock, A. (2021). Extreme Ozone Loss Following Nuclear War Results in Enhanced Surface Ultraviolet Radiation. Journal of Geophysical Research: *Atmospheres, 126*(18). https://doi.org/10.1029/2021JD035079

270. Tilmes, S., MacMartin, D. G., Lenaerts, J., van Kampenhout, L., Muntjewerf, L., Xia, L., Harrison, C. S., Krumhardt, K. M., Mills, M. J., & Kravitz, B. (2020). Reaching 1.5 and 2.0 °C global surface temperature targets using stratospheric aerosol geoengineering. *Earth System Dynamics, 11*(3), 579-601. https://doi.org/10.5194/esd-11-579-2020

271. Tilmes, S., Richter, J. H., Kravitz, B., MacMartin, D. G., Glanville, A. S., Visioni, D., Kinnison, D. E., & Müller, R. (2021). Sensitivity of total column ozone to stratospheric sulfur injection strategies. *Geophysical Research Letters, 48*(19). https://doi.org/10.1029/2021GL094058

272. Tilmes, S., Visioni, D., Jones, A., Haywood, J., Séférian, R., Nabat, P., Boucher, O., Bednarz, E. M., & Niemeier, U. (2022). Stratospheric ozone response to sulfate aerosol and solar dimming climate interventions based on the G6 Geoengineering Model Intercomparison Project (GeoMIP) simulations. *Atmospheric Chemistry and Physics, 22*(7), 4557-4579. https://doi.org/10.5194/acp-22-4557-2022

273. Robrecht, S., Vogel, B., Tilmes, S., & Müller, R. (2021). Potential of future stratospheric ozone loss in the midlatitudes under global warming and sulfate geoengineering. *Atmospheric Chemistry and Physics, 21*(4), 2427-2455. https://doi.org/10.5194/acp-21-2427-2021

274. Madronich, S., Tilmes, S., Kravitz, B., MacMartin, D., & Richter, J. (2018). Response of Surface Ultraviolet and Visible Radiation to Stratospheric SO_2 Injections. *Atmosphere, 9*(11), 432. https://doi.org/10.3390/atmos9110432

275. Durand, M., Murchie, E. H., Lindfors, A. V., Urban, O., Aphalo, P. J., & Robson, T. M. (2021). Diffuse solar radiation and canopy photosynthesis in a changing environment. *Agricultural and Forest Meteorology, 311*. https://doi.org/10.1016/j.agrformet.2021.108684

276. De Mazière, M., Thompson, A. M., Kurylo, M. J., Wild, J. D., Bernhard, G., Blumenstock, T., Braathen, G. O., Hannigan, J. W., Lambert, J.-C., Leblanc, T., McGee, T. J., Nedoluha, G., Petropavlovskikh, I., Seckmeyer, G., Simon, P. C., Steinbrecht, W., & Strahan, S. E. (2018). The Network for the Detection of Atmospheric Composition Change (NDACC): history, status and perspectives. *Atmospheric Chemistry and Physics, 18*(7), 4935-4964. https://doi.org/10.5194/acp-18-4935-2018

277. Hülsen, G., Gröbner, J., Bais, A., Blumthaler, M., Diémoz, H., Bolsée, D., Diaz, A., Fountoulakis, I., Naranen, E., Schreder, J., Stefania, F., & Manuel Vilaplana Guerrero, J. (2020). Second solar ultraviolet radiometer comparison campaign UVC-II. *Metrologia, 57*(3). https://doi.org/10.1088/1681-7575/ab74e5

278. Svendby, T. M., Johnsen, B., Kylling, A., Dahlback, A., Bernhard, G. H., Hansen, G. H., Petkov, B., & Vitale, V. (2021). GUV long-term measurements of total ozone column and effective cloud transmittance at three Norwegian sites. *Atmospheric Chemistry and Physics, 21*(10), 7881-7899. https://doi.org/10.5194/acp-21-7881-2021

279. Foster, T. M., Weide, E. L., Niedzwiedz, A., Duffert, J., & Seckmeyer, G. (2021). Characterization of the angular response of a multi-directional spectroradiometer for measuring spectral radiance. *EPJ Techniques and Instrumentation, 8*(1). https://doi.org/10.1140/epjti/s40485-021-00069-

280. Johnsen, B., Kjeldstad, B., Aalerud, T. N., Nilsen, L. T., Schreder, J., Blumthaler, M., Bernhard, G., Topaloglou, C., Meinander, O., Bagheri, A., Slusser, J. R., & Davis, J. (2008). Intercomparison and harmonization of UV Index measurements from multiband filter radiometers. *Journal of Geophysical Research: Atmospheres, 113*(D15). https://doi.org/10.1029/2007jd009731

281. Egli, L., Gröbner, J., Hülsen, G., Bachmann, L., Blumthaler, M., Dubard, J., Khazova, M., Kift, R., Hoogendijk, K., Serrano, A., Smedley, A., & Vilaplana, J. M. (2016). Quality assessment of solar UV irradiance measured with array spectroradiometers. *Atmospheric Measurement Techniques, 9*(4), 1553-1567. https://doi.org/10.5194/amt-9-1553-2016

282. Zuber, R., Ribnitzky, M., Tobar, M., Lange, K., Kutscher, D., Schrempf, M., Niedzwiedz, A., & Seckmeyer, G. (2018). Global spectral irradiance array spectroradiometer validation according to WMO. *Measurement Science and Technology, 29*(10). https://doi.org/10.1088/1361-6501/aada34

283. González, C., Vilaplana, J. M., Bogeat, J. A., & Serrano, A. (2022). Comparison of global UV spectral irradiance measurements between a BTS CCD-array and a Brewer spectroradiometer. *Atmospheric Measurement Techniques, 15*(13), 4125-4133. https://doi.org/10.5194/amt-15-4125-2022

284. Allen, M. W., Swift, N., Nield, K. M., Liley, B., & McKenzie, R. L. (2020). Use of electronic UV dosimeters in measuring personal UV exposures and public health education. *Atmosphere, 11*(7). https://doi.org/10.3390/atmos11070744

285. Diffey, B. (2020). The early days of personal solar ultraviolet dosimetry. *Atmosphere, 11*(2), 125. https://doi.org/10.3390/atmos11020125

286. Downs, N. J., Axelsen, T., Parisi, A. V., Schouten, P. W., & Dexter, B. R. (2020). Measured UV exposures of ironman, sprint and olympic-distance triathlon competitors. *Atmosphere, 11*(5). https://doi.org/10.3390/atmos11050440

287. Cai, S., Zuo, C., Zhang, J., Liu, H., & Fang, X. (2021). A paper-based wearable photodetector for simultaneous UV intensity and dosage measurement. *Advanced Functional Materials, 31*(20). https://doi.org/10.1002/adfm.202100026

288. Seckmeyer, G., Klingebiel, M., Riechelmann, S., Lohse, I., McKenzie, R. L., Ben Liley, J., Allen, M. W., Siani, A.-M., & Casale, G. R. (2012). A critical assessment of two types of personal UV dosimeters. *Photochemistry and Photobiology, 88*(1), 215-222. https://doi.org/10.1111/j.1751-1097.2011.01018.x

289. Gröbner, J., Schreder, J., Kazadzis, S., Bais, A. F., Blumthaler, M., Görts, P., Tax, R., Koskela, T., Seckmeyer, G., Webb, A. R., & Rembges, D. (2005). Traveling reference spectroradiometer for routine quality assurance of spectral solar ultraviolet irradiance measurements. *Applied Optics, 44*(25), 5321-5331. https://doi.org/10.1364/AO.44.005321

290. Cadet, J.-M., Portafaix, T., Bencherif, H., Lamy, K., Brogniez, C., Auriol, F., Metzger, J.-M., Boudreault, L.-E., & Wright, C. Y. (2020). Inter-comparison campaign of solar UVR instruments under clear sky conditions at Reunion Island (21°S, 55°E). *International Journal of Environmental Research and Public Health, 17*(8). https://doi.org/10.3390/ijerph17082867

291. Fountoulakis, I., Diémoz, H., Siani, A. M., Hülsen, G., & Gröbner, J. (2020). Monitoring of solar spectral ultraviolet irradiance in Aosta, Italy. *Earth System Science Data, 12*(4), 2787-2810. https://doi.org/10.5194/essd-12-2787-2020

292. Schinke, C., Pollex, H., Hinken, D., Wolf, M., Bothe, K., Kröger, I., Nevas, S., & Winter, S. (2020). Calibrating spectrometers for measurements of the spectral irradiance caused by solar radiation. *Metrologia, 57*(6). https://doi.org/10.1088/1681-7575/abafc5

293. Mayer, B., & Kylling, A. (2005). Technical note: The libRadtran software package for radiative transfer calculations – description and examples of use. *Atmospheric Chemistry and Physics, 5*, 1855-1877. https://doi.org/10.5194/acp-5-1855-2005

294. Ricchiazzi, P., Yang, S., Gautier, C., & Sowle, D. (1998). SBDART: A research and teaching software tool for plane-parallel radiative transfer in the Earth's atmosphere. *Bulletin of the American Meteorological Society, 7*9(10), 2101-2114. https://doi.org/10.1175/1520-0477(1998)079<2101:Sarats>2.0.Co;2

295. Gueymard, C. A. (2019). The SMARTS spectral irradiance model after 25 years: New developments and validation of reference spectra. *Solar Energy, 187*, 233-253. https://doi.org/10.1016/j.solener.2019.05.048

296. Madronich, S., & Flocke, S. (1997). Theoretical Estimation of Biologically Effective UV Radiation at the Earth's Surface. In C. S. Zerefos, & A. F. Bais (Eds.), *Solar Ultraviolet Radiation - Modeling, Measurements & Effects, 52*, 23-48. Springer, Berlin, Germany.

297. Madronich, S. (1992). Implications of recent total atmospheric ozone measurements for biologically active ultraviolet radiation reaching the earth's surface. *Geophysical Research Letters, 19*(1), 37-40. https://doi.org/10.1029/91GL02954

298. Emde, C., & Mayer, B. (2007). Simulation of solar radiation during a total eclipse: a challenge for radiative transfer. *Atmospheric Chemistry and Physics, 7*(9), 2259-2270. https://doi.org/10.5194/acp-7-2259-2007

299. Ockenfuß, P., Emde, C., Mayer, B., & Bernhard, G. (2020). Accurate 3-D radiative transfer simulation of spectral solar irradiance during the total solar eclipse of 21 August 2017. *Atmospheric Chemistry and Physics, 20*(4), 1961-1976. https://doi.org/10.5194/acp-20-1961-2020

300. Noebauer, U. M., & Sim, S. A. (2019). Monte Carlo radiative transfer. *Living Reviews in Computational Astrophysics, 5*(1). https://doi.org/10.1007/s41115-019-0004-9

301. Gueymard, C. A. (2018). Revised composite extraterrestrial spectrum based on recent solar irradiance observations. *Solar Energy, 169*, 434-440. https://doi.org/10.1016/j.solener.2018.04.067

302. Bak, J., Coddington, O., Liu, X., Chance, K., Lee, H.-J., Jeon, W., Kim, J.-H., & Kim, C.-H. (2021). Impact of using a new high-resolution solar reference spectrum on OMI ozone profile retrievals. *Remote Sensing, 14*(1). https://doi.org/10.3390/rs14010037

303. Schmid, B., & Wehrli, C. (1995). Comparison of Sun photometer calibration by use of the Langley technique and the standard lamp. *Applied Optics, 34*(21), 4500-4512. https://doi.org/10.1364/ao.34.004500

304. Gröbner, J., Kröger, I., Egli, L., Hülsen, G., Riechelmann, S., & Sperfeld, P. (2017). The high-resolution extraterrestrial solar spectrum (QASUMEFTS) determined from ground-based solar irradiance measurements. *Atmospheric Measurement Techniques, 10*, 3375–3383. https://doi.org/10.5194/amt-10-3375-2017

305. Richard, E., Harber, D., Coddington, O., Drake, G., Rutkowski, J., Triplett, M., Pilewskie, P., & Woods, T. (2020). SI-traceable spectral irradiance radiometric characterization and absolute calibration of the TSIS-1 Spectral Irradiance Monitor (SIM). *Remote Sensing, 12*(11). https://doi.org/10.3390/rs12111818

306. Coddington, O. M., Richard, E. C., Harber, D., Pilewskie, P., Woods, T. N., Chance, K., Liu, X., & Sun, K. (2021). The TSIS 1 Hybrid Solar Reference Spectrum. *Geophysical Research Letters, 48*(12). https://doi.org/10.1029/2020gl091709

307. Arola, A., Wandji Nyamsi, W., Lipponen, A., Kazadzis, S., Krotkov, N. A., & Tamminen, J. (2021). Rethinking the correction for absorbing aerosols in the OMI- and TROPOMI-like surface UV algorithms. *Atmospheric Measurement Techniques, 14*(7), 4947-4957. https://doi.org/10.5194/amt-14-4947-2021

308. Heath, D. F., Mateer, C. L., & Krueger, A. J. (1973). The Nimbus-4 Backscatter Ultraviolet (BUV) atmospheric ozone experiment — tow years' operation. *Pure and Applied Geophysics, 106-108*(1), 1238-1253. https://doi.org/10.1007/BF00881076

309. Frith, S. M., Kramarova, N. A., Stolarski, R. S., McPeters, R. D., Bhartia, P. K., & Labow, G. J. (2014). Recent changes in total column ozone based on the SBUV Version 8.6 Merged Ozone Data Set. *Journal of Geophysical Research: Atmospheres, 119*(16), 9735-9751. https://doi.org/10.1002/2014JD02188

310. Krotkov, N. A., Bhartia, P. K., Herman, J. R., Fioletov, V., & Kerr, J. (1998). Satellite estimation of spectral surface UV irradiance in the presence of tropospheric aerosols: 1. Cloud-free case. *Journal of Geophysical Research: Atmospheres, 103*(D8), 8779-8793. https://doi.org/10.1029/98jd00233

311. Krotkov, N. A., Herman, J. R., Bhartia, P. K., Fioletov, V., & Ahmad, Z. (2001). Satellite estimation of spectral surface UV irradiance: 2. Effects of homogeneous clouds and snow. *Journal of Geophysical Research: Atmospheres, 106*(D11), 11743-11759. https://doi.org/10.1029/2000jd900721

312. Burrows, J. P., Weber, M., Buchwitz, M., Rozanov, V., Ladstätter-Weißenmayer, A., Richter, A., DeBeek, R., Hoogen, R., Bramstedt, K., Eichmann, K.-U., Eisinger, M., & Perner, D. (1999). The Global Ozone Monitoring Experiment (GOME): Mission concept and first scientific results. *Journal of the Atmospheric Sciences, 56*(2), 151-175. https://doi.org/10.1175/1520-0469(1999)056<0151:Tgomeg>2.0.Co;2

313. Kujanpää, J., & Kalakoski, N. (2015). Operational surface UV radiation product from GOME-2 and AVHRR/3 data. *Atmospheric Measurement Techniques, 8*(10), 4399-4414. https://doi.org/10.5194/amt-8-4399-2015

314. Levelt, P. F., Joiner, J., Tamminen, J., Veefkind, J. P., Bhartia, P. K., Stein Zweers, D. C., Duncan, B. N., Streets, D. G., Eskes, H., van der A, R., McLinden, C., Fioletov, V., Carn, S., de Laat, J., DeLand, M., Marchenko, S., McPeters, R., Ziemke, J., Fu, D., Liu, X., et al. (2018). The Ozone Monitoring Instrument: overview of 14 years in space. *Atmospheric Chemistry and Physics, 18*(8), 5699-5745. https://doi.org/10.5194/acp-18-5699-2018

315. Herman, J., Huang, L., McPeters, R., Ziemke, J., Cede, A., & Blank, K. (2018). Synoptic ozone, cloud reflectivity, and erythemal irradiance from sunrise to sunset for the whole earth as viewed by the DSCOVR spacecraft from the earth–sun Lagrange 1 orbit. *Atmospheric Measurement Techniques, 11*(1), 177-194. https://doi.org/10.5194/amt-11-177-2018

316. Brogniez, C., Auriol, F., Deroo, C., Arola, A., Kujanpää, J., Sauvage, B., Kalakoski, N., Pitkänen, M. R. A., Catalfamo, M., Metzger, J. M., Tournois, G., & Da Conceicao, P. (2016). Validation of satellite-based noontime UVI with NDACC ground-based instruments: influence of topography, environment and satellite overpass time. *Atmospheric Chemistry and Physics, 16*(23), 15049-15074. https://doi.org/10.5194/acp-16-15049-2016

317. Arola, A., Kazadzis, S., Lindfors, A., Krotkov, N., Kujanpää, J., Tamminen, J., Bais, A., di Sarra, A., Villaplana, J. M., Brogniez, C., Siani, A. M., Janouch, M., Weihs, P., Webb, A., Koskela, T., Kouremeti, N., Meloni, D., Buchard, V., Auriol, F., Ialongo, I., et al. (2009). A new approach to correct for absorbing aerosols in OMI UV. *Geophysical Research Letters, 36*(22), L22805. https://doi.org/10.1029/2009gl041137

318. Bernhard, G., Arola, A., Dahlback, A., Fioletov, V., Heikkilä, A., Johnsen, B., Koskela, T., Lakkala, K., Svendby, T., & Tamminen, J. (2015). Comparison of OMI UV observations with ground-based measurements at high northern latitudes. *Atmospheric Chemistry and Physics, 15*(13), 7391-7412. https://doi.org/10.5194/acp-15-7391-2015

319. Kosmopoulos, P. G., Kazadzis, S., Schmalwieser, A. W., Raptis, P. I., Papachristopoulou, K., Fountoulakis, I., Masoom, A., Bais, A. F., Bilbao, J., Blumthaler, M., Kreuter, A., Siani, A. M., Eleftheratos, K., Topaloglou, C., Gröbner, J., Johnsen, B., Svendby, T. M., Vilaplana, J. M., Doppler, L., Webb, A. R., et al. (2021). Real-time UV index retrieval in Europe using Earth observation-based techniques: system description and quality assessment. *Atmospheric Measurement Techniques, 14*(8), 5657-5699. https://doi.org/10.5194/amt-14-5657-2021

320. Vuilleumier, L., Harris, T., Nenes, A., Backes, C., & Vernez, D. (2021). Developing a UV climatology for public health purposes using satellite data. *Environment International, 146*. https://doi.org/10.1016/j.envint.2020.106177

321. Fisher, D. (2020). Mission Status for Earth Science Constellation. In *NASA Goddard Space Flight Center Tech. Doc. Document ID 20205007514*, 1-41: Goddard Space Flight Center, Greenbelt, Maryland.

322. Flynn, L., Long, C., Wu, X., Evans, R., Beck, C. T., Petropavlovskikh, I., McConville, G., Yu, W., Zhang, Z., & Niu, J. (2014). Performance of the ozone mapping and profiler suite (OMPS) products. *Journal of Geophysical Research: Atmospheres, 119*(10), 6181-6195. https://doi.org/10.1002/2013JD020484

323. Lindfors, A. V., Kujanpää, J., Kalakoski, N., Heikkilä, A., Lakkala, K., Mielonen, T., Sneep, M., Krotkov, N. A., Arola, A., & Tamminen, J. (2018). The TROPOMI surface UV algorithm. *Atmospheric Measurement Techniques, 11*(2), 997-1008. https://doi.org/10.5194/amt-11-997-2018

324. Cortesi, U., Ceccherini, S., Del Bianco, S., Gai, M., Tirelli, C., Zoppetti, N., Barbara, F., Bonazountas, M., Argyridis, A., Bós, A., Loenen, E., Arola, A., Kujanpää, J., Lipponen, A., Wandji Nyamsi, W., van der A, R., van Peet, J., Tuinder, O., Farruggia, V., Masini, A., et al. (2018). Advanced Ultraviolet Radiation and Ozone Retrieval for Applications (AURORA): A project overview. *Atmosphere, 9*(11), 454. https://doi.org/10.3390/atmos9110454

325. Lakkala, K., Kujanpää, J., Brogniez, C., Henriot, N., Arola, A., Aun, M., Auriol, F., Bais, A. F., Bernhard, G., De Bock, V., Catalfamo, M., Deroo, C., Diémoz, H., Egli, L., Forestier, J.-B., Fountoulakis, I., Garcia, R. D., Gröbner, J., Hassinen, S., Heikkilä, A., et al. (2020). Validation of the TROPOspheric Monitoring Instrument (TROPOMI) surface UV radiation product. *Atmospheric Measurement Techniques, 13*(12), 6999–7024. https://doi.org/10.5194/amt-13-6999-2020

326. Tanskanen, A., Lindfors, A., Maatta, A., Krotkov, N., Herman, J., Kaurola, J., Koskela, T., Lakkala, K., Fioletov, V., Bernhard, G., McKenzie, R., Kondo, Y., O'Neill, M., Slaper, H., den Outer, P., Bais, A. F., & Tamminen, J. (2007). Validation of daily erythemal doses from Ozone Monitoring Instrument with ground-based UV measurement data. *Journal of Geophysical Research: Atmospheres, 112*(D24). https://doi.org/10.1029/2007JD008830

327. Zempila, M. M., Fountoulakis, I., Taylor, M., Kazadzis, S., Arola, A., Koukouli, M. E., Bais, A., Meleti, C., & Balis, D. (2018). Validation of OMI erythemal doses with multi-sensor ground-based measurements in Thessaloniki, Greece. *Atmospheric Environment, 183*, 106-121. https://doi.org/10.1016/j.atmosenv.2018.04.012

328. Lipponen, A., Ceccherini, S., Cortesi, U., Gai, M., Keppens, A., Masini, A., Simeone, E., Tirelli, C., & Arola, A. (2020). Advanced ultraviolet radiation and ozone retrieval for applications—surface ultraviolet radiation products. *Atmosphere, 11*(4). https://doi.org/10.3390/atmos11040324

329. Zhao, R., & He, T. (2022). Estimation of 1-km tesolution all-sky instantaneous erythemal UV-B with MODIS data based on a deep learning method. *Remote Sensing, 14*(2). https://doi.org/10.3390/rs14020384

330. Krzyścin, J. W., Guzikowski, J., Pietruczuk, A., & Sobolewski, P. S. (2019). Improvement of the 24 hr forecast of surface UV radiation using an ensemble approach. *Meteorological Applications, 27*(1). https://doi.org/10.1002/met.1865

331. Ahmed, A. A. M., Ahmed, M. H., Saha, S. K., Ahmed, O., & Sutradhar, A. (2022). Optimization algorithms as training approach with hybrid deep learning methods to develop an ultraviolet index forecasting model. *Stochastic Environmental Research and Risk Assessment, 36*(10), 3011-3039. https://doi.org/10.1007/s00477-022-02177-3

332. Scragg, R. K. R., Stewart, A. W., McKenzie, R. L., Reeder, A. I., Liley, J. B., & Allen, M. W. (2016). Sun exposure and 25-hydroxyvitamin D$_3$ levels in a community sample: quantifying the association with electronic dosimeters. *Journal of Exposure Science & Environmental Epidemiology, 27*(5), 471-477. https://doi.org/10.1038/jes.2016.51

333. Godar, D. E. (2005). UV Doses Worldwide. *Photochemistry and Photobiology, 81*(4). https://doi.org/10.1562/2004-09-07-ir-308r.1

334. Schmalwieser, A. W., & Siani, A. M. (2018). Review on nonoccupational personal solar UV exposure measurements. *Photochemistry and Photobiology, 94*(5), 900-915. https://doi.org/10.1111/php.12946

335. Schmalwieser, A. W., Casale, G. R., Colosimo, A., Schmalwieser, S. S., & Siani, A. M. (2021). Review on occupational personal solar UV exposure measurements. *Atmosphere, 12*(2). https://doi.org/10.3390/atmos12020142

336. Backes, C., Religi, A., Moccozet, L., Vuilleumier, L., Vernez, D., & Bulliard, J. L. (2018). Facial exposure to ultraviolet radiation: Predicted sun protection effectiveness of various hat styles. *Photodermatology, Photoimmunology and Photomedicine, 34*(5), 330-337.

337. Backes, C., Religi, A., Moccozet, L., Behar-Cohen, F., Vuilleumier, L., Bulliard, J.-L., & Vernez, D. (2019). Sun exposure to the eyes: predicted UV protection effectiveness of various sunglasses. *Journal of Exposure Science & Environmental Epidemiology, 29*(6), 753-764.

338. Mims III, F. M., McGonigle, A. J. S., Wilkes, T. C., Parisi, A. V., Grant, W. B., Cook, J. M., & Pering, T. D. (2019). Measuring and visualizing solar UV for a wide range of atmospheric conditions on Hawai'i island. *International Journal of Environmental Research and Public Health, 16*(6), 997. https://doi.org/10.3390/ijerph16060997

339. Wester, U., Pagels, P., & Boldemann, C. (2018). Solar ultraviolet radiation exposure proxy estimated by sky view fish eye photography—potentials and limitations from an exploratory correlation study. *Photochemistry and Photobiology, 95*(2), 656-661. https://doi.org/10.1111/php.13027

340. Schmalwieser, A. W., Lohr, M. A., Daly, S. M., & Williams, J. D. (2022). Modeling acute and cumulative erythemal sun exposure on vulnerable body sites during beach vacations utilizing behavior-encoded 3D body models. *Photochemical & Photobiological Sciences*. https://doi.org/10.1007/s43630-022-00293-1

341. Henning, A., J. Downs, N., & Vanos, J. K. (2021). Wearable ultraviolet radiation sensors for research and personal use. *International Journal of Biometeorology, 66*(3), 627-640. https://doi.org/10.1007/s00484-021-02216-8

342. Huang, X., & Chalmers, A. N. (2021). Review of wearable and portable sensors for monitoring personal solar UV exposure. *Annals of Biomedical Engineering, 49*(3), 964-978. https://doi.org/10.1007/s10439-020-02710-x

343. Zou, W., Sastry, M., Gooding, J. J., Ramanathan, R., & Bansal, V. (2020). Recent advances and a roadmap to wearable UV sensor technologies. *Advanced Materials Technologies, 5*(4). https://doi.org/10.1002/admt.201901036

344. Wilson, D. J., Martín-Martínez, F. J., & Deravi, L. F. (2022). Wearable light sensors based on unique features of a natural biochrome. *ACS Sensors, 7*(2), 523-533. https://doi.org/10.1021/acssensors.1c02342

345. Wang, J., Jeevarathinam, A. S., Jhunjhunwala, A., Ren, H., Lemaster, J., Luo, Y., Fenning, D. P., Fullerton, E. E., & Jokerst, J. V. (2018). A wearable colorimetric dosimeter to monitor sunlight exposure. *Advanced Materials Technologies, 3*(6). https://doi.org/10.1002/admt.201800037

346. Terenetskaya, I. (2019). How to provide adequate UV dosimetry to avoid Vitamin D deficiency and related neuropsychiatric disorders. *Archives in Neurology & Neuroscience, 6*(1). https://doi.org/10.33552/ANN.2019.06.000629

347. de Troya Martín, M., Blázquez Sánchez, N., García Harana, C., Alarcón Leiva, M. C., Aguilera Arjona, J., Rivas Ruiz, F., & de Gálvez Aranda, M. V. (2021). Beach lifeguards: sun exposure and sun protection in Spain. *Safety and Health at Work, 12*(2), 244-248. https://doi.org/10.1016/j.shaw.2020.10.003

348. Robinson, J. K., Durst, D. A., Gray, E., Kwasny, M., Heo, S. Y., Banks, A., & Rogers, J. A. (2020). Sun exposure reduction by melanoma survivors with wearable sensor providing real-time UV exposure and daily text messages with structured goal setting. *Archives of Dermatological Research, 313*(8), 685-694. https://doi.org/10.1007/s00403-020-02163-1

349. Modenese, A., Korpinen, L., & Gobba, F. (2018). Solar radiation exposure and outdoor work: an underestimated occupational risk. *International Journal of Environmental Research and Public Health, 15*(10). https://doi.org/10.3390/ijerph15102063

350. Robinson, J. K., Patel, S., Heo, S. Y., Gray, E., Lim, J., Kwon, K., Christiansen, Z., Model, J., Trueb, J., Banks, A., Kwasny, M., & Rogers, J. A. (2021). Real-time UV measurement with a sun protection system for warning young adults about sunburn: Prospective cohort study. *JMIR mHealth and uHealth, 9*(5). https://doi.org/10.2196/25895

351. Moldovan, H. R., Wittlich, M., John, S. M., Brans, R., Tiplica, G. S., Salavastru, C., Voidazan, S. T., Duca, R. C., Fugulyan, E., Horvath, G., Alexa, A., & Butacu, A. I. (2020). Exposure to solar UV radiation in outdoor construction workers using personal dosimetry. *Environmental Research, 181*. https://doi.org/10.1016/j.envres.2019.108967

352. Thieden, E., Holm-Schou, A.-S. S., Philipsen, P. A., Heydenreich, J., & Wulf, H. C. (2019). Adult UVR exposure changes with life stage – a 14-year follow-up study using personal electronic UVR dosimeters. *Photochemical & Photobiological Sciences, 18*(2), 467-476. https://doi.org/10.1039/c8pp00365c

353. De Castro-Maqueda, G., Gutierrez-Manzanedo, J. V., Ponce-González, J. G., Fernandez-Santos, J. R., Linares-Barrios, M., & De Troya-Martín, M. (2019). Sun protection habits and sunburn in elite aquatics athletes: Surfers, windsurfers and olympic sailors. *Journal of Cancer Education, 35*(2), 312-320. https://doi.org/10.1007/s13187-018-1466-x

354. Nakagawara, V. B., Montgomery, R. W., & Marshall, W. J. (2007). Optical radiation transmittance of aircraft windscreeens and pilot vision. Vol. DOT/FAA/AM-07/20. Office of Aerospace Medicine, Washington, DC.

355. International Commission on Non-Ionizing Radiation Protection (2004). Guidelines on limits of exposure to ultraviolet radiation of wavelengths between 180 nm and 400 nm (incoherent optical radiation). *Health Physics, 87*(2), 171-186.

356. Baczynska, K. A., Brown, S., Chorley, A. C., Lyachev, A., Wittlich, M., & Khazova, M. (2020). Measurements of UV-A exposure of commercial pilots using Genesis-UV dosimeters. *Atmosphere, 11*(5). https://doi.org/10.3390/atmos11050475

357. Turner, J., Igoe, D., Parisi, A. V., McGonigle, A. J., Amar, A., & Wainwright, L. (2020). A review on the ability of smartphones to detect ultraviolet (UV) radiation and their potential to be used in UV research and for public education purposes. *Science of the Total Environment, 706*. https://doi.org/10.1016/j.scitotenv.2019.135873

358. Salvadori, G., Leccese, F., Lista, D., Burattini, C., & Bisegna, F. (2020). Use of smartphone apps to monitor human exposure to solar radiation: Comparison between predicted and measured UV index values. *Environmental Research, 183*. https://doi.org/10.1016/j.envres.2020.109274

359. Kwon, K., Heo, S. Y., Yoo, I., Banks, A., Chan, M., Lee, J. Y., Park, J. B., Kim, J., & Rogers, J. A. (2019). Miniaturized, light-adaptive, wireless dosimeters autonomously monitor exposure to electromagnetic radiation. *Science Advances, 5*(12). https://doi.org/10.1126/sciadv.aay2462

360. Harris, T. C., Vuilleumier, L., Backes, C., Nenes, A., & Vernez, D. (2021). Satellite-based personal UV dose estimation. *Atmosphere, 12*(2). https://doi.org/10.3390/atmos12020268

361. Krzyścin, J. W., Lesiak, A., Narbutt, J., Sobolewski, P., & Guzikowski, J. (2018). Perspectives of UV nowcasting to monitor personal pro-health outdoor activities. *Journal of Photochemistry and Photobiology B: Biology, 184*, 27-33. https://doi.org/10.1016/j.jphotobiol.2018.05.012

362. Kohli, I., Zubair, R., Lyons, A. B., Nahhas, A. F., Braunberger, T. L., Mokhtari, M., Ruvolo, E., Lim, H. W., & Hamzavi, I. H. (2019). Impact of long-wavelength ultraviolet A1 and visible light on light-skinned individuals. *Photochemistry and Photobiology, 95*(6), 1285-1287. https://doi.org/10.1111/php.13143

363. Diffey, B., & Osterwalder, U. (2017). Labelled sunscreen SPFs may overestimate protection in natural sunlight. *Photochemical & Photobiological Sciences, 16*(10), 1519-1523. https://doi.org/10.1039/C7PP00260B

364. MacLaughlin, J. A., Anderson, R. R., & Holick, M. F. (1982). Spectral character of sunlight modulates photosynthesis of previtamin D_3 and its photoisomers in human skin. *Science, 216*(4549), 1001-1003. https://doi.org/10.1126/science.6281884

365. Bouillon, R., Eisman, J., Garabedian, M., Holick, M., Kleinschmidt, J., Suda, T., Terenetskaya, I., & Webb, A. (2006). *Action spectrum for the production of previtamin D_3 in human skin*. Vol. 174:2006, UDC: 612.014.481-06. CIE, Vienna, Austria.

366. Norval, M., Björn, L. O., & de Gruijl, F. R. (2010). Is the action spectrum for the UV-induced production of previtamin D_3 in human skin correct? P*hotochemical and Photobiological Sciences, 9*(1), 11-17. https://doi.org/10.1039/b9pp00012g

367. Young, A. R., Morgan, K. A., Harrison, G. I., Lawrence, K. P., Petersen, B., Wulf, H. C., & Philipsen, P. A. (2021). A revised action spectrum for vitamin D synthesis by suberythemal UV radiation exposure in humans in vivo. *Proceedings of the National Academy of Sciences, 118*(40). https://doi.org/10.1073/pnas.2015867118

368. Bolsée, D., Webb, A. R., Gillotay, D., Dörschel, B., Knuschke, P., Krins, A., & Terenetskaya, I. (2000). Laboratory facilities and recommendations for the characterization of biological ultraviolet dosimeters. *Applied Optics, 39*(16), 2813-2822. https://doi.org/10.1364/ao.39.002813

369. Olds, W. (2010). *Elucidating the links between UV radiation and vitamin D synthesis: Using an in vitro mode*l. PhD Thesis, Queensland University of Technology Brisbane, Australia.

370. van Dijk, A., den Outer, P., van Kranen, H., & Slaper, H. (2016). The action spectrum for vitamin D_3: initial skin reaction and prolonged exposure. *Photochemical & Photobiological Sciences, 15*(7), 896-909. https://doi.org/10.1039/C6PP00034G

371. Webb, A. R., Terenetskaya, I. P., Holick, M. F., van Dijk, A., McKenzie, R. L., Lucas, R. M., Young, A. R., Philipsen, P. A., & de Gruijl, F. R. (2022). Previtamin D action spectrum: Challenging CIE towards a standard. *Lighting Research & Technology*. https://doi.org/10.1177/14771535221122937

2

LINKAGES BETWEEN COVID–19, SOLAR UV RADIATION, AND THE MONTREAL PROTOCOL

G. H. Bernhard[47], S. Madronich[48], R. M. Lucas[49], S. N. Byrne[50], T. Schikowski[51], and R. E. Neale[52,53]

[47] Biospherical Instruments Inc., San Diego, California, USA.

[48] Atmospheric Chemistry Observations and Modeling Laboratory, National Center for Atmospheric Research, Boulder, USA.

[49] National Centre for Epidemiology and Population Health, Australian National University, Canberra, Australia.

[50] The University of Sydney, School of Medical Sciences, Faculty of Medicine and Health, Sydney, Australia.

[51] Leibniz Research Institute for Environmental Medicine, Düsseldorf, Germany.

[52] Population Health Program, QIMR Berghofer Medical Research Institute, Brisbane, Australia.

[53] School of Public Health, University of Queensland, Brisbane, Australia.

Table of contents

Summary

There are several connections between coronavirus disease 2019 (COVID-19), solar UV radiation, and the Montreal Protocol. Exposure to ambient solar UV radiation inactivates SARS-CoV-2, the virus responsible for COVID-19. An action spectrum describing the wavelength dependence of the inactivation of SARS-CoV-2 by UV and visible radiation has recently been published. In contrast to action spectra that have been assumed in the past for estimating the effect of UV radiation on SARS-CoV-2, the new action spectrum has a large sensitivity in the UV-A (315–400 nm) range. If this "UV-A tail" is correct, solar UV radiation could be much more efficient in inactivating the virus responsible for COVID-19 than previously thought. Furthermore, the sensitivity of inactivation rates to the total column ozone would be reduced because ozone absorbs only a small amount of UV-A radiation. By using solar simulators, the times for inactivating SARS-CoV-2 have been determined by several groups; however, many measurements are affected by poorly defined experimental setups. The most reliable data suggest that 90% of viral particles embedded in saliva are inactivated within ~7 minutes by solar radiation for a solar zenith angle (SZA) of 16.5° and within ~13 minutes for a SZA of 63.4°. Slightly longer inactivation times were found for aerosolised virus particles. These times can become considerably longer during cloudy conditions or if virus particles are shielded from solar radiation. Many publications have provided evidence of an inverse relationship between ambient solar UV radiation and the incidence or severity of COVID-19, but the reasons for these negative correlations have not been unambiguously identified and could also be explained by confounders, such as ambient temperature, humidity, visible radiation, daylength, temporal changes in risk and disease management, and the proximity of people to other people. Meta-analyses of observational studies indicate inverse associations between serum 25-hydroxy vitamin D (25(OH)D) concentration and the risk of SARS-CoV-2 positivity or severity of COVID-19, although the quality of these studies is largely low. Mendelian randomisation studies have not found statistically significant evidence of a causal effect of 25(OH)D concentration on COVID-19 susceptibility or severity, but a potential link between vitamin D status and disease severity cannot be excluded as some randomised trials suggest that vitamin D supplementation is beneficial for people admitted to a hospital. Several studies indicate significant positive associations between air pollution and COVID-19 incidence and fatality rates. Conversely, well-established cohort studies indicate no association between long-term exposure to air pollution and infection with SARS-CoV-2. By limiting increases in UV radiation, the Montreal Protocol has also suppressed the inactivation rates of pathogens exposed to UV radiation. However, there is insufficient evidence to conclude that the expected larger inactivation rates without the Montreal Protocol would have had tangible consequences on the progress of the COVID-19 pandemic.

1 Introduction

Coronavirus disease 2019 (COVID-19) is an infectious disease caused by severe acute respiratory syndrome coronavirus 2 (SARS-CoV-2). It was first identified in December 2019 in China and has resulted in a global pandemic. The 2020 Assessment Update [1] by the Environmental Effects Assessment Panel (EEAP) of the Montreal Protocol under the United Nations Environment Programme (UNEP) included a section on linkages between COVID-19, solar ultraviolet (UV) radiation, and the Montreal Protocol. At the time the publication was prepared, COVID-19 had been in existence for less than one year and research on the subject was incomplete with many papers still in review. The scientific literature is now more mature and we present an update on the current knowledge of the aspects of COVID-19 related to solar UV radiation and the Montreal Protocol.

SARS-CoV-2 is mainly transmitted from person to person through large respiratory droplets and aerosols (small droplets with diameters ≥ 5 μm [2]) generated by breathing, talking, sneezing, singing, and coughing in close proximity to another person [3-7]. The relative role of large droplets *vs* aerosols is still unclear [8], but aerosols can penetrate more deeply into the lungs than droplets [2]. Indirect transmission through fomites (defined as inanimate objects carrying pathogens) that have been contaminated by respiratory secretions is considered possible [9], but research suggests that this path of transmission is unlikely [4,10-12].

A 2021 review article concluded, based on 5 studies, that less than 10% of globally reported SARS-CoV-2 infections occurred outdoors [13]. The odds of indoor transmission was 18.7 (95% confidence interval (CI): 6.0, 57.9) times higher compared to outdoor transmission. Furthermore, in high- and middle-income countries, about 92% of time is spent indoors or in a vehicle [14]. Hence, it would be expected that more than 90% of transmissions occur indoors, even if the likelihood of in- and outdoors transmission were equal. These studies support the currently prevailing view that most transmissions occur indoors where there is essentially no exposure to solar UV-B (280–315 nm) radiation and greatly reduced exposure to ambient UV-A (315–400 nm) radiation.

Many publications (see Sect. 5) have provided evidence for an inverse relationship between ambient solar UV radiation and incidence or severity of COVID-19. However, the reasons for this negative correlation[54] are not clear. The following hypotheses may explain this association:

1. Exposure to ambient solar UV radiation inactivates SARS-CoV-2 particles, and higher intensity of UV radiation (e.g., at latitudes closer to the Equator) is more effective in inactivating the virus.

2. UV radiation is merely a proxy for other environmental factors such as air temperature that are responsible for the observed inverse correlation. For example, when UV radiation is low in winter, temperature is often also low, prompting humans to stay indoors in close proximity to others, thereby increasing the chance for SARS-CoV-2 transmission. Lower temperatures or other environmental factors such as air pollution may also compromise the immune system and may have a detrimental effect on disease outcome [15]

3. Higher intensity of UV-B radiation leads to more production of vitamin D (Sect. 6) or other substances produced in the skin upon exposure to UV radiation, such as nitric oxide, which may have benefits for disease prevention and severity.

These three hypotheses will be discussed in the following subsections.

Many experimental studies (often using unrealistically large virus concentrations) have shown that SARS-CoV-2 particles can remain viable on porous and non-porous surfaces for several days if they are shielded from UV radiation [16-20]. Survival times on porous surfaces are generally much shorter than on impermeable surfaces because of the different evaporation mechanisms for the two surface types [21]. Infectious SARS-CoV-2 viruses have been recovered from plastic, glass, and stainless steel surfaces after 3 days [16], 7 days [17] and 28 days [18]. SARS-CoV-2 virus particles have been shown to remain viable on banknotes for between four [17] and up to 28 days when the ambient temperature was maintained at 20 °C [18]. On the outer layer of a surgical mask, infectious viruses can survive up to 6 days after contamination. Increasing the ambient temperature greatly reduces the survivability of virus particles on all surfaces to as little as 24 h at 40 °C [18]. According to a recent study [22], the Alpha, Beta, Delta, and Omicron variants of SARS-CoV-2 exhibit more than two-fold longer survival on plastic and skin than the original Wuhan strain. As we will show below, these long lifetimes of SARS-CoV-2 particles decrease greatly upon exposure to UV radiation.

2 The action spectrum for the inactivation of SARS-CoV-2

Action spectra describe the wavelength dependence of biological effects caused by UV radiation. A biological effect is quantified by first multiplying the action spectrum for this effect with the spectrum of the incident radiation and then integrating this product over wavelength. The result is the biologically effective UV irradiance, UV_{BE}.

The action spectrum for the inactivation of SARS-CoV-2 has recently been measured by Biasin et al. [23] using light-emitting diode (LED) sources with ~10 nm bandwidth at wavelengths of 254, 278, 308, 366, and 405 nm. The experiment for establishing the action spectrum has several weaknesses: the uncertainties of the measurements at these wavelengths were not evaluated; the LED's bandwidth of 10 nm is large for measuring a function that varies over four decades; and interpolating measurements at only 5 wavelengths over the 150 nm wide wavelength range of interest is subject to large interpolation errors that have not been discussed. While these limitations are significant, we emphasise that these are the only measurements of the action spectrum for the inactivation of SARS-CoV-2 that are available to date (August 2022).

Figure 1 compares the action spectrum by Biasin et al. [23] with action spectra that have been used previously to estimate the effect of UV radiation on SARS-CoV-2. Of note, the new spectrum has a large sensitivity in the UV-A (315–400 nm) range, while the spectrum for generalised virus inactivation [24]—which has been used in several studies (discussed below) to estimate the inactivation times of SARS-CoV-2—has no sensitivity beyond 320 nm. If the "UV-A tail" measured by Biasin et al. [23] is correct, solar UV radiation could be much more efficient in inactivating the virus responsible for COVID-19, and inactivation would be less influenced by parameters that affect the UV-A and UV-B contributions to solar radiation differently, such as total column ozone[55] (TCO), time of the day, season, or latitude. While this large UV-A tail is missing in the generalised action spectrum for virus inactivation [24], there is evidence that this sensitivity in the UV-A range is real. First, the recently measured absorption spectrum of RNA of Torula yeast also has a large contribution from the UV-A range [26]. Second, the H1N1 influenza virus also seems to be highly sensitive to radiation in the UV-A range [27], and even the action spectrum for erythema [28] has a remarkable resemblance to that measured by Biasin et al. [23]. Third, the dependence of the

---

[54] A negative correlation expresses a statistical relationship between two variables whereby higher values of one variable tend to be associated with lower values of the other. Several essentially equal terms for "negative correlation" are being used, including anticorrelation, inverse correlation, and negative (or inverse) association.

[55] Ozone amounts integrated from the Earth's surface to the top of the atmosphere, measured in Dobson Units (DU). See [25] for more details.

inactivation times of SARS-CoV 2 on UV spectra simulated for various solar zenith angles (SZA) discussed below can only be explained if there is a significant contribution from UV-A wavelengths. This argument is also supported by theoretical calculations [29]. Fourth, it has recently been shown that exposing human coronavirus 229E (CoV-229E)—a virus associated with a range of respiratory symptoms including pneumonia and bronchiolitis—to UV-A radiation leads to a significant reduction in coronavirus spike protein and decreased virus-induced death of infected human tracheal epithelial cells [30]. Fifth, it has also been shown that many viruses can be damaged by peroxides and other reactive oxygen species, which are created by UV-A radiation [31]. However, whether a similar oxidative toxicity also affects SARS-CoV-2 has not yet been determined. Taken together, these considerations suggest that UV-A-mediated mechanisms in addition to RNA damage [26], which is predominantly caused by UV-B wavelengths, lead to the inactivation of SARS-CoV-2 upon exposure to UV radiation.
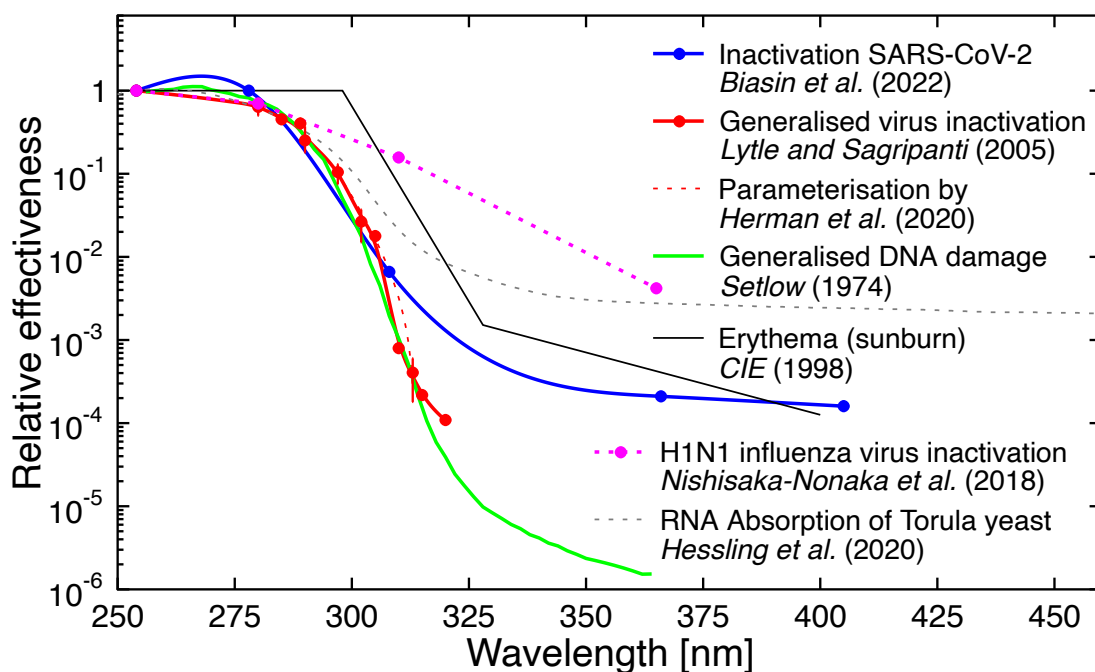
Fig. 1 Comparison of action spectra and other spectra relevant for discussing the wavelength dependence of inactivation of SARS-CoV-2 by UV radiation. All spectra are arbitrarily normalised at 254 nm. Biasin et al. [23] measured the relative effectiveness of UV radiation in inactivating SARS-CoV-2 at 278, 308, 366, and 405 nm (blue symbols). Data were interpolated with a spline approximation that also included a data point at 254 nm measured by Biasin et al. [32]. Note that this interpolation is uncertain between 280 and 305 nm due to the lack of intermediate measurements in this wavelength range. Lytle and Sagripanti [24] give the generalised action spectrum for virus inactivation (red symbols). The spectrum is based on data from up to 24 viruses (data at some wavelengths are based on fewer viruses). Data were interpolated with a spline approximation with little uncertainty (red line). The broken red line is a fit to the same data by Herman et al. [33] using an analytical function. Note that this function deviates significantly from the data points between 307 and 312 nm. Setlow [34] provides the generalised action spectrum for DNA damage as parameterised in the Tropospheric Ultraviolet and Visible (TUV) radiative transfer model (https://www.acom.ucar.edu/Models/TUV/Interactive_TUV/) (green line). CIE [28] shows the action spectrum for erythema (black line). The action spectrum from Nishisaka-Nonaka et al. [27] is for the inactivation of the H1N1 influenza virus by inhibiting replication and transcription of viral RNA in host cells (pink symbols). The spectrum from Heßling et al. [26] is not an action spectrum but the absorption spectrum of RNA of Torula yeast, normalised at 254 nm. (Absorption and action spectra would be identical if every absorbed photon were to lead to irreversible damage; however, this is not the case if repair mechanisms are at play [35].)

3 Inactivation times of SARS-CoV-2 virus particles with solar UV radiation

Several studies have determined the time needed to inactivate 90% of virus particles upon irradiation with UV radiation, based on: (i) direct measurements using solar simulators [36-41]; (ii) the action spectrum for the inactivation of SARS-CoV 2 particles measured by Biasin et al. [23], followed by theoretical calculations; or (iii) theoretical calculations using the standardised action spectrum for virus inactivation [33,42-44]. These studies are discussed in more detail below and results are summarised in Table 1.

All studies assume that the number of viable virus particles, N, decreases exponentially when exposed to germicidal radiation (either from artificial light sources or the Sun) for the time t [45]:

$$N = N_0 e^{-\alpha t} \qquad (1)$$

where N_0 is the number of viable particles at the start of the exposure and α is a decay constant. With t_{10} and t_1 defined as the times that reduce N to 10% and 1% of N_0, respectively, Eq. (1) implies that t_1 is twice as long as t_{10}. However, the time difference between t_{10} and t_1 can be considerably longer under certain conditions [46,47] because viruses in a real-world setting are embedded in a matrix of body fluids (e.g., saliva and mucus) or foreign objects, which partially shield viruses from exposure. Clustered populations of viruses can also protect each other from exposure to radiation [48]. Hence, there are large uncertainties in extrapolating t_{10} to t_1 and beyond (e.g., 0.1% and 0.0001% survival for disinfection and sterilisation levels, respectively [44]). This is particularly the case for virus particles that are embedded in porous materials, such as face masks and clothing, or otherwise shielded from UV radiation.

3.1   Measured inactivation times

Ratnesar-Shumate et al. [37] used a solar simulator to determine t_{10} for SARS-CoV-2 virus particles that were first suspended in either simulated saliva or a culture medium (gMEM[56]) and then dried on stainless steel surfaces. The solar simulator produced spectral irradiance resembling noon-time solar spectra at 40° N latitude (e.g., Philadelphia, Ankara, Beijing) for three days representative of summer, spring, and winter: 21 June (SZA=16.5°), 21 February (SZA=50.6°) and 21 December (SZA=63.4°). The three spectra were compared with spectra modelled with the Tropospheric Ultraviolet and Visible (TUV) radiative transfer model (https://www.acom.ucar.edu/Models/TUV/Interactive_TUV/), and the agreement was generally excellent. However, the simulated spectrum for 21 June (high sun conditions in summer of the Northern Hemisphere) underestimated the spectrum calculated by TUV at wavelengths less than 308 nm. This difference is significant because the product of the solar spectrum and any action spectra for virus inactivation typically peaks near 305 nm, but the consequence of this discrepancy cannot be quantitatively assessed from the data provided by Ratnesar-Shumate et al. [37]. Inactivation times t_{10} for virus particles embedded in saliva were 6.8, 8.0 and 12.8 minutes for the three spectra, respectively. For viruses enclosed in the culture medium, t_{10} was more than twice as long: 14.3, 17.6, and 54.4 minutes for the spectra simulated for 21 June, 21 February, and 21 December, respectively.

Using the same solar simulator, Schuit et al. [36] determined t_{10} for aerosolised virus particles. For viruses suspended in saliva, t_{10} was 7.5 and 19 minutes for exposure to simulated noon solar spectra for 21 June (SZA=16.5°) and 7 March (SZA=45.0°), respectively.

---

[56] Glasgow's Minimum Essential Medium

Table 1. Time to inactivate 90% (10% survival) of virus particles at 40° N upon irradiation with UV radiation.

Study	Time t_{10} = time to inactivate 90% of infectious virus (minutes)				Ratio
Measured inactivation times					
	21-Jun (Summer) SZA=16.6° UV-B=1.83 W m^{-2} UV-A=58.5 W m^{-2} UVI=10.2	7-Mar SZA=45.1° UV-B=0.92 W m^{-2} UV-A= 40.5 W m^{-2} UVI=4.8	21-Feb SZA=50.8° UV-B=0.70 W m^{-2} UV-A= 34.9 W m^{-2} UVI=3.6	21-Dec (Winter) SZA=63.4° UV-B=0.28 W m^{-2} UV-A= 21.5 W m^{-2} UVI=1.6	Winter / Summer
Saliva on steel [37]	6.8		8.0	12.8	1.9
Growth medium (gMEM) [37]	14.3		17.6	54.4	3.8
Aerosol in saliva [36]	7.5	19			
Aerosol in culture medium [36]	12.6	13.6			
Calculated inactivation times					
Calculated by us, based on the action spectrum by [23] and D_{10} inactivation dose of 8.1 J m^{-2} at 254 nm	4.4	7.4	9.1	16.5	3.8
Calculated by us, based on the action spectrum by Lytle and Sagripanti [24] and D_{10} inactivation dose of 3.2 J m^{-2} at 254 nm.	6.1	18.1	27.2	97.2	15.9
Calculated by Herman et al. [33]. Based on the action spectrum by Lytle and Sagripanti [24] as parameterised by Herman et al. [33] and D_{10} inactivation dose of 3.2 J m^{-2} at 254 nm.	4.8	13.4	19.8	69.3	14.6
Calculated by Sagripanti and Lytle [43]. Based on the action spectrum by Lytle and Sagripanti [24] and D_{10} inactivation dose of 6.9 J m^{-2} at 254 nm.	22	63*		> 300	> 14

* refers to spring equinox on 21 March instead of 7 March.

In addition to the two studies discussed above, Sloan et al. [41] determined inactivation times for SARS-CoV-2 using another solar simulator (SunLite Solar Simulator Model 11002 from Abet Technologies). The simulator was set to "1 Sun", defined as "full sunlight intensity on a bright clear day on Earth and measuring approximately 1000 W m^{-2}". According to data provided by the manufacturer, the simulator produces UV-A and UV-B irradiances of 41.46 W m^{-2} and 1.28 W m^{-2}, respectively, at these settings. These irradiances are reportedly similar to those measured at the equinox at 40° N latitude during noon. However, the authors do not show a spectrum of their solar simulator and we therefore could not determine whether the device does indeed simulate the solar spectrum accurately, in particular in the critical wavelength range of 300–320 nm. Viral solution was suspended in either culture medium or simulated mucus, and then deposited on stainless steel coupons, and desiccated. For virus suspended in culture medium, the inactivation time t_{10} was 23 minutes under controlled temperature (22.5 °C) and relative humidity (RH=34%). When the virus was suspended in simulated mucus, the inactivation time was significantly longer (t_{10}=91 minutes). These inactivation times are longer than those measured by Ratnesar-

Shumate et al. [37]; however, a direct comparison is not possible because of the uncertainty of the solar spectrum used by Sloan et al. [41]. While the study confirms that inactivation times depend on the medium enclosing the virus, the results contradict those by Ratnesar-Shumate et al. [37], which indicate shorter inactivation times for virus embedded in saliva versus a growth medium.

In another study, Raiteux et al. [39] irradiated stainless steel coupons loaded with a suspension containing SARS-CoV-2 virus with a solar simulator consisting of a Xenon lamp and a filter. The simulator was set to an illuminance[57] of either 10,000 lx, representing "a cloud-covered sky in autumn in France", or 56,000 lx, representing "a slightly cloudy sky in summer in France". No further description of the simulator's output is given and it is unknown whether the spectrum resembles that of sunlight in the UV-B and UV-A regions. Results of the study should therefore be considered only in a qualitative sense. The experiment revealed that no virus was detectable after a 20 minute exposure to an illuminance of 10,000 lx at either 20 or 35 °C and a relative humidity of 50%. For an illuminance of 56,000 lx, infectious virus was no longer detectable after 5 min of exposure. Ninety percent of viral load was lost every 9.2 minutes at 10,000 lx and every 2.1 minutes at 56,000 lx. The inactivation time was inversely proportional to the applied illuminance within the measurement uncertainty. This suggests that the UV-B and UV-A contributions of the lamp spectra scale linearly with illuminance. The results are qualitatively consistent with those by Ratnesar-Shumate et al. [37] and confirm that simulated sunlight rapidly inactivates SARS-CoV-2 at temperatures ranging from 20 °C to 35 °C.

Using a model 91293 solar simulator from Oriel Instruments, which was equipped with a filter to block visible and infrared radiation, Wondrak et al. [38] confirmed that "UV radiation at environmentally relevant doses" will inactivate SARS-CoV-2 coronaviruses. However, no inactivation times were calculated and the study therefore cannot be used for a quantitative assessment.

3.2   Calculated inactivation times

All studies discussed in the previous section used a solar simulator to determine inactivation times. In contrast, Carvalho et al. [44], Herman et al. [33], Nicastro et al. [40], and Sagripanti and Lytle [43] used an indirect method to estimate t_{10} based on the inactivation dose at 254 nm (a wavelength in the UV-C waveband produced by a mercury lamp) and an action spectrum for virus inactivation. The inactivation time t_{10} in minutes is then calculated from these quantities:

$$t_{10}[\min] = \frac{D_{10}(\lambda_r)}{60\mathrm{s} \times E_e} = \frac{D_{10}(\lambda_r)}{60\mathrm{s} \times \int E(\lambda)A(\lambda)\mathrm{d}\lambda}$$

where $D_{10}(\lambda_r)$ is the UV dose at 254 nm that results in 10% survival, $A(\lambda)$ is the action spectrum, and $E(\lambda)$ is the spectral irradiance of sunlight modelled for various SZAs and TCO. The integral is evaluated over a wavelength range where both $E(\lambda)$ and $A(\lambda)$ are different from zero. Of the three studies, the most reliable is the one by Nicastro et al. [40] because it uses the measured action spectrum by Biasin et al. [23] for the inactivation of SARS-CoV-2 particles and $D_{10}(\lambda_r)$ measured also for SARS-CoV-2. In contrast, Herman et al. [33] and Sagripanti and Lytle [43] use the action spectrum by Lytle and Sagripanti [24]. (See Fig. 1 for comparison of action spectra).

Using the action spectrum and dose $D_{10}(254)$ reported by Nicastro et al. [40], we calculated inactivation times of 3.5 and 12.2 minutes for noontime spectra on the summer solstice (21 June), and on the winter solstice (21 December) for northern latitudes of 40°. For similar conditions, Sagripanti and Lytle [43] calculate considerably longer times of 22 minutes and > 300 minutes because calculations are based on the action spectrum by Lytle and Sagripanti [24], which does not have a UV-A contribution (Fig. 1). Using the same action spectrum, Herman et al. [33] calculated inactivation times t_{10} for viruses adhered to fomites oriented horizontally under clear skies. For SZAs of less than 20°, 40°, and 60°, inactivation times were less than 8, 20, and 60 minutes, respectively. These times are generally smaller than those determined by Sagripanti and Lytle [43], mostly due to the difference in the inactivation dose at 254 nm assumed by the two studies. We note that the calculations by Herman et al. [33] are also affected by their poor parameterisation of the action spectrum (Fig. 1). Likewise, the interpolation of the measurements by Nicastro et al. [40] is uncertain because the action spectrum was measured at only five wavelengths with a relatively large bandwidth of ~10 nm (Sect (2)). We further note that the ratio of inactivation times for winter and summer (last column of Table 1) calculated by Nicastro et al. [40] agree much better with the times measured by Ratnesar-Shumate et al. [37] than the times calculated by Herman et al. [33] and Sagripanti and Lytle [43]. This observation is strong evidence that the action spectrum by Biasin et al. [23], with its large UV-A tail, is closer to the actual action spectrum.

Carvalho et al. [44] calculated inactivation times for locations across the globe based on UV radiation data from the Tropospheric Emission Monitoring Internet Service (TEMIS), which uses assimilated UV radiation fields from several space-borne instruments. These UV radiation data refer to the daily radiant exposure and were weighted with the DNA action spectrum [34] shown in Fig. 1. Hence, the effect from UV-A wavelengths was likely underestimated. In contrast to the studies discussed above, Carvalho et al. [44] took into

---

[57] Illuminance is expressed in the unit of lux (lx) and is the spectral irradiance weighted with the sensitivity of the human eye under daylight conditions, expressed by the photopic luminosity function, and scaled with 683.002 lx W^{-1} m^2.

account that virus particles embedded in aerosol are equally sensitive to radiation from all directions. They assumed inactivation doses $D_{10}(254)$ of 1.8 J m^{-2} (least conservative, based on [36]) and 7.0 J m^{-2} (most conservative, based on [37]), and calculated inactivation times t_{10} of ~5 minutes for overhead Sun (e.g., São Paulo (24° S), Brazil) for the least conservative scenario. During summer in Iceland, t_{10} was calculated to range between 30 to 100 min. These inactivation times are similar in magnitude to those listed in Table 1. Carvalho et al. [44] performed similar calculations for sterilisation level inactivation, where the fraction of "surviving" viruses is less than one millionth of the initial number of viable virus particles. Associated sterilisation times are naturally much longer than t_{10}; however, these times are of little practical use considering that neither the number of viable particles at the start of the exposure nor the number of virus particles that result in an infection is well known.

In summary, the uncertainty of inactivation times for SARS-CoV-2 is large and depends on many factors including uncertainties of the experiments used to determine inactivation times and the matrix in which the virus is embedded. Based on the studies discussed above we conclude that 90% of SARS-CoV-2 virus particles will be inactivated by solar UV radiation within 4 to 20 minutes under optimal conditions for SZA ≤ 40°. These times will become considerably larger for SZA > 40°, during cloudy conditions, if surfaces are not directly irradiated by sunlight, or if virus particles are shielded from solar exposure by other means (absorption by matrix material, deposition on a porous material, shade). Even inactivation times as short as 5 minutes may be too long to protect against transmission among people in the outdoors talking to each other in close proximity. Furthermore, most transmissions occur indoors where there is essentially no exposure to solar UV-B radiation (most glass windows do not transmit at UV-B wavelengths), and both UV-A and visible solar radiation are greatly reduced, in particular when direct sunlight is blocked by window shades or other means. Hence, while solar radiation helps to disinfect surfaces or exhaled aerosol contaminated with SARS-CoV-2 particles, one cannot rely on the Sun's germicidal effect in general and, in particular, early and late in the day, during winter, or at high latitudes during all seasons.

4 Radiation amplification factors for SARS-CoV-2 action spectra

Radiation Amplification Factors (RAFs) are used to approximately assess the sensitivity of effects of UV radiation to changes in the stratospheric ozone layer. Specifically, the dimensionless RAF describes the relative change in effective UV irradiance (UV$_{BE}$) in response to a relative change in TCO:

$$\Delta UV_{BE}/UV_{BE} = -RAF \times \Delta TCO/TCO \tag{3}$$

where the symbol Δ expresses a change in UV$_{BE}$ or TCO in absolute units. For example, a RAF of 1.5 means that a 1% change in TCO would lead to a 1.5% change in UV$_{BE}$. For larger (> 10%) changes in TCO, such as the decreases in TCO that would have occurred without the implementation of Montreal Protocol, the power form of Eq. (3) [49] is typically applied, but the definition of the RAF remains unchanged:

$$UV_{BE+}/UV_{BE-} = \left(TCO_-/TCO_+\right)^{RAF} \tag{4}$$

where the subscripts (+ and −) refer to the cases with higher or lower values of ozone and UV$_{BE}$, respectively.

RAFs for the action spectra by Biasin et al. [23] and Lytle and Sagripanti [24] are shown in Fig. 2. RAFs for the action spectrum of Biasin et al. [23] range between 0.3 and 1.3 for SZA ≤ 60° and TCO between 200 and 400 DU, which cover the majority of conditions outside the polar regions. The magnitude and pattern is similar to RAFs for the erythemal action spectrum [28], which is expected given the similarity of the two action spectra (Fig. 1). In contrast, RAFs for the action spectrum of Lytle and Sagripanti [24] are between 1.9 and 2.7 for the same range of SZAs and TCO, and similar to those of the DNA damage action spectrum [34]. Hence, the effect of changes in ozone is more than a factor of two larger on average for the spectrum by Lytle and Sagripanti [24] than for that by Biasin et al. [23].
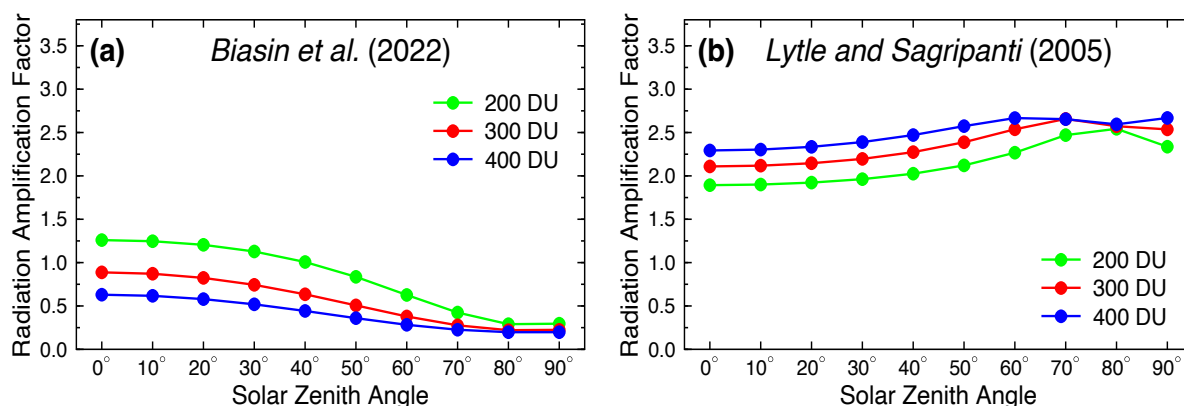
Fig. 2 Radiation amplification factors for the action spectra by (a) Biasin et al. [23] and (b) Lytle and Sagripanti [24]. RAFs are shown as a function of SZA for TCO of 200, 300, and 400 Dobson Units (DU).

5 Observed relationships between UV radiation and COVID-19 incidence

Many observational epidemiological studies have demonstrated an inverse relationship between some metric of UV radiation and COVID-19 incidence rates [50-60]. Most of these studies have flaws as discussed in the following. Many papers also report an inverse correlation with temperature and humidity; however, these relationships are not further discussed in depth.

Gorman and Weller [54] review the potential of UV radiation to alter morbidity and mortality from COVID-19 based on more than 30 studies from many countries. The article is based on knowledge as of October 2020 (less than one year after the start of the pandemic) and concludes that inverse associations have been observed between measures of ambient UV radiation and COVID-19 incidence and mortality in most, but not all studies. Depending on the study, UV intensities were quantified by the UV Index[58] (UVI); UV-A, UV-B, and UV-A+UV-B irradiance; and vitamin D-weighted UV irradiance. Gorman and Weller [54] also point out that many studies did not adjust for important confounders such as population demographics, temperature, and humidity.

Carleton et al. [53], Choi et al. [52], and Ma et al. [50] applied sophisticated statistical analyses and adjusted for several confounders to quantify the relationship between UV radiation and various measures of COVID-19 or SARS-CoV-2 activity. However, the three studies are based on UV fields from the ERA5 reanalysis [61], which are defined as the integration over wavelengths between 200 nm and 440 nm (https://docs.meteoblue.com/en/meteo/data-sources/era5). The contribution from the wavelength range 400–440 nm, which is in the visible part of the spectrum, accounts for almost 50% of radiative energy of the "UV" datasets used in these studies. Their conclusions that higher UV radiation dose is associated with lower COVID-19 growth rates are therefore questionable. Furthermore, the three studies analysed data for relatively short periods close to the start of the pandemic (Carleton et al. [53] used 1 January to 10 April 2020, Choi et al. [52] used 1 March 2020 to 13 March 2021, and Ma et al. [50] used 15 March to 31 December 2020). Public health policies (e.g., lock-downs, closing of borders, social distancing, and wearing of masks); strategies in managing the pandemic; and available treatments for COVID-19 changed rapidly during 2020. These changes are important confounding factors that are difficult to quantify. Statistical analyses based on data from many countries, as used by Carleton et al. [53] and Choi et al. [52],

---

[58] The UV Index is calculated by weighting solar UV spectra with the action spectrum of erythema [28] and scaling the result with 40 m^2/W.

are further hampered by the heterogeneity of the policies enacted around the world. Nevertheless, the three studies report strong inverse associations between solar radiation in the 290–440 nm range and various COVID-19 metrics. For example, Carleton et al. [53] conclude that the increase in seasonal "UV" exposure between January and June 2020 lowered extratropical Northern Hemisphere COVID-19 growth rates by 7.4%±2.9% (±1 standard deviation). Over the same period, the seasonal decline in exposure to UV radiation in the extratropical Southern Hemisphere raised growth rates by 7.3%±2.9%. However, they also conclude that UV radiation has a substantially smaller effect on the spread of the disease than social distancing policies. Ma et al. [50] found that the fraction of the reproduction number R_t (defined as the mean number of new infections caused by a single infected person), which are attributable to temperature, specific humidity, and UV radiation, were 3.73%, 9.35% and 4.44%, respectively. Hence, these meteorological factors account for a total 17.5% of R_t.

Moozhipurath et al. [56] reported that an increase in the daily maximum UVI by one unit was associated with a 1.2% decline in daily growth rates of cumulative COVID-19 deaths. UVI data were downloaded from https://darksky.net/ without identifying their source. The analysis is based on data from 183 countries and the period 22 January 2020 to 8 May 2020. The caveats of using heterogeneous data from a short period as noted above also apply here. In a follow-on study, Moozhipurath and Kraft [55] posit that reduced exposure to solar UV radiation during lockdowns, with people confined to their homes, reduced their vitamin D status (Sect. 6). This implies that the positive effect of lockdowns in reducing transmissions is partly offset by a greater risk of severe illness once an infection occurs. The authors conclude that lockdowns in conjunction with adequate exposure to UV-B radiation might have reduced the number of COVID-19 deaths more strongly than lockdowns alone, and estimate that there would be 11% fewer deaths on average with sufficient exposure to UV B irradiation during the period when people were recommended not to leave their house. However, a major weakness of the study is the lack of measurement of the vitamin D status at the population level. The vitamin D status was instead estimated from UVI data used in their earlier study [56] without explicitly describing the assumed relationship between UVI and vitamin D status and without taking behavioural changes into account. For example, there is no evidence that lockdowns reduced vitamin D status at the population level. Indeed the opposite may have occurred in some countries due to reduced office hours. Of note, according to the paper's "competing interests" statement, the lead author of the paper is a "full-time employee of a multinational chemical company involved in vitamin D business and holds shares in the company," which may have biased the study.

Isaia et al. [60] correlated death rates and incidence rates of infections against vitamin D-weighted UV irradiation, fraction of people in nursing homes, air temperature, and comorbidities across Italy. The study is based on the short period of 25 February to 31 May 2020 when policies and treatment options rapidly evolved, coinciding with seasonal increase in UV radiation. The authors found that the amount of solar UV radiation contributed the most to the observed correlation, explaining up to 83.2% of the variance in COVID-19-affected cases per population. This very high percentage contradicts the much lower numbers given in the studies discussed above and is not reconcilable with the fact that most COVID-19 transmissions occur indoors. While Isaia et al. [60] speculate that the effect of UV radiation is mediated by the synthesis of vitamin D, vitamin D status of the population was not assessed. Considering that vitamin D status is also influenced by individual behaviour (sun exposure, sun protection, and supplementation), the study merely presents a hypothesis.

The inverse correlation between UV radiation and COVID-19 incidence or deaths documented in the studies above is qualitatively consistent with the virucidal effect of UV radiation and its role in raising 25(OH)D levels. However, each of these studies has major limitations and none of them provides a clear causative pathway to explain the observed associations quantitatively.

UV radiation strongly covaries with visible radiation, and it is therefore very difficult to determine from observational studies like those cited above whether the perceived seasonality is driven by UV radiation (e.g., via its germicidal effects or the production of vitamin D); visible radiation, which controls the circadian and circannual rhythms; or other factors that co-vary with UV radiation, such as temperature. This assertion is demonstrated in Fig. 3, which correlates measurements of UV-B and UV irradiance at San Diego, California (32° N), with visible (VIS) irradiance in the 400–600 nm range. The coefficients of determination R^2 are 0.868 for UV-B *vs* VIS and 0.976 for UV *vs* VIS, suggesting that 86.8% and 97.6% of the variance in UV-B and UV irradiance, respectively, can be explained by the variance in visible irradiance. Compared to these strong associations, in particular for UV *vs* VIS, UV radiation and COVID-19 incidence rates are far less associated with each other; hence, studies that show a strong inverse correlation between the two variables would likely also show a strong inverse correlation between COVID-19 and visible irradiance even though visible radiation has little effect on virus survival and does not lead to vitamin D production.

Cherrie et al. [62] demonstrated a significant negative association between deaths from COVID-19 and ambient UV-A radiation and attribute this relationship to the release of nitric oxide (NO) from the skin upon exposure to UV-A radiation. Such release of NO has been shown to be associated with lower blood pressure [63] and reduced incidence of myocardial infarctions [64]. As there is evidence that hypertension and cardiometabolic disease also increase the risk of death from COVID-19 [65], Cherrie et al. [62] argue that UV-A-driven release of NO reduces the mortality from COVID-19. In a commentary to the paper, McKenzie and Liley [66] point out that the data could equally be explained by production of vitamin D by exposure to solar UV-B radiation considering the strong correlation between UV-A and UV-B radiation. Interestingly Guasp et al. [57] show a weaker inverse correlation between COVID-19 incidence and the UVI than with short-wave irradiance (300–3,000 nm; a wavelength range including UV and visible radiation plus a part of the infrared spectrum). While this study is based on data from the very beginning of the pandemic only, it suggests that visible radiation may be a stronger determinant of disease incidence than UV radiation for reasons discussed in more detail below.

When interpreting the studies cited above, it has to be noted that correlation does not imply causation. For example, Martinez [67] pointed out that the incidence of polio, which peaks in the summer, correlates with temperature, daylength, and the sale of bathing suits. A transmission model using any of the three drivers would capture the seasonal structure of the disease because all drivers contain a covariate with the necessary seasonal dependence, even though it is highly unlikely that sales of bathing suits cause polio. Applying this thought experiment—combined with the high covariance between UV and visible radiation—to the observed inverse correlations between UV radiation and COVID-19 incidence rate suggests that these correlations cannot prove that UV radiation is the causative factor for the perceived seasonality of COVID-19.
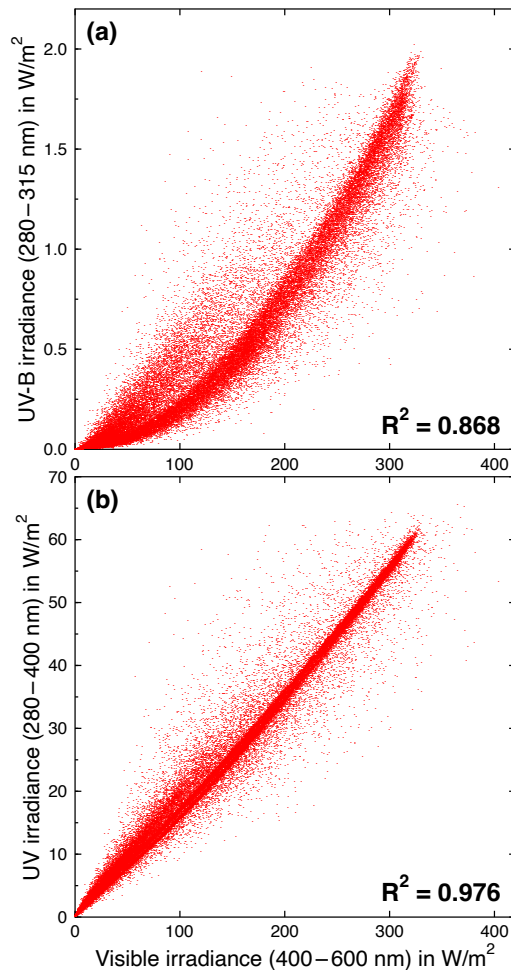
Fig. 3 Scatter plot of (a) UV-B irradiance (280–315 nm) and (b) UV irradiance (280–400 nm) versus visible irradiance (400–600 nm). Data were measured in San Diego (32° N) between 2005 and 2008 by a SUV-100 spectroradiometer of the former National Science Foundation's (NSF) UV monitoring network [68]. The coefficient of determination R^2 is 0.868 for (a) and 0.976 for (b). Some of the scatter is caused by the fact that the SUV-100 is a scanning instrument, which requires about 15 minutes of time to complete a spectrum between 280 and 600 nm. Cloud conditions may change over this period, thereby exacerbating the scatter between the two quantities. If the whole spectrum had been measured at the same time, the scatter between the quantities would be smaller and R^2 larger, suggesting that the actual covariance between UV and visible irradiance is even higher than indicated in the two plots.

The pilot phase of a prospective, double-blinded, randomised, placebo-controlled trial involving 30 patients has recently been completed that aimed to determine whether phototherapy with narrow-band UV radiation (NB-UVB) at 311 nm has an effect on the mortality of hospitalised, high-risk COVID-19 patients [69]. The trial was motivated by the observation that NB-UVB treatment stabilises the immune system relevant to autoimmune diseases. Considering that COVID-19 morbidity and mortality are partly driven by poor immune regulation (Sect. 6), it is therefore conceivable that treatments with NB-UVB may affect COVID-19 disease outcomes. The 30 enrolled patients were randomised 1:1 to NB-UVB or placebo phototherapy and treated daily with sub-erythemal doses for up to eight consecutive days. Although this pilot study was primarily to test safety and feasibility, it found that the twenty-eight-day mortality was 13.3% (2 patients) in the treatment and 33.3% (5 patients) for those receiving the placebo. However, the difference was not statistically significant (p=0.39). Results for a planned follow-on study with a larger sample size are not yet available. If such a larger study were to demonstrate the efficacy of NB-UVB treatment, the effect of UV radiation on COVID-19 disease outcome could be firmly established. Such an outcome would also inform the assessment of the effects of solar UV radiation on COVID-19.

After many years of research, the factors that drive the seasonality of common diseases (and the relative importance of the factors causing seasonality) have still not been unambiguously determined. For example, humidity, temperature, closeness of people, changes in diets, and vitamin D status have been suggested to explain why influenza is more prevalent in winter than summer [15]. In addition, the human immune system may change with season, becoming more resistant or more susceptible to different infections based on daylength, and the disease burden is therefore partly driven by the circannual rhythm [70], which is, in turn, partly driven by

visible radiation. For example, in one German cohort, expression in white blood cells of nearly one in four genes in the entire genome differed between seasons. Genes in the Northern Hemisphere tended to switch on when they were switched off south of the Equator, and *vice versa* [71]. Other factors that are potentially responsible for seasonality include: pathogen survival in the environment and transmissibility; changes over time in pathogen reservoirs (human and non-human); frequency of pathogen-host interactions (cultural, socioeconomic, linked to lifestyle and temperature); host susceptibility to infection; indoor heating systems that generate conditions of low relative humidity; and difference between indoor and outdoor temperatures [54,70,72-75]. Many of these factors co-vary with UV radiation. Diseases from enveloped viruses, such as SARS-CoV-2 and influenza viruses, generally have a stronger seasonality than those from viruses without an envelope, such as the rhinoviruses that cause the common cold [15]. It is therefore plausible that the factors that drive the seasonality of influenza are also predominantly responsible for the seasonality of SARS-CoV-2.

As mentioned in the introduction (Sect. 1), there is strong evidence that most SARS-CoV-2 infections occur indoors [13] where there is essentially no exposure to solar UV-B radiation. Furthermore, exposure studies have shown that adults working outdoors receive only about 10% of the total available annual UV radiation dose, while indoor-working adults and children get only about 2–4% of the available UV dose [76,77]. These fractions were likely even lower during lockdowns. Despite the observed inverse correlations between UV radiation and COVID-19 incidence, and after considering the many other factors that correlate with UV radiation discussed above, we conclude that it is premature to establish UV radiation as the key factor driving the seasonality of the COVID-19 pandemic.

6 Vitamin D and risk and severity of COVID-19

Vitamin D has important modulatory effects on the immune system that might reduce the risk and severity of COVID-19. The active form of vitamin D upregulates innate immunity by stimulating release of antimicrobial peptides, such as cathelicidin, which leads to an early defence against infection [78]. Vitamin D also influences the adaptive immune system, dampening down overproduction of pro-inflammatory cytokines, which can result in severe complications and organ damage (a cytokine storm). Vitamin D might also influence outcomes from COVID-19 through effects on the renin angiotensin aldosterone system, with important effects on vascular function, hypertension and cardiovascular remodelling [79]. Observational studies [80] and randomised controlled trials [81,82] suggest a beneficial effect of vitamin D supplementation on the incidence and severity of acute respiratory tract infection, but there is relatively limited high-quality information about SARS-CoV-2 infection and/or COVID-19.

Meta-analyses of observational studies indicate inverse associations between 25(OH)D concentration and risk of SARS-CoV-2 positivity or COVID-19 disease or severity [83-86]. However, the quality of the observational studies has largely been low and heterogeneity high. Notable potential biases relate to lack of adequate control of confounders, self-reported SARS-CoV-2 positivity, and measurement of 25(OH)D concentration many years before the SARS-CoV-2 outbreak. In addition, a range of assays, with potentially variable accuracy and precision, have been used to measure 25(OH)D concentration; thus, even if the association is causal, an optimal 25(OH)D concentration cannot be defined.

Mendelian randomisation (MR) studies can overcome the bias introduced by confounding factors and timing of measurement. These studies assess associations between genetically determined, rather than measured, 25(OH)D concentration. The relatively small proportion of variability in 25(OH)D concentration explained by genetic variants necessitates a large sample size to give sufficient statistical power to detect small effect sizes. There have been two MR studies conducted within the COVID-19 host genetics initiative [87,88]. The sample size and genetic instruments used varied somewhat, but both arrived at the same conclusions; that is, there is no statistically significant evidence of a causal effect of 25(OH)D concentration on COVID-19 susceptibility or severity, but small effects cannot be ruled out. In the larger of the two studies (total cases 17,964) [88], the odds ratio (OR) for risk of infection for each standard deviation increase in 25(OH)D (using the genetic instrument that explained the most variability) was 1.04 (95% CI: 0.92, 1.18). The OR for severe disease (n=4336 cases) compared with population controls was 0.96 (95% CI: 0.64, 1.43). While there was no association with having 25(OH)D concentration <50 or <75 nmol/L (commonly used cut-points to define vitamin D deficiency or insufficiency, respectively) [88], a link with more severe vitamin D deficiency (e.g., 25(OH)D < 30 nmol/L) cannot be excluded.

Several randomised trials have examined the effect of supplementing hospitalised COVID-19 patients with vitamin D on disease outcomes, with heterogeneous findings. A randomised placebo-controlled trial in Brazil supplemented patients (n=240) with a large single oral dose of 200,000 IU of vitamin D_3 or placebo[59] [89]. There was no difference in the length of stay (primary outcome; median 7 days in both groups) and no statistically significant difference in any of the secondary outcomes, specifically in-hospital mortality (vitamin D 7.6% *vs* placebo 5.1%; *p*=0.43), admission to the intensive care unit (16.0% *vs* 21.2%; *p*=0.30) or mechanical ventilation (7.6% *vs* 14.4%; *p*=0.09). Similarly, a study in Argentina did not find any benefit of high-dose vitamin D supplementation [90]. In this

---

[59] For comparison, the recommended daily intake of vitamin D_3 ranges from 400 IU to 800 IU/day in many countries.

multicentre randomised controlled trial, 218 hospitalised patients with confirmed COVID-19, mild-to-moderate symptoms, and risk factors for progression were randomised to a single oral dose of 500,000 IU of vitamin D_3 or placebo. There was no significant effect on the respiratory score of Sepsis-related Organ Failure Assessment (p=0.93), in-hospital mortality (4.3% vitamin D *vs* 1.9% placebo, *p*=0.45) or other secondary outcomes (length of stay and intensive care unit admission). In contrast, a pilot trial in Spain, in which 76 hospitalised patients were randomised to control (usual care) or supplementation with 0.532 mg of 25(OH)D (calcifediol) on the day of admission[60], day 3, and day 7, followed by a weekly dose of 0.266 mg until discharge, observed reduced admission to intensive care in the supplemented group (2% *vs* 50%; *p*<0.001) [91]. An open-label trial[61] in France, in which 254 hospitalised patients aged ≥65 years were randomised to a single oral dose of 400,000 IU or 50,000 IU of vitamin D_3, found reduced deaths at 14 days in the high-dose group (6%) compared with the lower-dose group (11%) (*p*=0.049) [92]. In addition to the inconsistency in the findings, and some limitations related to trial design in some studies, all used very large bolus doses (i.e., a single dose given all at once) of vitamin D, which are largely uninformative about the effects of vitamin D obtained through sunlight or usual supplementation doses.

In conclusion, the evidence supporting a role of vitamin D in the risk or severity of COVID-19 is currently inconsistent. In addition, there is limited information about the effect of severe vitamin D deficiency. Given the laboratory evidence supporting a role of vitamin D in the immune system, and the indications of benefit for other acute respiratory tract infections, it would be prudent to adopt a precautionary principle and develop policies to avoid vitamin D deficiency. However, routine supplementation of populations that are not experiencing vitamin D deficiency is currently not warranted.

7 Effect of ambient air pollution on SARS-CoV-2 infections

Ambient air quality is affected by pollutants that are emitted into the air. Photochemical smog is formed when these pollutants are exposed to solar UV radiation [93]. Several studies reported a decrease in air pollution following the enforcement of lockdowns in many countries worldwide resulting in a reduction of excess mortality [94,95]. The progression of the COVID-19 pandemic may also have been affected by changes in ambient air pollution. A study that analysed the effect of air pollution on the 2002–2004 outbreak of severe acute respiratory syndrome (SARS), a disease which predated COVID-19 and was caused by the severe acute respiratory syndrome coronavirus 1 (SARS-CoV-1), yielded mixed and inconclusive results [96]. On the other hand, several recent studies indicate significant associations between air pollution and COVID-19 incidence and fatality rates [97-100]. While factors associated with infection have been well established, such as the proximity to infected persons in indoor spaces through airborne transmission [101], the question of the role of ambient air pollution in the spread of SARS-CoV-2 and the development of the pandemic is still unclear. For the USA, Wu et al. [102] found that higher historical exposures to $PM_{2.5}$ (particles with a diameter of ≤ 2.5 micrometres) were positively associated with higher county-level COVID-19 mortality rates after accounting for many area-level confounders. Specifically, an increase of 1 µg m^{-3} in the long-term average of $PM_{2.5}$ was associated with a statistically significant 11% (95% CI: 6%, 17%) increase in the county's COVID-19 mortality rate. Similarly, by analysing data from China for the period 19 January 2020 to 15 March 2020 and applying a lag of 21 days between COVID-19 diagnosis and death, Yao et al. [103] found that a higher case-fatality rate of COVID-19 was associated with higher (historical, 2000-2016) daily concentrations of $PM_{2.5}$ and PM_{10} (particles with a diameter of ≤ 10 micrometres). There are several biological pathways that have been proposed whereby exposure to outdoor air pollution may relate to transmission, host susceptibility, and disease severity [104,105]. Air pollution has been postulated to affect the viability and transport of viral particles in the air [106] and hence increase respiratory infections. It is also possible that air pollution could increase severity of COVID-19 through its contribution to chronic conditions—such as chronic respiratory disease, diabetes, and heart disease—and through long-term effects on immune system function [107]. However, the first results in well-established cohort studies indicate no direct association between exposure to air pollution and infection with SARS-CoV-2 [108]. Hence, the role of air pollution in the transmission and severity of the disease is still not well established and results from epidemiological and experimental studies that could elucidate this issue further are still lacking.

---

[60] For comparison, the typical recommended dose in clinical settings is 50–100 µg (0.05–0.1 mg).

[61] An open-label trial is a medical study in which both investigators and trial participants are fully aware of which treatment group the participants are in and what treatments are assigned to them.

8 Link between the Montreal Protocol and the inactivation of SARS-CoV-2

While the Montreal Protocol has prevented run-away increases in solar UV radiation [Sect. 4.1 of Chapter 1, it may have also affected the inactivation rate of pathogens exposed to UV radiation. According to McKenzie et al. [109], the Montreal Protocol has averted increases of erythemal (sunburning) irradiances by approximately 20% between the early 1990s and 2018 at mid-latitudes. Under the presumption that the action spectrum measured by Biasin et al. [23] is correct, the sensitivity to changes in TCO should be similar for erythemal irradiance and the effective irradiance for the inactivation of SARS-CoV-2 virus particles (Sect. 4). This conclusion implies that inactivation times of SARS-CoV-2 viruses would be about 20% shorter today if the Montreal Protocol had not been implemented. However, a larger effect would be expected if the actual action spectrum were closer to that reported by Lytle and Sagripanti [24]. Whatever the actual sensitivity to changes in TCO may be, it is unlikely that this effect has any tangible consequences on the progress of the COVID-19 pandemic considering that: (i) fomites in the outdoors that are exposed to solar UV radiation provide the least likely mode of transmission; (ii) outdoor infections via exhaled droplets or aerosol are the exception; (iii) outdoor transmission in the few cases that have occurred were likely between people talking or acting in close proximity where inactivation times even in full sunlight are too long to have a significant effect; and (iv) the role of UV-B radiation in raising 25(OH)D levels, which may protect from severe disease progression, have not been convincingly documented (Sect. 6). On the other hand, the far-reaching, positive outcomes of the successful implementation of the Montreal Protocol for life on Earth [25,93,110-114] outweigh any potential advantage for disinfection by higher amounts of solar UV radiation.

9 Gaps in knowledge

Our assessment identified the following gaps in knowledge:

- To date, the action spectrum for the inactivation of SARS-CoV-2 has been measured by only one group [23] and the experiment for establishing this spectrum has several weaknesses (Sect. 2). Furthermore, this action spectrum has a relatively large contribution from wavelengths in the UV-A range, in contrast to action spectra published for many other viruses [24]. The reason for this discrepancy is presently unknown and the measurements by Biasin et al. [23] have not been independently confirmed.

- Several groups have measured inactivation times of SARS-CoV-2 upon exposure to simulated UV radiation. While all studies confirmed the germicidal effects of UV radiation, the measured inactivation times vary widely and depend on many factors, including experimental setup, sample preparation, and the medium in which the sample is embedded (e.g., saliva, growth medium, or aerosol). Inactivation times have not been measured yet under solar radiation and the extrapolation of the laboratory studies to real-world settings is therefore subject to large uncertainties.

- While many studies demonstrate inverse correlations between UV radiation and COVID-19 incidence or severity of disease, a convincing theory explaining these associations is still missing and the causative factors at play, and their relative contributions, are still unknown.

- It is not clear how research on the seasonality of common virus-caused diseases such as the common cold and influenza can be best applied to augment our understanding of the observed seasonality of COVID-19.

- While observational studies indicate inverse associations between 25(OH)D concentration and risk of SARS-CoV-2 positivity or COVID-19 severity, Mendelian randomisation studies have not found statistically significant evidence of a causal effect of 25(OH)D concentration on COVID-19 susceptibility or severity. Furthermore, randomised trials have generated mixed results. Hence, there is currently no reliable quantification of the role of vitamin D in reducing the susceptibility or severity of COVID-19.

- While several observational studies indicate significant associations between air pollution and COVID-19 incidence and fatality rates, results of well-established cohort studies indicate no association between long-term exposure to air pollution and infection with SARS-CoV-2. Hence, the role of air pollution in the transmission and severity of disease is still not well established.

10 Conclusions

By preventing large increases in UV radiation, the Montreal Protocol may have also affected the inactivation rates of SARS-CoV-2 exposed to solar UV radiation. Without the Montreal Protocol, these rates would have been larger; however, it is unlikely that this would have significantly changed the progression of the COVID-19 pandemic. The most reliable experimental data suggest that 90% of SARS-CoV-2 particles are inactivated by solar radiation within ~7 minutes for high sun and ~13 minutes for low sun. However, one cannot rely on the Sun's germicidal effect in general and, in particular, early and late in the day, during winter, or at high latitudes during all seasons. There is evidence of an inverse relationship between ambient solar UV radiation and the incidence or severity of COVID-19, but the reasons for this inverse correlation have not been unambiguously identified as they can also be explained by confounders, such as ambient temperature, humidity, visible radiation, daylength, temporal changes in risk and disease management, and the proximity of people to other people. Observational studies indicate that higher concentrations of vitamin D (specifically 25(OH)D) in the blood are correlated with lower risk of SARS-CoV-2 positivity or severity of COVID-19. While reasons for this inverse relationship have not been established, a potential link between vitamin D status and disease severity cannot be excluded at this time. Considering that laboratory studies support the role of vitamin D in the immune system, it would be prudent to advocate policies to avoid vitamin D deficiency. However, routine supplementation of populations that are not experiencing vitamin D deficiency is currently not warranted.

Assessments on the effect of solar UV radiation on COVID-19 prevalence and severity are impeded by: the uncertainty of the action spectrum for the inactivation of SARS-CoV-2; the lack of measurements of inactivation rates of SARS-CoV-2 under solar radiation; the dearth of controlled clinical trials investigating the causes of the inverse association between ambient UV radiation and incidence or severity of COVID-19, which is indicated by observational studies; and the inconsistency between the results of observational studies and randomised trials concerning the role of vitamin D and air pollution in the incidence and progression of COVID-19.

List of abbreviations

25(OH)D 25	25-hydroxy vitamin D
CI	confidence interval
CIE	Commission Internationale de l' Éclairage (engl.: International Commission on Illumination)
COVID-19	coronavirus disease 2019
DNA	deoxyribonucleic acid
EEAP	Environmental Effects Assessment Panel
gMEM	Glasgow's Minimum Essential Medium
LED	light-emitting diode
NB-UVB	narrow-band ultraviolet-B
$PM_{2.5}$	particulate matter composed of particles that have a diameter less than 2.5 micrometres
PM_{10}	particulate matter composed of particles that have a diameter less than 10 micrometres
RAF	Radiation Amplification Factor
RH	relative humidity
RNA	ribonucleic acid
SARS-CoV-1	severe acute respiratory syndrome coronavirus 1
SARS-CoV-2	severe acute respiratory syndrome coronavirus 2
SZA	solar zenith angle
TCO	total column ozone
TEMIS	Tropospheric Emission Monitoring Internet Service
TUV	Tropospheric Ultraviolet and Visible
UV-A	Ultraviolet-A (315–400 nm)
UV-B	Ultraviolet-B (280–315 nm)
UV-C	Ultraviolet-C (100–280 nm)
UVI	Ultraviolet Index
VIS	Visible (radiation)
WMO	World Meteorological Organization

Conflict of interest The authors have no conflict of interest.

References

1. Neale, R. E., Barnes, P. W., Robson, T. M., Neale, P. J., Williamson, C. E., Zepp, R. G., Wilson, S. R., Madronich, S., Andrady, A. L., Heikkilä, A. M., Bernhard, G. H., Bais, A. F., Aucamp, P. J., Banaszak, A. T., Bornman, J. F., Bruckman, L. S., Byrne, S. N., Foereid, B., Häder, D. P., Hollestein, L. M., et al. (2021). Environmental effects of stratospheric ozone depletion, UV radiation, and interactions with climate change: UNEP Environmental Effects Assessment Panel, Update 2020. *Photochemical & Photobiological Sciences*, 20(1), 1-67. https://doi.org/10.1007/s43630-020-00001-x

2. Prather, K. A., Wang, C. C., & Schooley, R. T. (2020). Reducing transmission of SARS-CoV-2. *Science*, 368(6498), 1422-1424. https://doi.org/10.1126/science.abc6197

3. Stadnytskyi, V., Bax, C. E., Bax, A., & Anfinrud, P. (2020). The airborne lifetime of small speech droplets and their potential importance in SARS-CoV-2 transmission. *Proceedings of the National Academy of Sciences*, 117(22), 11875-11877. https://doi.org/10.1073/pnas.2006874117

4. The Lancet Respiratory Medicine (2020). COVID-19 transmission—up in the air. *The Lancet Respiratory Medicine*, 8(12). https://doi.org/10.1016/S2213-2600(20)30514-2

5. Rahman, H. S., Aziz, M. S., Hussein, R. H., Othman, H. H., Salih Omer, S. H., Khalid, E. S., Abdulrahman, N. A., Amin, K., & Abdullah, R. (2020). The transmission modes and sources of COVID-19: a systematic review. *International Journal of Surgery Open*, 26, 125-136. https://doi.org/10.1016/j.ijso.2020.08.017

6. Zhou, L., Ayeh, S. K., Chidambaram, V., & Karakousis, P. C. (2021). Modes of transmission of SARS-CoV-2 and evidence for preventive behavioral interventions. *BMC Infectious Diseases*, 21(1). https://doi.org/10.1186/s12879-021-06222-4

7. Zhang, R., Li, Y., Zhang, A. L., Wang, Y., & Molina, M. J. (2020). Identifying airborne transmission as the dominant route for the spread of COVID-19. *Proceedings of the National Academy of Sciences*, 117(26), 14857-14863. https://doi.org/10.1073/pnas.2009637117

8. Klompas, M., Baker, M. A., & Rhee, C. (2020). Airborne transmission of SARS-CoV-2. *Journal of the American Medical Association*, 324(5). https://doi.org/10.1001/jama.2020.12458

9. Cai, J., Sun, W., Huang, J., Gamber, M., Wu, J., & He, G. (2020). Indirect virus transmission in cluster of COVID-19 cases, Wenzhou, China, 2020. *Emerging Infectious Diseases*, 26(6), 1343-1345. https://doi.org/10.3201/eid2606.200412

10. Colaneri, M., Seminari, E., Novati, S., Asperges, E., Biscarini, S., Piralla, A., Percivalle, E., Cassaniti, I., Baldanti, F., Bruno, R., Mondelli, M. U., Bruno, R., Mondelli, M. U., Brunetti, E., Di Matteo, A., Seminari, E., Maiocchi, L., Zuccaro, V., Pagnucco, L., Ludovisi, S., et al. (2020). Severe acute respiratory syndrome coronavirus 2 RNA contamination of inanimate surfaces and virus viability in a health care emergency unit. *Clinical Microbiology and Infection*, 26(8), 1094.e1091-1094.e1095. https://doi.org/10.1016/j.cmi.2020.05.009

11. Harvey, A. P., Fuhrmeister, E. R., Cantrell, M. E., Pitol, A. K., Swarthout, J. M., Powers, J. E., Nadimpalli, M. L., Julian, T. R., & Pickering, A. J. (2020). Longitudinal monitoring of SARS-CoV-2 RNA on high-touch surfaces in a community setting. *Environmental Science & Technology Letters*, 8(2), 168-175. https://doi.org/10.1021/acs.estlett.0c00875

12. Rocha, A. L. S., Pinheiro, J. R., Nakamura, T. C., da Silva, J. D. S., Rocha, B. G. S., Klein, R. C., Birbrair, A., & Amorim, J. H. (2021). Fomites and the environment did not have an important role in COVID-19 transmission in a Brazilian mid-sized city. *Scientific Reports*, 11(1). https://doi.org/10.1038/s41598-021-95479-5

13. Bulfone, T. C., Malekinejad, M., Rutherford, G. W., & Razani, N. (2021). Outdoor transmission of SARS-CoV-2 and other respiratory viruses: a systematic review. *The Journal of Infectious Diseases*, 223(4), 550-561. https://doi.org/10.1093/infdis/jiaa742

14. Klepeis, N. E., Nelson, W. C., Ott, W. R., Robinson, J. P., Tsang, A. M., Switzer, P., Behar, J. V., Hern, S. C., & Engelmann, W. H. (2001). The National Human Activity Pattern Survey (NHAPS): a resource for assessing exposure to environmental pollutants. *Journal of Exposure Science & Environmental Epidemiology*, 11(3), 231-252. https://doi.org/10.1038/sj.jea.7500165

15. Cohen, J. (2020). Sick time. *Science*, 367(6484), 1294-1297. https://doi.org/10.1126/science.367.6484.1294

16. van Doremalen, N., Bushmaker, T., Morris, D. H., Holbrook, M. G., Gamble, A., Williamson, B. N., Tamin, A., Harcourt, J. L., Thornburg, N. J., Gerber, S. I., Lloyd-Smith, J. O., de Wit, E., & Munster, V. J. (2020). Aerosol and surface stability of SARS-CoV-2 as compared with SARS-CoV-1. *New England Journal of Medicine*, 382(16), 1564-1567. https://doi.org/10.1056/NEJMc2004973

17. Chin, A. W. H., Chu, J. T. S., Perera, M. R. A., Hui, K. P. Y., Yen, H.-L., Chan, M. C. W., Peiris, M., & Poon, L. L. M. (2020). Stability of SARS-CoV-2 in different environmental conditions. *The Lancet Microbe*, 1(1), e10. https://doi.org/10.1016/s2666-5247(20)30003-3

18. Riddell, S., Goldie, S., Hill, A., Eagles, D., & Drew, T. W. (2020). The effect of temperature on persistence of SARS-CoV-2 on common surfaces. *Virology Journal*, 17(1), 145. https://doi.org/10.1186/s12985-020-01418-7

19. Kampf, G., Todt, D., Pfaender, S., & Steinmann, E. (2020). Persistence of coronaviruses on inanimate surfaces and their inactivation with biocidal agents. J*ournal of Hospital Infection*, 104(3), 246-251. https://doi.org/10.1016/j.jhin.2020.01.022

20. Pastorino, B., Touret, F., Gilles, M., de Lamballerie, X., & Charrel, R. N. (2020). Prolonged infectivity of SARS-CoV-2 in fomites. *Emerging Infectious Diseases*, 26(9). https://doi.org/10.3201/eid2609.201788

21. Chatterjee, S., Murallidharan, J. S., Agrawal, A., & Bhardwaj, R. (2021). Why coronavirus survives longer on impermeable than porous surfaces. *Physics of Fluids*, 33(2). https://doi.org/10.1063/5.0037924

22. Hirose, R., Itoh, Y., Ikegaya, H., Miyazaki, H., Watanabe, N., Yoshida, T., Bandou, R., Daidoji, T., & Nakaya, T. (2022). Differences in environmental stability among SARS-CoV-2 variants of concern: both omicron BA.1 and BA.2 have higher stability. *Clinical Microbiology and Infection*, 28(11), 1486-1491. https://doi.org/10.1016/j.cmi.2022.05.020

23. Biasin, M., Strizzi, S., Bianco, A., Macchi, A., Utyro, O., Pareschi, G., Loffreda, A., Cavalleri, A., Lualdi, M., Trabattoni, D., Tacchetti, C., Mazza, D., & Clerici, M. (2022). UV and violet light can neutralize SARS-CoV-2 infectivity. *Journal of Photochemistry and Photobiology*, 10. https://doi.org/10.1016/j.jpap.2021.100107

24. Lytle, C. D., & Sagripanti, J. L. (2005). Predicted inactivation of viruses of relevance to biodefense by solar radiation. *Journal of Virology*, 79(22), 14244-14252. https://doi.org/10.1128/JVI.79.22.14244-14252.2005

25. Bernhard, G. H., Bais, A. F., Aucamp, P. J., Klekociuk, A. R., Liley, J. B., & McKenzie, R. L. (2022). *Stratospheric ozone, UV radiation, and climate interactions. Chapter 1*

26. Heßling, M., Hönes, K., Vatter, P., & Lingenfelder, C. (2020). Ultraviolet irradiation doses for coronavirus inactivation–review and analysis of coronavirus photoinactivation studies. *GMS hygiene and infection control*, 15. https://doi.org/10.3205/dgkh000343

27. Nishisaka-Nonaka, R., Mawatari, K., Yamamoto, T., Kojima, M., Shimohata, T., Uebanso, T., Nakahashi, M., Emoto, T., Akutagawa, M., Kinouchi, Y., Wada, T., Okamoto, M., Ito, H., Yoshida, K.-i., Daidoji, T., Nakaya, T., & Takahashi, A. (2018). Irradiation by ultraviolet light-emitting diodes inactivates influenza a viruses by inhibiting replication and transcription of viral RNA in host cells. *Journal of Photochemistry and Photobiology B: Biology*, 189, 193-200. https://doi.org/10.1016/j.jphotobiol.2018.10.017

28. CIE. (1998). *Erythema reference action spectrum and standard erythema dose*. CIE Standard Bureau, Vol. ISO 17166:1999(E), CIE DS 007.1/E-1998. Commission Internationale de l'Eclairage, Vienna, Austria.

29. Luzzatto-Fegiz, P., Temprano-Coleto, F., Peaudecerf, F. J., Landel, J. R., Zhu, Y., & McMurry, J. A. (2021). UVB radiation alone may not explain sunlight inactivation of SARS-CoV-2. *The Journal of Infectious Diseases*, 223(8), 1500-1502. https://doi.org/10.1093/infdis/jiab070

30. Rezaie, A., Leite, G. G. S., Melmed, G. Y., Mathur, R., Villanueva-Millan, M. J., Parodi, G., Sin, J., Germano, J. F., Morales, W., Weitsman, S., Kim, S. Y., Park, J. H., Sakhaie, S., & Pimentel, M. (2020). Ultraviolet A light effectively reduces bacteria and viruses including coronavirus. *PloS One*, 15(7), e0236199. https://doi.org/10.1371/journal.pone.0236199

31. Wigginton, K. R., Pecson, B. M., Sigstam, T., Bosshard, F., & Kohn, T. (2012). Virus inactivation mechanisms: impact of disinfectants on virus function and structural integrity. *Environmental Science & Technology*, 46(21), 12069-12078. https://doi.org/10.1021/es3029473

32. Biasin, M., Bianco, A., Pareschi, G., Cavalleri, A., Cavatorta, C., Fenizia, C., Galli, P., Lessio, L., Lualdi, M., Tombetti, E., Ambrosi, A., Redaelli, E. M. A., Saulle, I., Trabattoni, D., Zanutta, A., & Clerici, M. (2021). UV-C irradiation is highly effective in inactivating SARS-CoV-2 replication. *Scientific Reports*, 11(1). https://doi.org/10.1038/s41598-021-85425-w

33. Herman, J., Biegel, B., & Huang, L. (2020). Inactivation times from 290 to 315 nm UVB in sunlight for SARS coronaviruses CoV and CoV-2 using OMI satellite data for the sunlit Earth. *Air Quality, Atmosphere & Health*, 14(2), 217-233. https://doi.org/10.1007/s11869-020-00927-2

34. Setlow, R. B. (1974). The wavelengths in sunlight effective in producing skin cancer: a theoretical analysis. *Proceedings of the National Academy of Sciences of the United States of America*, 71(9), 3363-3366. https://doi.org/10.1073/pnas.71.9.3363

35. Aas, P. A., Otterlei, M., Falnes, P. Ø., Vågbø, C. B., Skorpen, F., Akbari, M., Sundheim, O., Bjørås, M., Slupphaug, G., Seeberg, E., & Krokan, H. E. (2003). Human and bacterial oxidative demethylases repair alkylation damage in both RNA and DNA. *Nature, 421*(6925), 859-863. https://doi.org/10.1038/nature01363

36. Schuit, M., Ratnesar-Shumate, S., Yolitz, J., Williams, G., Weaver, W., Green, B., Miller, D., Krause, M., Beck, K., Wood, S., Holland, B., Bohannon, J., Freeburger, D., Hooper, I., Biryukov, J., Altamura, L. A., Wahl, V., Hevey, M., & Dabisch, P. (2020). Airborne SARS-CoV-2 is rapidly inactivated by simulated sunlight. *Journal of Infectious Diseases*, 222(4), 564-571. https://doi.org/10.1093/infdis/jiaa334

37. Ratnesar-Shumate, S., Williams, G., Green, B., Krause, M., Holland, B., Wood, S., Bohannon, J., Boydston, J., Freeburger, D., Hooper, I., Beck, K., Yeager, J., Altamura, L. A., Biryukov, J., Yolitz, J., Schuit, M., Wahl, V., Hevey, M., & Dabisch, P. (2020). Simulated sunlight rapidly inactivates SARS-CoV-2 on surfaces. *Journal of Infectious Diseases*, 222(2), 214-222. https://doi.org/10.1093/infdis/jiaa274

38. Wondrak, G. T., Jandova, J., Williams, S. J., & Schenten, D. (2021). Solar simulated ultraviolet radiation inactivates HCoV-NL63 and SARS-CoV-2 coronaviruses at environmentally relevant doses. *Journal of Photochemistry and Photobiology B: Biology, 224*. https://doi.org/10.1016/j.jphotobiol.2021.112319

39. Raiteux, J., Eschlimann, M., Marangon, A., Rogée, S., Dadvisard, M., Taysse, L., Larigauderie, G., & Sinclair, A. (2021). Inactivation of SARS-CoV-2 by simulated sunlight on contaminated surfaces. *Microbiology Spectrum, 9*(1). https://doi.org/10.1128/Spectrum.00333-21

40. Nicastro, F., Sironi, G., Antonello, E., Bianco, A., Biasin, M., Brucato, J. R., Ermolli, I., Pareschi, G., Salvati, M., Tozzi, P., Trabattoni, D., & Clerici, M. (2021). Solar UV-B/A radiation is highly effective in inactivating SARS-CoV-2. *Scientific Reports, 11*(1). https://doi.org/10.1038/s41598-021-94417-9

41. Sloan, A., Cutts, T., Griffin, B. D., Kasloff, S., Schiffman, Z., Chan, M., Audet, J., Leung, A., Kobasa, D., Stein, D. R., Safronetz, D., & Poliquin, G. (2021). Simulated sunlight decreases the viability of SARS-CoV-2 in mucus. *PloS One, 16*(6). https://doi.org/10.1371/journal.pone.0253068

42. Herman, J., & Piacentini, R. D. (2021). UVB (290–315 nm) inactivation of the SARS CoV-2 virus as a function of the standard UV index. *Air Quality, Atmosphere & Health, 15*(1), 85-90. https://doi.org/10.1007/s11869-021-01099-3

43. Sagripanti, J. L., & Lytle, C. D. (2020). Estimated inactivation of coronaviruses by solar radiation with special reference to COVID-19. *Photochemistry and Photobiology, 96*(4), 731-737. https://doi.org/10.1111/php.13293

44. Carvalho, F. R. S., Henriques, D. V., Correia, O., & Schmalwieser, A. W. (2021). Potential of solar UV radiation for inactivation of coronaviridae family estimated from satellite data. *Photochemistry and Photobiology, 97*(1), 213-220. https://doi.org/10.1111/php.13345

45. Blatchley, E. R. I., & Coohill, T. P. (2021). Ultraviolet disinfection. In G. McDonnell, & J. Hansen (Eds.), *Block's disinfection, sterilization, and preservation*, 171-191. Wolters Kluwer Health, Philadelphia, USA

46. Weiss, M., & Horzinek, M. C. (1986). Resistance of Berne virus to physical and chemical treatment. *Veterinary Microbiology, 11*(1-2), 41-49. https://doi.org/10.1016/0378-1135(86)90005-2

47. Kariwa, H., Fujii, N., & Takashima, I. (2006). Inactivation of SARS coronavirus by means of povidone-iodine, physical conditions and chemical reagents. *Dermatology, 212*, 119-123. https://doi.org/10.1159/000089211

48. Kowalski, W. J., Bahnfleth, W. P., Raguse, M., & Moeller, R. (2020). The cluster model of ultraviolet disinfection explains tailing kinetics. *Journal of Applied Microbiology, 128*(4), 1003-1014. https://doi.org/10.1111/jam.14527

49. Micheletti, M. I., Piacentini, R. D., & Madronich, S. (2003). Sensitivity of biologically active UV radiation to stratospheric ozone changes: effects of action spectrum shape and wavelength range. *Photochemistry and Photobiology, 78*(5), 456-461. https://doi.org/10.1562/0031-8655(2003)0780456SOBAUR2.0.CO2

50. Ma, Y., Pei, S., Shaman, J., Dubrow, R., & Chen, K. (2021). Role of meteorological factors in the transmission of SARS-CoV-2 in the United States. *Nature Communications, 12*(1). https://doi.org/10.1038/s41467-021-23866-7

51. Sfică, L., Bulai, M., Amihăesei, V.-A., Ion, C., & tefan, M. (2020). Weather conditions (with focus on UV radiation) associated with COVID-19 outbreak and worldwide climate-based prediction for future prevention. *Aerosol and Air Quality Research, 20*(9), 1862-1873. https://doi.org/10.4209/aaqr.2020.05.0206

52. Choi, Y. W., Tuel, A., & Eltahir, E. A. B. (2021). On the environmental determinants of COVID-19 seasonality. *GeoHealth, 5*(6). https://doi.org/10.1029/2021GH000413

53. Carleton, T., Cornetet, J., Huybers, P., Meng, K. C., & Proctor, J. (2020). Global evidence for ultraviolet radiation decreasing COVID-19 growth rates. *Proceedings of the National Academy of Sciences, 118*(1). https://doi.org/10.1073/pnas.2012370118

54. Gorman, S., & Weller, R. B. (2020). Investigating the potential for ultraviolet light to modulate morbidity and mortality from COVID-19: a narrative review and update. *Frontiers in Cardiovascular Medicine, 7*. https://doi.org/10.3389/fcvm.2020.616527

55. Moozhipurath, R. K., & Kraft, L. (2021). Association of lockdowns with the protective role of ultraviolet-B (UVB) radiation in reducing COVID-19 deaths. *Scientific Reports, 11*(1). https://doi.org/10.1038/s41598-021-01908-w

56. Moozhipurath, R. K., Kraft, L., & Skiera, B. (2020). Evidence of protective role of Ultraviolet-B (UVB) radiation in reducing COVID-19 deaths. *Scientific Reports, 10*(1). https://doi.org/10.1038/s41598-020-74825-z

57. Guasp, M., Laredo, C., & Urra, X. (2020). Higher solar irradiance is associated with a lower incidence of COVID-19. *Clinical Infectious Diseases, 71*(16), 2269-2271. https://doi.org/10.1093/cid/ciaa575

58. Nandin de Carvalho, H. (2022). Latitude impact on pandemic SARS-CoV-2 2020 outbreaks and possible utility of UV indexes in predictions of regional daily infections and deaths. *Journal of Photochemistry and Photobiology, 10*. https://doi.org/10.1016/j.jpap.2022.100108

59. Falzone, Y. M., Bosco, L., Sferruzza, G., Russo, T., Vabanesi, M., & Filippi, M. (2021). Evaluation of the combined effect of mobility and seasonality on the COVID-19 pandemic: a Lombardy-based study. *SSRN Electronic Journal*. https://doi.org/10.2139/ssrn.3778753

60.   Isaia, G., Diémoz, H., Maluta, F., Fountoulakis, I., Ceccon, D., di Sarra, A., Facta, S., Fedele, F., Lorenzetto, G., Siani, A. M., & Isaia, G. (2021). Does solar ultraviolet radiation play a role in COVID-19 infection and deaths? An environmental ecological study in Italy. *Science of the Total Environment, 757*. https://doi.org/10.1016/j.scitotenv.2020.143757

61.   Hersbach, H., Bell, B., Berrisford, P., Hirahara, S., Horányi, A., Muñoz-Sabater, J., Nicolas, J., Peubey, C., Radu, R., Schepers, D., Simmons, A., Soci, C., Abdalla, S., Abellan, X., Balsamo, G., Bechtold, P., Biavati, G., Bidlot, J., Bonavita, M., Chiara, G., et al. (2020). The ERA5 global reanalysis. *Quarterly Journal of the Royal Meteorological Society, 146*(730), 1999-2049. https://doi.org/10.1002/qj.3803

62.   Cherrie, M., Clemens, T., Colandrea, C., Feng, Z., Webb, D. J., Weller, R. B., & Dibben, C. (2021). Ultraviolet A radiation and COVID-19 deaths in the USA with replication studies in England and Italy. *British Journal of Dermatology, 185*(2), 363-370. https://doi.org/10.1111/bjd.20093

63.   Weller, R. B., Wang, Y., He, J., Maddux, F. W., Usvyat, L., Zhang, H., Feelisch, M., & Kotanko, P. (2020). Does incident solar ultraviolet radiation lower blood pressure? *Journal of the American Heart Association, 9*(5). https://doi.org/10.1161/JAHA.119.013837

64.   Mackay, D. F., Clemens, T. L., Hastie, C. E., Cherrie, M. P. C., Dibben, C., & Pell, J. P. (2019). UVA and seasonal patterning of 56 370 myocardial infarctions across Scotland, 2000–2011. *Journal of the American Heart Association, 8*(23). https://doi.org/10.1161/jaha.119.012551

65.   Li, F., Tao, L., Serruys, P. W., Onuma, Y., Soliman, O., McEvoy, J. W., Wijns, W., Hui, C., Yang, M., Wang, R., Zhang, R., Yin, Z., Liu, Y., Wang, H., Zhao, Y., Zhao, X., Yang, S., Li, W., Li, Q., Zhang, X., et al. (2020). Association of hypertension and antihypertensive treatment with COVID-19 mortality: a retrospective observational study. *European Heart Journal, 41*(22), 2058-2066. https://doi.org/10.1093/eurheartj/ehaa433

66.   McKenzie, R. L., & Liley, J. B. (2021). Yet another benefit from sunlight in the fight against COVID-19? *British Journal of Dermatology, 185*(2), 246-247. https://doi.org/10.1111/bjd.20516

67.   Martinez, M. E. (2018). The calendar of epidemics: seasonal cycles of infectious diseases. *PLoS Pathogens, 14*(11). https://doi.org/10.1371/journal.ppat.1007327

68.   Booth, C. R., Lucas, T. B., Morrow, J. H., Weiler, C. S., & Penhale, P. A. (1994). The United States National Science Foundation's polar network for monitoring ultraviolet radiation. In C. S. Weiler, & P. A. Penhale (Eds.), *Ultraviolet radiation in Antarctica: Measurements and biological effects, 62*, 17-37: American Geophysical Union, Washington, D.C. https://doi.org/10.1029/AR062p0017

69.   Lau, F. H., Powell, C. E., Adonecchi, G., Danos, D. M., DiNardo, A. R., Chugden, R. J., Wolf, P., & Castilla, C. F. (2022). Pilot phase results of a prospective, randomized controlled trial of narrowband ultraviolet B phototherapy in hospitalized COVID-19 patients. *Experimental Dermatology, 31*(7), 1109-1115. https://doi.org/10.1111/exd.14617

70.   Kronfeld-Schor, N., Stevenson, T. J., Nickbakhsh, S., Schernhammer, E. S., Dopico, X. C., Dayan, T., Martinez, M., & Helm, B. (2021). Drivers of infectious disease seasonality: potential implications for COVID-19. *Journal of Biological Rhythms, 36*(1), 35-54. https://doi.org/10.1177/0748730420987322

71.   Dopico, X. C., Evangelou, M., Ferreira, R. C., Guo, H., Pekalski, M. L., Smyth, D. J., Cooper, N., Burren, O. S., Fulford, A. J., Hennig, B. J., Prentice, A. M., Ziegler, A.-G., Bonifacio, E., Wallace, C., & Todd, J. A. (2015). Widespread seasonal gene expression reveals annual differences in human immunity and physiology. *Nature Communications, 6*(1). https://doi.org/10.1038/ncomms8000

72.   Lal, A., Hales, S., French, N., & Baker, M. G. (2012). Seasonality in human zoonotic enteric diseases: a systematic review. *PLoS One, 7*(4). https://doi.org/10.1371/journal.pone.0031883

73.   Moriyama, M., Hugentobler, W. J., & Iwasaki, A. (2020). Seasonality of respiratory viral infections. *Annual Review of Virology, 7*(1), 83-101. https://doi.org/10.1146/annurev-virology-012420-022445

74.   Nguyen, J. L., Schwartz, J., & Dockery, D. W. (2014). The relationship between indoor and outdoor temperature, apparent temperature, relative humidity, and absolute humidity. *Indoor Air, 24*(1), 103-112. https://doi.org/10.1111/ina.12052

75.   Nelson, R. J., Demas, G. E., Klein, S. L., & Kriegsfeld, L. J. (2002). *Seasonal patterns of stress, immune function, and disease*. Cambridge University Press, Cambridge, UK.

76.   Scragg, R. K. R., Stewart, A. W., McKenzie, R. L., Reeder, A. I., Liley, J. B., & Allen, M. W. (2016). Sun exposure and 25-hydroxyvitamin D_3 levels in a community sample: quantifying the association with electronic dosimeters. *Journal of Exposure Science & Environmental Epidemiology, 27*(5), 471-477. https://doi.org/10.1038/jes.2016.51

77.   Godar, D. E. (2005). UV Doses Worldwide. *Photochemistry and Photobiology, 81*(4). https://doi.org/10.1562/2004-09-07-ir-308r.1

78.   Pahar, B., Madonna, S., Das, A., Albanesi, C., & Girolomoni, G. (2020). Immunomodulatory role of the antimicrobial LL-37 peptide in autoimmune diseases and viral infections. *Vaccines, 8*(3). https://doi.org/10.3390/vaccines8030517

79. Bae, J. H., Choe, H. J., Holick, M. F., & Lim, S. (2022). Association of vitamin D status with COVID-19 and its severity. *Reviews in Endocrine and Metabolic Disorders, 23*(3), 579-599. https://doi.org/10.1007/s11154-021-09705-6

80. Pham, H., Rahman, A., Majidi, A., Waterhouse, M., & Neale, R. E. (2019). Acute respiratory tract infection and 25-Hydroxyvitamin D concentration: a systematic review and meta-analysis. *International Journal of Environmental Research and Public Health, 16*(17), 3020. https://doi.org/10.3390/ijerph16173020

81. Pham, H., Waterhouse, M., Baxter, C., Duarte Romero, B., McLeod, D. S. A., Armstrong, B. K., Ebeling, P. R., English, D. R., Hartel, G., Kimlin, M. G., Martineau, A. R., O'Connell, R., van der Pols, J. C., Venn, A. J., Webb, P. M., Whiteman, D. C., & Neale, R. E. (2021). The effect of vitamin D supplementation on acute respiratory tract infection in older Australian adults: an analysis of data from the D-Health Trial. *Lancet Diabetes Endocrinol, 9*(2), 69-81. https://doi.org/10.1016/S2213-8587(20)30380-6

82. Jolliffe, D. A., Camargo, C. A., Sluyter, J. D., Aglipay, M., Aloia, J. F., Ganmaa, D., Bergman, P., Bischoff-Ferrari, H. A., Borzutzky, A., Damsgaard, C. T., Dubnov-Raz, G., Esposito, S., Gilham, C., Ginde, A. A., Golan-Tripto, I., Goodall, E. C., Grant, C. C., Griffiths, C. J., Hibbs, A. M., Janssens, W., et al. (2021). Vitamin D supplementation to prevent acute respiratory infections: a systematic review and meta-analysis of aggregate data from randomised controlled trials. *Lancet Diabetes Endocrinol, 9*(5), 276-292. https://doi.org/10.1016/S2213-8587(21)00051-6

83. Petrelli, F., Luciani, A., Perego, G., Dognini, G., Colombelli, P. L., & Ghidini, A. (2021). Therapeutic and prognostic role of vitamin D for COVID-19 infection: A systematic review and meta-analysis of 43 observational studies. *The Journal of Steroid Biochemistry and Molecular Biology, 211*. https://doi.org/10.1016/j.jsbmb.2021.105883

84. Liu, N., Sun, J., Wang, X., Zhang, T., Zhao, M., & Li, H. (2021). Low vitamin D status is associated with coronavirus disease 2019 outcomes: a systematic review and meta-analysis. *International Journal of Infectious Diseases*, 104, 58-64. https://doi.org/10.1016/j.ijid.2020.12.077

85. Bassatne, A., Basbous, M., Chakhtoura, M., El Zein, O., Rahme, M., & El-Hajj Fuleihan, G. (2021). The link between COVID-19 and VItamin D (VIVID): A systematic review and meta-analysis. *Metabolism, 119*. https://doi.org/10.1016/j.metabol.2021.154753

86. Akbar, M. R., Wibowo, A., Pranata, R., & Setiabudiawan, B. (2021). Low serum 25-hydroxyvitamin D (Vitamin D) level is associated with susceptibility to COVID-19, severity, and mortality: a systematic review and meta-analysis. *Frontiers in Nutrition, 8*, 660420. https://doi.org/10.3389/fnut.2021.660420

87. Butler-Laporte, G., Nakanishi, T., Mooser, V., Morrison, D. R., Abdullah, T., Adeleye, O., Mamlouk, N., Kimchi, N., Afrasiabi, Z., Rezk, N., Giliberti, A., Renieri, A., Chen, Y., Zhou, S., Forgetta, V., & Richards, J. B. (2021). Vitamin D and COVID-19 susceptibility and severity in the COVID-19 Host Genetics Initiative: a Mendelian randomization study. *PLoS Medicine, 18*(6), e1003605-e1003605. https://doi.org/10.1371/journal.pmed.1003605

88. Patchen, B. K., Clark, A. G., Gaddis, N., Hancock, D. B., & Cassano, P. A. (2021). Genetically predicted serum vitamin D and COVID-19: a Mendelian randomisation study. *British Medical Journal Nutrition, Prevention & Health, 4*(1), 213-225. https://doi.org/10.1136/bmjnph-2021-000255

89. Murai, I. H., Fernandes, A. L., Sales, L. P., Pinto, A. J., Goessler, K. F., Duran, C. S. C., Silva, C. B. R., Franco, A. S., Macedo, M. B., Dalmolin, H. H. H., Baggio, J., Balbi, G. G. M., Reis, B. Z., Antonangelo, L., Caparbo, V. F., Gualano, B., & Pereira, R. M. R. (2021). Effect of a single high dose of vitamin D_3 on hospital length of stay in patients with moderate to severe COVID-19: a randomized clinical trial. *Journal of the American Medical Association, 325*(11), 1053-1060. https://doi.org/10.1001/jama.2020.26848

90. Mariani, J., Antonietti, L., Tajer, C., Ferder, L., Inserra, F., Sanchez Cunto, M., Brosio, D., Ross, F., Zylberman, M., López, D. E., Luna Hisano, C., Maristany Batisda, S., Pace, G., Salvatore, A., Hogrefe, J. F., Turela, M., Gaido, A., Rodera, B., Banega, E., Iglesias, M. E., et al. (2022). High-dose vitamin D versus placebo to prevent complications in COVID-19 patients: Multicentre randomized controlled clinical trial. *PloS One, 17*(5). https://doi.org/10.1371/journal.pone.0267918

91. Entrenas Castillo, M., Entrenas Costa, L. M., Vaquero Barrios, J. M., Alcalá Díaz, J. F., López Miranda, J., Bouillon, R., & Quesada Gomez, J. M. (2020). Effect of calcifediol treatment and best available therapy versus best available therapy on intensive care unit admission and mortality among patients hospitalized for COVID-19: a pilot randomized clinical study. *The Journal of Steroid Biochemistry and Molecular Biology, 203*. https://doi.org/10.1016/j.jsbmb.2020.105751

92. Annweiler, C., Beaudenon, M., Gautier, J., Gonsard, J., Boucher, S., Chapelet, G., Darsonval, A., Fougère, B., Guérin, O., Houvet, M., Ménager, P., Roubaud-Baudron, C., Tchalla, A., Souberbielle, J.-C., Riou, J., Parot-Schinkel, E., & Célarier, T. (2022). High-dose versus standard-dose vitamin D supplementation in older adults with COVID-19 (COVIT-TRIAL): A multicenter, open-label, randomized controlled superiority trial. *PLoS Medicine, 19*(5). https://doi.org/10.1371/journal.pmed.1003999

93. Madronich, S., Sulzberger, B., Longstreth, J., Schikowski, T., Andersen, M. P. S., Solomon, K. R., & Wilson, S. R. (2022). Changes in tropospheric air quality related to the protection of stratospheric ozone and a changing climate. *Chapter 6*

94. Vicedo-Cabrera, A. M., Sera, F., Liu, C., Armstrong, B., Milojevic, A., Guo, Y., Tong, S., Lavigne, E., Kyselý, J., Urban, A., Orru, H., Indermitte, E., Pascal, M., Huber, V., Schneider, A., Katsouyanni, K., Samoli, E., Stafoggia, M., Scortichini, M., Hashizume, M., et al. (2020). Short term association between ozone and mortality: global two stage time series study in 406 locations in 20 countries. *BMJ*. https://doi.org/10.1136/bmj.m108

95. Schneider, R., Masselot, P., Vicedo-Cabrera, A. M., Sera, F., Blangiardo, M., Forlani, C., Douros, J., Jorba, O., Adani, M., Kouznetsov, R., Couvidat, F., Arteta, J., Raux, B., Guevara, M., Colette, A., Barré, J., Peuch, V.-H., & Gasparrini, A. (2022). Differential impact of government lockdown policies on reducing air pollution levels and related mortality in Europe. *Scientific Reports, 12*(1). https://doi.org/10.1038/s41598-021-04277-6

96. Cui, Y., Zhang, Z.-F., Froines, J., Zhao, J., Wang, H., Yu, S.-Z., & Detels, R. (2003). Air pollution and case fatality of SARS in the People's Republic of China: an ecologic study. *Environmental Health, 2*(1), 15. https://doi.org/10.1186/1476-069X-2-15

97. Chen, C., Wang, J., Kwong, J., Kim, J., van Donkelaar, A., Martin, R. V., Hystad, P., Su, Y., Lavigne, E., Kirby-McGregor, M., Kaufman, J. S., Benmarhnia, T., & Chen, H. (2022). Association between long-term exposure to ambient air pollution and COVID-19 severity: a prospective cohort study. *Canadian Medical Association Journal, 194*(20), E693-E700. https://doi.org/10.1503/cmaj.220068

98. Sheridan, C., Klompmaker, J., Cummins, S., James, P., Fecht, D., & Roscoe, C. (2022). Associations of air pollution with COVID-19 positivity, hospitalisations, and mortality: Observational evidence from UK Biobank. *Environmental Pollution, 308*. https://doi.org/10.1016/j.envpol.2022.119686

99. Nobile, F., Michelozzi, P., Ancona, C., Cappai, G., Cesaroni, G., Davoli, M., Di Martino, M., Nicastri, E., Girardi, E., Beccacece, A., Scognamiglio, P., Sorge, C., Vairo, F., & Stafoggia, M. (2022). Air pollution, SARS-CoV-2 incidence and COVID-19 mortality in Rome: a longitudinal study. *European Respiratory Journal, 60*(3). https://doi.org/10.1183/13993003.00589-2022

100. English, P. B., Von Behren, J., Balmes, J. R., Boscardin, J., Carpenter, C., Goldberg, D. E., Horiuchi, S., Richardson, M., Solomon, G., Valle, J., & Reynolds, P. (2022). Association between long-term exposure to particulate air pollution with SARS-CoV-2 infections and COVID-19 deaths in California, U.S.A. *Environmental Advances, 9*. https://doi.org/10.1016/j.envadv.2022.100270

101. Azimi, P., Keshavarz, Z., Cedeno Laurent, J. G., Stephens, B., & Allen, J. G. (2021). Mechanistic transmission modeling of COVID-19 on the Diamond Princess cruise ship demonstrates the importance of aerosol transmission. *Proceedings of the National Academy of Sciences of the United States of America, 118*(8). https://doi.org/10.1073/pnas.2015482118

102. Wu, X., Nethery, R. C., Sabath, M. B., Braun, D., & Dominici, F. (2020). Air pollution and COVID-19 mortality in the United States: Strengths and limitations of an ecological regression analysis. *Science Advances, 6*(45). https://doi.org/10.1126/sciadv.abd4049

103. Yao, Y., Pan, J., Liu, Z., Meng, X., Wang, W., Kan, H., & Wang, W. (2020). Temporal association between particulate matter pollution and case fatality rate of COVID-19 in Wuhan. *Environmental Research, 189*, 109941. https://doi.org/10.1016/j.envres.2020.109941

104. Woodby, B., Arnold, M. M., & Valacchi, G. (2021). SARS-CoV-2 infection, COVID-19 pathogenesis, and exposure to air pollution: What is the connection? *Annals of the New York Academy of Sciences, 1486*(1), 15-38. https://doi.org/https://doi.org/10.1111/nyas.14512

105. Stieb, D. M., Evans, G. J., To, T. M., Lakey, P. S. J., Shiraiwa, M., Hatzopoulou, M., Minet, L., Brook, J. R., Burnett, R. T., & Weichenthal, S. A. (2021). Within-city variation in reactive oxygen species from fine particle air pollution and COVID-19. *American Journal of Respiratory and Critical Care Medicine, 204*(2), 168-177. https://doi.org/10.1164/rccm.202011-4142OC

106. Martelletti, L., & Martelletti, P. (2020). Air pollution and the novel Covid-19 disease: a putative disease risk factor. *SN Comprehensive Clinical Medicine, 2*(4), 383-387. https://doi.org/10.1007/s42399-020-00274-4

107. Bourdrel, T., Annesi-Maesano, I., Alahmad, B., Maesano, C. N., & Bind, M.-A. (2021). The impact of outdoor air pollution on COVID-19: a review of evidence from in vitro, animal, and human studies. *European Respiratory Review, 30*(159), 200242. https://doi.org/10.1183/16000617.0242-2020

108. Kogevinas, M., Castaño-Vinyals, G., Karachaliou, M., Espinosa, A., de Cid, R., Garcia-Aymerich, J., Carreras, A., Cortés, B., Pleguezuelos, V., Jiménez, A., Vidal, M., O'Callaghan-Gordo, C., Cirach, M., Santano, R., Barrios, D., Puyol, L., Rubio, R., Izquierdo, L., Nieuwenhuijsen, M., Dadvand, P., et al. (2021). Ambient air pollution in relation to SARS-CoV-2 infection, antibody response, and COVID-19 disease: A cohort study in Catalonia, Spain (COVICAT study). *Environmental Health Perspectives, 129*(11), 117003. https://doi.org/10.1289/ehp9726

109. McKenzie, R., Bernhard, G., Liley, B., Disterhoft, P., Rhodes, S., Bais, A., Morgenstern, O., Newman, P., Oman, L., Brogniez, C., & Simic, S. (2019). Success of Montreal Protocol demonstrated by comparing high-quality UV measurements with "World Avoided" calculations from two chemistry-climate models. *Scientific Reports, 9*(1), 12332. https://doi.org/10.1038/s41598-019-48625-z

110. Neale, R. E., Lucas, R. M., Byrne, S., Hollestein, L., Rhodes, L. E., Yasar, S., Young, A. R., Ireland, R., & Olsen, C. M. (2022). The effects of exposure to solar radiation on human health. *Chapter 3*

111. Barnes, P. W., Robson, T. M., Zepp, R. G., Bornman, J. F., Jansen, M. A. K., Ossola, R., Wang, Q.-W., Robinson, S. A., Foereid, B., Klekociuk, A. R., Martinez-Abaigar, J., Hou, W. C., & Paul, N. D. (2022). Interactive effects of changes in UV radiation and climate on terrestrial ecosystems, biogeochemical cycles, and feedbacks to the climate system. *Chapter 4*

112. Andrady, A. L., Heikkila, A. M., Pandey, K. K., Bruckman, L. S., White, C. C., Zhu, M., & Zhu, L. (2022). Effects of UV radiation on natural and synthetic materials. *Chapter 7*

113. Jansen, M. A. K., Barnes, P. W., Bornman, J. F., Rose, K. A., Madronich, S., White, C. C., Zepp, R. G., & Andrady, A. L. (2022). The Montreal Protocol and the fate of environmental plastic debris. *Chapter 8*

114. Neale, P. J., Williamson, C. E., Banaszak, A. T., Häder, D. P., Hylander, S., Ossola, R., Rose, K. A., Wängberg, S.-Å., & Zepp, R. G. (2022). The response of aquatic ecosystems to the interactive effects of stratospheric ozone depletion, UV radiation, and climate change. *Chapter 5*

3

THE EFFECTS OF EXPOSURE TO SOLAR RADIATION ON HUMAN HEALTH

R.E. Neale[62,63], R.M. Lucas[64], S.N. Byrne[65], L. Hollestein[66,67], L.E. Rhodes[68], S. Yazar[69], A.R. Young[70], M. Berwick[71], R.A. Ireland[64], and C.M. Olsen[61,72]

[62] Population Health Program, QIMR Berghofer Medical Research Institute, QLD, Australia

[63] School of Public Health, University of Queensland, QLD, Australia

[64] National Centre for Epidemiology and Population Health, Australian National University, ACT, Australia

[65] University of Sydney, School of Medical Science, Faculty of Medicine and Health, NSW Australia

[66] Erasmus MC Cancer Institute, The Netherlands

[67] Netherlands Comprehensive Cancer Organisation, The Netherlands

[68] Dermatology Research Centre, School of Biological Sciences, University of Manchester, and Salford Royal Hospital, Northern Care Alliance NHS Trust, Manchester, UK

[69] Garvan Medical Research Institute, NSW, Australia

[70] Kings College London, United Kingdom

[71] University of New Mexico Comprehensive Cancer Center, United States

[72] Frazer Institute, University of Queensland, QLD, Australia

Table of contents

Summary

This assessment by the Environmental Effects Assessment Panel (EEAP) of the Montreal Protocol under the United Nations Environment Programme (UNEP) evaluates the effects of UV (UV) radiation on human health within the context of the Montreal Protocol and its Amendments. We assess work published since our last comprehensive assessment in 2018. Over the last four years gains have been made in knowledge of the links between sun exposure and health outcomes, mechanisms, and estimates of disease burden, including economic impacts. Of particular note, there is new information about the way in which exposure to UV radiation modulates the immune system, causing both harms and benefits for health. The burden of skin cancer remains high, with many lives lost to melanoma and many more people treated for keratinocyte cancer, but it has been estimated that the Montreal Protocol will have prevented 11 million cases of melanoma and 432 million cases of keratinocyte cancer that would otherwise have occurred in the United States in people born between 1890 and 2100. While the incidence of skin cancer continues to rise, rates have stabilised in younger populations in some countries. Mortality has also plateaued, partly due to the use of systemic therapies for advanced disease. However, these therapies are very expensive, contributing to the extremely high economic burden of skin cancer, and emphasising the importance and comparative cost-effectiveness of prevention. Photodermatoses, inflammatory skin conditions induced by exposure to UV radiation, can have a marked detrimental impact on the quality of life of sufferers. More information is emerging about their potential link with commonly used drugs, particularly anti-hypertensives. The eyes are also harmed by over-exposure to UV radiation. The incidence of cataract and pterygium is continuing to rise, and there is now evidence of a link between intraocular melanoma and sun exposure. It has been estimated that the Montreal Protocol will have prevented 63 million cases of cataract that would otherwise have occurred in the United States in people born between 1890 and 2100. Despite the clearly established harms, exposure to UV radiation also has benefits for human health. While the best recognised benefit is production of vitamin D, beneficial effects mediated by factors other than vitamin D are emerging. For both sun exposure and vitamin D, there is increasingly convincing evidence of a positive role in diseases related to immune function, including both autoimmune diseases and infection. With its influence on the intensity of UV radiation and global warming, the Montreal Protocol has, and will have, both direct and indirect effects on human health, potentially changing the balance of the risks and benefits of spending time outdoors.

1 Introduction

The Montreal Protocol on Substances that Deplete the Ozone Layer and its Amendments (most recently Kigali in 2016) have prevented substantial depletion of stratospheric ozone and facilitated its recovery, with a marked effect on ultraviolet (UV) radiation and reduction in global warming. In the absence of the Montreal Protocol the erythemally weighted UV irradiance, indicated by the UV Index, would have increased by up to 20% between 1996 and 2020 in the region where most of the world's population lives (between 50 °N and 50 °S of the equator) [1]. With the Montreal Protocol it is projected that UV radiation will decline at mid-latitudes over the remainder of the 21st century, although in urban areas where air quality is improving, UV radiation at the Earth's surface is likely to increase. The Montreal Protocol has contributed to a reduction in global warming, as the ozone-depleting chemicals controlled under the Protocol are also potent greenhouse gases.

The changes brought about by the Montreal Protocol have important effects on human wellbeing, both directly and indirectly. In this assessment we focus largely on direct effects due to human exposure to UV radiation, but human health is also influenced by air quality [2] and impacts of UV radiation on terrestrial [3] and aquatic [4] ecosystems, and materials [5]. Direct effects occur due to ozone-driven changes in the intensity of UV radiation, influencing the time outdoors before damage to the skin and eyes occurs. These changes in UV irradiance, along with climate change, influence sun exposure and sun protection behaviour. However, changes in health outcomes linked to UV radiation also need be considered within the context of broader societal influences and changes in health service use. For example, over the past several decades day-to-day occupational and recreational activities have moved predominantly indoors, but in many countries with temperate climates, annual holidays in regions with high ambient UV radiation have become common and use of sunbeds has increased. Alongside this, the sun protection factor of sunscreens has increased and the public has been educated about how to protect the skin from the sun. In developed countries, changing practices in screening and diagnosis, particularly for skin cancer, make a considerable contribution to the observed trends. It is thus challenging to attribute trends in human health solely to changes in ambient UV radiation. However, with the increases in UV radiation that would have occurred in the absence of the Montreal Protocol, balancing the risks and benefits of sun exposure would have presented a far greater challenge.

We present an assessment of findings regarding the effect of UV radiation on health published since our previous Quadrennial Assessment [6]. This assessment is not a systematic literature review. Rather, we conducted a broad critical assessment of the literature to identify publications containing information that may be of interest to policy makers whose remit is to make decisions about controls of ozone-depleting substances.

2 New knowledge about mechanisms underpinning the effects of UV radiation on health

2.1 Genes and skin cancer

Skin cancer arises primarily as a consequence of UV-induced DNA damage that remains unrepaired, combined with immune suppression (Fig. 1). The past decade has seen an in-depth discovery of the genetic basis of skin cancers. Cutaneous melanomas carry distinct UV radiation mutational signatures (C>T substitutions at TpC dinucleotides (mutated base underlined), C>T substitutions at CpC and CpC dinucleotides, and high levels of T>C and T>A mutations (Appendix Fig. 1); the latter mutations may be caused by indirect DNA damage following exposure to UV radiation [7]. Melanocytes, from which melanomas arise, contain over 2000 genomic sites that are up to 170-fold more susceptible to UV radiation-induced damage than the average site in the genome [8]. These may serve as genetic dosimeters (i.e., indicators of UV radiation dose), which could be developed as a tool to determine risk of melanoma and thus the need for surveillance.

Until recently it was believed that cyclobutane pyrimidine dimers (CPDs) could only be formed during exposure to UV radiation. New studies have shown that CPDs can be formed after UV radiation exposure has ended, with maximal expression 2-3 hours post-irradiation, including in human skin in vivo [9]. These "dark CPDs" are formed by chemiexcitation, in which energy from UV radiation photons is transferred to chemical intermediates, including melanin intermediates, which then transfer energy to DNA, resulting in CPD formation. The biological significance of dark CPDs is unknown.

Many genetic loci associated with the risk of melanoma have been discovered. Additional variants have been identified through the use of multi-trait analysis of genome-wide association studies. Of note, new variants include those related to autoimmune traits; further functional analyses of these may identify new targets for chemoprevention of melanoma [10]. This method has also been used to identify new loci underpinning risk of keratinocyte cancer. Most variants affect both basal cell carcinoma (BCC) and squamous cell carcinoma (SCC) (collectively called keratinocyte cancer (KC)), demonstrating their shared susceptibility [11]. Loci in pigmentation, DNA repair and cell-cycle control, telomere length and immune response pathways have been identified.
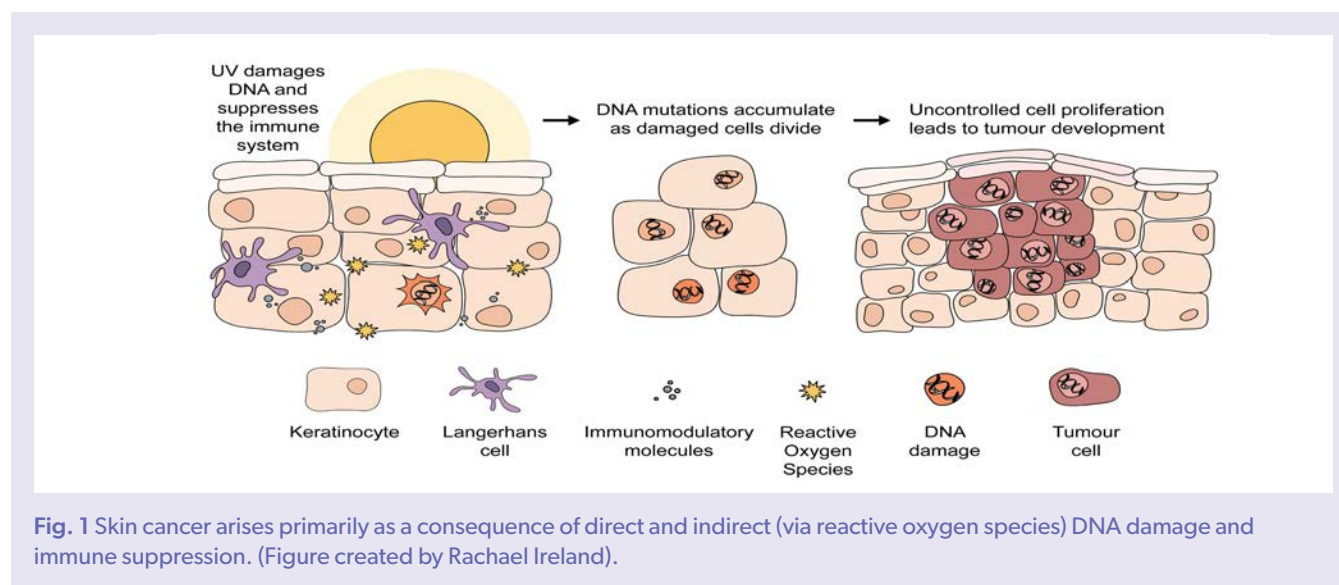

Fig. 1 Skin cancer arises primarily as a consequence of direct and indirect (via reactive oxygen species) DNA damage and immune suppression. (Figure created by Rachael Ireland).

2.2   The role of UV radiation-induced immune modulation in the harms and benefits of sun exposure

Many of the harmful and beneficial effects of exposure to UV radiation are mediated through UV-induced effects on the immune system, both locally and systemically. Our immune system is responsible for protecting us from pathogens and destroying aberrant (potentially malignant) cells. At the same time, it must self-regulate to avoid over-reactions to pathogens, and to tolerate 'self' by not attacking self-antigens that could lead to autoimmune diseases. In most people, exposing the skin to UV radiation suppresses local (skin) immune processes, enabling malignant cells to escape immune control, but it also upregulates antimicrobial processes in the skin. It also suppresses aberrant immune responses systemically; i.e. in other, non-sun exposed, parts of the body. Exposure to UV radiation is thus 'immune modulatory' rather than solely 'immune suppressive'.

2.3   Mechanisms and consequences of UV radiation-induced modulation of immunity

Modulation of the immune system occurs through the direct or indirect activation of cells that reside within the epidermis and dermis, including epidermal keratinocytes, dendritic cells such as Langerhans's cells, dermal lymphocytes, nerves, and mast cells [12]. Indirect pathways include UV radiation-induced changes in the action of cytokines and other mediators of the immune response, such as nitric oxide, *cis*-urocanic acid, ligands of the aryl hydrocarbon receptor, platelet-activating factor (PAF), prostaglandin E2, antimicrobial peptides, and vitamin D [13]. Some of these mediators lead to the recruitment of circulating immune cells from the blood. For example, following a sunburn (see Sect. 3.2), the skin is rapidly infiltrated by neutrophils, the most abundant leucocyte (white blood cell) in the circulation. Neutrophil infiltration peaks at ~24 hours after exposure to an inflammatory (3 minimal erythema dose (MED)) dose of broadband UV-B radiation, returning to baseline 7-14 days later [14]. Neutrophils perform important anti-bacterial functions which, together with the induction of anti-microbial peptides, partly explains why skin infections are uncommon following exposure of the skin to UV radiation. UV-recruited neutrophils also produce anti-inflammatory cytokines such as IL-4 which leads to local immune suppression.

Dendritic cells in the skin capture, process and present antigens to other immune cells, initiating an immune response. They are versatile and 'plastic' in their ability to take up, process and present foreign and tumour antigens to T cells. It is this property that makes dendritic cells the 'conductors' of the adaptive immune response. In response to UV radiation, dendritic cells and mast cells migrate from the site of exposure to the lymph nodes that drain the skin. There, they regulate T cell-dependent responses (reviewed in [15]) and activate immune regulatory B cells (B_{Regs} – Fig. 2) [16]. Importantly, in mouse models and using solar-simulated UV radiation, blocking this UV radiation-induced migration of mast cells [17] and/or the activity of UV-activated B cells [18] prevents carcinogenesis induced by UV radiation. Other regulatory immune cells are also activated and may migrate back to UV-irradiated skin [14]. There they suppress the skin and anti-tumour immune responses, modulate inflammation, potentially enhancing wound healing [19], and/or proliferate and migrate into the circulation (reviewed in [12]). Together, these events explain why UV radiation is considered a complete carcinogen; it is able to both mutate DNA and suppress the anti-tumour immune response.

Research published since our last assessment [6] has highlighted new mechanisms by which exposing the skin to UV radiation influences immunity, including upregulation of lipids, changes in white blood cells, and alterations in the skin microbiome and transcriptome. Exposing the skin to solar-simulated UV radiation causes an increase in the production of immunomodulatory lipids such as platelet-activating factor (PAF) and PAF-like species [20]. These bioactive lipids, and changes in lipid metabolism, directly affect immune-cell phenotype and function, including increasing the production of cytokines that suppress the immune system (Fig. 2). In addition, activation of the PAF receptor in human skin induces the release of large numbers of microvesicle particles [21]. These may transport PAF and other bioactive chemicals from epidermal keratinocytes to distant immune cells and organs, thus effecting UV-B-mediated systemic immune modulation [21]. This discovery provides crucial insight into the mechanism by which exposure to UV-B radiation alters the immune system at sites that are not directly exposed to the radiation.

The effects of exposure to UV radiation on white blood cell (leukocyte) subsets in blood have been recently reviewed [13]. Exposure of mice to a single 8 kJ m^{-2} dose of solar-simulated UV radiation induces changes in the number, phenotype and function of these cells in both the innate and adaptive immune systems that typically lead to reduced activity and capacity to recirculate [22], consistent with benefits for immune-mediated disorders such as multiple sclerosis (MS) and potentially COVID-19 [23].

Several studies have identified seasonal changes in the number of leukocytes and have found the overall inflammatory milieu to be more pro-inflammatory in winter and anti-inflammatory in summer. While vitamin D is known to have effects on immune function, the effects on leukocytes were independent of vitamin D status (reviewed in [13]). In support of this work, a randomised controlled trial (RCT) of low dose (400 IU/day) vitamin D$_3$ supplementation (compared to placebo) in vitamin D-deficient (mean 25-hydroxy vitamin D [25(OH)D[73]] blood concentration=36.1 nmol L^{-1}) but otherwise healthy participants in Aberdeen, Scotland, found seasonal variation in natural T-regulatory cell populations and functions that was independent of blood 25(OH)D concentration [24].

UV irradiation of the skin causes changes in the skin microbiome [25] and transcriptome (the set of coding and non-coding RNA in cells) [26]. In people with atopic dermatitis (the most common type of eczema), 12 to 25 treatments over 6 to 8 weeks with narrowband UV-B radiation caused a shift to greater microbial diversity accompanied by reduced skin inflammation [25]. Irradiation of the skin of

---

[73] 25(OH)D is the metabolite measured to determine vitamin D status

seven healthy male volunteers (skin type II) using solar-simulated UV radiation and doses equivalent to 0, 3 and 6 standard erythemal doses (SED) led to altered expression, mainly upregulation, of multiple genes (primarily related to DNA repair and apoptosis, immunity and inflammation, pigmentation, and vitamin D synthesis) [26]. The number of genes affected increased with increasing dose of UV radiation. UV-B (280-320 nm) and UV-A1 (340-400 nm) had similar effects on gene expression.

An abnormal cutaneous response to exposure to UV radiation may result in overactive immune responses to substances in the skin, resulting in UV-induced allergic skin conditions [27]. Evidence is also accruing to suggest that dysfunction of the skin's innate immune system contributes to some photodermatoses, including conditions aggravated by sun exposure such as systemic lupus erythematosus (SLE) [28] and rosacea [29] (Sect. 4.3). Abnormalities of innate immunity can explain the enhanced UV-B-induced keratinocyte damage observed in cutaneous manifestations of SLE [28], and the inflammatory response to UV-B-induced keratinocyte damage in rosacea [29].

Recent studies show that irradiating the skin of mice with UV-B radiation can lead to changes in distant organs. One study demonstrated changes in gene expression in the kidney, upregulating inflammatory responses [30]. This may be one mechanism by which sun exposure in people with SLE causes acute exacerbation of nephritis (inflammation of the kidney). In another study in mice, chronic exposure of the skin to broadband UV-B radiation (100–300 m J cm^{-2} for 3 days per week for 10 weeks) significantly reduced levels of dopamine and related enzymes (tyrosine hydroxylase and dopamine beta-hydroxylase) in the blood and adrenal glands and induced marked damage in the adrenal medulla [31]. These studies add to our emerging understanding of wide-ranging systemic effects of exposing the skin to UV radiation, noting that studies in mice do not always translate to humans but also that similar studies in humans may not be feasible.
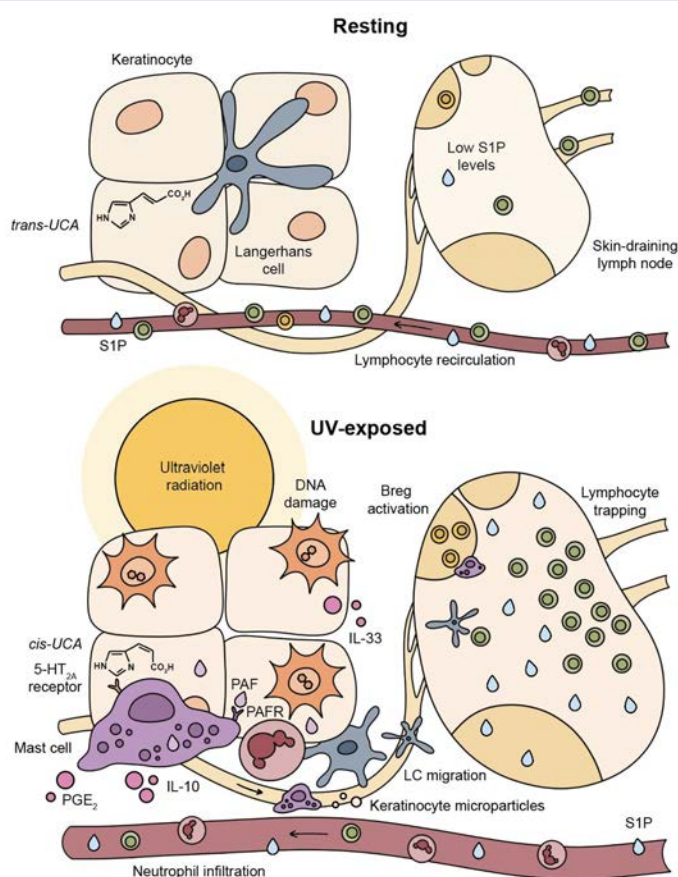
Fig. 2 Ultraviolet radiation is immunomodulatory. The absorption of UV radiation by chromophores in the skin directly and indirectly activates cells in the epidermis and dermis, including keratinocytes, Langerhans cells (LCs), mast cells and dermal lymphocytes. Exposing the skin to UV radiation stimulates keratinocytes and mast cells to release microvesicle particles, cytokines and immunomodulatory lipids such as platelet activating factor (PAF), which induce neutrophil and monocyte infiltration into the skin and can affect distant, non-skin cells. Skin mast cells and dendritic cells migrate into the skin-draining lymph nodes where they activate regulatory phenotypes (e.g. Breg). Elevated sphingosine-1-phosphate (S1P) lipid levels in the draining lymph nodes after exposure of the skin to UV radiation also contribute to systemic immune suppression by preventing lymphocyte circulation. UCA, urocanic acid; 5-HT, 5-hydroxytryptamine; PG, prostaglandin. (Figure created by Rachael Ireland).

3 Harms of exposure to UV radiation

Human exposure to UV radiation causes harms to the skin and eyes. For the skin in particular, the risks vary according to skin pigmentation. People with deeply pigmented skin are at particularly low risk of UV-induced skin cancer, due to the type of melanin and the degree of pigmentation. In contrast, people with lightly pigmented skin are at markedly increased risk of skin cancer, particularly if they reside in areas with high ambient UV radiation. Low-dose repeated exposures to UV radiation can increase pigmentation and skin thickness, offering some protection against skin damage during subsequent exposures, a concept called habituation. However, the protection afforded is modest, with photoprotection factors (interpreted similarly to the sun protection factor (SPF) used for sunscreens) of 2-3 for people with darker skin at high northern latitudes and 10-12 for people with lighter skin types at lower European latitudes (e.g. 35°North) [32].

3.1 Skin cancer

3.1.1 The association between exposure to UV radiation and skin cancer

Exposing the skin to UV radiation is the primary modifiable cause of melanoma and KC. The main mechanisms underlying UV-induced tumourigenesis are DNA mutation, suppression of anti-tumour immune responses, and promotion of cutaneous inflammation. However, the patterns of exposure that give rise to these tumours, and the proportion estimated to be attributable to exposure to UV radiation, differ by geographic location, skin type, and tumour type.

The association between sun exposure and melanoma is complex, and appears to differ according to the site of the tumour. A recent study supports the dual pathway hypothesis, where melanoma on sites that are less frequently exposed to the sun occurs in people with many naevi (moles), whereas melanomas on the head and neck are associated with cumulative sun exposure [33,34]. Despite their complex association with pattern and dose of sun exposure, 75% of melanomas globally are estimated to be attributable to population exposure to excess UV radiation compared with a reference population [35]. This figure is higher in countries with higher ambient UV radiation, particularly Australia and New Zealand (96%) [35], than in those where the intensity of UV radiation is lower, such as Canada (62%) [36] and France (83%) [37]. In people with skin of colour, melanomas tend to occur on the palms of the hands, soles of the feet, and mucosal surfaces, and UV radiation is not a risk factor for these lesions [38].

With respect to KCs, SCCs have a straightforward association with cumulative exposure to UV radiation. The pattern of exposure that gives rise to BCC is less well established, but intermittent exposure in both childhood and adulthood appears to play an important role. This notion is supported by a recent meta-analysis that found stronger associations between sunburns and sunbathing in adulthood and BCC than was apparent for SCC. Sunburn in adulthood was associated with a 1.85-fold increased risk of BCC (95% CI 1.15-3.00) and a 1.41-fold increased risk of SCC (95% CI 0.91-2.18). Similar findings were reported for sunbathing in adulthood [39]. Nevertheless, one study did find that cumulative sun exposure was associated with BCC but the association with exposure before the age of 25 years of age was stronger than the association with exposure in adulthood [40]. There is little information about the link between exposure to UV radiation and risk of KC in people with skin of colour. Studies in east Asia suggest associations with measures of sun exposure, such as UV Index, outdoors occupational exposure, and lifetime exposure, but the quality of the studies is low to moderate. There are no studies in people with black skin [41].

The strong association between exposure to UV radiation and KC, combined with high prevalence of exposure, translates into a very high proportion of KCs being attributable to this exposure factor. In Canada, estimates suggested that 81% of BCCs and 83% of SCCs diagnosed in 2015 were attributable to exposure to UV radiation [39]. Easily modifiable risk factors were responsible for BCC in particular; 19% of BCCs were attributable to sunburn in adulthood and 28% to adult sunbathing (the equivalent values for SCC were 10% and 17%).

Outdoor workers are at particular risk of developing KC [42]. In a systematic review, 18 of the 19 included studies suggested an increased risk of KC among outdoors workers, although estimates were imprecise in many studies [43]. In Canada 6% of KCs in 2011 were attributed to occupational exposure to UV radiation [44]. This is similar to previous studies, where in women 1% of skin cancer (i.e., KCs and rare skin cancers) cases and 4% of skin cancer deaths were attributable to exposure to UV radiation in an occupational setting. The equivalent numbers for men were 7% of cases and 13% of deaths [45,46].

A possible synergistic effect of simultaneous exposure to UV radiation and excessive alcohol consumption on sunburn and skin damage has previously been raised in epidemiological studies (reviewed in [47]). New work in mouse models and using human skin explants suggests that this is not due to alcohol-induced risky sun exposure behaviour, but rather that synergistic metabolic pathways induce more DNA mutations and immune dysfunction [47].

3.1.2 Skin cancers avoided by the Montreal Protocol

Estimates from the United States Environmental Protection Agency indicate that the Montreal Protocol will have prevented 11 million cases of melanoma and 432 million cases of KC that would have occurred in the United States in people born between 1890 and 2100 [48]. The model estimated that cohorts born in 2040 or later will not experience any excess incidence of skin cancer caused by the effects of ozone depletion, assuming continued compliance with the Montreal Protocol. While this highlights the critical importance of the Montreal Protocol, an important limitation is that these estimates assume no changes in sun exposure behaviour and skin cancer surveillance, and no changes in population structure, such as in the distribution of skin types. Other limitations include uncertainty regarding stratospheric ozone trends, the impacts of climate change, and the action spectrum for skin cancer development.

3.1.3 Geographic variability in the incidence of melanoma

Worldwide in 2020 an estimated 325,000 new cases of invasive melanoma were diagnosed and 57,000 people died from melanoma [49]. The estimated age-standardised (World Standard) incidence per 100,000 people per year of invasive cutaneous melanoma was 3.8 for men and 3.0 for women. Incidence was highest in Oceania (30.1) and lowest in Africa (0.9) and Asia (0.42). Australia and New Zealand continue to report the highest incidence of all countries (Fig. 3), and the highest burden in terms of disability-adjusted life years (DALYs) lost, followed by North America and Europe [50,51].

In 2018 it was estimated that melanoma accounted for 1.6% of all new cancer cases and was responsible for 0.6% of all cancer deaths worldwide [52]. In comparison, the most common cancer at that time (lung), excluding keratinocyte cancer, was responsible for 11.6% of cases and 18.4% of deaths. The cumulative risk of developing melanoma (birth to age 74 years, globally) was estimated to be 0.39% in men and 0.31% in women (noting that this is an average of the markedly different risks in people with light and dark skin); estimates of the cumulative risk of death from melanoma were 0.08% for men and 0.05% for women [52]. Melanoma constituted 11% of all cancer cases in Australia in 2019, and was responsible for 2.7% of deaths from cancer [53]. In Europe in 2018, melanoma accounted for 3.7% of all cancer cases (men: 3.5%; women: 3.9%), and was responsible for 2.5% of deaths from cancer (men: 3.2%; women: 1.9%) [54].

By 2040 the number of new melanoma cases globally is predicted to increase to 510,000 per year and deaths to 96,000, assuming changes in population size and age structure but no change in the incidence rates [49].
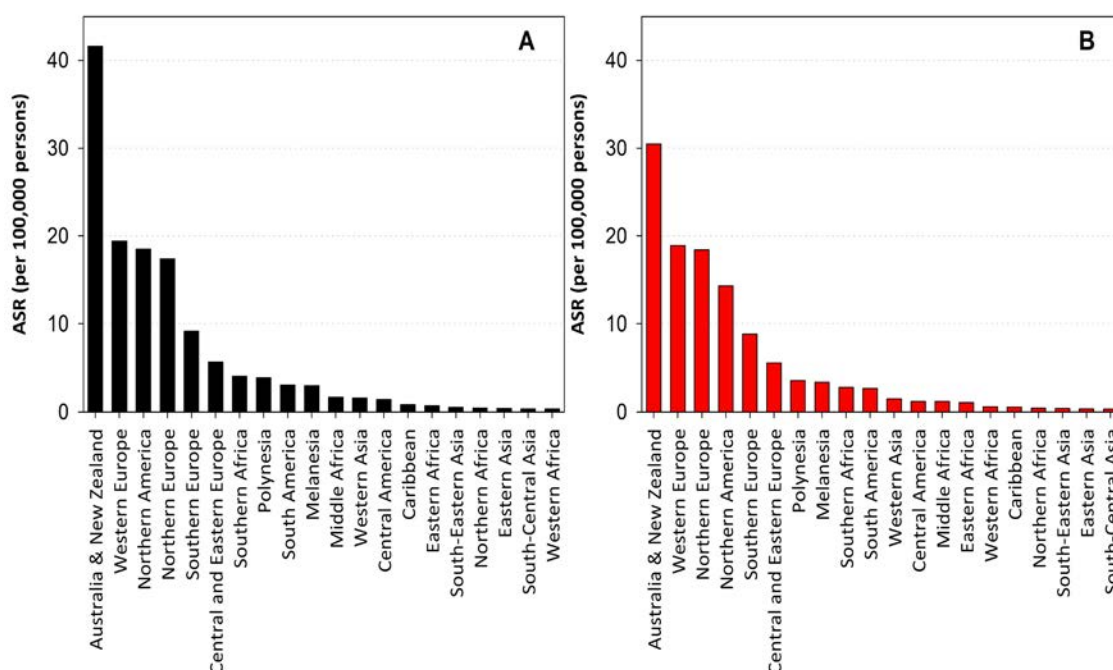

Fig. 3 Estimated age-standardised incidence rate (world-standard population) of invasive cutaneous melanoma in the year 2020, by world region: (A) men; and (B) women (Data from the Global Cancer Observatory Database).

3.1.4 Trends in the incidence of melanoma, based on published reports

Trends in melanoma incidence need to be interpreted in light of changing surveillance practices. In the United States [55,56], Australia [57], and Europe [58,59] there has been a much greater increase in the incidence of *in situ* (confined to the epidermis) and thin melanomas compared with thick melanomas. The increase in melanoma incidence has also greatly outstripped increases in the mortality rate. These patterns are thought to reflect the detection of lesions that are unlikely to cause significant morbidity or mortality within a person's lifetime, a phenomenon known as over-diagnosis, which is occurring due to the combined effect of an increase in skin examinations, lower clinical thresholds for taking a biopsy of pigmented lesions, and lower pathological thresholds for diagnosing melanomas [60,61]. Over-diagnosis of melanomas could lead to an under-estimate of the impact of the Montreal Protocol.

Recent trends in incidence of melanoma vary across populations. Incidence increased in the United Kingdom, Norway, Sweden and Canada (1982-2015) [62], particularly the Eastern Newfoundland and Labrador provinces (2007-2015) [63], and in France (1990-2018) [64]. Of recent reports from Eastern Europe, those from Lithuania (1991-2015) [65], Ukraine (2002-2013) [66], and the Czech Republic (1977-2018) [67] described increases for all age groups and in both men and women, while a study from Hungary found increases between 2011 and 2015 followed by a significant decrease between 2015 and 2019 [68]. For Australia, New Zealand and Denmark (1982-2015) there is a recent trend of stabilising or even declining incidence, likely due to concerted efforts in primary prevention over the past 2-4 decades [62].

While incidence is very low in China and South Korea, small increases in incidence were noted (from 0.4/100,000 in 1990 to 0.9/100,000 in 2019) in China [69] and in South Korea (from 2.6/100,000 in 2004 to 3.0/100,000 in 2017) [70]. In China in 2017, the highest incidence rates were recorded for the eastern and northeast provinces compared with the western provinces, a trend which may be due to heightened awareness and greater access to medical services in these regions [71]. A study from Singapore reported very low incidence among Chinese, Malay and Indian Singaporeans [72].

A study of trends in melanoma incidence using data from the Surveillance, Epidemiology, and End Results (SEER) program in the United States showed that across all ethnicities incidence stabilised between 2010 and 2018 (average annual percent change [AAPC], 0.39%; 95% CI, -0.40% to 1.18%), following five decades of continuous increases [73]. However, the incidence of the thickest melanomas (T4, >4.0 mm) continued to rise (AAPC 3.32%; 95% CI, 2.06%-4.60%). Populations with lower socioeconomic status or from minority groups were more likely to have thicker melanomas over the time period examined, likely due to poorer access to screening and early detection activities. While the incidence of melanoma in children is very low, between 2000 and 2015 in the United States declines in incidence were reported for children aged 10-19 years, while incidence in younger children remained stable [74].

Several studies have reported different trends according to age. Studies from Canada [75], Italy [76], and England [77] report increases in incidence in older age groups, possibly at least partly due to longer life-span, but a stabilisation or decline in younger age groups. In contrast, a Finnish study of melanoma incidence in children and adolescents reported a four-fold increase between 1990 and 2014, most notable among adolescents [78]. It is unclear whether this represents a true increase or is due to changes in diagnostic criteria and/or cancer registry coverage.

3.1.5 Trends in incidence of melanoma according to age: analysis of Global Cancer Observatory data

It is difficult to compare trends in incidence of melanoma based on reports from the published literature due to the use of different populations for standardising age, as has been noted in the Panel's annual assessments 2019-2021 [79-81]. We therefore extracted population-based registry statistics for six high-risk populations with data available for the period 1982-2016 (namely Australia, United States Whites, Norway, Sweden, Denmark and the United Kingdom) from the Global Cancer Observatory (age standardised to the World Standard Population) [82]. While incidence began to stabilise in Australia after 2005, it continues to increase in the other countries for both men (Fig. 4A) and women (Fig. 4B). However, there is marked variation with age, with modest increases among people aged less than 50 years (Fig. 4C and 4D) and much more notable increases among older age groups (50 years and over) (Fig. 4E and 4F). For Australia only, there has been a decline in incidence among younger age groups that began around 2007. In the most recent 10-year period, the estimated average annual percent change in incidence was highest for Norway (4.0% for men and 4.2% for women) and Sweden (3.8% for men and 4.0% for women). These trends are attributable to population-specific changes in time outdoors and implementation of sun-protection programs; these will influence trends into the future as younger cohorts, who have been exposed to these behavioural changes from a younger age, enter middle and older age.
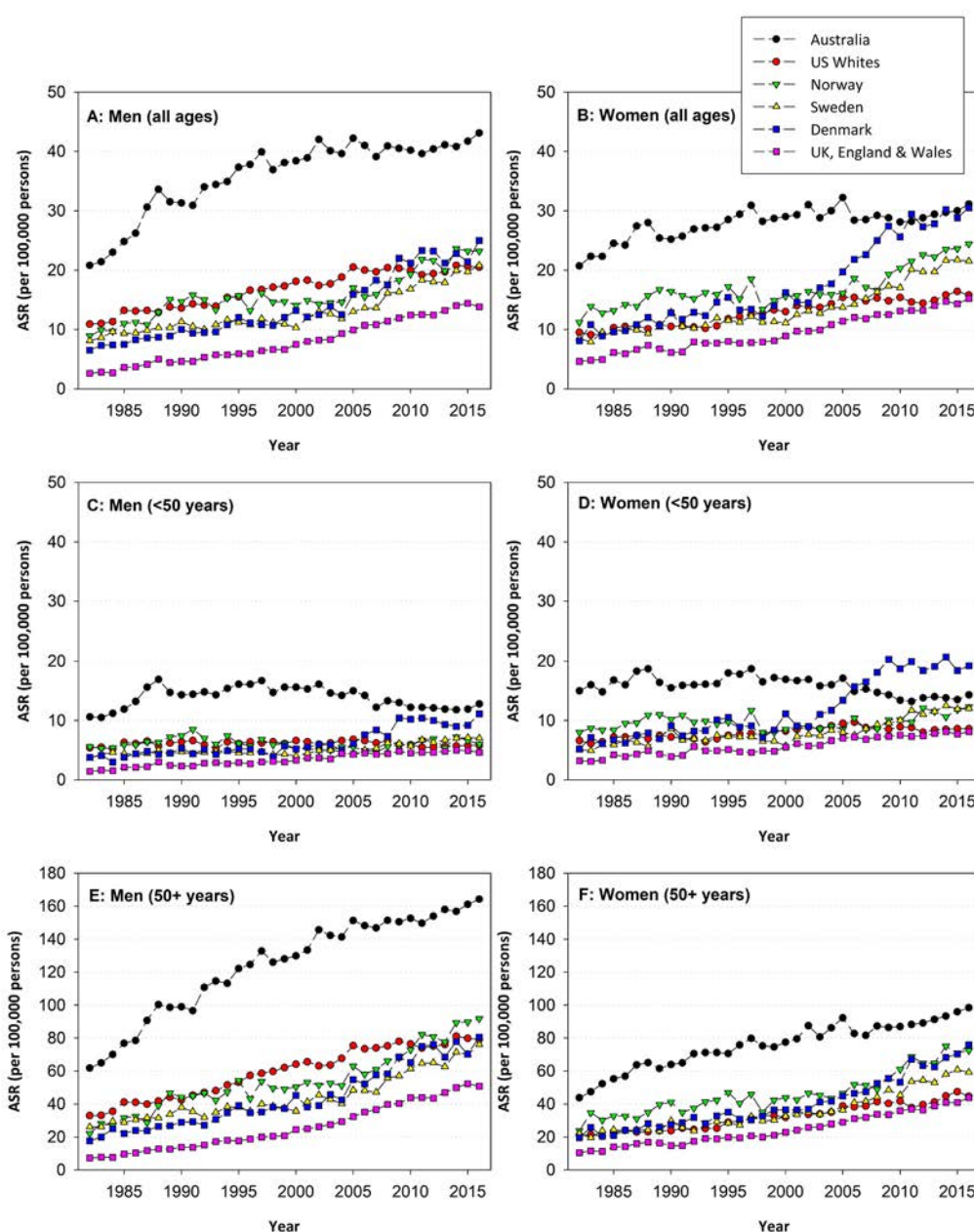
Fig. 4 Age standardised incidence rate (ASIR, World) of invasive cutaneous melanoma 1982-2016 in 6 populations [Australia, United States Whites, Norway, Sweden, Denmark and United Kingdom (England and Wales)] from 1982-2016. Trends presented separately for men and women, and for all ages and separately for those <50 years and ≥50 years.

3.1.6 Trends in melanoma mortality

Trends in mortality are underpinned by changes in incidence and case-fatality rates. The latter has been decreasing markedly in some countries in recent years due to the introduction of new and highly effective systemic therapies for advanced melanoma [83], and this will continue to affect mortality rates with increasing use for earlier stage disease.

A study using data from the WHO Mortality Database covering 31 countries over the time period 1985 to 2015 reported an overall increase in melanoma mortality for men in all countries, in contrast with stable or declining rates in women [84]. For the most recent time period (2013-2015) the median mortality rate was 2.6 deaths per 100,000 for males and 1.6 per 100,000 for females; the highest mortality rates were recorded for Australia and Norway for men, and Norway and Slovenia for women (noting that New Zealand, which has the highest mortality globally, was not included in the report). The increase in most countries reflected increasing mortality rates in

people aged 50 years or older; mortality rates were generally stable or declining in younger age groups. The latter trend likely reflects lower incidence among younger birth cohorts exposed to lower cumulative exposure to damaging UV radiation. A separate report for Spain over the period 1982-2016 showed a similar trend, with mortality rates stabilising in men and women younger than 64 years from the mid-90s, while rates continued to rise in older age groups [85].

Recent declines in melanoma mortality have been reported for New Zealand (2015-2018) [86] and China (1990-2019) [69], but increases were reported for the Netherlands (1950-2018) [87] and Brazil (1996-2016) [88], while mortality was stable in France (1990-2018) [64] and South Korea (2014-2017) [70]. These disparate trends are difficult to interpret given heterogeneity in the introduction (and timing thereof) of new systemic treatments (particularly immunotherapy about 10 years ago) across jurisdictions.

3.1.7   Trends in the incidence of Merkel cell carcinoma

Merkel cell carcinoma (MCC) is a rare skin cancer that may be associated with exposure to UV radiation. An increase in the incidence of MCC between 1997 and 2016 has been reported for the United States, Norway, Scotland, New Zealand, and Queensland, Australia at a rate of 2 to 4% per year [89]. Increases have been greater in Brazil, with average annual percent change from 2000 to 2017 of 9.4% for men and 3.1% for women [90]. These findings are consistent with an earlier report covering 20 countries for the period 1990-2007 [91]. The increase in the United States has been attributed to three factors: increased detection, an ageing population, and higher exposure to UV radiation in more recent birth cohorts [92].

The cause of MCC is not well understood; the Merkel cell polyomavirus (MCPyV) is clonally integrated in up to 80% of tumours [93]. While several studies have reported more mutations in MCPyV-negative tumours (dominated by UV signature mutations) [93,94], a new study based on 9 tumours reported more mutations in MCPyV-positive compared to MCPyV-negative tumours [95]. Because MCC is such a rare tumour, all existing studies are based on limited tumour series, and further studies using larger sample sizes are needed to understand the role of exposure to UV radiation in the aetiology of these cancers.

Survival from MCC is much lower than for melanoma (50% at 5-years for local and <14% for metastatic disease [96]), although immunotherapy trials are reporting improved outcomes [97-99]; the costs of treatment are likely to increase if these therapies are widely adopted.

3.1.8   Trends in incidence of keratinocyte cancer

Accurately reporting the burden, incidence, and trends in KC remains a challenge. KCs are not routinely reported in most cancer registries. Further, people frequently experience more than one lesion, but this multiplicity is often not considered, with only the first lesion in a person being reported. Accounting for multiple KCs per person results in an approximately 50% increase in incidence rates [100,101].

An analysis of Global Burden of Disease data found that in 2019 KC was the most common cancer globally, affecting almost 3 times as many people as the next most common cancer (lung – 2.2 million people) [102,103]; there were ~6.4 million new patients with KC. Death due to BCC is very rare, but ~56,000 people died due to SCC. The burden of disease, as measured by DALYs, increased by almost 25% between 2010 and 2019.

Age-standardised incidence rates of KC are highest and increasing in Australia and New Zealand [104-107], with age-standardised rates as high as 1907/100,000 (standardised to the 2001 Australian population). In Europe, increasing incidence of KC has been reported. For example, in Iceland there was a 2 to 4-fold increase in the incidence of BCC [108] and a 16-fold increase in incidence of SCC between 1981 and 2017 [109], attributed to increased holidays to destinations with high ambient UV radiation and use of sunbeds. In Serbia between 1999 and 2015 there was an annual increase in KCs of 2.3% [110]. In the United Kingdom, SCC incidence increased by 31% and BCC by 21% between 2004 and 2014 [111]. In the United States the incidence of KC increased from 1990 to 2004, but then remained fairly stable from 2005 to 2019 [112].

Among populations with predominantly light skin, the lifetime risk of KC is much higher in areas with high ambient UV radiation. In the United Kingdom, where ambient UV radiation is comparatively low, lifetime risk is estimated to be 20% [113]. In contrast, lifetime risk in Australia, where the ambient UV radiation is high, is estimated at 69% (73% for men and 65% for women) [114].

Benign and premalignant keratinocyte lesions caused by sun exposure add an additional burden to the already high cost of skin cancer for healthcare systems and individuals. The prevalence of actinic keratosis (benign lesions) is high and estimated to be between 25% (in a general practice population in Switzerland) and 29% (in patients attending dermatology outpatient clinics in Spain) in European populations [115,116]. The incidence of *in situ* skin cancers (premalignant lesions) is also increasing, and in some countries the incidence of these lesions is increasing more rapidly than that of invasive cancers. For example, in the Netherlands the incidence of SCC increased by 6-8% per year between 2002 and 2017, compared with a 12-14% annual increase since 2010 for SCC *in situ* [101,117].

3.1.9 Risks of skin cancer in people who are immunosuppressed

Immunosuppression is a risk factor for melanoma, BCC and SCC. Populations with compromised immunity at increased risk include organ transplant recipients [118], those diagnosed with HIV/AIDS (4-fold increased risk of melanoma) [119,120], and those treated for rheumatoid arthritis (~1.3-fold increased risk of KC and melanoma) [121], inflammatory bowel disease (~1.5-fold increased risk of KC), and some lymphoproliferative disorders including non-Hodgkin lymphoma and chronic lymphocytic leukemia (~2-fold increased risk of melanoma) [122]. In solid-organ transplant recipients the magnitude of the increased risk differs between skin cancer types: the increased risk in a high ambient UV radiation environment is 2- to 3-fold for melanoma, 6- to 10-fold for BCC, and as high as 100-fold for SCC [123].

3.1.10 Costs associated with skin cancer management

The average paid and unpaid productivity loss per premature death from melanoma in Europe is estimated to be €450,694 [124], the second highest loss of all cancer types after Hodgkin's lymphoma, likely due to the relatively earlier age of onset (and thus greater paid productivity losses).

The introduction of new systemic treatments for advanced melanoma and their increasing use as an adjuvant treatment for non-metastatic disease is causing a rise in the overall cost per capita associated with melanoma treatment globally. In the United States between 1997 and 2015, total expenditure for treatment of melanoma increased at a faster rate than for other cancers [125]. In the Netherlands malignant skin tumours were the 4th most costly cancer in 2017; drug costs increased from €0.7 million to €121 million from 2007 to 2017 [126]. The largest cost drivers in France, Germany and the United Kingdom are medications and hospitalisation and/or emergency department treatment [127]. Adverse events from the use of new treatments are also responsible for a sizable cost burden [128,129].

A modelling study on the cost of melanoma in Europe estimated national costs ranging between €1.1 million in Iceland and €543.8 million in Germany (€2.7 billion for all European Union states) [130]. A recent study estimated the national costs of treating newly diagnosed melanoma in Australia and New Zealand for the year 2021, and reported total costs of AUD 481.6 million (€310 million [73]),and NZD 74.5 million (€43 million), respectively [131]. In Australia, the mean cost per patient was AUD 14,268 (€9,198), ranging from AUD 644 (€415) for *in situ* melanoma to AUD 100,725 (€64,930) for stage III/IV (advanced) disease. These costs will increase as expensive immunotherapy becomes a therapy of choice for earlier stage melanoma, either alone or in combination with targeted therapies [132].

Examining the skin to identify melanoma can lead to the detection of benign lesions, often resulting in additional treatments that may or may not be needed. A study in the United States reported on the costs of diagnosis and treatment of actinic keratoses and other benign lesions associated with screening for melanoma via total body skin examination [133]. In an analysis of 36,647 total body skin examinations in 20,270 adults, the estimated cost of treatment (including consultation, biopsy and pathology charges) for each melanoma detected was USD 32,594 (€33,614), with an additional cost of USD 7,840 (€8,085) to treat actinic keratoses and other benign lesions.

Given the very high and escalating costs of treatment, public health agencies have strengthened their focus on primary prevention, for which there is evidence of cost-effectiveness. A modelling study to evaluate the cost-effectiveness of prevention compared with early detection for melanoma control [134] used data from two randomised controlled trials (RCTs) conducted in Australia [135,136]. Compared with annual clinical skin examinations (early detection), and no intervention, advice to use sunscreen daily (prevention) resulted in lower numbers of melanoma and KC cases, and significantly lower costs associated with diagnosis and treatment [134]. However, these findings may not be applicable to locations with lower ambient UV radiation, and potential costs of over-diagnosis have not yet been considered.

In Canada, the costs of KC and other rare skin cancers due to occupational exposure to UV radiation were estimated to be CAD (2011) 29 million (€22 million) in direct and indirect costs, and CAD (2011) 6 million (€4.5 million) in intangible (due to effects on quality of life) costs in 2011 [137]. These costs can be mitigated; estimates suggest that for every dollar invested in personal protective equipment and shade structures, CAD 0.49 and CAD 0.35 will be returned, respectively [138]. Another modelling study of cost-effectiveness showed that primary prevention by systematic use of sunscreen at a population level would prevent substantial numbers of new skin tumours (26% less excised KC), and save healthcare costs [134]. Among people at high risk of KC, costs for treatment of KC and actinic keratoses were reduced one year after treatment with topical 5-fluorouracil, showing that chemoprevention may be an option to reduce the incidence of skin cancer in this subgroup [139].

The very high and increasing costs of managing skin cancer underscore the need to protect the stratospheric ozone layer; in the absence of control of ozone-depleting substances, the intensity of UV radiation in some regions would increase to the point where many more people would be exposed to sufficient UV radiation to initiate skin cancers.

3.2 Sunburn

Sunburn is an acute inflammatory skin reaction caused by over-exposing the skin to UV radiation, primarily the UV-B wavelengths; it is clinically manifest as erythema (redness) in people with Fitzpatrick skin types I to IV[74] (modified from [140]), and may cause pain and blistering.

Despite the definition of sunburn varying between studies, it is a well-established risk factor for the development of cutaneous melanoma and KC [141,142], and number of severe sunburns may be associated with increased risk of herpes zoster (i.e., shingles) [143]. Moreover, inflammation from sunburn is a health burden, independently of its association with other conditions. In the United States National Emergency Department Sample, including information about presentations to 950 hospital emergency departments from 2013 to 2015, there were 82,048 visits for sunburn, with 21% classified as severe sunburn (second or third degree burns and/or requiring inpatient admission) [144]. The average cost of an emergency department visit for sunburn was USD 1132. Presentation for all sunburns and for severe sunburns showed highest frequency in lower-income young men, and the incidence was higher in the sunnier states.

3.2.1 Trends in rates of sunburn

Data from the United States National Health Interview Surveys reveal that 34% of community-dwelling adults reported one or more sunburns in the prior 12 months in both 2005 and 2015 (sample sizes 29,250 and 31,399 respectively) [145]. The percentage of adolescents reporting sunburn was considerably higher. Between 2015 and 2017, 57% of 21,894 people aged 14 to 18 years reported being sunburnt at least once in the previous 12 months [146]. Sunburn was also more common in adolescents than in adults in Spain; 75% of 776 adolescents reported being sunburnt in the previous year compared with ~54% of 632 adults and 44% of 324 children [147]. In Germany, 22% of children aged 1-10 years surveyed in 2020 had been sunburnt in the previous year, and there was a positive association with age [148].

In some countries there has been a reduction in the prevalence of sunburn, coinciding with increased use of sun protection behaviours. In Australia, a comprehensive skin cancer prevention campaign, SunSmart, began in 1988. Surveys conducted in the state of Victoria over the subsequent three decades, in which participants were asked about their sun protection behaviour on the weekend prior to the interview, showed a marked increase in the percentage of people using at least one sun protection behaviour (seeking shade, or using hat or sunscreen) in the first decade after SunSmart began (from 29% to 65%) and more modest increases thereafter [149]. Sunscreen use increased from 11% pre SunSmart to 68% in the 2010s. In the state of New South Wales, the percentage of people reporting often or always using sunscreen increased from ~30% in 2003 to ~40% in 2016, but there was no increase in use of hats [150]. The increase in sun protection is evident in sunburn trends. In Australian adults (n=3614), the percentage reporting sunburn during the previous weekend in summer decreased from 14% to 11% between 2003/2004 and 2016/2017 [151], accompanied by an increase in the percentage of people using two more sun protection behaviours (from 41% to 45%). Sunburn occurred more frequently in Australian adolescents than in adults, but there was a decline from 20% to 15% across this period. In adults in Denmark (n=33,315) a 1% annual decrease in sunburn in the previous 12 months was seen across 2007-2015, coinciding with a national sun safety campaign [152].

A birth cohort analysis of melanoma-prone families demonstrates changes in sun protection behaviour and sunburns over time. People from 17 centres in Europe, North and South America, Australia and the Middle East (n=2407) were questioned about sun exposure and sunburns at various anchor points across their lives [153]. These behaviours were analysed according to birth cohort (in decades from those born in the 1910s and 20s through to those born in the 1980s). There was a clear secular trend in the reported frequency of sunscreen use; people born more recently were more likely to use sunscreen at a younger age than those born earlier. Time outdoors on weekends at less than 20 years of age was lower in more recent birth cohorts. Within each birth cohort sunburn occurred more frequently in early *vs* later life, but more recent cohorts were less likely to experience early life sunburns.

Changes in sun exposure and prevention behaviour in some countries have been marked, which may be underpinned, at least in part, by sun protection campaigns. In the absence of the Montreal Protocol, however, it is likely that the benefits of these changes would have been less evident, as the time to sunburn would have been markedly shorter.

3.2.2 Sunburn prevalence in people of darker skin type

Skin melanisation provides some protection against sunburn and UV radiation-induced skin cancer. Traditionally, people with dark skin (skin types V-VI) have been thought to be at very low risk of sunburn [154]. However, the difficulties of detecting sunburn erythema in people with dark skin can contribute to an over-estimation of the amount of UV radiation required to cause sunburn, and an under-estimation of sunburn prevalence [155]. Known differences in sun protection behaviours between ethnically diverse populations could also influence sunburn prevalence [156].

In a survey of people of Black African or Black Caribbean heritage living in the United Kingdom (n=222 respondents), over 50% reported a lifetime history of sunburn [157], with frequencies of 47%, 54% and 71% in those self-classifying as dark, medium and light skin tone. In the United States, nearly 10% of 4,157 Non-Hispanic Black participants in the National Health Interview Survey 2015

---

[74] Fitzpatrick Skin Types: Type 1: Light white skin, always burns, never tans; Type 2: Light white skin, usually burns, tans minimally; Type 3: White skin, sometimes burns, tans moderately; Type 4: Olive-light brown skin, rarely burns, tans moderately-heavily; Type 5: Medium brown skin, rarely burns; Type 6: Dark brown-black skin, rarely to never burns.

reported being sunburnt in the previous year, compared with nearly 25% of Hispanic people (n=5208) and 42% of non-Hispanic Whites (n=19,784) [145]. These surveys suggest that sunburn occurs more frequently in people with darker skin types than traditionally appreciated, but in light of the lower severity of sunburn compared with that in people with light skin, and the extremely low risk of UV-induced skin cancer in these populations, the significance of this is unclear.

3.3 Photodermatoses

Photodermatoses are inflammatory skin disorders that are induced or exacerbated by exposure to UV radiation and, in certain conditions, visible light [27]. Both UV-B and UV-A radiation can contribute to the development of photodermatoses. Photodermatoses fall into aetiological groups: dysregulated immune responses to UV radiation; disorders of DNA repair; intrinsic biochemical defects; photosensitivity reactions to drugs and/or exogenous chemicals; and photoaggravated disorders.

3.3.1 The burden of photodermatoses and their impact on health and psychological wellbeing

The lack of registry data and of consistent case definition for the most common dermatoses make it very challenging to estimate the population prevalence of photodermatoses. However, some photodermatoses, such as the immune-mediated condition, polymorphic light eruption (PLE), have been reported commonly from dermatology clinics in light-skinned populations in temperate regions, particularly during spring [158]. Comprehensive reviews of data from photodiagnostic units in dermatology departments indicate that the photodermatoses most commonly seen are PLE, photoaggravated atopic dermatitis, actinic prurigo, chronic actinic dermatitis, solar urticaria and drug-induced photosensitivity. Photodermatoses occur in dark-skin populations, although with differing frequencies and characteristics from light-skin populations [159]. In a systematic review of population-based and dermatology outpatient studies of rosacea, a photoaggravated chronic inflammatory facial condition, a global prevalence of up to 5% was estimated; however studies in which rosacea was self-reported yielded higher prevalence than in those where the condition was determined by examination [160]. Studies of the prevalence of most photodermatoses are scarce; for example, there are no reported population-based studies in solar urticaria.

Photodermatoses involve a wide range of clinical features, which vary according to the individual condition; these include pain in the skin within a few minutes of sun exposure, severe itching, erythema, blistering, and scarring. The adverse impact on sufferers occurs both directly due to symptoms, and indirectly through restrictions imposed by sun avoidance. In a systematic review of 20 studies (2487 adult and 119 child participants), in which an assessment of quality of life or psychological wellbeing was performed, one-third of adults and children with photodermatoses were found to experience a very large negative impact on quality of life (Dermatology Life Quality index >10), and anxiety and depression occurred twice as frequently as in the unaffected population [161].

3.3.2 The association between commonly used photosensitising drugs and photodermatoses and skin cancer

The pathologic mechanisms underlying drug photosensitivity are broadly classified as phototoxic or photoallergic. Oral medication-induced photosensitivity commonly involves phototoxicity, which can theoretically occur in anyone upon exposure to sufficient dose of a drug and UV radiation. Clinically, drug phototoxicity most often manifests as skin redness, swelling and burning, and can be misdiagnosed as severe sunburn.

An analysis of more than 745 million drugs dispensed in Germany and Austria between 2010 and 2017 indicated that nearly 50% had photosensitising potential, with diuretics and anti-inflammatory drugs being primarily responsible [162]. However, the global incidence of drug photosensitivity is uncertain. Analysis of the Japanese Adverse Drug Event Report database (2004-2016) found less than 0.1% of 430,587 reports concerned photosensitivity reactions [163]. A systematic review identified 1134 reported cases of suspected drug phototoxicity associated with 129 oral drugs [164]. However, the quality of the evidence for an association with drugs is low; fewer than 25% of studies performed phototesting, and only 10% confirmed the diagnosis with drug challenge-rechallenge testing. In a report of 2243 patients with photodermatosis evaluated at a photodiagnostic unit, 5% were diagnosed with photodermatosis induced by oral medication. All underwent broadband UV radiation testing and monochromatic testing to wavelengths from 300 to 600 nm (i.e., in the UV-B, UV-A, and visible spectra). UV-A was the main provoking waveband with UV-B contributing in 15% of cases [165].

It is possible that commonly prescribed photosensitising drugs may induce skin cancer. Some mechanisms by which drugs induce acute photosensitivity are also relevant for skin cancer induction, such as promotion of UV-induced DNA damage. In a nested case-control study, using data from the Danish Cancer Registry, of people with their first diagnosis of BCC (n=71,533) or SCC (n=8,629) and population controls (n=1,430,883), there was an increased risk of KC with long-term use of hydrochlorothiazide (a diuretic medication commonly used for treatment of high blood pressure); adjusted odds ratios (ORs) for high use *vs* never use were 1.29 (95% CI 1.23-1.35) for BCC and 3.98 (95% CI 3.68-4.31) for SCC [166]. This led to the European Medicines Agency recommending that advice on increased risk of KC should be included in hydrochlorothiazide product information [167]. Further studies, based in different geographic locations and demographic groups, reveal heterogeneous and conflicting results for an increased risk of KC and melanoma with hydrochlorothiazide use [168-172]. Given its potential public health significance, this issue needs to be resolved.

3.4   Eye diseases associated with exposure to UV radiation

Exposure to UV radiation, either directly or through intermediate factors, is associated with increased risk of cataract of the lens, pterygium, squamous cell carcinoma of the cornea and/or conjunctiva, photokeratitis (affecting the cornea) and photoconjunctivitis, pinguecula, and possibly intra-ocular melanomas, macular degeneration and glaucoma. This section assesses evidence available since our last assessment [6] on conditions that are directly related to exposure to UV radiation.

The superficial layers of the eye are exposed to UV radiation and incur damage through the same pathways of DNA damage and production of reactive oxygen species as is seen in the skin. When the individual is in an upright position and the sun is overhead, there is some inherent protection from exposure to UV radiation provided by the protrusion of the brow, the eyebrows, and the eyelids. These provide less protection at other body positions (e.g., lying down), or when the sun is at a lower angle [173,174]. Wearing a hat and using shade can also reduce exposure, while high surface albedo can increase exposure; large and wraparound sunglasses that block both UV-A and UV-B radiation provide good sun protection [175-177]. UV wavelengths also penetrate to the deeper structures of the eye (reviewed in a previous assessment [178]). The cornea absorbs wavelengths below 295 nm, but allows longer wavelengths to reach the iris and lens. In adults, the lens of the eye absorbs all wavelengths below 370 nm, and greater than 98% of wavelengths between 370 and 400 nm, with higher absorbance in the posterior part of the lens [179]. Over time, the chemical changes induced by that absorption – direct UV-B induced damage and (indirect) UV-A induced photo-oxidation of soluble lens proteins – cause clouding of the lens; i.e., cataract [179]. In young children, the lens may transmit a greater proportion of shorter UV wavelengths, allowing these to reach, and potentially damage, the retina.

3.4.1   Trends in the prevalence and incidence of cataract

Cataract is the major eye condition associated with long-term exposure to UV radiation. The main types of cataracts, as defined by their location in the lens, are nuclear, cortical, or posterior subcapsular. In many cases, there is a mixed phenotype and, within any individual, the two eyes may contain cataracts with a different predominant phenotype. The two subtypes most clearly associated with exposure to UV radiation are nuclear and cortical cataracts.

According to the latest reports of the Vision Loss Expert Group of the Global Burden of Disease Study, cataract was the leading cause of blindness between 1990 and 2015 around the world, accounting for 35% (95% CI 26 - 44) of the total blindness in 2015 [180-184]. Projections to 2020 from several countries/regions indicate that cataract would remain the main cause of blindness in 2020 [180-185]. Compared with global figures, the proportion of moderate to severe vision impairment caused by cataract was estimated to be higher in East Asia [180], South-east Asia [182], Oceania [182] and Sub-Saharan Africa [184] where exposure to sunlight may be higher and access to suitable medical care may be limited. The disability from cataract (measured in DALYs) increased from 3.5 million in 1990 to 6.7 million in 2019 - an increase of 191% [186].

New studies further demonstrate the high prevalence of cataract. In the cross-sectional Ural Eye and Medical Study set in a rural area of Russia, the prevalence of cataract was 45% in people aged ≥ 40 years (of 5899 participants, 81% of eligible residents). Nuclear and cortical cataracts affected 38% and 15% of participants, respectively [187]. A population-based study conducted in Finland found that the prevalence of cataracts increased from 8.1% (95% CI 7.8-8.5) to 11.4% (95% CI 10.9-11.9) among individuals ≥ 30 years between 2000 and 2011 [188]. The annual average incidence over the 11-year period was estimated to be 109 cases per year per 10,000 people (95% CI 104-114) [188]. The cumulative incidence over a similar time period (baseline 2004-2006; follow-up 2011-2013) was greater in Singapore; in the Malay Eye Study the age-standardised cumulative incidence of nuclear and cortical cataract over this time period was estimated to be 13.6% and 14.1% (equating to an annual average crude incidence of 227 and 189 cases per year per 10,000 individuals), respectively [189].

Greater exposure to UV radiation has been clearly linked to an increased risk of cataract (reviewed in [179]). A recent study provides additional supporting evidence. In a population-based cross-sectional study in three different rural areas of India (n=12,021), 33% of participants aged 40 years and older had a cataract in at least one eye [190]. Compared with the lowest quintile of a lifetime effective sun exposure score (calculated taking into account the years of exposure, hours of sun exposure accounting for type of headgear used (none, caps, hats, umbrellas, veils, sunglasses)), the prevalence of cataract was significantly higher in the 3rd, 4th and 5th quintiles of exposure. Those in the fifth quintile were 9 times more likely to have cataracts than those in the first quintile (adjusted OR 9.4; 95% CI 7.9-11.2), rising to nearly 26 times more likely in analyses confined to the highest altitude region (Guwahati/Hills region). Differences in exposure to UV radiation, solar angle and sun protection behaviours each had an additional influence on prevalence of cataracts. Nevertheless, in data from the 2008-12 Korea National Health and Nutritional Examination Survey of economically active people, there was no significant association between higher sunlight exposure (≥ 5 hours *vs* <5 hours/day in the sun without sunglasses or hat) and medically diagnosed cataract (adjusted OR=0.88, 95% CI 0.77-1.00) [191].

Globally, and across diverse individual regions for which there are recent data, the incidence of cataract continues to increase, at least partly due to ageing populations. Where there is good access to high quality medical care, including cataract surgery, this may not contribute greatly to the burden of disability. However, in many regions, cataract remains a leading cause of blindness, resulting in considerable morbidity due to vision loss and its sequelae (e.g., falls) [192].

A recent study has estimated the effectiveness of the Montreal Protocol in preventing eye diseases, with a focus on cataract. It was estimated that the implementation of the Montreal Protocol with all of its Amendments and adjustments compared to a scenario of no control of ozone-depleting substances, will have prevented 63 million cataract cases in people born in the United States between 1890 and 2100. When the comparison scenario is the original Montreal Protocol, this figure is 33 million fewer cases of cataract, demonstrating the importance of the ongoing strengthening of the Protocol [48].

3.4.2 Prevalence of pterygium

Pterygium is a non-cancerous, self-limiting pink, fleshy tissue growth on the conjunctiva, that is initially induced by exposure to both UV-B and UV-A radiation. The mechanisms of how and why pterygium is self-limiting have been clarified by recent studies [193]. As this condition commonly occurs in surfers who are exposed to significant amounts of sunlight it is often referred to as 'surfer's eye'. The impact of pterygium on vision is minimal unless it reaches the cornea, but it is painful to remove and often recurs after surgical removal.

Evidence suggests that the prevalence of pterygium has slightly increased in recent years. In a recent meta-analysis of 55 studies (including data from >400,000 people in 24 countries), the overall prevalence of pterygium was estimated at 12% (95% CI 11-14) [194]. However, studies included a diverse range of age groups and not all were population based. The reported prevalence was higher than that from a 2013 meta-analysis based on 20 articles from 12 countries (10.2%; 95% CI 6.3-16.1%) [195].

Studies from Brazil demonstrate the high variability in prevalence estimates according to location and study methods. In a population-based study in the Brazilian Amazon, including 2041 people (86% of those eligible to participate) aged 45 years and over, the prevalence was 58% [196]. The recent meta-analysis estimated prevalence in Brazil to be 52.0% (in an ophthalmic clinic-based study in Manaus, age range 21-61 years); 21.2% in the Amazon rainforest (population-based study of people 11 years and older); 18.4% in the Brazilian rainforest (population-based, no age data); and 8.1% in São Paulo (population-based, median age 49.6 years) [194]. Such variability challenges the simple combining of estimates across studies. However, the prevalence of pterygium seems to be modest and consistent across various regions of China, estimated to be approximately 6% [197,198]. A population-based cohort study, the Gutenberg Health Study, including the German city of Mainz and the surrounding regions (latitude 50°N), found a very low prevalence of pterygium with an estimate for the weighted prevalence of 0.9% (95% CI 0.8-1.2) in people aged 40 to 80 years [199]. The presence of pterygium was associated with male sex, higher age, and migration from Arabic-Islam countries, the former Soviet Union, and former Yugoslavia. In a slightly higher latitude region, including both an urban and rural multi-ethnic population in Ufa city and surrounds in Russia, the prevalence of pterygium was 2.3% (95% CI 2.0-2.7) among people over 40 years [200]. Risk factors for pterygium were rural residence, higher age, and lower level of education.

The incidence of pterygium has been reported in two longitudinal studies. In Southern India, which lies within the 'pterygium belt' (37° north and south of the equator where pterygia are most common [201]), the age- and sex-adjusted incidence was 25.4 per 100 person years (95% CI 24.8, 25.7) over a 15-year period in residents (n=2290) of rural areas aged 30 years and older at baseline [202]. The overall incidence rate in 6122 adults aged 40 years and over was considerably lower (age-adjusted 6-year incidence=1.2%; 95% CI 1.0%-1.6%) over six years of follow-up in the Singapore Epidemiology of Eye Diseases Study [203].

In a meta-analysis of risk factors for pterygium several factors associated with solar exposure of the eyes increased the risk of pterygium, including spending more *vs* less than 5 hours outdoors per day (OR 1.24; 95% CI 1.11-1.36), or having outdoor *vs* indoor occupations (OR 1.46; 95% CI 1.36, 1.55). Furthermore, in a recent study reporting on findings from the Korean National Health and Nutritional Examination Survey, an average of ≥ 5 hours/day in the sun without sunglasses or hat, compared to <5 hours, was associated with an increased risk of pterygium in women (OR=1.47, 95% CI 1.16-1.73) but not men (OR=0.88, 95% CI 0.70, 1.10) [191]. There was a dose response apparent, with greater time outdoors associated with higher risk. Importantly, in the meta-analysis, wearing sunglasses reduced the odds of pterygium by approximately 50% (OR 0.47; 95% CI 0.19-0.74) [194]. In support of this finding, in a longitudinal study of young adults in Australia, wearing sunglasses for at least half of the time outdoors resulted in a significantly greater decline in the area of conjunctival UV fluorescence, a biomarker of sun exposure, over 8 years compared to never or seldom use [204].

3.4.3 The link between exposure to UV radiation and intraocular melanoma

Intraocular melanoma is the most common type of cancer that develops within the eyeball, but it is rare compared to cutaneous melanoma. Intraocular melanomas predominantly occur on the uvea and conjunctiva, but uveal are considerably more common than conjunctival melanomas.

Exposure to sunlight, light pigmentation of the eye and skin, and living at high latitudes are often reported as risk factors for both types of intraocular melanoma, akin to melanoma of the skin. We have previously assessed the epidemiological and genetic evidence regarding the role of UV radiation in the etiology of intraocular melanoma, with more convincing evidence for conjunctival *vs* uveal melanoma [178]. Recent genetic studies provide further evidence of similarity of intraocular to cutaneous melanoma and thus a possible causal role of exposure to UV radiation. A study comparing the genetic changes in uveal melanomas with those in cutaneous melanomas has shown many shared mutations, including UV signature mutations, suggesting that some uveal melanomas may be UV-dependent [205]. In a similar study, tissue samples from conjunctival melanomas displayed evidence of genetic changes consistent with UV-related damage similar to those found in melanoma of the skin [206].

Published recent incidence data for intraocular melanoma are available from four developed countries that have well-established cancer registries: United States, Canada, Australia and Ireland (Table 1). The age-standardised incidence rate ranged from 3.3 per million in Canada [207] to 9.5 per million in Ireland [208], but rates are not directly comparable due to the use of different populations for age

standardisation and different periods of observation. On average the age-adjusted incidence increased by 0.5% per year in the United States between 1973 and 2013 (p<0.05) [209]. In Canada there was minimal change from 1992 to 2010 [207]. In Australia there was an increase of 2.5% per year from 1982-1993, followed by a decrease of 1.2% per year from 1993-2014 [210]. Thus, in these countries, the incidence of intraocular melanomas has remained relatively constant over time, in contrast to that of cutaneous melanomas.

The incidence of conjunctival melanoma was substantially lower compared to uveal melanoma in incidence studies from Canada and Europe, replicating previous findings. The age-standardised incidence rate of conjunctival melanoma was 0.32 cases per million people per year (age-standardised to the World Standard Population) between 1992 and 2010 in Canada [211], while it was 0.42 cases per million people per year (age-standardised to the European Standard Population) in Europe [212].

Table 1 Age-standardised incidence rates of intraocular melanomas across developed countries and regions.

Study	Country/Region	Period	Age-standardised incidence rate per million person years (95% CI)
Uveal melanoma			
Aronow et al (2018) [209]	United States	1973 to 2013	5.2 (5.0, 5.4) [a]
Baily et al (2018) [208]	Ireland	2010 to 2015	9.5 (8.4, 10.7)[b]
Ghazawi et al (2019) [207]	Canada	1992 to 2010	3.3 (3.2, 3.5)[c]
Beasley et al (2021) [210]	Australia	1982 to 2014	7.6 (7.3, 7.9)[d]
Conjunctival melanoma			
Ghawazi et al (2020) [211]	Canada	1992 to 2010	0.32 (0.28, 0.37) [c]
Virgili et al (2020) [212]	Europe	1995 to 2007	overall 0.42[e]
Virgili et al (2020) [212]	Northern Europe	1995 to 2007	0.81 (0.59, 1.09) [e]
Virgili et al (2020) [212]	UK and Ireland	1995 to 2007	0.40 (0.36, 0.45) [e]
Virgili et al (2020) [212]	Central Europe	1995 to 2007	0.59 (0.51, 0.68) [e]
Virgili et al (2020) [212]	Southern Europe	1995 to 2007	0.35 (0.26, 0.47) [e]
Virgili et al (2020) [212]	Eastern Europe	1995 to 2007	0.27 (0.22, 0.33) [e]

[a]Age-adjusted to the US population 2000; [b]age-standardised using the 1976 European standard population; [c]age-standardised using the World Standard Population; [d]age-standardised using the 2001 Australian standard population; [e]age-standardised using the European standard population.

3.4.4 Damage to the eye from drug-induced phototoxicity

A number of drugs absorb in the UV range and have phototoxic side effects affecting various structures in the eye [213]. For example, fluoroquinolone antibiotics such as ciprofloxacin and norfloxacin (used to treat ocular infections), in the presence of UV-A radiation, caused damage to epithelial cells (in cell culture) and proteins of the lens. Exposure of the eye to UV-A radiation while using these compounds could accelerate the development of cataract [214]. Use of ophthalmic formulations containing ketoconazole, diclofenac, or sulphacetamide were found to be toxic or irritating in the presence of UV-A radiation [215]. While there is growing awareness of cutaneous photosensitivity in relation to systemic drugs, the focus for eyes appears to have been on exposure to UV-A radiation in conjunction with topical medications.

It will be important to better understand the potential photosensitisation resulting from both topical and systemic drugs for the eye, given its vulnerability to damage from exposure to UV-radiation and the clear protection that sunglasses provide.

3.5   Non-skin cancer-related harms of UV-induced immune suppression

3.5.1   Increased risk of systemic infections and reduced vaccine effectiveness

Hart and Norval [12] hypothesised that vaccination through acutely or chronically sun-exposed skin (e.g., the upper arm, a common site for intramuscular vaccination) may result in a less effective immune response compared to unexposed skin (e.g., buttock). However, there remains little confirmatory evidence for this at present. In a cluster randomised trial in children in rural South Africa, an intervention to protect vaccinees from solar UV radiation did not result in higher antibody levels following a measles booster [216]. However, in a small clinical trial testing the immune response to a novel antigen (keyhole limpet hemocyanin) — although higher natural exposure to UV radiation was not associated with a change in antigen-specific antibodies — there was a reduced T-cell response [217]. Any effect of exposure to UV radiation may be more important for vaccines that rely on a cell-mediated, rather than humoral (antibody), response to vaccination; e.g. Bacille Calmette Guerin (BCG) for tuberculosis, particularly in low latitude (higher UV radiation) locations.

3.5.2 UV radiation and reactivation of viruses

The association of intense exposure to UV radiation with subsequent reactivation of Herpes simplex virus 1 (HSV), causing cold sores of the lip, is well-described (reviewed in [178]). The presence of IgM class antibodies to HSV reflects recent viral activity, either primary or recurrent infection [218]. In a recent study from Sweden, the odds for anti-HSV IgM positivity were nearly two-fold higher (odds ratio=1.99 per mean MED difference) in summer than in winter (mean MED difference was 9.967 equivalent to 2093.1 J m^{-2}), consistent with UV-induced reactivation of HSV, with or without the manifestation of cold sores [218].

There is considerable current interest in another herpes virus, Epstein Barr virus (EBV), in relation to risk of multiple sclerosis (MS), nasopharyngeal carcinoma and other diseases. Results from a recent study from Hong Kong [219] suggest that higher personal sun exposure is associated with reactivation of EBV. The measures of personal exposure included ambient UV radiation at the date of blood collection, serum 25(OH)D concentration, and self-reported duration of sunlight exposure (hours/day) over four life periods (6-12 years, 13-18 years, 19-30 years, and 10 years prior to recruitment). EBV reactivation was measured as seropositivity to EBV viral capsid antigen (VCA) IgA. Only duration of sunlight exposure at 19-30 years and 10 years prior to recruitment (for ≥ 8 hours compared to <2 hours, OR=2.44, 95% CI 1.04-5.73, OR=3.59, 95% CI 1.46-8.77, respectively) were associated with increased odds of VCA-IgA seropositivity (inferred as evidence of reactivation). Reactivation of EBV may be a trigger of relapses in MS [220]. Thus, higher levels of sun exposure, leading to EBV reactivation, might be expected to also be associated with relapse. However, previous research suggests that higher sun exposure (over the life-course prior to MS onset) is associated with fewer relapses in people with MS [221]. Nevertheless, the time course of sun exposure may be of importance; higher sun exposure earlier in life may be protective for the development of MS through immune mechanisms, but after EBV infection higher sun exposure may be associated with increased risk of relapse through reactivation of EBV. Datasets are available that could test this hypothesis.

Varicella zoster virus is a herpesvirus that causes chicken pox during primary infection and shingles on reactivation. Using data from Thailand, a recent study examined seasonal variation in case reports of chickenpox and shingles [222]. Both chickenpox and shingles showed strong seasonality. Chickenpox was characterised by outbreaks beginning during November and December, with seasonal peaks in February and March (with deep troughs from June to October). The amplitude of the seasonal effect decreased closer to the equator. Shingles showed a peak in May-June, with a shallow trough in February-March and a deep trough in October-December. Again, higher latitudes had more pronounced seasonal cycles. Changes in ambient UV radiation were the main driver of the seasonal cycle for shingles reactivation, but not chickenpox, consistent with an effect of UV radiation on reactivation but not primary infection with Varicella zoster virus.

4 Benefits of exposure to UV radiation

Sun exposure has numerous benefits, many of which are mediated by exposure to UV radiation, and some by exposure to other wavelengths. People need to be able to safely spend time outdoors to gain these benefits. The Montreal Protocol has likely enabled the benefits to be gained, by preventing the intensity of ambient UV radiation from increasing to an extent where it would have been very difficult for light-skinned people in particular to spend time outdoors without markedly increasing their risk of UV-induced skin and eye diseases.

4.1   Health benefits of greater time outdoors and sun exposure

We have previously reported on the evidence of health benefits of exposure to sunlight for autoimmune and cardiovascular diseases, as well as myopia and some cancers [6]. It is challenging to generate high-quality evidence from human studies of benefits of exposure to UV radiation, primarily because it is difficult to capture accurate exposure data over a relevant time period. In addition, it is challenging to determine which wavelengths of sunlight are most important and further, how much of any effect of exposure to the sun is through vitamin D *vs* non-vitamin D pathways. Determining whether associations are causal, and thus whether the balance of risks and benefits of sun exposure needs to be reconsidered, will require accumulation of evidence across epidemiological and mechanistic studies [223]. Recent studies have been largely cross-sectional, and/or used population-level exposures such as sunshine duration [224], ambient UV radiation or location [225], or remote sensing of green space coverage [226]. From these studies, benefits of higher green space coverage, longer duration of sunshine, or higher individual levels of sun exposure have included lower blood pressure in adults [227] and children [226], and reduced prevalence of obesity [224] and depression [228].

In a large study (n=342,457) of patients undergoing dialysis in 2189 facilities across the United States, monthly average ambient UV irradiation at the clinic location had a linear inverse association with monthly average pre-dialysis systolic blood pressure, including after adjustment for ambient temperature [225]. The effect size was greater in Whites than in Blacks. These data are consistent with new analyses of the Melanoma in Southern Sweden study in which women with low or moderate past sun exposure (assessed by questionnaire including items on deliberate sun bathing, use of a sun bed, and travel for sunny holidays) had a greater risk of being prescribed anti-hypertensive medication by their physician than those with higher sun exposure; the association persisted after adjustment for being a smoker, exercise category, BMI, and education (adjusted OR=1.41, 95% CI 1.3-1.6; adjusted OR=1.15, 95% CI 1.1-1.2, respectively, for low and moderate sun exposure) [229]. In a recent study from South Korea, there were fewer cardiovascular (adjusted hazard ratio (HR)=0.68, 95% CI 0.49-0.94) and cerebrovascular (adjusted HR=0.60, 95% CI 0.47-0.77) events over 11 years in patients with vitiligo who had received long-term narrow-band UV-B phototherapy (≥ 100 sessions) compared with those who had received <3 phototherapy sessions [230]. There is accumulating evidence, including from small clinical trials, that UV-A (and possibly UV-B) irradiation influences blood pressure (and cardiovascular disease risk) through release of nitric oxide from stores in skin [231-233].

There is compelling evidence from multiple studies supporting reduced risk of myopia with greater exposure to UV radiation and/or high intensity visible light. Longitudinal cohort studies from China [234], the Netherlands [235], and Australia [236] show that more time spent outdoors during childhood, measured using a variety of metrics, was associated with reduced risk of developing myopia in childhood and young adulthood. Furthermore, two studies found that greater outdoor activity in childhood could reduce the adverse effect of higher levels of screen time [234,235]. Another study showed that lower area of conjunctival autofluorescence was associated with a greater risk of developing myopia between ages 20 and 28 years [237], suggesting that the protective effects of sun exposure may continue into young adulthood. In a cross-sectional analysis within the Singapore birth cohort study, more time outdoors, but not light levels or the timing and frequency of light exposure, was associated with lower odds of myopia [238]. Another study found that greater green space coverage was associated with lower prevalence of myopia [239]. While more time outdoors seems well-established as protective for the development of myopia, details of optimal exposure to minimise myopia are not fully elucidated. Of note, the effect of greater exposure to UV radiation appears to be distinct from any effect of varying focal length during time outdoors [240].

There is now considerable evidence that there may be benefits of spending more time outdoors/sun exposure for the onset and progression of MS in addition to those ascribed to vitamin D (see below). A recent multi-ethnic case-control study confirmed a protective effect of higher sun exposure on risk of developing MS in white populations, and extended this to show the benefits were also apparent for blacks and Hispanics [241]. In contrast, benefits of higher 25(OH)D concentration were apparent only in United States Whites, possibly because 25(OH)D concentration is a better indicator of recent sun exposure in people with lighter skin. A case-control study in Canada, Italy, and Norway demonstrated that an accumulation model for sun exposure to age 15 years, rather than a critical periods model, provided the best fit for the protective effects of higher sun exposure on risk of MS in adulthood [242]. Importantly, among those who spent a lot of time outdoors in summer, use of sun protection did not alter MS risk. These findings highlight the need to provide balanced sun exposure messages that take account of geographical differences in weather patterns, skin pigmentation, and cultural practices [242]. Another case-control study showed a strong protective effect of greater time outdoors in the summer prior to diagnosis or during the first year of life, as well as higher ambient UV radiation, on the risk of developing paediatric MS [243].

The focus in relation to MS has been largely on the risk of developing the disease. There is new evidence that higher sun exposure prior to developing MS, and increasing sun exposure post-diagnosis, are associated with a more favourable post-diagnostic disease course [221,244] [245], although there is some evidence that sun exposure may be detrimental for people with MS who have a sun-sensitive

genotype [244]. A trial of narrow-band UV-B radiation in people with clinically isolated syndrome to prevent the development of MS [246] found a lower risk of progression to MS in people receiving phototherapy than in the control group, although in this small study this was not statistically significant. Analyses of data from this trial have since revealed some novel potential pathways activated by narrowband (311 nm) UV-B, including transient changes in both the number of circulating leukocytes [247] and the production of pro-inflammatory cytokines [248]. Given the non-solar spectrum used, this is likely to be most relevant to a treatment setting, but it does indicate the possible importance of UV-B radiation for this condition.

There is also recent evidence that exposure to higher intensity of UV radiation during early life may protect from the development of type 1 diabetes – an autoimmune disease of the pancreas. In a data-linkage based cohort study of 29,078 children in Western Australia (~6% of whom were diagnosed with type 1 diabetes by age 16), higher ambient (erythemally weighted) UV radiation was associated with reduced risk of developing type 1 diabetes, but only in males and only for UV radiation during the 3rd trimester and 1st year of life [249]. The authors concluded, assuming a causal association, that for every 100 kJ m^{-2} increase in total lifetime dose of ambient UV radiation dose, the relative risk of developing type 1 diabetes in males decreased by 29%.

Emerging evidence suggests that higher antenatal sun exposure may reduce the risk of pre-term birth [250] and learning disabilities [251]. However, higher pre-delivery ambient temperatures have been linked to increased risk of pre-term birth [252,253], complicating analyses where data on personal exposures and potential confounders are not available, and multiple environmental exposures acting at different time-points during pregnancy need to be considered. Additional research will be required to clarify the role of personal sun exposure during pregnancy on the many facets of the health of the offspring.

Exposing the skin to UV radiation enhances feelings of well-being, possibly through the release of beta-endorphins following UV-B induced DNA damage in keratinocytes [254]. This could provide a biological underpinning to an 'addiction' to tanning. In addition, serotonin is produced in the brain in response to bright sunlight [255], with this pathway potentially important for seasonal variability in mood and seasonal affective disorder. Observational studies show links between higher exposure to sunlight and reduced risk of depressive disorders, but confounding and reverse causation are possible explanations for these findings. However, artificial light therapy is established as a treatment for disorders such as seasonal affective disorder [256], and a recent experimental study confirms the benefit of sunlight. The single-blind clinical trial tested the effect of sunlight therapy (exposure of sun-protected forearms or calves to sunlight on sunny days (at least 10,000 lux) in Taiwan for an accumulated minimum of 30 min/day for a total of 14 days in four weeks) on depression in participants who were at least one month post-stroke. Testing at one month after the completion of the intervention showed a significant reduction in the depression score in the group receiving the sunlight therapy compared to a control (usual treatment) group [257].

There is growing interest in better understanding the potential benefits of sun exposure and the pathways and wavelengths involved. This information is critical to providing appropriate messaging to different populations on safe sun exposure to balance harms and benefits.

4.2   Vitamin D

Perhaps the best known benefit of sun exposure to the skin, driven by UV-B radiation, is the synthesis in the skin of vitamin D. Most populations derive very little of their vitamin D needs from diet, thus relying primarily on this UV-B induced synthesis.

4.2.1   The role of vitamin D in health outcomes

Vitamin D is best known for its role in musculoskeletal health. Vitamin D status is defined according to the blood concentration of 25(OH)D, with a concentration of <50 nmol L^{-1} commonly considered vitamin D deficient (including here unless specifically stated otherwise). Vitamin D deficiency as defined at this concentration is associated with increased risk of hip fractures in people aged 60 years and over [258]. It has been estimated that, assuming this association is causal, approximately 8% of hip fractures occurring in adults aged ≥ 65 years in Australia are attributable to vitamin D deficiency (25(OH)D <50 nmol L^{-1}) [259]. Falls in older adults have also been linked to 25(OH)D concentration <50 nmol L^{-1} [260]. Despite the established link between vitamin D and musculoskeletal health, the optimal 25(OH)D concentration to minimize fractures and falls is uncertain. Meta-analyses of randomised controlled trials (RCTs) show that vitamin D supplementation alone is only of benefit in people who are vitamin D deficient (<50 nmol L^{-1}) [261] or that it has no effect [262]. The Vitamin D and Omega-3 Trial in the United States did not find any benefit of supplementing older adults with vitamin D for 5 years on fractures, including in people whose baseline 25(OH)D concentration was <50 nmol L^{-1} [263], but there was insufficient power to assess the effect in people with more severe vitamin D deficiency. These findings collectively suggest that the risk of falls and fractures may not increase until 25(OH)D concentration drops to the range currently considered to be severely deficient (<25 nmol L^{-1}).

The importance of vitamin D for other health outcomes remains unclear. Observational studies are prone to confounding or reverse causality. This can be overcome by Mendelian randomisaton (MR) studies (which examine the association between genetically determined, rather than measured 25(OH)D concentration, and health outcomes), although most MR studies have not allowed for non-linear associations between genetically predicted 25(OH)D concentration and disease, and are mostly silent on the consequences of severe vitamin D deficiency. RCTs provide additional information regarding the causality of associations. However, RCTs test the effect of a particular supplement dose and dosing regimen in a specific population for a set length of time during one life period. The absence of effect in an RCT cannot therefore be used as proof of lack of a causal association. With these cautions in mind, we present below a summary of recent evidence for some common disease conditions.

Low 25(OH)D concentration has been consistently linked with increased risk of depression in observational studies [264]. MR studies suggest that this association may not be causal [265,266], and it is likely that adequate vitamin D status is a good marker of exposure to other beneficial wavelengths in sunlight that have an important effect on mood. Data from RCTs are somewhat inconsistent. A meta-analysis revealed an effect of vitamin D on negative emotion, but with very high heterogeneity, and the effect was predominantly seen in people who were vitamin D deficient or who were depressed at study baseline [267]. In support of this, a very large trial in the United States among adults without depression at baseline did not find any benefit of 5 years of vitamin D supplementation [268].

There are similarly inconsistent findings for type 2 diabetes mellitus (T2DM). A meta-analysis of observational studies found that each 1 standard deviation (SD) higher 25(OH)D concentration was associated with a 20% lower risk of T2DM (p<0.001), but a genetically predicted 1 SD increase was not significantly associated with T2DM [269]. An MR study in a Chinese population also found no association between genetically predicted 25(OH)D and T2DM [270]. An RCT in which 2423 people with prediabetes were supplemented with 4000 IU of vitamin D per day for ~2.5 years did not find a statistically significant reduction in the incidence of T2DM, although it is important to note that the mean 25(OH)D concentration at baseline was in the sufficient range (70 nmol L^{-1}) and only 22% of participants were vitamin D deficient (<50 nmol L^{-1}) [271,272]. In a meta-analysis of RCTs in people without T2DM, vitamin D supplementation significantly reduced fasting glucose and fasting insulin but had no effect on incident T2DM overall or in progression from prediabetes to T2DM [273]. It is plausible that the findings in the observational studies reflect a non-vitamin D pathway of sun exposure, whereby higher 25(OH)D concentration is an indicator of having received sufficient sun exposure to gain the other benefits. This hypothesis is supported by mouse studies that suggest UV radiation-induced release of nitric oxide from the skin can suppress the development of glucose intolerance and hepatic lipid accumulation [274].

Observational studies consistently demonstrate inverse associations between 25(OH)D concentration and cancer incidence [275], but confounding and reverse causality are possible explanations for this finding, and this is not supported by MR studies [276] or RCTs [275]. Evidence is emerging, however, for a possible beneficial effect of vitamin D supplementation on cancer mortality [275,277].

Case-control and cohort studies support an increased risk of MS with low 25(OH)D concentration [278], and this is supported by MR studies [279]. The association is less clear for other autoimmune diseases such as type 1 diabetes mellitus [280] and inflammatory bowel disease [279]; although there are suggestive protective effects, confidence intervals are wide and small effects cannot be ruled out. In terms of infectious diseases, observational studies [281], RCTs [282], and MR studies [283] indicate that low 25(OH)D increases risk and severity [284] of respiratory tract infection.

A recent analysis including over 500,000 participants found strong evidence for a nonlinear association between serum 25(OH)D concentration and coronary heart disease, stroke, and all-cause mortality. This was supported by an MR analysis, which suggested the risk associated with low genetically predicted 25(OH)D was only evident in those with measured 25(OH)D below 40 nmol L^{-1} [285]. However, a recent re-analysis, using different model assumptions, found no significant association with genetically predicted 25(OH)D and mortality outcomes, irrespective of 25(OH)D concentration, suggesting that the earlier analysis may have generated incorrect findings (see https://pubmed.ncbi.nlm.nih.gov/36528346/).

Collectively, these findings suggest that vitamin D plays a causal role in some health outcomes, in addition to falls and fractures. However, there is no strong evidence to support increasing the recommended 25(OH)D target concentration to greater than 50 nmol L^{-1} [285], which is the concentration recommended by many organisations internationally.

4.2.2 Revised action spectrum for vitamin D

Action spectra are biological weighting functions that are used to assess the risks and benefits of exposure to different wavelengths of UV radiation. An action spectrum for the production of pre-vitamin D in the skin was produced by the Commission Internationale l'Éclairage (CIE) in 1982, showing a maximum effect at 297 nm, with essentially no production above 315 nm. However, the validity of this has been questioned because it is based on the use of human skin *ex vivo*. A recently published study calculated the action spectrum for serum 25(OH)D, the accepted molecule to determine vitamin D status, using an *in vivo* experiment [286]. The action spectrum was shifted 5 nm towards shorter wavelengths, suggesting that the CIE action spectrum may need to be revised. However, the effect of the shift is likely to be less relevant for natural sunlight than for artificial light sources [1]. Thus while further research is needed to elucidate the implications of a revised action spectrum for calculating the ratio of harms *vs* benefits of exposure to sunlight, the CIE action spectrum is likely to be adequate for risk benefit calculations.

4.2.3 Effect of clothing, sunscreen, and skin pigmentation on vitamin D production

Clothing provides good protection against erythema but also has a strong inhibitory effect on vitamin D synthesis. Full body clothing cover, especially in females, may contribute to the high prevalence of vitamin D deficiency in many countries with high insolation. Recent studies confirm the influence of clothing on 25(OH)D concentration [287,288].

Sunscreen reduces the risk of skin cancer and premalignant lesions and is a mainstay of sun protection globally, but concerns have been raised that regular application of sunscreen may increase the risk of vitamin D deficiency. Two reviews suggest this is not the case [289,290], although there are no RCTs of the effect of routine application of high SPF sunscreen on 25(OH)D concentration. Studies conducted since these reviews continue to suggest that sunscreen users have higher 25(OH)D concentration than those who do not use sunscreen [291,292]. This is most likely because sunscreen users spend more time outdoors, but these studies suggest that using sunscreen does not obviate the benefits for vitamin D of spending more time outdoors.

Dark-skinned immigrants to northern European countries tend to have lower 25(OH)D concentration than those with lighter skin. This is likely due to a combination of reduced vitamin D production in darker compared with lighter skins, and to behavioural differences. For example, an observational study comparing Danes with dark and light skin found that those with dark skin received a lower UV radiation dose and exposed less body surface area than those with lighter skin. There was only minimal difference in the increase in 25(OH)D concentration per joule of UV radiation exposure (light=0.63 nmol L^{-1} joule^{-1}; dark=0.53 nmol L^{-1} joule^{-1}) [293], although the analysis assumed a proportional response in 25(OH)D concentration with increasing body surface area exposed, which may not be the case. Experimental studies have generated discrepant estimates of the inhibitory effect of melanin. One study examined the effect on 25(OH)D concentration of exposing people with different skin types to five serial whole-body sub-erythemal exposures of solar-simulated UV radiation [294]. Comparing people with very light and very dark skin, the melanin inhibitory factor was estimated at ~1.3. In contrast, in a study in which the dose of solar-simulated radiation was given as a function of minimum erythemal dose (i.e., people with darker skins received a higher dose), and UV radiation was delivered to commonly exposed skin sites only, the melanin inhibitory factor was estimated to be ~8 [295]. This issue needs to be resolved as it has implications for public health advice for people with darker skin.

4.2.4 Prevalence of vitamin D deficiency

Vitamin D deficiency is prevalent across many parts of the world. However, obtaining accurate estimates is hampered by unreliable laboratory assays used in many studies. The prevalence of deficiency also depends on the 25(OH)D concentration used to define deficiency and on the time of year when samples were collected; these factors must be considered when interpreting these data. Figure 5 (with detailed data in Appendix Table 1) shows the prevalence of vitamin D deficiency (25(OH)D concentration < 50 nmol L^{-1}) derived from national studies (albeit using a range of assays, not all standardised to an international standard reference method) as well as some recent population studies. The results of these prevalence studies emphasise the apparent high prevalence of vitamin D deficiency in many parts of the world. With recovery of stratospheric ozone under the Montreal Protocol, projections are for lower UV-B radiation at high-latitude locations [1], which could increase the prevalence of vitamin D deficiency. This effect may be ameliorated by warming temperatures due to climate change, resulting in greater time outdoors, as demonstrated by a study from Germany, which found significantly higher 25(OH)D concentration in two extreme summers (2018 and 2019) compared with the preceding 4 summers [296]. However, in lower-latitude locations where the temperature is already high, warming temperatures due to climate change may reduce time outdoors and exacerbate the problem of vitamin D deficiency, particularly in urban populations.
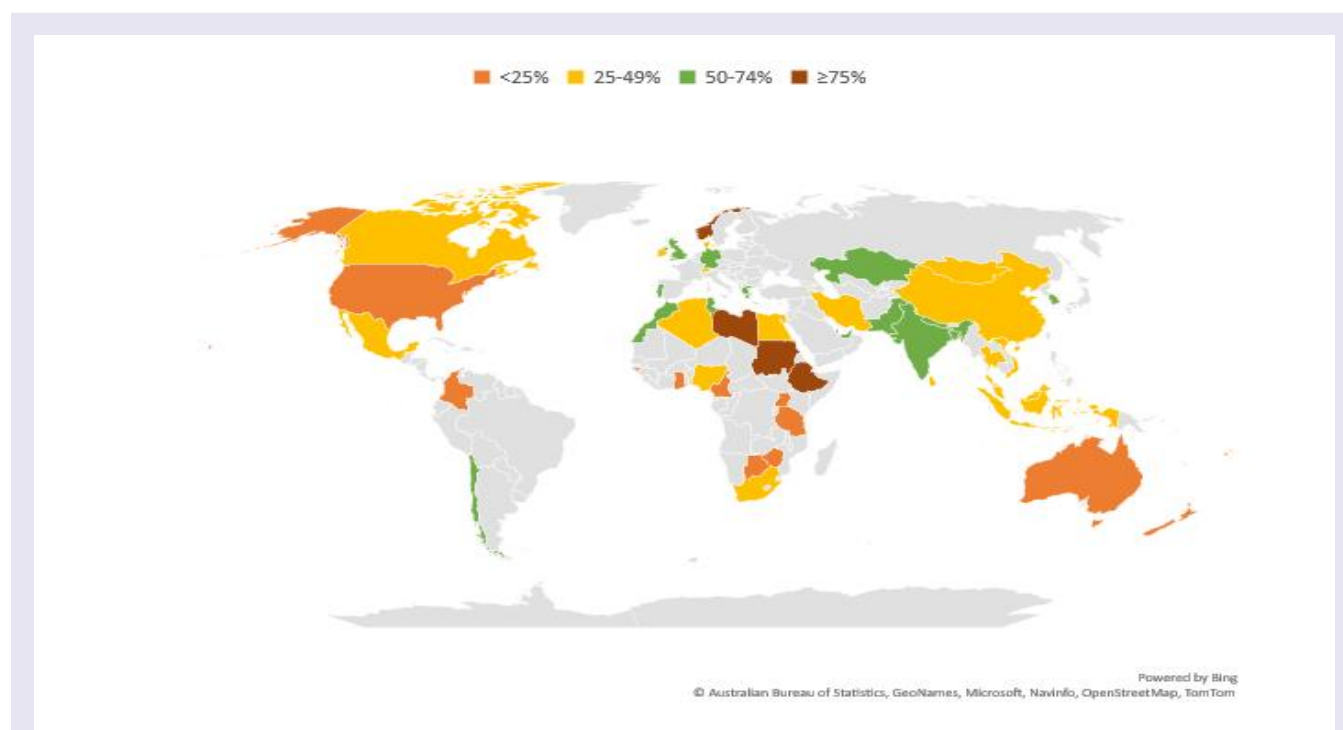
Fig. 5 Prevalence of vitamin D deficiency (25(OH)D<50 nmol/L). Figures for south-Asian countries (Sri Lanka, Nepal, Bangladesh, Pakistan, and India) are derived from a meta-analysis of studies (see Appendix Table 2) that included a range of different populations and 25(OH)D assays. Similarly, figures for African countries are derived from a meta-analysis of studies (see Appendix Table 3) that included a range of different populations and 25(OH)D assays. All other figures are based on population surveys. Data for Chile and Fiji are restricted to women. Data for Mongolia are restricted to men. Data for Denmark, Norway, Greece, Mexico, Ireland, and Iran are restricted to children and/or adolescents. For details of the adult age ranges for other countries see Appendix Table 1.

4.3   Climate change, depletion of stratospheric ozone, and human health

In a previous assessment [79] we comprehensively reviewed the links between climate change, stratospheric ozone depletion and recovery, and human health. Little has been published on this topic in the last four years. The Sixth Assessment of the IPCC Working Group II on the effects of climate change on human health does not mention skin cancer, or other UV-induced health outcomes. Projections for ambient UV radiation in the coming years [1] suggest that with recovery of stratospheric ozone there will be a reduction in the UVI of 2-5% in northern mid-latitudes, a reduction of 4-6% in southern mid-latitudes, and no change in the tropics. Although large reductions in the UV Index in southern high latitudes (>60°S) as stratospheric ozone recovers are projected, this is in a region with no resident populations (Ushuaia in southern Argentina has latitude of 55°S). However, with a growing number of tourists to Antarctica each summer season (approximately 170,000/season in recent years [297]) as well as base staff and researchers, the high variability in the UV Index, including maxima reaching UV Index of 14 [1] may pose risks to health. In addition to the effects of recovery of stratospheric ozone, reductions in cloud cover are projected to increase DNA-weighted UV radiation levels by 1.3% per decade from 2050, based on data from 1998-2016 at four mid-latitude sites (Lauder, New Zealand; Table Mountain, South Africa; Haute Provence, France; Hohenpeissenberg, Germany) and one tropical high altitude site (Mauna Loa, Hawaii) [298].

In an extension of a previous analysis [299], Piacentini and colleagues applied a temperature modification to the carcinogenicity of UV radiation ('effective carcinogenicity') to estimate the incidence of KC in current and next centuries as a result of rising ambient temperature under different climate change scenarios (RCP2.6, RCP4.5, RCP6.0, RCP 8.5) [300]. The model projects increases in incidence for SCC for 2100 of 5.8%, 10.4%, 13.8% and 21.4% (for respective RCPs), and for BCC, 2.1%, 4.9%, 6.5% and 9.9%. The model does not take account of changing UV radiation (as a result of changes in stratospheric ozone and/or cloud cover), or changes in sun exposure behaviour in relation to temperature.

5 Gaps in knowledge

During our assessment of the literature we identified the following gaps in knowledge:

- **Dynamic modelling is needed to better quantify the benefits of the Montreal Protocol:** Trends in skin cancer in different countries are likely to be due to a combination of: (1) immigration patterns, leading to changed distribution of skin types; (2) changing recreational and occupational exposures; (3) concerted efforts to encourage populations to adopt sun-protective behaviours; and (4) changing surveillance habits, potentially resulting in over-diagnosis. Importantly, any predictions will need to take account of the influence of climate change on human behaviour, which will be an increasingly important driver of exposure to UV radiation.

- **Better methods are needed to estimate prevalence of health conditions, including keratinocyte cancer, related to UV radiation:** Other than internal cancers and melanoma, the lack of population-based registries makes it extremely challenging to estimate the population incidence or prevalence of conditions, including keratinocyte cancers, related to exposure to sunlight. Harnessing the power of data linkage may be one way of resolving this problem, recognising that this may under-estimate the burden of conditions that present less frequently in the health system.

- **Photobiological studies to define the dose and pattern of UV radiation that confers minimal harm are required:** There is currently no known UV radiation dose or exposure pattern that confers minimal harm to the skin and eyes. Related to this, over-exposure is poorly defined and, in some settings, sunburn is considered the only relevant indicator of over-exposure. A greater understanding of this issue would enable messages to be developed that balance the benefits and harms of exposure to sunlight.

- **The extent of the problem relating to the use of photosensitising medications needs to be elucidated:** Photosensitising medications can result in damage to skin and eyes. However, the extent of the problem, particularly for the eyes, is unclear.

- **Studies are needed to better understand beneficial effects of exposure to UV radiation:** Exposing the skin and eyes to the sun is likely to have benefits beyond those mediated by production of vitamin D. However, while evidence of benefit and mechanisms is maturing, it is still in its infancy. Clearly defined non-vitamin D biomarkers of benefit are needed so that studies can be conducted to identify the mechanisms, along with the dose and pattern of exposure needed to confer benefits.

- **Public health messaging to guide personal sun exposure to minimise harms and maximise any benefits requires more detail on the relative effective doses of UV radiation:** In particular, we need to quantify the effect on the balance of risks and harms of smaller doses of UV radiation to a greater body surface area. For example, a comparison of the effect of exposure to UV radiation with 5% and 85% of the body surface area exposed suggests that there may not be a linear increase in 25(OH)D concentration, but there is little information about percentages between these extremes.

- **Current public health messages focus on lightly pigmented populations, with doses of UV radiation for harms and benefits uncertain for deeply pigmented skin:** Skin cancers are rare, but vitamin D deficiency common, in those with deeply pigmented skin. Skin melanin protects the skin from UV-B-induced harms (e.g., DNA damage) and reduces vitamin D production, but the UV radiation dose at which these events occur needs to be quantified. Further, the action spectrum for vitamin D production may vary with skin type, but this is not currently known. Resolving these questions is important, enabling the development of evidence-based messages that recognise the increasing diversity of populations within countries.

6 Conclusions

Exposure to UV radiation has multiple harms and benefits. By preventing large increases in UV-B radiation, the Montreal Protocol has avoided many adverse health outcomes, consistent with Sustainable Development Goal (SDG) 3 (Ensure healthy lives and promote well-being for all at all ages). Further, the costs of the adverse effects of exposure to UV radiation are high and increasing, and occupational exposures represent a considerable economic burden. The Montreal Protocol plays a role in protecting outdoor workers, consistent with SDG 8 (Promote sustained, inclusive and sustainable economic growth, full and productive employment and decent work for all).

In addition to avoiding large increases in UV radiation, the Montreal Protocol has stimulated research into the harms and benefits of sunlight exposure. The resulting knowledge has enabled harms to the skin and eyes to be ameliorated through the use of sun protection strategies. For the skin, this has been particularly important for people with lightly pigmented skin, and is evident in the plateauing trends in skin cancer seen in younger age groups in some countries. For the eyes, blindness caused by cataracts disproportionately affects people in developing countries due to lack of access to lens replacement surgery. These diverse effects are consistent with SDG 10 (Reduce inequality within and among countries).

Alongside the harms, increasing recognition of the benefits is informing public health and clinical practice. For people with lightly pigmented skin, this underpins strategies to balance the risks and benefits of sun exposure. For those with deeply pigmented skin, knowledge of the importance of sun exposure may be particularly relevant for those living in areas with low ambient UV radiation for whom the benefits of sun exposure for most people (with the exception of those at risk of inflammatory skin disorders) are likely to outweigh the harms.

In conclusion, sun exposure is critical for human life on Earth. The Montreal Protocol and its Amendments have prevented large increases in ambient UV-B radiation. This has both mitigated the adverse effects and enabled access to the beneficial effects of sun exposure, thus playing a vital role globally in health and economies.

References

1. Bernhard, G. H., Bais, A. F., Aucamp, P. J., Klekociuk, A. R., Liley, J. B., & McKenzie, R. L. (2022). Stratospheric ozone, UV radiation, and climate interactions. *Chapter 1*

2. Madronich, S., Sulzberger, B., Longstreth, J., Schikowski, T., Sulbæk Andersen, M.P., Solomon, K. R., & Wilson, S. R. (2022). Changes in tropospheric air quality related to the protection of stratospheric ozone and a changing climate. *Chapter 6*

3. Barnes, P. W., Robson, T. M., Zepp, R. G., Bornman, J. F., Jansen, M. A. K., Ossola, R., Wang, Q.-W., Robinson, S. A., Foereid, B., Klekociuk, A. R., Martinez-Abaigar, J., Hou, W. C., & Paul, N. D. (2022). Interactive effects of changes in UV radiation and climate on terrestrial ecosystems, biogeochemical cycles, and feedbacks to the climate system. *Chapter 4*

4. Neale, P. J., Williamson, C. E., Banaszak, A. T., Häder, D. P., Hylander, S., Ossola, R., Rose, K. A., Wängberg, S.-Å., & Zepp, R. G. (2022). The response of aquatic ecosystems to the interactive effects of stratospheric ozone depletion, UV radiation, and climate change. *Chapter 5*

5. Andrady, A. L., Heikkilä, A. M., Pandey, K. K., Bruckman, L. S., White, C. C., Zhu, M., & Zhu, L. (2022). Effects of UV radiation on natural and synthetic materials. *Chapter 7*

6. Lucas, R. M., Yazar, S., Young, A. R., Norval, M., de Gruijl, F. R., Takizawa, Y., Rhodes, L. E., Sinclair, C. A., & Neale, R. E. (2019). Human health in relation to exposure to solar ultraviolet radiation under changing stratospheric ozone and climate. *Photochemical & Photobiological Sciences, 18*(3), 641-680. https://doi.org/10.1039/c8pp90060d

7. Hayward, N. K., Wilmott, J. S., Waddell, N., Johansson, P. A., Field, M. A., Nones, K., Patch, A. M., Kakavand, H., Alexandrov, L. B., Burke, H., Jakrot, V., Kazakoff, S., Holmes, O., Leonard, C., Sabarinathan, R., Mularoni, L., Wood, S., Xu, Q., Waddell, N., Tembe, V., et al. (2017). Whole-genome landscapes of major melanoma subtypes. *Nature, 545*(7653), 175-180. https://doi.org/10.1038/nature22071

8. Premi, S., Han, L., Mehta, S., Knight, J., Zhao, D., Palmatier, M. A., Kornacker, K., & Brash, D. E. (2019). Genomic sites hypersensitive to ultraviolet radiation. *Proceedings of the National Academy of Sciences of the United States of America, 116*(48), 24196-24205. https://doi.org/10.1073/pnas.1907860116

9. Lawrence, K. P., Delinasios, G. J., Premi, S., Young, A. R., & Cooke, M. S. (2022). Perspectives on cyclobutane pyrimidine dimers—rise of the dark dimers. *Photochemistry and Photobiology, 98*(3), 609-616. https://doi.org/10.1111/php.13551

10. Liyanage, U. E., MacGregor, S., Bishop, D. T., Shi, J., An, J., Ong, J. S., Han, X., Scolyer, R. A., Martin, N. G., Medland, S. E., Byrne, E. M., Green, A. C., Saw, R. P. M., Thompson, J. F., Stretch, J., Spillane, A., Jiang, Y., Tian, C., Agee, M., Aslibekyan, S., et al. (2022). Multi-trait genetic analysis identifies autoimmune loci associated with cutaneous melanoma. *Journal of Investigative Dermatology, 142*(6), 1607-1616. https://doi.org/10.1016/j.jid.2021.08.449

11. Liyanage, U. E., Law, M. H., Han, X., An, J., Ong, J.-S., Gharahkhani, P., Gordon, S., Neale, R. E., Olsen, C. M., MacGregor, S., & Whiteman, D. C. (2019). Combined analysis of keratinocyte cancers identifies novel genome-wide loci. *Human Molecular Genetics 28*(18), 3148-3160. https://doi.org/10.1093/hmg/ddz121

12. Hart, P. H., & Norval, M. (2020). Are there differences in immune responses following delivery of vaccines through acutely or chronically sun-exposed compared with sun-unexposed skin? *Immunology, 159*(2), 133-141. https://doi.org/10.1111/imm.13128

13. Hart, P. H., & Norval, M. (2021). More than effects in skin: Ultraviolet radiation-induced changes in immune cells in human blood. *Frontiers in Immunology, 12*, 694086. https://doi.org/10.3389/fimmu.2021.694086

14. Hawkshaw, N. J., Pilkington, S. M., Murphy, S. A., Al-Gazaq, N., Farrar, M. D., Watson, R. E. B., Nicolaou, A., & Rhodes, L. E. (2020). UV radiation recruits CD4+GATA3+ and CD8+GATA3+ T cells while altering the lipid microenvironment following inflammatory resolution in human skin in vivo. *Clinical & Translational Immunology, 9*(4), e01104-n/a. https://doi.org/10.1002/cti2.1104

15. Bernard, J. J., Gallo, R. L., & Krutmann, J. (2019). Photoimmunology: how ultraviolet radiation affects the immune system. *Nature Reviews Immunology, 19*(11), 688-701. https://doi.org/10.1038/s41577-019-0185-9

16. Byrne, S. N., Limon-Flores, A. Y., & Ullrich, S. E. (2008). Mast cell migration from the skin to the draining lymph nodes upon ultraviolet irradiation represents a key step in the induction of immune suppression. *Journal of Immunology, 180*(7), 4648-4655. https://doi.org/10.4049/jimmunol.180.7.4648

17. Sarchio, S. N. E., Scolyer, R. A., Beaugie, C., McDonald, D., Marsh-Wakefield, F., Halliday, G. M., & Byrne, S. N. (2014). Pharmacologically antagonizing the CXCR4-CXCL12 chemokine pathway with AMD3100 inhibits sunlight-induced skin cancer. *Journal of Investigative Dermatology, 134*(4), 1091-1100. https://doi.org/10.1038/jid.2013.424

18. Kok, L.-F., Ferguson, A. L., Marshall, J. E., Tse, B. C. Y., Halliday, G. M., & Byrne, S. N. (2020). B cell-targeted immunotherapy limits tumor growth, enhances survival, and prevents lymph node metastasis of UV-induced keratinocyte cancers in mice. *Journal of Investigative Dermatology, 140*(7), 1459-1463. https://doi.org/10.1016/j.jid.2019.12.018

19. Shime, H., Odanaka, M., Tsuiji, M., Matoba, T., Imai, M., Yasumizu, Y., Uraki, R., Minohara, K., Watanabe, M., Bonito, A. J., Fukuyama, H., Ohkura, N., Sakaguchi, S., Morita, A., & Yamazaki, S. (2020). Proenkephalin(+) regulatory T cells expanded by ultraviolet B exposure maintain skin homeostasis with a healing function. *Proceedings of the National Academy of Sciences of the United States of America, 117*(34), 20696-20705. https://doi.org/10.1073/pnas.2000372117

20. Tse, B. C. Y., & Byrne, S. N. (2020). Lipids in ultraviolet radiation-induced immune modulation. *Photochemical & Photobiological Sciences, 19*(7), 870-878. https://doi.org/10.1039/d0pp00146e

21. Liu, L., Awoyemi, A. A., Fahy, K. E., Thapa, P., Borchers, C., Wu, B. Y., McGlone, C. L., Schmeusser, B., Sattouf, Z., Rohan, C. A., Williams, A. R., Cates, E. E., Knisely, C., Kelly, L. E., Bihl, J. C., Cool, D. R., Sahu, R. P., Wang, J., Chen, Y., Rapp, C. M., et al. (2021). Keratinocyte-derived microvesicle particles mediate ultraviolet B radiation-induced systemic immunosuppression. *Journal of Clinical Investigation, 131*(10), e144963. https://doi.org/10.1172/JCI144963

22. Tse, B. C. Y., Ireland, R. A., Lee, J. Y., Marsh-Wakefield, F., Kok, L. F., Don, A. S., & Byrne, S. N. (2021). Exposure to systemic immunosuppressive ultraviolet radiation alters T cell recirculation through sphingosine-1-phosphate. *Journal of Immunology 207*(9), 2278-2287. https://doi.org/10.4049/jimmunol.2001261

23. Lau, F. H., Powell, C. E., Adonecchi, G., Danos, D. M., DiNardo, A. R., Chugden, R. J., Wolf, P., & Castilla, C. F. (2022). Pilot phase results of a prospective, randomized controlled trial of narrowband ultraviolet B phototherapy in hospitalized COVID-19 patients. *Experimental Dermatology, 31*(7), 1109-1115. https://doi.org/10.1111/exd.14617

24. Maboshe, W., Macdonald, H. M., Wassall, H., Fraser, W. D., Tang, J. C. Y., Fielding, S., Barker, R. N., Vickers, M. A., Ormerod, A., & Thies, F. (2021). Low-dose vitamin D_3 supplementation does not affect natural regulatory T cell population but attenuates seasonal changes in T cell-produced IFN-gamma: Results from the D-SIRe2 randomized controlled trial. *Frontiers in Immunology, 12*, 623087. https://doi.org/10.3389/fimmu.2021.623087

25. Lossius, A. H., Sundnes, O., Ingham, A. C., Edslev, S. M., Bjornholt, J. V., Lilje, B., Bradley, M., Asad, S., Haraldsen, G., Skytt-Andersen, P., Holm, J. O., & Berents, T. L. (2022). Shifts in the skin microbiota after UVB treatment in adult atopic dermatitis. *Dermatology, 238*(1), 109-120. https://doi.org/10.1159/000515236

26. Bustamante, M., Hernandez-Ferrer, C., Tewari, A., Sarria, Y., Harrison, G. I., Puigdecanet, E., Nonell, L., Kang, W., Friedlander, M. R., Estivill, X., Gonzalez, J. R., Nieuwenhuijsen, M., & Young, A. R. (2020). Dose and time effects of solar-simulated ultraviolet radiation on the in vivo human skin transcriptome. *British Journal of Dermatology, 182*(6), 1458-1468. https://doi.org/10.1111/bjd.18527

27. Hart, P. H., Norval, M., Byrne, S. N., & Rhodes, L. E. (2019). Exposure to ultraviolet radiation in the modulation of human diseases. *Annual Review of Pathology, 14*(1), 55-81. https://doi.org/10.1146/annurev-pathmechdis-012418-012809

28. Sarkar, M. K., Hile, G. A., Tsoi, L. C., Xing, X., Liu, J., Liang, Y., Berthier, C. C., Swindell, W. R., Patrick, M. T., Shao, S., Tsou, P.-S., Uppala, R., Beamer, M. A., Srivastava, A., Bielas, S. L., Harms, P. W., Getsios, S., Elder, J. T., Voorhees, J. J., Gudjonsson, J. E., et al. (2018). Photosensitivity and type I IFN responses in cutaneous lupus are driven by epidermal-derived interferon kappa. *Annals of Rheumatic Diseases, 77*(11), 1653-1664. https://doi.org/10.1136/annrheumdis-2018-213197

29. Kulkarni, N. N., Takahashi, T., Sanford, J. A., Tong, Y., Gombart, A. F., Hinds, B., Cheng, J. Y., & Gallo, R. L. (2020). Innate immune dysfunction in rosacea promotes photosensitivity and vascular adhesion molecule expression. *Journal of Investigative Dermatology, 140*(3), 645-655.e646. https://doi.org/10.1016/j.jid.2019.08.436

30. Skopelja-Gardner, S., Tai, J., Sun, X., Tanaka, L., Kuchenbecker, J. A., Snyder, J. M., Kubes, P., Mustelin, T., & Elkon, K. B. (2021). Acute skin exposure to ultraviolet light triggers neutrophil-mediated kidney inflammation. *Proceedings of the National Academy of Sciences of the United States of America, 118*(3), e2019097118. https://doi.org/10.1073/pnas.2019097118

31. Lim, H.-S., Yoon, K.-N., Chung, J. H., Lee, Y.-S., Lee, D. H., & Park, G. (2021). Chronic ultraviolet irradiation to the skin dysregulates adrenal medulla and dopamine metabolism in vivo. *Antioxidants, 10*(6), 920. https://doi.org/10.3390/antiox10060920

32. Diffey, B. (2021). Erythema and acclimatization following repeated sun exposure: A modeling study. *Photochemistry and Photobiology, 97*(6), 1558-1567. https://doi.org/10.1111/php.13466

33. Laskar, R., Ferreiro-Iglesias, A., Bishop, D. T., Iles, M. M., Kanetsky, P. A., Armstrong, B. K., Law, M. H., Goldstein, A. M., Aitken, J. F., Giles, G. G., Australian Melanoma Family Study, I., Leeds Case-Control Study, I., Robbins, H. A., & Cust, A. E. (2021). Risk factors for melanoma by anatomical site: an evaluation of aetiological heterogeneity. *British Journal of Dermatology, 184*(6), 1085-1093. https://doi.org/10.1111/bjd.19705

34. Ghiasvand, R., Robsahm, T. E., Green, A. C., Rueegg, C. S., Weiderpass, E., Lund, E., & Veierød, M. B. (2018). Association of phenotypic characteristics and UV radiation exposure with risk of melanoma on different body sites. *JAMA Dermatology, 155*(1), 39-49. https://doi.org/10.1001/jamadermatol.2018.3964

35. Arnold, M., de Vries, E., Whiteman, D. C., Jemal, A., Bray, F., Parkin, D. M., & Soerjomataram, I. (2018). Global burden of cutaneous melanoma attributable to ultraviolet radiation in 2012. I*nternational Journal of Cancer, 143*(6), 1305-1314. https://doi.org/10.1002/ijc.31527

36. O'Sullivan, D. E., Brenner, D. R., Villeneuve, P. J., Walter, S. D., Demers, P. A., Friedenreich, C. M., King, W. D., & Com, P. S. T. (2019). Estimates of the current and future burden of melanoma attributable to ultraviolet radiation in Canada. *Preventive Medicine, 122*, 81-90. https://doi.org/10.1016/j.ypmed.2019.03.012

37. Arnold, M., Kvaskoff, M., Thuret, A., Guenel, P., Bray, F., & Soerjomataram, I. (2018). Cutaneous melanoma in France in 2015 attributable to solar ultraviolet radiation and the use of sunbeds. *Journal of the European Academy of Dermatology and Venereology, 32*(10), 1681-1686. https://doi.org/10.1111/jdv.15022

38. Lopes, F. C. P. S., Sleiman, M. G., Sebastian, K., Bogucka, R., Jacobs, E. A., & Adamson, A. S. (2021). UV exposure and the risk of cutaneous melanoma in skin of color: A systematic review. *JAMA Dermatology, 157*(2), 213-219. https://doi.org/10.1001/jamadermatol.2020.4616

39. O'Sullivan, D. E., Brenner, D. R., Villeneuve, P. J., Walter, S. D., Demers, P. A., Friedenreich, C. M., King, W. D., & Com, P. S. T. (2021). The current burden of non-melanoma skin cancer attributable to ultraviolet radiation and related risk behaviours in Canada. *Cancer Causes & Control, 32*(3), 279-290. https://doi.org/10.1007/s10552-020-01382-1

40. Little, M. P., Linet, M. S., Kimlin, M. G., Lee, T., Tatalovich, Z., Sigurdson, A. J., & Cahoon, E. K. (2019). Cumulative solar ultraviolet radiation exposure and basal cell carcinoma of the skin in a nationwide US cohort using satellite and ground-based measures. [Article]. *Environmental Health: A Global Access Science Source, 18*(1), 114. https://doi.org/10.1186/s12940-019-0536-9

41. Kolitz, E., Lopes, F. C. P. S., Arffa, M., Pineider, J., Bogucka, R., & Adamson, A. S. (2022). UV exposure and the risk of keratinocyte carcinoma in skin of color: A systematic review. *JAMA Dermatology, 158*(5), 542-546. https://doi.org/10.1001/jamadermatol.2022.0263

42. World Health Organisation. (2021). *The effect of occupational exposure to solar ultraviolet radiation on malignant skin melanoma and non-melanoma skin cancer: a systematic review and meta-analysis from the WHO/ILO joint estimates of the work-related burden of disease and injury*. https://apps.who.int/iris/handle/10665/350569.

43. Loney, T., Paulo, M. S., Modenese, A., Gobba, F., Tenkate, T., Whiteman, D. C., Green, A. C., & John, S. M. (2021). Global evidence on occupational sun exposure and keratinocyte cancers: a systematic review. *British Journal of Dermatology, 184*(2), 208-218. https://doi.org/10.1111/bjd.19152

44. Peters, C. E., Kim, J., Song, C., Heer, E., Arrandale, V. H., Pahwa, M., Labreche, F., McLeod, C. B., Davies, H. W., Ge, C. B., & Demers, P. A. (2019). Burden of non-melanoma skin cancer attributable to occupational sun exposure in Canada. I*nternational Archives of Occupational and Environmental Health, 92*(8), 1151-1157. https://doi.org/10.1007/s00420-019-01454-z

45. Nurminen, M., & Karjalainen, A. (2001). Epidemiologic estimate of the proportion of fatalities related to occupational factors in Finland. *Scandinavian Journal of Work, Environment & Health, 27*(3), 161-213. http://www.jstor.org/stable/40967134

46. Young, C., Rushton, L., & British Occupational Cancer Burden Study Group (2012). Occupational cancer in Britain. Skin cancer. *British Journal of Cancer, 107 Suppl 1*, S71-75. https://doi.org/10.1038/bjc.2012.120

47. Brand, R. M., Stottlemyer, J. M., Paglia, M. C., Carey, C. D., & Falo, L. D. (2021). Ethanol consumption synergistically increases ultraviolet radiation induced skin damage and immune dysfunction. *Journal of Dermatological Science, 101*(1), 40-48. https://doi.org/10.1016/j.jdermsci.2020.11.001

48. Madronich, S., Lee-Taylor, J. M., Wagner, M., Kyle, J., Hu, Z., & Landolfi, R. (2021). Estimation of skin and ocular damage avoided in the United States through implementation of the Montreal Protocol on Substances that Deplete the Ozone Layer. *ACS Earth and Space Chemistry, 5*(8), 1876-1888. https://doi.org/10.1021/acsearthspacechem.1c00183

49. Arnold, M., Singh, D., Laversanne, M., Vignat, J., Vaccarella, S., Meheus, F., Cust, A. E., de Vries, E., Whiteman, D. C., & Bray, F. (2022). Global burden of cutaneous melanoma in 2020 and projections to 2040. *JAMA Dermatology, 158*(5), 495-503. https://doi.org/10.1001/jamadermatol.2022.0160

50. Urban, K., Mehrmal, S., Uppal, P., Giesey, R. L., & Delost, G. R. (2021). The global burden of skin cancer: A longitudinal analysis from the Global Burden of Disease Study, 1990-2017. *JAAD International, 2*, 98-108. https://doi.org/10.1016/j.jdin.2020.10.013

51. Li, Z., Fang, Y., Chen, H., Zhang, T., Yin, X., Man, J., Yang, X., & Lu, M. (2022). Spatiotemporal trends of the global burden of melanoma in 204 countries and territories from 1990 to 2019: Results from the 2019 global burden of disease study. *Neoplasia, 24*(1), 12-21. https://doi.org/10.1016/j.neo.2021.11.013

52. Bray, F., Ferlay, J., Soerjomataram, I., Siegel, R. L., Torre, L. A., & Jemal, A. (2018). Global cancer statistics 2018: GLOBOCAN estimates of incidence and mortality worldwide for 36 cancers in 185 countries. *CA: A Cancer Journal for Clinicians, 68*(6), 394-424. https://doi.org/10.3322/caac.21492

53. Australian Institute of Health and Welfare (AIHW). (2021). Cancer in Australia 2021. Cancer series no. 133. Cat. no. CAN 144, 172 pp, Canberra: AIHW, https://doi.org/10.25816/ye05-nm50. Accessed 01 April 2022. Canberra, Australia.

54. Ferlay, J., Colombet, M., Soerjomataram, I., Dyba, T., Randi, G., Bettio, M., Gavin, A., Visser, O., & Bray, F. (2018). Cancer incidence and mortality patterns in Europe: Estimates for 40 countries and 25 major cancers in 2018. *European Journal of Cancer, 103*, 356-387. https://doi.org/10.1016/j.ejca.2018.07.005

55. Lashway, S. G., Harris, R. B., Farland, L. V., O'Rourke, M. K., & Dennis, L. K. (2021). Age and cohort trends of malignant melanoma in the United States. *Cancers (Basel)*, 13(15), 3866. https://doi.org/10.3390/cancers13153866

56. Kurtansky, N. R., Dusza, S. W., Halpern, A. C., Hartman, R. I., Geller, A. C., Marghoob, A. A., Rotemberg, V. M., & Marchetti, M. A. (2022). An epidemiologic analysis of melanoma overdiagnosis in the United States, 1975-2017. *Journal of Investigative Dermatology, 142*(7), 1804-1811. https://doi.org/10.1016/j.jid.2021.12.003

57. Aitken, J. F., Youlden, D. R., Baade, P. D., Soyer, H. P., Green, A. C., & Smithers, B. M. (2018). Generational shift in melanoma incidence and mortality in Queensland, Australia, 1995-2014. *International Journal of Cancer, 142*(8), 1528-1535. https://doi.org/10.1002/ijc.31141

58. Eriksson, H., Nielsen, K., Vassilaki, I., Lapins, J., Mikiver, R., Lyth, J., & Isaksson, K. (2021). Trend shifts in age-specific incidence for in situ and invasive cutaneous melanoma in Sweden. *Cancers (Basel)*, 13(11), 2838. https://doi.org/10.3390/cancers13112838

59. Sacchetto, L., Zanetti, R., Comber, H., Bouchardy, C., Brewster, D. H., Broganelli, P., Chirlaque, M. D., Coza, D., Galceran, J., Gavin, A., Hackl, M., Katalinic, A., Laronningen, S., Louwman, M. W. J., Morgan, E., Robsahm, T. E., Sanchez, M. J., Tryggvadottir, L., Tumino, R., Van Eycken, E., et al. (2018). Trends in incidence of thick, thin and in situ melanoma in Europe. *European Journal of Cancer, 92*, 108-118. https://doi.org/10.1016/j.ejca.2017.12.024

60. Welch, H. G., Mazer, B. L., & Adamson, A. S. (2021). The rapid rise in cutaneous melanoma diagnoses. The New England Journal of Medicine, 384(1), 72-79. https://doi.org/10.1056/NEJMsb2019760

61. Matsumoto, M., Wack, S., Weinstock, M. A., Geller, A., Wang, H., Solano, F. X., Kirkwood, J. M., & Ferris, L. K. (2022). Five-year outcomes of a melanoma screening initiative in a large health care system. *JAMA Dermatology, 158*(5), 504-512. https://doi.org/10.1001/jamadermatol.2022.0253

62. Olsen, C. M., Thompson, J. F., Pandeya, N., & Whiteman, D. C. (2020). Evaluation of sex-specific incidence of melanoma. *JAMA Dermatology, 156*(5), 553-560. https://doi.org/10.1001/jamadermatol.2020.0470

63. Gulliver, W., Gulliver, S., Power, R. J., Penney, M., & Lane, D. (2021). The incidence of cutaneous malignant melanoma in Eastern Newfoundland and Labrador, Canada, from 2007 to 2015. *Dermatology, 238*(3), 527-533. https://doi.org/10.1159/000519193

64. Defossez, G., Uhry, Z., Delafosse, P., Dantony, E., d'Almeida, T., Plouvier, S., Bossard, N., Bouvier, A. M., Molinié, F., Woronoff, A. S., Colonna, M., Grosclaude, P., Remontet, L., & Monnereau, A. (2021). Cancer incidence and mortality trends in France over 1990-2018 for solid tumors: the sex gap is narrowing. BMC Cancer, 21(1), 726. https://doi.org/10.1186/s12885-021-08261-1

65. Dulskas, A., Cerkauskaite, D., Vinceževskiene, I., & Urbonas, V. (2021). Trends in incidence and mortality of skin melanoma in Lithuania 1991-2015. *International Journal of Environmental Research and Public Health, 18*(8), 4165. https://doi.org/10.3390/ijerph18084165

66. Korovin, S., Fedorenko, Z., Michailovich, Y., Kukushkina, M., Sekerija, M., & Ryzhov, A. (2020). Burden of malignant melanoma in Ukraine in 2002-2013: incidence, mortality and survival. *Experimental Oncology, 42*(4), 324-329. https://doi.org/10.32471/exp-oncology.2312-8852.vol-42-no-4.15334

67. 67. Pehalova, L., Krejci, D., Snajdrova, L., & Dusek, L. (2021). Cancer incidence trends in the Czech Republic. *Cancer Epidemiology, 74*, 101975. https://doi.org/10.1016/j.canep.2021.101

68. Liszkay, G., Kiss, Z., Gyulai, R., Oláh, J., Holló, P., Emri, G., Csejtei, A., Kenessey, I., Benedek, A., Polányi, Z., Nagy-Erdei, Z., Daniel, A., Knollmajer, K., Várnai, M., Vokó, Z., Nagy, B., Rokszin, G., Fábián, I., Barcza, Z., & Polgár, C. (2020). Changing trends in melanoma incidence and decreasing melanoma mortality in Hungary between 2011 and 2019: A nationwide epidemiological study. *Frontiers in Oncology, 10*, 612459. https://doi.org/10.3389/fonc.2020.612459

69. Bai, R., Huang, H., Li, M., & Chu, M. (2021). Temporal trends in the incidence and mortality of skin malignant melanoma in China from 1990 to 2019. *Journal of Oncology, 2021*, 9989824. https://doi.org/10.1155/2021/9989824

70. Kim, T., Yoon, S., Shin, D. E., Lee, S. C., Oh, J., Lee, S. Y., Kim, D. K., Kim, S., Jung, B., Kim, M., & Lee, S. (2021). Incidence and survival rates of cutaneous melanoma in South Korea using nationwide health insurance claims data. *Cancer Research and Treatment, 54*(3), 937-949. https://doi.org/10.4143/crt.2021.871

71. Wu, Y., Wang, Y., Wang, L., Yin, P., Lin, Y., & Zhou, M. (2020). Burden of melanoma in China, 1990-2017: Findings from the 2017 global burden of disease study. *International Journal of Cancer, 147*(3), 692-701. https://doi.org/10.1002/ijc.32764

72. Oh, C. C., Jin, A., & Koh, W. P. (2021). Trends of cutaneous basal cell carcinoma, squamous cell carcinoma, and melanoma among the Chinese, Malays, and Indians in Singapore from 1968-2016. *JAAD International, 4*, 39-45. https://doi.org/10.1016/j.jdin.2021.05.006

73. Chen, M. L., de Vere Hunt, I. J., John, E. M., Weinstock, M. A., Swetter, S. M., & Linos, E. (2022). Differences in thickness-specific incidence and factors associated with cutaneous melanoma in the US from 2010 to 2018. *JAMA Oncology, 8*(5), 755-759. https://doi.org/10.1001/jamaoncol.2022.0134

74. Kelm, R. C., Ali, Y., Orrell, K., Rangel, S. M., Kruse, L., Wagner, A. M., Gerami, P., West, D. P., & Nardone, B. (2021). Age and sex differences for malignant melanoma in the pediatric population-childhood versus adolescence: analysis of current nationwide data from the National Cancer Institute Surveillance, Epidemiology, and End Results (SEER) program. J*AMA Dermatology, 84*(3), 862-864. https://doi.org/10.1016/j.jaad.2020.10.050

75. Heer, E. V., Harper, A. S., Sung, H., Jemal, A., & Fidler-Benaoudia, M. M. (2020). Emerging cancer incidence trends in Canada: The growing burden of young adult cancers. *Cancer, 126*(20), 4553-4562. https://doi.org/10.1002/cncr.33050

76. Bucchi, L., Mancini, S., Crocetti, E., Dal Maso, L., Baldacchini, F., Vattiato, R., Giuliani, O., Ravaioli, A., Caldarella, A., Carrozzi, G., Ferretti, S., Filiberti, R. A., Fusco, M., Gatti, L., Gili, A., Magoni, M., Mangone, L., Mazzoleni, G., Michiara, M., Panato, C., et al. (2021). Mid-term trends and recent birth-cohort-dependent changes in incidence rates of cutaneous malignant melanoma in Italy. *International Journal of Cancer, 148*(4), 835-844. https://doi.org/10.1002/ijc.33259

77. Memon, A., Banniser, P., Rogers, I., Sundin, J., Al-Ayadhy, B., James, P. W., & McNally, R. J. Q. (2021). Changing epidemiology and age-specific incidence of cutaneous malignant melanoma in England: An analysis of the national cancer registration data by age, gender and anatomical site, 1981–2018. *The Lancet Regional Health - Europe, 2*, 100024. https://doi.org/10.1016/j.lanepe.2021.100024

78. Rousi, E. K., Kallionpää, R. A., Kallionpää, R. E., Juteau, S. M., Talve, L. A. I., Hernberg, M. M., Vihinen, P. P., Kähäri, V. M., & Koskivuo, I. O. (2022). Increased incidence of melanoma in children and adolescents in Finland in 1990-2014: nationwide re-evaluation of histopathological characteristics. Annals of Medicine, 54(1), 244-252. https://doi.org/10.1080/07853890.2022.2026001

79. Bernhard, G. H., Neale, R. E., Barnes, P. W., Neale, P. J., Zepp, R. G., Wilson, S. R., Andrady, A. L., Bais, A. F., McKenzie, R. L., Aucamp, P. J., Young, P. J., Liley, J. B., Lucas, R. M., Yazar, S., Rhodes, L. E., Byrne, S. N., Hollestein, L. M., Olsen, C. M., Young, A. R., Robson, T. M., et al. (2020). Environmental effects of stratospheric ozone depletion, UV radiation and interactions with climate change: UNEP Environmental Effects Assessment Panel, update 2019. *Photochemical & Photobiological Sciences, 19*, 542-584. https://doi.org/10.1039/d0pp90011g

80. Neale, R. E., Barnes, P. W., Robson, T. M., Neale, P. J., Williamson, C. E., Zepp, R. G., Wilson, S. R., Madronich, S., Andrady, A. L., Heikkilä, A. M., Bernhard, G. H., Bais, A. F., Aucamp, P. J., Banaszak, A. T., Bornman, J. F., Bruckman, L. S., Byrne, S. N., Foereid, B., Häder, D. P., Hollestein, L. M., et al. (2021). Environmental effects of stratospheric ozone depletion, UV radiation, and interactions with climate change: UNEP Environmental Effects Assessment Panel, Update 2020. *Photochemical & Photobiological Sciences, 20*(1), 1-67. https://doi.org/10.1007/s43630-020-00001-x

81. Barnes, P. W., Robson, T. M., Neale, P. J., Williamson, C. E., Zepp, R. G., Madronich, S., Wilson, S. R., Andrady, A. L., Heikkilä, A. M., Bernhard, G. H., Bais, A. F., Neale, R. E., Bornman, J. F., Jansen, M. A. K., Klekociuk, A. R., Martinez-Abaigar, J., Robinson, S. A., Wang, Q. W., Banaszak, A. T., Häder, D. P., et al. (2022). Environmental effects of stratospheric ozone depletion, UV radiation, and interactions with climate change: UNEP Environmental Effects Assessment Panel, Update 2021. *Photochemical & Photobiological Sciences, 21*(3), 275-301. https://doi.org/10.1007/s43630-022-00176-5

82. Ferlay, J., Colombet, M., Soerjomataram, I., Parkin, D. M., Piñeros, M., Znaor, A., & Bray, F. (2021). Cancer statistics for the year 2020: An overview. *International Journal of Cancer, 149*(4), 778-789. https://doi.org/10.1002/ijc.33588

83. Berk-Krauss, J., Stein, J. A., Weber, J., Polsky, D., & Geller, A. C. (2020). New systematic therapies and trends in cutaneous melanoma deaths among US Whites, 1986-2016. *American Journal of Public Health, 110*(5), 731-733. https://doi.org/10.2105/AJPH.2020.305567

84. Yang, D. D., Salciccioli, J. D., Marshall, D. C., Sheri, A., & Shalhoub, J. (2020). Trends in malignant melanoma mortality in 31 countries from 1985 to 2015. *British Journal of Dermatology, 183*(6), 1056-1064. https://doi.org/10.1111/bjd.19010

85. Gutierrez-Gonzalez, E., Lopez-Abente, G., Aragones, N., Pollan, M., Pastor-Barriuso, R., Sanchez, M. J., & Perez-Gomez, B. (2019). Trends in mortality from cutaneous malignant melanoma in Spain (1982-2016): sex-specific age-cohort-period effects. *Journal of the European Academy of Dermatology and Venereology, 33*(8), 1522-1528. https://doi.org/10.1111/jdv.15565

86. Environmental Health Intelligence New Zealand (ehinz) (2020). Fact sheet: Melanoma mortality. https://www.ehinz.ac.nz/indicators/uv-exposure/melanoma/. Accessed 14 January 2021.

87. van Niekerk, C. C., Groenewoud, H. M. M., & Verbeek, A. L. M. (2021). Trends and projections in cutaneous melanoma death in the Netherlands from 1950 to 2045. *Medicine Open, 100*(48), e27784.

88. Nader Marta, G., Munhoz, R. R., Teixeira, M. P., Waldvogel, B. C., Pires de Camargo, V., Feher, O., & Sanches, J. A. (2020). Trends in melanoma mortality in Brazil: A registry-based study. *JCO Global Oncology, 6*, 1766-1771. https://doi.org/10.1200/go.20.00426

89. Olsen, C. M., Pandeya, N., & Whiteman, D. C. (2021). International increases in Merkel cell carcinoma incidence rates between 1997 and 2016. *Journal of Investigative Dermatology, 141*(11), 2596-2601. https://doi.org/10.1016/j.jid.2021.04.007

90. de Melo, A. C., & Santos Thuler, L. C. (2021). Trends in the incidence and morbidity of Merkel cell carcinoma in Brazil. *Future Oncology 17*(22), 2857-2865. https://doi.org/10.2217/fon-2020-1313

91.   Stang, A., Becker, J. C., Nghiem, P., & Ferlay, J. (2018). The association between geographic location and incidence of Merkel cell carcinoma in comparison to melanoma: An international assessment. *European Journal of Cancer, 94*, 47-60. https://doi.org/10.1016/j.ejca.2018.02.003

92.   Jacobs, D., Huang, H., Olino, K., Weiss, S., Kluger, H., Judson, B. L., & Zhang, Y. (2021). Assessment of age, period, and birth cohort effects and trends in Merkel cell carcinoma incidence in the United States. *JAMA Dermatology, 157*(1), 59-65. https://doi.org/10.1001/jamadermatol.2020.4102

93.   Feng, H., Shuda, M., Chang, Y., & Moore, P. S. (2008). Clonal integration of a polyomavirus in human Merkel cell carcinoma. *Science, 319*(5866), 1096-1100. https://doi.org/10.1126/science.1152586

94.   Goh, G., Walradt, T., Markarov, V., Blom, A., Riaz, N., Doumani, R., Stafstrom, K., Moshiri, A., Yelistratova, L., Levinsohn, J., Chan, T. A., Nghiem, P., Lifton, R. P., & Choi, J. (2016). Mutational landscape of MCPyV-positive and MCPyV-negative Merkel cell carcinomas with implications for immunotherapy. *Oncotarget, 7*(3), 3403-3415. https://doi.org/10.18632/oncotarget.6494

95.   Mokánszki, A., Méhes, G., Csoma, S. L., Kollár, S., & Chang Chien, Y. C. (2021). Molecular profiling of Merkel cell polyomavirus-associated Merkel cell carcinoma and cutaneous melanoma. *Diagnostics (Basel)*, 11(2), 212. https://doi.org/10.3390/diagnostics11020212

96.   Harms, K. L., Healy, M. A., Nghiem, P., Sober, A. J., Johnson, T. M., Bichakjian, C. K., & Wong, S. L. (2016). Analysis of prognostic factors from 9387 Merkel cell carcinoma cases forms the basis for the new 8th edition AJCC Staging System. *Annals of Surgical Oncology 23*(11), 3564-3571. https://doi.org/10.1245/s10434-016-5266-4

97.   D'Angelo, S. P., Bhatia, S., Brohl, A. S., Hamid, O., Mehnert, J. M., Terheyden, P., Shih, K. C., Brownell, I., Lebbé, C., Lewis, K. D., Linette, G. P., Milella, M., Georges, S., Shah, P., Ellers-Lenz, B., Bajars, M., Güzel, G., & Nghiem, P. T. (2020). Avelumab in patients with previously treated metastatic Merkel cell carcinoma: long-term data and biomarker analyses from the single-arm phase 2 JAVELIN Merkel 200 trial. *Journal for Immunotherapy of Cancer, 8*(1), e000674. https://doi.org/10.1136/jitc-2020-000674

98.   Chang, W. C., Lin, A. Y., Hsu, J. C., Wu, C. E., Goh, C., Chou, P., Kuo, K., Chang, A., & Palencia, R. (2021). A cost-utility analysis of avelumab for metastatic Merkel cell carcinoma in Taiwan. *Cancer Reports 4*(6), e1399. https://doi.org/10.1002/cnr2.1399

99.   Garza-Davila, V. F., Valdespino-Valdes, J., Barrera, F. J., Ocampo-Candiani, J., & Garza-Rodríguez, V. (2022). Clinical impact of immunotherapy in Merkel cell carcinoma patients: A systematic review and meta-analysis. *JAMA Dermatology, 87*(1), 121-130. https://doi.org/10.1016/j.jaad.2021.04.024

100.   Venables, Z. C., Nijsten, T., Wong, K. F., Autier, P., Broggio, J., Deas, A., Harwood, C. A., Hollestein, L. M., Langan, S. M., Morgan, E., Proby, C. M., Rashbass, J., & Leigh, I. M. (2019). Epidemiology of basal and cutaneous squamous cell carcinoma in the U.K. 2013–15: a cohort study. [Article in Press]. *British Journal of Dermatology, 181*(3), 474-482. https://doi.org/10.1111/bjd.17873

101.   Tokez, S., Hollestein, L., Louwman, M., Nijsten, T., & Wakkee, M. (2020). Incidence of multiple vs first cutaneous squamous cell carcinoma on a nationwide scale and estimation of future incidences of cutaneous squamous cell carcinoma. *JAMA Dermatology, 156*(12), 1300-1306. https://doi.org/10.1001/jamadermatol.2020.3677

102.   Global Burden of Disease 2019 Cancer Collaboration (2021). Cancer incidence, mortality, Years of Life Lost, Years Lived With Disability, and Disability-Adjusted Life Years for 29 cancer groups from 2010 to 2019: A systematic analysis for the Global Burden of Disease Study 2019. *JAMA Oncology, 8*(2), 420. https://doi.org/10.1001/jamaoncol.2021.6987

103.   Zhang, W., Zeng, W., Jiang, A., He, Z., Shen, X., Dong, X., Feng, J., & Lu, H. (2021). Global, regional and national incidence, mortality and disability-adjusted life-years of skin cancers and trend analysis from 1990 to 2019: An analysis of the Global Burden of Disease Study 2019. *Cancer Medicine, 10*(14), 4905-4922. https://doi.org/10.1002/cam4.4046

104.   Pondicherry, A., Martin, R., Meredith, I., Rolfe, J., Emanuel, P., & Elwood, M. (2018). The burden of non-melanoma skin cancers in Auckland, New Zealand. [Article]. *Australasian Journal of Dermatology, 59*(3), 210-213. https://doi.org/10.1111/ajd.12751

105.   Pandeya, N., Olsen, C. M., & Whiteman, D. C. (2017). The incidence and multiplicity rates of keratinocyte cancers in Australia. *Medical Journal of Australia, 207*(8), 339-343. https://doi.org/10.5694/mja17.00284 [pii]

106.   Staples, M. P., Elwood, M., Burton, R. C., Williams, J. L., Marks, R., & Giles, G. G. (2006). Non-melanoma skin cancer in Australia: the 2002 national survey and trends since 1985. *Medical Journal of Australia, 184*(1), 6-10. https://doi.org/10.5694/j.1326-5377.2006.tb00086.x

107.   Adelson, P., Sharplin, G. R., Roder, D. M., & Eckert, M. (2018). Keratinocyte cancers in South Australia: incidence, geographical variability and service trends. [Article]. *Australian and New Zealand Journal of Public Health, 42*(4), 329-333. https://doi.org/10.1111/1753-6405.12806

108.   Adalsteinsson, J. A., Ratner, D., Olafsdottir, E., Grant-Kels, J., Ungar, J., Silverberg, J. I., Kristjansson, A. K., Jonasson, J. G., & Tryggvadottir, L. (2020). Basal cell carcinoma: an emerging epidemic in women in Iceland. *British Journal of Dermatology, 183*(5), 847-856. https://doi.org/10.1111/bjd.18937

109. Adalsteinsson, J. A., Olafsdottir, E., Ratner, D., Waldman, R., Feng, H., Ungar, J., Silverberg, J. I., Kristjansson, A. K., Jonasson, J. G., & Tryggvadottir, L. (2021). Invasive and in situ squamous cell carcinoma of the skin: a nationwide study in Iceland. *British Journal of Dermatology, 185*(3), 537-547. https://doi.org/10.1111/bjd.19879

110. Ilić, D., Videnović, G., Kozomara, R., Radaković, S. S., Vlahović, Z., Matvijenko, V., & Živković, S. (2020). Non-melanoma skin cancers in Serbia (1999-2015) - the need for national prevention and control strategy. [Article]. *Vojnosanitetski Pregled, 77*(11), 1154-1160. https://doi.org/10.2298/vsp181112201i

111. Mirza, F. N., Yumeen, S., & Walter, F. M. (2021). The epidemiology of malignant melanoma, squamous cell carcinoma and basal cell carcinoma in the UK from 2004 to 2014: a population-based cohort analysis using the Clinical Practice Research Datalink. [Article]. *British Journal of Dermatology, 184*(2), 365-367. https://doi.org/10.1111/bjd.19542

112. Aggarwal, P., Knabel, P., & Fleischer, A. B., Jr. (2021). United States burden of melanoma and non-melanoma skin cancer from 1990 to 2019. *JAMA Dermatology, 85*(2), 388-395. https://doi.org/10.1016/j.jaad.2021.03.109

113. Kwiatkowska, M., Ahmed, S., Ardern-Jones, M. R., Bhatti, L. A., Bleiker, T. O., Gavin, A., Hussain, S., Huws, D. W., Irvine, L., Langan, S. M., Millington, G. W. M., Mitchell, H., Murphy, R., Paley, L., Proby, C. M., Thomson, C. S., Thomas, R., Turner, C., Vernon, S., & Venables, Z. C. (2022). A summary of the updated report on the incidence and epidemiological trends of keratinocyte cancers in the UK 2013–2018. [Letter]. *British Journal of Dermatology, 186*(2), 367-369. https://doi.org/10.1111/bjd.20764

114. Olsen, C. M., Pandeya, N., Green, A. C., Ragaini, B. S., Venn, A. J., & Whiteman, D. C. (2022). Keratinocyte cancer incidence in Australia: a review of population-based incidence trends and estimates of lifetime risk. *Public Health Research and Practice, 32*(1), e3212203. https://doi.org/10.17061/phrp3212203

115. Dziunycz, P. J., Schuller, E., & Hofbauer, G. F. L. (2018). Prevalence of actinic keratosis in patients attending general practitioners in Switzerland. [Article]. *Dermatology, 234*(5-6), 186-191. https://doi.org/10.1159/000491820

116. Ferrándiz-Pulido, C., Lera-Imbuluzqueta, M., Ferrándiz, C., & Plazas-Fernandez, M. J. (2018). Prevalence of actinic keratosis in different regions of Spain: The EPIQA Study. [Article]. *Actas Dermo-Sifiliográficas, 109*(1), 83-86. https://doi.org/10.1016/j.adengl.2017.05.023

117. Tokez, S., Wakkee, M., Louwman, M., Noels, E., Nijsten, T., & Hollestein, L. (2020). Assessment of cutaneous squamous cell carcinoma (cSCC) in situ incidence and the risk of developing invasive cSCC in patients with prior cSCC in situ vs the general population in the Netherlands, 1989-2017. *JAMA Dermatology, 156*(9), 973-981. https://doi.org/10.1001/jamadermatol.2020.1988

118. Friman, T. K., Jäämaa-Holmberg, S., Åberg, F., Helanterä, I., Halme, M., Pentikäinen, M. O., Nordin, A., Lemström, K. B., Jahnukainen, T., Räty, R., & Salmela, B. (2022). Cancer risk and mortality after solid organ transplantation: A population-based 30-year cohort study in Finland. *International Journal of Cancer, 150*(11), 1779-1791. https://doi.org/10.1002/ijc.33934

119. Poizot-Martin, I., Lions, C., Delpierre, C., Makinson, A., Allavena, C., Fresard, A., Brégigeon, S., Rojas, T. R., & Delobel, P. (2022). Prevalence and spectrum of second primary malignancies among people living with HIV in the French Dat'AIDS Cohort. *Cancers (Basel)*, 14(2), 401. https://doi.org/10.3390/cancers14020401

120. Yuan, T., Hu, Y., Zhou, X., Yang, L., Wang, H., Li, L., Wang, J., Qian, H.-Z., Clifford, G. M., & Zou, H. (2022). Incidence and mortality of non-AIDS-defining cancers among people living with HIV: A systematic review and meta-analysis. *eClinicalMedicine, 52*, 101613. https://doi.org/10.1016/j.eclinm.2022.101613

121. D'Arcy, M. E., Beachler, D. C., Pfeiffer, R. M., Curtis, J. R., Mariette, X., Seror, R., Mahale, P., Rivera, D. R., Yanik, E. L., & Engels, E. A. (2021). Tumor necrosis factor inhibitors and the risk of cancer among older Americans with rheumatoid arthritis. *Cancer Epidemiology, Biomarkers & Prevention, 30*(11), 2059-2067. https://doi.org/10.1158/1055-9965.EPI-21-0125

122. Turk, T., Saad, A. M., Al-Husseini, M. J., & Gad, M. M. (2020). The risk of melanoma in patients with chronic lymphocytic leukemia: a population-based study. *Current Problems in Cancer, 44*(2), 100511-100511. https://doi.org/10.1016/j.currproblcancer.2019.100511

123. Plasmeijer, E., Jiyad, Z., Way, M., Marquart, L., Miura, K., Campbell, S., Isbel, N., Fawcett, J., Ferguson, L. E., Davis, M., Whiteman, D. C., Soyer, H. P., O'Rourke, P., & Green, A. C. (2019). Extreme incidence of skin cancer in kidney and liver yransplant recipients living with high sun exposure. *Acta Dermato-Venereologica, 99*(10), 929-930. https://doi.org/10.2340/00015555-3234

124. Ortega-Ortega, M., Hanly, P., Pearce, A., Soerjomataram, I., & Sharp, L. (2021). Paid and unpaid productivity losses due to premature mortality from cancer in Europe in 2018. *International Journal of Cancer, 150*(4), 580-593. https://doi.org/10.1002/ijc.33826

125. Yang, J. J., Maloney, N. J., Cheng, K., & Bach, D. Q. (2021). Financial burden in US patients with melanoma from 1997 to 2015: Racial disparities, trends, and predictors of high expenditures. *JAMA Dermatology, 84*(3), 819-821. https://doi.org/10.1016/j.jaad.2020.07.051

126. Noels, E., Hollestein, L., Luijkx, K., Louwman, M., de Uyl-de Groot, C., van den Bos, R., van der Veldt, A., Grunhagen, D., & Wakkee, M. (2020). Increasing costs of skin cancer due to increasing incidence and introduction of pharmaceuticals, 2007-2017. *Acta Dermato-Venereologica, 100*(10), adv00147. https://doi.org/10.2340/00015555-3463

127. Grange, F., Mohr, P., Harries, M., Ehness, R., Benjamin, L., Siakpere, O., Barth, J., Stapelkamp, C., Pfersch, S., McLeod, L. D., Kaye, J. A., Wolowacz, S., & Kontoudis, I. (2017). Economic burden of advanced melanoma in France, Germany and the UK: a retrospective observational study (Melanoma Burden-of-Illness Study). *Melanoma Research, 27*(6), 607-618. https://doi.org/10.1097/cmr.0000000000000372

128. Fernandes, J., Bregman, B., Combemale, P., Amaz, C., de Leotoing, L., Vainchtock, A., & Gaudin, A. F. (2017). Hospitalisation costs of metastatic melanoma in France; the MELISSA study (MELanoma In hoSpital coSts Assessment). *BMC Health Services Research, 17*(1), 542. https://doi.org/10.1186/s12913-017-2472-0

129. Copley-Merriman, C., Stevinson, K., Liu, F. X., Wang, J., Mauskopf, J., Zimovetz, E. A., & Chmielowski, B. (2018). Direct costs associated with adverse events of systemic therapies for advanced melanoma: Systematic literature review. *Medicine (Baltimore), 97*(31), e11736. https://doi.org/10.1097/md.0000000000011736

130. Krensel, M., Schafer, I., & Augustin, M. (2019). Cost-of-illness of melanoma in Europe - a modelling approach. *Journal of the European Academy of Dermatology and Venereology, 33 Suppl 2*, 34-45. https://doi.org/10.1111/jdv.15308

131. Gordon, L. G., Leung, W., Johns, R., McNoe, B., Lindsay, D., Merollini, K. M. D., Elliott, T. M., Neale, R. E., Olsen, C. M., Pandeya, N., & Whiteman, D. C. (2022). Estimated healthcare costs of melanoma and keratinocyte skin cancers in Australia and Aotearoa New Zealand in 2021. *International Journal of Environmental Research and Public Health, 19*(6), 3178. https://doi.org/10.3390/ijerph19063178

132. Luke, J. J., Ascierto, P. A., Carlino, M. S., Gershenwald, J. E., Grob, J.-J., Hauschild, A., Kirkwood, J. M., Long, G., Mohr, P., Robert, C., Ross, M., Scolyer, R. A., Yoon, C. H., Poklepovic, A., Rutkowski, P., Anderson, J. R., Ahsan, S., Ibrahim, N., & Eggermont, A. M. M. (2020). KEYNOTE-716: Phase III study of adjuvant pembrolizumab versus placebo in resected high-risk stage II melanoma. *Future Oncology 16*(3), 4429-4438. https://doi.org/10.2217/fon-2019-0666

133. Anderson, A., Matsumoto, M., Secrest, A., Saul, M. I., Ho, J., & Ferris, L. K. (2021). Cost of treatment of benign and premalignant lesions during skin cancer screening. *JAMA Dermatology, 157*(7), 876-879. https://doi.org/10.1001/jamadermatol.2021.1953

134. Gordon, L., Olsen, C., Whiteman, D. C., Elliott, T. M., Janda, M., & Green, A. (2020). Prevention versus early detection for long-term control of melanoma and keratinocyte carcinomas: a cost-effectiveness modelling study. *BMJ Open, 10*(2), e034388. https://doi.org/10.1136/bmjopen-2019-034388

135. van der Pols, J. C., Williams, G. M., Neale, R. E., Clavarino, A., & Green, A. C. (2006). Long-term increase in sunscreen use in an Australian community after a skin cancer prevention trial. *Preventive Medicine, 42*(3), 171-176. https://doi.org/10.1016/j.ypmed.2005.10.007

136. Janda, M., Youl, P., Neale, R., Aitken, J., Whiteman, D., Gordon, L., & Baade, P. (2014). Clinical skin examination outcomes after a video-based behavioral intervention: analysis from a randomized clinical trial. *JAMA Dermatology, 150*(4), 372-379. https://doi.org/10.1001/jamadermatol.2013.9313

137. Mofidi, A., Tompa, E., Spencer, J., Kalcevich, C., Peters, C. E., Kim, J., Song, C., Mortazavi, S. B., & Demers, P. A. (2018). The economic burden of occupational non-melanoma skin cancer due to solar radiation. *Journal of Occupational and Environmental Hygiene, 15*(6), 481-491. https://doi.org/https://doi.org/10.1080/15459624.2018.1447118

138. Mofidi, A., Tompa, E., Song, C., Tenkate, T., Arrandale, V., J Jardine, K., Davies, H., & Demers, P. A. (2021). Economic evaluation of interventions to reduce solar ultraviolet radiation (UVR) exposure among construction workers. *Journal of Occupational and Environmental Hygiene, 18*(6), 250-264. https://doi.org/10.1080/15459624.2021.1910278

139. Yoon, J., Phibbs, C. S., Chow, A., & Weinstock, M. A. (2018). Impact of topical fluorouracil cream on costs of treating keratinocyte carcinoma (nonmelanoma skin cancer) and actinic keratosis. [Article]. *JAMA Dermatology, 79*(3), 501-507.e502. https://doi.org/10.1016/j.jaad.2018.02.058

140. Fitzpatrick, T. B. (1988). The validity and practicality of sun-reactive skin types I through VI. *Archives of Dermatology, 124*(6), 869-871. https://doi.org/10.1001/archderm.124.6.869

141. Olsen, C. M., Pandeya, N., Law, M. H., MacGregor, S., Iles, M. M., Thompson, B. S., Green, A. C., Neale, R. E., & Whiteman, D. C. (2020). Does polygenic risk influence associations between sun exposure and melanoma? A prospective cohort analysis. *British Journal of Dermatology, 183*(2), 303-310. https://doi.org/10.1111/bjd.18703

142. Savoye, I., Olsen, C. M., Whiteman, D. C., Bijon, A., Wald, L., Dartois, L., Clavel-Chapelon, F., Boutron-Ruault, M.-C., & Kvaskoff, M. (2018). Patterns of ultraviolet radiation exposure and skin cancer risk: the E3N-SunExp Study. *Journal of Epidemiology, 28*(1), 27-33. https://doi.org/10.2188/jea.JE20160166

143. Kawai, K., VoPham, T., Drucker, A., Curhan, S. G., & Curhan, G. C. (2020). Ultraviolet radiation exposure and the risk of Herpes zoster in three prospective cohort studies. *Mayo Clinic Proceedings, 95*(2), 283-292. https://doi.org/10.1016/j.mayocp.2019.08.022

144. Tripathi, R., Mazmudar, R. S., Knusel, K. D., Ezaldein, H. H., Bordeaux, J. S., & Scott, J. F. (2021). Trends in emergency department visits due to sunburn and factors associated with severe sunburns in the United States. *Archives of Dermatological Research, 313*(2), 79-88. https://doi.org/10.1007/s00403-020-02073-2

145. Holman, D. M., Ding, H., Berkowitz, Z., Hartman, A. M., & Perna, F. M. (2019). Sunburn prevalence among US adults, National Health Interview Survey 2005, 2010, and 2015. *JAMA Dermatology, 80*(3), 817-820. https://doi.org/10.1016/j.jaad.2018.10.044

146. Wei, G., Farooq, J., Castelo-Soccio, L., & Mhaskar, R. (2021). Correlates between physical activity and sunburn prevalence among a nationally representative sample of US high school students, 2015-2017. *Journal of Physical Activity and Health, 18*(9), 1113-1119. https://doi.org/10.1123/jpah.2020-0711

147. Blazquez-Sanchez, N., Rivas-Ruiz, F., Bueno-Fernandez, S., Fernandez-Morano, M. T., Arias-Santiago, S., Rodriguez-Martinez, A., DeCastro-Maqueda, G., & DeTroya-Martin, M. (2021). Photoprotection habits, attitudes and knowledge among school communities in the Costa del sol (Spain). *European Journal of Public Health, 31*(3), 508-514. https://doi.org/10.1093/eurpub/ckab010

148. Goerig, T., Soedel, C., Pfahlberg, A. B., Gefeller, O., Breitbart, E. W., & Diehl, K. (2021). Sun protection and sunburn in children aged 1-10 years in Germany: prevalence and determinants. *Children (Basel), 8*(8), 668. https://doi.org/10.3390/children8080668

149. Tabbakh, T., Volkov, A., Wakefield, M., & Dobbinson, S. (2019). Implementation of the SunSmart program and population sun protection behaviour in Melbourne, Australia: Results from cross-sectional summer surveys from 1987 to 2017. *PLoS Medicine, 16*(10), e1002932-e1002932. https://doi.org/10.1371/journal.pmed.1002932

150. Liew, A. Y. S., & Cust, A. E. (2021). Changes in sun protection behaviours, sun exposure and shade availability among adults, children and adolescents in New South Wales, 2003–2016. *Australian and New Zealand Journal of Public Health, 45*(5), 462-468. https://doi.org/10.1111/1753-6405.13112

151. Cancer Australia (2019). National Cancer Control Indicators: Sunburn and Sun Protection. https://ncci.canceraustralia.gov.au/prevention/sun-exposure/sunburn-and-sun-protection. Accessed 30/3/2022.

152. Køster, B., Meyer, M., Andersson, T., Engholm, G., & Dalum, P. (2018). Development in sunburn 2007-2015 and skin cancer projections 2007-2040 of campaign results in the Danish population. *Medicine (Baltimore), 97*(41), e12738-e12738. https://doi.org/10.1097/MD.0000000000012738

153. Lacson, J. C. A., Zamani, S. A., Froes Jr, L. A. R., Mitra, N., Qian, L., Doyle, S. H., Azizi, E., Balestrini, C., Bishop, D. T., Bruno, W., Carlos-Ortega, B., Cuellar, F., Cust, A. E., Elder, D. E., Gerdes, A.-M., Ghiorzo, P., Grazziotin, T. C., Gruis, N. A., Hansson, J., Hocevar, M., et al. (2021). Birth cohort-specific trends of sun-related behaviors among individuals from an international consortium of melanoma-prone families. *BMC Public Health, 21*(1), 692-692. https://doi.org/10.1186/s12889-021-10424-5

154. Fitzpatrick, T. B. (1988). The validity and practicality of sun-reactive skin types I through VI. *Archives of Dermatology, 124*(6), 869-871. https://doi.org/10.1001/archderm.1988.01670060015008

155. Shih, B. B., Allan, D., de Gruijl, F. R., & Rhodes, L. E. (2015). Robust detection of minimal sunburn in pigmented skin by 785 nm laser speckle contrast imaging of blood flux. *Journal of Investigative Dermatology, 135*(4), 1197-1199. https://doi.org/10.1038/jid.2014.507

156. Calderón, T. A., Bleakley, A., Jordan, A. B., Lazovich, D., & Glanz, K. (2019). Correlates of sun protection behaviors in racially and ethnically diverse U.S. adults. *Preventive Medicine Reports, 13*, 346-353. https://doi.org/10.1016/j.pmedr.2018.12.006

157. Bello, O., Sudhoff, H., & Goon, P. (2021). Sunburn prevalence is underestimated in UK-based people of African ancestry. *Clinical, Cosmetic and Investigational Dermatology, 14*, 1791-1797. https://doi.org/10.2147/CCID.S334574

158. Rhodes, L. E., Bock, M., Soe Janssens, A., Ling, T. C., Anastasopoulou, L., Antoniou, C., Aubin, F., Bruckner, T., Faivre, B., Gibbs, N. K., Jansen, C., Pavel, S., Stratigos, A. J., de Gruijl, F. R., & Diepgen, T. L. (2010). Polymorphic light eruption occurs in 18% of Europeans and does not show higher prevalence with increasing latitude: Multicenter survey of 6,895 individuals residing from the Mediterranean to Scandinavia. *Journal of Investigative Dermatology, 130*(2), 626-628. https://doi.org/10.1038/jid.2009.250

159. Gutierrez, D., Gaulding, J. V., Motta Beltran, A. F., Lim, H. W., & Pritchett, E. N. (2018). Photodermatoses in skin of colour. *Journal of the European Academy of Dermatology and Venereology, 32*(11), 1879-1886. https://doi.org/10.1111/jdv.15115

160. Gether, L., Overgaard, L. K., Egeberg, A., & Thyssen, J. P. (2018). Incidence and prevalence of rosacea: a systematic review and meta-analysis. *British Journal of Dermatology, 179*(2), 282-289. https://doi.org/10.1111/bjd.16481

161. Rutter, K. J., Ashraf, I., Cordingley, L., & Rhodes, L. E. (2020). Quality of life and psychological impact in the photodermatoses: a systematic review. *British Journal of Dermatology, 182*(5), 1092-1102. https://doi.org/10.1111/bjd.18326

162. Hofmann, G. A., Gradl, G., Schulz, M., Haidinger, G., Tanew, A., & Weber, B. (2020). The frequency of photosensitizing drug dispensings in Austria and Germany: a correlation with their photosensitizing potential based on published literature. *Journal of the European Academy of Dermatology and Venereology, 34*(3), 589-600. https://doi.org/10.1111/jdv.15952

163. Nakao, S., Hatahira, H., Sasaoka, S., Hasegawa, S., Motooka, Y., Ueda, N., Abe, J., Fukuda, A., Naganuma, M., Kanoh, H., Seishima, M., Ishiguro, M., Kinosada, Y., & Nakamura, M. (2017). Evaluation of drug-induced photosensitivity using the Japanese Adverse Drug Event Report (JADER) Database. *Biological and Pharmaceutical Bulletin, 40*(12), 2158-2165. https://doi.org/10.1248/bpb.b17-00561

164. Kim, W. B., Shelley, A. J., Novice, K., Joo, J., Lim, H. W., & Glassman, S. J. (2018). Drug-induced phototoxicity: A systematic review. *JAMA Dermatology, 79*(6), 1069-1075. https://doi.org/10.1016/j.jaad.2018.06.061

165. Alrashidi, A., Rhodes, L. E., Sharif, J. C. H., Kreeshan, F. C., Farrar, M. D., & Ahad, T. (2020). Systemic drug photosensitivity—Culprits, impact and investigation in 122 patients. *Photodermatology, Photoimmunology & Photomedicine, 36*(6), 441-451. https://doi.org/10.1111/phpp.12583

166. Pedersen, S. A., Gaist, D., Schmidt, S. A. J., Holmich, L. R., Friis, S., & Pottegard, A. (2018). Hydrochlorothiazide use and risk of nonmelanoma skin cancer: A nationwide case-control study from Denmark. *JAMA Dermatology, 78*(4), 673-681 e679. https://doi.org/10.1016/j.jaad.2017.11.042

167. Pharmacovigilance Risk Assessment Committee PRAC recommendations on signals, European Medicines Agency 2018. https://www.ema.europa.eu/en/documents/prac-recommendation/prac-recommendations-signals-adopted-3-6-september-2018-prac-meeting_en-0.pdf. Accessed 30/3/2022.

168. Pottegård, A., Pedersen, S. A., Schmidt, S. A. J., Lee, C.-N., Hsu, C.-K., Liao, T.-C., Shao, S.-C., & Lai, E. C.-C. (2019). Use of hydrochlorothiazide and risk of skin cancer: a nationwide Taiwanese case-control study. *British Journal of Cancer, 121*(11), 973-978. https://doi.org/10.1038/s41416-019-0613-4

169. Gallelli, L., Cione, E., Siniscalchi, A., Vasta, G., Guerra, A., Scaramuzzino, A., Longo, L., Muraca, L., De Sarro, G., Leuzzi, G., Gerace, A., Scuteri, A., Vasapollo, P., Natale, V., Zampogna, S., & Luciani, F. (2021). Is there a link between non-melanoma skin cancer and hydrochlorothiazide? *Current Drug Safety, 17*(3), 211-216. https://doi.org/10.2174/1574886316666211103164412

170. Daniels, B., Pearson, S. A., Vajdic, C. M., Pottegård, A., Buckley, N. A., & Zoega, H. (2020). Risk of squamous cell carcinoma of the lip and cutaneous melanoma in older Australians using hydrochlorothiazide: A population-based case-control study. *Basic and Clinical Pharmacology and Toxicology, 127*(4), 320-328. https://doi.org/10.1111/bcpt.13463

171. Bendinelli, B., Masala, G., Garamella, G., Palli, D., & Caini, S. (2019). Do thiazide diuretics increase the risk of skin cancer? A critical review of the scientific evidence and updated meta-analysis. *Current Cardiology Reports, 21*(9), 92. https://doi.org/10.1007/s11886-019-1183-z

172. Williams, N. M., Vincent, L. T., Rodriguez, G. A., & Nouri, K. (2020). Antihypertensives and melanoma: An updated review. *Pigment Cell & Melanoma Research, 33*(6), 806-813. https://doi.org/10.1111/pcmr.12918

173. Hatsusaka, N., Seki, Y., Mita, N., Ukai, Y., Miyashita, H., Kubo, E., Sliney, D., & Sasaki, H. (2021). UV Index does not predict ocular ultraviolet exposure. *Translational Vision Science & Technology, 10*(7), 1. https://doi.org/10.1167/tvst.10.7.1

174. Marro, M., Moccozet, L., & Vernez, D. (2022). Assessing human eye exposure to UV light: A narrative review. *Frontiers in Public Health, 10*, 900979-900979. https://doi.org/10.3389/fpubh.2022.900979

175. Lanca, C., Teo, A., Vivagandan, A., Htoon, H. M., Najjar, R. P., Spiegel, D. P., Pu, S.-H., & Saw, S.-M. (2019). The effects of different outdoor environments, sunglasses and hats on light levels: Implications for myopia prevention. *Translational Vision Science & Technology, 8*(4), 7-7. https://doi.org/10.1167/tvst.8.4.7

176. Backes, C., Religi, A., Moccozet, L., Behar-Cohen, F., Vuilleumier, L., Bulliard, J. L., & Vernez, D. (2019). Sun exposure to the eyes: predicted UV protection effectiveness of various sunglasses. J*ournal of Exposure Science & Environmental Epidemiology, 29*(6), 753-764. https://doi.org/10.1038/s41370-018-0087-0

177. Rabbetts, R., & Sliney, D. (2019). Technical report: Solar ultraviolet protection from sunglasses. *Optometry and Vision Science, 96*(7), 523-530. https://doi.org/10.1097/OPX.0000000000001397

178. Lucas, R. M., Norval, M., Neale, R. E., Young, A. R., de Gruijl, F. R., Takizawa, Y., & van der Leun, J. C. (2014). The consequences for human health of stratospheric ozone depletion in association with other environmental factors. *Photochemical & Photobiological Sciences, 14*(1), 53-87. https://doi.org/10.1039/c4pp90033b

179. Lofgren, S. (2017). Solar ultraviolet radiation cataract. *Experimental Eye Research, 156*, 112-116. https://doi.org/10.1016/j.exer.2016.05.026

180. Cheng, C.-Y., Wang, N., Wong, T. Y., Congdon, N., He, M., Wang, Y. X., Braithwaite, T., Casson, R. J., Cicinelli, M. V., Das, A., Flaxman, S. R., Jonas, J. B., Keeffe, J. E., Kempen, J. H., Leasher, J., Limburg, H., Naidoo, K., Pesudovs, K., Resnikoff, S., Silvester, A. J., et al. (2020). Prevalence and causes of vision loss in East Asia in 2015: magnitude, temporal trends and projections. *British Journal of Ophthalmology, 104*(5), 616-622. https://doi.org/10.1136/bjophthalmol-2018-313308

181. Kahloun, R., Khairallah, M., Resnikoff, S., Cicinelli, M. V., Flaxman, S. R., Das, A., Jonas, J. B., Keeffe, J. E., Kempen, J. H., Leasher, J., Limburg, H., Naidoo, K., Pesudovs, K., Silvester, A. J., Tahhan, N., Taylor, H. R., Wong, T. Y., Bourne, R. R. A., & Vision Loss Expert Group of the Global Burden of Disease, S. (2019). Prevalence and causes of vision loss in North Africa and Middle East in 2015: magnitude, temporal trends and projections. *British Journal of Ophthalmology, 103*(7), 863-870. https://doi.org/10.1136/bjophthalmol-2018-312068

182. Keeffe, J. E., Casson, R. J., Pesudovs, K., Taylor, H. R., Cicinelli, M. V., Das, A., Flaxman, S. R., Jonas, J. B., Kempen, J. H., Leasher, J., Limburg, H., Naidoo, K., Silvester, A. J., Stevens, G. A., Tahhan, N., Wong, T. Y., Resnikoff, S., & Bourne, R. R. A. (2019). Prevalence and causes of vision loss in South-east Asia and Oceania in 2015: magnitude, temporal trends and projections. *British Journal of Ophthalmology, 103*(7), 878-884. https://doi.org/10.1136/bjophthalmol-2018-311946

183. Leasher, J. L., Braithwaite, T., Furtado, J. M., Flaxman, S. R., Lansingh, V. C., Silva, J. C., Resnikoff, S., Taylor, H. R., Bourne, R. R. A., & Vision Loss Expert Group of the Global Burden of Disease, S. (2019). Prevalence and causes of vision loss in Latin America and the Caribbean in 2015: magnitude, temporal trends and projections. *British Journal of Ophthalmology, 103*(7), 885-893. https://doi.org/10.1136/bjophthalmol-2017-311746

184. Naidoo, K., Kempen, J. H., Gichuhi, S., Braithwaite, T., Casson, R. J., Cicinelli, M. V., Das, A., Flaxman, S. R., Jonas, J. B., Keeffe, J. E., Leasher, J., Limburg, H., Pesudovs, K., Resnikoff, S., Silvester, A. J., Tahhan, N., Taylor, H. R., Wong, T. Y., Bourne, R. R. A., & Vision Loss Expert Group of the Global Burden of Disease, S. (2020). Prevalence and causes of vision loss in sub-Saharan Africa in 2015: magnitude, temporal trends and projections. *British Journal of Ophthalmology, 104*(12), 1658-1668. https://doi.org/10.1136/bjophthalmol-2019-315217

185. Foreman, J., Keel, S., McGuiness, M., Liew, D., Wijngaarden, P., Taylor, H. R., & Dirani, M. (2020). Future burden of vision loss in Australia: Projections from the National Eye Health Survey. *Clinical & Experimental Ophthalmology, 48*(6), 730-738. https://doi.org/10.1111/ceo.13776

186. GBD results tool Available from: https://ghdx.healthdata.org/gbd-results-tool. Accessed Accessed 11 April 22.

187. Bikbov, M. M., Kazakbaeva, G. M., Gilmanshin, T. R., Zainullin, R. M., Nuriev, I. F., Zaynetdinov, A. F., Israfilova, G. Z., Panda-Jonas, S., Arslangareeva, I. I., Rakhimova, E. M., Rusakova, I. A., & Jonas, J. B. (2020). Prevalence and associated factors of cataract and cataract-related blindness in the Russian Ural Eye and Medical Study. *Scientific Reports, 10*(1), 18157. https://doi.org/10.1038/s41598-020-75313-0

188. Purola, P. K. M., Nättinen, J. E., Ojamo, M. U. I., Koskinen, S. V. P., Rissanen, H. A., Sainio, P. R. J., & Uusitalo, H. M. T. (2021). Prevalence and 11-year incidence of common eye diseases and their relation to health-related quality of life, mental health, and visual impairment. *Quality of Life Research, 30*(8), 2311-2327. https://doi.org/10.1007/s11136-021-02817-1

189. Tan, A. G., Tham, Y. C., Chee, M. L., Mitchell, P., Cumming, R. G., Sabanayagam, C., Wong, T. Y., Wang, J. J., & Cheng, C. Y. (2020). Incidence, progression and risk factors of age-related cataract in Malays: The Singapore Malay Eye Study. *Clinical & Experimental Ophthalmology, 48*(5), 580-592. https://doi.org/10.1111/ceo.13757

190. Vashist, P., Tandon, R., Murthy, G. V. S., Barua, C. K., Deka, D., Singh, S., Gupta, V., Gupta, N., Wadhwani, M., Singh, R., Vishwanath, K., & Group, I.-E. S. S. (2020). Association of cataract and sun exposure in geographically diverse populations of India: The CASE study. First Report of the ICMR-EYE SEE Study Group. *PLoS One, 15*(1), e0227868. https://doi.org/10.1371/journal.pone.0227868

191. Lee, J., Kim, U. J., Lee, Y., Han, E., Ham, S., Lee, W., Choi, W. J., & Kang, S. K. (2021). Sunlight exposure and eye disorders in an economically active population: data from the KNHANES 2008-2012. *Annals of Occupational and Environmental Medicine, 33*, e24. https://doi.org/10.35371/aoem.2021.33.e24

192. Global Burden of Disease Blindness and Vision Impairment Collaborators, & Vision Loss Expert Group of the Global Burden of Disease, S. (2021). Causes of blindness and vision impairment in 2020 and trends over 30 years, and prevalence of avoidable blindness in relation to VISION 2020: the Right to Sight: an analysis for the Global Burden of Disease Study. *The Lancet Global Health, 9*(2), e144-e160. https://doi.org/10.1016/S2214-109X(20)30489-7

193. Van Acker, S. I., van den Bogerd, B., Haagdorens, M., Siozopoulou, V., Ni Dhubhghaill, S., Pintelon, I., & Koppen, C. (2021). Pterygium - the good, the bad, and the ugly. *Cells (Basel), 10*(7), 1567. https://doi.org/10.3390/cells10071567

194. Rezvan, F., Khabazkhoob, M., Hooshmand, E., Yekta, A., Saatchi, M., & Hashemi, H. (2018). Prevalence and risk factors of pterygium: a systematic review and meta-analysis. *Survey of Ophthalmology, 63*(5), 719-735. https://doi.org/10.1016/j.survophthal.2018.03.001

195. Liu, L., Wu, J., Geng, J., Yuan, Z., & Huang, D. (2013). Geographical prevalence and risk factors for pterygium: a systematic review and meta-analysis. *BMJ Open, 3*(11), e003787. https://doi.org/10.1136/bmjopen-2013-003787

196. Fernandes, A. G., Salomão, S. R., Ferraz, N. N., Mitsuhiro, M. H., Furtado, J. M., Muñoz, S., Cypel, M. C., Cunha, C. C., Vasconcelos, G. C., Sacai, P. Y., Morales, P. H., Cohen, M. J., Cohen, J. M., Watanabe, S. S., Campos, M., Belfort Junior, R., & Berezovsky, A. (2020). Pterygium in adults from the Brazilian Amazon Region: Prevalence, visual status and refractive errors. *British Journal of Ophthalmology, 104*(6), 757-763. https://doi.org/10.1136/bjophthalmol-2019-314131

197. Pan, Z., Cui, J., Shan, G., Chou, Y., Pan, L., Sun, Z., Cui, Z., Sun, J., Cao, Y., Zhao, J., Ma, X., Ma, J., He, H., Ma, J., & Zhong, Y. (2019). Prevalence and risk factors for pterygium: a cross-sectional study in Han and Manchu ethnic populations in Hebei, China. *BMJ Open, 9*(2), e025725. https://doi.org/10.1136/bmjopen-2018-025725

198. Wang, Y., Shan, G., Gan, L., Qian, Y., Chen, T., Wang, H., Pan, X., Wang, W., Pan, L., Zhang, X., Wang, M., Ma, J., & Zhong, Y. (2020). Prevalence and associated factors for pterygium in Han and Mongolian adults: a cross-sectional study in inner Mongolian, China. *BMC Ophthalmology, 20*(1), 45. https://doi.org/10.1186/s12886-020-1324-6

199. Hampel, U., Wasielica-Poslednik, J., Ries, L., Faysal, R., Schulz, A., Nickels, S., Wild, P. S., Schmidtmann, I., Münzel, T., Beutel, M. E., Lackner, K. J., Pfeiffer, N., & Schuster, A. K. (2021). Prevalence of pterygium and identification of associated factors in a German population - results from the Gutenberg Health Study. *Acta Ophthalmologica, 99*(1), e130-e131. https://doi.org/10.1111/aos.14505

200. Bikbov, M. M., Zainullin, R. M., Kazakbaeva, G. M., Gilmanshin, T. R., Salavatova, V. F., Arslangareeva, I. I., Nikitin, N. A., Panda-Jonas, S., Zaynetdinov, A. F., Kazakbaev, R. A., Nuriev, I. F., Khikmatullin, R. I., Uzianbaeva, Y. V., Yakupova, D. F., Aminev, S. K., & Jonas, J. B. (2019). Pterygium prevalence and Its associations in a Russian population: The Ural Eye and Medical Study. *American Journal of Ophthalmology, 205*, 27-34. https://doi.org/10.1016/j.ajo.2019.02.031

201. Cameron, M. E. (1965). *Pterygium Throughout the World*: Thomas.

202. Khanna, R. C., Marmamula, S., Cicinelli, M. V., Mettla, A. L., Giridhar, P., Banerjee, S., Shekhar, K., Chakrabarti, S., Murthy, G. V. S., Gilbert, C. E., & Rao, G. N. (2021). Fifteen-year incidence rate and risk factors of pterygium in the Southern Indian state of Andhra Pradesh. *British Journal of Ophthalmology, 105*(5), 619-624. https://doi.org/10.1136/bjophthalmol-2020-316359

203. Fang, X. L., Chong, C. C. Y., Thakur, S., Da Soh, Z., Teo, Z. L., Majithia, S., Lim, Z. W., Rim, T. H., Sabanayagam, C., Wong, T. Y., Cheng, C.-Y., & Tham, Y.-C. (2021). Ethnic differences in the incidence of pterygium in a multi-ethnic Asian population: the Singapore Epidemiology of Eye Diseases Study. *Scientific Reports, 11*(1), 501. https://doi.org/10.1038/s41598-020-79920-9

204. Lingham, G., Kugelman, J., Charng, J., Lee, S. S., Yazar, S., McKnight, C. M., Coroneo, M. T., Lucas, R. M., Brown, H., Stevenson, L. J., Mackey, D. A., & Alonso-Caneiro, D. (2021). Conjunctival ultraviolet autofluorescence area decreases with age and sunglasses use. *British Journal of Ophthalmology*, epub ahead of print. https://doi.org/10.1136/bjophthalmol-2021-320284

205. Goh, A. Y., Ramlogan-Steel, C. A., Jenkins, K. S., Steel, J. C., & Layton, C. J. (2020). Presence and prevalence of UV related genetic mutations in uveal melanoma: similarities with cutaneous melanoma. *Neoplasma, 67*(5), 958-971. https://doi.org/10.4149/neo_2020_190815N768

206. Mundra, P. A., Dhomen, N., Rodrigues, M., Mikkelsen, L. H., Cassoux, N., Brooks, K., Valpione, S., Reis-Filho, J. S., Heegaard, S., Stern, M.-H., Roman-Roman, S., & Marais, R. (2021). Ultraviolet radiation drives mutations in a subset of mucosal melanomas. *Nature Communications, 12*(1), 259. https://doi.org/10.1038/s41467-020-20432-5

207. Ghazawi, F. M., Darwich, R., Le, M., Rahme, E., Zubarev, A., Moreau, L., Burnier, J. V., Sasseville, D., Burnier, M. N., & Litvinov, I. V. (2019). Uveal melanoma incidence trends in Canada: a national comprehensive population-based study. *British Journal of Ophthalmology, bjophthalmol-2018*. https://doi.org/10.1136/bjophthalmol-2018-312966

208. Baily, C., O'Neill, V., Dunne, M., Cunningham, M., Gullo, G., Kennedy, S., Walsh, P. M., Deady, S., & Horgan, N. (2019). Uveal melanoma in Ireland. *Ocular Oncology and Pathology, 5(*3), 195-204. https://doi.org/10.1159/000492391

209. Aronow, M. E., Topham, A. K., & Singh, A. D. (2018). Uveal melanoma: 5-Year update on incidence, treatment, and survival (SEER 1973-2013). *Ocular Oncology and Pathology, 4*(3), 145-151. https://doi.org/10.1159/000480640

210. Beasley, A. B., Preen, D. B., McLenachan, S., Gray, E. S., & Chen, F. K. (2021). Incidence and mortality of uveal melanoma in Australia (1982–2014). *British Journal of Ophthalmology,* epub ahead of print. https://doi.org/10.1136/bjophthalmol-2021-319700

211. Ghazawi, F. M., Darwich, R., Le, M., Jfri, A., Rahme, E., Burnier, J. V., Sasseville, D., Burnier, M. N., Jr., & Litvinov, I. V. (2020). Incidence trends of conjunctival malignant melanoma in Canada. *British Journal of Ophthalmology, 104*(1), 23-25. https://doi.org/10.1136/bjophthalmol-2019-313977

212. Virgili, G., Parravano, M., Gatta, G., Capocaccia, R., Mazzini, C., Mallone, S., Botta, L., & Group, R. A. W. (2020). Incidence and survival of patients with conjunctival melanoma in Europe. *JAMA Ophthalmology, 138*(6), 601-608. https://doi.org/10.1001/jamaophthalmol.2020.0531

213. Roberts, J. E. (2002). Screening for ocular phototoxicity. *International Journal of Toxicology, 21*(6), 491-500. https://doi.org/10.1080/10915810290169918

214. Zhao, B., Chignell, C. F., Rammal, M., Smith, F., Hamilton, M. G., Andley, U. P., & Roberts, J. E. (2010). Detection and prevention of ocular phototoxicity of ciprofloxacin and other fluoroquinolone antibiotics. *Photochemistry and Photobiology, 86*(4), 798-805. https://doi.org/10.1111/j.1751-1097.2010.00755.x

215. Sahu, R. K., Singh, B., Saraf, S. A., Kaithwas, G., & Kishor, K. (2014). Photochemical toxicity of drugs intended for ocular use. *Archives of Industrial Hygiene and Toxicology, 65*(2), 157-167. https://doi.org/10.2478/10004-1254-65-2014-2461

216. Wright, C. Y., Lucas, R. M., D'Este, C., Kapwata, T., Kunene, Z., Swaminathan, A., Mathee, A., & Albers, P. N. (2019). Effect of a sun protection intervention on the immune response to measles booster vaccination in infants in rural South Africa. *Photochemistry and Photobiology, 95*(1), 446-452. https://doi.org/10.1111/php.13004

217. Swaminathan, A., Harrison, S. L., Ketheesan, N., van den Boogaard, C. H. A., Dear, K., Allen, M., Hart, P. H., Cook, M., & Lucas, R. M. (2019). Exposure to solar UVR suppresses cell-mediated immunization responses in humans: The Australian Ultraviolet Radiation and Immunity Study. *Journal of Investigative Dermatology, 139*(7), 1545-1553.e1546. https://doi.org/10.1016/j.jid.2018.12.025

218. Lopatko Lindman, K., Lockman-Lundgren, J., Weidung, B., Olsson, J., Elgh, F., & Lövheim, H. (2022). Long-term time trends in reactivated herpes simplex infections and treatment in Sweden. *BMC Infectious Diseases, 22*(1), 547-547. https://doi.org/10.1186/s12879-022-07525-w

219. Mai, Z.-M., Lin, J.-H., Ngan, R. K.-C., Kwong, D. L.-W., Ng, W.-T., Ng, A. W.-Y., Ip, K.-M., Chan, Y.-H., Lee, A. W.-M., Ho, S.-Y., Lung, M. L., & Lam, T.-H. (2020). Solar ultraviolet radiation and vitamin D deficiency on Epstein-Barr Virus reactivation: Observational and genetic evidence from a nasopharyngeal carcinoma-endemic population. *Open Forum Infectious Diseases, 7*(10), ofaa426. https://doi.org/10.1093/ofid/ofaa426

220. Bar-Or, A., Pender, M. P., Khanna, R., Steinman, L., Hartung, H. P., Maniar, T., Croze, E., Aftab, B. T., Giovannoni, G., & Joshi, M. A. (2020). Epstein-Barr virus in multiple sclerosis: Theory and emerging immunotherapies. *Trends in Molecular Medicine, 26*(3), 296-310. https://doi.org/10.1016/j.molmed.2019.11.003

221. Simpson, S., van der Mei, I., Lucas, R. M., Ponsonby, A.-L., Broadley, S., Blizzard, L., & Taylor, B. (2018). Sun exposure across the life course significantly modulates early multiple sclerosis clinical course. *Frontiers in Neurology, 9*, 16. https://doi.org/10.3389/fneur.2018.00016

222. Bakker, K. M., Eisenberg, M. C., Woods, R., & Martinez, M. E. (2021). Exploring the seasonal drivers of Varicella zoster virus transmission and reactivation. *American Journal of Epidemiology, 190*(9), 1814-1820. https://doi.org/10.1093/aje/kwab073

223. Lucas, R. M., & Rodney Harris, R. (2018). On the nature of evidence and 'proving' causality: Smoking and lung cancer vs. sun exposure, vitamin D and multiple sclerosis. *International Journal of Environmental Research and Public Health, 15*(8), 1726. https://doi.org/10.3390/ijerph15081726

224. Chen, R., Yang, C., Li, P., Wang, J., Liang, Z., Wang, W., Wang, Y., Liang, C., Meng, R., Wang, H. Y., Peng, S., Sun, X., Su, Z., Kong, G., Wang, Y., & Zhang, L. (2021). Long-term exposure to ambient $PM_{2.5}$, sunlight, and obesity: A nationwide study in China. *Frontiers in Endocrinology, 12*, 790294. https://doi.org/10.3389/fendo.2021.790294

225. Weller, R. B., Wang, Y., He, J., Maddux, F. W., Usvyat, L., Zhang, H., Feelisch, M., & Kotanko, P. (2020). Does incident solar ultraviolet radiation lower blood pressure? *Journal of the American Heart Association, 9*(5), e013837. https://doi.org/10.1161/JAHA.119.013837

226. Luo, Y. N., Yang, B. Y., Zou, Z., Markevych, I., Browning, M., Heinrich, J., Bao, W. W., Guo, Y., Hu, L. W., Chen, G., Ma, J., Ma, Y., Chen, Y. J., & Dong, G. H. (2022). Associations of greenness surrounding schools with blood pressure and hypertension: A nationwide cross-sectional study of 61,229 children and adolescents in China. *Environmental Research, 204*(Pt A), 112004. https://doi.org/10.1016/j.envres.2021.112004

227. Twohig-Bennett, C., & Jones, A. (2018). The health benefits of the great outdoors: A systematic review and meta-analysis of greenspace exposure and health outcomes. *Environmental Research, 166*, 628-637. https://doi.org/10.1016/j.envres.2018.06.030

228. Cui, Y., Gong, Q., Huang, C., Guo, F., Li, W., Wang, Y., & Cheng, X. (2021). The relationship between sunlight exposure duration and depressive symptoms: A cross-sectional study on elderly Chinese women. *PLoS One, 16*(7), e0254856. https://doi.org/10.1371/journal.pone.0254856

229. Lindqvist, P. G., Landin-Olsson, M., & Olsson, H. (2021). Low sun exposure habits is associated with a dose-dependent increased risk of hypertension: a report from the large MISS cohort. *Photochemical & Photobiological Sciences, 20*(2), 285-292. https://doi.org/10.1007/s43630-021-00017-x

230. Bae, J. M., Kim, Y.-S., Choo, E. H., Kim, M.-Y., Lee, J. Y., Kim, H.-O., & Park, Y. M. (2021). Both cardiovascular and cerebrovascular events are decreased following long-term narrowband ultraviolet B phototherapy in patients with vitiligo: a propensity score matching analysis. *Journal of the European Academy of Dermatology and Venereology, 35*(1), 11-12. https://doi.org/https://doi.org/10.1111/jdv.17073

231. Mackay, D. F., Clemens, T. L., Hastie, C. E., Cherrie, M. P. C., Dibben, C., & Pell, J. P. (2019). UVA and seasonal patterning of 56 370 myocardial infarctions across Scotland, 2000-2011. *Journal of the American Heart Association, 8*(23), e012551. https://doi.org/10.1161/JAHA.119.012551

232. Liddle, L., Monaghan, C., Burleigh, M. C., Baczynska, K. A., Muggeridge, D. J., & Easton, C. (2022). Reduced nitric oxide synthesis in winter: A potential contributing factor to increased cardiovascular risk. *Nitric Oxide, 127*, 1-9. https://doi.org/10.1016/j.niox.2022.06.007

233. Weller, R. B., Macintyre, I. M., Melville, V., Farrugia, M., Feelisch, M., & Webb, D. J. (2022). The effect of daily UVA phototherapy for 2 weeks on clinic and 24-h blood pressure in individuals with mild hypertension. *Journal of Human Hypertension*. https://doi.org/10.1038/s41371-022-00729-2

234. Huang, L., Schmid, K. L., Yin, X. N., Zhang, J., Wu, J., Yang, G., Ruan, Z. L., Jiang, X. Q., Wu, C. A., & Chen, W. Q. (2021). Combination effect of outdoor activity and screen exposure on risk of preschool myopia: Findings from Longhua Child Cohort Study. *Frontiers in Public Health, 9*, 607911. https://doi.org/10.3389/fpubh.2021.607911

235. Enthoven, C. A., Tideman, J. W. L., Polling, J. R., Yang-Huang, J., Raat, H., & Klaver, C. C. W. (2020). The impact of computer use on myopia development in childhood: The Generation R study. *Preventive Medicine, 132*, 105988. https://doi.org/10.1016/j.ypmed.2020.105988

236. Lingham, G., Yazar, S., Lucas, R. M., Milne, E., Hewitt, A. W., Hammond, C. J., MacGregor, S., Rose, K. A., Chen, F. K., He, M., Guggenheim, J. A., Clarke, M. W., Saw, S. M., Williams, C., Coroneo, M. T., Straker, L., & Mackey, D. A. (2021). Time spent outdoors in childhood is associated with reduced risk of myopia as an adult. *Scientific Reports, 11*(1), 6337. https://doi.org/10.1038/s41598-021-85825-y

237. Lee, S. S.-Y., Lingham, G., Sanfilippo, P. G., Hammond, C. J., Saw, S.-M., Guggenheim, J. A., Yazar, S., & Mackey, D. A. (2022). Incidence and progression of myopia in early adulthood. *JAMA Ophthalmology, 140*(2), 162-169. https://doi.org/10.1001/jamaophthalmol.2021.5067

238. Li, M., Lanca, C., Tan, C. S., Foo, L. L., Sun, C. H., Yap, F., Najjar, R. P., Sabanayagam, C., & Saw, S. M. (2021). Association of time outdoors and patterns of light exposure with myopia in children. *British Journal of Ophthalmology*, epub ahead of print. https://doi.org/10.1136/bjophthalmol-2021-318918

239. Yang, X., Yang, Y., Wang, Y., Wei, Q., Ding, H., & Zhong, X. (2021). Protective effects of sunlight exposure against PRK-induced myopia in infant rhesus monkeys. *Ophthalmic and Physiological Optics, 41*(4), 911-921. https://doi.org/10.1111/opo.12826

240. Lingham, G., Mackey, D. A., Lucas, R., & Yazar, S. (2020). How does spending time outdoors protect against myopia? A review. *British Journal of Ophthalmology, 104*(5), 593-599. https://doi.org/10.1136/bjophthalmol-2019-314675

241. Langer-Gould, A., Lucas, R., Xiang, A. H., Chen, L. H., Wu, J., Gonzalez, E., Haraszti, S., Smith, J. B., Quach, H., & Barcellos, L. F. (2018). MS Sunshine Study: Sun exposure but not vitamin D is associated with multiple sclerosis risk in Blacks and Hispanics. *Nutrients, 10*(3), 268. https://doi.org/10.3390/nu10030268

242. Magalhaes, S., Pugliatti, M., Riise, T., Myhr, K. M., Ciampi, A., Bjornevik, K., & Wolfson, C. (2019). Shedding light on the link between early life sun exposure and risk of multiple sclerosis: results from the EnvIMS Study. *International Journal of Epidemiology, 48*(4), 1073-1082. https://doi.org/10.1093/ije/dyy269

243. Sebastian, P., Cherbuin, N., Barcellos, L. F., Roalstad, S., Casper, C., Hart, J., Aaen, G. S., Krupp, L., Benson, L., Gorman, M., Candee, M., Chitnis, T., Goyal, M., Greenberg, B., Mar, S., Rodriguez, M., Rubin, J., Schreiner, T., Waldman, A., Weinstock-Guttman, B., et al. (2022). Association between time spent outdoors and risk of multiple sclerosis. *Neurology, 98*(3), e267-e278. https://doi.org/10.1212/WNL.0000000000013045

244. Ostkamp, P., Salmen, A., Pignolet, B., Goerlich, D., Andlauer, T. F. M., Schulte-Mecklenbeck, A., Gonzalez-Escamilla, G., Bucciarelli, F., Gennero, I., Breuer, J., Antony, G., Schneider-Hohendorf, T., Mykicki, N., Bayas, A., Bergh, F. T., Bittner, S., Hartung, H.-P., Friese, M. A., Linker, R. A., Luessi, F., et al. (2021). Sunlight exposure exerts immunomodulatory effects to reduce multiple sclerosis severity. *Proceedings of the National Academy of Sciences of the United States of America, 118*(1), e2018457118. https://doi.org/10.1073/pnas.2018457118

245. Chapman, C., Lucas, R. M., Ponsonby, A. L., Taylor, B., & Ausimmune Investigator, G. (2022). Predictors of progression from a first demyelinating event to clinically definite multiple sclerosis. *Brain Communications, 4*(4), fcac181. https://doi.org/10.1093/braincomms/fcac181

246. Hart, P. H., Jones, A. P., Trend, S., Cha, L., Fabis-Pedrini, M. J., Cooper, M. N., d'Este, C., Geldenhuys, S., Carroll, W. M., Byrne, S. N., Booth, D. R., Cole, J. M., Lucas, R. M., & Kermode, A. G. (2018). A randomised, controlled clinical trial of narrowband UVB phototherapy for clinically isolated syndrome: The PhoCIS study. *Multiple Sclerosis Journal - Experimental, Translational and Clinical, 4*(2), 2055217318773112. https://doi.org/10.1177/2055217318773112

247. Trend, S., Jones, A. P., Cha, L., Cooper, M. N., Geldenhuys, S., Fabis-Pedrini, M. J., Carroll, W. M., Cole, J. M., Booth, D. R., Lucas, R. M., French, M. A., Byrne, S. N., Kermode, A. G., & Hart, P. H. (2019). Short-term changes in frequencies of circulating leukocytes associated with narrowband UVB phototherapy in people with clinically isolated syndrome. *Scientific Reports, 9*(1), 7980. https://doi.org/10.1038/s41598-019-44488-6

248. Trend, S., Leffler, J., Cooper, M. N., Byrne, S. N., Kermode, A. G., French, M. A., & Hart, P. H. (2020). Narrowband UVB phototherapy reduces TNF production by B cell subsets stimulated via TLR7 from individuals with early multiple sclerosis. *Clinical & Translational Immunology, 9*(10), e1197-n/a. https://doi.org/10.1002/cti2.1197

249. Miller, K. M., Hart, P. H., Lucas, R. M., Davis, E. A., & de Klerk, N. H. (2021). Higher ultraviolet radiation during early life is associated with lower risk of childhood type 1 diabetes among boys. *Scientific Reports, 11*(1), 18597. https://doi.org/10.1038/s41598-021-97469-z

250. Megaw, L., Clemens, T., Daras, K., Weller, R. B., Dibben, C., & Stock, S. J. (2021). Higher sun exposure in the first trimester Is associated with reduced preterm birth. A Scottish population cohort study using linked maternity and meteorological records. *Frontiers in Reproductive Health, 3*. https://doi.org/10.3389/frph.2021.674245

251. Hastie, C. E., Mackay, D. F., Clemens, T. L., Cherrie, M. P. C., King, A., Dibben, C., & Pell, J. P. (2019). Antenatal exposure to solar radiation and learning disabilities: Population cohort study of 422,512 children. *Scientific Reports, 9*(1), 9356-9356. https://doi.org/10.1038/s41598-019-45562-9

252. Chersich, M. F., Pham, M. D., Areal, A., Haghighi, M. M., Manyuchi, A., Swift, C. P., Wernecke, B., Robinson, M., Hetem, R., Boeckmann, M., & Hajat, S. (2020). Associations between high temperatures in pregnancy and risk of preterm birth, low birth weight, and stillbirths: systematic review and meta-analysis. *BMJ-British Medical Journal, 371*, m3811. https://doi.org/10.1136/bmj.m3811

253. Sun, S., Weinberger, K. R., Spangler, K. R., Eliot, M. N., Braun, J. M., & Wellenius, G. A. (2019). Ambient temperature and preterm birth: A retrospective study of 32 million US singleton births. *Environment International, 126*, 7-13. https://doi.org/10.1016/j.envint.2019.02.023

254. Yardman-Frank, J. M., & Fisher, D. E. (2021). Skin pigmentation and its control: From ultraviolet radiation to stem cells. *Experimental Dermatology, 30*(4), 560-571. https://doi.org/10.1111/exd.14260

255. Lambert, G. W., Reid, C., Kaye, D. M., Jennings, G. L., & Esler, M. D. (2002). Effect of sunlight and season on serotonin turnover in the brain. *Lancet, 360*(9348), 1840-1842. https://doi.org/10.1016/s0140-6736(02)11737-5

256. Wirz-Justice, A., Skene, D. J., & Münch, M. (2021). The relevance of daylight for humans. *Biochemical Pharmacology, 191*, 114304. https://doi.org/10.1016/j.bcp.2020.114304

257. Wang, S.-J., & Chen, M.-Y. (2020). The effects of sunlight exposure therapy on the improvement of depression and quality of life in post-stroke patients: A RCT study. *Heliyon, 6*(7), e04379-e04379. https://doi.org/10.1016/j.heliyon.2020.e04379

258. Wang, N., Chen, Y., Ji, J., Chang, J., Yu, S., & Yu, B. (2020). The relationship between serum vitamin D and fracture risk in the elderly: a meta-analysis. *Journal of Orthopaedic Surgery and Research, 15*(1), 81-81. https://doi.org/10.1186/s13018-020-01603-y

259. Neale, R. E., Wilson, L. F., Black, L. J., Waterhouse, M., Lucas, R. M., & Gordon, L. G. (2021). Hospitalisations for falls and hip fractures attributable to vitamin D deficiency in older Australians. *British Journal of Nutrition, 126*(11), 1682-1686. https://doi.org/10.1017/S0007114521000416

260. Annweiler, C., & Beauchet, O. (2015). Questioning vitamin D status of elderly fallers and nonfallers: a meta-analysis to address a 'forgotten step'. *Journal of Internal Medicine, 277*(1), 16-44. https://doi.org/10.1111/joim.12250

261. Ling, Y., Xu, F., Xia, X., Dai, D., Xiong, A., Sun, R., Qiu, L., & Xie, Z. (2021). Vitamin D supplementation reduces the risk of fall in the vitamin D deficient elderly: An updated meta-analysis. *Clinical Nutrition, 40*(11), 5531-5537. https://doi.org/10.1016/j.clnu.2021.09.031

262. Chakhtoura, M., Bacha, D. S., Gharios, C., Ajjour, S., Assaad, M., Jabbour, Y., Kahale, F., Bassatne, A., Antoun, S., Akl, E. A., Bouillon, R., Lips, P., Ebeling, P. R., & el-Hajj Fuleihan, G. (2022). Vitamin D supplementation and fractures in adults: A systematic umbrella review of meta-analyses of controlled trials. *Journal of Clinical Endocrinology & Metabolism, 107*(3), 882-898. https://doi.org/10.1210/clinem/dgab742

263. LeBoff, M. S., Chou, S. H., Ratliff, K. A., Cook, N. R., Khurana, B., Kim, E., Cawthon, P. M., Bauer, D. C., Black, D., Gallagher, J. C., Lee, I. M., Buring, J. E., & Manson, J. E. (2022). Supplemental vitamin D and incident fractures in midlife and older adults. *The New England Journal of Medicine, 387*(4), 299-309. https://doi.org/10.1056/NEJMoa2202106

264. Li, H., Sun, D., Wang, A., Pan, H., Feng, W., Ng, C. H., Ungvari, G. S., Tao, L., Li, X., Wang, W., Xiang, Y.-T., & Guo, X. (2019). Serum 25-hydroxyvitamin D levels and depression in older adults: A dose–response meta-analysis of prospective cohort studies. *American Journal of Geriatric Psychiatry, 27*(11), 1192-1202. https://doi.org/10.1016/j.jagp.2019.05.022

265. Libuda, L., Laabs, B.-H., Ludwig, C., Bühlmeier, J., Antel, J., Hinney, A., Naaresh, R., Föcker, M., Hebebrand, J., König, I. R., & Peters, T. (2019). Vitamin D and the risk of depression: A causal relationship? Findings from a Mendelian randomization study. *Nutrients, 11*(5), 1085. https://doi.org/10.3390/nu11051085

266. Arathimos, R., Ronaldson, A., Howe, L. J., Fabbri, C., Hagenaars, S., Hotopf, M., Gaughran, F., Lewis, C. M., & Dregan, A. (2021). Vitamin D and the risk of treatment-resistant and atypical depression: A Mendelian randomization study. T*ranslational Psychiatry, 11*(1), 561-561. https://doi.org/10.1038/s41398-021-01674-3

267. Cheng, Y. C., Huang, Y. C., & Huang, W. L. (2020). The effect of vitamin D supplement on negative emotions: A systematic review and meta analysis. *Depression and Anxiety, 37*(6), 549-564. https://doi.org/10.1002/da.23025

268. Okereke, O. I., Reynolds, C. F., Mischoulon, D., Chang, G., Vyas, C. M., Cook, N. R., Weinberg, A., Bubes, V., Copeland, T., Friedenberg, G., Lee, I. M., Buring, J. E., & Manson, J. E. (2020). Effect of long-term vitamin D_3 supplementation vs placebo on risk of depression or clinically relevant depressive symptoms and on change in mood scores: A randomized clinical trial. JAMA. *Journal of the American Medical Association, 324*(5), 471-480. https://doi.org/10.1001/jama.2020.10224

269. Zheng, J.-S., Luan, J. a., Sofianopoulou, E., Sharp, S. J., Day, F. R., Imamura, F., Gundersen, T. E., Lotta, L. A., Sluijs, I., Stewart, I. D., Shah, R. L., van der Schouw, Y. T., Wheeler, E., Ardanaz, E., Boeing, H., Dorronsoro, M., Dahm, C. C., Dimou, N., El-Fatouhi, D., Franks, P. W., et al. (2020). The association between circulating 25-hydroxyvitamin D metabolites and type 2 diabetes in European populations: A meta-analysis and Mendelian randomisation analysis. *PLoS Medicine, 17*(10), e1003394-e1003394. https://doi.org/10.1371/journal.pmed.1003394

270. Wang, N., Wang, C., Chen, X., Wan, H., Chen, Y., Chen, C., Han, B., & Lu, Y. (2019). Vitamin D, prediabetes and type 2 diabetes: bidirectional Mendelian randomization analysis. *European Journal of Nutrition, 59*(4), 1379-1388. https://doi.org/10.1007/s00394-019-01990-x

271. Pittas, A. G., Dawson-Hughes, B., Sheehan, P., Ware, J. H., Knowler, W. C., Aroda, V. R., Brodsky, I., Ceglia, L., Chadha, C., Chatterjee, R., Desouza, C., Dolor, R., Foreyt, J., Fuss, P., Ghazi, A., Hsia, D. S., Johnson, K. C., Kashyap, S. R., Kim, S., LeBlanc, E. S., et al. (2019). Vitamin D supplementation and prevention of type 2 diabetes. *The New England Journal of Medicine, 381*(6), 520-530. https://doi.org/10.1056/NEJMoa1900906

272. Pittas, A., Dawson-Hughes, B., & Staten, M. (2019). Vitamin D supplementation and prevention of type 2 diabetes. Reply. *The New England Journal of Medicine, 381*(18), 1785-1786. https://doi.org/10.1056/NEJMc1912185

273. Tang, H., Li, D., Li, Y., Zhang, X., Song, Y., & Li, X. (2018). Effects of vitamin D supplementation on glucose and insulin homeostasis and incident diabetes among nondiabetic adults: A meta-analysis of randomized controlled trials. *International Journal of Endocrinology, 2018*, 7908764-7908769. https://doi.org/10.1155/2018/7908764

274. Dhamrait, G. K., Panchal, K., Fleury, N. J., Abel, T. N., Ancliffe, M. K., Crew, R. C., Croft, K., Fernandez, B. O., Minnion, M., Hart, P. H., Lucas, R. M., Mark, P. J., Feelisch, M., Weller, R. B., Matthews, V., & Gorman, S. (2019). Characterising nitric oxide-mediated metabolic benefits of low-dose ultraviolet radiation in the mouse: a focus on brown adipose tissue. *Diabetologia, 63*(1), 179-193. https://doi.org/10.1007/s00125-019-05022-5

275. Sluyter, J. D., Manson, J. E., & Scragg, R. (2021). Vitamin D and clinical cancer outcomes: A review of meta analyses. J*BMR Plus, 5*(1), e10420-n/a. https://doi.org/10.1002/jbm4.10420

276. Ong, J.-S., Dixon-Suen, S. C., Han, X., An, J., Liyanage, U., Dusingize, J.-C., Schumacher, J., Gockel, I., Boehmer, A., Jankowski, J., Palles, C., O'Mara, T., Spurdle, A., Law, M. H., Iles, M. M., Pharoah, P., Berchuck, A., Zheng, W., Thrift, A. P., Olsen, C., et al. (2021). A comprehensive re-assessment of the association between vitamin D and cancer susceptibility using Mendelian randomization. *Nature Communications, 12*(1), 246-246. https://doi.org/10.1038/s41467-020-20368-w

277. Keum, N., Chen, Q. Y., Lee, D. H., Manson, J. E., & Giovannucci, E. (2022). Vitamin D supplementation and total cancer incidence and mortality by daily vs. infrequent large-bolus dosing strategies: a meta-analysis of randomised controlled trials. *British Journal of Cancer, 127*(5), 872-878. https://doi.org/10.1038/s41416-022-01850-2

278. Sintzel, M. B., Rametta, M., & Reder, A. T. (2018). Vitamin D and multiple sclerosis: A comprehensive review. *Neurology and Therapy, 7*(1), 59-85. https://doi.org/10.1007/s40120-017-0086-4

279. Jiang, X., Ge, T., & Chen, C.-Y. (2021). The causal role of circulating vitamin D concentrations in human complex traits and diseases: a large-scale Mendelian randomization study. *Scientific Reports, 11*(1), 184-184. https://doi.org/10.1038/s41598-020-80655-w

280. Manousaki, D., Harroud, A., Mitchell, R. E., Ross, S., Forgetta, V., Timpson, N. J., Smith, G. D., Polychronakos, C., & Richards, J. B. (2021). Vitamin D levels and risk of type 1 diabetes: A Mendelian randomization study. *PLoS Medicine, 18*(2), e1003536-e1003536. https://doi.org/10.1371/journal.pmed.1003536

281. Pham, H., Rahman, A., Majidi, A., Waterhouse, M., & Neale, R. E. (2019). Acute respiratory tract infection and 25-hydroxyvitamin D concentration: A systematic review and meta-analysis. I*nternational Journal of Environmental Research and Public Health, 16*(17), 3020. https://doi.org/10.3390/ijerph16173020

282. Jolliffe, D. A., Camargo, C. A., Sluyter, J. D., Aglipay, M., Aloia, J. F., Ganmaa, D., Bergman, P., Bischoff-Ferrari, H. A., Borzutzky, A., Damsgaard, C. T., Dubnov-Raz, G., Esposito, S., Gilham, C., Ginde, A. A., Golan-Tripto, I., Goodall, E. C., Grant, C. C., Griffiths, C. J., Hibbs, A. M., Janssens, W., et al. (2021). Vitamin D supplementation to prevent acute respiratory infections: a systematic review and meta-analysis of aggregate data from randomised controlled trials. *The Lancet Diabetes & Endocrinology, 9*(5), 276-292. https://doi.org/10.1016/S2213-8587(21)00051-6

283. Çolak, Y., Nordestgaard, B. G., & Afzal, S. (2021). Low vitamin D and risk of bacterial pneumonias: Mendelian randomisation studies in two population-based cohorts. *Thorax, 76*(5), 468-478. https://doi.org/10.1136/thoraxjnl-2020-215288

284. Pham, H., Waterhouse, M., Baxter, C., Duarte Romero, B., McLeod, D. S. A., Armstrong, B. K., Ebeling, P. R., English, D. R., Hartel, G., Kimlin, M. G., Martineau, A. R., O'Connell, R., van der Pols, J. C., Venn, A. J., Webb, P. M., Whiteman, D. C., & Neale, R. E. (2021). The effect of vitamin D supplementation on acute respiratory tract infection in older Australian adults: an analysis of data from the D-Health Trial. *The Lancet Diabetes & Endocrinology, 9*(2), 69-81. https://doi.org/10.1016/S2213-8587(20)30380-6

285. Emerging Risk Factors Collaboration/EPIC-CVD/Vitamin D Studies Collaboration (2021). Estimating dose-response relationships for vitamin D with coronary heart disease, stroke, and all-cause mortality: observational and Mendelian randomisation analyses. *The Lancet Diabetes & Endocrinology, 9*(12), 837-846. https://doi.org/10.1016/S2213-8587(21)00263-1

286. Young, A. R., Morgan, K. A., Harrison, G., Lawrence, K. P., Petersen, B., Wulf, H. C., & Philipsen, P. A. (2021). A revised action spectrum for vitamin D synthesis by suberythemal UV radiation exposure in humans in vivo. *Proceedings of the National Academy of Sciences of the United States of America, 118*(40), e2015867118. https://doi.org/10.1073/pnas.2015867118

287. Al Zarooni, A. A. R., Nagelkerke, N., Al Marzouqi, F. I., & Al Darmaki, S. H. (2022). Risk factors for vitamin D deficiency in Abu Dhabi Emirati population. *PLoS One, 17*(2), e0264064-e0264064. https://doi.org/10.1371/journal.pone.0264064

288. Al-Yatama, F. I., AlOtaibi, F., Al-Bader, M. D., & Al-Shoumer, K. A. (2019). The effect of clothing on vitamin D status, bone turnover markers, and bone mineral density in young Kuwaiti females. *International Journal of Endocrinology, 2019*, 6794837-6794810. https://doi.org/10.1155/2019/6794837

289. Passeron, T., Bouillon, R., Callender, V., Cestari, T., Diepgen, T. L., Green, A. C., van der Pols, J. C., Bernard, B. A., Ly, F., Bernerd, F., Marrot, L., Nielsen, M., Verschoore, M., Jablonski, N. G., & Young, A. R. (2019). Sunscreen photoprotection and vitamin D status. *British Journal of Dermatology, 181*(5), 916-931. https://doi.org/10.1111/bjd.17992

290. Neale, R. E., Khan, S. R., Lucas, R. M., Waterhouse, M., Whiteman, D. C., & Olsen, C. M. (2019). The effect of sunscreen on vitamin D: a review. *British Journal of Dermatology, 181*(5), 907-915. https://doi.org/10.1111/bjd.17980

291. Fayet-Moore, F., Brock, K. E., Wright, J., Ridges, L., Small, P., Seibel, M. J., Conigrave, A. D., & Mason, R. S. (2019). Determinants of vitamin D status of healthy office workers in Sydney, Australia. *Journal of Steroid Biochemistry and Molecular Biology, 189*, 127-134. https://doi.org/10.1016/j.jsbmb.2019.02.017

292. Feketea, G. M., Bocsan, I. C., Tsiros, G., Voila, P., Stanciu, L. A., & Zdrenghea, M. (2021). Vitamin D status in children in Greece and its relationship with sunscreen application. *Children (Basel), 8*(2), 111. https://doi.org/10.3390/children8020111

293. Datta, P., Philipsen, P. A., Idorn, L. W., & Wulf, H. C. (2021). Low vitamin D in dark-skinned immigrants is mainly due to clothing habits and low UVR exposure: a Danish observational study. *Photochemical & Photobiological Sciences, 20*(12), 1573-1584. https://doi.org/10.1007/s43630-021-00115-w

294. Young, A. R., Morgan, K. A., Ho, T.-W., Ojimba, N., Harrison, G. I., Lawrence, K. P., Jakharia-Shah, N., Wulf, H. C., Cruickshank, J. K., & Philipsen, P. A. (2020). Melanin has a small inhibitory effect on cutaneous vitamin D synthesis: A comparison of extreme phenotypes. *Journal of Investigative Dermatology, 140*(7), 1418-1426.e1411. https://doi.org/10.1016/j.jid.2019.11.019

295. Neville, J. J., Palmieri, T., & Young, A. R. (2021). Physical determinants of vitamin D photosynthesis: A review. *JBMR Plus, 5*(1), e10460-n/a. https://doi.org/10.1002/jbm4.10460

296. Kraus, F. B., Medenwald, D., & Ludwig-Kraus, B. (2020). Do extreme summers increase blood vitamin D (25-hydroxyvitamin D) levels? *PLoS One, 15*(11), e0242230. https://doi.org/10.1371/journal.pone.0242230

297. Boyall, L., & Samingpai, B. (2021). Tourism in Antarctica. Accessed 25/9/2022.

298. Eleftheratos, K., Kapsomenakis, J., Zerefos, C., Bais, A., Fountoulakis, I., Dameris, M., Jöckel, P., Haslerud, A., Godin-Beekmann, S., Steinbrecht, W., Petropavlovskikh, I., Brogniez, C., Leblanc, T., Liley, J. B., Querel, R., & Swart, D. (2020). Possible effects of greenhouse gases to ozone profiles and DNA active UV-B irradiance at ground level. *Atmosphere, 11*(3), 228. https://doi.org/10.3390/atmos11030228

299. van der Leun, J. C., Piacentini, R. D., & de Gruijl, F. R. (2008). Climate change and human skin cancer. *Photochemical & Photobiological Sciences, 7*(6), 730-733. https://doi.org/10.1039/b719302e

300. Piacentini, R. D., Della Ceca, L. S., & Ipiña, A. (2018). Climate change and its relationship with non-melanoma skin cancers. *Photochemical & Photobiological Sciences, 17*(12), 1913-1917. https://doi.org/10.1039/c7pp00405b

APPENDIX

The effects of exposure to solar radiation on human health

R.E. Neale, R.M. Lucas, S.N. Byrne, L. Hollestein, L.E. Rhodes, S. Yazar, A.R. Young, M. Berwick, R.A. Ireland, and C. M. Olsen

Appendix Table 1. Prevalence of vitamin D deficiency from national studies and published peer-reviewed papers

Author, year [Publication number]	Location	Study years	Population	Assay	Season	n	Age	Percent vitamin D deficient (25(OH)D< 50 nmol/L)
Australian Bureau of Statistics [1]	Australia	2011-3	Random sample	LC-MS/MS	Year round	~11,000	5+ years	23.5
Black et al 2021 [12]	Australia		Nationally representative, Aboriginal and Torres Strait Islanders	LC-MS/MS		3250	adult	27.0
New Zealand Ministry of Health [6]	New Zealand	2008-9	Nationally representative	LC-MS/MS	Year round	3099	15+ yr	32.0
Yousef et al 2021 [2]	Canada	2012-5	Random sampling of dwellings	Diasorin Immunoassay	Year round	11,579	3-79 yr	36.4
Herrick et al 2019 [3]	United States	2011-4	NHANES – probability sample	LC-MS/MS	South in winter, north in summer	16,180	≥1 yr	18.3
Cashman et al 2013 [5]	Ireland	2019-20	Nationally representative	LC-MS/MS	Year round	246	13-18 yr	54.8
	Ireland	2008-10	Random selection	ELISA (OCTEIA) LC-MS/MS	Year round	1132	18+ yr	40.1 45.9

Study	Country	Year	Sampling	Assay	Season	N	Age	%
Cashman et al 2016 [14]	Denmark	2011-2	Regionally representative	Variable, but standardised to the Vitamin D standardisation program		779	8-12 yr	36.8
	Norway	2010-11	Regionally representative			939	15-18 yr	76.1
	Greece	2007-9	Regionally representative			806	9-14 yr	62.4
	Germany	2003-6	Nationally representative			10,015	1-17 yr	45.6
	Germany	2008-11	Nationally representative			6995	18-79 yr	56.0
	United Kingdom	2008-12	Nationally representative			511	1-18 yr	53.4
	United Kingdom	2008-12	Nationally representative			977	19-91 yr	57.9
	Netherlands	2006-7	Regionally representative			2627	40-66 yr	33.6
	Iceland	2002-6	Regionally representative			5519	66-96 yr	33.6
Lin et al 2021 [15]	United Kingdom	2006-10	UK Biobank	Diasorin Liaison	Year round	449,943	40-69 yr	32.3
Kim et al 2020 [4]	South Korea	2008-14	Randomly selected households	Diasorin RIA	Year round	46,405	18-80 yr	66.7
Chile Ministry of Health [7]	Chile	2016-7	Nationally representative	LC-MS/MS		5520	15-49 yr females	54.8
Mongolia National Center for Public Health [8]	Mongolia	2016-7	Nationally representative	Enzyme-linked fluorescence assay	Sept-Nov	1711	6-59 m	61.0
					Sept-Nov	377	15-49 yr men	40.4
					Sept-Nov	924	Pregnant women	75.4
Heere et al 2010 [9]	Fiji	2004	Nationally representative	Diasorin RIA	Winter (May-Sept)	511	15-54 yr females	11.0
Marzban et al 2021 [10]	Iran		Randomly selected households living in rural areas of the Persian Gulf	IDS-ELISA		1806	Adults	28.0
Duarte et al 2020 [11]	Portugal		Nationwide, random sample of people living in private households	ADVIA competitive immunoassay		3092	18+ yr	67.0
Beer et al, 2020 [13]	Colombia		National survey	ADVIA competitive immunoassay			All ages	24.0
							Toddlers	43.0
							Adolescents	20.0
Flores et al 2017 28241892	Mexico	2012	Nationally representative	Chemi-luminescent microparticle immunoassay	Year round	2695	1-4 yr	25.9
							5-11 yr	36.6

Gromova et al 2020 [16]	Kazakhstan	2018	Systematic random sampling from outpatient clinics in each region	Abbott chemi-luminescence microparticle immunoassay (CMIA)	Summer (May to Aug)	1347	Adults females	79.0
							Adult males	56.1
Chen et al 2017 [17]	China	2010-2013	Nationally representative	Diasorin RIA	Year round	6014	60+ yr	39.1
Hu et al 2017 [18]	China	2010-2013	Nationally representative	Diasorin RIA	Year round	14,473	6-17 yr	53.2
Nikooyeh et al 2021 [19]	Iran	2013-4	Nationally representative	Direct enzyme Immunoassay	Year round	1111	19-65 yr	Winter: 90.1 Summer: 69.2
Nikooyeh et al 2017 [20]	Iran	2013-4	Nationally representative	Direct enzyme Immunoassay	Year round	667	5-18 yr	Mid-Winter: 93.2
Poh et al 2013 [21]	Malaysia	2010-1	Nationally representative	Diasorin Liaison	Year round	2056	4-12 yr	47.5
Poh et al 2016 [22]	Malaysia	2010-1	Nationally representative	Diasorin Liaison	Year round	861	2+ yr	43.7
	Thailand			Diasorin Liaison		495		33.7
	Indonesia			Immunoassay		276		44.0
	Vietnam			HPLC		384		48.2
Bani et al 2022 [23]	Switzerland, Canton Ticino			Chemi-luminescence microparticle capture immunoassay (CMIA)		18,131	All	35.5
Al Zarooni 2019 [24]	Abu Dhabi Emirates	2011-2	Adults presenting to preventive health screening program clinics	Not provided	Year round	12,346	18+ yr	72.0
Latif Zainel et al 2019 [25]	Qatar	2017	Adults presenting to primary care clinics	Abbott immunoassay; multiple labs	Year round	102,342	18-65 yr	Not treated: 71.4 Previously treated: 53.4

Values in **purple** show those selected for the map displayed in Figure 5 (main text).

Appendix Table 2. Prevalence of vitamin D deficiency in South Asian countries (results from a meta-analysis) [26

| Country	Percent vitamin D deficient (25(OH)D< 50 nmol/L)	Heterogeneity	No. studies
Sri Lanka	48		1
Nepal	57		2
Bangladesh	67		5
Pakistan	73	High (18% to 99%)	18
India	67	High (18% to 99%)	39

Appendix Table 3. Prevalence of vitamin D deficiency in African countries (results from a meta-analysis) [27]

Country	Percent vitamin D deficient (25(OH)D< 50 nmol/L)	Population	No. studies
Tunisia (2)	68	Adults	2
Libya (1)	80	Adults	1
Egypt (5)	45	Adults	5
Sudan (1)	99	Adults	1
Ethiopia (4)	86	Adults	4
Uganda (1)	20	Adults	1
Kenya (1)	17	Adults	1
Seychelles (1)	8	Adults	1
Tanzania (3)	3	Adults	3
Zimbabwe (1)	2	1-2 year-olds (but said to be similar to adult levels)	1
South Africa (7)	31	Adults	7
Botswana (1)	17	<2 year-old without tuberculosis	1
Cameroon (1)	3.2	Adults	1
Nigeria (5)	25	Adults	5
Ghana (3)	14	Adults	3
Cote d'Ivoire (1)	9	Adults	1
Guinea-Bissau (1)	13	Adults	1
Morocco (2)	74	Adults	2
Algeria (1)	29.9 September 41.4 March	5-15 year-old children	1

APPENDIX FIGURE 1. UV RADIATION-INDUCED SIGNATURE MUTATIONS IN DNA DNA contains 4 amino acid bases (thymine (T), adenine (A), guanine (G), cytosine (C)), linked by a sugar phosphate backbone. DNA is in the form of a double helix with two anti-parallel strands, one running in the 5' (5-prime) to 3' direction, and the other in the 3' to 5' direction (5' and 3' refer to carbon molecules in the sugar backbone). Thymine and cytosine are pyrimidines; guanine and adenine are purines. Thymine binds (with a weak hydrogen bond) only to adenine, cytosine to only guanine. DNA is 'read' to construct proteins – the correct sequence of bases is critical to ensure the correct structure of the proteins synthesised.
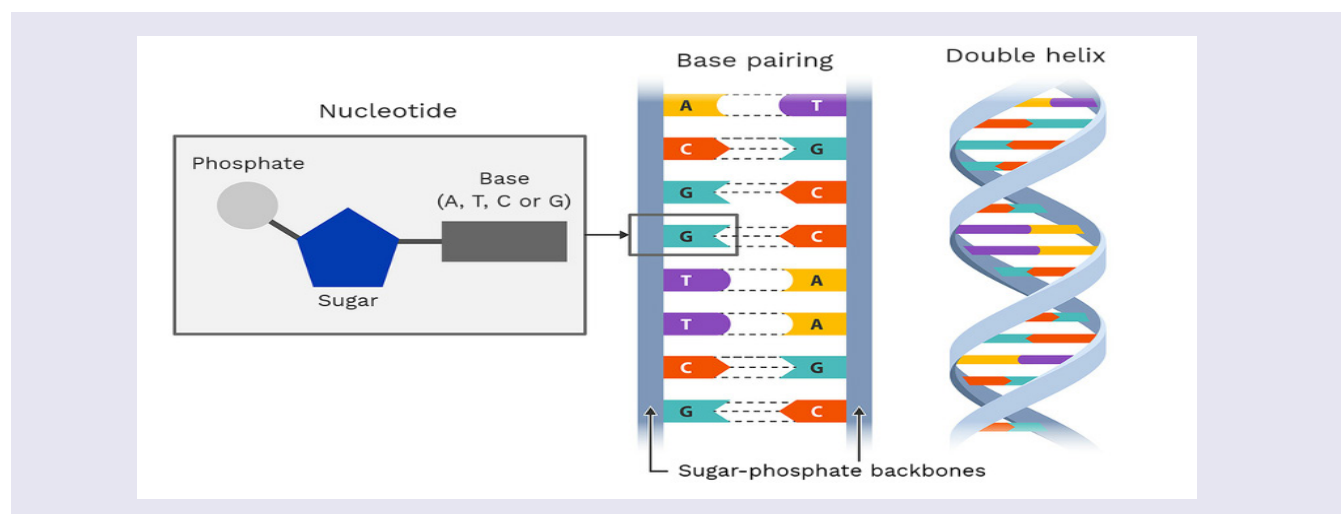
Nucleotides are composed of a sugar molecule, a phosphate group, and a base. TpC refers to two adjacent nucleotides, where a thymine nucleotide is followed by a cytosine nucleotide in the sequence going from the 5' to the 3' direction (for example in the red circle above), and similarly, CpC describes a cytosine followed by a cytosine in the 5' to 3' direction.

Absorption of UV-B radiation by DNA can cause adjacent thymine bases to 'join up' to form a thymine dimer (a form of cyclobutane pyrimidine dimer (CPD)).
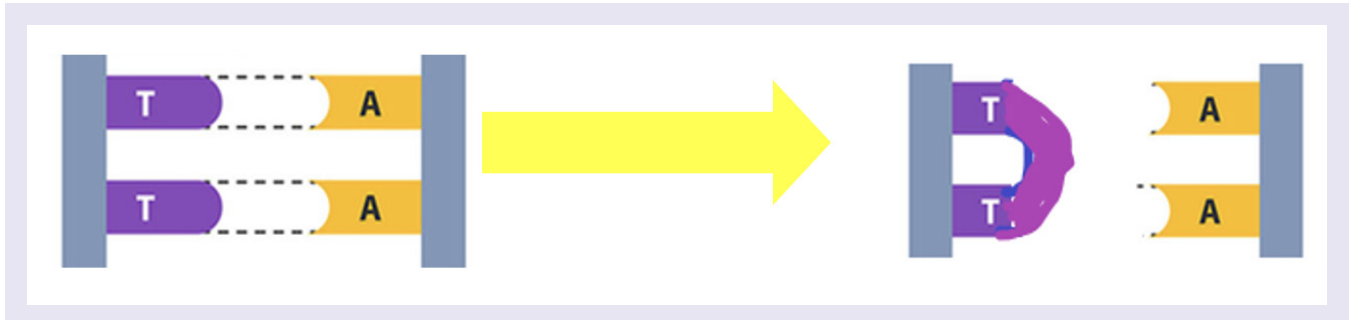
If thymine dimers are not repaired, the result can be death of the cell. Repair enzymes can locate the CPD, remove it, and use the other DNA strand as a guide to repair the DNA correctly. However, faulty DNA repair can lead to the original cytosine (C) base being replaced by a thymine base (T), resulting in a permanent change in the sequence of bases for that strand of DNA; i.e., a UV signature mutation. Mutations result in incorrect "reading" of DNA and production of abnormal proteins.

- a C>T transition at a TpC dinucleotide (see red circled area above) due to faulty DNA repair of a T-T dimer.
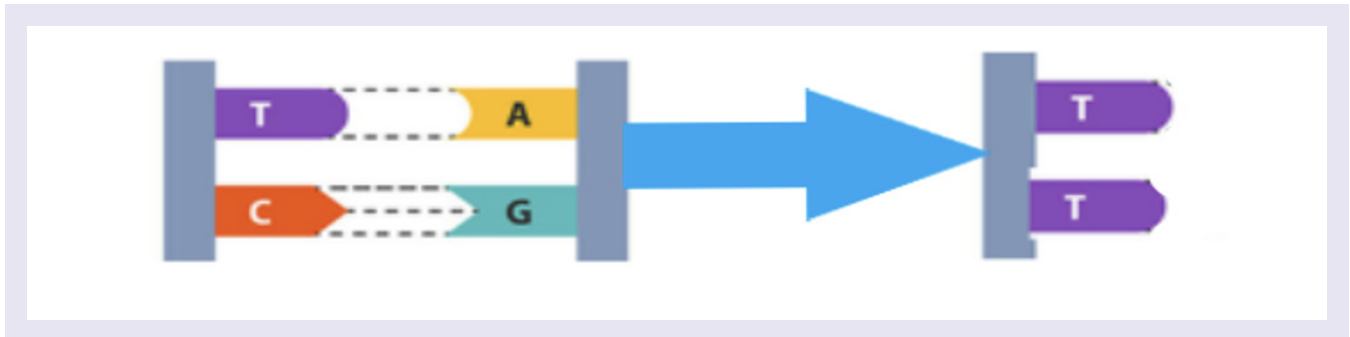
- a C>T transition at a CpC dinucleotide (either the first or second cytosine replaced, CpC and CpC, respectively) due to faulty DNA repair of UV-induced DNA damage.
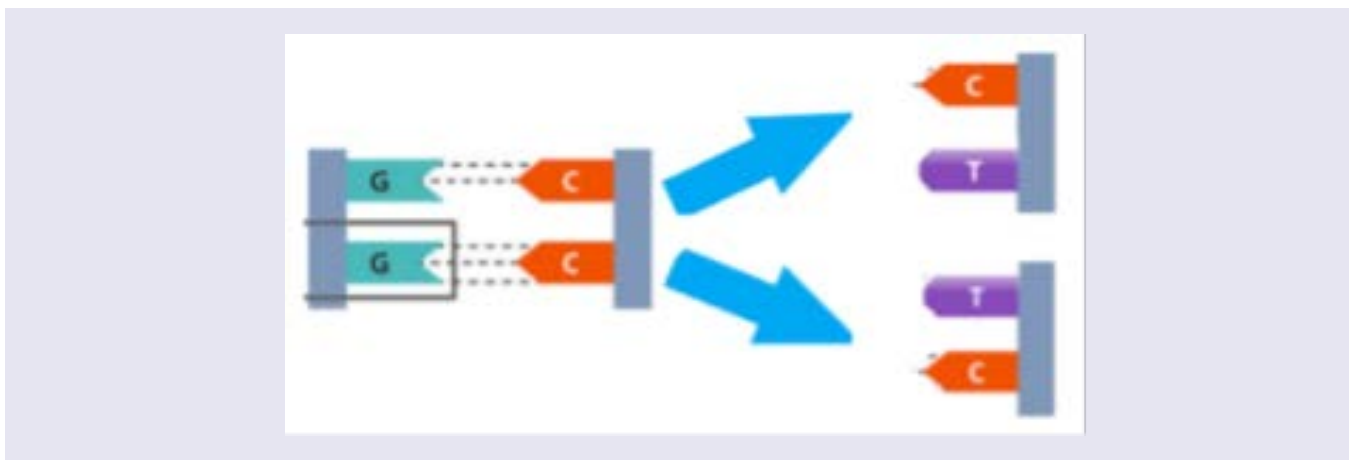
References

1. Australian Bureau of Statistics. The Australian Health Survey 2011-2013: Updated results, https://www.abs.gov.au/ausstats/abs@.nsf/Lookup/4364.0.55.003main+features12011-2012

2. Yousef, S., Manuel, D., Colman, I., Papadimitropoulos, M., Hossain, A., Faris, M., & Wells, G. A. (2021). Vitamin D status among first-generation immigrants from different ethnic groups and origins: An observational study using the Canadian Health Measures Survey. *Nutrients, 13*(8), https://doi.org/10.3390/nu13082702

3. Herrick, K. A., Storandt, R. J., Afful, J., Pfeiffer, C. M., Schleicher, R. L., Gahche, J. J., & Potischman, N. (2019). Vitamin D status in the United States, 2011-2014. *American Journal of Clinical Nutrition, 110*(1), 150-157, https://doi.org/10.1093/ajcn/nqz037

4. Kim, S. Y., Lee, M. H., Lim, W. J., Kim, S. I., & Lee, Y. J. (2020). Associations of 25-hydroxyvitamin D levels and arthritis with sleep duration: the Korean national health and nutrition examination survey 2008-2014. *Nature and Science of Sleep, 12*, 883-894, https://doi.org/10.2147/NSS.S275464

5. Cashman, K. D., Muldowney, S., McNulty, B., Nugent, A., FitzGerald, A. P., Kiely, M., Walton, J., Gibney, M. J., & Flynn, A. (2013). Vitamin D status of Irish adults: findings from the National Adult Nutrition Survey. *British Journal of Nutrition, 109*(7), 1248-1256, https://doi.org/10.1017/S0007114512003212

6. Ministry of Health (2012). Vitamin D status of New Zealand Adults: Findings from the 2008/09 New Zealand Adult Nutrition Survey. Wellington: Ministry of Health. https://www.health.govt.nz/publications/vitamin%20d%20status%20of%20new%20zealand%20adults

7. Chile Ministry of Health (2017). National Health Survey 2016/2017. http://epi.minsal.cl/wp-content/uploads/2018/03/Resultados-Vitamina-D.pdf. Accessed 11 October 2022.

8. National Center for Public Health (2017). Nutrition status of the population of Mongolia: Fifth National Health Survey report, https://www.unicef.org/mongolia/media/1116/file/NNS_V_undsen_tailan_EN.pdf

9. Heere, C., Skeaff, C. M., Waqatakirewa, L., Vatucawaqa, P., Khan, A. N., & Green, T. J. (2010). Serum 25-hydroxyvitamin D concentration of Indigenous-Fijian and Fijian-Indian women. *Asia Pacific Journal of Clinical Nutrition, 19*(1), 43-48.

10. Marzban, M., Kalantarhormozi, M., Mahmudpour, M., Ostovar, A., Keshmiri, S., Darabi, A. H., Khajeian, A., Bolkheir, A., Amini, A., & Nabipour, I. (2021). Prevalence of vitamin D deficiency and its associated risk factors among rural population of the northern part of the Persian Gulf. *BMC Endocrine Disorders, 21*(1), 219, https://doi.org/10.1186/s12902-021-00877-5

11. Duarte, C., Carvalheiro, H., Rodrigues, A. M., Dias, S. S., Marques, A., Santiago, T., Canhão, H., Branco, J. C., & da Silva, J. A. P. (2020). Prevalence of vitamin D deficiency and its predictors in the Portuguese population: a nationwide population-based study. *Archives of Osteoporosis, 15*(1), 36-36, https://doi.org/10.1007/s11657-020-0695-x

12. Black, L. J., Dunlop, E., Lucas, R. M., Pearson, G., Farrant, B., & Shepherd, C. C. J. (2021). Prevalence and predictors of vitamin D deficiency in a nationally representative sample of Australian Aboriginal and Torres Strait Islander adults. *British Journal of Nutrition, 126*(1), 101-109, https://doi.org/10.1017/S0007114520003931

13. Beer, R. J., Herran, O. F., & Villamor, E. (2020). Prevalence and correlates of vitamin D deficiency in a tropical setting: results from a nationally representative survey. *American Journal of Clinical Nutrition, 112*(4), 1088-1098, https://doi.org/10.1093/ajcn/nqaa197

14. Cashman, K. D., Dowling, K. G., Skrabakova, Z., Gonzalez-Gross, M., Valtuena, J., De Henauw, S., Moreno, L., Damsgaard, C. T., Michaelsen, K. F., Molgaard, C., Jorde, R., Grimnes, G., Moschonis, G., Mavrogianni, C., Manios, Y., Thamm, M., Mensink, G. B., Rabenberg, M., Busch, M. A., Cox, L., Meadows, S., Goldberg, G., Prentice, A., Dekker, J. M., Nijpels, G., Pilz, S., Swart, K. M., van Schoor, N. M., Lips, P., Eiriksdottir, G., Gudnason, V., Cotch, M. F., Koskinen, S., Lamberg-Allardt, C., Durazo-Arvizu, R. A., Sempos, C. T., & Kiely, M. (2016). Vitamin D deficiency in Europe: pandemic? *American Journal of Clinical Nutrition, 103*(4), 1033-1044, https://doi.org/10.3945/ajcn.115.120873

15. Lin, L. Y., Smeeth, L., Langan, S., & Warren-Gash, C. (2021). Distribution of vitamin D status in the UK: a cross-sectional analysis of UK Biobank. *BMJ Open, 11*(1), e038503, https://doi.org/10.1136/bmjopen-2020-038503

16. Gromova, O., Doschanova, A., Lokshin, V., Tuletova, A., Grebennikova, G., Daniyarova, L., Kaishibayeva, G., Nurpeissov, T., Khan, V., Semenova, Y., Chibisova, A., Suzdalskaya, N., Aitaly, Z., & Glushkova, N. (2020). Vitamin D deficiency in Kazakhstan: Cross-Sectional study. *Journal of Steroid Biochemistry and Molecular Biology, 199*, 105565, https://doi.org/10.1016/j.jsbmb.2019.105565

17. Chen, J., Yun, C., He, Y., Piao, J., Yang, L., & Yang, X. (2017). Vitamin D status among the elderly Chinese population: a cross-sectional analysis of the 2010-2013 China national nutrition and health survey (CNNHS). *Nutrition Journal, 16*(1), 3, https://doi.org/10.1186/s12937-016-0224-3

18. Hu, Y., Chen, J., Wang, R., Li, M., Yun, C., Li, W., Yang, Y., Piao, J., Yang, X., & Yang, L. (2017). Vitamin D nutritional status and its related factors for Chinese children and adolescents in 2010-2012. *Nutrients, 9*(9), https://doi.org/10.3390/nu9091024

19. Nikooyeh, B., Abdollahi, Z., Shariatzadeh, N., Kalayi, A., Zahedirad, M., & Neyestani, T. (2021). Effect of latitude on seasonal variations of vitamin D and some cardiometabolic risk factors: national food and nutrition surveillance. *Eastern Mediterranean Health Journal, 27*(3), 269-278, https://doi.org/10.26719/emhj.20.119

20. Nikooyeh, B., Abdollahi, Z., Hajifaraji, M., Alavi-Majd, H., Salehi, F., Yarparvar, A. H., & Neyestani, T. R. (2017). Vitamin D status, latitude and their associations with some health parameters in children: National food and nutrition surveillance. *Journal of Tropical Pediatrics, 63*(1), 57-64, https://doi.org/10.1093/tropej/fmw057

21. Poh, B. K., Ng, B. K., Siti Haslinda, M. D., Nik Shanita, S., Wong, J. E., Budin, S. B., Ruzita, A. T., Ng, L. O., Khouw, I., & Norimah, A. K. (2013). Nutritional status and dietary intakes of children aged 6 months to 12 years: findings of the Nutrition Survey of Malaysian Children (SEANUTS Malaysia). *British Journal of Nutrition, 110 Suppl 3*, S21-35, https://doi.org/10.1017/S0007114513002092

22. Poh, B. K., Rojroongwasinkul, N., Nguyen, B. K., Sandjaja, Ruzita, A. T., Yamborisut, U., Hong, T. N., Ernawati, F., Deurenberg, P., Parikh, P., & Group, S. S. (2016). 25-hydroxy-vitamin D demography and the risk of vitamin D insufficiency in the South East Asian Nutrition Surveys (SEANUTS). *Asia Pacific Journal of Clinical Nutrition, 25*(3), 538-548, https://doi.org/10.6133/apjcn.092015.02

23. Bani, P., Cingari, S., & Mathis, B. (2022). Study on the prevalence of vitamin D deficiency in the population of Canton Ticino. *La Rivista Italiana della Medicina di Laboratorio, 18*(1), 18-21, https://doi.org/10.23736/S1825-859X.22.00136-0

24. Al Zarooni, A. A. R., Al Marzouqi, F. I., Al Darmaki, S. H., Prinsloo, E. A. M., & Nagelkerke, N. (2019). Prevalence of vitamin D deficiency and associated comorbidities among Abu Dhabi Emirates population. *BMC Research Notes, 12*(1), 503, https://doi.org/10.1186/s13104-019-4536-1

25. Zainel, A. A. L., Qotba, H., Al Nuaimi, A., & Syed, M. (2019). Vitamin D status among adults (18-65 years old) attending primary healthcare centres in Qatar: a cross-sectional analysis of the Electronic Medical Records for the year 2017. *BMJ Open, 9*(8), e029334, https://doi.org/10.1136/bmjopen-2019-029334

26. Siddiqee, M. H., Bhattacharjee, B., Siddiqi, U. R., & MeshbahurRahman, M. (2021). High prevalence of vitamin D deficiency among the South Asian adults: a systematic review and meta-analysis. *BMC Public Health, 21*(1), 1823, https://doi.org/10.1186/s12889-021-11888-1

27. Mogire, R., Mutua, A., Kimita, W., Kamau, A., Bejon, P., Pettifor, J., Adeyemo, A., Williams, T., & Atkinson, S. (2020). Prevalence of vitamin D deficiency in Africa: a systematic review and meta-analysis. *The Lancet Global Health, 8*(1), e134-e142, https://doi.org/10.1016/S2214-109X(19)30457-7

4

INTERACTIVE EFFECTS OF CHANGES IN UV RADIATION AND CLIMATE ON TERRESTRIAL ECOSYSTEMS, BIOGEOCHEMICAL CYCLES, AND FEEDBACKS TO THE CLIMATE SYSTEM

P.W. Barnes[75], T.M. Robson[76],[77], R.G. Zepp[78], J.F. Bornman[79], M.A.K. Jansen[80], R. Ossola[81], Q.-W. Wang[82], S.A. Robinson[83], B. Foereid[84], A.R. Klekociuk[85], J. Martinez-Abaigar[86], W.-C. Hou[87], R. Mackenzie[88],[89], and N.D. Paul[90]

[75] Biological Sciences and Environment Program, Loyola University New Orleans, New Orleans, USA

[76] Organismal & Evolutionary Biology (OEB), Viikki Plant Sciences Centre (ViPS), Faculty of Biological and Environmental Sciences, University of Helsinki, Helsinki, Finland

[77] National School of Forestry, University of Cumbria, Ambleside, UK.

[78] ORD/CEMM, US Environmental Protection Agency, Athens, Georgia, USA

[79] Food Futures Institute, Murdoch University, Perth, Australia

[80] BEES, University College Cork, Cork, Ireland

[81] Department of Chemistry, Colorado State University, Fort Collins, USA

[82] Institute of Applied Ecology, Chinese Academy of Sciences (CAS), Shenyang, China

[83] Securing Antarctica's Environmental Future, Global Challenges Program & School of Earth, Atmospheric and Life Sciences, University of Wollongong, Wollongong, Australia

[84] Environment and Natural Resources, Norwegian Institute of Bioeconomy Research, Ås, Norway

[85] Antarctic Climate Program, Australian Antarctic Division, Kingston, Australia

[86] Faculty of Science and Technology, University of La Rioja, Logroño (La Rioja), Spain

[87] Department of Environmental Engineering, National Cheng Kung University, Tainan City

[88] Cape Horn International Center (CHIC), Puerto Williams, Chile

[89] Millennium Institute Biodiversity of Antarctic and Subantarctic Ecosystems (BASE), Chile

[90] Lancaster Environment Centre, Lancaster University, Lancaster, UK

Table of contents

Summary

Terrestrial organisms and ecosystems are being exposed to new and rapidly changing combinations of solar UV radiation and other environmental factors because of ongoing changes in stratospheric ozone and climate. In this Quadrennial Assessment we examine the interactive effects of changes in stratospheric ozone, UV radiation and climate on terrestrial ecosystems and biogeochemical cycles in the context of the Montreal Protocol. We specifically assess effects on terrestrial organisms, agriculture and food supply, biodiversity, ecosystem services and feedbacks to the climate system. Emphasis is placed on the role of extreme climate events in altering the exposure to UV radiation of organisms and ecosystems and the potential effects on biodiversity. We also address the responses of plants to increased temporal variability in solar UV radiation, the interactive effects of UV radiation and other climate change factors (e.g., drought, temperature) on crops, and the role of UV radiation in driving the breakdown of organic matter from dead plant material (i.e., litter) and biocides (pesticides and herbicides). Our assessment indicates that UV radiation and climate interact in various ways to affect the structure and function of terrestrial ecosystems, and that by protecting the ozone layer, the Montreal Protocol continues to play a vital role in maintaining healthy, diverse ecosystems on land that sustain life on Earth. Furthermore, the Montreal Protocol and its Kigali Amendment are mitigating some of the negative environmental consequences of climate change by limiting the emissions of greenhouse gases and protecting the carbon sequestration potential of vegetation and the terrestrial carbon pool.

1 Introduction

The Montreal Protocol and its Amendments have been highly effective in protecting the Earth's stratospheric ozone layer and preventing global-scale increases in solar ultraviolet-B radiation (UV-B; wavelengths between 280-315 nm) at the Earth's surface [1]. Consequently, this multilateral treaty, ratified by all 198 United Nations member states, has prevented large-scale detrimental effects of elevated UV-B radiation on agricultural productivity, terrestrial organisms and ecosystems [2-4]. Moreover, because many of the ozone-depleting compounds controlled by the Montreal Protocol are also potent greenhouse gases, this treaty and its Kigali Amendment are playing an important role in mitigating global warming and other environmental effects of climate change [5,6].

Changes in stratospheric ozone and climate are not independent of one another [7,8] and both can affect surface ultraviolet radiation (UV; 280-400 nm), especially UV-B radiation [9-11]. According to current projections, which assume full compliance with the Montreal Protocol, future changes in UV radiation reaching the Earth's surface are likely to be due primarily to changes in climate (i.e., mainly cloud cover, aerosols and surface reflectivity) rather than changes in stratospheric ozone [10,12,13]. However, future changes in UV radiation at the Earth's surface are uncertain: a new study projects an increase in the UV Index of 3-8% over the tropics and mid-latitudes, respectively, by 2100 depending on the greenhouse gas (GHG) scenario used in the model simulations, cloud cover, and aerosol concentrations [10,14]. Changes in the exposure of organisms and ecosystems to UV radiation also results from increased incidence and extent of wildfires, which generate aerosols (also causing further damage to the ozone layer), and from alterations in vegetation cover from land-use practices (e.g., deforestation), melting of snow and ice, and shifting distribution ranges of species responding to climate change [10,12,15-18] (Summarised in Table 1). In this assessment, we address how the expected, rather small changes in UV irradiation interact with the on-going changes in climate to affect food security, biodiversity, biogeochemical cycles and feedbacks to the climate system.

Since our last Quadrennial Assessment [12,19], the Earth's climate has continued to change and the frequency and intensity of extreme climate events (e.g., heat waves, droughts, and storms), and those events resulting from a combination of weather extremes and other drivers (e.g., wildfires), have increased [20,21]. As global warming and its consequences continue to increase, there is renewed interest in possible technological interventions to reduce the warming. Stratospheric Aerosol Injection (SAI), an intervention that involves Solar Radiation Management (SRM), has received the most attention due to its potential feasibility. SAI would involve injecting reflective aerosols, such as sulphate, into the stratosphere to reflect incoming solar radiation away from the Earth's surface [22]. There are many uncertainties associated with this intervention, including risks to the stratospheric ozone layer that could increase ground-level UV irradiance [23-25]. In addition to the risks associated with the initiation of SAI, once adopted, any subsequent termination of this climate intervention would lead to a rapid increase in temperature and extreme deleterious effects on ecosystems [26,27]. This, and other SRM interventions, would likely expose the Earth's ecosystems to new and potentially rapidly changing combinations of UV radiation and other biotic and abiotic environmental factors [28].

In this Quadrennial Assessment, we evaluate the current state of the science on the changes in stratospheric ozone, solar UV radiation and their interactions with climate change as they affect terrestrial ecosystems and biogeochemical cycles in the context of the Montreal Protocol [29]. We also address key gaps in knowledge and how these interacting effects and the Montreal Protocol will have a bearing on the targets of the United Nations Sustainable Development Goals (SDGs) and their targets.

Table 1 Summary of the effects of various climate change-driven factors on the potential exposure of terrestrial plants and animals to UV radiation. Effects show direction (i.e., decreases (-) or increases (+)) in exposure to UV radiation with the relative magnitude of these changes indicated by the number of negative and positive signs. In some cases (e.g., altered phenology), changes may either increase or decrease UV exposure depending on the circumstances and species. Changes in exposure to UV radiation resulting from modifications in land cover (i.e., deforestation and shrub encroachment) refer to effects on ground-dwelling, understorey organisms. The effects on exposure to UV radiation shown here do not include changes in stratospheric ozone. Additional information and relevant references are provided in the text that follows.

Climate change effect	Effect on exposure to UV radiation
Migration or range shift to higher elevations	+
Migration or range shift to higher latitudes	- -
Altered phenology (seasonal development)	-/+
Deforestation (wet regions)	+++
Shrub encroachment (dry regions)	- - -
Altered cloud cover	- - -/+++
Change in aerosols	- -/++
Decreased snow/ice cover	- /++

2 Effects of stratospheric ozone depletion on climate and extreme climate events on exposure to UV radiation

While both stratospheric ozone depletion and climate change can modify the amount of UV radiation reaching terrestrial ecosystems [8,10], ozone depletion itself can also contribute to climate change by modifying atmospheric circulation patterns and altering regional patterns of wind, precipitation and temperature [30-32]. The impacts of these changes in climate on terrestrial ecosystems have been most pronounced in Antarctica and in the high latitudes of the Southern Hemisphere, although there is evidence of ozone-driven climate change in Arctic regions as well [33]. In addition to the effects of climate change on UV irradiation outlined above (Table 1), extreme events linked to climate change (e.g., droughts, floods, heat waves, fires) may abruptly change UV radiation conditions for many organisms. Below, we assess recent findings on the effects of ozone-driven climate change on polar ecosystems and the potential effects of extreme events on the exposure of terrestrial ecosystems in general to UV radiation.

2.1 Recent stratospheric ozone depletion and climate change effects on polar ecosystems

The impact of stratospheric ozone depletion on polar ecosystems is a complex interplay between the consequences of changing surface UV radiation, and effects caused by shifts in the weather and climate due to the associated cooling of the lower stratosphere [12,29,34]. The increased UV irradiance in the polar regions as a direct result of ozone depletion has been documented since the late 1970s (ozone hole era) [8]. This has particularly been the case in the Antarctic region, where measurements show that the UV Index at the surface in late spring and early summer has, at times, been similar to that at mid- and subtropical latitudes [10,35]. In the past, it was assumed that snow and ice cover would provide plants and surface organisms some protection from the high UV irradiances that occur during the peak of ozone depletion, but with climate warming accelerating the melting of snow and sea ice, Antarctic organisms are increasingly being exposed to this elevated UV radiation. How these high UV irradiances in late springtime impact the resident plants and animals is not entirely clear; studies conducted at the end of the twentieth century found relatively small effects on plants exposed to the elevated UV radiation experienced at that time. This was likely due to the inherent adaptations, UV protective mechanisms and acclimation

responses of these species in order to survive extreme environments [36-38]. Without the Montreal Protocol, the maximum UV Index would have potentially increased from pre-ozone depletion levels of 6 to 20, exposing coastal Antarctic organisms to UV Indices at the end of this century that would be greater than those experienced today in the tropics [10]. These extreme UV radiation conditions would likely have exceeded the UV-tolerances of many Antarctic organisms. In the Arctic, surface UV-B irradiance has also been elevated in recent years (e.g., 2019/2020) when episodic large stratospheric ozone depletion has followed anomalously cold stratospheric winters [10]. However, unlike in the Antarctic, these events occur during early spring when most organisms are still protected by sea ice or snow cover.

Changes in the stratosphere driven by ozone depletion have also been clearly shown to cause seasonally-dependent shifts in near-surface patterns of wind, temperature and precipitation [39-42]. Knock-on effects on warming of oceans and melting sea ice cover have been investigated [40-49], but many uncertainties persist [50] as the effects of ozone depletion on weather patterns are occurring against a backdrop of climate change. Collectively, these changes have led to increased variability of weather and climate, which is most pronounced in the polar regions [51]. As documented in our previous assessments and elsewhere, these shifts in weather and climate have had pronounced impacts on many Antarctic organisms, from tiny moss and cushion plants to wandering albatross [12,34,52,53].

Since our last Quadrennial Assessment, extremes have occurred in both ozone depletion and climatic events that have led to observed or potential effects on plants and animals in polar regions (Table 2). Specific findings include:

- During spring 2019, the Antarctic stratosphere was strongly disturbed by meteorological influences from upward-propagating atmospheric waves [54-56] resulting in a small ozone hole. These stratospheric conditions played a role in enhancing prolonged drought over the 2019/2020 austral summer that exacerbated the unprecedented wildfires in eastern Australia [57-64]. Effects on stratospheric chemistry following the wildfires led to wider changes in both the chemical composition and temperature of the stratosphere across southern mid-latitudes [18,65-73]. Strong vertical and horizontal gradients in the ozone concentration of the Antarctic upper troposphere during the austral spring potentially delayed the subsequent effects on surface climate [32].The role of ozone depletion in modulating the dynamical coupling between the polar stratosphere and the surface at lower latitudes for this particular season is still under investigation. Nevertheless, it appears likely that the combined effects of climate change and ozone depletion could have impacted both the timing and magnitude of these wildfires with considerable consequences for ecosystems in this region.

- In contrast to 2019, a strong and persistent Antarctic ozone hole occurred in 2020 and 2021 [54,74-76] and this led to record surface UV irradiances at several sites across East Antarctica during early summer. It has been suggested that the Australian wildfires that occurred during the previous summer contributed to this strong ozone loss [18,54-56,71,72,74]. There is evidence that increased ozone depletion has tended to delay the annual breakdown of the Antarctic stratospheric vortex [77]. Modelling suggests that increasing greenhouse gas concentrations also favour a more persistent vortex [78], as well as reducing the likelihood of a weaker vortex [58]. While concentrations of ozone depleting substances (ODSs) remain elevated, later seasonal persistence of the Antarctic vortex could expose organisms to higher UV irradiances at times of year when young animals are born/hatch and when plants are actively growing. The loss of protective snow cover could exacerbate these effects [34].

- Since our last assessment there have been two widespread heatwave events in Antarctica, the first in summer 2019/2020 when heat records were broken around the continent [63]. In March 2022 (autumn) extreme temperatures, almost 40 ˚C higher than normal, were reported as an atmospheric river, or plume of warm, moist air, moved onto the Antarctic plateau. Heatwaves such as these accelerate melting of icebanks [79], potentially exposing vegetation to high springtime UV-B radiation from which they have previously been protected [36]. The impacts of these heatwaves and the subsequent ice melt have been poorly studied in Antarctica in part due to the lack of environmental monitoring with networks of sensors tracking temperature and climate variables at appropriate scales. This lack of data is well illustrated by the recently published global maps of soil temperature [80], which exclude Antarctica. Warming temperatures on the Antarctic Peninsula are opening up ice free areas [79] causing the expansion of vascular plants [81] and increasing the possibility of new plant and animal species invading the continent [21,82]. As in the Arctic, there are examples of both plant expansion (i.e., "greening", [81,83]) and death of plants by drought (i.e., "browning", [84-88]). Heatwaves may also be particularly detrimental to mosses, as they survive by creating warm microclimates in Antarctica's cold environments but this may become a disadvantage as air temperatures increase [89].

- In the Arctic, unprecedented low total column ozone values occurred in the 2020 boreal spring [90,91] due to strong stratospheric ozone depletion, and this resulted in record-breaking high solar UV-B irradiances [92,93]. These conditions were promoted by weak tropospheric wave activity [90,94], associated with anomalous sea surface temperature in the North Pacific [33], which caused the stratospheric vortex to become large and stable. Heatwave conditions that occurred in the Siberian Arctic in early 2020 [95] appear to have been aided by atmospheric circulation patterns that were affected by the strong ozone depletion [33,94]. Ozone depletion in March 2020 may also have aided the prevailing reduction of sea ice in the Arctic Ocean bordering Siberia [96]. As indicated above, most Arctic organisms are currently protected by snow and sea ice at the time of maximum ozone depletion and high UV radiation conditions at this time of year (i.e., early March to mid-April 2020), but changes in snow and ice cover resulting from climate change could increase exposure to UV radiation.

Table 2 Summary of environmental effects of stratospheric ozone changes and concurrent climate extremes from 2018-2022. The factors that affect the size of the Antarctic and Arctic ozone holes each spring bring widespread climate impacts that can extend far beyond the polar regions. For example, Antarctic ozone depletion varies with the phase of the southern annular mode (SAM). The SAM phase has been linked to the black summer (2019/2020) bushfires in Australia, which produced aerosols that contributed to further ozone depletion and smoke particles, which accelerated snow melt in New Zealand and Antarctica. Note that the assessment of the environmental impacts of heatwaves and anomalous ozone dynamics has been extremely limited due to the COVID-19 pandemic that prevented many planned scientific visits to remote polar regions.

Ozone effects	Climate extremes and associated effects	Plant responses	Animal responses, including humans
Antarctica and Southern Hemisphere (September 2019-February 2020)			
Anomalously small ozone hole.	Wildfires in Australia produced aerosols that caused ozone depletion and black carbon particles that accelerated snow melt [97].	Widespread loss of plant biomass in Australia [98].	Loss of human life and adverse health effects; loss of domestic animals and wildlife [99-102].
	Heatwaves in Antarctica [103].	Additional snow melt that caused temporary greening of some previously moribund moss beds in East Antarctica [53,104]. Vascular plants on the Antarctic Peninsula appear to be faring better than mosses under global warming and the grass *Deschampsia antarctica* appears to be quite tolerant of in-vitro high temperature shock treatments [105]. Extreme summer marine heatwaves increased chlorophyll a (an indicator of the abundance of phytoplankton) in the Southern Ocean [106]. Hotter and longer heatwaves increased the mortality and decreased post-heatwave growth rates in the Southern Ocean diatom *Actinocyclus actinochilus* relative to milder, shorter heatwaves [107].	Functional thermal limits for the Antarctic sea urchin (*Sterechinus neumayeri*) were determined under simulated marine heatwaves. Key biological functions vary in their thermal sensitivity and in their responses to different rates of warming [108].
Arctic (January – April 2020)			
Anomalously large ozone depletion [8].	Heatwave in the Siberian Arctic; accelerated loss of sea ice [96].	Permafrost warming and thaw lead to landscape changes (retrogressive thaw slumps) and increased greenhouse gas emissions [109].	Negative impacts on organisms that depend on sea ice; positive impacts on animals that thrive in open oceans [95,110,111].
Antarctica (November – December 2020 and November – December 2021)			
Persistent ozone hole producing anomalous surface UV irradiance [97]. See also [10].		Persistent ozone hole producing anomalous surface UV irradiance [97]. See also [10].	High potential for excessive exposure to UV radiation as animals return to breeding sites in spring and early summer [112]. Reductions in Antarctic sea-ice [21] will result in higher exposure to UV radiation in the water column.

2.2 Interactive effects of extreme climate events and UV radiation extending beyond polar ecosystems

Globally, extreme climate events (ECEs[91]) are increasing in frequency and severity with climate change and are projected to become even more prevalent in the future as the climate continues to change [20]. Examples of ECEs include stronger storms and tropical cyclones, catastrophic floods, protracted droughts, anomalous heat waves and freezes, and more intense wildfires [114-119]. ECEs cause long term disruption to ecosystem structure and function [120-123] and occur against a backdrop of more gradual changes in the environment (e.g., rising surface temperatures and atmospheric carbon dioxide (CO_2) concentrations). These disruptions to ecosystem function can exacerbate the deleterious effects of ECEs on plants and animals [124]. Extreme climate events also alter the amount of UV radiation reaching terrestrial ecosystems (Fig. 1). These changes in UV radiation can occur over short or long timeframes, which can then lead to acute or chronic effects on ecosystems, respectively. The changes in solar UV radiation together with other environmental factors (e.g., temperature, availability of moisture) may affect biodiversity, productivity, emissions of greenhouse gases [125-127], and ecosystem carbon storage [124]. For example, fires, floods, and tropical cyclones (hurricanes) all create openings in forest canopies [128,129], driving subsequent adjustment in the understorey vegetation to an acute or chronic increase in incident solar radiation; these increases in solar radiation are often accompanied by increases in temperature and decreases in soil moisture [130-132]. There is also an associated increase in the amplitude of fluctuations in these abiotic factors. Some plant species (e.g., shade-adapted specialists) may not be able to adjust to this new environment and will go locally extinct. However, other plant species can respond quickly to these environmental changes [133-135] and may increase in abundance. With respect to UV radiation, some plant species can respond rapidly to increases in amounts and variability in solar UV radiation through the production and accumulation of UV-protective pigments [132,136] (Sect. 3), and these attributes may allow these species to be successful in the changing conditions. From an ecosystem perspective, fires and hurricanes are among the most disruptive examples of ECEs as they can cause the loss of productivity and biodiversity, and increase the emissions of GHGs [137-139], which can be enhanced by UV radiation (Sect. 6).
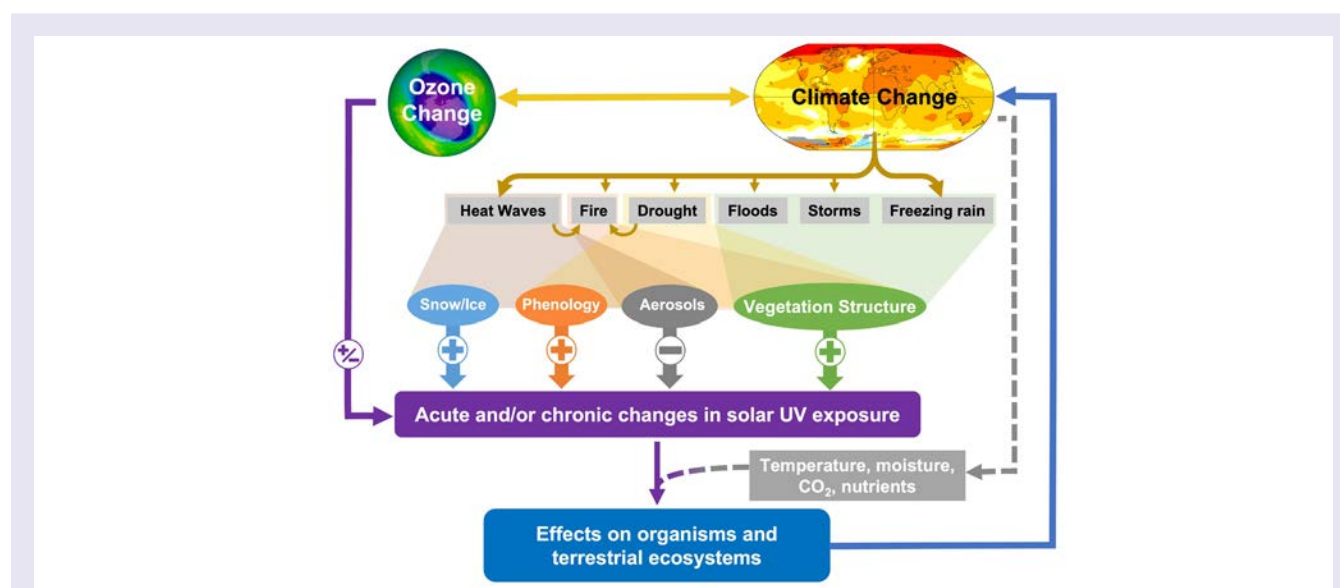
Fig. 1 Pathways by which extreme climate events (ECEs) driven by changes in stratospheric ozone and climate can affect exposure of terrestrial organisms and ecosystems to UV radiation. Changes in stratospheric ozone and climate interact to influence the frequency and intensity of a number of ECEs (upper-most grey rectangles). These ECEs in turn affect atmospheric and surface intermediaries (multi-coloured ovals connected with ECEs by overlapping shaded regions), which can increase (+) or decrease (-) the solar UV radiation reaching terrestrial organisms and ecosystems. Solid arrows show direct mediation by climate, ozone and UV radiation on ECEs and potential interactive and feedback effects. Dashed arrows show chronic effects of climate change factors.

The disruptive nature of ECEs also opens up the remaining ecological communities to invasive species, which can further destabilize these systems [12]. For example, certain invasive species that can tolerate high solar radiation and colonise open habitats may displace some native, specialised or endemic species [140]. To what extent differences among plant species in their tolerances to UV radiation influences species invasions into high UV environments remains unclear [141,142]. Recovery of ecosystems from these ECEs will largely depend on the species that colonise the more open habitats created, and their biodiversity value and traits that support ecosystem function [143].

Wildfires and droughts affect the amount of UV and photosynthetically active radiation (PAR, 400-700 nm) reaching terrestrial ecosystems due to increasing aerosols from smoke and dust, and volatile organic compounds released by plants [144]. These

[91] An extreme climate event has been defined as "an episode or occurrence in which a statistically rare or unusual climatic period alters ecosystem structure and/or function well outside the bounds of what is considered typical or normal variability" [113] or similarly according to the IPCC, "the occurrence of a value of a variable exceeds (or is below) a threshold" that is exceeded [20]. Compound extreme events are the "combination of multiple drivers and/or hazards that contribute to societal or environmental risk." An example of a compound extreme event would be fire weather conditions which are the combination of hot, dry, and windy conditions [20].

atmospheric changes not only reduce PAR and UV radiation, but also change the spectral composition of sunlight at ground level [145]. Importantly, changes in air quality resulting from fires and droughts can occur well beyond the location of these events [146-148]. Thus, these conditions arising from fires and droughts can potentially affect photosynthesis and light-driven development in plants [149], as well as litter decomposition and GHG emissions in ecosystems [19] not directly impacted by these extreme events (Sect. 6.1).

3 Effects of UV radiation and climate interactions on plants and animals

While moderate UV-B irradiance serves as an informational cue that facilitates the normal regulation of plant growth and metabolism, exposure to excessive UV radiation, and in particular short wavelength UV-B radiation, can have deleterious effects on terrestrial organisms [e.g., 150]. As sessile, photosynthetic organisms, plants require sunlight for their growth and reproduction, but this also means that they can receive a large cumulative amount of solar UV radiation over their lifetime. This cumulative amount would have been very high in the extreme UV irradiation conditions that would have occurred without the Montreal Protocol [1]; however, because of its implementation appreciable reductions in photosynthesis in terrestrial plants have been avoided. High UV irradiance conditions would also likely impair growth with severe consequences for global carbon storage and climate [3,10] (Box 1). Under current climate conditions, and in most regions of the world, land plants appear to show adequate protection against UV radiation that limits the deleterious effects of moderate UV-B radiation. There are physiological similarities in responses to adverse conditions (stress), that may determine the extent to which plants can tolerate increased UV radiation in combination with other abiotic factors (e.g., temperature, drought, elevated CO_2) that occur simultaneously. In this section, we highlight recent progress in identifying the mechanisms by which plants perceive and respond to UV radiation. These findings allow us to better assess the impacts of changes in UV radiation, plant response to rapid increases in UV radiation (as occur following many ECEs), and how UV radiation interacts with environmental stresses (e.g., climate change) to modulate their growth and productivity.

In contrast to the abundant literature on the effects of UV-B radiation on terrestrial plants, far less attention has been paid to the effects of UV-B radiation on terrestrial animals. What research there is on animals, typically addresses vision in the UV-A waveband and its effect on behaviour [151], and the application of these findings for controlling insect pests and pollinators of certain crops [152]. One exception is the increasing research, largely focussed on agricultural systems, showing that terrestrial invertebrates, including mites [153,154] and insects such as aphids [155-157], are vulnerable to direct damage from UV-B radiation. There are interesting parallels between invertebrate and plant responses to UV radiation; for example, in the role of DNA-repair [158,159], antioxidant metabolism [160-163] and pigments [156,157,162] in conferring UV-protection. This includes evidence that mites can obtain UV protective compounds by consuming pollen [161]. It is also clear that avoidance behaviour plays a major part in reducing the exposure of invertebrates to solar UV radiation [153-155,164].

3.1   Perception and response of plants to changing UV radiation

The need to better understand how organisms respond to elevated UV-B radiation, as occurs with stratospheric ozone depletion, stimulated research that eventually led to the discovery of a UV-B photoreceptor in plants (UVR8, which stands for Ultraviolet Resistance Locus 8) [165]. It is now well-documented that UVR8 mediates a number of plant responses to changes in UV-B radiation in the environment. Recently, UVR8 has been found to operate over a spectral region extending through the UV-B and part of the UV-A radiation wavebands [166]. Thus, variation in solar UV radiation attenuated by the stratospheric ozone layer (which screens UV radiation up to *ca*. 335 nm) is well matched to the action spectrum of UVR8 [167,168]. This might suggest that the evolution of UVR8 allowed plants to perceive and respond to environmental cues related to changes in stratospheric ozone.

The UVR8-signalling pathway likely evolved very early in the transition of plants from aquatic to terrestrial environments [169-171]. Two overlapping signalling pathways for UV responses (UVR8/WRKY36/HY5 and UVR8/COP1/SPA-HY5 pathways) have been conserved during the evolution of green plants [171,172]. These pathways regulate a series of genetic transcription factors that affect accumulation of flavonoids, functioning of the plant hormone auxin, and growth (i.e., through inhibition of elongation of lateral roots and hypocotyls [173]). Subsequently, diversification of signal transduction to increase crosstalk with other signalling pathways that control the production of additional secondary metabolites, such as brassinosteroids (hormones involved in plant development), enabled fine-tuning of tolerance to UV radiation in photosynthetic organisms.

Specific responses in plants that are involved in their acclimation to UV radiation include: the accumulation of flavonoid pigments as UV sunscreens, shorter stature with increased branching, and smaller leaves with thickened cell walls. These changes together with a more conservative strategy (i.e., slower but more efficient growth, photosynthesis, and water loss [174,175]) collectively mitigate the potentially deleterious effects of current levels of solar UV radiation on plants.

Among the diverse functions of phenolic compounds in growth, development and reproduction, certain flavonoids and related

phenolic acids (e.g., hydroxycinnamic acid derivatives) screen UV radiation in plant tissues and are therefore central to plant UV-acclimation responses. The accumulation of these compounds in leaves, flower petals and pollen is temperature dependent but is also driven by UV-B radiation [136,176,177]. Flavonoids fulfil many additional roles in plants, in that they are involved in ameliorating biotic and abiotic environmental-stress, regulating the transport of certain hormones (i.e., auxin) and are required in many species for successful germination and growth of the pollen tube on the stigma of flowers, where they participate in cell signalling and recognition [178-181]. There is also evidence that greater accumulation of flavonoids in pollen grains improves their germination (e.g. in *Clarkia unguiculata*; [182]) and flavonoids function in UV-screening in pollen, which is essential to maintain viability [183,184]. Additionally, flavonoid glycosides (quercetins and kaempferols), hydroxycinnamic acids and anthocyanins in leaves and pollen act as strong antioxidants, and, as such, they scavenge reactive oxygen species (ROS) produced by abiotic stressors such as excessive solar radiation, including UV-B radiation [179,185].

In assessing plant acclimation to increased UV radiation, it is relevant to consider responses to short-term, rapid fluctuations in UV radiation - as would occur with changing cloud cover or from day-to-day during the break-up of the stratospheric ozone hole - as well as to the longer-term (i.e., decade-scale changes that occur from anthropogenic changes in stratospheric ozone together with climate). The patterns of these responses can be used to evaluate whether plants' epidermal UV screening and photoprotection principally acclimate to immediate changes in UV radiation or if plants mainly rely on other mechanisms that allow trans-generational improvements in protection against UV radiation (i.e., genetic adaptation or epigenetics). There is increasing evidence that the accumulation of photoprotective compounds (including flavonoids, hydroxycinnamic acids and carotenoids) tracks seasonal and even daily variation in UV radiation [186-191]. In general, the magnitude of diurnal changes in UV screening is less than those that occur during the development of leaves. Diurnal changes in UV screening can, however, be of comparable size to the variation in screening that results from day-to-day fluctuations in UV radiation and temperature [177,187,192]. Rapid acclimation of UV-screening to short-term changes in UV radiation indicates a high level of phenotypic plasticity and suggests that many plants can acclimate to short-term fluctuations in UV irradiance arising from transient reductions in stratospheric ozone, reduced cloud cover or certain ECEs (Fig. 1; Sect. 2.2). In fact, a comparison of 629 taxa growing together at high elevation and high latitude locations subject to strongly contrasting UV irradiances, found phenotypic plasticity in epidermal UV screening according to their immediate growing microenvironment, and this outweighed any differences in adaptation arising from their evolutionary history under disparate climates [193]. Similarly, the importance of the local environment over the place of origin is also highlighted by experiments where species and populations are grown in the same location and habitat (i.e., common-garden experiments [194]).

Although the capacity for rapid acclimation may be advantageous for adjusting to short-term environmental variability, high phenotypic plasticity may interfere with the capacity for genetic adaptation to changing conditions over long time periods [195-197]. Understanding the relative importance of phenotypic plasticity vs genetic adaptation is needed to evaluate the consequences of climate change-induced range shifts that expose plant species to UV irradiances that might be beyond those experienced in their historic ranges (Sect. 4.1).

Studies examining the mechanisms by which native plant species tolerate naturally high UV-B environments can provide insights into the range of adaptive responses exhibited by plants to UV-B radiation. For example, *Rheum nobile* (Sikkim Rhubarb), an herbaceous plant that grows above 4000 m on the Tibetan Plateau, has large translucent flower bracts containing high concentrations of flavonoids, which form a protective cover over its flowers. This species can thus attenuate UV-B radiation within its floral tissues to similar levels across its elevation range [198]. In the same region, other herbaceous plants, such as *Megacarpaea delavayi* (a wild mustard; [199]) and five species in the genus *Saussurea* (thistle-like plants in the sunflower family; [200]) have a rapid DNA repair mechanism to mitigate the damaging effects of high UV-B irradiances. Comparative genomic analysis of 377 Tibetan peach populations showed that the expansion of SINE retrotransposons (genetic variations that regulate gene expression), promotes adaptation to UV-B radiation [201]. These, and other evolutionary adaptations of specialist alpine species to extreme UV radiation conditions indicate how plants in general might adapt to high UV-B irradiances. However, the rate of changes in UV irradiance as a result of ozone depletion or climate change is likely to outpace the rates of adaptation in many species, especially long-lived perennials such as trees. Additionally, plants endemic to high elevations often have limited distribution ranges and abundances, and may be among the most vulnerable to habitat loss due to climate change.

Box 1 The effect of terrestrial ecosystems on climate change in a world without successful controls of ozone-depleting substances.

A recent modelling exercise [3] estimated that large increases in plant effective UV-B radiation resulting from uncontrolled emissions of ozone-depleting substances (ODS) would have strongly reduced carbon dioxide uptake by terrestrial vegetation in the "world avoided" (i.e., a world without effective control of ODS by the Montreal Protocol) compared with the "world projected" (i.e., the actual world with the Montreal Protocol projected into the future). As a result of the control of ODS emissions, by 2100 it was estimated that:

- Carbon storage by terrestrial vegetation would have decreased by 325-690 billion tons;

- Atmospheric CO_2 concentrations would have increased by an additional 190 ppm, on average (range = 115-235 ppm; panel (a) in the figure below); and

- Global mean surface temperature would have risen an additional 2.5°C (range = 2.4-2.7°C; panel (b), which includes the ODS warming effect (1.7°C) and the UV plant effect (0.85°C).

Because of the relatively long time period involved, there are significant uncertainties associated with these projections. The size of the effect depends on the action spectrum used to describe the sensitivity of photosynthesis to different wavelengths of UV-B radiation and on extrapolating the dose response relationship between change in plant effective UV-B radiation and primary productivity (see Sect. 8 and [9]).

Nonetheless, this modelling highlights both the potential damage to terrestrial ecosystems in the world avoided scenario and the limits imposed on such models by the scope of known responses of plants and mixed vegetation to changes in UV-B radiation.
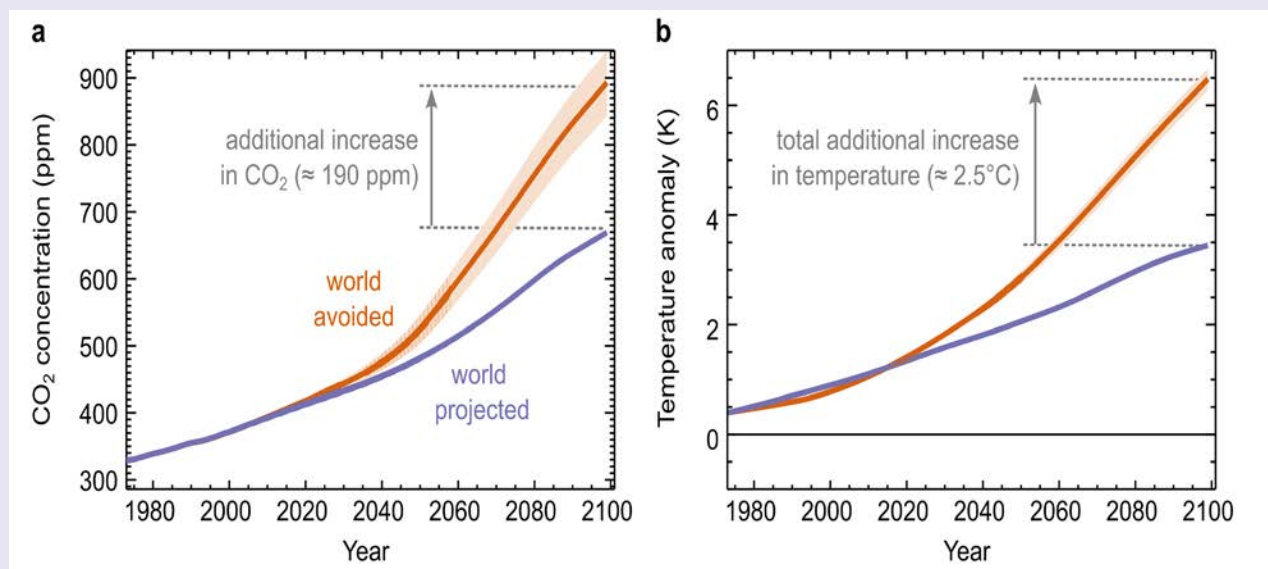
Changes in atmospheric CO_2 concentrations (a) and surface temperature (b) resulting from UV-B radiation under scenarios with (violet line) and without (orange line) the Montreal Protocol. Shading around the orange line represents the range of responses from simulations assuming a 50-150% range of plant responses to UV radiation. Figure adapted from [3], reproduced by permission.

3.2 Proxies for past solar UV irradiance based on acclimation responses of modern-day plants to UV radiation

Because many of the phenolic UV sunscreens accumulated by plants are resistant to decay, it may be possible to infer historical changes in solar UV radiation from tissue samples of plants that have been preserved in herbaria or in sediment cores. Herbarium specimens offer the potential to retrospectively infer past environmental conditions by assessing how plant traits have changed over the period of their collection (usually decades). However, to be reliable proxies for UV radiation, herbarium specimens must be sampled in a consistent and

unbiased manner over time (See [202] for a full discussion of necessary procedures). If these protocols are followed, and if other factors that can modify flavonoid and anthocyanin accumulation in plants (e.g., shading, changes in temperature, availability of moisture or total solar irradiance) are accounted for, one could associate trends in pigmentation of thermostable compounds with historical changes in UV radiation.

Over longer time frames the effects of major global events such as changes in solar activity, volcanic eruptions, or reversals in the Earth's magnetic field (e.g., at the Laschamps Excursion 42,000 years ago) might be examined through changes in the phenolic composition of pollen or spores. For example, the hydroxycinnamic acid *para*-coumaric acid, which is preserved in fossilised sporopollenin (a compound that forms the outer wall of spores and pollen), continues to be the focus of research seeking such a proxy for UV-B radiation over geological time periods. However, before it can be reliably used it is necessary to ascertain the action spectrum of its response to UV radiation, its rate of degradation, the response time of its synthesis, as well as the consistency of response among species and over time [203]. In the case of fossilised pollen from *Nitraria* (a steppe plant) and conifers, chemical signatures have been shown to differ from those of contemporary (extant) pollen in a predictable and consistent manner such that stable relationships can be modelled [204].

3.3   Interactive effects of UV radiation and climate change factors

Ongoing changes in climate, together with associated changes in plant species distribution, are exposing wild plants, forests and crops to new combinations of UV radiation and other climatic conditions [10,125]. Combinations of particular concern are high UV-B irradiance and drought or temperature, as climate change is increasing the frequency and severity of heat waves and droughts, and these events frequently coincide with high UV radiation, particularly at mid to low latitudes [205].

There are marked similarities in the acclimation responses of plants to increases in UV radiation and drought. A recent meta-analysis found these two sets of responses to be generally consistent irrespective of whether experiments were performed in controlled environments (i.e., growth chambers or greenhouses) or in the field [206]. In general, when plants are exposed to co-occurring drought and increased UV irradiance, the accumulation of defence compounds (e.g., proline and secondary antioxidants, such as flavonoids and anthocyanins) and other stress responses (e.g., decreased leaf area, reduced stomatal opening) is enhanced. Thus, the combined detrimental effects of these stressors on plant function are milder (i.e., reduced production of stress-associated malondialdehyde (MDA) and reactive oxygen species (ROS), and this reduces the negative effects on photosynthesis and biomass production [206,207]. The response of plants to increased UV radiation may therefore confer cross-protection against drought [206,208] and mitigate some of the detrimental effects of drought on plant growth and productivity, unless both stress factors are excessive. Further, it has been postulated that plants may use UV radiation as a signal of impending drought [209]. The functional association between exposure to drought and UV radiation exposure appears to involve common physiological defence and acclimation responses [209,210]. For example, multiple studies have shown that overexpression of protective pigments in plants results in enhanced protection against both drought and UV-B radiation [211,212]. UV-B radiation can even be exploited for seed priming, resulting in enhanced expression of drought tolerance of plants grown from such UV pre-treated seeds [213]. Certain agricultural practices may also negatively impact crop tolerance of both UV radiation and drought. For example, growth allocation to roots relative to shoots often increases in drought-stressed plants, as well as those exposed to high solar UV-B radiation (i.e., increased root:shoot ratios), but high nitrogen availability has the opposite effect on root:shoot allocation [214].

High UV-B irradiance often co-occurs with high temperatures. A recent study of a commercial tomato cultivar (*Solanum lycopersicum* cv. Money Maker) compared plants transferred under near-ambient solar UV radiation to those placed in a UV exclusion treatment in the field. Exposure to UV-B radiation led to partial closure of leaf stomatal pores, reducing transpiration and evaporative cooling, and thus increasing leaf temperature by up to 1.5°C [215]. These findings are relevant in warmer climates where even small increases in temperature may have substantial consequences for survival of crops [216], as high temperatures are well-known to negatively affect photosynthesis and growth of many plant species. More broadly, a recent meta-analysis across terrestrial, freshwater and marine plants, algae and animals [217] showed that any negative effects of UV-B radiation can be somewhat compensated for by elevated temperatures, although this depends on the habitat and organism involved. This positive effect of warming appears to be restricted to cool climates where organisms often function at temperatures below their physiological optima, and thus is not expected to occur in environments approaching the thermal and physiological limits of organisms [217]. Given the current context of global warming, more detailed temperature and UV-radiation dose-response studies are required to fill this knowledge gap. Furthermore, the scope of such studies needs to go beyond crop yield, as early evidence shows that interactive effects of heat and UV radiation can also affect crop quality [218] (Sect. 5.2).

Apart from high temperatures, the effects of UV radiation on plants can also be modified by low temperatures, and climate change is expected to increase the incidence of extreme cold events in some regions [20](Sect. 2.2). In studies with the model plant *Arabidopsis thaliana*, the synthesis of flavonoids is strongly enhanced in response to low temperatures (4/2°C, day/night) compared to moderate temperatures (18/20°C), just as it is by UV radiation. Where plants are simultaneously exposed to both cold and UV radiation, complex interactive effects are observed, with UV-B decoupling flavonoid accumulation from gene-expression, indicating post-translational regulation [219]. Low temperatures and UV-B radiation also produce a shift in the composition of flavonoid glycosides from kaempferols to quercetins [177]. The shift in composition towards quercetin synthesis at low temperatures suggests an enhancement in antioxidant function [177,220], which could increase overall plant hardiness.

Temperature is a cue for many organisms, controlling their seasonal development (i.e., phenology). Changes in thermal regime, such as periods of extreme heat or cold or even an absence of cold temperatures, can disrupt the timing of growth, reproduction, and other aspects of phenology [221,222]. Temporal shifts in phenology can also change the seasonal timing of exposure to UV radiation, as solar

UV radiation varies at high-to-mid latitudes over the course of the year. Shifts in phenology due to changes in climate and UV radiation may result in new combinations of biotic interactions (i.e., competitors and pests; Sect. 4.1) and abiotic stresses that may be outside the tolerances for some species. For plants, these new combinations of abiotic stresses can have detrimental effects on their growth and survival even though each individual stressor may have a negligible effect [223].

Complex effects on plants may also occur when other environmental factors interact with UV radiation. Recent studies have revisited the interactive effects of UV radiation and increased nitrogen deposition [224], ozone pollution [15,225] and elevated atmospheric CO_2 concentration, where short term stimulation can be outweighed by long-term downregulation of photosynthesis [226], as noted in our previous assessments [12,227]. Elucidation of the interactive effects of UV radiation and these other environmental factors is necessary to improve our ability to model and assess the effects of UV radiation on the carbon sequestration of terrestrial vegetation in a changing climate (e.g., Box 1).

4 Species distributions and biodiversity

Maintaining the wide variety of plants, animals, and microorganisms in terrestrial environments (i.e., biodiversity) is essential for ecosystem health, stability, and valuable services provided to humans. The loss of biodiversity can occur directly (e.g., hunting or harvesting) or indirectly (e.g., loss of habitat, climate change, and invasive species). While considerable attention has been given to the effects of climate change on biodiversity [21,228,229], far less is known about how solar UV radiation might interact with climate change to influence species distributions and diversity in ecological communities. We examine these effects from available studies and evaluate how the UV radiation exposures of species can potentially change as their distributions shift in response to climate change.

4.1   Potential effects of climate change and UV radiation on shifting species distributions

Plant and animal species are migrating or shifting their distribution ranges to higher elevations and latitudes in response to on-going changes in climate [230-232]. As species occupy higher elevations and latitudes, they may encounter increased or decreased UV radiation, respectively, because of the natural gradients in solar UV radiation that occur with elevation and latitude (Table 1). Some plants and animals are also shifting their ranges in the opposite direction, *viz.*, towards lower elevation (lower UV radiation) and latitude (higher UV radiation), to avoid the increased seasonality of temperature at higher latitudes [233,234]. How species respond to novel combinations of UV radiation and multiple climatic conditions has direct implications for how they will interact with other species, including their pests and pathogens (Sect. 5.3), with consequences for biodiversity [e.g., 235].

Latitudinal change. While the changes in UV radiation received by plants and animals resulting from latitudinal shifts in ranges are generally rather modest, they may affect terrestrial ecosystems and biodiversity. For instance, if one assumes species migrate at their maximal rates to keep pace with climate change (i.e., their average climate velocity for the period 2050-2090; [236]), the UV irradiance under clear sky conditions for herbaceous plants would decline by 4.5%, while that for more mobile plant-eating insects would decline by 16.2% after a century of climate change (Fig. 2A).

Plants encountering reduced UV-B irradiance resulting from range shifts would likely reduce their levels of UV-protective compounds (i.e., epidermal flavonoids and other phenolic compounds) [237,238]. The multiplicity of roles performed by these plant secondary compounds could, in turn, make some plants more vulnerable to herbivores [239,240] (Sect. 5.3) as some of these chemicals serve as deterrents for insect herbivores.

Accelerated loss of biodiversity will likely occur as climate change continues to exert its effects on range shifts on plants and animals. Plants use both temperature and day length (photoperiod) as environmental cues for regulation of phenology (flowering, dormancy, budburst, etc.). Trees with long generation times may be especially vulnerable to extinction because they have limited opportunities to genetically adapt to a changing photoperiod and their environmental cues such as UV radiation may be mismatched with their new environment [241-243].

At present, it is unclear how changes in UV radiation in combination with climate change will affect species migrations and adaptation as experimental and modelling data are not yet available to quantify and fully assess the risk of these interactive effects.

Elevational change. For many montane ecosystems, climate change is resulting in the migration of lower elevation species to higher elevations. Climate change is also reducing the envelope of suitable habitats for high elevation alpine species to survive, while increasing competition against emigrating species from lower elevations [21,244]. However, like latitudinal shifts towards the equator, elevational distribution changes also occur downslope for some species [233,234]. For species shifting their ranges to higher elevations, their exposure to solar UV radiation would be expected to increase, assuming no change in cloud cover (Fig. 2B). Further, reduced snow cover due to warmer temperatures exposes organisms to fluctuations in temperature and solar radiation, including UV-B radiation [245].

High elevation alpine plants often have heightened accumulation of UV-screening compounds and herbivore defence [141,246-249]. Across a diversity of plant species from alpine and subalpine zones in Bulgaria, improved photoprotection has been found to effectively prevent greater DNA damage caused by increased UV radiation at higher altitudes. These mechanisms were sufficiently effective since plants growing at the highest elevations had fewer UV-induced DNA dimers than those at lower elevations, with grasses (Family Poaceae) least susceptible to UV-induced DNA damage among a wide diversity of plant families tested [250]. Nevertheless, as species migrate to high elevations, more resources may be allocated towards protection against UV radiation, and this could in turn divert resources away from growth, which could then reduce competitive ability [251,252]. Depending on the availability of suitable habitats at higher elevations, these changes in species interactions have the potential to negatively affect biodiversity [253] by shifting the balance of competition between species [254,255].

While climate change is causing many species to migrate to higher elevations, these climate change-induced shifts in distribution ranges are often most pronounced for non-native, invasive species [256-258]. At present, it is unclear if UV radiation affects native and non-native invasive species differently [141,142,259-261]. However, invasive species are generally considered to exhibit greater phenotypic plasticity to new environments than native species, although this may depend on availability of resources [262,263]. In some cases, invasive species have been found to alter their production of UV screening compounds to a greater degree than native species [141]. This flexibility may allow non-native, invasive species to occupy new habitats more rapidly than native species and, in some cases, outcompete endemic alpine species [235].
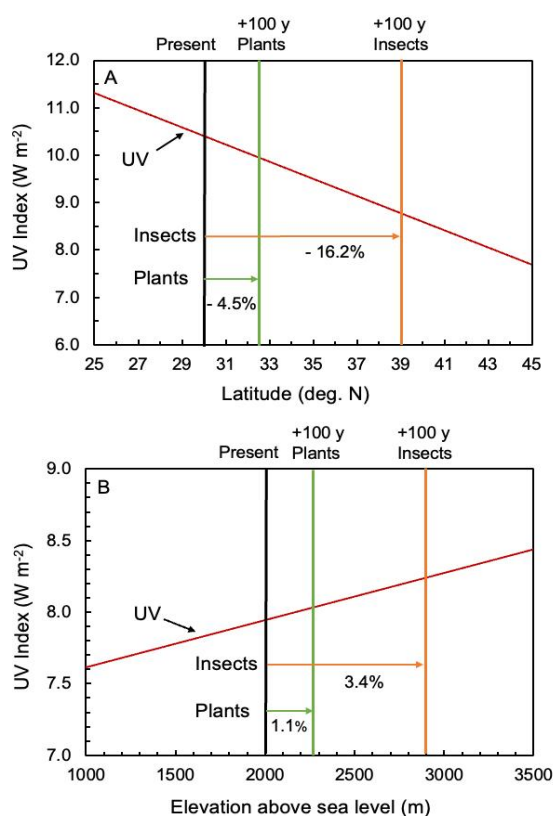

Fig. 2 Potential changes in exposure to UV radiation as plants and insects migrate to higher latitudes and elevations with climate change. Panel A shows the estimated changes in UV radiation as plants and their herbivorous insects migrate poleward after 100 years (y) of climate change. UV radiation data are simulated midday summer (June 21) UV irradiances (here reported as UV Index; red line) based on stratospheric ozone levels in 1980 at sea level (radiative transfer model TUV; [264]). Horizontal arrows show distances migrated for herbaceous plants (green arrow) and plant-eating insects (orange arrow) originating from 30° N after 100 years of climate change assuming maximum rates of migration and average climate velocity for 2050-2090 (from [236]). Panel B shows the simulated midday summer (June 21) clear sky UV Index changes with elevation in the European Alps (46° N latitude; red line) and the estimated changes in UV irradiance for plants (green line) and insects (orange line) as they migrate from 2000 m to higher elevations after 100 years of climate change, assuming average current rates of leading edge migration for Western European montane plants (28.2 m/decade) and insects (90.5 m/decade) [265].

4.2   Assessing the risks to biodiversity from the interactive effects of UV radiation and climate change

Climate change can cause declines in biodiversity by reducing the availability of suitable habitats for species and by differentially shifting their distribution ranges, which then disrupts species interactions and ecosystem function. If species cannot keep pace with climate change, then populations will decline leading to a loss of biodiversity. In this context, species distribution models (SDMs) are used to determine how climate change will affect future habitat suitability of species through changes in key abiotic drivers. These models can be used to inform species conservation as well as management for plant production in agriculture and forestry [266].

Several studies have shown that the inclusion of solar UV-B radiation in models forecasting future distribution ranges of ecologically and agriculturally important crop and tree species improves their statistical predictive power [267-273]. These models are based on different scenarios of climate change (i.e., IPCC scenarios of greenhouse gas emissions) and create projections based on correlative relationships

between climate and species occurrence. These projections suggest that the ranges of some species of native plants from open, dry habitats found in arid and semi-arid shrub-steppe biomes will expand to higher elevations [268-273], while the ranges of willows and other related species from wetter habitats will contract [267].

Some studies of plants native to China and central Asia include UV-B radiation among the potential explanatory climatic variables that contribute to species distributions, sourcing data from the global climatology [274]. Future habitat suitability estimated using Maximum Entropy models (MaxEnt; models that apply basic machine learning algorithms to resolve environmental conditions where the species is present across its distribution) reveal incident UV-B radiation together with precipitation and temperature as significant correlates of species occurrence. While these models do not identify the mechanisms underlying these results, the findings suggest that such models could be useful in assessing risks to biodiversity, as well as providing information on potential species distributions and suitable habitats for conservation and planting crops for different scenarios of climate and solar UV-B radiation.

Despite the inclusion of UV-B radiation among significant climatic variables in some studies of species distributions [267-273], most modelling studies to date do not include UV-B radiation and its interaction with other abiotic stressors as potential constraints on species distribution. As more detailed UV-B databases become available, it is likely that UV-B radiation will more routinely be included among climatic variables used to predict species occurrence and changes in biodiversity. As well as species distribution, climatological data that include regional UV-B irradiances can be applied to study whether climatic trends correlate with patterns in plant functional traits among species. For example, a large-scale study of 1192 grassland species found that UV radiation was negatively correlated with leaf size across the Mongolian and Tibetan Plateau [275], while leaf shape, reflectance, and thickness have also been found to covary with UV-B radiation along environmental gradients [276-278].

5 Effects on agriculture and food production

Some of the earliest concerns raised over stratospheric ozone depletion and the accompanying increase in solar UV-B radiation considered the potential for reductions in crop productivity and compromised food security [279,280]. A prior assessment [38] using results from field studies conducted at high latitude locations indicated that plant productivity declines by about 3% for every 10% increase in plant effective UV-B radiation (i.e., UV-B radiation weighted according to a generalised plant action spectrum [281]). These findings implied that the projected increases in solar UV radiation with changes in stratospheric ozone and climate, assuming full compliance with the Montreal Protocol, would have minimal effects on agricultural productivity. However, few experimental studies to date have been conducted on species growing in those regions with the highest natural levels of UV-B radiation on Earth (i.e., the tropics and high elevations). Previous studies also tended to focus on crop productivity but paid less attention to the effects of UV radiation on food quality. The effects of UV radiation on agroecosystems also extends beyond the direct effects on crop plants, as UV radiation can influence pest-pathogen interactions and the persistence and effectiveness of biocides and agricultural pollutants. The management of solar radiation in greenhouses and advances in artificial UV lighting are exploiting some of the beneficial effects of modest exposures to UV radiation to improve food quality, enhance plant defences against pest and pathogens, and contributing to more sustainable agricultural practices [282].

5.1   Agroecosystems vulnerable to changes in UV radiation and climate

As noted in our 2019 Update Assessment [283], and in other reports [284,285], most field research to date on the effects of UV radiation on crops has been concentrated on regions outside the tropics and at lower elevations. The tropics extend over approximately 33% of the Earth's land surface [286] and harbour a vast reservoir of biodiversity [287] that provides critical resources and essential services for agriculture and food security [288]. Thus, tropical agroecosystems warrant further attention to safeguard a sustainable future for life on Earth.

Because the projected recovery of stratospheric ozone is highly dependent on changes in GHG concentrations and lifetimes of ODS, there remains some uncertainty about how UV-B radiation might change in the future for tropical regions [10,289]. Under some scenarios, UV-B radiation could increase by 3% in the tropics due to interactions between stratospheric ozone, climate and aerosols [8,10]. This increase would further elevate the already high levels of UV-B radiation that occur naturally at low latitudes. At present, the consequences of these relatively modest percentage increases in UV-B radiation on crops or wild plants in this region are uncertain. Available evidence suggests that current levels of UV-B radiation in the tropics can alter the morphology (e.g., smaller leaves, reduced shoot height) and chemistry (e.g., increased flavonoid levels) of native, non-crop tropical plants, but that biomass production is rarely decreased in these species (e.g., [290]). By comparison, several field experiments have shown that certain varieties of temperate-zone crops (e.g., wheat and soybean) [291-293] show decreases in photosynthesis and yield when grown under ambient UV-B radiation in the tropics. These findings suggest that some important crop species grown in the tropics might be vulnerable to relatively small increases in UV-B radiation.

As noted above and in Sect. 4.1, climate change is shifting bioclimatic zones and this is allowing certain crops to be grown at higher elevations than was previously possible [294-299]. For some crop species originating from lower elevations, the more intense UV radiation at high elevations may exceed their tolerances to UV radiation with negative consequences for their physiology and growth [300]. As crop species are grown in these new habitats, they will also encounter new weeds, pests and pathogens, which may disrupt the structure and function of these agroecosystems [301,302]. Differential effects of climate change on range shifts and phenology can also lead to spatial and/or temporal or seasonal mismatches between pollinators and their plant hosts [303,304], posing additional risks to food security. Many of these high-elevation agroecosystems support community livelihoods and are important carbon sinks that help mitigate global warming. Thus, their risks from changes in climate and UV radiation are of particular concern.

5.2   Effects of UV radiation on food quality

Laboratory and field studies have found significant effects of UV radiation on crop quality with regard to texture, flavour, appearance and nutritional content. It is now well-established that the concentrations of a wide array of natural plant chemicals are modified by UV radiation [305-308] and these changes in chemical composition can have positive and negative effects on food quality. There is abundant research demonstrating that exposure to modest levels of UV radiation can improve food quality by enhancing crop flavour [309], taste [310], colour [311], nutritional content [312-315], and pharmaceutical content [316-318] in various plants. Given that the intake of fruits and vegetables of many consumers is well below recommended levels [319], the higher nutritional content of crops exposed to UV radiation may generate long-term health benefits. For example, Keflie et al. [320] used solar UV-B radiation to increase vitamin D in oyster mushrooms, which may alleviate vitamin D deficiency in humans. Some have proposed legal regulation for UV treatment of foods, including mushrooms [321].

In some cases, exposure of crops to UV radiation can lead to a decrease in their nutritional value for humans and livestock. For example, some species of tropical grasses show increases in tannins when grown under experimentally elevated UV-B radiation, and this would imply a reduced palatability of forage for cattle [322,323]. High levels of UV radiation may also increase amounts of other anti-nutritional compounds in plants, such as oxalates, which are generally associated with kidney problems [324]. At present, the full scope of UV-induced anti-nutritional compounds is not fully known nor is the identification of crops most at risk to these changes.

5.3   Effects of UV radiation on plant interactions with pests and pathogens

The Food and Agriculture Organization of the United Nations (FAO) estimates that plant pests[92] cause a 20-40% loss in global agricultural production per year, costing *ca*. $220 billion USD, with the impacts of invasive insect species adding another $70 billion USD [325]. It is expected that climate change, including ECEs, will increase the incidence and severity of pests and pathogens in some regions, as these organisms colonise new previously sub-optimal habitats along latitudinal and elevational gradients [326,327]. The climate-induced parallel range shifts of plants with latitude or elevation into new habitats may constitute additional stress from plant pests (Sect. 4.1) [328]. Rising concentrations of CO_2 and associated global warming together with regional increases in UV radiation may also act together to compromise food security through complex effects on plant pests and disease [329]. While our previous assessments have reported on UV-mediated increases in resistance to specific pests and pathogens [12,38], we note that there is a need for more detailed studies on the interactive effects of UV radiation, CO_2 and other climate change factors on plant interactions with pests and pathogens.

Exposure to UV radiation can confer increased resistance of certain crops to pests and diseases through changes in host physiology, morphology, and biochemistry. As noted in Sect. 3.1, UV radiation typically enhances the production of polyphenolic compounds, such as flavonoids. Some of these compounds enhance a plant's defence against herbivores and pathogens (e.g., viral, fungal or bacterial) [240,283,330]. Disease and pest attack will also elicit the production of increased amounts of these polyphenolic compounds that can make the host plant unpalatable or toxic (Sect. 5.2) and/or protect the plant through their antioxidant properties (e.g., scavenging of free radicals). These effects on pests or pathogen attack are part of a wider network of interactive effects on plant physiology and morphology potentially altering the susceptibility of crops to these threats [331].

Chemical biocides are widely employed to manage pests and pathogens in crops (Sect. 5.4). However, several biocontrol agents against insect pests have been developed and used as alternatives to chemical pesticides. Of particular interest is a group of fungi that are parasitic on insects (entomopathogenic fungi). Entomopathogenic fungi kill insects by penetrating the outer protective cuticle layer of specific hosts with the help of proteases [332]. These fungi live naturally in soils but can be mass-produced for application to crops where they have been used against pests including spittlebugs and locusts, which affect crops such as maize, sugarcane and beans [332], as well as against various insect pests in rice [333]. However, many of the entomopathogenic fungi are strongly inhibited by UV radiation and temperatures above 300 C, which affect their development and pathogenic function against certain insects. Therefore, these abiotic constraints are considered a major barrier to the use of entomopathogenic fungi in controlling insect pests [333-336]. However, the effect of solar UV-B radiation on these fungi remains to be confirmed through experiments where they are grown under realistic solar radiation conditions [337]. Such studies may also allow for selection of fungal biocontrol agents that are more tolerant to UV-B radiation and other climate factors, for use as biocontrol agents to safeguard economically important agricultural systems.

---

[92] A pest in this context is "any species, strain or biotype of plant, animal or pathogenic agent injurious to the plants or plant products", as per the definition in the International Standard for Phytosanitary Measures No. 5 (ISPM) adopted by the Commission on Phytosanitary Measures of the International Plant Protection Convention.

5.4   Effects of UV radiation on agricultural biocides

The widespread application of biocides (herbicides and pesticides) for controlling or killing harmful organisms in agricultural field settings results in some accumulation of these chemicals in water, soil, and atmosphere, and may also result in residues in agricultural products. Given that biocides are designed to be bioactive, their adverse effects on non-target organisms and humans are of concern. Direct and indirect photodegradation by solar UV radiation can potentially reduce the environmental residence time of pesticides [19]. However, photochemical degradation can also reduce the functional effectiveness of biocides as crop protectants, which may lead to greater amounts being administered by growers [338,339]. Direct photodegradation of biocides occurs when a chemical absorbs UV radiation, leading to its breakdown into various degradation products [340]. Indirect photodegradation involves the reaction of the biocide with reactive intermediates formed when natural photosensitisers (e.g., nitrate) absorb solar radiation [341]. Not all biocides are subject to direct photodegradation under solar radiation. For biocides with an action spectrum for direct photodegradation only in the UV-C region (wavelengths 100-280 nm) and not extending into the solar UV-B, only indirect photodegradation occurs under solar radiation.

In the field, the exposure of biocides to solar radiation depends on the manner in which they are applied to crops, as well as the specific characteristics of the crops, including age and canopy structure, which determines their exposure to solar radiation. These factors, together with the chemical composition of the pesticide formulation determine the extent to which they are photodegraded in the field. For example, the additive (co-formulation compound) benoxacor, which is used as a safener (i.e., a compound used in combination with herbicides to reduce negative effects on crops) of the herbicide metolachlor, accelerates the photodegradation of the active ingredient on soil surfaces, lessening its toxicity [342]. The extent to which biocides are photodegraded is also highly dependent on where the biocide residues occur. For example, the photodegradation rate of the herbicide imazethapyr is two orders of magnitude slower when applied to maize and soybean leaves than in aqueous solutions [343]. The leaves of aromatic herbs like thyme emit volatile organic compounds that can further affect the photodegradation of biocides deposited on their leaf surfaces, resulting in the formation of different photoproducts [342,344-346]. Thus, the importance of direct *vs* indirect UV-mediated photodegradation of biocides in the environment appears highly context dependent, and requires further research across a range of crops, environmental conditions and methods of application to clarify modes of action.

Climate change may be an additional factor impacting pesticide photodegradation on leaf surfaces. While photodegradation kinetics typically have a weak temperature dependence, pyrethroid insecticides applied onto spinach plants grown at 16 – 21∘C degraded up to 2 times slower than when plants were grown at lower temperatures (10 - 15°C), likely due to differences in the chemical composition of leaf wax [347].

As observed for other contaminants [e.g., 348,112] biocide photodegradation products can be more toxic than their parent compounds. For example, some breakdown products generated by UV-B radiation of the fungicide chlorothalonil and the insecticide imidacloprid on plant leaves are more toxic to fish than their parent compounds [345].

Functional nano-pesticides are being developed using nano-emulsion technologies as an alternative to traditional pesticide applications [349-352]. Encapsulated pesticides in nano-carriers, such as polymers, nanoclays, and metal organic frameworks provide controlled-release kinetics and improved stability against environmental degradation by UV radiation. The use of encapsulated pesticides prevents undesirable pesticide losses and release into the environment that otherwise would cause ecological and health concerns [353]. The development of nano-biocides may contribute to more environmentally friendly and sustainable food production systems (Sect. 7), potentially protecting the integrity of biocides during their application on crops, while still facilitating subsequent degradation of their residues.

5.5   Development and application of UV lighting systems in agriculture

Concerns over the effects of elevated UV-B radiation resulting from ozone depletion on food production stimulated considerable research into the effects of UV-B radiation on crops, and much of this early research focused mainly on the leaf-level physiology and shoot growth of traditional crop plants (e.g., soybean, rice, maize; [354]). More recently, studies have examined effects of UV-B radiation on plants of medicinal value, mushrooms and algae [355]. For example, mushrooms [356,357] and certain microalgae [358] synthesise increased amounts of vitamin D after being exposed to UV-B radiation (Sect. 5.2) [358,359]. In addition, more attention is being given to studying the effects of UV-B radiation on seeds, fruits, subterranean organs (e.g., roots and tubers), and on derived products, such as wine and olive oil [313,360-363].

Results from these studies indicate that plants exposed to low or moderate levels of UV-B radiation in controlled environments (e.g., greenhouses, growth chambers) often have improved vigour, enhanced nutraceutical quality and are more resistant to pest and pathogens compared to plants that are grown in the absence of UV-B radiation, as typically occurs in commercial production glasshouses [282].

Other studies have shown how the application of UV-B radiation can modulate different physiological processes important for agriculture. These advances include, 1) accumulation of anthocyanins and other antioxidants in different coloured fruits, such as peach, apple, grapes, and blueberry [314,363-366] (Sect. 5.2); 2) improving the tolerance of rice and tomato to low temperatures, salinity and drought [367,368]; 3) the manipulation of flavonoid accumulation in vegetables [369]; 4) the production of smaller cucumber plants for targeted commercialisation [175]; 5) an increase in anticancer compounds in *Catharanthus roseus* [370] following treatment with a combination of hormones and UV radiation; and 6) extending the shelf-life of fruit by reducing the activity of enzymes involved in fruit rotting [371]. Also, the accumulation of bioactive compounds can be triggered more effectively by applying high UV-B radiation during

short periods in specific developmental stages (frequently near harvest) rather than using UV-B radiation over longer periods. This approach has been successfully applied in kale and grapes [362,372,373]. These advances have been achieved by translating research that was conducted to better understand the effects of increased UV-B radiation resulting from ozone depletion into commercial practices to improve food quality and production (Sect. 7).

One of the more significant technological advances in plant UV research and horticulture has been the development and use of UV light-emitting diodes (LEDs). Increasingly, LED lighting systems are being used by growers before and after harvest to improve food value. LEDs are more energy-efficient and environmentally friendly than most traditional light sources used in horticulture (e.g., high-pressure sodium vapour or metal halide lamps), and by utilising LEDs that emit both in the UV and PAR regions the control of the spectral composition, intensity and exposure period can be attuned to the light requirements of specific plants and crops [374,375]. However, at present, only UV-A LEDs have been widely adopted to stimulate the accumulation of desirable plant compounds [376]. There are also some examples of successful application of UV LEDs in reducing certain plant diseases [377] and increasing nutritional quality [376].

6 Effects on biogeochemical cycles and climate feedbacks

Terrestrial ecosystems provide many valuable services, including the processing of dead organic material and the storage and recycling of essential nutrients. Both land vegetation and soils are also important carbon sinks that influence the concentrations of atmospheric CO_2 and hence climate. Solar UV radiation affects carbon storage and atmospheric CO_2 by influencing plant productivity [3], and the photodegradation of modern dead plant material (litter) and ancient organic matter preserved in permafrost soils [378,379], which becomes exposed to solar radiation because of climate change-induced thawing [380-384] (Box 2). Changes in climate and UV radiation can further interact to alter the cycling of other elements (nitrogen being the most important) and the emissions of GHGs other than CO_2, which can affect stratospheric ozone and climate. Below we evaluate new findings that address the underlying mechanisms and climate consequences of the interactive effects of UV radiation and climate change on biogeochemical cycles.

6.1   Photodegradation of plant litter

The decomposition of plant litter is a key biogeochemical process determining rates of nutrient cycling and energy flow in terrestrial ecosystems. This process affects vegetation productivity, carbon storage and soil fertility, and releases CO_2 and other GHGs to the atmosphere [385]. Thus, decomposition of litter has important feedback effects to the climate system.

In general, the rate of litter decomposition is regulated by climatic factors (temperature and moisture) and the chemical composition of litter (primarily the amount of lignin and the ratio of carbon to nitrogen (C:N ratio) in the litter), which modifies the activity and composition of the decomposer organisms (fungi, bacteria and invertebrate decomposers). Exposure of litter to solar UV radiation and short wavelength visible radiation (i.e., blue and green light), can cause the direct breakdown of lignin and other plant cell wall constituents forming non-volatile and volatile compounds (e.g., CO_2 which is released to the atmosphere). This process is referred to as photochemical mineralisation or photomineralisation [385,386] (Fig. 3a, right panel). Additionally, UV and short-wavelength visible radiation can also accelerate the breakdown of litter by changing its chemistry, making it more palatable to microbes and thereby enhancing microbial decomposition (Fig. 3a, left panel) [387-389]. Promotion of microbial activity can also occur by the photodegradation of waxy surfaces layers (i.e., leaf cuticle) that allows moisture to more readily penetrate litter [390]. These indirect effects of solar radiation on microbial decomposition are collectively referred to as photo-priming or photofacilitation [391,392]. In some situations, solar UV radiation can negatively affect litter decomposition by altering the composition and activities of the decomposer community (not shown in Fig. 3) [393]. The overall effect of solar radiation on litter decomposition reflects the net effect of these three processes [391].

Among litter components, lignin has been identified as the most photoreactive due to its absorption in the UV and blue-green region of the solar spectrum [385,392]. However, recent studies have found that cellulose and hemicellulose are even more susceptible to photodegradation than lignin [394,395]. These discrepancies are an unresolved knowledge gap that could be addressed by identifying differences in the photodegradation action spectra for lignin, cellulose, and hemicellulose. The presence of polyphenolic compounds in plant litter (Sect. 3.1) decreases photodegradation under natural [396] and controlled laboratory conditions [397]. This result suggests that the accumulation of polyphenolic secondary metabolites in green leaves may persist during the early phase of litter decomposition and attenuate the penetration of UV-B radiation into litter. The surface area of litter exposed to solar radiation is also an important predictor of litter decomposition rate and carbon turnover [398-400].
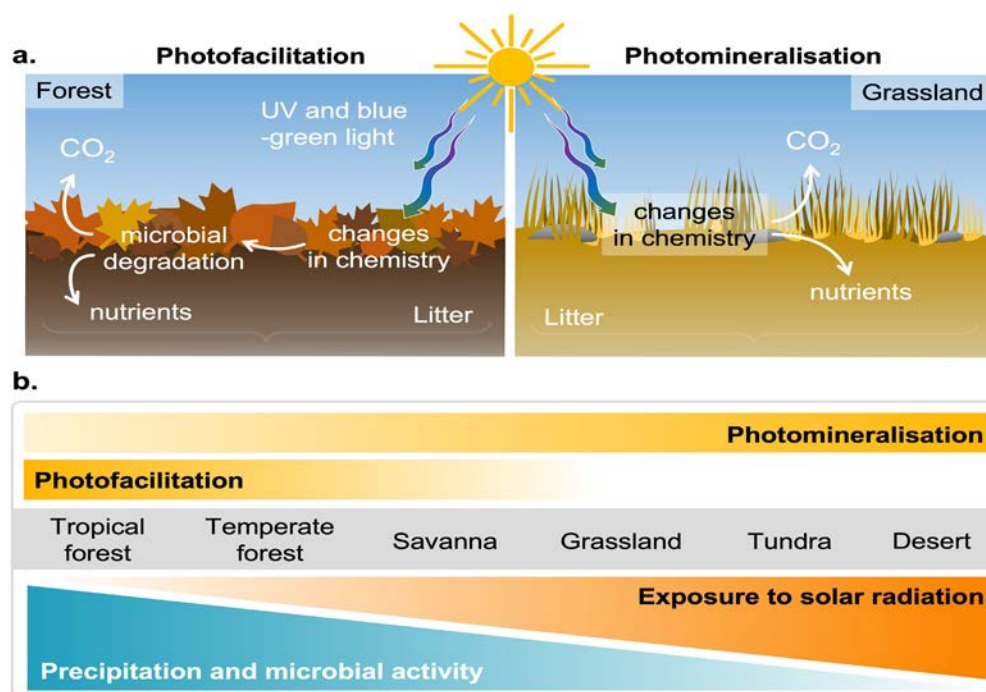
Fig. 3 The relative importance of photomineralisation and photofacilitation in litter decomposition across terrestrial biomes and environments. Panel **a** illustrates the processes of photofacilitation and photomineralisation in the photodegradation of surface litter exposed to solar radiation (UV radiation and blue-green light) in representative wet (forest; greater photofaciliation) and dry (grassland; greater photomineralisation) ecosystems. Panel **b** shows relative changes in photofacilitation and photomineralisation across biomes and along gradients of moisture, microbial activity and exposure to solar radiation. Not shown in this figure is the potential leaching of non-volatile breakdown compounds resulting from photodegradation of litter that can occur when it rains, and possible negative direct effects of UV radiation on microbes.

Photodegradation of litter was initially thought to be important only in dryland ecosystems (e.g., deserts and grasslands) where low moisture and high temperatures often constrain the activities of decomposing microbes. Recent studies have established that photodegradation of litter is important not only in semi-arid [401-403] and arid [404-407] ecosystems but also in moist environments that support tropical [408], subtropical [409], temperate and boreal forests [393,396,397], alpine steppe [410], and marshes [411].

Calculations of the strength of the terrestrial carbon sink have typically excluded photodegradation of litter in mesic ecosystems (having moderate water supply) due to their high vegetation cover. However, recent field studies found that photodegradation of litter facilitates carbon cycling in canopy openings of temperate and tropical forests, even where understory solar radiation is relatively low [396,397,408,412]. Exposure to the full solar spectrum, resulting from the formation of a forest gap, can increase litter photodegradation rates by up to 120% relative to shaded conditions across a wide diversity of plant species [396]. This number is considerably higher than that for photodegradation in semi-arid regions (60%) [413] or across several habitats or biomes (23%) [387], underscoring the importance of forest disturbance in mesic ecosystems. Exposure to solar radiation alters lignin structure of litter in the early stages of decomposition, promoting litter degradation via photofacilitation. This fact highlights the role of photofacilitation in mesic ecosystems, where higher water availability favours microbial decomposition compared to drylands [388,414] (Fig. 3). On the other hand, relatively high UV radiation, which occurs during the time of the year when the forest canopy is leafless, may also have an inhibitory effect on microbial decomposers [397]. The seasonal consequences of these effects of UV radiation on understory microbes and overall ecosystem health and function remain unclear.

Recent studies have clarified the relative importance of the different wavelengths of solar radiation (i.e., UV-B, UV-A and blue-green) in driving photodegradation of litter and these findings have implications for the effects of ozone depletion on this process. A recent meta-analysis found that, globally, solar radiation increases litter mass loss by 15.3 (± 1.0)% relative to litter that has not been exposed to solar radiation [415]. The contribution of UV-B radiation was found to be significant only in specific environments, causing an 18% and 23% loss of litter mass in semi-arid regions and polar regions, respectively. The relatively limited importance of UV-B radiation in promoting loss of litter mass agrees with the results obtained with a new spectral weighting function for litter photomineralisation, which showed that UV-B and UV-A radiation, together with visible blue-green light, are responsible for 9%, 61% and 30%, respectively, of total photochemical (abiotic) carbon loss [405] (Fig. 4). Overall, these rather small effects of UV-B radiation suggests that litter photodegradation would be minimally affected by further changes in stratospheric ozone.
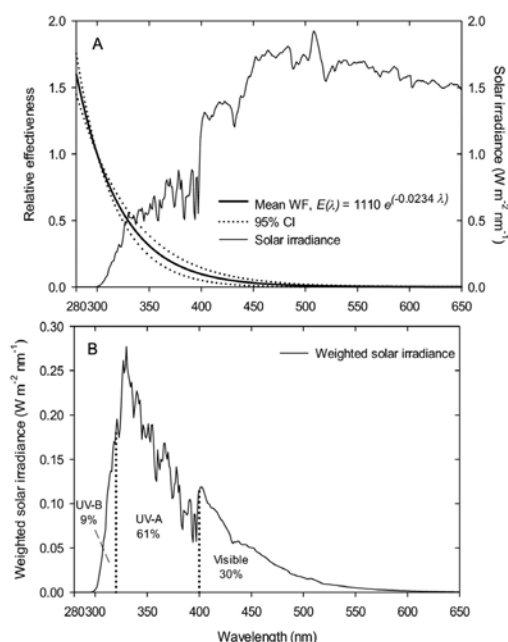
Fig. 4 Action spectrum and weighted solar radiation for the photo-mineralisation of litter from plants in the North American Sonoran Desert. Panel A shows the mean weighting function/action spectrum for the photo-mineralisation of plant litter (heavy solid line; measured as CO_2 loss), with 95% confidence interval (dotted line; CI), along with the average solar noon spectral irradiance over the time period of the study (thin solid line). Panel B shows solar radiation at solar noon weighted according to the action spectrum in Panel A, along with the total % effectiveness of the solar UV-B, UV-A and visible wavebands. Adapted from [405].

Photodegradation can also be influenced by changes in vegetation cover and soil erosion that result from changes in land use and climate, including ECEs (Sect. 2.2). The loss of forests and other natural or semi-natural vegetation cover due to agricultural practices increases photo-degradation of surface litter [19,398], such that deforestation and land clearing will accelerate release of carbon from the ecosystem and alter patterns of greenhouse gas emissions and nutrient cycling [396,403,416,417]. In dryland ecosystems, litter position (e.g., at the soil surface *vs* buried or covered in dust) is the predominant factor determining carbon loss from photodegradation [418,399]. In contrast to forests, these dryland systems are experiencing an increase in woody plant cover as a result of changes in land use and climate and these vegetation shifts result in more shading of ground litter and increased soil erosion and deposition, which decrease litter photodegradation [419,420]. Additional environmental changes such as increased nitrogen deposition and abandonment or less intensive use of agricultural land may slow litter decomposition through the attenuation of surface UV radiation by increased plant canopy development [410].

Rainfall is another factor affecting litter photodegradation. In an experiment performed in drylands, the addition of supplemental precipitation (simulating a 2.7 times increased rainfall) accelerated loss of litter mass by a factor of 2.6 under near-ambient solar radiation but had no effect if litter was not previously exposed to solar radiation [389]. This result suggests that photodegradation followed by leaching may be another significant mechanism of loss of litter mass in arid ecosystems [389,421].

Collectively, these findings indicate that the overall effect of photodegradation on the decomposition of plant litter depends on environmental conditions (primarily moisture and temperature), litter quality, the degree of exposure of litter to solar radiation (as influenced by vegetation cover, litter position and degree of soil-litter mixing), and the solar spectral composition of radiation reaching the litter layer [12]. Given the relatively small contribution of UV-B radiation to loss of litter mass and photomineralisation, ongoing and projected changes in stratospheric ozone and their interaction with climate and land-use changes are likely to impact litter photodegradation mainly by modifying its exposure to total solar radiation [12,19,146].

6.2   Photochemical release of nutrients from terrestrial ecosystems

Most studies of photodegradation of organic matter in terrestrial ecosystems have focussed on effects on carbon but, as demonstrated in aquatic ecosystems [112], UV radiation can also affect the storage and cycling of other elements, such as nitrogen and phosphorous. Even in understory environments, where the amount and spectral composition of solar radiation is greatly modified by canopy structure and phenology, UV-B radiation [396], UV-A radiation and blue light can promote the conversion of organic nitrogen into inorganic compounds (nitrogen mineralisation) [412,416].

A recent meta-analysis of litter degradation studies found that the amount of UV radiation received affected the timing of nitrogen and phosphorous loss compared to that of carbon [414] due to differences in the relative contribution of microbial vs photochemical degradation. Under reduced UV radiation, nutrient mineralisation was slow and poorly correlated with overall loss of litter mass, whereas, under increased UV radiation, phosphorous and nitrogen mineralisation was rapid and correlated with carbon mineralisation. These results suggest that microbial processes dominate nutrient cycling under low levels of UV radiation, while abiotic processes, which are characterised by a simultaneous release of nutrients and carbon, are more important at higher UV irradiances. Thus, under conditions of high UV irradiation the nutrients in litter may be made more rapidly available to plants, potentially reducing competition

for nutrients between plants and microbes. These effects could play a significant role in ecosystem functioning but have not yet been thoroughly studied. The release of mineral forms of nitrogen is also likely to produce volatile nitrogen compounds including nitrous oxide (N_2O), which is both a powerful GHG and ODS [19]. Given the obvious implications for climate and stratospheric ozone, the effect of UV radiation on N_2O emissions by litter remains a critical knowledge gap to be addressed in future studies.

Box 2 Biogeochemical cycling of warming permafrost under climate change

The world's soils store large amounts of carbon, approximately two-to-three times more than the atmosphere (Panel A below; [378]). Therefore, even small instability or degradation of soils driven by perturbations in climate can lead to large releases of carbon. A large proportion of soil carbon is stored at high northern latitudes, where it has remained stable in peatlands and permafrost soils over long time periods; often many thousands of years.

Permafrost is defined as any ground that remains completely frozen for at least two consecutive years. There is extensive evidence that climate warming is causing permafrost to thaw [381]. This releases large amounts of organic carbon that was previously locked underground, whereby it becomes available for microbial and photochemical decomposition [384]. These two processes release dissolved organic matter (DOM) and greenhouse gases (GHGs) such as CO_2 [382, 383]

The effects of climate change on vegetation growing at high latitudes differ according to the region and vegetation type. These effects are illustrated in Panel B below. Warmer winters and springs mean that less precipitation falls as snow, and that the snowpack melts earlier. Reduced snow cover allows more solar radiation to reach the soil, thereby increasing photodegradation (B, circle a). A smaller snowpack also exposes vegetation to the environment above the snowpack for longer, leaving it more susceptible to damage and desiccation (referred to as Arctic browning; [84]). The resultant loss of vegetation cover can lead to soil erosion and loss of ecosystem stability [86, 87]. In this scenario, these ecosystems become sources of carbon and release nutrients. Moribund vegetation is unable to take up these nutrients, more of which are leached into waterways or emitted as gases [384], including the potent greenhouse gas N_2O (Sect. 6.2). Elsewhere, warmer temperatures may extend the growing season and nutrient release from thawing permafrost, which will increase plant growth and vegetation cover (Arctic greening). Additional shade from vegetation intercepts solar radiation before it reaches the soil, thereby limiting photodegradation (B, circle b). However, warming also leads to increased disturbance in these ecosystems, including more frequent wildfires, drought, floods, heatwaves, and herbivore outbreaks. Disturbance events generally destabilise the soil and contribute to the release of organic carbon from permafrost to waterbodies (B, circles c-d) [80], where it is subject to continued photodegradation to CO_2 (B, circle d.; see also [112]).
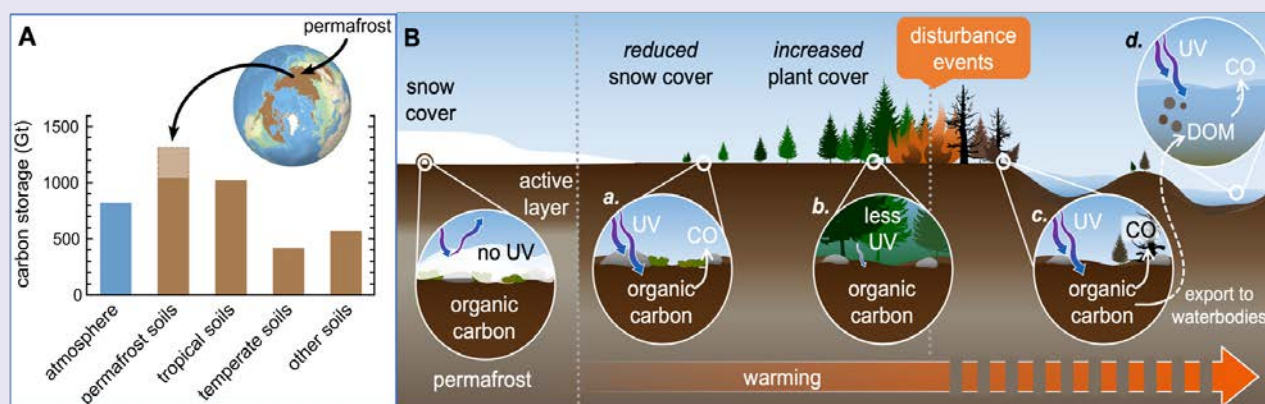
Panel A, comparison of carbon stocks in various type of soils (brown bars) and the atmosphere (blue bar). The lighter extended bar gives the contribution from permafrost soils greater than 3 m depths that is not relevant to the other soil types. Reproduced and modified from [378]. **Panel B,** schematic showing the effect of warming on permafrost. Prior to climate change, soils and vegetation were covered for much of the year (left). Warming leads to reduced snow cover, permafrost thaw, and subsequent increased frequency of disturbance events like fire, floods, droughts and insect damage causing dieback. Inset circles illustrate how solar UV radiation interacts with these climate driven processes in soil (a-c) and waterbodies (d). Climate change is causing the active top layer of soil to thaw during the summer and freeze again in the autumn – this active layer is becoming deeper and staying unfrozen for longer.

6.3   Methane emissions, UV radiation and plants

Methane (CH_4) is a potent greenhouse gas, such that relatively small changes in its emissions can make a significant contribution to climate change [422]. In addition to anthropogenic emissions, methane is released naturally by terrestrial ecosystems, particularly wetlands [423,424]. At present, solar UV radiation is not considered an important driver of methane emission from terrestrial ecosystems [9,425,112]. However, there is concern that climate changes associated with stratospheric ozone depletion at high latitudes (tundra and taiga ecosystems in the Northern Hemisphere and peatlands or wetlands in the Southern Hemisphere) may enhance methane emissions [19].

Plants often serve as conduits of methane produced by bacteria in damp soils [426]. They also contribute to methane emissions through photochemical mineralisation of pectin, waxes, and lignin by UV-B radiation, although this effect is deemed rather small [427]. Methane emission from plants is accelerated by interaction with other stressors such as herbivore damage and high temperatures [428]. Controlled experiments with Scots pine and Norway spruce under ambient conditions in Finland found a positive relationship between methane emissions and solar radiation, which was steeper at warmer temperatures [429]. Even then, in most habitats, direct emission from plants through photodegradation of pectin [430] is considered only a minor contributor to global terrestrial methane emissions [429,422].

Methane emission from plants also occurs through microbial methane production in the heartwood of trees (reviewed by [422,425,431]). From there, methane can be released to the atmosphere by passing through the bark or through the plant's vascular system. This process is currently thought to be the main avenue of plant methane emissions in non-wetland environments, and it is modulated by the moisture and phenolic content of heartwood rather than by UV radiation [432]. Reactive oxygen species (ROS), which are produced in all organisms and can be enhanced by oxidative stress, also take part in reactions that can release methane. Additional research is required to at the global scale to provide for a more complete understanding of the effects of climate and UV radiation on terrestrial methane emissions [428,425,433,422].

6.4   Interactions of UV radiation with fire-derived carbon

Forest fires are increasing in severity and frequency and will become even more prevalent as the climate continues to change [20]. Boreal forests are particularly vulnerable to fires as extreme warming is expected in this region [434-440] close to the Arctic circle. Forest fires directly contribute to climate change by releasing GHGs such as CO_2, methane, and nitrous oxide [15,435]. Wildfires also provide an important pathway for opening soil surfaces to UV irradiation, leading to enhanced photodegradation of organic matter with consequent release of CO_2 (Sect. 6.1; Box 2). Due to the incomplete combustion of wood and other biomass, fires convert a substantial fraction of vegetation into burnt biomass, termed charcoal or pyrogenic carbon (PyC) [437]. Recent estimates indicate that *ca*. 256 Tg carbon (TgC) yr^{-1} (range = 196–340 TgC yr^{-1}; 1 teragram = 1012 grams) of biomass were converted into pyrogenic carbon between 1997 and 2016 [441]. During rainfall events following a wildfire, ash and pyrogenic carbon (estimated up to 203 TgC yr^{-1} in a modelling study [442]) reach nearby watersheds, resulting in increased loads of organic carbon, nutrients, and metals [443,444]. The impact of wildfires on surrounding water bodies can last for years, affecting biogeochemical processes and drinking water quality [445,443]. In addition, fire-derived aerosols can temporarily reduce incident UV radiation reaching the Earth's surface [145] and slow down UV-driven chemical processes in the troposphere [15].

Pyrogenic carbon includes a broad suite of chemicals such as anhydrous sugars, condensed aromatics (often named black carbon), and graphitic carbon [441]. The specific chemical composition of PyC depends on biomass type and charring temperature, and this composition affects its solubility, bioavailability, and photoreactivity [441,444,446,447]. Adding to previous findings [441], recent studies confirmed that black carbon is the most photoreactive fraction of PyC [448] and that microbial mineralisation of PyC can be enhanced by prior exposure to UV radiation (i.e., photofacilitation) [444,447], similar to plant litter (Sect. 6.1) and dissolved organic matter in water [112].

7 Sustainability and the Montreal Protocol

By protecting the stratospheric ozone layer and mitigating some of the effects of climate change, the Montreal Protocol and its Amendments are assisting in the implementation of several of the United Nations Sustainable Development Goals (SDGs). Many findings in our Quadrennial Assessment address SDGs and specific targets that are relevant to agriculture (*SDG 2: Zero hunger*) and terrestrial ecosystems (*SDG 15: Life on land*) (Fig. 5). Other relevant contributions of the Montreal Protocol are related to pollution and contamination (*SDG 3: Good health and well-being*), and climate change (*SGD 13: Climate action*). Specific SDG targets addressed by our findings are described below.

SDG 2: Zero hunger

While small increases in solar UV-B radiation do not appear to pose a threat to crop yield, extreme increases in UV-B radiation, as would have occurred without the Montreal Protocol, would likely have significantly decreased agricultural productivity (Sect. 5) and jeopardised SDG 2 and particularly 2.4 (*Sustainable food production and resilient agricultural practices*). Several studies have shown that moderate UV radiation can alter the chemical composition of food and medicinal plants (Fig. 5a). In most cases, UV radiation increases the nutritional profile of some crop species (e.g., by increasing the concentration of certain antioxidants, e.g., flavonoids), with potential long-term positive outcomes for human health (Sect. 5.2). The latter finding has motivated the development of agricultural practices (e.g., UV-transparent greenhouse coverings and UV-emitting LEDs) that exploit low and medium levels of UV-B radiation to enhance the nutraceutical properties of crops (Sect. 5.5). These practices can be directly deployed in both developed and developing countries to obtain food with an improved nutritional profile for increased food security.

SDG 3: Good health and well-being

Plants exposed to modest levels of UV radiation often display some increase in resistance to pests and pathogens (Sect. 5.3), which could lead to reduced use of pesticides. However, solar UV radiation also degrades certain pesticides (Fig. 5a). This may lead to increased application of pesticides (Sect. 5.4), which could increase the risk of exposure of workers and consumers to these chemicals as well as adding to soil pollution and contamination (SDG 3.9). The net result on pesticide use likely depends on many factors, including changes in UV irradiance, cropping system, and types of pesticides.

SDG 13: Climate action

Modelling studies indicate that the Montreal Protocol and its Amendments have played a critical role in protecting global carbon sequestration by terrestrial vegetation, which has, in turn, slowed the build-up of CO_2 in the atmosphere and reduced a certain amount of global warming (Box 1). Also, exposure of plants to modest levels of UV radiation, that would not have continued to occur without the Montreal Protocol, can improve their tolerances to drought (Fig. 5b) and enhance resistance to pests and pathogens, thereby making crops and natural ecosystems more resilient to climate change (Sect. 2.2, 3.3; *SDG Target 13.1: Improve resilience to climate change*). Finally, this Assessment prepared for the Parties to the Montreal Protocol and as a scientific publication contributes to *SDG Target 13.3 (Improve education, awareness-raising and human and institutional capacity on climate change mitigation, adaptation, impact reduction and early warning*).
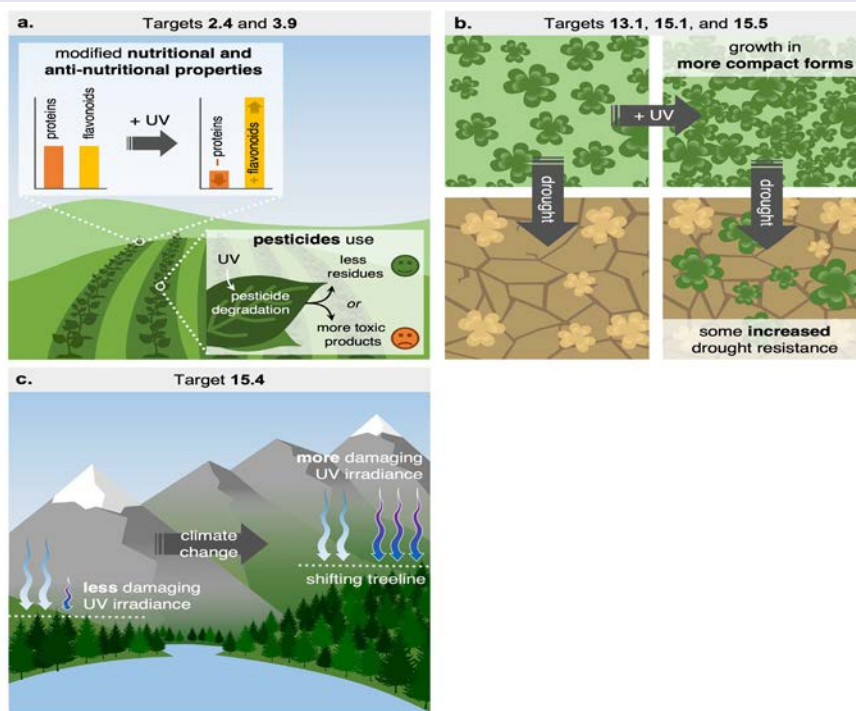
Fig. 5 Pictorial representation of how the Montreal Protocol and its Amendments align with several Sustainable Development Goals (SDG) and their targets. Panel **a** shows SDGs 2.4 (*Sustainable food production and resilient agricultural practices*) and 3.9 (*Deaths and illnesses from hazardous chemicals and soil pollution and contamination*). Panels **b** and c show SDGs 13.1 (*Strengthen resilience and adaptive capacity to climate related disasters;* centre panel) and 15.1, 15.4, 15.5 (*Protect, restore and promote sustainable use of terrestrial ecosystems, sustainably manage forests, combat desertification, and halt and reverse land degradation and halt biodiversity loss*).

SDG 15: Life on land

Increasing temperatures due to climate change are shifting the distribution ranges of plants and animals to higher elevations and latitudes, which changes their exposure to solar UV irradiation (Fig. 5c; Sect. 4.1). Some modelling studies suggest that UV radiation can be important in influencing the distribution shifts in plants (Sect. 4.2), which have the potential to negatively impact biodiversity (*SDG Target 15.1: Conservation of terrestrial ecosystems*). For mountain ecosystems, the shift to higher altitudes is often more pronounced for invasive species, which then occupy ecological niches of endemic alpine species with negative outcomes for biodiversity (*SDG Target 15.4: Conservation of mountain ecosystems).*

SDG 17: Partnership

Monitoring of the stratospheric ozone layer and its interactions with climate change are key to understanding the effects of UV radiation on terrestrial ecosystems, therefore the assessment of how species respond to this climatic pressure represents a challenge imposed on all countries. Partnerships between countries in Northern and Southern Hemispheres have been facilitated by the Montreal Protocol, which has stimulated technology transfer and innovation on the effects of UV radiation on plants and animals among scientific communities worldwide (*SDG targets 17.6, 17.7 and 17.8: North-South cooperation to access science, technology and innovation; Promote development, transfer and dissemination of environmentally sound technologies; and Science, technology and innovation capacity-building mechanisms for least developed countries*). This partnership has facilitated international support for data acquisition and sharing on the stratospheric ozone layer and the effect of UV radiation on terrestrial ecosystems (*SDG target 17.9: Enhance international capacity-building to achieve SDGs*). This has assisted least developed countries to have first-hand information for the implementation of environmental policies towards the achievement of SDGs (*SDG target 17.14: Enhance policy coherence for sustainable development*).

8 Gaps in knowledge

In this assessment we have identified several important knowledge gaps. These include:

- **Additional well-designed field studies are needed on all the topics addressed here to increase the confidence in our assessment.** It is well-established that the responses of plants and other organisms to UV radiation are heavily dependent on other wavelengths of solar radiation as well as environmental factors such as temperature and moisture availability. There is also large inter- and intraspecific variation in sensitivity to UV radiation. Thus, the assessment of the effects of changes in solar UV radiation, stratospheric ozone and climate requires research conducted on a variety of species under natural, field conditions. However, studies conducted under controlled environmental conditions (e.g., growth chambers and glasshouses) can provide important insights into the mechanisms of effects of UV radiation. In our assessment we have included certain studies carried out under controlled conditions when the results appear plausible and/or are useful for increasing awareness of potential effects and outcomes, but more field studies are clearly needed to reduce many of the uncertainties identified in this assessment.

- **Research into the impacts of Solar Radiation Management (SRM), such as Stratospheric Aerosol Injection (SAI), is needed to keep pace with policy-makers' interest in these technologies.** This is of particular concern, given that the existing evidence might suggest that impacts on terrestrial ecosystems of adopting SAI, and in particular any eventual termination or interruption of SAI following its adoption, are likely to be considerable, persistent and in some cases irreversible [24,26-28,449]. Importantly, some models of the effects of SRM on primary productivity by terrestrial ecosystems only draw on estimates derived from relatively simple and short-term calculations of changing canopy-level light-use efficiency under SAI scenarios. Experimental evidence of the relative importance of short-term responses *vs* the long-term acclimation of photosynthesis to the changes in spectral composition and irradiance brought by SAI have yet to be assessed through controlled experiments. Thus, we are not in a position to confidently assess the effects of SAI on ecosystem-level carbon assimilation at this time.

- **Experimental studies are needed to verify findings from modelling studies aimed at quantifying the environmental consequences of extreme levels of solar UV-B radiation, as would have occurred with uncontrolled emissions of ODS.** While these modelling studies are powerful approaches to understanding the benefits of the Montreal Protocol, and assessing the risks of future changes in the stratospheric ozone layer [e.g., 3], they rely on several assumptions that can lead to large uncertainties in the findings. As experimental studies on organisms exposed to these extreme amounts of UV radiation are lacking, it is often assumed that the effects of UV-B radiation on growth, productivity and reproduction observed under current UV radiation can be linearly extrapolated to higher amounts of UV radiation. This assumption is likely unrealistic, especially for the more extreme ozone depletion scenarios that would have eventually occurred without the Montreal Protocol. In addition, little is known about how the photomorphogenic responses of plants, which are driven by photoreceptors such as UVR8, are affected by extreme levels of UV-B radiation, or about the levels of UV irradiation where damage by the UV-B waveband supersedes the regulatory, photomorphogenic effects.

- **There is a critical need to develop action spectra for plants and other organisms, which more accurately describe biological responses to the different wavelengths of UV radiation under the full solar spectrum.** Action spectra are fundamental to interpreting biological responses to changes in UV radiation that occur with stratospheric ozone depletion and they also serve as spectral weighting functions in both laboratory and field experiments [450]. Large uncertainties in assessing the effects of ozone depletion can occur if inappropriate action spectra are used [451].

- **The establishment of long-term biomonitoring studies would improve our ability to assess how organisms and ecosystems will respond to the ongoing changes in UV radiation and climate.** Changes in UV radiation and climate, especially extreme climate events and combined extreme events (e.g., wildfires), pose significant risks to the health, stability, and biodiversity of terrestrial ecosystems, but little experimental or modelling data exist to quantify these effects. These studies are critically needed for organisms and ecosystems in polar regions, the tropics and high elevation mountains.

- **The establishment of a global UV radiation biomonitoring network using material from selected organisms (from pollen to plants and animals) could further increase our knowledge and reduce uncertainties on the use of biological proxies for solar UV radiation.** Certain plant material and tissues, such as herbarium specimens and pollen in sediment cores, have the potential to serve as proxies for reconstructing past UV radiation environments on Earth, but presently there are large uncertainties associated with these techniques.

- **Studies are needed to characterise a wider array of interactive effects to adequately assess the consequences and map potential mitigation options of ongoing changes in solar UV radiation together with other contemporary environmental changes.** Advances have been made in understanding how UV radiation interacts with other climate change factors (e.g., UV radiation and drought) to affect the growth and physiology of plants [452] but studies need to be expanded to include multiple interactive factors (e.g., UV radiation, temperature, drought, CO_2 concentrations).

- **There is a need for additional biomedical research examining how UV radiation-induced changes in plant secondary metabolites affects dietary availability of metabolites, and the impacts of these changes on food quality and the epidemiology of human diseases.** Evidence continues to mount showing that exposure of plants to UV radiation alters their secondary chemistry and nutritional quality. But how these changes affect human health is largely unknown. This knowledge gap needs to be addressed to gain a fuller understanding of climate change-associated effects of UV radiation and their consequences for consumers, as well as the development of more sustainable agricultural practices (Sect. 5.5 and 7).

- **Research is needed to better understand the effects of UV-B radiation on animals.** In comparison to terrestrial plants and ecosystems, there are far fewer studies on the effects of UV-B radiation on animals. While there are some similarities in experimental approaches used to study plant and animal responses to UV-B radiation (e.g., providing different UV-B radiation treatments using UV-emitting lamps) there are also some important differences that often limit the applicability of UV radiation research on animals. For example, plant research typically uses a filter material (e.g. cellulose diacetate) to remove the short wavelength UV radiation that is present in lamps but not in solar radiation [337]. Most plant research has also taken into account the effects of different UV wavelengths by using action spectra as biological spectral weighting functions in designing and interpreting experiments using UV radiation produced by lamps [337]. Not all studies of the responses of terrestrial animals, including insects and other invertebrates, adopt these approaches. In our assessment, these experimental deficiencies represent a significant limit in placing current understanding of invertebrate responses, mostly obtained using UV-emitting lamps, in the context of variation in solar UV-B radiation in the field.

- **Despite recent advances in understanding the ecological significance of photodegradation in the decomposition of plant litter, further research is needed to refine our mechanistic understanding of this process and assess its importance in the cycling of carbon and other nutrients, and feedbacks to the climate system.** Findings since our last Quadrennial Assessment have revealed that photodegradation of plant litter is not only important in drylands, but across all terrestrial ecosystems. These findings explain, in part, why traditional biogeochemical models of litter decomposition that do not include photodegradation are often inadequate in reproducing measured mass and carbon losses [402,453,454]. Despite this general finding, many knowledge gaps remain, notably the quantification of the relative importance of photomineralisation vs photofacilitation in both dry and mesic environments, and whether the spectral weighting function derived from studies in drylands also applies to mesic ecosystems. Nutrient cycling has also been much less studied than carbon cycling, and particularly how changes in nitrogen cycling caused by UV irradiance could feedback on climate change and stratospheric ozone depletion. Open questions also remain concerning the underlying chemistry controlling litter photomineralisation and the role of UV radiation in driving GHG emissions from the thawing of permafrost. Reducing these uncertainties would improve our ability to assess how changes in UV radiation and climate will impact carbon cycling and feedbacks to the climate system.

9 Conclusions

The findings presented in this Quadrennial Assessment indicate that changes in stratospheric ozone, UV radiation and climate can interact in various ways to modify terrestrial ecosystems and biogeochemical cycles. While exposure to solar UV radiation, and in particular the short wavelength UV-B radiation, has the potential to cause deleterious effects on plants, animals, and microorganisms, most species have evolved mechanisms to tolerate or avoid harmful solar UV radiation at the Earth's surface within the range experienced without significant ozone depletion. The extreme UV irradiances that would have occurred without the Montreal Protocol (i.e., "World-Avoided" scenarios) would likely have exceeded these tolerance limits and greatly reduced the productivity and biodiversity of terrestrial ecosystems. These conditions would also have driven increased photodegradation of organic matter and nutrient cycling, which would have increased emission of GHGs, including nitrous oxide, an ozone-depleting and greenhouse gas. Our findings further indicate that, in some cases, moderate levels of solar UV radiation (i.e., ambient UV irradiances without appreciable ozone depletion) can have some positive effects on organisms and the environment (e.g., improved food quality, enhanced plant defence against pests, improved plant vigour and resistance to other abiotic stresses, and the photodegradation of pesticides). Maintaining these beneficial effects of moderate UV radiation would have been impossible without the Montreal Protocol. Thus, the Montreal Protocol and its Amendments have played, and continue to play, a vital role in maintaining healthy, diverse ecosystems on land that can sustain life on Earth. The Montreal Protocol and its Kigali Amendment are also directly and indirectly protecting the Earth's climate and mitigating some of the negative consequences of climate change by limiting the emissions of GHGs and protecting the carbon sequestration potential of vegetation and the terrestrial carbon pool [3,5].

Since our last full assessment [12], there have been additional extreme weather events (e.g., heat waves, droughts, and hurricanes) and events resulting from a combination of weather extremes and other drivers (e.g., wildfires) that have all contributed to the disruption and destabilisation of terrestrial ecosystems. These have been particularly pronounced in polar regions where anomalies in stratospheric ozone and ozone-driven climate change have occurred in the last three years [10]. Ozone depletion over Antarctica in certain years has coincided with early summer and has likely resulted in greater exposure to UV radiation of animals, plants and microbes. These, and other extreme events (as outlined in Sect. 2.2), are expected to increase in frequency and intensity in the future because of climate change [20]. Together with other aspects of climate change, these extreme events will likely alter the UV radiation received by terrestrial organisms to a greater degree than the expected changes in the stratospheric ozone layer—assuming continued and full compliance with the Montreal Protocol. While understanding of the mechanisms of these UV-climate interactions is improving, the scale of their effects in terrestrial ecosystems remain poorly defined at present. Nonetheless, our findings indicate that the Montreal Protocol and its Amendments continue to make valuable contributions towards mitigating some of the negative environmental consequences of climate change as well as addressing several of the SDG targets established in the United Nations 2030 Agenda for Sustainable Development.

Author contributions All authors contributed to the conception and assessment, and carried out extensive revisions of content.

Conflict of interest The authors have no conflicts of interest.

References

1. McKenzie, R., Bernhard, G., Liley, B., Disterhoft, P., Rhodes, S., Bais, A., Morgenstern, O., Newman, P., Oman, L., Brogniez, C., & Simic, S. (2019). Success of Montreal Protocol demonstrated by comparing high-quality UV measurements with "World Avoided" calculations from two chemistry-climate models. *Scientific Reports, 9*(1), 12332, https://doi.org/10.1038/s41598-019-48625-z.

2. Barnes, P. W., Bornman, J. F., Pandey, K. K., Bernhard, G. H., Bais, A. F., Neale, R. E., Robson, T. M., Neale, P. J., Williamson, C. E., Zepp, R. G., Madronich, S., Wilson, S. R., Andrady, A. L., Heikkilä, A. M., & Robinson, S. A. (2021). The success of the Montreal Protocol in mitigating interactive effects of stratospheric ozone depletion and climate change on the environment. *Global Change Biology, 27*(22), 5681-5683, https://doi.org/10.1111/gcb.15841.

3. Young, P. J., Harper, A. B., Huntingford, C., Paul, N. D., Morgenstern, O., Newman, P. A., Oman, L. D., Madronich, S., & Garcia, R. R. (2021). The Montreal Protocol protects the terrestrial carbon sink. *Nature, 596*(7872), 384-388, https://doi.org/10.1038/s41586-021-03737-3.

4. Smith, S. L., O'Neill, H. B., Isaksen, K., Noetzli, J., & Romanovsky, V. E. (2022). The changing thermal state of permafrost. *Nature Reviews Earth & Environment, 3*(1), 10-23, https://doi.org/10.1038/s43017-021-00240-1.

5. Goyal, R., England, M. H., Sen Gupta, A., & Jucker, M. (2019). Reduction in surface climate change achieved by the 1987 Montreal Protocol. *Environmental Research Letters, 14*(12), 124041, https://doi.org/10.1088/1748-9326/ab4874.

6. Purohit, P., Borgford-Parnell, N., Klimont, Z., & Höglund-Isaksson, L. (2022). Achieving Paris climate goals calls for increasing ambition of the Kigali Amendment. *Nature Climate Change, 12*(4), 339-342, https://doi.org/10.1038/s41558-022-01310-y.

7. WMO (2018). *Scientific Assessment of Ozone Depletion: 2018*, Global Ozone Research and Monitoring Project-Report No. 58, 588 pp., Geneva, Switzerland, http://ozone.unep.org/science/assessment/sap

8. WMO (2022). *Scientific Assessment of Ozone Depletion: 2022,* GAW Report No. 278. 509 pp., World Meteorological Organization, Geneva, Switzerland, https://ozone.unep.org/science/assessment/sap

9. Bais, A. F., Bernhard, G., McKenzie, R. L., Aucamp, P. J., Young, P. J., Ilyas, M., Jöckel, M., & Deushi, M. (2019). Ozone-climate interactions and effects on solar ultraviolet radiation. *Photochemical & Photobiological Sciences, 18*, 602-640, https://doi.org/10.1039/C8PP90059K.

10. Bernhard, G. H., Bais, A. F., Aucamp, P. J., Klekociuk, A. R., Liley, J. B., & McKenzie, R. L. (2022). Stratospheric ozone, UV radiation, and climate interactions. *Chapter 1*

11. Wang, J. A., & Friedl, M. A. (2019). The role of land cover change in Arctic-Boreal greening and browning trends. *Environmental Research Letters, 14*(12), 125007, https://doi.org/10.1088/1748-9326/ab5429.

12. Bornman, J. F., Barnes, P. W., Robson, T. M., Robinson, S. A., Jansen, M. A. K., Ballaré, C. L., & Flint, S. D. (2019). Linkages between stratospheric ozone, UV radiation and climate change and their implications for terrestrial ecosystems. *Photochemical & Photobiological Sciences, 18*, 681-716, https://doi.org/10.1039/C8PP90061B.

13. Bais, A. F., McKenzie, R. L., Bernhard, G., Aucamp, P. J., Ilyas, M., Madronich, S., & Tourpali, K. (2015). Ozone depletion and climate change: impacts on UV radiation. *Photochemical & Photobiological Sciences, 14*(1), 19-52, https://doi.org/10.1039/c4pp90032d.

14. Lamy, K., Portafaix, T., Josse, B., Brogniez, C., Godin-Beekmann, S., Bencherif, H., Revell, L., Akiyoshi, H., Bekki, S., Hegglin, M. I., Jöckel, P., Kirner, O., Liley, B., Marecal, V., Morgenstern, O., Stenke, A., Zeng, G., Abraham, N. L., Archibald, A. T., Butchart, N., Chipperfield, M. P., Di Genova, G., Deushi, M., Dhomse, S. S., Hu, R.-M., Kinnison, D., Kotkamp, M., McKenzie, R., Michou, M., Connor, F. M., Oman, L. D., Pitari, G., Plummer, D. A., Pyle, J. A., Rozanov, E., Saint-Martin, D., Sudo, K., Tanaka, T. Y., Visioni, D., & Yoshida, K. (2019). Clear-sky ultraviolet radiation modelling using output from the Chemistry Climate Model Initiative. *Atmospheric Chemistry and Physics, 19*(15), 10087-10110, https://doi.org/10.5194/acp-19-10087-2019.

15. Madronich, S., Sulzberger, B., Longstreth, J. D., Schikowski, T., Sulbæk Andersen, M.P., Soloman, K. R., & Wilson, S. R. (2022). Changes in tropospheric air quality related to the protection of stratospheric ozone in a changing climate. *Chapter 6*

16. Pu, W., Cui, J., Wu, D., Shi, T., Chen, Y., Xing, Y., Zhou, Y., & Wang, X. (2021). Unprecedented snow darkening and melting in New Zealand due to 2019–2020 Australian wildfires. *Fundamental Research, 1*(3), 224-231, https://doi.org/10.1016/j.fmre.2021.04.001.

17. Damany-Pearce, L., Johnson, B., Wells, A., Osborne, M., Allan, J., Belcher, C., Jones, A., & Haywood, J. (2022). Australian wildfires cause the largest stratospheric warming since Pinatubo and extends the lifetime of the Antarctic ozone hole. *Scientific Reports, 12*(1), 12665, https://doi.org/10.1038/s41598-022-15794-3.

18. Bernath, P., Boone, C., & Crouse, J. (2022). Wildfire smoke destroys stratospheric ozone. *Science, 375*(6586), 1292-1295, https://doi.org/10.1126/science.abm5611.

19. Sulzberger, B., Austin, A. T., Cory, R. M., Zepp, R. G., & Paul, N. D. (2019). Solar UV radiation in a changing world: Roles of cryosphere-land-water-atmosphere interfaces in global biogeochemical cycles. *Photochemical & Photobiological Sciences, 18*, 747-774, https://doi.org/10.1039/C8PP90063A.

20. IPCC (2021). Climate Change 2021: The Physical Science Basis. Contribution of Working Group I to the Sixth Assessment Report of the Intergovernmental Panel on Climate Change. [V. Masson-Demotte, P. Zhai, A. Pirani, S.L. Connors, C.Péan, S. Berger, N. Caud, Y. Chen, L. Goldfarb, M.I. Gomis, M. Huang, K. Leitzell, E. Lonnoy, J.B.R. Matthews, T.K. Maycock, T. Waterfield, O. Yelekçi, R. Yu and B. Zhou (Eds)], doi.org/10.1017/9781009157896

21. IPCC (2022). Climate change 2022: Impacts, adaptation, and vulnerability. Contribution of Working Group II to the Sixth Assessment Report of the Intergovernmental Panel on Climate Change. [H.-O. Pörtner, D.C. Roberts, M. Tignor, E.S. Poloczanska, K. Mintenbeck, A. Alegría, M. Craig, S. Langsdorf, S. Löschke, V. Möller, A. Okem, B. Rama (eds.)]. Cambridge University Press. Cambridge University Press, Cambridge, UK and New York, NY, USA, 3056 pp., doi:10.1017/9781009325844

22. Crutzen, P. J. (2006). Albedo enhancement by stratospheric sulfur injections: A contribution to resolve a policy dilemma? *Climatic Change, 77*(3-4), 211-220, https://doi.org/10.1007/s10584-006-9101-y.

23. Kravitz, B., & MacMartin, D. G. (2020). Uncertainty and the basis for confidence in solar geoengineering research. *Nature Reviews Earth & Environment, 1*(1), 64-75, https://doi.org/10.1038/s43017-019-0004-7.

24. Madronich, S., Tilmes, S., Kravitz, B., MacMartin, D., & Richter, J. (2018). Response of surface ultraviolet and visible radiation to stratospheric SO_2 injections. *Atmosphere, 9*(11), https://doi.org/10.3390/atmos9110432.

25. Tilmes, S., Müller, R., & Salawitch, R. (2008). The sensitivity of Polar ozone depletion to proposed geoengineering schemes. *Science, 320*(5880), 1201, https://doi.org/10.1126/science.1153966.

26. Trisos, C. H., Amatulli, G., Gurevitch, J., Robock, A., Xia, L., & Zambri, B. (2018). Potentially dangerous consequences for biodiversity of solar geoengineering implementation and termination. *Nature Ecology & Evolution, 2*(3), 475-482, https://doi.org/10.1038/s41559-017-0431-0.

27. Lockley, A., Xu, Y., Tilmes, S., Sugiyama, M., Rothman, D., & Hindes, A. (2022). 18 Politically relevant solar geoengineering scenarios. *Socio-Environmental Systems Modelling, 4*, 18127, https://doi.org/10.18174/sesmo.18127.

28. Zarnetske, P. L., Gurevitch, J., Franklin, J., Groffman, P. M., Harrison, C. S., Hellmann, J. J., Hoffman, F. M., Kothari, S., Robock, A., Tilmes, S., Visioni, D., Wu, J., Xia, L., & Yang, C. E. (2021). Potential ecological impacts of climate intervention by reflecting sunlight to cool Earth. *Proceedings of the National Academy of Sciences USA, 118*(15), https://doi.org/10.1073/pnas.1921854118.

29. Barnes, P. W., Robson, T. M., Neale, P. J., Williamson, C. E., Zepp, R. G., Madronich, S., Wilson, S. R., Andrady, A. L., Heikkilä, A. M., Bernhard, G. H., Bais, A. F., Neale, R. E., Bornman, J. F., Jansen, M. A. K., Klekociuk, A. R., Martinez-Abaigar, J., Robinson, S. A., Wang, Q. W., Banaszak, A. T., Häder, D. P., Hylander, S., Rose, K. C., Wängberg, S. Å., Foereid, B., Hou, W. C., Ossola, R., Paul, N. D., Ukpebor, J. E., Andersen, M. P. S., Longstreth, J., Schikowski, T., Solomon, K. R., Sulzberger, B., Bruckman, L. S., Pandey, K. K., White, C. C., Zhu, L., Zhu, M., Aucamp, P. J., Liley, J. B., McKenzie, R. L., Berwick, M., Byrne, S. N., Hollestein, L. M., Lucas, R. M., Olsen, C. M., Rhodes, L. E., Yazar, S., & Young, A. R. (2022). Environmental effects of stratospheric ozone depletion, UV radiation, and interactions with climate change: UNEP Environmental Effects Assessment Panel, Update 2021. *Photochemical & Photobiological Sciences,* https://doi.org/10.1007/s43630-022-00176-5.

30. Friedel, M., Chiodo, G., Stenke, A., Domeisen, D., Fueglistaler, S., Anet, J., & Peter, T. (2022). Sprintime arctic ozone depletion forces northern hemisphere climate anomalies. Nature Geosciences, 15, 541-547, https://doi.org/10.1038/s41561-022-00974-7.

31. Kwon, H., Choi, H., Kim, B.-M., Kim, S.-W., & Kim, S.-J. (2020). Recent weakening of the southern stratospheric polar vortex and its impact on the surface climate over Antarctica. *Environmental Research Letters, 15*(9), https://doi.org/10.1088/1748-9326/ab9d3d.

32. Jucker, M., & Goyal, R. (2021). Ozone-forced southern annular mode during Antarctic stratospheric warming events. *Geophysical Review Letters, 10*.1002/essoar.10507626.1, https://doi.org/10.1029/2021GL095270.

33. Xia, Y., Hu, Y., Huang, Y., Zhao, C., Xie, F., & Yang, Y. (2021). Significant contribution of severe ozone loss to the Siberian-Arctic surface warming in spring 2020. *Geophysical Research Letters, 48*(8), e2021GL092509, https://doi.org/10.1029/2021GL092509.

34. Robinson, S. A., & Erickson III, D. J. (2015). Not just about sunburn--the ozone hole's profound effect on climate has significant implications for Southern Hemisphere ecosystems. *Global Change Biology, 21*(2), 515-527, https://doi.org/10.1111/gcb.12739.

35. Bernhard, G. H., McKenzie, R. L., Lantz, K., & Stierle, S. (2022). Updated analysis of data from Palmer Station, Antarctica (64° S), and San Diego, California (32° N), confirms large effect of the Antarctic ozone hole on UV radiation. *Photochemical & Photobiological Sciences, 21*(3), 373-384, https://doi.org/10.1007/s43630-022-00178-3.

36. Robinson, S. A., Wasley, J., & Tobin, A. K. (2003). Living on the edge - plants and global change in continental and maritime Antarctica. *Global Change Biology, 9*(12), 1681-1717, https://doi.org/10.1046/j.1365-2486.2003.00693.x.

37.   Newsham, K. K., & Robinson, S. A. (2009). Responses of plants in polar regions to UVB exposure: a meta-analysis. *Global Change Biology, 15*(11), 2574-2589, https://doi.org/10.1111/j.1365-2486.2009.01944.x.

38.   Ballaré, C. L., Caldwell, M. M., Flint, S. D., Robinson, S. A., & Bornman, J. F. (2011). Effects of solar ultraviolet radiation on terrestrial ecosystems. Patterns, mechanisms, and interactions with climate change. *Photochemical & Photobiological Sciences, 10*(2), 226-241, https://doi.org/10.1039/c0pp90035d.

39.   Banerjee, A., Fyfe, J. C., Polvani, L. M., Waugh, D., & Chang, K.-L. (2020). A pause in Southern Hemisphere circulation trends due to the Montreal Protocol. *Nature, 579*(7800), 544-548, https://doi.org/10.1038/s41586-020-2120-4.

40.   Fogt, R. L., & Marshall, G. J. (2020). The Southern Annular Mode: Variability, trends, and climate impacts across the Southern Hemisphere. *WIREs Climate Change, 11*(4), e652, https://doi.org/10.1002/wcc.652.

41.   Gillett, Z. E., Arblaster, J. M., Dittus, A. J., Deushi, M., Jöckel, P., Kinnison, D. E., Morgenstern, O., Plummer, D. A., Revell, L. E., Rozanov, E., Schofield, R., Stenke, A., Stone, K. A., & Tilmes, S. (2019). Evaluating the relationship between interannual variations in the Antarctic ozone hole and Southern Hemisphere surface climate in chemistry–climate models. *Journal of Climate, 32*(11), 3131-3151, https://doi.org/10.1175/jcli-d-18-0273.1.

42.   Morales, M. S., Cook, E. R., Barichivich, J., Christie, D. A., Villalba, R., LeQuesne, C., Srur, A. M., Ferrero, M. E., Gonzalez-Reyes, A., Couvreux, F., Matskovsky, V., Aravena, J. C., Lara, A., Mundo, I. A., Rojas, F., Prieto, M. R., Smerdon, J. E., Bianchi, L. O., Masiokas, M. H., Urrutia-Jalabert, R., Rodriguez-Caton, M., Munoz, A. A., Rojas-Badilla, M., Alvarez, C., Lopez, L., Luckman, B. H., Lister, D., Harris, I., Jones, P. D., Williams, A. P., Velazquez, G., Aliste, D., Aguilera-Betti, I., Marcotti, E., Flores, F., Munoz, T., Cuq, E., & Boninsegna, J. A. (2020). Six hundred years of South American tree rings reveal an increase in severe hydroclimatic events since mid-20th century. *Proceedings of the National Academy of Sciences USA, 117*(29), 16816-16823, https://doi.org/10.1073/pnas.2002411117.

43.   Damiani, A., Cordero, R. R., Llanillo, P. J., Feron, S., Boisier, J. P., Garreaud, R., Rondanelli, R., Irie, H., & Watanabe, S. (2020). Connection between Antarctic Ozone and climate: Interannual precipitation changes in the Southern Hemisphere. *Atmosphere, 11*(6), 579, https://doi.org/10.3390/atmos11060579.

44.   Doddridge, E. W., Marshall, J., Song, H., Campin, J.-M., & Kelley, M. (2021). Southern Ocean heat storage, reemergence, and winter sea ice decline induced by summertime winds. *Journal of Climate, 34*(4), 1403-1415, https://doi.org/10.1175/jcli-d-20-0322.1.

45.   England, M., Polvani, L., & Sun, L. (2018). Contrasting the Antarctic and Arctic atmospheric responses to projected sea ice loss in the late twenty-first century. *Journal of Climate, 31*(16), 6353-6370, https://doi.org/10.1175/JCLI-D-17-0666.1

46.   Li, S., Liu, W., Lyu, K., & Zhang, X. (2021). The effects of historical ozone changes on Southern Ocean heat uptake and storage. *Climate Dynamics, 57*(7-8), 2269-2285, https://doi.org/10.1007/s00382-021-05803-y.

47.   Marshall, J., Ferreira, D., Bitz, C. M., Solomon, S., & Plumb, A. (2015). Antarctic Ocean and sea ice response to ozone depletion: A two-time-scale problem. *Journal of Climate, 28*(3), 1206-1226, https://doi.org/10.1175/jcli-d-14-00313.1.

48.   Son, S.-W., Han, B.-R., Garfinkel, C. I., Kim, S.-Y., Park, R., Abraham, N. L., Akiyoshi, H., Archibald, A. T., Butchart, N., Chipperfield, M. P., Dameris, M., Deushi, M., Dhomse, S. S., Hardiman, S. C., Jöckel, P., Kinnison, D., Michou, M., Morgenstern, O., O'Connor, F. M., Oman, L. D., Plummer, D. A., Pozzer, A., Revell, L. E., Rozanov, E., Stenke, A., Stone, K., Tilmes, S., Yamashita, Y., & Zeng, G. (2018). Tropospheric jet response to Antarctic ozone depletion: An update with Chemistry-Climate Model Initiative (CCMI) models. *Environmental Research Letters, 13*(5), 054024, https://doi.org/10.1088/1748-9326/aabf21.

49.   Waugh, D. W., Thomas, J. L., Polvani, L. M., Marshall, J., Kostov, Y., Kelley, M., Gnanadesikan, A., Ferreira, D., Doddridge, E. W., Codron, F., & Seviour, W. J. M. (2019). The Southern Ocean sea surface temperature response to ozone depletion: A multimodel comparison. *Journal of Climate, 32*(16), 5107-5121, https://doi.org/10.1175/jcli-d-19-0109.1.

50.   Polvani, L. M., Banerjee, A., Chemke, R., Doddridge, E. W., Ferreira, D., Gnanadesikan, A., Holland, M. A., Kostov, Y., Marshall, J., Seviour, W. J. M., Solomon, S., & Waugh, D. W. (2021). Interannual SAM modulation of Antarctic sea ice extent does not account for its long-term trends, pointing to a limited role for ozone depletion. *Geophysical Research Letters, 48*(21), https://doi.org/10.1029/2021gl094871.

51.   Stuecker, M. F., Bitz, C. M., Armour, K. C., Proistosescu, C., Kang, S. M., Xie, S.-P., Kim, D., McGregor, S., Zhang, W., Zhao, S., Cai, W., Dong, Y., & Jin, F.-F. (2018). Polar amplification dominated by local forcing and feedbacks. *Nature Climate Change, 8*(12), 1076-1081, https://doi.org/10.1038/s41558-018-0339-y.

52.   Bergstrom, D. M., Dickson, C. R., Baker, D. J., Winham, J., Selkirk, P. M., & McGeoch, M. A. (2021). Ecosystem collapse on a Sub-Antarctic island. In J. G. Canadell, & R. B. Jackson (Eds.), *Ecosystem Collapse and Climate Change* (pp. 13-25). Cham: Springer International Publishing.

53.   Robinson, S. A., King, D. H., Bramley-Alves, J., Waterman, M. J., Ashcroft, M. B., Wasley, J., Turnbull, J. D., Miller, R. E., Ryan-Colton, E., Benny, T., Mullany, K., Clarke, L. J., Barry, L. A., & Hua, Q. (2018). Rapid change in East Antarctic terrestrial vegetation in response to regional drying. *Nature Climate Change, 8*(10), 879-884, https://doi.org/10.1038/s41558-018-0280-0.

54. Kramarova, N., Newman, P. A., Nash, E. R., Strahan, S. E., Long, C. S., Johnson, B., Pitts, M., Santee, M. L., Petropavlovskikh, I., Coy, L., & de Laat, J. (2020). 2019 Antarctic ozone hole In J. Blunden, & D. S. Arndt (Eds.), *"State of the Climate in 2019", Bulletin of the American Meteorological Society* (Vol. 101, pp. S310-S312).

55. Milinevsky, G., Evtushevsky, O., Klekociuk, A., Wang, Y., Grytsai, A., Shulga, V., & Ivaniha, O. (2019). Early indications of anomalous behaviour in the 2019 spring ozone hole over Antarctica. *International Journal of Remote Sensing, 4*1(19), 7530-7540, https://doi.org/10.1080/2150704X.2020.1763497.

56. Shen, X., Wang, L., & Osprey, S. (2020). Tropospheric forcing of the 2019 Antarctic sudden stratospheric warming. *Geophysical Research Letters*, https://doi.org/10.1029/2020gl089343.

57. Hendon, H. H., Thompson, D. J. W., Lim, E.-P., Butler, A. H., Newman, P. A., Coy, L., Scaife, A., Polichtchouk, I., Garreaud, R. S., T.G., S., & Nakamura, H. (2019). Rare forecasted climate event under way in the Southern Hemisphere. *Nature, 573*(7775), 495, https://doi.org/10.1038/d41586-019-02858-0.

58. Jucker, M., Reichler, T., & Waugh, D. W. (2021). How frequent are Antarctic sudden stratospheric warmings in present and future climate? *Geophysical Research Letters, 48*(11), https://doi.org/10.1029/2021gl093215.

59. Lim, E.-P., Hendon, H. H., Boschat, G., Hudson, D., Thompson, D. W. J., Dowdy, A. J., & Arblaster, J. M. (2019). Australian hot and dry extremes induced by weakenings of the stratospheric polar vortex. *Nature Geoscience*, https://doi.org/10.1038/s41561-019-0456-x.

60. Lim, E.-P., Hendon, H. H., Butler, A. H., Garreaud, R. D., Polichtchouk, I., Shepherd, T. G., Scaife, A., Comer, R., Coy, L., Newman, P. A., Thompson, D. J. W., & Nakamura, H. (2020). The 2019 Antarctic sudden stratospheric warming. *SPARC Newsletter, 54*, 10-13.

61. Newman, P., Nash, E. R., Kramarova, N., & Butler, A. (2020). The 2019 southern stratospheric warming. In T. Scambos, & S. Stammerjohn (Eds.), *"State of the Climate in 2019", Bulletin of the American Meteorological Society* (Vol. 101, pp. S297-S298, Vol. 8).

62. 62. Noguchi, S., Kuroda, Y., Kodera, K., & Watanabe, S. (2020). Robust enhancement of tropical convective activity by the 2019 Antarctic sudden stratospheric warming. *Geophysical Research Letters, 47*(15), e2020GL088743, https://doi.org/10.1029/2020GL088743.

63. Robinson, S. A., Klekociuk, A. R., King, D. H., Pizarro Rojas, M., Zúñiga, G. E., & Bergstrom, D. M. (2020). The 2019/2020 summer of Antarctic heatwaves. *Global Change Biology, 26*(6), 3178-3180, https://doi.org/10.1111/gcb.15083.

64. Yamazaki, Y., Matthias, V., Miyoshi, Y., Stolle, C., Siddiqui, T., Kervalishvili, G., Laštovička, J., Kozubek, M., Ward, W., Themens, D. R., Kristoffersen, S., & Alken, P. (2020). September 2019 Antarctic sudden stratospheric warming: quasi-6-Day wave burst and ionospheric effects. *Geophysical Research Letters, 47*(1), https://doi.org/10.1029/2019gl086577.

65. Allen, D. R., Fromm, M. D., Kablick III, G. P., & Nedoluha, G. E. (2020). Smoke with induced rotation and lofting (SWIRL) in the stratosphere. *Journal of the Atmospheric Sciences, 77*(12), 4297-4316, https://doi.org/10.1175/JAS-D-20-0131.1.

66. Boone, C. D., Bernath, P. F., & Fromm, M. D. (2020). Pyrocumulonimbus stratospheric plume injections measured by the ACE-FTS. *Geophysical Research Letters, 47*(15), e2020GL088442, https://doi.org/10.1029/2020GL088442.

67. Hirsch, E., & Koren, I. (2021). Record-breaking aerosol levels explained by smoke injection into the stratosphere. *Science, 371*(6535), 1269-1274, https://doi.org/10.1126/science.abe1415.

68. Kablick III, G. P., Allen, D. R., Fromm, M. D., & Nedoluha, G. E. (2020). Australian PyroCb smoke generates synoptic-scale stratospheric anticyclones. *Geophysical Research Letters, 47*(13), e2020GL088101, https://doi.org/10.1029/2020GL088101.

69. Khaykin, S., Legras, B., Bucci, S., Sellitto, P., Isaksen, L., Tencé, F., Bekki, S., Bourassa, A., Rieger, L., Zawada, D., Jumelet, J., & Godin-Beekmann, S. (2020). The 2019/20 Australian wildfires generated a persistent smoke-charged vortex rising up to 35 km altitude. *Communications Earth & Environment, 1*(1), 1-12, https://doi.org/10.1038/s43247-020-00022-5.

70. Ohneiser, K., Ansmann, A., Baars, H., Seifert, P., Barja, B., Jimenez, C., Radenz, M., Teisseire, A., Floutsi, A., Haarig, M., Foth, A., Chudnovsky, A., Engelmann, R., Zamorano, F., Bühl, J., & Wandinger, U. (2020). Smoke of extreme Australian bushfires observed in the stratosphere over Punta Arenas, Chile, in January 2020: optical thickness, lidar ratios, and depolarization ratios at 355 and 532 nm. *Atmospheric Chemistry and Physics, 20*(13), 8003-8015, https://doi.org/10.5194/acp-20-8003-2020.

71. Schwartz, M. J., Santee, M. L., Pumphrey, H. C., Manney, G. L., Lambert, A., Livesey, N. J., Millán, L., Neu, J. L., Read, W. G., & Werner, F. (2020). Australian new year's pyroCb impact on stratospheric composition. *Geophysical Research Letters, 47*(24), e2020GL090831, https://doi.org/10.1029/2020GL090831.

72. Solomon, S., Dube, K., Stone, K., Yu, P., Kinnison, D., Toon, O. B., Strahan, S. E., Rosenlof, K. H., Portmann, R., Davis, S., Randel, W., Bernath, P., Boone, C., Bardeen, C. G., Bourassa, A., Zawada, D., & Degenstein, D. (2022). On the stratospheric chemistry of midlatitude wildfire smoke. *Proceedings of the National Academy of Sciences USA, 119*(10), e2117325119, https://doi.org/10.1073/pnas.2117325119.

73. Yu, P., Davis, S. M., Toon, O. B., Portmann, R. W., Bardeen, C. G., Barnes, J. E., Telg, H., Maloney, C., & Rosenlof, K. H. (2021). Persistent stratospheric warming due to 2019–2020 Australian wildfire smoke. *Geophysical Research Letters, 48*(7), e2021GL092609, https://doi.org/10.1029/2021GL092609.

74. Klekociuk, A. R., Tully, M. B., Krummel, P. B., Henderson, S. I., Smale, D., Querel, R., Nichol, S., Alexander, S. P., Fraser, P. J., & Nedoluha, G. (2022). The Antarctic ozone hole during 2020. *Journal of Southern Hemisphere Earth Systems Science*, https://doi.org/10.1071/es21015.

75. Stone, K. A., Solomon, S., Kinnison, D. E., & Mills, M. J. (2021). On recent large Antarctic ozone holes and ozone recovery metrics. *Geophysical Research Letters, 48*(22), https://doi.org/10.1029/2021gl095232.

76. Yook, S., Thompson, D. W. J., & Solomon, S. (2022). Climate impacts and potential drivers of the unprecedented Antarctic ozone holes of 2020 and 2021. *Geophysical Research Letters, 49*(10), e2022GL098064, https://doi.org/10.1029/2022GL098064.

77. Lecouffe, A., Godin-Beekmann, S., Pazmiño, A., & Hauchecorne, A. (2022). Evolution of the intensity and duration of the Southern Hemisphere stratospheric polar vortex edge for the period 1979–2020. A*tmospheric Chemistry and Physics, 22*(6), 4187-4200, https://doi.org/10.5194/acp-22-4187-2022.

78. Ceppi, P., & Shepherd, T. G. (2019). The role of the stratospheric polar vortex for the austral jet response to greenhouse gas forcing. *Geophysical Research Letters, 46*(12), 6972-6979, https://doi.org/10.1029/2019gl082883.

79. Lee, J. R., Waterman, M. J., Shaw, J. D., Bergstrom, D. M., Lynch, H. J., Wall, D. H., & Robinson, S. A. (2022). Islands in the ice: Potential impacts of habitat transformation on Antarctic biodiversity. *Global Change Biology*, https://doi.org/10.1111/gcb.16331.

80. Lembrechts, J. J., van den Hoogen, J., Aalto, J., Ashcroft, M. B., De Frenne, P., Kemppinen, J., Kopecky, M., Luoto, M., Maclean, I. M. D., Crowther, T. W., Bailey, J. J., Haesen, S., Klinges, D. H., Niittynen, P., Scheffers, B. R., Van Meerbeek, K., Aartsma, P., Abdalaze, O., Abedi, M., Aerts, R., Ahmadian, N., Ahrends, A., Alatalo, J. M., Alexander, J. M., Allonsius, C. N., Altman, J., Ammann, C., Andres, C., Andrews, C., Ardo, J., Arriga, N., Arzac, A., Aschero, V., Assis, R. L., Assmann, J. J., Bader, M. Y., Bahalkeh, K., … & Lenoir, J. (2022). Global maps of soil temperature. *Global Change Biology, 28*(9), 3110-3144, https://doi.org/10.1111/gcb.16060.

81. Cannone, N., Malfasi, F., Favero-Longo, S. E., Convey, P., & Guglielmin, M. (2022). Acceleration of climate warming and plant dynamics in Antarctica. *Current Biology, 32*(7), 1599-1606, https://doi.org/10.1016/j.cub.2022.01.074.

82. Chown, S. L., Leihy, R. I., Naish, T. R., Brooks, C. M., Convey, P., Henley, B. J., Mackintosh, A. N., Phillips, L. M., Kennicutt II, M. C., & Grant, S. M. (Eds.). (2022). *Antarctic climate change and the environment: A decadal synopsis and recommendations for action.* Cambridge, United Kingdom: Scientific Committee on Antarctic Research

83. Myers-Smith, I. H., Kerby, J. T., Phoenix, G. K., Bjerke, J. W., Epstein, H. E., Assmann, J. J., John, C., Andreu-Hayles, L., Angers-Blondin, S., Beck, P. S. A., Berner, L. T., Bhatt, U. S., Bjorkman, A. D., Blok, D., Bryn, A., Christiansen, C. T., Cornelissen, J. H. C., Cunliffe, A. M., Elmendorf, S. C., Forbes, B. C., Goetz, S. J., Hollister, R. D., de Jong, R., Loranty, M. M., Macias-Fauria, M., Maseyk, K., Normand, S., Olofsson, J., Parker, T. C., Parmentier, F.-J. W., Post, E., Schaepman-Strub, G., Stordal, F., Sullivan, P. F., Thomas, H. J. D., Tømmervik, H., Treharne, R., Tweedie, C. E., Walker, D. A., Wilmking, M., & Wipf, S. (2020). Complexity revealed in the greening of the Arctic. *Nature Climate Change, 10*(2), 106-117, https://doi.org/10.1038/s41558-019-0688-1.

84. Callaghan, T. V., Cazzolla Gatti, R., & Phoenix, G. (2022). The need to understand the stability of arctic vegetation during rapid climate change: An assessment of imbalance in the literature. *Ambio, 51*(4), 1034-1044, https://doi.org/10.1007/s13280-021-01607-w.

85. Phoenix, G. K., & Treharne, R. (2022). Arctic greening and browning: Challenges and a cascade of complexities. *Global Change Biology, 28*(11), 3481-3483, https://doi.org/10.1111/gcb.16118.

86. Treharne, R., Bjerke, J. W., Tommervik, H., Stendardi, L., & Phoenix, G. K. (2019). Arctic browning: Impacts of extreme climatic events on heathland ecosystem CO_2 fluxes. *Global Change Biology, 25*(2), 489-503, https://doi.org/10.1111/gcb.14500.

87. Robinson, S. A. (2022). Climate change and extreme events are changing the biology of Polar Regions. *Global Change Biology*, https://doi.org/10.1111/gcb.16309.

88. Bokhorst, S., Cornelissen, J. H. C., & Veraverbeke, S. (2022). Long-term legacies of seasonal extremes in Arctic ecosystem functioning. *Global Change Biology, 28*(10), 3161-3162, https://doi.org/10.1111/gcb.16078.

89. Perera-Castro, A. V., Waterman, M. J., Turnbull, J. D., Ashcroft, M. B., McKinley, E., Watling, J. R., Bramley-Alves, J., Casanova-Katny, A., Zuniga, G., Flexas, J., & Robinson, S. A. (2020). It is hot in the sun: Antarctic mosses have high temperature optima for photosynthesis despite cold climate. *Frontiers in Plant Science, 11*, 1178, https://doi.org/10.3389/fpls.2020.01178.

90. Lawrence, Z. D., Perlwitz, J., Butler, A. H., Manney, G. L., Newman, P. A., Lee, S. H., & Nash, E. R. (2020). The remarkably strong Arctic stratospheric polar vortex of winter 2020: Links to record-breaking Arctic oscillation and ozone loss. *Journal of Geophysical Research: Atmospheres, 125*(22), e2020JD033271, https://doi.org/10.1029/2020JD033271.

91. Manney, G. L., Livesey, N. J., Santee, M. L., Froidevaux, L., Lambert, A., Lawrence, Z. D., Millán, L. F., Neu, J. L., Read, W. G., Schwartz, M. J., & Fuller, R. A. (2020). Record-low Arctic stratospheric ozone in 2020: MLS observations of chemical processes and comparisons with previous extreme winters. *Geophysical Research Letters, 47*(16), http://doi.org/10.1029/2020gl089063.

92. Bernhard, G. H., Fioletov, V. E., Grooß, J.-U., Ialongo, I., Johnsen, B., Lakkala, K., Manney, G. L., Müller, R., & Svendby, T. (2021). Ozone and ultraviolet radiation. In J. Blunden, & T. Boyer (Eds.), *"State of the Climate in 2020", Bulletin of the American Meteorological Society,* (Vol. 102, pp. S299–S303, Vol. 8).

93. Bernhard, G. H., Fioletov, V. E., Grooß, J. U., Ialongo, I., Johnsen, B., Lakkala, K., Manney, G. L., Müller, R., & Svendby, T. (2020). Record-breaking increases in Arctic solar ultraviolet radiation caused by exceptionally large ozone depletion in 2020. *Geophysical Research Letters, 47*(24), https://doi.org/10.1029/2020gl090844.

94. Domeisen, D. I. V., & Butler, A. H. (2020). Stratospheric drivers of extreme events at the Earth's surface. *Communications Earth & Environment, 1*(1), https://doi.org/10.1038/s43247-020-00060-z.

95. Overland, J. E., & Wang, M. (2021). The 2020 Siberian heat wave. I*nternational Journal of Climatology, 41*, E2341-E2346, https://doi.org/10.1002/joc.6850.

96. Zhang, J., Tian, W., Pyle, J. A., Keeble, J., Abraham, N. L., Chipperfield, M. P., Xie, F., Yang, Q., Mu, L., Ren, H.-L., Wang, L., & Xu, M. (2022). Responses of Arctic sea ice to stratospheric ozone depletion. *Science Bulletin, 67*(11), 1182-1190, https://doi.org/10.1016/j.scib.2022.03.015.

97. Yook, S., Thompson, D. W. J., & Solomon, S. (2022). Climate impacts and potential drivers of the unprecedented antarctic ozone holes of 2020 and 2021. *Geophysical Research Letters, 49*(10), https://doi.org/10.1029/2022gl098064.

98. Abram, N. J., Henley, B. J., Sen Gupta, A., Lippmann, T. J. R., Clarke, H., Dowdy, A. J., Sharples, J. J., Nolan, R. H., Zhang, T., Wooster, M. J., Wurtzel, J. B., Meissner, K. J., Pitman, A. J., Ukkola, A. M., Murphy, B. P., Tapper, N. J., & Boer, M. M. (2021). Connections of climate change and variability to large and extreme forest fires in southeast Australia. *Communications Earth & Environment, 2*(1), https://doi.org/10.1038/s43247-020-00065-8.

99. Zhang, Y., Beggs, P. J., McGushin, A., Bambrick, H., Trueck, S., Hanigan, I. C., Morgan, G. G., Berry, H. L., Linnenluecke, M. K., Johnston, F. H., Capon, A. G., & Watts, N. (2020). The 2020 special report of the MJA–Lancet Countdown on health and climate change: lessons learnt from Australia's "Black Summer". *Medical Journal of Australia, 213*(11), 490-492.e410, https://doi.org/10.5694/mja2.50869.

100. Graham, A. M., Pringle, K. J., Pope, R. J., Arnold, S. R., Conibear, L. A., Burns, H., Rigby, R., Borchers-Arriagada, N., Butt, E. W., Kiely, L., Reddington, C., Spracklen, D. V., Woodhouse, M. T., Knote, C., & McQuaid, J. B. (2021). Impact of the 2019/2020 Australian megafires on air quality and health. *Geohealth, 5*(10), e2021GH000454, https://doi.org/10.1029/2021GH000454.

101. Cowled, B. D., Hillman, A., Ward, M. P., Clutterbuck, H., Doyle, M., Webb Ware, J., Thomas, M., Plain, K., Barwell, R., Laurence, M., & Pfeiffer, C. (2022). The black summer bushfires: impacts and risk factors for livestock bushfire injury in south-eastern Australia. *Australian Veterinary Journal, 100*(7), 306-317, https://doi.org/10.1111/avj.13165.

102. Dickman, C. R. (2021). Ecological consequences of Australia's "Black Summer" bushfires: Managing for recovery. [https://doi.org/10.1002/ieam.4496]. *Integrated Environmental Assessment and Management, 17*(6), 1162-1167, https://doi.org/10.1002/ieam.4496.

103. González-Herrero, S., Barriopedro, D., Trigo, R. M., López-Bustins, J. A., & Oliva, M. (2022). Climate warming amplified the 2020 record-breaking heatwave in the Antarctic Peninsula. *Communications Earth & Environment, 3*(1), https://doi.org/10.1038/s43247-022-00450-5.

104. Bergstrom, D. M., Wienecke, B. C., van den Hoff, J., Hughes, L., Lindenmayer, D. B., Ainsworth, T. D., Baker, C. M., Bland, L., Bowman, D. M. J. S., Brooks, S. T., Canadell, J. G., Constable, A. J., Dafforn, K. A., Depledge, M. H., Dickson, C. R., Duke, N. C., Helmstedt, K. J., Holz, A., Johnson, C. R., McGeoch, M. A., Melbourne-Thomas, J., Morgain, R., Nicholson, E., Prober, S. M., Raymond, B., Ritchie, E. G., Robinson, S. A., Ruthrof, K. X., Setterfield, S. A., Sgrò, C. M., Stark, J. S., Travers, T., Trebilco, R., Ward, D. F. L., Wardle, G. M., Williams, K. J., Zylstra, P. J., & Shaw, J. D. (2021). Combating ecosystem collapse from the tropics to the Antarctic. *Global Change Biology, 27*(9), 1692-1703, https://doi.org/10.1111/gcb.15539.

105. Cortes-Antiquera, R., Pizarro, M., Contreras, R. A., Kohler, H., & Zuniga, G. E. (2021). Heat shock tolerance in Deschampsia antarctica desv. cultivated in vitro is mediated by enzymatic and non-enzymatic antioxidants. *Frontiers in Plant Science, 12*, 635491, https://doi.org/10.3389/fpls.2021.635491.

106. Montie, S., Thomsen, M. S., Rack, W., & Broady, P. A. (2020). Extreme summer marine heatwaves increase chlorophyll a in the Southern Ocean. *Antarctic Science, 32*(6), 508-509, https://doi.org/10.1017/S0954102020000401.

107. Samuels, T., Rynearson, T. A., & Collins, S. (2021). Surviving heatwaves: Thermal experience predicts life and death in a southern ocean diatom. *Frontiers in Marine Science, 8*, https://doi.org/10.3389/fmars.2021.600343.

108. De Leij, R., Grange, L. J., & Peck, L. S. (2022). Functional thermal limits are determined by rate of warming during simulated marine heatwaves. *Marine Ecology Progress Series, 685*, 183-196, https://doi.org/10.3354/meps13980

109. Bernhard, P., Zwieback, S., & Hajnsek, I. (2022). Accelerated mobilization of organic carbon from retrogressive thaw slumps on the northern Taymyr Peninsula. *The Cryosphere, 16*(7), 2819-2835, https://doi.org/10.5194/tc-16-2819-2022.

110. Boonstra, R., Bodner, K., Bosson, C., Delehanty, B., Richardson, E. S., Lunn, N. J., Derocher, A. E., & Molnár, P. K. (2020). The stress of Arctic warming on polar bears. [https://doi.org/10.1111/gcb.15142]. *Global Change Biology, 26*(8), 4197-4214, https://doi.org/10.1111/gcb.15142.

111. Stirling, I., & Derocher, A. E. (2012). Effects of climate warming on polar bears: a review of the evidence. *Global Change Biology, 18*(9), 2694-2706, https://doi.org/10.1111/j.1365-2486.2012.02753.x.

112. Neale, P. J., Williamson, C. E., Banaszak, A. T., Häder, D.-P., Hylander, S., Ossola, R., Rose, K. A., Wängberg, S. Å., & Zepp, R. G. (2022). The response of aquatic ecosystems to the interactive effects of stratospheric ozone depletion, UV radiation, and climate change. *Chapter 5*

113. Smith, M. D. (2011). The ecological role of climate extremes: current understanding and future prospects. *Journal of Ecology, 99*(3), 651-655, https://doi.org/10.1111/j.1365-2745.2011.01833.x.

114. Chen, Y., Liao, Z., Shi, Y., Tian, Y., & Zhai, P. (2021). Detectable increases in sequential flood-heatwave events across China during 1961–2018. *Geophysical Research Letters, 48*(6), e2021GL092549, https://doi.org/10.1029/2021GL092549.

115. Fischer, E. M., Sippel, S., & Knutti, R. (2021). Increasing probability of record-shattering climate extremes. *Nature Climate Change, 11*(8), 689-695, https://doi.org/10.1038/s41558-021-01092-9.

116. Goss, M., Swain, D. L., Abatzoglou, J. T., Sarhadi, A., Kolden, C. A., Williams, A. P., & Diffenbaugh, N. S. (2020). Climate change is increasing the likelihood of extreme autumn wildfire conditions across California. *Environmental Research Letters, 15*(9), 094016, https://doi.org/10.1088/1748-9326/ab83a7.

117. Kennard, D. K., Matlaga, D., Sharpe, J., King, C., Alonso-Rodríguez, A. M., Reed, S. C., Cavaleri, M. A., & Wood, T. E. (2020). Tropical understory herbaceous community responds more strongly to hurricane disturbance than to experimental warming. *Ecology and Evolution, 10*(16), 8906-8915, https://doi.org/10.1002/ece3.6589.

118. Li, F., Wan, X., Wang, H., Orsolini, Y. J., Cong, Z., Gao, Y., & Kang, S. (2020). Arctic sea-ice loss intensifies aerosol transport to the Tibetan Plateau. *Nature Climate Change, 10*(11), 1037-1044, https://doi.org/10.1038/s41558-020-0881-2.

119. Musselman, K. N., Addor, N., Vano, J. A., & Molotch, N. P. (2021). Winter melt trends portend widespread declines in snow water resources. *Nature Climate Change, 2021*, https://doi.org/10.1038/s41558-021-01014-9.

120. Dodd, R. J., Chadwick, D. R., Harris, I. M., Hines, A., Hollis, D., Economou, T., Gwynn-Jones, D., Scullion, J., Robinson, D. A., & Jones, D. L. (2021). Spatial co-localisation of extreme weather events: a clear and present danger. *Ecology Letters, 24*(1), 60-72, https://doi.org/10.1111/ele.13620.

121. Filazzola, A., Matter, S. F., & MacIvor, J. S. (2021). The direct and indirect effects of extreme climate events on insects. *Science of the Total Environment, 769*, 145161, https://doi.org/10.1016/j.scitotenv.2021.145161.

122. IPCC (2019). Summary for Policymakers. In: Climate Change and Land: an IPCC special report on climate change, desertification, land degradation, sustainable land management, food security, and greenhouse gas fluxes in terrestrial ecosystems. In J. S. P.R. Shukla, E. Calvo Buendia, V. Masson-Delmotte, H.- O. Pörtner, D. C. Roberts, P. Zhai, R. Slade, S. Connors, R. van Diemen, M. Ferrat, E. Haughey, S. Luz, S. Neogi, M. Pathak, J. Petzold, J. Portugal Pereira, P. Vyas, E. Huntley, K. Kissick, M. Belkacemi, J. Malley (Ed.). Geneva, Switzerland.

123. Ruthrof, K. X., Fontaine, J. B., Breshears, D. D., Field, J. P., & Allen, C. D. (2021). Extreme events trigger terrestrial and marine ecosystem collapses in the Southwestern USA and Southwestern Australia. In *Ecosystem Collapse and Climate Change* (pp. 187-217, Ecological Studies), https//doi.org/10.1007/978-3-030-71330-0_8

124. Walsh, J. E., Ballinger, T. J., Euskirchen, E. S., Hanna, E., Mård, J., Overland, J. E., Tangen, H., & Vihma, T. (2020). Extreme weather and climate events in northern areas: A review. *Earth-Science Reviews, 209*, https://doi.org/10.1016/j.earscirev.2020.103324.

125. Neale, R. E., Barnes, P. W., Robson, T. M., Neale, P. J., Williamson, C. E., Zepp, R. G., Wilson, S. R., Madronich, S., Andrady, A. L., Heikkilä, A. M., Bernhard, G. H., Bais, A. F., Aucamp, P. J., Banaszak, A. T., Bornman, J. F., Bruckman, L. S., Byrne, S. N., Foereid, B., Häder, D. P., Hollestein, L. M., Hou, W.-C. C., Hylander, S., Jansen, M. A. K., Klekociuk, A. R., Liley, J. B., Longstreth, J., Lucas, R. M., Martinez-Abaigar, J., McNeill, K., Olsen, C. M., Pandey, K. K., Rhodes, L. E., Robinson, S. A., Rose, K. C., Schikowski, T., Solomon, K. R., Sulzberger, B., Ukpebor, J. E., Wang, Q.-W., Wängberg, S.-Å., White, C. C., Yazar, S., Young, A. R., Young, P. J., Zhu, L., & Zhu, M. (2021). Environmental effects of stratospheric ozone depletion, UV radiation, and interactions with climate change: UNEP Environmental Effects Assessment Panel, Update 2020. *Photochemical & Photobiological Sciences, 20*, 1-67, https://doi.org/10.1007/s43630-020-00001-x.

126. Silva, C. A., Santilli, G., Sano, E. E., & Laneve, G. (2021). Fire occurrences and greenhouse gas emissions from deforestation in the Brazilian Amazon. *Remote Sensing, 13*(3), https://doi.org/10.3390/rs13030376.

127. Shiraishi, T., & Hirata, R. (2021). Estimation of carbon dioxide emissions from the megafires of Australia in 2019-2020. *Scientific Reports, 11*(1), 8267, https://doi.org/10.1038/s41598-021-87721-x.

128. Leitold, V., Morton, D. C., Martinuzzi, S., Paynter, I., Uriarte, M., Keller, M., Ferraz, A., Cook, B. D., Corp, L. A., & González, G. (2022). Tracking the rates and mechanisms of canopy damage and recovery following hurricane Maria using multitemporal Lidar data. *Ecosystems, 25*(4), 892-910, https://doi.org/10.1007/s10021-021-00688-8

129. Wang, J. A., Randerson, J. T., Goulden, M. L., Knight, C. A., & Battles, J. J. (2022). Losses of tree cover in California driven by increasing fire disturbance and climate stress. *AGU Advances, 3*(4), https://doi.org/10.1029/2021av000654.

130. Messier, C., Parent, S., & Bergeron, Y. (1998). Effects of overstory and understory vegetation on the understory light environment in mixed boreal forests. [https://doi.org/10.2307/3237266]. *Journal of Vegetation Science, 9*(4), 511-520, https://doi.org/10.2307/3237266.

131. Tanner, E. V., Kapos, V., & Healey, J. (1991). Hurricane effects on forest ecosystems in the Caribbean. *Biotropica, 513*-521, https://www.jstor.org/stable/2388274.

132. Wang, Q. W., Robson, T. M., Pieristè, M., Oguro, M., Oguchi, R., Murai, Y., & Kurokawa, H. (2020). Testing trait plasticity over the range of spectral composition of sunlight in forb species differing in shade tolerance. *Journal of Ecology*, https://doi.org/10.1111/1365-2745.13384.

133. Lovelock, C. E., Osmond, C. B., & Jebb, M. (1994). Photoinhibition and recovery in tropical plant species: response to disturbance. *Oecologia, 97*(3), 297-307, https://doi.org/10.1007/BF00317318.

134. Nichol, C. J., Pieruschka, R., Takayama, K., B, F. R., Kolber, Z., Rascher, U., Grace, J., Robinson, S. A., Pogson, B., & Osmond, B. (2012). Canopy conundrums: building on the Biosphere 2 experience to scale measurements of inner and outer canopy photoprotection from the leaf to the landscape. *Functional Plant Biology, 39*(1), 1-24, https://doi.org/10.1071/fp11255.

135. Barnes, P. W., Kersting, A. R., Flint, S. D., Beyschlag, W., & Ryel, R. J. (2013). Adjustments in epidermal UV-transmittance of leaves in sun-shade transitions. *Physiologia Plantarum, 149*, 200-213, https://doi.org/10.1111/ppl.12025.

136. Barnes, P. W., Robson, T. M., Tobler, M. A., Bottger, I. N., & Flint, S. D. (2017). Plant responses to fluctuating UV environments. In B. Jordan (Ed.), *UV-B Radiation and Plant Life: Molecular Biology to Ecology* (pp. 72-89). Oxfordshire, UK: CABI, https://doi.org/

137. Dahal, D., Liu, S., & Oeding, J. (2014). The carbon cycle and hurricanes in the United States between 1900 and 2011. *Scientific Reports, 4*, https://doi.org/10.1038/srep05197.

138. Veraverbeke, S., Delcourt, C. J. F., Kukavskaya, E., Mack, M., Walker, X., Hessilt, T., Rogers, B., & Scholten, R. C. (2021). Direct and longer-term carbon emissions from arctic-boreal fires: A short review of recent advances. *Current Opinion in Environmental Science & Health, 23*, https://doi.org/10.1016/j.coesh.2021.100277.

139. Prestes, N. C. C. d. S., Massi, K. G., Silva, E. A., Nogueira, D. S., de Oliveira, E. A., Freitag, R., Marimon, B. S., Marimon-Junior, B. H., Keller, M., & Feldpausch, T. R. (2020). Fire effects on understory forest regeneration in Southern Amazonia. *Frontiers in Forests and Global Change, 3*, https://doi.org/10.3389/ffgc.2020.00010.

140. Knuesting, J., Brinkmann, M. C., Silva, B., Schorsch, M., Bendix, J., Beck, E., & Scheibe, R. (2018). Who will win where and why? An ecophysiological dissection of the competition between a tropical pasture grass and the invasive weed Bracken over an elevation range of 1000 m in the tropical Andes. *Plos One, 13*(8), e0202255, https://doi.org/10.1371/journal.pone.0202255.

141. Barnes, P. W., Ryel, R. J., & Flint, S. D. (2017). UV screening in native and non-native plant species in the tropical alpine: Implications for climate change-driven migration of species to higher elevations. *Frontiers in Plant Science, 8*(1451), 12-21, https://doi.org/10.3389/fpls.2017.01451.

142. Watermann, L. Y., Hock, M., Blake, C., & Erfmeier, A. (2019). Plant invasion into high elevations implies adaptation to high UV-B environments: a multi-species experiment. *Biological Invasions*, https://doi.org/10.1007/s10530-019-02173-9.

143. Rammer, W., Braziunas, K. H., Hansen, W. D., Ratajczak, Z., Westerling, A. L., Turner, M. G., & Seidl, R. (2021). Widespread regeneration failure in forests of Greater Yellowstone under scenarios of future climate and fire. *Global Change Biology, 27*(18), 4339-4351, https://doi.org/10.1111/gcb.15726.

144. Werner, C., Meredith, L. K., Ladd, S. N., Ingrisch, J., Kübert, A., van Haren, J., Bahn, M., Bailey, K., Bamberger, I., Beyer, M., Blomdahl, D., Byron, J., Daber, E., Deleeuw, J., Dippold, M. A., Fudyma, J., Gil-Loaiza, J., Honeker, L. K., Hu, J., Huang, J., Klüpfel, T., Krechmer, J., Kreuzwieser, J., Kühnhammer, K., Lehmann, M. M., Meeran, K., Misztal, P. K., Ng, W.-R., Pfannerstill, E., Pugliese, G., Purser, G., Roscioli, J., Shi, L., Tfaily, M., & Williams, J. (2021). Ecosystem fluxes during drought and recovery in an experimental forest. *Science, 374*(6574), 1514-1518, https://doi.org/10.1126/science.abj6789.

145. Scordo, F., Chandra, S., Suenaga, E., Kelson, S. J., Culpepper, J., Scaff, L., Tromboni, F., Caldwell, T. J., Seitz, C., Fiorenza, J. E., Williamson, C. E., Sadro, S., Rose, K. C., & Poulson, S. R. (2021). Smoke from regional wildfires alters lake ecology. *Scientific Reports, 11*(1), 10922, https://doi.org/10.1038/s41598-021-89926-6.

146. Wilson, S. R., Madronich, S., Longstreth, J. D., & Solomon, K. R. (2019). Interactive effects of changing stratospheric ozone and climate on composition of the troposphere, air quality, and consequences for human and ecosystem health. *Photochemical & Photobiological Sciences, 18*, 775-803, https://doi.org/10.1039/C8PP90064G

147. Francis, D., Fonseca, R., Nelli, N., Cuesta, J., Weston, M., Evan, A., & Temimi, M. (2020). The atmospheric drivers of the major Saharan dust storm in June 2020. *Geophysical Research Letters, 47*(24), https://doi.org/10.1029/2020gl090102.

148. Zheng, G., Sedlacek, A. J., Aiken, A. C., Feng, Y., Watson, T. B., Raveh-Rubin, S., Uin, J., Lewis, E. R., & Wang, J. (2020). Long-range transported North American wildfire aerosols observed in marine boundary layer of eastern North Atlantic. *Environment International, 139*, 105680, https://doi.org/10.1016/j.envint.2020.105680.

149. Durand, M., Murchie, E. H., Lindfors, A. V., Urban, O., Aphalo, P. J., & Robson, T. M. (2021). Diffuse solar radiation and canopy photosynthesis in a changing environment. *Agricultural and Forest Meteorology, 311*, 108684, https://doi.org/10.1016/j.agrformet.2021.108684.

150. Chen, Z., Gao, W., Reddy, K. R., Chen, M., Taduri, S., Meyers, S. L., & Shankle, M. W. (2020). Ultraviolet (UV) B effects on growth and yield of three contrasting sweet potato cultivars. *Photosynthetica, 58*(1), 37-44, https://doi.org/10.32615/ps.2019.137.

151. Cronin, T. W., & Bok, M. J. (2016). Photoreception and vision in the ultraviolet. *Journal of Experimental Biology, 219*(18), 2790-2801, https://doi.org/10.1242/jeb.128769.

152. Fennell, J. T., Fountain, M. T., & Paul, N. D. (2019). Direct effects of protective cladding material on insect pests in crops. *Crop Protection, 121*, 147-156, https://doi.org/10.1016/j.cropro.2019.04.003.

153. Onzo, A., Sabelis, M. W., & Hanna, R. (2010). Effects of ultraviolet radiation on predatory mites and the role of refuges in plant structures. *Environmental Entomology, 39*(2), 695-701, https://doi.org/10.1603/en09206.

154. Ohtsuka, K., & Osakabe, M. (2009). Deleterious effects of UV-B radiation on herbivorous spider mites: They can avoid it by remaining on lower leaf surfaces. *Environmental Entomology, 38*(3), 920-929, https://doi.org/10.1603/022.038.0346.

155. Yin, W. D., Hoffmann, A. A., Gu, X. B., & Ma, C. S. (2018). Behavioral thermoregulation in a small herbivore avoids direct UVB damage. *Journal of Insect Physiology, 107*, 276-283, https://doi.org/10.1016/j.jinsphys.2017.12.002.

156. Hu, Z. Q., Zhao, H. Y., & Thieme, T. (2013). The effects of enhanced ultraviolet-B radiation on the biology of green and brown morphs of *Sitobion avenae* (Hemiptera: Aphididae). *Environmental Entomology, 42*(3), 578-585, https://doi.org/10.1603/en12136.

157. Burdick, S. C., Prischmann-Voldseth, D. A., & Harmon, J. P. (2015). Density and distribution of soybean aphid, *Aphis glycines* Matsumura (Hemiptera: Aphididae) in response to UV radiation. *Population Ecology*, 1-10, https://doi.org/10.1007/s10144-015-0501-6.

158. Yoshioka, Y., Gotoh, T., & Suzuki, T. (2018). UV-B susceptibility and photoreactivation in embryonic development of the two-spotted spider mite, *Tetranychus urticae*. *Experimental and Applied Acarology, 75*(2), 155-166, https://doi.org/10.1007/s10493-018-0263-x.

159. Murata, Y., & Osakabe, M. (2017). Photo-enzymatic repair of UVB-induced DNA damage in the two-spotted spider mite *Tetranychus urticae*. *Experimental and Applied Acarology, 71*(1), 15-34, https://doi.org/10.1007/s10493-016-0100-z.

160. Tian, C. B., Li, Y. Y., Wang, X., Fan, W. H., Wang, G., Liang, J. Y., Wang, Z. Y., & Liu, H. (2019). Effects of UV-B radiation on the survival, egg hatchability and transcript expression of antioxidant enzymes in a high-temperature adapted strain of *Neoseiulus barkeri*. *Experimental and Applied Acarology, 77*(4), 527-543, https://doi.org/10.1007/s10493-019-00361-9.

161. Sugioka, N., Kawakami, M., Hirai, N., & Osakabe, M. (2018). A pollen diet confers ultraviolet-B resistance in phytoseiid mites by providing antioxidants. *Frontiers in Ecology and Evolution, 6*, 133, https://doi.org/10.3389/fevo.2018.00133.

162. Koveos, D. S., Suzuki, T., Terzidou, A., Kokkari, A., Floros, G., Damos, P., & Kouloussis, N. A. (2017). Egg hatching response to a range of ultraviolet-B (UV-B) radiation doses for four predatory mites and the herbivorous spider mite *Tetranychus urticae*. *Experimental and Applied Acarology, 71*(1), 35-46, https://doi.org/10.1007/s10493-016-0102-x.

163. Cui, H. Y., Zeng, Y. Y., Reddy, G. V. P., Gao, F., Li, Z. H., & Zhao, Z. H. (2021). UV radiation increases mortality and decreases the antioxidant activity in a tephritid fly. *Food and Energy Security, 10*(3), https://doi.org/10.1002/fes3.297.

164. Fennell, J. T., Wilby, A., Sobeih, W., & Paul, N. D. (2020). New understanding of the direct effects of spectral balance on behaviour in *Myzus persicae*. *Journal of Insect Physiology, 126*, 104096, https://doi.org/10.1016/j.jinsphys.2020.104096.

165. Rizzini, L., Favory, J.-J., Cloix, C., Faggionato, D., O'Hara, A., Kaiserli, E., Baumeister, R., Schaefer, E., Nagy, F., Jenkins, G. I., & Ulm, R. (2011). Perception of UV-B by the *Arabidopsis* UVR8 protein. *Science, 332*(6025), 103-106, https://doi.org/10.1126/science.1200660.

166. Rai, N., O'Hara, A., Farkas, D., Safronov, O., Ratanasopa, K., Wang, F., Lindfors, A. V., Jenkins, G. I., Lehto, T., Salojarvi, J., Brosche, M., Strid, A., Aphalo, P. J., & Morales, L. O. (2020). The photoreceptor UVR8 mediates the perception of both UV-B and UV-A wavelengths up to 350 nm of sunlight with responsivity moderated by cryptochromes. *Plant, Cell & Environment*, https://doi.org/10.1111/pce.13752.

167. Rai, N., Morales, L. O., & Aphalo, P. J. (2021). Perception of solar UV radiation by plants: photoreceptors and mechanisms. *Plant Physiology, 186*(3), 1382-1396, https://doi.org./10.1093/plphys/kiab162.

168. Madronich, S., Mckenzie, R. L., Caldwell, M., & Björn, L. O. (1995). Changes in ultraviolet radiation reaching the earth's surface. *Ambio: a Journal of Human Environment, 24*(3), 143-152.

169. Fernández, M. B., Tossi, V., Lamattina, L., & Cassia, R. (2016). A comprehensive phylogeny reveals functional conservation of the UV-B photoreceptor UVR8 from green algae to higher plants. *Frontiers in Plant Science, 7*, 1698, https://doi.org/10.3389/fpls.2016.01698.

170. Balcerowicz, M. (2022). Ancient sun protection: the evolutionary origin of plant UV-B signaling. *Plant Physiology, 188*(1), 29-31, https://doi.org/10.1093/plphys/kiab517

171. Zhang, Z., Xu, C., Zhang, S., Shi, C., Cheng, H., Liu, H., & Zhong, B. (2022). Origin and adaptive evolution of UV RESISTANCE LOCUS 8-mediated signaling during plant terrestrialization. *Plant Physiology, 188*(1), 332-346, https://doi.org/10.1093/plphys/kiab486.

172. Podolec, R., Demarsy, E., & Ulm, R. (2021). Perception and signaling of ultraviolet-B radiation in plants. *Annual Review of Plant Biology, 72*, 793-822, https://doi.org/10.1146/annurev-arplant-050718-095946.

173. Podolec, R., Lau, K., Wagnon, T. B., Hothorn, M., & Ulm, R. (2021). A constitutively monomeric UVR8 photoreceptor confers enhanced UV-B photomorphogenesis. *Proceedings of the National Academy of Sciences USA, 118*(6), https://doi.org/10.1073/pnas.2017284118.

174. Wang, D., Sun, Y., Tu, M., Zhang, P., Wang, X., Wang, T., & Li, J. (2021). Response of *Zebrina pendula* leaves to enhanced UV-B radiation. *Functional Plant Biology, 48*(9), 851-859, https://doi.org/10.1071/FP20274.

175. Qian, M., Rosenqvist, E., Prinsen, E., Pescheck, F., Flygare, A.-M., Kalbina, I., Jansen, M. A. K., & Strid, Å. (2021). Downsizing in plants - UV induces pronounced morphological changes in cucumber in the absence of stress. *bioRxiv*, 2021.2002.2027.432481, https://doi.org/10.1101/2021.02.27.432481.

176. Bidel, L. P. R., Meyer, S., Talhouet, A. C., Baudin, X., Daniel, C., Cazals, G., & Streb, P. (2020). Epidermal UVA screening capacity measured *in situ* as an indicator of light acclimation state of leaves of a very plastic alpine plant *Soldanella alpina* L. *Plant Physiology and Biochemistry, 151*, 10-20, https://doi.org/10.1016/j.plaphy.2020.02.045.

177. Nichelmann, L., & Pescheck, F. (2021). Solar UV-B effects on composition and UV screening efficiency of foliar phenolics in *Arabidopsis thaliana* are augmented by temperature. *Physiologia Plantarum*, https://doi.org/10.1111/ppl.13554.

178. Mo, Y., Nagel, C., & Taylor, L. P. (1992). Biochemical complementation of chalcone synthase mutants defines a role for flavonols in functional pollen. *Proceedings of the National Academy of Sciences USA, 89*(15), 7213-7217, https://doi.org/10.1073/pnas.89.15.7213.

179. Muhlemann, J. K., Younts, T. L. B., & Muday, G. K. (2018). Flavonols control pollen tube growth and integrity by regulating ROS homeostasis during high-temperature stress. *Proceedings of the National Academy of Sciences of the Unites States of America, 115*(47), E11188-E11197, https://doi.org/10.1073/pnas.1811492115.

180. Wang, L., Lam, P. Y., Lui, A. C. W., Zhu, F. Y., Chen, M. X., Liu, H., Zhang, J., & Lo, C. (2020). Flavonoids are indispensable for complete male fertility in rice. *Journal of Experimental Botany, 71*(16), 4715-4728, https://doi.org/10.1093/jxb/eraa204.

181. Brunetti, C., Di Ferdinando, M., Fini, A., Pollastri, S., & Tattini, M. (2013). Flavonoids as antioxidants and developmental regulators: Relative significance in plants and humans. *International Journal of Molecular Sciences, 14*(2), 3540-3555, https://doi.org/10.3390/ijms14023540.

182. Peach, K., Liu, J. W., & Mazer, S. J. (2020). Climate predicts uv floral pattern size, anthocyanin concentration, and pollen performance in *Clarkia unguiculata*. *Frontiers in Plant Science, 11*, 847, https://doi.org/10.3389/fpls.2020.00847.

183. Koski, M. H., Berardi, A. E., & Galloway, L. F. (2020). Pollen colour morphs take different paths to fitness. *Journal of Evolionary Biology, 33*, 388-400, https://doi.org/10.1111/jeb.13599.

184. Xue, J. S., Zhang, B., Zhan, H., Lv, Y. L., Jia, X. L., Wang, T., Yang, N. Y., Lou, Y. X., Zhang, Z. B., Hu, W. J., Gui, J., Cao, J., Xu, P., Zhou, Y., Hu, J. F., Li, L., & Yang, Z. N. (2020). Phenylpropanoid derivatives are essential components of sporopollenin in vascular plants. *Molecular Plant, 13*(11), 1644-1653, https://doi.org/10.1016/j.molp.2020.08.005.

185. Agati, G., Brunetti, C., Fini, A., Gori, A., Guidi, L., Landi, M., Sebastiani, F., & Tattini, M. (2020). Are flavonoids effective antioxidants in plants? Twenty years of our investigation. *Antioxidants (Basel), 9*(11), https://doi.org/10.3390/antiox9111098.

186. Barnes, P. W., Tobler, M. A., Keefover-Ring, K., Flint, S. D., Barkley, A. E., Ryel, R. J., & Lindroth, R. L. (2016). Rapid modulation of ultraviolet shielding in plants is influenced by solar ultraviolet radiation and linked to alterations in flavonoids. *Plant, Cell & Environment, 39*(1), 222-230, https://doi.org/10.1111/pce.12609.

187. Neugart, S., Tobler, M. A., & Barnes, P. W. (2021). Rapid adjustment in epidermal UV sunscreen: Comparison of optical measurement techniques and response to changing solar UV radiation conditions. *Physiologia Plantarum, 173*(3), 725-735, https://doi.org/10.1111/ppl.13517.

188. Gori, A., Nascimento, L. B., Ferrini, F., Centritto, M., & Brunetti, C. (2020). Seasonal and diurnal variation in leaf phenolics of three medicinal Mediterranean wild species: What is the best harvesting moment to obtain the richest and the most antioxidant extracts? *Molecules, 25*(4), 956, https://doi.org/10.3390/molecules25040956.

189. Badmus, U. O., Ač, A., Klem, K., Urban, O., & Jansen, M. A. K. (2022). A meta-analysis of the effects of UV radiation on the plant carotenoid pool. *Plant Physiology and Biochemistry, 183*, 36-45, https://doi.org/10.1016/j.plaphy.2022.05.001.

190. Piccolella, S., Crescente, G., Pacifico, F., & Pacifico, S. (2018). Wild aromatic plants bioactivity: a function of their (poly)phenol seasonality? A case study from Mediterranean area. *Phytochemistry Reviews, 17*(4), 785-799, https://doi.org/10.1007/s11101-018-9558-0.

191. Gori, A., Brunetti, C., Dos Santos Nascimento, L. B., Marino, G., Guidi, L., Ferrini, F., Centritto, M., Fini, A., & Tattini, M. (2021). Photoprotective role of photosynthetic and non-photosynthetic pigments in *Phillyrea latifolia*: Is their "antioxidant" function prominent in leaves exposed to severe summer drought? I*nternational Journal of Molecular Sciences, 22*(15), https://doi.org/10.3390/ijms22158303.

192. Neugart, S., Tobler, M. A., & Barnes, P. W. (2021). The function of flavonoids in the diurnal rhythm under rapidly changing UV conditions-A model study on okra. *Plants (Basel), 10*(11), https://doi.org/10.3390/plants10112268.

193. Hartikainen, S. (2021). *Adjustment of optically measured leaf traits to patterns of solar spectral irradiance in plant taxa from high elevations and from forest understoreys*. University of Helsinki, Helsinki, Finland, hartikainen_saara_dissertation_2021.pdf

194. Zhou, S., Yan, X., Yang, J., Qian, C., Yin, X., Fan, X., Fang, T., Gao, Y., Chang, Y., & Liu, W. (2021). Variations in flavonoid metabolites along altitudinal gradient in a desert medicinal plant *Agriophyllum squarrosum. Frontiers in Plant Science, 12*, 1306, https://doi.org/10.3389/fpls.2021.683265.

195. Eriksson, M., & Rafajlovic, M. (2022). The role of phenotypic plasticity in the establishment of range margins. *Philosophical Transactions of the Royal Society of London B Biological Sciences, 377*(1846), 20210012, https://doi.org/10.1098/rstb.2021.0012.

196. Schmid, M., & Guillaume, F. (2017). The role of phenotypic plasticity on population differentiation. *Heredity, 119*(4), 214-225, https://doi.org/10.1038/hdy.2017.36.

197. Crispo, E. (2008). Modifying effects of phenotypic plasticity on interactions among natural selection, adaptation and gene flow. *Journal of Evolutionary Biology, 21*(6), 1460-1469, https://doi.org/10.1111/j.1420-9101.2008.01592.x.

198. Song, B., Gao, Y., Stöcklin, J., Song, M., Sun, L., & Sun, H. (2020). Ultraviolet screening increases with elevation in translucent bracts of *Rheum nobile* (Polygonaceae), an alpine 'glasshouse' plant from the high Himalayas. *Botanical Journal of the Linnean Society*, https://doi.org/10.1093/botlinnean/boaa005.

199. Yang, Q., Bi, H., Yang, W., Li, T., Jiang, J., Zhang, L., Liu, J., & Hu, Q. (2020). The genome sequence of alpine M*egacarpaea delavayi* Identifies species-specific whole-genome duplication. *Frontiers in Genetics, 11*, https://doi.org/10.3389/fgene.2020.00812.

200. Zhang, X., Sun, Y., Landis, J. B., Shen, J., Zhang, H., Kuang, T., Sun, W., Sun, J., Tiamiyu, B. B., Deng, T., Sun, H., & Wang, H. (2021). Transcriptomes of *Saussurea* (Asteraceae) provide insights into high-altitude adaptation. *Plants-Basel, 10*(8), https://doi.org/10.3390/plants10081715.

201. Wang, X., Liu, S., Zuo, H., Zheng, W., Zhang, S., Huang, Y., Pingcuo, G., Ying, H., Zhao, F., Li, Y., Liu, J., Yi, T.-S., Zan, Y., Larkin, R. M., Deng, X., Zeng, X., & Xu, Q. (2021). Genomic basis of high-altitude adaptation in Tibetan *Prunus* fruit trees. *Current Biology, 31*(17), 3848-+, https://doi.org/10.1016/j.cub.2021.06.062.

202. Panchen, Z. A., Doubt, J., Kharouba, H. M., & Johnston, M. O. (2019). Patterns and biases in an Arctic herbarium specimen collection: Implications for phenological research. *Applications in Plant Sciences, 7*(3), e1229, https://doi.org/10.1002/aps3.1229.

203. Seddon, A. W. R., Festi, D., Robson, T. M., & Zimmermann, B. (2019). Fossil pollen and spores as a tool for reconstructing ancient solar-ultraviolet irradiance received by plants: an assessment of prospects and challenges using proxy-system modelling. *Photochemical & Photobiological Sciences, 18*(2), 275-294, https://doi.org/10.1039/C8PP00490K.

204. Jardine, P. E., Hoorn, C., Beer, M. A. M., Barbolini, N., Woutersen, A., Bogota Angel, G., Gosling, W. D., Fraser, W. T., Lomax, B. H., Huang, H., Sciumbata, M., He, H., Dupont-Nivet, G., & Kustatscher, E. (2021). Sporopollenin chemistry and its durability in the geological record: an integration of extant and fossil chemical data across the seed plants. *Palaeontology, 64*(2), 285-305, https://doi.org/10.1111/pala.12523.

205. IPCC (2022). Summary for Policymakers In D. C. R. H.-O. Pörtner, E.S. Poloczanska, K. Mintenbeck, M. Tignor, A. Alegría, M. Craig, S. Langsdorf, S. Löschke, V. Möller, A. Okem (Ed.), *Climate Change 2022: Impacts, Adaptation, and Vulnerability. Contribution of Working Group II to the Sixth Assessment Report of the Intergovernmental Panel on Climate Change*. Cambridge University Press.

206. Jansen, M. A. K., Ač, A., Klem, K., & Urban, O. (2022). A meta-analysis of the interactive effects of UV and drought on plants. *Plant, Cell & Environment, 45*(1), 41-54, https://doi.org/10.1111/pce.14221.

207. Díaz-Guerra, L., Llorens, L., Julkunen-Tiitto, R., Nogués, I., Font, J., González, J. A., & Verdaguer, D. (2019). Leaf biochemical adjustments in two Mediterranean resprouter species facing enhanced UV levels and reduced water availability before and after aerial biomass removal. *Plant Physiology and Biochemistry, 137*, 130-143, https://doi.org/10.1016/j.plaphy.2019.01.031.

208. Verdaguer, D., Díaz-Guerra, L., Font, J., González, J. A., & Llorens, L. (2018). Contrasting seasonal morphological and physio-biochemical responses to UV radiation and reduced rainfall of two mature naturally growing Mediterranean shrubs in the context of climate change. *Environmental and Experimental Botany, 147*, 189-201, https://doi.org/10.1016/j.envexpbot.2017.12.007.

209. Aphalo, P. J., & Sadras, V. O. (2021). Explaining preemptive acclimation by linking information to plant phenotype. *Journal of Experimental Botany*, *erab537*, https://doi.org/10.1093/jxb/erab537.

210. Sàenz-de la O, D., Morales, L. O., Strid, A., Torres-Pacheco, I., & Guevara-Gonzalez, R. G. (2021). Ultraviolet-B exposure and exogenous hydrogen peroxide application lead to cross-tolerance toward drought in *Nicotiana tabacum* L. *Physiologia Plantarum*, https://doi.org/10.1111/ppl.13448.

211. Gourlay, G., Hawkins, B. J., Albert, A., Schnitzler, J. P., & Peter Constabel, C. (2022). Condensed tannins as antioxidants that protect poplar against oxidative stress from drought and UV-B. *Plant, Cell & Environment, 45*(2), 362-377, https://doi.org/10.1111/pce.14242.

212. Wang, H., Liu, S., Wang, T., Liu, H., Xu, X., Chen, K., & Zhang, P. (2020). The moss flavone synthase I positively regulates the tolerance of plants to drought stress and UV-B radiation. *Plant Science, 298*, 110591, https://doi.org/10.1016/j.plantsci.2020.110591.

213. Thomas T.T, D., & Puthur, J. T. (2017). UV radiation priming: A means of amplifying the inherent potential for abiotic stress tolerance in crop plants. *Environmental and Experimental Botany, 138*, 57-66, https://doi.org/10.1016/j.envexpbot.2017.03.003.

214. Klem, K., Oravec, M., Holub, P., Šimor, J., Findurová, H., Surá, K., Veselá, B., Hodaňová, P., Jansen, M. A. K., & Urban, O. (2022). Interactive effects of nitrogen, UV and PAR on barley morphology and biochemistry are associated with the leaf C:N balance. *Plant Physiology and Biochemistry, 172*, 111-124, https://doi.org/10.1016/j.plaphy.2022.01.006.

215. Williams, T. B., Dodd, I. C., Sobeih, W. Y., & Paul, N. D. (2022). Ultraviolet radiation causes leaf warming due to partial stomatal closure. *Horticulture Research, 9*, uhab066, https://doi.org/10.1093/hr/uhab066.

216. Ribeiro, A. F., Russo, A., Gouveia, C. M., & Pires, C. A. (2020). Drought-related hot summers: A joint probability analysis in the Iberian Peninsula. *Weather and Climate Extremes, 30*, 100279, https://doi.org/10.1016/j.wace.2020.100279.

217. Jin, P., Overmans, S., Duarte, C. M., Agustí, S., & Bates, A. (2019). Increasing temperature within thermal limits compensates negative ultraviolet-B radiation effects in terrestrial and aquatic organisms. *Global Ecology and Biogeography*, https://doi.org/10.1111/geb.12973.

218. Fang, H. C., Dong, Y. H., Yue, X. X., Chen, X. L., He, N. B., Hu, J. F., Jiang, S. H., Xu, H. F., Wang, Y. C., Su, M. Y., Zhang, J., Zhang, Z. Y., Wang, N., & Chen, X. S. (2019). MdCOL4 interaction mediates crosstalk between UV-B and high temperature to control fruit coloration in apple. *Plant and Cell Physiology, 60,* 1055-1066, https://doi.org/10.1093/pcp/pcz023.

219. Schulz, E., Tohge, T., Winkler, J. B., Albert, A., Schäffner, A. R., Fernie, A. R., Zuther, E., & Hincha, D. K. (2021). Natural variation among *Arabidopsis* accessions in the regulation of flavonoid metabolism and stress gene expression by combined UV radiation and cold. *Plant and Cell Physiology, 62*(3), 502-514, https://doi.org/10.1093/pcp/pcab013.

220. Coffey, A., & Jansen, M. A. K. (2019). Effects of natural solar UV-B radiation on three *Arabidopsis* accessions are strongly affected by seasonal weather conditions. *Plant Physiology and Biochemistry, 134*, 64-72, https://doi.org/10.1016/j.plaphy.2018.06.016.

221. Sangüesa-Barreda, G., Di Filippo, A., Piovesan, G., Rozas, V., Di Fiore, L., García-Hidalgo, M., García-Cervigón, A. I., Muñoz-Garachana, D., Baliva, M., & Olano, J. M. (2021). Warmer springs have increased the frequency and extension of late-frost defoliations in southern European beech forests. *Science of the Total Environment, 775*, 145860, https://doi.org/10.1016/j.scitotenv.2021.145860.

222. Slatyer, R. A., Umbers, K. D. L., & Arnold, P. A. (2021). Ecological responses to variation in seasonal snow cover. *Conservation Biology*, n/a(n/a), https://doi.org/10.1111/cobi.13727.

223. Zandalinas, S. I., Sengupta, S., Fritschi, F. B., Azad, R. K., Nechushtai, R., & Mittler, R. (2021). The impact of multifactorial stress combination on plant growth and survival. *New Phytologist, 230*(3), 1034-1048, https://doi.org/10.1111/nph.17232.

224. Deng, B., Liu, X., Zheng, L., Liu, Q., Guo, X., & Zhang, L. (2019). Effects of nitrogen deposition and UV-B radiation on seedling performance of Chinese tallow tree (*Triadica sebifera*): A photosynthesis perspective. *Forest Ecology and Management, 433*, 453-458, https://doi.org/10.1016/j.foreco.2018.11.038.

225. Tripathi, R., Rai, K., Singh, S., Agrawal, M., & Agrawal, S. (2019). Role of supplemental UV-B in changing the level of ozone toxicity in two cultivars of sunflower: growth, seed yield and oil quality. *Ecotoxicology, 28*(3), 277-293, https://doi.org/10.1007/s10646-019-02020-6.

226. Urban, O., Hrstka, M., Holub, P., Veselá, B., Večeřová, K., Novotná, K., Grace, J., & Klem, K. (2019). Interactive effects of ultraviolet radiation and elevated CO_2 concentration on photosynthetic characteristics of European beech saplings during the vegetation season. *Plant Physiology and Biochemistry, 134*, 20-30, https://doi.org/10.1016/j.plaphy.2018.08.026.

227. Bornman, J. F., Barnes, P. W., Robinson, S. A., Ballaré, C. L., Flint, S. D., & Caldwell, M. M. (2015). Solar ultraviolet radiation and ozone depletion-driven climate change: effects on terrestrial ecosystems, *Photochemical & Photobiological Sciences, 14*(1), 88-107, 10.1039/c4pp90034k.

228. Nunez, S., Arets, E., Alkemade, R., Verwer, C., & Leemans, R. (2019). Assessing the impacts of climate change on biodiversity: is below 2 °C enough? *Climatic Change, 154*(3-4), 351-365, https://doi.org/10.1007/s10584-019-02420-x.

229. Weiskopf, S. R., Rubenstein, M. A., Crozier, L. G., Gaichas, S., Griffis, R., Halofsky, J. E., Hyde, K. J. W., Morelli, T. L., Morisette, J. T., Muñoz, R. C., Pershing, A. J., Peterson, D. L., Poudel, R., Staudinger, M. D., Sutton-Grier, A. E., Thompson, L., Vose, J., Weltzin, J. F., & Whyte, K. P. (2020). Climate change effects on biodiversity, ecosystems, ecosystem services, and natural resource management in the United States. *Science of the Total Environment, 733*, 137782, https://doi.org/10.1016/j.scitotenv.2020.137782.

230. Pecl, G. T., Araújo, M. B., Bell, J. D., Blanchard, J., Bonebrake, T. C., Chen, I.-C., Clark, T. D., Colwell, R. K., Danielsen, F., Evengård, B., Falconi, L., Ferrier, S., Frusher, S., Garcia, R. A., Griffis, R. B., Hobday, A. J., Janion-Scheepers, C., Jarzyna, M. A., Jennings, S., Lenoir, J., Linnetved, H. I., Martin, V. Y., McCormack, P. C., McDonald, J., Mitchell, N. J., Mustonen, T., Pandolfi, J. M., Pettorelli, N., Popova, E., Robinson, S. A., Scheffers, B. R., Shaw, J. D., Sorte, C. J. B., Strugnell, J. M., Sunday, J. M., Tuanmu, M.-N., Vergés, A., Villanueva, C., Wernberg, T., Wapstra, E., & Williams, S. E. (2017). Biodiversity redistribution under climate change: Impacts on ecosystems and human well-being. *Science, 355*(6332), eaai9214, https://doi.org/10.1126/science.aai9214.

231. Vitasse, Y., Ursenbacher, S., Klein, G., Bohnenstengel, T., Chittaro, Y., Delestrade, A., Monnerat, C., Rebetez, M., Rixen, C., Strebel, N., Schmidt, B. R., Wipf, S., Wohlgemuth, T., Yoccoz, N. G., & Lenoir, J. (2021). Phenological and elevational shifts of plants, animals and fungi under climate change in the European Alps. *Biological Reviews, 96*(5), 1816-1835, https://doi.org/10.1111/brv.12727.

232. Chowdhury, S., Fuller, R. A., Dingle, H., Chapman, J. W., & Zalucki, M. P. (2021). Migration in butterflies: a global overview. *Biological Reviews, 96*(4), 1462-1483, https://doi.org/10.1111/brv.12714.

233. Lenoir, J., Gégout, J.-C., Guisan, A., Vittoz, P., Wohlgemuth, T., Zimmermann, N. E., Dullinger, S., Pauli, H., Willner, W., & Svenning, J.-C. (2010). Going against the flow: potential mechanisms for unexpected downslope range shifts in a warming climate. *Ecography, 33*(2), 295-303, https://doi.org/10.1111/j.1600-0587.2010.06279.x.

234. Tagliari, M. M., Danthu, P., Leong Pock Tsy, J.-M., Cornu, C., Lenoir, J., Carvalho-Rocha, V., & Vieilledent, G. (2021). Not all species will migrate poleward as the climate warms: The case of the seven baobab species in Madagascar. *Global Change Biology, 27*(23), 6071-6085, https://doi.org/10.1111/gcb.15859.

235. Tomiolo, S., & Ward, D. (2018). Species migrations and range shifts: A synthesis of causes and consequences. *Perspectives in Plant Ecology, Evolution and Systematics, 33*, 62-77, https://doi.org/10.1016/j.ppees.2018.06.001.

236. IPCC. (2014). Climate Change 2014: Impacts, Adaptation, and Vulnerability. Part A: Global and Sectoral Aspects. Contribution of Working Group II to the Fifth Assessment Report of the Intergovernmental Panel on Climate Change [Field, C.B., V.R. Barros, D.J. Dokken, K.J. Mach, M.D. Mastrandrea, T.E. Bilir, M. Chatterjee, K.L. Ebi, Y.O. Estrada, R.C. Genova, B. Girma, E.S. Kissel, A.N. Levy, S. MacCracken, P.R. Mastrandrea, and L.L. White (eds.)]. Cambridge University Press, Cambridge, United Kingdom and New York, NY, USA, 1132 pp., https://www.ipcc.ch/report/ar5/wg2/

237. Tripp, E. A., Zhuang, Y., Schreiber, M., Stone, H., & Berardi, A. E. (2018). Evolutionary and ecological drivers of plant flavonoids across a large latitudinal gradient. *Molecular Phylogenetics and Evolution, 128*, 147-161, https://doi.org/10.1016/j.ympev.2018.07.004.

238. Castagna, A., Csepregi, K., Neugart, S., Zipoli, G., Večeřová, K., Jakab, G., Jug, T., Llorens, L., Martínez-Abaigar, J., Martínez-Lüscher, J., Núñez-Olivera, E., Ranieri, A., Schoedl-Hummel, K., Schreiner, M., Teszlák, P., Tittmann, S., Urban, O., Verdaguer, D., Jansen, M. A. K., & Hideg, É. (2017). Environmental plasticity of Pinot noir grapevine leaves; a trans-European study of morphological and biochemical changes along a 1500 km latitudinal climatic gradient. *Plant, Cell & Environment, 40*(11), 2790-2805, https://doi.org/10.1111/pce.13054.

239. Escobar-Bravo, R., Klinkhamer, P. G. L., & Leiss, K. A. (2017). Interactive effects of UV-B light with abiotic factors on plant growth and chemistry, and their consequences for defense against arthropod herbivores. *Frontiers in Plant Science, 8*, 278, https://doi.org/10.3389/fpls.2017.00278.

240. Escobar-Bravo, R., Nederpel, C., Naranjo, S., Kim, H. K., Rodríguez-López, M. J., Chen, G., Glauser, G., Leiss, K. A., & Klinkhamer, P. G. (2021). Ultraviolet radiation modulates both constitutive and inducible plant defenses against thrips but is dose and plant genotype dependent. *Journal of Pest Science, 94*(1), 69-81, https://doi.org/10.1007/s10340-019-01166-w.

241. Tedla, B., Dang, Q.-L., & Inoue, S. (2019). White birch has limited phenotypic plasticity to take advantage of increased photoperiods at higher latitudes north of the seed origin. *Forest Ecology and Management, 451*, 117565, https://doi.org/10.1016/j.foreco.2019.117565.

242. Way, D. A., & Montgomery, R. A. (2014). Photoperiod constraints on tree phenology, performance and migration in a warming world. *Plant, Cell & Environment, 38*(9), 1725-1736, https://doi.org/10.1111/pce.12431.

243. Tedla, B., Dang, Q. L., & Inoue, S. (2020). CO_2 elevation and photoperiods north of seed origin change autumn and spring phenology as well as cold hardiness in boreal white birch. *Frontiers in Plant Science, 11*, 506, https://doi.org/10.3389/fpls.2020.00506.

244. Mamantov, M. A., Gibson-Reinemer, D. K., Linck, E. B., & Sheldon, K. S. (2021). Climate-driven range shifts of montane species vary with elevation. *Global Ecology and Biogeography, 30*(4), 784-794, https://doi.org/10.1111/geb.13246.

245. Wu, Y., Yang, Y., Liu, C., Hou, Y., Yang, S., Wang, L., & Zhang, X. (2021). Potential suitable habitat of two economically important forest trees (*Acer truncatum* and *Xanthoceras sorbifolium*) in east Asia under current and future climate scenarios. *Forests, 12*(9), https://doi.org/10.3390/f12091263.

246. Kergunteuil, A., Descombes, P., Glauser, G., Pellissier, L., & Rasmann, S. (2018). Plant physical and chemical defence variation along elevation gradients: a functional trait-based approach. *Oecologia, 187*(2), 561-571, https://doi.org/10.1007/s00442-018-4162-y.

247. Pellissier, L., Moreira, X., Danner, H., Serrano, M., Salamin, N., van Dam, N. M., & Rasmann, S. (2016). The simultaneous inducibility of phytochemicals related to plant direct and indirect defences against herbivores is stronger at low elevation. *Journal of Ecology, 104*(4), 1116-1125, https://doi.org/10.1111/1365-2745.12580.

248. Moreira, X., Petry, W. K., Mooney, K. A., Rasmann, S., & Abdala-Roberts, L. (2018). Elevational gradients in plant defences and insect herbivory: recent advances in the field and prospects for future research. *Ecography, 41*(9), 1485-1496, https://doi.org/10.1111/ecog.03184.

249. Fernández-Marín, B., Sáenz-Ceniceros, A., Solanki, T., Robson, T. M., & García-Plazaola, J. I. (2021). Alpine forbs rely on different photoprotective strategies during spring snowmelt. *Physiologia Plantarum, 172*(3), 1506-1517, https://doi.org/10.1111/ppl.13342.

250. Gateva, S. P., Jovtchev, G., V. Angelova, T., P. Nonova, T., Tyutyundzhiev, N., G. Geleva, E., Katrandzhiev, K., A. Nikolova, N., Dimitrov, D., & V. Angelov, C. (2022). Effect of UV radiation and other abiotic stress factors on DNA of different wild plant species grown in three successive seasons in alpine and subalpine regions. *Phyton, 91*(2), 293-313, https://doi.org/10.32604/phyton.2022.016397.

251. Fraser, D. P., Sharma, A., Fletcher, T., Budge, S., Moncrieff, C., Dodd, A. N., & Franklin, K. A. (2017). UV-B antagonises shade avoidance and increases levels of the flavonoid quercetin in coriander (*Coriandrum sativum*). *Scientific Reports, 7*(1), 17758, https://doi.org/10.1038/s41598-017-18073-8.

252. Ballaré, C. L., & Austin, A. T. (2019). Recalculating growth and defense strategies under competition: Key roles of photoreceptors and jasmonates. *Journal of Experimental Botany, 70,* 3425-3434, https://doi.org/10.1093/jxb/erz237.

253. Seastedt, T., & Oldfather, M. (2021). Climate change, ecosystem processes and biological diversity responses in high elevation communities. *Climate, 9*(5), https://doi.org/10.3390/cli9050087.

254. Robson, T. M., Klem, K., Urban, O., & Jansen, M. A. K. (2015). Re-interpreting plant morphological responses to UV-B radiation. *Plant, Cell & Environment, 38*(5), 856-866, https://doi.org/10.1111/pce.12374.

255. Barnes, P. W., Ballaré, C. L., & Caldwell, M. M. (1996). Photomorphogenic effects of UV-B radiation on plants: Consequences for light competition. *Journal of Plant Physiology, 148*(1-2), 15-20, https://doi.org/10.1016/S0176-1617(96)80288-4.

256. Wolf, A., Zimmerman, N. B., Anderegg, W. R. L., Busby, P. E., & Christensen, J. (2016). Altitudinal shifts of the native and introduced flora of California in the context of 20th-century warming. *Global Ecology and Biogeography, 25*(4), 418-429, https://doi.org/10.1111/geb.12423.

257. Dainese, M., Aikio, S., Hulme, P. E., Bertolli, A., Prosser, F., & Marini, L. (2017). Human disturbance and upward expansion of plants in a warming climate. *Nature Climate Change, 7,* 577-580, https://doi.org/10.1038/nclimate3337.

258. Mosena, A., Steinlein, T., & Beyschlag, W. (2018). Reconstructing the historical spread of non-native plants in the North American West from herbarium specimens. *Flora, 242,* 45-52, https://doi.org/10.1016/j.flora.2018.03.002.

259. Wang, H., Ma, X. C., Zhang, L., Siemann, E., & Zou, J. W. (2016). UV-B has larger negative impacts on invasive populations of *Triadica sebifera* but ozone impacts do not vary. *Journal of Plant Ecology, 9*(1), 61-68, https://doi.org/10.1093/jpe/rtv045.

260. Václavík, T., Beckmann, M., Cord, A. F., & Bindewald, A. M. (2017). Effects of UV-B radiation on leaf hair traits of invasive plants—Combining historical herbarium records with novel remote sensing data. *Plos One, 12*(4), e0175671, https://doi.org/10.1371/journal.pone.0175671.

261. Hock, M., Hofmann, R. W., Müller, C., & Erfmeier, A. (2019). Exotic plant species are locally adapted but not to high ultraviolet-B radiation: a reciprocal multispecies experiment. *Ecology, 100*(5), e02665, https://doi.org/10.1002/ecy.2665.

262. Jovtchev, G., Stankov, A., Ravnachka, I., Gateva, S., Dimitrov, D., Tyutyundzhiev, N., Nikolova, N., & Angelov, C. (2019). How can the natural radiation background affect DNA integrity in angiosperm plant species at different altitudes in Rila Mountain (Southwest Bulgaria)? *Environmental Science and Pollution Research, 26*(13), 13592-13601, https://doi.org/10.1007/s11356-019-04872-1.

263. Davidson, A. M., Jennions, M., & Nicotra, A. B. (2011). Do invasive species show higher phenotypic plasticity than native species and, if so, is it adaptive? A meta-analysis. *Ecology Letters, 14*(4), 419-431, https://doi.org/10.1111/j.1461-0248.2011.01596.x.

264. Madronich, S. (1987). Photodissociation in the atmosphere: 1. Actinic flux and the effects of ground reflections and clouds. *Journal of Geophysical Research: Atmospheres, 92*(D8), 9740-9752, https://doi.org/10.1029/JD092iD08p09740.

265. Zu, K., Wang, Z., Zhu, X., Lenoir, J., Shrestha, N., Lyu, T., Luo, A., Li, Y., Ji, C., Peng, S., Meng, J., & Zhou, J. (2021). Upward shift and elevational range contractions of subtropical mountain plants in response to climate change. *Science of the Total Environment, 783*, 146896, https://doi.org/10.1016/j.scitotenv.2021.146896.

266. Benito Garzon, M., Robson, T. M., & Hampe, A. (2019). DeltaTraitSDMs: species distribution models that account for local adaptation and phenotypic plasticity. *New Phytologist, 222*(4), 1757-1765, https://doi.org/10.1111/nph.15716.

267. Li, W., Shi, M., Huang, Y., Chen, K., Sun, H., & Chen, J. (2019). Climatic change can influence species diversity patterns and potential habitats of Salicaceae plants in China. *Forests, 10*(3), 220, https://doi.org/10.3390/f10030220.

268. Wang, D., Cui, B., Duan, S., Chen, J., Fan, H., Lu, B., & Zheng, J. (2019). Moving north in China: The habitat of *Pedicularis kansuensis* in the context of climate change. *Science of the Total Environment, 697*, 133979, https://doi.org/10.1016/j.scitotenv.2019.133979.

269. Li, M., He, J., Zhao, Z., Lyu, R., Yao, M., Cheng, J., & Xie, L. (2020). Predictive modelling of the distribution of *Clematis* sect. *Fruticella s*. str. under climate change reveals a range expansion during the Last Glacial Maximum. *PeerJ, 8*, e8729, https://doi.org/10.7717/peerj.8729.

270. Zhang, K., Yao, L., Meng, J., & Tao, J. (2018). Maxent modeling for predicting the potential geographical distribution of two peony species under climate change. *Science of the Total Environment, 634*, 1326-1334, https://doi.org/10.1016/j.scitotenv.2018.04.112.

271. Peng, L. P., Cheng, F. Y., Hu, X. G., Mao, J. F., Xu, X. X., Zhong, Y., Li, S. Y., & Xian, H. L. (2019). Modelling environmentally suitable areas for the potential introduction and cultivation of the emerging oil crop *Paeonia ostii* in China. *Scientific Reports, 9*(1), 3213, https://doi.org/10.1038/s41598-019-39449-y.

272. Zhang, K., Zhang, Y., & Tao, J. (2019). Predicting the potential distribution of Paeonia veitchii (Paeoniaceae) in China by incorporating climate change into a Maxent model. *Forests, 10*(2), https://doi.org/10.3390/f10020190.

273. Hu, X. G., Jin, Y. Q., Wang, X. R., Mao, J. F., & Li, Y. (2015). Predicting impacts of future climate change on the distribution of the widespread conifer Platycladus orientalis. *Plos One, 10*(7), e0132326, https://doi.org/10.1371/journal.pone.0132326.

274. Beckmann, M., Vaclavik, T., Manceur, A. M., Sprtova, L., von Wehrden, H., Welk, E., & Cord, A. F. (2014). glUV: a global UV-B radiation data set for macroecological studies. *Methods in Ecology and Evolution, 5*(4), 372-383, https://doi.org/10.1111/2041-210x.12168.

275. Ren, T., He, N., Liu, Z., Li, M., Zhang, J., Li, A., Wei, C., Lü, X., & Han, X. (2021). Environmental filtering rather than phylogeny determines plant leaf size in three floristically distinctive plateaus. *Ecological Indicators, 130*, https://doi.org/10.1016/j.ecolind.2021.108049.

276. Ye, M., Zhu, X., Gao, P., Jiang, L., & Wu, R. (2020). Identification of quantitative trait loci for altitude adaptation of tree leaf shape with *Populus szechuanica* in the Qinghai-Tibetan Plateau. *Frontiers in Plant Science, 11*, 632, https://doi.org/10.3389/fpls.2020.00632.

277. Li, X., Ke, X., Zhou, H., & Tang, Y. (2019). Contrasting altitudinal patterns of leaf UV reflectance and absorbance in four herbaceous species on the Qinghai–Tibetan Plateau. *Journal of Plant Ecology, 12*(2), 245-254, https://doi.org/10.1093/jpe/rty016.

278. Wang, Q.-W., Liu, C., Robson, T. M., Hikosaka, K., & Kurokawa, H. (2021). Leaf density and chemical composition explain variation in leaf mass area with spectral composition among 11 widespread forbs in a common garden. P*hysiologia Plantarum, 173*(3), 698-708, https://doi.org/10.1111/ppl.13512.

279. Teramura, A. H. (1980). Effects of ultraviolet-B irradiances on soybean. I. Importance of photosynthetically active radiation in evaluating ultraviolet-B irradiance effects on soybean and wheat growth. *Physiologia Plantarum, 48*, 333-339, https://doi.org/10.1111/j.1399-3054.1980.tb03264.x.

280. Sisson, W. B., & Caldwell, M. M. (1977). Atmospheric ozone depletion: Reduction of photosynthesis and growth of a sensitive higher plant exposed to enhanced UV-B radiation. *Journal of Experimental Botany, 28*(104), 691-705, https://doi.org/10.1093/jxb/28.3.691.

281. Caldwell, M. M. (1971). Solar UV irradiation and the growth and development of higher plants. *Photophysiology, 6*, 131-177.

282. Robson, T. M., Pieristè, M., Durand, M., Kotilainen, T. K., & Aphalo, P. J. (2022). The benefits of informed management of sunlight in production greenhouses and polytunnels. *Plants People Plane*t, https://doi.org/10.1002/ppp3.10258.

283. Bernhard, G. H., Neale, R. E., Barnes, P. W., Neale, P. J., Zepp, R. G., Wilson, S. R., Andrady, A. L., Bais, A. F., McKenzie, R. L., Aucamp, P. J., Young, P. J., Liley, J. B., Lucas, R. M., Yazar, S., Rhodes, L. E., Byrne, S. N., Hollestein, L. M., Olsen, C. M., Young, A. R., Robson, T. M., Bornman, J. F., Jansen, M. A. K., Robinson, S. A., Ballare, C. L., Williamson, C. E., Rose, K. C., Banaszak, A. T., Hader, D. P., Hylander, S., Wangberg, S. A., Austin, A. T., Hou, W. C., Paul, N. D., Madronich, S., Sulzberger, B., Solomon, K. R., Li, H., Schikowski, T., Longstreth, J., Pandey, K. K., Heikkila, A. M., & White, C. C. (2020). Environmental effects of stratospheric ozone depletion, UV radiation and interactions with climate change: UNEP Environmental Effects Assessment Panel, update 2019.

Photochemical & Photobiological Sciences, 19, 542-584, https://doi.org/10.1039/d0pp90011g.

284. Feeley, K. J., Stroud, J. T., & Perez, T. M. (2017). Most 'global' reviews of species' responses to climate change are not truly global. *Diversity and Distributions, 23*(3), 231-234, https://doi.org/10.1111/ddi.12517.

285. Sheldon, K. S. (2019). Climate change in the tropics: Ecological and evolutionary responses at low latitudes. *Annual Review of Ecology, Evolution, and Systematics, 50*(1), 303-333, https://doi.org/10.1146/annurev-ecolsys-110218-025005.

286. Feeley, K. J., & Stroud, J. T. (2018). Where on Earth are the "tropics"? *Frontiers of Biogeography, 10*(1-2), https://doi.org/10.21425/f5fbg38649.

287. Raven, P. H., Gereau, R. E., Phillipson, P. B., Chatelain, C., Jenkins, C. N., & Ulloa Ulloa, C. The distribution of biodiversity richness in the tropics. *Science Advances, 6*(37), eabc6228, https://doi.org/10.1126/sciadv.abc6228.

288. Secretariat of the Convention on Biological Diversity (2008). *Biodiversity and agriculture: Safeguarding biodiversity and securing food for the world*. Montreal, Canada, 56 pp., https://www.cbd.int/doc/bioday/2008/ibd-2008-booklet-en.pdf

289. Chipperfield, M. P., Bekki, S., Dhomse, S., Harris, N. R. P., Hassler, B., Hossaini, R., Steinbrecht, W., Thieblemont, R., & Weber, M. (2017). Detecting recovery of the stratospheric ozone layer. *Nature, 549*(7671), 211-218, https://doi.org/10.1038/nature23681.

290. Krause, G. H., Jahns, P., Virgo, A., Garcia, M., Aranda, J., Wellmann, E., & Winter, K. (2007). Photoprotection, photosynthesis and growth of tropical tree seedlings under near-ambient and strongly reduced solar ultraviolet-B radiation. *Journal of Plant Physiology, 164*, 1311-1322, https://doi.org/10.1016/j.jplph.2006.09.004.

291. Kataria, S., & Guruprasad, K. N. (2015). Exclusion of solar UV radiation improves photosynthetic performance and yield of wheat varieties. *Plant Physiology and Biochemistry, 97*, 400-411, https://doi.org/10.1016/j.plaphy.2015.10.001.

292. Kataria, S., & Baghel, L. (2016). Influence of UV exclusion and selenium on carbon fixation, nitrogen fixation and yield of soybean variety JS-335. *South African Journal of Botany, 103*, 126-134, https://doi.org/10.1016/j.sajb.2015.09.003.

293. Mazza, C. A., Gimenez, P. I., Kantolic, A. G., & Ballaré, C. L. (2013). Beneficial effects of solar UV-B radiation on soybean yield mediated by reduced insect herbivory under field conditions. *Physiologia Plantarum, 147*(3), 307-315, https://doi.org/10.1111/j.1399-3054.2012.01661.x.

294. Mansour, G., Ghanem, C., Mercenaro, L., Nassif, N., Hassoun, G., & Del Caro, A. (2022). Effects of altitude on the chemical composition of grapes and wine: a review. *OENO One, 56*(1), 227-239, https://doi.org/10.20870/oeno-one.2022.56.1.4895.

295. Hinojos Mendoza, G., Gutierrez Ramos, C. A., Heredia Corral, D. M., Soto Cruz, R., & Garbolino, E. (2020). Assessing suitable areas of common grapevine (Vitis vinifera l.) for current and future climate situations: The CDS Toolbox SDM. *Atmosphere, 11*(11), 1201, https://doi.org/10.3390/atmos11111201.

296. Moriondo, M., Jones, G. V., Bois, B., Dibari, C., Ferrise, R., Trombi, G., & Bindi, M. (2013). Projected shifts of wine regions in response to climate change. *Climatic Change, 119*(3), 825-839, https://doi.org/10.1007/s10584-013-0739-y.

297. Hannah, L., Roehrdanz, P. R., Ikegami, M., Shepard, A. V., Shaw, M. R., Tabor, G. M., Zhi, L., Marquet, P. A., & Hijmans, R. J. (2013). Climate change, wine, and conservation. *Proceedings of the National Academy of Sciences, 110*(17), 6907-6912, https://doi.org/10.1073/pnas.1210127110.

298. Malhotra, S. (2017). Horticultural crops and climate change: A review. *Indian Journal of Agricultural Sciences, 87*(1), 12-22.

299. Ginbo, T. (2022). Heterogeneous impacts of climate change on crop yields across altitudes in Ethiopia. *Climatic Change, 170*(1), 1-21, Vol.:(0123456789) https://doi.org/10.1007/s10584-022-03306-1.

300. Derebe, A. D., Gobena Roro, A., Tessfaye Asfaw, B., Worku Ayele, W., & Hvoslef-Eide, A. K. (2019). Effects of solar UV-B radiation exclusion on physiology, growth and yields of taro (*Colocasia esculenta* (L.)) at different altitudes in tropical environments of Southern Ethiopia. *Scientia Horticulturae, 256*, 108563, https://doi.org/10.1016/j.scienta.2019.108563.

301. Tonnang, H. E., Sokame, B. M., Abdel-Rahman, E. M., & Dubois, T. (2022). Measuring and modelling crop yield losses due to invasive insect pests under climate change. *Current Opinion in Insect Science, 100873*, https://doi.org/10.1016/j.cois.2022.100873.

302. Wallingford, P. D., Morelli, T. L., Allen, J. M., Beaury, E. M., Blumenthal, D. M., Bradley, B. A., Dukes, J. S., Early, R., Fusco, E. J., Goldberg, D. E., Ibáñez, I., Laginhas, B. B., Vilà, M., & Sorte, C. J. B. (2020). Adjusting the lens of invasion biology to focus on the impacts of climate-driven range shifts. *Nature Climate Change, 10*(5), 398-405, https://doi.org/10.1038/s41558-020-0768-2.

303. Schweiger, O., Biesmeijer, J. C., Bommarco, R., Hickler, T., Hulme, P. E., Klotz, S., Kühn, I., Moora, M., Nielsen, A., Ohlemüller, R., Petanidou, T., Potts, S. G., Pyšek, P., Stout, J. C., Sykes, M. T., Tscheulin, T., Vilà, M., Walther, G.-R., Westphal, C., Winter, M., Zobel, M., & Settele, J. (2010). Multiple stressors on biotic interactions: how climate change and alien species interact to affect pollination. *Biological Reviews, 85*(4), 777-795, https://doi.org/10.1111/j.1469-185X.2010.00125.x.

304. Weaver, S. A., & Mallinger, R. E. (2022). A specialist bee and its host plants experience phenological shifts at different rates in response to climate change. *Ecology, e3658*, https://doi.org/10.1002/ecy.3658.

305. Jaiswal, D., Pandey, A., Mukherjee, A., Agrawal, M., & Agrawal, S. B. (2020). Alterations in growth, antioxidative defense and medicinally important compounds of *Curcuma caesia* Roxb. under elevated ultraviolet-B radiation. *Environmental and Experimental Botany, 177*, 104152, https://doi.org/10.1016/j.envexpbot.2020.104152.

306. Neugart, S., & Schreiner, M. (2018). UVB and UVA as eustressors in horticultural and agricultural crops. *Scientia Horticulturae, 234*, 370-381, https://doi.org/10.1016/j.scienta.2018.02.021.

307. Robson, T. M., Aphalo, P. J., Banas, A. K., Barnes, P. W., Brelsford, C. C., Jenkins, G. I., Kotilainen, T., Labuz, J., Martínez-Abaigar, J., Morales, L. O., Neugart, S., Pieristè, M., Rai, N., Vandenbussche, F., & Jansen, M. (2019). A perspective on ecologically relevant plant-UV research and its practical application. *Photochemical & Photobiological Sciences, 18*, 970-988, https://doi.org/10.1039/c8pp00526e.

308. Takshak, S., & Agrawal, S. B. (2019). Defense potential of secondary metabolites in medicinal plants under UV-B stress. *Journal of Photochemistry and Photobiology B: Biology, 193*, 51-88, https://doi.org/10.1016/j.jphotobiol.2019.02.002.

309. Lin, N., Liu, X. Y., Zhu, W. F., Cheng, X., Wang, X. H., Wan, X. C., & Liu, L. L. (2021). Ambient Ultraviolet B signal modulates tea flavor characteristics via shifting a metabolic flux in flavonoid biosynthesis. *Journal of Agricultural and Food Chemistry, 69*, 3401-3414, https://doi.org/10.1021/acs.jafc.0c07009.

310. Falcato Fialho Palma, C., Castro-Alves, V., Rosenqvist, E., Ottosen, C. O., Strid, Å., & Morales, L. O. (2021). Effects of UV radiation on transcript and metabolite accumulation are dependent on monochromatic light background in cucumber *Physiologia Plantarum, 173*, 750-761, https://doi.org/10.1111/ppl.13551.

311. Quintero-Arias, D. G., Acuña-Caita, J. F., Asensio, C., & Valenzuela, J. L. (2021). Ultraviolet transparency of plastic films determines the quality of lettuce (*Lactuca sativa*, l.) grown in a greenhouse. *Agronomy, 11*(2), 358, https://doi.org/10.3390/agronomy11020358.

312. Ma, M., Wang, P., Yang, R., Zhou, T., & Gu, Z. (2019). UV-B mediates isoflavone accumulation and oxidative-antioxidant system responses in germinating soybean. *Food Chemistry, 275*, 628-636, https://doi.org/10.1016/j.foodchem.2018.09.158

313. Qi, W., Ma, J., Zhang, J., Gui, M., Li, J., & Zhang, L. (2020). Effects of low doses of UV-B radiation supplementation on tuber quality in purple potato (*Solanum tuberosum* L.). *Plant Signaling & Behavior, 15*(9), 1783490, https://doi.org/10.1080/15592324.2020.1783490.

314. Santin, M., Castagna, A., Miras-Moreno, B., Rocchetti, G., Lucini, L., Hauser, M. T., & Ranieri, A. (2020). Beyond the visible and below the peel: How UV-B radiation influences the phenolic profile in the pulp of peach fruit. A biochemical and molecular study. *Frontiers in Plant Science, 11*, 579063, https://doi.org/10.3389/fpls.2020.579063

315. Ferreyra, M. L. F., Serra, P., & Casati, P. (2021). Recent advances on the roles of flavonoids as plant protective molecules after UV and high light exposure. *Physiologia Plantarum, 173*(3), 736-749, https://doi.org/10.1111/ppl.13543.

316. Brousseau, V. D., Wu, B.-S., MacPherson, S., Morello, V., & Lefsrud, M. (2021). Cannabinoids and terpenes: How production of photo-protectants can be manipulated to enhance *Cannabis sativa* l. *Phytochemistry. Frontiers in Plant Science, 12*, 620021, https://doi.org/10.3389/fpls.2021.620021

317. Tripathi, D., Meena, R. P., & Pandey-Rai, S. (2021). Short term UV-B radiation mediated modulation of physiological traits and withanolides production in *Withania coagulans* (L.) Dunal under in-vitro condition. *Physiology and Molecular Biology of Plants, 27*(8), 1823-1835, https://doi.org/10.1007/s12298-021-01046-7

318. Zhong, Z., Liu, S., Han, S., Li, Y., Tao, M., Liu, A., He, Q., Chen, S., Dufresne, C., Zhu, W., & Tian, J. (2021). Integrative omic analysis reveals the improvement of alkaloid accumulation by ultraviolet-B radiation and its upstream regulation in *Catharanthus roseus*. *Industrial Crops and Products, 166*, 113448, https://doi.org/10.1016/j.indcrop.2021.113448.

319. FAO (2020). Fruit and vegetables—your dietary essentials. The international year of fruits and vegetables, 2021, background paper. (pp. 82). Rome, Italy, https://doi.org/10.4060/cb2395en

320. Keflie, T. S., Samuel, A., Woldegiorgis, A. Z., Lambert, C., Nohr, D., & Biesalski, H. K. (2021). Consumption of sun-exposed oyster mushrooms help patients fight tuberculosis. *Asian Journal of Complementary and Alternative Medicine. Volume, 9*(2).

321. Efsa Panel on Nutrition, N. F. a. F. A., Turck, D., Bohn, T., Castenmiller, J., De Henauw, S., Hirsch-Ernst, K. I., Maciuk, A., Mangelsdorf, I., McArdle, H. J., Naska, A., Pelaez, C., Pentieva, K., Siani, A., Thies, F., Tsabouri, S., Vinceti, M., Cubadda, F., Frenzel, T., Heinonen, M., Marchelli, R., Neuhäuser-Berthold, M., Poulsen, M., Prieto Maradona, M., Schlatter, J. R., van Loveren, H., Gerazova-Efremova, K., Roldán-Torres, R., & Knutsen, H. K. (2022). Safety of vitamin D_2 mushroom powder as a Novel food pursuant to Regulation (EU) 2015/2283 (NF 2019/1471). [https://doi.org/10.2903/j.efsa.2022.7326]. *European Food Safety Authority Journal, 20*(6), e07326, https://doi.org/10.2903/j.efsa.2022.7326.

322. Hamid, A., Singh, S., Agrawal, M., & Agrawal, S. B. (2019). *Heteropogon contortus* bl-1 (pilli grass) and elevated UV-B radiation: The role of growth, physiological, and biochemical traits in determining forage productivity and quality. *Photochemistry and Photobiology, 95*(2), 572-580, https://doi.org/10.1111/php.12990.

323. Hamid, A., Singh, S., Agrawal, M., & Agrawal, S. B. (2020). Effects of plant age on performance of the tropical perennial fodder grass, *Cenchrus ciliaris* L. subjected to elevated ultraviolet-B radiation. *Plant Biology 22*(5), 805-812, https://doi.org/10.1111/plb.13116.

324. Golob, A., Stibilj, V., Kreft, I., Vogel-Mikus, K., Gaberscik, A., & Germ, M. (2018). Selenium treatment alters the effects of UV radiation on chemical and production parameters in hybrid buckwheat. *Acta Agriculturae Scandinavica Section B-Soil and Plant Science, 68*, 5-15.

325. FAO (2019). New standards to curb the global spread of plant pests and diseases. http://www.fao.org/news/story/en/item/1187738/icode/

326. Jones, R. A. C., & Naidu, R. A. (2019). Global dimensions of plant virus diseases: Current status and future perspectives. *Annual Review of Virology, 6*(1), 387-409, https://doi.org/10.1146/annurev-virology-092818-015606.

327. Bebber, D. P., Ramotowski, M. A., & Gurr, S. J. (2013). Crop pests and pathogens move polewards in a warming world. *Nature Climate Change, 3*(11), 985-988, https://doi.org/10.1038/nclimate1990.

328. Chaloner, T. M., Gurr, S. J., & Bebber, D. P. (2021). Plant pathogen infection risk tracks global crop yields under climate change. *Nature Climate Change, 11*(8), 710-715, https://doi.org/10.1038/s41558-021-01104-8.

329. Juroszek, P., Racca, P., Link, S., Farhumand, J., & Kleinhenz, B. (2020). Overview on the review articles published during the past 30 years relating to the potential climate change effects on plant pathogens and crop disease risks. *Plant Pathology, 69*(2), 179-193, https://doi.org/10.1111/ppa.13119.

330. Pierik, R., & Ballaré, C. L. (2021). Control of plant growth and defense by photoreceptors: From mechanisms to opportunities in agriculture. *Molecular Plant, 14*(1), 61-76, https://doi.org/10.1016/j.molp.2020.11.021.

331. Pérez-Hedo, M., Alonso-Valiente, M., Vacas, S., Gallego, C., Pons, C., Arbona, V., Rambla, J. L., Navarro-Llopis, V., Granell, A., & Urbaneja, A. (2021). Plant exposure to herbivore-induced plant volatiles: a sustainable approach through eliciting plant defenses. *Journal of Pest Science, 94*(4), 1221-1235, https://doi.org/10.1007/s10340-021-01334-x.

332. Brunner-Mendoza, C., Reyes-Montes, M. d. R., Moonjely, S., Bidochka, M. J., & Toriello, C. (2019). A review on the genus *Metarhizium* as an entomopathogenic microbial biocontrol agent with emphasis on its use and utility in Mexico. *Biocontrol Science and Technology, 29*(1), 83-102, https://doi.org/10.1080/09583157.2018.1531111.

333. Tong, S. M., & Feng, M. G. (2022). Molecular basis and regulatory mechanisms underlying fungal insecticides' resistance to solar ultraviolet irradiation. *Pest Management Science, 78*(1), 30-42, https://doi.org/10.1002/ps.6600.

334. Mann, A. J., & Davis, T. S. (2021). Entomopathogenic fungi to control bark beetles: a review of ecological recommendations. *Pest Management Science, 77*(9), 3841-3846, https://doi.org/10.1002/ps.6364.

335. Sutanto, K. D., Husain, M., Rasool, K. G., Malik, A. F., Al-Qahtani, W. H., & Aldawood, A. S. (2022). Persistency of indigenous and exotic entomopathogenic fungi isolates under Ultraviolet B (UV-B) irradiation to enhance field application efficacy and obtain sustainable control of the red palm weevil. *Insects, 13*(1), 103, https://doi.org/10.3390/insects13010103.

336. Bernardo, C. d. C., Pereira-Junior, R. A., Luz, C., Mascarin, G. M., & Kamp Fernandes, É. K. (2020). Differential susceptibility of blastospores and aerial conidia of entomopathogenic fungi to heat and UV-B stresses. *Fungal Biology, 124*(8), 714-722, https://doi.org/10.1016/j.funbio.2020.04.003.

337. Aphalo, P. J., Albert, A., Björn, L. O., McLeod, A., Robson, T. M., & Rosenqvist, E. (Eds.). (2012). *Beyond the visible: A handbook of best practice in plant UV photobiology* (COST Action FA0906 UV4growth). Helsinki, Finland http://hdl.handle.net/10138/37558: University of Helsinki, Department of Biosciences, Division of Plant Biology

338. Puglis, H. J., & Boone, M. D. (2011). Effects of technical-grade active ingredient vs. commercial formulation of seven pesticides in the presence or absence of UV radiation on survival of green frog tadpoles. *Archives of Environmental Contamination and Toxicology, 60*(1), 145-155, https://doi.org/10.1007/s00244-010-9528-z.

339. Kah, M., Walch, H., & Hofmann, T. (2018). Environmental fate of nanopesticides: durability, sorption and photodegradation of nanoformulated clothianidin. *Environmental Science: Nano, 5*(4), 882-889, https://doi.org/10.1039/c8en00038g.

340. Schwarzenbach, R. P., Gschwend, P. M., & Imboden, D. M. (2002). Direct Photolysis. In R. P. Schwarzenbach, P. M. Gschwend, & D. M. Imboden (Eds.), *Environmental Organic Chemistry* (pp. 611-654): John Wiley & Sons.

341. Schwarzenbach, R. P., Gschwend, P. M., & Imboden, D. M. (2002). Indirect Photolysis: Reactions with Photooxidants in Natural Waters and in the Atmosphere. In R. P. Schwarzenbach, P. M. Gschwend, & D. M. Imboden (Eds.), *Environmental Organic Chemistry* (pp. 655-686): John Wiley & Sons.

342. Su, L., Caywood, L. M., Sivey, J. D., & Dai, N. (2019). Sunlight photolysis of safener benoxacor and herbicide metolachlor as mixtures on simulated soil surfaces. *Environmental Science & Technology, 53*(12), 6784-6793, https://doi.org/10.1021/acs.est.9b01243.

343. Anderson, S. C., Chu, L., Bouma, C., Beukelman, L., McLouth, R., Larson, E., & Nienow, A. M. (2019). Comparison of the photodegradation of imazethapyr in aqueous solution, on epicuticular waxes, and on intact corn (*Zea mays*) and soybean (*Glycine max*) leaves. *Journal of Environmental Science and Health, Part B, 54*(2), 129-137, https://doi.org/10.1080/03601234.2018.1511400.

344. Buyl Lee, S., & Chung Suh, M. (2021). Regulatory mechanisms underlying cuticular wax biosynthesis. *Journal of Experimental Botany, 73*(9), 2799-2816, https://doi.org/10.1093/jxb/erab509.

345. Arbid, Y., Sleiman, M., & Richard, C. (2022). Photochemical interactions between pesticides and plant volatiles. *Science of the Total Environment, 807*(1), 150716, https://doi.org/10.1016/j.scitotenv.2021.150716.

346. Palma, D., Arbid, Y., Sleiman, M., de Sainte-Claire, P., & Richard, C. (2020). New route to toxic nitro and nitroso products upon irradiation of micropollutant mixtures containing imidacloprid: Role of NOx and effect of natural organic matter. *Environmental Science & Technology, 54*(6), 3325-3333, https://doi.org/10.1021/acs.est.9b07304.

347. Xi, N., Li, Y., Chen, J., Yang, Y., Duan, J., & Xia, X. (2021). Elevated temperatures decrease the photodegradation rate of pyrethroid insecticides on spinach leaves: Implications for the effect of climate warming. *Environmental Science & Technology, 55*(2), 1167-1177, https://doi.org/10.1021/acs.est.0c06959.

348. Qu, S., Kolodziej, E. P., Long, S. A., Gloer, J. B., Patterson, E. V., Baltrusaitis, J., Jones, G. D., Benchetler, P. V., Cole, E. A., Kimbrough, K. C., Tarnoff, M. D., & Cwierny, D. M. (2013). Product-to-parent reversion of Trenbolone: Unrecognized risks for endocrine disruption. *Science, 342*(6156), 347-351, https://doi.org/10.1126/science.1243192.

349. Mishra, P., Tyagi, B. K., Mukherjee, A., & Chandrasekaran, N. (2019). Potential application of nanopesticides to pest control in the food and agriculture sector. In *Food Applications of Nanotechnology* (pp. 493-509): CRC Press, https://doi.org/10.1201/9780429297038

350. Côa, F., Bortolozzo, L. S., Petry, R., Da Silva, G. H., Martins, C. H. Z., de Medeiros, A. M. Z., Sabino, C. M. S., Costa, R. S., Khan, L. U., Delite, F. S., & Martinez, D. S. T. (2020). Environmental toxicity of nanopesticides against non-target organisms: The state of the art. In L. F. Fraceto, V. L. S.S. de Castro, R. Grillo, D. Ávila, H. Caixeta Oliveira, & R. Lima (Eds.), *Nanopesticides: From research and development to mechanisms of action and sustainable use in agriculture* (pp. 227-279). Cham: Springer International Publishing, https://doi.org/10.1007/978-3-030-44873-8_8

351. Mishra, P., Dutta, S., Haldar, M., Dey, P., Kumar, D., Mukherjee, A., & Chandrasekaran, N. (2019). Enhanced mosquitocidal efficacy of colloidal dispersion of pyrethroid nanometric emulsion with benignity towards non-target species. *Ecotoxicology and Environmental Safety, 176*, 258-269, https://doi.org/10.1016/j.ecoenv.2019.03.096.

352. Wang, D., Saleh, N. B., Byro, A., Zepp, R., Sahle-Demessie, E., Luxton, T. P., Ho, K. T., Burgess, R. M., Flury, M., White, J. C., & Su, C. (2022). Nano-enabled pesticides for sustainable agriculture and global food security. *Nature Nanotechnology, 17*(4), 347-360, https://doi.org/10.1038/s41565-022-01082-8.

353. Kumar, S., Nehra, M., Dilbaghi, N., Marrazza, G., Hassan, A. A., & Kim, K.-H. (2019). Nano-based smart pesticide formulations: Emerging opportunities for agriculture. *Journal of Controlled Release, 294*, 131-153, https://doi.org/10.1016/j.jconrel.2018.12.012.

354. Teramura, A. H. (1983). Effects of ultraviolet-B radiation on the growth and yield of crop plants. *Physiologia Plantarum, 58*, 415-427, https://doi.org/10.1111/j.1399-3054.1983.tb04203.x.

355. Takshak, S., & Agrawal, S. B. (2019). Defense potential of secondary metabolites in medicinal plants under UV-B stress. *Journal of Photochemistry & Photobiology*, *B: Biology, 193*, 51-88, https://doi.org/10.1016/j.jphotobiol.2019.02.002.

356. Jiang, Q. Y., Zhang, M., & Mujumdar, A. S. (2020). UV induced conversion during drying of ergosterol to vitamin D in various mushrooms: Effect of different drying conditions. *Trends in Food Science & Technology, 105*, 200-210, https://doi.org/10.1016/j.tifs.2020.09.011.

357. Leung, M. F., & Cheung, P. C. K. (2021). Vitamins D and D_2 in cultivated mushrooms under ultraviolet irradiation and their bioavailability in humans: A mini-review. *International Journal of Medicinal Mushrooms, 23*, 1-15, https://doi.org/10.1615/IntJMedMushrooms.2021040390.

358. Ljubic, A., Thulesen, E. T., Jacobsen, C., & Jakobsen, J. (2021). UVB exposure stimulates production of vitamin D_3 in selected microalgae. *Algal Research-Biomass Biofuels and Bioproducts, 59*, 102472, https://doi.org/10.1016/j.algal.2021.102472.

359. Cardwell, G., Bornman, J. F., James, A. P., & Black, L. J. (2018). *A review of mushrooms as a potential source of dietary vitamin D. Nutrients, 10*(10), 1498, https://doi.org/10.3390/nu10101498.

360. Mariz-Ponte, N., Martins, S., Goncalves, A., Correia, C. M., Ribeiro, C., Dias, M. C., & Santos, C. (2019). The potential use of the UV-A and UV-B to improve tomato quality and preference for consumers. *Scientia Horticulturae, 246*, 777-784, https://doi.org/10.1016/j.scienta.2018.11.058.

361. Muller, R., Acosta-Motos, J. R., Grosskinsky, D. K., Hernandez, J. A., Lutken, H., & Barba-Espin, G. (2019). UV-B exposure of black carrot (*Daucus carota* ssp. *sativus* var. atrorubens) plants promotes growth, accumulation of anthocyanin, and phenolic compounds. *Agronomy-Basel, 9*, 323, https://doi.org/10.3390/agronomy9060323.

362. Del-Castillo-Alonso, M. Á., Monforte, L., Tomás-Las-Heras, R., Núñez-Olivera, E., & Martínez-Abaigar, J. (2020). A supplement of ultraviolet-B radiation under field conditions increases phenolic and volatile compounds of Tempranillo grape skins and the resulting wines. *European Journal of Agronomy, 121*, 126150, https://doi.org/10.1016/j.eja.2020.126150.

363. Del-Castillo-Alonso, M. A., Monforte, L., Tomas-Las-Heras, R., Ranieri, A., Castagna, A., Martinez-Abaigar, J., & Nunez-Olivera, E. (2021). Secondary metabolites and related genes in *Vitis vinifera* L. cv. Tempranillo grapes as influenced by ultraviolet radiation and berry development. *Physiologia Plantarum*, https://doi.org/10.1111/ppl.13483.

364. Santin, M., Lucini, L., Castagna, A., Rocchetti, G., Hauser, M. T., & Ranieri, A. (2019). Comparative "phenol-omics" and gene expression analyses in peach (Prunus persica) skin in response to different postharvest UV-B treatments. *Plant Physiology and Biochemistry, 135*, 511-519, https://doi.org/10.1016/j.plaphy.2018.11.009.

365. Ding, R. R., Che, X. K., Shen, Z., & Zhang, Y. H. (2021). Metabolome and transcriptome profiling provide insights into green apple peel reveals light- and UV-B-responsive pathway in anthocyanins accumulation. *BMC Plant Biology, 21*, 351, https://doi.org/10.1186/s12870-021-03121-3.

366. Li, T. S., Yamane, H., & Tao, R. (2021). Preharvest long-term exposure to UV-B radiation promotes fruit ripening and modifies stage-specific anthocyanin metabolism in highbush blueberry. *Horticulture Research, 8*, 67, https://doi.org/10.1038/s41438-021-00503-4.

367. Thomas, T. T. D., & Puthur, J. T. (2020). UV-B priming enhances specific secondary metabolites in *Oryza sativa* (L.) empowering to encounter diverse abiotic stresses. *Plant Growth Regulation, 92*(2), 169-180, https://doi.org/10.1007/s10725-020-00628-x.

368. Jiang, Z. F., Xu, M. F., Dong, J. F., Zhu, Y., Lou, P. P., Han, Y. D., Hao, J., Yang, Y. J., Ni, J., & Xu, M. J. (2022). UV-B pre-irradiation induces cold tolerance in tomato fruit by SlUVR8-mediated upregulation of superoxide dismutase and catalase. *Postharvest Biology and Technology, 185*, 111777, https://doi.org/10.1016/j.postharvbio.2021.111777.

369. Neugart, S., & Bumke-Vogt, C. (2021). Flavonoid glycosides in *Brassica* species respond to UV-B depending on exposure time and adaptation time. *Molecules, 26*, 494, https://doi.org/10.3390/molecules26020494.

370. Rady, M. R., Gierczik, K., Ibrahem, M. M., Matter, M. A., & Galiba, G. (2021). Anticancer compounds production in *Catharanthus roseus* by methyl jasmonate and UV-B elicitation. *South African Journal of Botany, 142*, 34-41, https://doi.org/10.1016/j.sajb.2021.05.024.

371. Santin, M., Giordani, T., Cavallini, A., Bernardi, R., Castagna, A., Hauser, M. T., & Ranieri, A. (2019). UV-B exposure reduces the activity of several cell wall-dismantling enzymes and affects the expression of their biosynthetic genes in peach fruit (*Prunus persica* L., cv. Fairtime, melting phenotype). *Photochemical & Photobiological Sciences, 18*, 1280-1289, https://doi.org/10.1039/c8pp00505b.

372. Yoon, H. I., Kim, D., & Son, J. E. (2020). Spatial and temporal bioactive compound contents and chlorophyll fluorescence of kale (*Brassica oleracea* l.) under UV-B exposure near harvest time in controlled environments. [Article; Early Access]. *Photochemistry and Photobiology, 96*, 845-852, https://doi.org/10.1111/php.13237.

373. Castillejo, N., Martinez-Zamora, L., & Artes-Hernandez, F. (2021). Periodical UV-B radiation hormesis in biosynthesis of kale sprouts nutraceuticals. *Plant Physiology and Biochemistry, 165*, 274-285, https://doi.org/10.1016/j.plaphy.2021.05.022.

374. Virsile, A., Samuoliene, G., Miliauskiene, J., & Duchovskis, P. (2019). Applications and advances in LEDs for horticulture and crop production. In T. Koutchma (Ed.), Ultraviolet LED Technology for Food Applications. From *Farms to Kitchens* (pp. 35-65). London: Elsevier, https://doi.org/10.1016/B978-0-12-817794-5.00003-0

375. Khan, S., Dar, A. H., Shams, R., Aga, M. B., Siddiqui, M. W., Mir, S. A., Rizvi, Q.-U.-e. H., Khan, S. A., & Altaf, A. (2021). Applications of ultraviolet light–emitting diode technology in horticultural produce: A systematic review and meta-analysis. *Food and Bioprocess Technology, 15*, 487-497, https://doi.org/10.1007/s11947-021-02742-8.

376. Yoon, H. I., Kim, H. Y., Kim, J., Oh, M.-M., & Son, J. E. (2021). Quantitative analysis of UV-B radiation interception in 3D plant structures and intraindividual distribution of phenolic contents. *International Journal of Molecular Sciences, 22(5), 2701,* https://doi.org/10.3390/ijms22052701

377. McLay, E. R., Pontaroli, A. C., & Wargent, J. J. (2020). UV-B induced flavonoids contribute to reduced biotrophic disease susceptibility in lettuce seedlings. *Frontiers in Plant Science, 11*, 594681, https://doi.org/10.3389/fpls.2020.594681.

378. Strauss, J., Schirrmeister, L., Grosse, G., Fortier, D., Hugelius, G., Knoblauch, C., Romanovsky, V., Schädel, C., Schneider von Deimling, T., Schuur, E. A. G., Shmelev, D., Ulrich, M., & Veremeeva, A. (2017). Deep Yedoma permafrost: A synthesis of depositional characteristics and carbon vulnerability. *Earth-Science Reviews, 172*, 75-86, https://doi.org/10.1016/j.earscirev.2017.07.007.

379. Hugelius, G., Strauss, J., Zubrzycki, S., Harden, J. W., Schuur, E. A. G., Ping, C. L., Schirrmeister, L., Grosse, G., Michaelson, G. J., Koven, C. D., O'Donnell, J. A., Elberling, B., Mishra, U., Camill, P., Yu, Z., Palmtag, J., & Kuhry, P. (2014). Estimated stocks of circumpolar permafrost carbon with quantified uncertainty ranges and identified data gaps. *Biogeosciences, 11*(23), 6573-6593, https://doi.org/10.5194/bg-11-6573-2014.

380. Biskaborn, B. K., Smith, S. L., Noetzli, J., Matthes, H., Vieira, G., Streletskiy, D. A., Schoeneich, P., Romanovsky, V. E., Lewkowicz, A. G., Abramov, A., Allard, M., Boike, J., Cable, W. L., Christiansen, H. H., Delaloye, R., Diekmann, B., Drozdov, D., Etzelmüller, B., Grosse, G., Guglielmin, M., Ingeman-Nielsen, T., Isaksen, K., Ishikawa, M., Johansson, M., Johannsson, H., Joo, A., Kaverin, D., Kholodov, A., Konstantinov, P., Kröger, T., Lambiel, C., Lanckman, J.-P., Luo, D., Malkova, G., Meiklejohn, I., Moskalenko, N., Oliva, M., Phillips, M., Ramos, M., Sannel, A. B. K., Sergeev, D., Seybold, C., Skryabin, P., Vasiliev, A., Wu, Q., Yoshikawa, K., Zheleznyak, M., & Lantuit, H. (2019). Permafrost is warming at a global scale. *Nature Communications, 10*(1), 264, https://doi.org/10.1038/s41467-018-08240-4.

381. IPCC (2019). Summary for Policymakers. In: IPCC Special Report on the Ocean and Cryosphere in a Changing Climate In H.-O. Pörtner, D. C. Roberts, V. Masson-Delmotte, P. C. Zhai, M. Tignor, E. Poloczanska, et al. (Eds.). Cambridge, UK and New York, NY, USA, https://doi.org/10.1017/9781009157964.001

382. Cory, R. M., Ward, C. P., Crump, B. C., & Kling, G. W. (2014). Sunlight controls water column processing of carbon in arctic fresh waters. *Science, 345*(6199), 925-928, https://doi.org/10.1126/science.1253119

383. Cory, R. M., Crump, B. C., Dobkowski, J. A., & Kling, G. W. (2013). Surface exposure to sunlight stimulates CO_2 release from permafrost soil carbon in the Arctic. *Proceedings of the National Academy of Sciences of the United States of America, 110(9)*, 3429-3434, https://doi.org/10.1073/pnas.1214104110.

384. Turetsky, M. R., Abbott, B. W., Jones, M. C., Anthony, K. W., Olefeldt, D., Schuur, E. A. G., Koven, C. D., McGuire, A. D., Grosse, G., & Kuhry, P. (2019). Permafrost collapse is accelerating carbon release. *Nature, 569*, 32-34.

385. Austin, A. T., & Ballaré, C. L. (2010). Dual role of lignin in plant litter decomposition in terrestrial ecosystems. *Proceedings of the National Academy of Sciences USA, 107*(10), 4618-4622, https://doi.org/10.1073/pnas.0909396107.

386. Day, T. A., & Bliss, M. S. (2020). Solar photochemical emission of CO_2 from leaf litter: Sources and significance to C loss. *Ecosystems, 23*, 1344-1361, https://doi.org/10.1007/s10021-019-00473-8.

387. King, J. Y., Brandt, L. A., & Adair, E. C. (2012). Shedding light on plant litter decomposition: advances, implications and new directions in understanding the role of photodegradation. *Biogeochemistry, 111*(1-3), 57-81, https://doi.org/10.1007/s10533-012-9737-9.

388. Keiser, A. D., Warren, R., Filley, T., & Bradford, M. A. (2021). Signatures of an abiotic decomposition pathway in temperate forest leaf litter. *Biogeochemistry, 153*(2), 177-190, https://doi.org/10.1007/s10533-021-00777-9.

389. Day, T. A., Urbine, J. M., & Bliss, M. S. (2022). Supplemental precipitation accelerates decay but only in photodegraded litter and implications that sunlight promotes leaching loss. *Biogeochemistry, 158*(1), 113-129, https://doi.org/10.1007/s10533-022-00888-x.

390. Logan, J. R., Barnes, P., & Evans, S. E. (2022). Photodegradation of plant litter cuticles enhances microbial decomposition by increasing uptake of non-rainfall moisture. *Functional Ecology, 36*, 1727-1738, https://doi.org/10.1111/1365-2435.14053.

391. Barnes, P. W., Throop, H. L., Archer, S. R., Breshears, D. D., McCulley, R. L., & Tobler, M. A. (2015). Sunlight and soil-litter mixing: drivers of litter decomposition in drylands. *Progress in Botany, 76*, 273-302, https://doi.org/10.1007/978-3-319-08807-5_11.

392. Austin, A. T., Méndez, M. S., & Ballaré, C. L. (2016). Photodegradation alleviates the lignin bottleneck for carbon turnover in terrestrial ecosystems. *Proceedings of the National Academy of Sciences USA, 113*(16), 4392-4397, https://doi.org/10.1073/pnas.1516157113.

393. Pieristè, M., Forey, E., Lounès-Hadj Sahraoui, A., Meglouli, H., Laruelle, F., Delporte, P., Robson, T. M., & Chauvat, M. (2020). Spectral composition of sunlight affects the microbial functional structure of Beech leaf litter during the initial phase of decomposition. *Plant and Soil*, https://doi.org/10.1007/s11104-020-04557-6.

394. Cuadra, P., Guajardo, J., Carrasco-Orellana, C., Stappung, Y., Fajardo, V., & Herrera, R. (2020). Differential expression after UV-B radiation and characterization of chalcone synthase from the Patagonian hairgrass *Deschampsia antarctica*. *Phytochemistry, 169*, 112179, https://doi.org/10.1016/j.phytochem.2019.112179.

395. Ruhland, C. T., & Niere, J. A. (2019). The effects of surface albedo and initial lignin concentration on photodegradation of two varieties of *Sorghum bicolor* litter. *Scientific Reports, 9*(1), 18748, https://doi.org/10.1038/s41598-019-55272-x.

396. Wang, Q.-W., Pieristè, M., Liu, C., Kenta, T., Robson, M. T., & Kurokawa, H. (2021). The contribution of photodegradation to litter decomposition in a temperate forest gap and understorey. *New Phytologist, 229*(5), 2625-2636, https://doi.org/10.1111/nph.17022.

397. Pieristè, M., Neimane, S., Solanki, T., Nybakken, L., Jones, A. G., Forey, E., Chauvat, M., Ņečajeva, J., & Robson, T. M. (2020). Ultraviolet radiation accelerates photodegradation under controlled conditions but slows the decomposition of senescent leaves from forest stands in southern Finland. *Plant Physiology and Biochemistry, 146*, 42-54, https://doi.org/10.1016/j.plaphy.2019.11.005.

398. Araujo, P. I., Grasso, A. A., González-Arzac, A., Méndez, M. S., & Austin, A. T. (2022). Sunlight and soil biota accelerate decomposition of crop residues in the Argentine Pampas. *Agriculture, Ecosystems & Environment, 330*, 107908, https://doi.org/10.1016/j.agee.2022.107908.

399. Liu, G. F., Wang, L., Jiang, L., Pan, X., Huang, Z. Y., Dong, M., & Cornelissen, J. H. C. (2018). Specific leaf area predicts dryland litter decomposition via two mechanisms. *Journal of Ecology, 106*(1), 218-229, https://doi.org/10.1111/1365-2745.12868.

400. Erdenebileg, E., Wang, C., Ye, X., Cui, Q., Du, J., Huang, Z., Liu, G., & Cornelissen, J. H. (2020). Multiple abiotic and biotic drivers of long-term wood decomposition within and among species in the semiarid inland dunes: A dual role for stem diameter. *Functional Ecology*, https://doi.org/10.1111/1365-2435.13559.

401. Esch, E. H., King, J. Y., & Cleland, E. E. (2019). Foliar litter chemistry mediates susceptibility to UV degradation in two dominant species from a semi-arid ecosystem. *Plant and Soil, 440*(1-2), 265-276, https://doi.org/10.1007/s11104-019-04069-y.

402. Berenstecher, P., Vivanco, L., Pérez, L. I., Ballaré, C. L., & Austin, A. (2020). Sunlight doubles aboveground carbon loss in a seasonally dry woodland in Patagonia. *Current Biology, 30*(16), P3243-3251.E3243, https://doi.org/10.1016/j.cub.2020.06.005.

403. Méndez, M. S., Martinez, M. L., Araujo, P. I., & Austin, A. T. (2019). Solar radiation exposure accelerates decomposition and biotic activity in surface litter but not soil in a semiarid woodland ecosystem in Patagonia, Argentina. *Plant and Soil*, https://doi.org/10.1007/s11104-019-04325-1.

404. Asao, S., Parton, W. J., Chen, M. S., & Gao, W. (2018). Photodegradation accelerates ecosystem N cycling in a simulated California grassland. *Ecosphere, 9*(8), e02370, https://doi.org/10.1002/ecs2.2370.

405. Day, T. A., & Bliss, M. S. (2019). A spectral weighting function for abiotic photodegradation based on photochemical emission of CO_2 from leaf litter in sunlight. *Biogeochemistry, 146*(2), 173-190, https://doi.org/10.1007/s10533-019-00616-y.

406. Logan, J. R., Jacobson, K. M., Jacobson, P. J., & Evans, S. E. (2021). Fungal communities on standing litter are structured by moisture type and constrain decomposition in a hyper-arid grassland. *Frontiers in Microbiology, 12*, 596517, https://doi.org/10.3389/fmicb.2021.596517.

407. Ball, B. A., Christman, M. P., & Hall, S. J. (2019). Nutrient dynamics during photodegradation of plant litter in the Sonoran Desert. *Journal of Arid Environments, 160*, 1-10, https://doi.org/10.1016/j.jaridenv.2018.09.004.

408. Marinho, O. A., Martinelli, L. A., Duarte-Neto, P. J., Mazzi, E. A., & King, J. Y. (2020). Photodegradation influences litter decomposition rate in a humid tropical ecosystem, Brazil. *Science of the Total Environment, 715*, 136601, https://doi.org/10.1016/j.scitotenv.2020.136601.

409. Wu, C. S., Wang, H. K., Mo, Q. F., Zhang, Z. J., Huang, G. X., Kong, F. Q., Liu, Y. Q., & Wang, G. G. (2019). Effects of elevated UV-B radiation and N deposition on the decomposition of coarse woody debris. *Science of the Total Environment, 663*, 170-176, https://doi.org/10.1016/j.scitotenv.2019.01.271.

410. Wei, B., Zhang, D., Kou, D., Yang, G., Liu, F., Peng, Y., & Yang, Y. (2022). Decreased ultraviolet radiation and decomposer biodiversity inhibit litter decomposition under continuous nitrogen inputs. *Functional Ecology, 36*, 998-1009, https://doi.org/10.1111/1365-2435.14015.

411. Shelton, S., Neale, P., Pinsonneault, A., & Tzortziou, M. (2022). Biodegradation and photodegradation of vegetation-derived dissolved organic matter in tidal marsh ecosystems. *Estuaries and Coasts, 45*, 1324-1342, https://doi.org/10.1007/s12237-021-00982-7.

412. Pieristè, M., Chauvat, M., Kotilainen, T. K., Jones, A. G., Aubert, M., Robson, M. T., & Forey, E. (2019). Solar UV-A radiation and blue light enhance tree leaf litter decomposition in a temperate forest. *Oecologia, 191*(1), 191-203, https://doi.org/10.1007/s00442-019-04478-x.

413. Austin, A. T., & Vivanco, L. (2006). Plant litter decomposition in a semi-arid ecosystem controlled by photodegradation. *Nature, 442*, 555-558, https://doi.org/10.1038/nature05038.

414. Yan, W., Shangguan, Z., & Zhong, Y. (2021). Responses of mass loss and nutrient release in litter decomposition to ultraviolet radiation. *Journal of Soils and Sediments, 21*(2), 698-704, https://doi.org/10.1007/s11368-020-02810-0.

415. Wang, Q.-W., Pieristè, M., Kotilainen, T., Forey, E., Chauvat, M., Kurokawa, H., Robson, M., & Jones, A. (2022). Meta-analysis of ecological studies attenuating solar radiation illustrates the importance of blue light over ultraviolet radiation in driving photodegradation of litter in terrestrial ecosystems. https://doi.org/10.21203/rs.3.rs-1377521/v1.

416. Wang, Q.-W., Robson, T. M., Pieristè, M., Kenta, T., Zhou, W., & Kurokawa, H. (2022). Canopy structure and phenology modulate the impacts of solar radiation on C and N dynamics during litter decomposition in a temperate forest. *Science of the Total Environment, 820*, 153185, https://doi.org/10.1016/j.scitotenv.2022.153185.

417. Landuyt, D., Ampoorter, E., Bastias, C. C., Benavides, R., & Müller, S. (2020). Importance of overstorey attributes for understorey litter production and nutrient cycling in European forests. *Forest Ecosystems, 7*, 45, https://doi.org/10.1186/s40663-020-00256-x.

418. Berenstecher, P., Araujo, P. I., & Austin, A. T. (2021). Worlds apart: Location above-or below-ground determines plant litter decomposition in a semi-arid Patagonian steppe. *Journal of Ecology, 109*(8), 2885-2896, https://doi.org/10.1111/1365-2745.13688.

419. Predick, K. I., Archer, S. R., Aguillon, S. M., Keller, D. A., Throop, H. L., & Barnes, P. W. (2018). UV-B radiation and shrub canopy effects on surface litter decomposition in a shrub-invaded dry grassland. *Journal of Arid Environments, 157*, 13-21, https://doi.org/10.1016/j.jaridenv.2018.06.007.

420. Barnes, P. W., Throop, H. L., Hewins, D. B., Abbene, M. L., & Archer, S. R. (2012). Soil coverage reduces photodegradation and promotes the development of soil-microbial films on dryland leaf litter. *Ecosystems, 15*(2), 311-321, https://doi.org/10.1007/s10021-011-9511-1.

421. Lee, H.-S., Hur, J., Lee, M.-H., Brogi, S. R., Kim, T.-W., & Shin, H.-S. (2019). Photochemical release of dissolved organic matter from particulate organic matter: Spectroscopic characteristics and disinfection by-product formation potential. *Chemosphere, 235*, 586-595, https://doi.org/10.1016/j.chemosphere.2019.06.127.

422. Saunois, M., Stavert, A. R., Poulter, B., Bousquet, P., Canadell, J. G., Jackson, R. B., Raymond, P. A., Dlugokencky, E. J., Houweling, S., Patra, P. K., Ciais, P., Arora, V. K., Bastviken, D., Bergamaschi, P., Blake, D. R., Brailsford, G., Bruhwiler, L., Carlson, K. M., Carrol, M., Castaldi, S., Chandra, N., Crevoisier, C., Crill, P. M., Covey, K., Curry, C. L., Etiope, G., Frankenberg, C., Gedney, N.,… & Zhuang, Q. (2020). The global methane budget 2000–2017. *Earth System Science Data, 12*(3), 1561-1623, https://doi.org/10.5194/essd-12-1561-2020.

423. Jackson, R. B., Saunois, M., Bousquet, P., Canadell, J. G., Poulter, B., Stavert, A. R., Bergamaschi, P., Niwa, Y., Segers, A., & Tsuruta, A. (2020). Increasing anthropogenic methane emissions arise equally from agricultural and fossil fuel sources. *Environmental Research Letters, 15*(7), https://doi.org/10.1088/1748-9326/ab9ed2.

424. Dean, J. F., Middelburg, J. J., Röckmann, T., Aerts, R., Blauw, L. G., Egger, M., Jetten, M. S. M., de Jong, A. E. E., Meisel, O. H., Rasigraf, O., Slomp, C. P., in't Zandt, M. H., & Dolman, A. J. (2018). Methane feedbacks to the global climate system in a warmer world. *Reviews of Geophysics, 56*(1), 207-250, https://doi.org/10.1002/2017RG000559.

425. Covey, K. R., & Megonigal, J. P. (2019). Methane production and emissions in trees and forests. *New Phytologist, 222*(1), 35-51, https://doi.org/10.1111/nph.15624.

426. Pitz, S. L., Megonigal, J. P., Chang, C.-H., & Szlavecz, K. (2018). Methane fluxes from tree stems and soils along a habitat gradient. *Biogeochemistry, 137*(3), 307-320, https://doi.org/10.1007/s10533-017-0400-3.

427. Fraser, W. T., Blei, E., Fry, S. C., Newman, M. F., Reay, D. S., Smith, K. A., & McLeod, A. R. (2015). Emission of methane, carbon monoxide, carbon dioxide and short-chain hydrocarbons from vegetation foliage under ultraviolet irradiation. *Plant, Cell & Environment, 38*(5), 980-989, https://doi.org/10.1111/pce.12489.

428. Barba, J., Poyatos, R., & Vargas, R. (2019). Automated measurements of greenhouse gases fluxes from tree stems and soils: magnitudes, patterns and drivers. *Scientific Reports, 9*(1), 4005, https://doi.org/10.1038/s41598-019-39663-8.

429. Tenhovirta, S. A. M., Kohl, L., Koskinen, M., Patama, M., Lintunen, A., Zanetti, A., Lilja, R., & Pihlatie, M. (2022). Solar radiation drives methane emissions from the shoots of Scots pine. *New Phytologist*, 235(1), 66-77. https://doi.org/10.1111/nph.18120.

430. McLeod, A. R., Fry, S. C., Loake, G. J., Messenger, D. J., Reay, D. S., Smith, K. A., & Yun, B.-W. (2008). Ultraviolet radiation drives methane emissions from terrestrial plant pectins. *New Phytologist, 180*(1), 124-132, https://doi.org/10.1111/j.1469-8137.2008.02571.x.

431. Yip, D. Z., Veach, A. M., Yang, Z. K., Cregger, M. A., & Schadt, C. W. (2019). Methanogenic Archaea dominate mature heartwood habitats of eastern cottonwood (*Populus deltoides*). *New Phytologist, 222*(1), 115-121, https://doi.org/10.1111/nph.15346.

432. Li, H.-L., Zhang, X.-M., Deng, F.-D., Han, X.-G., Xiao, C.-W., Han, S.-J., & Wang, Z.-P. (2019). Microbial methane production is affected by secondary metabolites in the heartwood of living trees in upland forests. *Trees, 34*(1), 243-254, https://doi.org/10.1007/s00468-019-01914-6.

433. Feng, H., Guo, J., Han, M., Wang, W., Peng, C., Jin, J., Song, X., & Yu, S. (2020). A review of the mechanisms and controlling factors of methane dynamics in forest ecosystems. *Forest Ecology and Management, 455*, https://doi.org/10.1016/j.foreco.2019.117702.

434. Abatzoglou, J. T., Williams, A. P., Boschetti, L., Zubkova, M., & Kolden, C. A. (2018). Global patterns of interannual climate–fire relationships. *Global Change Biology, 24*(11), 5164-5175, https://doi.org/10.1111/gcb.14405.

435. Andreae, M. O. (2019). Emission of trace gases and aerosols from biomass burning – an updated assessment. *Atmosphere Chemistry and Physics, 19*, 8523-8546, https://doi.org/10.5194/acp-19-8523-2019.

436. Hart, S. J., Henkelman, J., McLoughlin, P. D., Nielsen, S. E., Truchon-Savard, A., & Johnstone, J. F. (2019). Examining forest resilience to changing fire frequency in a fire-prone region of boreal forest. *Global Change Biology, 25*(3), 869-884, https://doi.org/10.1111/gcb.14550.

437. Jones, M. W., Santín, C., van der Werf, G. R., & Doerr, S. H. (2019). Global fire emissions buffered by the production of pyrogenic carbon. *Nature Geoscience, 12*(9), 742-747, https://doi.org/10.1038/s41561-019-0403-x.

438. Rumpel, C. (2019). Soils linked to climate change. *Nature, 572*(7770), 442-443, https://doi.org/10.1038/d41586-019-02450-6.

439. Walker, X. J., Baltzer, J. L., Cumming, S. G., Day, N. J., Ebert, C., Goetz, S., Johnstone, J. F., Potter, S., Rogers, B. M., & Schuur, E. A. G. (2019). Increasing wildfires threaten historic carbon sink of boreal forest soils. *Nature, 572*(7770), 520-523, https://doi.org/10.1038/s41586-019-1474-y.

440. Williams, A. P., & Abatzoglou, J. T. (2016). Recent advances and remaining uncertainties in resolving past and future climate effects on global fire activity. *Current Climate Change Reports, 2*(1), 1-14, https://doi.org/10.1007/s40641-016-0031-0.

441. Wagner, S., Jaffé, R., & Stubbins, A. (2018). Dissolved black carbon in aquatic ecosystems. *Limnology Oceanography Letters, 3*(3), 168-185, https://doi.org/10.1002/lol2.10076.

442. Bostick, K. W., Zimmerman, A. R., Wozniak, A. S., Mitra, S., & Hatcher, P. G. (2018). Production and composition of pyrogenic dissolved organic matter from a logical series of laboratory-generated chars. *Frontiers in Earth Science, 6*, Article 43, https://doi.org/10.3389/feart.2018.00043.

443. Hohner, A. K., Rhoades, C. C., Wilkerson, P., & Rosario-Ortiz, F. L. (2019). Wildfires alter forest watersheds and threaten drinking water quality. *Accounts of Chemical Research, 52*(5), 1234-1244, https://doi.org/10.1021/acs.accounts.8b00670.

444. Goranov, A. I., Wozniak, A. S., Bostick, K. W., Zimmerman, A. R., Mitra, S., & Hatcher, P. G. (2022). Microbial labilization and diversification of pyrogenic dissolved organic matter. *Biogeosciences, 19*(5), 1491-1514, https://doi.org/10.5194/bg-19-1491-2022.

445. Rust, A. J., Hogue, T. S., Saxe, S., & McCray, J. (2018). Post-fire water-quality response in the western United States. *International Journal of Wildland Fire, 27*(3), 203-216, https://doi.org/10.1071/WF17115.

446. Wagner, S., Coppola, A. I., Stubbins, A., Dittmar, T., Niggemann, J., Drake, T. W., Seidel, M., Spencer, R. G. M., & Bao, H. (2021). Questions remain about the biolability of dissolved black carbon along the combustion continuum. *Nature Communications, 12*(1), 4281, https://doi.org/10.1038/s41467-021-24477-y.

447. Bostick, K. W., Zimmerman, A. R., Goranov, A. I., Mitra, S., Hatcher, P. G., & Wozniak, A. S. (2021). Biolability of fresh and photodegraded pyrogenic dissolved organic matter from laboratory-prepared chars. *Journal of Geophysical Research: Biogeosciences, 126*(5), e2020JG005981, https://doi.org/10.1029/2020JG005981.

448. Bostick, K. W., Zimmerman, A. R., Goranov, A. I., Mitra, S., Hatcher, P. G., & Wozniak, A. S. (2020). Photolability of pyrogenic dissolved organic matter from a thermal series of laboratory-prepared chars. *Science of the Total Environment, 724*, 138198, https://doi.org/10.1016/j.scitotenv.2020.138198.

449. Tilmes, S., Kinnison, D. E., Garcia, R. R., Salawitch, R., Canty, T., Lee-Taylor, J., Madronich, S., & Chance, K. (2012). Impact of very short-lived halogens on stratospheric ozone abundance and UV radiation in a geo-engineered atmosphere. *Atmospheric Chemistry and Physics, 12*(22), 10945-10955, https://doi.org/10.5194/acp-12-10945-2012.

450. Flint, S. D., Ryel, R. J., & Caldwell, M. M. (2003). Ecosystem UV-B experiments in terrestrial communities: a review of recent findings and methodologies. *Agricultural and Forest Meteorology, 120*(1-4), 177-189, https://doi.org/10.1016/j.agrformet.2003.08.014.

451. Caldwell, M. M., & Flint, S. D. (2006). Use and evaluation of biological spectral UV weighting functions for the ozone reduction issue. In F. Ghetti, G. Checcucci, & J. F. Bornman (Eds.), *Environmental UV radiation: Impact on ecosystems and human health and predictive models* (pp. 71-84, Environmental UV Radiation: Impact on Ecosystems and Human Health and Predictive Models). Dordrecht: Springer Netherlands, https//doi.org/10.1007/1-4020-3697-3_6

452. Carvalho, L. C., & Amâncio, S. (2019). Cutting the Gordian Knot of abiotic stress in grapevine: From the test tube to climate change adaptation. *Physiologia Plantarum, 165*(2), 330-342, https://doi.org/10.1111/ppl.12857.

453. Day, T. A., Bliss, M. S., Tomes, A. R., Ruhland, C. T., & Guenon, R. (2018). Desert leaf litter decay: Coupling of microbial respiration, water-soluble fractions and photodegradation. *Global Change Biology, 24*(11), 5454-5470, https://doi.org/10.1111/gcb.14438.

454. Parton, W., Silver, W. L., Burke, I. C., Grassens, L., Harmon, M. E., Currie, W. S., King, J. Y., Adair, E. C., Brandt, L. A., Hart, S. C., & Fasth, B. (2007). Global-scale similarities in nitrogen release patterns during long-term decomposition. *Science, 315*, 361-364, https://doi.org/10.1126/science.1134853.

5

THE RESPONSE OF AQUATIC ECOSYSTEMS TO THE INTERACTIVE EFFECTS OF STRATOSPHERIC OZONE DEPLETION, UV RADIATION, AND CLIMATE CHANGE

P. J. Neale[93], C. E. Williamson[94], A. T. Banaszak[95], D.-P. Häder[96], S. Hylander[97], R. Ossola[98], K. C. Rose[99], S.-Å. Wängberg[100], and R. Zepp[101]

[93] Smithsonian Environmental Research Center, Edgewater, USA

[94] Miami University of Ohio, Oxford, USA

[95] Universidad Nacional Autónoma de México, Unidad Académica de Sistemas Arrecifales, Puerto Morelos, Mexico

[96] Friedrich-Alexander University, Möhrendorf, Germany

[97] Linnaeus University, Kalmar, Sweden

[98] Colorado State University, Fort Collins, USA

[99] Rensselaer Polytechnic Institute, Troy, USA

[100] University of Gothenburg, Gothenburg, Sweden

[101] ORD/CEMM, US Environmental Protection Agency, Athens, USA

Table of contents

Summary

Variations in stratospheric ozone and changes in the aquatic environment by climate change and human activity are modifying exposure of aquatic ecosystems to UV radiation. These shifts in exposure have consequences for distributions of species, biogeochemical cycles, and services provided by aquatic ecosystems. This Quadrennial Assessment presents the latest knowledge on the multi-faceted interactions between the effects of UV irradiation and of climate change, and of other anthropogenic activities, and how these conditions are changing aquatic ecosystems. Climate change results in variations in the depth of mixing, thickness of ice cover, the duration of ice-free conditions and inputs of dissolved organic matter, all of which can either increase or decrease exposure to UV radiation. Anthropogenic activities release oil, UV filters in suncreens, and microplastics into the aquatic environment that are then modified by UV radiation, frequently amplifying adverse effects on aquatic organisms and their environments. The impacts of these changes in combination with factors such as warming and ocean acidification are considered for aquatic micro-organisms, macroalgae, plants, and animals (floating, swimming, and attached). Minimising the disruptive consequences of these effects on critical services provided by the world's rivers, lakes and oceans (freshwater supply, recreation, transport and food security) will not only require continued adherence to the Montreal Protocol but also a wider inclusion of solar UV radiation and its effects in studies and/or models of aquatic ecosystems under conditions of the future global climate.

1 Introduction

The exposure of aquatic ecosystems to solar UV-B[102] radiation is changing due to variations in stratospheric ozone as well as shifts in many other factors affected by global climate change. Together, these shifts in exposure have consequences for distributions of species, biogeochemical cycles, and services provided by aquatic ecosystems, including human health, fisheries, and recreation. Whereas stratospheric ozone only affects radiation in the UV-B region of the solar spectrum, alterations of the aquatic environment by climate change and human activity either increase or decrease exposure over the full UV spectrum. Particularly important is the amount and timing of terrestrial runoff, which decreases the transparency of aquatic ecosystems to UV radiation mainly due to inputs of dissolved organic matter (DOM). Other alterations increase or decrease exposure, including changes in the depth of mixing, thickness of ice cover and the duration of ice-free conditions. Seasonal variations in exposure are also modulated as UV radiation itself photobleaches the DOM. This has the further consequence of generating greenhouse gases and enhancing the breakdown of DOM by micro-organisms. In turn, aquatic micro-organisms, macroalgae, plants, and animals (floating, swimming, and attached) respond to changes in UV irradiance, and their responses also depend on other effects of climate change, including warming and ocean acidification.

Substances released into the environment by humans, such as oil, UV filters in sunscreens, and microplastics are modified by UV radiation, which in turn can change their effects on aquatic organisms and their environments. We provide an assessment of the knowledge about the interactive effects of UV radiation and climate change on aquatic ecosystems, emphasising new findings since the last Quadrennial Assessment by the Environmental Effects Assessment Panel (EEAP) of the Montreal Protocol under the United Nations Environment Programme (UNEP) [1]. We start by assessing recent advances in understanding the major factors controlling underwater exposure to UV radiation, and then discuss both the beneficial and adverse effects of UV radiation on aquatic ecosystems in the context of interactions with climate and other environmental changes.

---

[102] A list of all abbreviations with their definitions follows Sect. 7

2 Changes in abiotic conditions alter exposure of aquatic ecosystems to underwater UV radiation

Exposure of aquatic ecosystems to UV radiation in marine and inland surface waters is determined by the combined effects of incident irradiance, ice and snow cover, water transparency, and the depth to which organisms passively circulate or, if motile, actively position. Depletion of stratospheric ozone specifically affects exposure by increasing incident UV-B radiation, whereas other factors influence exposure over the full spectrum (UV-B, UV-A and visible or photosynthetically active radiation [PAR]). After incident irradiance, transparency is the most important factor determining the exposure of aquatic organisms and materials to UV radiation, usually limiting penetration of UV-B radiation to just the upper zone of the surface layer, which is the warmest, most biologically active section of aquatic ecosystems. Within the surface layer, penetration of UV radiation can vary through space and time. For example, the depth at which UV-B radiation is reduced to 1% of its incident value ranges from tens of metres in the clearest ocean waters to tens of centimetres in inland waters that have high concentrations of dissolved organic matter [2, 3]. The overall exposure of organisms and materials present throughout the full depth of the surface mixed layer thus depends on how often they move (or are moved) into this upper zone of high exposure (Fig. 1). Above the water surface, ice and snow cover, when they are present, are important barriers to the penetration of UV radiation into underlying waters.
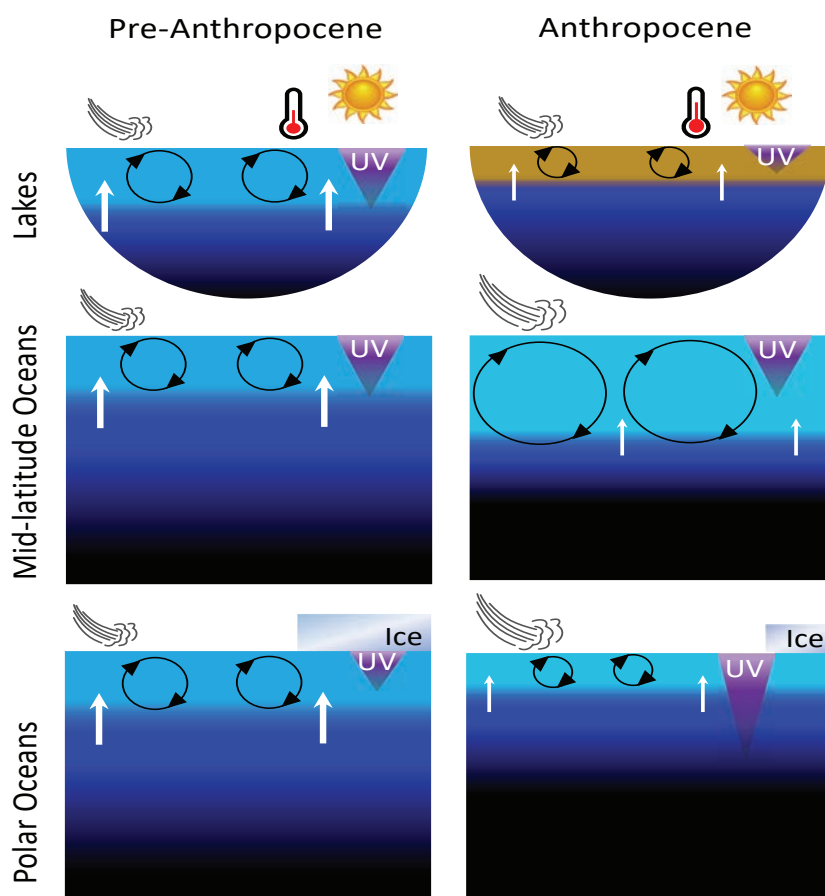
Fig. 1 Schematic depiction of processes controlling exposure to UV-B radiation in aquatic ecosystems comparing before and after the "Anthropocene", i.e. the current period of significant human impact on the Earth's ecosystems. In general, exposure to UV-B radiation is limited to the surface layer (light blue/brown), the mixing of which depends on the stratifying effect of surface warming and inputs of fresh water *vs* the stirring effects of surface winds and currents. Ice cover shields the polar ocean and wintertime lakes (not shown). In the Anthropocene ocean, there is more warming, more wind, and a greater mixed layer depth (MLD), while sharpening the density barrier (pycnocline, dark blue) to nutrient transport (arrows) from deep water (black). Ice melt reduces shielding and freshens the polar ocean reducing the MLD. Terrestrial run-off from rain events browns lake surface water, lowers UV-B transparency and warms surface waters due to enhanced absorption of solar radiation. Drought would have the opposite effect. The warming results in shallower mixed layers, as do weaker winds. Dimensions are not to scale.

While the Montreal Protocol has been successful in limiting the increase in incident UV-B radiation due to ozone depletion, other factors that change the exposure to UV-B radiation are shifting with climate change. In this section, we discuss how these factors can combine in different ways across various regions to either increase or decrease exposure to UV radiation in the aquatic environment.

2.1   Factors mediating the effect of climate change on UV radiation in the aquatic environment

2.1.1   Water transparency

Inputs of terrestrially-derived dissolved organic matter control the transparency to UV-B radiation in most inland and coastal waters because they contain a large portion of chromophoric (coloured) dissolved organic matter (CDOM), the fraction of terrestrially-derived DOM that absorbs UV and visible radiation. CDOM is the most important contributor to decreased UV transparency of all surface waters, but suspended sediments, organic particulates and algal pigments also contribute [2]. Algal-derived CDOM and pigments are the main controls of UV transparency in the open ocean [4]. Climate change and anthropogenic activities are causing long-term changes in these factors, which are increasing the transparency in some regions while decreasing it in others. In this section we assess these region-specific trends in UV transparency.

Where the inputs of CDOM have increased, transparency to both visible and UV radiation has decreased. This "browning" of surface waters has been mainly documented for boreal lakes in North America and Europe affected in the past by atmospheric deposition and surface runoff [5, 1]. More recently, reductions in exposure to UV radiation have also been reported for three lakes in eastern and southwestern China. Modelled UV-B radiation at 1 m depth (relative to the surface incidence) decreased 12-39% over the period 1961-2014 due to decreased transparency [6]. The suggested causes of decreased transparency included increases in CDOM, algal pigments and suspended sediments, the importance of each driver varying among the lakes.

There are many more long-term datasets covering broad geographical regions that focus on transparency of visible radiation, which can be an indicator of transparency to UV-B radiation. These datasets show a diversity of trends, with both increases and decreases in transparency. Only some of the decreases were due to browning. For example, browning was observed in about half of the lakes in a large database covering the Northeast and Midwest United States over the period 1980-2013. These lakes were concentrated in the Adirondack mountains, an area which is recovering from acid deposition after the installation of acidification pollution controls [7]. The consequent increases in soil pH causes greater dissolution of soil-bound organic matter [8]. Similarly, there is a wide range of water transparency trends in the period 1991 – 2012 for thousands of lakes in Wisconsin as estimated from remotely sensed reflectance data [9]. For most lakes there was no change, but in those where there was a change in transparency, more exhibited declines (– 23%) than increases in transparency (+ 6%). Most recently, remote-sensing lake data have been analysed for the whole continental United States and the results show that average lake water transparency has actually increased since 1984 [10]. Remotely-sensed lake transparency has also increased, on average, for 153 large lakes in China [11]. Importantly, these studies only deal with visible transparency, but changes could also apply to average underwater exposure to UV-B radiation. Establishing relationships between visible and UV transparency across broad lake regions is a current knowledge gap. This gap could be filled by following a modelling approach similar to that used for the previously cited study of the three Chinese lakes [6], and can involve CDOM, algal biomass and suspended sediments (which can all be remotely sensed), analogous to relationships already established for estuarine waters [12] discussed below.

Assuming that trends in visible transparency indicate a change in UV transparency in a similar direction, if not magnitude, it is relevant to consider how variations in trends relate to drivers in watersheds. Increasing precipitation mainly drives browning in clear lakes where CDOM is the primary determinant of water transparency [13, 9]. Land-use was the primary driver in the Wisconsin lakes, with a high percentage of agriculture in the watershed linked to low transparency [9]. This implied that nutrient inputs exercised control on transparency in these lakes by encouraging algal growth. However, the effect of increased runoff is different for eutrophic lakes already turbid due to algal growth. There, runoff from increased precipitation tended to dilute the concentration of algae and increase transparency [13]. In the continental scale studies, the greatest increase in visible transparency occurred for lakes in densely settled areas of the United States (1984-2018) and eastern China (2000-2017) as improvements in water quality reduced suspended sediments and nutrients [10, 11]. Remotely-sensed data also showed increased visible transparency of lakes in arid regions of the Southwest US and the Qinghai-Tibet Plateau of China [10, 11] due to reduced precipitation and associated runoff or, for China, inputs of warming-induced glacial meltwater (except when transporting fine suspended sediment from glaciers). Overall, there is an improved understanding of which land-use and climate factors tend to increase or decrease the visible transparency of lakes, and a key need for the future is extending this understanding to how these factors affect UV transparency.

In coastal waters, extreme events such as flooding are increasing with climate change and result in large pulses of terrestrially-derived DOM that affect both UV transparency and carbon cycling (e.g., [14,15]), (see also Sect. 3.4). While extreme events cause large, short-term pulses of DOM into coastal and estuarine waters, other factors are causing long-term decreases in UV radiation. For example, variations in CDOM are the main source of seasonal changes in transparency in the Rhode River sub-estuary of the Chesapeake Bay, but increased suspended particulate matter is the main cause of a long-term decline in transparency to UV-B and UV-A radiation, and to PAR [12]. Similar long-term trends of increasing inputs of sediment and terrestrially-derived DOM are causing decreased water transparency in the North Sea, a phenomenon termed "coastal darkening" [16]. In the Southern Hemisphere, climate change is also altering rainfall patterns and increasing inputs of terrestrial material into coastal environments, for example in coastal Patagonian waters [17].

CDOM is also the most important factor causing decreases in UV transparency in oligotrophic waters such as the Red Sea [3] and waters around the Great Barrier Reef [18]. CDOM is typically low in the waters of the Great Barrier Reef but average UV absorbance (at 350 nm) more than doubles during the wet season [18]. The main sources of CDOM are rivers flowing into Northeast Australian coastal waters. Spatial variation in the amount of CDOM in the Red Sea causes the penetration of UV-B radiation to 1% of surface incident to range from 35 m in the North to 13 m in the South [3]. However, in the Red Sea (surrounded by desert) CDOM is derived mainly from the breakdown of marine organisms and is photodegraded under summertime conditions. Photodegradation is also the most important process reducing CDOM content around the Great Barrier Reef during the dry season [18]. Photodegradation decreases both the amount of CDOM and changes its chemical structure such that it absorbs less UV radiation (Sect. 3.4). The breakdown can occur both via abiotic and a combination of abiotic and biotic processes, which are discussed in more detail in Sect. 3.4. Increased UV transparency in the Red Sea due to photodegradation coincides with the peak in surface water temperature, subjecting corals to a combination of high UV-B radiation and thermal stress (Sect. 5.3). Internal loading of CDOM also occurs in shallow lakes due to the breakdown of litter from aquatic plants; this CDOM is highly susceptible to photodegradation [19].

2.1.2 Mixed layer depth

Water bodies and the organisms within them are in constant motion. After water transparency, the main determinant of how much something in the water is exposed to UV radiation is how long and how often it is near the surface where UV radiation is most intense. The oceans and most lakes are stratified (at least seasonally) between surface and deep layers having different densities due to different temperatures and salinities (Fig. 1). In the ocean, the surface layer is generally 20-100 m deep but is much shallower in lakes at only a few to tens of metres. The depth to which the surface water circulates (the Mixed Layer Depth, MLD) is determined by the balance between two opposing forces: The resistance to movement created when surface waters are warmed and become less dense than deeper layers *vs* the strength of the wind in overpowering the density differences and mixing shallow and deep water together (Fig. 1). Adding to the density balance in the ocean, seawater becomes lighter with freshwater inputs (rain/ice melt) and both fresh- and seawater become heavier as they cool. These changes in circulation directly affect exposure to UV radiation: Deeper circulation means that plankton spend less time near the surface and are exposed to less UV radiation over their lifetime, while shallow circulation increases exposure to UV radiation.

Oceans - There has been a shift over time in our understanding of how climate change might affect the balance between the forces of mixing and stratification, with implications for exposure to UV radiation in the mixed layer. Early studies highlighted in past EEAP assessments (e.g. [20]) focused on how warming will lighten surface layers leading to shallower MLDs [21]. More recently, it has become clear that climate change does not have a uniform effect on MLDs [22]. In some cases, there are shallower MLDs, but in many others the resistance to mixing due to the increased density difference has been counterbalanced, or even overpowered, by stronger winds [23]. A trend of no change or deepening in MLD was first detected from long-term (1990-2015) ocean time series observations in three study areas of the Atlantic and Pacific oceans [22]. At one of the Atlantic sites and the Pacific site, both the depth of mixing and UV radiation transparency have been monitored. These combined data sets also showed either no trend or a net decrease (~5% per decade) in average exposure to UV radiation in the mixed layer at these sites [24].
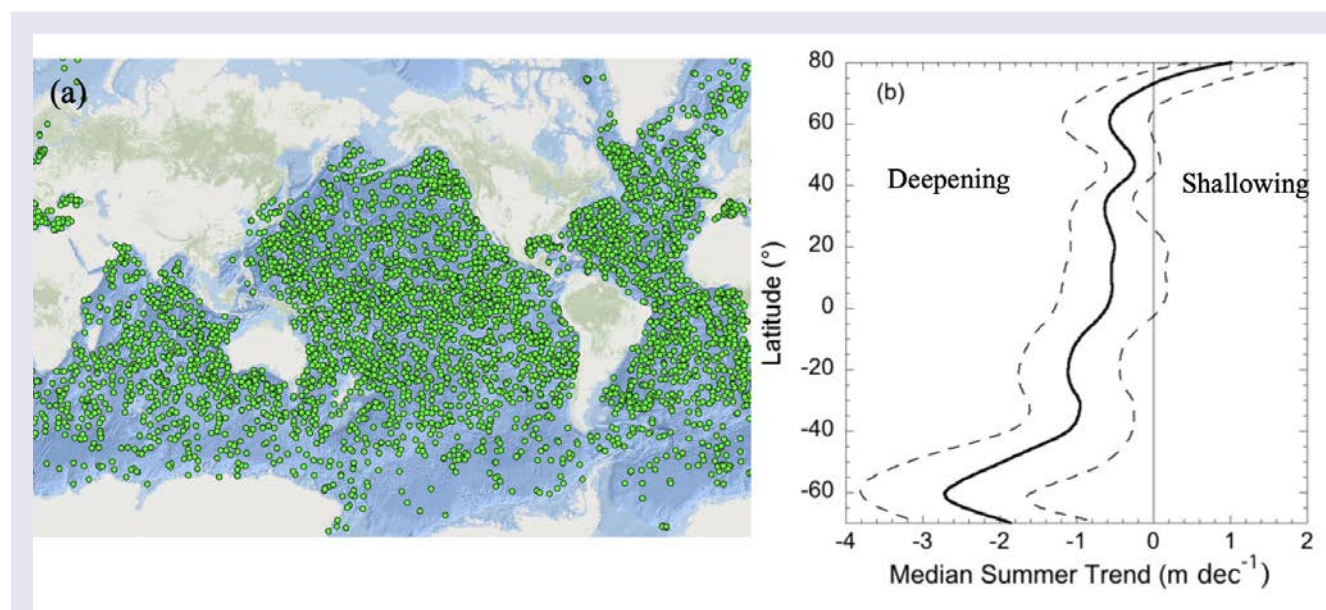

Fig. 2 (a) Illustration of the locations of profiling ARGO floats on 22 March, 2022 to show density of global coverage used to observe mixed-layer depth (source ocean-ops.org) (b) latitudinal variation in the trend (1970-2018) in summertime mixed layer depth, median (solid line) and 33rd and 66th percentiles (dashed lines), negative values indicate deepening, redrawn from [25].

Confirmation that these MLD trends apply more widely throughout the ocean has been obtained by analysing the records of an international programme of free-floating, autonomously-diving ocean sensors, known as the "Array for Real-Time Geostrophic Oceanography" (ARGO), which have now comprehensively profiled all parts of the global ocean (Fig. 2a). An analysis of almost 50 years (1970-2018) of density profiles from these floats as well as data from ships show that, on average, over the global ocean, the MLD has deepened by 2.9% per decade, adding around 5-10 m per decade to the MLD [25]. The trend varies regionally, with greater deepening in much of the Southern Ocean and less deepening in the North Atlantic, whereas shallowing is occurring for some areas near the Equator and in high Arctic latitudes (Fig. 2b). Deeper mixing in the Southern Ocean is linked to the strengthening of surface winds associated with the positive phase of the Southern Annular Mode (in turn an effect of ozone depletion [26]; see also Chapter 1, *Bernhard et al. [27]*). Shallowing in some parts of the equatorial region has been attributed to higher precipitation and freshening of the surface layer [28].

Lakes - A "mixed" picture is also emerging for changes in MLDs and exposure to UV radiation in lakes and reservoirs. Long time-series data (1970-2010) from 26 lakes around the globe show no significant trend in MLD despite surface warming trends [29]. On the other hand, the MLD declined (became shallower) for most European lakes observed over the period 1981-2019 (n=51). Nevertheless, only 14 (27%) exhibited statistically significant trends [30]. Despite the lack of clear trends in lacustrine MLDs over time, the phenomenon of atmospheric stilling, i.e. declining wind speeds, is associated with shallower MLDs in large lakes [31, 32]. In clear lakes like Crater Lake (United States), these shallower MLDs can cause substantially more exposure to UV radiation and consequent damage to organisms [31]. In general, surface wind speeds on continents were declining over the period 1979-2008, but have increased since then [33, 34]. The causes and future of atmospheric stilling are unclear, as is whether the reversal in atmospheric stilling will continue in the future [34, 35]. Hence, it is unclear if MLDs, and therefore exposure to UV radiation, will continue to exhibit long-term or widespread changes, especially in larger lakes that are more sensitive to wind.

In many lakes of the Northern Hemisphere there is an increased CDOM concentration resulting in "browning" (Sect. 2.1.1). The extra energy absorbed by CDOM has enhanced surface warming and led to shallower mixed layers (known as shoaling), especially in smaller lakes (e.g., [24, 36]). However, the decreased transparency outweighs the shoaling effect, so the average UV irradiation and PAR in the surface mixed layer have decreased [24]. Together, these results indicate decreasing exposures to UV radiation in the surface mixed layer of lakes with increased CDOM.

In addition to changes in MLD, the seasonal length of stratification has increased in many regions, which is important for cumulative exposure to UV radiation. Most temperate lakes mix at least seasonally in the spring and autumn and are stratified during the summer. In these lakes, there is a trend towards longer seasons of stratification [37] and/or less frequent episodes of full water column mixing [38]. These trends are expected to continue in the future. Under representative concentration pathways 2.6, 6.0 and 8.5 for emission of greenhouse gases (see [39]), models predict that the average duration of stratification will increase by 13, 22, and 33 days, respectively, by the end of the century [37]. Empirical evidence demonstrates that longer duration of stratification is associated with stronger summer stratification and more stable mixed layers [40]. An increase in the seasonal duration of stratification can increase the cumulative annual exposure of organisms and materials in the surface mixed layer to UV-B radiation.

2.1.3 Ice and snow cover

Ice cover shades the water column from UV-B radiation and its duration and extent have exhibited substantial declines in recent decades. Clean ice has very little absorbance in the UV range between 200 and 400 nm [41]. However, when produced under natural conditions, ice includes air bubbles and brine inclusions (for sea ice) that scatter solar radiation and reduce UV transmittance. Due to these other characteristics, ice thickness alone explains only a small amount of variation in light transmittance [42]. Additionally, the transmittance of light through ice-cover varies greatly depending on the upper surface conditions such as presence and condition of snow cover and presence of melt ponds on the ice [43].

Snow on ice scatters solar radiation, although the degree depends on grain size, for example, melted, refrozen snow has large grains and low albedo (reflection) [42]. Snow melting also produces standing water (ponds) on the ice that increases UV transmission. For example, seasonal studies in Baffin Bay in 2016 [44, 45] showed that when ponds developed, average transmittance increased about ten times for PAR and UV-A radiation (325, 340 and 379 nm) (Fig. 3). UV-B radiation (305 nm) was nearly undetectable before snow melt, but average transmittance was greater than 5% afterwards (Fig. 3). Ponding also causes spatial variability in transmittance. For example, in Baffin Bay on 2 July the transmittance of UV-B radiation through the ice was twice as high (11-14%) in areas with ponded ice compared to those without ponds [44] (Fig. 3b). For the short wavelength UV-A (325 nm), the maximum transmission was much higher, reaching 22-35% when ice was ponded. One can assume that for long UV-B wavelengths, e.g., 315 nm, transmission would be somewhere in between those values. The formation of ponds may be more important in the Arctic than on Antarctic sea ice, since sublimation (i.e. where ice converts directly to water vapour) is the main process of snow loss in the Antarctic [43].
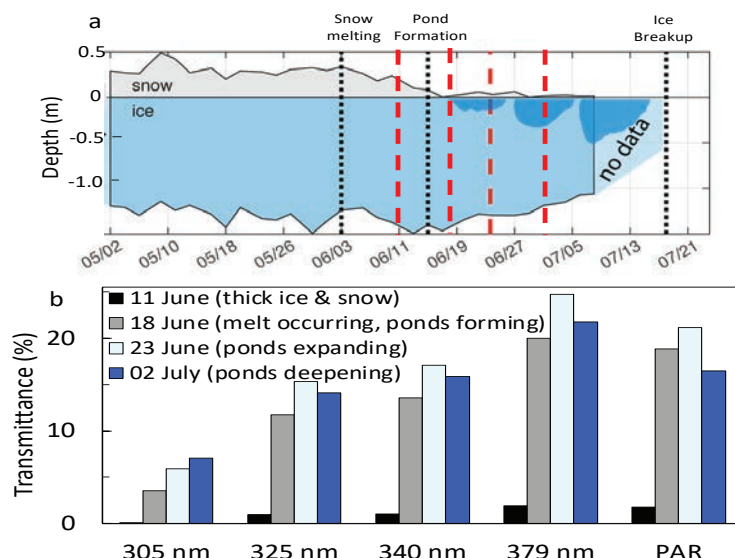
Fig. 3 Effect of Arctic ice cover on transparency of UV radiation and PAR. (a) Thickness of ice, snow and pond depth through the spring, dotted black lines mark start of snow melting, start of pond development, and ice break-up. Dark blue areas indicate pond development. Red dashed lines indicate dates when transmission was measured (b) Average (n>100) transmittance to 2 metres depth of UV-B, UV-A and PAR under combined snow and ice cover (11 June), melting snow with initiation of pond development (18 June), melting snow and shallow pond formation (23 June), and low snow and deeper pond (2 July). Adapted from [44, 45].

Polar oceans - The spatial extent and seasonal duration of ice-cover in the polar oceans has decreased substantially in recent decades [46, 47]. Sea-ice cover in the Arctic has, per decade, decreased by 2.6% in May, 7.4% in July and 13% in September between 1978 and 2017 ([46, 47], Fig. 4). Over this time span, the area of the Arctic Ocean with ice cover has reduced from over 60% to about 30% [47] (Fig. 4). While ice melt is directly attributable to warming, recent global climate modelling suggests about half of the Arctic warming responsible for ice loss over this period was caused by ozone depleting substances acting as powerful greenhouse gasses [48, 49]. Consistent with controls implemented under the Montreal Protocol and its Amendments, the global warming effects of ozone depleting substances are now decreasing. To the extent that they continue to decrease, the rate of Arctic warming, and hence ice melt and consequent increases in exposure to UV radiation, may be tempered in future decades [48].
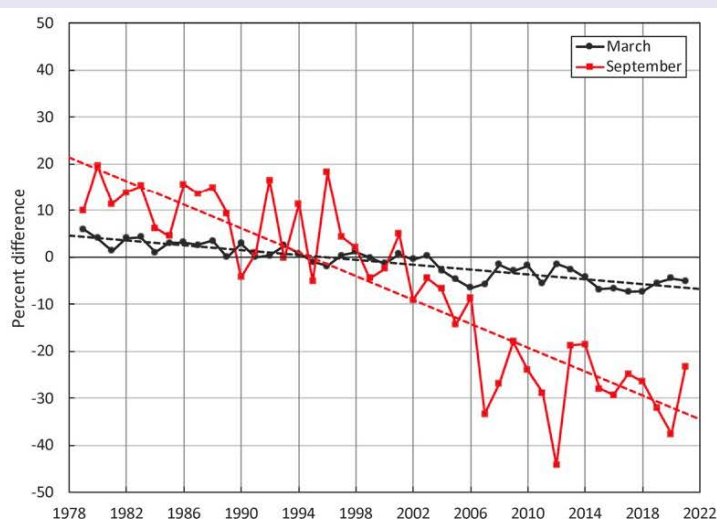
Fig. 4 Time series of change as percent difference in maximum ice cover (black, March) and minimum ice cover (red, September) and linear trend lines (dashed) for the Arctic relative to the 1981 to 2010 average for March and September (Source: [46]).

Sea ice dynamics regulate the long-term changes and seasonal variations in exposure to UV radiation and are substantially different around Antarctica when compared to the Arctic. For example, while Arctic ice cover has rapidly declined in extent in recent decades, ice extent in the Antarctic lacks strong trends ([50, 47], Fig. 5). This polar difference is due to differences in warming rates and the fact that ice cover has been increasing in the Ross Sea, while it has been decreasing in the area around the Antarctic peninsula (the Amundsen-Bellingshausen Sea) and in the Weddell Sea. Most models, however, predict that the ice cover will decrease over time even in Antarctica [51]. While ice cover loss in Antarctica has been limited, there is considerably more exposure to UV radiation on a seasonal basis associated with seasonality in ice cover. This is because only 15% of Antarctic winter sea ice remains at the summer minimum, as compared to 40% in the Arctic [46].
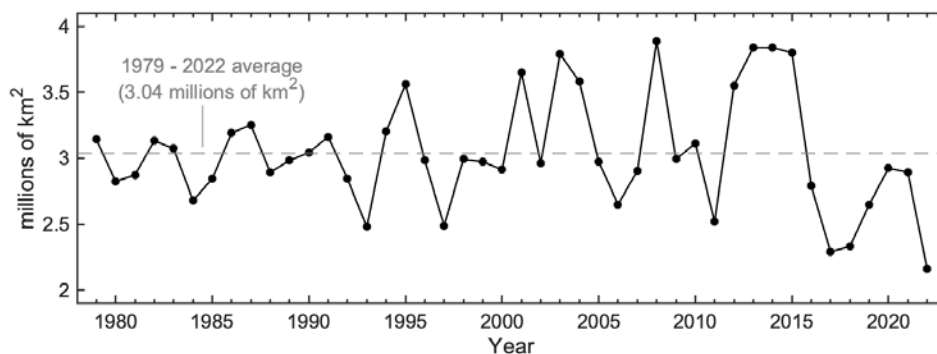
Fig. 5 Sea ice extent around Antarctica in February (summer minimum) (data from [50]).

Lakes - Like ice cover in the oceans, high latitude lakes have also exhibited rapid and substantial declines in ice cover [52]. Data from 60 lakes with records ranging from 107 to 204 years show an acceleration of loss of ice cover in recent decades. For example, trends in the later onset of seasonal ice formation and shorter seasonal duration were six times faster in the last 25-year period (1992–2016) compared with previous quarter centuries [53]. Similarly, extreme events, such as years without any ice cover on lakes that historically had ice every winter, are becoming more common [54]. Lake ice thickness has also declined, especially in subarctic lakes [30]. Overall, it has been estimated that the number of lakes in the Northern Hemisphere experiencing intermittent winter ice cover will double or increase 15-fold with 2 or 8 °C of warming, respectively [55]. For ice-covered lakes at low latitudes (i.e. mountain lakes), ice loss is likely to increase exposure to UV radiation even more since the higher position of the sun in the sky and (generally) lower attenuation by atmospheric aerosols results in higher incident UV radiation [56].

In general, reduced ice cover in lakes and seas opens up aquatic ecosystems to higher UV irradiation, as well as PAR. The shortened period with ice cover in lakes is manifested as an earlier breakup in the spring that is followed by stratification and a later ice-on in the autumn [37]. Earlier ice thaw could possibly expose more aquatic habitats to UV-B radiation during the early-spring period when ozone depletion is often most severe. For the Arctic sea, however, spring is a period of near maximum ice-coverage (March in the Arctic) and so-far the reduction in ice-cover at this time of the year has been small ([46], Fig. 4). During the spring season, surface conditions, such as increases in melt pools and snow cover losses, may be the most important drivers of increases in exposure to UV radiation in the Arctic.

3 UV radiation in combination with climate change can have adverse effects at the ecosystem level

Aquatic organisms differ in their sensitivity to solar UV radiation and their effectiveness in mitigating and repairing induced damage. When these differences in sensitivity combine with the effects of climate change, the species composition of aquatic ecosystems can shift [57]. Differential responses to changes in UV radiation and increasing temperature favour more resilient species. This is the case for the floating microalgae (phytoplankton) which are the base of the food chain in many aquatic ecosystems. For example, two microalgae in the genus *Thalassiosira* (marine diatoms, cell size and shape shown in Fig. 6a) differed in how they responded to UV-B irradiation from a solar simulator under a global warming scenario. Considering the inhibitory effect of UV-B radiation on growth at temperatures normally experienced by these species (16°C), warming to 20°C moderated the inhibition in one species but intensified it in another [58].
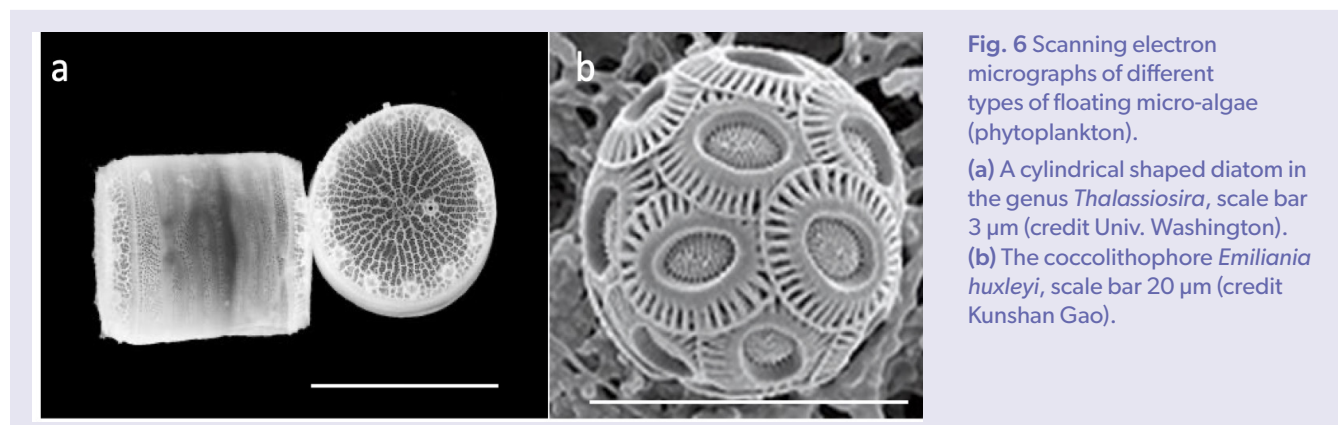
Fig. 6 Scanning electron micrographs of different types of floating micro-algae (phytoplankton).

(a) A cylindrical shaped diatom in the genus *Thalassiosira*, scale bar 3 µm (credit Univ. Washington). **(b)** The coccolithophore *Emiliania huxleyi*, scale bar 20 µm (credit Kunshan Gao).

Organisms in coastal ecosystems are usually more sensitive to solar UV radiation than open ocean species [59, 60], but are better protected due to the lower transparency of coastal waters (section 2.1). In addition, productivity in coastal ecosystems is augmented by high nutrient input from terrestrial runoff and higher temperatures [17]. Both environmental factors favour enzymatic mechanisms present in many aquatic organisms that repair UV-induced damage of DNA [1] and the recovery from UV-induced damage to the photosynthetic apparatus in many species of microalgae (e.g., [61, 58]).

Warming caused by greenhouse gases increases the temperature difference between the surface and bottom layers of lakes and the ocean [25]. For example, two large-scale analyses of hundreds of lakes showed that surface waters have been warming at median rates of 0.37–0.39 °C decade-1, while temperature has remained stable in deep waters [40, 62]. These temperature trends are sharpening the vertical temperature gradient at the boundary between surface and deep water, reinforcing it as a barrier limiting nutrient supply from deep water to phytoplankton in the surface layer (Fig. 1, [25]). Nutrient limitation not only reduces productivity but also hampers repair of cellular damage, which will generally increase the severity of UV-induced damage [63, 64].

3.1 Interactive effects of UV radiation, climate change, and other stressors on aquatic ecosystems

In addition to excessive UV radiation, aquatic organisms are exposed to a plethora of other concurrent environmental stress factors such as warming, eutrophication and acidification [65, 66]. The combined effects differ among species and physiological processes and can be antagonistic, neutral, or synergistic depending on species, strain, and experimental conditions [65, 67].

Anthropogenic emissions have resulted in increasing CO_2 concentrations in both the atmosphere and dissolved in aquatic ecosystems. In turn, increasing CO_2 in water decreases the pH and results in ocean acidification [68]. Ocean acidification reduces the calcium carbonate incorporation of calcifying algae such as *Corallina* and *Acetabularia* as well as in many zoological taxa such as worms, bivalves, and corals [69, 66]. In terms of the effects of UV radiation, inhibition of photosynthesis is more severe under elevated CO_2 for some freshwater phytoplankton populations [70] and marine diatoms [66]. In other microalgae, sensitivity to photoinhibition is only slightly enhanced or not affected at all by growth under elevated CO_2 [66, 71]. For example, in the coccolithophore *Emiliana huxleyi* (Fig. 6b), sensitivity of photosynthesis to inhibition by UV radiation, and in particular by UV-B radiation, was not affected by elevated CO_2 [71]. While the calcified scales (coccoliths) of coccolithophores (Fig. 6b) attenuate the effects of UV radiation [72], the loss of calcification in coccoliths of *E. huxleyi* grown at elevated CO_2 did not increase its sensitivity to UV radiation [71].

The causes of these variations in species-specific sensitivity remain to be determined and leave a knowledge gap in our understanding of how these primary producers will respond to UV radiation in the future (acidified) ocean.

To understand the overall effect on the aquatic ecosystem, one of the best ways to study the interactive effects of elevated CO_2 and solar UV radiation in the ocean is to use large (thousands of L) experimental enclosures called mesocosms, which are often floated in the ocean. However, to be ecologically relevant, these enclosures need to be transparent to UV radiation. Unfortunately, some common designs for mesocosms use UV-opaque materials (e.g., [73]) or covers (e.g., [74]), which leaves open the question of how representative the results of some multi-stressor experiments are with respect to natural conditions that include exposure to UV radiation – such as the finding that ocean acidification encourages the growth of toxic microalgae [75].

There are relatively few reports of the biological responses of marine ecosystems that combine solar UV radiation with other multiple stressors including warming, elevated CO_2, and nutrient limitation or eutrophication. The multiple stressor studies that have been done, including effects of UV radiation, are more frequent in freshwater systems, where smaller (tens of L) "microcosms" have been used. For example, exposure to solar UV radiation under present day conditions inhibited both phytoplankton and bacterial production in an oligotrophic (low nutrient content), high-mountain lake in southern Spain with low watershed inputs of CDOM [76]. Under a global change scenario of increased temperature and nutrient inputs from dust-storms, the inhibitory effects of solar UV radiation were reduced, but bacteria benefited more than phytoplankton. This result suggests that ambient UV radiation in combination with climate change could shift this lake, and other similar oligotrophic systems, towards higher heterotrophy (enhanced consumption of oxygen).

3.2 Photoinactivation by UV-B radiation of pathogens and parasites in the aquatic environment

Exposure to UV radiation is one of several factors leading to reduced infectivity of parasites and pathogens in aquatic systems. Photoinactivation has been studied in a number of parasites and pathogens affecting human health [77, 78]. Viruses are thought to be responsible for most gastrointestinal illnesses contracted in recreational waters contaminated by human faeces. Representative human sewage-borne viruses include enteroviruses, noroviruses, and adenoviruses. Inactivation of viruses and bacteria upon exposure to solar UV radiation can contribute to reduction of their densities in aquatic environments [78, 79]. Inactivation can occur by direct absorption of UV-B radiation by microbial nucleic acids or proteins and/or by photo-oxidative damage to the same structures sensitised by chromophores present either inside the bacterial cell or in the environment surrounding the pathogens (Fig. 7) [78]. CDOM can screen out UV-B radiation, thus reducing direct damage, but it also can sensitise photooxidative damage via indirect, exogenous processes. The net effect depends, inter alia, on depth and spectral attenuation in the water column, biological weighting functions, and mixing dynamics [78,80].

Fig. 7 Conceptual model of inactivation mechanisms by solar radiation in viruses and bacteria. The direct mechanism involves photon absorption by viral or bacterial proteins or nucleic acids (orange stars), which triggers their photodegradation. In indirect mechanisms, the photon is absorbed by a sensitiser (Sens) present either inside (endogenous) or outside (exogenous) the pathogen. This process generates photochemically produced reactive intermediates (PPRIs) that include, among others, singlet oxygen, hydroxyl radicals, and triplet excited states that further damage the pathogen's proteins and nucleic acids (orange stars). Green shapes represent proteins. Modified from [78].
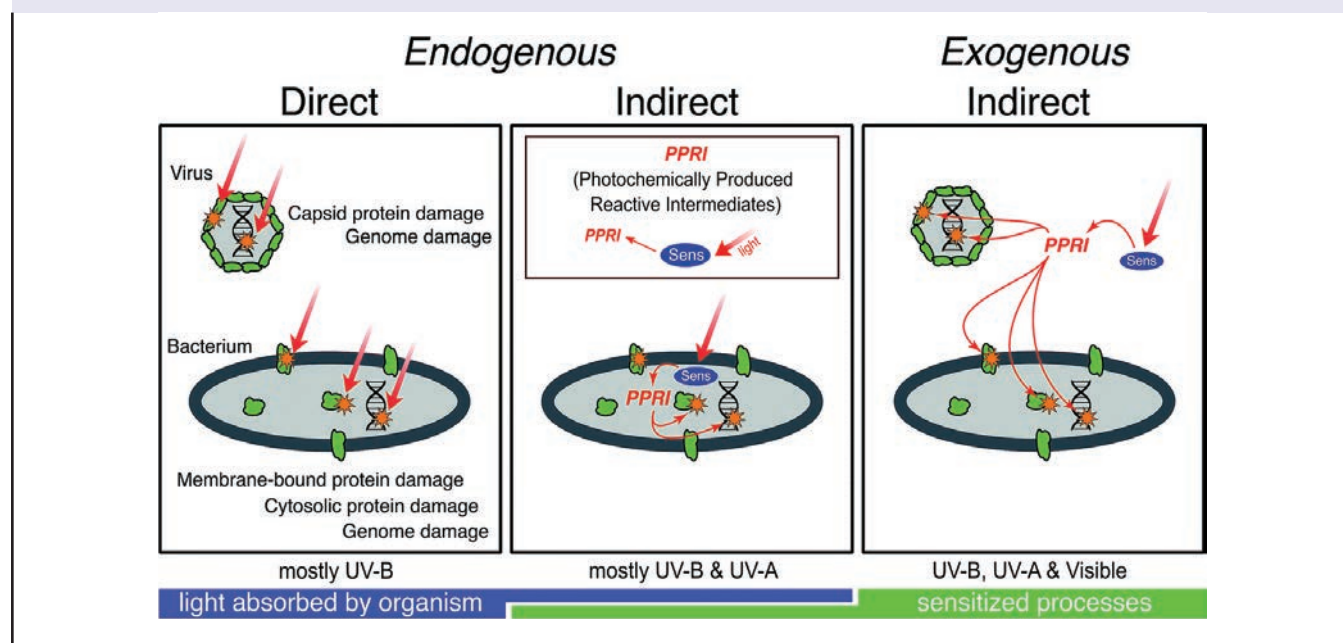
Biological weighting functions (BWFs), which are related to action spectra (Chapter 1, *Bernhard et al. [27]*), are used to quantify wavelength effects on direct photoinactivation of microorganisms and to better understand the role of microbial characteristics and environmental changes in their sensitivity to UV radiation [78, 81-83]. BWFs are used in photobiological models to evaluate effects of changes in location and time on direct photoinactivation of these microorganisms in the aquatic environment [78, 81-83]. For example, the effects of attenuation of solar radiation on photoinactivation of pathogen indicators in various swim areas of the Great Lakes (United States) were assessed using models that integrate BWFs and UV attenuation coefficients to estimate depth dependence and thus UV attenuation effects on inactivation rates [79].

Although BWFs for photoinactivation have been established for some water-borne pathogens, less is known about UV photoinactivation of the SARS-CoV-2 virus causing the COVID-19 pandemic. The SARS-CoV-2 virus has been detected in wastewater streams and rivers (e.g., [84, 85]). The virus can be photo-inactivated by UV-C radiation (e.g. [86]) but the rate of this process in water in response to solar radiation is not well-known [87]. The action spectrum of inactivation by UV radiation of SARS-CoV-2 in the air [88] is somewhat different from other viruses (either DNA or RNA based) in that it shows some sensitivity to UV-A radiation (Chapter 2, *Bernhard et al. [89]*). This suggests that inactivation of SARS-CoV-2 by solar UV radiation in water could be faster than for other viruses, but more study is needed. UV radiation in the aquatic environment also has implications for human health via effects on parasite-carrying insect vectors, e.g., by mosquitos. Mosquito larvae are sensitive to UV-B irradiation, and thus a reduced UV-transparency caused by high concentrations of dissolved organic matter (cf. Sect. 2.1) would increase their survival [90].

Not only humans, but all organisms, are affected by pathogens and parasites. Host-pathogen interactions differentially affect the growth and survival of individual species and thus the species composition of aquatic ecosystems [91]. For example, experiments suggest that the zooplankton parasite, *Pasteuria ramosa*, is more sensitive to UV radiation compared to its host [92]; however, this parasite may partially adapt to its ambient regime of UV radiation. Although experimental UV irradiation reduced the transmission potential (i.e. reduced spore production), treated parasites from high transparency lakes were more successful at infecting hosts than parasites from lakes with lower UV transparency [93]. Furthermore, zooplankton parasites have larger and longer outbreaks in less transparent systems than in systems with higher transparency [94]. Hence, factors that reduce exposure to UV radiation, such as low UV-transparency, extended ice cover, or deep MLDs etc. (Sect. 2), will also reduce the UV-disinfection rate and allow greater spread of pathogen vectors in natural waters. In all, this suggests that exposure to UV radiation (especially UV-B radiation) is an important factor affecting overall pathogen and parasite prevalence as well as infectivity such that decreased exposures have negative consequences for host-pathogen interactions and human health.

While UV irradiation may inactivate some parasites and pathogens, it also acts as a stressor to many organisms, which in turn may make them more sensitive to infections and parasites. For example, ulcerative dermal necrosis is a disease found in Atlantic salmon [95]. The disease develops from small grey to white areas of skin to deep ulcers covering much of the head, primarily affecting salmon upon return to freshwaters from the ocean. It was recently hypothesised that high UV irradiation in shallow freshwaters increased stress on salmon, making them more susceptible to secondary infections by pathogens such as *Saprolegnia parasitica* [95]. This interaction between the effect of UV radiation and disease susceptibility could have adverse effects on farmed salmon populations but the extent of these issues is not well known.

3.3   Reduced production of the marine planktonic community due to exposure to UV-B radiation

After the realisation in the 1990s that ozone depletion increased the exposure of aquatic ecosystems to UV-B radiation, many studies demonstrated that photosynthesis by aquatic primary producers, mainly phytoplankton, was inhibited by UV-B radiation (reviewed by [96]). However, left largely undetermined has been the integrated effect of UV radiation on the net metabolism of all organisms, photosynthetic and non-photosynthetic. Such a measure is the Net Community Production (NCP), the overall increase or decrease in oxygen over the course of a 24-h *in situ* incubation in a transparent enclosure. NCP reflects the balance between the productivity of microalgae (autotrophs), which generates oxygen, *vs* the breakdown and consumption of organic material by all microorganisms and higher organisms (heterotrophs), which consume oxygen. The effect of UV-B radiation on NCP at the ocean's surface was recently measured at sites near the west Australian coast. In a productive area that is typically net autotrophic, incubations in containers transmitting UV-B radiation had a 33% lower daily NCP, on average, compared to NCP incubations that excluded UV-B radiation [97]. Thus, exposure to UV-B radiation shifted the metabolic balance towards heterotrophy. In contrast, there was little or no effect of excluding UV-B radiation in low productivity waters. These results complement previous measurements in productive waters such as those near Antarctica, where exposure to UV-B radiation also shifted the community towards heterotrophy, while there was little effect on NCP in low productivity, open ocean waters [98]. The emerging picture is that shifts towards greater heterotrophy due to exposure of the planktonic community to UV-B radiation are only important in high productivity waters, e.g., coastal and polar oceans. Increased UV-B radiation could result in high productivity waters sequestering less carbon, with potential implications for the global carbon cycle. However, these results only relate to NCP right at the ocean's surface. In the ocean, oxygen production and consumption occur over the whole surface layer (see Fig. 1). The overall effect of UV-B radiation on the NCP of the entire water column remains unknown, but is expected to be much less than at the surface due to the attenuation of UV-B radiation with depth (Sect. 2.1). The effects of UV-B radiation could become more important if the surface mixed layer becomes more shallow with global climate change – however, at present, this is not the case in most marine surface layers (Sect. 2.1.2).

3.4   Aquatic cycling of carbon and other elements via photodegradation and photofacilitation

DOM is one of the main chromophores in aquatic ecosystems[103] [99]. By absorbing UV and visible radiation, chromophoric dissolved organic matter (CDOM) controls water transparency (Sect. 2.1.1). However, the process of absorption, particularly of UV radiation, also triggers the breakdown of DOM, both its chromophoric and non-chromophoric forms (referred to as DOM photodegradation). Once in an electronically excited state, CDOM can either breakdown via direct photolysis or produce reactive species (e.g., singlet oxygen, hydroxyl radicals, triplet excited states, and hydrated electrons) that further react with both chromophoric and non-chromophoric DOM.
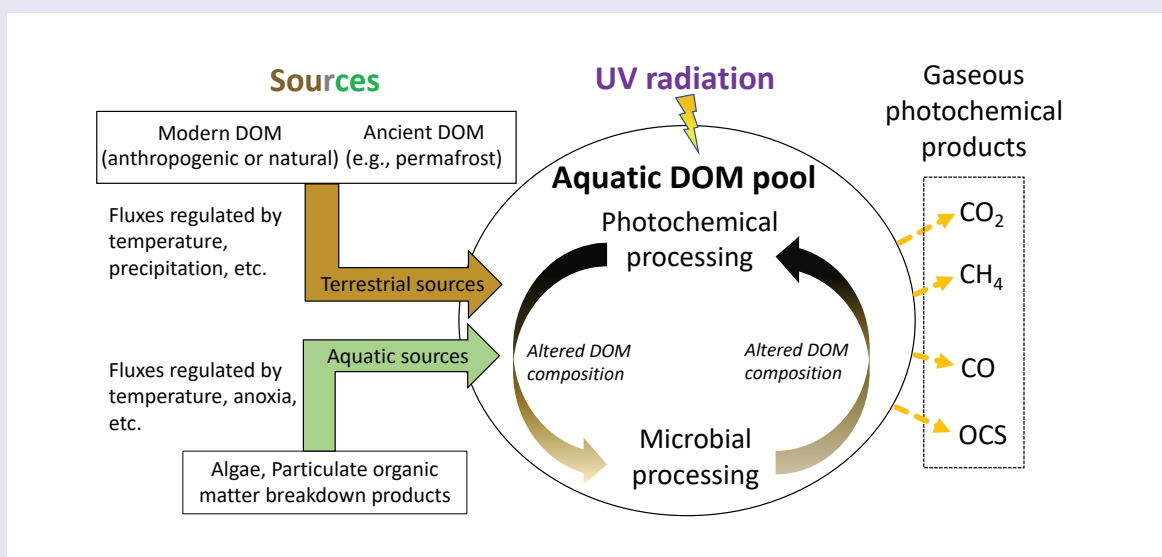
Fig. 8 Schematic of the sources and processing of dissolved organic matter (DOM) in the aquatic environment. DOM has both terrestrial and aquatic sources, whose inputs are controlled by rate of production and transport. Terrestrial sources include ancient DOM released during permafrost thaw. Once in the water, DOM undergoes photochemical and microbial processing, with the former usually enhancing the latter. These processes alter DOM composition and produce low molecular weight products, some of which are greenhouse gases. Products include carbon dioxide (CO_2), methane (CH_4), carbon monoxide (CO) and carbonyl sulphide (OCS).

Regardless of the specific mechanism, DOM photodegradation leads to loss of CDOM content (i.e., photobleaching) and formation of degradation products. DOM photoproducts include trace gases such as carbon dioxide (CO_2), carbon monoxide (CO), and methane (CH_4), among others, nutrients such as ammonia and phosphate, low-molecular-weight compounds, and partially photo-oxidised DOM [99]. For inorganic end-products (e.g., CO_2 or ammonia), the process is referred to as photomineralisation. The chemical changes induced by UV irradiation of DOM also affect its bioavailability, often leading to increased microbial utilisation or potential for mineralisation to CO_2. This combined process involving UV radiation, DOM, and microbes (photofacilitation) has been reported in both aquatic and terrestrial ecosystems (Fig. 8, and for more discussion of terrestrial ecosystems, see Chapter 4, *Barnes et al.* [100]).

Some DOM photoproducts, such as CO_2 and CH_4, are greenhouse gases and have the potential to directly exacerbate climate change, while others can have indirect impacts. For example, CO can influence atmospheric methane concentrations by competing for OH radicals (Chapter 6, *Madronich et al.* [101]). Climate change is already impacting DOM biogeochemistry by enhancing terrestrial runoff to lakes, rivers, and coastal systems (Sect. 2.1.1), which increases the amount of DOM that can be photodegraded. Another important source of DOM are the permafrost soils of the Northern Hemisphere; this reservoir of terrestrial organic carbon is estimated to be about 1300 petagrams C (PgC = 10^{15} g C), which is about twice as large as the carbon reservoir in the atmosphere [102] (also see Chapter 4, Barnes et al. [100]).

---

[103] A chromophore is a molecule that absorbs radiation, either UV or visible. Hence, CDOM is the fraction of dissolved organic matter able to absorb solar radiation. Other chromophores present in surface waters are nitrate, nitrite, particulate organic matter, and iron complexes.

As climate warms, permafrost is melting and a part of this carbon pool is especially susceptible to abrupt thaw [103]. DOM released from thawed permafrost soils impacts surface water composition and is susceptible to photodegradation by solar UV radiation ([104] also see Sect. 3.4.1). In addition, reductions in ice and snow, changes in cloud cover, and local changes in UV irradiation (Sect. 2.1) modify exposure of DOM to UV radiation, which influences the magnitude of photodegradation processes.

3.4.1 Photodegradation of dissolved organic matter by UV radiation releases greenhouse gases that may exacerbate climate change

Emissions of CO_2 resulting from photodegradation of DOM at mid-latitudes are generally negligible compared to emissions from microbial mineralisation of DOM but may play a large role at high latitudes. Outside of the Arctic, photomineralisation typically explains < 15% of total organic carbon loss from aquatic ecosystems, namely 9–12% in Scandinavian lakes [105, 106], 3–5% in rivers [107], and 0.08–0.3% in estuaries [108, 109]. Photomineralisation could be much higher in Arctic watersheds rich in yedoma (organic-rich permafrost, [110]) but the magnitude is still uncertain, with photochemical contributions ranging from negligible [111-113] to 75–90% of total CO_2 emissions [114-116]. Recent work highlighted that seasonality [114, 116] and iron levels [114] are critical controls of DOM photomineralisation in this environment and may justify the contrasting literature results. The use of different protocols for sample handling, data collection, and data analyses also contribute to this variability [117]. Understanding how DOM photoreactivity varies across seasons and with water chemistry is crucial to predicting the extent of photochemical CO_2 emissions in high latitude ecosystems and their variations induced by changes in climate and UV radiation.

Photodegradation of DOM by UV radiation also produces CO and CH_4, which are then released into the atmosphere. Although this can elevate concentrations of these gases near the ocean surface, current estimates suggest that emissions from aquatic environments are negligible at the global scale. Global CO sources are 2.6 Pg CO yr^{-1} (=2,600 Tg CO yr^{-1}) [118], while photochemical processes in the ocean produce 44 Tg CO yr^{-1} [119] [104]. Of the photochemically produced CO, a large portion is consumed in situ by microbial processes, resulting in a net release to the atmosphere of 9.3 Tg CO yr^{-1}. As a result, oceanic photoproduction is responsible for 0.36% of global CO emissions. These estimates are restricted to the open ocean, thereby excluding potential CO hotspots that may increase the relative importance of processes driven by UV radiation. Specifically, coastal and freshwaters have more terrestrial DOM than the open ocean and produce CO more rapidly than marine DOM ([120] and references therein). High latitude watersheds in spring may also represent an overlooked source of this gas, as CO is always produced alongside CO_2 during DOM photodegradation (CO_2/CO ratio ranges from 4 to 73 [121]). CO production from the photodegradation of DOM and particulate organic matter in the Arctic Ocean is also not yet included in CO estimates, and its contribution is expected to increase due to climate change [122, 123].

Global CH_4 emissions are 576 Tg CH_4 yr^{-1} [124], while photochemical production from the ocean surface is 121 Gg CH_4 yr^{-1} (Gg = 10^9 g) [125], yielding 0.02% of total methane emissions. Research on photochemical CH_4 emission is still limited but available data indicate that terrestrial DOM is up to 30 times less efficient than marine DOM in releasing CH_4 and that CH_4 is not a major DOM photodegradation product (CH_4/CO = 0.05×10^{-3} – 2.5×10^{-3}) [125]. For these reasons, incorporation of freshwater and coastal contributions is unlikely to substantially affect current estimates of global CH_4 emissions.

Carbonyl sulphide (OCS) is the only greenhouse gas for which DOM photodegradation in the ocean contributes significantly to emissions on a global scale (≥16%; [126]). To date, large uncertainties still exist regarding the importance of DOM photodegradation as a source of OCS, which ranges from 41 to 813 Gg OCS yr^{-1} [127-129, 126]. Lack of an understanding of spatial, temporal, and spectral variations in apparent OCS quantum yields and limited knowledge of additional non-photochemical sources justify this wide range [126]. Refined estimates of the oceanic source of OCS would help constrain other components of the global OCS budget related to terrestrial plant uptake and aerosol formation [126].

3.4.2 Partial photo-oxidation modifies the chemical composition of dissolved organic material and can trigger its microbial mineralisation to carbon dioxide

Partial photooxidation of DOM by UV radiation is increasingly recognised as a key trigger of cycling of elements in aquatic systems because of the direct impact that DOM chemistry has on microbial processes [108, 130, 111, 131]. Partial photooxidation is a complex process that involves, among other things, cleavage of aromatic rings, decarboxylation, degradation of chromophores, increase in the overall oxidation state, and decrease in molecular weight [132, 133]. Carboxylic-rich alicyclic molecules are among the products of partial DOM photooxidation and are predominantly formed via singlet oxygen oxidation [134, 133]. While the exact structure and reactivity of carboxylic-rich alicyclic molecules and other partial photooxidation products are unknown, they are analogous to the compounds generated during breakdown of DOM by natural microbial communities [132].

New findings have highlighted the importance of partial photooxidation in facilitating microbial mineralisation of terrestrial DOM to CO_2. Based on a new model for photodegradation of DOM, 13% of DOM present in estuarine environments undergoes partial photooxidation, while direct photomineralisation to CO_2 accounts for 0.2% of total C fluxes [135].

---

[104] Conte et al. [119] report carbon monoxide (CO) as carbon mass equivalents. In their report, the yearly fluxes of 19 Tg C yr^{-1} (photochemical CO production) and 4 Tg C yr^{-1} (net oceanic emission) were converted to mass of CO using the ratio of CO to C molecular weight (28 *vs* 12 g mol^{-1}). Tg = 10^{12} g.

Photodegradation converts 48% of biologically recalcitrant and 4% of semi-labile DOM into the labile pool, which is readily mineralised by microorganisms [135]. Microbial mineralisation elicited by partial photooxidation may also release more CO_2 than direct DOM photomineralisation in Arctic watersheds [111, 133, 131] but the magnitude of this coupled photochemical-microbial CO_2 emission, its seasonality, and its variation in response to climate change and changes in UV radiation have not yet been estimated.

3.4.3 Photodegradation of dissolved organic material in aquatic ecosystems releases nutrients

Most studies of photooxidation and photofacilitation in aquatic ecosystems focus on carbon but these processes can also affect the inorganic components of DOM. Of particular interest are processes involving nitrogen and phosphorous due to their role as nutrients, albeit recent work showed that sulphur is also efficiently photomineralised to sulphate [136], in addition to other trace gases such as OCS.

It is well acknowledged that UV irradiation of dissolved organic nitrogen (DON) releases ammonia [137, 120, 80], a process with the potential of sustaining microbial activity in nitrogen-limited ecosystems such as Arctic waterbodies [137, 138]. Photochemical production of ammonia from DON was recently determined to contribute on average up to 5% (range 1– 44%) of microbial nitrogen uptake in Arctic freshwaters, with variations depending on light intensity, water depth, and microbial activity [139]. The average value is comparable to previous estimates for boreal lakes [140]. Substrate limitations [139] and variations in DOM chemistry across seasons [141] can justify contrasting literature results in DON photomineralisation – as ammonia photoproduction has been inconsistently observed across studies (see [120] and references therein).

In addition to nitrogen species, UV-irradiation of dissolved and particulate organic matter in aquatic ecosystems releases phosphate [142, 120], which may fuel algal blooms. This process is particularly prevalent in shallow eutrophic lakes, where sediments have high phosphorous loads, are resuspended frequently, and are thus susceptible to photochemical processing [142, 143]. Specifically, the amount of phosphate released is directly proportional to sedimentary phosphorous content, and rates of release increased over a group of four increasingly eutrophic lakes in China [142]. This photochemical release of phosphate may provide a positive feedback loop for eutrophication but it is unknown whether this process has general applicability to all shallow lakes.

4 Environmental contaminants exposed to UV radiation and UV filters are toxic to aquatic organisms

4.1   Role of UV irradiation in the formation and potential toxicity of microplastics in the aquatic environment

There is increasing concern about the prevalence and risks of microplastics (defined as plastic particles and fibres < 5 mm in size) in terrestrial and aquatic ecosystems globally. UV radiation plays a key role in the formation of microplastics, as well as in their absorptive capacity and release of associated leachates and bound substances [144]. Evidence is growing that microplastics and associated chemicals can have detrimental effects on organisms and ecosystems, but the effects are highly variable across species that have been studied so far. The relationship of microplastics to UV radiation, stratospheric ozone depletion and their interactions with climate change is a cross-cutting issue that involves processes in both terrestrial and aquatic ecosystems, as well as studies in the fields of toxicology, chemistry, and materials science. For details, the reader is referred to a separate assessment that covers the role of UV radiation in the formation of microplastics and current research about how microplastics may be affecting ecosystems and human health (Chapter 8, *Jansen et al.* [145]).

4.2   Ecological impacts of the release of UV filters into the aquatic environment

While UV filters in topical sunscreens are effective at reducing UV-induced damage during recreational or occupational exposure in humans [146], some sunscreen components are considered contaminants of concern due to their potential negative impacts on aquatic life [147-150]. UV filters are categorised as either organic or inorganic and work by reflecting and/or absorbing harmful UV radiation. Two of the most common organic UV filters in sunscreens are oxybenzone and avobenzone, while inorganic UV filters often include the "white" compounds TiO_2 and ZnO, which reflect both UV and visible radiation. Nanoparticle formulations of inorganic UV filters are common, as they often have a lower reflectance in the visible light range and therefore are perceived as more aesthetically acceptable [148].

Organic and inorganic UV filters have been detected in surface waters, sediments, and in organisms [151]. Organic UV filters such as oxybenzone, octinoxate, octocrylene and benzophenones are toxic to a wide range of aquatic organisms, including corals, zooplankton, and marine bacteria [152, 153]. The toxicity of oxybenzone in corals and sea anemones can arise in part from its conversion in animal tissue to derivatives which are phototoxic upon exposure to solar UV radiation [154]. These organisms normally have symbiotic algae that can suppress the toxicity by sequestering the derivative but this protection is lost if the algae are expelled [154]. The latter phenomenon is known as "bleaching" and is discussed in Sect. 5.3.2.

The applicability of many toxicity studies has been questioned because they were conducted at concentrations that exceed ecological relevance [155]. For example, sunscreen compounds such as oxybenzone have been found in coral tissues and at concentrations of 0.1-136 ng/L in coastal waters near Oahu, Hawaii [151] and 114, 11, and 118 ng/L in Chesapeake Bay water, sediments, and oyster tissues, respectively [156]. These concentrations are substantially below the effective concentrations that would adversely affect 50% (EC50) of a population of the alga *Chlorella vulgaris* (96 h EC50 at 2.98 mg/L, 95% CI = 2.70-3.39 mg/L), the zooplankton *Daphnia magna* (48 h EC50 at 1.09 mg/L, 95% CI = 0.76-1.73 mg/L), or the fish *Brachydania rerio* (96 h EC50 at 3.98 mg/L, 95% CI = 2.86-6.53 mg/L) [157]. In a large study of benzophenones, over 90% of examined sites had concentrations below predicted no-effect concentrations (Guo et al., 2020). However, concentrations can be high in some locations at specific times. For example, the concentration of oxybenzone ranged from 30 ng/L to 27,880 ng/L in near-shore waters in Hanauma Bay, Hawai'i [158]. Considering studies conducted to date, the effects of UV sunscreen compounds on corals and coral reefs have been highly variable, and the methods used to examine potential toxicity (e.g., species, life stages, field *vs* laboratory, exposure times, nominal *vs* test concentrations) have varied [159]. Exposure methods can also influence observed responses [160]. The lack of consistent and standardised testing makes comparisons between and among studies difficult and reduces the ability to infer the most likely ecological effects of sunscreen compounds in aquatic ecosystems. Therefore, caution is warranted in extrapolating the findings of many of these studies.

Recent laboratory studies have reported that the toxicity of sunscreens can depend on the interaction between different sunscreen components. A study involving two species of corals, the bush coral, *Seriatopora caliendrum*, and the cauliflower coral, *Pocillopora damicornis*, found that other ingredients present in commercial formulations may increase the bioavailability of the active ingredients and exacerbate their toxicity to adult corals [161]. In a second study, toxicities and bioaccumulation of 4 benzophenones were tested in larvae and adults of the same two species [162]. Larvae of *S. caliendrum* suffered settlement failure, bleaching, and mortality upon exposure to benzophenones BP-1 and BP-8, whereas *P. damicornis* larvae were unaffected. Small fragments of adults of both species were more sensitive to benzophenones BP-1, BP-8, and BP-3 than the larval stages [162].

In addition to impacting corals, avobenzone can adversely affect survivourship and behaviour in other organisms, such as the zooplankton species *Daphnia magna* [67]. At the highest concentration tested (228 μg/L), oxybenzone caused erratic swimming patterns and high mortality in larvae and decreased metamorphosis of the larvae to the polyp stage in the upside down medusae *Cassiopea xamachana* and *C. frondosa* [163]. In a separate study on loggerhead turtles (*Caretta caretta*), researchers found evidence of bioaccumulation and observed that gene biomarkers for inflammation, oxidative stress, and hormonal activity increased with plasma concentrations of UV filters [164].

In general, inorganic mineral UV filters are considered less toxic and safer for aquatic organisms compared to their organic counterparts [165] and have therefore been suggested as environmentally safer alternatives [148]. Supporting this claim, researchers reported no significant harmful effects of TiO_2 on sea urchin pluteus-stage embryo growth and immune-cell viability in adults [166]. However, some studies on inorganic UV filters report environmental effects. Nanoparticle ZnO negatively impacted *Acropora* spp. corals by disrupting the symbiosis with their algal symbionts, thereby accelerating damage through coral bleaching [167]. Similarly, ZnO reduced the efficiency of photosynthesis in the Indo-Pacific smooth cauliflower coral, *Stylophora pistillata*, compared to controls [168], and exposure of California purple sea urchins (*Strongylocentrotus purpuratus*) to ZnO resulted in embryonic malformations [169]. Moreover, TiO_2 and ZnO nanoparticles released into the aquatic environment generate damaging reactive oxygen species (ROS) under UV radiation [170]. Therefore, concerns remain as to the utility of ZnO as an alternative to organic UV filters.

Climate change may amplify the toxicity of sunscreen compounds. For example, toxicity of both organic and inorganic sunscreen compounds to sea urchins, diatoms, and amphipods increases with increasing salinity [171], and salinity is increasing in regions where evaporation exceeds precipitation. Also, ocean acidification amplified the potential toxicity (as measured by biomarkers) of the benzophenone BP-3 for the yellow clam *Amarilladesma mactroides* [172]. In another study, mortality of the coral *Acropora tenuis* was higher when exposed to the sunscreen, oxybenzone, and high temperatures as compared to high temperatures alone [173]. Exposure of organisms to oxybenzone at 23°C also increased gene expression associated with detoxification, the endocrine system, and stress responses relative to the control at 18.5°C.

There continues to be a growing interest in the use of natural products as the active ingredients in sunscreens due to the toxicity of many common UV filters. Mycosporine-like amino acids (MAAs) are UV-absorbing compounds produced by marine macroalgae [174-177], fungi, phytoplankton, plants and bacteria [176, 178] and have been investigated as natural alternatives to commercial sunscreen components (see [179] for a database of these compounds). Additional information on the production and function of MAAs in organisms is provided in Sect. 5.2. Among the various compounds, there is a particular interest in mycosporine-glycine [180], palythine [181], palythene [182], shinorine [183], porphyra-334 [184] and scytonemin as UV filters for sunscreen [185], skin care [186], and cosmetic formulations [187, 188] due to their availability, stability, and antioxidant properties. Genetic engineering of bacteria to overproduce MAAs is also being considered as a cost-efficient form of production [183].

The balance between potential ecological damage *vs* concerns regarding human skin cancer risks have to be carefully considered. Health care professionals encourage alternative methods to reduce exposure to UV radiation, including the use of photoprotective clothing. However, some UV filters are now being incorporated into fabrics to increase their UV shielding capacity (Chapter 7, *Andrady et al.* [189]), and it is presently unknown how much of these UV filters could be released into the natural environment.

4.3   UV radiation degrades oil pollutants but enhances their toxicity to aquatic organisms

New lines of evidence confirmed that UV radiation is a key factor contributing to the removal of pollution from oil spills (reviewed by [190]). During the 102 days of the Deepwater Horizon spill, UV-driven production of water soluble organic carbon (also referred to as photodissolution) accounted for about 8% (estimated range: 3-17%) of overall oil removal, an amount comparable to other widely acknowledged removal processes (evaporation and coastal stranding) [191]. Both UV and visible radiation are important regulators of photo-dissolution rates, with UV radiation becoming less important as oil slick thickness increases. Even though these results are based on photodissolution of a single oil type, they motivate more research into the ecological effects of oil photooxidation products in aquatic environments [191, 192].

Several studies evaluated the effect of co-exposure of coral reef invertebrates to both UV radiation and oil pollutants (reviewed by [193]). Shallow coral reefs are routinely exposed to high levels of solar UV radiation, which can increase the toxicity of some oil components. Results from 66 studies showed that oil toxicity increased on average 7.2 times when corals, sponges, molluscs, polychaetes, and crustaceans are exposed to UV radiation in the presence of oil pollutants [193]. Co-exposure with other environmental stressors also increases oil toxicity, although not as much as co-exposure with UV irradiation. For example, co-exposure of oil-pollutants and elevated temperature (12 studies) or low pH (6 studies) increased oil toxicity by 3.0- and 1.3-fold, respectively [193]. In addition, exposure of corals in a laboratory study to a combination of UV-B and UV-A radiation exacerbated the toxicity of heavy fuel oil, decreasing the threshold concentration for 50% lethality or effect by 1.3-fold on average [194]. These tests covered 8 different development and survival endpoints in early life stages such as gametes, developing embryos, and planula larvae (the free-swimming dispersal stage) of the staghorn coral, *Acropora millepora*, (cf. life stages of related coral *A. palmata* shown in Fig. 9). In this and earlier studies, increased toxicity from co-exposure to oil and UV radiation was considered to result from oil components that sensitised organisms to UV radiation, which adds to their inherent toxicity.

UV irradiation following exposure to polycyclic aromatic hydrocarbons, which are found in oil spills, can increase mortality due to the phototoxicity of bioaccumulated polycyclic aromatic hydrocarbons. For example, exposure of fiddler crab eggs to polycyclic aromatic hydrocarbons, which can occur as they incubate in estuarine sediments, resulted in enhanced mortality when the free-swimming larvae were exposed to solar UV radiation upon hatching [195]. Overall, these findings of interactive effects of UV radiation and oil spill components indicate the need for a more routine inclusion of UV radiation treatments in oil toxicity studies so that identified hazard thresholds are environmentally relevant [195].

4.4   Improved prediction of UV-induced photoreactions of contaminants in the aquatic environment

Significant advances have been achieved in the simulation of photoreactions of contaminants in aquatic environments including those involving solar UV-B radiation [196, 197, 78]. The Water Quality Assessment Simulation Program (WASP) is a framework widely used to model contaminants in surface waters [196]. The latest version, WASP8, which has been updated to simulate light penetration and photoreactions for five wavelength bands in the ultraviolet (two of which in the UV-B waveband) and to model nanoparticle-specific processes. The updated program can now simulate the direct phototransformation of nanomaterials and other contaminants taking into account the full solar spectrum [196, 198]. Potentially, WASP8 can use projected variations in UV-B radiation to predict changes in contaminant phototransformation that can impact aquatic ecosystems and the services they provide.

5 The adverse effects of UV radiation and the defences against those effects vary among aquatic organisms

5.1 Exposure to UV radiation increases the toxicity of some harmful microalgae

A primary effect of UV-B radiation on microalgae is inhibition of photosynthesis and DNA damage, with cumulative exposure causing decreases in growth rate. However, the sensitivity of microalgae to the adverse effects of UV-B radiation varies among species. For example, the decrease in photosynthetic efficiency (the initial conversion of light into cellular energy) upon exposure to inhibiting intensities of simulated solar radiation, including UV-B radiation, often differs among groups of microalgae. A study of freshwater algae found that chlorophyte algae were the least sensitive, diatoms had intermediate sensitivity, and cyanobacteria were the most sensitive [199]. Given that there are differences in sensitivity among microalgal species, there is concern that undesirable strains might be more resistant to UV-B radiation, and be favoured by increased UV-B radiation. Particularly undesirable are toxic microalgae that accumulate in harmful algal blooms that are a hazard to public health (reviewed by [200]). Growth of the toxic marine dinoflagellate *Karenia mikimotoi* was unaffected by exposure to solar UV radiation, ocean acidification, or a combination of the two treatments [201]. Toxicity, on the other hand, was enhanced by each of these treatments, although the combined treatment (UV radiation and ocean acidification) did not increase toxin content further.

Other studies have examined the interactive effects of UV radiation and nutrient availability on toxic cyanobacteria, which cause harmful algal blooms in freshwater environments. When a toxic strain of *Microcystis aeruginosa* was grown with large amounts of phosphorus, as would occur in a nutrient rich lake, photosynthesis and growth were little affected by UV radiation compared to the moderate or severe inhibition observed under low or depleted phosphorous conditions, respectively [202]. In addition, short-term inhibition of photosynthesis occurs in the toxic strain of *M. aeruginosa* under UV irradiation but it recovers rapidly. As a result, the toxic strain has better overall performance under repeated exposures (daily for a week) when compared to a non-toxic strain [203]. Moreover, UV irradiation enhanced the accumulation of the toxin, microcystin [203]. Hence, the effects of UV radiation on microalgae are species-specific, but there are several examples suggesting that exposure to UV radiation enhances the toxicity and/or abundance of toxic strains, which would make their accumulation in harmful algal blooms more hazardous.

5.2 Aquatic organisms synthesise or accumulate photoprotective substances that ameliorate the effects of UV radiation

UV radiation is an important physical factor that controls the depth distribution of sessile species (e.g. corals and macroalgae) in aquatic environments [204]. In turn, many aquatic species produce photoprotective substances to counteract damage induced by UV radiation. These substances are pigments or compounds that intercept solar UV radiation before it can damage biologically important molecules such as DNA and structures such as the photosynthetic apparatus [205, 206].

The most common photoprotective pigments in marine organisms that specifically absorb UV radiation are mycosporine-like amino acids (MAAs), which are low molecular weight, water soluble compounds. There are more than 20 types of MAAs with absorption maxima at wavelengths ranging from 309 to 362 nm [207] and broad absorption bands of up to 50 nm at full width half maximum, which can effectively absorb UV-B and UV-A wavelengths [208]. Their high molar absorptivity, stability, and dissipation of UV radiation energy as heat means these compounds are particularly effective photoprotectants against UV-B and UV-A damage in aquatic organisms ([208] and refs. therein). These compounds are only synthesised by bacteria, cyanobacteria, fungi and algae [209]. Recent research has demonstrated that MAAs are found widely in macroalgae [210-213]. While zooplankton and higher organisms cannot synthesise these substances, they can take them up in their diet or from associated microorganisms and incorporate them into outer tissue cells where they protect the organisms from damage by UV radiation [214, 174]. Sea urchins and other marine herbivores use the same protective mechanism ([215] and Sect. 5.4). In addition to MAAs, several cyanobacteria use a different class of pigments called scytonemins to screen UV radiation. These substances are effective UV absorbers since they protect cyanobacteria on sun-exposed surfaces of rocks, trees and buildings [216].

The concentration and number of MAAs in any given organism is probably related to the potential for exposure to damaging UV radiation such that macroalgae that are adapted to surface waters synthesise higher amounts of MAAs than at depth [213]. This conclusion is driven by observations on the effects of exposure to UV radiation for macroalgae growing at different depths, for example, UV-induced inhibition in growth and photosynthesis occurred in rhodophytes when grown in surface waters but not when grown at a depth of 1.7 m [217]. The vertical distribution of macroalgae in coastal waters of Antarctica is also strongly influenced by the penetration of solar UV radiation [218]. Finally, there is a strong seasonal variability in protective MAAs with low concentrations in winter concomitant with low stress from exposure to UV radiation [219, 220].

Certain antioxidants also protect macroalgae from UV radiation [221-224]. Although most of these compounds absorb some UV radiation, they mainly provide protection by scavenging UV-induced reactive oxygen species. For example, carotenoids perform this function in brown macroalgae [223]. Among chlorophytes (green macroalgae), some species such as *Cladophora sp*. rely on screening pigments, whereas others such as Ulva intestinalis lack such pigments and instead photorepair UV-B-induced DNA damage

[225]. Hence, a wide variety of photoprotective substances are produced by bacteria, fungi as well as by micro- and macroalgae, which suggests that they provide an important and effective mechanism in aquatic organisms to ameliorate the negative effects of UV radiation.

5.3 Interactive effects of UV radiation and thermal stress on corals

Tropical coral reefs, which are based on the symbiotic association between reef-building corals and symbiotic dinoflagellates (Symbiodiniaceae), are highly diverse and economically important ecosystems. These ecosystems are naturally exposed to high levels of UV radiation because of low solar zenith angles and the natural thinness of the stratospheric ozone layer over tropical latitudes, as well as high transparency of the water column over coral reefs. Therefore, it is not surprising that coral reef dwelling organisms have evolved photoprotective mechanisms [208]. However, tropical dwelling corals often live near their upper thermal limit [226], and therefore are particularly vulnerable to thermal stress associated with increased sea surface temperatures as a result of climate change. Increased sea surface temperatures by 1°C to 2°C can cause coral bleaching [227]. Most studies on the impact of UV radiation on coral-reef dwelling organisms have used the full-spectrum of solar radiation or combinations of artificial lamps, so the relative importance of UV-B *vs* other spectral bands is uncertain at present. Assessments of recent findings on the interactive effects of UV radiation and other stressors on corals are summarised in Table 5.1 and discussed in more detail below.

5.3.1 Direct effects of UV-B radiation on symbionts versus corals

It has been suggested that exposure to UV-B radiation has a greater effect on symbionts than on the coral host. For example, in the Indo-Pacific staghorn coral (*Acropora muricata*), exposure to solar UV radiation decreased photosynthetic efficiency in the symbiont but otherwise had no effect on the holobiont (i.e., the integrated assemblage of the coral, symbiotic microalgae, and associated microbiome) [228]. Similarly, in the Indo-Pacific bush coral (*Seriatopora caliendrum*), UV-B irradiation (295-320 nm) reduced pigment concentrations of the symbiont but had no effect on coral larval survival, metamorphosis, or settlement (life stages illustrated in Fig. 9) [229]. For symbionts in another Indo-Pacific species, the cauliflower coral (*Pocillopora damicornis*), chronic exposure to solar radiation including UV-B radiation reduced photosynthetic efficiency and pigment concentrations of the symbionts [230]. Despite this evident impairment of the symbionts, which in the long term could lead to expulsion from the host, short-term (3-day) exposure to solar and UV-B radiation did not significantly increase symbiont expulsion beyond that occurring without UV-B irradiation [230].

Symbiont expulsion from the coral host can lead to bleaching. Due to climate change causing increased sea surface temperatures, reports of coral bleaching are becoming more common, therefore the negative impact of UV-B radiation on symbiont health is a concern, since it can compound the effects of thermal stress as detailed in the next section and increase coral bleaching.
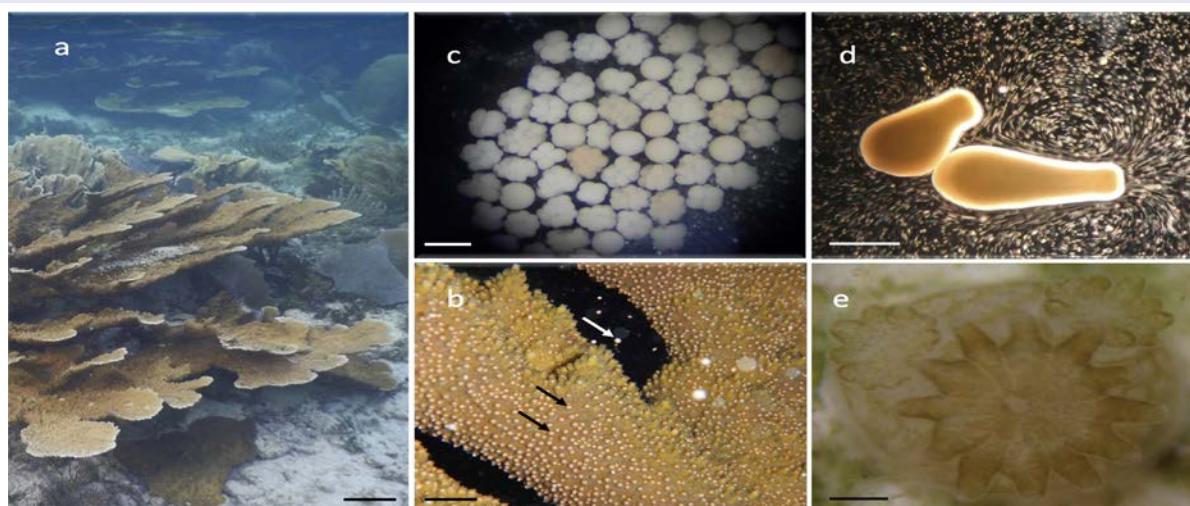
Fig. 9 Life cycle of the Caribbean coral *Acropora palmata* **(a)** showing an adult colony (scale bar = 10 cm). **(b)** During summer months in the evening colonies synchronously spawn (scale bar = 2 cm) gamete bundles (seen as many pink spheres on the coral branches, two of which are indicated by black arrows) that contain eggs and sperm. The eggs are rich in lipids such that when the bundles are released (indicated by white arrow) and rise to the surface, they break up due to wave action and fertilisation can occur between gametes of distinct colonies. (c) The embryos (scale bar = 600 μm) develop into (d) pear-shaped planula larvae (scale bar = 1 mm), both of which float at the water surface for three to five days exposed to summer-time peaks of UV radiation. Once the larvae begin to swim, they search for suitable substrate to settle, followed by metamorphosis into (e) a coral primary polyp (scale bar = 1 mm), which undergoes asexual reproduction to form the colony. Photo credits: Sandra Mendoza Quiroz.

Table 1 An assessment of the biological effects on different stages of the life cycle of corals (see Fig. 9) as a result of exposure to UV-B radiation, another stressor, or UV-B radiation and another stressor in combination.

Life cycle stage	Stressor	Biological effect	Species	Reference
Adult (sessile)	UV-B radiation	No effect in coral host, decreased photosynthetic efficiency in symbiont	*Acropora muricata*	[228]
		No effect in coral host, decreased photosynthetic efficiency in symbiont	*Pocillopora damicornis*	[230]
		No effect in coral host, reduced pigment concentration in symbiont	*Seriatopora caliendrum*	[229]
	Increased water transparency and peak temperatures coincide with high UV-B radiation	Coral bleaching	Mixed, natural assemblage, Red Sea	[3]
	Microplastic degradation	Decreased growth and food capture rates	*Lophelia pertusa, Madrepora oculata*	[231]
	Organic UV filters	Coral bleaching and death	*Pocillopora damicornis, Seriatopora caliendrum*	[161, 162]
	Increased toxicity of organic UV filters in combination with increased temperature	Coral death	*Acropora tenuis*	[173]
	Inorganic UV filters	Coral bleaching	*Acropora spp.*	[167]
		Reduced photosystem II activity	*Stylophora pistillata*	[168]
Gametes	Phototoxicity of heavy fuel oil	Reduced fertilisation success	*Acropora millepora*	[194]
Embryos (floating at water surface)	Phototoxicity of heavy fuel oil	Fragmentation of embryos resulting in smaller larvae	*Acropora millepora*	[194]
Planula larvae (free-swimming dispersal stage)	Exposure to UV-B radiation	No effect on larval survival, metamorphosis or settlement	*Seriatopora caliendrum*	[229]
	Organic UV filters	Bleaching, settlement failure, mortality	*Pocillopora damicornis, Seriatopora caliendrum*	[162]
	Phototoxicity of marine fuels	Reduced metamorphosis success	*Acropora tenuis*	[232]
	Phototoxicity of heavy fuel oil	Reduced survival, deformed larvae, reduced metamorphosis success	*Acropora millepora*	[194]

5.3.2 Response to UV radiation and thermal stress

Climate change associated thermal stress causes coral bleaching (i.e., loss of symbiotic algae) and may be lethal or, at the very least, affect metabolic processes including photosynthesis, respiration, and calcification. The effects of thermal stress are exacerbated by exposure to the naturally high UV radiation levels characteristic of many tropical coral reef environments [208]. Some coral reef dwelling

organisms, such as the Caribbean octocorals *Pseudoplexaura crucis* and *Eunicea tourneforti* [233] and the Indo-Pacific scleractinian[105] coral *Acropora muricata* [228] have proven to be resistant to the effects of UV irradiation alone or in combination with thermal stress [233]. The presence of UV absorbing compounds such as MAAs in *A. muricata* [228] may provide protection against the damaging effects of UV radiation as they do for other corals ([234], more details in Sect. 5.4). However, the induction of bleaching in the Indo-Pacific coral *P. damicornis* by thermal stress was the same whether or not it was exposed to UV radiation [235]. The main effect of UV radiation in this coral (independent of thermal stress) was to depress the nitrogen content of organic matter that it released into reef waters [235]. Since this release is a major source of organic matter to reef waters, UV radiation could cause significant changes in the nutrient biogeochemistry of tropical reef surface waters, resulting in higher C:N:P ratios. This imbalance could lead to higher levels of nitrogen fixation by the coral microbiome and other reef-dwelling organisms. On the other hand, exposure to low levels of artificial, full-spectrum UV radiation (equivalent to 15 m depth on tropical coral reefs) was shown to mitigate thermal stress and nitrate-induced inhibition of photosynthesis by promoting the synthesis of antioxidant compounds and MAAs in *P. damicornis* [236]. Thus, mild UV irradiation can protect corals against the effects of other types of stress.

The impact of combined thermal and UV radiation stress on tropical corals can be species-specific and depend on whether photoprotective MAAs are produced by the symbiotic algae and are lost during bleaching, or are produced by the host and retained even after bleaching [237]. Although exposure to UV radiation in combination with thermal stress generally has adverse effects on tropical corals, responses and resistance to long term damage appear to be species-dependent. The interactive effects of UV radiation and thermal stress add to the list of factors that are likely to negatively affect persistence of corals and impact species distribution of tropical coral reefs as climate change continues in the future.

5.4   Photoprotection in corals and invertebrates

Aquatic invertebrates use a range of photoprotective mechanisms to offset potential damage by UV irradiation including morphological changes, avoidance of exposure, synthesis of antioxidant and photoprotective compounds such as carotenoids and MAAs, and molecular defence mechanisms such as activation of DNA repair mechanisms and up-regulation of stress genes [238, 239]. Examples of the latter are expression of genes for heat shock proteins and signalling kinases [239]. Suites of MAAs have been detected in tropical reef-dwelling corals, which provide broad-band protection from damage due to UV irradiation [240]. Concentrations of MAAs tend to positively correlate with exposure to UV radiation such that there are documented decreases with depth, fluctuations with seasonal cycles and in experiments that manipulate exposures to UV radiation [208]. However, MAA content in the estuarine-dwelling anemone *Anthopleura hermaphroditica*, endemic to Chile, did not fluctuate despite large seasonal variations in UV-B radiation [241]. Instead, this anemone accumulates antioxidants and phenolic compounds to protect from UV radiation. Overall, different mechanisms or combinations of mechanisms are used by aquatic organisms to offset the deleterious effects of UV radiation.

Sea urchins, like other invertebrates, have developed a host of protective strategies. These strategies include accumulation of photoprotective compounds (such as MAAs and carotenoids), avoidance of exposure to UV radiation, and other defence mechanisms [239]. In addition to MAAs, sea urchins synthesise the "black" type spinochrome (polyhydroxy-1,4-naphthoquinone), a UV-protective compound that is the most abundant pigment in sea urchins associated with coral reef environments [242]. Sea urchin embryos, long used as model organisms to study the effects of chemical stressors on marine organisms, are potential model systems for also studying the effects of physical stressors such as UV radiation including UV-B wavebands. Sea urchins play an important ecological role as herbivores controlling the biomass of attached (benthic) algae through grazing. The most common impacts of exposure to UV radiation in developing embryos of sea urchins are deviations in skeleton formation and patterning, with damage being dependent on cumulative exposure [239].

To summarise, tropical coral reef dwelling organisms have developed a wide range of strategies for adapting to UV irradiation. However, there is still limited information about how they respond to UV-B radiation in combination with global change stressors. More information is needed to predict how these organisms will respond in the future and how that may affect the coral reef landscape.

5.5   Effects of UV radiation on zooplankton including sub-lethal, mortality and defence mechanisms

5.5.1 Exposure to UV-B radiation and fitness of zooplankton

Experimental studies using lamps that mimic the full spectrum of solar UV radiation demonstrated that lifetime reproductive success of zooplankton (a proxy for fitness) can be reduced by exposure to broad-band UV radiation [243]. However, it is crucial to also understand how effects on organismal fitness and survival vary across the UV spectrum. A type of action spectrum describing the variation in zooplankton mortality due to exposure to different wavelengths of UV radiation, the biological weighting function, has been previously defined for *Daphnia* [244]. Recent work has shown that this function is also applicable to mortality of a freshwater ciliate (*Pelagodileptus trachelioides*) due to UV irradiation [245, 246]. For both *Daphnia* and the ciliate, short-wavelength UV-B radiation is the most effective

---

[105] Octocorals and scleractinian corals resemble each other in general appearance, but octocorals do not deposit a calcium carbonate-based skeleton whereas scleratinian corals do. Also, octocorals have eight-fold symmetry whereas scleractinian corals (also known as hexacorals) have six-fold symmetry.

at causing mortality, similar to the wavelengths most effective for damaging DNA and RNA (see action spectra discussion in the COVID assessment, Chapter 2, *Bernhard et al.* [89]). Collectively, these experiments illustrate that UV-B radiation is detrimental to zooplankton and exposure leads to reduced fitness.

UV radiation can also cause sub-lethal effects, such as reduced feeding rates, reduced growth and morphological changes in many organisms [247, 248]. These effects have been previously documented in all types of major zooplankton taxa [249-251], and in recent years include reports on less studied taxa such as ciliates and crab larvae [252, 253, 245]. Other recent examples of sub-lethal effects include reduced body length, width and tail spine length in juvenile *Daphnia* [254] as well as reduced moulting and growth in *Daphnia* upon exposure to combined UV-A and UV-B radiation [248]. Furthermore, a variable exposure to UV radiation (combined UV-A and UV-B) mimicking the natural situation with cloudiness led to lower fitness in *Daphnia* compared to a constant exposure [255].

Defence mechanisms in zooplankton mitigate some of the damage from UV irradiation, for example by repair systems, photoprotection or avoiding surface waters during times of high UV irradiance [256, 214, 257-259]. However, defences may come with some costs, e.g., a reduced predator avoidance capacity [252, 253]. Recent studies illustrate that the level of expression of these defences not only depends on phenotypic plasticity but also on the evolutionary history [260]. For example, *Daphnia* isolated from a high-UV environment displayed intense UV-avoidance and induced photoprotective pigmentation compared to individuals of the same species coming from a low-UV environment [260]. Furthermore, *Daphnia* was able to diminish the negative effects of long-term, multi-generational, exposure to UV radiation by progressively altering pigmentation, life-history and probably other types of defences [261]. These transgenerational adaptations increased UV-tolerance and reversed the effect of UV radiation on offspring production within three generations. The overall outcome of exposure to UV radiation in terms of effects on population sizes is not known. Attempts have recently been made to model the outcome of exposure to UV-B radiation on reproduction in zooplankton [262]. However, parameterisation of such models using realistic biological weighting functions is still lacking.

5.5.2 Exposure to UV radiation modulates zooplankton interactions in the food web

Zooplankton respond to several challenges at the same time, including exposure to UV radiation, predation risk, and searching for food. An important way that exposure to UV-B radiation can affect zooplankton is by modifying how they respond to these other challenges. Predation risk is perceived in several ways, for example by detecting the chemical signals (kairomones) emitted by an invertebrate predator.

In the trade-off between avoiding the effects of exposure to UV radiation *vs* predation, avoidance of exposure to the radiation was recently suggested to be the most important factor, as shown for the zooplankton, *Daphnia*. Depth migration experiments show that two species (large and small) avoided exposure to levels of UV-A and UV-B radiation typical of surface waters by downward migration even when that increased their vulnerability to a macroinvertebrate predator [263]. The presence of a surface visual predator (fish) did not induce any deeper migration than that needed to avoid UV radiation. On the other hand, zooplankton reduced UV-avoidance to access food, showing that feeding opportunities are favoured in the trade-off with avoiding the damaging effects of UV radiation [264].

UV-avoidance is furthermore dependent on water transparency. Reduced penetration of UV radiation into the water column, which can be caused by factors such as extreme precipitation events and smoke haze (Sect. 2.1), reduce zooplankton migration to deeper waters [265-267]. However, a recent field study demonstrated that reduced exposure to UV radiation created by smoke haze does not always reduce zooplankton migration [268]. Despite the lower risk of damage by UV radiation, zooplankton still migrated downward during the day to avoid predation by fish, illustrating the multiple challenges to zooplankton that need to be considered in understanding food web interactions. UV avoidance has also been studied in water bodies at low latitudes where UV radiation is relatively high year round. Evidence from these environments suggests that zooplankton rely less on vertical migration and more on other defences such as accumulation of photoprotective substances to avoid damage due to exposure to UV radiation [269]. It has been demonstrated multiple times that the accumulation of photoprotective compounds in zooplankton reduces the negative effects of UV radiation but increases their vulnerability to fish predators that track their prey by visually perceiving UV-absorbing pigments [256]. Recent studies extend this knowledge, demonstrating the importance of the composition of the fish community with a negative association between photoprotective compounds and the density of visual predators such as sticklebacks [270].

At larger geographic scales, changes in UV-transparency can lead to range expansions, modulated zooplankton interactions (see above), as well as changes in community composition [256, 271, 272]. More recently, zooplankton predators such as the phantom midge larvae *Chaoborus*, and the freshwater jellyfish (*Craspedacusta sowerbii*) have been shown to be sensitive to UV radiation and mainly invade habitats with low UV transparency [273, 274]. Such invasions may increase with decreased UV transparency (Sect. 2.1.1) and are expected to result in selective predation on certain species and changes in the composition of the zooplankton community. These changes can have cascading effects on other parts of the aquatic food web, including fish stocks. Hence, changes in UV radiation combined with the effects of climate change will lead to changes in species interactions and the resulting food web structure.

5.6   Harmful effects of UV-B radiation on fish

Exposure of fish to UV radiation, and particularly UV-B radiation, has negative effects on physiology, behaviour, morphology and in some cases leads to mortality of eggs, juveniles and adult fish [275, 276]. The latest laboratory studies illustrate this fact, showing that early developmental stages of the Senegalese sole (*Solea senegalesis*) changed pigmentation, behaviour, and reduced growth upon exposure to UV radiation (combined UV-B and UV-A) [277]. Additional sub-lethal and lethal effects have been demonstrated in response to exposure to both UV-B and UV-A radiation and in different life stages of many fish species [275, 276]. These negative effects of UV

irradiation have been mostly observed in laboratory settings using artificial radiation, while fewer examples exist in field experiments using natural solar radiation. Thus, there is a need to understand to what extent the laboratory-based results are realistic and can be extrapolated to effects on population sizes and yields in the wild and in aquaculture. Furthermore, the UV lamps used in the laboratory need to be selected with great care to exclude unrealistic shortwave UV-B radiation (below 300 nm) and weighting exposures with action spectra need to be carried out to ensure that environmentally relevant doses are applied.

Laboratory studies also do not take into account that fish have a number of mechanisms to avoid damage by UV radiation in the natural environment including behavioural avoidance, cellular repair mechanisms, accumulation of photoprotective compounds (including pigments), and physical barriers such as scales [275, 276]. One recent example of a potential additional adaptation to avoid damage is the variable buoyancy in eggs of several species that reproduce in oceanic surface waters (Fig. 10).
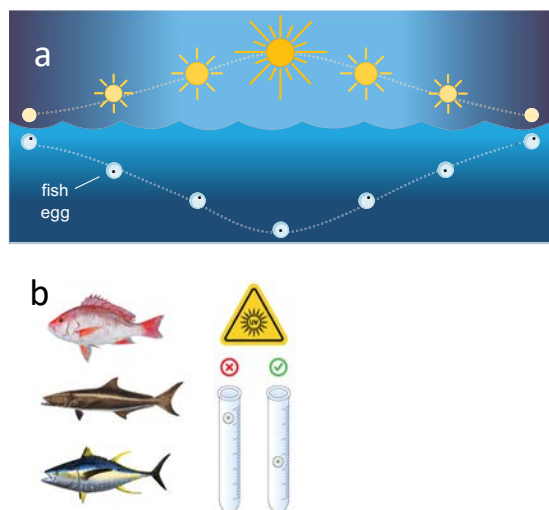

Fig. 10 Fish have several mechanisms to avoid UV-damage. Recent laboratory studies have demonstrated that fish eggs can sink in response to UV-A irradiation. **(a)** The diel expression of this in the ocean helps to avoid potential damage from concomitant solar UV-B radiation, since eggs will sink as UV-B irradiation increases.

(b) This mechanism is active in red snapper (*Lutjanus campechanus*), cobia (*Rachycentron canadum*), and yellowfin tuna (*Thunnus albacares*). On the right, a schematic of the experiment with eggs in tubes either protected (x) or exposed (√) to UV-A radiation (Figure redrawn from [278,279]).

The embryos sank down to greater depths when exposed to UV- A radiation and recovered a surface position when released from UV-stress [278, 279]. Although the response is induced by UV-A irradiation, in the ocean this mechanism would concomitantly reduce exposure to solar UV-B radiation. In all, these findings suggest that fish are negatively affected if exposed to UV radiation but have a wide range of adaptations that can help to mitigate damage due to such exposure.

6 Knowledge gaps

Based on this most recent assessment, we can identify several important knowledge gaps, new and continuing. These include:

- Models are needed that demonstrate the benefits to aquatic ecosystems derived from the implementation of the Montreal Protocol and avoidance of large increases in incident UV-B radiation. Demonstrating such benefits will help sustain commitments to the multinational treaty. A key knowledge gap for implementing these models in the aquatic environment is defining more spectral weighting functions that quantify the response of a variable (e.g., virus inactivation) to exposure to UV radiation as a function of wavelength. This gap has been noted also in previous assessments [1]. Spectral weighting functions are known for some biogeochemical processes ([120] and references therein) and organismal responses (e.g. coliphage inactivation [82], phytoplankton photosynthesis [71], *Daphnia* mortality [244], and others described in Sect. 3.2, 4.4 and 5.5.1). However, there are many processes in the aquatic environment for which information on spectral weighting functions is limited or unknown, including breakdown of oil contaminants, photoinactivation of pathogens and mortality of various taxa. While the required investment of time and cost has been a barrier in the past, a novel, light emitting diode-based, exposure system now makes it easier to estimate spectral weighting functions for aquatic samples [280]. Besides spectral weighting functions, models need to take into account various feedbacks, UV adaptations among organisms, and the interactive effects with other factors. Progress on this front is possible using whole ecosystem manipulations combined with models, such as those described in Dur et al. [262], as long as those models use realistic biological

weighting functions (see Sect. 5.5.1).

- Improved methods for estimating UV transparency from remote-sensing data will enable better estimates of exposure to UV radiation in lakes around the globe (Sect. 2.1).

- The Arctic is undergoing rapid environmental changes, the effect of which includes the release of photoreactive organic matter to surface waters as a result of permafrost thawing. Photodegradation of dissolved organic matter releases CO_2 and other greenhouse gases and impacts its bioavailability, but there is a lack of agreement on the magnitude of these processes and on their seasonal and geographical variability (Sect. 3.4.1). This information is crucial to predicting the extent of photochemical CO_2 emissions in high latitude ecosystems and their variations induced by changes in climate and UV radiation.

- UV-B radiation should be included in more studies of the effects of contaminants introduced into and/or are affecting aquatic ecosystems due to human activities. Particularly important is determining how UV radiation affects the fate of microplastics and to what extent microplastics pose a danger to aquatic ecosystems (Chapter 8, *Jansen et al*. [145]). Recent research assessed here also shows the importance of UV radiation, including UV-B wavebands, in dispersing and degrading oil pollutants, which can then be phototoxic in the marine environment. This topic has been under-appreciated in the past and is an area that needs more attention in the future.

- There is a need for more assessment of the environmental impact and toxicity of UV filters. Considering that use of these filters in topical sunscreens is important in preventing skin cancer, a recent report from the National Academies of Sciences, Engineering and Medicine of the United States [150] has highlighted the urgent need for more studies of their environmental impact. This includes whether impacts can be lessened by using inorganic or "natural" organic filters.

More studies using solar UV radiation (*vs* artificial sources of UV radiation) are needed to better assess how the responses of fish to UV-B radiation affect fisheries and aquaculture. Compared to studies on most other groups of aquatic organisms, there are very few studies of fish using ecologically relevant exposures of solar UV radiation.

7 Conclusions

Our assessment has shown that considerable knowledge continues to be acquired about how solar UV-B radiation impacts aquatic organisms and their ecosystems, whether marine, estuarine, or freshwater. As documented in this and previous assessments (e.g. [1]), exposure to solar UV-B radiation most frequently has undesirable effects, such as reduced productivity or survival, but in some cases there are desirable results (at least for humans), such as inactivation of pathogens. Given that most of the effects are negative, the large increases in incident UV-B irradiance that have been avoided by adherence to the Montreal Protocol (Chapter 1, *Bernhard et al*. [27]) can be viewed as being largely beneficial to aquatic ecosystems and the services they provide, supporting progress toward the Sustainable Development Goals, especially SDG14 (Life Below Water) [281]. While the world has avoided increased UV-B radiation due to stratospheric ozone depletion, UV-B radiation in the aquatic environment is nevertheless changing due to global climate change and other anthropogenic effects such as increased environmental pollution, both in the air and water. Our current assessment shows that climate change has variable effects on exposure to UV-B radiation, either increasing or decreasing exposure in the aquatic environment (Sect. 2). All organisms have a set of adaptations that enable them to reduce damage from UV radiation, but these may not be as effective when combined with other stressors such as increased sea-surface temperatures and ocean acidification. Moreover, other factors such as variation in temperature and pH, and presence of pollutants can increase the sensitivity of organisms to damage from UV radiation and impact biogeochemical processes (Sect. 3).

In summary, this latest assessment of the effects of UV-B radiation and stratospheric ozone depletion on aquatic ecosystems reflects a realisation of how effects increasingly depend on the multi-faceted interaction between exposure to UV radiation and changes resulting from climate change and other anthropogenic activities. Minimising the disruptive consequences of these effects on critical services provided by the world's rivers, lakes and oceans (freshwater supply, recreation, transport and food security) will not only require continued adherence to the Montreal Protocol but also a wider inclusion of solar UV radiation and its effects in studies and/or models of aquatic ecosystems under conditions of a future global climate.

List of abbreviations

ARGO   Array for Real-time Geostrophic Oceanography

BWF   Biological Weighting Function

CDOM   Chromophoric Dissolved Organic Matter

DOM   Dissolved Organic Matter

EEAP   Environmental Effects Assessment Panel

MAA   Mycosporine-like Amino Acid

MLD   Mixed Layer Depth

NCP   Net Community Production

PAR   Photosynthetically Available Radiation (same as visible radiation) (400-700 nm)

UV-A   Ultraviolet-A (315–400 nm)

UV-B   Ultraviolet-B (280–315 nm)

UV-C   Ultraviolet-C (100–280 nm)

WASP   Water Quality Assessment Simulation Program

Author contributions All authors contributed to the conception and assessment, and carried out extensive revisions of content.

Conflict of interest The authors have no conflicts of interest.

References

1. Williamson, C. E., Neale, P. J., Hylander, S., Rose, K. C., Figueroa, F. L., Robinson, S. A., Häder, D.-P., Wängberg, S.-Å., & Worrest, R. C. (2019). The interactive effects of stratospheric ozone depletion, UV radiation, and climate change on aquatic ecosystems. *Photochemical & Photobiological Sciences*, 18(3), 717-746. https://doi.org/10.1039/c8pp90062k

2. Neale, P. J., Williamson, C. E., & Morris, D. P. (2021). Optical properties of water. In K. Tockner, & T. Mehner (Eds.), *Encyclopedia of Inland Waters*, (2nd ed.), pp. 73-82. Elsevier. https://doi.org/10.1016/B978-0-12-819166-8.00020-7

3. Overmans, S., & Agustí, S. (2020). Unraveling the seasonality of UV exposure in reef waters of a rapidly warming (sub-)tropical sea. *Frontiers in Marine Science*, 7, 111. https://doi.org/10.3389/fmars.2020.00111

4. Overmans, S., Duarte, C. M., Sobrino, C., Iuculano, F., Álvarez-Salgado, X. A., & Agustí, S. (2022). Penetration of Ultraviolet-B radiation in oligotrophic regions of the oceans during the Malaspina 2010 expedition. *Journal of Geophysical Research: Oceans, 127*(5) e2021JC017654. https://doi.org/10.1029/2021jc017654

5. de Wit, H. A., Valinia, S., Weyhenmeyer, G. A., Futter, M. N., Kortelainen, P., Austnes, K., Hessen, D. O., Räike, A., Laudon, H., & Vuorenmaa, J. (2016). Current browning of surface waters will be further promoted by wetter climate. *Environmental Science & Technology Letters, 3*(12), 430-435. https://doi.org/10.1021/acs.estlett.6b00396

6. Zhang, Y., Shi, K., Zhou, Q., Zhou, Y., Zhang, Y., Qin, B., & Deng, J. (2020). Decreasing underwater ultraviolet radiation exposure strongly driven by increasing ultraviolet attenuation in lakes in eastern and southwest China. *Science of the Total Environment, 720*, 137694. https://doi.org/10.1016/j.scitotenv.2020.137694

7. Lapierre, J.-F., Collins, S. M., Oliver, S. K., Stanley, E. H., & Wagner, T. (2021). Inconsistent browning of northeastern U.S. lakes despite increased precipitation and recovery from acidification. *Ecosphere, 12*(3), e03415. https://doi.org/10.1002/ecs2.3415

8. Monteith, D. T., Stoddard, J. L., Evans, C. D., de Wit, H. A., Forsius, M., Høgåsen, T., Wilander, A., Skjelkvåle, B. L., Jeffries, D. S., Vuorenmaa, J., Keller, B., Kopácek, J., & Vesely, J. (2007). Dissolved organic carbon trends resulting from changes in atmospheric deposition chemistry. *Nature, 450*, 537. https://doi.org/10.1038/nature06316

9. Rose, K. C., Greb, S. R., Diebel, M., & Turner, M. G. (2017). Annual precipitation regulates spatial and temporal drivers of lake water clarity. *Ecological Applications, 27*(2), 632-643. https://doi.org/10.1002/eap.1471

10. Topp, S. N., Pavelsky, T. M., Stanley, E. H., Yang, X., Griffin, C. G., & Ross, M. R. V. (2021). Multi-decadal improvement in US lake water clarity. *Environmental Research Letters, 16*(5), 055025. https://doi.org/10.1088/1748-9326/abf002

11. Wang, S., Li, J., Zhang, B., Lee, Z., Spyrakos, E., Feng, L., Liu, C., Zhao, H., Wu, Y., Zhu, L., Jia, L., Wan, W., Zhang, F., Shen, Q., Tyler, A. N., & Zhang, X. (2020). Changes of water clarity in large lakes and reservoirs across China observed from long-term MODIS. *Remote Sensing of Environment, 247*, 111949. https://doi.org/10.1016/j.rse.2020.111949

12. Rose, K. C., Neale, P. J., Tzortziou, M., Gallegos, C. L., & Jordan, T. E. (2019). Patterns of spectral, spatial, and long-term variability in light attenuation in an optically complex sub-estuary. *Limnology and Oceanography, 64*(S1), S257-S272. https://doi.org/10.1002/lno.11005

13. Lisi, P. J., & Hein, C. L. (2019). Eutrophication drives divergent water clarity responses to decadal variation in lake level. *Limnology and Oceanography, 64*(S1), S49-S59. https://doi.org/10.1002/lno.11095

14. Osburn, C. L., Atar, J. N., Boyd, T. J., & Montgomery, M. T. (2019). Antecedent precipitation influences the bacterial processing of terrestrial dissolved organic matter in a North Carolina estuary. *Estuarine, Coastal and Shelf Science, 221*, 119-131. https://doi.org/10.1016/j.ecss.2019.03.016

15. Qu, L., Wu, Y., Li, Y., Stubbins, A., Dahlgren, R. A., Chen, N., & Guo, W. (2020). El Niño-driven dry season flushing enhances dissolved organic matter export From a subtropical watershed. *Geophysical Research Letters, 47*(19), e2020GL089877. https://doi.org/10.1029/2020GL089877

16. Opdal, A. F., Lindemann, C., & Aksnes, D. L. (2019). Centennial decline in North Sea water clarity causes strong delay in phytoplankton bloom timing. *Global Change Biology, 25*(11), 3946-3953. https://doi.org/10.1111/gcb.14810

17. Vizzo, J. I., Cabrerizo, M. J., Villafañe, V. E., & Helbling, E. W. (2021). Input of terrestrial material into coastal Patagonian waters and its effects on phytoplankton communities from the Chubut River Estuary (Argentina). In *Anthropogenic Pollution of Aquatic Ecosystems*, (pp. 131-155). Springer. https://doi.org/10.1007/978-3-030-75602-4_7

18. Lønborg, C., McKinna, L. I. W., Slivkoff, M. M., & Carreira, C. (2021). Coloured dissolved organic matter dynamics in the Great Barrier Reef. *Continental Shelf Research, 219*, 104395. https://doi.org/10.1016/j.csr.2021.104395

19. Song, N., & Jiang, H. L. (2020). Coordinated photodegradation and biodegradation of organic matter from macrophyte litter in shallow lake water: Dual role of solar irradiation. *Water Research, 172*, 115516. https://doi.org/10.1016/j.watres.2020.115516

20. Häder, D.-P., Williamson, C. E., Wangberg, S.-A., Rautio, M., Rose, K. C., Gao, K., Helbling, E. W., Sinha, R. P., & Worrest, R. (2015). Effects of UV radiation on aquatic ecosystems and interactions with other environmental factors. *Photochemical & Photobiological Sciences, 14*(1), 108-126. https://doi.org/10.1039/C4PP90035A

21. Sarmiento, J. L., Slater, R., Barber, R., Bopp, L., Doney, S. C., Hirst, A. C., Kleypas, J., Matear, R., Mikolajewicz, U., Monfray, P., Soldatov, V., Spall, S. A., & Stouffer, R. (2004). Response of ocean ecosystems to climate warming. *Global Biogeochemical Cycles, 18*(3), GB3003. https://doi.org/10.1029/2003GB002134

22. Somavilla, R., González-Pola, C., & Fernández-Diaz, J. (2017). The warmer the ocean surface, the shallower the mixed layer. How much of this is true? *Journal of Geophysical Research: Oceans, 122*(9), 7698-7716. https://doi.org/10.1002/2017JC013125

23. Young, I. R., & Ribal, A. (2019). Multiplatform evaluation of global trends in wind speed and wave height. *Science, 364*(6440), 548-552. https://doi.org/10.1126/science.aav9527

24. Neale, P. J., & Smyth, R. L. (2018). Are warmer waters, brighter waters? An examination of the irradiance environment of lakes and oceans in a changing climate. In D. P. Hader, & K. Gao (Eds.), *Aquatic Ecosystems in a Changing Climate*, (pp. 89-115). CRC. https://doi.org/10.1201/9780429436130

25. Sallée, J. B., Pellichero, V., Akhoudas, C., Pauthenet, E., Vignes, L., Schmidtko, S., Garabato, A. N., Sutherland, P., & Kuusela, M. (2021). Summertime increases in upper-ocean stratification and mixed-layer depth. *Nature, 591*(7851), 592-598. https://doi.org/10.1038/s41586-021-03303-x

26. Waugh, D. W., Garfinkel, C. I., & Polvani, L. M. (2015). Drivers of the recent tropical expansion in the southern hemisphere: Changing SSTs or ozone depletion? *Journal of Climate, 28*(16), 6581-6586. https://doi.org/10.1175/jcli-d-15-0138.1

27. Bernhard, G. H., Bais, A. F., Aucamp, P. J., Klekociuk, A. R., Liley, J. B., & McKenzie, R. L. (2022). Stratospheric ozone, UV radiation, and climate interactions. *Chapter 1*

28. Li, K.-x., & Zheng, F. (2022). Effects of a freshening trend on upper-ocean stratification over the central tropical Pacific and their representation by CMIP6 models. *Deep Sea Research Part II: Topical Studies in Oceanography, 195*, 104999. https://doi.org/10.1016/j.dsr2.2021.104999

29. Kraemer, B. M., Anneville, O., Chandra, S., Dix, M., Kuusisto, E., Livingstone, D. M., Rimmer, A., Schladow, S. G., Silow, E., Sitoki, L. M., Tamatamah, R., Vadeboncoeur, Y., & McIntyre, P. B. (2015). Morphometry and average temperature affect lake stratification responses to climate change. *Geophysical Research Letters, 42*(12), 4981-4988. https://doi.org/10.1002/2015GL064097

30. Stefanidis, K., Varlas, G., Papaioannou, G., Papadopoulos, A., & Dimitriou, E. (2022). Trends of lake temperature, mixing depth and ice cover thickness of European lakes during the last four decades. *Science of the Total Environment, 830*, 154709. https://doi.org/10.1016/j.scitotenv.2022.154709

31. Stetler, J., Girdner, S., Mack, J., Winslow, L., Leach, T., & Rose, K. (2020). Atmospheric stilling and warming air temperatures drive long-term changes in lake stratification in a large oligotrophic lake. *Limnology and Oceanography, 66*(3), 954-964. https://doi.org/10.1002/lno.11654

32. Woolway, R. I., Meinson, P., Nõges, P., Jones, I. D., & Laas, A. (2017). Atmospheric stilling leads to prolonged thermal stratification in a large shallow polymictic lake. *Climatic Change, 141*(4), 759-773. https://doi.org/10.1007/s10584-017-1909-0

33. Vautard, R., Cattiaux, J., Yiou, P., Thépaut, J.-N., & Ciais, P. (2010). Northern Hemisphere atmospheric stilling partly attributed to an increase in surface roughness. *Nature Geoscience, 3*(11), 756-761. https://doi.org/10.1038/ngeo979

34. Zeng, Z., Ziegler, A. D., Searchinger, T., Yang, L., Chen, A., Ju, K., Piao, S., Li, L. Z. X., Ciais, P., Chen, D., Liu, J., Azorin-Molina, C., Chappell, A., Medvigy, D., & Wood, E. F. (2019). A reversal in global terrestrial stilling and its implications for wind energy production. *Nature Climate Change, 9*(12), 979-985. https://doi.org/10.1038/s41558-019-0622-6

35. Zhang, Z., Wang, K., Chen, D., Li, J., & Dickinson, R. (2019). Increase in surface friction dominates the observed surface wind speed decline during 1973–2014 in the northern hemisphere lands. *Journal of Climate, 32*(21), 7421-7435. https://doi.org/10.1175/jcli-d-18-0691.1

36. Pilla, R. M., Williamson, C. E., Zhang, J., Smyth, R. L., Lenters, J. D., Brentrup, J. A., Knoll, L. B., & Fisher, T. J. (2018). Browning-related decreases in water transparency lead to long-term increases in surface water temperature and thermal stratification in two small lakes. *Journal of Geophysical Research: Biogeosciences, 123*(5), 1651-1665. https://doi.org/10.1029/2017jg004321

37. Woolway, R. I., Sharma, S., Weyhenmeyer, G. A., Debolskiy, A., Golub, M., Mercado-Bettín, D., Perroud, M., Stepanenko, V., Tan, Z., Grant, L., Ladwig, R., Mesman, J., Moore, T. N., Shatwell, T., Vanderkelen, I., Austin, J. A., DeGasperi, C. L., Dokulil, M., La Fuente, S., Mackay, E. B., et al. (2021). Phenological shifts in lake stratification under climate change. *Nature Communications, 12*(1), 2318. https://doi.org/10.1038/s41467-021-22657-4

38. Woolway, R. I., & Merchant, C. J. (2019). Worldwide alteration of lake mixing regimes in response to climate change. *Nature Geoscience, 12*(4), 271-276. https://doi.org/10.1038/s41561-019-0322-x

39. van Vuuren, D. P., Edmonds, J., Kainuma, M., Riahi, K., Thomson, A., Hibbard, K., Hurtt, G. C., Kram, T., Krey, V., Lamarque, J.-F., Masui, T., Meinshausen, M., Nakicenovic, N., Smith, S. J., & Rose, S. K. (2011). The representative concentration pathways: an overview. *Climatic Change, 109*(1-2), 5-31. https://doi.org/10.1007/s10584-011-0148-z

40. Jane, S. F., Hansen, G. J. A., Kraemer, B. M., Leavitt, P. R., Mincer, J. L., North, R. L., Pilla, R. M., Stetler, J. T., Williamson, C. E., Woolway, R. I., Arvola, L., Chandra, S., DeGasperi, C. L., Diemer, L., Dunalska, J., Erina, O., Flaim, G., Grossart, H.-P., Hambright, K. D., Hein, C., et al. (2021). Widespread deoxygenation of temperate lakes. *Nature, 594*(7861), 66-70. https://doi.org/10.1038/s41586-021-03550-y

41. Warren, S. G. (2019). Optical properties of ice and snow. Philosophical Transactions of the Royal Society A: Mathematical, *Physical and Engineering Sciences, 377*(2146), 20180161. https://doi.org/10.1098/rsta.2018.0161

42. Katlein, C., Arndt, S., Belter, H. J., Castellani, G., & Nicolaus, M. (2019). Seasonal evolution of light transmission distributions through Arctic sea ice. *Journal of Geophysical Research: Oceans, 124*(8), 5418-5435. https://doi.org/10.1029/2018jc014833

43. Arndt, S., Meiners, K. M., Ricker, R., Krumpen, T., Katlein, C., & Nicolaus, M. (2017). Influence of snow depth and surface flooding on light transmission through Antarctic pack ice. *Journal of Geophysical Research: Oceans, 122*(3), 2108-2119. https://doi.org/10.1002/2016jc012325

44. Matthes, L. C., Mundy, C. J., L.-Girard, S., Babin, M., Verin, G., & Ehn, J. K. (2020). Spatial heterogeneity as a key variable influencing spring-summer progression in UVR and PAR transmission through Arctic sea ice. *Frontiers in Marine Science, 7*, 183. https://doi.org/10.3389/fmars.2020.00183

45. Oziel, L., Massicotte, P., Randelhoff, A., Ferland, J., Vladoiu, A., Lacour, L., Galindo, V., Lambert-Girard, S., Dumont, D., Cuypers, Y., Bouruet-Aubertot, P., Mundy, C. J., Ehn, J., Bécu, G., Marec, C., Forget, M. H., Garcia, N., Coupel, P., Raimbault, P., Houssais, M. N., et al. (2019). Environmental factors influencing the seasonal dynamics of spring algal blooms in and beneath sea ice in western Baffin Bay. *Elementa: Science of the Anthropocene, 7*(1), 34. https://doi.org/10.1525/elementa.372

46. Meier, W. N., Perovich, D., Farrell, S., Haas, C., Hendricks, S., Petty, A. A., Webster, M., Divine, D., Gerland, S., Kaleschke, L., Ricker, R., Steer, A., Tian-Kunze, X., Tschudi, M., & Wood, K. (2021). Sea Ice. In T. A. Moon, M. L. Druckenmiller, & R. L. Thoman (Eds.), *Arctic Report Card: Update for 2021*, (pp. NOAA Technical Report OAR ARC. https://doi.org/10.25923/y2wd-fn85

47. Serreze, M. C., & Meier, W. N. (2019). The Arctic's sea ice cover: trends, variability, predictability, and comparisons to the Antarctic. *Annals of the New York Academy of Sciences, 1436*(1), 36-53. https://doi.org/10.1111/nyas.13856

48. Goyal, R., England, M. H., Sen Gupta, A., & Jucker, M. (2019). Reduction in surface climate change achieved by the 1987 Montreal Protocol. *Environmental Research Letters, 14*(12), 124041. https://doi.org/10.1088/1748-9326/ab4874

49. Polvani, L. M., Previdi, M., England, M. R., Chiodo, G., & Smith, K. L. (2020). Substantial twentieth-century Arctic warming caused by ozone-depleting substances. *Nature Climate Change, 10*(2), 130-133. https://doi.org/10.1038/s41558-019-0677-4

50. Fetterer, F., Knowles, K., Meier, W. N., Savoie, M., & Windnagel, A. K. (2021). Sea Ice Index, Version 3. National Snow and Ice Data Center.

51. Moore, J. K., Fu, W., Primeau, F., Britten, G. L., Lindsay, K., Long, M., Doney, S. C., Mahowald, N., Hoffman, F., & Randerson, J. T. (2018). Sustained climate warming drives declining marine biological productivity. *Science, 359*(6380), 1139. https://doi.org/10.1126/science.aao6379

52. Woolway, R. I., Kraemer, B. M., Lenters, J. D., Merchant, C. J., O'Reilly, C. M., & Sharma, S. (2020). Global lake responses to climate change. *Nature Reviews Earth & Environment, 1*(8), 388-403. https://doi.org/10.1038/s43017-020-0067-5

53. Sharma, S., Richardson, D. C., Woolway, R. I., Imrit, M. A., Bouffard, D., Blagrave, K., Daly, J., Filazzola, A., Granin, N., Korhonen, J., Magnuson, J., Marszelewski, W., Matsuzaki, S. I. S., Perry, W., Robertson, D. M., Rudstam, L. G., Weyhenmeyer, G. A., & Yao, H. (2021). Loss of ice cover, shifting phenology, and more extreme events in Northern Hemisphere lakes. *Journal of Geophysical Research: Biogeosciences, 126*(10), e2021JG006348. https://doi.org/10.1029/2021jg006348

54. Filazzola, A., Blagrave, K., Imrit, M. A., & Sharma, S. (2020). Climate change drives increases in extreme events for lake ice in the Northern Hemisphere. *Geophysical Research Letters, 47*(18), e2020GL089608. https://doi.org/10.1029/2020gl089608

55. Sharma, S., Blagrave, K., Magnuson, J. J., O'Reilly, C. M., Oliver, S., Batt, R. D., Magee, M. R., Straile, D., Weyhenmeyer, G. A., Winslow, L., & Woolway, R. I. (2019). Widespread loss of lake ice around the Northern Hemisphere in a warming world. *Nature Climate Change, 9*(3), 227-231. https://doi.org/10.1038/s41558-018-0393-5

56. Häder, D. P., & Cabrol, N. A. (2020). Monitoring of solar irradiance in the high Andes. *Photochemistry and Photobiology, 96*(5), 1133-1139. https://doi.org/10.1111/php.13276

57. Häder, D.-P., & Barnes, P. W. (2019). Comparing the impacts of climate change on the responses and linkages between terrestrial and aquatic ecosystems. *Science of the Total Environment, 682*, 239-246. https://doi.org/10.1016/j.scitotenv.2019.05.024

58. Wu, Y., Zhang, M., Li, Z., Xu, J., & Beardall, J. (2020). Differential responses of growth and photochemical performance of marine diatoms to ocean warming and high light irradiance. *Photochemistry and photobiology, 96*(5), 1074-1082. https://doi.org/10.1111/php.13268

59. Li, G., Gao, K., & Gao, G. (2011). Differential impacts of solar UV radiation on photosynthetic carbon fixation from the coastal to offshore surface waters in the South China Sea. *Photochemistry and Photobiology, 87*(2), 329-334. https://doi.org/10.1111/j.1751-1097.2010.00862.x

60. Valiñas, M. S., Villafañe, V. E., & Walter Helbling, E. (2018). Effects of global change on aquatic lower trophic levels of coastal south west Atlantic Ocean environments. In D. P. Häder, & K. Gao (Eds.), *Aquatic Ecosystems in a Changing Climate*, (pp. 116-145). https://doi.org/10.1201/9780429436130-7

61. Chen, J., Wang, H., Yang, A. Q., Si, R. R., & Guan, W. C. (2018). Short-term and diurnal temperature changes alter the response of harmful algal blooms of *Pseudo-nitzschia pungens* to solar ultraviolet radiation. *New Zealand Journal of Marine and Freshwater Research, 52*(1), 69-81. https://doi.org/10.1080/00288330.2017.1331454

62. Pilla, R. M., Williamson, C. E., Adamovich, B. V., Adrian, R., Anneville, O., Chandra, S., Colom-Montero, W., Devlin, S. P., Dix, M. A., Dokulil, M. T., Gaiser, E. E., Girdner, S. F., Hambright, K. D., Hamilton, D. P., Havens, K., Hessen, D. O., Higgins, S. N., Huttula, T. H., Huuskonen, H., Isles, P. D. F., et al. (2020). Deeper waters are changing less consistently than surface waters in a global analysis of 102 lakes. *Scientific Reports, 10*(1), 20514. https://doi.org/10.1038/s41598-020-76873-x

63. Jiang, X., Zhang, Y., Hutchins, D. A., & Gao, K. (2022). Nitrogen-limitation exacerbates the impact of ultraviolet radiation on the coccolithophore *Gephyrocapsa oceanica*. *Journal of Photochemistry and Photobiology B: Biology, 226*, 112368. https://doi.org/https://doi.org/10.1016/j.jphotobiol.2021.112368

64. Zhang, Y., Li, K., Zhou, Q., Chen, L., Yang, X., & Zhang, H. (2021). Phytoplankton responses to solar UVR and its combination with nutrient enrichment in a plateau oligotrophic Lake Fuxian: a mesocosm experiment. *Environmental Science and Pollution Research, 28*(23), 29931-29944. https://doi.org/10.1007/s11356-021-12705-3

65. Birk, S., Chapman, D., Carvalho, L., Spears, B. M., Andersen, H. E., Argillier, C., Auer, S., Baattrup-Pedersen, A., Banin, L., Beklioğlu, M., Bondar-Kunze, E., Borja, A., Branco, P., Bucak, T., Buijse, A. D., Cardoso, A. C., Couture, R.-M., Cremona, F., de Zwart, D., Feld, C. K., et al. (2020). Impacts of multiple stressors on freshwater biota across spatial scales and ecosystems. *Nature Ecology & Evolution, 4*(8), 1060-1068. https://doi.org/10.1038/s41559-020-1216-4

66. Gao, K., Beardall, J., Häder, D. P., Hall-Spencer, J. M., Gao, G., & Hutchins, D. A. (2019). Effects of ocean acidification on marine photosynthetic organisms under the concurrent influences of warming, UV radiation and deoxygenation. *Frontiers in Marine Science, 6*, 322. https://doi.org/10.3389/fmars.2019.00322

67. Boyd, P., Collins, S., Dupont, S., Fabricius, K., Gattuso, J.-P., Havenhand, J., Hutchins, D., Riebesell, U., Rintoul, M., Vichi, M., Biswas, H., Gao, K., Gehlen, M., Hurd, C., Kurihara, H., McGraw, C., Navarro, J., Nilsson, G., Passow, U., & Pörtner, H.-O. (2018). Experimental strategies to assess the biological ramifications of multiple drivers of ocean global ocean - a review. *Global Change Biology, 24*, 2239-2261. https://doi.org/10.1111/gcb.14102

68. Gao, K., & Häder, D.-P. (2020). Photosynthetic performances of marine microalgae under influences of rising CO_2 and solar UV radiation. In Q. Wang (Ed.), *Microbial photosynthesis,* (pp. 139-150). Springer. https://doi.org/10.1007/978-981-15-3110-1_7

69. Byrne, M., & Fitzer, S. (2019). The impact of environmental acidification on the microstructure and mechanical integrity of marine invertebrate skeletons. *Conservation Physiology, 7*(1), coz062. https://doi.org/10.1093/conphys/coz062

70. Sobrino, C., Neale, P. J., Phillips-Kress, J. D., Moeller, R. E., & Porter, J. (2009). Elevated CO_2 increases sensitivity to ultraviolet radiation in lacustrine phytoplankton assemblages. *Limnology and Oceanography, 54*, 2448-2459. https://doi.org/10.4319/lo.2009.54.6_part_2.2448

71. Lorenzo, M. R., Neale, P. J., Sobrino, C., León, P., Vázquez, V., Bresnan, E., & Segovia, M. (2019). Effects of elevated CO_2 on growth, calcification and spectral dependence of photoinhibition in the coccolithophore *Emiliania huxleyi* (Prymnesiophyceae) *Journal of Phycology, 55*(4), 775-778. https://doi.org/10.1111/jpy.12885

72. Miao, H., Beardall, J., & Gao, K. (2018). Calcification moderates the increased susceptibility to UV radiation of the coccolithophorid *Gephryocapsa oceanica* grown under elevated CO_2 concentration: Evidence based on calcified and non calcified cells. *Photochemistry and Photobiology, 94*(5), 994-1002. https://doi.org/10.1111/php.12928

73. Riebesell, U., Czerny, J., von Bröckel, K., Boxhammer, T., Büdenbender, J., Deckelnick, M., Fischer, M., Hoffmann, D., Krug, S. A., Lentz, U., Ludwig, A., Muche, R., & Schulz, K. G. (2013). Technical Note: A mobile sea-going mesocosm system – new opportunities for ocean change research. *Biogeosciences, 10*(3), 1835-1847. https://doi.org/10.5194/bg-10-1835-2013

74. Ma, K., Powers, L. C., Seppälä, J., Norkko, J., & Brandes, J. A. (2022). Effects of added humic substances and nutrients on photochemical degradation of dissolved organic matter in a mesocosm amendment experiment in the Gulf of Finland, Baltic Sea. *Photochemistry and Photobiology, 98*(5), 1025-1042. https://doi.org/10.1111/php.13597

75. Riebesell, U., Aberle-Malzahn, N., Achterberg, E. P., Algueró-Muñiz, M., Alvarez-Fernandez, S., Arístegui, J., Bach, L. T., Boersma, M., Boxhammer, T., & Guan, W. (2018). Toxic algal bloom induced by ocean acidification disrupts the pelagic food web. *Nature Climate Change, 8*(12), 1082-1086. https://doi.org/10.1038/s41558-018-0344-1

76. Duran-Romero, C., Medina-Sanchez, J. M., & Carrillo, P. (2020). Uncoupled phytoplankton-bacterioplankton relationship by multiple drivers interacting at different temporal scales in a high-mountain Mediterranean lake. *Scientific Reports, 10*(1), 350. https://doi.org/10.1038/s41598-019-57269-y

77. Boehm, A. B., Silverman, A. I., Schriewer, A., & Goodwin, K. (2019). Systematic review and meta-analysis of decay rates of waterborne mammalian viruses and coliphages in surface waters. *Water Research, 164*, 114898. https://doi.org/10.1016/j.watres.2019.114898

78. Nelson, K. L., Boehm, A. B., Davies-Colley, R. J., Dodd, M. C., Kohn, T., Linden, K. G., Liu, Y., Maraccini, P. A., McNeill, K., Mitch, W. A., Nguyen, T. H., Parker, K. M., Rodriguez, R. A., Sassoubre, L. M., Silverman, A. I., Wigginton, K. R., & Zepp, R. G. (2018). Sunlight-mediated inactivation of health-relevant microorganisms in water: a review of mechanisms and modeling approaches. *Environmental Science: Processes & Impacts, 20*(8), 1089-1122. https://doi.org/10.1039/c8em00047f

79. Zepp, R. G., Cyterski, M., Wong, K., Georgacopoulos, O., Acrey, B., Whelan, G., Parmar, R., & Molina, M. (2018). Biological weighting functions for evaluating the role of sunlight-induced inactivation of coliphages at selected beaches and nearby tributaries. *Environmental Science & Technology, 52*(22), 13068-13076. https://doi.org/10.1021/acs.est.8b02191

80. Sulzberger, B., Austin, A. T., Cory, R. M., Zepp, R. G., & Paul, N. D. (2019). Solar UV radiation in a changing world: roles of cryosphere–land–water–atmosphere interfaces in global biogeochemical cycles. *Photochemical & Photobiological Sciences, 18*(3), 747-774. https://doi.org/10.1039/C8PP90063A

81. Silverman, A. I., & Boehm, A. B. (2020). Systematic review and meta-analysis of the persistence and disinfection of human coronaviruses and their viral surrogates in water and wastewater. *Environmental Science & Technology Letters, 7*, 544-553. https://doi.org/10.1021/acs.estlett.0c00313

82. Silverman, A. I., Tay, N., & Machairas, N. (2019). Comparison of biological weighting functions used to model endogenous sunlight inactivation rates of MS2 coliphage. *Water Research, 151*, 439-446. https://doi.org/10.1016/j.watres.2018.12.015

83. Bernhard, G. H., Neale, R. E., Barnes, P. W., Neale, P. J., Zepp, R. G., Wilson, S. R., Andrady, A. L., Bais, A. F., McKenzie, R. L., & Aucamp, P. J. (2020). Environmental effects of stratospheric ozone depletion, UV radiation and interactions with climate change: UNEP Environmental Effects Assessment Panel, update 2019. *Photochemical & Photobiological Sciences, 19*(5), 542-584. https://doi.org/10.1039/D0PP90011G

84. Medema, G., Heijnen, L., Elsinga, G., Italiaander, R., & Brouwer, A. (2020). Presence of SARS-Coronavirus-2 RNA in sewage and correlation with reported COVID-19 prevalence in the early stage of the epidemic in the Netherlands. *Environmental Science & Technology Letters, 7*(7), 511-516. https://doi.org/10.1021/acs.estlett.0c00357

85. Rimoldi, S. G., Stefani, F., Gigantiello, A., Polesello, S., Comandatore, F., Mileto, D., Maresca, M., Longobardi, C., Mancon, A., Romeri, F., Pagani, C., Cappelli, F., Roscioli, C., Moja, L., Gismondo, M. R., & Salerno, F. (2020). Presence and infectivity of SARS-CoV-2 virus in wastewaters and rivers. *Science of the Total Environment, 744*, 140911. https://doi.org/10.1016/j.scitotenv.2020.140911

86. Seyer, A., & Sanlidag, T. (2020). Solar ultraviolet radiation sensitivity of SARS-CoV-2. *The Lancet Microbe, 1*(1), e8-e9. https://doi.org/10.1016/s2666-5247(20)30013-6

87. Paul, D., Kolar, P., & Hall, S. G. (2021). A review of the impact of environmental factors on the fate and transport of coronaviruses in aqueous environments. *npj Clean Water, 4*(1), 7. https://doi.org/10.1038/s41545-020-00096-w

88. Biasin, M., Strizzi, S., Bianco, A., Macchi, A., Utyro, O., Pareschi, G., Loffreda, A., Cavalleri, A., Lualdi, M., Trabattoni, D., Tacchetti, C., Mazza, D., & Clerici, M. (2022). UV and violet light can Neutralize SARS-CoV-2 Infectivity. *Journal of Photochemistry and Photobiology, 10*, 100107. https://doi.org/10.1016/j.jpap.2021.100107

89. Bernhard, G. H., Madronich, S., Lucas, R. M., Byrne, S. Schikowski, T., & Neale, R. E. (2022). Linkages between COVID-19, solar UV radiation, and the Montreal Protocol. *Chapter 2*

90. Berry, N. L., Overholt, E. P., Fisher, T. J., & Williamson, C. E. (2020). Dissolved organic matter protects mosquito larvae from damaging solar UV radiation. *Plos One, 15*(10), e0240261. https://doi.org/10.1371/journal.pone.0240261

91. Wood, C. L., & Johnson, P. T. (2015). A world without parasites: exploring the hidden ecology of infection. *Frontiers in Ecology and the Environment, 13*(8), 425-434. https://doi.org/10.1890/140368

92. Overholt, E. P., Duffy, M. A., Meeks, M. P., Leach, T. H., & Williamson, C. E. (2020). Light exposure decreases infectivity of the Daphnia parasite Pasteuria ramo*sa. Journal of Plankton Research, 42*(1), 41-44. https://doi.org/10.1093/plankt/fbz070

93. Rogalski, M. A., & Duffy, M. A. (2020). Local adaptation of a parasite to solar radiation impacts disease transmission potential, spore yield, and host fecundity. *Evolution, 74*, 1856-1864. https://doi.org/10.1111/evo.13940

94. Shaw, C. L., Hall, S. R., Overholt, E. P., Cáceres, C. E., Williamson, C. E., & Duffy, M. A. (2020). Shedding light on environmentally transmitted parasites: lighter conditions within lakes restrict epidemic size. *Ecology, 101*(11), e03168. https://doi.org/10.1002/ecy.3168

95. Henard, C., Saraiva, M. R., Ściślak, M. E., Ruba, T., McLaggan, D., Noguera, P., & van West, P. (2022). Can ulcerative dermal necrosis (UDN) in Atlantic salmon be attributed to ultraviolet radiation and secondary *Saprolegnia parasitica* infections? *Fungal Biology Reviews, 40*, 70-75. https://doi.org/10.1016/j.fbr.2022.02.002

96. Villafañe, V., Sundbäck, K., Figueroa, F., & Helbling, E. (2003). Photosynthesis in the aquatic environment as affected by UVR. In E. W. Helbling, & H. E. Zagarese (Eds.), *UV effects in aquatic organisms and ecosystems*, (pp. 357-397). Royal Society of Chemistry. https://doi.org/10.1039/9781847552266-00357

97. García-Corral, L. S., Duarte, C. M., & Agusti, S. (2020). Impact of UV radiation on plankton net community production: responses in Western Australian estuarine and coastal waters. *Marine Ecology Progress Series, 651*, 45-56. https://doi.org/10.3354/meps13456

98. Regaudie-de-Gioux, A., Agustí, S., & Duarte, C. M. (2014). UV sensitivity of planktonic net community production in ocean surface waters. *Journal of Geophysical Research: Biogeosciences, 119*(5), 929-936. https://doi.org/10.1002/2013jg002566

99. Ossola, R. (2021). *Advancing the Photochemistry of Dissolved Organic Matter: Quantification of Singlet Oxygen and Formation Mechanism of Selected Photoproducts*. PhD Dissertation, ETH Zurich. https://doi.org/10.3929/ethz-b-000482128

100. Barnes, P. W., Robson, T. M., Zepp, R. G., Bornman, J. F., Jansen, M. A. K., Ossola, R., Wang, Q.-W., Robinson, S. A., Foereid, B., Klekociuk, A. R., Martinez-Abaigar, J., Hou, W.-C., Mackenzie, R. L., & Paul, N. D. (2022). Interactive effects of changes in UV radiation and climate on terrestrial ecosystems, biogeochemical cycles, and feedbacks to the climate system. *Chapter 4*

101. Madronich, S., Sulzberger, B., Longstreth, J. D., Schikowski, T., Andersen, M. P. S., Solomon, K. R., & Wilson, S. R. (2022). Changes in tropospheric air quality related to the protection of stratospheric ozone and a changing climate. *Chapter 6*

102. Hugelius, G., Strauss, J., Zubrzycki, S., Harden, J. W., Schuur, E. A. G., Ping, C. L., Schirrmeister, L., Grosse, G., Michaelson, G. J., Koven, C. D., O'Donnell, J. A., Elberling, B., Mishra, U., Camill, P., Yu, Z., Palmtag, J., & Kuhry, P. (2014). Estimated stocks of circumpolar permafrost carbon with quantified uncertainty ranges and identified data gaps. *Biogeosciences, 11*(23), 6573-6593. https://doi.org/10.5194/bg-11-6573-2014

103. Hugelius, G., Loisel, J., Chadburn, S., Jackson, R. B., Jones, M., MacDonald, G., Marushchak, M., Olefeldt, D., Packalen, M., Siewert, M. B., Treat, C., Turetsky, M., Voigt, C., & Yu, Z. (2020). Large stocks of peatland carbon and nitrogen are vulnerable to permafrost thaw. *Proceedings of the National Academy of Sciences, 117*(34), 20438-20446. https://doi.org/10.1073/pnas.1916387117

104. Gagné, K. R., Ewers, S. C., Murphy, C. J., Daanen, R., Walter Anthony, K., & Guerard, J. J. (2020). Composition and photo-reactivity of organic matter from permafrost soils and surface waters in interior Alaska. *Environmental Science: Processes & Impacts*, 22(7), 1525-1539. https://doi.org/10.1039/d0em00097c

105. Allesson, L., Koehler, B., Thrane, J.-E., Andersen, T., & Hessen, D. O. (2021). The role of photomineralization for CO_2 emissions in boreal lakes along a gradient of dissolved organic matter. *Limnology and Oceanography, 66*(1), 158-170. https://doi.org/10.1002/lno.11594

106. Koehler, B., Landelius, T., Weyhenmeyer, G. A., Machida, N., & Tranvik, L. J. (2014). Sunlight-induced carbon dioxide emissions from inland waters. *Global Biogeochemical Cycles, 28*(7), 2014GB004850. https://doi.org/10.1002/2014GB004850

107. Maavara, T., Logozzo, L., Stubbins, A., Aho, K., Brinkerhoff, C., Hosen, J., & Raymond, P. (2021). Does photomineralization of dissolved organics matter in temperate rivers? *Journal of Geophysical Research: Biogeosciences, 126*(7), e2021JG006402. https://doi.org/10.1029/2021JG006402

108. Clark, J. B., Long, W., & Hood, R. R. (2020). A comprehensive estuarine dissolved organic carbon budget using an enhanced biogeochemical model. *Journal of Geophysical Research: Biogeosciences, 125*(5), e2019JG005442. https://doi.org/10.1029/2019JG005442

109. Stubbins, A., Law, C. S., Uher, G., & Upstill-Goddard, R. C. (2011). Carbon monoxide apparent quantum yields and photoproduction in the Tyne estuary. *Biogeosciences, 8*(3), 703-713. https://doi.org/10.5194/bg-8-703-2011

110. Zimov, S. A., Schuur, E. A. G., & Chapin, F. S. (2006). Permafrost and the global carbon budget. *Science, 312*(5780), 1612-1613. https://doi.org/10.1126/science.1128908

111. Grunert, B. K., Tzortziou, M., Neale, P., Menendez, A., & Hernes, P. (2021). DOM degradation by light and microbes along the Yukon River-coastal ocean continuum. *Scientific Reports, 11*(1), 10236. https://doi.org/10.1038/s41598-021-89327-9

112. Rocher-Ros, G., Harms, T. K., Sponseller, R. A., Väisänen, M., Mörth, C.-M., & Giesler, R. (2021). Metabolism overrides photo-oxidation in CO_2 dynamics of Arctic permafrost streams. *Limnology and Oceanography, 66*(S1), 11564. https://doi.org/10.1002/lno.11564

113. Stubbins, A., Mann, P. J., Powers, L., Bittar, T. B., Dittmar, T., McIntyre, C. P., Eglinton, T. I., Zimov, N., & Spencer, R. G. M. (2017). Low photolability of yedoma permafrost dissolved organic carbon. *Journal of Geophysical Research: Biogeosciences, 122*(1), 200-211. https://doi.org/10.1002/2016JG003688

114. Bowen, J. C., Ward, C. P., Kling, G. W., & Cory, R. M. (2020). Arctic amplification of global warming strengthened by sunlight oxidation of permafrost carbon to CO_2. *Geophysical Research Letters, 47*(12), e2020GL087085. https://doi.org/10.1029/2020GL087085

115. Cory, R. M., Ward, C. P., Crump, B. C., & Kling, G. W. (2014). Sunlight controls water column processing of carbon in arctic fresh waters. *Science, 345*(6199), 925-928. https://doi.org/10.1126/science.1253119

116. Mazoyer, F., Laurion, I., & Rautio, M. (2022). The dominant role of sunlight in degrading winter dissolved organic matter from a thermokarst lake in a subarctic peatland. *Biogeosciences. 19*(17), 3959-3977. https://doi.org/10.5194/bg-19-3959-2022

117. Koehler, B., Powers, L. C., Cory, R. M., Einarsdóttir, K., Gu, Y., Tranvik, L. J., Vähätalo, A. V., Ward, C. P., & Miller, W. L. (2022). Inter-laboratory differences in the apparent quantum yield for the photochemical production of dissolved inorganic carbon in inland waters and implications for photochemical rate modeling. *Limnology and Oceanography: Methods, 20*(6), 320-337. https://doi.org/10.1002/lom3.10489

118. Zheng, B., Chevallier, F., Yin, Y., Ciais, P., Fortems-Cheiney, A., Deeter, M. N., Parker, R. J., Wang, Y., Worden, H. M., & Zhao, Y. (2019). Global atmospheric carbon monoxide budget 2000–2017 inferred from multi-species atmospheric inversions. *Earth System Science Data, 11*(3), 1411-1436. https://doi.org/10.5194/essd-11-1411-2019

119. Conte, L., Szopa, S., Séférian, R., & Bopp, L. (2019). The oceanic cycle of carbon monoxide and its emissions to the atmosphere. *Biogeosciences, 16*(4), 881-902. https://doi.org/10.5194/bg-16-881-2019

120. Mopper, K., Kieber, D. J., & Stubbins, A. (2015). Marine photochemistry of organic matter: Processes and impacts. In C. A. Carlson (Ed.), *Biogeochemistry of Marine Dissolved Organic Matter,* (2nd ed., pp. 389-450). Academic Press. https://doi.org/10.1016/B978-0-12-405940-5.00008-X

121. Reader, H. E., & Miller, W. L. (2012). Variability of carbon monoxide and carbon dioxide apparent quantum yield spectra in three coastal estuaries of the South Atlantic Bight. *Biogeosciences, 9*(11), 4279-4294. https://doi.org/10.5194/bg-9-4279-2012

122. Campen, H. I., Arévalo-Martínez, D. L., Artioli, Y., Brown, I. J., Kitidis, V., Lessin, G., Rees, A. P., & Bange, H. W. (2022). The role of a changing Arctic Ocean and climate for the biogeochemical cycling of dimethyl sulphide and carbon monoxide. *Ambio, 51*(2), 411-422. https://doi.org/10.1007/s13280-021-01612-z

123. Song, G., & Xie, H. (2017). Spectral efficiencies of carbon monoxide photoproduction from particulate and dissolved organic matter in laboratory cultures of Arctic sea ice algae. *Marine Chemistry, 190*, 51-65. https://doi.org/10.1016/j.marchem.2017.02.002

124. Saunois, M., Stavert, A. R., Poulter, B., Bousquet, P., Canadell, J. G., Jackson, R. B., Raymond, P. A., Dlugokencky, E. J., Houweling, S., Patra, P. K., Ciais, P., Arora, V. K., Bastviken, D., Bergamaschi, P., Blake, D. R., Brailsford, G., Bruhwiler, L., Carlson, K. M., Carrol, M., Castaldi, S., et al. (2020). The global methane budget 2000–2017. *Earth System Science Data, 12*(3), 1561-1623. https://doi.org/10.5194/essd-12-1561-2020

125. Li, Y., Fichot, C. G., Geng, L., Scarratt, M. G., & Xie, H. (2020). The contribution of methane photoproduction to the oceanic methane paradox. *Geophysical Research Letters, 47*(14), e2020GL088362. https://doi.org/10.1029/2020GL088362

126. Whelan, M. E., Lennartz, S. T., Gimeno, T. E., Wehr, R., Wohlfahrt, G., Wang, Y., Kooijmans, L. M. J., Hilton, T. W., Belviso, S., Peylin, P., Commane, R., Sun, W., Chen, H., Kuai, L., Mammarella, I., Maseyk, K., Berkelhammer, M., Li, K.-F., Yakir, D., Zumkehr, A., et al. (2018). Reviews and syntheses: Carbonyl sulfide as a multi-scale tracer for carbon and water cycles. *Biogeosciences, 15*(12), 3625-3657. https://doi.org/10.5194/bg-15-3625-2018

127. Launois, T., Belviso, S., Bopp, L., Fichot, C. G., & Peylin, P. (2015). A new model for the global biogeochemical cycle of carbonyl sulfide - Part 1: Assessment of direct marine emissions with an oceanic general circulation and biogeochemistry model. *Atmospheric Chemistry and Physics, 15*(5), 2295-2312. https://doi.org/https://doi.org/10.5194/acp-15-2295-2015

128. Lennartz, S. T., Marandino, C. A., von Hobe, M., Cortes, P., Quack, B., Simo, R., Booge, D., Pozzer, A., Steinhoff, T., Arevalo-Martinez, D. L., Kloss, C., Bracher, A., Röttgers, R., Atlas, E., & Krüger, K. (2017). Direct oceanic emissions unlikely to account for the missing source of atmospheric carbonyl sulfide. *Atmospheric Chemistry and Physics, 17*(1), 385-402. https://doi.org/10.5194/acp-17-385-2017

129. Lennartz, S. T., von Hobe, M., Booge, D., Bittig, H. C., Fischer, T., Gonçalves-Araujo, R., Ksionzek, K. B., Koch, B. P., Bracher, A., Röttgers, R., Quack, B., & Marandino, C. A. (2019). The influence of dissolved organic matter on the marine production of carbonyl sulfide (OCS) and carbon disulfide (CS2) in the Peruvian upwelling. *Ocean Science, 15*(4), 1071-1090. https://doi.org/10.5194/os-15-1071-2019

130. Cory, R. M., & Kling, G. W. (2018). Interactions between sunlight and microorganisms influence dissolved organic matter degradation along the aquatic continuum. *Limnology and Oceanography Letters, 3*(3), 102-116. https://doi.org/10.1002/lol2.10060

131. Ward, C. P., Nalven, S. G., Crump, B. C., Kling, G. W., & Cory, R. M. (2017). Photochemical alteration of organic carbon draining permafrost soils shifts microbial metabolic pathways and stimulates respiration. *Nature Communications, 8*(1), 772. https://doi.org/10.1038/s41467-017-00759-2

132. Nalven, S. G., Ward, C. P., Payet, J. P., Cory, R. M., Kling, G. W., Sharpton, T. J., Sullivan, C. M., & Crump, B. C. (2020). Experimental metatranscriptomics reveals the costs and benefits of dissolved organic matter photo-alteration for freshwater microbes. *Environmental Microbiology, 22*(8), 3505-3521. https://doi.org/10.1111/1462-2920.15121

133. Ward, C. P., & Cory, R. M. (2020). Assessing the prevalence, products, and pathways of dissolved organic matter partial photo-oxidation in arctic surface waters. *Environmental Science: Processes & Impacts, 22*, 1214-1223. https://doi.org/10.1039/C9EM00504H

134. Cory, R. M., McNeill, K., Cotner, J. B., Amado, A., Purcell, J. M., & Marshall, A. G. (2010). Singlet oxygen in the coupled photochemical and biochemical oxidation of dissolved organic matter. *Environmental Science & Technology, 44*(10), 3683-3689. https://doi.org/10.1021/es902989y

135. Clark, J. B., Neale, P., Tzortziou, M., Cao, F., & Hood, R. R. (2019). A mechanistic model of photochemical transformation and degradation of colored dissolved organic matter. *Marine Chemistry, 214*, 103666. https://doi.org/10.1016/j.marchem.2019.103666

136. Ossola, R., Tolu, J., Clerc, B., Erickson, P. R., Winkel, L. H. E., & McNeill, K. (2019). Photochemical production of sulfate and methanesulfonic acid from dissolved organic sulfur. *Environmental Science & Technology, 53*(22), 13191-13200. https://doi.org/10.1021/acs.est.9b04721

137. Doane, T. A. (2017). The abiotic nitrogen cycle. *ACS Earth and Space Chemistry, 1*(7), 411-421. https://doi.org/10.1021/acsearthspacechem.7b00059

138. von Friesen, L. W., & Riemann, L. (2020). Nitrogen fixation in a changing Arctic ocean: An overlooked source of nitrogen? *Frontiers in Microbiology, 11*, 596426. https://doi.org/10.3389/fmicb.2020.596426

139. Bowen, J. (2021). *Impact of Dissolved Organic Matter Photodegradation on Carbon and Nitrogen Cycling in Freshwaters*. Thesis, University of Michigan. https://doi.org/10.7302/3033

140. Vähätalo, A. V., Salonen, K. M., & Wetzel, R. G. (2003). Photochemical transformation of allochthonous organic matter provides bioavailable nutrients in a humic lake. *Archiv für Hydrobiologie, 156*(3), 287-324. https://doi.org/10.1127/0003-9136/2003/0156-0287

141. Yang, Y., Sun, P., Padhye, L. P., & Zhang, R. (2020). Photo-ammonification in surface water samples: Mechanism and influencing factors. *Science of the Total Environment, 759*, 143547. https://doi.org/10.1016/j.scitotenv.2020.143547

142. Guo, M., Li, X., Song, C., Liu, G., & Zhou, Y. (2020). Photo-induced phosphate release during sediment resuspension in shallow lakes: A potential positive feedback mechanism of eutrophication. *Environmental Pollution, 258*, 113679. https://doi.org/10.1016/j.envpol.2019.113679

143. Li, X., Zhou, Y., Liu, G., Lei, H., & Zhu, D. (2017). Mechanisms of the photochemical release of phosphate from resuspended sediments under solar irradiation. *Science of the Total Environment, 595*(Supplement C), 779-786. https://doi.org/10.1016/j.scitotenv.2017.04.039

144. Cheng, F., Zhang, T., Liu, Y., Zhang, Y., & Qu, J. (2021). Non-negligible effects of UV irradiation on transformation and environmental risks of microplastics in the water environment. *Journal of Xenobiotics, 12*(1), 1-12. https://doi.org/10.3390/jox12010001

145. Jansen, M. A. K., Barnes, P. W., Bornman, J. F., Rose, K. C., Madronich, S., White, C. C., Zepp, R. G., & Andrady, A. L. (2022). The Montreal Protocol and the fate of environmental plastic debris. *Chapter 8*

146. Wilson, B. D., Moon, S., & Armstrong, F. (2012). Comprehensive review of ultraviolet radiation and the current status on sunscreens. *The Journal of Clinical and Aesthetic Dermatology, 5*(9), 18-23.

147. Downs, C. A., Cruz, O. T., & Remengesau, T. E. (2022). Sunscreen pollution and tourism governance: Science and innovation are necessary for biodiversity conservation and sustainable tourism. *Aquatic Conservation: Marine and Freshwater Ecosystems, 32*(5), 896-906. https://doi.org/10.1002/aqc.3791

148. Schneider, S. L., & Lim, H. W. (2019). Review of environmental effects of oxybenzone and other sunscreen active ingredients. *Journal of the American Academy of Dermatology, 80*(1), 266-271. https://doi.org/10.1016/j.jaad.2018.06.033

149. Tovar-Sanchez, A., Sanchez-Quiles, D., & Rodriguez-Romero, A. (2019). Massive coastal tourism influx to the Mediterranean Sea: The environmental risk of sunscreens. *Science of the Total Environment, 656*, 316-321. https://doi.org/10.1016/j.scitotenv.2018.11.399

150. National Academies of Sciences, Engineering, and Medicine. (2022). *Review of Fate, Exposure, and Effects of Sunscreens in Aquatic Environments and Implications for Sunscreen Usage and Human Health*. The National Academies Press, Washington, D.C. https://doi.org/10.17226/26381

151. Mitchelmore, C. L., He, K., Gonsior, M., Hain, E., Heyes, A., Clark, C., Younger, R., Schmitt-Kopplin, P., Feerick, A., Conway, A., & Blaney, L. (2019). Occurrence and distribution of UV-filters and other anthropogenic contaminants in coastal surface water, sediment, and coral tissue from Hawaii. *Science of the Total Environment, 670*, 398-410. https://doi.org/10.1016/j.scitotenv.2019.03.034

152. de Miranda, L. L. R., Harvey, K. E., Ahmed, A., & Harvey, S. C. (2021). UV-filter pollution: current concerns and future prospects. *Environmental Monitoring and Assessment, 193*(12), 840. https://doi.org/10.1007/s10661-021-09626-6

153. Lozano, C., Matallana-Surget, S., Givens, J., Nouet, S., Arbuckle, L., Lambert, Z., & Lebaron, P. (2020). Toxicity of UV filters on marine bacteria: Combined effects with damaging solar radiation. *Science of the Total Environment, 722*, 137803. https://doi.org/10.1016/j.scitotenv.2020.137803

154. Vuckovic, D., Tinoco, A. I., Ling, L., Renicke, C., Pringle, J. R., & Mitch, W. A. (2022). Conversion of oxybenzone sunscreen to phototoxic glucoside conjugates by sea anemones and corals. *Science, 376*(6593), 644-648. https://doi.org/10.1126/science.abn2600

155. Yuan, S., Huang, J., Jiang, X., Huang, Y., Zhu, X., & Cai, Z. (2022). Environmental fate and toxicity of sunscreen-derived Inorganic ultraviolet filters in aquatic environments: A review. *Nanomaterials, 12*(4), 699. https://doi.org/10.3390/nano12040699

156. He, K., Hain, E., Timm, A., Tarnowski, M., & Blaney, L. (2019). Occurrence of antibiotics, estrogenic hormones, and UV-filters in water, sediment, and oyster tissue from the Chesapeake Bay. *Science of the Total Environment, 650*(Pt 2), 3101-3109. https://doi.org/10.1016/j.scitotenv.2018.10.021

157. Du, Y., Wang, W. Q., Pei, Z. T., Ahmad, F., Xu, R. R., Zhang, Y. M., & Sun, L. W. (2017). Acute toxicity and ecological risk assessment of benzophenone-3 (BP-3) and benzophenone-4 (BP-4) in ultraviolet (UV)-filters. *International Journal of Environmental Research and Public Health, 14*(11), 1414. https://doi.org/10.3390/ijerph14111414

158. Downs, C. A., Bishop, E., Diaz-Cruz, M. S., Haghshenas, S. A., Stien, D., Rodrigues, A. M. S., Woodley, C. M., Sunyer-Caldú, A., Doust, S. N., Espero, W., Ward, G., Farhangmehr, A., Tabatabaee Samimi, S. M., Risk, M. J., Lebaron, P., & DiNardo, J. C. (2022). Oxybenzone contamination from sunscreen pollution and its ecological threat to Hanauma Bay, Oahu, Hawaii, U.S.A. *Chemosphere, 291*, 132880. https://doi.org/10.1016/j.chemosphere.2021.132880

159. Moeller, M., Pawlowski, S., Petersen-Thiery, M., Miller, I. B., Nietzer, S., Heisel-Sure, Y., Kellermann, M. Y., & Schupp, P. J. (2021). Challenges in current coral reef protection – Possible impacts of UV filters used in sunscreens, a critical review. *Frontiers in Marine Science, 8*, 665548. https://doi.org/10.3389/fmars.2021.665548

160. Araújo, C. V. M., Rodríguez-Romero, A., Fernández, M., Sparaventi, E., Medina, M. M., & Tovar-Sánchez, A. (2020). Repellency and mortality effects of sunscreens on the shrimp Palaemon varians: Toxicity dependent on exposure method. *Chemosphere, 257*, 127190. https://doi.org/10.1016/j.chemosphere.2020.127190

161. He, T., Tsui, M. M. P., Tan, C. J., Ma, C. Y., Yiu, S. K. F., Wang, L. H., Chen, T. H., Fan, T. Y., Lam, P. K. S., & Murphy, M. B. (2019). Toxicological effects of two organic ultraviolet filters and a related commercial sunscreen product in adult corals. *Environmental Pollution, 245*, 462-471. https://doi.org/10.1016/j.envpol.2018.11.029

162. He, T., Tsui, M. M. P., Tan, C. J., Ng, K. Y., Guo, F. W., Wang, L. H., Chen, T. H., Fan, T. Y., Lam, P. K. S., & Murphy, M. B. (2019). Comparative toxicities of four benzophenone ultraviolet filters to two life stages of two coral species. *Science of the Total Environment, 651*, 2391-2399. https://doi.org/10.1016/j.scitotenv.2018.10.148

163. Fitt, W. K., & Hofmann, D. K. (2020). The effects of the UV-blocker oxybenzone (benzophenone-3) on planulae swimming and metamorphosis of the Scyphozoans *Cassiopea xamachana* and *Cassiopea frondosa*. *Oceans, 1*(4), 174-180. https://doi.org/10.3390/oceans1040013

164. Cocci, P., Mosconi, G., & Palermo, F. A. (2020). Sunscreen active ingredients in loggerhead turtles (*Caretta caretta*) and their relation to molecular markers of inflammation, oxidative stress and hormonal activity in wild populations. *Marine Pollution Bulletin, 153*, 111012. https://doi.org/10.1016/j.marpolbul.2020.111012

165. Raffa, R. B., Pergolizzi, J. V., Taylor, R., & Kitzen, J. M. (2019). Sunscreen bans: Coral reefs and skin cancer. *Journal of Clinical Pharmacy and Therapeutics, 44*(1), 134-139. https://doi.org/10.1111/jcpt.12778

166. Catalano, R., Labille, J., Gaglio, D., Alijagic, A., Napodano, E., Slomberg, D., Campos, A., & Pinsino, A. (2020). Safety evaluation of TiO_2 nanoparticle-based sunscreen UV Filters on the development and the immunological state of the sea urchin *Paracentrotus lividus*. *Nanomaterials, 10*(11), 2102. https://doi.org/10.3390/nano10112102

167. Corinaldesi, C., Marcellini, F., Nepote, E., Damiani, E., & Danovaro, R. (2018). Impact of inorganic UV filters contained in sunscreen products on tropical stony corals (*Acropora* spp.). *Science of the Total Environment, 637-638*, 1279-1285. https://doi.org/10.1016/j.scitotenv.2018.05.108

168. Fel, J.-P., Lacherez, C., Bensetra, A., Mezzache, S., Béraud, E., Léonard, M., Allemand, D., & Ferrier-Pagès, C. (2018). Photochemical response of the scleractinian coral *Stylophora pistillata* to some sunscreen ingredients. *Coral Reefs, 38*(1), 109-122. https://doi.org/10.1007/s00338-018-01759-4

169. Cunningham, B., Torres-Duarte, C., Cherr, G., & Adams, N. (2020). Effects of three zinc-containing sunscreens on development of purple sea urchin (*Strongylocentrotus purpuratus*) embryos. *Aquatic Toxicology, 218*, 105355. https://doi.org/10.1016/j.aquatox.2019.105355

170. Hanigan, D., Truong, L., Schoepf, J., Nosaka, T., Mulchandani, A., Tanguay, R. L., & Westerhoff, P. (2018). Trade-offs in ecosystem impacts from nanomaterial versus organic chemical ultraviolet filters in sunscreens. *Water Research, 139*, 281-290. https://doi.org/10.1016/j.watres.2018.03.062

171. Fastelli, P., & Renzi, M. (2019). Exposure of key marine species to sunscreens: Changing ecotoxicity as a possible indirect effect of global warming. *Marine Pollution Bulletin, 149*, 110517. https://doi.org/10.1016/j.marpolbul.2019.110517

172. Chaves Lopes, F., Rosa de Castro, M., Caldas Barbosa, S., Primel, E. G., & de Martinez Gaspar Martins, C. (2020). Effect of the UV filter, Benzophenone-3, on biomarkers of the yellow clam (*Amarilladesma mactroides*) under different pH conditions. *Marine Pollution Bulletin, 158*, 111401. https://doi.org/10.1016/j.marpolbul.2020.111401

173. Wijgerde, T., van Ballegooijen, M., Nijland, R., van der Loos, L., Kwadijk, C., Osinga, R., Murk, A., & Slijkerman, D. (2020). Adding insult to injury: Effects of chronic oxybenzone exposure and elevated temperature on two reef-building corals. *Science of the Total Environment, 733*, 139030. https://doi.org/10.1016/j.scitotenv.2020.139030

174. Rosic, N. N. (2019). Mycosporine-like amino acids: Making the foundation for organic personalised sunscreens. *Marine drugs, 17*(11), 638. https://doi.org/10.3390/md17110638

175. Sen, S., & Mallick, N. (2021). Mycosporine-like amino acids: Algal metabolites shaping the safety and sustainability profiles of commercial sunscreens. *Algal Research, 58*, 102425. https://doi.org/10.1016/j.algal.2021.102425

176. Singh, A., Čížková, M., Bišová, K., & Vítová, M. (2021). Exploring mycosporine-like amino acids (MAAs) as safe and natural protective agents against UV-induced skin damage. *Antioxidants, 10*(5), 683. https://doi.org/10.3390/antiox10050683

177. Rangel, K. C. (2020). Assessment of the photoprotective potential and toxicity of Antarctic red macroalgae extracts from *Curdiea racovitzae* and I*ridaea cordata* for cosmetic use. *Algal Research, 50*, 101984. https://doi.org/10.1016/j.algal.2020.101984

178. Woolley, J. M., Staniforth, M., Horbury, M. D., Richings, G. W., Wills, M., & Stavros, V. G. (2018). Unravelling the photoprotection properties of mycosporine amino acid motifs. *The Journal of Physical Chemistry Letters, 9*(11), 3043-3048. https://doi.org/10.1021/acs.jpclett.8b00921

179. Geraldes, V., & Pinto, E. (2021). Mycosporine-like amino acids (MAAs): Biology, chemistry and identification features. *Pharmaceuticals, 14*(1), 63. https://doi.org/10.3390/ph14010063

180. Bhatia, S., Sardana, S., Sharma, A., Vargas De La Cruz, C. B., Chaugule, B., & Khodaie, L. (2019). Development of broad spectrum mycosporine loaded sunscreen formulation from *Ulva fasciata* delile. *BioMedicine, 9*(3), 17. https://doi.org/10.1051/bmdcn/2019090317

181. Lawrence, K. P., Long, P. F., & Young, A. R. (2019). Mycosporine-like amino acids for skin photoprotection. *Current Medicinal Chemistry, 25*(40), 5512-5527. https://doi.org/10.2174/0929867324666170529124237

182. Prasedya, E. S., Syafitri, S. M., Geraldine, B. A., Hamdin, C. D., Frediansyah, A., Miyake, M., Kobayashi, D., Hazama, A., & Sunarpi, H. (2019). UVA photoprotective activity of Brown macroalgae *Sargassum cristafolium*. *Biomedicines, 7*(4), 77. https://doi.org/10.3390/biomedicines7040077

183. Yang, G., Cozad, M. A., Holland, D. A., Zhang, Y., Luesch, H., & Ding, Y. (2018). Photosynthetic production of sunscreen shinorine using an engineered cyanobacterium. *ACS Synthetic Biology, 7*(2), 664-671. https://doi.org/10.1021/acssynbio.7b00397

184. Bhatia, S., Al-Harrasi, A., Behl, T., Anwer, M. K., Ahmed, M. M., Mittal, V., Kaushik, D., Chigurupati, S., Kabir, M. T., Sharma, P. B., Chaugule, B., & Vargas-de-la-Cruz, C. (2021). Unravelling the photoprotective effects of freshwater alga *Nostoc commune* Vaucher ex Bornet et Flahault against ultraviolet radiations. *Environmental Science and Pollution Research, 29*(10), 14380-14392. https://doi.org/10.1007/s11356-021-16704-2

185. Amador-Castro, F., Rodriguez-Martinez, V., & Carrillo-Nieves, D. (2020). Robust natural ultraviolet filters from marine ecosystems for the formulation of environmental friendlier bio-sunscreens. *Science of the Total Environment, 749*, 141576. https://doi.org/10.1016/j.scitotenv.2020.141576

186. Sánchez-Suárez, J., Villamil, L., Coy-Barrera, E., & Díaz, L. (2021). *Cliona varians*-derived actinomycetes as bioresources of photoprotection-related Bioactive end-products. *Marine Drugs, 19*(12), 674. https://doi.org/10.3390/md19120674

187. Brunt, E. G., & Burgess, J. G. (2018). The promise of marine molecules as cosmetic active ingredients. *International Journal of Cosmetic Science, 40*(1), 1-15. https://doi.org/10.1111/ics.12435

188. Vega, J., Bonomi-Barufi, J., Gómez-Pinchetti, J. L., & Figueroa, F. L. (2020). Cyanobacteria and red macroalgae as potential sources of antioxidants and UV radiation-absorbing compounds for cosmeceutical applications. *Marine Drugs, 18*(12), 659. https://doi.org/10.3390/md18120659

189. Andrady, A. L., Heikkilä, A. M., Pandey, K. K., Bruckman, L. S., White, C. C., Zhu, M., & Zhu, L. (2022). Effects of UV radiation on natural and synthetic materials. *Chapter 7*

190. Ward, C. P., & Overton, E. B. (2020). How the 2010 Deepwater Horizon spill reshaped our understanding of crude oil photochemical weathering at sea: a past, present, and future perspective. *Environmental Science: Processes & Impacts, 22*(5), 1125-1138. https://doi.org/10.1039/d0em00027b

191. Freeman, D. H., & Ward, C. P. (2022). Sunlight-driven dissolution is a major fate of oil at sea. *Science Advances, 8*(7), eabl7605. https://doi.org/10.1126/sciadv.abl7605

192. Zito, P., Podgorski, D. C., Bartges, T., Guillemette, F., Roebuck, J. A., Spencer, R. G. M., Rodgers, R. P., & Tarr, M. A. (2020). Sunlight-induced molecular progression of oil into oxidized oil soluble species, interfacial material, and dissolved organic matter. *Energy & Fuels, 34*(4), 4721-4726. https://doi.org/10.1021/acs.energyfuels.9b04408

193. Nordborg, F. M., Jones, R. J., Oelgemoller, M., & Negri, A. P. (2020). The effects of ultraviolet radiation and climate on oil toxicity to coral reef organisms - A review. *Science of the Total Environment, 720*, 137486. https://doi.org/10.1016/j.scitotenv.2020.137486

194. Nordborg, F. M., Brinkman, D. L., Ricardo, G. F., Agustí, S., & Negri, A. P. (2021). Comparative sensitivity of the early life stages of a coral to heavy fuel oil and UV radiation. *Science of the Total Environment, 781*, 146676. https://doi.org/10.1016/j.scitotenv.2021.146676

195. Nielsen, K. M., Alloy, M. M., Damare, L., Palmer, I., Forth, H. P., Morris, J., Stoeckel, J. A., & Roberts, A. P. (2020). Planktonic fiddler crab (*Uca longisignalis*) are susceptible to photoinduced toxicity following in ovo exposure in oiled mesocosms. *Environmental Science & Technology, 54*(10), 6254-6261. https://doi.org/10.1021/acs.est.0c00215

196. Knightes, C. D., Ambrose Jr, R. B., Avant, B., Han, Y., Acrey, B., Bouchard, D. C., Zepp, R., & Wool, T. (2019). Modeling framework for simulating concentrations of solute chemicals, nanoparticles, and solids in surface waters and sediments: WASP8 Advanced Toxicant Module. *Environmental Modelling & Software, 111*, 444-458. https://doi.org/10.1016/j.envsoft.2018.10.012

197. Vione, D., & Scozzaro, A. (2019). Photochemistry of surface fresh waters in the framework of climate change. *Environmental Science & Technology, 53*(14), 7945-7963. https://doi.org/10.1021/acs.est.9b00968

198. Han, Y., Knightes, C. D., Bouchard, D., Zepp, R., Avant, B., Hsieh, H.-S., Chang, X., Acrey, B., Henderson, W. M., & Spear, J. (2019). Simulating graphene oxide nanomaterial phototransformation and transport in surface water. *Environmental Science: Nano, 6*(1), 180-194. https://doi.org/10.1039/C8EN01088A

199. Beecraft, L., Watson, S. B., & Smith, R. E. H. (2019). Innate resistance of PSII efficiency to sunlight stress is not an advantage for cyanobacteria compared to eukaryotic phytoplankton. *Aquatic Ecology, 53*(3), 347-364. https://doi.org/10.1007/s10452-019-09694-4

200. Paerl, H. W., Otten, T. G., & Kudela, R. (2018). Mitigating the expansion of harmful algal blooms across the freshwater-to-marine continuum. *Environmental Science & Technology, 52*(10), 5519-5529. https://doi.org/10.1021/acs.est.7b05950

201. Wang, X., Feng, X., Zhuang, Y., Lu, J., Wang, Y., Gonçalves, R. J., Li, X., Lou, Y., & Guan, W. (2019). Effects of ocean acidification and solar ultraviolet radiation on physiology and toxicity of dinoflagellate *Karenia mikimotoi*. *Harmful Algae, 81*, 1-9. https://doi.org/10.1016/j.hal.2018.11.013

202. Ren, L., Wang, P., Wang, C., Paerl, H. W., & Wang, H. (2020). Effects of phosphorus availability and phosphorus utilization behavior of *Microcystis aeruginosa* on its adaptation capability to ultraviolet radiation. *Environmental Pollution, 256*, 113441. https://doi.org/10.1016/j.envpol.2019.113441

203. Xu, Z., Gao, G., Tu, B., Qiao, H., Ge, H., & Wu, H. (2019). Physiological response of the toxic and non-toxic strains of a bloom-forming cyanobacterium Microcystis aeruginosa to changing ultraviolet radiation regimes. *Hydrobiologia, 833*(1), 143-156. https://doi.org/10.1007/s10750-019-3896-9

204. Jokiel, P. L. (1980). Solar ultraviolet radiation and coral reef epifauna. *Science, 207*(4435), 1069-1071. https://doi.org/10.1126/science.207.4435.1069

205. Figueroa, F. L. (2021). Mycosporine-like amino acids from marine resource. *Marine Drugs, 19*(1), 18. https://doi.org/10.3390/md19010018

206. Llewellyn, C. A., & Airs, R. L. (2010). Distribution and abundance of MAAs in 33 species of microalgae across 13 classes. *Marine Drugs, 8*(4), 1273-1291. https://doi.org/10.3390/md8041273

207. Bandaranayake, W. M. (1998). Mycosporines: are they nature's sunscreens? *Natural Product Reports, 15*(2), 159-172. https://doi.org/10.1039/A815159Y

208. Banaszak, A. T., & Lesser, M. P. (2009). Effects of solar ultraviolet radiation on coral reef organisms. *Photochemical & Photobiological Sciences, 8*(9), 1276-1294. https://doi.org/10.1039/b902763g

209. Bentley, R. (1990). The shikimate pathway--a metabolic tree with many branches. *Critical Reviews in Biochemistry and Molecular Biology, 25*(5), 307-384. https://doi.org/10.3109/10409239009090615

210. Lalegerie, F., Stiger-Pouvreau, V., & Connan, S. (2020). Temporal variation in pigment and mycosporine-like amino acid composition of the red macroalga *Palmaria palmata* from Brittany (France): Hypothesis on the MAA biosynthesis pathway under high irradiance. *Journal of Applied Phycology, 32*(4), 2641-2656. https://doi.org/10.1007/s10811-020-02075-7

211. Nishida, Y., Kumagai, Y., Michiba, S., Yasui, H., & Kishimura, H. (2020). Efficient extraction and antioxidant capacity of mycosporine-like amino acids from red alga dulse *Palmaria palmata* in Japan. *Marine Drugs, 18*(10), 502. https://doi.org/10.3390/md18100502

212. Orfanoudaki, M., Hartmann, A., Karsten, U., Ganzera, M., & Müller, K. (2019). Chemical profiling of mycosporine-like amino acids in twenty-three red algal species. *Journal of Phycology, 55*(2), 393-403. https://doi.org/10.1111/jpy.12827

213. Sun, Y., Zhang, N., Zhou, J., Dong, S., Zhang, X., Guo, L., & Guo, G. (2020). Distribution, contents, and types of mycosporine-like amino acids (MAAs) in marine macroalgae and a database for MAAs based on these characteristics. *Marine Drugs, 18*(1), 43. https://doi.org/10.3390/md18010043

214. Hylander, S. (2020). Mycosporine-like amino acids (MAAs) in zooplankton. *Marine Drugs, 18*(2), 72. https://doi.org/10.3390/md18020072

215. Kokabi, M., Yousefzadi, M., Nejad Ebrahimi, S., & Zarei, M. (2020). Extraction and characterization of UV-absorbing compounds from sea urchin *Echinometra mathaei*. *Aquatics Physiology and Biotechnology, 8*(8), 99-115. https://doi.org/10.22124/japb.2020.14293.1346

216. Pathak, J., Ahmed, H., Singh, P. R., Singh, S. P., Häder, D.-P., & Sinha, R. P. (2019). Mechanisms of photoprotection in cyanobacteria. In A. K. Mishra, D. N. Tiwari, & A. N. Rai (Eds.), *Cyanobacteria*, (pp. 145-171). Elsevier. https://doi.org/10.1016/b978-0-12-814667-5.00007-6

217. Xu, J., Zhang, X., Fu, Q., Gao, G., & Gao, K. (2018). Water depth-dependant photosynthetic and growth rates of *Gracilaria lemaneiformis*, with special reference to effects of solar UV radiation. *Aquaculture, 484*, 28-31. https://doi.org/10.1016/j.aquaculture.2017.10.035

218. Gómez, I., Navarro, N. P., & Huovinen, P. (2019). Bio-optical and physiological patterns in Antarctic seaweeds: A functional trait based approach to characterize vertical zonation. *Progress in Oceanography, 174*, 17-27. https://doi.org/10.1016/j.pocean.2018.03.013

219. Jofre, J., Celis-Plá, P. S. M., Figueroa, F. L., & Navarro, N. P. (2020). Seasonal variation of mycosporine-like amino acids in three subantarctic red seaweeds. *Marine Drugs, 18*(2), 75. https://doi.org/10.3390/md18020075

220. Lalegerie, F., Gager, L., Stiger-Pouvreau, V., & Connan, S. (2020). The stressful life of red and brown seaweeds on the temperate intertidal zone: Effect of abiotic and biotic parameters on the physiology of macroalgae and content variability of particular metabolites. In N. Bourgougnon (Ed.), *Seaweeds Around the World: State of Art and Perspectives, 95*, (pp. 247-287). https://doi.org/10.1016/bs.abr.2019.11.007

221. Gómez, I., & Huovinen, P. (2020). Brown algal phlorotannins: an overview of their functional roles. In I. Gómez, & P. Huovinen (Eds.), *Antarctic Seaweeds*, (pp. 365-388). Springer Cham, Switzerland. https://doi.org/10.1007/978-3-030-39448-6_18

222. Mannino, A. M., & Micheli, C. (2020). Ecological function of phenolic compounds from mediterranean fucoid algae and seagrasses: An overview on the genus *Cystoseira* sensu lato and *Posidonia oceanica* (L.) Delile. *Journal of Marine Science and Engineering, 8*(1), 19. https://doi.org/10.3390/jmse8010019

223. Polo, L. K., & Chow, F. (2020). Physiological performance by growth rate, pigment and protein content of the brown seaweed Sargassum filipendula (Ochrophyta: Fucales) induced by moderate UV radiation exposure in the laboratory. *Scientia Marina, 84*(1), 59. https://doi.org/10.3989/scimar.04982.22A

224. Schmitz, C., Ramlov, F., de Lucena, L. A. F., Uarrota, V., Batista, M. B., Sissini, M. N., Oliveira, I., Briani, B., Martins, C. D. L., Nunes, J. M. d. C., Rörig, L., Horta, P. A., Figueroa, F. L., Korbee, N., Maraschin, M., & Bonomi-Barufi, J. (2018). UVR and PAR absorbing compounds of marine brown macroalgae along a latitudinal gradient of the Brazilian coast. *Journal of Photochemistry and Photobiology B: Biology, 178*, 165-174. https://doi.org/10.1016/j.jphotobiol.2017.10.029

225. Pescheck, F. (2019). UV-A screening in *Cladophora* sp. lowers internal UV-A availability and photoreactivation as compared to non-UV screening in Ulva intestinalis. *Photochemical & Photobiological Sciences, 18*(2), 413-423. https://doi.org/10.1039/C8PP00432C

226. Berkelmans, R., & Willis, B. L. (1999). Seasonal and local spatial patterns in the upper thermal limits of corals on the inshore Central Great Barrier Reef. *Coral Reefs, 18*(3), 219-228. https://doi.org/10.1007/s003380050186

227. Hoegh-Guldberg, O. (1999). Climate change, coral bleaching and the future of the world's coral reefs. *Marine and Freshwater Research, 50*(8), 839-866. https://doi.org/10.1071/mf99078

228. van de Water, J. A. J. M., Courtial, L., Houlbrèque, F., Jacquet, S., & Ferrier-Pagès, C. (2018). Ultraviolet radiation has a limited impact on seasonal differences in the *Acropora muricata* holobiont. *Frontiers in Marine Science, 5*, 275. https://doi.org/10.3389/fmars.2018.00275

229. Zhou, J., Fan, T.-Y., Beardall, J., & Gao, K. (2017). UV-A induced delayed development in the larvae of coral *Seriatopora caliendrum*. *Journal of Photochemistry and Photobiology B: Biology, 167*, 249-255. https://doi.org/10.1016/j.jphotobiol.2017.01.007

230. Zhou, J., Huang, H., Beardall, J., & Gao, K. (2017). Effect of UV radiation on the expulsion of *Symbiodinium* from the coral *Pocillopora damicornis*. *Journal of Photochemistry and Photobiology B: Biology, 166*, 12-17. https://doi.org/10.1016/j.jphotobiol.2016.11.003

231. Mouchi, V., Chapron, L., Peru, E., Pruski, A. M., Meistertzheim, A. L., Vetion, G., Galand, P. E., & Lartaud, F. (2019). Long-term aquaria study suggests species-specific responses of two cold-water corals to macro-and microplastics exposure. *Environmental Pollution, 253*, 322-329. https://doi.org/10.1016/j.envpol.2019.07.024

232. Nordborg, F. M., Flores, F., Brinkman, D. L., Agustí, S., & Negri, A. P. (2018). Phototoxic effects of two common marine fuels on the settlement success of the coral *Acropora tenuis*. *Scientific Reports, 8*(1), 8635. https://doi.org/10.1038/s41598-018-26972-7

233. McCauley, M., Banaszak, A. T., & Goulet, T. L. (2018). Species traits dictate seasonal-dependent responses of octocoral–algal symbioses to elevated temperature and ultraviolet radiation. *Coral Reefs, 37*(3), 901-917. https://doi.org/10.1007/s00338-018-1716-8

234. Banaszak, A. T., Barba Santos, M. G., LaJeunesse, T. C., & Lesser, M. P. (2006). The distribution of mycosporine-like amino acids (MAAs) and the phylogenetic identity of symbiotic dinoflagellates in cnidarian hosts from the Mexican Caribbean. *Journal of Experimental Marine Biology and Ecology, 337*(2), 131-146. https://doi.org/10.1016/j.jembe.2006.06.014

235. Courtial, L., Planas Bielsa, V., Houlbrèque, F., & Ferrier-Pagès, C. (2018). Effects of ultraviolet radiation and nutrient level on the physiological response and organic matter release of the scleractinian coral *Pocillopora damicornis* following thermal stress. *Plos One, 13*(10), e0205261. https://doi.org/10.1371/journal.pone.0205261

236. Blanckaert, A. C. A., de Barros Marangoni, L. F., Rottier, C., Grover, R., & Ferrier-Pagès, C. (2021). Low levels of ultra-violet radiation mitigate the deleterious effects of nitrate and thermal stress on coral photosynthesis. *Marine Pollution Bulletin, 167*, 112257. https://doi.org/10.1016/j.marpolbul.2021.112257

237. Henley, E. M., Quinn, M., Bouwmeester, J., Daly, J., Zuchowicz, N., Lager, C., Bailey, D. W., & Hagedorn, M. (2021). Reproductive plasticity of Hawaiian *Montipora* corals following thermal stress. *Scientific Reports, 11*(1), 12525 https://doi.org/10.1038/s41598-021-91030-8

238. Álvarez-Gómez, F., Korbee, N., Casas-Arrojo, V., Abdala-Díaz, R., & Figueroa, F. (2019). UV Photoprotection, cytotoxicity and immunology capacity of red algae extracts. *Molecules, 24*(2), 341. https://doi.org/10.3390/molecules24020341

239. Bonaventura, R., & Matranga, V. (2017). Overview of the molecular defense systems used by sea urchin embryos to cope with UV radiation. *Marine Environmental Research, 128*, 25-35. https://doi.org/10.1016/j.marenvres.2016.05.019

240. Shick, J. M., Romaine-Lioud, S., Romaine-Lioud, S., Ferrier-Pagès, C., & Gattuso, J. P. (1999). Ultraviolet-B radiation stimulates shikimate pathway-dependent accumulation of mycosporine-like amino acids in the coral *Stylophora pistillata* despite decreases in its population of symbiotic dinoflagellates. *Limnology and Oceanography, 44*(7), 1667-1682. https://doi.org/10.4319/lo.1999.44.7.1667

241. Cubillos, V. M., Ramírez, E. F., Cruces, E., Montory, J. A., Segura, C. J., & Mardones, D. A. (2018). Temporal changes in environmental conditions of a mid-latitude estuary (southern Chile) and its influences in the cellular response of the euryhaline anemone Anthopleura hermaphroditica. *Ecological Indicators, 88*, 169-180. https://doi.org/10.1016/j.ecolind.2018.01.015

242. Brasseur, L., Demeyer, M., Decroo, C., Caulier, G., Flammang, P., Gerbaux, P., & Eeckhaut, I. (2018). Identification and quantification of spinochromes in body compartments of Echinometra mathaei's coloured types. *Royal Society Open Science, 5*(8), 171213. https://doi.org/10.1098/rsos.171213

243. Hylander, S., Grenvald, J. C., Kiørboe, T., & Pfrender, M. (2014). Fitness costs and benefits of ultraviolet radiation exposure in marine pelagic copepods. *Functional Ecology, 28*(1), 149-158. https://doi.org/10.1111/1365-2435.12159

244. Williamson, C. E., Neale, P. J., Grad, G., De Lange, H. J., & Hargreaves, B. R. (2001). Beneficial and detrimental effects of UV radiation: Implications of variation in the spectral composition of environmental radiation for aquatic organisms. *Ecological Applications, 11*, 1843-1857. https://doi.org/10.1890/1051-0761(2001)011[1843:BADEOU]2.0.CO;2

245. Sonntag, B., & Sommaruga, R. (2020). Effectiveness of photoprotective strategies in three mixotrophic planktonic ciliate species. *Diversity, 12*(6), 252. https://doi.org/10.3390/d12060252

246. Neale, R. E., Barnes, P. W., Robson, T. M., Neale, P. J., Williamson, C. E., Zepp, R. G., Wilson, S. R., Madronich, S., Andrady, A. L., Heikkila, A. M., Bernhard, G. H., Bais, A. F., Aucamp, P. J., Banaszak, A. T., Bornman, J. F., Bruckman, L. S., Byrne, S. N., Foereid, B., Hader, D. P., Hollestein, L. M., et al. (2021). Environmental effects of stratospheric ozone depletion, UV radiation, and interactions with climate change: UNEP Environmental Effects Assessment Panel, Update 2020. *Photochemical & Photobiological Sciences, 20*(1), 1-67. https://doi.org/10.1007/s43630-020-00001-x

247. Laspoumaderes, C., Bastidas Navarro, M., Souza, M. S., Modenutti, B., & Balseiro, E. (2019). Effect of ultraviolet radiation on clearance rate of planktonic copepods with different photoprotective strategies. *International Review of Hydrobiology, 104*(1-2), 34-44. https://doi.org/10.1002/iroh.201801960

248. Wolinski, L., Souza, M. S., Modenutti, B., & Balseiro, E. (2020). Effect of chronic UVR exposure on zooplankton molting and growth. *Environmental Pollution, 267*, 115448. https://doi.org/10.1016/j.envpol.2020.115448

249. Bancroft, B. A., Baker, N. J., & Blaustein, A. R. (2007). Effects of UVB radiation on marine and freshwater organisms: a synthesis through meta-analysis. *Ecology Letters, 10*(4), 332-345. https://doi.org/10.1111/j.1461-0248.2007.01022.x

250. Llabrés, M., Agustí, S., Fernández, M., Canepa, A., Maurin, F., Vidal, F., Duarte, C. M., & Rex, M. (2013). Impact of elevated UVB radiation on marine biota: a meta-analysis. *Global Ecology and Biogeography, 22*(1), 131-144. https://doi.org/10.1111/j.1466-8238.2012.00784.x

251. Peng, X., Fan, Y., Jin, J., Xiong, S., Liu, J., & Tang, C. (2017). Bioaccumulation and biomagnification of ultraviolet absorbents in marine wildlife of the Pearl River Estuarine, South China Sea. *Environmental Pollution, 225*, 55-65. https://doi.org/10.1016/j.envpol.2017.03.035

252. Bashevkin, S. M., Christy, J. H., & Morgan, S. G. (2020). Costs and compensation in zooplankton pigmentation under countervailing threats of ultraviolet radiation and predation. *Oecologia, 193*(1), 111-123. https://doi.org/10.1007/s00442-020-04648-2

253. Bashevkin, S. M., Christy, J. H., Morgan, S. G., & Clusella Trullas, S. (2019). Adaptive specialization and constraint in morphological defences of planktonic larvae. *Functional Ecology, 34*(1), 217-228. https://doi.org/10.1111/1365-2435.13464

254. Eshun-Wilson, F., Wolf, R., Andersen, T., Hessen, D. O., & Sperfeld, E. (2020). UV radiation affects antipredatory defense traits in Daphnia pulex. *Ecology and Evolution, 10*(24), 14082-14097. https://doi.org/10.1002/ece3.6999

255. Stabile, F., Bronmark, C., Hansson, L. A., & Lee, M. (2021). Fitness cost from fluctuating ultraviolet radiation in *Daphnia magna*. *Biology Letters, 17*(8), 20210261. https://doi.org/10.1098/rsbl.2021.0261

256. Hansson, L.-A., & Hylander, S. (2009). Effects of ultraviolet radiation on pigmentation, photoenzymatic repair, behavior, and community ecology of zooplankton. *Photochemical & Photobiological Sciences, 8*(9), 1266. https://doi.org/10.1039/b908825c

257. Lee, M., Zhang, H., Sha, Y., Hegg, A., Ugge, G. E., Vinterstare, J., Škerlep, M., Pärssinen, V., Herzog, S. D., Björnerås, C., Gollnisch, R., Johansson, E., Hu, N., Nilsson, P. A., Hulthén, K., Rengefors, K., Langerhans, R. B., Brönmark, C., & Hansson, L.-A. (2019). Low-latitude zooplankton pigmentation plasticity in response to multiple threats. *Royal Society Open Science, 6*(7), 190321. https://doi.org/10.1098/rsos.190321

258. Marcoval, M. A., Pan, J., Diaz, A. C., & Fenucci, J. L. (2021). Dietary bioaccumulation of UV-absorbing compounds, and post-ingestive fitness in larval planktotrophic crustaceans from coastal SW Atlantic. *Marine Environmental Research, 170*, 105433. https://doi.org/10.1016/j.marenvres.2021.105433

259. Wolinski, L., Modenutti, B., & Balseiro, E. (2020). Melanin and antipredatory defenses in *Daphnia dadayana* under UVR exposure. *International Review of Hydrobiology, 105*(3-4), 106-114. https://doi.org/10.1002/iroh.201902033

260. Fernandéz, C. E., Campero, M., Bianco, G., Ekvall, M. T., Rejas, D., Uvo, C. B., & Hansson, L. A. (2020). Local adaptation to UV radiation in zooplankton: a behavioral and physiological approach. *Ecosphere, 11*, e03081. https://doi.org/10.1002/ecs2.3081

261. Sha, Y., Tesson, S. V. M., & Hansson, L. A. (2020). Diverging responses to threats across generations in zooplankton. *Ecology, 101* e03145. https://doi.org/10.1002/ecy.3145

262. Dur, G., Won, E.-J., Han, J., Lee, J.-S., & Souissi, S. (2021). An individual-based model for evaluating post-exposure effects of UV-B radiation on zooplankton reproduction. *Ecological Modelling, 441*, 109379. https://doi.org/10.1016/j.ecolmodel.2020.109379

263. Ekvall, M. T., Sha, Y., Palmér, T., Bianco, G., Bäckman, J., Åström, K., & Hansson, L. A. (2020). Behavioural responses to co-occurring threats of predation and ultraviolet radiation in *Daphnia*. *Freshwater Biology, 65*(9), 1509-1517. https://doi.org/10.1111/fwb.13516

264. Lee, M., & Hansson, L. A. (2021). Daphnia magna trade-off safety from UV radiation for food. *Ecology and Evolution, 11*(24), 18026-18031. https://doi.org/10.1002/ece3.8399

265. Rose, K. C., Williamson, C. E., Fischer, J. M., Connelly, S. J., Olson, M., Tucker, A. J., & Noe, D. A. (2012). The role of ultraviolet radiation and fish in regulating the vertical distribution of *Daphnia*. *Limnology and Oceanography, 57*(6), 1867-1876. https://doi.org/10.4319/lo.2012.57.6.1867

266. Urmy, S. S., Williamson, C. E., Leach, T. H., Schladow, S. G., Overholt, E. P., & Warren, J. D. (2016). Vertical redistribution of zooplankton in an oligotrophic lake associated with reduction in ultraviolet radiation by wildfire smoke. *Geophysical Research Letters, 43*(8), 3746-3753. https://doi.org/10.1002/2016gl068533

267. Williamson, C. E., Overholt, E. P., Brentrup, J. A., Pilla, R. M., Leach, T. H., Schladow, S. G., Warren, J. D., Urmy, S. S., Sadro, S., Chandra, S., & Neale, P. J. (2016). Sentinel responses to droughts, wildfires, and floods: Ultraviolet radiation and the consequences for lakes and their ecosystem services. *Frontiers in Ecology and Environment, 14*, 102-109. https://doi.org/10.1002/fee.1228

268. Scordo, F., Chandra, S., Suenaga, E., Kelson, S. J., Culpepper, J., Scaff, L., Tromboni, F., Caldwell, T. J., Seitz, C., Fiorenza, J. E., Williamson, C. E., Sadro, S., Rose, K. C., & Poulson, S. R. (2021). Smoke from regional wildfires alters lake ecology. *Scientific Reports, 11*(1), 10922. https://doi.org/10.1038/s41598-021-89926-6

269. Sha, Y., Zhang, H., Lee, M., Björnerås, C., Škerlep, M., Gollnisch, R., Herzog, S. D., Ekelund Ugge, G., Vinterstare, J., Hu, N., Pärssinen, V., Hulthén, K., Nilsson, P. A., Rengefors, K., Brönmark, C., Langerhans, R. B., & Hansson, L.-A. (2020). Diel vertical migration of copepods and its environmental drivers in subtropical Bahamian blue holes. *Aquatic Ecology, 55*(4), 1157-1169. https://doi.org/10.1007/s10452-020-09807-4

270. Oester, R., Greenway, R., Moosmann, M., Sommaruga, R., Tartarotti, B., Brodersen, J., & Matthews, B. (2022). The influence of predator community composition on photoprotective traits of copepods. *Ecology and Evolution, 12*(4), e8862. https://doi.org/10.1002/ece3.8862

271. Marinone, M. C., Marque, S. M., Suárez, D. A., del Carmen Diéguez, M., Pérez, P., De Los Ríos, P., Soto, D., & Zagarese, H. E. (2006). UV radiation as a potential driving force for zooplankton community structure in Patagonian lakes. *Photochemistry and Photobiology, 82*(4), 962. https://doi.org/10.1562/2005-09-09-ra-680

272. Williamson, C. E., Olson, O. G., Lott, S. E., Walker, N. D., Engstrom, D. R., & Hargreaves, B. R. (2001). Ultraviolet radiation and zooplankton community structure following deglaciation in Glacier Bay, Alaska. *Ecology, 82*(6), 1748-1760. https://doi.org/10.1890/0012-9658(2001)082[1748:Urazcs]2.0.Co;2

273. Caputo, L., Huovinen, P., Sommaruga, R., & Gómez, I. (2018). Water transparency affects the survival of the medusa stage of the invasive freshwater jellyfish *Craspedacusta sowerbii*. *Hydrobiologia, 817*(1), 179-191. https://doi.org/10.1007/s10750-018-3520-4

274. Lindholm, M., Wolf, R., Finstad, A., & Hessen, D. O. (2016). Water browning mediates predatory decimation of the Arctic fairy shrimp *Branchinecta paludosa*. *Freshwater Biology, 61*(3), 340-347. https://doi.org/10.1111/fwb.12712

275. Alves, R. N., & Agustí, S. (2020). Effect of ultraviolet radiation (UVR) on the life stages of fish. *Reviews in Fish Biology and Fisheries, 30*(2), 335-372. https://doi.org/10.1007/s11160-020-09603-1

276. Lawrence, K. P., Young, A. R., Diffey, B. L., & Norval, M. (2019). The impact of solar ultraviolet radiation on fish: Immunomodulation and photoprotective strategies. *Fish and Fisheries, 21*(1), 104-119. https://doi.org/10.1111/faf.12420

277. Araujo, M. J., Quintaneiro, C., Soares, A., & Monteiro, M. S. (2021). Effects of ultraviolet radiation to *Solea senegalensis* during early development. *Science of the Total Environment, 764*, 142899. https://doi.org/10.1016/j.scitotenv.2020.142899

278. Pasparakis, C., Wang, Y., Heuer, R. M., Zhang, W., Stieglitz, J. D., McGuigan, C. J., Benetti, D. D., Scholey, V. P., Margulies, D., & Grosell, M. (2022). Ultraviolet avoidance by embryonic buoyancy control in three species of marine fish. *Science of the Total Environment, 806*(Pt 3), 150542. https://doi.org/10.1016/j.scitotenv.2021.150542

279. Pasparakis, C., Wang, Y., Stieglitz, J. D., Benetti, D. D., & Grosell, M. (2019). Embryonic buoyancy control as a mechanism of ultraviolet radiation avoidance. *Science of the Total Environment, 651*(Pt 2), 3070-3078. https://doi.org/10.1016/j.scitotenv.2018.10.093

280. Ward, C. P., Bowen, J. C., Freeman, D. H., & Sharpless, C. M. (2021). Rapid and reproducible characterization of the wavelength dependence of aquatic photochemical reactions using light-emitting diodes. *Environmental Science & Technology Letters, 8*(5), 437-442. https://doi.org/10.1021/acs.estlett.1c00172

281. Pandey, U. C., Nayak, S. R., Roka, K., & Jain, T. K. (2021). *SDG14 – Life Below Water: Towards Sustainable Management of Our Oceans*. https://doi.org/10.1108/9781800717091

6

CHANGES IN TROPOSPHERIC AIR QUALITY RELATED TO THE PROTECTION OF STRATOSPHERIC OZONE IN A CHANGING CLIMATE

S. Madronich[106],[107], B. Sulzberger[108], J. D. Longstreth[109], T. Schikowski[110], M. P. Sulbæk Andersen[111], K. R. Solomon[112], and S. R. Wilson[113]

---

[106] National Center for Atmospheric Research, Boulder, USA

[107] USDA UV-B Monitoring and Research Program, Natural Resource Ecology Laboratory, Colorado State University, Fort Collins, USA.

[108] Academic Guest after retirement from Swiss Federal Institute of Aquatic Science and Technology, CH-8600 Duebendorf, Switzerland.

[109] The Institute for Global Risk Research, LLC, Bethesda, USA.

[110] IUF-Leibniz Research Institute for Environmental Medicine, Dusseldorf, Germany.

[111] Department of Chemistry and Biochemistry, California State University, Northridge, USA.

[112] School of Environmental Sciences, University of Guelph, Guelph, Canada.

[113] School of Earth, Atmospheric and Life Sciences, University of Wollongong, Wollongong, Australia.

Table of contents

Summary

Ultraviolet (UV) radiation drives the net production of tropospheric ozone (O_3) and a large fraction of particulate matter (PM) including sulfate, nitrate, and secondary organic aerosols. Ground-level O_3 and PM are detrimental to human health, leading to several million premature deaths per year globally, and have adverse effects on plants and the yields of crops. The Montreal Protocol has prevented large increases in UV radiation that would have had major impacts on air quality. Future scenarios in which stratospheric O_3 returns to 1980 values or even exceeds them (the so-called super-recovery) will tend to ameliorate urban ground-level O_3 slightly but worsen it in rural areas. Furthermore, recovery of stratospheric O_3 is expected to increase the amount of O_3 transported into the troposphere by meteorological processes that are sensitive to climate change.

UV radiation also generates hydroxyl radicals (OH) that control the amounts of many environmentally important chemicals in the atmosphere including some greenhouse gases, e.g., methane (CH_4), and some short-lived ozone-depleting substances (ODSs). Recent modelling studies have shown that the increases in UV radiation associated with the depletion of stratospheric ozone over 1980-2020 have contributed a small increase (~3%) to the globally averaged concentrations of OH.

Replacements for ODSs include chemicals that react with OH radicals, hence preventing the transport of these chemicals to the stratosphere. Some of these chemicals, e.g., hydrofluorocarbons that are currently being phased out, and hydrofluoroolefins now used increasingly, decompose into products whose fate in the environment warrants further investigation. One such product, trifluoroacetic acid (TFA), has no obvious pathway of degradation and might accumulate in some water bodies, but is unlikely to cause adverse effects out to 2100.

1 Introduction

The protection of stratospheric ozone (O_3) has had important consequences for the chemical composition of the lower atmosphere (the troposphere) and the quality of the air that humans and many other organisms breathe. Ultraviolet (UV) radiation plays an essential role in the generation of photochemical smog, exposure to which is associated with widespread health effects, reductions in life expectancies, damage to forests, and smaller agricultural yields. Given the number of populations and ecosystems currently affected by photochemical smog, even small changes in UV radiation are important, such as those associated with the few percent depletion of stratospheric O_3 that occurred at midlatitudes over 1980-2000. By limiting the depletion of stratospheric O_3, the Montreal Protocol has avoided large increases in tropospheric UV radiation that would have exacerbated photochemical air pollution in urban areas.

On the global scale, UV-B radiation (280-315 nm) controls the self-cleaning capacity of the troposphere by generating hydroxyl radicals (OH). These radicals react with many chemicals emitted to the troposphere, including greenhouse gases such as methane, facilitating their removal from the atmosphere and essentially determining their atmospheric lifetime. The Montreal Protocol has maintained the troposphere's self-cleaning capacity at near natural levels, but future changes remain a concern, especially if the intensity of UV-B radiation decreases substantially due to increasing stratospheric ozone under some future scenarios.

Actions under the Montreal Protocol have led to the introduction of new chemicals to the atmosphere as replacements to some of the ozone-depleting substances, including hydrofluorochlorocarbons (HCFCs), hydrofluorocarbons (HFCs), hydrofluoroethers (HFEs), hydrofluoroolefins (HFOs) and hydrochlorofluoroolefins (HCFOs). However, their atmospheric photo-degradation can lead to persistent secondary pollutants such as trifluoroacetic acid (TFA), whose ultimate fate in the environment remains unclear, requiring continued monitoring and assessment relative to other natural and/or anthropogenic sources.

We have reported on these issues in our previous assessments [1-6] and our objective here is to provide an updated overview and assessment of the scientific evidence. As will be presented in the following sections, our previous conclusions remain qualitatively unchanged and consistent with increasingly available observations and numerical simulations. This assessment consists of two parts: The first part (Sect. 2) focuses on the effects of depletion of stratospheric ozone, solar UV radiation (particularly UV-B), and interactions with climate change on tropospheric air quality and how changes in tropospheric air quality affect human health and ecosystems. The second part (Sect. 3) assesses the known sources of trifluoroacetic acid (TFA), including those related to the replacement chemicals under the purview of the Montreal Protocol, and their potential risk to humans and ecosystems.

In conducting this assessment, we have searched the literature through PubMed®, Google Scholar, ScienceDirect®, and relevant journals to obtain peer-reviewed papers from the recent literature (2018–2022) as well as reports from recognised international agencies (e.g., World Health Organization) and government agencies (e.g., US Environmental Protection Agency). We have critically evaluated these papers and reports before including information from them in this Quadrennial Assessment.

2 UV-dependent air pollutants and their effects on human health, plants, and the self-cleaning capacity of the troposphere

The importance of UV radiation to the formation of some types of air pollution has been known at least since the studies of photochemical smog in Los Angeles in the 1950s, when it was shown that ambient O_3 was generated by UV-induced reactions involving nitrogen oxides (NOx) and volatile organic compounds (VOCs) [7]. Since then, many details of these photochemical reactions have been elucidated, such as the central role of UV-generated OH radicals in controlling the overall reactivity; and the formation of O_3, peroxides, acids, and other harmful gaseous intermediates, including some that can condense to form particulate matter (PM). This gas- and solid-phase chemistry is complex, involving hundreds of different chemicals, often with rapidly changing emissions and different environmental conditions.

A brief overview/summary of tropospheric chemistry, with emphasis on the distinct roles of UV-B and UV-A radiation, is provided in Sect. 2.1. The formation of photochemical smog, specifically its ground-level O_3 and UV-sensitive PM components, is discussed in Sect. 2.2 and 2.3, including an assessment of the possible effects of changes in UV radiation related to the recovery of stratospheric ozone over the coming decades. Exposure to photochemical smog can have large impacts on human health, particularly in vulnerable populations even at low concentrations of pollutants (Sect. 2.4). Tropospheric O_3 and PM can also affect plant health (Sect. 2.5). UV-B radiation has beneficial effects by causing the formation of OH, the cleaning agent of the troposphere (Sect. 2.6). Finally, changes in atmospheric circulation and the transport of pollutants affects the tropospheric air quality (Sect. 2.7). A summary of our assessment is provided in Sect. 2.8.

2.1   Background: The UV photochemistry of tropospheric air

The most important UV-induced processes that control air quality in the troposphere are shown in Fig. 1. UV-B radiation is responsible for the formation of the OH radical, the major oxidising agent in the troposphere. This occurs through the photolysis of O_3 and subsequent reaction of an electronically excited oxygen atom with water (H_2O). Hydroxyl radicals are lost by reaction with reduced chemicals, including carbon monoxide (CO), methane (CH_4), VOCs, sulfur dioxide (SO_2), and nitrogen dioxide (NO_2) (Fig. 1). Hydroxyl radicals control the atmospheric amounts of these chemicals as well as those of many other important trace gases, e.g., HFCs, HCFCs, HFOs, and very-short-lived substances (VSLSs, e.g., halo-organics with a lifetime of less than or equal to 6 months). Chemicals such as chlorofluorocarbons (CFCs) that do not react with OH have the potential to reach the stratosphere in large amounts; the CFCs were therefore replaced with chemicals that react with OH (HCFCs, HFCs, HFOs, etc.).

UV-B and UV-A radiation are together responsible for the net production of O_3 in the troposphere. This occurs via photo-dissociation of nitrogen dioxide (NO_2) to NO and O, mainly by UV-A radiation, and subsequent reaction of the oxygen atom with molecular oxygen (Fig.1). Nitrogen oxides (NOx = NO + NO_2) are emitted primarily as NO, and the NO_2 is produced via the re-cycling of the hydroxyl radical (OH) generated from the UV-B photolysis of O_3. Due to this autocatalytic production of O_3 involving OH, the net production of O_3 depends not only on UV A radiation but also on UV-B radiation. The different effects of UV-B and UV-A radiation are discussed in more detail in Box 1. Note that Fig.1 is restricted to reactions occurring in the gas phase, while heterogeneous, UV-induced processes involving aerosols are discussed in Sect. 2.3.
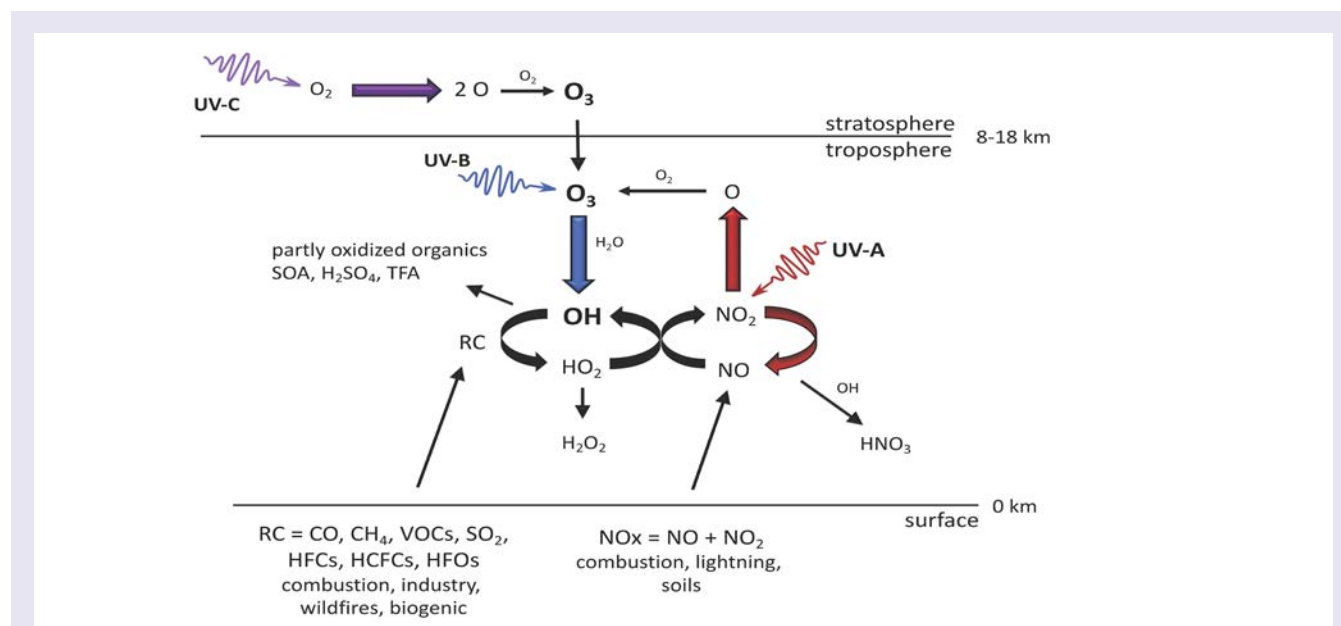
Fig. 1 Simplified schematic of tropospheric photochemistry. UV-C radiation (100-280 nm) in the stratosphere generates ozone, O_3, some of which is transported to the troposphere. UV-B radiation initiates tropospheric chemistry by photo-dissociating O_3 and generating highly reactive hydroxyl radicals (OH). These react with many compounds emitted by human activities and natural processes, e.g., carbon monoxide, methane, volatile organic compounds including halocarbons, and others, all generalised in the figure as RC (reduced compounds). By removing these compounds, the concentration of OH controls the self-cleaning capacity of the atmosphere. Nitrogen oxides (NOx = NO + NO_2) catalyze the photo-oxidation by regenerating OH via reaction of NO with HO_2. This coupling of the NOx and HOx (OH + HO_2) cycles also leads to autocatalytic production of O_3, often in amounts larger than lost initially via its UV-B photolysis, since NOx and HOx molecules can cycle many times before being removed. The cycles are terminated by reaction with OH to make nitric acid, (HNO_3) or by reaction of HO_2 to inorganic or organic peroxides, e.g., hydrogen peroxide (H_2O_2). Other products, depending on the reduced compounds being oxidised by OH, could include partly oxidised organics, secondary organic aerosols (SOA), sulfuric acid (H_2SO_4), and trifluoroacetic acid (TFA).

2.2   UV radiation and ground-level ozone

Ground-level O_3 continues to be a major environmental problem, with costly impacts on human health and vegetation. Most ground-level O_3 is produced by the UV photochemical processing of pollutants (see Sect. 2.1), with occasional contributions from downward transport of ozone-rich stratospheric air (see Sect. 2.7). It is generally accepted that concentrations of O_3 have increased throughout the global troposphere over the past century, due to increasing emissions of VOCs and NOx. This is borne out in numerical simulations with chemistry-climate models, as shown in Fig. 2. Contributions from stratospheric ozone de-pletion (1980 to current) and the associated increases in UV-B radiation have been negligible by comparison, at least for the global scale. Future project-ions tend to show an increasing global burden of O_3, although the details depend on the assumed scenario of greenhouse gas emissions (only one shown in the figure, SSP370).
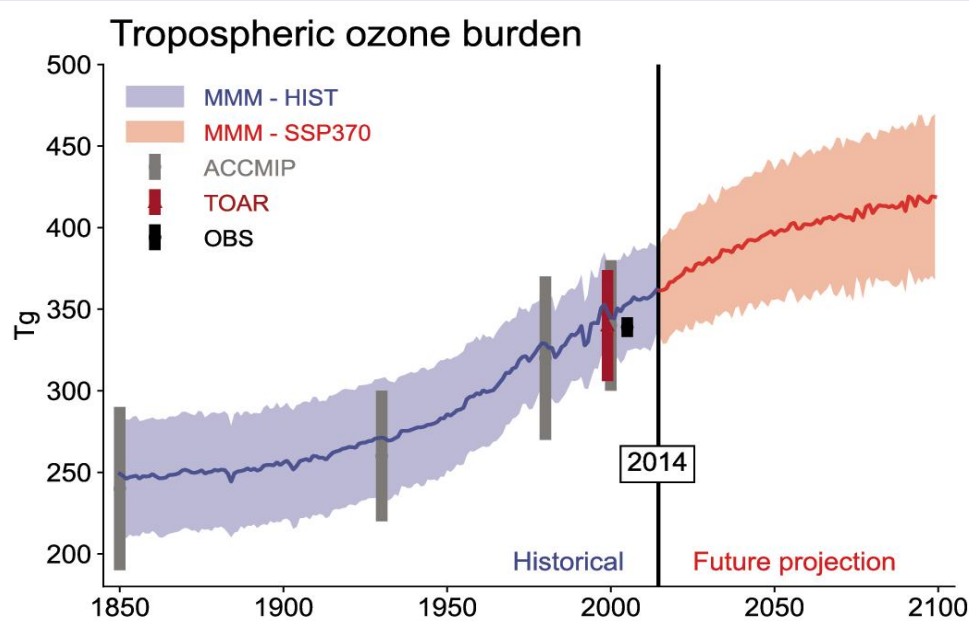

Fig. 2 Global tropospheric ozone (Tg) estimated by multi-model assessments (MMM, ACCMIP, TOAR) and observations (OBS, for the year 2000). Future projections are for one Shared Socioeconomic Pathway (SSP370 scenario). From IPCC 2021 Ch. 6 [11].

Box 1. Effects of different UV wavelengths on the photochemistry of ozone and hydroxyl radicals in the troposphere

Photochemical reactions in the troposphere are controlled by UV-B (280-315 nm) and UV-A (315-400 nm) radiation, while UV-C (100-280 nm) photons are absorbed entirely by stratospheric O_2 and O_3. Among its many important effects, tropospheric UV radiation generates hydroxyl radicals (the self-cleaning agent of the atmosphere; Sect. 2.6),

$O_3 + h\nu(\lambda < 330 \text{ nm}) \rightarrow O^* + O_2$

$O^* + H_2O \rightarrow OH + OH$

and is the final step in the production of tropospheric O_3 (Sect. 2.2)

$NO_2 + h\nu (\lambda < 420 \text{ nm}) \rightarrow NO + O$

$O + O_2 \rightarrow O_3$
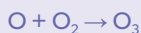
Quantification of how UV radiation regulates the chemistry of the troposphere is fundamental to the development of scientifically sound models of air quality and chemistry-climate interactions. In general, for a photo-dissociation (or photolysis) reaction,

$\qquad AB + h\nu \rightarrow A + B$

where its rate is proportional to the first-order rate coefficient, J_{AB} (s^{-1}), which can be calculated as an integral over relevant wavelengths λ,

$\qquad J_{AB} = \int F(\lambda)\ \sigma(\lambda)\ \varphi(\lambda)\ d\lambda$ (Equation 1)

where $F(\lambda)$ is the spectral actinic flux (quanta $cm^{-2}\ s^{-1}$) at a location and time, $\sigma(\lambda)$ is the absorption cross section (cm^2 $molecule^{-1}$) of the photo-labile molecule AB, and $\varphi(\lambda)$ is the efficiency or yield (molecule $quantum^{-1}$) of the products of interest (the photo-fragments A and B, above).
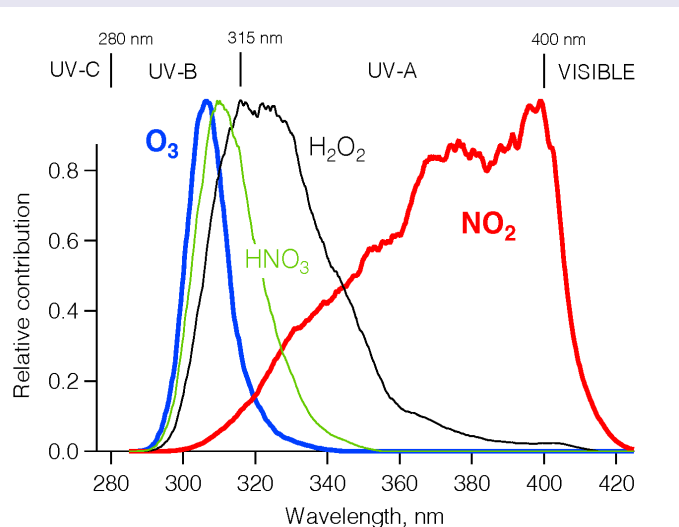
Box 1. *Continued*

The graph shows the spectral dependence (the integrand of Eq. 1) for several photolysis reactions that are of major importance in tropospheric chemistry. Both UV-B and UV-A radiation are relevant, but with different roles because UV-B affects primarily the photo-dissociation of O_3 (J_{O_2}), while UV-A dominates the photolysis of NO_2 (J_{NO_2}). Other UV photo-dissociation reactions, for example of HNO_3, H_2O_2, and numerous organic chemicals (carbonyls, nitrates, peroxides, not shown in the graph), also contribute to the rates of formation and destruction of photochemical smog.

Contribution of different wavelengths to the photolysis rate coefficient for ozone (O_3, blue), nitric acid (HNO_3, green), hydrogen peroxide (H_2O_2, black) and nitrogen dioxide (NO_2, red). Each curve has been normalised to 1.0 at its maximum.

Box 2 Major UV photo-dissociation reactions in the troposphere. The sensitivity is the percentage increase in the rate of reaction for each 1 percent decrease in the O_3 column. The sensitivity is the percentage increase in the rate of reaction for each 1 percent decrease in the O_3 column.

The table shows the estimated sensitivity of key photolysis reactions to the amount of overhead O_3. Specifically, the sensitivity gives the percentage increase in the photo-dissociation rate coefficient (J) for a 1% decrease in the O_3 column. Reactions which are mostly in the UV-B waveband have the largest sensitivities. Changes in UV-B radiation (i.e., those that occur with stratospheric ozone depletion) have a different effect on tropospheric chemistry than changes in UV-A radiation (which might be due to, for example, clouds or aerosols). This is illustrated in the graph of Box 3 with a highly simplified kinetic model. It can be seen that (i) O_3 is produced rapidly in the first few hours (near sources, often in urban settings) but decreases gradually on longer timescales and thus distance from sources; (ii) decreases in the NO_2 photolysis rate coefficient (J_{NO_2}, due mostly to UV-A wavelengths) cause lower O_3 in the urban region but make little or no difference far from sources; and (iii) decreasing the O_3 photolysis rate coefficient J_{O_3} due mostly to UV-B wavelengths) decreases near-source O_3 (even more than the J_{NO_2} decrease), but at longer times it causes an increase in O_3. Thus, both positive and negative changes of ambient O_3 concentrations can be expected in response to changes in UV-B radiation. Specifically, higher (lower) UV-B amounts imply faster (slower) production as well as faster (slower) destruction.

While the overall principles are well understood [9,10], the precise values and timing of these changes depend on the specific chemical mixtures and geographic scales of interest and are not fully known. Accurate prediction of how multiple secondary pollutants (O_3, secondary PM, peroxides) respond to changes in UV radiation remains a fundamental challenge to the modeling of air quality.

Trends in local and regional concentrations of tropospheric O_3 vary greatly as shown in Fig. 3. Over the past few decades, concentrations of O_3 at ground-level and in the lower atmosphere have been generally decreasing in most developed countries, while increasing greatly in some locations including East and South Asia, in response to changes in emissions of NOx and VOCs. Reductions in emissions of NOx and VOCs will be necessary to reverse the observed increasing trends, but any substantial future changes in UV radiation could modify the effectiveness of such reductions.
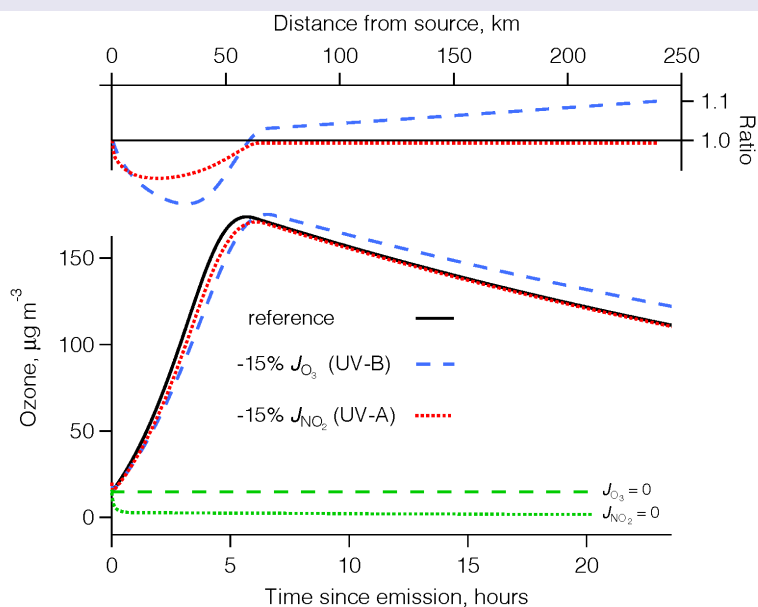
Box 3. Illustration of the response of ground-level ozone to changes in J_{O3} (mostly UV-B) and J_{NO_2} (mostly UV-A), calculated with a simplified kinetic model. Ozone is produced rapidly near sources of pollution (e.g., cities), but is destroyed slowly as air parcels are transported away by winds (taken here as 10 km h^{-1}). Less intense UV-A radiation generates less ozone initially but not at later times. Less intense UV-B radiation leads to even less initial production of O_3, but also to a slower decrease at longer times. The lower panel shows O_3 concentrations, while the upper panel shows the changes as ratios to the reference. Values of the maximum in O_3 concentration and its timing are illustrative only, with actual values sensitive to the spatial and temporal patterns of emissions, the chemical nature of the emissions, day/night cycles, and details of meteorological transport. The reference chemical mechanism is: $O_3+UV\text{-}B \rightarrow 2OH$ (7×10^{-6}); $OH+RC \rightarrow HO_2$ (10^{-11}); $HO_2+NO \rightarrow OH+NO_2$ (8.1×10^{-12}); $O_3+NO \rightarrow NO_2$ (1.9×10^{-14}); $NO_2+UV\text{-}A \rightarrow NO+O_3$ (10^{-2}); $NO_2+OH \rightarrow HNO_3$ (1.1×10^{-11}); $2HO_2 \rightarrow H_2O_2$ (2.90×10^{-12}), with rate coefficient units of s^{-1} for photolysis and cm^3 molec^{-1} s^{-1} for biomolecular reactions, and initial concentrations of O_3 (20 µg m^{-3}), NO (12.5 µg m^{-3}), and RC (10 x NO, molar basis).
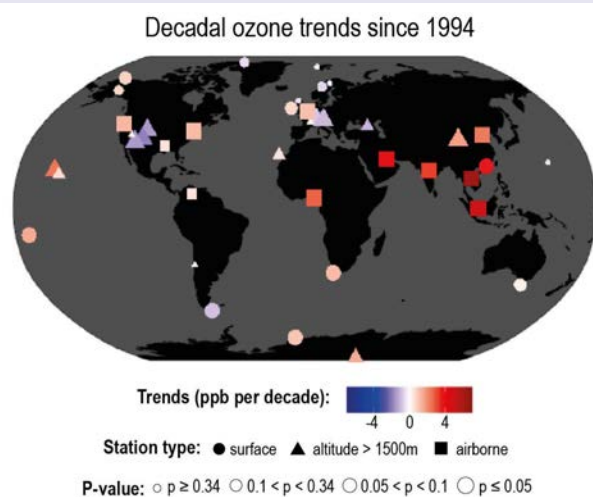
Fig. 3 Regional and local trends in tropospheric ozone at the surface and lower atmosphere. From IPCC 2021 Ch. 6 [11].

The possibility that ground level O_3 can be affected by changes in UV related to depletion of stratospheric ozone was first pointed out by Liu and Trainer [12] and has since been confirmed by several studies using numerical models [13-17], as well as observations at the South Pole [18] and at mid-latitudes [19]. More intense UV-B irradiation generally induces faster chemical reactivity in air parcels (Box 1), leading

to faster removal of primary chemicals, but also more rapid and intense build up (and removal) of intermediate or secondary pollutants, such as hetero-organics (e.g., aldehydes, ketones, and organic nitrates) and other byproducts including O_3, peroxides, and secondary PM. Conversely, reductions in UV radiation decrease chemical reactivity, causing slower production of O_3 and other photochemical pollutants near source regions, e.g., urban areas, while slowing the destruction on regional and global scales.

The decreases in UV radiation at the surface, expected from the recovery of stratospheric O_3, to 1980 levels are estimated to have only a small impact on ambient O_3, as reported previously [14,15], since reductions of O_3 at midlatitudes have been limited to only a few percent (relative to a 1980 baseline). For the United States, the recovery to 1980 levels will increase the O_3 column by 4–6%, and the resulting lower levels of UV radiation will tend to lower ambient O_3 over a few large urban areas, while raising it slightly elsewhere, consistent with an overall slower chemical reactivity. However, recent climate model simulations [20-22], also reviewed in Chapter 1 (Bernhard et al. [23], suggest that under some scenarios of increasing greenhouse gas emissions, stratospheric O_3 could exceed the 1980 baseline (the so-called "super-recovery"). By 2100, stratospheric O_3 could increase by an additional 10% (above the 1980 levels) under high emission scenarios (SSP3-7.0, SSP4-6.0 and SSP5-8.5; see Fig. 3 in Chapter 1 [23]). This would decrease tropospheric J_{O3} by about 14% (Box 2), like the changes used in the sensitivity calculation shown in Box3. Under these scenarios, the changes in tropospheric O_3 (urban declines and regional increases) would be about three times greater than those estimated for recovery limited to 1980 levels [14,15]. Even at current levels (see Fig. 2 and 3), ground level O_3 damages vegetation and causes economically significant reductions in crop yields (see Sect. 2.4 and 2.5). Additional increases due to the recovery (or super-recovery) of stratospheric O_3 are of concern but could be offset by more stringent reductions in emissions of NOx and VOCs.
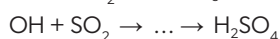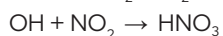
Much larger changes would have occurred without the implementation of the Montreal Protocol (the "world avoided"), where unabated growth of emissions of CFCs would have resulted in catastrophic global loss of stratospheric O_3 [24], with major impacts on UV radiation [25], incidence of skin cancer [26,27], and reduction of the global carbon sink by damage to vegetation [28]. However, to our knowledge, calculations of the impacts of such large increases in UV radiation on air quality, particularly ambient O_3 and secondary aerosols, have not been carried out.

While large changes in UV-B radiation have been avoided by the Montreal Protocol (see Chapter 1 [23]), trends and variability in UV radiation exist also for other reasons (especially due to aerosols and clouds), and these changes provide ongoing opportunities to better understand and quantify the representation of UV-driven chemical processes in models for air quality. Reduced emissions have systematically improved air quality in many locations, but this has increased UV radiation near the surface, potentially negating some of the benefits of the reduced emissions. For example, aerosol haze in China was reduced substantially during the last decade due to lower emissions of NOx and SO_2. This has led to surface brightening (e.g., by 0.70–1.16 W m^{-2} yr^{-1} in eastern China over 2014–2019) [29] but also to undesirable increases in ambient O_3 [30-33] (e.g., by 2–6 µg m^{-3} yr^{-1} in megacity clusters of Beijing and Shanghai over 2013–2017) [34]. Simulations with numerical models show several possible reasons including increases in UV radiation [31,33-39], shifts in the VOC/NOx chemical regime resulting in increased production of O_3 efficiency [35,40], higher emissions of biogenic VOC due to rising temperatures [30], and decreased competition for gas-phase radicals by aerosol surfaces [34,40], with reality likely being a combination of these factors.

Long-term increases in UV radiation at the surface due to improved local air quality have been recorded in many other locations. For example, increasing trends in UV radiation over 1996–2016 were found [41] for stations in Japan and Greece, and were attributed to reductions in absorbing aerosols. More recently, *Ipiña et al.* [42] found that the UV Index in Mexico City increased by *ca.* 20% over 2000–2019 (due to reductions in PM, SO_2, O_3, and NO_2) and estimated that such increases in UV radiation would require an additional 10% reduction in VOC emissions to meet the same ground-level O_3 concentrations had the UV remained constant. Brief increases in UV radiation at the surface have been observed during the economic slowdowns related to the COVID-19 pandemic, e.g., in Brazil [43], East Asia [44], India [45], and likely in many other locations. Analysis of these data is ongoing and should yield insights on how atmospheric pollution responds to changes in UV radiation under different conditions.

2.3   UV radiation and particulate matter

Particulate matter is a major component of air pollution, and particles smaller than about 2.5 µm ($PM_{2.5}$) are believed to be particularly damaging due to their ability to penetrate deeply into lungs. A large fraction of $PM_{2.5}$ is formed by UV-initiated photochemistry. While "primary" PM is emitted directly (e.g., dust, black carbon, or sea spray) "secondary" PM is produced in the atmosphere, typically by condensation of gases having low saturation vapour pressures. These condensable gases are mostly produced by reactions of OH with pollutants such as SO_2, NO_2, or VOCs, to yield sulfate, nitrate, or secondary organic aerosols (SOA), respectively:

$$OH + NO_2 \rightarrow HNO_3$$
$$OH + SO_2 \rightarrow \ldots \rightarrow H_2SO_4$$
$$OH + VOC \rightarrow \ldots \rightarrow OVOC \text{ (various partly oxidised VOCs)} \rightarrow SOA$$

where the last two reactions involve several intermediate steps. The rate-limiting step in the production of these particles is the reaction of OH with the precursors (NO_2, SO_2, or VOCs), so that the dependence of OH on UV radiation (see Sect. 2.1) applies directly to the rate of formation of secondary PM as well. Decreases (increases) in stratospheric O_3 lead to increases (decreases) in tropospheric UV-B radiation and concentrations of OH radicals, and therefore to faster (slower) formation of these PM. The Montreal Protocol, through its influence on the amount of UV radiation reaching the troposphere, has direct consequences for the formation of secondary PM. Primary PM, on the other hand, is not expected to depend strongly on UV irradiation.

The relative amounts of primary and secondary PM vary greatly in time and space, and estimates exist only for regions where reliable emission inventories exist. For the contiguous United States (Fig. 4) modeling studies indicate that more than half of the $PM_{2.5}$ is secondary in origin, and thus directly sensitive to variations in UV radiation [46]. Globally, major contributors to $PM_{2.5}$ are sulfate, nitrate, organics, ammonium, and black carbon (see Fig. 6.7 of IPCC 2021 [11]). While sulfate and nitrate PM are of secondary origin, for organics the relative global contribution of primary and secondary PM is less clear. Satellite-based observations of aerosol optical properties provide only very limited information about chemical composition [47,48]. A better understanding of the secondary/primary ratio of $PM_{2.5}$ in all populated regions is required to fully assess the role of UV radiation and hence the relevance of the Montreal Protocol to this global air pollution problem.
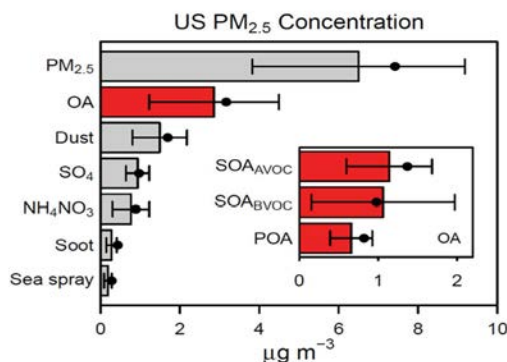

Fig. 4 Composition of $PM_{2.5}$ over the contiguous United States calculated with a chemistry-transport model. Particles produced by UV photochemical reactions (secondary aerosols) include sulfate (SO_4), ammonium nitrate (NH_4NO_3) and secondary organic aerosols (SOA) from anthropogenic or biogenic precursors (SOAAVOC and SOABVOC, respectively), and account for more than half of the total $PM_{2.5}$, compared to directly emitted particles (primary aerosols) such as dust, soot, and sea spray. VOC, volatile organic compounds. From Pye et al. [46].

An emerging and rapidly evolving topic is the effect of UV radiation on chemical reactions within and on the surface of aerosol particles. These heterogeneous processes are extremely complex and still poorly understood, at least in part because aerosols may be composed of many different chemicals, often mixed within the same particle, and each with different UV-absorbing properties and different photolytic fragments. Depending on the specific particle, several UV-mediated processes have already been identified: (a) photolysis of particle-bound organic chemicals into volatile gases (e.g., CO and CO_2), leading to loss of particle mass [49-54]; (b) photolysis of particle-bound inorganic and organic nitrogen into gaseous NO, NO_2, or HONO, potentially increasing the oxidising capacity of the atmosphere [55-58]; (c) conversion of SO_2 gas on the surface of particles to particulate sulfate (thus increasing the mass of the particle) [59-61]; (d) formation of molecular chlorine (Cl_2) leading to enhanced reactivity of a daytime suburban atmosphere [62], (e) increased absorption of shortwave radiation (from formation of brown carbon) with consequences for radiative forcing of climate [63-67]; and (f) formation of various reactive oxygen species (ROS), some of which (e.g., peroxides) are sufficiently long-lived that they may persist during inhalation and play a major role in deleterious health effects of air pollution [61,64,68-72].

Ultraviolet-induced photo-processes within and on the surface of aerosols can also increase the ability of aerosols to act as cloud condensation nuclei (CCN) [73,74], which can change cloud properties and therefore indirectly impact climate. UV-B irradiation (~4.5 days solar radiation equivalent) of dissolved organic matter (DOM, used as a surrogate for organic aerosols) from freshwaters resulted in an increase of hygroscopicity by up to 2.5 times [73]. This is a result of the photodegradation of DOM into hydrophilic low molecular weight chemicals, a process that has been reported in sunlit surface waters [75,76]. A similar effect on CCN was also observed upon UV-B irradiation of SOA formed from the oxidation of α-pinene and naphthalene [74], which are biogenic and anthropogenic SOA precursors, respectively. Considering that CCN are central to the lifecycle of clouds, this represents a newly recognised and potentially important dependence of the hydrological cycle (and climate in general) on UV radiation.

In most cases, the spectral dependence of these heterogeneous photo-processes is still unknown, so that it is not yet possible to assess reliably how much they would be influenced by changes in UV-B radiation resulting from changes in stratospheric ozone. As more spectral data become available, our understanding of the multiple ways in which UV radiation influences aerosol properties and lifetimes will increase and illuminate what role this plays in the natural and perturbed atmosphere.

In summary, changes in UV radiation affect the formation, transformation, and destruction of PM. Quantification of these effects of UV radiation is still somewhat problematic because it involves complex chemical feedbacks that depend on specific physical and chemical variables, such as temperature, humidity, and the amounts of VOCs and NOx present. However, despite this uncertainty, even small changes in UV radiation should be of concern, because of the large number of people currently exposed to poor air quality and its significance to human health.

2.4 Health impacts of photochemical smog

Air pollution is a major public health concern. Estimates of the impacts vary but are consistently large. Thus, the World Health Organization (WHO) estimates that 4.2 million deaths every year occur because of exposure to ambient (outdoor) air pollution which includes particulates and gases, such as O_3, NOx, etc. [77]. These values are somewhat higher than the values reviewed in our previous assessment, which ranged from 1.75 to 4.3 million, depending on year and source of estimates [6]. Regular reports on concentrations of tropospheric O_3 and its effects on humans and the environment are published in Tropospheric Ozone Assessment Reports, e.g., [78]. Our previous Quadrennial Assessment [6] provided an overview of the effects of air pollution on human health with much of the information focusing on respiratory and cardiovascular morbidity and mortality, although reproductive and neurological effects were also briefly addressed. Information on these and other effects from exposure to air pollution continues to accumulate.

An umbrella review (a review of systematic reviews and meta-analyses) [79] evaluated 548 meta-analyses derived from 75 systematic reviews on non-region-specific associations between outdoor air pollution and human health. Of these meta-analyses, 57% (313) were not statistically significant. Of the 235 nominally significant meta-analyses, all but 5 indicated an adverse effect on human health. Analyses were graded as strong (13), highly suggestive (23), suggestive (67) or weak (132). Strong evidence for an association between outdoor air pollution exposure and cardiorespiratory diseases was found for:

- an increased risk of stroke-related mortality per 10 µg m-3 increase of PM_{10} and $PM_{2.5}$ (short-term exposure; relative risk (RR): 1.005 95% CI: 1.003 to 1.007 and RR: 1.014, 95% CI: 1.009 to 1.020, respectively);

- hypertension per 10 µg m-3 increase of $PM_{2.5}$ (short-term exposure; odds ratio (OR) 1.097, 95% CI: 1.060 to 1.136);

- asthma-related admissions per 10 µg m-3 increase of $PM_{2.5}$ and NO_2 levels (short-term exposure; OR: 1.022, 95% CI: 1.014 to 1.031 and OR: 1.019, 95% CI: 1.1013 to 1.024, respectively);

- chronic obstructive pulmonary disease (COPD) and asthma-related admissions of the elderly per 10 µg m-3 increase of NO_2 (24 h average; RR: 1.386%, 95% CI: 1.110% to 1.661%);

- mortality due to pneumonia per 10 µg m-3 increase NO_2 levels (long-term exposure; Hazard Ratio (HR): 1.077, 95% CI: 1.060 to 1.094).

2.4.1 Health impacts at low concentrations of air pollution

New studies, assessed here, indicate that even relatively low levels of pollution may be detrimental [80-82]. Many countries have acted by regulating concentrations of key pollutants and there has been a remarkable decrease in air pollution levels in almost all countries with developed economies leading to levels below the air pollution standards. With the decrease in concentrations of key pollutants, studies now show the detrimental effects on health at relatively low levels of air pollution. Many show effects at concentrations lower than the current annual average standard. In response to this, the World Health Organization (WHO) updated its 2005 Global Air Quality Guidelines (AQG) in September 2021 [83,84]. These new air quality guidelines [83] set ambitious goals, which will be difficult to achieve in most countries. They reflect the large impact that air pollution has on health globally. The new guidelines are aiming for annual mean concentrations of $PM_{2.5}$ not exceeding 5 µg m-3 and NO_2 not exceeding 10 µg m-3, and the peak season mean 8-hour O_3 concentration not exceeding 60 µg m-3 [83]. For comparison, the corresponding 2005 WHO guideline values for $PM_{2.5}$ and NO_2 were 10 µg m-3 and 40 µg m-3 with no recommendation issued for long-term concentrations of O_3 [85]. Table 1 presents the new WHO guidelines in comparison to standards from the European Union, the EPA (USA) and China. Note that UV radiation is involved in the formation of many of these pollutants, including O_3, NO_2, and a large fraction of PM_{10} and $PM_{2.5}$, including sulfate, nitrate, and secondary organic aerosols. Furthermore, UV radiation may make PM_{10} and $PM_{2.5}$ more toxic by generating ROS (Sect. 2.3).

Table 1 Summary of air quality guidelines in several jurisdictions. EU, European Union; EPA, Environmental Protection Agency, USA.

Air pollutant	Time frame, h	WHO new	WHO old	EU	EPA USA	China– Grade 1*	China– Grade 2**
$PM_{2.5}$ µg m-3	24-h	15	25		35	35	75
	annual	5	10	25	12	15	35
PM_{10} µg m-3	24-h	45	50	50	150	50	150
	annual	15	20	40		40	70
NO_2 µg m-3	24-h	25				80	80
	annual	10	40	40	100	40	40
	1-h		200	200	190	200	200

Air pollutant	Time frame, h	WHO new	WHO old	EU	EPA USA	China–Grade 1*	China–Grade 2**
SO_2 µg m^{-3}	24-h	40	20	125		50	150
	annual					20	60
	1-h			350	200	150	500
CO mg m^{-3}	24-h	4				4	4
	1 h				40	10	10
	daily, 8-h max	10	10	10	10		
O_3 µg m^{-3}	1 h					160	200
	daily, 8-h max	100	100	120	140	100	160

$PM_{2.5}$, particles with a diameter of 2.5 µm or less ($\leq PM_{2.5}$); PM_{10}, particles diameter of 10 µm or less ($\leq PM_{10}$); NO_2, nitrogen dioxide; SO_2, sulfur dioxide; CO, carbon monoxide; O_3, ozone.
*China Grade 1 Road: National Highways; **China Grade 2 Roads: Provincial Highway

Evidence continues to accumulate demonstrating that exposure to air pollution can have serious effects on nearly all organ systems of the human body. As outlined in our earlier assessment, the health effects of air pollution include cardiovascular and respiratory disease, cancer, effects on the brain and the reproductive system including adverse birth outcomes [6]. Much of the more recent support documenting the effects of low-level exposure has come from the study of large cohorts in Canada [80], Europe [81] and the United States [82], where regulatory efforts have reduced the average level of exposure. These studies have consistently shown that the adverse effects of air pollution are not limited to high exposures; harmful health effects can be observed at very low concentrations (see below), with no observable thresholds below which exposure can be considered safe.

Research conducted as part of the 'Effects of Low-Level Air Pollution: A Study in Europe' (ELAPSE) [81,86-92] examined the mortality and morbidity effects of exposure to low concentrations of four air pollutants: $PM_{2.5}$, NO_2, black carbon (BC), and tropospheric warm season O_3, with some of the research also investigating the importance of elemental components of $PM_{2.5}$ [88,92-94]. The ELAPSE study consisted of two sets of cohorts: The first was a pooled cohort of up to 15 conventional research cohorts, most of which were in a region with at least one large city with an associated smaller town. This resulted in a rich amount of individual data for up to 325,000 participants. The second set of cohorts comprised seven large administrative cohorts, which were formed by linking census data, population registries, and death registries. These were analysed individually, and, in some cases, meta-analyses were conducted to produce overall results. The key strength of the administrative cohorts was their large sample size (about 28 million) and national representativeness.

The effect of low-level air pollution exposure in 22 cohorts (a combination of research and administrative cohorts) across Europe was associated with several health outcomes and mortality [81]. Almost all participants had annual average exposures below the European Union guidance values (Table 1) for $PM_{2.5}$ and NO_2, and about 14% had mean annual exposures below the United States National Ambient Air Quality Standards for $PM_{2.5}$ (12 µg m^{-3}). In the pooled analysis of the research cohorts, participants had been exposed to 15 µg m^{-3} $PM_{2.5}$, 1.5×10^{-5} m^{-1} black carbon (BC), 25 µg m^{-3} NO_2, and 67 µg m^{-3} O_3 on average. Among the cohorts, mean concentrations of $PM_{2.5}$ ranged from 12 to 19 µg m^{-3}, except for the Norwegian cohort (8 µg m^{-3}). The study followed 325,367 adults and found significant positive associations between even low exposure to $PM_{2.5}$, BC, and NO_2 and mortality from natural-causes as well as cause-specific mortality such as cardiovascular and ischemic heart disease, cerebrovascular disease, respiratory disease, COPD, diabetes, cardiometabolic disease, and lung cancer mortality [91]. An increase of 5 µg m^{-3} in $PM_{2.5}$ was associated with 13% (95% CI: 10.6% to 15.5%) increase in natural deaths. For participants with exposures below the United States standard of 12 µg m^{-3}, an increase of 5 µg m^{-3} $PM_{2.5}$ was associated with nearly a 30% [29.6% (95% CI: 14% to 47.4%)] increase in natural deaths. For NO_2, hazard ratios remained elevated and significant when analyses were restricted to observations below 20 µg m^{-3}.

Liu and colleagues [95] analysed the association between the incidence of asthma and low concentrations of air pollution using three large cohorts from Scandinavia (n = 98,326). They found a hazard ratio of 1.22 (95% CI: 1.04–1.43) per 5 µg m^{-3} increase in $PM_{2.5}$, 1.17 (95% CI: 1.10–1.25) per 10 µg m^{-3} for NO_2 and 1.15 (95% CI: 1.08–1.23) per 0.5×10^{-5} m^{-1} for BC. Hazard ratios were larger in cohort subsets with exposure levels below the annual average limits for the European Union and United States (Table 1) and proposed World Health Organization guidelines for $PM_{2.5}$ and NO_2 (Table 1) compared to the hazard ratios in cohorts exposed to levels above the annual limits.

A meta-analysis [96] of 107 studies on the effect of long-term exposure to air pollution on mortality showed that there was strong evidence that exposure to $PM_{2.5}$ and PM_{10} is associated with increased mortality from all causes, cardiovascular disease, respiratory disease, and lung cancer. The combined Hazard Ratios (HRs) for natural-cause mortality were 1.08 (95% CI: 1.06, 1.09) per 10 µg m^{-3} increase in $PM_{2.5}$, and 1.04 (95% CI: 1.03, 1.06) per 10 µg m^{-3} increase in PM_{10}. This study also indicated that associations with $PM_{2.5}$ remained relevant below the current WHO standards of 10 µg $PM_{2.5}$ m^{-3}.

2.4.2 Health impacts due to components of particulate matter

Studies are only beginning to link health effects to specific chemicals identified in aerosols. Current guidelines and standards for PM are based on the mass of $PM_{2.5}$, without consideration of chemical composition of the particles. Although it stands to reason that the chemical composition would be an important determinant of health impacts, relatively few studies have examined this specific issue. In the context of the Montreal Protocol, UV-dependent secondary PM (sulfate, nitrate, and secondary organics) is chemically distinct from primary, UV-independent, PM. Thus, the relative health impacts of secondary *vs* primary PM are central to this assessment.

Several groups have examined exposure to elemental constituents of aerosols, e.g., Cu, Fe, K, Ni, S, Si, V and Zn in $PM_{2.5}$ [92,93,97]. While most show increases in HRs with increasing atomic abundances, they cannot identify the contribution of secondary particulates, such as secondary organics, sulfates, and nitrates, that depend on UV radiation.

The composition of PM across the United States was modeled recently by Pye et al. [46], using the Community Multiscale Air Quality (CMAQ) model with improved representation of aerosol composition, and was analysed for associations with mortality data (for 2016) for cardiovascular and respiratory disease. The median county-level cardiovascular and respiratory disease age-adjusted death rate was 320 per 100,000 population across 2708 counties, while the average concentration of $PM_{2.5}$ was 6.5 µg m^{-3}, with organic aerosols (OA) being the most abundant component at 2.9 µg m^{-3}. They estimated that, across the United States, for every 1 µg m^{-3} increase in $PM_{2.5}$, 'there is an increase of 1.4 (95% CI:0.5-2.3) cardiovascular and respiratory deaths per 100,000 people. The sensitivity appears much greater for OA, with increases of 1 µg m^{-3} leading to an increase of 8.1 (95% CI:5.4-11) cardiovascular and respiratory deaths per 100,000 people. Subdivision of OA into primary and secondary types showed greater sensitivity for the latter, especially for PM formed by the OH-initiated oxidation of natural VOCs, such as isoprene and terpenes, commonly emitted by vegetation. The importance of secondary organic PM is consistent with a likely role of ROS in tissue damage (Sect. 2.3).

In conclusion, early indications are that secondary aerosols, including SOA, may be particularly damaging. This is of direct relevance to the Montreal Protocol, since secondary aerosols are generated by UV-driven photochemistry. In many locations (e.g., the contiguous United States, see Fig. 4), secondary aerosols may be the largest and the most detrimental fraction of $PM_{2.5}$.

2.4.3 Interactions of air pollution and temperature on health

Episodes of air pollution frequently occur in combination with extremes in temperature with synergistic effects on health depending on the pollutant(s) involved, the degree and direction of temperature change, and the characteristics of the geographic area and the populations affected. Reviews and meta-analyses of the adverse health effects from extremes of temperature (both highs and lows) have proliferated in recent years indicating just how much research in this area is being done due to concerns about climate change [98-106].

A study from nine European cities by Analitis et al. [107] reported that the daily number of deaths increases by 2.20% (95% CI: 1.28–3.13) on days with high O_3 per 1 °C increase in temperature. The interaction of temperature with PM_{10} was significant for cardiovascular causes of death for all ages (2.24% on days with low PM_{10} (95% CI: 1.01–3.47), while it was 2.63% (95% CI: 1.57–3.71) on days with high PM_{10}.

In a recent meta-analysis, Areal et al. [108] showed that effects of air pollutants were modified by high temperatures, leading to higher mortality from respiratory diseases and an increase in hospital admissions. The effect of PM_{10} during higher temperatures increased the risk of mortality by 2.1%, and for hospital admissions the effects increased by 11%. The effects of ground-level O_3 during high temperatures were similar [108].

2.4.4 Health impacts of air pollution in vulnerable populations

Air pollution affects people from the beginning to the end of life, causing a wide range of acute and chronic diseases. Sensitive populations include, among others, children, the elderly, and people with existing chronic diseases. Accordingly, people with cardiovascular diseases are more likely to suffer a heart attack, stroke, or death when exposed to air pollution [109].

Ambient air pollution not only contributes to adverse health outcomes in individuals after birth, but it may also have immediate adverse impacts on reproductive processes. Animal and epidemiological evidence demonstrates that air pollution may influence fertility. A large Danish study investigated 10,183 participants between 2007 and 2018 [110] who were trying to conceive. The study showed that higher concentrations of PM_{10} and $PM_{2.5}$ were associated with small reductions in fecundability, for example, the reductions in fecundability ratios from a one interquartile range (IQR) increase in $PM_{2.5}$ (IQR = 3.2 µg m^{-3}) and PM_{10} (IQR = 5.3 µg m^{-3}) during each menstrual cycle were 0.93 (95% CI: 0.87–0.99) and 0.91 (95% CI: 0.84–0.99).

In another study on exposure to air pollution and the risk of pre-term birth, the authors investigated 2.7 million births across the state of California from 2011-2017 [111]. This study found an increased risk of pre-term birth with higher concentrations of $PM_{2.5}$ [adjusted relative risks (aRR) (per interquartile increase)] 1.04, (95% CI: 1.04–1.05) and particulate matter from diesel exhaust, aRR = 1.02 (95% CI: 1.01–1.03). Similar results were observed in another study from California, where the authors investigated 196,970 singleton pregnancies between 2007-2015. These authors found that, during cold seasons, increased exposure to $PM_{2.5}$ during the three days prior to the premature birth was associated with 5-6% increased odds of very-early pre-term birth (OR_{lag3} 1.06, 95% CI: 1.02–1.11). These studies confirm results from human and other animal studies that air pollutants can enter a pregnant female's circulatory system and exert many deleterious health effects in multiple body organs including the placenta and the developing foetus [111].

In the umbrella review discussed above, *Markozannes et al.* [79] also found strong associations for a number of pregnancy/birth related outcomes. These included a:

- 10 µg m^{-3} increase in PM$_{2.5}$ for various durations of exposure was associated with an increased risk of having an infant born small for gestational age, a) long-term exposure entire pregnancy OR: 1.151, 95% CI: 1.104–1.200; b) long-term exposure first trimester: OR: 1.074, 95% CI: 1.046–1.103; c) long-term exposure last trimester: OR: 1.062, 95% CI: 1.042–1.083.

- 13 µg m^{-3} increase in SO$_2$, (24 h average) was associated with an increased risk of low birthweight OR: 1.035, 95% CI: 1.031–1.049 as was

- 10 µg m^{-3} increase in PM$_{10}$ (long-term exposure; mean difference 7.42 g, 95% CI: 8.10–6.75.

- 10-µg m^{-3} increase in PM$_{2.5}$ for the third trimester was associated with an increased risk for hypertension during pregnancy OR: 2.177 95% CI: 1.710–2.773.

There is also growing evidence that exposure to air pollutants maybe detrimental to the central nervous system and contribute to deficits in cognitive development, neurodegenerative diseases and dementia [112,113]. A recent review [113] found that, despite a substantial increase in publications, there is only suggestive evidence that air pollution may influence late-life cognitive health as there is still substantial heterogeneity of findings across the studies. The strongest effect found was with respect to PM$_{2.5}$ and cognitive decline. The review included two different outcomes, namely, incidence of dementia and abnormal neuroimaging. Since then, a large Canadian study investigated the effect of exposure to air pollution and incidence of dementia in ~2.1 million individuals [114]. The study identified 257,816 incident cases of dementia and found a positive association between an interquartile range (IQR) increase in PM$_{2.5}$ of 4.8 µg m^{-3} and incidence of dementia, with a hazard ratio (HR) of 1.04 (95% CI: 1.03–1.05) and an IQR increase of 26.7 µg m^{-3} in NO$_2$ HR = 1.10 (95% CI: 1.08–1.12) over a 5-year period, respectively. A similar large study using data from Medicare from the United States examined ~2.0 million incidences of dementia cases [115]. Per IQR increase in the 5-year average PM$_{2.5}$ (3.2 µg m^{-3}) and NO$_2$ (22 µg m^{-3}), they found an association with the development of dementia HR= 1.060 (95% CI: 1.054–1.066) and with exposure to NO$_2$ HR=1.019 (95% CI: 1.012–1.026), respectively. The authors also observed significant associations between exposure to PM$_{2.5}$ and the development of Alzheimer's disease HR=1.078 (95% CI: 1.070–1.086) and NO$_2$ exposure HR = 1.031 (95% CI: 1.023–1.039). The results of these new studies lend support to the theory that there is an association between air pollution and dementia and Alzheimer's disease.

2.5 Effects of tropospheric ozone and particulates on plants

Photochemical air pollution can damage plants, with potentially adverse effects on agriculture and other natural resources. Ground-level ozone is a particular concern, since numerous studies have demonstrated significant damage [78,116]. Other air pollutants co-produced with O$_3$, e.g., peroxyacetyl nitrate (CH$_3$C(O)O$_2$NO$_2$) are also phytotoxic, although their specific effects are difficult to separate from those of O$_3$ [117]. The understanding of mechanisms and mitigation of these effects has improved, and some effects of particulates on plants are assessed below.

2.5.1 Effects of tropospheric ozone on health and yields of plants

In the previous Quadrennial Assessment [6], we evaluated the adverse effects of O$_3$ on crop and other plants. We noted that tropospheric O$_3$ could contribute to significant losses in quality and yield of crops, e.g., 10–36% for wheat and 7–24% for rice. The adverse effects of O$_3$ on plants continue to be documented in the literature. A metanalysis of 48 studies on the exposure of soybeans to tropospheric O$_3$ conducted between 1980 and 2019 showed increases in degradation of chlorophyll and foliar injury. Leaf-area was reduced by 21%, biomass of leaves by 14%, shoots by 23%, and roots by 17% [118]. Chronic exposure to O$_3$ of about 150 µg m^{-3} caused a decrease in yield of seed by 28%. In a study in Argentina [119], exposures of soybeans (a sensitive crop) to O$_3$ at a concentration of 274 µg m^{-3} for 7 days resulted in a reduction in below-ground biomass of 25%, a 30% reduction of nodule biomass, and a 21% reduction of biological nitrogen fixation. Effects were more severe in tests with soils of low fertility where production of seed and seed protein was reduced by 10% and 12%, respectively. These effects in soybean exposed to O$_3$ at 160 µg m^{-3} for 7 days were linked to decreases in metabolism of carbon and capacity for detoxification in the roots of soybean [120]. A study on the historical losses to air pollutants in maize and soybean grown in the United States showed that improvements in the control of O$_3$, SO$_2$, PM, and NO$_2$ have improved yields by an average of 20% [121]. Of these pollutants, PM and NO$_2$ appeared to cause more damage than O$_3$ and SO$_2$. Overall, the improvement in yields was equivalent to *ca* US$ 5 billion.

Observations between 2015 and 2018 in the province of Henan in China [122] showed that annual losses in yield of wheat exposed to O$_3$ at concentrations above 80 µg m^{-3} were 12.8, 8.9, 10.8, and 14.1%. These were equivalent to annual losses of US$ 2.14, 1.32, 1.68, and 2.16 billion, respectively. A model was developed to extrapolate these losses to other crops in China [123]. Based on a four-year average of tropospheric concentration of O$_3$, estimated losses in wheat were 50 million tonnes per year, mostly in winter wheat (48 million tonnes); 21 million tonnes in rice; 18 million tonnes in maize and 1.6 million tonnes in soybeans [123]. A separate modelling study estimated that current concentrations of O$_3$ reduced yield by 6.9% for rice and 10.4% for wheat [124]. Clearly, tropospheric O$_3$ has significant adverse effects on food security in some countries and this might be exacerbated in the event of super-recovery of stratospheric ozone.

A modeling study on the effects of measured concentrations of O$_3$ on grapes in the Demarcated Region of Douro in Portugal indicated that, in two years of high levels of O$_3$, productivity of grapes was reduced by 27% and sugar content by 32% [125]. Similar effects were echoed in other grape-growing regions across the globe [126].

Crops are not the only class of plants to suffer reductions in yields from exposure to air pollutants. Forests are important sources of wood and fibre and can be affected by tropospheric air pollutants such as O_3. In an analysis of the impacts of O_3 on production of forests in Italy, Sacchelli et al. [127] calculated that the average cost of potential O_3 damage to forests in Italy in 2005 ranged from 31.6 to 57.1 million € (i.e., 10–17 € ha^{-1} year^{-1}). This damage resulted in a 1.1% reduction in the profitable forest areas. Estimated decreases in the annual national production of firewood, timber for poles, roundwood and wood for pulp and paper were 7.5, 7.4, 5.0, and 4.8%, respectively. A study on the effects of O_3 on trees in Mediterranean forests in Istria and Dalmatia showed that current levels cause inhibition of growth for two species of oak (*Quercus pubescens* and *Q. ilex*) as well as pine (*Pinus nigra*) [128]. A climatological modelling study in European forests has shown that climate change has lengthened the growing season by ca 7 days decade^{-1} [129]. Because of this, the total phytotoxic dose of O_3 taken up by trees over the season has increased and outweighs the benefits of a decrease in concentration of tropospheric O_3 (1.6%) that resulted from measures to control pollution between 2000–2014.

Because of their sensitivity, the potential effects of O_3 in the environment have been more extensively studied in plants than in animals. However, a recent study has focused on the effects of O_3 in amphibians [130]. The authors exposed tadpoles of the midwife toad (*Alytes obstetricans*) to airborne O_3 at concentration up to 180–220 µg g m^{-3} for 8 h per day from an early stage of development (limbs not yet formed) to metamorphosis. This is equivalent to the maximum concentrations observed in the Sierra de Guadarrama Mountains over a period of 10 years. The measured responses were successful development and infection of the developing tadpoles with the aquatic fungus *Batrachochytrium dendrobatidis*, which causes the disease known as chytridiomycosis. Airborne concentrations of O_3 were measured in the exposure chambers but not in the water containing the tadpoles, so that actual dose could not be calculated. Results suggested that, at the greatest airborne exposure, development of the tadpole was delayed and that susceptibility to *B. dendrobatidis* was increased. This study is preliminary and further work is needed to elucidate potential effects.

In summary, future changes in UV-B radiation will influence ground-level O_3 and other pollutants. The recovery of stratospheric O_3 to 1980 levels is expected to contribute 1–2 µg m^{-3} to ground-level O_3 outside major urban areas [14,15,36], but super-recovery under some future climate scenarios could lead to larger increases (Sect. 2.2, and Box 1). This could be offset by further reductions in NO and VOC emissions, so the actual O_3 concentrations will depend on local and regional air quality control measures, as well as the impacts of climate change and the Montreal Protocol on stratospheric O_3. These impacts could affect both food security and forests.

2.5.2 Toxicological mechanisms

Effects of ozone on plants are mediated by the formation of free radicals in the tissues of the plants. Ozone enters the leaf of the plant through the stomata and forms ROS, which include $O_2^{\cdot-}$, H_2O_2, OH, $^1O_2$, as well as reactive carbonyl species such as malondialdehyde and methylglyoxal [131]. These reaction products damage components of the cells but also stimulate signaling systems, such as the release of isoprene [132] to activate defense mechanisms. These defences include physical actions, such as closure of the stomata, biochemical responses such as the release of superoxide dismutase, catalase, and peroxidases to destroy the ROS, and release of chemical buffers, such as ascorbic acid, glutathione, phenolic chemicals, flavonoids, proline [133], and other amino acids, carotenoids, tocopherols, polyamines, and sugars [131].

Some adverse effects of tropospheric air pollutants on plants are indirect. For example, air-pollutants can affect visual and chemical signals that mediate interaction between plants, and organisms that depend on plants or that are needed for the sustainability of plant communities [134] (see Fig. 5). For example, tropospheric O_3 can destroy or change biogenic volatile chemicals and thus interfere with attraction of pollinators or pests to plants [135]. O_3 could also interfere with sensory organs and the ability of pollinators to sense sources of nectar or the ability of biological-control organisms to sense their target hosts [134]. Also, physiological responses to damage from O_3 might alter the ratios of pigments in plants, the phenology (seasonal development) of flowers and whole plants [136], or the time of flowering, thus affecting host recognition and pollinators. Pollutants may also affect reproduction in plants by directly damaging air-borne pollen through stimulating repair mechanisms and redirecting resources to cell repair rather than reproduction [137,138]. In addition, the allergenicity of pollen can be enhanced with implications for human health [137].
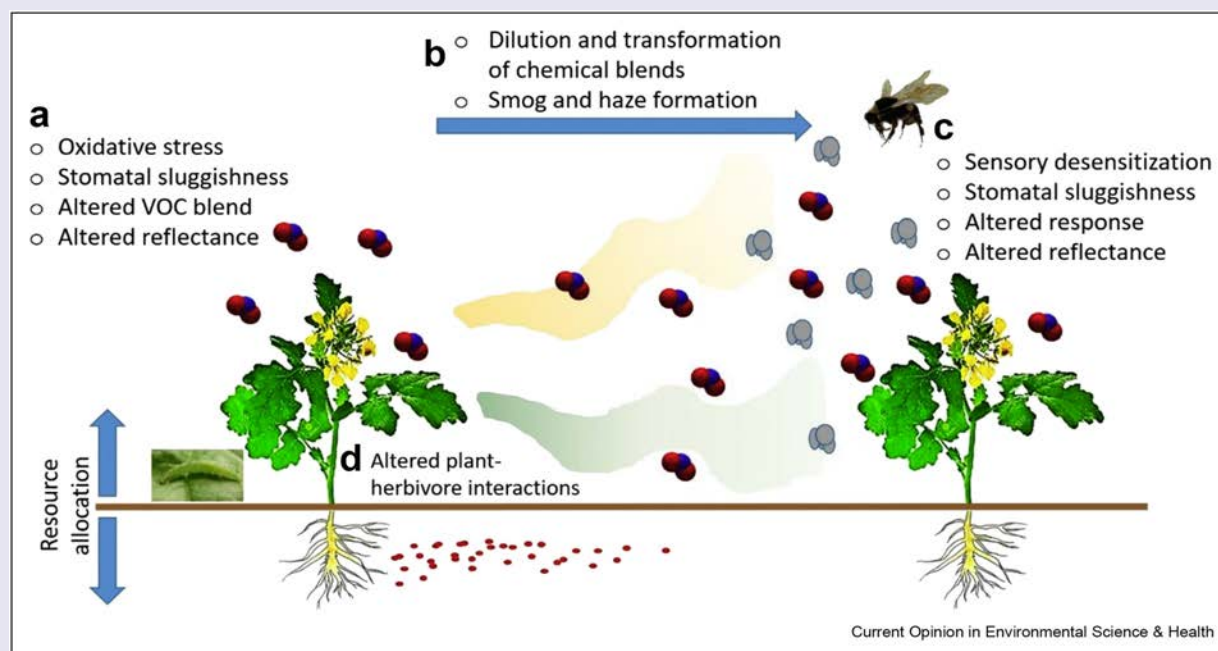
Fig. 5 Sites at which air pollution can affect interactions mediated by olfactory or visual cues between plants and their associated community. a) Effects of pollutants on signal-emitting organisms. **b)** The degradation of VOCs by air pollutants and formation of reaction products and secondary organic aerosol (SOA). **c)** Effects on the signal receiving organisms, e.g., pollinating insects. In addition, exposure to air pollution can influence the interactions between herbivores and plants. **d)** From [134], reproduced with permission.

2.5.3 Effects of particulates on plants

The effects of PM on plants were previously assessed to be few and minor [5,6], but new studies suggest they may be important particularly in polluted areas. In a study of water-extractable chemicals collected from $PM_{2.5}$ samplers on roadsides in Hungary, 13 common roadside plants were tested for sensitivity using the OECD-227 guideline test [139]. Endpoints measured in the study were shoot weight, shoot height, visible symptoms of damage on the plants, growth rate, photosynthetic pigments, and activity of peroxidase enzyme. The authors concluded that particulate pollution derived from traffic added substantial additional stress to communities of plants found on roadsides. The study was conducted during mid-winter and near sources, implying that most of the PM was primary rather than secondary, and hence insensitive to any changes in UV radiation. It is unclear if similar plant damage would have been caused by UV-dependent secondary aerosols.

In another study, the combined effects of ambient atmospheric O_3 and particulate matter on wheat were assessed [140]. The cumulative concentration of ambient O_3 above the threshold of 80 µg m^{-3} h^{-1} during the 4-month study was 453 µg m^{-3} h^{-1}. Concentrations of ambient $PM_{2.5}$ and PM_{10} ranged between 45–412 µg m^{-3} and 103–580 µg m^{-3}, respectively. Controls were cleaned of particulates and were protected from O_3 by treatment with ethylene diurea, a mitigator of ozone-stress. Economic yield was reduced 34% in wheat exposed to O_3 and PM, 44% in wheat exposed to PM only and 52% in plants exposed to O_3 alone. Similar observations were reported in a modeling analysis of the effects of O_3 and PM on the yields of wheat and rice in China [124]. Based on current levels of O_3 and aerosols, their results indicated that anthropogenic aerosols reduced yield of rice and wheat by 4.6 and 4.7%, respectively. The authors suggested that this was because of the effect of dimming of photosynthetically active radiation by aerosols but that there were some benefits from cooling and nutrients provided via the aerosols. The losses due to both O_3 and aerosols were estimated to be 11.3 for rice and 14.6% for wheat. The relative contributions of primary and secondary PM were not reported, so that the sensitivity to changes in UV radiation remains unclear.

Overall, these results indicate that aerosols and tropospheric O_3 alone, or in combination, have adverse effects on plants and yields of crops. The loss from O_3 is greater than that from aerosols but they do act additively. With few studies on this interaction, the potential for additive and/or synergistic effects of O_3 and particulates, the significance to crop plants and human activities is uncertain. However, it is likely that these effects will be localised and could be mitigated by increased controls of tropospheric air pollutants.

2.6   Self-cleaning capacity of the atmosphere

The hydroxyl radical (OH) is the major oxidant in the troposphere and its concentration largely determines the lifetime of many tropospheric pollutants. It is produced via UV-B photolysis of O_3 (see Fig. 1). Hence, increases in the tropospheric concentration of OH are, in part, a consequence of increasing emissions of ODSs. The tropospheric concentration of OH is a balance between OH production and consumption, where both rates are also affected by climate change.

Global mean concentrations of tropospheric OH have been calculated to have changed little from 1850 to around 1980 [141,142]. However, in the period 1980-2010 the modeled global tropospheric concentration of OH has increased, mainly because of increasing concentrations of precursors of tropospheric O_3, and UV radiation [141]. According to the combined output of three computer models (Fig. 6), there was a net increase in OH of about 8% (mean value of the models). The main precursor of tropospheric O_3 is NOx, the tropospheric concentration of which has increased over 1980-2010 (Fig. 6). Global emissions of NOx peaked around 2012, followed by reductions [143]. In addition to NOx, also ODSs and factors underlying climate change such as rising water vapour have contributed to the net increase in modeled OH from 1980-2010. Increasing atmospheric CH_4 was the main factor countering the trend of rising OH (by about -8%, see Fig. 6) in this period.
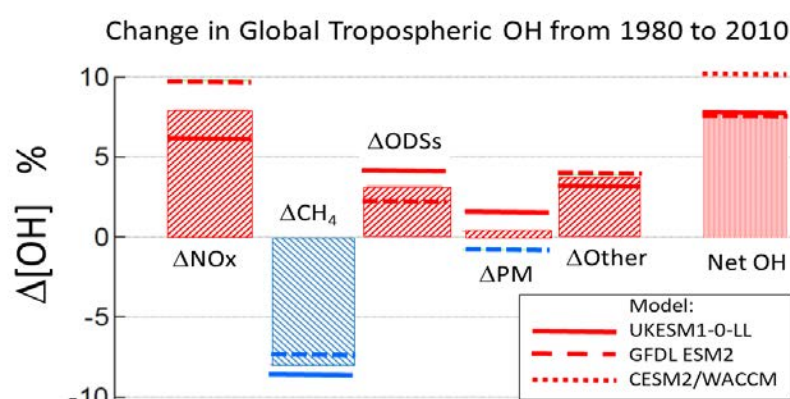

Fig. 6 Relative change in global concentrations of tropospheric OH from 1980 to 2020, estimated with three different Earth System Models (ESMs). The net change in OH (rightmost column) has contributions from increased emissions of nitrogen oxides and other precursors of tropospheric ozone (ΔNOx); increased emissions of methane (ΔCH₄); accumulation of ozone-depleting substances now regulated under the Montreal Protocol (ΔODSs); emissions of particulate matter and its precursors (ΔPM); and other undifferentiated changes attributed to underlying climate change (e.g., water vapour), as well as interactions among these separate factors (ΔOther) (modified from [141]).

Studies that infer concentrations of OH by the rate of removal of chemicals from the atmosphere have generally indicated a decreasing trend in OH after 2000 [144]. However, the interannual variability in OH from these studies was large, i.e., the difference between modeled and measured OH trends were not statistically significant [141]. For such studies, methyl chloroform (CH_3CCl_3) is often used [145] to infer concentrations of OH. The drawback of this method is that the emissions (almost entirely anthropogenic) of CH_3CCl_3 have declined substantially in the last 30 years [145], thus affecting the accuracy and precision of derived amounts of global OH.

Future trends in tropospheric concentrations of OH not only depend on solar UV-B radiation and on the concentration of precursors of OH but also on OH sinks, particularly CO and CH_4. As discussed above, the increasing global concentration of CH_4 was the main factor countering positive modeled OH trends in the period 1980-2010 (Fig. 6). Total global emissions of CH_4 are currently ~525 Tg yr^{-1} [146]. If emissions of CH_4 from anthropogenic and natural sources continue to rise as they have since 2007, this could decrease global mean OH by up to 10% by 2050 [147], increasing the atmospheric lifetime and concentrations of CH_4 in a positive feedback. Also, emissions of CO, the major sink of OH, may increase as a result of more frequent and longer lasting wildfires related to climate change. A change in the average concentration of OH in the troposphere would have large impacts on the cleaning capacity of the troposphere.

Finally, we note the importance of reactions between tropospheric OH and gases that affect stratospheric ozone (Fig. 7). These include anthropogenic halogenated organics (the HCFCs and HFCs, specifically selected for their reactivity with OH so that they are removed in the troposphere), as well as gases such as CH_4 and VSLSs. Hydroxyl radicals control the tropospheric lifetimes of these gases, and hence their ability to reach the stratosphere. VSLSs are important pollutants since they can reach the lower stratosphere, despite their tropospheric lifetime of less than 6 months, and contribute to depletion of stratospheric O_3 [148,149]. These chemicals are not controlled by the Montreal Protocol and include chlorinated, brominated, and iodinated VSLSs (Cl-VSLSs, Br-VSLSs, and I-VSLSs, respectively). Cl-VSLSs are mostly of anthropogenic origin, while I-VSLSs and Br-VSLSs, particularly bromoform ($CHBr_3$) and dibromomethane (CH_2Br_2) are mainly produced in biotic processes and are affected by climate change, including increased coastal runoff and thawing of permafrost [148]. The contribution of BrVSLSs to the total stratospheric bromine loading was estimated to be ≈ 25% (in 2016) [150].

The mixing ratio of Br-VSLS at the tropopause has been measured to increase with latitude in the Northern Hemisphere, particularly during polar winter [149] when photochemically driven losses are smallest. This results (via troposphere-to-stratosphere transport) in higher concentrations of Br-VLSLs in the extratropical lower stratosphere, as compared to those in the tropical lower stratosphere [149].

The major sink of halogenated VSLSs is reaction with OH. Hence the tropospheric lifetime of VSLSs mainly depends on the tropospheric concentration of OH. For example, *Rex et al.* [151] found a lifetime of dibromomethane (CH_2Br_2) as long as 188 days inside an OH minimum zone over the West Pacific, while outside the OH minimum zone, the lifetime of CH_2Br_2 was 55 days. In addition to $CHBr_3$ and CH_2Br_2, methyl bromide (CH_3Br) is an ODS. Due to the Montreal Protocol and its Amendments, atmospheric mole fractions of CH_3Br have declined considerably and, at present, emissions of CH_3Br primarily stem from natural sources [152], with some anthropogenic sources related to commercial quarantine and pre-shipment applications. The production of CH_3Br in seawater is a biological process mediated by phytoplankton such as diatoms [153]. The interannual variability of atmospheric CH_3Br concentrations cannot be solely explained by changes in the biological production of CH_3Br due to changes in sea-surface temperatures (SSTs) and stratification [152]. Also, sinks of CH_3Br have to be considered, where the major atmospheric sink of CH_3Br is reaction with OH. *Nicewonger et al.* [152] found a strong correlation between the interannual variability of CH_3Br and the Oceanic Niño Index (ONI) from 1995 to 2020. About 36% of the variability in global atmospheric CH_3Br was explained by the variability in El Niño Southern Ocean (ENSO) during this period, with increases in CH_3Br during El Niño and decreases during La Niña [152]. One reason for increases in atmospheric CH_3Br concentrations during El Niño years (positive ONI) could be a global reduction in OH during El Niño years. Based on modeling studies for the period 1980 to 2010, *Zhao et al.* [142] found decreases in global concentrations of OH during El Niño years that were mainly driven by an elevated loss of OH via reaction with CO from enhanced burning of biomass (Fig. 7). The longer the tropospheric lifetime of halogenated VSLSs, the higher is the probability that they reach the stratosphere and contribute to depletion of stratospheric O_3 with impacts on ground-level UV-B radiation. Since UV-B radiation, together with tropospheric O_3 and water vapour enhance the formation of OH, increased levels of UV-B radiation could counterbalance decreasing concentrations of OH due to wildfires and thawing of permafrost soils (Fig. 7).

2.7 Changes in atmospheric circulation and transport of pollutants

2.7.1 Ozone from the stratosphere

Ozone as an air quality issue has normally been considered as a local or regional issue. However, O_3 from the stratosphere is also transported to the troposphere where it contributes an important but variable fraction of O_3 at ground level and represents a baseline upon which locally or regionally generated O_3 is added. This is known as stratospheric-tropospheric exchange (STE). The magnitude of the contribution of stratospheric O_3 to tropospheric O_3 is difficult to quantify but important. A comparison of measurements and 3 different models estimated the influence of stratospheric O_3 on tropospheric O_3, highlighting the challenges of obtaining consistent results [154]. The study estimated the fraction of O_3 near the Earth's surface that can be attributed to O_3 transported down from the stratosphere. This was found to vary between 10% year-round in the tropics increasing to greater than 50% at mid to high latitudes in winter.
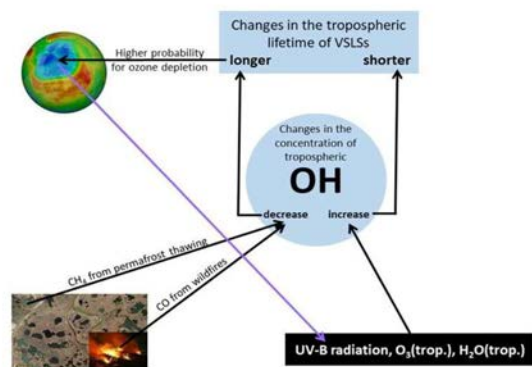
Fig. 7 Interacting effects of UV-B radiation and climate change on tropospheric concentrations of OH and on the lifetime of very-short-lived substances (VSLSs). Effects of climate change include more frequent wildfires and thawing of permafrost soils with the formation of thermokarst lakes, which are important sources of CO and CH_4, respectively. Increased emissions of CO and CH_4 tend to decrease the tropospheric OH concentration, which in turn results in longer lifetime of VSLSs and thus a higher probability of stratospheric ozone depletion.

Estimates of STE are poorly characterised by observations and atmospheric models. An assessment of amounts of O_3 in the troposphere shows that model estimates of STE were around 1000 Tg yr^{-1} O_3 for results reported in 1995 but by 2015 models provided estimates approaching 400 Tg yr^{-1}, with a multi-model estimate of 535 ± 160 Tg yr^{-1} for the year 2000 [155]. The IPCC AR6 assessment reports a value of 628 ± 800 Tg yr^{-1} for 2010, with the large uncertainty highlighting how poorly this value is known [11]. Other recent estimates include 347 ± 12 Tg yr^{-1} (2007–2010) [156] and 400 ± 60 Tg yr^{-1} (1990–2017) [157].

Typically, the magnitude of the STE is inferred as the difference between the calculated production and loss of O_3 (termed the residual) rather than modelling STE transport itself [158]. These production and loss terms are an order of magnitude larger (around 5000 Tg yr^{-1}) than the estimated transport [e.g., 159], so that their difference is highly uncertain. A second confounding factor is that models have used different definitions of the upper boundary (tropopause) of the troposphere.

The modelling of the impact of STE on tropospheric O_3 for the period 1850 – 2100 shows a significant decrease in O_3 from the stratosphere by the year 2000 [158] (see Fig. 9). A modelling study focusing on the period 1980–2010 calculated a decrease in the transport of O_3 from the stratosphere to the troposphere due to the impact of ODSs on stratospheric O_3 [160]. The model estimated a 4% decrease (14 Tg O_3) in global tropospheric O_3 resulting from ODS up until 1994. Another study using measurements of N_2O to constrain the atmospheric modelling estimated an average decrease in STE due to the Antarctic ozone hole (1990–2017) of 30 Tg yr^{-1} with a range of 5–55 Tg yr^{-1}, depending on year [157].
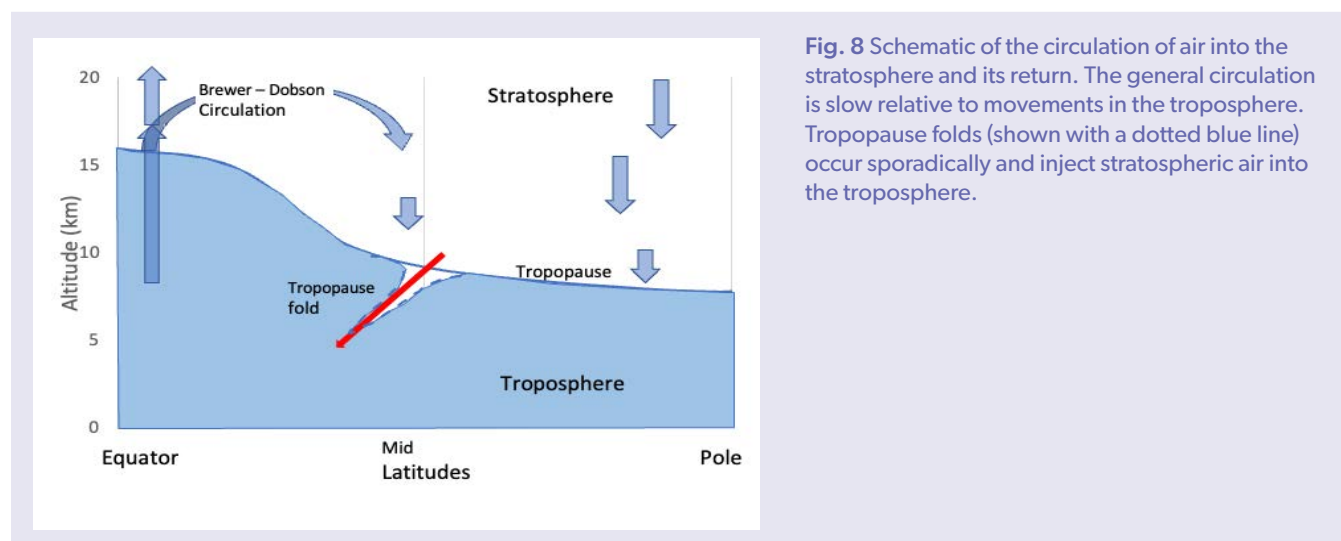

Fig. 8 Schematic of the circulation of air into the stratosphere and its return. The general circulation is slow relative to movements in the troposphere. Tropopause folds (shown with a dotted blue line) occur sporadically and inject stratospheric air into the troposphere.

In contrast, the results of a modelling and observational study of the regional changes in O_3 concentration in the troposphere for the period 1980–1990 through to 2000–2010 [154] suggest an increase in the concentration of O_3 at the Earth's surface, but the other studies (noted above) found that stratospheric O_3 led to a small increase over this period in the Northern Hemisphere and no significant change in the Southern Hemisphere. Clearly more work is needed in this area.

For the period from 2000–2100, substantial increases in the amount of O_3 transported from the stratosphere to the troposphere are predicted [158]. Estimates using the output from seven atmospheric models and focusing primarily on RCP6.0, [161] suggest a 10¬–16% increase in the amount of O_3 in the troposphere from STE in the 21st century. When assessing the relative importance of changes in GHGs *vs* ODSs in driving the changes in STE, they did not obtain a consistent picture from the models, although it appears that the two factors are of similar magnitude [161]. However, there is insufficient agreement between models to quantify trends. The net change in the concentration of O_3 in the troposphere by 2100 is very dependent on the magnitude of anthropogenic emissions. The decrease in net chemical production (red curve, Fig. 9) is driven by the predicted controls on the emission of air pollutants. Calculations using the RCP8.5 scenario showed a marked increase in the concentration of O_3 in the troposphere, with a 3-fold larger amount of O_3 transported from the stratosphere than the RCP6.0 scenario [161]. It is not possible to infer the magnitude of the changes in O_3 at ground level from these models, as they report O_3 concentrations averaged for the entire vertical extent of the troposphere, and the impact of stratospheric O_3 is much larger in the upper troposphere than at the Earth's surface.

Folds in the tropopause have a direct impact on air quality at ground level. These folds are not uniformly distributed longitudinally [162,163] and are common over the Eastern Mediterranean, where they have been identified as a significant cause of elevated concentrations of O_3 at ground level that are greater than the European Union air-quality standards [164]. The equivalent effect is also observed in the Southern Hemisphere over the Indian and Southern Oceans. A modelling study of tropopause folds for the period 1960–2100, using emissions as specified in RCP6.0 and including stratospheric O_3 recovery, suggests that folds will increase during this period. Statistically significant changes in the number of tropopause folds of around 3 % have been identified in regions that coincide with a calculated increase of 6 μg m^{-3} in O_3 near the Earth's surface [165].
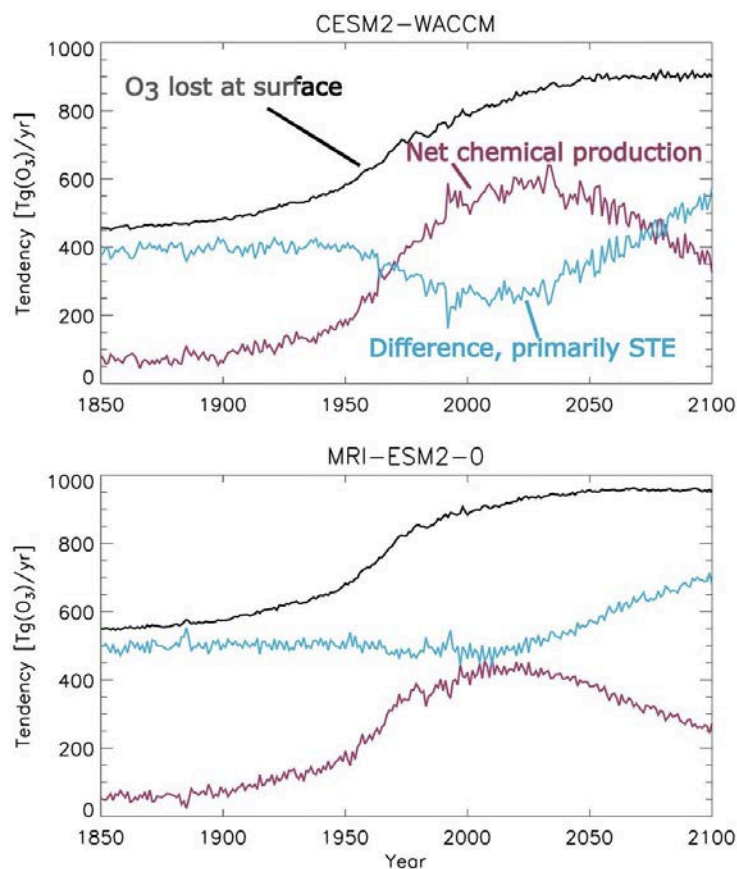
Fig. 9 Drivers of tropospheric ozone concentration (redrawn with permission and assistance from Guang Zeng from Fig. 13, in [158]). The deposition amount is directly related to the concentration of O_3 at the surface of the Earth. The two panels represent the output of different chemistry-climate models considered in the study. STE, stratospheric-tropospheric exchange.

Quantifying the transport of O_3 from the stratosphere is therefore important to understanding tropospheric air quality but remains difficult. The challenge in measuring and modelling STE of O_3 is partially due to the mechanism by which the downward transport occurs. Air rich in O_3 is injected into the troposphere at the edges of the tropics via "folds" (Fig. 8), where thin layers of air from the stratosphere are surrounded (vertically) by air from the troposphere and *vice versa*. These layers then mix. Methods for identifying folds within model output are being improved [e.g., 165] and showing some promising consistency among different models [162].

The modelling of STE is also hampered by the relatively few measurements of the chemical composition and physical structure of the atmosphere in the upper troposphere and lower stratosphere. As a result, there is little information that can be used to constrain atmospheric models. Efforts are now underway to use measurements of the chemical composition of air on commercial aircraft to build up a robust climatology, which can help modelling. [166] Similarly, there are ongoing efforts to improve the use of measurements of O_3 by satellites in atmospheric modelling [167], and potentially O_3 sondes and *in situ* measurements. Using observations to constrain models introduces sensitivity to changes in quality and calibration of the input data and this requires careful assessment [167,168] In future, these data should allow better quantification of the changes in tropospheric O_3 that are caused by changes in stratospheric O_3.

2.7.2 Effects of circulation changes on extreme weather events and air quality

Air quality is also affected by extreme weather events, such as wildfires. Changes in weather patterns, including extreme weather events, are not only caused by climate change but also by polar stratospheric ozone depletion, which strengthens the stratospheric polar vortex. Changing weather patterns due to the Antarctic ozone hole have been observed in the Southern Hemisphere (see Chapters 1 and 3 [23,169], and [170]. For example, anomalies in rainfall and droughts in the Southern Hemisphere are correlated with the duration of the Antarctic Ozone hole [171]. In addition to the strength of the stratospheric polar vortex, the El Niño Southern Oscillation and the Indian Ocean Dipole also affect weather conditions in Australia [172]. Hot and dry weather increases the risk of wildfires. The severe fire season in Australia 2019-2020 led to significant degradation of air quality within Australia and a smoke plume that was traced around the globe [173-175]. The likelihood of wildfires is increasing globally, a trend that is expected to continue [176]. However, the recovery of stratospheric O_3 should decrease the stability of the Antarctic polar vortex, which should lead to wetter conditions in the Southern Hemisphere in the near future for this region.

Similarly to the effects of the atmospheric dynamics of the Antarctic ozone hole, Arctic stratospheric ozone depletion results in a shift of the Arctic Oscillation (AO) to more positive values (e.g., [177]) and a more zonal Northern Hemisphere jet stream. Consequences are colder than normal surface temperatures in southeastern Europe and southern Asia, but warmer than normal surface temperatures in Western Europe, Russia, and northern Asia [178]. For example, a likely consequence of the unprecedented Arctic stratospheric ozone depletion in spring 2020 was the heat wave in Siberia accompanied by wildfires in this region [179]. Whether such events will occur in the future depends on trends in the emissions of ODSs and GHGs, since GHGs affect the Arctic stratosphere via radiative cooling [180]. Hence, the frequency of extreme weather events such as droughts and therefore wildfires in both hemispheres is influenced by direct effects of climate change and by changes in atmospheric circulation and in polar stratospheric O_3. Wildfires decrease tropospheric air quality with the emission of PM, CO, and other tropospheric pollutants, which impact human health.

2.8   Conclusions

Changes in stratospheric O_3 concentrations and thus in ground-level UV-B radiation affect tropospheric air quality. Poor air quality remains a major health problem globally, despite progress in reducing emissions of air primary pollutants. Much of the impact of air pollutants is due to chemicals produced by UV-B-initiated photochemistry, including O_3 and PM, i.e., secondary inorganic and organic aerosols. PM and tropospheric O_3 pose a significant health risk. Overall, recovery of stratospheric O_3, and hence lower intensity of ground-level UV-B radiation, is expected to slightly improve air quality in cities in mid-latitudes but slightly worsen air quality in rural areas. For PM, the impacts of changes in UV-B radiation on the amount and chemical composition of PM are still poorly understood.

Transport of O_3 from the stratosphere into the troposphere adds to tropospheric O_3 concentrations. This transport is expected to increase because of the recovery of stratospheric O_3 and changes in global circulation driven by climate change. Given the current state of knowledge, estimating the magnitude of these changes remains a significant challenge.

UV-B radiation is also involved in the formation of OH, the major cleaning agent of the troposphere. Hence, UV-B radiation has some beneficial effects on tropospheric air quality. Reaction with OH drives the atmospheric removal of many problematic tropospheric gases including some pollutants and GHGs such as CH_4, and VSLSs (noting also that GHGs and VSLSs affect stratospheric O_3). Given current global CH_4 emission of ~500 Tg yr^{-1}, a 1% decrease of the global OH concentration would result in an increase of ~1% in tropospheric CH_4 concentrations, equivalent to a sustained increase in emissions of CH_4 of ~5 Tg yr^{-1}.

The main sink of OH is reaction with CO. An important natural source of CO is wildfires, which have increased in frequency and intensity due to climate change. Hence, UV-B radiation and climate change affect concentrations of tropospheric OH with potential feedbacks on climate change and on stratospheric ozone.

The impact of poor air quality is not limited to human health; it affects plants and other organisms as well. This has had a substantial impact on food production and forests through exposure to ground-level O_3. There is also evidence of reduced food production due to PM. The magnitude of these impacts will be altered by climate change and the future evolution of stratospheric O_3.

3 Trifluoroacetic acid in the global environment with relevance to the Montreal Protocol

3.1   Background

Trifluoroacetic acid (TFA) is the terminal breakdown product of many fluorinated chemicals, including those that fall under the purview of the Montreal Protocol and its Amendments. Its properties (discussed below) include very low reactivity, high stability, and recalcitrance to breakdown in the environment. This has raised concerns about the use of fluorinated substitutes for the ozone-depleting and the fluorinated greenhouse gases. The formation, fate, and potential effects of TFA have been the remit of the EEAP for the last two decades, and this overview is a continuation of this activity with a primary focus on new information since the last Quadrennial Assessment [6] to the Parties of the Montreal Protocol.

3.1.1   Classification of trifluoroacetic acid as a per- and poly-fluoroalkyl chemical

Trifluoroacetic acid CF_3-COOH (CAS# 76-05-1) is a perfluorinated chemical, meaning that, aside from its functional group (-COOH), all hydrogen atoms in the molecule have been replaced with fluorine. The European Chemicals Agency has proposed that this chemical be included in a class, the per- and poly-fluoroalkyl substances (PFAS) [181]. Others have suggested that the definition of PFAS should exclude TFA and chemicals that degrade to just give TFA [182]. In 2022, there were 4730 chemicals in the PFAS class, which had been expanded to include all chemicals with at least one aliphatic -CF_2- or -CF_3 moiety. The PFAS class includes gases (such as those under

the purview of the Montreal Protocol), low boiling point liquids, high boiling point liquids and lubricants, and solid polymers used in industry, medicine, and domestic equipment. As has been pointed out [183], a small number (about 256) of these PFAS are currently used commercially and *"grouping and categorizing PFAS using fundamental classification criteria based on composition and structure can be used to identify appropriate groups of PFAS substances for risk assessment."* [183] More recently, a majority of a panel of experts agreed that "*all PFAS should not be grouped together, persistence alone is not sufficient for grouping PFAS for the purposes of assessing human health risk, and that the definition of appropriate subgroups can only be defined on a case-by-case manner.*" [184]. In addition, the majority opinion with respect to toxicology was that "*it is inappropriate to assume equal toxicity/potency across the diverse class of PFAS*" [184].

This same argument applies to the inclusion of TFA, with a two-carbon chain and a single CF_3 group, into a class with longer chain PFAS. These longer chain PFAS have key chemical, physical, and biological properties that become quite different with increasing length of the carbon-chain (Table 2 and Appendix Table 1). For example (see Table 2), log K_{OW} (a measure of partitioning between lipids in organisms and water); Henry's Law Constant (a measure of partitioning between water and air); K_{OC} (a measure of adsorption to soil and sediment); and the half-life in humans (related to chronic exposure and chronic toxicity) all vary with changes in the length of the carbon chain. These relationships are well recognised [185-189] as they are important drivers of adsorption, distribution, and excretion in animals, which are major determinants of adverse effects.

Table 2 Key physical, chemical, and biological properties of the linear perfluorinated carboxylic acids from 2-8 carbons.

Property	Trifluoro-acetic acid	Perfluoro-propanonic acid	Perfluoro-butanoic acid	Perfluoro-pentanoic acid	Perfluoro-hexanoic acid	Perfluoro-heptanoic acid	Perfluoro-octanoic acid
Abbreviation	TFA	PF TFA	PFBA	PFPeA	PFHxA	PFHpA	PFOA
CAS#	76-05-1	422-64-0	375-22-4	2706-90-3	307-24-4	375-85-9	335-67-1
Molecular formula	CF_3COOH	CF_3CF_2COOH	$CF_3(CF_2)_2COOH$	$CF_3(CF_2)_3COOH$	$CF_3(CF_2)_4COOH$	$CF_3(CF_2)_5COOH$	$CF_3(CF_2)_6COOH$
Number of carbon atoms	2	3	4	5	6	7	8
Log K_{OW}	0.5	1.5 [a]	2.43 [a]	3.262 [a]	3.48	5.024 [a]	5.905 [a]
Henry's Law Constant (atm m^{-3} mol^{-1})	1.11×10^{-7}	4.43×10^{-6} [a]	0.0051 [a]	0.029 [a]	0.174 [a]	1.521 [a]	3.044 [a]
K_{OC} (L kg^{-1})	0.17-20	12.7 [a]	58 [a]	270 [a]	1247 [a]	5761	30,440
NOEC most sensitive aquatic plant (ng L^{-1})	2.5×10^6 [b]	1.44×10^7 [c]	6.21×10^8 [c]	$> 1.00 \times 10^9$ [c]	NA	$> 1.02 \times 10^9$ [c]	5.80×10^3 [c]
NOEC most sensitive aquatic animal (ng L^{-1})	LC50 = 7×10^7 [d]	LC50 = 8.0×10^7 [d]	LC50 = 1.1×10^8 [d]	LC50 = 1.3×10^8 [d]	LC50 = 1.4×10^8 [d]	LC50 $> 1.02 \times 10^6$ [d]	LC50 = 1.5×10^8
Half-life in humans [f]	16 h	NA	72-81 h	NA	14-49 d [e]	1.2-1.5 yr	2.1-10 yr

Unless otherwise stated, references are from [190]. Other sources are: [a] [191] [b] [192] [c] [193] [d] [194] [e] [187] [f] [195]. NOEC, no observed effect concentration; NA, not applicable.

There has been considerable discussion as to the inclusion of TFA in the class PFAS for regulatory purposes [182,183,196-199]. Regulatory agencies in North America acknowledge the physical, chemical, and biological properties of chemicals in the class of PFAS [189] and, in particular, the influence of chain length on these properties [188,189,200]. A sound assessment of the environmental impact of TFA needs to consider the relevant physical, chemical, and toxicological data and realistic environmental concentrations (see discussion in Sect. 3.2 to 3.6). We are of the opinion that the properties of TFA indicate that it should not be included in this class for the purposes of generic regulatory risk assessment.

The PFAS class also includes other perfluorinated chemicals that are of concern, e.g., perfluorooctanesulfonic acid, (PFOS). PFOS differs from TFA and its homologues because it is a sulfonic acid and is also more toxic than its alkanoic homolog. Therefore, as these chemicals do not fall under the purview of the Montreal Protocol, they have not been included in this discussion or in Table 2.

3.1.2 Properties of trifluoroacetic acid

The physical and chemical properties of TFA are well known [201] but key to assessing environmental risk is that it is a strong acid with a pKa of 0.3 and is completely miscible with water [190]. In the environment, it forms salts with alkali metals, which are also very soluble in water. These properties indicate that TFA and its salts will not bioaccumulate in organisms other than terrestrial plants and will not biomagnify in food chains. The carbon-fluorine bond is the strongest of all bonds with carbon and TFA and its salts are very recalcitrant in the environment. Studies on degradation by microbiota, including species and strains from contaminated areas, have not shown any evidence of TFA being susceptible to microbiological degradation [202,203].

3.2 Chemical pathways for degradation of precursors to trifluoroacetic acid

HCFCs and HFCs have found widespread use as replacements in applications that previously used CFCs. More recently, short-chain halogenated alkenes (hydrofluoroolefins, HFOs) are finding increasing use in several commercial applications. For example, E-CF$_3$CH=CHF (HFO-1234ze(E)) and E-CF$_3$-CH=CHCl (HCFO-1233zd(E)) are being used for foam blowing and in large chillers, whereas 2,3,3,3-tetrafluoropropene, CF$_3$CF=CH$_2$ (HFO-1234yf) is used as a replacement for 1,1,1,2-tetrafluoroethane, CF$_3$CH$_2$F (HFC-134a), in vehicle air conditioning units [204]. These chemicals are anthropogenic and there are no known natural sources of HCFCs, HFCs, and HFOs.

Tropospheric degradation of HCFCs, HFCs and HFOs is initiated by reaction with OH radicals, leading to formation of small terminal degradation products including CO, CO$_2$, and the halo-acids hydrogen fluoride (HF) and hydrogen chloride (HCl). Some of the degradation products are also atmospheric precursors of TFA through hydrolysis of acyl halides, e.g., CF$_3$CFO, or via secondary photochemistry of trifluoroacetaldehyde (CF$_3$CHO) [205,206]. The chemistry by which the CFC replacements are converted into precursors of TFA has been extensively studied over the last few decades and recently summarised [207,208]. Figure 10 illustrates how atmospheric degradation of different CFC replacements, belonging to three successive generations of CFC replacements, can lead to the formation of TFA in significantly different yields. For instance, the dominant atmospheric fate of CF$_3$CClO and CF$_3$CFO, generated in the atmospheric processing of HCFC-123 and HFC-134a, respectively, is uptake into cloud water, followed by effective hydrolysis to yield TFA, on a timescale of approximately 5-30 days [205]. However, due to competing fates of the intermediary alkoxy radicals (marked with asterisks in Fig. 10), the effective yields of TFA are significantly different (e.g., ~ 60% for HCFC-123 and 7–20% for HFC-134a). In the case of HFO-1234yf, no significant competition exists in the degradation pathway and the expected yield of TFA is ~ 100% through the hydrolysis of CF$_3$CFO.
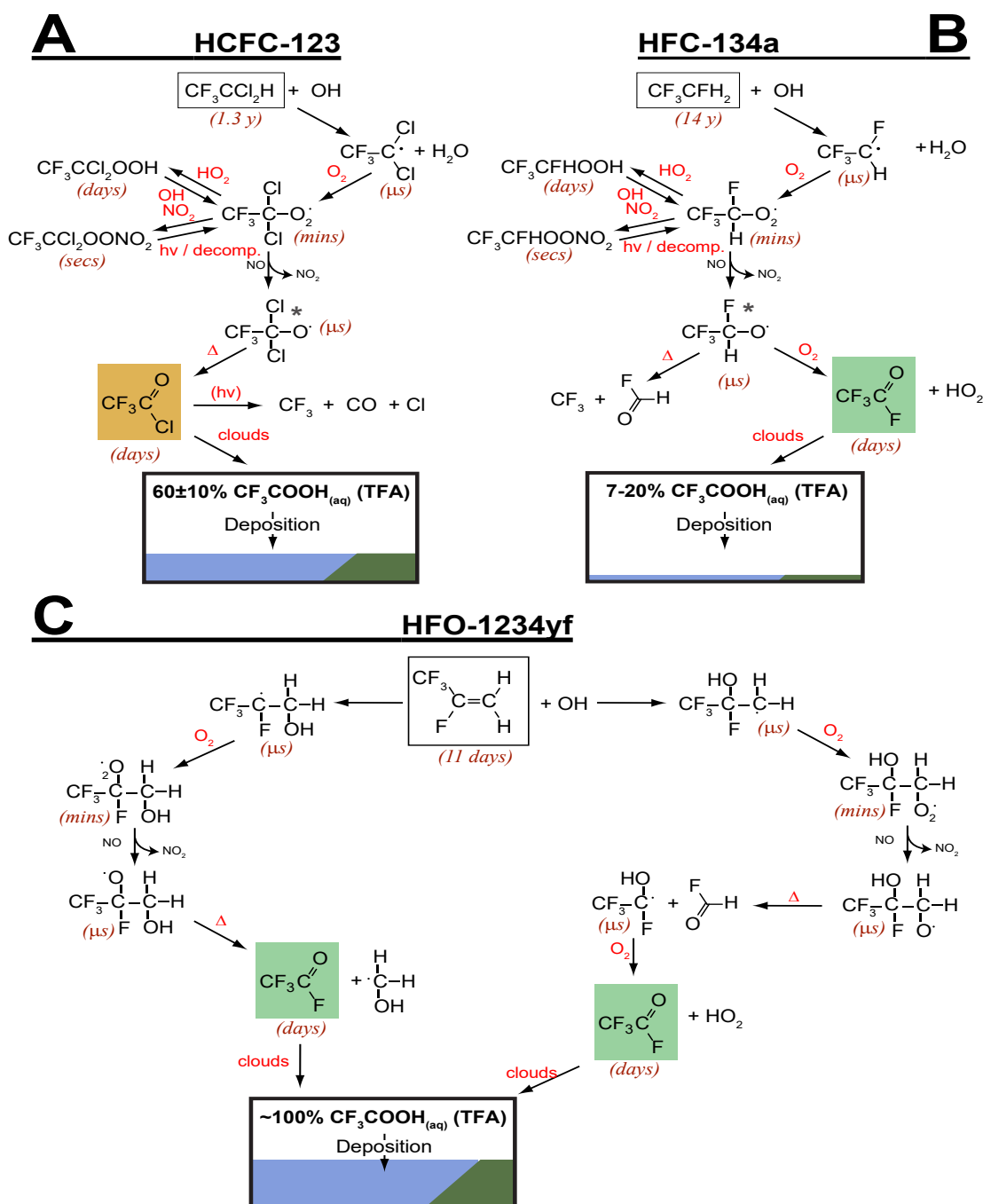
Fig. 10 Atmospheric degradation pathways and corresponding yields of TFA for HFCF-123 (Panel A), HFC-134a (Panel B) and HFO-1234yf (Panel C) representing three generations of important CFC replacements. Approximate atmospheric lifetimes for the chemical species involved are indicated in parenthesis. Species marked by an asterisk have significant competing fates in the atmosphere [205,206].

Even if they are not producing acid-halides during their atmospheric degradation, some other CFC replacements can still form TFA in small yields through the formation of trifluoroaldehyde, CF_3CHO. This aldehyde is the primary degradation product from several CFC replacements, including HCFCs, HFCs, HFOs and HCFOs, e.g., HCFC-234fb ($CF_3CH_2CCl_2F$, τ = 45 years), HFC-143a (CF_3CH_3, τ = 51 years) and HFO-1234ze(E) (E-$CF_3CH=CHF$, τ = 19 days) and HCFO-1233zd(E) ($CF_3CH=CHCl$, τ = 42 days) [209]. Here τ is the atmospheric lifetime defined as the reciprocal of the pseudo first order rate constants for the removal of the chemical species, also sometimes referred to as the "e-folding lifetime".

Figure 11 illustrates the atmospheric degradation of HCFO-1233zd(E), which produces CF_3CHO in essentially 100% yield. CF_3CHO has three competing fates in the atmosphere. First, it undergoes photolysis (annually averaged diurnal atmospheric lifetime in the troposphere of ≤ 2 days at 40° latitude) giving CF_3 and HCO radicals [210] (see also Sect. 3.7). Second, oxidation initiated by OH produces acyl peroxy radicals, which can react with HO2, NO, or NO_2. Reaction of these acyl peroxy radicals with HO_2 radicals can lead to the formation of TFA as a minor product. Third, contact with liquid water produces hydrates, which can react with OH radicals leading to the formation of TFA [211]. The latter two processes are currently thought to be minor fates of CF_3CHO. The reaction of the hydrate with OH radicals is an efficient pathway for generating TFA; however, the importance of hydrolysis of CF_3CHO to give TFA is uncertain (see Sect. 3.7.3). Due to these competing fates, an estimated 2-30% of atmospheric CF_3CHO is converted into TFA (see Appendix Sect. 4).

3.3 Contribution of chemicals under the purview of the Montreal Protocol to the global load of trifluoroacetic acid

Several CFC replacements give rise to the formation of TFA as an atmospheric oxidation product. Figure 12 provides an overview of estimated yields of TFA (%) for CFC replacements, as well as selected chemicals not under the purview of the Montreal Protocol (non-MP). In addition, some replacements such as HCFC-225ca ($CF_3CF_2CHCl_2$) yield longer-chain PFCAs, CF_2CF_2COOH (100%). HFC-134a and HFO-1234yf are the two substitutes that have the largest predicted contribution to global TFA concentrations among those gases that fall under the purview of the Montreal Protocol. The Science Assessment Panel (SAP) and the Technology and Economic Assessment Panel (TEAP) of the Montreal Protocol under the United Nations Environment Programme (UNEP) have projected future uses and potential releases from 2020 to 2100 for these two substitutes. A summary of the projected yield of TFA from degradation in the troposphere (Fig. 12) is provided in Table 3.
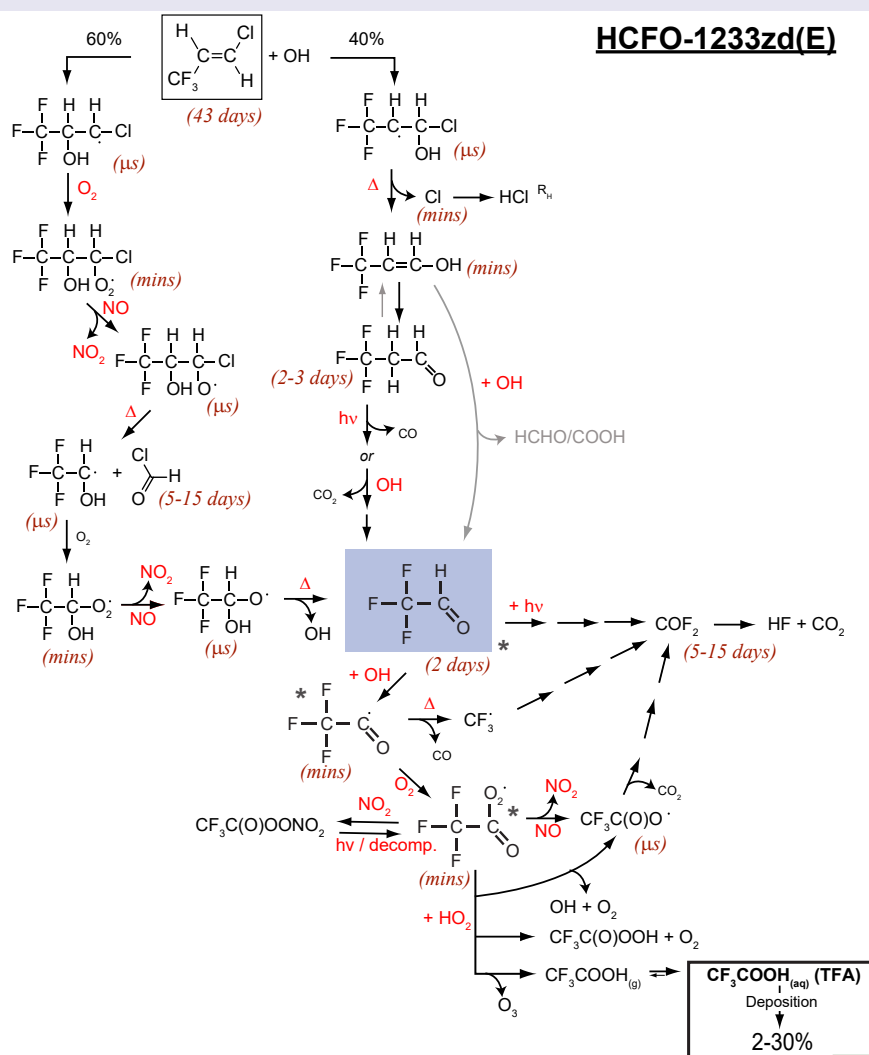

Fig. 11 Atmospheric degradation of HCFO-1233zd. The OH initiated oxidation of the product, CF_3CHO, is a minor source of TFA. Based on [207] and [208].
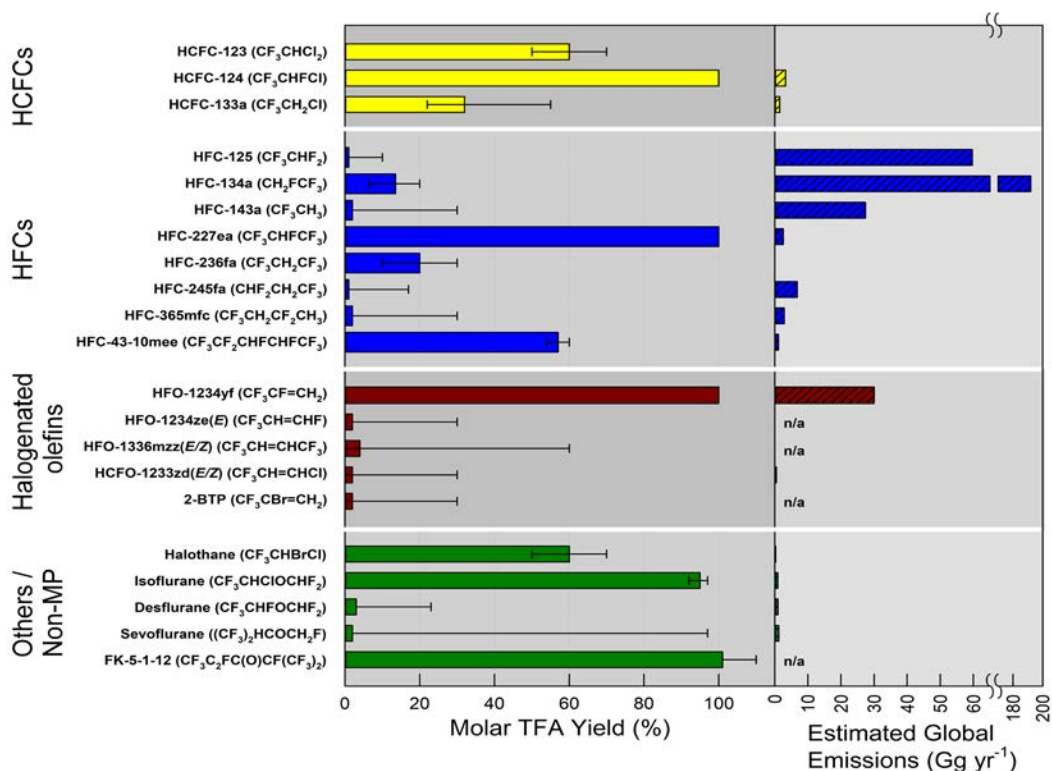
Fig. 12 Yields of TFA from selected individual CFC replacement compounds, and their estimated global emissions. Also included are selected compounds not under the purview of the Montreal Protocol and Amendments. Error bars represent both experimental uncertainties and upper and lower yield ranges due to competing reaction channels that depends on environmental conditions. Yields of TFA from individual compounds are estimated based on evaluations of the available literature as described in Online Resource Sect. 4. Note split scale for the emission of HFC-134a is much higher than that of other compounds.

Table 3 Projected global yields of TFA from HFC-134a and HFO-1234yf and total deposition between 2020 and 2100.

	HFC-134a	HFO-1234yf	Sum
Annual formation of TFA (a.e., acid equivalents)			
2020	0.01–0.03 Tg yr^{-1}	0.03–0.03 Tg yr^{-1}	0.04–0.06 Tg yr^{-1}
2050	0.02–0.05 Tg yr^{-1}	0.34–0.49 Tg yr^{-1}	0.36–0.54 Tg yr^{-1}
2100	0.01–0.02 Tg yr^{-1}	0.63–1.03 Tg yr^{-1}	0.64–1.05 Tg yr^{-1}
Sums of deposited TFA (a.e.)			
2020–2050	0.5–1.5 Tg	5.3–6.6 Tg	5.8–8.1 Tg
2020–2100	1.0–2.9 Tg	30.5–49.0 Tg	31.5–51.9 Tg
Concentration of TFA as the sodium salt in the oceans in	**2050**		**244–246 ng L^{-1}**
	2100		**266–284 ng L^{-1}**

These data are taken from Table 7.3 of the 2022 report of the Science Assessment Panel [212] and currently are best estimates for the two listed refrigerants. Releases of other potential sources of TFA (see Fig. 12) have not been included but are expected to be much smaller. Estimated future concentration in the oceans is based on the nominal value of 200 ng a.e. L^{-1} in 2020 and a total volume of 1.36 x 10^9 km^{-3}. For comparison to toxicity values, concentrations have been converted to sodium salt.

These amounts of TFA are estimated to increase concentrations in the global oceans from the nominal value of 200 ng a.e. L^{-1} (equivalent to 239 ng TFA sodium salt L^{-1}) estimated by *Frank et a*l. [213] to 266–284 ng sodium salt L^{-1} in 2100 if evenly distributed across all oceans. If the actual concentrations were less than the nominal value (239 ng TFA sodium salt L^{-1}), the predicted values for 2100 would be smaller. In a recent study in Germany, the contribution of currently used refrigerants to the formation of TFA was estimated [214]. The worst-case annual formation of TFA from refrigerant R134a was estimated at 1050 tonnes yr^{-1}, 1170 tonnes yr^{-1} from refrigerant R1234yf, and 141 tonnes yr^{-1} from all other refrigerants. If the proportions of TFA from other refrigerants in Germany are applied to the global estimate of deposition, the maximum value for contributions from all refrigerants would be about 6% greater i.e., 302 ng sodium salt L^{-1}.

It should be noted that the geographic distribution of TFA released into the atmosphere across the globe has changed with the introduction of refrigerants and blowing agents such as HFOs with short atmospheric lifetimes (days). The longer atmospheric lifetimes of the older generation HFCs allowed wider and more even distribution of parent HFCs and deposition of TFA, across the globe [215-217]. The HFOs will be degraded by tropospheric OH radicals closer to the source of release with resulting steeper gradients of concentration depending on wind direction and velocity [see examples of modeling of deposition in 217]. As a result of this uneven deposition, concentrations of TFA in surface waters will vary with flow rates and volumes of water. Prediction of concentrations of TFA in surface waters will require the development of hydrologic models, such as those now used to model distribution and concentrations of other pollutants in water. These types of models are available from the EPA (USA) [218] but would need to be modified for modeling of the dispersion of HFOs and TFA once it reaches the surface.

3.4   Trifluoroacetic acid in precipitation

The presence of TFA in precipitation continues to be studied, with several new reports published since the last Quadrennial Assessment [6]. Unless otherwise stated, only those studies with complete descriptions of analytical methods have been included. Analysis of rainwater samples collected in 2016 in 28 cities across China showed detectable amounts of TFA in all samples [219]. Concentrations ranged from a low of 9.1 to a high of 320 ng TFA a.e. L^{-1} and fluxes from 160 to 16,000 ng TFA a.e. m^{-2} day^{-1} (Tables S7 and S8 in [219]). A study on concentrations of TFA present in rainwater samples in eight locations across Germany from February 2018 to February 2019 showed a seasonal range of concentrations over one year [220]. Across all sites, frequency of detection was greater than 90% except in December, January, and February. The greatest median concentration, 703 ng TFA a.e. L^{-1}, was in June 2018. Over the year, daily fluxes across collection sites showed less variability with the greatest median flux of 774 ng TFA a.e. m^{-2} day^{-1} and the smallest of about 205 ng m^{-2} day^{-1} [Table 2 in 220]. This study was continued for an additional year [220] and a similar pattern was observed (Fig. 13). The source of the TFA was most likely degradation of fluorinated gases in the troposphere and the authors suggest that the seasonality is because of seasonal changes in solar UV-radiation and the photochemical formation of OH radicals responsible for production of TFA in the troposphere [220]. Fluxes of TFA in rainwater in Germany [220] were less than those reported from China [219], probably because of the release of more precursors in greater concentrations in the latter location. A recent study on temporal trends in concentrations of TFA in surface waters reported increases in concentrations of 6-fold between samples collected in 1998 and those collected in 2021 [221]. Concentrations in samples collected down-wind from the San Francisco Bay area were greater in 2021 (up to 2790 ng L^{-1}) than in 1998 (up to 287 ng L^{-1}). The author suggests that these residues of TFA are from the breakdown of fluorinated refrigerants, but fluxes were not reported so the role of reduced precipitation in generating the greater concentrations is unknown. Once reaching the surface, TFA will form salts with alkali metals and mix with surface- or interstitial-water in the soil. These salts can be taken up by plants (see below) and accumulate in plant tissues, particularly leaves. Based on this property, archived samples of various leaves of some species of trees from the German Environmental Specimen Bank were analysed for the presence of TFA [222]. The leaves collected spanned the period from 1989 to 2020 and showed an increase in concentrations of TFA. For example, concentrations of TFA in leaves of Lombardy poplar increased from ca 160 µg kg^{-1} (d.w.) in 1991 to ca 970 µg kg^{-1} in 2019. The authors suggest that the sources of TFA are replacements for the CFCs, mostly from precipitation. The authors are likely correct in this conclusion.

Breakdown products of some fluorinated chemicals include hydrofluoric acid (HF) and TFA, which are strong acids. However, the amounts generated from the oxidation of HFOs represent only a small (< 0.5%) contribution to the formation of acid rain in comparison to other sources such as sulfur and nitrogen oxides [223] and this is judged to not be of concern.

3.5   Other sources of trifluoroacetic acid in the global environment

In previous assessments [6,224,225], we have discussed other potential sources of TFA that are not related to the chemicals under the purview of the Montreal Protocol. In the global context, there is a paucity of information on these sources, but they fall into some general groupings, *inter alia*:

- Geogenic sources

- Effluents and releases from the manufacture of fluorinated chemicals, including chemicals under the purview of the Montreal Protocol and Amendments

- Combustion and degradation of fluorinated chemicals in commercial and household waste

- Biological and environmental degradation of chemicals such as pharmaceuticals and pesticides that contain fluorine atoms, specifically the -CF$_3$ moiety.

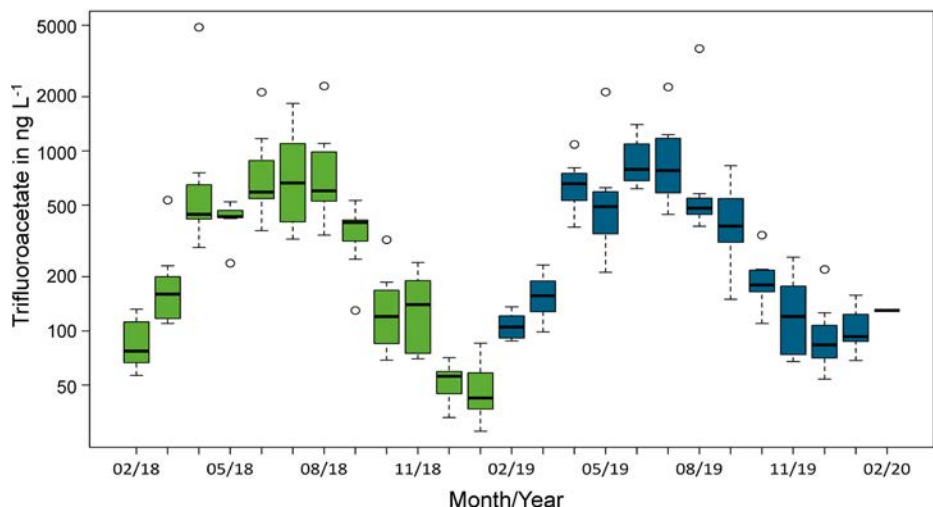These are discussed in more detail below.

Fig. 13 Concentration of trifluoroacetate in composite precipitation samples from eight sites in Germany from February 2018 to February 2020. The y-axis is on a binary logarithmic scale (log2) and the solid horizontal bar is the median, the box indicates the upper and lower quartiles, the whiskers the upper of lower quartile – or + the interquartile range x 1.5, and the data symbols are the outliers. From Fig. 27 in [220].

3.5.1 Geogenic sources

Since the early reports of the widespread presence of TFA in marine waters [213,226] and its association with ^{14}C-dated deep waters older than 1000 years [227], it was believed that there are natural sources of TFA. This is consistent with the report that concentrations of TFA increase with proximity to locations of undersea volcanic vents [227,228].

However, the theory that TFA can be formed from geogenic sources has been challenged [229]. This challenge was partially based on potential analytical errors and lack of information on levels of detection and quantitation, and high variance in concentrations measured in samples at different depths and in different oceanic basins. The authors focused on atmospheric sources of TFA in surface waters and ice, which originates in precipitation and did not consider measurements in other bodies of water such as endorheic lakes and playas located in areas of low precipitation and little fluorochemical industry. One of these locations, the Dead Sea, had a reported concentration of 6400 ng L^{-1} [226]. The Dead Sea is in a rift valley with a history of geological faulting and with a volume of 114 km^3, so that this concentration is equivalent to 730 tonnes of TFA. That this amount of TFA (measured in the 1990s) is all from anthropogenic sources is very unlikely, and geogenic sources are more plausible.

Another argument put forward that TFA does not originate from geogenic sources is the lack of TFA in older (> 2000 year-old) samples of glacial melt, surface, and ground water. These older waters originated from precipitation from evaporated (distilled) marine and surface waters. Like chloride, TFA from oceans (and possible endorheic lakes) could be carried to land close to the shore. However, this transport would only be for short distances and is unlikely to be a significant source of TFA and other PFAS in precipitation and/or ice cores [220]. While it is possible that TFA could have been released from surficial volcanos, these potential sources lack the combinations of high temperature and high pressures found in thermal vents in the deep ocean. It should be noted that some authors have reported the presence of fluorinated and/or chlorinated short-chain and aromatic carbon compounds (but not TFA) in emissions from surficial volcanos [reviewed in 230,231].

The background value of 200 ng TFA L^{-1} in the oceans as suggested by Frank et al. [213] would be equivalent to 268 x 106 tonnes of TFA in the global oceans if well mixed globally. However, based on analyses in several oceanic basins, lesser amounts (a range of 61–205 x 10^6 tonnes equivalent to 45–152 ng L^{-1}) were suggested by Scott et al. [227]. From the total known use and release of HFC-134a, HFC-143a, and HFC-227ea between 1990 and 2015, the total amount of TFA that could theoretically have been produced is 4.5 x 10^6 tonnes. This is very much less than the total based on the range of concentrations measured in the oceans, which, using an estimated ten-fold range, would be equivalent to 27–270 x 106 tonnes. Even with this assumption, this is equivalent to a discrepancy of 6 to 60-fold that is much larger than would be explainable by anthropogenic activity in relation to use of the HFCs. This gap is most likely from natural sources.

In the absence of more rigorous and consistent sampling of the oceans, these concentrations and amounts are speculative. For the purposes of comparisons to toxicity values and risk assessment, the EEAP [6,224,225,232] used the larger value to err on the side of caution when estimating further contribution from the chemicals under the purview of the Montreal Protocol to the total load in the global oceans.

Another major unknown in characterising the source of reported concentrations of TFA in the oceans is the degradation half-life of TFA in the environment. As discussed above, TFA is very recalcitrant and is essentially unreactive under normal environmental conditions. If, as seems to be the case, the half-life is likely very long (≈ centuries), very small amounts could accumulate over time to explain the amounts observed in oceans and endorheic basins.

3.5.2 Manufacturing of fluorinated chemicals

In the 1990s, there was only one manufacturer of TFA in the USA [201] and relatively few manufacturers of fluorinated refrigerants that fall under the purview of the Montreal Protocol. Since that time, the manufacture of fluorinated chemicals has increased, and these facilities are found in many countries around the world. Details on the amounts produced, use, and release of most of these chemicals and by-products are not reported in a way that is accessible to the public or the scientific community such as it is for chemicals under the purview of the Montreal Protocol. Several recent papers have reported measurements of TFA and potential precursors in locations near manufacturing facilities. Here we focus mostly on publications in the last four years.

A study of leachates and effluents from municipal waste disposal sites and landfills in the environs of Tianjin (China), the location of several fluorochemical manufacturing facilities, showed the presence of many PFAS as well as TFA at all sampling sites [233]. Greatest amounts of TFA (60,000 and 50,000 ng a.e. L^{-1}) were measured in leachates from two incineration plants, although leachates from one landfill and one transfer-site had similarly high concentrations approaching 40,000 ng a.e. L^{-1}. TFA was detected in samples of surface water and soils near a fluorochemical complex in Jinan (China) [234]. Concentration of TFA in lotic (flowing) surface waters ranged from 300 to 1000 ng L^{-1} but two lentic (still water sites) had mean concentrations of 1700 and 2600 ng a.e. L^{-1}. Well- and tap-water had concentrations of about 250 ng a.e. L^{-1}. In the same study, concentrations of TFA in soil samples close to factories ranged from 59 to 2081 ng a.e. kg^{-1}. Uptake of TFA from nutrient solution (containing 2,000,000,000 ng a.e. L^{-1}) by roots and leaves of wheat plants resulted in accumulated concentrations 170,000,000 ng kg^{-1} in roots and 100,000,000 ng kg^{-1} in shoots after exposure for 80 h [235]. Given the large and unrealistic concentrations in the nutrient solution, this is not surprising. Other PFAS were also taken up but to a lesser extent than TFA. This study did demonstrate uptake of TFA by plants. As discussed in the previous update report [225], maize and poplar plants take up TFA from contaminated soils [236]. Transport to the leaves was greater than to the stalk or the maize kernels. This is consistent with transport with water to the sites of transpiration and loss of water vapour through the leaves, resulting in accumulation of non-volatile salts of TFA. The median bioaccumulation factor (soil:leaf) was about 200. When these authors fed maize leaves to herbivores (locusts) the leaf-to-locust transfer factors were < 1 (0.028–0.185), indicative of negative trophic magnification (trophic dilution), most likely because locusts can excrete TFA, as has been demonstrated in mammals [201]. The large concentrations of TFA found in the environments around factories and plants manufacturing fluorinated chemicals indicate large fugitive emissions from some facilities that manufacture these chemicals. Given the small number of studies, the total load to the environment is very uncertain but it is an issue that needs to be addressed regionally, even if it is outside the scope of the Montreal Protocol.

3.5.3 Combustion and thermolysis of fluorinated chemicals

Polymers containing fluorine, such as polytetrafuoroethylene (PTFE) and related products, are heavily used in urban and industrial areas [237]. Data on amounts of fluoropolymers produced each year are not easily obtained; median estimates of value are in the region of 8 billion US dollars; however, there were no data on the mass of the products. When these polymers are subjected to high temperatures, they can degrade to yield TFA or precursors of TFA [238]. When heated to 500°C in the presence of air, PTFE, polychlorotrifluoroethylene (CPTFE), ethylene chlorotrifluoroethylene (ECTFE), and polytetrafluoroethylene-co-tetrafluoroethylene perfluoropropylether (PFEPE) yielded 7.8, 9.5, 6.3, and 2.5% TFA, respectively (Ellis et al., 2001). A similar study on this source of TFA in Beijing (China) indicated yields of TFA from thermolysis of PTFE, poly(vinylidene fluoride-hexafluoropropylene) (PVDF-HFP), and poly(vinylidene fluoride-co-chlorotrifluoroethylene) (PVDF-CTFE) were 1.2%, 0.9% and 0.3%, respectively, which was estimated to contribute 0.6–6.1 ng a.e. L^{-1} to precipitation over this city [239]. These are potential sources of TFA to the environment but little information was found in the literature on the effect of conditions of combustion (ranging from very high incineration temperature of waste to open-burning) on the rates of formation of TFA. However, this does remain a possible, but globally uncertain, source of TFA. A recent laboratory study of degradation of PFCAs [240], has shown that exposure of PFCAs (see Table 2) to sodium hydroxide in a polar aprotic solvent (e.g., dimethyl sulfoxide) resulted in degradation to fluoride ions in yields between 78 and 100% in 24 h.

TFA was formed in amounts of 19 to 39 mol% for PFCAs with 5 to 9 carbon chains. The authors suggest that this observation might lead to the development of methods for disposing of PFCAs. However, the TFA produced in the process might become a source of TFA to the environment.

3.5.4 Unidentified sources of exposure to trifluoroacetic acid

A review of the global occurrence of PFCs in water from wastewater treatment plants identified only two studies (included in previous reports from the EEAP) that had reported the presence of TFA [241]. Whether the TFA was formed during treatment of the wastewater or was present in the incoming effluent could not be determined; however, the authors speculated that it could have been formed from degradation of longer-chain PFAS precursors.

In a study of the concentrations of PFAS in the serum of staff and support workers in Nankai University in Tianjin (China), a location where fluorochemicals are manufactured, TFA and other PFAS were detected [242]. The frequency of detection of TFA was 97% but 12 other PFAS had greater frequencies of detection. The median concentration of TFA in serum of the volunteers was 8460 ng L^{-1} and

the 75th centile was 12,550 ng a.e. L^{-1}. Given the high solubility in water as noted above (and low K_{OW}, Table 2), this concentration is likely equivalent to a systemic burden of the same values in ng kg^{-1}. These values are 4.4 orders of magnitude less than the NOED (No Observed Effect Dose) for TFA in rats (discussed below) and do not suggest biologically significant risks for humans. Concentrations of PFOS and PFOA were greater than TFA and these chemicals are more toxic than TFA and are retained in the body for longer periods (Table 2). The authors reported an association between the sum of the concentrations of PFAS and biomarkers of diabetes but offered no insight as to causality by a specific chemical or the route of exposure to these chemicals.

Residues of TFA have been found in beverages such as beer and herbal infusions (teas) [243]. Analysis of samples of beer from 23 countries spanning the globe provided a range of concentrations with a median of 6100 ng L^{-1} and a maximum of 51,000 ng a.e. L^{-1}. The authors opined that the source of TFA in the beer and teas was not the water used to make the beverage, suggesting rather that the barley or the hops and the dried leaf of the tea(s) was the source of the contamination. Measurements of TFA in barley have not yet been reported in the literature but uptake of TFA from soil into maize kernels (discussed above) resulted in accumulations with a range of 40,400 to 102,000 ng a.e. kg^{-1} [236]. If accumulation in barley is like maize, this is a possible explanation; however, the source of the TFA in the barley is uncertain. It could originate from industrial sources of contamination or pesticides used in agriculture that break down to produce TFA and a terminal residue (see below).

An earlier paper from China [244] had reported the detection of many PFAS in outdoor dust; however, they did not analyse for TFA. Residues of TFA (and other PFAS) have now been detected in indoor and outdoor dust in China [245]. Median concentrations of TFA in outdoor dust from six locations in China ranged from 61,000 to 222,000 µg a.e. kg^{-1} with no consistent differences between rural and urban sites. In urban sites, concentrations of TFA in indoor dust from six locations in China ranged from 117,000 to 470,000 µg a.e. kg^{-1}. Concentrations of other PFAS were much smaller [245]. Using procedures from the EPA (USA), these authors also estimated daily intake values of PFAS of toddlers and adults that could result from ingestion of dust. The 95th centile estimated daily intakes of TFA for toddlers and adults were 5.3 and 0.55 ng a.e. kg^{-1} body weight, respectively for indoor dust. The 95th centile estimated daily intakes for toddlers and adults from outdoor dust were 3.2 and 0.33 ng a.e. kg^{-1} body weight. The original source(s) of the contamination in the dusts are unknown but there were amounts of unknown precursors (37−67 mol %) for PFAS in the dust [245].

3.5.5 Pharmaceuticals and pesticides

Fluorine atoms are frequently added to pharmaceuticals and pesticides to enhance or modify their biological properties. The most common use is replacement of a hydrogen with a fluorine atom. The van der Waals radii for hydrogen (0.12 nm) and fluorine (0.14 nm) are similar and small compared to that of other halogens such as chlorine (0.18 nm) [246]. Thus, fluorine-substituted chemicals are more likely to successfully dock with receptor sites than chemicals substituted with larger halogens such as Cl. The C-F bond is one of the strongest in organic chemistry, so this substitution tends to make the molecule more resistant to biochemical breakdown, which prolongs biological activity. In addition, substitution of hydrogen with fluorine can change other properties of the chemical, especially of adjacent chemical groups. For example, the F atom is a much stronger withdrawer of electrons than an H atom. As compared to hydrogen with a Hammett sigma value of zero, the Hammett for a single fluorine substituent on a benzene ring is +0.062 for para-effect and +0.337 for the meta-affect. For a $-CF_3$ on a benzene ring, the Hammett sigma values are +0.54 and +0.43, respectively.

For comparison with the precursors of TFA that are under the purview of the Montreal Protocol, the following discussion is focused on chemicals with a $C-CF_3$ moieties since these could potentially degrade to produce TFA as a terminal residue. It is estimated that about 20% of pharmaceuticals currently in commerce contain one or more fluorine atoms. As of 2020, the number of pharmaceuticals containing fluorine atom(s) was 369 [247] and in 2021, 13 new products containing fluorine were added [248]. Of these, 77 contain $C-CF_3$ moieties [from Fig. 4 in 247]. Some bacteria use fluoxetine (Prozac®, CAS# 54910-89-3) as a sole source of carbon and the terminal metabolite is TFA [249], which is not further metabolised. These authors also reported photolytic defluorination of intermediates formed in the degradation of fluoxetine [Fig. 7 in 249] but did not specify intensity or wavelength. Whether this photolytic defluorination occurs under environmental conditions is unknown. TFA can also be formed from some fluoro-pharmaceuticals during treatment of water with O_3. The molar yield of TFA from fluoxetine solutions treated with O_3 at 4 mg L^{-1} was as large as 40% [202].

Pharmaceuticals are used globally but there is a paucity of information on the amounts produced and used in the treatment of humans and other animals. However, these pharmaceuticals and/or their breakdown products are excreted and thus enter the environment. For example, anaesthetic procedures involving halothane ($CF_3CHClBr$), isoflurane ($CF_3CHClOCHF_2$), and desfluorane ($CF_3CHFOCHF_2$) are known to produce TFA as a metabolite in humans. Anaesthesia using halothane can result in significant levels of TFA in blood (20,000-110,000 µg L^{-1}), which is excreted in urine [250-253]. Those pharmaceuticals that contain the $C-CF_3$ moiety are expected to be a source of TFA in the environment but there are two unknowns, the yield of TFA from the breakdown of the pharmaceutical and the amounts of pharmaceuticals that are used. More publicly available information is needed to even begin to address this uncertainty. To estimate the contribution of pharmaceuticals to the total global load of TFA would be highly speculative but they are a potential source of TFA.

Some pesticides also contain one or more $C-CF_3$ moieties [254] and are potential sources of TFA in the environment [225]. Breakdown of some of these pesticides to TFA has been investigated. For example, ozonation (4 mg L^{-1}) of solutions of trembotrione (mesotrione, CAS# 104206-82-8), flufenacet (CAS# 142459-58-3), flurtamone (CAS# 96525-23-4), and fluopyram (CAS# 658066-35-4) at 100 µg L^{-1} for times between 5 and 60 min resulted in 5, 20, 43, and 32% production of TFA on a molar basis (Fig. 7 in [202]). Whether ozonation is a good model for the formation of TFA from pesticides in agricultural soils or not is unknown. The yield of TFA from the degradation of pesticides is dependent on the other substituents on the molecule and the environmental conditions. Studies on the photolysis of the lampricide 3-trifluoromethyl-4-nitrophenol (TFM CAS# 88-30-2) used to control the sea lamprey in the North American Great Lakes have shown that photolysis (365 nm) results in the formation of TFA [255]. Yields were dependent on the pH of the solution and ranged

from 5–18%. Conversion of the nitro-group to an amino-group increased the rate of conversion but not the yield. In another study, yields of TFA from photolysis of the penoxsulam (an herbicide) and sulfoxaflor (an insecticide) exposed to UV radiation in river water were less than 5% under laboratory conditions [256]. Neither of these pesticides were included in Table 4. Yields of TFA from penoxsulam were greater in river water than in distilled water at pH 7 (Fig. S18 in [256]). This dependence of the formation of TFA on environmental conditions and substituents on the other parts of the molecule likely applies to other pesticides and to pharmaceuticals and other potential precursors of TFA.

Similarly, as for pharmaceuticals, the amounts of pesticides used across the globe are not known at the level of individual chemicals. The Food and Agricultural Organization of the United Nations collects data on pesticide use by country, but these data are grouped by chemical class of pesticide and information on individual products is not available. However, data on annual estimates of the use of individual pesticides are available in the United States through the database on Estimated Annual Agricultural Pesticide Use, maintained by the US Geological Survey through the National Water-Quality Assessment Project [257].

To obtain a better understanding of the possible contributions of pesticides to the global load of TFA, we estimated the use of those pesticides containing one or more C-CF$_3$ moieties from data available in the United States. Maps and associated estimates of amount of pesticide applied [257] were downloaded and then compiled. As a worst case, upper estimates of use were selected and all data from 1992 to 2018 were collected, summed, and converted to tonnes of active ingredient. The molar yield of TFA was calculated using the ratio of the molecular weight of TFA (114.02 Daltons) and the pesticide (from Table S3 in [254]). This is a conservative assumption as the actual yield of TFA is dependent on other substituents on the molecule and the primary driver(s) of degradation. The potential total tonnage of TFA released from these pesticides was then calculated. These results are shown in Table 4.

Table 4 Potential release of TFA from fluorinated-pesticides used in the USA from 1992-2018.

Name[a]	MW[a]	Formula[a]	Number of C-CF$_3$ moieties[a]	Molar yield of TFA	Estimated tonnes of TFA
Acifluorfen	361.657	$C_{14}H_7ClF_3NO_5$	1	0.315	3,332
Bicyclopyrone	399.366	$C_{19}H_2OF_3NO_5$	1	0.286	117
Bifenthrin	422.872	$C_{23}H_{22}ClF_3O_2$	1	0.270	2,116
Chlorfenapyr	407.615	$C_{15}H_{11}BrClF_3N_2O$	1	0.280	315
Cyflumetofen	447.454	$C_{24}H_{24}F_3NO_4$	1	0.255	28
Cyhalothrin-gamma	449.854	$C_{23}H_{19}ClF_3NO_3$	1	0.253	73
Cyhalothrin-lambda	449.854	$C_{23}H_{19}ClF_3NO_3$	1	0.253	1,431
Dithiopyr	401.41	$C_{15}H_{16}F_5NO_2S_2$	1	0.284	1
Ethalfluralin	333.267	$C_{13}H_{14}F_3N_3O_4$	1	0.342	11,437
Fipronil	437.141	$C_{12}H_4Cl_{12}F_6N_4OS$	2	0.522	809
Flonicamid	229.162	$C_9H_6F_3N_3O$	1	0.498	168
Fluazifop	327.259	$C_{15}H_{12}F_3NO_4$	1	0.348	1,887
Fluazinam	465.089	$C_{13}H_4Cl_2F_6N_4O_4$	2	0.490	407
Flubendiamide	682.392	$C_{23}H_{22}F_7IN_2O_4S$	2	0.334	233

Flucarbazone	396.297	$C_{12}H_{11}F_3N_4O_6S$	1	0.288	105
Flufenacet	363.331	$C_{14}H_{13}F_4N_3O_2S$	1	0.314	2,623
Flumetralin	421.733	$C_{16}H_{12}ClF_4N_3O_4$	1	0.270	306
Fluometuron	232.206	$C_{10}H_{11}F_3N_2O$	1	0.491	12,618
Fluopicolide	383.576	$C_{14}H_8Cl_3F_3N_2O$	1	0.297	30
Fluopyram	396.717	$C_{16}H_{11}ClF_6N_2O$	2	0.575	292
Fluridone	329.322	$C_{19}H_{14}F_3NO$	1	0.346	27
Flutolanil	323.315	$C_{17}H_{16}F_3NO_2$	1	0.353	1,229
Fluvalinate	502.918	$C_{26}H_{22}ClF_3N_2O_3$	1	0.227	4
Fomesafen	438.758	$C_{15}H_{10}ClF_3N_2O_6S$	1	0.260	6,519
Isoxaflutole	359.319	$C_{15}H_{12}F_3NO_4S$	1	0.317	1,405
Lactofen	461.774	$C_{19}H_{15}ClF_3NO_7$	1	0.247	1,120
Mesotrione (trembotrione)	461.774	$C_{17}H_{16}ClF_3O_6S$	1	0.259	4,565
Novaluron	492.706	$C_{17}H_9ClF_8N_2O_4$	1	0.231	221
Oxyfluorfen	361.701	$C_{15}H_{11}ClF_3NO_4$	1	0.315	3,117
Prosulfuron	419.379	$C_{15}H_{16}F_3N_5O_4S$	1	0.272	151
Saflufenacil	500.85	$C_{17}H_{17}ClF_4N_4O_5S$	1	0.228	525
Tefluthrin	418.736	$C_{17}H_{14}ClF_7O_2$	1	0.272	1,893
Thiazopyr	396.376	$C_{16}H_{17}F_5N_2O_2S$	1	0.288	7
Trifloxystrobin	408.377	$C_{20}H_{19}F_3N_2O_4$	1	0.279	1,492
Trifluralin	335.283	$C_{13}H_{16}F_3N_3O_4$	1	0.340	65,327
Triflusulfuron	478.403	$C_{16}H_{17}F_3N_6O_6S$	1	0.238	30
Total					**122,604**

^a Data from [254]. Data on use of pesticides in the United States are from [257]. See Appendix Table 2 for annual quantities.

It should be noted that these estimated values are based on worst case assumption of highest estimated use and complete conversion of all C-CF$_3$ moieties in the chemical to TFA. Global use of pesticides in 2019 was estimated as 4,190,985 tonnes with 495,475 tonnes in North America [259], approximately 12% of the global use. Because of selection for resistance and the availability of alternatives, some of the pesticides included in Table 4 are no longer in use and the use-pattern of those currently in use will likely change in the future. For this reason and the lack of data on global pesticide use, the estimates of total global contribution to loads of TFA are uncertain; however, in comparison to future loads of TFA resulting from the release of chemicals under the purview of the Montreal Protocol, the potential contribution from pesticides is small.

A recent analysis of sources of TFA in the environment from the German Environment Agency [259] reported on precursors of TFA and included uses of refrigerants gases and other uses of chemicals for 2016–2018. Most of the TFA was estimated to be sourced from five products. The potential annual production of TFA from use of pesticides in Germany was 504 tonnes per year (Fig. 14), based on a mean of 3 years) but should not be compared directly with the data from the United States (Table 4), which presents total estimated use over 26 years.
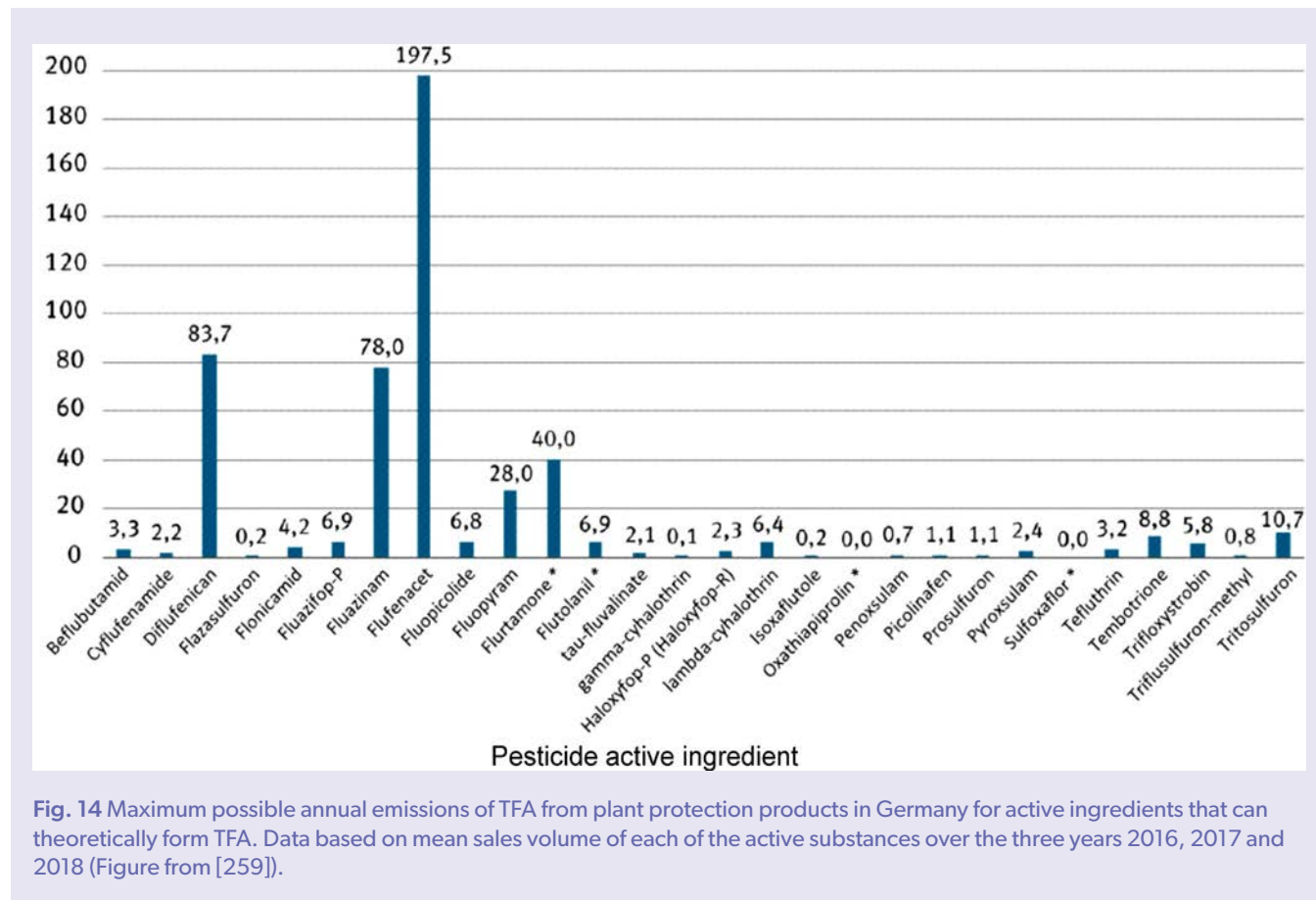

Fig. 14 Maximum possible annual emissions of TFA from plant protection products in Germany for active ingredients that can theoretically form TFA. Data based on mean sales volume of each of the active substances over the three years 2016, 2017 and 2018 (Figure from [259]).

3.6   Human and environmental risks associated with trifluoroacetic acid in the environment

3.6.1   Risks from exposure to TFA in terrestrial animals

Since the last Quadrennial Assessment, only one report on the potential effects of TFA in mammals was found in the literature [260]. This was a report on the effects of exposure to TFA salts via drinking water in male laboratory rats. The tests followed OECD guidelines (Tests 417 and 452 [261]) and exposures were for 90, 370, and 412 days at concentrations in the drinking water of 0 (control), 30, 120, and 600 mg TFA a.e. L^{-1}. The latter concentration was equivalent to a daily intake of 37.8 mg TFA kg^{-1} (b.m.). Responses measured were activity of the enzymes alanine-amino-transferase (ALT) and glutamate-pyruvate-transferase (GPT) in the blood. No significant effects were observed at 30 mg L^{-1} for any time of exposure but a significant increase in ALT activity was observed at 120 and 600 mg TFA a.e. L^{-1} at 370 days but not at 412 days. No effects on GPT were reported. In a second study with exposures for 14, 28, and 90 days to 0, 600, 1200, and 2400 mg TFA a.e. L^{-1}, no significant effects on ALT were observed. Increases in the activity of enzymes in or originating from the liver are considered as compensatory unless accompanied by physiological responses such as loss of weight. This reported effect does not change the conclusion that TFA is of low toxicity in mammals.

An extensive review of the potential effects of TFA in the environment published by the German Environmental Agency [214] did not identify any risks other than the persistence of TFA in the environment, which is a legislative rather than toxicological criterion. The concentrations of TFA in beer and tea discussed above are small when compared to the NOED of TFA in mammals. This indicates that the risk to humans from residues of TFA in beer and tea are *de minimis* (of little importance).

3.6.2 Risks of exposure to TFA in aquatic organisms

Since the last Quadrennial Assessment, one new toxicity test for an aquatic organism was located. This was a retest of the most sensitive alga (*Raphidocelis subcapitata*) conducted on behalf of Solvay [192]. The study protocol followed OECD guideline 201 [261]. Effect values were based on growth. A no observed effect concentration (NOEC) of 2.5 mg a.e. L^{-1} (2,500,000 ng L^{-1}) was reported based on inhibition of growth. Being a more recent study conducted under OECD guidelines, this data point was substituted for the older (1999) study used in the 2016 risk assessment [232] and is illustrated in Fig. 15. Although this new study on *R. subcapitata* has not been published in the literature, the study was conducted under Good Laboratory Practice Guidelines with Quality Assurance and Quality Control [262]. The detailed report of the study was reviewed by ECHA [263] and was classified as "*reliable without restriction*", hence it has been used here in the characterisation of the toxicity of TFA to aquatic organisms.

The margin of exposure between the distribution of NOECs and the observed and expected concentrations in the oceans and endorheic basins is several orders of magnitude and is indicative of *de minimis* risk.
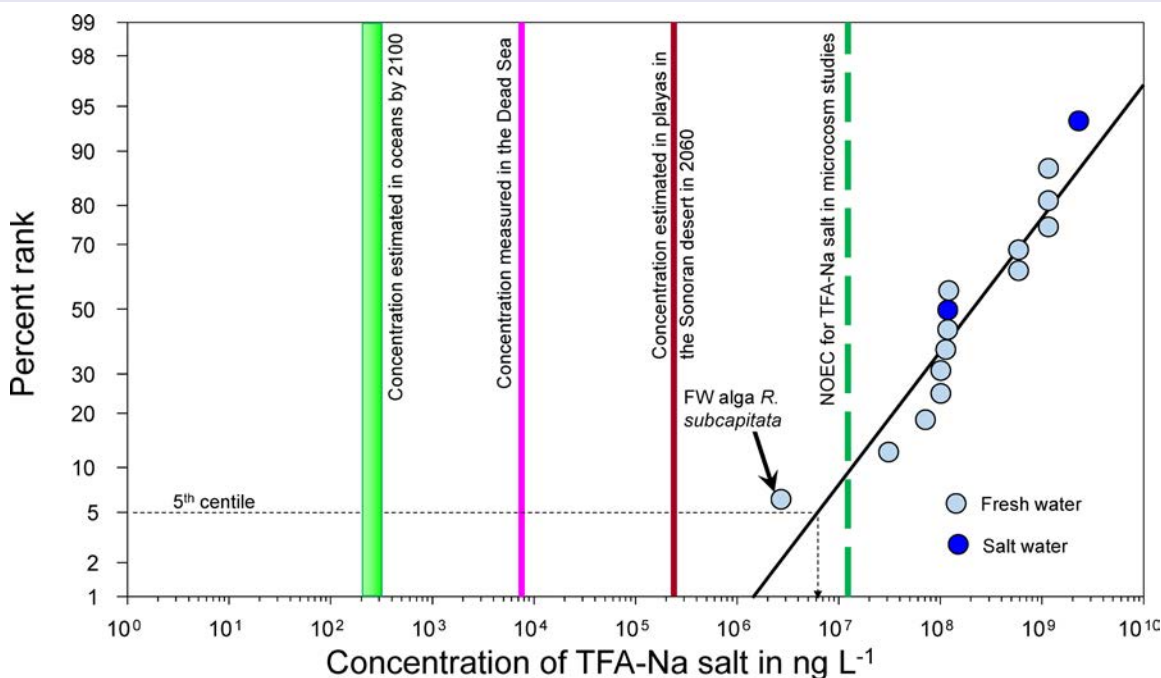

Fig. 15 A log-probability cumulative frequency plot of no observed effect concentrations (NOEC) of trifluoroacetic acid salt compared to various environmental concentrations in water. The dashed vertical green line indicates the NOEC for TFA-Na salt in microcosms is a toxicology-based criterion.

3.6.3 Environmental persistence of TFA as an assessment criterion

Environmental persistence is one of the criteria used to identify persistent organic pollutants (POPs), such as those regulated under the purview of the Stockholm convention. Persistence alone has been suggested to be a criterion for regulatory action [264]. The suggested threshold for this classification is a degradation half-life > 6 months. The stability of TFA and its salts indicates a half-life >> 6 months, but our opinion is that persistence should only be considered as a regulatory criterion for substances that are moderately or highly toxic and/or are bioaccumulative in organisms and/or undergo trophic magnification. TFA does not bioaccumulate nor is it toxic at the low to moderate exposures currently measured in the environment or those predicted in the distant future.

3.7   Other issues relevant to the degradation of fluorinated chemicals and release of TFA

3.7.1   Potential effects of hydrofluorocarbons and hydrofluoroolefins on tropospheric ozone

The photochemistry of CFC replacements, including HFCs and halogenated olefins, could impact air quality through formation of tropospheric O_3 on urban or regional scales. The spatial and temporal variation in VOC emissions, non-linear chemistry of the reacting chemical species, and complex atmospheric mixing and transport factors, all contribute to large uncertainties and thus complicate this assessment. In the past, e.g., [265], the potential impact has been addressed based on the indices of either the photochemical ozone creation potential (POCP) [266] or the Maximum Incremental Reactivity (MIR) index [267]. The MIR index values reflect the mass (grams) of ozone formed relative to the mass (grams) of VOC emitted. The POCP is a relative potential determined from the effect of a small incremental increase in the emission of a chemical on the calculated amount of O_3 formed, relative to the effect of an identical mass emission of ethene as a reference chemical. The former was developed with a focus on ozone formation in urban plumes and mainly in a United States urban-scale context. The latter addresses ground-level ozone formation on the regional, multi-day episode scale, as it most often occurs in Europe, here being predominantly a long-range transboundary and transport air quality issue. Both indices require fully speciated emission inventories and non-trivial model calculations. However, the POCP values can also be estimated to a first approximation based on structure and reactivity of the VOC, which is especially useful for VOCs for which no full chemical mechanisms have been implemented in atmospheric model studies, i.e., for many of the HFCs and HFOs discussed here.

With the exception of a 3-D global modeling study (Geos Chem) of the impact of HCFO-1233zd(E) [215], there have been no new reports of POCPs/MIR values for the HFCs and HFOs/HCFOs in the literature over the last review period. Recently, a methodological update to the original POCP estimation method has become available [268] (see Appendix, SI Sect. 3 for details). Table SI 3 (Appendix) lists the updated POCP values for CFCs and their replacements, based on the most recent reactivity evaluations and estimated for both north-west European and United States urban reference conditions. These values now provide index values on the same comparable scale and can be used as an approximate indicator of the potential impact on tropospheric ozone from the CFC replacements. In general, first- and second-generation CFC replacements, HCFCs and HFCs, have very small POCP values. Many of the common HFOs, with some exceptions, have POCP values that lie between those for methane (0.57/0.22) and ethane (10.91/4.52). The POCP values for HFOs are generally larger than those for the analogous HFCs, but much smaller than those for the parent alkenes. This is consistent with the few explicit MIR modeling studies of HFOs available in the literature. e.g., [267,269]. It is clear from these studies, and from the values in Table SI 3 (Appendix) that substitution of e.g., HFC-134a emissions for an equal mass of HFO-1234yf emissions, would lead to an increase in POCP-weighted emissions (two orders of magnitude). Still, MIR studies and atmospheric modeling studies of HFO-1234yf, have shown that O_3 production from HFO-1234yf is indistinguishable from that from ethane (also consistent with Table SI 3, Appendix), and that replacing HFC-134a in vehicle air conditioning units with HFO-1234yf across the United States has a negligible impact (< 0.01 %) on the formation of tropospheric ozone. It is clear from the above, that the small increases in tropospheric ozone formation generated from a transition from HFC emissions to emissions of HFOs would not be of concern.

3.7.2   Relevance of trifluoroacetaldehyde, a precursor of TFA, is increasing

With the transition from HFCs to third-generation alternatives such as HFO-1234ze(E) and HCFO-1233zd(E), the atmospheric abundance of CF_3CHO, (estimated 40° latitude, annually averaged diurnal tropospheric lifetime of ≤ 2 days [210]) is expected to increase in source regions. Ambient concentrations of HFO-1234ze and HCFO-1233zd(E) have been measured in central Europe (Germany) at urban, semi-urban, and remote sites from 2011 onwards [270-272]. As discussed in Sect. 3.2, these chemicals give CF_3CHO as an intermediary product of atmospheric degradation, with a yield of 100%. In 2020 the measured mean abundances of HFO-1234ze and HCFO-1233zd(E) in central Europe at Jungfraujoch (remote, 3580 m above sea level) were 0.98 ng m^{-3} (0.21 pptv) and 1.01 ng m^{-3} (0.19 pptv), respectively. This is an increase from 0.18 ng m^{-3} (0.039 pptv) and 0.02 ng m^{-3} (0.003 pptv) in 2013 at this same measurement station. A recent 3D global chemistry and transport model study [273] suggests significant increases in the abundance of CF_3CHO in source regions, as well as in the global background, however, it appears that the model of Wang et al. does not include photolysis of CF_3CHO, which is the major tropospheric sink for CF_3CHO (see above). They employed a high and a low emissions scenario for HFO-1234ze (12.6 or 124.4 ktonne yr^{-1} by 2050) and predicted annual average mixing ratios of 11 ng m^{-3} (2.7 pptv) for CF_3CHO in China (source region) and 0.7 ng m^{-3} (0.18 pptv) as a global average for their low emissions scenario. For their high emissions scenario, they predict annual mixing ratios in China of 413 ng m^{-3} (103 pptv). These values are all significantly larger than those (< 5 pg m^{-3} level) which can be inferred from a 3-D global chemistry model study of the atmospheric degradation of HCFO-1233zd(E) with contemporary emissions estimates (0.5 Gg yr^{-1}) [215]. The stark difference in the two studies can be explained by the difference in CF_3CHO chemistry employed by the two models. Due to the fast photolysis of CF_3CHO, concentrations of CF_3CHO are unlikely to build up to ng m^{-3} levels locally or globally.

3.7.3   Sinks for CF_3CHO: A photolytic source of HFC-23 and CF_3CHO-hydrate formation

The dominant overall sink for CF_3CHO is thought to be photolysis [210]. The photolysis can proceed through three principal pathways:

(1a) $CF_3CHO + h\nu \rightarrow CF_3 + HCO$

(1b) $CF_3CHO + h\nu \rightarrow CF_3H + CO$

(1c) $CF_3CHO + h\nu \rightarrow CF_3CO + H$
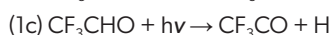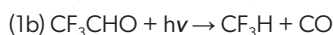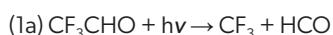
Chiappero et al. [210] reported a quantum yield of $\varphi_{1a} = 0.17 \pm 0.03$ and no indication of reaction 1b occurring in the 308 nm photolysis of CF_3CHO. However, a recent study by Campbell et al. reported that reaction 1b has a quantum yield at 308 nm of $\varphi_{1b} = 0.01 \pm 0.005$, and that in effect $11 \pm 5.5\%$ of CF_3CHO would undergo reaction via reaction 1b in the atmosphere to yield CF_3H (HFC-23) [274]. CF_3H is a strong GHG (GWP = 12,690), and its photochemical formation through reaction 1b could, in effect, present an additional and potentially significant contribution to the radiative forcing of climate of the parent CFC alternatives. The study of Campbell et al. 2020 [274] was based on an indirect technique using CO as a marker for pathway 1b and conducted at very low, sub-atmospheric pressure and temperatures. A subsequent chamber study at atmospheric pressures by Sulbæk Andersen and Nielsen [275] using broad-band actinic radiation shows no formation of CF_3H in the tropospheric photolysis of CF_3CHO and an estimated upper limit for the yield of CF_3H of 0.3 % was established. Whereas the study of Sulbæk Andersen and Nielsen [275] was carried out under tropospheric conditions, none of the past photolytic studies were performed using the same photolysis sources and detection methods. As suggested by Sulbæk Andersen and Nielsen [275], investigations of the photolysis at wavelengths relevant to the upper troposphere/lower stratosphere would be of interest for a more comprehensive modeling of the atmospheric photolysis of CF_3CHO.

The yield of TFA from CF_3CHO may depend on whether it remains in gaseous form. It has been reported that formaldehyde is efficiently converted to gaseous formic acid via a multiphase pathway involving a hydrated form of formaldehyde [276]. Earlier, using computational methods, Rayne and Forest [277] suggested that CF_3CHO will be dominantly present as the hydrated form in aqueous solution. The reaction of OH radicals with the hydrated form of CF_3CHO in the gas phase is known to be an effective route for formation of TFA (100%) [211]; however, to what extent CF_3CHO could be removed from the atmosphere through wet scavenging and undergo multiphase chemistry is unknown.

3.7.4 CF_3CHO and TFA: Interactions with particle growth and formation of new particles

Recent simulations have shown that both CF_3CHO and TFA can participate in particle growth and particle formation processes [278-280] However, these processes are highly dependent on season and atmospheric conditions. The reaction of $CF_3CHO/(CH_3)_2NH/H_2O$ can compete well as a sink for CF_3CHO at night (when photolysis is not occurring and concentrations of OH radical are low) if relative humidity and dimethylamine concentrations are high.

TFA enhances the formation rate of new dimethylamine/sulfuric particles significantly (up to 227-fold [278]), but only under conditions of relatively low temperatures and sulfuric acid concentrations, and relatively high TFA and dimethylamine concentration. With increasingly effective regulations on emissions of sulfur-containing pollutants, the enhancement of new particle formation by TFA may become increasingly important in urban areas where emissions of sulfur are expected to decline.

3.7.5   Potential impact of reactions of TFA with stabilised Criegee intermediates

Stabilised Criegee intermediates (SCI), highly reactive chemicals formed in the atmosphere, react rapidly with perfluorinated carboxylic acids (PFCAs), including TFA, producing hydroperoxyfluoroesters. This is likely the dominant gas-phase fate of PFCAs [281], although this only constitutes a temporary reservoir. SCIs exist in the greatest concentrations over forested regions, where emissions of biogenic alkene are high. The lifetime of TFA would be as short as 2 days over land areas with significant SCI-mediated loss, such as in tropical forests [216]. However, hydrolysis of the ester products, and reaction with OH, simply regenerates TFA; therefore, reactions of TFA with SCI are unlikely to have a substantial impact on the overall loss of gas-phase TFA [281]. In effect, the SCI-mediated oxidation products were found to have no significant impact on concentrations or distributions of TFA in the atmosphere [216] and this is not a pathway for net destruction of TFA in the environment.

3.8   Conclusions and uncertainties

TFA is a perfluorinated acid that has been included in the class of per- and polyfluoroalkyl substances (PFAS). This class of chemicals contains 4730 substances, of which about 256 are in commercial use. Even in the subclass of perfluorinated alkanoic acids, the physical, chemical, and biological properties of these substances differ widely, mostly in relation to length of the alkyl chain. To regulate these substances as a class (as has been suggested) is not scientifically defensible and TFA should be treated as a unique chemical for the purposes of regulation.

TFA is an acid when formed in the atmosphere but on reaching the surface (soil or water) it forms salts with alkali metals (e.g., sodium, potassium, calcium etc.). Because of its lack of reactivity, TFA salts are persistent in the environment and estimates of half-life are uncertain but could be in the range of centuries or millennia. This persistence is not a major concern because it does not react with biomolecules. TFA and its salts are easily excreted by animals and do not bioaccumulate in food chains. Salts of TFA have low toxicity to animals and plants and there are very wide margins between current/projected exposures and toxicity values.

One source of TFA in the environment is the degradation of replacements for chemicals that contribute to the destruction of stratospheric O_3. These are the HCFCs, HFCs, and HFOs, all of which are replacements for chemicals that fall under the purview of the Montreal Protocol. Some of these products are greenhouse gases and contribute to global climate change. Because of this, there is a trend to replace long-lived HCFCs and HFCs with HFOs, which have very short atmospheric lifespans and do not contribute to climate change. The use of these replacements is monitored under the auspices of the Montreal Protocol and estimates of current and future releases of TFA are regularly assessed. These releases will add to the existing load of TFA in the environment but predicted amounts are well below the threshold for concern with respect to human and environmental health.

Initial reactions in the atmospheric degradation of HCFCs, HFCs, and HFOs that lead to TFA are well understood. Some uncertainties still exist for the atmospheric fate of CF_3CHO. With the transition from HFCs to HFOs, the importance of the degradation product, CF_3CHO, in the environment is increasing. Nevertheless, CF_3CHO is likely to be only a minor source of TFA. Other than HCFCs, HFCs, and HFOs, there are additional sources of TFA in the environment. TFA is used as a laboratory reagent and is the starting material for many industrial products. It is formed from combustion of fluoropolymers and as a terminal breakdown product of fluorinated pharmaceuticals and pesticides. Fugitive releases have resulted in high levels of contamination near manufacturing facilities and TFA is routinely detected in surface waters. Other than precipitation, which contains TFA formed in the atmosphere, the sources for TFA in surface waters are uncertain. However, preliminary estimates of possible releases from use of pesticides in the United States and Germany suggest that total amounts are less than those from HCFCs, HFCs, and HFOs. Amounts released from degradation of pharmaceuticals are very uncertain and amounts from fugitive releases from manufacturing are completely unknown.

TFA released into the environment will eventually collect in terminal basins such as endorheic lakes or the oceans. Because the HCFCs and HFCs are long-lived in the atmosphere, they distribute globally and TFA from these substances is more evenly deposited. The HFOs and HCFOs have shorter lifetimes in the atmosphere and deposition of TFA from these substances is likely to be more localised. This will result in greater concentrations near the locations of release. This is unlikely to present a risk to humans or the environment in these locations but changes in concentration in surface water (or soil) would respond rapidly to releases. Monitoring of the environment for residues of TFA would provide an early warning if trends in concentration indicate rapid increases.

Presence of TFA in precipitation and flowing waters will be driven by release from precursors and other sources as well as the hydrology and will likely fluctuate. Concentrations in terminal basins such as the oceans will fluctuate less but will be dependent on rates of inputs from precipitation and rivers. Once in the oceans, concentrations will be influenced by rates of input of fresh water as well as currents and mixing in the oceans. Current and projected (to 2100) concentrations of TFA in the oceans provide a very large margin of exposure (thousand-fold) when compared to thresholds of toxicity and risks to the environment and human health are *de minimis*. However, there is some uncertainty in the environmental toxicity values because only two marine species are included in the toxicity data set for aquatic species; and marine macrophytes, which are keystone species with respect to habitat, have not been tested.

There are several national and regional programmes that monitor and report on concentrations of chemicals such as pesticides in surface water. For example, the National Water-Quality Assessment programme in the United States [257] and NAIADES programme in France [282]. These programmes have the infrastructure to routinely sample flowing waters from many watersheds and analyse these for residues of pesticides. It should not be difficult or costly to include TFA in these analyses. If started soon, these data could be useful in characterising inputs of TFA from the short-lived HFOs as well as in identifying point-sources of industrial inputs.

4 Knowledge gaps

There have been significant efforts to improve air quality through reductions in VOCs and NOx emissions. However, major uncertainties remain for future emissions scenarios, as well as changes in environmental conditions such as UV-B radiation, temperature, and humidity, which are sensitive to changes in stratospheric O_3 and climate. Furthermore, models need to be improved to better characterise the production and destruction of ground-level O_3 in complex urban VOC-NOx mixtures, the propensity for producing SOA, and the contribution of the transport of stratospheric O_3 to the troposphere.

Knowledge of global OH concentrations and their variability must be enhanced to constrain the estimated atmospheric lifetime of the many gases removed by OH. This will require improved assessment of anthropogenic and natural emissions of species that control the concentration of atmospheric OH, including CO, methane, and NOx. Better methods are needed to estimate global-scale OH concentrations, since the use of methyl chloroform for this purpose has become less reliable due to its rapidly decreasing emissions.

Some uncertainties remain in our understanding of the sources, routes of formation, and environmental fate of TFA. Identification and quantification of potential natural sources of TFA are urgently needed.

Similarly, better local/regional emission inventories are needed for short-lived precursors of TFA arising from CFC-replacements, as well as characterisation of all other anthropogenic sources of TFA. In addition, reliable estimates of yields of TFA are required for current and new replacement compounds and their partially oxidised degradation intermediates. Finally, there is some uncertainty in toxicity values for TFA because of the limited number of marine species tested.

5 Conclusions

UV-B radiation has positive and negative impacts on tropospheric air quality. UV-B radiation is essential to the formation of photochemical smog, including ground-level O_3, particulate matter, but is also essential for removing pollutants from the atmosphere. Thus, changes in UV-B radiation have consequences for both air quality and the lifetime of many gases, including some GHGs and VSLSs. Poor air quality remains a major health problem globally, despite progress in reducing anthropogenic emissions of air pollutants. The Montreal Protocol has prevented large increases in UV-B radiation; however, interactions with climate change complicate predictions. Future changes in UV-B radiation are uncertain but present substantial dangers given the widespread vulnerability of humans to e.g., photochemical smog.

The Montreal Protocol has led to the replacement of ODSs with fluorinated chemicals, some of which can undergo degradation in the atmosphere to give TFA in various yields. TFA is known to have a long environmental lifetime and accumulates in surface and ground waters. At present, there are large uncertainties associated with the concentrations of TFA in various environmental compartments in some regions, as well as the relative proportion of anthropogenic sources related to the Montreal Protocol, compared to the other anthropogenic and natural sources. There is some uncertainty in toxicity values because of the limited number of marine species tested. Current and predicted concentrations (to year 2100) of TFA in the oceans provide a large margin of exposure (thousand-fold) when compared to thresholds of toxicity.

The topics of this assessment align closely with several of the Sustainable Development Goals (SDGs) [283]. Issues in air-quality (Sect. 2) specifically relate to SDG 3 (*Good Health and Well-being*), but also inform SDG 2 (*Zero Hunger – via damage to crops*), SDG 11 (*Sustainable Cities and Communities – via impacts on livability*), and SDG 13 (*Climate Action – via OH controlling the lifetimes of many climate-relevant gases*). Atmospheric processing of CFC-replacements leading to persistent chemicals such as TFA (Sect. 3) raises concerns about SDG 12 (*Responsible Consumption and Production*) and in the context of SDG 6 (*Clean Water and Sanitation – via accumulation in sources of drinking water*).

References

1. Tang, X., Madronich, S., Wallington, T., & Calamari, D. (1998). Changes in tropospheric composition and air quality. *Journal of Photochemistry and Photobiology B: Biology, 46*, 83–95. https://doi.org/10.1016/S1011-1344(98)00187-0

2. Solomon, K. R., Tang, X., Wilson, S. R., Zanis, P., & Alkiviadis F Bais (2003). Changes in tropospheric composition and air quality due to stratospheric ozone depletion. *Photochemical & Photobiological Sciences, 2*, 62–67. https://doi.org/10.1039/B211086E

3. Wilson, S. R., Solomon, K. R., & Tang, X. (2007). Changes in tropospheric composition and air quality due to stratospheric ozone depletion and climate change. *Photochemical & Photobiological Sciences, 6*, 301-310. https://doi.org/10.1039/B700022G

4. Tang, X., Wilson, S. R., Solomon, K. R., Shao, M., & Madronich, S. (2011). Changes in tropospheric composition and air quality due to stratospheric ozone depletion and interactions with changes in climate. *Photochemical & Photobiological Sciences, 10*, 280–291. https://doi.org/10.1039/C0PP90039G

5. Madronich, S., Shao, M., Wilson, S. R., Solomon, K. R., Longstreth, J. D., & Tang, X. Y. (2015). Changes in air quality and tropospheric composition due to depletion of stratospheric ozone and interactions with changing climate: implications for human and environmental health. *Photochemical & Photobiological Sciences, 14*, 149-169. https://doi.org/10.1039/c4pp90037e

6. Wilson, S. R., Madronich, S., Longstreth, J. D., & Solomon, K. R. (2019). Interactive effects of changing stratospheric ozone and climate on tropospheric composition and air quality, and the consequences for human and ecosystem health. Photochemical & Photobiological Sciences, 18, 775-803. https://doi.org/10.1039/c8pp90064g

7. Haagen-Smit, A. J., Bradley, C. E., & Fox, M. M. (1953). Ozone formation in photochemical oxidation of organic substances. Industrial & Engineering Chemistry, 45(9), 2086-2089. https://doi.org/10.1021/ie50525a044

8. McKenzie, R. L., Aucamp, P. J., Bais, A. F., Bjoern, L. O., Ilyas, M., & Madronich, S. (2011). Ozone depletion and climate change: Impacts on UV radiation. *Photochemical & Photobiological Sciences, 10*(2), 182-198. https://doi.org/10.1039/c0pp90034f

9. Seinfeld, J. H., & Pandis, S. N. (2016). *Atmospheric Chemistry and Physics: From Air Pollution to Climate Change* (3rd ed.): John Wiley and Sons

10. Brasseur, G. P., & Jacob, D. J. (2017). *Modeling of Atmospheric Chemistry*: Cambridge University Press.

11. Szopa, S., Naik, V., Adhikary, B., Artaxo, P., Berntsen, T., Collins, W. D., Fuzzi, S., Gallardo, L., Scharr, A. K., Z.Klimont, Liao, H., Unger, N., & Zanis, P. (2021). Short-Lived Climate Forcers. In V. Masson-Delmotte, P. Zhai, A. Pirani, S. L. Connors, C. Péan, S. Berger, N. Caud, Y. Chen, L. Goldfarb, M. I. Gomis, M. Huang, K. Leitzell, E. Lonnoy, J. B. R. Matthews, T. K. Maycock, T. Waterfield, O. Yelekçi, R. Yu, & B. Zhou (Eds.), *Climate Change 2021: The Physical Science Basis. Contribution of Working Group I to the Sixth Assessment Report of the Intergovernmental Panel on Climate Change*: Cambridge University Press

12. Liu, S. C., & Trainer, M. (1988). Responses of the tropospheric ozone and odd hydrogen radicals to column ozone change. *Journal of Atmospheric Chemistry, 6*(3), 221-233. https://doi.org/10.1007/bf00053857

13. Thompson, A. M., Stewart, R. W., Owens, M. A., & Herwehe, J. A. (1989). Sensitivity of tropospheric oxidants to global chemical and climate change. *Atmospheric Environment (1967)*, 23(3), 519-532. https://doi.org/10.1016/0004-6981(89)90001-2

14. Zhang, H., Wu, S., Huang, Y., & Wang, Y. (2014). Effects of stratospheric ozone recovery on photochemistry and ozone air quality in the troposphere. *Atmospheric Chemistry and Physics, 14*(8), 4079-4086. https://doi.org/10.5194/acp-14-4079-2014

15. Hodzic, A., & Madronich, S. (2018). Response of surface ozone over the continental United States to UV radiation declines from the expected recovery of stratospheric ozone. *npj Climate and Atmospheric Science, 1*(1), 35. https://doi.org/10.1038/s41612-018-0045-5

16. Bekki, S., Law, K. S., & Pyle, J. A. (1994). Effect of ozone depletion on atmospheric CH_4 and CO concentrations. *Nature, 371*(6498), 595-597. https://doi.org/10.1038/371595a0

17. Fuglestved, J. S., Jonson, J. E., & Isaksen, I. S. A. (1994). Effects of reductions in stratospheric ozone on tropospheric chemistry through changes in photolysis rates. *Tellus B: Chemical and Physical Meteorology, 46*(3), 172-192. https://doi.org/10.3402/tellusb.v46i3.15790

18. Schnell, R. C., Liu, S. C., Oltmans, S. J., Stone, R. S., Hofmann, D. J., Dutton, E. G., Deshler, T., Sturges, W. T., Harder, J. W., Sewell, S. D., Trainer, M., & Harris, J. M. (1991). Decrease of summer tropospheric ozone concentrations in Antarctica. *Nature, 351*(6329), 726-729. https://doi.org/10.1038/351726a0

19. Isaksen, I. S. A., Zerefos, C., Kourtidis, K., Meleti, C., Dalsøren, S. B., Sundet, J. K., Grini, A., Zanis, P., & Balis, D. (2005). Tropospheric ozone changes at unpolluted and semipolluted regions induced by stratospheric ozone changes. [https://doi.org/10.1029/2004JD004618]. *Journal of Geophysical Research: Atmospheres, 110*(D2). https://doi.org/https://doi.org/10.1029/2004JD004618

20. Butler, A. H., Daniel, J. S., Portmann, R. W., Ravishankara, A. R., Young, P. J., Fahey, D. W., & Rosenlof, K. H. (2016). Diverse policy implications for future ozone and surface UV in a changing climate. *Environmental Research Letters, 11*(6), 064017. https://doi.org/10.1088/1748-9326/11/6/064017

21. Keeble, J., Hassler, B., Banerjee, A., Checa-Garcia, R., Chiodo, G., Davis, S., Eyring, V., Griffiths, P. T., Morgenstern, O., Nowack, P., Zeng, G., Zhang, J., Bodeker, G., Burrows, S., Cameron-Smith, P., Cugnet, D., Danek, C., Deushi, M., Horowitz, L. W., Kubin, A., et al. (2021). Evaluating stratospheric ozone and water vapour changes in CMIP6 models from 1850 to 2100. *Atmospheric Chemistry and Physics, 21*(6), 5015-5061. https://doi.org/10.5194/acp-21-5015-2021

22. Shepherd, T. G. (2008). Dynamics, stratospheric ozone, and climate change. *Atmosphere-Ocean, 46*(1), 117-138. https://doi.org/10.3137/ao.460106

23. Bernhard, G. H., Bais, A. F., Aucamp, P. J., Klekociuk, A. R., Liley, J. B., & McKenzie, R. L. (2022). Stratospheric ozone, UV radiation, and climate interactions. *Chapter 1*

24. Newman, P. A., Oman, L. D., Douglass, A. R., Fleming, E. L., Frith, S. M., Hurwitz, M. M., Kawa, S. R., Jackman, C. H., Krotkov, N. A., Nash, E. R., Nielsen, J. E., Pawson, S., Stolarski, R. S., & Velders, G. J. M. (2009). What would have happened to the ozone layer if chlorofluorocarbons (CFCs) had not been regulated? *Atmospheric Chemistry and Physics, 9*(6), 2113-2128. https://doi.org/10.5194/acp-9-2113-2009

25. McKenzie, R., Bernhard, G., Liley, B., Disterhoft, P., Rhodes, S., Bais, A., Morgenstern, O., Newman, P., Oman, L., Brogniez, C., & Simic, S. (2019). Success of Montreal Protocol demonstrated by comparing high-quality UV measurements with "World Avoided" calculations from two chemistry-climate models. *Scientific Reports, 9*, 13. https://doi.org/10.1038/s41598-019-48625-z

26. 26. van Dijk, A., Slaper, H., den Outer, P. N., Morgenstern, O., Braesicke, P., Pyle, J. A., Garny, H., Stenke, A., Dameris, M., Kazantzidis, A., Tourpali, K., & Bais, A. F. (2013). Skin cancer risks avoided by the Montreal Protocol--worldwide modeling integrating coupled climate-chemistry models with a risk model for UV. *Photochemistry & Photobiology, 89*(1), 234-246. https://doi.org/10.1111/j.1751-1097.2012.01223.x

27. Madronich, S., Lee-Taylor, J. M., Wagner, M., Kyle, J., Hu, Z., & Landolfi, R. (2021). Estimation of skin and ocular damage avoided in the United States through implementation of the Montreal Protocol on substances that deplete the ozone layer. A*CS Earth and Space Chemistry, 5*(8), 1876-1888. https://doi.org/10.1021/acsearthspacechem.1c00183

28. Young, P. J., Harper, A. B., Huntingford, C., Paul, N. D., Morgenstern, O., Newman, P. A., Oman, L. D., Madronich, S., & Garcia, R. R. (2021). The Montreal Protocol protects the terrestrial carbon sink. *Nature, 596*(7872), 384-388. https://doi.org/10.1038/s41586-021-03737-3

29. Shi, H., Zhang, J., Zhao, B., Xia, X., Hu, B., Chen, H., Wei, J., Liu, M., Bian, Y., Fu, D., Gu, Y., & Liou, K.-N. (2021). Surface brightening in Eastern and Central China since the implementation of the Clean Air Action in 2013: Causes and implications. *Geophysical Research Letters, 48(*3), e2020GL091105. https://doi.org/https://doi.org/10.1029/2020GL091105

30. Ma, M., Gao, Y., Wang, Y., Zhang, S., Leung, L. R., Liu, C., Wang, S., Zhao, B., Chang, X., Su, H., Zhang, T., Sheng, L., Yao, X., & Gao, H. (2019). Substantial ozone enhancement over the North China Plain from increased biogenic emissions due to heat waves and land cover in summer 2017. *Atmospheric Chemistry and Physics, 19*(19), 12195-12207. https://doi.org/10.5194/acp-19-12195-2019

31. Wang, W., Li, X., Shao, M., Hu, M., Zeng, L., Wu, Y., & Tan, T. (2019). The impact of aerosols on photolysis frequencies and ozone production in Beijing during the 4-year period 2012–2015. *Atmospheric Chemistry and Physics, 19*(14), 9413-9429. https://doi.org/10.5194/acp-19-9413-2019

32. Wang, Y., Gao, W., Wang, S., Song, T., Gong, Z., Ji, D., Wang, L., Liu, Z., Tang, G., Huo, Y., Tian, S., Li, J., Li, M., Yang, Y., Chu, B., Petaja, T., Kerminen, V. M., He, H., Hao, J., Kulmala, M., et al. (2020). Contrasting trends of $PM_{2.5}$ and surface-ozone concentrations in China from 2013 to 2017. *National Science Review, 7,* 1331-1339. https://doi.org/10.1093/nsr/nwaa032

33. Wu, J., Bei, N., Hu, B., Liu, S., Wang, Y., Shen, Z., Li, X., Liu, L., Wang, R., Liu, Z., Cao, J., Tie, X., Molina, L. T., & Li, G. (2020). Aerosol-photolysis interaction reduces particulate matter during wintertime haze events. *Proceedings of the National Academy of Sciences of the United States of America, 117*(18), 9755-9761. https://doi.org/10.1073/pnas.1916775117

34. Li, K., Jacob, D. J., Liao, H., Shen, L., Zhang, Q., & Bates, K. H. (2019). Anthropogenic drivers of 2013-2017 trends in summer surface ozone in China. *Proceedings of the National Academy of Sciences of the United States of America, 116*(2), 422-427. https://doi.org/10.1073/pnas.1812168116

35. Liu, Y., & Wang, T. (2020). Worsening urban ozone pollution in China from 2013 to 2017 – Part 2: The effects of emission changes and implications for multi-pollutant control. *Atmospheric Chemistry and Physics, 20*(11), 6323-6337. https://doi.org/10.5194/acp-20-6323-2020

36. Hollaway, M., Wild, O., Yang, T., Sun, Y., Xu, W., Xie, C., Whalley, L., Slater, E., Heard, D., & Liu, D. (2019). Photochemical impacts of haze pollution in an urban environment. *Atmospheric Chemistry and Physics, 19*(15), 9699-9714. https://doi.org/10.5194/acp-19-9699-2019

37. Tian, R., Ma, X., Jia, H., Yu, F., Sha, T., & Zan, Y. (2019). Aerosol radiative effects on tropospheric photochemistry with GEOS-Chem simulations. *Atmospheric Environment, 208*, 82-94. https://doi.org/10.1016/j.atmosenv.2019.03.032

38. Gao, J., Li, Y., Zhu, B., Hu, B., Wang, L., & Bao, F. (2020). What have we missed when studying the impact of aerosols on surface ozone via changing photolysis rates? *Atmospheric Chemistry and Physics, 20*, 10831-10844. https://doi.org/10.5194/acp-2020-140

39. Gao, J., Li, Y., Xie, Z., Hu, B., Wang, L., Bao, F., & Fan, S. (2022). The impact of the aerosol reduction on the worsening ozone pollution over the Beijing-Tianjin-Hebei region via influencing photolysis rates. *Science of the Total Environment, 153197*. https://doi.org/10.1016/j.scitotenv.2022.153197

40. Ma, X., Huang, J., Zhao, T., Liu, C., Zhao, K., Xing, J., & Xiao, W. (2020). Rapid increase in summer surface ozone over the North China Plain during 2013–2019: A side effect of particulate matters reduction control? *Atmospheric Chemistry and Physics, 20*. https://doi.org/10.5194/acp-2020-385

41. Fountoulakis, I., Zerefos, C. S., Bais, A. F., Kapsomenakis, J., Koukouli, M.-E., Ohkawara, N., Fioletov, V., De Backer, H., Lakkala, K., Karppinen, T., & Webb, A. R. (2018). Twenty-five years of spectral UV-B measurements over Canada, Europe and Japan: Trends and effects from changes in ozone, aerosols, clouds, and surface reflectivity. *Comptes Rendus de l'Academie d'Geoscience de France, 350*(7), 393-402. https://doi.org/10.1016/j.crte.2018.07.011

42. Ipiña, A., López-Padilla, G., Retama, A., Piacentini, R. D., & Madronich, S. (2021). Ultraviolet radiation environment of a tropical megacity in transition: Mexico City 2000–2019. *Environmental Science & Technology*. https://doi.org/10.1021/acs.est.0c08515

43. Becerra-Rondón, A., Ducati, J., & Haag, R. (2021). Partial COVID-19 lockdown effect in atmospheric pollutants and indirect impact in UV radiation in Rio Grande do Sul, Brazil. *Atmósfera*. https://doi.org/10.20937/atm.53027

44. Ming, Y., Lin, P., Naik, V., Paulot, F., Horowitz, L. W., Ginoux, P. A., Ramaswamy, V., Loeb, N. G., Shen, Z., Singer, C. E., Ward, R. X., Zhang, Z., & Bellouin, N. (2021). Assessing the influence of COVID-19 on the shortwave radiative fluxes over the East Asian marginal seas. *Geophysical Research Letters, 48*(3), e2020GL091699. https://doi.org/https://doi.org/10.1029/2020GL091699

45. Bera, B., Bhattacharjee, S., Shit, P. K., Sengupta, N., & Saha, S. (2022). Variation and correlation between ultraviolet index and tropospheric ozone during COVID-19 lockdown over megacities of India. *Stochastic Environmental Research and Risk Assessment, 36*(2), 409-427. https://doi.org/10.1007/s00477-021-02033-w

46. Pye, H. O. T., Ward-Caviness, C. K., Murphy, B. N., Appel, K. W., & Seltzer, K. M. (2021). Secondary organic aerosol association with cardiorespiratory disease mortality in the United States. *Nature Communications, 12*(1), 7215. https://doi.org/10.1038/s41467-021-27484-1

47. Sowden, M., & Blake, D. (2021). Using infrared geostationary remote sensing to determine particulate matter ground-level composition and concentration. *Air Quality, Atmosphere & Health, 1-10*. https://doi.org/10.1007/s11869-021-01061-3

48. Si, Y., Lu, Q., Zhang, X., Hu, X., Wang, F., Li, L., & Gu, S. (2021). A review of advances in the retrieval of aerosol properties by remote sensing multi-angle technology. *Atmospheric Environment, 244*, 117928. https://doi.org/10.1016/j.atmosenv.2020.117928

49. Hodzic, A., Kasibhatla, P. S., Jo, D. S., Cappa, C. D., Jimenez, J. L., Madronich, S., & Park, R. J. (2016). Rethinking the global secondary organic aerosol (SOA) budget: Stronger production, faster removal, shorter lifetime. *Atmospheric Chemistry and Physics, 16*(12), 7917-7941. https://doi.org/10.5194/acp-16-7917-2016

50. O'Brien, R. E., & Kroll, J. H. (2019). Photolytic aging of secondary organic aerosol: Evidence for a substantial photo-recalcitrant fraction. *Journal of Physical Chemistry Letters*, *10*(14), 4003-4009. https://doi.org/10.1021/acs.jpclett.9b01417

51. Baboomian, V. J., Gu, Y., & Nizkorodov, S. A. (2020). Photodegradation of secondary organic aerosols by long-term exposure to solar actinic radiation. *ACS Earth and Space Chemistry, 4*(7), 1078-1089. https://doi.org/10.1021/acsearthspacechem.0c00088

52. Wang, T., Liu, Y., Deng, Y., Cheng, H., Yang, Y., Feng, Y., Zhang, L., Fu, H., & Chen, J. (2020). Photochemical oxidation of water-soluble organic carbon (WSOC) on mineral dust and enhanced organic ammonium formation. *Environmental Science & Technology, 54*, 15631-15642. https://doi.org/10.1021/acs.est.0c04616

53. Zawadowicz, M. A., Lee, B. H., Shrivastava, M., Zelenyuk, A., Zaveri, R. A., Flynn, C., Thornton, J. A., & Shilling, J. E. (2020). Photolysis controls atmospheric budgets of biogenic secondary organic aerosol. *Environmental Science & Technology, 54*(7), 3861-3870. https://doi.org/10.1021/acs.est.9b07051

54. Hodzic, A., Madronich, S., Kasibhatla, P. S., Tyndall, G., Aumont, B., Jimenez, J. L., Lee-Taylor, J., & Orlando, J. (2015). Organic photolysis reactions in tropospheric aerosols: Effect on secondary organic aerosol formation and lifetime. *Atmospheric Chemistry and Physics, 15*(16), 9253-9269. https://doi.org/10.5194/acp-15-9253-2015

55. Ndour, M., Conchon, P., D'Anna, B., Ka, O., & George, C. (2009). Photochemistry of mineral dust surface as a potential atmospheric renoxification process. *Geophysical Research Letters, 36*(5). https://doi.org/10.1029/2008gl036662

56. Tuite, K., Thomas, J. L., Veres, P. R., Roberts, J. M., Stevens, P. S., Griffith, S. M., Dusanter, S., Flynn, J. H., Ahmed, S., Emmons, L., Kim, S. W., Washenfelder, R., Young, C., Tsai, C., Pikelnaya, O., & Stutz, J. (2021). Quantifying nitrous acid formation mechanisms using measured vertical profiles during the CalNex 2010 Campaign and 1D Column Modeling. *Journal of Geophysical Research-Atmospheres, 126*(13). https://doi.org/10.1029/2021jd034689

57. Ye, C., Heard, D. E., & Whalley, L. K. (2017). Evaluation of novel routes for NOx formation in remote regions. *Environmental Science & Technology, 51*(13), 7442-7449. https://doi.org/10.1021/acs.est.6b06441

58. Reed, C., Evans, M. J., Crilley, L. R., Bloss, W. J., Sherwen, T., Read, K. A., Lee, J. D., & Carpenter, L. J. (2017). Evidence for renoxification in the tropical marine boundary layer. *Atmospheric Chemistry and Physics, 17*(6), 4081-4092. https://doi.org/10.5194/acp-17-4081-2017

59. Wang, X., Gemayel, R., Hayeck, N., Perrier, S., Charbonnel, N., Xu, C., Chen, H., Zhu, C., Zhang, L., Wang, L., Nizkorodov, S. A., Wang, X., Wang, Z., Wang, T., Mellouki, A., Riva, M., Chen, J., & George, C. (2020). Atmospheric photosensitization: A new pathway for sulfate formation. *Environmental Science & Technology, 54*(6), 3114-3120. https://doi.org/10.1021/acs.est.9b06347

60. Chen, Y., Tong, S., Li, W., Liu, Y., Tan, F., Ge, M., Xie, X., & Sun, J. (2021). Photocatalytic oxidation of SO_2 by TiO_2: Aerosol formation and the key role of gaseous reactive oxygen species. *Environmental Science & Technology, 55*(14), 9784-9793. https://doi.org/10.1021/acs.est.1c01608

61. Ye, C., Chen, H., Hoffmann, E. H., Mettke, P., Tilgner, A., He, L., Mutzel, A., Bruggemann, M., Poulain, L., Schaefer, T., Heinold, B., Ma, Z., Liu, P., Xue, C., Zhao, X., Zhang, C., Zhang, F., Sun, H., Li, Q., Wang, L., et al. (2021). Particle-phase photoreactions of HULIS and TMIs establish a strong source of H2O2 and particulate sulfate in the winter North China Plain. *Environmental Science & Technology*. https://doi.org/10.1021/acs.est.1c00561

62. Chen, Q., Xia, M., Peng, X., Yu, C., Sun, P., Li, Y., Liu, Y., Xu, Z., Xu, Z., & Wu, R. (2022). Large daytime molecular chlorine missing source at a suburban site in East China. Journal of Geophysical Research: *Atmospheres, 127*(4), e2021JD035796. https://doi.org/10.1029/2021JD035796

63. Laskin, A., Laskin, J., & Nizkorodov, S. A. (2015). Chemistry of atmospheric brown carbon. *Chemical Reviews, 115*(10), 4335-4382. https://doi.org/10.1021/cr5006167

64. Aiona, P. K., Luek, J. L., Timko, S. A., Powers, L. C., Gonsior, M., & Nizkorodov, S. A. (2018). Effect of photolysis on absorption and fluorescence spectra of light-absorbing secondary organic aerosols. *ACS Earth and Space Chemistry, 2*(3), 235-245. https://doi.org/10.1021/acsearthspacechem.7b00153

65. Walhout, E. Q., Yu, H., Thrasher, C., Shusterman, J. M., & O'Brien, R. E. (2019). Effects of photolysis on the chemical and optical properties of secondary organic material over extended time scales. *ACS Earth and Space Chemistry, 3*(7), 1226-1236. https://doi.org/10.1021/acsearthspacechem.9b00109

66. Fleming, L. T., Lin, P., Roberts, J. M., Selimovic, V., Yokelson, R., Laskin, J., Laskin, A., & Nizkorodov, S. A. (2020). Molecular composition and photochemical lifetimes of brown carbon chromophores in biomass burning organic aerosol. *Atmospheric Chemistry and Physics, 20*(2), 1105-1129. https://doi.org/10.5194/acp-20-1105-2020

67. Vo, L., Legaard, E., Thrasher, C., Jaffe, A., Berden, G., Martens, J., Oomens, J., & O'Brien, R. E. (2021). UV/Vis and IRMPD spectroscopic analysis of the absorption properties of methylglyoxal brown carbon. *ACS Earth and Space Chemistry*. https://doi.org/10.1021/acsearthspacechem.1c00022

68. Li, N., Xia, T., & Nel, A. E. (2008). The role of oxidative stress in ambient particulate matter-induced lung diseases and its implications in the toxicity of engineered nanoparticles. *Free Radical Biology & Medicine, 44*(9), 1689-1699. https://doi.org/10.1016/j.freeradbiomed.2008.0128

69. Bates, J. T., Fang, T., Verma, V., Zeng, L., Weber, R. J., Tolbert, P. E., Abrams, J. Y., Sarnat, S. E., Klein, M., Mulholland, J. A., & Russell, A. G. (2019). Review of acellular assays of ambient particulate matter oxidative potential: Methods and relationships with composition, sources, and health effects. *Environmental Science & Technology, 53*(8), 4003-4019. https://doi.org/10.1021/acs.est.8b03430

70. Manfrin, A., Nizkorodov, S. A., Malecha, K. T., Getzinger, G. J., McNeill, K., & Borduas-Dedekind, N. (2019). Reactive oxygen species production from secondary organic aerosols: The importance of singlet oxygen. *Environmental Science & Technology, 53*(15), 8553-8562. https://doi.org/10.1021/acs.est.9b01609

71. Liu, F., Whitley, J., Ng, N. L. S., & Lu, H. (2020). Time-resolved single-cell assay for measuring intracellular reactive oxygen species upon exposure to ambient particulate matter. *Environmental Science & Technology*. https://doi.org/10.1021/acs.est.0c02889

72. Hwang, B., Fang, T., Pham, R., Wei, J., Gronstal, S., Lopez, B., Frederickson, C., Galeazzo, T., Wang, X., Jung, H., & Shiraiwa, M. (2021). Environmentally persistent free radicals, reactive oxygen species generation, and oxidative potential of highway $PM_{2.5}$. *ACS Earth and Space Chemistry*. https://doi.org/10.1021/acsearthspacechem.1c00135

73. Borduas-Dedekind, N., Ossola, R., David, R. O., Boynton, L. S., Weichlinger, V., Kanji, Z. A., & McNeill, K. (2019). Photomineralization mechanism changes the ability of dissolved organic matter to activate cloud droplets and to nucleate ice crystals. *Atmospheric Chemistry and Physics, 19*(19), 12397-12412. https://doi.org/10.5194/acp-19-12397-2019

74. Borduas-Dedekind, N., Nizkorodov, S., & McNeill, K. (2020). UVB-irradiated laboratory-generated secondary organic aerosol extracts have increased cloud condensation nuclei abilities: Comparison with dissolved organic matter and implications for the photomineralization mechanism. *Chimia (Aarau), 74*(3), 142-148. https://doi.org/10.2533/chimia.2020.142

75. Erickson, D. J. I., Sulzberger, B., Zepp, R. G., & Austin, A. T. (2015). Effects of stratospheric ozone depletion, solar UV radiation, and climate change on biogeochemical cycling: interactions and feedbacks. [10.1039/C4PP90036G]. *Photochemical & Photobiological Sciences, 14*(1), 127-148. https://doi.org/10.1039/C4PP90036G

76. Sulzberger, B., Austin, A. T., Cory, R. M., Zepp, R. G., & Paul, N. D. (2019). Solar UV radiation in a changing world: roles of cryosphere–land–water–atmosphere interfaces in global biogeochemical cycles. [10.1039/C8PP90063A]. *Photochemical & Photobiological Sciences, 18*(3), 747-774. https://doi.org/10.1039/C8PP90063A

77. WHO (2022). Air Pollution. https://www.who.int/health-topics/air-pollution#tab=tab_1. Accessed April 2022.

78. Lefohn, A. S., Malley, C. S., Smith, L., Wells, B., Hazucha, M., Simon, H., Naik, V., Mills, G., Schultz, M. G., Paoletti, E., De Marco, A., Xu, X., Zhang, L., Wang, T., Neufeld, H. S., Musselman, R. C., Tarasick, D., Brauer, M., Feng, Z., Tang, H., et al. (2018). Tropospheric ozone assessment report: Global ozone metrics for climate change, human health, and crop/ecosystem research. *Elementa: Science of the Anthropocene, 6*. https://doi.org/10.1525/elementa.279

79. Markozannes, G., Pantavou, K., Rizos, E. C., Sindosi, O., Tagkas, C., Seyfried, M., Saldanha, I. J., Hatzianastassiou, N., Nikolopoulos, G. K., & Ntzani, E. (2022). Outdoor air quality and human health: An overview of reviews of observational studies. *Environmental Pollution, 306*, 119309. https://doi.org/10.1016/j.envpol.2022.119309

80. Brauer, M., Brook, J. R., Christidis, T., Chu, Y., Crouse, D. L., Erickson, A., Hystad, P., Li, C., Martin, R. V., Meng, J., Pappin, A. J., Pinault, L. L., Tjepkema, M., van Donkelaar, A., Weichenthal, S., & Burnett, R. T. (2019). Mortality-air pollution associations in low-exposure environments (MAPLE): Phase 1. *Research Reports: Health Effects Institute(203)*, 1-87.

81. Brunekreef, B., Strak, M., Chen, J., Andersen, Z. J., Atkinson, R., Bauwelinck, M., Bellander, T., Boutron-Ruault, M. C., Brandt, J., Carey, I., Cesaroni, G., Forastiere, F., Fecht, D., Gulliver, J., Hertel, O., Hoffmann, B., de Hoogh, K., Houthuijs, D., Hvidtfeldt, U. A., Janssen, N. A. H., et al. (2021). *Mortality and morbidity effects of long-term exposure to low-level PM$_{2.5}$, BC, NO$_2$, and O$_3$: An analysis of European cohorts in the ELAPSE project* (Vol. Vol. WA 754 R432 No. 208, HEI Report Series): Health Effects Institute.

82. Dominici, F., Schwartz, J., Di, Q., Braun, D., Choirat, C., & Zanobetti, A. (Eds.). (2022). *Assessing Adverse Health Effects of Long-Term Exposure to Low Levels of Ambient Air Pollution: Phase 1* (2020/01/08 ed., Vol. 211, HEI Research Reports): Health Effects Institute.

83. WHO (2021). *WHO Global Air Quality Guidelines: Particulate Matter (PM$_{2.5}$ and PM$_{10}$), Ozone, Nitrogen Dioxide, Sulfur Dioxide and Carbon Monoxide*. Geneva: World Health Organization.

84. WHO (2017). *Evolution of WHO Air Quality Guidelines: Past, Present and Future (2017)*. Geneva: World Health Organization.

85. WHO (2006). *Air Quality Guidelines: Global Update 2005: Particulate Matter, Ozone, Nitrogen Dioxide and Sulfur Dioxide* (Vol. EUR/05/5046029). Copenhagen: World Health Organization. Regional Office for Europe.

86. Liu, S., Jørgensen, J. T., Ljungman, P., Pershagen, G., Bellander, T., Leander, K., Magnusson, P. K. E., Rizzuto, D., Hvidtfeldt, U. A., Raaschou-Nielsen, O., Wolf, K., Hoffmann, B., Brunekreef, B., Strak, M., Chen, J., Mehta, A., Atkinson, R. W., Bauwelinck, M., Varraso, R., Boutron-Ruault, M. C., et al. (2021). Long-term exposure to low-level air pollution and incidence of chronic obstructive pulmonary disease: The ELAPSE project. *Environment International, 146*, 106267. https://doi.org/10.1016/j.envint.2020.106267

87. Wolf, K., Hoffmann, B., Andersen, Z. J., Atkinson, R. W., Bauwelinck, M., Bellander, T., Brandt, J., Brunekreef, B., Cesaroni, G., Chen, J., de Faire, U., de Hoogh, K., Fecht, D., Forastiere, F., Gulliver, J., Hertel, O., Hvidtfeldt, U. A., Janssen, N. A. H., Jørgensen, J. T., Katsouyanni, K., et al. (2021). Long-term exposure to low-level ambient air pollution and incidence of stroke and coronary heart disease: a pooled analysis of six European cohorts within the ELAPSE project. *Lancet Planet Health, 5*(9), e620-e632. https://doi.org/10.1016/s2542-5196(21)00195-9

88. Chen, J., Rodopoulou, S., Strak, M., de Hoogh, K., Taj, T., Poulsen, A. H., Andersen, Z. J., Bellander, T., Brandt, J., Zitt, E., Fecht, D., Forastiere, F., Gulliver, J., Hertel, O., Hoffmann, B., Hvidtfeldt, U. A., Verschuren, W. M. M., Jørgensen, J. T., Katsouyanni, K., Ketzel, M., et al. (2022). Long-term exposure to ambient air pollution and bladder cancer incidence in a pooled European cohort: the ELAPSE project. *British Journal of Cancer*. https://doi.org/10.1038/s41416-022-01735-4

89. Samoli, E., Rodopoulou, S., Hvidtfeldt, U. A., Wolf, K., Stafoggia, M., Brunekreef, B., Strak, M., Chen, J., Andersen, Z. J., Atkinson, R., Bauwelinck, M., Bellander, T., Brandt, J., Cesaroni, G., Forastiere, F., Fecht, D., Gulliver, J., Hertel, O., Hoffmann, B., de Hoogh, K., et al. (2021). Modeling multi-level survival data in multi-center epidemiological cohort studies: Applications from the ELAPSE project. *Environment International, 147*, 106371. https://doi.org/10.1016/j.envint.2020.106371

90. Stafoggia, M., Oftedal, B., Chen, J., Rodopoulou, S., Renzi, M., Atkinson, R. W., Bauwelinck, M., Klompmaker, J. O., Mehta, A., Vienneau, D., Andersen, Z. J., Bellander, T., Brandt, J., Cesaroni, G., de Hoogh, K., Fecht, D., Gulliver, J., Hertel, O., Hoffmann, B., Hvidtfeldt, U. A., et al. (2022). Long-term exposure to low ambient air pollution concentrations and mortality among 28 million people: results from seven large European cohorts within the ELAPSE project. *Lancet Planet Health, 6*(1), e9-e18. https://doi.org/10.1016/s2542-5196(21)00277-1

91. Strak, M., Weinmayr, G., Rodopoulou, S., Chen, J., de Hoogh, K., Andersen, Z. J., Atkinson, R., Bauwelinck, M., Bekkevold, T., Bellander, T., Boutron-Ruault, M. C., Brandt, J., Cesaroni, G., Concin, H., Fecht, D., Forastiere, F., Gulliver, J., Hertel, O., Hoffmann, B., Hvidtfeldt, U. A., et al. (2021). Long term exposure to low level air pollution and mortality in eight European cohorts within the ELAPSE project: Pooled analysis. *British Medical Journal, 374*, n1904. https://doi.org/10.1136/bmj.n1904

92. Rodopoulou, S., Stafoggia, M., Chen, J., de Hoogh, K., Bauwelinck, M., Mehta, A. J., Klompmaker, J. O., Oftedal, B., Vienneau, D., Janssen, N. A. H., Strak, M., Andersen, Z. J., Renzi, M., Cesaroni, G., Nordheim, C. F., Bekkevold, T., Atkinson, R., Forastiere, F., Katsouyanni, K., Brunekreef, B., et al. (2022). Long-term exposure to fine particle elemental components and mortality in Europe: Results from six European administrative cohorts within the ELAPSE project. *Science of the Total Environment, 809,* 152205. https://doi.org/10.1016/j.scitotenv.2021.152205

93. Chen, J., Rodopoulou, S., de Hoogh, K., Strak, M., Andersen, Z. J., Atkinson, R., Bauwelinck, M., Bellander, T., Brandt, J., Cesaroni, G., Concin, H., Fecht, D., Forastiere, F., Gulliver, J., Hertel, O., Hoffmann, B., Hvidtfeldt, U. A., Janssen, N. A. H., Jöckel, K. H., Jørgensen, J., et al. (2021). Long-Term Exposure to Fine Particle Elemental Components and Natural and Cause-Specific Mortality-a Pooled Analysis of Eight European Cohorts within the ELAPSE Project. *Environmental Health Perspectives, 129*(4), 47009. https://doi.org/10.1289/ehp8368

94. So, R., Chen, J., Mehta, A. J., Liu, S., Strak, M., Wolf, K., Hvidtfeldt, U. A., Rodopoulou, S., Stafoggia, M., Klompmaker, J. O., Samoli, E., Raaschou-Nielsen, O., Atkinson, R., Bauwelinck, M., Bellander, T., Boutron-Ruault, M. C., Brandt, J., Brunekreef, B., Cesaroni, G., Concin, H., et al. (2021). Long-term exposure to air pollution and liver cancer incidence in six European cohorts. *International Journal of Cancer, 149*(11), 1887-1897. https://doi.org/10.1002/ijc.33743

95. Liu, S., Jørgensen, J. T., Ljungman, P., Pershagen, G., Bellander, T., Leander, K., Magnusson, P. K. E., Rizzuto, D., Hvidtfeldt, U. A., Raaschou-Nielsen, O., Wolf, K., Hoffmann, B., Brunekreef, B., Strak, M., Chen, J., Mehta, A., Atkinson, R. W., Bauwelinck, M., Varraso, R., Boutron-Ruault, M. C., et al. (2021). Long-term exposure to low-level air pollution and incidence of asthma: The ELAPSE project. *European Respiratory Journal, 57*(6). https://doi.org/10.1183/13993003.03099 2020

96. Chen, J., & Hoek, G. (2020). Long-term exposure to PM and all-cause and cause-specific mortality: A systematic review and meta-analysis. *Environment International, 143*, 105974. https://doi.org/10.1016/j.envint.2020.105974

97. Chowdhury, S., Pozzer, A., Haines, A., Klingmuller, K., Munzel, T., Paasonen, P., Sharma, A., Venkataraman, C., & Lelieveld, J. (2022). Global health burden of ambient $PM_{2.5}$ and the contribution of anthropogenic black carbon and organic aerosols. *Environment International, 159*, 107020. https://doi.org/10.1016/j.envint.2021.107020

98. Chersich, M. F., Pham, M. D., Areal, A., Haghighi, M. M., Manyuchi, A., Swift, C. P., Wernecke, B., Robinson, M., Hetem, R., Boeckmann, M., Hajat, S., Nakstad, B., Wright, C. Y., Harvey, C., Wang, C., Durusu, D., Scorgie, F., Rees, H., Harden, L., Roos, N., et al. (2020). Associations between high temperatures in pregnancy and risk of preterm birth, low birth weight, and stillbirths: Systematic review and meta-analysis. *British Medical Journal, 371*, m3811. https://doi.org/10.1136/bmj.m3811

99. Liu, Z., Meng, Y., Xiang, H., Lu, Y., & Liu, S. (2020). Association of short-term exposure to meteorological factors and risk of hand, foot, and mouth disease: A systematic review and meta-analysis. *International Journal of Environmental Research and Public Health, 17*(21). https://doi.org/10.3390/ijerph17218017

100. Moghadamnia, M. T., Ardalan, A., Mesdaghinia, A., Keshtkar, A., Naddafi, K., & Yekaninejad, M. S. (2017). Ambient temperature and cardiovascular mortality: A systematic review and meta-analysis. *PeerJ, 5*. https://doi.org/10.7717/peerj.3574

101. Gronlund, C. J., Sullivan, K. P., Kefelegn, Y., Cameron, L., & O'Neill, M. S. (2018). Climate change and temperature extremes: a review of heat- and cold-related morbidity and mortality concerns of municipalities. *Maturitas, 114*, 54-59. https://doi.org/10.1016/j.maturitas.2018.06.002

102. Ryti, N. R., Guo, Y., & Jaakkola, J. J. (2016). Global association of cold spells and adverse health effects: A systematic review and meta-analysis. *Environmental Health Perspectives, 124*(1), 12-22. https://doi.org/10.1289/ehp.1408104

103. Sharpe, I., & Davison, C. M. (2022). A scoping review of climate change, climate-related disasters, and mental disorders among children in low- and middle-income countries. *International Journal of Environmental Research and Public Health, 19*(5). https://doi.org/10.3390/ijerph19052896

104. Syed, S., O'Sullivan, T. L., & Phillips, K. P. (2022). Extreme heat and pregnancy outcomes: A scoping review of the epidemiological evidence. *International Journal of Environmental Research and Public Health, 19*(4). https://doi.org/10.3390/ijerph19042412

105. Vu, A., Rutherford, S., & Phung, D. (2019). Heat health prevention measures and adaptation in older populations—A systematic review. *International Jorunal of Environmental Research and Public Health, 16*(22). https://doi.org/10.3390/ijerph16224370

106. Zanobetti, A., & O'Neill, M. S. (2018). Longer-term outdoor temperatures and health effects: A review. *Current Epidemiology Reports, 5*(2), 125-139. https://doi.org/10.1007/s40471-018-0150-3

107. Analitis, A., De' Donato, F., Scortichini, M., Lanki, T., Basagana, X., Ballester, F., Astrom, C., Paldy, A., Pascal, M., Gasparrini, A., Michelozzi, P., & Katsouyanni, K. (2018). Synergistic effects of ambient temperature and air pollution on health in Europe: Results from the PHASE Project. *International Journal of Environmental Research and Public Health, 15*(9). https://doi.org/10.3390/ijerph15091856

108. Areal, A. T., Zhao, Q., Wigmann, C., Schneider, A., & Schikowski, T. (2022). The effect of air pollution when modified by temperature on respiratory health outcomes: A systematic review and meta-analysis. *Science of the Total Environment, 811*, 152336. https://doi.org/10.1016/j.scitotenv.2021.152336

109. Rajagopalan, S., Al-Kindi, S. G., & Brook, R. D. (2018). Air pollution and cardiovascular disease: JACC state-of-the-art review. *Journal of the American College of Cardiologists, 72*(17), 2054-2070. https://doi.org/10.1016/j.jacc.2018.07.099

110. Wesselink, A. K., Wang, T. R., Ketzel, M., Mikkelsen, E. M., Brandt, J., Khan, J., Hertel, O., Laursen, A. S. D., Johannesen, B. R., Willis, M. D., Levy, J. I., Rothman, K. J., Sørensen, H. T., Wise, L. A., & Hatch, E. E. (2022). Air pollution and fecundability: Results from a Danish preconception cohort study. *Pediatric and Perinatal Epidemiology, 36*(1), 57-67. https://doi.org/10.1111/ppe.12832

111. Costello, J. M., Steurer, M. A., Baer, R. J., Witte, J. S., & Jelliffe-Pawlowski, L. L. (2022). Residential particulate matter, proximity to major roads, traffic density and traffic volume as risk factors for preterm birth in California. *Paediatric and Perinatal Epidemiology, 36*(1), 70-79. https://doi.org/10.1111/ppe.12820

112. Tham, R., & Schikowski, T. (2021). The role of traffic-related air pollution on neurodegenerative diseases in older people: An epidemiological perspective. *Journal of Alzheimer's Disease, 79*(3), 949-959. https://doi.org/10.3233/jad-200813

113. Weuve, J., Bennett, E. E., Ranker, L., Gianattasio, K. Z., Pedde, M., Adar, S. D., Yanosky, J. D., & Power, M. C. (2021). Exposure to air pollution in relation to risk of dementia and related outcomes: An updated systematic review of the epidemiological literature. *Environmental Health Perspectives, 129*(9), 96001. https://doi.org/10.1289/EHP8716

114. Chen, H., Kwong, J. C., Copes, R., Hystad, P., van Donkelaar, A., Tu, K., Brook, J. R., Goldberg, M. S., Martin, R. V., Murray, B. J., Wilton, A. S., Kopp, A., & Burnett, R. T. (2017). Exposure to ambient air pollution and the incidence of dementia: A population-based cohort study. *Environment International, 108*, 271-277. https://doi.org/10.1016/j.envint.2017.08.020

115. Shi, L., Steenland, K., Li, H., Liu, P., Zhang, Y., Lyles, R. H., Requia, W. J., Ilango, S. D., Chang, H. H., Wingo, T., Weber, R. J., & Schwartz, J. (2021). A national cohort study (2000-2018) of long-term air pollution exposure and incident dementia in older adults in the United States. *Nature Communications, 12*(1), 6754. https://doi.org/10.1038/s41467-021-27049-2

116. Paoletti, E., Feng, Z., De Marco, A., Hoshika, Y., Harmens, H., Agathokleous, E., Domingos, M., Mills, G., Sicard, P., Zhang, L., & Carrari, E. (2020). Challenges, gaps and opportunities in investigating the interactions of ozone pollution and plant ecosystems. *Science of the Total Environment, 709*, 136188. https://doi.org/10.1016/j.scitotenv.2019.136188

117. Gaffney, J. S., & Marley, N. A. (2021). The impacts of peroxyacetyl nitrate in the atmosphere of megacities and large urban areas: A historical perspective. *ACS Earth and Space Chemistry, 5*(8), 1829-1841.

118. Li, C., Gu, X., Wu, Z., Qin, T., Guo, L., Wang, T., Zhang, L., & Jiang, G. (2021). Assessing the effects of elevated ozone on physiology, growth, yield and quality of soybean in the past 40 years: A meta-analysis. *Ecotoxicology and Environmental Safety, 208*, 111644. https://doi.org/10.1016/j.ecoenv.2020.111644

119. Biancari, L., Cerrotta, C., Menéndez, A. I., Gundel, P. E., & Martínez-Ghersa, M. A. (2021). Episodes of high tropospheric ozone reduce nodulation, seed production and quality in soybean (*Glycine max* (L.) merr.) on low fertility soils. *Environmental Pollution, 269*, 116117. https://doi.org/10.1016/j.envpol.2020.116117

120. Tisdale, R. H., Zobel, R. W., & Burkey, K. O. (2021). Tropospheric ozone rapidly decreases root growth by altering carbon metabolism and detoxification capability in growing soybean roots. *Science of the Total Environment, 766*, 144292. https://doi.org/10.1016/j.scitotenv.2020.144292

121. Lobell, D. B., & Burney, J. A. (2021). Cleaner air has contributed one-fifth of US maize and soybean yield gains since 1999. *Environmental Research Letters, 16*(7), 074049. https://doi.org/10.1088/1748-9326/ac0fa4

122. Wang, T., Zhang, L., Zhou, S., Zhang, T., Zhai, S., Yang, Z., Wang, D., & Song, H. (2021). Effects of ground-level ozone pollution on yield and economic losses of winter wheat in Henan, China. *Atmospheric Environment, 262*, 118654. https://doi.org/10.1016/j.atmosenv.2021.118654

123. Wang, Y., Wild, O., Ashworth, K., Chen, X., Wu, Q., Qi, Y., & Wang, Z. (2022). Reductions in crop yields across China from elevated ozone. *Environmental Pollution, 292*(Pt A), 118218. https://doi.org/10.1016/j.envpol.2021.118218

124. Zhang, T., Yue, X., Unger, N., Feng, Z., Zheng, B., Li, T., Lei, Y., Zhou, H., Dong, X., & Liu, Y. (2021). Modeling the joint impacts of ozone and aerosols on crop yields in China: An air pollution policy scenario analysis. *Atmospheric Environment, 247*, 118216. https://doi.org/10.1016/j.atmosenv.2021.118216

125. Ascenso, A., Gama, C., Blanco-Ward, D., Monteiro, A., Silveira, C., Viceto, C., Rodrigues, V., Rocha, A., Borrego, C., & Lopes, M. (2021). Assessing Douro vineyards exposure to tropospheric ozone. *Atmosphere, 12*(2), 200. https://doi.org/10.3390/atmos12020200

126. Blanco-Ward, D., Ribeiro, A., Paoletti, E., & Miranda, A. (2021). Assessment of tropospheric ozone phytotoxic effects on the grapevine (*Vitis vinifera* L.): A review. *Atmospheric Environment, 244*, 117924. https://doi.org/10.1016/j.atmosenv.2020.117924

127. Sacchelli, S., Carrari, E., Paoletti, E., Anav, A., Hoshika, Y., Sicard, P., Screpanti, A., Chirici, G., Cocozza, C., & De Marco, A. (2021). Economic impacts of ambient ozone pollution on wood production in Italy. *Scientific Reports, 11*(1), 1-9. https://doi.org/10.1038/s41598-020-80516-6

128. Jakovljevic, T., Lovreskov, L., Jelic, G., Anav, A., Popa, I., Fornasier, M. F., Proietti, C., Limic, I., Butorac, L., Vitale, M., & De Marco, A. (2021). Impact of ground-level ozone on Mediterranean forest ecosystems health. *Science of the Total Environment, 783*, 147063. https://doi.org/10.1016/j.scitotenv.2021.147063

129. Anav, A., De Marco, A., Friedlingstein, P., Savi, F., Sicard, P., Sitch, S., Vitale, M., & Paoletti, E. (2019). Growing season extension affects ozone uptake by European forests. *Science of the Total Environment, 669*, 1043-1052. https://doi.org/10.1016/j.scitotenv.2019.03.020

130. Bosch, J., Elvira, S., Sausor, C., Bielby, J., Gonzalez-Fernandez, I., Alonso, R., & Bermejo-Bermejo, V. (2021). Increased tropospheric ozone levels enhance pathogen infection levels of amphibians. *Science of the Total Environment, 759*, 143461. https://doi.org/10.1016/j.scitotenv.2020.143461

131. Oksanen, E., & Kontunen-Soppela, S. (2021). Plants have different strategies to defend against air pollutants. Current Opinion in *Environmental Science & Health, 19*, 100222. https://doi.org/10.1016/j.coesh.2020.10.010

132. Li, S., Yuan, X., Feng, Z., Du, Y., Agathokleous, E., & Paoletti, E. (2022). Whole-plant compensatory responses of isoprene emission from hybrid poplar seedlings exposed to elevated ozone. *Science of the Total Environment, 806*(Pt 4), 150949. https://doi.org/10.1016/j.scitotenv.2021.150949

133. Boublin, F., Cabassa-Hourton, C., Leymarie, J., & Leitao, L. (2021). Potential involvement of proline and flavonols in plant responses to ozone. *Environmental Research, 207*, 112214. https://doi.org/10.1016/j.envres.2021.112214

134. Blande, J. D. (2021). Effects of air pollution on plant–insect interactions mediated by olfactory and visual cues. Current Opinion in *Environmental Science & Health, 19*, 100228. https://doi.org/10.1016/j.coesh.2020.100228

135. Masui, N., Agathokleous, E., Mochizuki, T., Tani, A., Matsuura, H., & Koike, T. (2021). Ozone disrupts the communication between plants and insects in urban and suburban areas: an updated insight on plant volatiles. *Journal of Forest Research, 32*, 1337–1349. https://doi.org/10.1007/s11676-020-01287-4

136. Duque, L., Poelman, E. H., & Steffan-Dewenter, I. (2021). Effects of ozone stress on flowering phenology, plant-pollinator interactions and plant reproductive success. *Environmental Pollution, 272*, 115953. https://doi.org/10.1016/j.envpol.2020.115953

137. Galveias, A., Arriegas, R., Mendes, S., Ribeiro, H., Abreu, I., Costa, A., & Antunes, C. (2021). Air pollutants NO_2- and O_3-induced *Dactylis glomerata* L. pollen oxidative defences and enhanced its allergenic potential. *Aerobiologia, 37*(1), 127-137. https://doi.org/10.1007/s10453-020-09676-2

138. Pereira, S., Fernández-González, M., Guedes, A., Abreu, I., & Ribeiro, H. (2021). The strong and the stronger: The effects of increasing ozone and nitrogen dioxide concentrations in pollen of different forest species. *Forests, 12*(1), 88. https://doi.org/10.3390/f12010088

139. Kováts, N., Hubai, K., Diósi, D., Sainnokhoi, T.-A., Hoffer, A., Tóth, Á., & Teke, G. (2021). Sensitivity of typical European roadside plants to atmospheric particulate matter. *Ecological Indicators, 124*, 107428. https://doi.org/10.1016/j.ecolind.2021.107428

140. Mina, U., Smiti, K., & Yadav, P. (2021). Thermotolerant wheat cultivar (*Triticum aestivum* L. var. WR544) response toe, EDU, and particulate matter interactive exposure. *Environmental Monitoring and Assessment, 193*(6), 1-16. https://doi.org/10.1007/s10661-021-09079-x

141. Stevenson, D. S., Zhao, A., Naik, V., O'Connor, F. M., Tilmes, S., Zeng, G., Murray, L. T., Collins, W. J., Griffiths, P. T., Shim, S. B., Horowitz, L. W., Sentman, L. T., & Emmons, L. (2020). Trends in global tropospheric hydroxyl radical and methane lifetime since 1850 from AerChemMIP. *Atmospheric Chemistry and Physics, 20*(21), 12905-12920. https://doi.org/10.5194/acp-20-12905-2020

142. Zhao, Y. H., Saunois, M., Bousquet, P., Lin, X., Berchet, A., Hegglin, M. I., Canadell, J. G., Jackson, R. B., Deushi, M., Jockel, P., Kinnison, D., Kirner, O., Strode, S., Tilmes, S., Dlugokencky, E. J., & Zheng, B. (2020). On the role of trend and variability in the hydroxyl radical (OH) in the global methane budget. *Atmospheric Chemistry and Physics, 20*(21), 13011-13022. https://doi.org/10.5194/acp-20-13011-2020

143. McDuffie, E. E., Smith, S. J., O'Rourke, P., Tibrewal, K., Venkataraman, C., Marais, E. A., Zheng, B., Crippa, M., Brauer, M., & Martin, R. V. (2020). A global anthropogenic emission inventory of atmospheric pollutants from sector- And fuel-specific sources (1970-2017): An application of the Community Emissions Data System (CEDS). *Earth System Science Data, 12*(4), 3413-3442. https://doi.org/10.5194/essd-12-3413-2020

144. Patra, P. K., Krol, M. C., Prinn, R. G., Takigawa, M., Mühle, J., Montzka, S. A., Lal, S., Yamashita, Y., Naus, S., Chandra, N., Weiss, R. F., Krummel, P. B., Fraser, P. J., O'Doherty, S., & Elkins, J. W. (2021). Methyl chloroform continues to constrain the hydroxyl (OH) variability in the troposphere. *Journal of Geophysical Research-Atmospheres, 126*(4), e2020JD033862. https://doi.org/10.1029/2020JD033862

145. Naus, S., Montzka, S. A., Patra, P. K., & Krol, M. C. (2021). A three-dimensional-model inversion of methyl chloroform to constrain the atmospheric oxidative capacity. *Atmospheric Chemistry and Physics, 21*(6), 4809-4824. https://doi.org/10.5194/acp-21-4809-2021

146. Worden, J. R., Cusworth, D. H., Qu, Z., Yin, Y., Zhang, Y., Bloom, A. A., Ma, S., Byrne, B. K., Scarpelli, T., Maasakkers, J. D., Crisp, D., Duren, R., & Jacob, D. J. (2022). The 2019 methane budget and uncertainties at 1° resolution and each country through Bayesian integration Of GOSAT total column methane data and a priori inventory estimates. *Atmospheric Chemistry and Physics, 22*(10), 6811-6841. https://doi.org/10.5194/acp-22-6811-2022

147. Turner, A. J., Frankenberg, C., & Kort, E. A. (2019). Interpreting contemporary trends in atmospheric methane. *Proceedings of the National Academy of Sciences of the United States of America, 116*(8), 2805-2813. https://doi.org/10.1073/pnas.1814297116

148. Fang, X. K., Pyle, J. A., Chipperfield, M. P., Daniel, J. S., Park, S., & Prinn, R. G. (2019). Challenges for the recovery of the ozone layer. *Nature Geoscience, 12*(8), 592-596. https://doi.org/10.1038/s41561-019-0422-7

149. Keber, T., Bonisch, H., Hartick, C., Hauck, M., Lefrancois, F., Obersteiner, F., Ringsdorf, A., Schohl, N., Schuck, T., Hossaini, R., Graf, P., Jockel, P., & Engel, A. (2020). Bromine from short-lived source gases in the extratropical northern hemispheric upper troposphere and lower stratosphere (UTLS). *Atmospheric Chemistry and Physics, 20*(7), 4105-4132. https://doi.org/10.5194/acp-20-4105-2020

150. Engel, A., Rigby, M., Burkholder, J. B., Fernandez, R. P., Froidevaux, L., Hall, B. D., Hossaini, R., Saito, T., Vollmer, M. K., & Yao, B. (2018). *Update on Ozone-Depleting Substances (ODS) and Other Gases of Interest to the Montreal Protocol, Chap. 1.* Scientific Assessment of Ozone Depletion: 2018, Global Ozone Research and Monitoring Project-Report No. 58, World Meteorological Organization. World Meteorological Organization, Geneva, Switzerland.

151. Rex, M., Wohltmann, I., Ridder, T., Lehmann, R., Rosenlof, K., Wennberg, P., Weisenstein, D., Notholt, J., Kruger, K., Mohr, V., & Tegtmeier, S. (2014). A tropical West Pacific OH minimum and implications for stratospheric composition. *Atmospheric Chemistry and Physics, 14*(9), 4827-4841. https://doi.org/10.5194/acp-14-4827-2014

152. Nicewonger, M. R., Saltzman, E. S., & Montzka, S. A. (2022). ENSO-driven fires cause large interannual variability in the naturally emitted, ozone-depleting trace gas CH_3Br. *Geophysical Research Letters, 49*, e2021GL094756. https://doi.org/10.1029/2021GL094756

153. Liu, S. S., Yang, G. P., He, Z., Gao, X. X., & Xu, F. (2021). Oceanic emissions of methyl halides and effect of nutrients concentration on their production: A case of the western Pacific Ocean (2 degrees N to 24 degrees N). *Science of the Total Environment, 769*, 144488. https://doi.org/10.1016/j.scitotenv.2020.144488

154. Williams, R. S., Hegglin, M. I., Kerridge, B. J., Jöckel, P., Latter, B. G., & Plummer, D. A. (2019). Characterising the seasonal and geographical variability in tropospheric ozone, stratospheric influence and recent changes. *Atmospheric Chemistry and Physics, 19*(6), 3589-3620. https://doi.org/10.5194/acp-19-3589-2019

155. Archibald, A. T., Neu, J. L., Elshorbany, Y. F., Cooper, O. R., Young, P. J., Akiyoshi, H., Cox, R. A., Coyle, M., Derwent, R. G., Deushi, M., Finco, A., Frost, G. J., Galbally, I. E., Gerosa, G., Granier, C., Griffiths, P. T., Hossaini, R., Hu, L., Jöckel, P., Josse, B., et al. (2020). Tropospheric Ozone Assessment Report: A critical review of changes in the tropospheric ozone burden and budget from 1850 to 2100. *Elementa: Science of the Anthropocene, 8*(1). https://doi.org/10.1525/elementa.2020.034

156. Wang, M., & Fu, Q. (2021). Stratosphere-troposphere exchange of air masses and ozone concentrations based on reanalyses and observations. *Journal of Geophysical Research: Atmospheres, 126*(18), e2021JD035159. https://doi.org/10.1029/2021JD035159

157. Ruiz, D. J., & Prather, M. J. (2022). From the middle stratosphere to the surface, using nitrous oxide to constrain the stratosphere–troposphere exchange of ozone. *Atmospheric Chemistry and Physics, 22*(3), 2079-2093. https://doi.org/10.5194/acp-22-2079-2022

158. Griffiths, P. T., Murray, L. T., Zeng, G., Shin, Y. M., Abraham, N. L., Archibald, A. T., Deushi, M., Emmons, L. K., Galbally, I. E., Hassler, B., Horowitz, L. W., Keeble, J., Liu, J., Moeini, O., Naik, V., O'Connor, F. M., Oshima, N., Tarasick, D., Tilmes, S., Turnock, S. T., et al. (2021). Tropospheric ozone in CMIP6 simulations. *Atmospheric Chemistry and Physics, 21*(5), 4187-4218. https://doi.org/10.5194/acp-21-4187-2021

159. Hu, L., Jacob, D. J., Liu, X., Zhang, Y., Zhang, L., Kim, P. S., Sulprizio, M. P., & Yantosca, R. M. (2017). Global budget of tropospheric ozone: Evaluating recent model advances with satellite (OMI), aircraft (IAGOS), and ozonesonde observations. *Atmospheric Environment, 167*, 323-334. https://doi.org/10.1016/j.atmosenv.2017.08.036

160. Griffiths, P. T., Keeble, J., Shin, Y. M., Abraham, N. L., Archibald, A. T., & Pyle, J. A. (2020). On the changing role of the stratosphere on the tropospheric ozone budget: 1979–2010. *Geophysical Research Letters, 47*, 9. https://doi.org/10.1029/2019gl086901

161. Abalos, M., Orbe, C., Kinnison, D. E., Plummer, D., Oman, L. D., Jöckel, P., Morgenstern, O., Garcia, R. R., Zeng, G., Stone, K. A., & Dameris, M. (2020). Future trends in stratosphere-to-troposphere transport in CCMI models. *Atmospheric Chemistry and Physics, 20*(11), 6883-6901. https://doi.org/10.5194/acp-20-6883-2020

162. Akritidis, D., Pozzer, A., Flemming, J., Inness, A., & Zanis, P. (2021). A global climatology of tropopause folds in CAMS and MERRA-2 reanalyses. *Journal of Geophysical Research: Atmospheres, 126*(8), e2020JD034115. https://doi.org/10.1029/2020JD034115

163. Liu, J. H., Rodriguez, J. M., Oman, L. D., Douglass, A. R., Olsen, M. A., & Hu, L. (2020). Stratospheric impact on the Northern Hemisphere winter and spring ozone interannual variability in the troposphere. *Atmospheric Chemistry and Physics, 20*(11), 6416-6432. https://doi.org/10.5194/acp-20-6417-2020

164. Dafka, S., Akritidis, D., Zanis, P., Pozzer, A., Xoplaki, E., Luterbacher, J., & Zerefos, C. (2021). On the link between the Etesian winds, tropopause folds and tropospheric ozone over the Eastern Mediterranean during summer. *Atmospheric Research, 248*. https://doi.org/10.1016/j.atmosres.2020.105161

165. Akritidis, D., Pozzer, A., & Zanis, P. (2019). On the impact of future climate change on tropopause folds and tropospheric ozone. *Atmospheric Chemistry and Physics, 19*(22), 14387-14401. https://doi.org/10.5194/acp-19-14387-2019

166. Cohen, Y., Marecal, V., Josse, B., & Thouret, V. (2021). Interpol-IAGOS: a new method for assessing long-term chemistry-climate simulations in the UTLS based on IAGOS data, and its application to the MOCAGE CCMI REF-C1SD simulation. *Geoscientific Model Development, 14*(5), 2659-2689. https://doi.org/10.5194/gmd-14-2659-2021

167. Huijnen, V., Miyazaki, K., Flemming, J., Inness, A., Sekiya, T., & Schultz, M. G. (2020). An intercomparison of tropospheric ozone reanalysis products from CAMS, CAMS interim, TCR-1, and TCR-2. *Geoscientific Model Development, 13*(3), 1513-1544. https://doi.org/10.5194/gmd-13-1513-2020

168. Krizan, P., Kozubek, M., & Lastovicka, J. (2019). Discontinuities in the ozone concentration time series from MERRA 2 reanalysis. *Atmosphere, 10*(12). https://doi.org/10.3390/atmos10120812

169. Barnes, P. W., Robson, T. M., Zepp, R. G., Bornman, J. F., Jansen, M. A. K., Ossola, R., Wang, Q.-W., Robinson, S. A., Foereid, B., Klekociuk, A. R., Martinez-Abaigar, J., Hou, W. C., & Paul, N. D. (2022). Interactive effects of changes in UV radiation and climate on terrestrial ecosystems, biogeochemical cycles, and feedbacks to the climate system. *Chapter 4*

170. Robinson, S. A., & Erickson Iii, D. J. (2015). Not just about sunburn – the ozone hole's profound effect on climate has significant implications for Southern Hemisphere ecosystems. *Global Change Biology, 21*(2), 515-527. https://doi.org/https://doi.org/10.1111/gcb.12739

171. Damiani, A., Cordero, R. R., Llanillo, P. J., Feron, S., Boisier, J. P., Garreaud, R., Rondanelli, R., Irie, H., & Watanabe, S. (2020). Connection between Antarctic Ozone and climate: interannual precipitation changes in the southern hemisphere. *Atmosphere, 11*(6), 579. https://doi.org/10.3390/atmos11060579

172. Lim, E.-P., Hendon, H. H., Boschat, G., Hudson, D., Thompson, D. W. J., Dowdy, A. J., & Arblaster, J. M. (2019). Australian hot and dry extremes induced by weakenings of the stratospheric polar vortex. *Nature Geoscience, 12*(11), 896-901. https://doi.org/10.1038/s41561-019-0456-x

173. Santee, M. L., Lambert, A., Manney, G. L., Livesey, N. J., Froidevaux, L., Neu, J. L., Schwartz, M. J., Millán, L. F., Werner, F., Read, W. G., Park, M., Fuller, R. A., & Ward, B. M. (2022). Prolonged and pervasive perturbations in the composition of the southern hemisphere midlatitude lower stratosphere from the Australian New Year's fires. *Geophysical Research Letters, 49*(4), e2021GL096270. https://doi.org/10.1029/2021GL096270

174. Tencé, F., Jumelet, J., Bekki, S., Khaykin, S., Sarkissian, A., & Keckhut, P. (2022). Australian black summer smoke observed by lidar at the French Antarctic station Dumont d'Urville. *Journal of Geophysical Research: Atmospheres, 127*(4), e2021JD035349. https://doi.org/10.1029/2021JD035349

175. NASA Goddard Space Flight Center (2021). Global Transport of Australian Bushfire Smoke. https://climate.nasa.gov/climate_resources/202/global-transport-of-australian-bushfire-smoke/. Accessed 16 March 2022 2022.

176. Jia, G., Shevliakova, E., Artaxo, P., Noblet-Ducoudré, N. D., Houghton, R., House, J., Kitajima, K., Lennard, C., Popp, A., Sirin, A., Sukumar, R., & Verchot, L. (2019). Land–climate interactions. In P. R. Shukla, J. Skea, E. C. Buendia, V. Masson-Delmotte, H.-O. Pörtner, D. C. Roberts, P. Zhai, R. Slade, S. Connors, R. v. Diemen, M. Ferrat, E. Haughey, S. Luz, S. Neogi, M. Pathak, J. Petzold, J. P. Pereira, P. Vyas, E. Huntley, et al. (Eds.), *Climate Change and Land: an IPCC special report on climate change, desertification, land degradation, sustainable land management, food security, and greenhouse gas fluxes in terrestrial ecosystems*. https://doi.org/https://www.ipcc.ch/srccl/

177. Lawrence, Z. D., Perlwitz, J., Butler, A. H., Manney, G. L., Newman, P. A., Lee, S. H., & Nash, E. R. (2020). The remarkably strong arctic stratospheric polar vortex of winter 2020: Links to record-breaking Arctic oscillation and ozone loss. *Journal of Geophysical Research: Atmospheres, 125*(22). https://doi.org/10.1029/2020jd033271

178. Friedel, M., Chiodo, G., Stenke, A., Domeisen, D. I. V., Fueglistaler, S., Anet, J. G., & Peter, T. (2022). Springtime arctic ozone depletion forces northern hemisphere climate anomalies. *Nature Geoscience, 15*(7), 541-547. https://doi.org/10.1038/s41561-022-00974-7

179. Overland, J. E., & Wang, M. Y. (2021). The 2020 Siberian heat wave. *International Journal of Climatology, 41*, E2341-E2346. https://doi.org/10.1002/joc.6850

180. von der Gathen, P., Kivi, R., Wohltmann, I., Salawitch, R. J., & Rex, M. (2021). Climate change favours large seasonal loss of Arctic ozone. *Nature Communications, 12*(1), 1-17. https://doi.org/10.1038/s41467-021-24089-6

181. OECD (2022). Per- and polyfluoroalkyl substances (PFAS). https://www.oecd.org/chemicalsafety/portal-perfluorinated-chemicals/. Accessed February 2022.

182. Wallington, T. J., Sulbæk Andersen, M. P., & Nielsen, O. J. (2021). The case for a more precise definition of regulated PFAS. *Environmental Science: Processes & Impacts, 23*(12), 1834-1838. https://doi.org/10.1039/d1em00296a

183. Buck, R. C., Korzeniowski, S. H., Laganis, E., & Adamsky, F. (2021). Identification and classification of commercially relevant per- and poly-fluoroalkyl substances (PFAS). *Integrated Environmental Assessment and Management, 17*, 1045-1055. https://doi.org/10.1002/ieam.4450

184. Anderson, J. K., Brecher, R. W., Cousins, I. T., DeWitt, J., Fiedler, H., Kannan, K., Kirman, C. R., Lipscomb, J., Priestly, B., Schoeny, R., Seed, J., Verner, M., & Hays, S. M. (2022). Grouping of PFAS for human health risk assessment: Findings from an independent panel of experts. *Regulatory Toxicology and Pharmacology, 105226*. https://doi.org/10.1016/j.yrtph.2022.105226

185. DEPA. (2015). *Short-chain Polyfluoroalkyl Substances (PFAS)*. Vol. 1707. Danish Environmental Protection Agency, Copenhagen.

186. EFSA (2020). Risk to human health related to the presence of perfluoroalkyl substances in food. *EFSA Journal, 18*(9), e06223. https://doi.org/10.2903/j.efsa.2020.6223

187. NICNAS. (2016). *Short Chain Perfluorocarboxylic Acids and their Direct Precursors: Human Health Tier II Assessment. National Industrial Chemicals Notification and Assessment Scheme (NICNAS)*, Canberra AU.

188. ECCC. (2022). Canada's Great Lakes Strategy for PFOS, PFOA, and LC-PFCAs Risk Management. Environment and Climate Change Canada, Ottawa, ON.

189. United States Environmental Protection Agency (EPA) (2022). *PFAS Master List of PFAS Substances* https://comptox.epa.gov/dashboard/chemical_lists/pfasmaster. Accessed April 2022.

190. PubChem (2022). *Trifluoroacetic acid*. https://pubchem.ncbi.nlm.nih.gov/compound/6422. Accessed January 2022.

191. RSC (2022). *ChemSpider*. http://www.chemspider.com/. Accessed May 2022.

192. Chabot, L. (2017). Chabot L. (2017). *ALGA, GROWTH INHIBITION TEST Effect of the trifuoroacetic acid on the growth of the unicellular alga Pseudokirchneriella subcapitata, according to OECD guideline 201* (Study conducted for RHODIA OPERATIONS – SOLVAY). Vol. 17-005-167094. Verneuil-En-Halatte, Verneuil-En-Halatte, France.

193. Boudreau, T. M. (2002). Toxicity of Perfluorinated Organic Acids to Selected Freshwater Organisms under Laboratory and Field Conditions. M.Sc., University of Guelph, Guelph.

194. Wang, Y., Niu, J., Zhang, L., & Shi, J. (2014). Toxicity assessment of perfluorinated carboxylic acids (PFCAs) towards the rotifer *Brachionus calyciflorus*. *The Science of the Total Environment, 491-492*, 266-270. https://doi.org/10.1016/j.scitotenv.2014.02.028

195. ATSDR. (2021). *Toxicological Profile for Perfluoroalkyls*. Agency for Toxic Substances and Disease Registry, Washington DC.

196. Kwiatkowski, C. F., Andrews, D. Q., Birnbaum, L. S., Bruton, T. A., DeWitt, J. C., Knappe, D. R. U., Maffini, M. V., Miller, M. F., Pelch, K. E., Reade, A., Soehl, A., Trier, X., Venier, M., Wagner, C. C., Wang, Z., & Blum, A. (2020). Scientific basis for managing PFAS as a chemical class. *Environmental Science & Technology Letters, 7*(8), 532-543. https://doi.org/10.1021/acs.estlett.0c00255

197. Cousins, I. T., Dewitt, J. C., Glüge, J., Goldenman, G., Herzke, D., Lohmann, R., Ng, C. A., Scheringer, M., & Wang, Z. (2020). The high persistence of PFAS is sufficient for their management as a chemical class. *Environmental Science: Processes & Impacts, 22*(12), 2307-2312. https://doi.org/10.1039/d0em00355g

198. Singh, R. R., & Papanastasiou, D. K. (2021). Comment on "Scientific basis for managing PFAS as a chemical class". *Environmental Science & Technology Letters, 8*(2), 192-194. https://doi.org/10.1021/acs.estlett.0c00765

199. Kwiatkowski, C. F., Andrews, D. Q., Birnbaum, L. S., Bruton, T. A., DeWitt, J. C., Knappe, D. R. U., Maffini, M. V., Miller, M. F., Pelch, K. E., Reade, A., Soehl, A., Trier, X., Venier, M., Wagner, C. C., Wang, Z., & Blum, A. (2021). Response to "Comment on scientific basis for managing PFAS as a chemical class". *Environmental Science & Technology Letters, 8*(2), 195-197. https://doi.org/10.1021/acs.estlett.1c00049

200. Hogue, C. (2022, July 4. 2022). How to define PFAS. *Chemical & Engineering News*, pp. 18-19.

201. Boutonnet, J. C., Bingham, P., Calamari, D., Rooij, C. d., Franklin, J., Kawano, T., Libre, J.-M., McCul-Loch, A., Malinverno, G., & Odom, J. M. (1999). Environmental risk assessment of trifluoroacetic acid. *Human and Ecological Risk Assessment, 5*, 59-124. https://doi.org/10.1080/10807039991289644

202. Scheurer, M., Nödler, K., Freeling, F., Janda, J., Happel, O., Riegel, M., Müller, U., Storck, F. R., Fleig, M., Lange, F. T., Brunsch, A., & Brauch, H.-J. (2017). Small, mobile, persistent: Trifluoroacetate in the water cycle – Overlooked sources, pathways, and consequences for drinking water supply. *Water Research, 126*, 460-471. https://doi.org/10.1016/j.watres.2017.09.045

203. Alexandrino, D. A. M., Ribeiro, I., Pinto, L. M., Cambra, R., Oliveira, R. S., Pereira, F., & Carvalho, M. F. (2018). Biodegradation of mono-, di- and trifluoroacetate by microbial cultures with different origins. *New Biotechnology, 43*, 23-29. https://doi.org/10.1016/j.nbt.2017.08.005

204. Wallington, T. J., Sulbæk Andersen, M. P., & Nielsen, O. J. (2015). Atmospheric chemistry of short-chain haloolefins: Photochemical ozone creation potentials (POCPs), global warming potentials (GWPs), and ozone depletion potentials (ODPs). *Chemosphere, 129*, 135-141. https://doi.org/10.1016/j.chemosphere.2014.06.092

205. Wallington, T. J., Schneider, W. F., Worsnop, D. R., Nielsen, O. J., Sehested, J., Debruyn, W. J., & Shorter, J. A. (1994). The environmental impact of CFC replacements HFCs and HCFCs. *Environmental Science & Technology, 28*(7), 320A-326A. https://doi.org/10.1021/es00056a714

206. Hurley, M. D., Wallington, T. J., Javadi, M. S., & Nielsen, O. J. (2008). Atmospheric chemistry of CF_3CFCH_2: Products and mechanisms of Cl atom and OH radical initiated oxidation. *Chemical Physics Letters, 450*(4-6), 263-267. https://doi.org/10.1016/j.cplett.2007.11.051

207. Burkholder, J. B., Cox, R. A., & Ravishankara, A. R. (2015). Atmospheric degradation of ozone depleting substances, their substitutes, and related species. *Chemical Reviews, 115*(10), 3704-3759. https://doi.org/10.1021/cr5006759

208. Wallington, T. J., Andersen, M. P. S., & Nielsen, O. J. (2017). Atmospheric Chemistry of Halogenated Organic Compounds. In J. R. Barker, A. L. Steiner, & T. J. Wallington (Eds.), *Advances in Atmospheric Chemistry, 2*, 305-402. New Jersey: World Scientific. https://doi.org/10.1142/9789813147355_0005

209. IPCC (2021). *Climate Change 2021: The Physical Science Basis. Contribution of Working Group I to the Sixth Assessment Report of the Intergovernmental Panel on Climate Change*. Cambridge, U.K.: Cambridge University Press.

210. Chiappero, M. S., Malanca, F. E., Argüello, G. A., Wooldridge, S. T., Hurley, M. D., Ball, J. C., Wallington, T. J., Waterland, R. L., & Buck, R. C. (2006). Atmospheric chemistry of perfluoroaldehydes ($C_xF2_{x+1}CHO$) and fluorotelomer aldehydes ($C_xF_{2x+1}CH_2CHO$): Quantification of the important role of photolysis. *The Journal of Physical Chemistry A, 110*(43), 11944-11953. https://doi.org/10.1021/jp064262k

211. Sulbæk Andersen, M. P., Toft, A., Nielsen, O. J., Hurley, M. D., Wallington, T. J., Chishima, H., Tonokura, K., Mabury, S. A., Martin, J. W., & Ellis, D. A. (2006). Atmospheric chemistry of perfluorinated aldehyde hydrates (n-$C_xF_{2x+1}CH(OH)_2$, x = 1, 3, 4): Hydration, dehydration, and kinetics and mechanism of Cl atom and OH radical initiated oxidation. *The Journal of Physical Chemistry A, 110*(32), 9854-9860. https://doi.org/10.1021/jp060404z

212. WMO (2022). Scientific Assessment of Ozone Depletion: *2022,* GAW Report No. 278. World Meteorological Organization, Geneva, Switzerland.

213. Frank, H., Christoph, E. H., Holm-Hansen, O., & Bullister, J. L. (2002). Trifluoroacetate in ocean waters. *Environmental Science & Technology, 36*, 12-15. https://doi.org/10.1021/es0101532

214. UBA. (2021). *Persistent Degradation Products of Halogenated Refrigerants and Blowing Agents in the Environment: Type, Environmental Concentrations, and Fate with Particular Regard to New Halogenated Substitutes with Low Global Warming Potential*. Vol. FB000452/ENG. Umwelt Bundesamt, Dessau-Roßlau.

215. Sulbæk Andersen, M. P., Schmidt, J. A., Volkova, A., & Wuebbles, D. J. (2018). A three-dimensional model of the atmospheric chemistry of E and Z-$CF_3CH=CHCl$ (HCFO-1233(zd) (E/Z)). *Atmospheric Environment, 179*, 250-259. https://doi.org/10.1016/j.atmosenv.2018.02.018

216. Holland, R., Khan, M. A. H., Driscoll, I., Chhantyal-Pun, R., Derwent, R. G., Taatjes, C. A., Orr-Ewing, A. J., Percival, C. J., & Shallcross, D. E. (2021). Investigation of the production of trifluoroacetic acid from two halocarbons, HFC-134a and HFO-1234yf and its fates using a global three-dimensional chemical transport model. *ACS Earth and Space Chemistry, 5*, 849–857. https://doi.org/10.1021/acsearthspacechem.0c00355

217. David, L. M., Barth, M., Höglund-Isaksson, L., Purohit, P., Velders, G. J., Glaser, S., & Ravishankara, A. R. (2021). Trifluoroacetic acid deposition from emissions of HFO-1234yf in India, China, and the Middle East. *Atmospheric Chemistry and Physics, 21*(19), 14833-14849. https://doi.org/10.5194/acp-21-14833-2021

218. United States Environmental Protection Agency (EPA). (2020). Models for Pesticide Risk Assessment. https://www.epa.gov/pesticide-science-and-assessing-pesticide-risks/models-pesticide-risk-assessment#AgDrift. Accessed January 2022.

219. Chen, H., Zhang, L., Li, M., Yao, Y., Zhao, Z., Munoz, G., & Sun, H. (2019). Per-and polyfluoroalkyl substances (PFASs) in precipitation from mainland China: Contributions of unknown precursors and short-chain (C2C3) perfluoroalkyl carboxylic acids. *Water Research, 153*, 169-177. https://doi.org/10.1016/j.watres.2019.01.019

220. Freeling, F., Behringer, D., Heydel, F., Scheurer, M., Ternes, T. A., & Nödler, K. (2020). Trifluoroacetate in precipitation: Deriving a benchmark dataset. Environmental Science & Technology, 54, 11210–11219. https://doi.org/10.1021/acs.est.0c02910

221. Cahill, T. M. (2022). Increases in trifluoroacetate concentrations in surface waters over two decades. *Environmental Science & Technology, 56*(13), 9428–9434. https://doi.org/10.1021/acs.est.2c01826

222. Freeling, F., Scheurer, M., Koschorreck, J., Hoffmann, G., Ternes, T. A., & Nödler, K. (2022). Levels and temporal trends of trifluoroacetate (TFA) in archived plants: evidence for increasing emissions of gaseous TFA precursors over the last decades. *Environmental Science & Technology Letters, 5*, 400-405. https://doi.org/10.1021/acs.estlett.2c00164

223. Lindley, A., McCulloch, A., & Vink, T. (2019). Contribution of hydrofluorocarbons (HFCs) and hydrofluoro-olefins (HFOs) atmospheric breakdown products to acidification ("Acid Rain") in the EU at present and in the future. *Open Journal of Air Pollution, 8*, 81-95. https://doi.org/doi: 10.4236/ojap.2019.84004

224. Bernhard, G. H., Neale, R. E., Barnes, P. W., Neale, P. J., Zepp, R. G., Wilson, S. R., Andrade, A. J., Bais, A. F., McKenzie, R. L., Aucamp, P. J., Young, P. J., Liley, B. J., Lucas, R. M., Yazar, S., Rhodes, L. E., Byrne, S. N., Hollestein, L. M., Olsen, L. M., Young, A. R., Robson, T. M., et al. (2020). Environmental effects of stratospheric ozone depletion, UV radiation and interactions with climate change: UNEP Environmental Effects Assessment Panel, update 2019. *Photochemical & Photobiological Sciences, 19*, 542-584. https://doi.org/10.1039/d0pp90011g

225. Neale, R. E., Barnes, P. W., Robson, T. M., Neale, P. J., Bernhard, G. H., Neale, R. E., Williamson, C. E., Zepp, R. G., Wilson, S. R., Madronich, S., Andrade, A. J., Heikkila, A. M., Bernhard, G. H., Bais, A. F., Aucamp, P. J., Banaszak, A. T., Bornman, J. F., Bruckman, L. S., Byrne, S. N., Føreid, B., et al. (2021). Environmental effects of stratospheric ozone depletion, UV radiation and interactions with climate change: UNEP Environmental Effects Assessment Panel, Update 2020. *Photochemical & Photobiological Sciences, 20*, 1-67. https://doi.org/10.1007/s43630-020-00001-x

226. Frank, H., Klein, A., & Renschen, D. (1996). *Environmental trifluoroacetate. Nature, 382*, 34-34. https://doi.org/10.1038/382034a0

227. Scott, B., Macdonald, R., Kannan, K., Fisk, A., Witter, A., Yamashita, N., Durham, L., Spencer, C., & Muir, D. (2005). Trifluoroacetate profiles in the Arctic, Atlantic, and Pacific oceans. *Environmental Science & Technology, 39*, 6555-6560. https://doi.org/10.1021/es047975u

228. Scott, B. F., Spencer, C., Martin, J. W., Barra, R., Bootsma, H. A., Jones, K. C., Johnston, A. E., & Muir, D. C. G. (2005). Comparison of haloacetic acids in the environment of the Northern and Southern Hemispheres. *Environmental Science & Technology, 39*(22), 8664-8670. https://doi.org/10.1021/es050118L

229. Joudan, S., DeSilva, A. O., & Young, C. (2021). Insufficient evidence for the existence of natural trifluoroacetic acid. *Environmental Science: Processes & Impacts, 23*, 1641–1649. https://doi.org/10.1039/d1em00306b

230. Klobas, J. E., & Wilmouth, D. M. (2019). V*olcanogenic Chlorofluorocarbons and the Recent CFC Anomalies. A white paper prepared at the request of the Scientific Assessment Panel (SAP) of the Montreal Protocol.* Harvard University Library, Boston.

231. Gribble, G. W. (2002). Fluorine in the Environment, a Review of its Sources and Geochemistry. In A. H. Neilson (Ed.), T*he Handbook of Environmental Chemistry, 3*, 121-136. Berlin Heidelberg: Springer-Verlag

232. Solomon, K., Velders, G., Wilson, S., Madronich, S., Longstreth, J., Aucamp, P., & Bornman, J. (2016). Sources, fates, toxicity, and risks of trifluoroacetic acid and its salts: Relevance to substances regulated under the Montreal and Kyoto protocols. *Journal of Toxicology and Environmental Health B, 19*, 289-304. https://doi.org/10.1080/10937404.2016.1175981

233. Wang, B., Yao, Y., Chen, H., Chang, S., Tian, Y., & Sun, H. (2020). Per-and polyfluoroalkyl substances and the contribution of unknown precursors and short-chain (C2–C3) perfluoroalkyl carboxylic acids at solid waste disposal facilities. *Science of the Total Environment, 705*, 135832. https://doi.org/10.1016/j.scitotenv.2019.135832

234. Xie, G., Zhai, Z., & Zhang, J. (2020). Distribution characteristics of trifluoroacetic acid in the environments surrounding fluorochemical production plants in Jinan, China. *Environmental Science and Pollution Research, 27*, 983-991. https://doi.org/10.1007/s11356-019-06689-4

235. Zhang, L., Sun, H., Wang, Q., Chen, H., Yao, Y., Zhao, Z., & Alder, A. C. (2019). Uptake mechanisms of perfluoroalkyl acids with different carbon chain lengths (C2-C8) by wheat (*Triticum aestivum* L.). *Science of the Total Environment, 654*, 19-27. https://doi.org/10.1016/j.scitotenv.2018.10.443

236. Lan, Z., Yao, Y., Xu, J., Chen, H., Ren, C., Fang, X., Zhang, K., Jin, L., Hua, X., & Alder, A. C. (2020). Novel and legacy per-and polyfluoroalkyl substances (PFASs) in a farmland environment: Soil distribution and biomonitoring with plant leaves and locusts. *Environmental Pollution, 263*, 114487. https://doi.org/10.1016/j.envpol.2020.114487

237. Gardiner, J. (2015). Fluoropolymers: Origin, production, and industrial and commercial applications. *Australian Journal of Chemistry, 68*(1), 13-22. https://doi.org/10.1071/CH14165

238. Ellis, D. A., Mabury, S. A., Martin, J. W., & Muir, D. C. (2001). Thermolysis of fluoropolymers as a potential source of halogenated organic acids in the environment. *Nature, 412*, 321-324. https://doi.org/10.1038/35085548

239. Cui, J. N., Guo, J. Y., Zhai, Z. H., & Zhang, J. B. (2019). The contribution of fluoropolymer thermolysis to trifluoroacetic acid (TFA) in environmental media. *Chemosphere, 222*, 637-644. https://doi.org/10.1016/j.chemosphere.2019.01.174

240. Trang, B., Li, Y., Xue, X.-S., Ateia, M., Houk, K. N., & Dichtel, W. R. (2022). Low-temperature mineralization of perfluorocarboxylic acids. *Science, 377*(6608), 839-845. https://doi.org/doi:10.1126/science.abm8868

241. Lenka, S. P., Kah, M., & Padhye, L. P. (2021). A review of the occurrence, transformation, and removal of poly- and perfluoroalkyl substances (PFAS) in wastewater treatment plants. *Water Research, 199*, 117187. https://doi.org/10.1016/j.watres.2021.117187

242. Duan, Y., Sun, H., Yao, Y., Meng, Y., & Li, Y. (2020). Distribution of novel and legacy per-/polyfluoroalkyl substances in serum and its associations with two glycemic biomarkers among Chinese adult men and women with normal blood glucose levels. *Environment International, 134*, 105295. https://doi.org/10.1016/j.envint.2019.105295

243. Scheurer, M., & Nödler, K. (2021). Ultrashort-chain perfluoroalkyl substance trifluoroacetate (TFA) in beer and tea–An unintended aqueous extraction. *Food Chemistry, 351*, 129304. https://doi.org/10.1016/j.foodchem.2021.129304

244. Yao, Y., Sun, H., Gan, Z., Hu, H., Zhao, Y., Chang, S., & Zhou, Q. (2016). Nationwide distribution of per- and polyfluoroalkyl substances in outdoor dust in Mainland China from eastern to western areas. *Environmental Science & Technology, 50*(7), 3676-3685. https://doi.org/10.1021/acs.est.6b00649

245. Wang, B., Yao, Y., Wang, Y., Chen, H., & Sun, H. (2021). Per-and polyfluoroalkyl substances in outdoor and indoor dust from Mainland China: Contributions of unknown precursors and implications for human exposure. *Environmental Science & Technology, 56*(10), 6036–6045. https://doi.org/10.1021/acs.est.0c08242

246. Siegemund, G., Schwertfeger, W., Feiring, A., Smart, B., Behr, F., Vogel, H., McKusick, B., & Kirsch, P. (2016). Fluorine Compounds, Organic. In *Ullmann's Encyclopedia of Industrial Chemistry*, n/a. Hoboken, NJ: Wiley-VCH Verlag GmbH & Co

247. Inoue, M., Sumii, Y., & Shibata, N. (2020). Contribution of organofluorine compounds to pharmaceuticals. *ACS Omega, 5*(19), 10633-10640. https://doi.org/10.1021/acsomega.0c00830

248. Yu, Y., Liu, A., Dhawan, G., Mei, H., Zhang, W., Izawa, K., Soloshonok, V. A., & Han, J. (2021). Fluorine-containing pharmaceuticals approved by the FDA in 2020: Synthesis and biological activity. *Chinese Chemical Letters*. https://doi.org/10.1016/j.cclet.2021.05.042

249. Khan, M. F., & Murphy, C. D. (2021). Bacterial degradation of the anti-depressant drug fluoxetine produces trifluoroacetic acid and fluoride ion. *Applied Microbiology and Biotechnology, 105*, 9359-9369. https://doi.org/10.1007/s00253-021-11675-3

250. Morio, M., Fujii, K., Takiyama, R., Chikasue, F., Kikuchi, H., & Ribarić, L. (1980). Quantitative analysis of trifluoroacetate in the urine and blood by isotachophoresis. *Anesthesiology, 53*(1), 56-59. https://doi.org/10.1097/00000542-198007000-00011

251. Mirkov, M. I., Morio, M., Kawahara, M., Yuge, O., Kinoshita, H., & Fujii, K. (1988). Excretion of trifluoroacetic acid as a metabolite of halothane in digestive juices. *Journal of Anesthesia, 2*(2), 133-138. https://doi.org/10.1007/s0054080020133

252. Sutton, T. S., Koblin, D. D., Gruenke, L. D., Weiskopf, R. B., Rampil, I. J., Waskell, L., & Eger 2nd, E. (1991). Fluoride metabolites after prolonged exposure of volunteers and patients to desflurane. *Anesthesia and Analgesia, 73*(2), 180-185. https://doi.org/10.1213/00000539-199108000-00011

253. Wark, H., Earl, J., Chau, D. D., & Overton, J. (1990). Halothane metabolism in children. *British Journal of Anaesthesia, 64*, 474-481. https://doi.org/10.1093/bja/64.4.474

254. Ogawa, Y., Tokunaga, E., Kobayashi, O., Hirai, K., & Shibata, N. (2020). Current contributions of organofluorine compounds to the agrochemical industry. *Iscience, 23*, 101467. https://doi.org/10.1016/j.isci.2020.101467

255. Ellis, D. A., & Mabury, S. A. (2000). The aqueous photolysis of TFM and related trifluoromethylphenols. An alternate source of trifluoroacetic acid in the environment. *Environmental Science & Technology, 34*, 632-637. https://doi.org/10.1021/es990422c

256. Bhat, A. P., Pomerantz, W. C. K., & Arnold, W. A. (2022). Finding fluorine: Photoproduct formation during the photolysis of fluorinated pesticides. *Environmental Science & Technology, 56*(17), 12336-12346. https://doi.org/10.1021/acs.est.2c04242

257. NAWQA, U. (2021). National Water-Quality Assessment (NAWQA) Project. Estimated Annual Agricultural Pesticide Use. https://water.usgs.gov/nawqa/pnsp/usage/maps/compound_listing.php. Accessed December 2021.

258. FAO STAT (2021). *Pesticide Use*. https://www.fao.org/faostat/en/?#data/RP. Accessed December 2021.

259. UBA. (2021). *Reducing Chemical Input into Water Bodies – Trifluoroacetate (TFA) as a Persistent and Mobile Substance from Many Sources*. Vol. ISSN 2363-829X. Umweld Bundesampt, German Environment Agency, Dessau-Roßlau.

260. UBA. (2019). *Ableitung Eines Gesundheitlichen Leitwertes für Trifluoressigsäure (TFA)*. Umwelt Bundesampt.

261. OECD (2022). OECD Test Guidelines for Chemicals https://www.oecd.org/chemicalsafety/testing/oecdguidelinesforthetestingofchemicals.htm. Accessed April 2022.

262. OECD (2022). Good Laboratory Practice (GLP) https://www.oecd.org/chemicalsafety/testing/good-laboratory-practiceglp.htm. Accessed April 2022.

263. ECHA (2021). Trifluoroacetic Acid: Toxicity to Aquatic Algae and Cyanobacteria. https://echa.europa.eu/registration-dossier/-/registered-dossier/5203/6/2/6/?documentUUID=9e9959f8-a994-4b8c-93d7-de7a1a3c1cfa. Accessed December 2021.

264. Cousins, I. T., Ng, C. A., Wang, Z., & Scheringer, M. (2019). Why is high persistence alone a major cause of concern? *Environmental Science: Processes & Impacts, 21*(5), 781-792. https://doi.org/10.1039/c8em00515J

265. IPCC/TEAP. (2005). *Special Report Safeguarding the Ozone Layer and the Global Climate System: Issues Related to Hydrofluorocarbons and Perfluorocarbons.* World Meteorological Organization (WMO) ; Intergovernmental Panel on Climate Change ; United Nations Environment Programme.

266. Derwent, R. G., Jenkin, M. E., & Saunders, S. M. (1996). Photochemical ozone creation potentials for a large number of reactive hydrocarbons under European conditions. *Atmospheric Environment, 30*(2), 181-199. https://doi.org/10.1016/1352-2310(95)00303-g

267. Carter, W. P. L. (1994). Development of ozone reactivity scales for volatile organic compounds. *Air & Waste, 44*, 881-899. https://doi.org/10.1080/1073161X.1994.10467290

268. Jenkin, M. E., Derwent, R. G., & Wallington, T. J. (2017). Photochemical ozone creation potentials for volatile organic compounds: Rationalization and estimation. *Atmospheric Environment 163*, 128–137. https://doi.org/10.1016/j.atmosenv.2017.05.024

269. Carter, W. P. L. (2009). *Investigation of Atmospheric Ozone Impacts of Trans 2,3,3,3-Tetrafluoropropene, Final Report for Contract UCR-09010016*. Center for Environmental Research and Technology, College of Engineering, University of California, Riverside, California.

270. Lefrancois, F., Jesswein, M., Thoma, M., Engel, A., Stanley, K., & Schuck, T. (2021). An indirect-calibration method for non-target quantification of trace gases applied to a time series of fourth-generation synthetic halocarbons at the Taunus Observatory (Germany). *Atmospheric Measurement Techniques, 14*(6), 4669-4687. https://doi.org/10.5194/amt-14-4669-2021

271. Vollmer, M. K., Reimann, S., Hill, M., & Brunner, D. (2015). First observations of the fourth generation synthetic halocarbons HFC-1234yf, HFC-1234ze(E), and HCFC-1233zd(E) in the atmosphere. *Environmental Science & Technology, 49*(5), 2703-2708. https://doi.org/10.1021/es505123x

272. Vollmer, M. K., Reimann, S., Hill, M., & Brunner, D. (2020). Update to Vollmer, M. K., S. Reimann, M. Hill, D. Brunner, First observations of the fourth generation synthetic halocarbons HFC-1234yf, HFC-1234ze(E), and HCFC-1233zd(E) in the atmosphere, *Environ. Sci. Technol., 49*, 2703-2708, https://doi.org/doi/10.1021/es505123x, 2015. https://www.empa.ch/documents/56101/190047/HFO+update+Report/fe3b26b5-fcb6-4cd9-a6f6-5c39ac01f20a. Accessed 2/7/2022.

273. Wang, Y., Wang, Z., Sun, M., Guo, J., & Zhang, J. (2021). Emissions, degradation and impact of HFO-1234ze from China PU foam industry. *Science of the Total Environment, 780*, 146631. https://doi.org/10.1016/j.scitotenv.2021.146631

274. Campbell, J. S., Hansen, C. S., & Kable, S. (2020). New HFO refrigerants transform in the atmosphere to ultimately produce problematic old HFCs. Paper presented at the American Geophysical Union Fall Metting 2020,

275. Sulbæk Andersen, M. P., & Nielsen, O. J. (2022). Tropospheric photolysis of CF_3CHO. *Atmospheric Environment, 272*, 118935. https://doi.org/10.1016/j.atmosenv.2021.118935

276. Franco, B., Blumenstock, T., Cho, C., Clarisse, L., Clerbaux, C., Coheur, P. F., De Mazière, M., De Smedt, I., Dorn, H. P., Emmerichs, T., Fuchs, H., Gkatzelis, G., Griffith, D. W. T., Gromov, S., Hannigan, J. W., Hase, F., Hohaus, T., Jones, N., Kerkweg, A., Kiendler-Scharr, A., et al. (2021). Ubiquitous atmospheric production of organic acids mediated by cloud droplets. *Nature, 593*(7858), 233-237. https://doi.org/10.1038/s41586-021-03462-x

277. Rayne, S., & Forest, K. (2016). Aqueous phase hydration and hydrate acidity of perfluoroalkyl and n:2 fluorotelomer aldehydes. *Journal of Environmental Science and Health, Part A, 51*(7), 579-582. https://doi.org/10.1080/10934529.2016.1141625

278. Liu, L., Yu, F., Tu, K., Yang, Z., & Zhang, X. (2021). Influence of atmospheric conditions on the role of trifluoroacetic acid in atmospheric sulfuric acid–dimethylamine nucleation. *Atmospheric Chemistry and Physics, 21*(8), 6221-6230. https://doi.org/10.5194/acp-21-6221-2021

279. Lu, Y., Liu, L., Ning, A., Yang, G., Liu, Y., Kurtén, T., Vehkamäki, H., Zhang, X., & Wang, L. (2020). Atmospheric sulfuric acid-dimethylamine nucleation enhanced by trifluoroacetic acid. *Geophysical Research Letters, 47*(2), e2019GL085627. https://doi.org/10.1029/2019GL085627

280. Dong, Z.-G., Xu, F., Mitchell, E., & Long, B. (2021). Trifluoroacetaldehyde aminolysis catalyzed by a single water molecule: An important sink pathway for trifluoroacetaldehyde and a potential pathway for secondary organic aerosol growth. *Atmospheric Environment, 249*, 118242. https://doi.org/10.1016/j.atmosenv.2021.118242

281. Taatjes, C. A., Khan, M. A. H., Eskola, A. J., Percival, C. J., Osborn, D. L., Wallington, T. J., & Shallcross, D. E. (2019). Reaction of perfluorooctanoic acid with Criegee intermediates and implications for the atmospheric fate of perfluorocarboxylic acids. *Environmental Science & Technology, 53*(3), 1245-1251. https://doi.org/10.1021/acs.est.8b05073

282. NAIADES (2022). Données sur la qualité des eaux de surface. http://www.naiades.eaufrance.fr/acces-donnees#/physicochimie. Accessed April 2022.

283. UN (2022). Sustainable Development Goals (SDGs). https://www.un.org/sustainabledevelopment/sustainable-development-goals/. Accessed September 2022

APPENDIX

Changes in tropospheric air quality related to the protection of stratospheric ozone in a changing climate

S. Madronich, B. Sulzberger, J. D. Longstreth, T. Schikowski, M. P. Sulbæk Andersen, K. R. Solomon, and S. R. Wilson

SI 1 Physical, chemical, and biological properties of the linear perfluorinated carboxylic acids

SI Table 1. Physical, chemical, and biological properties of the linear perfluorinated carboxylic acids from 2-8 carbons. BP, boiling point; NOEL, no observed effect level; NOEC, no observed effect concentration.

Property	Trifluoro-acetic acid	Perfluoro-propanonic acid	Perfluoro-butanoic acid	Perfluoro-pentanoic acid	Perfluoro-hexanoic acid	Perfluoro-heptanoic acid	Perfluoro-octanoic acid
Abbreviation	TFA	PFPrA	PFBA	PFPeA	PFHxA	PFHpA	PFOA
CAS#	76-05-1	422-64-0	375-22-4	2706-90-3	307-24-4	375-85-9	335-67-1
Molecular formula	CF_3COOH	$CF_3CF_2CO\,OH$	$CF_3(CF_2)_2CO\,OH$	$CF_3(CF_2)_3COOH$	$CF_3(CF_2)_4COOH$	$CF_3(CF_2)_5COOH$	$CF_3(CF_2)_6COOH$
# of C atoms	2	3	4	5	6	7	8
Molecular weight	114.02	164.03	214.04	264.05	314.05	414.0	464.08
BP (°C)	73	96.5	121.0	140 a	157	188-192	189 f
Solubility (H_2O mg L^{-1})	Miscible	Miscible	Miscible	122,600	21,700	3400-9500	9500
Vapour pressure (Pa)	11	3.93*	1307 [a]	1057	263	1.77 [a]	1.72 [a]
Log K_{OW}	0.5	1.5 [a]	2.43 [a]	3.262 [a]	3.48	5.024 [a]	5.905 [a]
Henry's Law Constant (atm m^{-3} mol^{-1})	$1.11 \times 10{-7}$	$4.43 \times 10{-6}$ [a]	0.0051 [a]	0.029 [a]	0.174 [a]	1.521 [a]	3.044 [a]
pKa	0.3	0.38 [a]	-0.2-0.7	-0.06	-0.13	-0.15	-0.16-3.8
K_{OC} (L kg^{-1})	0.17-20	12.7 [a]	58 [a]	270 [a]	1247 [a]	5761	30,440
Acute oral toxicity in rat (mg kg^{-1})	> 500	> 750	NA	NA	1750-5000[a]	NA	NA
NOEL (rat mg kg^{-1})	114 [b]	NA	3.01	NA	15-30 [b]	NA	NA

Property	Trifluoro-acetic acid	Perfluoro-propanonic acid	Perfluoro-butanoic acid	Perfluoro-pentanoic acid	Perfluoro-hexanoic acid	Perfluoro-heptanoic acid	Perfluoro-octanoic acid
NOEL Repro. (rat, mg kg^{-1})	NA	NA	50	NA	35 [j]	100 [c]	0.1 [c]
NOEC most sensitive aquatic plant (ng L^{-1})	2.5×10^{6} [d]	1.44×10^{7} [e]	6.21×10^{8} [e]	$> 1.00 \times 10^{9}$ [e]	NA	$> 1.02 \times 10^{9}$ [e]	5.80×10^{3} [e]
NOEC most sensitive aquatic animal (ng L^{-1})	LC50 = 7×10^{7} [e]	LC50 = 8.0×10^{7} [f]	LC50 = 1.1×10^{8} [f]	LC50 = 1.3×10^{8} [f]	LC50 = 1.4×10^{8} [f]	LC50 > 1.02×10^{6} [f]	LC50 = 1.5×10^{8}
Half-life in rats [g]	34–48 h [i]	NA	1-9 h	NA	2-5 h	1.4-2.4 h	44-322 h
Half-life in humans [g]	16 h	NA	72-81 h	NA	14-49 d [j]	1.2-1.5 y	2.1-10 y

Unless otherwise stated, references are from (PubChem, 2022). Other sources are: [a] (RSC, 2022) [b] (NICNAS, 2016) [c] (EFSA, 2020) [d] (Chabot, 2017) [e] (Boudreau, 2002) [f] (Wang et al., 2014) [g] (ATSDR, 2021) [h] (Boutonnet et al., 1999).

SI 2. Pesticide usage in the USA

SI Table 2. Annual usage of pesticides containing one or more trifluoromethyl moieties in the USA from 1992 to 2018.

SI Table 2. Annual usage of pesticides containing one or more trifluoromethyl moieties in the USA from 1992 to 2018.

Name	MW	Formula	#C-CF3	Molar Yield TFA	Molar Yield TFA-Na salt	Multiplier in lb	1992	1993	1994	1995	1996	1997	1998	1999	2000	2001	2002	2003	2004	2005	2006	2007	2008	2009	2010	2011	2012	2013	2014	2015	2016	2017	2018	TFA tonnes	TFA-Na tonnes
aciflufen	361.657	C$_{14}$H$_7$ClF$_3$NO$_5$	1	0.315	0.376	1000000	1.5	1.4	2.1	1.6	2.2	1.7	1	0.7	0.7	0.7	0.5	0.4	0.4	0.4	0.3	0.2	0.2	0.4	0.3	0.3	0.3	0.8	1.2	1	1.1	1	1.3	3332	3975
bicyclopyrone	399.366	C$_{19}$H$_{20}$F$_3$NO$_5$	1	0.286	0.341	1000000																								0	0.2	0.3	0.4	117	139
bifenthrin	422.872	C$_{23}$H$_{22}$ClF$_3$O$_2$	1	0.270	0.322	1000000	0.2	0.2	0.2	0.2	0.2	0.2	0.2	0.2	0.2	0.4	0.4	0.4	0.4	0.3	0.2	0.4	0.5	0.8	0.8	0.8	1.6	1.6	1.5	1.3	1.4	1.7	1.8	2116	2524
chlorfenapyr	407.615	C$_{15}$H$_{11}$BrClF$_3$N$_2$O	1	0.280	0.334	1000000						0.1	1.4	0.1	0.9	0	0																	315	376
cyflumetofen	447.454	C$_{24}$H$_{24}$F$_3$NO$_4$	1	0.255	0.304	1000																							1	40	70	65	66	28	33
cyhalothrin-gamma	449.854	C$_{23}$H$_{19}$ClF$_3$NO$_3$	1	0.253	0.302	1000000													0	0	0	0	0	0	0	0.1	0.1	0.1	0	0.1	0.1			73	88
cyhalothrin-lambda	449.854	C$_{23}$H$_{19}$ClF$_3$NO$_3$	1	0.253	0.302	1000000	0.2	0.2	0.1	0.3	0.3	0.3	0.4	0.3	0.3	0.3	0.4	0.3	0.3	0.4	0.4	0.4	0.6	0.6	0.6	0.6	0.6	0.8	0.8	0.8	0.8	0.8	0.9	1431	1707
dithiopyr	401.41	C$_{15}$H$_{16}$F$_6$N$_2$O$_2$S$_2$	1	0.284	0.339	1000																	0.1	0.1	0.3	0.2	0.3	0.5	0.8	1.1	1.8	2.2	1.7	1	1
ethalfluralin	333.267	C$_{13}$H$_{14}$F$_3$N$_3$O$_4$	1	0.342	0.408	1000000	4.8	4	4.6	5.1	4.2	3.2	4.6	4.5	3	2.8	2.2	2.7	2.7	2	1.8	1.5	1.5	1.7	1.6	1.2	1.5	1.4	1.6	1.7	1.4	4	2.4	11437	13643
fipronil	437.141	C$_{12}$H$_4$Cl$_2$F$_6$N$_4$OS	2	0.522	0.622	1000000							0.2	0.2	0.3	0.4	0.4	0.2	0.3	0.4	0.1	0.2	0.1	0.2	0.2	0.1	0	0	0	0	0	0	0	809	965
flonicamid	229.162	C$_9$H$_6$F$_3$N$_3$O	1	0.498	0.594	1000000																		0	0	0	0.1	0.1	0.1	0.1	0.1	0.1	0.1	168	201
fluazifop	327.259	C$_{15}$H$_{12}$F$_3$NO$_4$	1	0.348	0.416	1000000	0.8	0.9	0.9	1.1	1	0.1	0.8	0.6	0.6	0.5	0.3	0.4	0.3	0.2	0.3	0.3	0.2	0.4	0.3	0.1	0.2	0.2	0.2	0.4	0.4	0.2	0.4	1887	2251
fluazinam	465.089	C$_{13}$H$_4$Cl$_2$F$_6$N$_4$O$_4$	2	0.490	0.585	1000000										0	0	0	0.1	0.2	0.1	0.1	0	0.1	0.1	0.1	0.1	0.1	0.1	0.2	0.1	0.2	0.2	407	485
flubendiamide	682.392	C$_{23}$H$_{22}$F$_7$IN$_2$O$_4$S	2	0.334	0.399	1000000																		0.1	0	0.1	0.3	0.3	0.2	0.3	0.2	0.1	0	233	278
flucarbazone	396.297	C$_{12}$H$_{11}$F$_3$N$_4$O$_6$S	1	0.288	0.343	1000										10	18	19	42	35	60	30	62	33	35	55	82	54	58	55	41	32	80	105	125
flufenacet	363.331	C$_{14}$H$_{13}$F$_4$N$_3$O$_2$S	1	0.314	0.374	1000000							0.9	1.2	1.5	1.4	1.3	1.4	1.5	1.3	0.9	1.3	0.9	1.4	0.7	0.4	0.8	0.3	0.1	0.9	0.1	0	0.6	2623	3129
flumetralin	421.733	C$_{16}$H$_{12}$ClF$_3$N$_3$O$_4$	1	0.270	0.323	1000000					0.1	0.1	0.1	0.2	0.1	0.1	0.1	0.1	0.1	0.1	0.1	0.1	0.1	0.1	0.1	0.1	0.1	0.1	0.2	0.1	0.1	0.1	0.1	306	365
fluometuron	232.206	C$_{10}$H$_{11}$F$_3$N$_2$O	1	0.491	0.586	1000000	4.7	4.9	6	7.2	5.8	4.9	4.9	3.2	1	0.6	1.1	0.7	0.8	0.6	0.6	0.7	0.5	0.5	0.8	1.1	0.8	0.6	0.7	0.8	1	1	1.2	12618	15051
fluopicolide	383.576	C$_{14}$H$_8$Cl$_2$F$_3$N$_2$O	1	0.297	0.355	1000																	3	7	8	17	26	31	29	31	19	22	32	30	36
fluopyram	396.717	C$_{16}$H$_{11}$ClF$_6$N$_2$O	2	0.575	0.686	1000000																					0	0.1	0.1	0.2	0.2	0.3	0.3	292	348
fluridone	329.322	C$_{19}$H$_{14}$F$_3$NO	1	0.346	0.413	1000			42																					29	56	24	24	27	33
flutolanil	323.315	C$_{17}$H$_{16}$F$_3$NO$_2$	1	0.353	0.421	1000000				0.1	0.2	0.1	0.1	0.1	0.1	0.1	0.2	0.2	0.2	0.2	0.1	0.2	0.1	0.3	0.4	0.5	0.6	0.4	0.6	0.9	0.7	0.9	0.7	1229	1465
fluvalinate	502.918	C$_{26}$H$_{22}$ClF$_3$N$_2$O$_3$	1	0.227	0.270	1000		5.7	1.8	2.5	6.5	2.6	1.7	1.5	1.5	1.4	1.4	1.2	0.8	0.7	0.6	0.6	0.5	0.6	0.6	0.5	0.5	0.7	0.8	0.8	0.9	0.8	0.7	4	5
fomesafen	438.758	C$_{15}$H$_{10}$ClF$_3$N$_2$O$_6$S	1	0.260	0.310	1000000			0.4	0.5	0.6	0.7	1.3	1.2	1.3	1.2	1.4	0.8	0.7	0.7	0.8	0.7	0.7	0.7	1.6	2	2.6	3	3.6	5.1	6.7	7	6.3	6519	7776
isoxaflutole	359.319	C$_{15}$H$_{12}$F$_3$NO$_4$S	1	0.317	0.379	1000000									0.3	0.3	0.4	0.5	0.5	0.5	0.5	0.4	0.3	0.4	0.4	0.6	0.7	0.7	0.8	0.7	0.7	0.7	0.7	1495	1784
lactofen	461.774	C$_{19}$H$_{15}$ClF$_3$NO$_7$	1	0.247	0.295	1000000			0.3	0.2	0.3	0.4	0.4	0.4	0.2	0.2	0.2	0.2	0.1	0.1	0.1	0.1	0.1	0.3	0.3	0.3	0.5	0.8	0.8	0.9	0.8	0.5	1.2	1120	1336
mesotrione (tembotri...	440.814	C$_{17}$H$_{16}$ClF$_3$O$_6$S	1	0.259	0.309	1000000										0	0.5	0.8	1.5	1.8	2	2.1	1.9	1.8	2	2.1	2.5	2.6	2.5	2.9	3.4	4.1	4.4	4565	5446
novaluron	492.706	C$_{17}$H$_9$ClF$_8$N$_2$O$_4$	1	0.231	0.276	1000000														0	0.1	0	0.1	0.1	0.1	0.1	0.1	0.1	0.1	0.1	0.9	0.1	0.1	221	263
oxyfluorfen	361.701	C$_{15}$H$_{11}$ClF$_3$NO$_4$	1	0.315	0.376	1000000	0.4	0.5	0.5	0.7	1.2	0.7	0.8	1	0.7	0.7	0.6	0.7	0.7	0.7	0.8	0.7	0.7	0.7	0.6	0.9	0.9	1.1	0.9	0.9	1	1.2	1.6	3117	3718
prosulfuron	419.379	C$_{15}$H$_{16}$F$_3$N$_5$O$_4$S	1	0.272	0.324	1000000								0	0.1	0.1	0.1	0.1	0.1	0.1	0.1	0.1	0.1	0.1	0	0.1	0	0	0	0	0.1	0	0	151	181
saflufenacil	500.85	C$_{17}$H$_{17}$ClF$_4$N$_4$O$_5$S	1	0.228	0.272	1000000																				0.2	0.3	0.4	0.5	0.6	0.8	0.7	0.8	525	626
tefluthrin	418.736	C$_{17}$H$_{14}$ClF$_7$O$_2$	1	0.272	0.325	1000000	0.4	0.4	0.5	0.5	0.9	0.8	0.8	0.6	0.7	0.6	0.8	1	0.8	0.8	0.8	0.7	0.6	0.4	0.3	0.3	0.5	0.6	0.5	0.4	0.4	0.3	0.2	1893	2259
thiazopyr	396.376	C$_{16}$H$_{17}$F$_5$N$_2$O$_2$S	1	0.288	0.343	1000							2	0	1.8	3.2	2.6	6.7	2.6	1.8	6.3	14	2.6	3.6	0	0	3	3.5	3					7	9
trifloxystrobin	408.377	C$_{20}$H$_{19}$F$_3$N$_2$O$_4$	1	0.279	0.333	1000000									0.1	0.1	0.1	0.2	0.2	0.3	0.3	0.4	0.5	0.8	0.6	0.7	1	1.1	1.8	1	0.8	1.2	0.9	1492	1780
trifluralin	335.283	C$_{13}$H$_{16}$F$_3$N$_3$O$_4$	1	0.340	0.406	1000000	27	28	31	29	28	27	23	21	14	13	13	12	11	11	11	11	7.5	8	8.5	10	8	12	11	8	10	8		65327	77926
triflusulfuron	478.403	C$_{16}$H$_{17}$F$_3$N$_6$O$_6$S	1	0.238	0.284	1000					15	22	22	19	17	20	23	17	19	23	18	30	10	2	3	3.5	1	1	1	2	2.5	2.5	1	30	35

US use data from https://water.usgs.gov/nawqa/pnsp/usage/maps/compound_listing.php
Upper estimate of use.

SI 3 Estimated photochemical ozone creation potentials (POCP s) for ODSs, replacement compounds and related VOCs

The POCP estimation method employed here (Jenkin, 2017) is based on structure and reactivity for the species and different parameters for each geographical region (Northwest European or urban USA), and follows the equation $POCP\epsilon = (A \times \acute{Y}_S \times R \times S \times F) + P + R_{O3}) - Q$, where A is a simple multiplier, $\acute{Y}_S$ describes the structure of the VOC, R is a OH reactivity element, S is a parameter related to the size of the VOC, and F is parameter that can account for the impact of unreactive carbonyl degradation products (set to 1 for all chemicals in SI Table 3). P applies only for chemicals that undergo photolysis at tropospheric conditions (set to 0 for all chemicals in Table 6) and R_{o3} accounts for the formation of free radicals through the direct reaction of O_3 with the VOC. The latter is only included for the aliphatic alkenes in SI Table 3, as a) of the compounds in SI Table 3, only these compounds have significant reactivities towards O_3, b) the main OH formation mechanism requires at least one H atom attached to the carbon adjacent to the double bond – none of the HFO/HCFOs have this (Cox et al., 2020), and c) any additional OH formation routes (e.g., from excited CH_2OO radicals) are likely to be unimportant. Finally, Q applies only for a specific set of aromatic VOCs.

It is germane to note that the POCP estimation method was developed and tested for application on hydrocarbons, aliphatic olefins, and oxygenated VOCs. It was not developed explicitly cover halogenated compounds. Note also that the most recent POCP estimation equation published by Jenkin and co-workers (Jenkin, 2017) "*for alkenes and unsaturated oxygenates that react significantly with O_3*", contains an error in Eq. (9), which should correctly read "$R_{O3} = E \times m$" (Jenkin, 2022). The values below are POCPs estimated for both North-West European and USA urban conditions, using updated OH radical kinetics.

SI Table 3. Atmospheric lifetimes, OH radical rate coefficients, estimated photochemical ozone creation potentials (POCPε) for olefins and related chemicals, calculated for North-West European conditions and USA urban conditions. Unless otherwise noted, estimated total atmospheric lifetimes are those quoted in IPCC AR6 (Smith, 2021) and OH rate coefficients are from Burkholder et al. (Burkholder et al., 2020). POCP calculated using the (updated) approach by Jenkin et al. (Jenkin, 2022; Jenkin, 2017). See main text for details.

Chemical	Industrial Designation	Total Atmospheric Lifetime	OH radical rate-coefficient, (k_{OH}, cm^3 molecule^{-1}s^{-1}, 298 K, 1 atm)	POCPε, North-west European conditions (relative units)	POCPε, USA urban conditions (relative units)
Alkanes					
CH_4	*Methane*	11.8 years	6.3×10^{-15}	0.6	0.2
CH_3CH_3	*Ethane*	58 days	2.4×10^{-13}	10.9	4.5
Alkenes					
$CH_2{=}CH_2$	*Ethene*	1.5 days [a]	7.9×10^{-15}	100.4	98.6
$CH_3CH{=}CH_2$	*Propene*	0.4 days [a]	2.5×10^{-13}	110.6	134.5
$CH_3CH_2CH{=}CH_2$	*But-1-ene*	0.4 days [a]	3.2×10^{-15}	107.1	127.3
ODSs					
CH_3CCl_3	*Methyl chloroform*	5 years	1.0×10^{-14}	0.11	0.04
$CHCl_2F$	*HCFC-21*	1.7 years	2.9×10^{-14}	0.38	0.16
$CHClF_2$	*HCFC-22*	11.9 years	4.0×10^{-15}	0.08	0.03
HFCs					
CHF_3	*HFC-23*	228 years	3.0×10^{-16}	0.01	<0.01

Chemical	Industrial Designation	Total Atmospheric Lifetime	OH radical rate-coefficient, (k_{OH}, cm^3 molecule^{-1} s^{-1}, 298 K, 1 atm)	POCPε, North-west European conditions (relative units)	POCPε, USA urban conditions (relative units)
HFCs					
CH_2F_2	*HFC-32*	5.4 years	1.0×10-14	0.30	0.12
CF_3CHF_2	*HFC-125*	30 years	1.0×10-15	0.02	0.01
CF_3CH_3	*HFC-143a*	3.6 years	1.0×10-15	0.02	0.01
CF_3CH_2F	*HFC-134a*	14 years	4.0×10-15	0.06	0.02
CHF_2CH_3	*HFC-152a*	1.6 years	3.0×10-14	0.70	0.27
CF_3CHFCF_3	*HFC-227ea*	36 years	1.0×10-15	0.01	<0.01
CF_3CH_2FCHF	*HFC-245eb*	3.2 years	1.0×10-14	0.18	0.07
CHF_2CHFCF_3	*HFC-236ea*	11.4 years	5.2×10-15	0.05	0.02
HFOs/HCFOs					
$CF_2{=}CH_2$	*HFO-1132a*	4.7 days	2.8×10^{-12}	19.8	15.6
$CHF{=}CF_2$	*HFO-1123*	1.5 days	8.1×10^{-12}	15.1	17.5
$CH_2{=}CHF$	*HFO-1141*	2.6 days	5.0×10^{-12}	38.0	33.6
$CF_2{=}CF_2$	*HFO-1114*	1.1 days	1.0×10^{-11}	8.69	11.3
$CF_3CH{=}CH_2$	*HFO-1243zf*	9.1 days	1.5×10^{-12}	11.2	6.56
$CF_3CF{=}CH_2$	*HFO-1234yf*	12 days	1.1×10^{-12}	7.32	4.23
$CF_3CF{=}CF_2$	*HFO-1216*	5.5 days	2.2×10^{-12}	4.65	4.16
Z-$CF_3CF{=}CHF$	*HFO-1225ye(Z)*	9.9 days	1.3×10^{-12}	5.91	3.92
E-$CF_3CF{=}CHF$	*HFO-1225ye(E)*	5.8 days	2.3×10^{-12}	7.25	5.81
E-$CF_3CH{=}CHF$	*HFO-1234ze(E)*	19 days	7.0×10^{-13}	5.60	2.88
Z-$CF_3CH{=}CHF$	*HFO-1234ze(Z)*	9.9 days	1.4×10^{-12} [c]	1.51	0.61
$CF_3CF_2CH{=}CH_2$	*HFO-1345zfc*	9 days	1.4×10^{-12}	6.96	3.96
E-$CF_3CH{=}CHCF_3$	*HFO-1336mzz(E)*	122 days	1.3×10^{-13}	*0.98*	*0.39*

Chemical	Industrial Designation	Total Atmospheric Lifetime	OH radical rate-coefficient, (k_{OH}, cm^3 molecule^{-1} s^{-1}, 298 K, 1 atm)	POCPε, North-west European conditions (relative units)	POCPε, USA urban conditions (relative units)
HFOs/HCFOs					
Z-CF$_3$CH=CHCF$_3$	*HFO-1336mzz(Z)*	27 days	4.8 × 10^{-13}	2.90	1.35
E-CF$_3$CF=CFCF$_3$	*Octafluoro-2-butene*	31 days	5.8 × 10^{-13}	2.07	1.19
(CF$_3$)$_2$C=CH$_2$	*3,3,3-Trifluoro-2-(trifluoromethyl)-prop-1-ene*	10 days	7.8 × 10$^{-13\,d}$	4.02	2.08
E-(CF$_3$)$_2$CFCH=CHF	*HFO-1438ezy(E)*	43 days [b]	3.2 × 10^{-13}	1.55	0.65
E-CF$_3$CH=CHCl	*HCFO-1233zd(E)*	42 days	3.5 × 10^{-13}	0.55	0.21
Z-CF$_3$CH=CHCl	*HCFO-1233zd(Z)*	13 days	9.4 × 10^{-13}	1.64	0.67
cyc(-CH=CFCF$_2$CF$_2$-)	*1,3,3,4,4-Pentafluoro-cyclobutene*	270 days	6.2 × 10^{-14}	2.97	1.34
cyc(-CH=CHCF$_2$CF$_2$-)	*3,3,4,4-Tetrafluoro-cyclobutene*	84 days	1.7 × 10$^{-13\,d}$	5.86	3.24

[a] Estimated total lifetime as quoted in Calvert et al. (Calvert et al., 2000).

[b] IPCC AR6 (Smith, 2021) erroneously gives an atmospheric lifetime of 122 days for this species. The atmospheric lifetime of 43 days quoted here is calculated as the tropospheric partial lifetime only due reaction with the OH radical. The value is a scaling to the lifetime for CH$_3$CCl$_3$ (6.1 years) using k(OH+CH$_3$CCl$_3$, 272 K) = 6.14 × 10^{-15} cm^3 molecule^{-1} s^{-1} (Burkholder et al., 2020), and the OH rate-coefficient listed in SI Table 3 for E-(CF$_3$)$_2$CFCH=CHF which is essentially temperature independent from 214-296 K (Papadimitriou & Burkholder, 2016).

[c] JPL Evaluation Number 19 (Burkholder et al., 2020) lists this as 1.35 × 10^{-13} but it should be 1.37 × 10^{-12} cm^3 molecule^{-1} s^{-1} (Zhang et al., 2015).

[d] OH rate coefficient from Papadimitriou et al. (Papadimitriou et al., 2015).

SI 4 Estimated molar yields (%) of TFA from ODS replacements

Emissions and TFA yields in Figure 12 of the main text were estimated as outlined below.

SI 4.1.1 HCFC-123 (CF$_3$CHCl$_2$), 60 ± 10 %

CF$_3$CHCl$_2$ has a global annually averaged lifetime of 1.3 years (Smith, 2021). The main atmospheric fate of CF$_3$CHCl$_2$ is reaction with OH radicals in the troposphere. Atmospheric degradation leads to CF$_3$CCl$_2$O alkoxy radicals. Reaction of CF$_3$CCl$_2$O with O$_2$ is of minor importance and CF$_3$CCl$_2$O is converted to CF$_3$CClO through Cl elimination (Edney et al., 1991; Hayman et al., 1994; Tuazon & Atkinson, 1993). The estimated tropospheric photolytic lifetime for CF$_3$CClO for an overhead sun is 23 days (Calvert et al., 2008). The atmospheric lifetime of CF$_3$CClO with respect to uptake and hydrolysis in cloud water is 5-30 days (Wallington et al., 1994). On average about 60% of CF$_3$CClO is converted into TFA (Hayman et al., 1994) (see Figure 10 in the main text). The uncertainty in this yield is of the order of ± 5%. The yield of TFA in the atmospheric degradation of CF$_3$CHCl$_2$ is expected to be 60 ± 10 %.

CF$_3$CHCl$_2$ has been used as a refrigerant and a fire suppressant. Global annual emissions have been provided in a bottom-up estimate by Wuebbles & Patten (Wuebbles & Patten, 2009) as 0.130-0.135 Gg yr^{-1} for 2009.

SI 4.1.2 HCFC-124 (CF$_3$CHFCl), ~100%

CF$_3$CHFCl has a global annually averaged lifetime of 5.9 years (Smith, 2021). The main atmospheric fate of CF$_3$CHFCl is reaction with OH radicals in the troposphere. Atmospheric degradation of CF$_3$CHFCl leads to CF$_3$CFClO alkoxy radicals. The dominant, if not sole,

fate of CF_3CFClO is decomposition to give CF_3CFO and Cl (Bhatnagar & Carr, 1995; Tuazon & Atkinson, 1993). The atmospheric fate of CF_3CFO is incorporation into water droplets followed by hydrolysis to give TFA, occurring on a time scale of 5-15 days (Wallington et al., 1994). The yield of TFA in the atmospheric degradation of CF_3CHFCl is expected to be very close to 100%.

CF_3CHFCl has been used as a refrigerant and fire suppressant. Global annual emissions have been estimated by Simmonds et al. (Simmonds et al., 2017) as 3.3±0.89 Gg yr^{-1} for 2015.

SI 4.1.3 HCFC-133a (CF_3CH_2Cl), 22 – 55 %

CF_3CH_2Cl has a global annually averaged lifetime of 4.6 years (Smith, 2021). The main atmospheric fate of CF_3CH_2Cl is reaction with OH radicals in the troposphere. The degradation initiated by OH radicals leads to the formation CF_3CHClO alkoxy radicals. The atmospheric fate of CF_3CHClO is decomposition and reaction with O_2 (Møgelberg, Nielsen, et al., 1995). Reaction with O_2 gives CF_3CClO and HO_2 while decomposition can proceed through three channels:

$$CF_3CHClO + M \rightarrow CF_3 + HCOCl + M \qquad (1)$$
$$CF_3CHClO + M \rightarrow CF_3CO + HCl + M \qquad (2)$$
$$CF_3CHClO + M \rightarrow CF_3CHO + Cl + M \qquad (3)$$
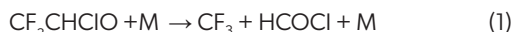
At ground level and at room temperature, decomposition and reaction with O_2 are of equal importance, i.e., the yield of CF_3CClO is 52% (Møgelberg, Nielsen, et al., 1995).

At higher altitudes, the importance of reaction with O_2 will increase. If CH_3CHClO is formed through reaction of CF_3CHClO_2 radicals with NO this can result in chemical activation of the resulting CF_3CHClO radicals, and in turn lead to enhanced decomposition.

The O_2 reaction channel product, CF_3CClO, undergoes photolysis in competition with incorporation into water droplets. The estimated tropospheric photolytic lifetime for CF_3CClO for an overhead sun is 23 days (Calvert et al., 2008). The atmospheric lifetime of CF_3CClO with respect to uptake and hydrolysis in cloud water is 5-30 days (Wallington et al., 1994). It has been estimated that, on average, 60% of CF_3CClO is converted into TFA (Hayman et al., 1994). Further reactions of CF_3CHClO decomposition products from reaction 2 and 3, CF_3CHO and CF_3CO, have the potential to yield TFA. Current understanding of the atmospheric fate of CF_3CHO suggests that its atmospheric fate is dominated by destruction by photolysis resulting in an atmospheric lifetime of the order of two days (Chiappero et al., 2006) (see also Sections 3.2 and 3.7.2 in the main text). Photolysis of CF_3CHO leads to CF_3 and CHO radicals which cannot contribute to the formation of TFA (Sulbæk Andersen & Nielsen, 2022). The rate of reaction of CF_3CHO with OH radicals is slow (atmospheric lifetime of approximately 20 days), and thus of less importance in the fate of CF_3CHO. Any oxidation of CF_3CHO initiated by OH radicals will produce CF_3CO radicals, which undergo reaction with O_2 to yield acyl peroxy radicals, $CF_3C(O)O_2$. These acyl peroxy radicals can react with HO_2, NO, or NO_2. Reaction of $CF_3C(O)O_2$ with HO_2 radicals can lead to the formation of TFA (39% yield) (Hurley et al., 2006). Finally, on contact with liquid water, CF_3CHO can produce aldehyde hydrates (gem-diols). These can, at least in the gas-phase, react with OH radicals (lifetime of approximately 90 days) and present an efficient way of generating TFA (Sulbæk Andersen et al., 2006). The latter two processes are likely minor fates for CF_3CHO. The importance of formation of TFA from the reaction of OH with CF_3CHO was indirectly accessed by Sulbæk Andersen et al. (Sulbæk Andersen, Schmidt, et al., 2018) in a global modeling study of HCFO-1233(zd). This model, which did not include potential CF_3CHO-hydrate formation, suggested a 2% yield of TFA from CF_3CHO. The contribution to TFA from CF_3CHO hydrate formation and processing remains highly uncertain (Franco et al., 2021; Sulbæk Andersen et al., 2006). Assuming that uptake into cloud water and hydration is efficient, effectively converting CF_3CHO into TFA on a timescale of 5 days (only limited by transport limitations, i.e., the lower limit for the time taken for transport into clouds (Wallington et al., 1994)), then a maximum TFA yield of 27% can be expected from the hydrate formation. Thus, the TFA yield from processing of CF_3CHO is estimated at 2% with an upper theoretical limit of ~ 30%.

The acyl radical, CF_3CO, generated directly in reaction 2 can also lead to formation of TFA, though the reaction with O_2 and subsequent reaction of the acyl peroxy acyl radical with HO_2, as described above. Reaction with HO_2 radicals occurs in competition with reaction with NO which significantly reduces the maximum possible yield (39%) of TFA from the HO_2 reaction with $CF_3C(O)OO$ (Hurley et al., 2006). If the atmospheric lifetimes for CF_3CHO are 2 days and 20 days with respect to photolysis and reaction with OH radicals, respectively, then the model results of Sulbæk Andersen and co-workers (Sulbæk Andersen, Schmidt, et al., 2018) suggest, that the molar yield of TFA, starting with CF_3CO, can be on the order of ~20 ± 10 %.

Based on the discussion above regarding the fate of CF_3CClO, the yield of TFA from hydrolysis of CF_3CClO can be calculated as 0.52 × (60%) = 31%. An uncertainty of ± 10% is estimated for this yield. Additional contributions from the atmospheric processing of CF_3CHO or CF_3CO could be as much as 0.48 × (2-30%) = 1-14%. Hence, the best estimate of the yield of TFA in the atmospheric degradation of CF_3CH_2Cl is 32%, but with an upper limit of 55% and a lower limit of 22%. Without a detailed atmospheric chemistry and transport model study, a more quantitative assessment of the yield of TFA is not possible.

CF_3CH_2Cl has been used as a chemical feedstock/ intermediate. Global annual emissions have been estimated by Vollmer et al. (Vollmer, Rigby, et al., 2015) as ~1.5 Gg yr^{-1} for 2014.

SI 4.2.1 HFC-125 (CF_3CF_2H), ~1–10%

CF_3CF_2H has an atmospheric lifetime of approximately 30 years (Smith, 2021). The atmospheric fate of CF_3CF_2H is reaction with OH radicals. Reaction with OH produces an alkyl radical that reacts with oxygen to give the peroxy radical $CF_3CF_2O_2$. The peroxy radical

reacts with NO to yield the alkoxy radical CF_3CF_2O which decomposes to give COF_2 and CF_3 radicals. However, Ellis et al. (Ellis et al., 2004) suggested a mechanism by which $CF_3CF_2O_2$ radicals can react with α-hydrogen containing peroxy radicals (e.g., CH_3O_2) in the atmosphere to give CF_3CF_2OH in small amounts (1-10%) (Wallington et al., 2006)). CF_3CF_2OH will eliminate HF to give CF_3CFO. The sole atmospheric fate of CF_3CFO is incorporation into water droplets followed by hydrolysis, occurring on a time scale of 5-15 days to give TFA (Wallington et al., 1994). Thus, the yield of TFA from CF_3CF_2H is estimated as 1–10%.

CF_3CF_2H is used as a fire suppressant. Global annual emissions have been estimated as 59.7±9.5 Gg yr^{-1} in 2015 (Simmonds et al., 2017).

SI 4.2.2 HFC-134a (CF_3CH_2F), 7–20 %

CF_3CH_2F has an atmospheric lifetime of 14 years (Smith, 2021). Reaction of OH radicals with CF_3CH_2F yields CF_3CHFO_2 radicals, which react with either other peroxy radicals, RO_2, or NO. Reaction with RO_2 yields a stabilized CF_3CHFO radical, which can either decompose or react with O_2 to give CF_3CFO. The atmospheric fate of CF_3CFO is incorporation into water droplets occurring on a time scale of 5–15 days (Wallington et al., 1994) and subsequent hydrolysis yields TFA. Reaction of CF_3CFO_2 with NO can produce excited peroxy radicals, CF_3CFHO, which undergo rapid decomposition and limit the formation of CF_3CFO to a range of 7 to 20 %, depending on conditions (see Figure 10 in the main text) (Wallington et al., 1996). Thus, the TFA yield is estimated as 7–20%.

CF_3CH_2F is used as a refrigerant. Global annual emissions in 2015 were estimated at 209.0±42.9 Gg yr^{-1} (Simmonds et al., 2017) and estimated in the Science Assessment Panel 2022 report (WMO (2022) as 64-192 Gg yr^{-1} for 2020. The latter is currently the best estimate for this refrigerant (see also Table 3 in the main text).

SI 4.2.3 HFC-143a (CF_3CH_3), 2–30%

CH_3CF_3 has a global annually averaged lifetime of 51 years (Smith, 2021). The atmospheric fate of CH_3CF_3 is reaction with OH radicals. Reaction with OH produces an alkyl radical that reacts with O_2 and NO to yield the alkoxy radical, CF_3CH_2O. The dominant fate of CF_3CH_2O in the atmosphere is reaction with O_2 to give CF_3CHO and HO_2 (Nielsen et al., 1994). Current understanding of the atmospheric fate of CF_3CHO suggests that its atmospheric lifetime is dominated by photolysis. As discussed in SI Section 4.1.3, atmospheric processing of CF_3CHO can lead to formation of TFA in small amounts. Thus, the TFA yield from processing of CH_3CF_3 is estimated at 2%, with an upper limit of ~ 30%.

CH_3CF_3 is used as a refrigerant. Global annual emissions in 2015 have been estimated as 27.4±3.0 Gg yr^{-1} (Simmonds et al., 2017).

SI 4.2.4 HFC-227ea (CF_3CHFCF_3), ~100%

CF_3CHFCF_3 has an atmospheric lifetime of 36 years (Smith, 2021). The atmospheric fate of CF_3CHFCF_3 is reaction with OH radicals. Reaction with OH produces an alkyl radical that reacts with O_2 and NO to yield the alkoxy radical CF_3CFOCF_3. The atmospheric fate of CF_3CFOCF_3 is decomposition via C-C cleavage to give CF_3CFO and CF_3 radicals (Zellner et al., 1994). The atmospheric fate of CF_3CFO is incorporation into water droplets followed by hydrolysis to give TFA, occurring on a time scale of 5-15 days (Wallington et al., 1994). The yield of TFA in the atmospheric degradation of CF_3CHFCF_3 is 100%.

CF_3CHFCF_3 is used as a fire extinguishant. Global annual emissions have been estimated as 2.53±0.99 Gg yr^{-1} for 2010 (Vollmer et al., 2011).

SI 4.2.5 HFC-236fa ($CF_3CH_2CF_3$), 20 ± 10 %

$CF_3CH_2CF_3$ has an atmospheric lifetime of 213 years (Smith, 2021). Reaction of OH radicals with $CF_3CH_2CF_3$ generate CF_3CHCF_3 radicals which react with oxygen and NO to yield the alkoxy radicals, CF_3CHOCF_3. The sole fate of CF_3CHOCF_3 is reaction with O_2 to yield CF_3COCF_3 (Møgelberg, Platz, et al., 1995). The dominant fate of CF_3COCF_3 is likely tropospheric photolysis to give CF_3 and CF_3CO radicals. As discussed in SI Section 4.1.3, further reaction of CF_3CO radicals with O_2 and HO_2 radicals can lead to formation of TFA in small amounts. Thus, the yield of TFA in the atmospheric oxidation of $CF_3CH_2CF_3$ is estimated at 20% (± 10%).

$CF_3CH_2CF_3$ is used as a fire suppressant. Global annual emissions have been estimated as 0.16±0.11 Gg yr^{-1} for 2010 (Vollmer et al., 2011).

SI 4.2.6 HFC-245fa ($CHF_2CH_2CF_3$) 1 – 17%

$CHF_2CH_2CF_3$ has an atmospheric lifetime of 7.9 years (Smith, 2021). The atmospheric fate of $CHF_2CH_2CF_3$ is reaction with OH radicals. Structure activity relationships (SAR) suggests that approximately 56% of the reaction of OH radicals with $CHF_2CH_2CF_3$ proceeds through hydrogen abstraction from the terminal $-CHF_2$ group (Calvert et al., 2008). This will lead to the formation of COF_2 and CF_3CHO as major products (Chen et al., 1997). Hydrogen abstraction from the $-CH_2-$ group is expected to produce a ketone, $CHF_2C(O)CF_3$, through reaction of CHF_2CHOCF_3 with O_2. By analogy to CF_3COCH_3 (Wallington et al., 1994), the main sink for $CHF_2C(O)CF_3$ is expected to be photolysis, yielding COF_2 and CO_2. Thus, the expected yield of TFA in the atmospheric oxidation of $CF_3CH_2CF_2CH_3$ is 0.56 × (2 – 30%) = 1%, with 17% as an upper limit.

$CHF_2CH_2CF_3$ is used as a blowing agent. Global annual emissions have been estimated as 6.77±0.79 Gg yr^{-1} for 2010 (Vollmer et al., 2011).

SI 4.2.7 HFC-365mfc ($CF_3CH_2CF_2CH_3$), 2–30%

$CF_3CH_2CF_2CH_3$ has an atmospheric lifetime of 8.9 years (Smith, 2021). The atmospheric fate of $CF_3CH_2CF_2CH_3$ is reaction with OH radicals. The reaction of OH radicals with $CF_3CH_2CF_2CH_3$ proceeds mainly via attack on the –CH_3 group leading to formation of $CF_3CH_2CF_2CHO$, which in turn is oxidized to CF_3CHO and COF_2 (Inoue et al., 2008). Oxidation of $CF_3CH_2CF_2CHO$ will generate CF_3CHO and COF_2 as secondary products. The only study in the literature on the atmospheric oxidation mechanism of $CF_3CH_2CF_2CHO$ used Cl atoms as a surrogate for OH radicals. However, based on SAR, approximately 76% of the reaction of OH radicals, proceeds through abstraction at the -CH_3 site (Calvert et al., 2008). Reaction at the -CH_2- group would produce a ketone, $CF_3C(O)CF_2CH_3$. Further oxidation of $CF_3C(O)CF_2CH_3$ initiated by OH radicals will generate CF_3CO radicals (and COF_2, CO and CO_2). As discussed in SI Section 4.1.3 both CF_3CHO and CF_3CO radicals can lead to formation of TFA in small amounts. Thus, the expected yield of TFA in the atmospheric oxidation of $CF_3CH_2CF_2CH_3$ is 2%, with 30% as the upper limit. $CF_3CH_2CF_2CH_3$ is used as a blowing agent and refrigerant. Global annual emissions have been estimated as 2.87±0.60 Gg yr^{-1} for 2010 (Vollmer et al., 2011).

SI 4.2.8 HFC-43-10mee ($CF_3CF_2CFHCFHCF_3$), 54 – 60%

$CF_3CF_2CFHCFHCF_3$ has an atmospheric lifetime of 17 years (Smith, 2021). The atmospheric fate of $CF_3CF_2CFHCFHCF$ is reaction with OH radicals. There has been no mechanistic study conducted on the atmospheric degradation of $CF_3CF_2CFHCFHCF_3$. SAR suggests that approximately half of the reaction proceeds through hydrogen abstraction from the -CHF- group, alpha to the terminal CF_3 group. (Calvert et al., 2008). Reaction of OH radicals with $CF_3CF_2CFHCFHCF_3$ followed by reactions with O_2 and NO will therefore yield both $CF_3CF_2CFOCFHCF_3$ and $CF_3CF_2CFHCFOCF_3$ radicals. These will likely undergo decomposition to the give acyl fluorides, CF_3CF_2CFO and CF_3CFO, and radicals $CFHCF_3$ and CF_3CF_2CFH. The latter two will react with O_2 and RO_2/NO yielding CF_3CHFO and CF_3CF_2CHFO radicals. Reaction of CF_3CHFO and CF_3CF_2CHFO (Møgelberg et al., 1997) with NO can produce excited peroxy radicals which undergo rapid decomposition (see discussion in SI Section 4.2.2 and Figure 10 in the main text). The decomposition pathways will give CFHO, CF_3 and CF_3CF_2 radicals. Reaction with O_2 will lead to CF_3CFO, and CF_3CF_2CFO. The atmospheric fate of CF_3CFO, and likely also CF_3CF_2CFO, is incorporation into water droplets followed by hydrolysis to give TFA and CF_3CF_2COOH, occurring on a time scale of 5-15 days (Wallington et al., 1994). Thus, the yield of TFA in the atmospheric oxidation of $CF_3CF_2CFHCFHCF_3$ is estimated as 50% + ~0.5 × (7 – 20%) = 54 – 60%. A similar yield of CF_3CF_2COOH is also expected.

$CF_3CF_2CFHCFHCF_3$ is used a solvent. Annual global emissions of $CF_3CF_2CFHCFHCF$ have been estimated as 1.13±0.31 Gg yr^{-1} for 2012 (Arnold et al., 2014).

SI 4.3.1 HFO-1234yf ($CF_3CF=CH_2$), ~100%

$CF_3CF=CH_2$ has an atmospheric lifetime of 12 days (Smith, 2021). Atmospheric oxidation of $CF_3CF=CH_2$ proceeds through OH addition to the double bond (see Fig. 10 in the main text). CF_3CFO is subsequently formed in a yield of 100%, independent of which side of the double bond is involved in the initial OH-addition step (Hurley et al., 2008). The atmospheric fate of CF_3CFO is incorporation into water droplets occurring on a time scale of 5–15 days (Wallington et al., 1994), and subsequent hydrolysis yields TFA. The yield of TFA in the atmospheric oxidation of $CF_3CF=CH_2$ is estimated at 100%.

$CF_3CF=CH_2$ is used as a refrigerant. Annual global emissions of $CF_3CF=CH_2$ have been estimated in the Science Assessment Panel 2022 report (WMO 2022) as 30 Gg yr^{-1} for 2020 (see also Table 3 in the main text).

SI 4.3.2 HFO-1234ze(E) ($CF_3CH=CHF$), 2–30%

$CF_3CF=CH_2$ has an atmospheric lifetime of 19 days (Smith, 2021). Atmospheric oxidation of $CF_3CH=CHF$ proceeds through OH addition to the double bond (Javadi et al., 2008). Subsequent reaction with O_2 and NO/RO_2 leads to the formation of CF_3CHO and HC(O)F in yields indistinguishable from 100%. As discussed in SI Section 4.1.3, atmospheric processing of CF_3CHO can lead to formation of TFA in small amounts. Thus, the TFA yield from processing of $CF_3CF=CH_2$ is estimated at 2%, with an upper limit of ~ 30%.

$CF_3CH=CHF$ is used as an aerosol propellant, in expanded polystyrene (styrofoam) insulation industry, and as a refrigerant. Annual global emissions of $CF_3CH=CHF$ are not known.

SI 4.3.3 HFO-1336mzz(E) (E-$CF_3CH=CHCF_3$) and HFO-1336mzz(Z) (Z-$CF_3CH=CHCF_3$), 4–60%

E- and Z- $CF_3CH=CHCF_3$ have atmospheric lifetimes of 122 and 27 days, respectively (Smith, 2021). Atmospheric oxidation of E- and Z- $CF_3CH=CHCF_3$ proceeds through OH addition to the double bond. Østerstrøm et al. (Østerstrøm et al., 2017) used Cl atoms in their study of the atmospheric oxidation of E- and Z- $CF_3CH=CHCF_3$. The OH initiated mechanism has not been studied in detail and remains speculative. The initially formed hydroxy-substituted alkoxy radicals will have competing fates of decomposition and reaction with O_2. It is possible that CF_3CHO is formed in this initial step through decomposition, or later through further reactions of possible degradation products, such as $CF_3CH(OH)C(O)CF_3$. An upper limit for the yield of CF_3CHO is 200%. As discussed in SI Section 4.1.3, atmospheric processing of CF_3CHO can lead to formation of TFA in small amounts. Thus, the TFA yield from processing of CF_3CHO is estimated at 4%, with an upper limit of ~ 60%.

E- and Z- $CF_3CH=CHCF_3$ are used as refrigerants. Annual global emissions are not known.

SI 4.3.4 HCFO-1233zd(E) (E-CF$_3$CH=CHCl) and HCFO-1233zd(Z) (Z-CF$_3$CH=CHCl), 2–30%

E- and Z- CF$_3$CH=CHCl have atmospheric lifetimes of 42 and 13 days, respectively (Smith, 2021). Atmospheric oxidation of E- and Z- CF$_3$CH=CHCl proceeds through OH addition to the double bond (Sulbæk Andersen et al., 2012; Sulbæk Andersen, Sølling, et al., 2018). The atmospheric degradation pathway for CF$_3$CH=CHCl is complex and produces CF$_3$CHO with estimated yield of 100% (see Section 3.2 and Figure 11 in the main text). As discussed in detail in SI Section 4.1.3, atmospheric processing of CF$_3$CHO can lead to formation of TFA in small amounts. Thus, the TFA yield from processing of CF$_3$CH=CHCl is estimated at 2%, with an upper limit of ~ 30%.

E-CF$_3$CH=CHCl is used as a polyurethane foam blowing agent and as a refrigerant. Z- CF$_3$CH=CHCl is used for degreasing of mechanical parts and dry cleaning. Annual global emissions for E- CF$_3$CH=CHCl have been estimated by Vollmer et al. (Vollmer, Reimann, et al., 2015) as 0.5 Gg yr^{-1} for 2014.

SI 4.3.5 2-BTP (CF$_3$CBr=CH$_2$), 2–30%

CF$_3$CBr=CH$_2$ has an estimated atmospheric lifetime of approximately 3 days (Sulbæk Andersen et al., 2009). Atmospheric oxidation of CF$_3$CBr=CH$_2$ proceeds through OH addition to the double bond. There is no mechanistic study available in the literature of the atmospheric oxidation of CF$_3$CBr=CH$_2$. Sulbæk Andersen et al. (Sulbæk Andersen et al., 2009) speculate that the OH relation leads to the formation of an enol CF$_3$C(OH)=CH$_2$ or a carbonyl/alcohol compound, CF$_3$C(O)-CH$_2$OH. These oxidation products would be reactive towards OH radicals and, in the case of CF$_3$C(OH)=CH$_2$, possibly undergo keto-enol tautomerization. It is possible that CF$_3$CHO is formed though reaction of OH radicals with the oxidation products or though photolysis of the carbonyl products. An upper limit for the yield of CF$_3$CHO is 100%. As discussed in SI Section 4.1.3, atmospheric processing of CF$_3$CHO can lead to formation of TFA in small amounts. Thus, the TFA yield from atmospheric processing of CF$_3$CBr=CH$_2$ is estimated at 2%, with an upper limit of ~ 30%.

CF$_3$CBr=CH$_2$ is used as a fire extinguishant. Global annual emissions are not known.

SI 4.4.1 Halothane (CF$_3$CHBrCl), 60 ± 10%

CF$_3$CHBrCl has an atmospheric lifetime of 1 year (Smith, 2021). The reaction of OH radicals with CF$_3$CHBrCl proceeds via hydrogen abstraction followed by reaction with O$_2$ and NO, and subsequent Br elimination, to give CF$_3$CClO in a yield indistinguishable from 100% (Bilde et al., 1998). The estimated tropospheric photolytic lifetime for CF$_3$CClO for an overhead sun is 23 days (Calvert et al., 2008). The atmospheric lifetime of CF$_3$CClO with respect to uptake and hydrolysis in cloud water is 5-30 days (Wallington et al., 1994). It has been estimated that, on average, 60% of CF$_3$CClO is converted into TFA (Hayman et al., 1994). The uncertainty on this yield is likely on the order of ± 10%. Thus, the TFA yield from atmospheric processing of CF$_3$CHBrCl is estimated at 60 ±10%.

Halothane is used as an inhaled anesthetic agent. Global annual emissions have been estimated by Vollmer et al. (Vollmer, Rhee, et al., 2015) as 0.25 Gg yr^{-1} for 2014.

SI 4.4.2 Isoflurane (CF$_3$CHClOCHF$_2$), 95 ± 3%

CF$_3$CHClOCHF$_2$ has an atmospheric lifetime of approximately 3 years (Mads P. Sulbæk Andersen et al., 2012). The atmospheric oxidation of CF$_3$CHClOCHF$_2$ proceeds via OH-mediated hydrogen abstraction. An estimated 95% of the reaction occurs at the -CHCl- group. Cl elimination subsequently yields the main oxidation product, CF$_3$C(O)OCHF$_2$ (95 ± 3%) (Wallington et al., 2002). The atmospheric lifetime of CF$_3$C(O)OCHF$_2$ with respect to reaction with OH is unknown. The atmospheric lifetime for a similar ester, CF$_3$C(O)OCH$_3$ is approximately 7.5 months (Blanco et al., 2010; Wallington et al., 1988). The atmospheric lifetime is likely to be longer for CF$_3$C(O)OCHF$_2$. Reaction of OH with CF$_3$C(O)OCHF$_2$ is not expected to lead to the formation of TFA. Loss of CF$_3$C(O)OCHF$_2$ via uptake into sea water followed by hydrolysis to give TFA is therefore estimated to be a major atmospheric sink for CF$_3$C(O)OCHF$_2$ (Kutsuna et al., 2004). The expected yield of TFA in the atmospheric oxidation of CF$_3$CHClOCHF$_2$ is 95 ± 3%.

Isoflurane is used as an inhaled anesthetic agent. Global annual emissions have been estimated by Vollmer et al. (Vollmer, Rhee, et al., 2015) as 0.88 Gg yr^{-1} for 2014.

SI 4.4.3 Desflurane (CF$_3$CHFOCHF$_2$), 3–20%

CF$_3$CHFOCHF$_2$ has an atmospheric lifetime of 9 years (Smith, 2021). The atmospheric fate of CF$_3$CHFOCHF$_2$ is reaction with OH radicals. No study of the OH initiated oxidation mechanism for CF$_3$CHFOCHF$_2$ exists in the literature. Based on a study of the chlorine atom initiated oxidation, Sulbæk Andersen et al. (2012) proposed that the hydrogen abstraction reaction proceeds predominantly from the -CHF- carbon group (83%). Only hydrogen abstraction from the terminal carbon will have the potential to lead to TFA (Sulbæk Andersen et al., 2012). Hydrogen abstraction from the terminal carbon (17%) will generate CF$_3$CHFOCF$_2$ radicals, which will react with O$_2$ and NO to give CF$_3$CHFOCF$_2$O radicals. These will undergo decomposition to give COF$_2$ and CF$_3$CHFO radicals. The latter will in one atmosphere of air react with O$_2$ to give CF$_3$CFO (18%) (Sulbæk Andersen et al., 2012). The atmospheric fate of CF$_3$CFO is incorporation into water droplets followed by hydrolysis to give TFA, occurring on a time scale of 5-15 days (Wallington et al., 1994). The TFA yield from atmospheric processing of CF$_3$CHClOCHF$_2$ can be estimated as 0.17 × 0.18 × (100%) = 3 %. A 20% upper limit of the estimate to account for possible differences in the location of hydrogen abstraction for the OH mediated abstraction, i.e., 3 – ~20%.

Desflurane is used as an inhaled anesthetic agent. Global annual emissions have been estimated as 0.96 Gg yr^{-1} for 2014 (Vollmer, Rhee, et al., 2015).

SI 4.4.4 Sevoflurane ($(CF_3)_2HCOCH_2F$), 2–95%

$(CF_3)_2HCOCH_2F$ has an atmospheric lifetime of 1.4 years (Sulbæk Andersen et al., 2021). The atmospheric fate of $(CF_3)_2HCOCH_2F$ is reaction with OH radicals. No study of the OH initiated oxidation mechanism for $CF_3CHFOCHF_2$ exists in the literature. Based on a study of the chlorine atom initiated oxidation, Sulbæk Andersen et al. (2012) proposed that the hydrogen abstraction reaction proceeds exclusively from the terminal -CH_2F group. Reaction of the initially formed alkoxy radical with O_2 and NO yields $(CF_3)_2HCOCHFO$, which in one atmosphere of air was found to give 7% CF_3COCF_3 (through decomposition) and 93% $(CF_3)_2HCOCFO$ (through reaction with O_2). The dominant fate of CF_3COCF_3 is likely tropospheric photolysis to give CF_3 and CF_3CO radicals (Calvert et al., 2008). As discussed in SI Section 4.1.3, further reaction of CF_3CO radicals with O_2 and HO_2 radicals can lead to formation of TFA in small amounts (20 ± 10%). The major fate of $(CF_3)_2HCOCFO$ will be dissolution into seawater followed by hydrolysis (Kutsuna et al., 2004). Hydrolysis would possibly result in the formation of $(CF_3)_2HCOCOOH(aq)$, but it is unclear if the hydrolysis of $(CF_3)_2HCOCFO$ would also lead to TFA. A possible upper limit for the estimated yield of TFA from ocean uptake and hydrolysis of $(CF_3)_2HCOCFO$ is 93%. Thus, the yield of TFA from atmospheric processing of $(CF_3)_2HCOCH_2F$ can be estimated as 2% (photolysis of CF_3COCF_3), with an upper limit of 95% (ocean uptake and hydrolysis of $(CF_3)_2HCOCFO$).

Sevoflurane is used as an inhaled anesthetic agent. Global annual emissions have been estimated as 1.20 Gg yr^{-1} for 2014 (Vollmer, Rhee, et al., 2015).

SI 4.4.5 FK-5-1-12 ($CF_3CF_2C(O)CF(CF_3)_2$), 101-110%

$CF_3CF_2C(O)CF(CF_3)_2$ has an atmospheric lifetime of 7 days (Smith, 2021). The atmospheric oxidation of $CF_3CF_2C(O)CF(CF_3)_2$ has been studied by Taniguchi et al. (Taniguchi et al., 2003). The main atmospheric fate of $CF_3CF_2C(O)CF(CF_3)_2$ is removal by photolysis. Photolysis yields CF_3CF_2 + $C(O)CF(CF_3)_2$ radicals and subsequent reactions of the $C(O)CF(CF_3)_2$ yields CF_3CFO in a molar yield of unity. The atmospheric fate of CF_3CFO is incorporation into water droplets followed by hydrolysis to give TFA, occurring on a time scale of 5-15 days (Wallington et al., 1994). CF_3CF_2 will react with O_2 and NO to give CF_3CF_2O radicals. Ellis et al. (Ellis et al., 2004) suggested a mechanism by which the reaction of molecules such as CF_3CF_2O react with α-hydrogen containing peroxy radicals (e.g., CH_3O_2) in the atmosphere to give CF_3CF_2OH in small amounts (1-10%) (Wallington et al., 2006)). CF_3CF_2OH will eliminate HF to give CF_3CFO. Thus, the yield of TFA in the atmospheric degradation of $CF_3CF_2C(O)CF(CF_3)_2$ is expected to be essentially 101%, with an upper limit of 110%. $CF_3CF_2(O)CF(CF_3)_2$ is used as a fire suppressant. Global annual emissions are unknown.

References

1. Arnold, T., Ivy, D. J., Harth, C. M., Vollmer, M. K., Mühle, J., Salameh, P. K., Paul Steele, L., Krummel, P. B., Wang, R. H. J., Young, D., Lunder, C. R., Hermansen, O., Rhee, T. S., Kim, J., Reimann, S., O'Doherty, S., Fraser, P. J., Simmonds, P. G., Prinn, R. G., & Weiss, R. F. (2014). HFC-43-10mee atmospheric abundances and global emission estimates. *Geophysical Research Letters, 41*(6), 2228-2235. https://doi.org/https://doi.org/10.1002/2013GL059143

2. ATSDR. (2021). *Toxicological Profile for Perfluoroalkyls*. ATSDR. https://www.atsdr.cdc.gov/toxprofiles/tp200.pdf

3. Bhatnagar, A., & Carr, R. W. (1995). Temperature dependence of the reaction of CF_3CFClO_2 Radicals with NO and the unimolecular decomposition of the CF_3CFClO radical. *The Journal of Physical Chemistry, 99*(49), 17573-17577. https://doi.org/10.1021/j100049a017

4. Bilde, M., Wallington, T. J., Ferronato, C., Orlando, J. J., Tyndall, G. S., Estupiñan, E., & Haberkorn, S. (1998). Atmospheric chemistry of CH_2BrCl, $CHBrCl_2$, $CHBr_2Cl$, $CF_3CHBrCl$, and CBr_2Cl_2. *The Journal of Physical Chemistry A, 102*(11), 1976-1986. https://doi.org/10.1021/jp9733375

5. Blanco, M. B., Bejan, I., Barnes, I., Wiesen, P., & Teruel, M. a. (2010). Atmospheric photooxidation of fluoroacetates as a source of fluorocarboxylic acids. *Environmental Science & Technology, 44*(7), 2354-2359. https://doi.org/10.1021/es903357j

6. Boudreau, T. M. (2002). *Toxicity of Perfluorinated Organic Acids to Selected Freshwater Organisms under Laboratory and Field Conditions* [M.Sc., University of Guelph]. Guelph.

7. Boutonnet, J. C., Bingham, P., Calamari, D., Rooij, C. d., Franklin, J., Kawano, T., Libre, J.-M., McCul-Loch, A., Malinverno, G., & Odom, J. M. (1999). *Environmental risk assessment of trifluoroacetic acid. Human and Ecological Risk Assessment, 5*, 59-124. https://doi.org/10.1080/10807039991289644

8. Burkholder, J. B., Sander, S. P., Abbatt, J., Barker, J. R., Cappa, C., Crounse, J. D., Dibble, T. S., Huie, R. E., Kolb, C. E., Kurylo, M. J., Orkin, V. L., Perciva, C. J., Wilmouth, D. M., & Wine, P. H. (2020). *Chemical Kinetics and Photochemical Data for Use in Atmospheric Studies*. http://jpldataeval.jpl.nasa.gov

9. Calvert, J. G., Atkinson, R., Kerr, J. A., & Madronich, S., Moortgat, G., Wallington, T. J., & Yarwood, G. (2000). *The Mechanisms of Atmospheric Oxidation of the Alkenes*. Oxford University Press.

10. Calvert, J. G., Derwent, R. G., Orlando, J. J., Tyndall, G. S., & Wallington, T. J. (2008). *Mechanisms of Atmospheric Oxidation of the Alkanes*. Oxford University Press.

11. Chabot, L. (2017). Chabot L. (2017). *ALGA, GROWTH INHIBITION TEST Effect of the trifuoroacetic acid on the growth of the unicellular alga Pseudokirchneriella subcapitata, according to OECD guideline 201 (Study conducted for RHODIA OPERATIONS – SOLVAY).*

12. Chen, J., Young, V., Niki, H., & Magid, H. (1997). Kinetic and Mechanistic Studies for Reactions of $CF_3CH_2CHF_2$ (HFC-245fa) Initiated by H-Atom Abstraction Using Atomic Chlorine. *The Journal of Physical Chemistry A, 101*(14), 2648-2653. https://doi.org/10.1021/jp963735s

13. Chiappero, M. S., Malanca, F. E., Argüello, G. A., Wooldridge, S. T., Hurley, M. D., Ball, J. C., Wallington, T. J., Waterland, R. L., & Buck, R. C. (2006). Atmospheric chemistry of perfluoroaldehydes ($C_xF_{2X+1}CHO$) and fluorotelomer aldehydes ($C_xF_{2X+1}CH_2CHO$): Quantification of the important role of photolysis. *The Journal of Physical Chemistry A, 110*(43), 11944-11953. https://doi.org/10.1021/jp064262k

14. Cox, R. A., Ammann, M., Crowley, J. N., Herrmann, H., Jenkin, M. E., McNeill, V. F., Mellouki, A., Troe, J., & Wallington, T. J. (2020). Evaluated kinetic and photochemical data for atmospheric chemistry: Volume VII – Criegee intermediates. *Atmospheric Chemistry and Physics, 20*(21), 13497-13519. https://doi.org/10.5194/acp-20-13497-2020

15. Edney, E. O., Gay, B. W., & Driscoll, D. J. (1991). Chlorine initiated oxidation studies of hydrochlorofluorocarbons: Results for HCFC-123 (CF_3CHCl_2) and HCFC-141b ($CFCl_2CH_3$). *Journal of Atmospheric Chemistry, 12*(2), 105-120. https://doi.org/10.1007/BF00115774

16. EFSA. (2020). Risk to human health related to the presence of perfluoroalkyl substances in food. *EFSA Journal, 18*(9), e06223. https://doi.org/10.2903/j.efsa.2020.6223

17. Ellis, D. A., Martin, J. W., De Silva, A. O., Mabury, S. A., Hurley, M. D., Sulbæk Andersen, M. P., & Wallington, T. J. (2004). Degradation of fluorotelomer alcohols: A likely atmospheric source of perfluorinated carboxylic acids. *Environmental Science & Technology, 38*, 3316-3321. https://doi.org/10.1021/es049860w

18. Franco, B., Blumenstock, T., Cho, C., Clarisse, L., Clerbaux, C., Coheur, P. F., De Mazière, M., De Smedt, I., Dorn, H. P., Emmerichs, T., Fuchs, H., Gkatzelis, G., Griffith, D. W. T., Gromov, S., Hannigan, J. W., Hase, F., Hohaus, T., Jones, N., Kerkweg, A., . . . Taraborrelli, D. (2021). Ubiquitous atmospheric production of organic acids mediated by cloud droplets. *Nature, 593*(7858), 233-237. https://doi.org/10.1038/s41586-021-03462-x

19. Hayman, G. D., Jenkin, M. E., Murrells, T. P., & Johnson, C. E. (1994). Trospospheric degradation chemistry of HCFC-123 (CF$_3$CHCl$_2$): A proposed replacement chlorofluorocarbon. *Atmospheric Environment, 28*(3), 421-437. https://doi.org/https://doi.org/10.1016/1352-2310(94)90121-X

20. Hurley, M. D., Ball, J. C., Wallington, T. J., Sulbæk Andersen, M. P., Nielsen, O. J., Ellis, D. A., Martin, J. W., & Mabury, S. A. (2006). Atmospheric chemistry of n-C$_x$F$_{2X+1}$CHO (x = 1, 2, 3, 4): Fate of n-C$_x$F$_{2X+1}$C(O) radicals. *The Journal of Physical Chemistry A, 110*(45), 12443-12447. https://doi.org/10.1021/jp064029m

21. Hurley, M. D., Wallington, T. J., Javadi, M. S., & Nielsen, O. J. (2008). Atmospheric chemistry of CF$_3$CFCH$_2$: Products and mechanisms of Cl atom and OH radical initiated oxidation. *Chemical Physics Letters, 450*(4-6), 263-267. https://doi.org/10.1016/j.cplett.2007.11.051

22. Inoue, Y., Kawasaki, M., Wallington, T. J., & Hurley, M. D. (2008). Atmospheric chemistry of CF$_3$CH$_2$CF$_2$CH$_3$ (HFC-365mfc): Kinetics and mechanism of chlorine atom initiated oxidation, infrared spectrum, and global warming potential. *Chemical Physics Letters, 462*(4), 164-168. https://doi.org/https://doi.org/10.1016/j.cplett.2008.07.054

23. Javadi, M. S., Søndergaard, R., Nielsen, O. J., Hurley, M. D., & Wallington, T. J. (2008). Atmospheric chemistry of trans-CF$_3$CH=CHF: products and mechanisms of hydroxyl radical and chlorine atom initiated oxidation. *Atmospheric Chemistry and Physics, 8*(12), 3141-3147. https://doi.org/10.5194/acp-8-3141-2008

24. Jenkin, M. E. (2022). Personal Communication.

25. Jenkin, M. E., Derwent, R.G., Wallington, T.J. (2017). Photochemical ozone creation potentials for volatile organic compounds: Rationalization and estimation. *Atmospheric Environment 163*, 128–137. https://doi.org/10.1016/j.atmosenv.2017.05.024

26. Kutsuna, S., Chen, L., Ohno, K., Tokuhashi, K., & Sekiya, A. (2004). Henry's law constants and hydrolysis rate constants of 2,2,2-trifluoroethyl acetate and methyl trifluoroacetate. *Atmospheric Environment, 38*(5), 725-732. https://doi.org/https://doi.org/10.1016/j.atmosenv.2003.10.019

27. Møgelberg, T. E., Nielsen, O. J., Sehested, J., & Wallington, T. J. (1995). Atmospheric chemistry of HCFC-133a: the UV absorption spectra of CF$_3$CClH and CF$_3$CClHO$_2$ radicals, reactions of CF$_3$CClHO$_2$ with NO and NO$_2$, and fate of CF$_3$CClHO radicals. *The Journal of Physical Chemistry, 99*(36), 13437-13444. https://doi.org/10.1021/j100036a018

28. Møgelberg, T. E., Platz, J., Nielsen, O. J., Sehested, J., & Wallington, T. J. (1995). Atmospheric chemistry of HFC-236fa: spectrokinetic investigation of the CF$_3$CHO$_2$CF$_3$ radical, its reaction with NO, and the fate of the CF$_3$CHOCF$_3$ radical. *The Journal of Physical Chemistry, 99*(15), 5373-5378. https://doi.org/10.1021/j100015a021

29. Møgelberg, T. E., Sehested, J., Tyndall, G. S., Orlando, J. J., Fracheboud, J.-M., & Wallington, T. J. (1997). Atmospheric chemistry of HFC-236cb: Fate of the alkoxy radical CF$_3$CF$_2$CFHO. *The Journal of Physical Chemistry A, 101*(15), 2828-2832. https://doi.org/10.1021/jp963021h

30. NICNAS. (2016). *Short Chain Perfluorocarboxylic Acids and their Direct Precursors: Human Health Tier II Assessment.* N. I. C. N. a. A. S. (NICNAS). https://www.nicnas.gov.au/chemical-information/imap-assessments/imap-group-assessment-report?assessment_id=1686

31. Nielsen, O. J., Gamborg, E., Sehested, J., Wallington, T. J., & Hurley, M. D. (1994). Atmospheric chemistry of HFC-143a: Spectrokinetic investigation of the CF$_3$CH$_2$O$_2$ radical, its reactions with NO and NO$_2$, and the fate of CF$_3$CH$_2$O. *The Journal of Physical Chemistry, 98*(38), 9518-9525. https://doi.org/10.1021/j100089a026

32. Østerstrøm, F. F., Andersen, S. T., Sølling, T. I., Nielsen, O. J., & Sulbæk Andersen, M. P. (2017). Atmospheric chemistry of Z- and E-CF$_3$CH=CHCF$_3$ [10.1039/C6CP07234H]. *Physical Chemistry Chemical Physics, 19*(1), 735-750. https://doi.org/10.1039/C6CP07234H

33. Papadimitriou, V. C., & Burkholder, J. B. (2016). OH radical reaction rate coefficients, infrared spectrum, and global warming potential of (CF$_3$)$_2$CFCH=CHF (HFO-1438ezy(E)). *The Journal of Physical Chemistry A, 120*(33), 6618-6628. https://doi.org/10.1021/acs.jpca.6b06096

34. Papadimitriou, V. C., Spitieri, C. S., Papagiannakopoulos, P., Cazaunau, M., Lendar, M., Daële, V., & Mellouki, A. (2015). Atmospheric chemistry of (CF$_3$)$_2$C=CH$_2$: OH radicals, Cl atoms and O$_3$ rate coefficients, oxidation end-products and IR spectra [10.1039/C5CP03840E]. *Physical Chemistry Chemical Physics, 17*(38), 25607-25620. https://doi.org/10.1039/C5CP03840E

35. PubChem. (2022). *Trifluoracetic acid*. National Center for Biotechnology Information, U.S. National Library of Medicine. Retrieved January 2022 from https://pubchem.ncbi.nlm.nih.gov/compound/6422

36. RSC. (2022). *ChemSpider*. Royal Society of Chemistry. Retrieved May from http://www.chemspider.com/

37. Simmonds, P. G., Rigby, M., McCulloch, A., O'Doherty, S., Young, D., Mühle, J., Krummel, P. B., Steele, P., Fraser, P. J., Manning, A. J., Weiss, R. F., Salameh, P. K., Harth, C. M., Wang, R. H. J., & Prinn, R. G. (2017). Changing trends and emissions of hydrochlorofluorocarbons (HCFCs) and their hydrofluorocarbon (HFCs) replacements. *Atmospheric Chemistry and Physics, 17*(7), 4641-4655. https://doi.org/10.5194/acp-17-4641-2017

38. Smith, C., Z.R.J. Nicholls, K. Armour, W. Collins, P. Forster, M. Meinshausen, M.D. Palmer, M. Watanabe. (2021). The Earth's Energy Budget, Climate Feedbacks, and Climate Sensitivity Supplementary Material. In V. Masson-Delmotte, P. Zhai, A. Pirani, S.L. Connors, C. Péan, S. Berger, N. Caud, Y. Chen, L. Goldfarb, M.I. Gomis, M. Huang, K. Leitzell, E. Lonnoy, J.B.R. Matthews, T.K. Maycock, T. Waterfield, O. Yelekçi, R. Yu, B. Zhou (Ed.), *Climate Change 2021: The Physical Science Basis. Contribution of Working Group I to the Sixth Assessment Report of the Intergovernmental Panel on Climate Change*

39. Sulbæk Andersen, M. P., Hurley, M. D., & Wallington, T. J. (2009). Kinetics of the gas phase reactions of chlorine atoms and OH radicals with $CF_3CBr=CH_2$ and $CF_3CF_2CBr=CH_2$. *Chemical Physics Letters, 482*(1), 20-23. https://doi.org/https://doi.org/10.1016/j.cplett.2009.09.056

40. Sulbæk Andersen, M. P., & Nielsen, O. J. (2022). Tropospheric photolysis of CF_3CHO. *Atmospheric Environment, 272*, 118935. https://doi.org/10.1016/j.atmosenv.2021.118935

41. Sulbæk Andersen, M. P., Nielsen, O. J., Hurley, M. D., & Wallington, T. J. (2012). Atmospheric chemistry of t-$CF_3CH=CHCl$: products and mechanisms of the gas-phase reactions with chlorine atoms and hydroxyl radicals [10.1039/C1CP22925G]. *Physical Chemistry Chemical Physics, 14*(5), 1735-1748. https://doi.org/10.1039/C1CP22925G

42. Sulbæk Andersen, M. P., Nielsen, O. J., Karpichev, B., Wallington, T. J., & Sander, S. P. (2012). Atmospheric chemistry of isoflurane, desflurane, and sevoflurane: Kinetics and mechanisms of reactions with chlorine atoms and OH radicals and global warming potentials. *The Journal of Physical Chemistry A, 116*(24), 5806-5820. https://doi.org/10.1021/jp2077598

43. Sulbæk Andersen, M. P., Nielsen, O. J., & Sherman, J. D. (2021). The global warming potentials for anesthetic gas sevoflurane need significant corrections. *Environmental Science & Technology, 55*(15), 10189-10191. https://doi.org/10.1021/acs.est.1c02573

44. Sulbæk Andersen, M. P., Schmidt, J. A., Volkova, A., & Wuebbles, D. J. (2018). A three-dimensional model of the atmospheric chemistry of E and Z-$CF_3CH=CHCl$ (HCFO-1233(zd) (E/Z)). *Atmospheric Environment, 179*, 250-259. https://doi.org/10.1016/j.atmosenv.2018.02.018

45. Sulbæk Andersen, M. P., Sølling, T. I., Andersen, L. L., Volkova, A., Hovanessian, D., Britzman, C., Nielsen, O. J., & Wallington, T. J. (2018). Atmospheric chemistry of (Z)-$CF_3CH=CHCl$: products and mechanisms of the Cl atom, OH radical and O_3 reactions, and role of (E)–(Z) isomerization [10.1039/C8CP04903C]. *Physical Chemistry Chemical Physics, 20*(44), 27949-27958. https://doi.org/10.1039/C8CP04903C

46. Sulbæk Andersen, M. P., Toft, A., Nielsen, O. J., Hurley, M. D., Wallington, T. J., Chishima, H., Tonokura, K., Mabury, S. A., Martin, J. W., & Ellis, D. A. (2006). Atmospheric chemistry of perfluorinated aldehyde hydrates (n-$C_xF_{2x+1}CH(OH)_2$, x = 1, 3, 4): Hydration, dehydration, and kinetics and mechanism of Cl atom and OH radical initiated oxidation. *The Journal of Physical Chemistry A, 110*(32), 9854-9860. https://doi.org/10.1021/jp060404z

47. Taniguchi, N., Wallington, T. J., Hurley, M. D., Guschin, A. G., Molina, L. T., & Molina, M. J. (2003). Atmospheric chemistry of $C_2F_5C(O)CF(CF_3)_2$: Photolysis and reaction with Cl atoms, OH radicals, and ozone. *The Journal of Physical Chemistry A, 107*(15), 2674-2679. https://doi.org/10.1021/jp0220332

48. Tuazon, E. C., & Atkinson, R. (1993). Tropospheric transformation products of a series of hydrofluorocarbons and hydrochlorofluorocarbons. *Journal of Atmospheric Chemistry, 17*(2), 179-199. https://doi.org/10.1007/BF00702825

49. Vollmer, M. K., Miller, B. R., Rigby, M., Reimann, S., Mühle, J., Krummel, P. B., O'Doherty, S., Kim, J., Rhee, T. S., Weiss, R. F., Fraser, P. J., Simmonds, P. G., Salameh, P. K., Harth, C. M., Wang, R. H. J., Steele, L. P., Young, D., Lunder, C. R., Hermansen, O., . . . Prinn, R. G. (2011). Atmospheric histories and global emissions of the anthropogenic hydrofluorocarbons HFC-365mfc, HFC-245fa, HFC-227ea, and HFC-236fa. *Journal of Geophysical Research: Atmospheres, 116*(D8). https://doi.org/https://doi.org/10.1029/2010JD015309

50. Vollmer, M. K., Reimann, S., Hill, M., & Brunner, D. (2015). First observations of the fourth generation synthetic halocarbons HFC-1234yf, HFC-1234ze(E), and HCFC-1233zd(E) in the atmosphere. *Environmental Science & Technology, 49*(5), 2703-2708. https://doi.org/10.1021/es505123x

51. Vollmer, M. K., Rhee, T. S., Rigby, M., Hofstetter, D., Hill, M., Schoenenberger, F., & Reimann, S. (2015). Modern inhalation anesthetics: Potent greenhouse gases in the global atmosphere. *Geophysical Research Letters, 42*(5), 1606-1611. https://doi.org/https://doi.org/10.1002/2014GL062785

52. Vollmer, M. K., Rigby, M., Laube, J. C., Henne, S., Rhee, T. S., Gooch, L. J., Wenger, A., Young, D., Steele, L. P., Langenfelds, R. L., Brenninkmeijer, C. A. M., Wang, J.-L., Ou-Yang, C.-F., Wyss, S. A., Hill, M., Oram, D. E., Krummel, P. B., Schoenenberger, F., Zellweger, C., . . . Reimann, S. (2015). Abrupt reversal in emissions and atmospheric abundance of HCFC-133a (CF_3CH_2Cl). *Geophysical Research Letters, 42*(20), 8702-8710. https://doi.org/https://doi.org/10.1002/2015GL065846

53. Wallington, T. J., Hurley, M. D., Fedotov, V., Morrell, C., & Hancock, G. (2002). Atmospheric Chemistry of $CF_3CH_2OCHF_2$ and $CF_3CHClOCHF_2$: Kinetics and mechanisms of reaction with Cl atoms and OH radicals and atmospheric fate of $CF_3C(O•)HOCHF_2$ and $CF_3C(O•)ClOCHF_2$ Radicals. *The Journal of Physical Chemistry A, 106*(36), 8391-8398. https://doi.org/10.1021/jp020017z

54. Wallington, T. J., Hurley, M. D., Fracheboud, J. M., Orlando, J. J., Tyndall, G. S., Sehested, J., Møgelberg, T. E., & Nielsen, O. J. (1996). Role of excited CF_3CFHO radicals in the atmospheric chemistry of HFC-134a. *The Journal of Physical Chemistry, 100*(46), 18116-18122. https://doi.org/10.1021/jp9624764

55. Wallington, T. J., Hurley, M. D., Xia, J., Wuebbles, D. J., Sillman, S., Ito, A., Penner, J. E., Ellis, D. A., Martin, J., Mabury, S. A., Nielsen, O. J., & Sulbæk Andersen, M. P. (2006). Formation of $C_7F_{15}COOH$ (PFOA) and other perfluorocarboxylic acids during the atmospheric oxidation of 8:2 fluorotelomer alcohol. *Environmental Science & Technology, 40*(3), 924-930. https://doi.org/10.1021/es051858x

56. Wallington, T. J., Liu, R., Dagaut, P., & Kurylo, M. J. (1988). The gas phase reactions of hydroxyl radicals with a series of aliphatic ethers over the temperature range 240–440 K. *International Journal of Chemical Kinetics, 20*(1), 41-49. https://doi.org/https://doi.org/10.1002/kin.550200106

57. Wallington, T. J., Schneider, W. F., Worsnop, D. R., Nielsen, O. J., Sehested, J., Debruyn, W. J., & Shorter, J. A. (1994). The environmental impact of CFC replacements HFCs and HCFCs. *Environmental Science & Technology, 28*(7), 320A-326A. https://doi.org/10.1021/es00056a714

58. Wang, Y., Niu, J., Zhang, L., & Shi, J. (2014). Toxicity assessment of perfluorinated carboxylic acids (PFCAs) towards the rotifer *Brachionus calyciflorus* [Research Support, Non-U.S. Gov't]. *The Science of the Total Environment, 491-492*, 266-270. https://doi.org/10.1016/j.scitotenv.2014.02.028

59. WMO (2022). Scientific Assessment of Ozone Depletion: 2022. GAW Report No. 278. World Meteorological Organization, Geneva, Switzerland. https://ozone.unep.org/science/assessment/sap

60. Wuebbles, D. J., & Patten, K. O. (2009). Three-dimensional modeling of HCFC-123 in the atmosphere: Assessing its potential environmental impacts and rationale for continued use. *Environmental Science & Technology, 43*(9), 3208-3213. https://doi.org/10.1021/es802308m

61. Zellner, R., Bednarek, G., Hoffmann, A., Kohlmann, J. P., Mörs, V., & Saathoff, H. (1994). Rate and mechanism of the atmospheric degradation of 2H-heptafluoropropane (HFC-227), *Berichte der Bunsengesellschaft für physikalische Chemie, 98*(2), 141-146. https://doi.org/10.1002/bbpc.19940980202

62. Zhang, N., Chen, L., Mizukado, J., Quan, H., & Suda, H. (2015). Rate constants for the gas-phase reactions of (Z)-CF_3CHCHF and (E)-CF_3CHCHF with OH radicals at 253–328K. *Chemical Physics Letters, 621*, 78-84. https://doi.org/10.1016/j.cplett.2014.12.044

7

EFFECTS OF UV RADIATION ON NATURAL AND SYNTHETIC MATERIALS

A. L. Andrady[114], A. M. Heikkilä[115], K. K. Pandey[116], L. S. Bruckman[117], C.C. White[118], M. Zhu[119], and L. Zhu[120]

[114] Chemical and Biomolecular Engineering, North Carolina State University, Raleigh, NC, USA

[115] Finnish Meteorological Institute, Helsinki, Finland

[116] Indian Academy of Wood Science, Bangalore, India

[117] Department of Materials Science and Engineering, Case Western Reserve University, Cleveland, OH, USA

[118] Exponent Inc, Bowie MD, USA

[119] College of Materials Science and Engineering, Donghua University, Shanghai, China

[120] State Key Laboratory for Modification of Chemical Fibres and Polymer Materials, Donghua University, Shanghai, China

Table of contents

Summary

The deleterious effects of solar ultraviolet (UV) radiation on construction materials, especially wood and plastics, and their consequent impacts on their useful lifetimes, are well documented in scientific literature. Any future increase in solar UV radiation and ambient temperature due to climate change will therefore shorten service lifetimes of materials, which will require higher levels of stabilisation or other interventions to maintain their lifetimes at the present levels. The implementation of the Montreal Protocol and its Amendments on Substances that Deplete the Ozone Layer controls the solar UV-B radiation received on Earth. This current Quadrennial Assessment provides a comprehensive update on the deleterious effects of solar UV radiation on the durability of natural and synthetic materials, as well as recent innovations in better stabilising materials against solar UV radiation-induced damage. Pertinent emerging technologies for wood and plastics used in construction, composite materials used in construction, textile fibres, comfort fabric, and photovoltaic materials are addressed in detail. Also addressed are the trends in technology designed to increase sustainability via replacing toxic, unsustainable legacy additives with 'greener' benign substitutes that may indirectly affect the UV-stability of the redesigned materials. An emerging class of efficient photostabilisers are the nanoscale particles that include oxide fillers and nanocarbons used in high-performance composites, which provide good UV stability to materials. They also allow the design of UV-shielding fabric materials with impressive UV protection factors. An emerging environmental issue related to the photodegradation of plastics is the generation of ubiquitous micro-scale particles from plastic litter exposed to solar UV radiation.

1 Introduction

The Montreal Protocol and its Amendments over the last 35 years have successfully contributed to the stability of the stratospheric ozone layer, limiting the solar ultraviolet (UV) radiation, particularly the UV-B wavebands (280-315 nm) of terrestrial solar radiation reaching the Earth's surface. Any future increase in solar UV radiation reaching the Earth, particularly the UV-B radiation, especially if accompanied by higher ambient temperatures, will shorten the service lifetimes of wood, plastics, and other organic materials. Given the low to moderate activation energies of photodegradation of these materials, even a small increase in the ambient temperature due to climate change, may accelerate degradation and shorten their service life. The presently available UV-stabilisation and coating technologies are expected to be adequate to mitigate these changes and maintain the service lifetimes of materials at the present level. However, elevated amounts of solar UV radiation in terrestrial solar radiation would require using correspondingly higher levels of UV stabilisers or more frequent surface treatment in the case of wood to ensure adequate service lifetimes. This strategy could invariably add significantly to the lifetime cost of materials. The materials industry is continuously researching more efficient and lower cost UV stabiliser systems for wood and plastics. In recent years, this search has been increasingly guided by long-term sustainability considerations that encourage the preferred development of 'greener' additives, such as natural UV stabilisers in place of conventional synthetic additives for both plastics and wood [1]. Using nanoparticles (NPs) as stabiliser/fillers in coatings, plastics, or textile fibres, which results in efficient light-shielding at very low fractions, is an especially promising development in new stabilisers.

With the projected increase in world population, the demand for wood and plastic materials popularly used in building construction will increase in the medium term. Global production volumes for both these are the highest reported over the past 70 years. For instance, 2.03 billion m^3 of industrial round wood processed in 2018 was mostly used as building materials [2]. Of the 359 million metric tons (MMTs) of plastic resins produced in 2018, about 30 % was used in building applications [3]. With the number of buildings worldwide estimated to double by 2060 [4], with the addition of 230 billion m^2 of new floor area (relative to 2017), the demand for construction materials will correspondingly increase. This increase will likely have significant environmental impacts at the global scale. The construction industry already accounts for 36% of energy expenditure and 37% of carbon dioxide (CO_2) emissions globally [5]. Increased sustainability requirements in the industry will be critical in the coming decade. The trend towards sustainability is already apparent in the sector; the global investment in certified energy-efficient buildings increased by 11 % in 2020, reflecting this trend.

Wood is a traditional, low-cost, and sustainable building material that has a relatively small carbon footprint relative to concretes, metals, or plastics [6]. For instance, a recent analysis illustrated the advantages of using wood over plastics as the material for fabricating pallets, a product with an annual global demand of 6.87 billion units [7]. Life cycle analysis (LCA) found wood to have a significant advantage over plastics in this application. Assuming incineration as the disposal method, the carbon footprint of a wood pallet was 0.34 kg of carbon dioxide equivalent (CO_2-e) four times lower than that of a plastic unit [8]. A Finnish study [7] agreed with the finding, but found wood-plastic composites (WPC) to have even a lower carbon footprint relative to wood. Using recycled post-consumer plastics in the WPC further decreases emissions. A similar comparison between metal, poly(vinyl chloride) (PVC), and wood used in constructing window frames found the latter to have the least environmental costs as measured by embodied non-renewable energy and carbon

emissions [9]. Findings from LCA studies can vary with location because of transportation and energy mix used. Therefore, they are not necessarily comparable across studies. These sustainability advantages make wood, especially the new 'mass timber' (or the engineered wood designed to compete with concrete or metal in strength), extremely attractive for use in buildings. Cross-laminated timber, a popular category of mass timber, was recently used to replace concrete in a high-rise building that is 18 stories high [10].

Materials used in building construction, transportation, and outdoor furniture are routinely exposed to solar UV radiation and undergo gradual photodegradation. The duration of their exposure to solar UV radiation determines the service life of these products such as composites used in vehicles, exterior panels in buildings, greenhouse glazing in agriculture, stadium seating, and synthetic turf. Photodegradation negatively affects appearance, compromises mechanical integrity, and encourages subsequent biodegradation, which all limit their service life [11]. With plastics, it is the UV-induced autocatalytic photo-oxidation reactions that result in surface discolouration or cracking accompanied by the loss of mechanical integrity over time. Photodamage to plastics, however, is mostly limited to a thin surface layer, resulting in damage modes such as yellowing, chalking, and cracking. As the base plastic resins are inherently photolabile, several groups of additives (UV-stabilisers) are typically compounded with plastics intended for extended outdoor use to mitigate the damaging effects of solar UV radiation [12-14]. These include UV-absorbers, insoluble pigments that absorb or scatter UV radiation, and additives that inhibit oxidative reactions. Potent radical traps, such as tertiary amines of tertiary phenols, are often used to inhibit the free-radical photodegradation reactions [15,16].

For instance, weathering of high-density polyethylene (HDPE) stabilised with UV-absorbers under accelerated weathering using a Xenon lamp (generally following ASTM G155), showed that the non-stabilised HDPE was embrittled, with its tensile strength extensibility reducing to 21 %, in 300 h of exposure, while the UV-stabilised HDPE was stable up to 900 h of exposure [17]. However, the combination of a UV-absorber (0.15 wt.%) with the radical-quencher hindered amine stabilisers (HALS) used at 0.45 wt.%, yields synergistic stabilisation with little degradation up to 1300 h of exposure. Accelerated weathering of polypropylene (PP) with a HALS (0.5 wt.%) and the UV screener, nano-ZnO (0.5 wt.%), showed synergistic stabilisation [15]. However, the latter study used a high-intensity UV-A lamp. The effect of this high-intensity UV lamp with a narrow wavelength emission range (very different from spectral qualities of solar radiation) cannot be reasonably compared to that of natural weathering exposure. A recent investigation [18] on the natural weathering of UV-stabilised plastics over 4 years at a total UV irradiance of 1020 MJ m^{-2}, ranked the durability of common plastic materials used in building. Their ranking was based on percentage retention of fracture strain after exposure. PP, poly(butylene terephthalate) (PBT), HDPE, and polycarbonate (PC) showed 47, 27, 20, and 17 % retention of the property, respectively. The result, however, cannot be generalised as it will strongly depend on the additives, especially UV stabilisers, used in plastics.

Studies on the photodegradation of plastics mostly focus on polyethylene (PE), polystyrene (PS), PVC, and poly(ethylene terephthalate) (PET). These plastics are also found in solid waste stream, urban litter, fresh waters, and especially marine debris. A recent summary of the existing data on plastics degradation in air and aquatic environments in terms of mass or area loss rates was carried out [19,20]. However, it relates primarily to fragmentation losses and perhaps including some photo-mineralisation. The latter process that converts the polymer into simple products such as CO_2 and water, defines the environmentally desirable endpoint of biological degradation. Using a simple model, the study [19] demonstrates the geometry-dependence of the kinetics of photodegradation of HDPE (Fig. 1). Despite the simplifying assumptions used in the analysis, it highlights the significance of the geometric form of a plastic material in determining degradation rates, a factor often overlooked in other studies. Another model on the rate of surface area loss on degradation in environmental degradation is based on polymer characteristics, such as the hydrophobicity, glass transition temperature, and the fractional crystallinity [21].
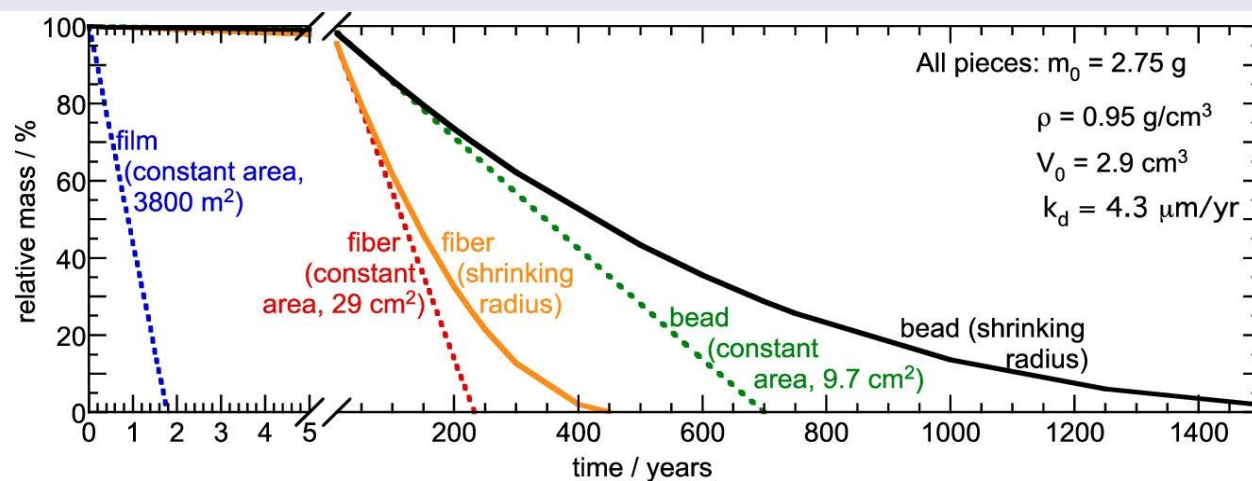

Fig. 1 A comparison of predicted degradation profiles for high-density polyethylene (HDPE) pieces with the same mass (mo), density (m$_o$), and surface loss rate for different shapes (thin film, fibre, and bead). The dashed lines correspond to extrapolations assuming constant surface area; the solid lines correspond to a model that assumes a shrinking radius, and therefore a surface area, decreasing with duration of degradative exposure. Figure from [19], CC BY 4.0.

The predominant type of plastic used in building construction is PVC, which is particularly susceptible to damage by solar UV radiation. The polymer undergoes photo-dehydrochlorination, releasing hydrogen chloride and yielding conjugated unsaturation. The PVC surface appears yellow to orange in colour on weathering, depending on the sequence lengths of the unsaturated units generated on the polymer molecules.

Degradation of the PVC surface releases the opacifier, titanium dioxide (TiO_2), compounded into the plastic and results in chalking or removal of the loose oxide on handling. However, it is the uneven discolouration of PVC products used in residential construction that determines their useful service life. Therefore, effective photo-stabilisers are critical to maintaining their outdoor service life under solar UV irradiation. In outdoor uses such as siding or panels, PVC is compounded with rutile titania as an opacifier and tin-based organic photostabilisers to control UV-induced degradation and thermal oxidation, respectively.

Several studies investigated the use of tin-based stabilisers for this purpose. A novel tin-based stabiliser, tin-sulfadiazine complexes, at a 0.5 wt.% in rigid PVC, reduced the dehydrochlorination rate constants to less than half that for control PVC samples in accelerated weathering studies [22]. Different organotin complexes with similar stabiliser function include fusidate [23], captopril [24], atenolol [25], mefenamic acid [26], naphthalene sulfonic acid [27], 4-methoxybenzoic acid [28], and carvedilol tin complexes [29]. While some of these show good stabiliser effectiveness, further development in terms of cost-effective manufacture and their environmental impacts will be needed before their commercialisation is considered.

In wood products, the photoreactions generally increase surface hydrophilicity that encourages subsequent biological degradation [30]. Using opaque or UV-absorbing surface coatings on wood ensures good stability under UV radiation [31]. However, the solvent-borne coatings contribute to the release of volatile organic chemicals (VOCs) into the atmosphere. Biodegradation, that also takes place concurrently on weathering can be controlled by treating the wood thermally or chemically. Chemicals typically used in treated wood (chromated copper arsenate, creosotes, and chlorophenols), however, can leach into the environment. As with plastics, the emphasis on developing sustainable strategies also guides the criteria in selecting coatings and stabilisers for wood, with candidates for substitutes of legacy additives such as plasticisers, fillers, thermal stabilisers, colourants, and flame retardants. The incidental effects of these 'greener' substitute additives such as natural oil preservatives on the UV-stability of wood still needs to be evaluated.

1.1   Building industry trends and materials use

Several emerging trends in the building industry will indirectly affect the mix of organic building materials to be used in future buildings. These may have important implications on their useful life under projected climate warming and increased UV radiation in areas of reduced cloud cover (Chapter 1, Bernhard et al. [32]). There are two such trends apparent in the building industry that may indirectly impact the choice of materials and their durability. Among these are 3-D printed homes and waste plastic utilisations in building technology. The trend in the building industry towards environmental sustainability encourages builders to qualify for LEED (Leadership in Energy and Environmental Design) [33] certification in the USA or BREEAM (Building Research Establishment Environmental Assessment Method) in Europe [34]. Carbon emissions in the sector are mostly due to the use of Portland cement and neither engineered wood products [35] nor plastic materials typically have comparably high carbon emissions. The ambitious LEED Zero program [33] aims at offsetting all energy, carbon emissions, and waste costs associated with future buildings.

A recent sustainable approach to building is 3-D printing that promises lower cost, comparable durability, and increased design freedom, with at least the same durability as conventional-built homes [36]. At this time these structures are mostly based on inorganic materials (mortar, clay, concrete), but plastic-based 3-D homes are feasible. At least two commercial operations, one using polyurethane-carbon fibre composites (PassivDom in Ukraine) and another using waste plastic as the primary material (Azure Homes, Los Angeles, CA) have started operations. With just $10 million revenue in 2020, the printed-home industry has a high compound annual growth rate of >91% in the near term with revenues increasing to over $1 billion by 2028 [37]. Using large volumes of plastics in printed homes would require managing the large VOC emissions, associated occupational hygiene concerns, waste disposal issues, and water contamination. While the approach will conserve wood, the effect of solar UV radiation on the entire printed plastic structure will need to be carefully evaluated in their use.

The recycled plastic waste is formed into plastic blocks or bricks for building [38], especially in emerging economies [39]. The mixed plastic waste stream composed primarily of PE, PP, PS, and PET will continue to increase in step with the world population and provide a low-cost reliable raw material. Being mostly thermoplastic, plastic waste can be readily melted into low-cost geocomposites for drainage systems and infill material for geosynthetic-encased granular columns [40]. Not only do they provide excellent durability at a low cost, but they also attain very significant labour savings in building operations compared to conventional materials. However, the material must be rendered fire resistant and the possibility of outgassing from slow degradation reactions in bricks needs to be addressed for the approach to be viable. Several commercial vendors offer such homes, including Conceptos Plásticos (Columbia) and Othalo (Norway). This trend will also reduce the demand for wood in buildings, contributing towards a more sustainable future.

1.2   Greener additives used in plastics and wood

An integral aspect of the drive toward sustainable building materials is the replacement of toxic legacy additives that are harmful to the environment with 'greener' alternatives [41-43]. In selecting additives, including UV-stabilisers [44] for plastics or coatings, increasing attention is being paid to minimising their potential ecotoxicity as these additives often leach out to contaminate the environment [45]. Wang et al. [46] reported the presence of UV absorbers at ~100 ng/g level in marine organisms including fish. In the plastics industry, this trend is illustrated by the phase-out of two classes of additives, phthalate plasticiser, and brominated flame retardants, a process

well underway in Europe, USA, and Japan. While greener additives selected for their functionality may improve the overall sustainability of plastics or coatings, their use may inadvertently compromise the UV-stability of materials, requiring a reassessment of the UV-stability of plastic compounds that carry the new 'greener' additives. However, the present phase of R&D appears to be primarily devoted to identifying substitutes with comparable functionality and increased sustainability. Two classes of additives, both toxic endocrine disruptor chemicals, that can potentially leach out to contaminate the environment [47], deserve special attention.

Of the 10.4 million metric tons (MMT) of plasticisers manufactured worldwide in 2021 [48], about 55 % were phthalates intended for use in poly(vinyl chloride) (PVC), primarily in the building and packaging sectors. Flexible PVC compounds that may carry up to 60 wt.% of phthalates account for 80-90 % of the consumption. Phthalates, identified as a common pollutant in the environment [49,50], are also endocrine disruptor (ED) chemicals, that may cause inter-generational adverse impacts on reproductive and neurological health, especially in children [51]. In July 2020, the EU restricted the use of bis (2-ethylhexyl) phthalate (DEHP), benzyl butyl phthalate (BBP), dibutyl phthalate (DBP), and di-isobutyl phthalate (DIBP) in consumer goods or products that posed risks to humans through dermal contact or by inhalation. Likewise, responding to consumer and regulatory pressure, the USA has restricted the use of particular phthalates in plastics.

The validation of sustainable alternatives for phthalates in PVC is well underway [52] and several classes of candidates have been identified: a) branched and hyperbranched plastics [53-55]; b) vegetable oil-based plasticisers [56,57]; and c) other promising compounds such as esters derived from biomass [58,59]. These are being evaluated for their efficacy as plasticisers, especially in PVC, and their migration resistance from moulded plastic products. While selected on the criterion of having effective plasticiser performance, these green substitutes can also affect the UV-stability of PVC. Encouraging results were reported for cardanol, a 'green' plasticiser for PVC derived from waste cashew nut shells, which also displayed UV-stabiliser properties that are superior to the dioctyl phthalate (DOT) it replaced [60].

Another class of additives being phased out because of their activity as endocrine disruptors and toxicity are flame retardants based on polybrominated diphenyl ether (PBDE) used at 10-20 wt.% in some plastic compounds [61-63]. As with plasticisers, the phase-out of PBDEs does not significantly reduce the levels of these compounds in the environment in the medium term, because of persisting residue from their early use since 2004 [64]. PBDE levels in human serum and breast milk are up to 160.3 ng/g [61]. The levels reported in e-waste workers in China are over twice that [65]. The concentration of PBDE replacements in the aquatic environment is higher than that of legacy PBDE's and these are often bio-accumulative [66]. Exposure to PBDE adversely affects reproductive and neurological health [67,68]. It is an additive listed in the Stockholm Convention and was phased out in the EU. In the USA, penta- and octa-PBDEs have been banned since 2004 [69], while the decabromo-PBDE, which was excluded, was regulated under the Toxic Substances Control Act in 2021 [70]. China, the largest producer and consumer of fire retardant chemicals, has regulated the levels of penta- and octa-PBDEs but only in electronic goods that use them in circuit boards [71].

Several 'greener' alternatives to PBDEs have emerged, including different (non-PBDE) brominated compounds, organophosphates [72,73], dechlorane compounds, and aluminium hydroxides [74]. The potential toxicity of the substitute fire retardants are being investigated [75]. The presence of conventional fire retardant additives in the compound often decreases the UV stability of polymers [76]. Whether or not the alternative fire retardants also have this problem has not been fully investigated.

2 Wood in building applications

Wood used in building applications, including that exposed routinely to the elements, is expected to be durable over extended periods. Solar UV radiation is well known to cause photodegradation of wood [77-79] as well as of protective paints and coatings used on wood products [80]. Routine exposure of wood to solar UV radiation results in the loss of both their aesthetic and mechanical properties [81]. These changes occur in in both natural and artificial weathering, primarily due to primarily due to photodegradation. Photodamage to wood surfaces is quantified as: a) changes in surface colour, an important criterion of consumer acceptability of wood [77,81-83]; and b) chemical analysis using Fourier transform infrared spectroscopy to assess the extent of oxidative changes [82,84,85]. In accelerated weathering of wood [86], a higher intensity of UV radiation and increased temperatures are typically employed, as with plastics; in some instances, a water spray is also used to simulate the effect of rain [87]. Photodegraded wood contains compounds extracted by water [85] making this a reasonable test parameter.

Cellulose and hemicellulose in wood (unlike its lignin fraction) are structurally saturated compounds carrying no chromophores. It is the absorption of solar UV radiation (290-400 nm) by lignin in wood that initiates the degradation and discolouration often accompanied by surface cracking [77,78,88]. Lignin is a strong light absorber with broad absorption in the UV-B (280-315 nm) and UV-A (315−400 nm) wavebands. Higher-density wood species appear to be relatively more stable against UV-induced colour changes [89]. Given the complexity of the mix of products formed and concurrent biodegradation of the surface, colour changes are only suited for assessing the early stages of weathering [78]. Preferential photodegradation of lignin leaves the wood surface rich in carbohydrate fraction,

which encourages biological decay [30]; non-degraded lignin, being phenolic in nature, is more resistant to microbial attack. The rate of photodegradation depends on the anatomical structure of wood species [88]. An exponential dependence of the rate of photodegradation of lignin with temperature was reported in a study based on changes in diffuse reflectance infrared spectroscopy [90]. Surface cracking due to destruction of the middle lamella (that holds adjacent cells together) with a high lignin content, is a major cause of the loss of mechanical properties [81] accompanying the weathering of wood.

Accelerated weathering in the laboratory, where the test conditions can be controlled, results in faster degradation than natural weathering. However, correlating durations of laboratory accelerated exposure with natural weathering remains elusive [91]. The correlation depends on the test parameters employed [92].

2.1 Thermal treatment for improved resistance to UV radiation

Heat-treated wood is a sustainable alternative to pressure-impregnated wood that is resistant to UV-induced and biological degradation. Environmental considerations have made the chemical-free heat treatment of wood an increasingly popular approach to increase durability. Subjecting wood to high temperatures under humid conditions in heat treatment results primarily in the cleavage of the acetyl groups of the hemicellulose fraction and its hydrolysis into oligomeric products. Thermal treatment yields appealingly darker [93,94] treated wood that is less hygroscopic and has improved dimensional stability [95]. Neural network-based algorithms that predict the properties of treated wood as a function of variables such as temperature, are being developed [96]. However, these improvements are obtained at the expense of its UV resistance with the treated wood discolouring readily on exposure to solar UV radiation [97,98]. Coating the treated surface can address this limitation. However, designing chemically coatings that adhere well to the hydrophobic surface of treated wood is a challenge, but several promising candidates have been identified.

Impregnating Scots pine wood with a titania sol in paraffin (at 212 °C) improved its UV resistance [98], with the colour change and lignin degradation reduced by more than 50 % with the treatment compared to the control, after 1176 h of accelerated weathering. Ashwood heat-treated at 192-212 °C and clear-coated with polyurethane coating also yielded good resistance to discolouration in laboratory exposure of up to 2000 h under UV-340 fluorescent lamps [99]. Further treatment of hardened surfaces with air saturated with steam at 95 °C to 135 °C enhances the colour stability of wood. For instance, change in surface colour after 298 h exposure to a xenon Weather-O-meter (simulates solar radiation with filtering systems designed for weathering) of untreated maple wood was reduced by 31.8, 43.8, and 61.1 % with steam treatment at 95, 115, and 135 °C, respectively [100]. While thermal treatment improves the desirable characteristics of wood, the accompanying reduced outdoor lifetimes under solar UV irradiation needs to be controlled using cost-effective surface coatings for wider acceptance of the approach.

2.2 Sustainable stabilisers derived from wood

As with plastics, sustainability considerations drive the search for non-toxic sustainable UV stabilisers for protecting the wood in outdoor applications. Plant-based compounds have shown promise as efficient UV stabilisers controlling surface discolouration in a range of wood species [101-105]. Flavonoids extracted from *Acacia confusa* heartwood significantly reduced the UV-induced degradation of lignin in wood [101]. Two most abundant flavones (okanin and melanoxetin) in *Acacia confusa* sp., have marked radical-scavenging and singlet-oxygen quenching properties [102]. Extractives of the wood of other species, such as that of Japanese cedar (*Cryptomeria japonica*) [106], Merbau (*Intsia* sp.) [31,107] *Dalbergia cohinchinensis* [31] as well as the bark of Trembling Aspen (*Populus tremuloides*), lodgepole pine (*Pinus contorta*), and western red cedar (*Thuja plicata*) [108] have all been demonstrated to have UV-stabilising activity either in wood or wood composites.

Wood bark extracts are particularly rich in polyphenols including condensed tannins and flavonoids, which are very good absorbers of UV radiation. For instance, a 1 wt.% solution of the extractive of *Phoebe zhennan* wood by polar solvent ethyl acetate completely absorbs solar UV-A and UV-B wavelengths in laboratory studies [109]. The extractives accounted for 3.8 wt.% of the wood. Such extracts can be used to stabilise surface coatings on wood as well. Polyurethane-acrylate wood coatings stabilised with 2 wt.% of the bark extracts from Chinese fir, for instance, effectively controlled the photo-discolouration of wood [108]. The colour change on exposure to a UV source for 898 h was reduced by ca 67 % compared to a control coated with polyurethane without any extractive. Also, extracts from the bark of alder and maritime pine species at a concentration of 5 % in alkyd-based coatings provided excellent UV-protection of Scot pine surfaces [110]. These stabilisers also work well in WPCs that also undergo UV-induced discolouration and loss of mechanical integrity [111]. Bark extractives from Western red cedar (*Thuja plicata*) at 2 wt.% mixed into bulk wood-plastic showed good stabiliser effectiveness, yielding about 25 % less discolouration at 1200 h of accelerated weathering, with less severe surface cracking and chemical degradation as indicated by Fourier transform infrared spectroscopy [1].

Lignin is the second most abundant biopolymer after cellulose in wood and is rich in UV-absorbing chromophores. It can therefore serve as a promising 'greener' substitute for synthetic UV-absorbers [112,113]. The UV-shielding properties of lignin depend upon its extraction process, methoxyl content, and the shape and size of lignin domains. Lignin NPs have even better UV-shielding properties. However, the undesirable dark colour of lignin is a drawback with lignin-based UV-absorbing products. Laboratory exposures of coatings with lignin NPs derived from waste wood on beech wood panels show good control of UV-induced discolouration [114].

2.3 Novel wood-based building materials

A novel, scalable, and optically transparent UV-blocking wood composite is a potential sustainable replacement for glazing (plastics or glass) in buildings and in greenhouse applications. Some of these novel transparent wood composite (TWC) materials have better UV

stability compared to polycarbonates used in glazing. In this technology, the lignin fraction of wood is replaced by either a synthetic [115] or a biopolymer [116,117], to obtain a composite of cellulosic materials and polymer (Fig. 2). For instance, a 2 mm thick sample of Douglas fir wood/epoxy TWC transmits 80 % of visible light but blocks UV radiation over the wavelength range of 200–400 nm [115]. A luminescent TWC was reported from Basswood with poly(methyl methacrylate) (PMMA) [118]. The synthetic fraction included the additives, ammonium polyphosphate (APP), and lanthanide-doped strontium aluminate (LSA; $SrAl2O4:Eu^{2+}$, Dy^{3+}) phosphor nanoparticles. The luminescent material is suited for applications such as smart windows, lighting, and safety directional signs in buildings. With good thermal stability up to 315 °C, TWCs can be designed to filter out UV-B radiation and have potential applications in smart building technology [119,120]. TWC materials based on biopolymers such as chitosan or cellulose in place of synthetic resins, have also been synthesised [116]. For instance the use of cellulose–lignin slurry from poplar wood displays high mechanical strength, excellent water stability, resistance to UV radiation, and improved thermal stability [121].

However, even with the chromophore-carrying lignin removed, TWCs still undergo some photo-discolouration and degradation on extended exposure to solar UV radiation [122,123] that might be due to photodegradation of residual lignin or the polymeric component (epoxy in this case). With extended exposure to solar UV radiation, the transparency of the material is compromised. This drawback, however, can be addressed using established UV stabiliser technologies. Blending 1.0 wt.% of a conventional UV stabiliser (2-(2H-benzotriazol-2-yl)-4, 6-di-tert-pentylphenol) into the epoxy resin used in epoxy/poplar wood TWC, reduced the loss in transmittance of visible light on weathering. For example, after 250 h of irradiation under UVA-340 fluorescent lamps, only a 1.4 % loss in transmittance was obtained with the stabilised TWC at 550 nm compared to a 27.5 % decrease in the untreated controls [122].
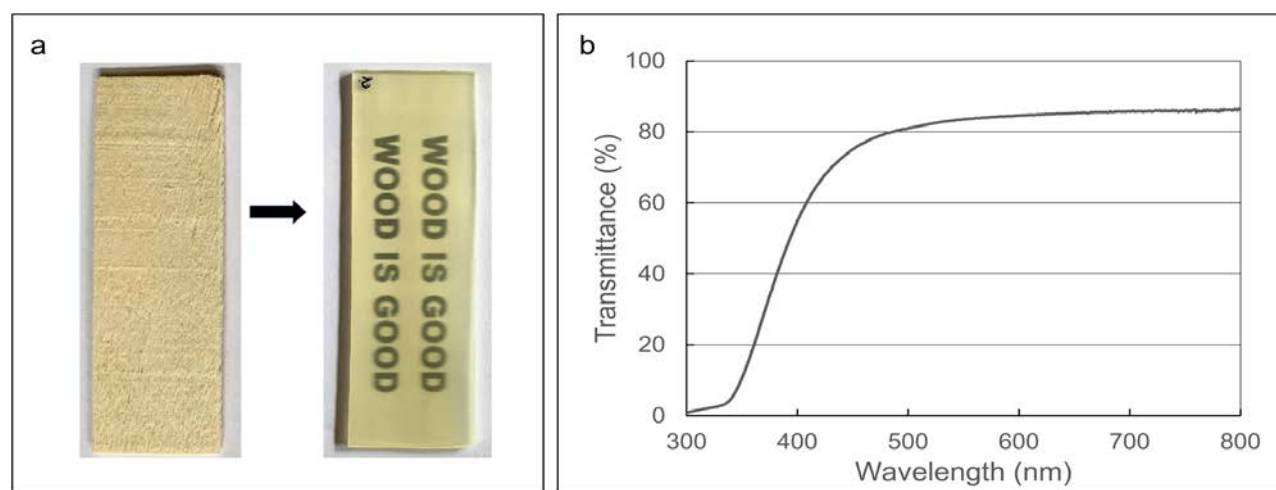
Fig. 2 (a) Piece of poplar wood (left) and piece of transparent wood composite (TWC, right) prepared using poplar wood and epoxy resin; **(b)** optical transmittance of TWC of 2 mm thickness.

3 Nanoparticulate filler-UV stabilisers

3.1   Nano-oxides and aramid fibres

Aramids constitute a high-value, high-performance class of industrial fibres that account for a few percent of the global synthetic fibre production. These fibres with exceptionally high strength (2.4-3 GPa) and modulus of elasticity (45-160 GPa) [124] are well suited for demanding applications such as bullet-proof vests, firefighter protective garments, and in military applications [125-127]. Nanofibres of aramids in the size range of 10-100 nm are also used to reinforce nanocomposites [128]. However, a significant drawback of the material is their inherent poor UV stability mostly because of their aromatic structural features, limiting their use in outdoor applications [129]. It is challenging to incorporate UV stabilisers into aramids, as organic compounds do not dissolve well in the highly crystalline fibre.

Nano-fillers of wide-band-gap oxides, which decorate the fibre surface or are grown on the fibre's surface [130] are especially effective stabilisers. Different strategies based on nanoscale oxide fillers are being developed to improve the UV stability of aramids.

Ma et al. [130] functionalised aramid fibres with nano-ZnO-structures grown on the fibre surface, resulting in improved UV resistance. After 168 h of UV irradiation under a 3-kW source with a wavelength range of 290–365 nm, the loss in tensile strength of the surface-modified was less than 5 %, while it was 20 % in the unmodified fibre. Seeding ZnO NPs onto aramid fibre surfaces coated with poly L-3,4-dihydroxyphenylalanine resulted in ZnO nanowires growing in the seeded layer as illustrated in Fig. 3 [131]. After 168 h of UV irradiation of 0.76 W m^{-2} nm^{-1} at 340 nm, the retention of the tensile strength for the modified oxide and control fibres was 97.2 and 80.4 %, respectively. ZnO NPs have also been crystallised onto aramid fibres by a sol-gel process with drying in supercritical CO_2. Subsequent exposure to UV radiation for up to 216 h, under a 40 W UV lamp (wavelength range 280–315 nm, complying with the Chinese Standard GB/T 14522-93) at 60 °C, the treated aramid fibres retained 93 % of their average tensile strength, while that of control fibres was only ca 25 % [132]. While the quantitative results of these studies are not comparable due to differences in the experimental settings, they indicate the potential of these techniques in improving the performance of aramid fibres in a way that could be transferable to functionalisation of other materials.

Sun et al. [129] used drying in supercritical CO_2 to improve the UV resistance and durability of aramid fibres treated with TiO_2 NPs. When exposed for 168 h under a UV-B lamp (40 W, wavelength range 280-315 nm, lamp length of 1220 mm, Dongguan Instrument Co. Ltd., Guangzhou, China; yielding an exposure of 40 W m^{-2} complying with the Chinese Standard GB/T 14522-93), absorption of UV-B radiation increased by ~15 % at a TiO_2 loading of 2.38 wt.% on the fibre surface. The tensile strength and modulus retention also improved by 5-14 %. Surface decoration of fibres with nano-oxides suggests a useful approach to improving the UV stability of other fibres. Where supercritical CO_2 is used, the technique needs to be evaluated for economic feasibility.
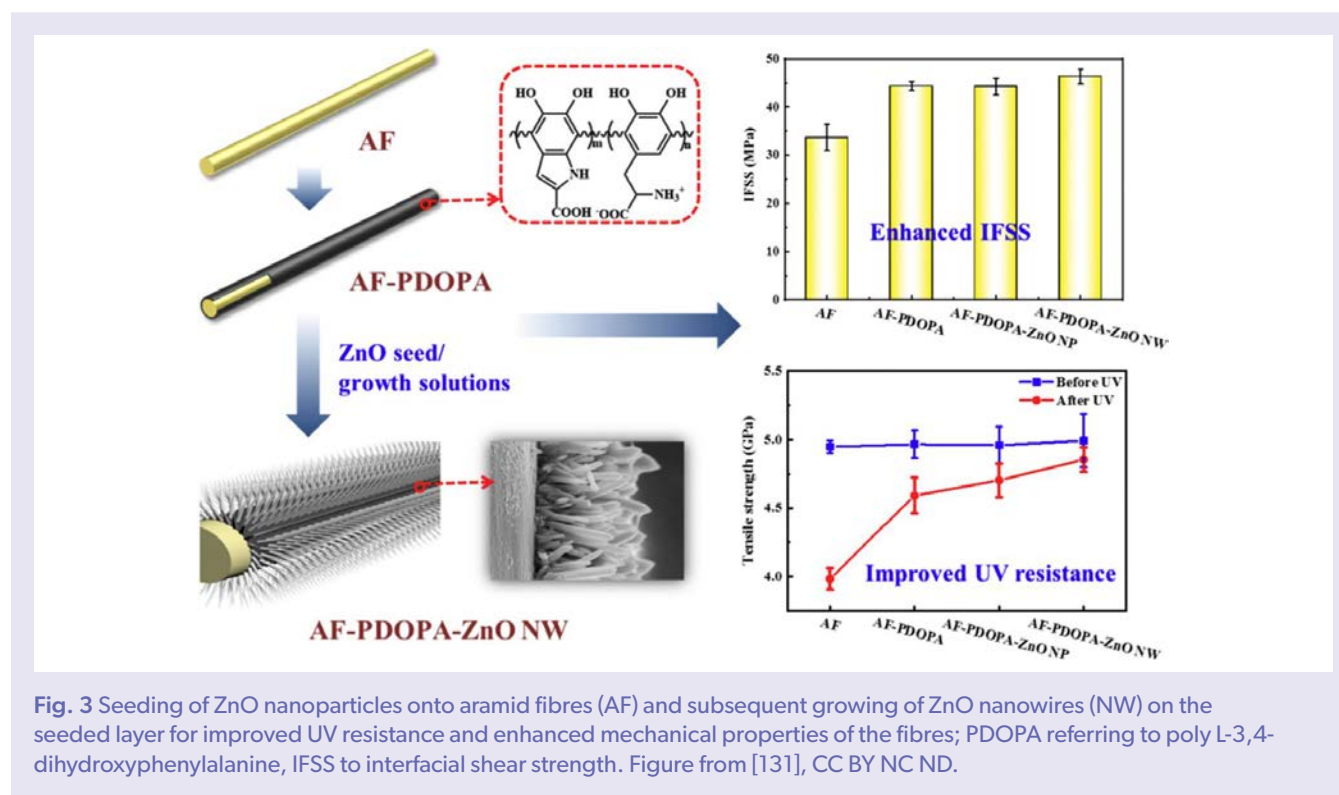
Fig. 3 Seeding of ZnO nanoparticles onto aramid fibres (AF) and subsequent growing of ZnO nanowires (NW) on the seeded layer for improved UV resistance and enhanced mechanical properties of the fibres; PDOPA referring to poly L-3,4-dihydroxyphenylalanine, IFSS to interfacial shear strength. Figure from [131], CC BY NC ND.

3.2   Nanocomposite films

Nanoparticle (NP) additives increasingly find application as UV stabilisers in films, as demonstrated by their use in greenhouse covers; for instance, incorporation of 2 wt.% each (total 6 wt.%) of ZnO, TiO_2, and SiO_2 NPs in a size range of 20-45 nm as light stabilisers, into PET films [133]. The mixture of three NPs improved the UV-blocking properties (94 % under UV-B and 60 % under UV-A radiation). A reduction of 57 % in UV-B and 36 % in UV-A transmission relative to that by a control film was achieved without affecting the high photosynthetically active radiation (PAR, 400-700 nm) transmittance of the film. Moreover, these properties persisted over 90 days of irradiation under a Xe lamp (Air Mass 1.5 Standard Spectrum, 60 W m^{-2}). Functionalised NPs, such as those coated to obtain a double-shell structure, are sophisticated nanofillers with tailored properties. ZnO NPs coated with amphiphilic polyurethane (APU) was investigated as a stabiliser in UV-cured poly(urethane acrylate) (PUA) [134]. Transparent polymer films with NP loading of 0.3 wt.% exhibited a >50 % increase in tensile strength and up to 80 % absorbance of UV-B radiation compared to the untreated PUA. The APU-functionalised ZnO are effective multifunctional fillers even at the low concentrations used in these studies. TiO_2 NPs have been

coated with SiO_2 and then poly(D-lactide) (PDLA) grafted onto the coated surface to obtain a double-shell (TiO_2@SiO_2-g-PDLA) hybrid nanoparticle [135]. When incorporated into a poly(L-lactide) (PLLA) matrix (at a loading of 2 wt.% TiO_2), the hybrid nanocomposite showed almost a 10-fold increase in UV absorbance at 350 nm relative to the untreated PLLA and with a higher tensile strength, even after 72 h irradiation under a 300 W UV lamp. Sophisticated core-shell or double-core-shell NPs used in these studies may be expensive relative to NP-fillers. The fact that they are used at such low weight fractions to obtain desirable multiple functionalities may offset their cost at least in some film applications.

3.3   Nanoscale carbon fillers in plastics

Carbon materials are excellent absorbers of both visible and UV radiation. They may also be used as reinforcing fillers in polymer composites. [136]. In addition to reinforcement, fillers like carbon nanotubes (CNTs) and graphene-family nanomaterials (GFNs) also impart increased UV stability to polymer composites. GFNs and CNTs are used, for instance, in batteries, sensors, and biomedical (antibacterial) applications. [137,138]. Because of their small dimensions, nanomaterials are very efficient in UV-shielding photostabilisation.

UV-resistant glass-fibre-reinforced composites have been produced by dispersing 0.25–1.0 wt.% of multi-walled carbon nanotubes in fibre-filled epoxy matrices [139]. When exposed under a UV radiation source (six spectral UVA-365 lamps with nominal wavelength 365 nm, Worldwide Specialty Lamp, Austell, GA, yielding 0.77–0.95 W m^{-2} nm^{-1} to comply with the ASTM specification of 0.89 W m^{-2} nm^{-1}) for 2160 h in cycles of exposure (4 h light and 4 h darkness), the filled composites showed very good UV resistance as evidenced by the absence of microcracks typically observed in untreated composite samples. Epoxy nanocomposites have been studied that contain 0.5 wt.% multiwalled carbon nanotubes (MWCNTs) (outer / inner diameter < 20 nm / 4 nm, length 1-12 µm) dispersed in the resin that was based on diglycidyl ether of bisphenol A (DGEBA) and cured with 2,2,4-trimethylene-1,6-hexadiamine (TMDA) [140]. These were subjected to accelerated weathering under UV-A lamps (140 W m^{-2} over 295–400 nm range) in alternating humidity and temperature conditions for a total irradiation time of 1-6 months. The DGEBA–TMDA/0.5 wt.% MWCNT samples displayed improved resistance against UV-degradation compared to the DGEBA–TMDA samples with no carbon filler. A novel UV-stabiliser for polypropylene has also been synthesised, based on functionalised graphene oxide (GO, thickness 3.4–7 nm, diameter 10–50 µm), where a hindered amine stabiliser was grafted onto GO nanoplatelets [141]. Samples of the plastic stabilised with 0.5 wt.% of GO and functionalised GO were artificially aged under OSRAM Ultra Vitalux 300 W sunlamp up to 600 h. The functionalised filler efficiently retarded the rate of photo-oxidation, as measured by the retention of tensile properties. Hybrids of graphene (8 nm flakes) and MWCNTs (length 5-15 µm, diameter 10-30 nm) have been used in waterborne polymer coating synthesised via mini-emulsion polymerisation [142]. Only 1 wt.% of hybrid G/CNT was used in the resin of 50 wt.% MMA and 50 wt.% butyl acrylate (BA). This was adequate to completely suppress photodegradation in accelerated aging of 400 h under a UV lamp (nominal wavelength 366 nm, P-Lab, 550 mW cm^{-2}, distance 15 cm) at 55 °C [142].

Studies reporting on the enhanced performance of materials with nanoscale carbon fillers are specific in terms of the size of the filler, the technique applied, the polymers and fillers used, the ageing conditions and the characterisation methods employed. However, it would seem that these kinds of fillers are finding more applications as the demand for more durable and more sustainable materials increases. In these recent studies it is significant that less than 1 wt.% of the carbonaceous filler was able to impart very significant improvements in UV-stability of the thermoset composites studied.

Graphene is currently used in electronics as well as in composites to take advantage of its unique electrical and reinforcing characteristics. The accompanying photo-stabilisation can be important in composite applications. High-volume use of graphene in composites is currently limited by the high manufacturing costs and uncertainties related to their lifetime, operational stability, and reproducibility [143]. In the future, graphene is nevertheless expected to find ever more applications (e.g., sensors, solar cells, and self-cleaning surfaces) [144-146].

---

4 Photovoltaic module components

Solar photovoltaic (PV) energy is a leading sustainable substitute for fossil-fuel energy and its rapid installation is critical to meeting the agreed-upon reductions in future global CO_2 emissions [5]. This will require the continuation of the accelerated growth of the PV industry globally. In 2020 there was ~940 gigawatt peak (GWp) of installed capacity. The newly installed 173 GWp in 2021 was the largest ever installed capacity in a single year. The continued competitiveness of PV power generation will be supported by the reduction in PV system costs by optimising manufacturing and having increased cell and module performance. The market is still dominated by crystalline silicon modules, but has shifted to mono-silicon cells with new cell types being commercialised. Bi-facial modules have been introduced in the market. The production capacity of PV has increased to over 470 GWp with the expansion of larger wafers and improved module area efficiency. Modules have grown in efficiency with passivated emitter and rear contact (PERC)

module and half-cell interconnect technologies. Maintaining long service lifetimes with minimal failure rates for PV modules is essential to meet the ambitious rates of growth expected of the technology [147]. Given the recent large-scale installations of PV modules and their long lifetimes (warranties of 25-30 years on performance), accelerated laboratory testing is also used in addition to field data to identify potential degradation mechanisms and failure risks. Accelerated laboratory testing has been changing to better understand the different degradation mechanisms that are present in PV modules; however, these types of testing do not always provide accurate prediction of degradation under in-use conditions and correlation between accelerated testing and in-use conditions is still lacking [148,149].

The basic structure of a crystalline silicon PV module is shown in Fig. 4. The encapsulant is a protective adhesive layer of a soft polymer that is used to cover the top and the bottom of the active layer (the solar cells). The encapsulant provides electrical insulation and physical support for the fragile cells and has historically been made of ethylene vinyl acetate (EVA) copolymers. A second plastic component is the backsheet, which provides environmental protection for the module and safety for humans to the high voltage. It is typically made of three polymer layers (outer or air-side, core, and inner layer construction) with the inner layer typically consisting of PET. In the majority of backsheets, the multiple layers are combined with an adhesive layer while some backsheets are coextruded [150]. Encapsulant and backsheet materials are key to ensuring PV module lifetime and are major components of the cost of the module. Degradation in each component layer in a PV module can accelerate degradation in other component layers (Fig. 5).

Transparent EVA is the most common encapsulant and will continue to be the most widely used encapsulant (~52 % in the next 10 years). Additionally, EVA with TiO_2 filler (white) will claim ~10 % of the market share to be used with bifacial cells. Polyolefin is expected to be 20 % and extruded EVA with polyolefin ~10 % in the next 10 years [147]. Polymer backsheets will continue to be the most common materials, with PET core-layers continuing to be used to provide electrical resistance, and with the outer-layer of poly(vinylidene difluoride) (PVDF) as the main backsheet type. However, in the next 10 years polymer backsheets are expected to decrease from ~75 to 45 % of the market share with glass-glass modules increasing over that time [147]. Solar UV radiation-induced degradation of these plastic components is a major factor in PV module failure [151] and many material failures in PV modules observed in the field involve encapsulant degradation, backsheet failure, or de-bonding of elements due to adhesive failure [151-154].

4.1　Durable encapsulation strategies

It is critical to select encapsulants that are durable under continuous outdoor exposure; discolouration of encapsulants accounts for about 10% of the module failure [153]. Transparent EVA is the most common encapsulant in PV modules [147]. Still, there is a need for a more durable, UV-stable material for next-generation encapsulants. Degradation of EVA encapsulant appears to be a complex inhomogeneous process involving solar UV radiation, temperature, and moisture. The installation location and how the modules are installed, especially their tilt angle (e.g., normal through 90°) can affect the amount of UV irradiance the module is exposed to [155]. The overall microclimate or stressor conditions within a PV module are non-uniform due to differences in moisture ingress, oxygen diffusion, module temperature, and physical strain within the module. There is a relationship between the photodegradation of the frontside EVA encapsulant and the location of the EVA in the module. Oxygen and moisture diffuse through the backsheet and the edges of the module; therefore, frontside EVA has lower transmittance at the centre of the cell compared to the edges of the cells. This is due to oxygen bleaching of photodegradation produced chromophores [156]. EVA is impacted on the edges of the solar cells more so than other locations, resulting in the formation of acetic acid, which leads to corrosion of metallisation and power loss [157]. A range of EVAs with different copolymer compositions are available commercially. Based on an accelerated weathering study of several candidate EVA copolymers, one with 18–33% by weight of vinyl acetate was found to be the most UV stable, making it potentially well suited for PV use [158].

The ongoing effort to find a better replacement for the encapsulant material has yielded several candidate polymers, such as ionomers and thermoplastic polyolefin (TPO) [159]. TPO has been investigated as an alternative to EVA [160,161] and has superior thermal stability, adhesive strength and resistance to discolouration. For instance, the discolouration of TPO on exposure to UV radiation of 365 nm from an LED light source at 900 W m^{-2} at 90 °C and 10-13 % RH was found to be nine times slower relative to EVA, and the polymer may also be easier to process [160]. While the initial research on TPO is promising, developmental work to validate its efficacy and economic feasibility is necessary especially in field studies of operational PV modules [162].

Among the candidate polymers being investigated is thermoplastic polyurethane (TPU). A multi-laboratory study compared five representative formulations of EVA encapsulants to TPU encapsulants of unknown formulation. Different sources including xenon, UVA 340, and metal-halide lamps with different filter types were used in the study. Samples were continuously exposed for 180 days at a relative humidity (RH) ranging from 7–50 % and temperatures from 40 – 90 °C. The encapsulants, EVA and TPU, exposed in the dark conditions showed minimal degradation compared to those exposed to UV radiation, which drives degradation. UV radiation-induced degradation was synergistically impacted at higher temperatures and humidity over the duration of exposure. The TPU in this particular study had the largest decrease in transmittance compared to the EVA formulations. The variability in degradation behaviour of the five EVAs suggests that their copolymer composition, residual monomer, and additives are important determinants of their UV degradation behaviour [163]. The synergy between UV radiation and temperature identifies climate change as a possible risk factor in reducing the service lifetime of these modules.

The UV degradation of four different encapsulants, TPO, TPU, silicone, and EVA was determined under accelerated aging while laminated between glass. A 1000 W Hg-Xe arc lamp was used with an accelerated exposure over 1694 h. This was calculated to be equivalent to 2.74 years of natural exposure to UV radiation in Atacama Desert conditions, corresponding to 1.34 years of UV-A and 24.7 years of exposure to UV-B radiation [164]. The TPU and silicone candidate materials yielded a 5 and 0.9 % loss in the transmittance

in visible light, respectively. TPO and EVA underwent similar chemical changes determined by Raman spectroscopy, but EVA showed a slightly lower reduction in light transmittance [164]. One study suggests that the more UV-transparent the encapsulant is, the higher the short circuit (I_{sc}) losses in heterojunction (HJT) PV cells will be, which is not the case with other architectures [165]. Although silicon HJT cells are presently a small fraction of the commercial PV market, they are currently being considered as the next step in technology because of their ability to respond to a broader spectrum compared to current PERC technology [147]. This suggests that UV radiation through the encapsulant has different degradation on the cell technology.

4.2   Durable backsheets

The most common types of backsheet have an outer layer made of either PVDF, PET, polyvinyl fluoride (PVF), polyamide (PA), or fluoroethylene vinyl ether (FEVE). Additional research on new types of backsheets is underway [166]. These polymeric backsheets can fail if they crack due to environmental degradation, leading to potential electrical leakage causing PV modules to be replaced or repaired to address the safety concern [154]. Repairing defects in PV module backsheets in the field has become a new approach in order to prevent the need to fully replace existing installed modules [167,168]. Backsheets are exposed to UV irradiance from the front side of the PV module in between the PV cells and from the rear-side albedo. White backsheets often turn yellow due to UV degradation and although these backsheets do not have an optical function, yellowing can cause an aesthetic problem especially in PV modules mounted in car parks. Importantly, yellowing is an indicator of degradation in progress of the backsheet, which can lead to more severe degradation. Advanced stages of degradation lead to delamination, embrittlement, or cracking resulting in the backsheet no longer providing electrical insulation [154,169-171]. Cross-sections of weathered-adhered laminate sandwich constructions of a PV module (glass/encapsulate/backsheet), using spatially resolved fluorescence imaging, for instance, show disproportionately high UV radiation damage to the adhesive layers [170].

The drive to reduce cost in PV modules is one reason for the use of materials of relatively lower UV stability in PV modules. Backsheet design would benefit from inherently more UV-stable outer layers, such as fluoropolymers. The addition of UV stabilisers in these long-lived materials is problematic due to stabiliser loss by leaching and bleaching over the greater than 25-year lifetime [172]. However, many backsheets are now coextruded, which removes the need for adhesive layers between the three layers.

The backsheets installed in PV modules in commercial fields had non-uniform degradation at the edges of racks/rows due to the increased UV albedo from the ground that is reflected on the backsheets that are less shaded than the interior of the modules [173-176]. The ground cover under the backsheets influences the amount of reflected UV radiation on the backsheet. For example, grass has a lower albedo than white rock [173,175] and leads to less degradation by UV radiation on the backsheet. The mounting configuration and module design could be improved to reduce the effect of the UV albedo on PV module backsheets [173,175,177]. The rear-side albedo (visible irradiance) helps increase power production in bifacial PV modules and sites would be designed to maximise albedo. This needs to be considered in bifacial modules with transparent polymeric backsheets [174].

The stability and insulation efficiency of the backsheet is related to the choice of encapsulant in the module. UV-induced degradation coupled with hydrolysis of EVA can produce acetic acid that can affect the backsheet, as illustrated by the crack formation in polyamide backsheets [170,178-180]. EVA copolymer is sometimes used as an inner layer in multi-layer backsheet construction. The EVA inner layer on exposure to UV radiation causes polyamide to crack [178,179]. In these complex systems, it is very important to study the interfaces between layers because degradation in one component can initiate additional degradation in other components. This means that accelerated testing needs to account for the synergistic impacts of the system and changes to materials in a PV module can impact the lifetime of other materials. Currently ~12 GW of installed modules with polyamide backsheets have failed due to cracking, which has a large impact on the installed PV power plants [180].

Backsheets with a PET outer layer readily undergo degradation under exposure to UV radiation as demonstrated in a study conducted in the NIST Simulated Photodegradation via High Energy Radiant Exposure (SPHERE) weathering chamber (170 W m^{-2} irradiation with a wavelength range of 290–400 nm) for 1800 h [181]. However, this surface degradation has not been shown to impact electrical output of the module. Upon UV degradation, (PET)/PET/EVA backsheets developed surface cracks (in the white TiO_2 filled PET outer/air-side layer) [182]. Cracking was absent in samples aged without UV irradiation. Moisture and UV irradiance appear to have synergistic roles with UV radiation initiating the surface cracking, while moisture enhances the surface degradation, decreasing the fracture toughness [182].

Novel transparent backsheets designed to work specifically with bifacial PV cells and modules are being introduced. These modules will collect the reflected albedo light on the back side of the module to increase power generation per unit area. Bifacial modules have been designed with the back surface metalised. Three types of transparent backsheets (outer/core/inner) have been tested including a PVF/PET/FEVE1 coating backsheet, PVDF/PET/FEVE2, and a FEVE3/PET/ EVA [183]. The backsheets and laminates (glass, encapsulant, transparent backsheet) were exposed to UV irradiance in the NIST SPHERE under ca 140 W m^{-2} (295 to 400 nm) at 75 °C/50 % RH (transparent films) and 65 °C/50 % RH (laminates). For all three backsheets, the PET core layer demonstrated the greatest material property changes after UV irradiation. This layer is the most susceptible to degradation by UV radiation. After exposure to the radiation, the outer layer of the fluoropolymer showed an increase in modulus and hardness, indicating this layer had become brittle due to degradation. The FEVE3/PET/EVA showed the most deterioration in optical, chemical, mechanical, and thermal properties after exposure, which eventually led to cracks within layers of the PET core, adhesive, and EVA inner layers, while the FEVE outer layer largely remained intact.

4.3   Cable sheath

Contributing to electrical power loss in PV systems and in electricity transport is the degradation of cable sheaths, which cause power loss and safety concerns. These undergo oxidation under solar UV irradiation causing brittleness [184,185]. For instance, crosslinked polyethylene (XLPE) material, widely used for manufacturing high-voltage cables as an electrical insulation material, was exposed to 36 W low-pressure vapour fluorescent lamps with radiation ranging from 350 to 400 nm for 200 h, resulting in a change in colour from grey to dark yellow following the exposure [186]. Photo-oxidation results in polymer chain breakage and the formation of unsaturated groups, such as vinylidene and vinyl groups in the PE. After weathering exposure, the surface of the XLPE insulating material is rough and degraded. The surface becomes non-uniform, since the material is semicrystalline and photo-oxidation occurs preferentially in the amorphous region. These surface changes from laboratory-based exposure lead to fatigue in the XLPE surface resulting in breakage in the insulating material [186].
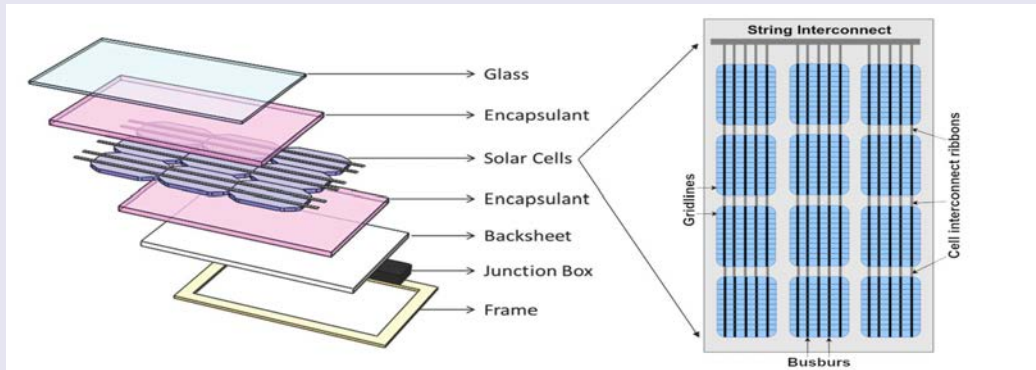
Fig. 4 Components of a crystalline silicon photovoltaic (PV) module illustrating the placement of encapsulants and backsheet, both made of plastic materials prone to degradation by solar UV radiation (modified from [187]).
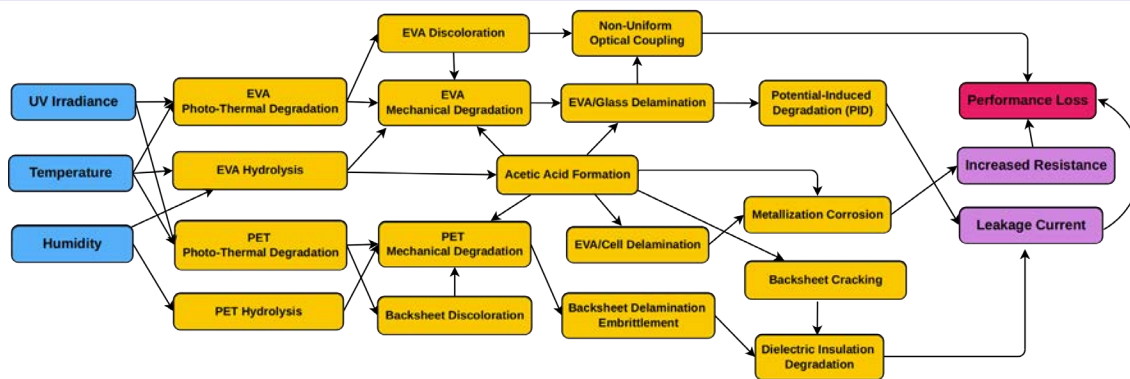
Fig. 5 An example of potential degradation pathways in a photovoltaic (PV) module showing that there are synergistic effects from different stressors (blue) including ultraviolet (UV) radiation that lead to degradation mechanisms and mode (orange). This degradation then causes overall performance loss (purple, red) such as power loss in PV modules (modified from [187]). PET, poly(ethylene terephthalate); EVA, ethylene vinyl acetate.

5 Micro- and nano-particle and composite fibres

Nanoparticles are used to coat or decorate the surface of textile fibres to impart specialised properties to the fibre and fabric such as antibacterial action using silver particles [188,189], wound healing [190], and solar energy harvesting [191]. When the NPs are also UV-absorbing or scattering, these fabrics display incidental UV-shielding to protect wearers from solar UV radiation. For instance, textile fibres surface-coated with silver NPs for antibacterial performance also provide a high degree of UV-screening because of the opacity of the particles [192]. However, the decorating NPs can also be selected primarily for their UV-screening to develop effective fabric. The approach is not entirely novel, but the use of well-defined nanoparticles provide impressive UV-shielding (Table 1). The UV protection factor (UPF) quantifies the efficiency of the fabric, and would also depend on weave characteristics; a UPF of x would mean that only 1/x of the solar UV-A and UV-B radiation would be transmitted through the fabric.

5.1 UV-protection fabrics based on nano-oxides in textile fibres

UV-absorbing oxide particles used either as a nanofiller or surface application to decorate the fibres can decrease the UV transmittance of fabrics incorporating them [193-196], as shown in Fig. 6. Their use is an effective and practical strategy in UV-protective fabrics. As the UV-shielding capacity of the oxide particles is determined by their specific surface area, using nanoscale particles obtains very effective UV-protection at low loadings. In general, it is the TiO_2 [197-200] and ZnO [201-203] that are mostly used as nanoparticles applied to increase the UV protective properties of fabrics and fibres, although MgO [201] and Ag nanoparticles [204] are also used for UV blocking. Exceptional UV blocking film is achieved by using TiO_2 nanoparticles [198]. Table 1 summarises the use of oxide nanoparticles in textile fibres/fabrics and their UV-shielding effectiveness. The high UPF values of the fabric at low nanoparticle loadings (Table 1) illustrates the efficacy of this approach.
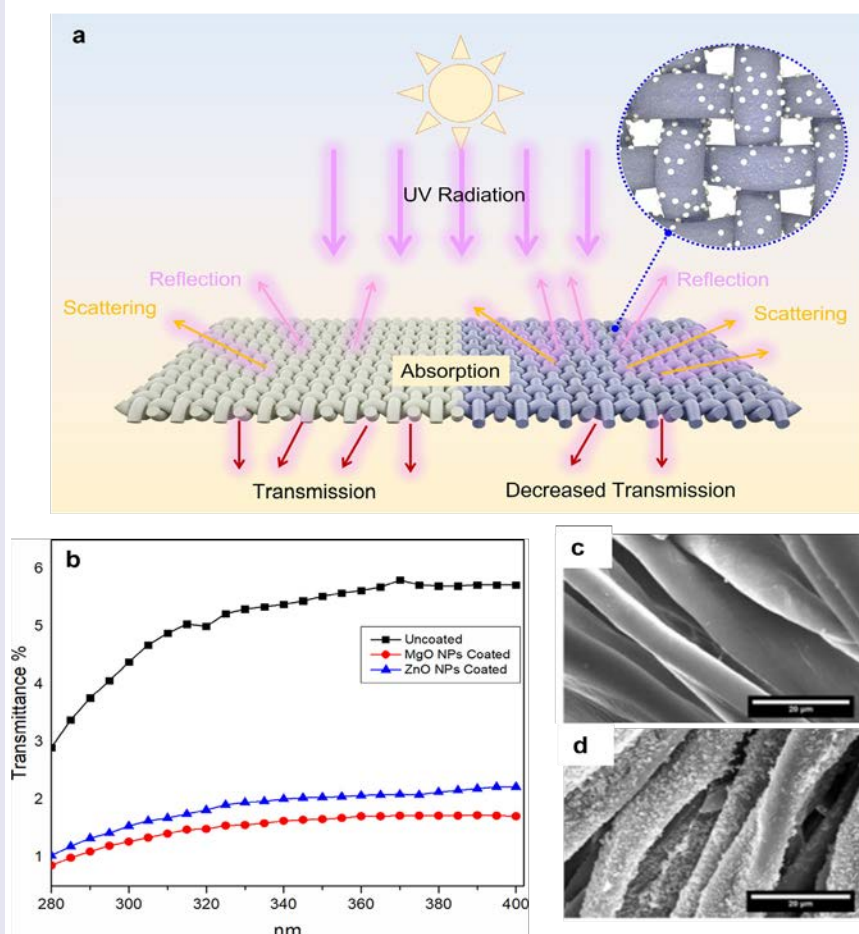
Fig. 6 (a) Illustrated ultraviolet (UV) shielding mechanism of the textile fabric treated with oxide nanoparticles (right) by scattering, absorbing, or reflecting the UV radiation when compared to the untreated fabric (left). (b) UV transmittance spectrum of cotton fabric treated with 2 % ZnO NPs, with a crystallite size of 20 nm and an aggregated particle size of 80-85 nm; or 2 % MgO NPs with a crystallite size of 9 nm and an aggregated particle size of 30-40 nm. Adapted from [201]. (c) and (d) SEM images of cotton fabric without (c) and with (d) decorated ZnO nanoparticles. The precursor solution (0.1 M zinc salt) was sonicated with fibres for 1.5 h to obtain the particle density shown in (d). Scale bar is 20 μm. Adapted from [202].

Personal thermal-management textiles are considered as next-generation textiles [205,206] and usually consist of multi-layered fabric constructs [207] that can block UV radiation while transmitting visible and reflecting near-infrared light [208]. One design approach is to incorporate nanofillers in some of the layers. For example, strong UV reflection was provided when TiO_2 NPs were used to form a composite woven textile based on poly(lactic acid) fibres in a multilayer metafabric consisting of two layers [209]. A hybrid film made with cellulose nanofibre (CNF)/antimony tin oxide (ATO) also blocks 91.07 % UV radiation, reflecting 95.19 % near-infrared (NIR), and transmitting 44.89 % visible (VIS) light [208]. Such films or fabrics not only can be used in textiles but also can be applied as window thermal barrier films [208].

Table 1 Nanoparticles used as surface treatment on textile fibres to increase their UV-shielding.

Materials	Particles			UPF (max)	Comments	Reference
	Type	Size	Amount			
Cotton fabric	TiO_2	17.9 nm (crystallite)	2.61 % Atomic Ti	220	Maintained appreciable UPF after 15–20 washing cycles	[199]
Cotton fabric	TiO_2	90–150 nm	Treated with 1 % wt./v TiO_2 NPs sol.	277	UPF reduced by 64.9 % after 15 wash cycles	[197]
PVDF film	TiO_2	TiO_2 pigment	10.55 % Atomic Ti	Only 0.01% UV transmittance in the entire spectrum	Less strength loss after natural weathering for 30 days	[198]
Poly(ethylene oxide) (PEO) nanofibre	TiO_2	100 nm	3.81% Atomic Ti	2751.65	Transmittance values of UV-A & UV-B reduced to 0.0525 % and 0.0207 %	[200]
Cotton fabric	ZnO	20 nm (crystallite); 80–85 nm (agglomerated)	Treated with 2 % ZnO NPs sol.	58	Significantly enhanced self-cleaning/stain removal properties	[201]
Cotton fabric	ZnO	38 nm	22.8 % Atomic Zn	102.88	Little decrease in UPF after 20 washing cycles	[202]
Cotton fabric	ZnO	35–42 nm (crystallite), 2405 nm (aggregate)	Treated with 20 mM Zn^{2+} precursor sol.	>96 % blocking in UV-A and UV-B wavebands	Good efficiency in methylene blue (MB) degradation, self-cleaning properties	[203]
Cotton fabric	Ag	35–80 nm	Treated with 4 wt.% silver carbamate sol.	2396	Improved photochemical degradation of MB under UV radiation	[204]
Cotton fabric	MgO	9 nm (crystallite); 3040 nm	Treated with 2 % MgO NPs sol.	71	Significantly enhanced self-cleaning/stain removal properties	[201]

5.2   Solar UV radiation generates micro- and nanofibres and particles

Textile fibres in fabric exposed to solar UV radiation for extended periods of time can fragment and, because of the uniaxial orientation of polymer molecules, yield microfibres (MF) or nanofibres (NF) as reported for wool and synthetic fibres [210,211]. The ecotoxicological effects of MFs are still largely unproven [212-214]. However, there is some concern for ecological effects given that microplastics by weight were estimated to exceed that of zooplankton in surface waters of the North Pacific sub-tropical circulating ocean current [215].

However, not all types of plastics readily photo-fragment into MFs or NFs. For instance, a laboratory exposure of different types of plastic pellets for a duration equivalent to 44 days of natural weathering in simulated seawater showed that the pellets of HDPE and nylon 6 degraded into MFs, but high impact PS and PP pellets under the same conditions did not generate MFs [216]. However, the study employed a photoreactor with UV-C radiation not found in solar radiation, and whether MFs will be derived from virgin pellets

undergoing photodegradation in nature is unclear. Macrofibre-yielding MFs under mechanical stress or photodegradation is to be expected. Wool and synthetic textile fibres (~2 mm long) exposed to simulated solar (Xenon source) radiation in natural seawater (for a duration equivalent to 1.5 years of natural exposure) showed such fragmentation [211]. Scanning electron micrographs showed evidence of fragmentation into microfibres of short fibres of PET and those of wool in less than two months of exposure to the simulated solar radiation. The exposure to the simulated solar radiation also resulted in the release of additive chemicals such as stabilisers and degradation products of PET, including glycol and terephthalic acid [211]. Generally, leached additives from plastics will also be prone to UV degradation, but the rates of their photoreaction and toxicity of any intermediates are unknown. While the UV wavelengths primarily responsible for this fragmentation are unknown, UV-B radiation is a good candidate, since it promotes oxidation of plastics. MFs can also be generated without the involvement of UV radiation, due to mechanical stress, for instance during laundering [217-220]. It is worth noting that the widespread use of face masks and personal protective equipment during the spread of COVID-19 aggravated the plastic fibre pollution and biomedical waste worldwide [221-224].

A similar environmental issue is posed by nanocomposite materials including composite fibres, where the release of nanoscale particles can occur during use (especially working) and with weathering [225]. For example, PP-CNT nanocomposites loaded with MWCNTs released both carbon nanofiller, plastic fragments, and metal (used as a catalyst in nanotube manufacture) when exposed to simulated solar radiation and subjected to mechanical stress [226].

5.3   Role of UV radiation in the fate of micro- and nanoplastics in the environment

It is well established that solar UV radiation facilitates the fragmentation of plastic litter in land and aquatic environments. With micro- and nanoscale plastics reported in food, water, human blood, and placenta in recent studies, this effect of UV radiation is receiving close attention. Photodegradative chemical changes on the surface of plastics also influence the diversity and rate of foulant species settling on them in aquatic environments. The composition of the foulant layer determines the rates of biodegradation and especially biomineralisation, and these processes are modified by UV radiation. The sorption of environmental pollutant species including antibiotics, endocrine disruptor chemicals, and metals by plastic debris may also be modified by UV radiation.

6 Knowledge gaps

Even though the degradation of plastics on exposure to solar UV radiation has been widely studied, some fundamental questions remain unanswered. Data on how the common additives used in plastic compounds affect the action spectra of deterioration of key properties of materials and how they change the dose-response of those properties are not available. Another knowledge gap is the synergistic effect of UV radiation and other weathering agents (e.g., moisture, heat, and air pollutants). Furthermore, reciprocity data that would help better relate the results of accelerated weathering to weathering in outdoor service environments are scarce. In wood materials, the chemistry of UV-induced degradation is relatively better understood but the variability between the diverse commercial wood species has not been adequately explored. An especially promising area of investigation might be the wood-derived antioxidant and UV-stabiliser compounds that can serve as sustainable replacements for the current conventional, often toxic additives.

Use of nanoscale pigments in plastics, textiles, and coatings have been increasingly advocated to protect these materials from UV radiation and to improve other properties. However, disposal and release of nanomaterial during use and at the end of service life remains a concern. The environmental effects of these nano materials are still not clear.

7 Conclusions

The service lives of materials routinely used outdoors are limited by the rate of their solar UV radiation-induced degradation as well as by ambient temperatures and are therefore closely linked to the amounts of exposure to UV radiation and climate change. Long service lifetimes of outdoor materials are critical in photovoltaic energy technologies and in building construction. While efficient UV-stabiliser technologies are available to address weathering degradation of materials such as wood and plastics, they invariably add to the lifetime costs of the relevant products. The role played by the Montreal Protocol as well as any measures on climate change mitigation are therefore directly pertinent to economic use of materials. Emerging UV-screening technologies for use in plastics and in wood coatings assessed in this assessment offer promise, but often require further techno-economic validation before commercialisation.

Development of high-efficiency UV-protective fibres is also an important aspect of the effect of solar UV radiation on the use of materials. There has been considerable progress on developing fibres with high-UPF values for textiles since our last Quadrennial Assessment ([227]). Again, their commercialisation requires information on launderability, retention of UPF, and potential release of nanoparticle additives into the environment. With the use of nanocomposites and coatings that incorporate nanoscale pigments, release of nanoscale particles during use or disposal of the products is an emerging concern. When plastics undergo UV-facilitated weathering they undergo fragmentation releasing microplastics and nanoplastics into the environment.

8 Montreal Protocol and the Sustainable Development Goals

Several of the United Nations Sustainable Development Goals (SDGs, adopted as part of the 2030 Agenda, [228]) are aligned with the Montreal Protocol and its Amendments aiming at protection of the stratospheric ozone layer and mitigation of climate change through phase-out of ozone-depleting substances and their replacements, many of which have large global warming potential. Issues addressed in this assessment are connected to sustainability of energy production (*SDG 7: Affordable and clean energy / Goal 7a*) and safety of the built environment (*SDG 9: Industry, innovation, and infrastructure / Goals 9.1 and 9.4*). In addition, they contribute to evidence-informed policies to be followed when formulating sustainable strategies for production of materials that are needed for our everyday commodities and the infrastructure around us (*SDG 17: Partnership for the goals / Goal 17.14*).

References

1. Peng, Y., Wang, Y., Zhang, R., Wang, W., & Cao, J. (2021). Improvement of wood against UV weathering and decay by using plant origin substances: Tannin acid and tung oil. *Industrial Crops and Products, 168*, 113606. https://doi.org/10.1016/j.indcrop.2021.113606

2. FAO. (2018). *Global Forest Products Facts and Figures 2018. FAO Report*. Food and Agriculture Organization of the United Nations (FAO).

3. BIR. (2020). *Recycling Plastics: Facts Data Policy recommendations. A report by the Bureau of International Recycling*. https://www.bir.org/publications/facts-figures/download/737/1000000832/36?method=view

4. Gamboa, C. (2020). Towards zero-carbon building. https://www.climate2020.org.uk/towards-zero-carbon-building/.

5. IEA. (2021). *World Energy Outlook 2021, Paris,* International Energy Agency, https://www.iea.org/reports/world-energy-outlook-2021

6. Sahoo, K., Bergman, R., Alanya-Rosenbaum, S., Gu, H., & Liang, S. (2019). Life cycle assessment of forest-based products: A review. *Sustainability, 11*(17), 4722. https://doi.org/10.3390/su11174722

7. Khan, M., Hussain, M., Deviatkin, I., Havukainen, J., & Horttanainen, M. (2021). Environmental impacts of wooden, plastic, and wood-polymer composite pallet: A life cycle assessment approach. *The International Journal of Life Cycle Assessment, 26*(8), 1607–1622. https://doi.org/10.1007/s11367-021-01953-7

8. Deviatkin, I., & Horttanainen, M. (2020). Carbon footprint of an EUR-sized wooden and a plastic pallet. In *2019 7th International Conference on Environment Pollution and Prevention (ICEPP 2019)*, (Vol. 158, pp. 03001, E3S Web of Conferences): EDP Sciences. https://doi.org/10.1051/e3sconf/202015803001

9. Asdrubali, F., Roncone, M., & Grazieschi, G. (2021). Embodied energy and embodied GWP of windows: A critical review. *Energies, 14*(13), 3788. https://doi.org/10.3390/en14133788

10. Korody, N. (2022). World's tallest wood building constructed in Vancouver. Archinect. https://archinect.com/news/article/149968916/world-s-tallest-wood-building-constructed-in-vancouver. Accessed Sep 20 2022.

11. Ainali, N. M., Bikiaris, D. N., & Lambropoulou, D. A. (2021). Aging effects on low-and high-density polyethylene, polypropylene and polystyrene under UV irradiation: An insight into decomposition mechanism by Py-GC/MS for microplastic analysis. *Journal of Analytical and Applied Pyrolysis, 158*, 105207. https://doi.org/10.1016/j.jaap.2021.105207

12. Jamal, M., Lanotte, M., & Giustozzi, F. (2022). Exposure of crumb rubber modified bitumen to UV radiation: A waste-based sunscreen for roads. *Journal of Cleaner Production, 348*, 131372. https://doi.org/10.1016/j.jclepro.2022.131372

13. Turner, A., & Filella, M. (2021). Polyvinyl chloride in consumer and environmental plastics, with a particular focus on metal-based additives. *Environmental Science: Processes & Impacts, 23*(9), 1376–1384. https://doi.org/10.1039/D1EM00213A

14. Vohlídal, J. (2021). Polymer degradation: A short review. *Chemistry Teacher International, 3*(2), 213–220. https://doi.org/10.1515/cti-2020-0015

15. Brostow, W., Lu, X., Gencel, O., & Osmanson, A. T. (2020). Effects of UV stabilizers on polypropylene outdoors. *Materials, 13*(7), 1626. https://doi.org/10.3390/ma13071626

16. El-Hiti, G. A., Ahmed, D. S., Yousif, E., Al-Khazrajy, O. S., Abdallh, M., & Alanazi, S. A. (2021). Modifications of polymers through the addition of ultraviolet absorbers to reduce the aging effect of accelerated and natural irradiation. *Polymers, 14*(1), 20. https://doi.org/10.3390/polym14010020

17. Koriem, A., Ollick, A., & Elhadary, M. (2021). The effect of artificial weathering and hardening on mechanical properties of HDPE with and without UV stabilizers. *Alexandria Engineering Journal, 60*(4), 4167–4175. https://doi.org/10.1016/j.aej.2021.03.024

18. Kim, S., Lee, Y., Kim, C., & Choi, S. (2022). Analysis of mechanical property degradation of outdoor weather-exposed polymers. *Polymers, 14*(2), 357. https://doi.org/10.3390/polym14020357

19. Chamas, A., Moon, H., Zheng, J., Qiu, Y., Tabassum, T., Jang, J. H., Abu-Omar, M., Scott, S. L., & Suh, S. (2020). Degradation rates of plastics in the environment. *ACS Sustainable Chemistry & Engineering, 8*(9), 3494–3511. https://doi.org/10.1021/acssuschemeng.9b06635

20. Li, C., Busquets, R., & Campos, L. C. (2020). Assessment of microplastics in freshwater systems: *A review. Science of the Total Environment, 707*, 135578. https://doi.org/10.1016/j.scitotenv.2019.135578

21. Min, K., Cuiffi, J. D., & Mathers, R. T. (2020). Ranking environmental degradation trends of plastic marine debris based on physical properties and molecular structure. *Nature communications, 11*(1), 1–11. https://doi.org/10.1038/s41467-020-14538-z

22. Ahmed, D. S., El-Hiti, G. A., Ibraheem, H., Alotaibi, M. H., Abdallh, M., Ahmed, A. A., Ismael, M., & Yousif, E. (2020). Enhancement of photostabilization of poly (vinyl chloride) doped with sulfadiazine tin complexes. *Journal of Vinyl and Additive Technology, 26*(3), 370–379. https://doi.org/10.1002/vnl.21752

23. Mahmood, Z. N., Yousif, E., Alias, M., El-Hiti, G. A., & Ahmed, D. S. (2020). Synthesis, characterization, properties, and use of new fusidate organotin complexes as additives to inhibit poly (vinyl chloride) photodegradation. *Journal of Polymer Research, 27*(9), 1–12. https://doi.org/10.1007/s10965-020-02245-8

24. Majeed, A., Yousif, E., El-Hiti, G. A., Ahmed, D. S., & Ahmed, A. A. (2020). Stabilization of poly (vinyl chloride) containing captopril tin complexes against degradation upon exposure to ultraviolet light. *Journal of Vinyl and Additive Technology, 26*(4), 601–612. https://doi.org/10.1002/vnl.21774

25. Salam, B., El-Hiti, G. A., Bufaroosha, M., Ahmed, D. S., Ahmed, A., Alotaibi, M. H., & Yousif, E. (2020). Tin complexes containing an atenolol moiety as photostabilizers for poly (vinyl chloride). *Polymers, 12*(12), 2923. https://doi.org/10.3390/polym12122923

26. Ahmed, A., El-Hiti, G. A., Hadi, A. G., Ahmed, D. S., Baashen, M. A., Hashim, H., & Yousif, E. (2021). Photostabilization of poly (vinyl chloride) films blended with organotin complexes of mefenamic acid for outdoor applications. *Applied Sciences, 11*(6), 2853. https://doi.org/10.3390/app11062853

27. Jasem, H., Hadi, A. G., El-Hiti, G. A., Baashen, M. A., Hashim, H., Ahmed, A. A., Ahmed, D. S., & Yousif, E. (2021). Tin-naphthalene sulfonic acid complexes as photostabilizers for poly (vinyl chloride). *Molecules, 26*(12), 3629. https://doi.org/10.3390/molecules26123629

28. Hadi, A. G., Baqir, S. J., Ahmed, D. S., El-Hiti, G. A., Hashim, H., Ahmed, A., Kariuki, B. M., & Yousif, E. (2021). Substituted organotin complexes of 4-methoxybenzoic acid for reduction of poly(vinyl chloride) photodegradation. *Polymers, 13*(22), 3946. https://doi.org/10.3390/polym13223946

29. Mousa, O. G., El-Hiti, G. A., Baashen, M. A., Bufaroosha, M., Ahmed, A., Ahmed, A. A., Ahmed, D. S., & Yousif, E. (2021). Synthesis of carvedilol-organotin complexes and their effects on reducing photodegradation of poly(vinyl chloride). *Polymers, 13*(4), 500. https://doi.org/10.3390/polym13040500

30. Buchner, J., Irle, M., Belloncle, C., Michaud, F., & Macchioni, N. (2019). Fungal and bacterial colonies growing on weathered wood surfaces. *Wood Material Science & Engineering, 14*(1), 33–41. https://doi.org/10.1080/17480272.2018.1443975

31. Zhu, T., Sheng, J., Chen, J., Ren, K., Wu, Z., Wu, H., Li, J., & Lin, J. (2021). Staining of wood veneers with anti-UV property using the natural dye extracted from *Dalbergia cohinchinensis*. *Journal of Cleaner Production, 284*, 124770. https://doi.org/10.1016/j.jclepro.2020.124770

32. Bernhard, G. H., Bais, A. F., Aucamp, P. J., Klekociuk, A. R., Liley, J. B., & McKenzie, R. L. (2022). Stratospheric ozone, UV radiation, and climate interactions. *Chapter 1*

33. USGBC. (2020). *LEED Zero Program Guide*. The US Green Building Council, Atlanta (GA). https://www.usgbc.org/sites/default/files/2020-04/LEED_Zero_Program%20Guide_April%202020.pdf

34. BRE Group (2022). BREEAM - BRE Group. https://bregroup.com/products/breeam/. Accessed Oct 10 2022.

35. Guan, Q.-F., Han, Z.-M., Yang, H.-B., Ling, Z.-C., & Yu, S.-H. (2021). Regenerated isotropic wood. *National Science Review, 8*(7), nwaa230. https://doi.org/10.1093/nsr/nwaa230

36. XHI. (2021). *Research and Feasibility Study on 3D Printed Homes in Rural Alaska July 2021*. Xtreme Habitats Institute (XHI), Anchorage, Alaska. https://www.ahfc.us/application/files/9016/2913/7446/3D_Printed_Home_Feasibility_Study_FINAL_2021_AHFC_Branded.pdf

37. GVR (2022). Grand View Research, 3D Printing Construction Market Size, Share & Trends Analysis Report by Construction Method (Extrusion, Powder Bonding), by Material Type, by End User (Building, Infrastructure), by Region, and Segment Forecasts, 2021 - 2028. Report ID: GVR-4-68039-084-2 Grand View Research, San Francisco, CA.

38. Awoyera, P., & Adesina, A. (2020). Plastic wastes to construction products: Status, limitations and future perspective. *Case Studies in Construction Materials, 12*, e00330. https://doi.org/10.1016/j.cscm.2020.e00330

39. Haque, M. S., & Islam, S. (2021). Effectiveness of waste plastic bottles as construction material in Rohingya displacement camps. *Cleaner Engineering and Technology, 3*, 100110. https://doi.org/10.1016/j.clet.2021.100110

40. Palmeira, E. M., Araújo, G. L. S., & Santos, E. C. G. (2021). Sustainable solutions with geosynthetics and alternative construction materials—a review. *Sustainability, 13*(22), 12756. https://doi.org/10.3390/su132212756

41. Gunaalan, K., Fabbri, E., & Capolupo, M. (2020). The hidden threat of plastic leachates: A critical review on their impacts on aquatic organisms. Water Research, 184, 116170. https://doi.org/10.1016/j.watres.2020.116170

42. Hassan, A. A., Abbas, A., Rasheed, T., Bilal, M., Iqbal, H. M., & Wang, S. (2019). Development, influencing parameters and interactions of bioplasticizers: An environmentally friendlier alternative to petro industry-based sources. *Science of the Total Environment, 682*, 394–404. https://doi.org/10.1016/j.scitotenv.2019.05.140

43. Najafi, V., & Abdollahi, H. (2020). Internally plasticized PVC by four different green plasticizer compounds. *European Polymer Journal, 128*, 109620. https://doi.org/10.1016/j.eurpolymj.2020.109620

44. Tipton, D. A., & Lewis, J. W. (2008). Effects of a hindered amine light stabilizer and a UV light absorber used in maxillofacial elastomers on human gingival epithelial cells and fibroblasts. *The Journal of Prosthetic Dentistry, 100*(3), 220–231. https://doi.org/10.1016/S0022-3913(08)60182-1

45. Barrick, A., Champeau, O., Chatel, A., Manier, N., Northcott, G., & Tremblay, L. A. (2021). Plastic additives: challenges in ecotox hazard assessment. *PeerJ, 9*, e11300. https://doi.org/10.7717/peerj.11300

46. Wang, W., Lee, I.-S., & Oh, J.-E. (2022). Specific-accumulation and trophic transfer of UV filters and stabilizers in marine food web. *Science of the Total Environment, 825*, 154079. https://doi.org/10.1016/j.scitotenv.2022.154079

47. Flaws, J., Damdimopoulou, P., Patisaul, H. B., Gore, A., Raetzman, L., & Vandenberg, L. N. (2022). *Plastics, EDCs & Health: A Guide for Public Interest Organizations and Policy-Makers on Endocrine Disrupting Chemicals & Plastics*. Endocrine Society & International Pollutants Elimination Network (IPEN). https://www.endocrine.org/-/media/endocrine/files/topics/edc_guide_2020_v1_6bhqen.pdf

48. Statista (2022). Market volume of plasticizer worldwide from 2015 to 2021, with a forecast for 2022 to 2029. https://www.statista.com/statistics/1245193/plasticizer-market-volume-worldwide/. Accessed Oct 12 2022.

49. Lee, Y.-M., Lee, J.-E., Choe, W., Kim, T., Lee, J.-Y., Kho, Y., Choi, K., & Zoh, K.-D. (2019). Distribution of phthalate esters in air, water, sediments, and fish in the Asan Lake of Korea. *Environment International, 126*, 635–643. https://doi.org/10.1016/j.envint.2019.02.059

50. Zhang, Q., Song, J., Li, X., Peng, Q., Yuan, H., Li, N., Duan, L., & Ma, J. (2019). Concentrations and distribution of phthalate esters in the seamount area of the Tropical Western Pacific Ocean. *Marine Pollution Bulletin, 140*, 107–115. https://doi.org/10.1016/j.marpolbul.2019.01.015

51. Engel, S. M., Patisaul, H. B., Brody, C., Hauser, R., Zota, A. R., Bennet, D. H., Swanson, M., & Whyatt, R. M. (2021). Neurotoxicity of ortho-phthalates: recommendations for critical policy reforms to protect brain development in children. *American Journal of Public Health, 111*(4), 687–695. https://doi.org/10.2105/AJPH.2020.306014

52. Rouane, A., Zerrouki, D., Aillerie, M., & Henni, A. (2019). Spectroscopic and mechanical properties of PVC plasticized by bio-plasticizer ESO. *Journal of Polymer Research, 27*(1), 12. https://doi.org/10.1007/s10965-019-1984-1

53. Chen, J., Nie, X., & Jiang, J. (2020). Synthesis of a novel bio-oil-based hyperbranched ester plasticizer and its effects on poly (vinyl chloride) soft films. *ACS Omega, 5*(10), 5480–5486. https://doi.org/10.1021/acsomega.0c00119

54. Li, Y., Yu, E., Yang, X., & Wei, Z. (2020). Multiarm hyperbranched polyester-b-poly (ε caprolactone): Plasticization effect and migration resistance for PVC. *Journal of Vinyl and Additive Technology, 26*(1), 35–42. https://doi.org/10.1002/vnl.21713

55. Pereira, V. A., Fonseca, A. C., Costa, C. S., Ramalho, A., Coelho, J. F., & Serra, A. C. (2020). End-capped biobased saturated polyesters as effective plasticizers for PVC. *Polymer Testing, 85*, 106406. https://doi.org/10.1016/j.polymertesting.2020.106406

56. Chen, J., Liu, Z., Wang, K., Huang, J., Li, K., Nie, X., & Jiang, J. (2019). Epoxidized castor oil-based diglycidyl-phthalate plasticizer: Synthesis and thermal stabilizing effects on poly (vinyl chloride). *Journal of Applied Polymer Science, 136*(9), 47142. https://doi.org/10.1002/app.47142

57. Tan, J., Liu, B., Fu, Q., Wang, L., Xin, J., & Zhu, X. (2019). Role of the oxethyl unit in the structure of vegetable oil-based plasticizer for PVC: an efficient strategy to enhance compatibility and plasticization. *Polymers, 11*(5), 779. https://doi.org/10.3390/polym11050779

58. Ji, S., Gao, C., Wang, H., Liu, Y., Zhang, D., Zhang, S., Lu, X., Wu, Y., & Hu, Z. (2019). Application of a bio-based polyester plasticizer modified by hydrosilicon-hydrogenation reaction in soft PVC films. *Polymers for Advanced Technologies, 30*(4), 1126–1134. https://doi.org/10.1002/pat.4546

59. Nguyen, T., Kim, Y. J., Park, S.-K., Lee, K.-Y., Park, J.-w., Cho, J. K., & Shin, S. (2020). Furan-2,5- and Furan-2,3-dicarboxylate esters derived from marine biomass as plasticizers for poly(vinyl chloride). *ACS Omega, 5*(1), 197–206.

60. Greco, A., Ferrari, F., & Maffezzoli, A. (2017). UV and thermal stability of soft PVC plasticized with cardanol derivatives. *Journal of Cleaner Production, 164*, 757–764. https://doi.org/10.1016/j.jclepro.2017.07.009

61. Nzangya, J. M., Ndunda, E. N., Bosire, G. O., Martincigh, B. S., & Nyamori, V. O. (2021). Polybrominated Diphenyl Ethers (PBDEs) as Emerging Environmental Pollutants: Advances in Sample Preparation and Detection Techniques. In *Emerging Contaminants*, 1–22: IntechOpen London, UK. https://doi.org/10.5772/intechopen.93858

62. Wang, J., Yan, Z., Zheng, X., Wang, S., Fan, J., Sun, Q., Xu, J., & Men, S. (2021). Health risk assessment and development of human health ambient water quality criteria for PBDEs in China. *Science of the Total Environment, 799*, 149353. https://doi.org/10.1016/j.scitotenv.2021.149353

63. Zhang, T., Zhou, X., Xu, A., Tian, Y., Wang, Y., Zhang, Y., Gu, Q., Wang, S., & Wang, Z. (2020). Toxicity of polybrominated diphenyl ethers (PBDEs) on rodent male reproductive system: a systematic review and meta-analysis of randomized control studies. *Science of the Total Environment, 720*, 137419. https://doi.org/10.1016/j.scitotenv.2020.137419

64. Abbasi, G., Li, L., & Breivik, K. (2019). Global historical stocks and emissions of PBDEs. *Environmental Science & Technology, 53*(11), 6330–6340. https://doi.org/10.1021/acs.est.8b07032

65. Kuo, L.-J., Cade, S. E., Cullinan, V., & Schultz, I. R. (2019). Polybrominated diphenyl ethers (PBDEs) in plasma from E-waste recyclers, outdoor and indoor workers in the Puget Sound, WA region. *Chemosphere, 219*, 209–216. https://doi.org/10.1016/j.chemosphere.2018.12.006

66. Hou, R., Lin, L., Li, H., Liu, S., Xu, X., Xu, Y., Jin, X., Yuan, Y., & Wang, Z. (2021). Occurrence, bioaccumulation, fate, and risk assessment of novel brominated flame retardants (NBFRs) in aquatic environments—A critical review. *Water Research, 198*, 117168. https://doi.org/10.1016/j.watres.2021.117168

67. Luan, M., Liang, H., Yang, F., Yuan, W., Chen, A., Liu, X., Ji, H., Wen, S., & Miao, M. (2019). Prenatal polybrominated diphenyl ethers exposure and anogenital distance in boys from a Shanghai birth cohort. *International Journal of Hygiene and Environmental Health, 222*(3), 513–523. https://doi.org/10.1016/j.ijheh.2019.01.008

68. Mutic, A. D., Barr, D. B., Hertzberg, V. S., Brennan, P. A., Dunlop, A. L., & McCauley, L. A. (2021). Polybrominated diphenyl ether serum concentrations and depressive symptomatology in pregnant African American women. *International Journal of Environmental Research and Public Health, 18*(7), 3614. https://doi.org/10.3390/ijerph18073614

69. Siddiqi, M. A., Laessig, R. H., & Reed, K. D. (2003). Polybrominated diphenyl ethers (PBDEs): New pollutants–old diseases. *Clinical Medicine & Research, 1*(4), 281–290. https://doi.org/10.3121/cmr.1.4.281

70. EPA (2021). Decabromodiphenyl Ether (DecaBDE); Regulation of Persistent, Bioaccumulative, and Toxic Chemicals Under TSCA Section 6(h). A Rule by the Environmental Protection Agency on 01/06/2021. The Federal Register : Doc. 2020-28686. In E. P. A. (EPA) (Ed.), (Vol. 86 FR 880, pp. 880–894).

71. Sharkey, M., Harrad, S., Abou-Elwafa Abdallah, M., Drage, D. S., & Berresheim, H. (2020). Phasing-out of legacy brominated flame retardants: The UNEP Stockholm Convention and other legislative action worldwide. *Environment International, 144*, 106041. https://doi.org/10.1016/j.envint.2020.106041

72. Blum, A., Behl, M., Birnbaum, L. S., Diamond, M. L., Phillips, A., Singla, V., Sipes, N. S., Stapleton, H. M., & Venier, M. (2019). Organophosphate ester flame retardants: are they a regrettable substitution for polybrominated diphenyl ethers? *Environmental science & technology letters, 6*(11), 638-649. https://doi.org/10.1016/j.jphotochem.2019.111948

73. Yang, X., Liu, X., Yang, X., Zhang, Q., Zheng, Y., Ren, Y., & Cheng, B. (2022). A phosphorous/nitrogen-containing flame retardant with UV-curing for polyester/cotton fabrics. *Cellulose, 29*(2), 1263–1281. https://doi.org/10.1021/acs.estlett.9b00582

74. Zhao, S., Tian, L., Zou, Z., Liu, X., Zhong, G., Mo, Y., Wang, Y., Tian, Y., Li, J., & Guo, H. (2021). Probing legacy and alternative flame retardants in the air of Chinese cities. *Environmental Science & Technology, 55*(14), 9450-9459. https://doi.org/10.1021/acs.est.0c07367

75. Bajard, L., Melymuk, L., & Blaha, L. (2019). Prioritization of hazards of novel flame retardants using the mechanistic toxicology information from ToxCast and Adverse Outcome Pathways. *Environmental Sciences Europe, 31*(1), 14. https://doi.org/10.1186/s12302-019-0195-z

76. Li, Y., Xue, B., Qi, P., Gu, X., Sun, J., Li, H., Lin, J., & Zhang, S. (2022). The synergistic effect between bis(2,2,6,6-tetramethyl-4-piperidyl) sebacate and polysiloxane on the photo-aging resistance and flame retardancy of polypropylene. *Composites Part B: Engineering, 234*, 109666. https://doi.org/10.1016/j.compositesb.2022.109666

77. Forsthuber, B., & Grüll, G. (2018). Prediction of wood surface discoloration for applications in the field of architecture. *Wood Science and Technology, 52*(4), 1093–1111. https://doi.org/10.1007/s00226-018-1015-0

78. Liu, R., Zhu, H., Li, K., & Yang, Z. (2019). Comparison on the aging of woods exposed to natural sunlight and artificial xenon light. *Polymers, 11*(4), 709. https://doi.org/10.3390/polym11040709

79. Mattonai, M., Watanabe, A., Shiono, A., & Ribechini, E. (2019). Degradation of wood by UV light: A study by EGA-MS and Py-GC/MS with on line irradiation system. *Journal of Analytical and Applied Pyrolysis, 139*, 224–232. https://doi.org/10.1016/j.jaap.2019.02.009

80. Davis, K., Leavengood, S., & Morrell, J. J. (2022). Effects of climate on exterior wood coating performance: A comparison of three industrial coatings in a warm-summer Mediterranean and a semi-arid climate in Oregon, USA. *Coatings, 12*(1), 85. https://doi.org/10.3390/coatings12010085

81. Nasir, V., Fathi, H., Fallah, A., Kazemirad, S., Sassani, F., & Antov, P. (2021). Prediction of mechanical properties of artificially weathered wood by color change and machine learning,. *Materials, 14*, 6314. https://doi.org/10.3390/ma14216314

82. Bansal, R., Nair, S., & Pandey, K. K. (2022). UV resistant wood coating based on zinc oxide and cerium oxide dispersed linseed oil nano-emulsion. *Materials Today Communications, 30*, 103177. https://doi.org/10.1016/j.mtcomm.2022.103177

83. Kržišnik, D., Lesar, B., Thaler, N., & Humar, M. (2018). Influence of natural and artificial weathering on the colour change of different wood and wood-based materials. *Forests, 9*(8), 488. https://doi.org/10.3390/f9080488

84. Cirule, D., Kuka, E., Kevers, M., Andersone, I., & Andersons, B. (2021). Photodegradation of unmodified and thermally modified wood due to indoor lighting. *Forests, 12*(8), 1060. https://doi.org/10.3390/f12081060

85. Varga, D., Tolvaj, L., Molnar, Z., & Pasztory, Z. (2020). Leaching effect of water on photodegraded hardwood species monitored by IR spectroscopy. *Wood Science and Technology, 54*(6), 1407–1421. https://doi.org/10.1007/s00226-020-01204-2

86. Kropat, M., Hubbe, M. A., & Laleicke, F. (2020). Natural, accelerated, and simulated weathering of wood: A review. *BioResources, 15*(4), 9998–10062. https://doi.org/10.15376/biores.15.4.Kropat

87. Bejo, L., Tolvaj, L., Kannar, A., & Preklet, E. (2019). Effect of water leaching on photodegraded spruce wood monitored by IR spectroscopy. *Journal of Photochemistry and Photobiology A: Chemistry, 382*, 111948. https://doi.org/https://doi.org/10.1016/j.jphotochem.2019.111948

88. Petrillo, M., Sandak, J., Grossi, P., & Sandak, A. (2019). Chemical and appearance changes of wood due to artificial weathering–dose–response model. *Journal of Near Infrared Spectroscopy, 27*(1), 26–37. https://doi.org/10.1177/0967033518825364

89. Arpaci, S. S., Tomak, E. D., Ermeydan, M. A., & Yildirim, I. (2021). Natural weathering of sixteen wood species: Changes on surface properties. *Polymer Degradation and Stability, 183*, 109415. https://doi.org/10.1016/j.polymdegradstab.2020.109415

90. Preklet, E., Tolvaj, L., Bejo, L., & Varga, D. (2018). Temperature dependence of wood photodegradation. Part 2: evaluation by Arrhenius law. *Journal of Photochemistry and Photobiology A: Chemistry, 356*, 329–333. https://doi.org/10.1016/j.jphotochem.2018.01.008

91. Pánek, M., & Reinprecht, L. (2019). Critical view on the possibility of color changes prediction in the surfaces of painted wood exposed outdoors using accelerated weathering in Xenotest. *Journal of Coatings Technology and Research, 16*(2), 339–352. https://doi.org/10.1007/s11998-018-0125-9

92. de Almeida, T. H., de Almeida, D. H., Chahud, E., Branco, L. A. M. N., Pinheiro, R. V., Christoforo, A. L., & Lahr, F. A. R. (2019). Mechanical performance of wood under artificial and natural weathering treatments. *BioResources, 14*(3), 6267–6277. https://doi.org/10.15376/biores.14.3.6267-6277

93. Gašparík, M., Gaff, M., Kačík, F., & Sikora, A. (2019). Color and chemical changes in teak (*Tectona grandis* L. f.) and meranti (*Shorea* spp.) wood after thermal treatment. *BioResources, 14*(2), 2667–2683. https://doi.org/10.15376/biores.14.2.2667-2683

94. Kučerová, V., Lagaňa, R., & Hýrošová, T. (2019). Changes in chemical and optical properties of silver fir (*Abies alba* L.) wood due to thermal treatment. *Journal of wood science, 65*(1), 1–10. https://doi.org/10.1186/s10086-019-1800-x

95. Zhang, N., Xu, M., & Cai, L. (2019). Improvement of mechanical, humidity resistance and thermal properties of heat-treated rubber wood by impregnation of SiO_2 precursor. *Scientific Reports, 9*(1), 1–9. https://doi.org/10.1038/s41598-018-37363-3

96. Li, N., & Wang, W. (2022). Prediction of mechanical properties of thermally modified wood based on TSSA-BP model. *Forests, 13*(2), 160. https://doi.org/10.3390/f13020160

97. Jirouš-Rajković, V., & Miklečić, J. (2019). Heat-treated wood as a substrate for coatings, weathering of heat-treated wood, and coating performance on heat-treated wood. *Advances in Materials Science and Engineering, 2019*, Article ID 8621486. https://doi.org/10.1155/2019/8621486

98. Shen, H., Zhang, S., Cao, J., Jiang, J., & Wang, W. (2018). Improving anti-weathering performance of thermally modified wood by TiO_2 sol or/and paraffin emulsion. *Construction and Building Materials, 169*, 372–378. https://doi.org/10.1016/j.conbuildmat.2018.03.036

99. Herrera, R., Sandak, J., Robles, E., Krystofiak, T., & Labidi, J. (2018). Weathering resistance of thermally modified wood finished with coatings of diverse formulations. *Progress in Organic Coatings, 119*, 145–154. https://doi.org/10.1016/j.porgcoat.2018.02.015

100. Dzurenda, L., Dudiak, M., & Výbohová, E. (2022). Influence of UV radiation on the color change of the surface of steamed maple wood with saturated water steam. *Polymers, 14*(1), 217. https://doi.org/10.3390/polym14010217

101. Chang, T.-C., & Chang, S.-T. (2017). Multiple photostabilization actions of heartwood extract from *Acacia confusa*. *Wood Science and Technology, 51*(5), 1133–1153. https://doi.org/10.1007/s00226-017-0930-9

102. Chang, T.-C., & Chang, S.-T. (2019). Photostabilization mechanisms of the main wood photostabilizers from the heartwood extract in Acacia confusa: okanin and melanoxetin. *Wood Science and Technology, 53*(2), 335–348. https://doi.org/10.1007/s00226-019-01084-1

103. Chang, T.-C., Yeh, T.-F., & Chang, S.-T. (2019). Investigation of photo-induced discoloration on wood treated with the polyphenols from *Acacia confusa* heartwood. *Journal of Wood Chemistry and Technology, 39*(4), 270–281. https://doi.org/10.1080/02773813.2019.1578376

104. Grigsby, W., & Steward, D. (2018). Applying the protective role of condensed tannins to acrylic-based surface coatings exposed to accelerated weathering. *Journal of Polymers and the Environment, 26*(3), 895–905. https://doi.org/10.1007/s10924-017-0999-0

105. Grigsby, W. J. (2017). Simulating the protective role of bark proanthocyanidins in surface coatings: Unexpected beneficial photo-stabilisation of exposed timber surfaces. *Progress in Organic Coatings, 110*, 55–61. https://doi.org/10.1016/j.porgcoat.2017.03.007

106. Kanbayashi, T., Matsunaga, M., & Kobayashi, M. (2021). Effects of natural weathering on the chemical composition of cell walls in sapwood and heartwood of Japanese cedar. *Wood Science and Technology, 55*(4), 1013–1024. https://doi.org/10.1007/s00226-021-01301-w

107. Hsiao, N.-C., Chang, T.-C., & Chang, S.-T. (2021). Influences of merbau heartwood extracts and their metal complexes on wood photodegradation. *European Journal of Wood and Wood Products, 79*(1), 207–216. https://doi.org/10.1007/s00107-020-01603-z

108. Peng, Y., Wang, Y., Chen, P., Wang, W., & Cao, J. (2020). Enhancing weathering resistance of wood by using bark extractives as natural photostabilizers in polyurethane-acrylate coating. *Progress in Organic Coatings, 145,* 105665. https://doi.org/10.1016/j.porgcoat.2020.105665

109. Pan, F., Chen, L., He, L., Jiang, Y., Qi, J., Xiao, H., Chen, Y., Huang, X., Hu, H., & Tu, L. (2020). Characterization of ethyl acetate and trichloromethane extracts from *Phoebe zhennan* wood residues and application on the preparation of UV shielding films. *Molecules, 25*(5), 1145. https://doi.org/10.3390/molecules25051145

110. Özgenç, Ö., Durmaz, S., Şahin, S., & Boyaci, I. H. (2020). Evaluation of the weathering resistance of waterborne acrylic-and alkyd-based coatings containing HALS, UV absorber, and bark extracts on wood surfaces. *Journal of Coatings Technology and Research, 17*(2), 461–475. https://doi.org/10.1007/s11998-019-00293-4

111. Vedrtnam, A., Kumar, S., & Chaturvedi, S. (2019). Experimental study on mechanical behavior, biodegradability, and resistance to natural weathering and ultraviolet radiation of wood-plastic composites. *Composites Part B: Engineering, 176*, 107282. https://doi.org/10.1016/j.compositesb.2019.107282

112. Sadeghifar, H., & Ragauskas, A. (2020). Lignin as a UV light blocker—a review. *Polymers, 12*(5), 1134. https://doi.org/10.3390/polym12051134

113. Zhang, Y., & Naebe, M. (2021). Lignin: A review on structure, properties, and applications as a light-colored UV absorber. *ACS Sustainable Chemistry & Engineering, 9*(4), 1427–1442. https://doi.org/10.1021/acssuschemeng.0c06998

114. Zikeli, F., Vinciguerra, V., D'Annibale, A., Capitani, D., Romagnoli, M., & Scarascia Mugnozza, G. (2019). Preparation of lignin nanoparticles from wood waste for wood surface treatment. *Nanomaterials, 9*(2), 281. https://doi.org/10.3390/nano9020281

115. Mi, R., Chen, C., Keplinger, T., Pei, Y., He, S., Liu, D., Li, J., Dai, J., Hitz, E., & Yang, B. (2020). Scalable aesthetic transparent wood for energy efficient buildings. *Nature communications, 11*(1), 1–9. https://doi.org/10.1038/s41467-020-17513-w

116. van Hai, L., Muthoka, R. M., Panicker, P. S., Agumba, D. O., Pham, H. D., & Kim, J. (2021). All-biobased transparent-wood: A new approach and its environmental-friendly packaging application. *Carbohydrate Polymers, 264*, 118012. https://doi.org/10.1016/j.carbpol.2021.118012

117. Rao, A. N. S., Nagarajappa, G. B., Nair, S., Chathoth, A. M., & Pandey, K. K. (2019). Flexible transparent wood prepared from poplar veneer and polyvinyl alcohol. *Composites Science and Technology, 182*, 107719. https://doi.org/10.1016/j.compscitech.2019.107719

118. Aldalbahi, A., El-Naggar, M. E., Khattab, T. A., & Hossain, M. (2021). Preparation of flame-retardant, hydrophobic, ultraviolet protective, and luminescent transparent wood. *Luminescence, 36*(8), 1922–1932. https://doi.org/10.1002/bio.4126

119. Höglund, M., Garemark, J., Nero, M., Willhammar, T., Popov, S., & Berglund, L. A. (2021). Facile processing of transparent wood nanocomposites with structural color from plasmonic nanoparticles. *Chemistry of Materials, 33*(10), 3736–3745. https://doi.org/10.1021/acs.chemmater.1c00806

120. Montanari, C., Ogawa, Y., Olsén, P., & Berglund, L. A. (2021). High performance, fully bio-based, and optically transparent wood biocomposites. *Advanced Science*, 2100559. https://doi.org/10.1002/advs.202100559

121. Xia, Q., Chen, C., Yao, Y., Li, J., He, S., Zhou, Y., Li, T., Pan, X., Yao, Y., & Hu, L. (2021). A strong, biodegradable and recyclable lignocellulosic bioplastic. *Nature Sustainability, 4*(7), 627–635. https://doi.org/10.1038/s41893-021-00702-w

122. Bisht, P., Pandey, K. K., & Barshilia, H. C. (2021). Photostable transparent wood composite functionalized with an UV-absorber. *Polymer Degradation and Stability, 189*, 109600. https://doi.org/10.1016/j.polymdegradstab.2021.109600

123. Wachter, I., Štefko, T., Rantuch, P., Martinka, J., & Pastierová, A. (2021). Effect of UV radiation on optical properties and hardness of transparent wood. *Polymers, 13*(13), 2067. https://doi.org/10.3390/polym13132067

124. Final Advanced Materials (2022). Aramid Fibre. https://www.final-materials.com/gb/21-aramid-fibre. Accessed Oct 12 2022.

125. da Silva, A. O., de Castro Monsores, K. G., Oliveira, S. d. S. A., Weber, R. P., & Monteiro, S. N. (2018). Ballistic behavior of a hybrid composite reinforced with curaua and aramid fabric subjected to ultraviolet radiation. *Journal of Materials Research and Technology, 7*(4), 584–591. https://doi.org/10.1016/j.jmrt.2018.09.004

126. Mishra, N., Madhad, H., & Vasava, D. (2021). Progress in the chemistry of functional aramids properties. *Journal of Heterocyclic Chemistry, 58*(10), 1887–1913. https://doi.org/10.1002/jhet.4336

127. Nascimento, R. F., da Silva, A. O., Weber, R. P., & Monteiro, S. N. (2020). Influence of UV radiation and moisten associated with natural weathering on the ballistic performance of aramid fabric armor. *Journal of Materials Research and Technology, 9*(5), 10334–10345. https://doi.org/10.1016/j.jmrt.2020.07.046

128. Fan, Y., Li, Z., & Wei, J. (2021). Application of Aramid Nanofibers in Nanocomposites: A Brief Review. *Polymers, 13*(18), 3071. https://doi.org/10.3390/polym13183071

129. Sun, H., Kong, H., Ding, H., Xu, Q., Zeng, J., Jiang, F., Yu, M., & Zhang, Y. (2020). Improving UV resistance of aramid fibers by simultaneously synthesizing TiO_2 on their surfaces and in the interfaces between fibrils/microfibrils using supercritical carbon dioxide. *Polymers, 12*(1), 147. https://doi.org/10.3390/polym12010147

130. Ma, L., Zhang, J., & Teng, C. (2020). Covalent functionalization of aramid fibers with zinc oxide nano-interphase for improved UV resistance and interfacial strength in composites. *Composites Science and Technology, 188*, 107996. https://doi.org/10.1016/j.compscitech.2020.107996

131. Zhang, J., & Teng, C. (2020). Nondestructive growing nano-ZnO on aramid fibers to improve UV resistance and enhance interfacial strength in composites. *Materials & Design, 192*, 108774. https://doi.org/10.1016/j.matdes.2020.108774

132. Zhang, L., Kong, H., Qiao, M., Ding, X., & Yu, M. (2020). Supercritical CO_2-induced nondestructive coordination between ZnO nanoparticles and aramid fiber with highly improved interfacial-adhesion properties and UV resistance. A*pplied Surface Science, 521*, 146430. https://doi.org/10.1016/j.apsusc.2020.146430

133. Bahramian, A. (2021). Poly (ethylene terephthalate)-based nanocomposite films as greenhouse covering material: Environmental sustainability, mechanical durability, and thermal stability. *Journal of Applied Polymer Science, 138*(10), 49991. https://doi.org/10.1002/app.49991

134. Zhang, S., Zhang, D., Bai, H., & Ming, W. (2020). ZnO nanoparticles coated with amphiphilic polyurethane for transparent polyurethane nanocomposites with enhanced mechanical and UV-shielding performance. *ACS Applied Nano Materials, 3*(1), 59–67. https://doi.org/10.1021/acsanm.9b01540

135. Cao, Y., Xu, P., Lv, P., Lemstra, P. J., Cai, X., Yang, W., Dong, W., Chen, M., Liu, T., & Du, M. (2020). Excellent UV resistance of polylactide by interfacial stereocomplexation with double-shell-structured TiO_2 nanohybrids. *ACS Applied Materials & Interfaces, 12*(43), 49090–49100. https://doi.org/10.1021/acsami.0c14423

136. Murphy, J. (2001). *Additives for plastics handbook*: Elsevier.

137. Raidongia, K., Tan, A. T., & Huang, J. (2014). Graphene oxide: some new insights into an old material. In *Carbon Nanotubes and Graphene*, 341–374: Elsevier. https://doi.org/10.1016/B978-0-08-098232-8.00014-0

138. Shearer, C. J., Cherevan, A., & Eder, D. (2014). Application of functional hybrids incorporating carbon nanotubes or graphene. In *Carbon Nanotubes and Graphene*, 387–433: Elsevier. https://doi.org/10.1016/B978-0-08-098232-8.00016-4

139. Chennareddy, R., Tuwair, H., Kandil, U. F., ElGawady, M., & Taha, M. R. (2019). UV-resistant GFRP composite using carbon nanotubes. *Construction and Building Materials, 220*, 679–689. https://doi.org/10.1016/j.conbuildmat.2019.05.167

140. Awad, S. A., Fellows, C. M., & Mahini, S. S. (2019). Evaluation of bisphenol A-based epoxy resin containing multiwalled carbon nanotubes to improve resistance to degradation. *Journal of Composite Materials, 53*(21), 2981–2991. https://doi.org/10.1177/0021998318816784

141. Chavoshi, N., & Jahanmardi, R. (2019). Chemical functionalization of graphene oxide by a hindered amine stabilizer and evaluation of the product as a UV-stabilizer for polypropylene. *Fullerenes, Nanotubes and Carbon Nanostructures, 27*(1), 1–9. https://doi.org/10.1080/1536383X.2018.1472084

142. Prosheva, M., Aboudzadeh, M. A., Leal, G. P., Gilev, J. B., & Tomovska, R. (2019). High-performance UV protective waterborne polymer coatings based on hybrid graphene/carbon nanotube radicals scavenging filler. *Particle & Particle Systems Characterization, 36*(7), 1800555. https://doi.org/10.1002/ppsc.201800555

143. Lawal, A. T. (2019). Graphene-based nano composites and their applications. A review. *Biosensors and Bioelectronics, 141*, 111384. https://doi.org/10.1016/j.bios.2019.111384

144. Huang, H., Shi, H., Das, P., Qin, J., Li, Y., Wang, X., Su, F., Wen, P., Li, S., & Lu, P. (2020). The chemistry and promising applications of graphene and porous graphene materials. *Advanced Functional Materials, 30*(41), 1909035. https://doi.org/10.1002/adfm.201909035

145. Olabi, A. G., Abdelkareem, M. A., Wilberforce, T., & Sayed, E. T. (2021). Application of graphene in energy storage device–A review. *Renewable and Sustainable Energy Reviews, 135*, 110026. https://doi.org/10.1016/j.rser.2020.110026

146. Padmanabhan, N. T., Thomas, N., Louis, J., Mathew, D. T., Ganguly, P., John, H., & Pillai, S. C. (2021). Graphene coupled TiO$_2$ photocatalysts for environmental applications: A review. *Chemosphere*, *271*, 129506. https://doi.org/10.1016/j.chemosphere.2020.129506

147. VDMA. (2022). *International Technology Roadmap for Photovoltaic (ITRPV)*. Frankfurt am Main: VDMA e.V.

148. Ottersböck, B., Oreski, G., & Pinter, G. (2022). How to accelerate natural weathering of polymeric photovoltaic backsheets – A comparison with standardized artificial aging. *Solar Energy Materials and Solar Cells, 244*, 111819. https://doi.org/10.1016/j.solmat.2022.111819

149. Weiß, K.-A., Bruckman, L. S., French, R. H., Oreski, G., Tanahashi, T., Ascéncio-Vásquez, J., Castillion-Gandara, L. F., Eder, G., Hrelja, N., Iseghem, M. v., Kaaya, I., Lindig, S., Liu, J., Mitterhofer, S., Neumaier, L., Rath, K., Venkat, S. N., & Wieser, R. J. (2021). Service Life Estimation for Photovoltaic Modules. Report IEA-PVPS T13-16:2021. Vol. T13-16:2021. IEA-PVPS.

150. Fairbrother, A., Phillips, N., & Gu, X. (2019). 7 - Degradation Processes and Mechanisms of Backsheets. In H. E. Yang, R. H. French, & L. S. Bruckman (Eds.), *Durability and Reliability of Polymers and Other Materials in Photovoltaic Modules*, 153–174: William Andrew Publishing. https://doi.org/10.1016/B978-0-12-811545-9.00007-0

151. Noman, M., Tu, S., Ahmad, S., Zafar, F. U., Khan, H. A., Rehman, S. U., Waqas, M., Khan, A. D., & Rehman, O. u. (2022). Assessing the reliability and degradation of 10–35 years field-aged PV modules. *PLOS ONE, 17*(1), e0261066. https://doi.org/10.1371/journal.pone.0261066

152. Julien, S. E., Kempe, M. D., Eafanti, J. J., Morse, J., Wang, Y., Fairbrother, A. W., Napoli, S., Hauser, A. W., Ji, L., O'Brien, G. S., Gu, X., French, R. H., Bruckman, L. S., Wan, K.-t., & Boyce, K. P. (2020). Characterizing photovoltaic backsheet adhesion degradation using the wedge and single cantilever beam tests, Part II: Accelerated tests. *Solar Energy Materials and Solar Cells, 211*, 110524. https://doi.org/10.1016/j.solmat.2020.110524

153. Kim, J., Rabelo, M., Padi, S. P., Yousuf, H., Cho, E.-C., & Yi, J. (2021). A Review of the degradation of photovoltaic modules for life expectancy. *Energies, 14*(14), 4278. https://doi.org/10.3390/en14144278

154. Tracy, J., Gambogi, W., Felder, T., Garreau-Iles, L., Hu, H., Trout, T. J., Khatri, R., Ji, X., Heta, Y., & Choudhury, K. R. Survey of Material Degradation in Globally Fielded PV Modules. In *2019 IEEE 46th Photovoltaic Specialists Conference (PVSC), 2019-06 2019* (pp. 0874–0879). https://doi.org/10.1109/PVSC40753.2019.8981140

155. Kumar, S., Alhamadani, H., Hassan, S., Alheloo, A., Hanifi, H., John, J. J., Mathiak, G., & Alberts, V. Comparative investigation and analysis of encapsulant degradation and glass abrasion in desert exposed photovoltaic modules. In *2021 IEEE 48th Photovoltaic Specialists Conference (PVSC), 2021* (pp. 0793–0798): IEEE. https://doi.org/10.1109/PVSC43889.2021.9519122

156. Han, H., Yan, H., Wang, X., Zhang, K., Huang, J., Sun, Y., Liu, J., Verlinden, P. J., Altermatt, P., Liang, Z., & Shen, H. (2019). Analysis of the degradation of encapsulant materials used in photovoltaic modules exposed to different climates in China. S*olar Energy, 194*, 177–188. https://doi.org/10.1016/j.solener.2019.10.014

157. Hara, K. (2022). Raman spectroscopic analysis of encapsulants in aged photovoltaic modules. *Journal of Photochemistry and Photobiology A: Chemistry, 425*, 113721. https://doi.org/10.1016/j.jphotochem.2021.113721

158. Sharma, B. K., Desai, U., Singh, A., & Singh, A. (2020). Effect of vinyl acetate content on the photovoltaic-encapsulation performance of ethylene vinyl acetate under accelerated ultra-violet aging. *Journal of Applied Polymer Science, 137*(2), 48268. https://doi.org/10.1002/app.48268

159. Tracy, J., Bosco, N., Delgado, C., & Dauskardt, R. (2020). Durability of ionomer encapsulants in photovoltaic modules. *Solar Energy Materials and Solar Cells, 208*, 110397. https://doi.org/10.1016/j.solmat.2020.110397

160. Adothu, B., Bhatt, P., Chattopadhyay, S., Zele, S., Oderkerk, J., Sagar, H. P., Costa, F. R., & Mallick, S. (2019). Newly developed thermoplastic polyolefin encapsulant–A potential candidate for crystalline silicon photovoltaic modules encapsulation. *Solar Energy, 194*, 581–588. https://doi.org/10.1016/j.solener.2019.11.018

161. Oreski, G., Omazic, A., Eder, G. C., Voronko, Y., Neumaier, L., Mühleisen, W., Hirschl, C., Ujvari, G., Ebner, R., & Edler, M. (2020). Properties and degradation behaviour of polyolefin encapsulants for photovoltaic modules. *Progress in Photovoltaics: Research and Applications, 28*(12), 1277–1288. https://doi.org/10.1002/pip.3323

162. Neale, R. E., Barnes, P. W., Robson, T. M., Neale, P. J., Williamson, C. E., Zepp, R. G., Wilson, S. R., Madronich, S., Andrady, A. L., Heikkilä, A. M., Bernhard, G. H., Bais, A. F., Aucamp, P. J., Banaszak, A. T., Bornman, J. F., Bruckman, L. S., Byrne, S. N., Foereid, B., Häder, D.-P., Hollestein, L. M., et al. (2021). Environmental effects of stratospheric ozone depletion, UV radiation, and interactions with climate change: UNEP Environmental Effects Assessment Panel, Update 2020. *Photochemical & Photobiological Sciences, 20*(1), 1–67. https://doi.org/10.1007/s43630-020-00001-x

163. Miller, D. C., Bokria, J. G., Burns, D. M., Fowler, S., Gu, X., Hacke, P. L., Honeker, C. C., Kempe, M. D., Köhl, M., Phillips, N. H., Scott, K. P., Singh, A., Suga, S., Watanabe, S., & Zielnik, A. F. (2019). Degradation in photovoltaic encapsulant transmittance: Results of the first PVQAT TG5 artificial weathering study. *Progress in Photovoltaics: Research and Applications, 27*(5), 391–409. https://doi.org/10.1002/pip.3103

164. Correa-Puerta, J., Ferrada, P., Häberle, P., Díaz-Almeida, D., Sanz, A., Zubillaga, O., Marzo, A., Portillo, C., & del Campo, V. (2021). Comparing the effects of ultraviolet radiation on four different encapsulants for photovoltaic applications in the Atacama Desert. *Solar Energy, 228*, 625–635. https://doi.org/10.1016/j.solener.2021.10.003

165. Lelièvre, J.-F., Couderc, R., Pinochet, N., Sicot, L., Munoz, D., Kopecek, R., Ferrada, P., Marzo, A., Olivares, D., Valencia, F., & Urrejola, E. (2022). Desert label development for improved reliability and durability of photovoltaic modules in harsh desert conditions. *Solar Energy Materials and Solar Cells, 236*, 111508. https://doi.org/10.1016/j.solmat.2021.111508

166. Oreski, G., Eder, G. C., Voronko, Y., Omazic, A., Neumaier, L., Mühleisen, W., Ujvari, G., Ebner, R., & Edler, M. (2021). Performance of PV modules using co-extruded backsheets based on polypropylene. *Solar Energy Materials and Solar Cells, 223*, 110976. https://doi.org/10.1016/j.solmat.2021.110976

167. Beaucarne, G., Eder, G., Jadot, E., Voronko, Y., & Mühleisen, W. (2022). Repair and preventive maintenance of photovoltaic modules with degrading backsheets using flowable silicone sealant. *Progress in Photovoltaics: Research and Applications, 30*(8), 1045-1053. https://doi.org/10.1002/pip.3492

168. Voronko, Y., Eder, G. C., Breitwieser, C., Mühleisen, W., Neumaier, L., Feldbacher, S., Oreski, G., & Lenck, N. (2021). Repair options for PV modules with cracked backsheets. *Energy Science & Engineering, 9*(9), 1583–1595. https://doi.org/10.1002/ese3.936

169. Han, H., Xia, J., Hu, H., Liu, R., Liu, J., Choudhury, K. R., Gambogi, W. J., Felder, T., Rodriguez, M., Simon, E., Zhang, Z., & Shen, H. (2021). Aging behavior and degradation of different backsheets used in the field under various climates in China. *Solar Energy Materials and Solar Cells, 225*, 111023. https://doi.org/10.1016/j.solmat.2021.111023

170. Lyu, Y., Fairbrother, A., Gong, M., Kim, J. H., Gu, X., Kempe, M., Julien, S., Wan, K.-T., Napoli, S., Hauser, A., O'Brien, G., Wang, Y., French, R., Bruckman, L., Ji, L., & Boyce, K. (2020). Impact of environmental variables on the degradation of photovoltaic components and perspectives for the reliability assessment methodology. *Solar Energy, 199*, 425–436. https://doi.org/10.1016/j.solener.2020.02.020

171. Moffitt, S. L., Pan, P.-C., Perry, L., Tracy, J., Choudhury, K. R., Kempe, M. D., & Gu, X. (2022). Microstructure changes during failure of PVDF-based photovoltaic backsheets. *Progress in Photovoltaics: Research and Applications, 1–10*. https://doi.org/10.1002/pip.3605

172. Kempe, M. D., Lyu, Y., Kim, J. H., Felder, T., & Gu, X. (2021). Fragmentation of photovoltaic backsheets after accelerated weathering exposure. *Solar Energy Materials and Solar Cells, 226*, 111044. https://doi.org/10.1016/j.solmat.2021.111044

173. Fairbrother, A., Boyd, M., Lyu, Y., Avenet, J., Illich, P., Wang, Y., Kempe, M., Dougherty, B., Bruckman, L., & Gu, X. (2018). Differential degradation patterns of photovoltaic backsheets at the array level. *Solar Energy, 163*, 62–69. https://doi.org/10.1016/j.solener.2018.01.072

174. Kobayashi, Y., Morita, H., Mori, K., & Masuda, A. (2019). Investigation of UV and hygrothermal stress on back side of rack-mounted photovoltaic modules. *Renewable Energy Focus, 29*, 107–113. https://doi.org/10.1016/j.ref.2019.03.008

175. Wang, Y., Huang, W.-H., Fairbrother, A., Fridman, L. S., Curran, A. J., Wheeler, N. R., Napoli, S., Hauser, A. W., Julien, S., Gu, X., O'Brien, G. S., Wan, K.-T., Ji, L., Kempe, M. D., Boyce, K. P., French, R. H., & Bruckman, L. S. (2019). Generalized spatio-temporal model of backsheet degradation from field surveys of photovoltaic modules. *IEEE Journal of Photovoltaics, 9*(5), 1374–1381. https://doi.org/10.1109/JPHOTOV.2019.2928700

176. Wieser, R. J., Rath, K., Moffitt, S. L., Zabalza, R., Boucher, E., Ayala, S., Brown, M., Gu, X., Ji, L., O'Brien, C., Hauser, A. W., O'Brien, G. S., French, R. H., Kempe, M. D., Tracy, J., Choudhury, K. R., Gambogi, W. J., Bruckman, L. S., & Boyce, K. P. Spatio-Temporal Modeling of Field Surveyed Backsheet Degradation. In *2021 IEEE 48th Photovoltaic Specialists Conference (PVSC), 2021-06 2021* (pp. 1383–1388). https://doi.org/10.1109/PVSC43889.2021.9519128

177. Lv, Y., Fan, D., & Kong, M. (2021). Reliability assessment on PV backsheets with and without considering spectral UV albedo effects: A theoretical comparison. *Solar Energy Materials and Solar Cells, 230*, 111230. https://doi.org/10.1016/j.solmat.2021.111230

178. Eder, G. C., Voronko, Y., Oreski, G., Mühleisen, W., Knausz, M., Omazic, A., Rainer, A., Hirschl, C., & Sonnleitner, H. (2019). Error analysis of aged modules with cracked polyamide backsheets. *Solar Energy Materials and Solar Cells, 203*, 110194. https://doi.org/10.1016/j.solmat.2019.110194

179. Lyu, Y., Fairbrother, A., Gong, M., Kim, J. H., Hauser, A., O'Brien, G., & Gu, X. (2020). Drivers for the cracking of multilayer polyamide-based backsheets in field photovoltaic modules: In-depth degradation mapping analysis. *Progress in Photovoltaics: Research and Applications, 28*(7), 704–716. https://doi.org/10.1002/pip.3260

180. Owen-Bellini, M., Moffitt, S. L., Sinha, A., Maes, A. M., Meert, J. J., Karin, T., Takacs, C., Jenket, D. R., Hartley, J. Y., Miller, D. C., Hacke, P., & Schelhas, L. T. (2021). Towards validation of combined-accelerated stress testing through failure analysis of polyamide-based photovoltaic backsheets. *Scientific Reports, 11*(1), 2019. https://doi.org/10.1038/s41598-021-81381-7

181. Julien, S. E., Kim, J. H., Lyu, Y., Miller, D. C., Gu, X., & Wan, K.-t. (2021). Cohesive and adhesive degradation in PET-based photovoltaic backsheets subjected to ultraviolet accelerated weathering. *Solar Energy, 224*, 637–649. https://doi.org/10.1016/j.solener.2021.04.065

182. Lin, C.-C., Lyu, Y., Jacobs, D. S., Kim, J. H., Wan, K.-T., Hunston, D. L., & Gu, X. (2019). A novel test method for quantifying cracking propensity of photovoltaic backsheets after ultraviolet exposure. *Progress in Photovoltaics: Research and Applications, 27*(1), 44–54. https://doi.org/10.1002/pip.3038

183. Smith, S., Perry, L., Watson, S., Moffitt, S. L., Shen, S.-J., Mitterhofer, S., Sung, L.-P., Jacobs, D., & Gu, X. (2022). Transparent backsheets for bifacial photovoltaic (PV) modules: Material characterization and accelerated laboratory testing. *Progress in Photovoltaics: Research and Applications, 30*(8), 959-969.

184. Lokanath, S. V., Skarbek, B., & Schindelholz, E. J. (2019). 9 - Degradation Processes and Mechanisms of PV Wires and Connectors. In H. E. Yang, R. H. French, & L. S. Bruckman (Eds.), *Durability and Reliability of Polymers and Other Materials in Photovoltaic Modules*, 217–233: William Andrew Publishing. https://doi.org/10.1016/B978-0-12-811545-9.00009-4

185. Santhakumari, M., & Sagar, N. (2019). A review of the environmental factors degrading the performance of silicon wafer-based photovoltaic modules: Failure detection methods and essential mitigation techniques. *Renewable and Sustainable Energy Reviews, 110*, 83–100. https://doi.org/10.1016/j.rser.2019.04.024

186. Hedir, A., Moudoud, M., Lamrous, O., Rondot, S., Jbara, O., & Dony, P. (2020). Ultraviolet radiation aging impact on physicochemical properties of crosslinked polyethylene cable insulation. *Journal of Applied Polymer Science, 137*(16), 48575. https://doi.org/10.1002/app.48575

187. Gok, A., Gordon, D. A., Wang, M., French, R. H., & Bruckman, L. S. (2019). 3 - Degradation Science and Pathways in PV Systems. In H. E. Yang, R. H. French, & L. S. Bruckman (Eds.), *Durability and Reliability of Polymers and Other Materials in Photovoltaic Modules*, 47–93: William Andrew Publishing. https://doi.org/10.1016/B978-0-12-811545-9.00003-3

188. Syafiuddin, A., Fulazzaky, M. A., Salmiati, S., Roestamy, M., Fulazzaky, M., Sumeru, K., & Yusop, Z. (2020). Sticky silver nanoparticles and surface coatings of different textile fabrics stabilised by *Muntingia calabura* leaf extract. *SN Applied Sciences, 2*(4), 1–10. https://doi.org/10.1007/s42452-020-2534-5

189. Xu, Q., Zheng, W., Duan, P., Chen, J., Zhang, Y., Fu, F., Diao, H., & Liu, X. (2019). One-pot fabrication of durable antibacterial cotton fabric coated with silver nanoparticles via carboxymethyl chitosan as a binder and stabilizer. *Carbohydrate Polymers, 204*, 42–49. https://doi.org/10.1016/j.carbpol.2018.09.089

190. Gedanken, A., Perkas, N., Perelshtein, I., & Lipovsky, A. (2018). Imparting pharmaceutical applications to the surface of fabrics for wound and skin care by ultrasonic waves. *Current Medicinal Chemistry, 25*(41), 5739–5754. https://doi.org/10.2174/0929867325666171229141635

191. Harifi, T., Montazer, M., Dillert, R., & Bahnemann, D. W. (2018). $TiO_2/Fe_3O_4/Ag$ nanophotocatalysts in solar fuel production: New approach to using a flexible lightweight sustainable textile fabric. *Journal of Cleaner Production, 196*, 688–697. https://doi.org/10.1016/j.jclepro.2018.06.031

192. Čuk, N., Šala, M., & Gorjanc, M. (2021). Development of antibacterial and UV protective cotton fabrics using plant food waste and alien invasive plant extracts as reducing agents for the in-situ synthesis of silver nanoparticles. *Cellulose, 28*(5), 3215–3233. https://doi.org/10.1007/s10570-021-03715-y

193. Rabiei, H., Dehghan, S. F., Montazer, M., Khaloo, S. S., & Koozekonan, A. G. (2022). UV protection properties of workwear fabrics coated with TiO_2 nanoparticles. *Frontiers in Public Health, 10*. https://doi.org/10.3389/fpubh.2022.929095

194. Rashid, M. M., Simončič, B., & Tomšič, B. (2021). Recent advances in TiO_2-functionalized textile surfaces. *Surfaces and Interfaces, 22*, 100890. https://doi.org/10.1016/j.surfin.2020.100890

195. Tang, Q., Zhang, H., Han, Y., Wang, D., & Wu, H. (2021). Photostability of TiO_2-coated wool fibers exposed to ultraviolet B, ultraviolet A, and visible light irradiation. *AUTEX Research Journal, 21*(1), 1–12. https://doi.org/10.2478/aut-2019-0055

196. Zhu, T., Li, S., Huang, J., Mihailiasa, M., & Lai, Y. (2017). Rational design of multi-layered superhydrophobic coating on cotton fabrics for UV shielding, self-cleaning and oil-water separation. *Materials & Design, 134*, 342–351. https://doi.org/10.1016/j.matdes.2017.08.071

197. Ahmed, N. A.-M. H., Kishk, D. M., & Nada, A. A. (2021). Green and durable treatment for multifunctional cellulose-containing woven fabrics via TiO_2-NP and HMTAP processed in semi-pilot machine. *Fibers and Polymers, 22*(10), 2815–2825. https://doi.org/10.1007/s12221-021-0755-x

198. Dasaradhan, B., Das, B. R., Goswami, T. H., & Prasad, N. E. (2022). Exploration of polyvinylidene difluoride (PVDF) for improvement of weathering resistance of textile substrates. *The Journal of the Textile Institute, 113*(9), 1845–1853. https://doi.org/10.1080/00405000.2021.1952806

199. Safdar, F., Javid, A., & Ashraf, M. (2021). Single step synthesis and functionalization of nano titania for development of multifunctional cotton fabrics. *Materials, 15*(1), 38. https://doi.org/10.3390/ma15010038

200. Zheng, G., Peng, H., Jiang, J., Kang, G., Liu, J., Zheng, J., & Liu, Y. (2021). Surface functionalization of PEO nanofibers using a TiO_2 suspension as sheath fluid in a modified coaxial electrospinning process. *Chemical Research in Chinese Universities, 37*(3), 571–577. https://doi.org/10.1007/s40242-021-1118-2

201. Faisal, S., Naqvi, S., Ali, M., & Lin, L. (2021). Comparative study of multifunctional properties of synthesised ZnO and MgO NPs for textiles applications. *Pigment & Resin Technology, 51*(3), 301–308. https://doi.org/10.1108/PRT-02-2021-0017

202. Javed, A., Azeem, M., Wiener, J., Thukkaram, M., Saskova, J., & Mansoor, T. (2021). Ultrasonically assisted in situ deposition of ZnO nano particles on cotton fabrics for multifunctional textiles. *Fibers and Polymers, 22*(1), 77–86. https://doi.org/10.1007/s12221-021-0051-9

203. Tănase, M. A., Soare, A. C., Oancea, P., Răducan, A., Mihăescu, C. I., Alexandrescu, E., Petcu, C., Dițu, L. M., Ferbinteanu, M., Cojocaru, B., & Cinteza, L. O. (2021). facile *in situ* synthesis of ZnO flower-like hierarchical nanostructures by the microwave irradiation method for multifunctional textile coatings. *Nanomaterials, 11*(10), 2574. https://doi.org/10.3390/nano11102574

204. El-Naggar, M. E., Khattab, T. A., Abdelrahman, M. S., Aldalbahi, A., & Hatshan, M. R. (2021). Development of antimicrobial, UV blocked and photocatalytic self-cleanable cotton fibers decorated with silver nanoparticles using silver carbamate and plasma activation. *Cellulose, 28*(2), 1105–1121. https://doi.org/10.1007/s10570-020-03537-4

205. Farooq, A. S., & Zhang, P. (2021). Fundamentals, materials and strategies for personal thermal management by next-generation textiles. *Composites Part A: Applied Science and Manufacturing, 142*, 106249. https://doi.org/10.1016/j.compositesa.2020.106249

206. Peng, Y., & Cui, Y. (2020). Advanced textiles for personal thermal management and energy. *Joule, 4*(4), 724–742. https://doi.org/10.1016/j.joule.2020.02.011

207. Yue, X., Zhang, T., Yang, D., Qiu, F., Wei, G., & Zhou, H. (2019). Multifunctional Janus fibrous hybrid membranes with sandwich structure for on-demand personal thermal management. *Nano Energy, 63*, 103808. https://doi.org/10.1016/j.nanoen.2019.06.004

208. Fang, D., Yu, H., Dirican, M., Tian, Y., Xie, J., Jia, D., Yan, C., Liu, Y., Li, C., & Liu, H. (2021). Disintegrable, transparent and mechanically robust high-performance antimony tin oxide/nanocellulose/polyvinyl alcohol thermal insulation films. *Carbohydrate Polymers, 266*, 118175. https://doi.org/10.1016/j.carbpol.2021.118175

209. Zeng, S., Pian, S., Su, M., Wang, Z., Wu, M., Liu, X., Chen, M., Xiang, Y., Wu, J., Zhang, M., & others (2021). Hierarchical-morphology metafabric for scalable passive daytime radiative cooling. *Science, 373*(6555), 692–696. https://doi.org/10.1126/science.abi5484

210. Sait, S. T., Sørensen, L., Kubowicz, S., Vike-Jonas, K., Gonzalez, S. V., Asimakopoulos, A. G., & Booth, A. M. (2021). Microplastic fibres from synthetic textiles: Environmental degradation and additive chemical content. *Environmental Pollution, 268*, 115745. https://doi.org/10.1016/j.envpol.2020.115745

211. Sørensen, L., Groven, A. S., Hovsbakken, I. A., Del Puerto, O., Krause, D. F., Sarno, A., & Booth, A. M. (2021). UV degradation of natural and synthetic microfibers causes fragmentation and release of polymer degradation products and chemical additives. *Science of the Total Environment, 755*, 143170. https://doi.org/10.1016/j.scitotenv.2020.143170

212. Jansen, M. A. K., Barnes, P. W., Bornman, J. F., Rose, K. C., Madronich, S., White, C. C., Zepp, R. G., & Andrady, A. L. (2022). The Montreal Protocol and the fate of environmental plastic debris. *Chapter 8*

213. Kim, D., Kim, H., & An, Y.-J. (2021). Effects of synthetic and natural microfibers on *Daphnia magna*–Are they dependent on microfiber type? *Aquatic Toxicology, 240,* 105968. https://doi.org/10.1016/j.aquatox.2021.105968

214. Kwak, J. I., Liu, H., Wang, D., Lee, Y. H., Lee, J.-S., & An, Y.-J. (2022). Critical review of environmental impacts of microfibers in different environmental matrices. *Comparative Biochemistry and Physiology Part C: Toxicology & Pharmacology, 251*, 109196. https://doi.org/10.1016/j.cbpc.2021.109196

215. Moore, C. J. (2019). Invasion of the biosphere by synthetic polymers: What our current knowledge may mean for our future. *Acta Oceanologica Sinica, 38*(5), 161–164. https://doi.org/10.1007/s13131-019-1424-4

216. Naik, R. A., Rowles III, L. S., Hossain, A. I., Yen, M., Aldossary, R. M., Apul, O. G., Conkle, J., & Saleh, N. B. (2020). Microplastic particle versus fiber generation during photo-transformation in simulated seawater. *Science of the Total Environment, 736*, 139690. https://doi.org/10.1016/j.scitotenv.2020.139690

217. Cai, Y., Yang, T., Mitrano, D. M., Heuberger, M., Hufenus, R., & Nowack, B. (2020). Systematic study of microplastic fiber release from 12 different polyester textiles during washing. *Environmental Science & Technology, 54*(8), 4847–4855. https://doi.org/10.1021/acs.est.9b07395

218. Cesa, F. S., Turra, A., Checon, H. H., Leonardi, B., & Baruque-Ramos, J. (2020). Laundering and textile parameters influence fibers release in household washings. *Environmental Pollution, 257,* 113553. https://doi.org/10.1016/j.envpol.2019.113553

219. De Falco, F., Cocca, M., Avella, M., & Thompson, R. C. (2020). Microfiber release to water, via laundering, and to air, via everyday use: a comparison between polyester clothing with differing textile parameters. *Environmental Science & Technology, 54*(6), 3288–3296. https://doi.org/10.1021/acs.est.9b06892

220. Kärkkäinen, N., & Sillanpää, M. (2021). Quantification of different microplastic fibres discharged from textiles in machine wash and tumble drying. *Environmental Science and Pollution Research, 28*(13), 16253–16263. https://doi.org/10.1007/s11356-020-11988-2

221. Abedin, M., Khandaker, M. U., Uddin, M., Karim, M., Ahamad, M., Islam, M., Arif, A. M., Sulieman, A., Idris, A. M., & others (2022). PPE pollution in the terrestrial and aquatic environment of the Chittagong city area associated with the COVID-19 pandemic and concomitant health implications. *Environmental Science and Pollution Research, 29*(18), 27521–27533. https://doi.org/10.1007/s11356-021-17859-8

222. Ardusso, M., Forero-López, A., Buzzi, N., Spetter, C., & Fernández-Severini, M. (2021). COVID-19 pandemic repercussions on plastic and antiviral polymeric textile causing pollution on beaches and coasts of South America. *Science of the Total Environment, 763*, 144365. https://doi.org/10.1016/j.scitotenv.2020.144365

223. Mejjad, N., Cherif, E. K., Rodero, A., Krawczyk, D. A., El Kharraz, J., Moumen, A., Laqbaqbi, M., & Fekri, A. (2021). Disposal behavior of used masks during the COVID-19 pandemic in the moroccan community: potential environmental impact. *International Journal of Environmental Research and Public Health, 18*(8), 4382. https://doi.org/10.3390/ijerph18084382

224. Shammi, M., Behal, A., & Tareq, S. M. (2021). The escalating biomedical waste management to control the environmental transmission of COVID-19 pandemic: A perspective from two south Asian countries. *Environmental Science & Technology, 55*(7), 4087–4093. https://doi.org/10.1021/acs.est.0c05117

225. Sánchez, M. B., Fito-López, C., & Cajaraville, M. (2021). A life cycle perspective of the exposure to airborne nanoparticles released from nanotechnology enabled products and applications. In *Health and Environmental Safety of Nanomaterials*, 173–194: Elsevier. https://doi.org/10.1016/B978-0-12-820505-1.00004-3

226. Han, C., Sahle-Demessie, E., Varughese, E., & Shi, H. (2019). Polypropylene–MWCNT composite degradation, and release, detection and toxicity of MWCNTs during accelerated environmental aging. *Environmental Science: Nano, 6*(6), 1876–1894. https://doi.org/10.1039/C9EN00153K

227. Andrady, A., Pandey, K., & Heikkilä, A. (2019). Interactive effects of solar UV radiation and climate change on material damage. *Photochemical & Photobiological Sciences, 18*(3), 804-825.

228. UN/DESA. (2015). *Trasforming our World: The 2030 Agenda for Sustainable Development A/RES/70/1*. United Nations / Department of Economic and Social Affairs (UN/DESA).

8

THE MONTREAL PROTOCOL AND THE FATE OF ENVIRONMENTAL PLASTIC DEBRIS

M. A. K. Jansen[121], P. W. Barnes[122], J. F. Bornman[123], K.C. Rose[124], S. Madronich[125], C. C. White[126], R. G. Zepp[127], and A. L. Andrady[128]

[121] School of Biological, Earth and Environmental Sciences, Environmental Research Institute, University College Cork, Cork, Ireland

[122] Biological Sciences and Environmental Program, Loyola University New Orleans, New Orleans, LA, USA

[123] Food Futures Institute, Murdoch University, Perth, Australia

[124] Biological Sciences, Rensselaer Polytechnic Institute, Troy, USA

[125] Atmospheric Chemistry Observations and Modeling Laboratory, National Center for Atmospheric Research, Boulder, CO, USA

[126] Exponent, Inc, Bowie, MD 20715, USA

[127] ORD/CEMM, US Environmental Protection Agency, Athens, GA, USA

[128] Chemical and Biomolecular Engineering, North Carolina State University, Raleigh, NC, USA

Table of contents

Summary

Microplastics (MPs) are an emerging class of pollutants in air, soil and especially in all aquatic environments. Secondary MPs are generated in the environment during fragmentation of photo-oxidised plastic litter. Photo-oxidation is mediated primarily by solar UV radiation. The implementation of the Montreal Protocol and its Amendments, which have resulted in controlling the tropospheric UV-B (280-315 nm) radiation load, is therefore pertinent to the fate of environmental plastic debris. Due to the Montreal Protocol high amounts of solar UV-B radiation at the Earth's surface have been avoided, retarding the oxidative fragmentation of plastic debris, leading to a slower generation and accumulation of MPs in the environment. Quantifying the impact of the Montreal Protocol in reducing the abundance of MPs in the environment, however, is complicated as the role of potential mechanical fragmentation of plastics under environmental mechanical stress fields is poorly understood.

1 Introduction

Plastic debris in the environment is an increasing pollution problem, and a multitude of studies has convincingly demonstrated the ubiquity of plastic debris, including microplastic (MP) particles, across planet Earth. An estimated 8300 million metric tons of plastics have been produced since the 1950s, of which ca 80% has ended in landfills and the natural environment [1]. As of 2016, *ca*. 19-23 million metric tons per year, or 11% of all plastic waste generated, was estimated to have entered aquatic ecosystems [2]. Polyethylene (PE), polypropylene (PP), polystyrene (PS), and poly(ethylene terephthalate) (PET) account for *ca*. 70% of all MPs in freshwater ecosystems [3]. An estimated 11.6-21.1 million tons of MPs made of PE, PP and PS occur in the top 200 m of the Atlantic Ocean [4]. Concerns about potential risks posed by MPs to the environment and human health have prompted much research. There are also calls for a global treaty on plastics towards a more sustainable future [5].

Breakdown of plastics occurs due to abiotic and biotic factors [6]. Micro- and nanoplastics (typically defined as plastic particles < 5 mm, and < 0.1 μm in size, respectively (but see [7]) are generated in the natural environment as a result of solar ultraviolet (UV)-driven weathering of plastic debris in combination with fragmentation due to exposure to mechanical forces [6]. These micro- and nanoplastics are widely distributed in aquatic and terrestrial ecosystems and also pose a potential risk to humans through inhalation [8], ingestion [9] and dermal contact [10]. MPs have been found, for example, in bottled drinking water [11], table salt [12], and seafood [13]. A recent estimate [9] places the annual human intake of MPs from all sources to be 105 particles. Small MPs (1-5μm) may enter systemic circulation and translocate into cellular compartments [14, 15].

Recently, MPs in human placenta have been detected in studies carried out in clinical settings. In one of these, PP particles, 5-10 μm in size, were found in placenta samples from vaginal deliveries [16]. A second study detected even larger MPs > 50 μm of PE, PS, and PP in human placenta and meconium from caesarean delivery [17], where the chance of contamination via the birth canal is excluded. Although some of the MPs crossed the placental barrier into the foetal side, no foetal translocation was noted, unlike in studies on inhaled MPs in rats where foetal translocation was observed [18]. Despite these concerning findings, negative human physiological impacts of micro- and nanoplastics have not been conclusively established [19].

Assuming current trends in global production of plastics, and no improvements in waste management infrastructure worldwide, releases into the environment may grow to 90 million metric tons per year by 2030 [2]. Given the recalcitrance of plastics to environmental degradation as well as potential negative biological and health impacts [20], there is particular concern about the risks posed by micro- and nanoplastic particles and similarly sized plastic fibres in terrestrial and aquatic ecosystems globally.

This current assessment focuses on the interactive effects of solar radiation, its UV component, and climate change on the fate of environmental plastic debris, with regard to degradation and fragmentation and their potential consequences.

2 Photo-oxidation and plastic persistence

A major barrier towards a realistic assessment of the global impacts of plastics is the incomplete knowledge of the fate, and particularly the degradation and fragmentation of plastics in the environment [21]. Exposure to solar UV radiation is the primary weathering mechanism of plastics debris (Fig. 1), making plastics prone to subsequent fragmentation into smaller particles [20, 22 – 26]. Photo-oxidation of plastic debris under extended outdoor exposure makes the material weak, brittle and prone to subsequent fragmentation [26, 27]. Fragmentation occurs when plastics are subjected to, for example, wave action or encounters with animals, resulting in the generation of secondary micro- or nano-particles[129] (Fig. 1).
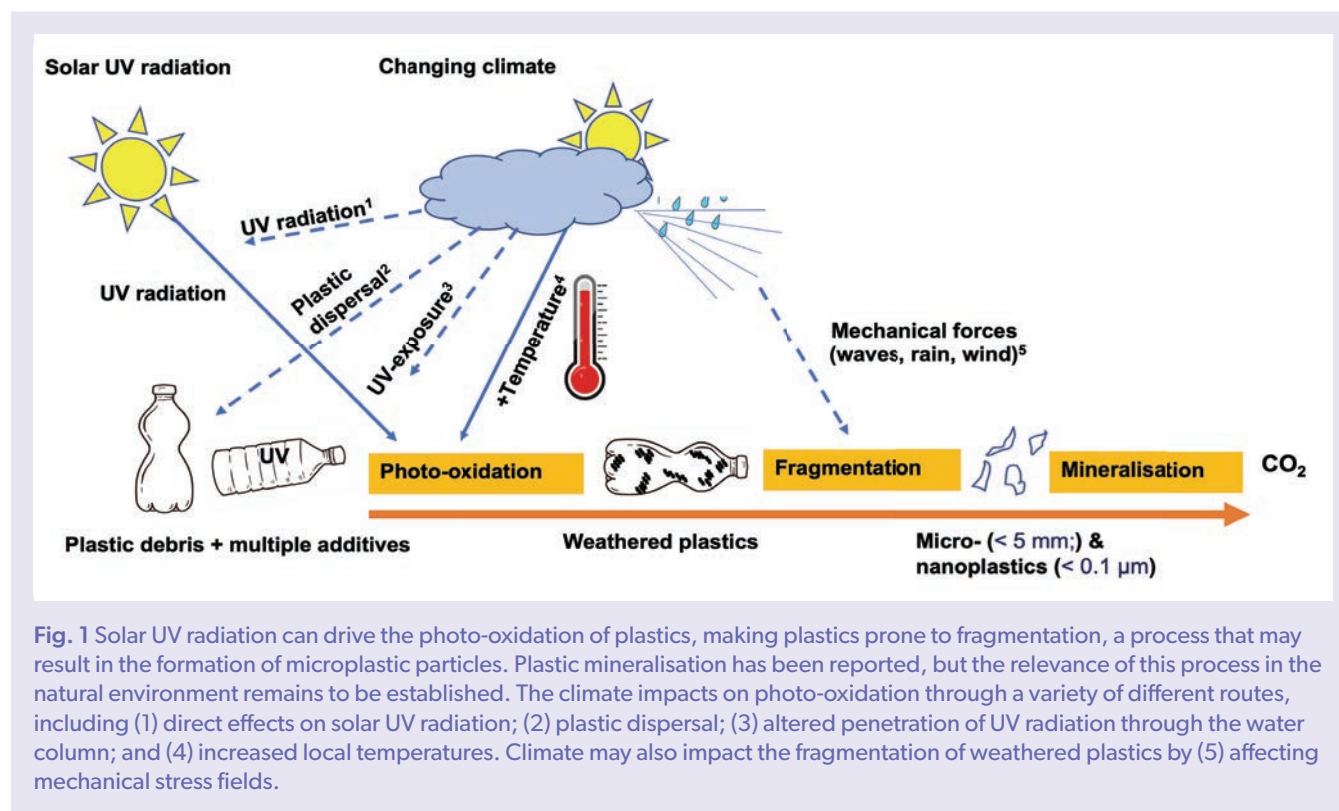
Fig. 1 Solar UV radiation can drive the photo-oxidation of plastics, making plastics prone to fragmentation, a process that may result in the formation of microplastic particles. Plastic mineralisation has been reported, but the relevance of this process in the natural environment remains to be established. The climate impacts on photo-oxidation through a variety of different routes, including (1) direct effects on solar UV radiation; (2) plastic dispersal; (3) altered penetration of UV radiation through the water column; and (4) increased local temperatures. Climate may also impact the fragmentation of weathered plastics by (5) affecting mechanical stress fields.

MPs sampled from beach and surface water environments show spectroscopic signatures of photo-oxidation, primarily the presence of surface carbonyl groups [28, 29], as well as increased fractional crystallinity [30]. While UV irradiation drives photooxidation, and therefore contributes to the fragmentation of plastic debris into progressively smaller sizes, it may also help remove plastic particles from the environment through photo-mineralisation [21, 27, 31]. There is evidence from laboratory-accelerated approaches that MPs can undergo UV-induced mineralisation into carbon dioxide (CO_2) and water [21, 31] (Fig. 1). However, the phenomenon has not been conclusively shown to occur in natural environments, and if it does occur in nature, only a small fraction of the already highly-fragmented plastics with a large specific surface area, is likely to be involved.

[129] Microplastics is a misnomer as it is generally taken to mean all plastic fragments < 5 mm in dimension. Nanoplastics has been used, depending on the publication, to mean fragments that are < 1000 nm or 100 nm.

3 Different plastics and photo-oxidation

In addition to base polymers, plastics generally contain catalyst residues and unreacted monomers, as well as intentionally added chemicals including plasticisers, dyes, antioxidants, flame retardants and/or UV stabilisers [32, 33]. Said mixture has a considerable impact on the rate of photo-oxidation and subsequent fragmentation of plastics. For example, high-density PE and nylon-6 plastics generate MPs when exposed to the equivalent of 44 days of solar irradiation, whereas high-impact PS and PP did not [34]. It remains to be determined whether differences in photo-oxidation relate to the base polymer, or rather specific additives. There is a substantial knowledge gap concerning action spectra of photo-oxidation, and dose-response curves, in the context of the composite characteristics of commercial plastics. Further, laboratory studies have shown that UV-associated degradation rates in simulated aquatic conditions are also mediated by other environmental factors, including temperature, oxygen availability and salinity [35].

4 The Montreal Protocol and photo-oxidation

The anticipated significant increase ("the World avoided") in terrestrial solar UV radiation, avoided by the implementation of the Montreal Protocol and its Amendments, would have increased the rates of photodegradation, and consequently fragmentation of plastic debris. It is currently not known whether a critical threshold of photo-oxidation for a given plastic is required to facilitate fragmentation. This presents a significant gap in knowledge. Also, little is known about the quantitative mechanical forces required to cause fragmentation, and how this force requirement is affected by the photo-oxidation state. Even non-oxidised plastics can be fragmented if mechanical forces are large enough [36]. However, how these forces compare with naturally-occurring stress-fields has not been well studied. There is evidence that virgin plastics can be fragmented in the gut of ingesting crustaceans [37, 38]; similarly, MPs can be generated as a consequence of the mechanical forces imposed on objects as diverse as car tyres [39] or artificial sports turf [40]. Thus, at this stage the relative importance of solar radiation, and weathering of plastics in facilitating fragmentation is not clear.

5 Plastic degradation and UV radiation in a changing climate

Both stratospheric ozone depletion and climate change can alter the irradiance of solar UV radiation reaching the Earth's surface [41], thus affecting photo-oxidation of plastics. Locally, strong increases in temperature under future climate scenarios may further accelerate the rate of photo-oxidation leading to fragmentation (Fig. 1). At present, there are very significant gaps in knowledge pertaining to the impact of global changes on plastic persistence. Increased temperature consequent to climate change is not the only factor that may affect the rate of plastic degradation. For example, increased stress-fields in aquatic environments cause fragmentation, changes in relative humidity alter photodegradation rates, sedimentation rates affect biodegradation, and increased rainfall patterns that control runoff have an effect on plastic dispersal, vertical mixing and transparency of aquatic ecosystems [42] (Chapter 5, Fig. 1). Conversely, plastics also affect climate change by being a significant sink of global carbon [43]. Other, more subtle impacts of MPs will affect carbon storage. For example, ingestion of MPs by a zooplankton species, *Salpa fusiformis* (also known as the common salp), increases the buoyancy of faecal pellets thereby decreasing downward transport and burial of marine carbon in a process called the "biological pump" [44]. Projected future increases in marine MP concentrations may thus reduce carbon sinking rates in the oceans, and therefore alter ocean carbon cycling [44]. Thus, there is a myriad of poorly detailed interactions between UV radiation, global change and plastics, affecting, amongst others, the fate of plastics in the natural environment.

6 Exposure of environmental plastic debris to UV radiation

In order to quantify the environmental rate of UV-driven photodegradation, it is necessary to evaluate the dispersal and distribution, i.e. exposure to UV radiation, of plastic debris [31, 45]. Especially significant from a UV-exposure perspective are air-borne, floating and beach debris. Airborne particles are dominated by fibres, including microplastic fibres [46]. Smaller plastic particles, including abrasive tyre wear[130] [47], may remain airborne for weeks [48, 49], and this is associated with strong UV irradiance. In the terrestrial environment there has been a rapid growth in the use of plastics in agricultural systems, for example, the use of plastic mulch to reduce weed growth and maintain optimal soil moisture and temperature. Such applications are associated with exposure to UV radiation, and fragments may enter the atmosphere and reach remote ecosystems [47, 50]. Conversely, other uses of plastics such as soil improvement using polyurethane foam [22] will not typically result in exposure to UV radiation of the plastics.

In the aquatic environment, exposure to UV radiation depends strongly on buoyancy, although advective water flow and turbulence results in sedimentation of larger numbers of MPs than would be expected from gravitational sedimentation alone in both the freshwater [51] and marine environments [52]. In the oceans, the global mass of floating plastic debris represents only a small percentage of the estimated annual influx of plastics into the aquatic environment, based on production volumes [43, 45, 53, 54], and only these floating plastics will experience UV irradiation. In contrast, sedimentation of plastics will minimise exposure to UV radiation. Sedimentation is linked to geometric and other physical properties of marine MPs, as well as biofouling [55], i.e. the development of a surface layer of microorganisms, algae, and small shelled species on the plastics. This increases the density of plastic debris [4, 56] driving sedimentation. Nevertheless, sedimentation is far from a one-way process. In a well-mixed ocean, biofouled MPs can oscillate vertically in the water column, with the depth of the oscillation depending on, for example, algal growth and light penetration [57]. Still, the nett, long-term sedimentation removes plastics from the photic zone, thus slowing down photo-oxidation.

7 Biological consequences of photo-oxidation and fragmentation

UV radiation-driven photo-oxidation of plastic debris, and subsequent fragmentation following exposure to mechanical forces, will alter the size distribution of plastics in the natural environment. However, the quantification of the UV-mediated changes in this plastic size distribution is lacking. In fact, a major deficiency in the study of the biological impacts of all plastics in the environment is the lack of reliable, quantitative knowledge of environmentally relevant concentrations of micro- and nanoplastics in different environments. This, in turn, relates to a lack of adequate, and standardised, monitoring technology, particularly in complex matrices such as, for example, soil [58]. Concentrations of larger MPs are best known. For example, Sembiring et al. [59] estimated MP (>125 μm) concentrations in an Indonesian river and the downstream seawater to be 0.06 and 3000 particles/m^3, respectively. The average MP concentration in river sediment was 16.7 particles/100 g and in marine sediment 3.3 particles/100 g. However, such numbers may vary considerably depending on the sampling and monitoring approach, as well as the actual location [60].

At present there is a lack of quantitative information on the presence of nano- and smaller microplastics in diverse environments. Given that it has been speculated that nano- and smaller microplastics will have a greater impact on organisms than larger plastics as a result of their transport properties, bioavailability, relative surface area and scope for additive leaching, ingestion and/or uptake in cells [61], this does hamper the assessments of risks associated with plastic pollution.

Both hazards and risks associated with MPs have been analysed and reported, although at present much uncertainty remains concerning biological impacts under realistic environmental concentrations of plastics. Large research gaps exist in the quantitative analysis of the relationship between various exposure routes of MPs, and the actual measured MP or NP toxicity [60]. For example, as the distribution of MPs in the environment is heterogeneous, different organisms will be exposed to different plastics. For example, PE and PP will (initially) float, while plastics such as poly(vinyl chloride) (PVC) sink more readily and as a consequence, organisms with different feeding habits will be differently exposed. Publication bias is also of some concern, with results showing a lack of biological impacts less likely to be published [62]. Nevertheless, and despite above mentioned reservations, research shows that plastics can potentially exert significant negative impacts on selected species of a very broad range of marine, freshwater and terrestrial species [63]. However, other studies fail to observe significant negative impact [62, 64]. This apparent lack of consistency across large numbers of studies suggests that experimental conditions, including MP concentration, size, shape and composition as well as the chosen test organism all play a role in the different outcomes of toxicity [64].

---

[130] A wide range of micro-sized particles in the environment are either non-plastic, or part-plastic anthropogenic particles, including tyre wear, paint particles and fibres. For example, tyres are made of elastomeric polymers (or rubber) and are not thermoplastic but thermosets. However, they have been generally included in the category 'microplastics' along with other thermosets such as polyurethane foam and epoxy.

Historically, toxicological studies have predominantly focused on marine taxa with relatively small sized organisms [3], with less data on the impacts of MPs on large animals, at high trophic levels or terrestrial biota [10]. Effects of MPs on plants and ecosystem productivity remain uncertain [20, 65 - 67]. Marine studies have indicated that zooplankton are more affected by plastics than many other taxa, with obvious consequences for the entire food web. The transfer of plastics up the food chain from primary producers to consumers is also of some concern [68, 69], although evidence of accumulation at higher trophic levels remains limited at present. Finally, understanding of the exposure to and uptake and effects of various types (synthetic, semi-synthetic or natural) of anthropogenic fibres is still in its infancy, notwithstanding the ubiquitous presence of these fibres in the natural environment [70].

A particular difficulty in exposure studies is the fact that plastics are a complex material comprised of different polymers, stabilisers, dyes and other additives. Many of these additives can leach out and exert toxic effects in their own right [32]. Thus, the same plastic base material may exert different toxic effects depending on the additives used in them. UV radiation may drive photo-oxidation, and ultimately photofragmentation, leading to increasing numbers of MPs with increased fragment surface area. This, in turn, can stimulate the leaching of plastic additives, such as endocrine disrupting chemicals that adversely affect organisms [71]. Plastic leachates activate oxidative stress responses in cell-based bioassays [72]. However, low environmental concentrations of leached chemicals indicate that effects in the natural environment may be limited [3]. UV radiation-driven photo-oxidation of plastic surface area can also decrease binding capacity for some organic substances [73], although increased absorptive capacity of plastics towards substances such as the antibiotic ciprofloxacin and the endocrine disruptor bisphenol-A has been reported [74]. Similarly, prior exposure to UV radiation can increase the binding capacity of plastics for heavy metals [75, 76].

Overall, a substantial knowledge gap remains concerning the effects of UV-mediated photo-oxidation and fragmentation, with expected impacts on size distribution of environmental plastics, as well as additive leaching and contaminant binding, all of which are likely to depend on plastic type, duration of exposure, and contaminant chemistry [25, 26, 77].

8 Knowledge gaps

The links between UV irradiation, the stratospheric ozone layer, and MP pollution, although highly relevant, are still poorly understood and scarcely addressed by the scientific community working on MPs. Major knowledge gaps relate to environmental distribution of plastics, and consequent exposure to UV radiation. While it is recognised that some plastics will be buried in sediments where penetration of UV radiation will be virtually nil, others will be airborne and potentially exposed to considerable amounts of UV radiation. Furthermore, where plastics are exposed to UV radiation, uncertainties about the UV dose-response of photo-oxidative reactions impede assessments of weathering and subsequent fragmentation. Thus, while UV-driven photo-oxidation of plastics, and subsequent fragmentation are well known, the quantitative impact of these processes on plastic longevity and MP generation remains unknown.

9 Conclusions

UV-driven weathering, followed by subsequent fragmentation can lead to a decrease in plastic macro-debris in the environment, yet increase the concentration of MPs. By integrating existing surface UV irradiation data with better knowledge of the distribution of plastics across various environmental niches, there is an opportunity to generate quantitative predictions of plastic persistence at a global scale. In turn, such insights can inform the design of more environmentally friendly plastics. However, this approach will require better knowledge of action spectra and dose-response relationships of UV driven oxidation of common compounded plastics, which include intentionally added chemicals such as plasticisers, dyes, antioxidants, flame retardants and/or UV stabilisers [32, 33]. It is also recognised that quantitative predictions of plastic persistence will be subject to effects of climate change, which may affect processes as diverse as the penetration of UV radiation into the water column, sedimentation rates and/or air movements. Furthermore, UV irradiation can also affect the chemical or toxicological properties of MPs and may play a key role in determining hazards and risks associated with MPs. Therefore, there is an urgent need to better understand the interactions between plastics in the environment, climate change, and UV radiation.

10 Relevance to the Sustainable Development Goals

The Montreal Protocol and its Amendments contribute to several of the United Nations Sustainable Development Goals (SDG) through protection of the stratospheric ozone layer and the mitigation of climate change. SDG targets addressed in this section are detailed below.

SDG 6: Clear Water and Sanitation

There is ample evidence that MPs are ubiquitous in freshwater and marine environments. Consequently, essential products such as drinking water can be contaminated by MPs. The implementation of the Montreal Protocol has resulted in the avoidance of high UV irradiation, which is a key driver of plastic weathering, and ultimately, generation of MPs.

SDG 14: Life below water

Macro-, micro,- and nanoplastic pollutants are ubiquitous in freshwater and marine environments. Consequently, aquatic organisms and ecosystems are exposed to these man-made pollutants. The hazardous character of MPs to aquatic organisms has been shown in some studies, although ecological risks remain to be established. The implementation of the Montreal Protocol has resulted in the avoidance of high UV irradiation, and this is likely to have resulted in decreased weathering, and ultimately, decreased generation of MPs. Conversely, implementation of the Montreal Protocol is likely to have resulted in increased persistence of macroplastic debris, which has been widely shown to have negative impacts on animals due to entanglement or accumulation in, for example, the stomach.

SDG 15: Life on Land

Climate change is impacting agricultural practices and has, amongst others, been associated with the increased use of plastics in farming. In turn, this may result in the accumulation of an appreciable plastic burden in agricultural soils with consequences for soil biochemistry, including soil microbiology and nitrogen cycling. The implementation of the Montreal Protocol has led to the avoidance of high UV irradiation but this, in turn, can extend plastic longevity and lead to land degradation and soil biodiversity loss.

Author contributions All authors contributed to the conception and assessment and carried out extensive revisions of content.

Conflict of interest The authors have no conflicts of interest.

References

1. Geyer, R., Jambeck, J. R., & Law, K. L. (2017). Production, use, and fate of all plastics ever made. *Science Advances, 3*(7), e1700782. https://www.science.org/doi/10.1126/sciadv.1700782

2. Borrelle, S. B., Ringma, J., Law, K. L., Monnahan, C. C., Lebreton, L., McGivern, A., Murphy, E., Jambeck, J., Leonard, G. H., Hilleary, M. A., & Eriksen, M. (2020). Predicted growth in plastic waste exceeds efforts to mitigate plastic pollution. *Science 369*(6510), 1515-1518. https://www.science.org/doi/full/10.1126/science.aba3656

3. Li, C., Busquets, R., & Campos, L. C. (2020). Assessment of microplastics in freshwater systems: A review. *Science of the Total Environment, 707*, 135578. https://doi.org/10.1016/j.scitotenv.2019.135578

4. Pabortsava, K., & Lampitt, R. S. (2020). High concentrations of plastic hidden beneath the surface of the Atlantic Ocean. *Nature communications, 11*(1), 1-11. https://doi.org/10.1038/s41467-020-17932-9

5. Geneva Environment Network. (2022). Update Plastics and the Environment. https://www.genevaenvironmentnetwork.org/resources/updates/plastics-and-the-environment/ (accessed 21 June 2022)

6. Andrady, A. L., Barnes, P. W., Bornman, J. F., Gouin, T., Madronich, S., White, C. C., Zepp, R. G., & Jansen, M. A. K. (2022). Oxidation and fragmentation of plastics in a changing environment; from UV-radiation to biological degradation. S*cience of the Total Environment, 158022*. https://doi.org/10.1016/j.scitotenv.2022.158022

7. Frias, J. P., & Nash, R. (2019). Microplastics: Finding a consensus on the definition. *Marine Pollution Bulletin, 138*, 145-147. https://doi.org/10.1016/j.marpolbul.2018.11.022

8. Amato-Lourenço, L. F., Carvalho-Oliveira, R., Júnior, G. R., dos Santos Galvão, L., Ando, R. A., & Mauad, T. (2021). Presence of airborne microplastics in human lung tissue. *Journal of Hazardous Materials, 416*, 126124. https://doi.org/10.1016/j.jhazmat.2021.126124

9. Cox, K. D., Covernton, G. A., Davies, H. L., Dower, J. F., Juanes, F., & Dudas, S. E. (2019). Human consumption of microplastics. *Environmental Science & Technology. 53* (12), 7068-7074. https://doi.org/10.1021/acs.est.9b01517

10. Zhang, S., Wang, J., Liu, X., Qu, F., Wang, X., Wang, X., Li, Y., & Sun, Y. (2019). Microplastics in the environment: A review of analytical methods, distribution, and biological effects. *TrAC Trends in Analytical Chemistry, 111*, 62-72. https://doi.org/10.1016/j.trac.2018.12.002

11. Mason, S. A., Welch, V. G., & Neratko, J. (2018). Synthetic polymer contamination in bottled water. *Frontiers in Chemistry 6*, 407. https://doi.org/10.3389/fchem.2018.00407

12. Smith, M., Love, D. C., Rochman, C. M., & Neff, R. A. (2018). Microplastics in seafood and the implications for human health. *Current Environmental Health Reports, 5*(3), 375–386. https://doi.org/10.1007/s40572-018-0206-z

13. Nicole, W. (2021) Microplastics in seafood: How much are people eating? *Environmental Health Perspectives, 129*(3), 034001. https://doi.org/10.1289/EHP8936

14. Lehner, R., Weder, C., Petri-Fink, A., & Rothen-Rutishauser, B. (2019). Emergence of nanoplastic in the environment and possible impact on human health. *Environmental Science & Technology, 53*(4), 1748-1765. https://doi.org/10.1021/acs.est.8b05512

15. Stock, V., Laurisch, C., Franke, J., Dönmez, M. H., Voss, L., Böhmert, L., Braeuning, A., & Sieg, H. (2021). Uptake and cellular effects of PE, PP, PET and PVC microplastic particles. *Toxicology in Vitro, 70*, 105021. https://doi.org/10.1016/j.tiv.2020.105021

16. Ragusa, A., Svelato, A., Santacroce, C., Catalano, P., Notarstefano, V., Carnevali, O., Papa, F., Rongioletti, M. C. A., Baiocco, F., Draghi, S., & D'Amore, E. (2021). Plasticenta: First evidence of microplastics in human placenta. *Environment International, 146*, 106274. https://doi.org/10.1016/j.envint.2020.106274

17. Braun, T., Ehrlich, L., Henrich, W., Koeppel, S., Lomako, I., Schwabl, P. and Liebmann, B. (2021). Detection of microplastic in human placenta and meconium in a clinical setting. *Pharmaceutics, 13*(7), 921. https://doi.org/10.3390/pharmaceutics13070921

18. Fournier, S. B., D'Errico, J. N., Adler, D. S., Kollontzi, S., Goedken, M. J., Fabris, L., Yurkow, E. J., & Stapleton, P. A. (2020). Nanopolystyrene translocation and fetal deposition after acute lung exposure during late-stage pregnancy. *Particle and Fibre Toxicology, 17*(1), 1-11. https://doi.org/10.1186/s12989-020-00385-9

19. Rahman, A., Sarkar, A., Yadav, O. P., Achari, G., Slobodnik, J. (2021). Potential human health risks due to environmental exposure to nano-and microplastics and knowledge gaps: a scoping review. *Science of the Total Environment, 757*, 143872. https://doi.org/10.1016/j.scitotenv.2020.143872

20. World Health Organization. (2019). *Microplastics in drinking-water*. Retrieved from: https://www.who.int/publications/i/item/9789241516198 (ISBN 978-92-4-151619-8)

21.   Ward, C. P., & Reddy, C. M. (2020). Opinion: we need better data about the environmental persistence of plastic goods. *Proceedings of the National Academy of Sciences, 117*(26), 14618-14621. https://doi.org/10.1073/pnas.2008009117

22.   Wong, J. K. H., Lee, K. K., Tang, K. H. D., & Yap, P.-S. (2020). Microplastics in the freshwater and terrestrial environments: Prevalence, fates, impacts and sustainable solutions. *Science of the Total Environment, 719*. 137512 https://doi.org/10.1016/j.scitotenv.2020.137512

23.   Qi, R., Jones, D. L., Li, Z., Liu, Q., & Yan, C. (2020). Behavior of microplastics and plastic film residues in the soil environment: A critical review. *Science of the Total Environment, 703*, 134722. https://doi.org/10.1016/j.scitotenv.2019.134722

24.   Masry, M., Rossignol, S., Gardette, J.L., Therias, S., Bussière, P.O., & Wong-Wah-Chung, P. (2021). Characteristics, fate, and impact of marine plastic debris exposed to sunlight: A review. *Marine Pollution Bulletin, 171*, 112701. https://doi.org/10.1016/j.marpolbul.2021.112701

25.   Liu, P., Zhan, X., Wu, X., Li, J., Wang, H., & Gao, S. (2020). Effect of weathering on environmental behavior of microplastics: Properties, sorption and potential risks. *Chemosphere, 242*, 125193. https://doi.org/10.1016/j.chemosphere.2019.125193

26.   Alimi, O., Claveau-Mallet, D., Kurusu, R., Lapointe, M., Bayen, S., & Tufenkji, N. (2021). Weathering pathways and protocols for environmentally relevant microplastics and nanoplastics: What are we missing? *Journal of Hazardous Materials, 423*, 126955. https://doi.org/10.1016/j.jhazmat.2021.126955

27.   Garvey, J. G., Imeror-Clerc, M., Rouzière, S., Gouadec, G., Boyron, O., Rowenczyk, L., Mingotaud, A.F., & Ter Halle, A. (2020). et al. (2020). Molecular-scale understanding of the embrittlement in polyethylene ocean debris. *Environmental Science & Technology, 54*, 11173−11181. https://doi.org/10.1021/acs.est.0c02095

28.   Andrady, A. L., Law, K. L., Donohue, J., & Koongolla, B. (2022). Accelerated degradation of low-density polyethylene in air and in sea water. *Science of the Total Environment, 811*, 151368. https://doi.org/10.1016/j.scitotenv.2021.151368

29.   Sorasan, C., Ortega-Ojeda, F.E., Rodríguez, A., & Rosal, R. (2022). Modelling the photodegradation of marine microplastics by means of infrared spectrometry and chemometric techniques. *Microplastics 1*(1), 198-210. https://doi.org/10.3390/microplastics1010013

30.   Menzel, T., Meides, N., Mauel, A., Mansfeld, U., Kretschmer, W., Kuhn, M., Herzig, E. M., Altstädt, V., Strohriegl, P., Senker, J., & Ruckdäschel, H. (2022). Degradation of low-density polyethylene to nanoplastic particles by accelerated weathering, *Science of the Total Environment, 826*,154035. https://doi.org/10.1016/j.scitotenv.2022.154035

31.   Zhu, L., Zhao, S., Bittar, T. B., Stubbins, A., & Li, D. (2020). Photochemical dissolution of buoyant microplastics to dissolved organic carbon: Rates and microbial impacts. *Journal of Hazardous Materials, 383*, 121065. https://doi.org/10.1016/j.jhazmat.2019.121065

32.   Sendra, M., Pereiro, P., Figueras, A. & Novoa, B. (2021). An integrative toxicogenomic analysis of plastic additives. *Journal of Hazardous Materials, 409*, 124975. https://doi.org/10.1016/j.jhazmat.2020.124975

33.   Gouin, T. (2021). Addressing the importance of microplastic particles as vectors for long-range transport of chemical contaminants: perspective in relation to prioritizing research and regulatory actions. *Microplastics and Nanoplastics, 1*(1), 1-19. https://doi.org/10.1186/s43591-021-00016-w

34.   Naik, R. A., Rowles III, L. S., Hossain, A. I., Yen, M., Aldossary, R. M., Apul, O. G., Conkle, J., & Saleh, N. B. (2020). Microplastic particle versus fiber generation during photo-transformation in simulated seawater. *Science of the Total Environment, 736*, 139690. https://doi.org/10.1016/j.scitotenv.2020.139690

35.   Ranjan Ved, P., & Goel, S. (2019). Degradation of low-density polyethylene film exposed to UV radiation in four environments. *Journal of Hazardous, Toxic, and Radioactive Waste, 23*(4), 04019015. https://doi.org/10.1061/(ASCE)HZ.2153-5515.0000453

36.   Chubarenko, I., Efimova, I., Bagaeva, M., Bagaev, A., & Isachenko, I. (2020). On mechanical fragmentation of single-use plastics in the sea swash zone with different types of bottom sediments: Insights from laboratory experiments. *Marine Pollution Bulletin, 150*, 110726. https://doi.org/10.1016/j.marpolbul.2019.110726

37.   Dawson, A. L., Kawaguchi, S., King, C. K., Townsend, K. A., King, R., Huston, W. M., & Bengtson Nash, S. M. (2018). Turning microplastics into nanoplastics through digestive fragmentation by Antarctic krill. *Nature Communications, 9*(1), 1-8. https://doi.org/10.1038/s41467-018-03465-9

38.   Mateos-Cárdenas, A., O'Halloran, J., van Pelt, F. N., & Jansen, M. A. K. (2020). Rapid fragmentation of microplastics by the freshwater amphipod *Gammarus duebeni* (Lillj.). *Scientific Reports, 10*(1), 1-12. https://doi.org/10.1038/s41598-020-69635-2

39.   Luo, Z., Zhou, X., Su, Y., Wang, H., Yu, R., Zhou, S., Xu, E. G., & Xing, B. (2021). Environmental occurrence, fate, impact, and potential solution of tire microplastics: Similarities and differences with tire wear particles. *Science of the Total Environment, 795*, 148902. https://doi.org/10.1016/j.scitotenv.2021.148902

40.   Clausen, L. P. W., Hansen, O. F. H., Oturai, N. B., Syberg, K., & Hansen, S. F. (2020). Stakeholder analysis with regard to a recent European restriction proposal on microplastics. *PloS One, 15(*6), p.e0235062. https://doi.org/10.1371/journal.pone.0235062

41. Barnes, P. W., Robson, T. M., Neale, P. J., Williamson, C. E., Zepp, R. G., Madronich, S., Wilson, S. R., Andrady, A. L., Heikkilä, A. M., Bernhard, G. H., & Bais, A. F. (2022). Environmental effects of stratospheric ozone depletion, UV radiation, and interactions with climate change: UNEP Environmental Effects Assessment Panel, Update 2021. *Photochemical & Photobiological Sciences, 21*(3), 275-301. https://doi.org/10.1007/s43630-022-00176-5

42. Neale, P. J., Williamson, C. E., Banaszak, A. T., Häder, D. P., Hylander, S., Ossola, R., Rose, K. A., Wängberg, S.-Å., & Zepp, R. G. (2022). The response of aquatic ecosystems to the interactive effects of stratospheric ozone depletion, UV radiation, and climate change. *Chapter 5*

43. Dees, J. P., Ateia, M., & Sanchez, D.L. (2020). Microplastics and their degradation products in surface waters: A missing piece of the global carbon cycle puzzle. *ACS ES&T Water, 1*(2), 214-216. https://doi.org/10.1021/acsestwater.0c00205

44. Wieczorek, A. M., Croot, P. L., Lombard, F., Sheahan, J. N., & Doyle, T. K. (2019). Microplastic ingestion by gelatinous zooplankton may lower efficiency of the biological pump. *Environmental Science & Technology, 53*(9), 5387-5395. https://doi.org/10.1021/acs.est.8b07174

45. Stubbins, A., Law, K. L., Muñoz, S. E., Bianchi, T. S., & Zhu, L. (2021). Plastics in the Earth system. *Science, 373*(6550), 51-55. https://www.science.org/doi/10.1126/science.abb0354

46. Welsh, B., Aherne, J., Paterson, A. M., Yao, H., & McConnell, C. (2022). Atmospheric deposition of anthropogenic particles and microplastics in south-central Ontario, Canada. *Science of the Total Environment, 835*, 155426. https://doi.org/10.1016/j.scitotenv.2022.155426

47. Brahney, J., Mahowald, N., Prank, M., Cornwell, G., Klimont, Z., Matsui, H., & Prather, K.A. (2021). Constraining the atmospheric limb of the plastic cycle. *Proceedings of the National Academy of Sciences, 118*(16), e2020719118. https://doi.org/10.1073/pnas.2020719118

48. Allen, S., Allen, D., Phoenix, V. R., Le Roux, G., Durántez Jiménez, P., Simonneau, A., Binet, S., & Galop, D. (2019). Atmospheric transport and deposition of microplastics in a remote mountain catchment. *Nature Geoscience, 12*(5), 339-344. https://doi.org/10.1038/s41561-019-0335-5

49. Evangeliou, N., Grythe, H., Klimont, Z., Heyes, C., Eckhardt, S., Lopez-Aparicio, S., & Stohl, A. (2020). Atmospheric transport is a major pathway of microplastics to remote regions. *Nature Communications, 11*(1), 1-11. https://doi.org/10.1038/s41467-020-17201-9

50. Brahney, J., Hallerud, M., Heim, E., Hahnenberger, M., & Sukumaran, S. (2020). Plastic rain in protected areas of the United States. *Science, 368*(6496), 1257-1260. https://www.science.org/doi/10.1126/science.aaz5819

51. Drummond, J. D., Schneidewind, U., Li, A., Hoellein, T. J., Krause, S., & Packman, A. I. (2022). Microplastic accumulation in riverbed sediment via hyporheic exchange from headwaters to mainstems. *Science Advances, 8*(2), eabi9305. https://www.science.org/doi/10.1126/sciadv.abi9305

52. Li, Y., Zhang, H., & Tang, C. (2020). A review of possible pathways of marine microplastics transport in the ocean. *Anthropocene Coasts, 3*(1), 6-13. https://doi.org/10.1139/anc-2018-0030

53. Barrett, J., Chase, Z., Zhang, J., Holl, M. M. B., Willis, K., Williams, A., Hardesty, B. D., & Wilcox, C. (2020). Microplastic pollution in deep-sea sediments from the Great Australian Bight. *Frontiers in Marine Science, 7*, 808. https://doi.org/10.3389/fmars.2020.576170

54. Zhang, Y., Kang, S., Allen, S., Allen, D., Gao, T., & Sillanpää, M. (2020). Atmospheric microplastics: A review on current status and perspectives. *Earth-Science Reviews, 203*, 103118. https://doi.org/10.1016/j.earscirev.2020.103118

55. Chubarenko, I., Bagaev, A., Zobkov, M., & Esiukova, E. (2016). On some physical and dynamical properties of microplastic particles in marine environment. *Marine Pollution Bulletin, 108*(1-2), 105-112. https://doi.org/10.1016/j.marpolbul.2016.04.048

56. Póvoa, A. A., Skinner, L. F., & de Araújo, F. V. (2021). Fouling organisms in marine litter (rafting on abiogenic substrates): A global review of literature. *Marine Pollution Bulletin, 166*, 112189. https://doi.org/10.1016/j.marpolbul.2021.112189

57. Kreczak, H., Willmott, A. J., & Baggaley, A. W. (2021). Subsurface dynamics of buoyant microplastics subject to algal biofouling. *Limnology and Oceanography, 66*(9), 3287-3299. https://doi.org/10.1002/lno.11879

58. Yang, L., Zhang, Y., Kang, S., Wang, Z., & Wu, C. (2021). Microplastics in soil: A review on methods, occurrence, sources, and potential risk. *Science of the Total Environment, 780*, 146546. https://doi.org/10.1016/j.scitotenv.2021.146546

59. Sembiring, E., Fareza, A. A., Suendo, V., & Reza, M. (2020). The Presence of microplastics in water, sediment, and milkfish (*Chanos chanos*) at the downstream area of Citarum River, Indonesia. *Water, Air, & Soil Pollution, 231*(7), 1-14. https://doi.org/10.1007/s11270-020-04710-y

60. Wang, C., Zhao, J., & Xing, B. (2021). Environmental source, fate, and toxicity of microplastics. *Journal of Hazardous Materials, 407*, 124357. https://doi.org/10.1016/j.jhazmat.2020.124357

61. Gigault, J., El Hadri, H., Nguyen, B., Grassl, B., Rowenczyk, L., Tufenkji, N., Feng, S., & Wiesner, M. (2021). Nanoplastics are neither microplastics nor engineered nanoparticles. *Nature Nanotechnology, 16*(5), 501-507. https://doi.org/10.1038/s41565-021-00886-4

62. Foley, C. J., Feiner, Z. S., Malinich, T. D., & Höök, T. O. (2018). A meta-analysis of the effects of exposure to microplastics on fish and aquatic invertebrates. *Science of the Total Environment, 631*, 550-559. https://doi.org/10.1016/j.scitotenv.2018.03.046

63. Vivekanand, A. C., Mohapatra, S., & Tyagi, V. K. (2021). Microplastics in aquatic environment: Challenges and perspectives. *Chemosphere, 282*, 131151. https://doi.org/10.1016/j.chemosphere.2021.131151

64. Bucci, K., Tulio, M., & Rochman, C. M. (2020). What is known and unknown about the effects of plastic pollution: A meta-analysis and systematic review. *Ecological Applications, 30*(2), e02044. https://doi.org/10.1002/eap.2044

65. Mateos-Cárdenas, A., van Pelt, F. N., O'Halloran, J., & Jansen, M. A. K. (2021). Adsorption, uptake and toxicity of micro- and nanoplastics: Effects on terrestrial plants and aquatic macrophytes. *Environmental Pollution, 284*, 117183. https://doi.org/10.1016/j.envpol.2021.117183

66. Maity, S., & Pramanick, K. (2020). Perspectives and challenges of micro/nanoplastics-induced toxicity with special reference to phytotoxicity. *Global Change Biology, 26*(6), 3241-3250. https://doi.org/10.1111/gcb.15074

67. Rillig, M. C., & Lehmann, A. (2020). Microplastic in terrestrial ecosystems. *Science, 368*(6498), 1430. https://www.science.org/doi/10.1126/science.abb5979

68. Sarker, S., Huda, A. S., Niloy, M. N. H., & Chowdhury, G. W. (2022). Trophic transfer of microplastics in the aquatic ecosystem of Sundarbans mangrove forest, Bangladesh. *Science of the Total Environment, 155896*. https://doi.org/10.1016/j.scitotenv.2022.155896

69. Hasegawa, T., & Nakaoka, M. (2021). Trophic transfer of microplastics from mysids to fish greatly exceeds direct ingestion from the water column. *Environmental Pollution, 273*, 116468. https://doi.org/10.1016/j.envpol.2021.116468

70. Athey, S. N., & Erdle, L. M. (2022). Are we underestimating anthropogenic microfiber pollution? A critical review of occurrence, methods, and reporting. *Environmental Toxicology and Chemistry, 41*(4), 822-837. https://doi.org/10.1002/etc.5173

71. Chen, Q., Allgeier, A., Yin, D., & Hollert, H. (2019). Leaching of endocrine disrupting chemicals from marine microplastics and mesoplastics under common life stress conditions. *Environment International, 130*, 104938. https://doi.org/10.1016/j.envint.2019.104938

72. Rummel, C. D., Escher, B. I., Sandblom, O., Plassmann, M. M., Arp, H. P. H., MacLeod, M., & Jahnke, A. (2019). Effects of leachates from UV-weathered microplastic in cell-based bioassays. *Environmental Science & Technology, 53*(15), 9214-9223. https://doi.org/10.1021/acs.est.9b02400

73. Hüffer, T., Weniger, A.-K., & Hofmann, T. (2018). Sorption of organic compounds by aged polystyrene microplastic particles. *Environmental Pollution, 236*, 218-225. https://doi.org/10.1016/j.envpol.2018.01.022

74. Xiong, Y., Zhao, J., Li, L., Wang, Y., Dai, X., Yu, F., & Ma, J. (2020). Interfacial interaction between micro/nanoplastics and typical PPCPs and nanoplastics removal via electrosorption from an aqueous solution. *Water Research, 184*, 116100. https://doi.org/10.1016/j.watres.2020.116100

75. Mao, R., Lang, M., Yu, X., Wu, R., Yang, X., & Guo, X. (2020). Aging mechanism of microplastics with UV irradiation and its effects on the adsorption of heavy metals. *Journal of Hazardous Materials, 393*. https://doi.org/10.1016/j.jhazmat.2020.122515

76. Yu, F., Yang, C., Huang, G., Zhou, T., Zhao, Y., & Ma, J. (2020). Interfacial interaction between diverse microplastics and tetracycline by adsorption in an aqueous solution. *Science of the Total Environment, 721*, 137729. https://doi.org/10.1016/j.scitotenv.2020.137729

77. Zhang, P., Huang, P., Sun, H., Ma, J., & Li, B. (2020). The structure of agricultural microplastics (PT, PU and UF) and their sorption capacities for PAHs and PHE derivates under various salinity and oxidation treatments. *Environmental Pollution, 257*, 113525. https://doi.org/10.1016/j.envpol.2019.113525

Members of the Environmental Effects Assessment Panel and Co-authors (2018-2022)

Dr Anthony L. Andrady
Department of Chemical and Biomolecular Engineering
North Carolina State University
Raleigh, NC 27695-7901
United States

Dr Pieter J. Aucamp
Ptersa Environmental Consultants
Faerie Glen 0043
South Africa

Prof. Alkiviadis F. Bais
Aristotle University of Thessaloniki
Department of Physics
54124 Thessaloniki
Greece

Prof. Paul W. Barnes (Co-chair)
Department of Biological Sciences
Loyola University
6363 St. Charles Ave.
New Orleans, LA 70118
United States

Dr Germar H. Bernhard
Biospherical Instruments Inc.
5340 Riley Street
San Diego, CA 92110-2621
United States

Prof. Janet F. Bornman (Co-chair)
Food Futures Institute
Murdoch University
South St, Murdoch WA 6150
Australia

Prof. D.-P. Häder
Department of Biology
Friedrich-Alexander University
Erlangen-Nürnberg, Möhrendorf
Germany

Dr Anu M. Heikkilä
Finnish Meteorological Institute R&D
Climate Research
00101 Helsinki
Finland

Assoc. Prof. Samuel Hylander
Centre for Ecology and Evolution in Microbial Model Systems
Linnaeus University
Kalmar
Sweden

Dr Janice Longstreth
The Institute for Global Risk Research
9119 Kirkdale Rd, Ste 200
Bethesda, MD 20817
United States

Dr Sasha Madronich
National Center for Atmospheric Research
Boulder, Colorado, 80307
United States

Dr Patrick J. Neale
Smithsonian Environmental Research Center
Edgewater, Maryland 21037
United States

Prof. Rachel Neale
QIMR Berghofer Medical Research Institute
Locked Bag 2000
Royal Brisbane Hospital
Brisbane, QLD, 4029
Australia

Dr Krishna K. Pandey (Co-chair)
Institute of Wood Science and Technology
18th Cross Malleswaram
Bengaluru – 560003
India

Co-authors

Assoc. Prof. Mads P. Sulbæk Andersen
Department of Chemistry and Biochemistry
California State University
18111 Nordhoff St
Northridge, CA 91330-8262
United States

Dr Anastazia T. Banaszak
Unidad Académica de Sistemas Arrecifales
Instituto de Ciencias del Mar y Limnología Universidad Nacional
Autónoma de México Prolongación Avenida Niños Héroes S/N
Dom. Con. Puerto Morelos, Delegación Benito Juárez 77580
Quintana Roo
Mexico

Professor Marianne Berwick
CRF 03
2325 Camino de Salud,
Albuquerque, New Mexico, 87131
United States

Prof. Scott N. Byrne
The University of Sydney
School of Medical Sciences
Faculty of Medicine and Health; Westmead Institute for Medical
Research Centre for Immunology & Allergy Research
Westmead, NSW 2145
Australia

Dr Laura S. Bruckman
School of Engineering
Department of Materials Science and Engineering
Case Western Reserve University
Cleveland, Ohio
United States

Dr Bente Føreid
Norwegian Institute of Bioeconomy Research (NIBIO), Fredrik A.
Dahls vei
1430 Ås
Norway

Dr Loes Hollestein
Erasmus MC
University Medical Center Rotterdam
Dr Molewaterplein 40, 3015 GD Rotterdam
The Netherlands

Assoc. Prof. Wen-Che Hou
Department of Environmental Engineering
National Cheng Kung University
No.1 University Road, Tainan City
Taiwan 70101, Republic of China

Prof. Marcel A.K. Jansen
School of Biological, Earth and Environmental Sciences,
Environmental Research Institute
University College Cork, Cork
Ireland

Dr Andrew R. Klekociuk
Australian Antarctic Division
203 Channel Highway
Kingston, Tasmania 7050
Australia

Dr Hong Li
Institute of Atmospheric Environment
Chinese Research Academy of Environmental Sciences, Chaoyang
District, Beijing
China

J. Ben Liley
National Institute of Water & Atmospheric Research
Private Bag 50061, Omakau, Central Otago
New Zealand

Prof. Javier Martínez-Abaigar
University of La Rioja
Faculty of Science and Technology
CCT, Madre de Dios 51
26006 Logroño (La Rioja)
Spain

Co-authors

Dr Richard L. McKenzie
National Institute of Water and Atmospheric Research (NIWA),
Lauder
Private Bag 50061 Omakau
Central Otago 9352
New Zealand

Assoc. Prof. Catherine Olsen
Department of Population Health
Queensland Institute of Medical Research
Berghofer Medical Research Institute
300 Herston Road, Herston 4029
Queensland
Australia

Dr Rachele Ossola
Department of Chemistry
1301 Center Avenue
Colorado State University
Fort Collins, CO 80523-1872
United States

Prof. Nigel D. Paul
Lancaster Environment Centre
Lancaster University
Lancaster, LA1 4YQ
United Kingdom

Dr Tamara Schikowski
Leibniz Research Institute for Environmental Medicine (IUF)
Auf'm Hennekamp 50
DE-40225 Düsseldorf
Germany

Prof. (Emeritus) Keith R. Solomon
Centre for Toxicology, School of Environmental Sciences
University of Guelph
Guelph, ON N1G 2W1
Canada

Assoc. Prof. Justina Ukpebor
Chemistry Department
Faculty of Physical Sciences
University of Benin
Benin City
Nigeria

Dr Qing-Wei Wang
Institute of Applied Ecology
Chinese Academy of Sciences (CAS)
72 Wenhua, Shenhe, Shenyang 110016
China

Prof. Meifang Zhu
College of Materials Science & Engineering
2999 North Renmin Road, Songjiang District
Donghua University
Shanghai 201620
China

Dr Liping Zhu
Center for Advanced Low-dimension Materials
2999 North Renmin Rd, Songjiang District
Donghua University
Shanghai 201620
China

Contributing author
Dr Roy Mackenzie
Cape Horn International Center (CHIC), Puerto Williams
Millennium Institute Biodiversity of Antarctic and Subantarctic
Ecosystems
Chile

Reviewers of the 2022 Assessment of the UNEP Environmental Effects Assessment Panel

Julie Newton-Bishop
University of Leeds
Leeds, United Kingdom

Rubén Piacentini
Institute of Physics Rosario (CONICET - National Univerisity of Rosario)
Rosario, Argentina

Halim Redhwi
King Fahad University of Petroleum & Minerals
Dhahran, Saudi Arabia

Miguel Rivas Avila
Universidad de Tarapaca
Arica, Chile

Eva Rosenqvist
University of Copenhagen
Taastrup, Denmark

Jonathan Shanklin
British Antarctic Survey
Cambridge, United Kingdom

Craig Sinclair
Cancer Council Victoria
Melbourne, Australia

Knut Asbjørn Solhaug
Norwegian University of Life Sciences
Ås, Norway

Helen Tope
Technology and Economic Assessment Panel
Melbourne, Australia

Matthew Tully
Bureau of Meteorology
Melbourne, Australia

Emilie van Deventer
World Health Organization
Geneva, Switzerland

Jason Wargent
Massey University
Palmerston North, New Zealand

Richard Weller
University of Edinburgh
Edinburgh, United Kingdom

Jana Barbro Winkler
Helmholtz Association of German Research Centres
Munich, Germany

Otmar Urban
Global Change Research Institute
Brno, Czechoslovakia

Arjan van Dijk
RIVM
Bilthoven, The Netherlands

Ann Webb
University of Manchester
Manchester, United Kingdom

David Whiteman
QIMR Berghofer Medical Research Institute
Brisbane, Australia

Hans Christian Wulf
Bispebjerg Hospital
Copenhagen, Denmark

Rubén Piacentini
Institute of Physics Rosario (CONICET - National Univerisity of Rosario)
Rosario, Argentina

Halim Redhwi
King Fahad University of Petroleum & Minerals
Dhahran, Saudi Arabia

Miguel Rivas Avila
Universidad de Tarapaca
Arica, Chile

Eva Rosenqvist
University of Copenhagen
Taastrup, Denmark

Jonathan Shanklin
British Antarctic Survey
Cambridge, United Kingdom

Reviewers

Craig Sinclair
Cancer Council Victoria
Melbourne, Australia

Knut Asbjørn Solhaug
Norwegian University of Life Sciences
Ås, Norway

Helen Tope
Technology and Economic Assessment Panel
Melbourne, Australia

Matthew Tully
Bureau of Meteorology
Melbourne, Australia

Emilie van Deventer
World Health Organization
Geneva, Switzerland

Jason Wargent
Massey University
Palmerston North, New Zealand

Richard Weller
University of Edinburgh
Edinburgh, United Kingdom

Jana Barbro Winkler
Helmholtz Association of German Research Centres
Munich, Germany

Otmar Urban
Global Change Research Institute
Brno, Czechoslovakia

Arjan van Dijk
RIVM
Bilthoven, The Netherlands

Ann Webb
University of Manchester
Manchester, United Kingdom

David Whiteman
QIMR Berghofer Medical Research Institute
Brisbane, Australia

Hans Christian Wulf
Bispebjerg Hospital
Copenhagen, Denmark